frontiers | Research Topics

Neural bases of neurological and psychiatric disorders and their neuromodulation treatments

Edited by
Kai Wang, Jiaojian Wang, Yanghua Tian, Bochao Cheng and Hongming Li

Published in
Frontiers in Psychiatry
Frontiers in Human Neuroscience
Frontiers in Neuroscience

ISSN 1664-8714
ISBN 978-2-83251-009-4
DOI 10.3389/978-2-83251-009-4

About Frontiers

Frontiers is more than just an open access publisher of scholarly articles: it is a pioneering approach to the world of academia, radically improving the way scholarly research is managed. The grand vision of Frontiers is a world where all people have an equal opportunity to seek, share and generate knowledge. Frontiers provides immediate and permanent online open access to all its publications, but this alone is not enough to realize our grand goals.

Frontiers journal series

The Frontiers journal series is a multi-tier and interdisciplinary set of open-access, online journals, promising a paradigm shift from the current review, selection and dissemination processes in academic publishing. All Frontiers journals are driven by researchers for researchers; therefore, they constitute a service to the scholarly community. At the same time, the *Frontiers journal series* operates on a revolutionary invention, the tiered publishing system, initially addressing specific communities of scholars, and gradually climbing up to broader public understanding, thus serving the interests of the lay society, too.

Dedication to quality

Each Frontiers article is a landmark of the highest quality, thanks to genuinely collaborative interactions between authors and review editors, who include some of the world's best academicians. Research must be certified by peers before entering a stream of knowledge that may eventually reach the public - and shape society; therefore, Frontiers only applies the most rigorous and unbiased reviews. Frontiers revolutionizes research publishing by freely delivering the most outstanding research, evaluated with no bias from both the academic and social point of view. By applying the most advanced information technologies, Frontiers is catapulting scholarly publishing into a new generation.

What are Frontiers Research Topics?

Frontiers Research Topics are very popular trademarks of the *Frontiers journals series*: they are collections of at least ten articles, all centered on a particular subject. With their unique mix of varied contributions from Original Research to Review Articles, Frontiers Research Topics unify the most influential researchers, the latest key findings and historical advances in a hot research area.

Find out more on how to host your own Frontiers Research Topic or contribute to one as an author by contacting the Frontiers editorial office: frontiersin.org/about/contact

Neural bases of neurological and psychiatric disorders and their neuromodulation treatments

Topic editors

Kai Wang — Anhui Medical University, China

Jiaojian Wang — Kunming University of Science and Technology, China

Yanghua Tian — First Affiliated Hospital of Anhui Medical University, China

Bochao Cheng — Sichuan University, China

Hongming Li — University of Pennsylvania, United States

Citation

Wang, K., Wang, J., Tian, Y., Cheng, B., Li, H., eds. (2023). *Neural bases of neurological and psychiatric disorders and their neuromodulation treatments*. Lausanne: Frontiers Media SA. doi: 10.3389/978-2-83251-009-4

Table of contents

frontiers in Psychiatry

ORIGINAL RESEARCH
published: 26 November 2020
doi: 10.3389/fpsyt.2020.608928

Association Between Trait Empathy and Resting Brain Activity in Women With Primary Dysmenorrhea During the Pain and Pain-Free Phases

Wanghuan Dun[1,2†], Tongtong Fan[3†], Qiming Wang[4], Ke Wang[3], Jing Yang[3], Hui Li[3], Jixin Liu[4] and Hongjuan Liu[1*]*

[1] Department of Intensive Care Unit, First Affiliated Hospital of Xi'an Jiaotong University, Xi'an, China, [2] Department of Rehabilitation Medicine, First Affiliated Hospital of Xi'an Jiaotong University, Xi'an, China, [3] Department of Medical Imaging, First Affiliated Hospital of Xi'an Jiaotong University, Xi'an, China, [4] School of Life Science and Technology, Center for Brain Imaging, Xidian University, Xi'an, China

OPEN ACCESS

Edited by:
Jiaojian Wang,
University of Electronic Science and Technology of China, China

Reviewed by:
Xianglin Li,
Binzhou Medical University, China
Xun Yang,
Sichuan University, China

***Correspondence:**
Jixin Liu
liujixin@xidian.edu.cn
Hongjuan Liu
liuhj423@163.com

[†] These authors have contributed equally to this work

Specialty section:
This article was submitted to Neuroimaging and Stimulation, a section of the journal Frontiers in Psychiatry

Received: 23 September 2020
Accepted: 04 November 2020
Published: 26 November 2020

Citation:
Dun W, Fan T, Wang Q, Wang K, Yang J, Li H, Liu J and Liu H (2020) Association Between Trait Empathy and Resting Brain Activity in Women With Primary Dysmenorrhea During the Pain and Pain-Free Phases. Front. Psychiatry 11:608928. doi: 10.3389/fpsyt.2020.608928

Empathy refers to the ability to understand someone else's emotions and fluctuates with the current state in healthy individuals. However, little is known about the neural network of empathy in clinical populations at different pain states. The current study aimed to examine the effects of long-term pain on empathy-related networks and whether empathy varied at different pain states by studying primary dysmenorrhea (PDM) patients. Multivariate partial least squares was employed in 46 PDM women and 46 healthy controls (HC) during periovulatory, luteal, and menstruation phases. We identified neural networks associated with different aspects of empathy in both groups. Part of the obtained empathy-related network in PDM exhibited a similar activity compared with HC, including the right anterior insula and other regions, whereas others have an opposite activity in PDM, including the inferior frontal gyrus and right inferior parietal lobule. These results indicated an abnormal regulation to empathy in PDM. Furthermore, there was no difference in empathy association patterns in PDM between the pain and pain-free states. This study suggested that long-term pain experience may lead to an abnormal function of the brain network for empathy processing that did not vary with the pain or pain-free state across the menstrual cycle.

Keywords: empathy, primary dysmenorrhea, interpersonal reactivity index, partial least squares, functional MRI

SIGNIFICANCE

This study reveals the association of resting brain activity and different trait empathy scores, and suggests that repeated menstrual pain had an effect on empathy processing that did not vary with the pain or pain-free states. It provides valuable insights into the neural mechanisms of empathy in primary dysmenorrhea.

INTRODUCTION

Empathy is a complex psychological construct that enable the sharing of the emotions, pain, and sensations of others, and also allow the exertion of cognitive ability in our interactions (1). The capacity to resonate with others may be influenced by many factors, such as motivational factors (2), gender differences (3), or current states (4). The ability to understand the pain in fellow human beings may be inhibited when individuals experience anger or depressed emotions (5). However, mechanisms of empathy in chronic pain are still unclear and have not received scientific attention compared with those related with healthy individuals.

Neuroimaging has been developed to assess the neural mechanisms of empathy in healthy individuals, and has consistently identified a core network comprising the anterior insula (AI) and the mid-cingulate cortex (MCC) in empathic states (6). Given that empathy can fluctuate in character in different states, a limited number of neuroimaging studies assessed empathy with subjects in different states. An electroencephalographic (EEG) study showed that the motor component of empathy for pain can be influenced by the mood states (5). Mira and colleagues reported that participants who were exposed to pressure pain yielded a lower activity in AI and the aMCC (7). Additionally, functional magnetic resonance imaging (fMRI) on subjects with congenital insensitivity to pain suggested that the empathy for pain in patients was regulated by different mechanics (8). Given that long-term pain can lead to maladaptive alteration in the central nervous system, including regions associated with empathy (9), whether empathy in clinical populations with pain can be influenced by prior pain experiences is still unknown. Primary dysmenorrhea (PDM), a very common type of cyclic menstrual pain without organic causes in female adolescents, induces recurrent, spontaneous, painful and pain-free states (10). Women with PDM have a poorer mood state during menstruation than preovulatory phases (11). Hence, PDM can be used as a great clinical model to study both the effects of long-term menstrual pain on empathy and the difference of the empathy between painful and pain-free states.

The interpersonal reactivity index (IRI) is the most common psychometric tool used to measure an individual's empathy. It uses four subscales including perspective taking, fantasy, empathic concern, and personal distress (12). Despite the findings of prior neuroimaging studies that examined the relationship between the brain and empathy based on IRI, all of them employed the mass-univariate general linear models (GLM) (1). In addition to the assumptions that must be met, mass-univariate tests increase the occurrence of false positive findings owing to multiple comparisons, and thus attenuate minor effects caused by corrections (13).

In the current study, our main aims were to investigate: (1) whether or not the empathy related to the resting brain activity could be affected by long-term pain, and (2) whether or not there were differences in empathy between painful and pain-free phases in women with PDM. Resting-state functional data and clinical variables were collected from 46 PDM women and 46 healthy controls (HC) during the periovulatory, luteal, and menstruation phases. We used the multivariate analysis method partial least squares (PLS) correlation to explore the relationship between patients' trait empathy and brain resting activity at three time points.

MATERIALS AND METHODS

Subjects

In the present study, we recruited 57 right-handed PDM patients and 53 age- and education-matched healthy participants from a local university with advertisements. All the subjects were diagnosed by a gynecologist and took part in conventional MRI scans to exclude pelvic or anatomical brain abnormalities. The following are inclusion criteria for PDMs: (1) menstrual cycle regularity of approximately 27–32 days, (2) menstrual pain during the past 6 months, (3) averaged pain intensity score >4 on a visual analog scale (($0 =$ no pain, $10 =$ worst imaginable pain) during the past 6 months. The inclusion criteria for HCs was similar to PDMs but without menstrual pain. Subject exclusion criteria were: (1) psychological or neurologic disease, (3) organic pelvic disease, (4) smoking, alcohol, or drug abuse, (5) childbirth or plan for pregnancy, (6) a history of other comorbid chronic pain conditions (e.g., irritable bowel syndrome, fibromyalgia, etc.), (7) use of oral contraceptives, hormonal supplements, Chinese medication, or the intake of central-acting medication during the last 6 months before MRI, or (8) any MRI contraindications. Resting-state functional (fMRI) data and various pathopsychological data were collected during the periovulatory, luteal, and menstruation phases. Urine kits were used to quantify luteinizing hormone to verify the periovulatory phase of participants. Eight PDMs and five HCs were excluded for missing fMRI data. Three patients and two healthy individuals lost their questionnaire information. Thus, 46 PDMs and 46 HCs were used in subsequent analyses.

Informed consent was obtained from all the participants and the experimental procedures were explained. The Institutional Review Board of the First Affiliated Hospital of the Medical College Xi'an Jiaotong University approved the study that complied with the Declaration of Helsinki.

Trait Empathy Assessment

The Chinese version of the IRI was used in this study. It is a self-report questionnaire designed to assess participants' trait empathy. It consists of four subscales, each of which measures a separate aspect of empathy: perspective taking (PT), fantasy scale (FS), empathic concern (EC), and personal distress (PD). PT refers to the ability to spontaneously adopt the perspectives of other people and see things from their points-of-view, FS refers to the tendency to transpose themselves into fictional situations, EC refers to a tendency to experience feelings of compassion and concern for the observed individual, and PD is self-oriented and measures feelings of anxiety and distress that result from witnessing another person's negative experience (14).

Each subscale contains seven items and participants rate the degree to which each item describes them on a five-point Likert scale ranging from 0 ("Does not describe me well") to 4

("Describes me very well"). For each subscale, a total score is calculated with higher scores indicating a higher functional level at the aspect of empathy.

MRI Data Acquisition

MRI was conducted at the Xi'an Jiaotong University during the menstruation, luteal, and periovulation phases, using a 3 T scanner (GE Signa HDxt, Milwaukee, WI, USA) with an eight-channel phased array head coil. The participants were told to close their eyes during the scans, but were instructed to remain awake and not to think about anything in particular. We obtained high-resolution three-dimensional (3D) longitudinal relaxation (T1) structural images with an axial fast spoiled gradient recalled sequence (FSGR) with the following parameters: voxel size = 1 mm^3, repetition time (TR)/echo time (TE) = 1,900 ms/2.6 ms, field-of-view (FOV) = 256 × 256 mm, acquisition matrix =256 × 256, flip angle = 12°, and slices = 140. Resting-state functional images were obtained using transverse relaxation star (T2*)-weighted, single-shot gradient-recalled echo-planar-imaging (EPI) sequence (TR = 2,000 ms, TE = 30 ms, matrix size = 64 × 64, slices = 35, slice thickness = 4.0 mm, FOV = 240 × 240 mm, flip angle = 90°.

MRI Data Preprocessing

Imaging data were analyzed using the FSL and Automated Functional Neuro-Imaging (http://afni.nimh.nih.gov/afni) software. Scripts containing the processing commands used in the current study have been released as part of the 1,000 Functional Connectome Project (http://www.nitrc.org/projects/fcon_1000) (15). A standard data preprocessing strategy was performed. Specifically, (1) the first five EPI volumes of each subject were discarded to allow subjects to become familiar with the scanning environment and eliminate magnetization variations to the steady state, and (2) the remaining images were corrected for slice timing, 3D head motion, time series despiking effects, and spatial smoothing and four-dimensional (4D) mean-based intensity normalization; (3) the time series from each voxel in the corrected images was temporally filtered with a bandpass filter (0.01–0.08 Hz) that eliminated the linear and quadratic trends. (4) The remaining images were then spatially normalized to the Montreal Neurological Institute 152 space and resampled to 2 mm isotropic voxels, and (5) eight nuisance signals (WM, cerebrospinal fluid signals and 24 motion parameters) were regressed out.

MRI DATA ANALYSIS

Regional Homogeneity (ReHo)

ReHo is a data-driven method evaluated using Kendall's coefficient of concordance (KCC) (16). It characterizes the local functional connectivity (FC) between a given voxel and its nearest neighboring voxels, and can integrate regional homogeneity in both structure and function. A previous study reported that ReHo obtained highly reliable (test-retest) results in a resting-state fMRI data analysis (17). Thus, ReHo is regarded as a robust and crucial measure of brain activity (18).

We used the resting-state fMRI data analysis toolkit (http://www.restfmri.net/forum/index.php) to evaluate the ReHo values in our fMRI datasets. First, ReHo maps of each subject were generated by computing the KCC of the time series of each voxel with its nearest 26 neighboring voxels. To eliminate the influence of individual variability, individual KCC images among each voxel were divided by their own mean KCC values estimated within a whole-brain mask for standardization. Finally, a Gaussian kernel (full-width at half-maximum: 4 mm) was used to smooth the standardized ReHo images to reduce noise and residual differences.

Statistical Analysis on Demographic and Clinical Data

Statistical tests were performed using SPSS Statistics 20.0 (SPSS Inc, Chicago, IL). Two-sample *t*-test was used to evaluate the differences in demographic characteristics (age, education, menstrual cycle, etc.) and clinical information (VAS, IRI) between HC and PDM. We then applied repeated measures analysis of variance (ANOVA) to test for a significant difference between clinical information within the group and the interaction effect between groups during the three phases. Normality of the data was examined and confirmed prior to statistical analysis. Results were considered significant at $p < 0.05$.

Statistical Analysis of MRI Data Using PLS Correlation Analysis

Behavior PLSC was used to explore resting brain activity associated with different dimensions of empathy. Behavior variables for each individual are entered into one matrix (behavior matrix), and resting brain activity in each voxel across the brains of each individual was expressed by another matrix (brain matrix). Herein, we included the four behavior variables: PT, FS, EC, and PD.

The first step is to compute the cross-covariance between behavior and brain matrix (19). The cross-covariance matrix was then subjected to singular value decomposition (SVD). A set of orthogonal latent variables (LVs) was generated and represented the maximal covariance between brain and behavioral measures (20). LVs consisted of d (the singular value that characterize the brain-behavior correlation strength), brain saliences (weightings across voxels that best express the contributions of every voxel to the brain-behavior correlation explained by this LV), and behavior saliences (weights across behavioral variables that indicate the intensity of the contribution of each behavioral variable to the brain-behavior correlation explained by this LV). The number of LVs is equal to the rank of the number of behavioral variables multiplied by the number of groups (20). Therefore, the PLS analysis in our study produced eight LVs, as we have two groups and four behavioral variables.

Additionally, we calculated brain scores for each participant as the dot product of the resting brain activity and the brain saliences used to quantify the contribution of each individual to each LV. Brain scores are the projections of every participant's brain data onto the salient brain pattern. Large absolute values of

TABLE 1 | Demographics of the studied participants.

Characteristic	HC ($n = 44$) mean (SE)	PDM ($n = 44$) mean (SE)	t	p
Age (years)	24.11 (0.21)	23.93 (0.34)	0.46	0.647
Education (years)	17.45 (0.15)	17.61 (0.23)	−0.57	0.568
Menstrual cycle (days)	29.14 (0.23)	29.34 (0.27)	−0.57	0.568
Age of menarche (years)	12.48 (0.14)	12.57 (0.17)	−0.42	0.674
History of menstrual pain (years)	—	10.48 (0.25)	—	—
Duration of menstrual pain (days)	—	1.94 (0.14)	—	—

PDM, primary dysmenorrhea; HC, healthy controls; SE, standard error. Comparisons of the subjects' basic information between PDM and HC groups were conducted with two-sample t-tests ($p < 0.05$ was considered significant).

TABLE 2 | Clinical comparison at periovulatory, luteal, and menstruation phases.

Behavior assessment		Time 1 mean (SE)	Time 2 mean (SE)	Time 3 mean (SE)	p^a	p^b
VAS	HC	0.07 (0.03)	0.31 (0.14)	0.47 (0.14)	0.056	0.000*
	PDM	1.07 (0.31)	1.30 (0.31)	4.27 (0.31)	0.000*	
	p^c	0.002*	0.005*	0.000*		
Perspective taking	HC	11.18 (0.53)	10.61 (0.51)	10.82 (0.56)	0.426	0.93
	PDM	11.52 (0.59)	10.95 (0.47)	10.93 (0.56)	0.264	
	p^c	0.666	0.626	0.887		
Fantasy scale	HC	13.89 (0.61)	14.86 (0.57)	14.25 (0.53)	0.083	0.15
	PDM	16.25 (0.56)	16.00 (0.58)	16.16 (0.65)	0.833	
	p^c	0.004*	0.159	0.020*		
Empathic concern	HC	16.45 (0.54)	16.84 (0.45)	15.98 (0.42)	0.196	0.30
	PDM	18.00 (0.41)	17.39 (0.46)	16.86 (0.49)	0.074	
	p^c	0.024*	0.400	0.173		
Personal distress	HC	7.36 (0.53)	7.43 (0.55)	7.32 (0.60)	0.969	0.61
	PDM	8.16 (0.54)	8.68 (0.59)	8.59 (0.66)	0.502	
	p^c	0.296	0.126	0.157		

*PDM, primary dysmenorrhea; HC, healthy controls; SE, standard error. Repeated measurements ANOVA: a, comparison of data at different times within the group; b, comparison of interactions (Group*Times) between groups at different times. Two-sample t-test: c, Comparison of differences between groups at the same period (*: $p < 0.05$).*

brain scores represent a strong contribution to the pattern and the scores closer to zero demonstrate a weaker contribution.

To determine the statistical significance of each LV in the PLS correlation analysis, we applied permutation testing with the use of 5,000 permutations. These reordered randomly the rows of the data matrix and maintained the behavior matrix unchanged. The LVs with $p < 0.05$ were considered significant so that the LVs were generalizable to the population. In the last step, we repeated bootstrap resampling 5,000 times to assess reliability of the effect in each voxel. Bootstrap ratios (BSRs: original saliences/bootstrap standard errors) were then obtained. The absolute values of saliences with BSR thresholds >3 were considered reliable, and were equivalent to p-values of approximately 0.01 (21). Otherwise, this involves random sampling (with replacement) of the brain and behavior matrices.

Subsequently, we obtained the distribution of the Pearson's correlation coefficient among the brain scores and each level of trait empathy in the two groups at each period. Finally, two-sample t-tests were performed between groups during the three phases.

RESULTS

Demographic Data and Clinical Characteristics

Forty-six right-handed patients with PDM and forty-six gender-matched HCs were recruited in the study. There was no significant difference between PDM patients and HCs in age, years of education, menstrual cycle, and age at menarche ($p > 0.05$). In this study, all PDM patients had a long history of menstrual pain (10.48 ± 0.25 years, **Table 1**).

PDM patients had significantly higher VAS scores than HCs during the periovulatory, luteal, and menstruation phases (**Table 2**). Additionally, repeated measures ANOVA test demonstrated that VAS scores yielded significant group-time interactions and significant differences within the PDM group at the three time points. For IRI subscales, two-sample t-tests yielded significant group differences with respect to the FS both in the periovulatory and menstruation phases, and empathic concern in the periovulatory phase ($p < 0.05$). No significant differences were found between groups and group-time interactions at perspective taking and personal distress.

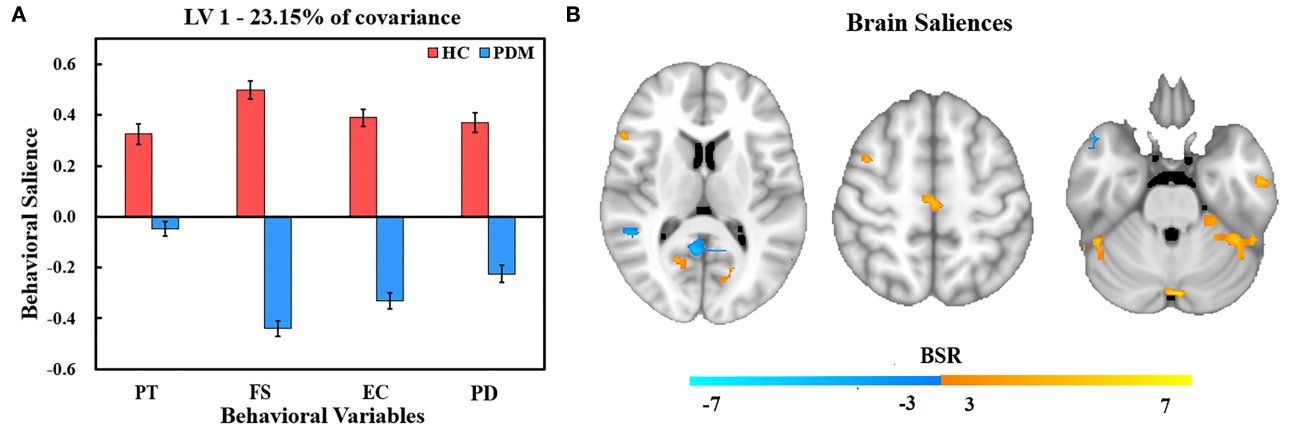

FIGURE 1 | PLS correlation analysis results of LV 1. **(A)** Bar graph of behavioral salience with stability estimated using the bootstrap method in the two studied groups. **(B)** Resting brain activity showing brain regions in which variations were associated with trait empathy. The map is generated with the threshold set at $p = 0.01$ (BSR = ±3). In the HC group, warm regions indicated a positive correlation between resting brain activity, empathy scores, and cool regions showed a negative correlation between the resting brain activity and empathy scores. In contrast, the association was reversed in the PDM group (warm, negative correlation; cool, positive correlation). PT, perspective taking; FS, fantasy; EC, empathic concern; PD, personal distress.

Association Patterns Between Resting Brain and Empathy

The PLS analysis generated 10 latent variables (LVs), but only the first significant LV (LV1) and the second significant LV (LV2) were statistically significant in relation to trait empathy and corresponding resting brain patterns in PDM patients and HCs. LV1 accounted for 23.15% of the shared covariance between clinical and resting brain measures and identified abnormal regulation brain patterns to trait empathy in PDM women compared with HCs (**Figure 1**). LV2 accounted for 19.31% covariance and identified similar regulation patterns between groups (**Figure 2**).

Abnormal Regulation Brain Patterns to Trait Empathy in PDM Women Compared With HCs

Figure 1A shows behavior salience characteristics corresponding to the first significant LV for PLS correlation analysis. In HCs group, FS was the strongest contributor to LV1, followed by EC, PD, and PT. Different dimensions of trait empathy have similar contributions to the brain-behavior correlation in PDM patients with the highest behavior salience in FS, followed by EC, PD, and PT. This indicates that all dimensions of trait empathy contributed to the brain-behavior correlation. However, the correlation patterns for behaviors and resting brain activities of the HC and PDM groups were different. This indicates an abnormal regulation pattern to empathy by brain regions in PDM women compared with HCs.

The brain regions that showed an association with trait empathy identified in LV1 are shown in **Figure 1B**. Trait empathy was correlated with both decreased and increased regional resting brain activity. In the HC group, we found that the resting brain activity was negatively correlated with trait empathy in the middle temporal gyrus, superior temporal gyrus, right lingual gyrus, middle occipital gyrus, posterior cingulate, right inferior parietal lobule (IPL), postcentral gyrus, and left supramarginal gyrus (**Table 3**). Positive associations between trait empathy and resting brain activity were in the right inferior temporal gyrus, left middle frontal gyrus, left fusiform gyrus, left precuneus, superior frontal gyrus, inferior frontal gyrus (IFG), and right supplementary motor area. The brain regions that correlated with trait empathy in PDM patients were abnormal. This identified opposite associations with trait empathy in these regions.

Correlation plots of brain scores with different dimensions of trait empathy are shown in **Figure 2**. In the HC group, brain scores are positively correlated with all dimensions of trait empathy in the periovulatory, luteal, and menstruation phases. In contrast to the HCs, there is a negative correlation in the PDM group regardless of the moderate positive correlation with PT in the periovulatory phase. Brain score correlations at each level of empathy yielded significant differences between HC and PDM in the periovulatory, luteal, and menstruation phases (none of the bootstrapped 95% confidence intervals of the correlation coefficients shown in **Figure 2** crosses zero). Moreover, significant changes of the correlation in both groups did not occur in the three phases.

Similar Brain Regulation Patterns to Trait Empathy Between PDM Women and HCs

Behavior salience contributing to LV2 are shown in **Figure 3A**. In comparison with LV1, LV2 reflects a similar regulation pattern of brain to trait empathy between PDM women and HCs. We found that FS was the strongest contributor to LV2, followed by PD, EC,

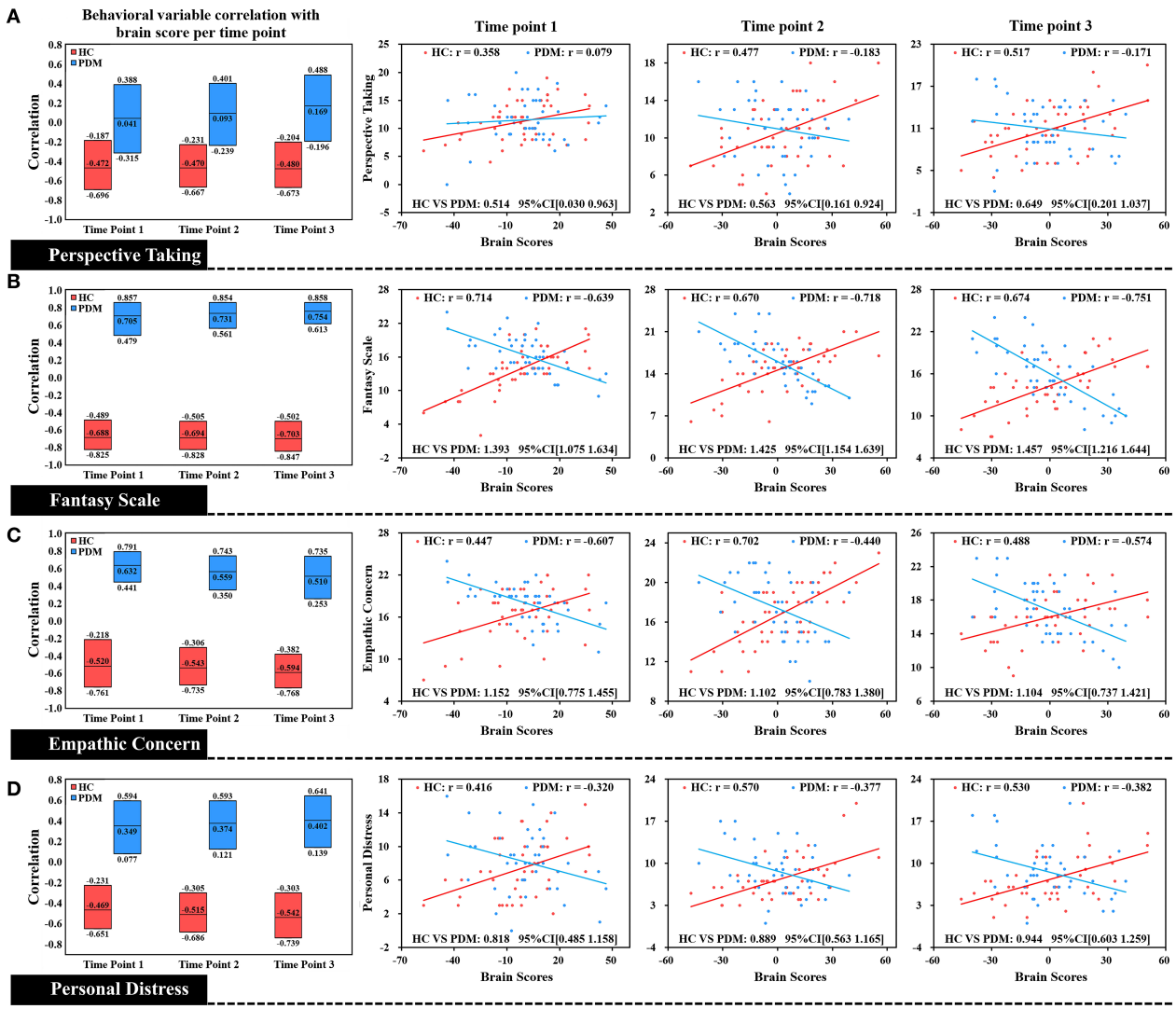

FIGURE 2 | Correlation of each level of trait empathy with brain scores of LV 1. In the box plot, the middle line of the box was the original correlation between empathy and brain score in the same phase, and the boundary of the box was the 95% CI of the trait empathy correlation with brain scores based on the use of 5,000 bootstraps. The original correlation between empathy and brain scores is shown by the scatter plot. There was a significant difference between HC and PDM in different dimensions of trait empathy in correlation with brain scores at the periovulatory, luteal, and menstruation phases through the effect-size analysis. There were no significant correlation changes in both groups during the three phases. HC, red; PDM, blue.

and PT in HCs. The highest behavior salience was also found in FS, followed by EC, PD, and PT in the PDM group.

The correlation of resting brain and trait empathy between the groups in LV2 was similar (**Figure 3B**). There was a significantly negative association in brain regions in both groups that involved the inferior temporal gyrus, right middle temporal gyrus, lingual gyrus, right anterior insula, middle frontal gyrus, IFG, and left IPL (**Table 4**). Positive association between trait empathy and resting brain activity were found in the left superior temporal gyrus, left inferior occipital gyrus, right posterior cingulate, right precuneus, and middle frontal gyrus.

Brain scores correlated with different dimensions of trait empathy in three phases in both groups is shown in **Figure 4**. We found that brain scores were negatively correlated with FS, EC, and PD, in the three phases in the HC group. There was also a negative correlation in the PDM group of the brain scores with all dimensions of trait empathy. Specifically, no significant difference between HC and PDM was found in the correlations of the brain scores with EC, FS, and PD, based on effect-size analysis (all of the bootstrapped 95% confidence intervals of the correlation coefficients shown in **Figure 4** cross zero). Similar to LV1, the correlation in both groups did not significantly change during the three phases.

DISCUSSION

In this study, it was shown based on the use of multivariate PLS correlation analyses that part of the identified empathy-related brain network in the PDM yielded an opposite activity compared with HC that indicated an abnormal regulation pattern to empathy in PDM. Additionally, these abnormal networks in PDM did not change across the menstrual cycle. This suggested that long-term menstrual pain may affect different aspects of trait empathy regardless of the pain or pain-free phases.

Trait Empathy-Related Brain Functional Networks in HCs

In our findings, we found that a set of brain regions were involved in different dimensions of trait empathy in HCs. These brain regions mainly included the right anterior insula, IFG, IPL, middle and superior temporal gyri, posterior cingulate,

TABLE 3 | The brain regions that have reliability contribution to behavior-brain covariance in LV 1.

Region of activation	Side	Sizes	Peak coordinates			
			x	y	z	BSRs
Inferior Temporal Gyrus	R	54	48	−48	−30	5.705
Middle Temporal Gyrus	L	54	−39	18	39	6.626
Middle Temporal Gyrus	R	20	48	−45	12	−6.453
Superior Temporal Gyrus	R	21	48	12	−21	−6.112
Lingual Gyrus	R	24	3	−87	−18	−5.071
Middle Occipital Gyrus	R	25	48	−69	−12	−4.785
Posterior Cingulate	R	58	12	−57	12	−5.854
Fusiform Gyrus	L	24	−54	−12	−30	5.422
Inferior Parietal Lobule	R	22	57	−33	36	−5.101
Precuneus	L	52	−12	−48	39	5.654
Superior Frontal Gyrus	L	37	−15	6	72	6.043
Inferior Frontal Gyrus	R	31	60	18	15	5.536
supplementary motor area	R	31	3	−21	60	5.967
Postcentral Gyrus	R	16	12	−51	72	−6.159
Supramarginal Gyrus	L	24	−54	−42	15	−5.818

BSRs, Original saliences/bootstrap standard errors; R, right hemisphere; L, left hemisphere; Peak coordinates refer to the MNI space; MNI, Montreal Neurological Institute.

TABLE 4 | Brain regions with reliability contributions to the behavioral brain covariance in LV 2.

Region of activation	Side	Sizes	Peak coordinates			
			x	y	z	BSRs
Inferior Temporal Gyrus	R	22	63	−15	−30	5.477
Inferior Temporal Gyrus	L	20	−54	−12	−36	5.782
Middle Temporal Gyrus	R	28	−42	−78	15	4.868
Superior Temporal Gyrus	L	20	−42	3	−24	−5.983
Lingual Gyrus	R	28	18	−90	−3	4.448
Inferior Occipital Gyrus	L	21	−42	−75	−9	−4.724
Posterior Cingulate	R	17	6	−42	3	−4.924
Insula	R	21	39	9	9	5.4
Precuneus	R	29	27	−87	27	−4.9459
Middle Frontal Gyrus	R	85	42	27	33	6.849
Middle Frontal Gyrus	L	51	−45	33	24	6.521
Middle Frontal Gyrus	R	42	36	6	57	−6.736
Inferior Frontal Gyrus	L	20	−42	9	30	6.191
Inferior Parietal Lobule	L	16	−42	−51	51	5.119

BSRs, Original saliences/bootstrap standard errors; R, right hemisphere; L, left hemisphere Peak coordinates refer to the MNI space; MNI, Montreal Neurological Institute.

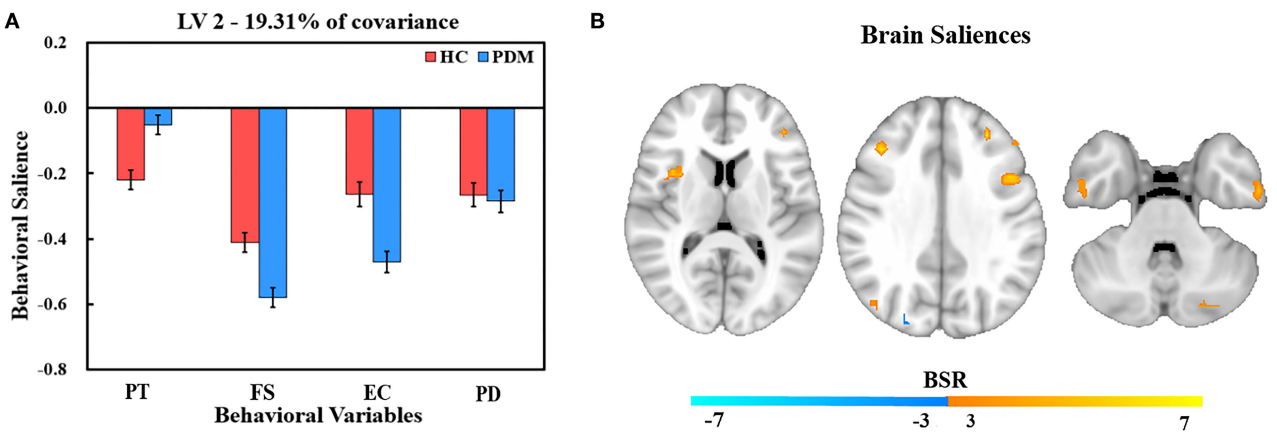

FIGURE 3 | PLS correlation analysis results of LV 2. **(A)** Bar graph of behavioral salience with stability estimated based on the use of bootstraps in the two groups. **(B)** Resting brain activity showing brain regions in which variations were associated with trait empathy. The map is the threshold at the equivalent value of $p = 0.01$ (BSR = ±3). Owing to the negative salience in both groups, warm regions indicated a negative correlation between resting brain activity and empathy, while cool regions showed a positive correlation between resting brain activity and empathy.

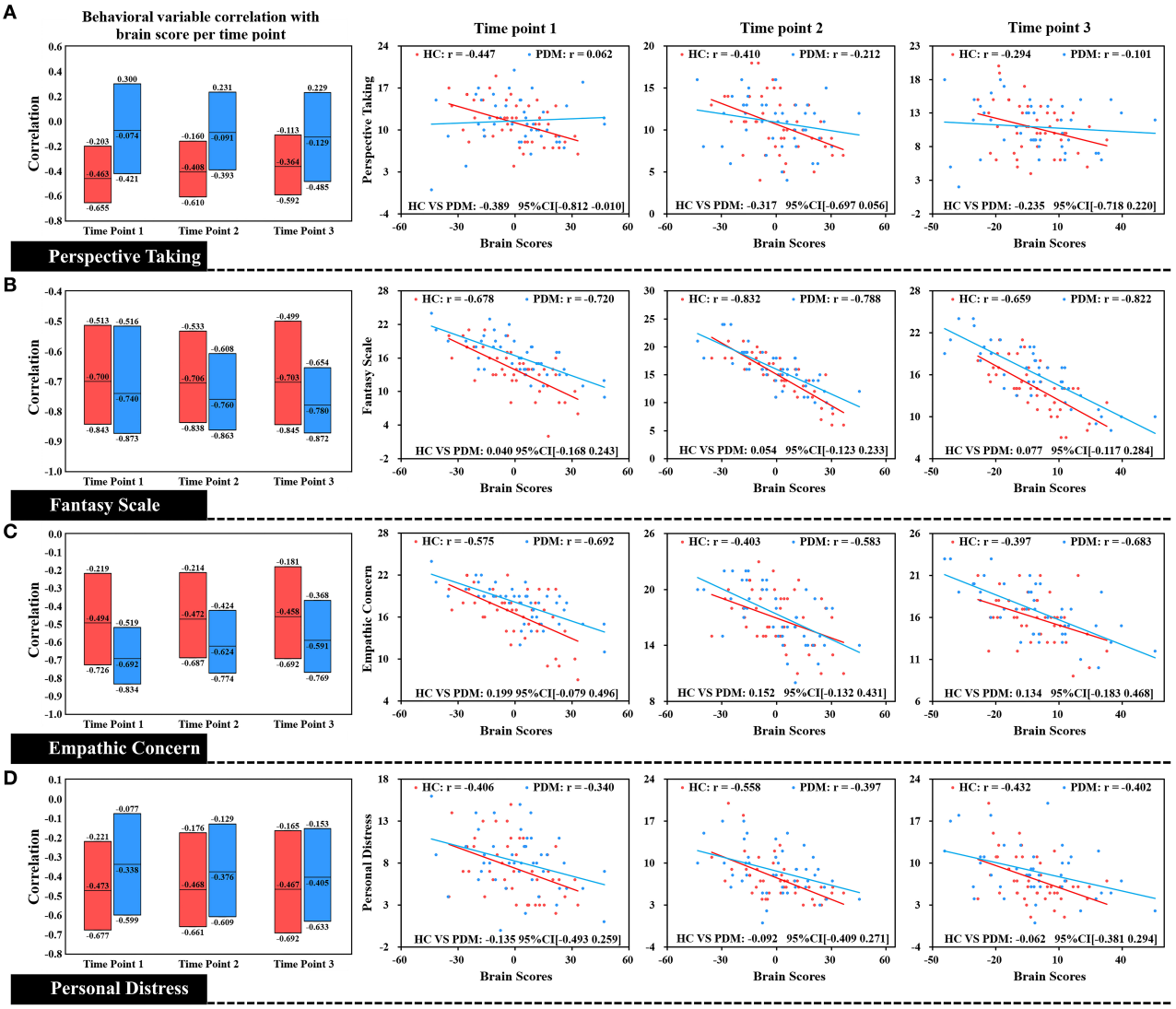

FIGURE 4 | Correlation of each level of trait empathy with brain scores of LV 2. In the box plot, the middle line of the box is the original correlation between empathy and brain score in the same phase. The boundary of the box was the 95% CI of the trait empathy correlation with brain scores based on the use of 5,000 bootstraps. The original correlation between empathy and brain score is shown by the scatter plot. There were no significant differences between HC and PDM in the EC, FS, and PD correlations with brain scores at the periovulatory, luteal, and menstruation phases based on effect-size analysis. The correlations in both groups did not significantly change during the three phases.

and precuneus. Functional neuroimaging studies on the neural mechanisms of empathy highlighted the AI, IFG, and IPL as parts of common networks in empathy for pain (22). Neuropsychological data provided further evidence that the lesions that involved the AI (23) and IFG (24) were associated with impairments of empathy. Additionally, the posterior cingulate, precuneus, and temporal gyri were also reported in research of empathy (25). With respect to the subscale of IRI, in a gray matter study of trait levels of empathy, Banissy et al. revealed that affective empathy scores on the PD and EC was linked with reduced gray matter volume in the insula, and EC scores were negatively related to gray matter volume both in the left precuneus and the left IFG (1). Levels of gray matter volume in the temporal gyrus were reported to be associated with participant PT and EC scores (26). Our data that related brain activity in the insula, IFG, temporal gyrus, and precuneus to empathy concern abilities were therefore in line with the studies of structural correlates of empathy. It is necessary to note that empathy is a multifaceted construct and consists of an emotional system and a cognitive system (27). The present theories propose that empathy relies strongly on the involvement of various neural networks (22), and is mediated by different series of

interaction regions (28). Based on the multivariable analysis of PLS correlation, our study was consistent with the above, and further suggested a comprehensive interaction network related to different aspects of empathy.

Brain Dysfunction Networks Associated With Empathy in PDM Women

In our results, a brain network that had an opposite regulation pattern to empathy as compared with the HC group was found in the PDM, and mainly involved the posterior cingulate, precuneus, IPL and IFG. PCC and precuneus are considered as parts of the default mode network (DMN) that has contributed immensely to various cognitive processing and has generated tremendous scientific attention (29, 30). Abnormal function of DMN have been found in a broad range of pain disorders as well as significant correlations between DMN and current clinical pain. Besides, alterations of DMN function indicate brain reorganization due to chronic pain (31). As DMN is recruited in attention related events (32), disengagement of attention to pain, such as mind wandering, is of benefit to individuals to cope with pain, and has an effect on the activity of the DMN network (33). In our study, it is likely that women with prolonged menstrual pain have a tendency to raise their attention to pain that leads to abnormal activities in the PCC and the precuneus. On the other hand, neuroimaging studies have indicated that the DMN networks involved in self-referential processing (34, 35). Specifically, empathy is inextricably associated with self-referential cognition (36). This suggested that empathy relied on self-referential processing to infer and represent the feelings of others (37). Moreover, dynamic causal modeling combined with canonical variance analysis revealed that functional integration within the DMN is associated with self-reported empathy (38). The DMN network plays a prominent role in empathy-related processing, and altered function may be linked with aberrant empathy. Our findings may indicate that long-term menstrual pain entails changes of activity and structure in PCC and precuneus that leads to changes of empathic processing.

The IPL and IFG are the two components of the newly defined frontoparietal network. Previous studies have reported abnormalities of frontoparietal network in chronic pain conditions (39). There is also converging evidence that this network was associated with endogenous pain modulation. For instance, Kong et al. indicated that functional connectivity of the frontoparietal network was involved in the prediction of the modulation of pain (40). Using a pattern-based regression method, Wager et al. mentioned that the anticipatory activity of the frontoparietal network reliably contributed to the prediction of placebo analgesia response (41). It is plausible to hypothesize that the alert structure of the IPL and IFG may reflect a dysfunctional pain modulation response. In addition, the frontoparietal network plays a critical role in the circuit of imitation and action representation that modulates and shapes emotional processing to impact empathy processing along with superior temporal sulcus (42). In this circuit, the IPL receives visual description of the action from superior temporal sulcus and code for precise kinesthetic properties, and then sends the information to IFG mirror neurons to code the goal of the action. The IFG sends copies of the motor plans back to superior temporal sulcus (43). Furthermore, a neuroimaging study has identified shared representation in empathy for pain (44). It is conceivable that the network underlying empathy partially overlaps with pain-related network (including IFG and IPL), and persistent pain can cause dysregulation of the empathy pathway by affecting the overlapping network.

Another interesting finding was that AI, middle, and superior temporal gyri, and the inferior occipital gyrus had similar activities compared with HC. There is accumulating evidence supporting the fact that the insula cortex plays an important role in the mediation of pain perception (45). Chronic pain studies have indicated that the morphometric abnormalities of the insula have been mentioned in chronic low-back pain studies (46). However, our results did not find any abnormal activity of AI in PDM women. The human insula has been divided into several subdivisions, including the ventral anterior insula (vAI) and dorsal anterior insula (dAI) (47), each of which has an influence on cognitive and affective processing (48). Recently, a meta-analysis that examined gray matter (GM) changes indicated that chronic pain led to increased GM in the dAI but decreased GM in the vAI (49). As noted, chronic pain alters both the cognitive and emotional domains (50). Accordingly, the increase in dAI may be equal to a decrease in vAI and represents normal activity in the entire AI in chronic pain. In our research, the empathic processing ability and intrinsic structure of AI may be disrupted by menstrual pain, but the overall activity appears to be normal. These findings provide novel insights into the impact of chronic pain on brain processing of empathy.

The underlying functional role of the temporal and inferior occipital gyri in chronic pain is not clear. Hence, the reason for which the temporal and inferior occipital gyri maintain similar activities in relation with empathy in PDM is difficult to explain. We have to consider the possibility that these regions were not affected by long-term menstrual pain and operated normally in empathic processing. There is another possibility that the intensity of menstrual pain is not high enough to affect the regulation of the temporal and inferior occipital gyri in empathy. To reach a full understanding of this issue, more research is needed on the empathy of pain disorders.

Changing Patterns of the Relationship Between Brain Regions and Empathy During the Menstrual Pain

In our results, the correlation of each aspect of empathy trait with brain scores yielded significant differences between PDM and HC during the periovulatory, luteal, and menstruation phases. As it was reported, prolonged nociceptive stimulus induced a form of adaptive reorganization and maladaptive plasticity in the brain (51). Neuroimaging studies with positron emission tomography and voxel-based morphometry disclosed state-related brain changes in metabolism and morphology in the various pain states (52, 53). There were also findings that indicated trait-related abnormal structure and functional connectivity during pain-free phases without menstrual pain

(51, 54, 55). Our results showed significantly different FS and EC scores as well as correlation of empathy with brain scores between two groups in periovulatory phases that suggested that repeated menstrual pain might have an effect on different levels of empathy in the painful and in the pain-free phases. Additionally, there were no differences in the correlation patterns to empathy in pain and pain-free phases. This indicated that the aberrant trait empathy in PDM does not vary with the pain or pain-free state throughout the menstrual cycle.

DATA AVAILABILITY STATEMENT

The raw data supporting the conclusions of this article will be made available by the authors, without undue reservation.

ETHICS STATEMENT

The studies involving human participants were reviewed and approved by The Institutional Review Board of the First Affiliated Hospital of the Medical College Xi'an Jiaotong University. The patients/participants provided their written informed consent to participate in this study. Written informed consent was obtained from the individual(s) for the publication of any potentially identifiable images or data included in this article.

AUTHOR CONTRIBUTIONS

HLiu and JL conceived the idea of this study and conducted the experiment. WD and TF detailedly analyzed results and writing the paper. QW helped with the data analysis and processing. KW, JY, and HLi contributed to the collection of data and samples. All authors revised the manuscript.

FUNDING

This work was supported by the National Natural Science Foundation of China (Grant Nos. 81901723, 81871331, and 81871330), the Natural Science Basic Research Program of Shaanxi (Program Nos. 2018JM7127 and 2019JQ-565) and the Fundamental Research Funds for Central Universities (Grant No. xjj2018261).

ACKNOWLEDGMENTS

We wish to thank Ming Zhang for his help in the field.

REFERENCES

1. Banissy MJ, Kanai R, Walsh V, Rees G. Inter-individual differences in empathy are reflected in human brain structure. *NeuroImage.* (2012) 62:2034–9. doi: 10.1016/j.neuroimage.2012.05.081
2. Yamada M, Decety J. Unconscious affective processing and empathy: an investigation of subliminal priming on the detection of painful facial expressions. *Pain.* (2009) 143:71–5. doi: 10.1016/j.pain.2009.01.028
3. Longobardi E, Spataro P, Rossi-Arnaud C. Direct and indirect associations of empathy, theory of mind, and language with prosocial behavior: gender differences in primary school children. *J Genet Psychol.* (2019) 180:266–79. doi: 10.1080/00221325.2019.1653817
4. Baron-Cohen S, Wheelwright S. The empathy quotient: an investigation of adults with Asperger syndrome or high functioning autism, and normal sex differences. *J Autism Dev Disord.* (2004) 34:163–75. doi: 10.1023/B:JADD.0000022607.19833.00
5. Li X, Meng X, Li H, Yang J, Yuan J. The impact of mood on empathy for pain: evidence from an EEG study. *Psychophysiology.* (2017) 54:1311–22. doi: 10.1111/psyp.12882
6. Li Y, Zhang T, Li W, Zhang J, Jin Z, Li L. Linking brain structure and activation in anterior insula cortex to explain the trait empathy for pain. *Hum Brain Mapp.* (2020) 41:1030–42. doi: 10.1002/hbm.24858
7. Preis MA, Schmidt-Samoa C, Dechent P, Kroener-Herwig B. The effects of prior pain experience on neural correlates of empathy for pain: an fMRI study. *Pain.* (2013) 154:411–8. doi: 10.1016/j.pain.2012.11.014
8. Danziger N, Prkachin KM, Willer JC. Is pain the price of empathy? The perception of others' pain in patients with congenital insensitivity to pain. *Brain*. (2006) 129:2494–507. doi: 10.1093/brain/awl155
9. Dun WH, Yang J, Yang L, Ding D, Ma XY, Liang FL, et al. Abnormal structure and functional connectivity of the anterior insula at pain-free periovulation is associated with perceived pain during menstruation. *Brain Imaging Behav.* (2017) 11:1787–95. doi: 10.1007/s11682-016-9646-y
10. Low I, Wei SY, Lee PS, Li WC, Lee LC, Hsieh JC, et al. Neuroimaging studies of primary dysmenorrhea. *Adv Exp Med Biol.* (2018) 1099:179–99. doi: 10.1007/978-981-13-1756-9_16
11. Yang L, Dun W, Li K, Yang J, Wang K, Liu H, et al. Altered amygdalar volume and functional connectivity in primary dysmenorrhoea during the menstrual cycle. *Eur J Pain.* (2019) 23:994–1005. doi: 10.1002/ejp.1368
12. Davis M. A multidimensional approach to individual differences in empathy. *JSAS Catalog Sel Doc Psychol.* (1980) 10:85.
13. Monti MM. Statistical analysis of fMRI time-series: a critical review of the GLM approach. *Front Hum Neurosci.* (2011) 5:28. doi: 10.3389/fnhum.2011.00028
14. Davis MH, Luce C, Kraus SJ. The heritability of characteristics associated with dispositional empathy. *J Pers.* (1994) 62:369–91. doi: 10.1111/j.1467-6494.1994.tb00302.x
15. Biswal BB, Mennes M, Zuo XN, Gohel S, Kelly C, Smith SM, et al. Toward discovery science of human brain function. *Proc Natl Acad Sci U S A.* (2010) 107:4734–9. doi: 10.1073/pnas.0911855107
16. Zang Y, Jiang T, Lu Y, He Y, Tian L. Regional homogeneity approach to fMRI data analysis. *NeuroImage.* (2004) 22:394–400. doi: 10.1016/j.neuroimage.2003.12.030
17. Zuo XN, Xu T, Jiang L, Yang Z, Cao XY, He Y, et al. Toward reliable characterization of functional homogeneity in the human brain: preprocessing, scan duration, imaging resolution and computational space. *NeuroImage.* (2013) 65:374–86. doi: 10.1016/j.neuroimage.2012.10.017
18. Fox SS, Norman RJ. Functional congruence: an index of neural homogeneity and a new measure of brain activity. *Science (New York, NY).* (1968) 159:1257–9. doi: 10.1126/science.159.3820.1257
19. Krishnan A, Williams LJ, McIntosh AR, Abdi H. Partial Least Squares (PLS) methods for neuroimaging: a tutorial and review. *NeuroImage.* (2011) 56:455–75. doi: 10.1016/j.neuroimage.2010.07.034
20. Wiebels K, Waldie KE, Roberts RP, Park HR. Identifying grey matter changes in schizotypy using partial least squares correlation. *Cortex.* (2016) 81:137–50. doi: 10.1016/j.cortex.2016.04.011
21. Ziegler G, Dahnke R, Winkler AD, Gaser C. Partial least squares correlation of multivariate cognitive abilities and local brain structure in children and adolescents. *NeuroImage.* (2013) 82:284–94. doi: 10.1016/j.neuroimage.2013.05.088
22. Wang C, Liu Y, Dun W, Zhang T, Yang J, Wang K, et al. Effects of repeated menstrual pain on empathic neural responses in women with

primary dysmenorrhea across the menstrual cycle. *Hum Brain Mapp.* (2020). doi: 10.1002/hbm.25226. [Epub ahead of print].
23. Gu X, Gao Z, Wang X, Liu X, Knight RT, Hof PR, et al. Anterior insular cortex is necessary for empathetic pain perception. *Brain.* (2012) 135:2726–35. doi: 10.1093/brain/aws199
24. Shamay-Tsoory SG, Aharon-Peretz J, Perry D. Two systems for empathy: a double dissociation between emotional and cognitive empathy in inferior frontal gyrus versus ventromedial prefrontal lesions. *Brain.* (2009) 132:617–27. doi: 10.1093/brain/awn279
25. Bzdok D, Schilbach L, Vogeley K, Schneider K, Laird AR, Langner R, et al. Parsing the neural correlates of moral cognition: ALE meta-analysis on morality, theory of mind, and empathy. *Brain Struct Funct.* (2012) 217:783–96. doi: 10.1007/s00429-012-0380-y
26. Rankin KP, Gorno-Tempini ML, Allison SC, Stanley CM, Glenn S, Weiner MW, et al. Structural anatomy of empathy in neurodegenerative disease. *Brain.* (2006) 129:2945–56. doi: 10.1093/brain/awl254
27. Cox CL, Uddin LQ, Di Martino A, Castellanos FX, Milham MP, Kelly C. The balance between feeling and knowing: affective and cognitive empathy are reflected in the brain's intrinsic functional dynamics. *Soc Cognit Affective Neurosci.* (2012) 7:727–37. doi: 10.1093/scan/nsr051
28. Shamay-Tsoory SG. Dynamic functional integration of distinct neural empathy systems. *Soc Cognit Affective Neurosci.* (2014) 9:1–2. doi: 10.1093/scan/nst107
29. Fransson P. How default is the default mode of brain function? Further evidence from intrinsic BOLD signal fluctuations. *Neuropsychologia.* (2006) 44:2836–45. doi: 10.1016/j.neuropsychologia.2006.06.017
30. Mars RB, Neubert FX, Noonan MP, Sallet J, Toni I, Rushworth MF. On the relationship between the "default mode network" and the "social brain". *Front Hum Neurosci.* (2012) 6:189. doi: 10.3389/fnhum.2012.00189
31. Ceko M, Frangos E, Gracely J, Richards E, Wang B, Schweinhardt P, et al. Default mode network changes in fibromyalgia patients are largely dependent on current clinical pain. *NeuroImage.* (2020) 216:116877. doi: 10.1016/j.neuroimage.2020.116877
32. Kaboodvand N, Iravani B, Fransson P. Dynamic synergetic configurations of resting-state networks in ADHD. *NeuroImage.* (2020) 207:116347. doi: 10.1016/j.neuroimage.2019.116347
33. Kucyi A, Salomons TV, Davis KD. Mind wandering away from pain dynamically engages antinociceptive and default mode brain networks. *Proc Natl Acad Sci U S A.* (2013) 110:18692–7. doi: 10.1073/pnas.1312902110
34. Molnar-Szakacs I, Uddin LQ. Self-processing and the default mode network: interactions with the mirror neuron system. *Front Hum Neurosci.* (2013) 7:571. doi: 10.3389/fnhum.2013.00571
35. Sajonz B, Kahnt T, Margulies DS, Park SQ, Wittmann A, Stoy M, et al. Delineating self-referential processing from episodic memory retrieval: common and dissociable networks. *NeuroImage.* (2010) 50:1606–17. doi: 10.1016/j.neuroimage.2010.01.087
36. Lombardo MV, Barnes JL, Wheelwright SJ, Baron-Cohen S. Self-referential cognition and empathy in autism. *PLoS ONE.* (2007) 2:e883. doi: 10.1371/journal.pone.0000883
37. Bilevicius E, Kolesar TA, Smith SD, Trapnell PD, Kornelsen J. Trait emotional empathy and resting state functional connectivity in default mode, salience, and central executive networks. *Brain Sci.* (2018) 8. doi: 10.3390/brainsci8070128
38. Esménio S, Soares JM, Oliveira-Silva P, Zeidman P, Razi A, Gonçalves ÓF, et al. Using resting-state DMN effective connectivity to characterize the neurofunctional architecture of empathy. *Sci Rep.* (2019) 9:2603. doi: 10.1038/s41598-019-38801-6
39. Ning Y, Zheng R, Li K, Zhang Y, Lyu D, Jia H, et al. The altered Granger causality connection among pain-related brain networks in migraine. *Medicine.* (2018) 97:e0102. doi: 10.1097/MD.0000000000010102
40. Kong J, Jensen K, Loiotile R, Cheetham A, Wey HY, Tan Y, et al. Functional connectivity of the frontoparietal network predicts cognitive modulation of pain. *Pain.* (2013) 154:459–67. doi: 10.1016/j.pain.2012.12.004
41. Wager TD, Atlas LY, Leotti LA, Rilling JK. Predicting individual differences in placebo analgesia: contributions of brain activity during anticipation and pain experience. *J Neurosci.* (2011) 31:439–52. doi: 10.1523/JNEUROSCI.3420-10.2011
42. Carr L, Iacoboni M, Dubeau MC, Mazziotta JC, Lenzi GL. Neural mechanisms of empathy in humans: a relay from neural systems for imitation to limbic areas. *Proc Natl Acad Sci U S A.* (2003) 100:5497–502. doi: 10.1073/pnas.0935845100
43. Rizzolatti G, Craighero L. The mirror-neuron system. *Annu Rev Neurosci.* (2004) 27:169–92. doi: 10.1146/annurev.neuro.27.070203.144230
44. Singer T, Seymour B, O'Doherty J, Kaube H, Dolan RJ, Frith CD. Empathy for pain involves the affective but not sensory components of pain. *Science (New York, NY).* (2004) 303:1157–62. doi: 10.1126/science.1093535
45. Lu C, Yang T, Zhao H, Zhang M, Meng F, Fu H, et al. Insular cortex is critical for the perception, modulation, and chronification of pain. *Neurosci Bull.* (2016) 32:191–201. doi: 10.1007/s12264-016-0016-y
46. Fritz HC, McAuley JH, Wittfeld K, Hegenscheid K, Schmidt CO, Langner S, et al. Chronic back pain is associated with decreased prefrontal and anterior insular gray matter: results from a population-based cohort study. *J Pain.* (2016) 17:111–8. doi: 10.1016/j.jpain.2015.10.003
47. Deen B, Pitskel NB, Pelphrey KA. Three systems of insular functional connectivity identified with cluster analysis. *Cereb Cortex.* (2011) 21:1498–506. doi: 10.1093/cercor/bhq186
48. Nomi JS, Schettini E, Broce I, Dick AS, Uddin LQ. Structural connections of functionally defined human insular subdivisions. *Cereb Cortex.* (2018) 28:3445–56. doi: 10.1093/cercor/bhx211
49. Cauda F, Palermo S, Costa T, Torta R, Duca S, Vercelli U, et al. Gray matter alterations in chronic pain: a network-oriented meta-analytic approach. *NeuroImage Clin.* (2014) 4:676–86. doi: 10.1016/j.nicl.2014.04.007
50. Bushnell MC, Ceko M, Low LA. Cognitive and emotional control of pain and its disruption in chronic pain. *Nat Rev Neurosci.* (2013) 14:502–11. doi: 10.1038/nrn3516
51. Tu CH, Niddam DM, Chao HT, Chen LF, Chen YS, Wu YT, et al. Brain morphological changes associated with cyclic menstrual pain. *Pain.* (2010) 150:462–8. doi: 10.1016/j.pain.2010.05.026
52. Tu CH, Niddam DM, Chao HT, Liu RS, Hwang RJ, Yeh TC, et al. Abnormal cerebral metabolism during menstrual pain in primary dysmenorrhea. *NeuroImage.* (2009) 47:28–35. doi: 10.1016/j.neuroimage.2009.03.080
53. Tu CH, Niddam DM, Yeh TC, Lirng JF, Cheng CM, Chou CC, et al. Menstrual pain is associated with rapid structural alterations in the brain. *Pain.* (2013) 154:1718–24. doi: 10.1016/j.pain.2013.05.022
54. Dun W, Yang J, Yang L, Ma S, Guo C, Zhang X, et al. Abnormal white matter integrity during pain-free periovulation is associated with pain intensity in primary dysmenorrhea. *Brain Imaging Behav.* (2017) 11:1061–70. doi: 10.1007/s11682-016-9582-x
55. Han F, Liu H, Wang K, Yang J, Yang L, Liu J, et al. Correlation between thalamus-related functional connectivity and serum BDNF levels during the periovulatory phase of primary dysmenorrhea. *Front Hum Neurosci.* (2019) 13:333. doi: 10.3389/fnhum.2019.00333

Conflict of Interest: The authors declare that the research was conducted in the absence of any commercial or financial relationships that could be construed as a potential conflict of interest.

frontiers in Human Neuroscience

ORIGINAL RESEARCH
published: 11 December 2020
doi: 10.3389/fnhum.2020.619839

Abnormal Whole Brain Functional Connectivity Pattern Homogeneity and Couplings in Migraine Without Aura

Yingxia Zhang[1,2], *Hong Chen*[2], *Min Zeng*[2], *Junwei He*[2], *Guiqiang Qi*[2], *Shaojin Zhang*[2] and *Rongbo Liu*[1]*

[1] Department of Radiology, West China Hospital of Sichuan University, Chengdu, China, [2] Department of Radiology, The Third Affiliated Hospital of Chengdu Medical College, Pidu District People's Hospital, Chengdu, China

Previous studies have reported abnormal amplitude of low-frequency fluctuation and regional homogeneity in patients with migraine without aura using resting-state functional magnetic resonance imaging. However, how whole brain functional connectivity pattern homogeneity and its corresponding functional connectivity changes in patients with migraine without aura is unknown. In the current study, we employed a recently developed whole brain functional connectivity homogeneity (FcHo) method to identify the voxel-wise changes of functional connectivity patterns in 21 patients with migraine without aura and 21 gender and age matched healthy controls. Moreover, resting-state functional connectivity analysis was used to reveal the changes of corresponding functional connectivities. FcHo analyses identified significantly decreased FcHo values in the posterior cingulate cortex (PCC), thalamus (THA), and left anterior insula (AI) in patients with migraine without aura compared to healthy controls. Functional connectivity analyses further found decreased functional connectivities between PCC and medial prefrontal cortex (MPFC), between AI and anterior cingulate cortex, and between THA and left precentral gyrus (PCG). The functional connectivities between THA and PCG were negatively correlated with pain intensity. Our findings indicated that whole brain FcHo and connectivity abnormalities of these regions may be associated with functional impairments in pain processing in patients with migraine without aura.

Keywords: migraine without aura, FCHo, functional connectivity, resting-state, functional magnetic resonance imaging

OPEN ACCESS

Edited by:
Jiaojian Wang,
University of Electronic Science and Technology of China, China

Reviewed by:
Heng Chen,
Guizhou University, China
Yifeng Wang,
Sichuan Normal University, China

***Correspondence:**
Rongbo Liu
medicalimage@163.com

Specialty section:
This article was submitted to Brain Imaging and Stimulation, a section of the journal Frontiers in Human Neuroscience

Received: *21 October 2020*
Accepted: *18 November 2020*
Published: *11 December 2020*

Citation:
Zhang Y, Chen H, Zeng M, He J, Qi G, Zhang S and Liu R (2020) Abnormal Whole Brain Functional Connectivity Pattern Homogeneity and Couplings in Migraine Without Aura. Front. Hum. Neurosci. 14:619839. doi: 10.3389/fnhum.2020.619839

INTRODUCTION

Migraine is a common chronic and idiopathic disorder characterized by recurrent moderate to severe headaches (Kruit et al., 2004). Migraine is an important healthcare and social problem affecting the patients' quality of life. Moreover, frequent migraine attacks cause loss of pain, sensitivity and functional lesions in brain regions (Tietjen, 2004; Borsook et al., 2012). With structural and diffusion magnetic resonance imaging (MRI) techniques, a few previous studies have demonstrated that migraine results in reduced gray matter volume and disrupted white matter

microstructural integrity (DaSilva et al., 2007; Kim et al., 2008; Schmidt-Wilcke et al., 2008; Valfrè et al., 2008). Based on resting-state functional MRI (fMRI), abnormal amplitudes of low-frequency fluctuation and regional homogeneity (ReHo) were also reported (Yu et al., 2012; Xue et al., 2013). All these studies demonstrated that migraine leads to progressive changes of brain structures and functions in patients.

Resting-state fMRI mainly reflects spontaneous fluctuations and has been widely used to study the intrinsic functional abnormalities in diseases (Fox et al., 2006; Yeo et al., 2011; Wang et al., 2017, 2020b). To characterize the functional activity similarities, ReHo was proposed to describe the similarity of time series (Zang et al., 2004). Given that more and more studies have demonstrated brain functions determined by its connectivity patterns with other brain areas (Passingham et al., 2002; Wang et al., 2015, 2019a), thus, to quantitatively characterize the voxel-wise similarity of whole brain functional connectivity pattern is vital to better reveal the functional abnormalities in brain. Recently, Wang et al. (2018a) developed a whole brain functional connectivity homogeneity (FcHo) method to delineate the voxel-wise whole brain functional connectivity pattern similarity. FcHo is defined by measuring the similarity of the whole brain functional connectivity pattern of a specific voxel with that of its nearest 26 neighborhood voxels. Compared to the ReHo approach, FcHo can better identify the association cortex areas with higher FcHo values than primary cortical areas, but for ReHo distribution, some primary cortical areas also represent high ReHo values (Wang et al., 2018a). Compared to functional connectivity density (FCD) and functional connectivity strength (FCS) methods, FcHo directly measures the similarity of the whole brain functional connectivity map of a given voxel with the nearest neighborhood voxels instead of counting the number of connectivities above a specific threshold (Wang et al., 2019b). Recently, the FcHo method has been used to explore the functional abnormalities in depression and its neuromodulation treatment mechanism (Wang et al., 2019b, 2020a). The FcHo method provides a new approach to exactly localize the functional abnormality in brain disorders.

In the current study, a fully data-driven FcHo method without any hypothesis was applied to reveal the abnormal functional connectivity patterns in 21 patients with migraine without aura and 21 gender and age matched healthy controls using resting-state fMRI data. Resting-state functional connectivity of the brain areas with changed FcHo was also performed to further reveal the corresponding disrupted functional networks in patients with migraine without aura.

MATERIALS AND METHODS

Subjects

Twenty-one patients with migraine without aura (16 female and five male; mean age = 31.19 ± 6.38 years) and 21 healthy controls (13 female and eight male; mean age = 30.19 ± 6.3 years) were recruited at the Third Affiliated Hospital of Chengdu Medical College, Pidu District People's Hospital. All participants were right-handed. The diagnosis of migraine without aura was made according to the International Headache Society criteria. The inclusion criteria for patients with migraine without aura were follows: (1) Must not have suffered from a migraine attack for at least 72 h before experiment; (2) Must not have a migraine precipitated during or on the day after the scan; (3) for migraine and healthy controls, no lifetime history of head trauma, seizures, serious medical or surgical illness, substance abuse or dependence, or contraindications for MRI. The participants were excluded if structural abnormalities were detected on MRI examination. Written informed consent was provided and obtained from all the subjects. This study was approved by the local ethics committees of the Third Affiliated Hospital of Chengdu Medical College, Pidu District People's Hospital.

Resting-State fMRI Data Acquisition

MRI data was acquired on a 3-Tesla Siemens MRI scanner in the Department of Radiology, the Pidu District People's Hospital of the third Affiliated Hospital of Chengdu Medical College, Chengdu, China. Foam padding and earplugs were used to reduce head motion and scanner noise. The participants were instructed to close their eyes and not fall asleep during scanning. Resting-state fMRI images were acquired using a gradient-echo echo-planar imaging (GRE-EPI) sequence with parameters: repetition time (TR) = 2000 ms, echo time (TE) = 30 ms, flip angle (FA) = 90^0, matrix = 64 × 64, field of view (FOV) = 220 × 220 mm, slice thickness = 4 mm with inter-slice gap = 0.6 mm, 32 axial slices, and 250 time points.

Resting-State fMRI Data Pre-processing

The resting-state fMRI data was pre-processed using DPARSFA software (https://www.nitrc.org/projects/dparsf/). The preprocessing steps include: discarding the first 10 volumes to facilitate magnetization equilibrium; after slice timing, the remaining images realigned to the first volume to correct head motion; normalizing all the images to the EPI template in MNI space and resampled to a $3 \times 3 \times 3 mm^3$; regression of Friston 24-parameter model of head motion, white matter, cerebrospinal fluid, and global mean signals and filtered with a temporal band-pass of 0.01–0.1 Hz. To exclude the head motion effects, the subjects with head-movement that exceeded 3 mm of translation or 3° of rotation in any direction were discarded. Under this criterion, no subject was discarded. Moreover, "scrubbed" was performed to censor the bad images before 2 time points and after 1 time points exceeding the pre-set criteria (frame displacement: FD, FD < 0.5) (Power et al., 2012). For the following functional connectivity analyses, the fMRI data were normalized to the EPI template and smoothed using a Gaussian kernel of 6 mm full-width at half maximum (FWHM).

Whole Brain Voxel-Wise FcHo Analyses

FcHo, measured using Kendall's coefficient concordance (KCC) (Kendall and Gibbons, 1990), was calculated for each voxel to describe the whole brain connectivity pattern similarity. The FcHo of a given voxel was defined by computing a KCC value of the whole brain functional connectivity of this voxel with those of its nearest 26 neighbors (see the following formula). Finally, a whole FcHo map for each subject was obtained and smoothed

with 6 mm FWHM for statistical analyses. To determine the FcHo differences between patients with migraine and healthy controls, a two-sample *t*-test was performed to compare the FcHo maps between the two groups. The significance was determined using the Alphasim correction method in the DPARBI toolkit (http://rfmri.org/dpabi) with a threshold of $p < 0.05$ (cluster-forming threshold at voxel-level $p < 0.001$, cluster size 53).

$$KCC = \frac{\sum (R_i)^2 - K(\overline{R})^2}{\frac{1}{12}N^2(K^3 - K)}$$

Where: R_i is the sum rank of the i th voxel of the whole brain; $\overline{R} = [(K+1)\times N]/2$ is the mean of the R_i; N is the number of a given voxel and its nearest neighbors ($N = 26$); K is the number of whole brain voxels.

Functional Connectivity Analyses

Seed-based whole brain functional connectivity analysis was used to further identify changed resting-state functional connectivity of the brain areas with different FcHo between patients with migraine and healthy controls. Functional connectivity was measured using Pearson's correlation coefficient between the averaged time series of the seed and target brain areas. Next, the Fisher's z transformation was applied to change functional connectivity to Z value to improve normality. The two-sample *t*-test was performed to identify brain areas with significantly different functional connectivity between patients with migraine without aura and healthy controls. The significance in the present study was determined using the Alphasim correction method in the DPARBI toolkit with a threshold of $p < 0.05$ (cluster-forming threshold at voxel-level $p < 0.001$, cluster size 47).

Correlation Analyses

To determine the relationship between clinical assessments including visual analog scale (VAS), duration of illness and FcHo, and functional connectivities in brain areas showing differences between patients with migraine without aura and healthy controls, Spearman correlation analyses were performed, and the significance was set at $p < 0.05$.

RESULTS

Demographics and Clinical Characteristics

The demographics and clinical characteristics of the subjects are shown in **Table 1**. No significant differences in gender ($p = 0.51$) and age ($p = 0.61$) were observed between patients with migraine without aura and healthy controls.

Changed FcHo in MDD

Significantly reduced FcHos in the posterior cingulate cortex (PCC), thalamus (THA), and left anterior insula (AI) were found in patients with migraine without aura compared with healthy controls (**Figure 1** and **Table 2**).

Changed Functional Connectivity

Seed-based whole brain functional connectivity analyses were performed and decreased functional connection was identified between THA and left precentral gyrus (PCG), between AI and anterior cingulate cortex (ACC), and between PCC and medial prefrontal cortex (MPFC) in patients with migraine without aura compared with healthy controls (**Figure 2** and **Table 2**).

TABLE 1 | Demographics and clinical characteristics of the subjects used in the present study.

	Migraine ($n = 21$)	Controls ($n = 21$)	*p*-value
Gender (male/female)	16/5	13/8	0.51
Age (mean ± SD)	31.19 ± 6.38	30.19 ± 6.3	0.61
VAS (mean ± SD)	4.33 ± 1.46		
HAMD (mean ± SD)	6.71 ± 6.25		
HAMA (mean ± SD)	7.95 ± 6.77		
Duration of illness (months)	44.69 ± 61.13		
FD values	0.16 ± 0.29	0.15 ± 0.027	0.49

A Pearson chi-squared test was used for gender comparison. Two-sample t-tests were used for age comparisons.
VAS, visual analog scale; HAMD, Hamilton Depression Rating Scale; HAMA, Hamilton Anxiety Scale.

Correlation Analyses

Correlation analyses found that functional connectivities of THA with left PCG were significantly negatively correlated with the VAS scores ($r = -0.49$, $p < 0.025$) in patients with migraine without aura (**Figure 3**).

DISCUSSION

In the present study, whole brain functional connectivity patterns homogeneity (FcHo) and functional connectivity were used to localize functionally abnormal brain areas and their corresponding circuits in patients with migraine without aura. FcHo analysis revealed significantly decreased FcHo in PCC, AI, and THA in migraine without aura patients. Resting-state functional connectivity analysis further identified decreased functional connectivity between PCC and MPFC, between AI and ACC, and between THA and left PCG in patients with migraine without aura. Moreover, the changed functional connectivities of THA with left PCG were negatively associated with pain intensity. Our findings provide the neuroanatomical basis for migraine without aura and could help improve our understanding of the neuropathology of migraine.

Thalamus, as a relay hub, participates in the transmission of nociceptive inputs to the cortical areas (Kupers and Kehlet, 2006). The abnormal functional activities in thalamus during spontaneous attacks of migraine have been reported in previous studies (Kobari et al., 1989; Kupers and Kehlet, 2006). Thalamus and precentral gyrus are two important nodes in sensorimotor network which plays a key role in pain intensity processing and discrimination of the sensory components of pain perception (Kanda et al., 2000; Peyron et al., 2000). The correlation analysis in our study found that the functional connectivities between thalamus and precentral gyrus were closely related to pain intensity, suggesting the important role of sensorimotor

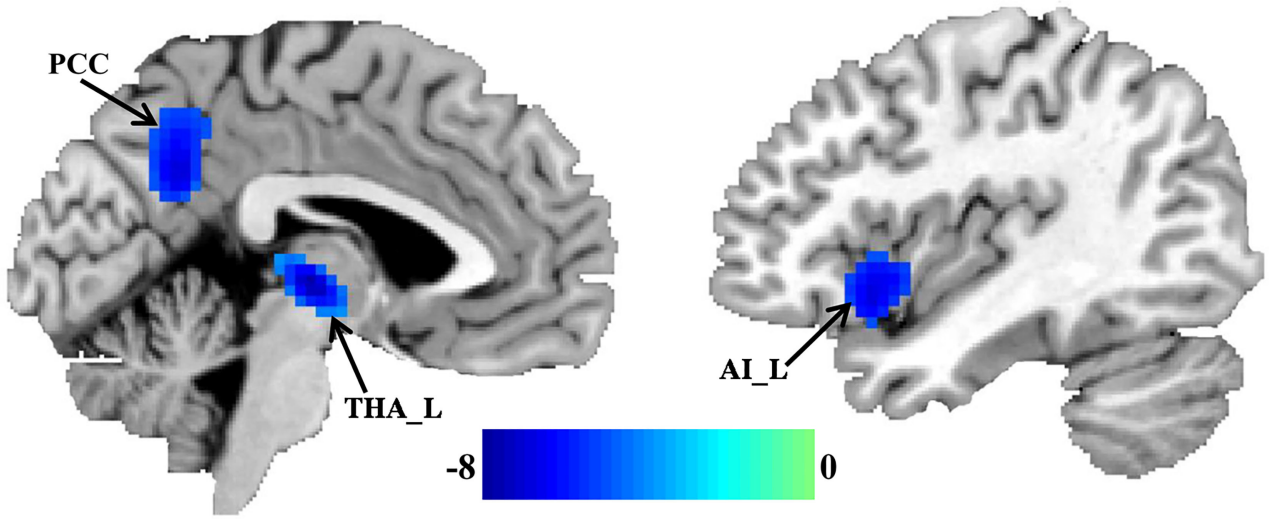

FIGURE 1 | Decreased whole brain functional connectivity pattern homogeneity (FcHo) in patients with migraine without aura. Two-sample *t*-test was used to compare the FcHo maps between healthy controls and patients with migraine without aura and identified significantly decreased FcHo in the posterior cingulate cortex (PCC), thalamus (THA), and left anterior insula (AI) in patients with migraine without aura.

TABLE 2 | Regions with changed FcHo and functional connectivities in migraine patients.

Parameters	Brain regions	Peak MNI coordinates			*T* values	Cluster size
		X	Y	Z		
FcHo:	Anterior insula	−45	15	−12	−7.61	143
	Posterior cingulate cortex	0	−54	30	−6.87	129
	Thalamus	−3	−18	0	−7.12	159
FC:	Anterior cingulate cortex	0	27	27	−7.28	126
	Medial prefrontal cortex	0	57	15	−7.76	106
	Precentral gyrus	30	−3	57	−6.93	75

FcHo, whole brain functional connectivity pattern homogeneity; FC, functional connectivity; MNI, Montreal Neurological Institute; L, left hemisphere; R, right hemisphere.

network in pain perception and pain intensity coding. Thus, the decreased whole brain functional connectivity pattern similarity, and disrupted functional connections between the thalamus and precentral gyrus, indicated the abnormal pain perception and sensation processing in patients with migraine without aura.

Decreased whole brain functional connectivity pattern similarity in posterior cingulate cortex (PCC) and functional connections between PCC and medial prefrontal cortex (MPFC) were also found in patients with migraine without aura. PCC and MPFC are two core regions of default mode network (DMN), and have been reported to be associated with social cognition, emotional, and self-referential processing (Gusnard et al., 2001; Amodio and Frith, 2006; Etkin et al., 2011; Wang et al., 2019a). The abnormal functional activities in DMN found in our study were supported by previous studies which found changed local regional homogeneity (ReHo) and amplitude of low frequency fluctuations (ALFF) in patients with migraine without aura (Yu et al., 2012; Xue et al., 2013). Xue et al. (2013) found decreased ALFF values in the left rostral anterior cingulate cortex, bilateral prefrontal cortex, and increased ALFF values in the right thalamus. Yu et al. (2012) found decreased ReHo values in the right rostral anterior cingulate cortex, the prefrontal cortex, the orbitofrontal cortex, and the supplementary motor area. The abnormal prefrontal cortex and anterior cingulate cortex were consistently found in our study. The different change patterns may result from different analytical methods suggesting different methods could provide **Supplementary Material**. In addition, Xue et al. (2013) found increased ALFF in thalamus but we found decreased FcHo in this area. The inconsistency may be related to different analytical methods which reflect different functional information of this area.

In addition, decreased whole brain functional connectivity pattern similarity in anterior insula (AI) and functional connections between AI and dorsal anterior cingulate cortex (ACC) were identified in patients with migraine without aura. Our finding was consistent with the previous reports which also found structural and functional abnormalities in insula and

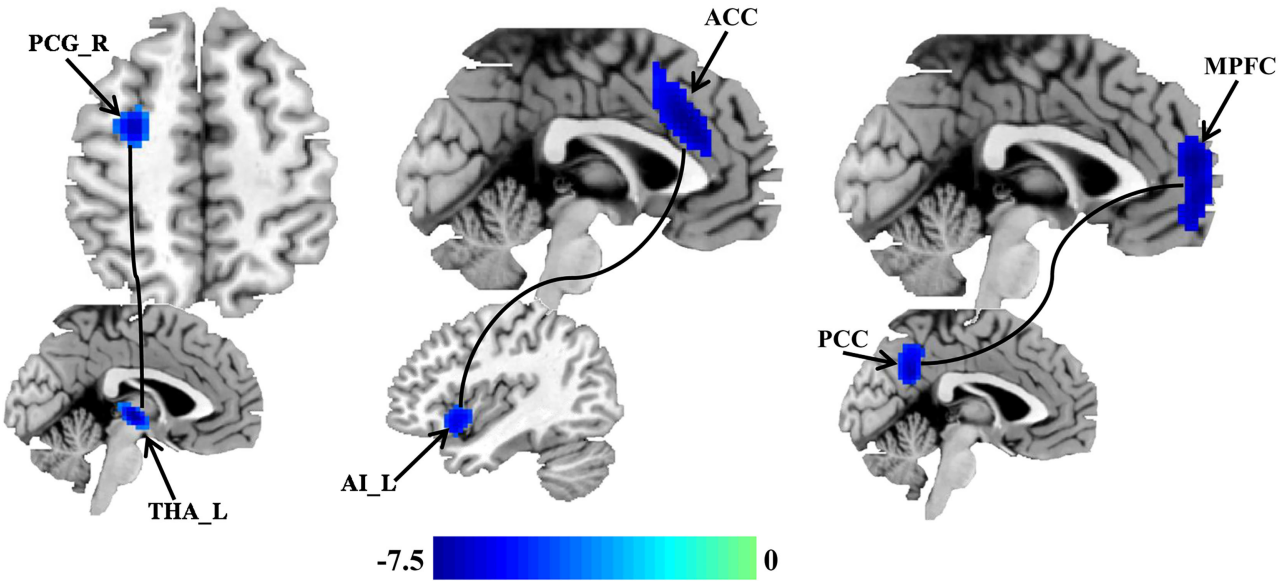

FIGURE 2 | Disrupted resting-state functional connectivities in patients with migraine without aura. Seed based whole brain resting-state functional connectivities analyses of PCC, THA, and AI were performed, and two-sample *t*-tests were used to identify the significant differences in functional connectivities between patients with migraine without aura and healthy control groups. Seed-based functional connectivity analyses identified disrupted functional connection between the THA and left precentral gyrus (PCG), between the AI and anterior cingulate cortex (ACC), and between the PCC and medial prefrontal cortex (MPFC) in patients with migraine without aura.

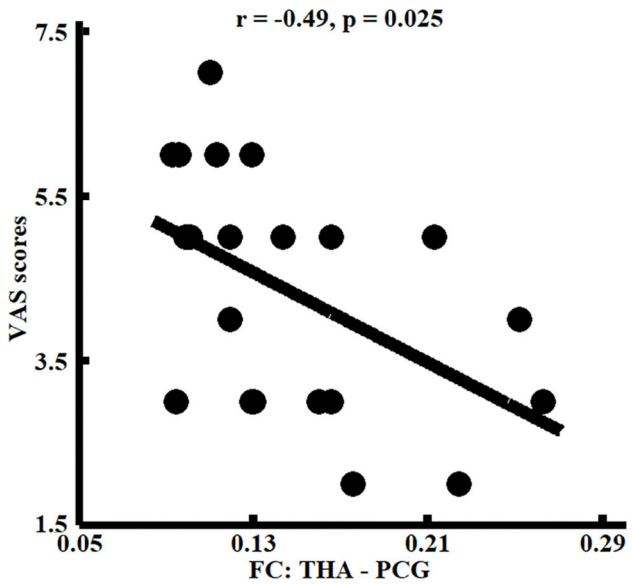

FIGURE 3 | Correlation analyses between whole brain functional connectivity homogeneity (FcHo) and functional connectivities parameters and clinical performances. Significant correlation between the functional connectivities of THA with PCG and pain intensity (i.e., VAS scores) was identified in patients with migraine without aura.

ACC (Peyron et al., 2000; Kim et al., 2008; Valfrè et al., 2008). Insula plays a key role in integrating multimodal information including cognition, emotion, pain and homeostasis (Kong et al., 2006; Craig, 2011; Kelly et al., 2012; Simmons et al., 2013). ACC mainly integrates the positive and negative affective responses of pain (Vogt, 2005; Shackman et al., 2011). AI and ACC are important parts of salience network for accommodating the dynamic interaction between the internal self-perception and external orient stimulus (Menon and Uddin, 2010; Menon, 2011). ACC mainly includes the rostral rACC and dorsal dACC, and rACC is manly involved in endogenous pain control through the endogenous opioid systems (Petrovic et al., 2002; Wager et al., 2004), whereas dACC is primarily involved in motor control and cognitive processing, especially attention (Touroutoglou et al., 2012). Therefore, the abnormal FcHo in AI and functional couplings between AI and dACC suggest impaired cognitive processing or motor control in patients with migraine without aura.

Global signal regression (GSR) is a controversial problem in fMRI study. Some studies considered that GSR could increase the negative correlation and exaggerate the between-group differences (Gotts et al., 2013; Saad et al., 2013), but a recent study demonstrated that GSR could better exclude head motion effects than no GSR for functional connectivity analyses (Satterthwaite et al., 2019). In our study, we found the similar results using the fMRI data with and without GSR, which suggests that our findings are robust and the intrinsic functional abnormalities in migraine.

The previous studies have demonstrated that chronic pain patients showed increased high-frequency BOLD oscillations (0.12–0.20 Hz) in the medial prefrontal cortex and parts of default mode network (Baliki et al., 2011). Recently,

frequency-dependent bilateral anterior insular networks were identified (Wang et al., 2018b, 2020c). In our study, decreased FcHo and functional connectivities of default mode network in the frequency band of 0.01–0.1 Hz were found suggesting that the functional abnormalities of the default mode network are present in both low and high frequencies. Additionally, we also found abnormal FcHo and functional connectivities in sensorimotor and salience networks in the frequency band of 0.01–0.1 Hz. Given the frequency-dependent functional circuits of salience network (Wang et al., 2018b, 2020c), whether the differences in the two networks are frequency-specific needs to be further investigated in future studies.

There are some limitations in our study. First, we only recruited a small sample size of patients with migraine without aura, and a large dataset is necessary to provide more convincing evidence. Second, all the analyses in the current study were performed only in the band of 0.01–0.1 Hz. Given that the pain related effect may be located in the frequency band >0.1 Hz, band-limited or coherence methods may be used in our future study to further reveal the pain effects.

CONCLUSION

In conclusion, this study revealed abnormal whole brain functional connectivity pattern homogeneity in THA, PCC, and AI and abnormal resting-state functional connectivities between THA and PCG, between PCC and MPFC, and between AI and ACC patients with migraine without aura. These findings indicate abnormal emption, pain, and cognitive processing in patients with migraine without aura. The dysfunctions of these areas may contribute to the onset of migraine in patients.

DATA AVAILABILITY STATEMENT

The raw data supporting the conclusions of this article will be made available by the authors, without undue reservation.

ETHICS STATEMENT

The studies involving human participants were reviewed and approved by the Third Affiliated Hospital of Chengdu Medical College, Pidu District People's Hospital. The patients/participants provided their written informed consent to participate in this study.

AUTHOR CONTRIBUTIONS

All authors listed have made a substantial, direct and intellectual contribution to the work, and approved it for publication.

SUPPLEMENTARY MATERIAL

The Supplementary Material for this article can be found online at: https://www.frontiersin.org/articles/10.3389/fnhum.2020.619839/full#supplementary-material

REFERENCES

Amodio, D. M., and Frith, C. D. (2006). Meeting of minds: the medial frontal cortex and social cognition. *Nat. Rev. Neurosci.* 7, 268–277. doi: 10.1038/nrn1884

Baliki, M. N., Baria, A. T., and Apkarian, A. V. (2011). The cortical rhythms of chronic back pain. *J. Neurosci.* 31, 13981–13990. doi: 10.1523/JNEUROSCI.1984-11.2011

Borsook, D., Maleki, N., Becerra, L., and McEwen, B. (2012). Understanding migraine through the lens of maladaptive stress responses: a model disease of allostatic load. *Neuron* 73, 219–234. doi: 10.1016/j.neuron.2012.01.001

Craig, A. D. (2011). Significance of the insula for the evolution of human awareness of feelings from the body. *Ann. N. Y. Acad. Sci. U. S. A.* 1225, 72–82. doi: 10.1111/j.1749-6632.2011.05990.x

DaSilva, A. F., Granziera, C., Tuch, D. S., Snyder, J., Vincent, M., and Hadjikhani, N. (2007). Interictal alterations of the trigeminal somatosensory pathway and periaqueductal gray matter in migraine. *Neuroreport* 18, 301–305. doi: 10.1097/WNR.0b013e32801776bb

Etkin, A., Egner, T., and Kalisch, R. (2011). Emotional processing in anterior cingulate and medial prefrontal cortex. *Trends Cogn. Sci.* 15, 85–93. doi: 10.1016/j.tics.2010.11.004

Fox, M. D., Corbetta, M., Snyder, A. Z., Vincent, J. L., and Raichle, M. E. (2006). Spontaneous neuronal activity distinguishes human dorsal and ventral attention systems. *Proc. Natl. Acad. Sci. U. S. A.* 103, 10046–10051. doi: 10.1073/pnas.0604187103

Gotts, S. J., Saad, Z. S., Jo, H. J., Wallace, G. L., Cox, R. W., and Martin, A. (2013). The perils of global signal regression for group comparisons: a case study of autism spectrum disorders. *Front. Hum. Neurosci.* 7:356. doi: 10.3389/fnhum.2013.00356

Gusnard, D. A., Akbudak, E., Shulman, G. L., and Raichle, M. E. (2001). Medial prefrontal cortex and self-referential mental activity: relation to a default mode of brain function. *Proc. Natl. Acad. Sci. U. S. A.* 98, 4259–4264. doi: 10.1073/pnas.071043098

Kanda, M., Nagamine, T., Ikeda, A., Ohara, S., Kunieda, T., Fujiwara, N., et al. (2000). Primary somatosensory cortex is actively involved in pain processing in human. *Brain Res.* 853, 282–289. doi: 10.1016/S0006-8993(99)02274-X

Kelly, C., Toro, R., Di Martino, A., Cox, C. L., Bellec, P., Castellanos, F. X., et al. (2012). A convergent functional architecture of the insula emerges across imaging modalities. *Neuroimage* 61, 1129–1142. doi: 10.1016/j.neuroimage.2012.03.021

Kendall, M. G., and Gibbons, J. D. (1990). *Rank Correlation Methods*. Oxford: Oxford University Press.

Kim, J. H., Suh, S. I., Seol, H. Y., Oh, K., Seo, W. K., Yu, S. W., et al. (2008). Regional grey matter changes in patients with migraine: a voxel-based morphometry study. *Cephalalgia* 28, 598–604. doi: 10.1111/j.1468-2982.2008.01550.x

Kobari, M., Meyer, J. S., Ichijo, M., Imai, A., and Oravez, W. T. (1989). Hyperperfusion of cerebral cortex, thalamus and basal ganglia during spontaneously occurring migraine headaches. *Headache* 29, 282–289. doi: 10.1111/j.1526-4610.1989.hed2905282.x

Kong, J., White, N. S., Kwong, K. K., Vangel, M. G., Rosman, I. S., Gracely, R. H., et al. (2006). Using fMRI to dissociate sensory encoding from cognitive evaluation of heat pain intensity. *Hum. Brain Mapp.* 27, 715–721. doi: 10.1002/hbm.20213

Kruit, M. C., van Buchem, M. A., Hofman, P. A. M., Bakkers, J. T. N., Terwindt, G. M., Ferrari, M. D., et al. (2004). Migraine as a risk factor for subclinical brain lesions. *JAMA* 291, 427–434. doi: 10.1001/jama.291.4.427

Kupers, R., and Kehlet, H. (2006). Brain imaging of clinical pain states: a critical review and strategies for future studies. *Lancet Neurol.* 5, 1033–1044. doi: 10.1016/S1474-4422(06)70624-X

Menon, V. (2011). Large-scale brain networks and psychopathology: a unifying triple network model. *Trends Cogn. Sci.* 15, 483–506. doi: 10.1016/j.tics.2011.08.003

Menon, V., and Uddin, L. Q. (2010). Saliency, switching, attention and control: a network model of insula function. *Brain Struct. Funct*. 214, 655–667. doi: 10.1007/s00429-010-0262-0

Passingham, R. E., Stephan, K. E., and Kotter, R. (2002). The anatomical basis of functional localization in the cortex. *Nat. Rev. Neurosci*. 3, 606–616. doi: 10.1038/nrn893

Petrovic, P., Kalso, E., Petersson, K. M., and Ingvar, M. (2002). Placebo and opioid analgesia– imaging a shared neuronal network. *Science* 295, 1737–1740. doi: 10.1126/science.1067176

Peyron, R., Laurent, B., and Garcia-Larrea, L. (2000). Functional imaging of brain responses to pain. a review and meta-analysis (2000). *Neurophysiol. Clin*. 30, 263–288. doi: 10.1016/S0987-7053(00)00227-6

Power, J. D., Barnes, K. A., Snyder, A. Z., Schlaggar, B. L., and Petersen, S. E. (2012). Spurious but systematic correlations in functional connectivity MRI networks arise from subject motion. *Neuroimage* 59, 2142–2154. doi: 10.1016/j.neuroimage.2011.10.018

Saad, Z. S., Reynolds, R. C., Jo, H. J., Gotts, S. J., Chen, G., Martin, A., et al. (2013). Correcting brain-wide correlation differences in resting-state FMRI. *Brain Connect*. 3, 339–352. doi: 10.1089/brain.2013.0156

Satterthwaite, T. D., Ciric, R., Roalf, D. R., Davatzikos, C., Bassett, D. S., and Wolf, D. H. (2019). Motion artifact in studies of functional connectivity: characteristics and mitigation strategies. *Hum. Brain Mapp*. 40, 2033–2051. doi: 10.1002/hbm.23665

Schmidt-Wilcke, T., Gänssbauer, S., Neuner, T., Bogdahn, U., and May, A. (2008). Subtle grey matter changes between migraine patients and healthy controls. *Cephalalgia* 28, 1–4. doi: 10.1111/j.1468-2982.2007.01428.x

Shackman, A. J., Salomons, T. V., Slagter, H. A., Fox, A. S., Winter, J. J., and Davidson, R. J. (2011). The integration of negative affect, pain and cognitive control in the cingulate cortex. *Nat. Rev. Neurosci*. 12, 154–167. doi: 10.1038/nrn2994

Simmons, W. K., Avery, J. A., Barcalow, J. C., Bodurka, J., Drevets, W. C., and Bellgowan, P. (2013). Keeping the body in mind: insula functional organization and functional connectivity integrate interoceptive, exteroceptive, and emotional awareness. *Hum. Brain Mapp*. 34, 2944–2958. doi: 10.1002/hbm.22113

Tietjen, G. E. (2004). Stroke and migraine linked by silent lesions. *Lancet Neurol*. 3:267. doi: 10.1016/S1474-4422(04)00729-X

Touroutoglou, A., Hollenbeck, M., Dickerson, B. C., and Feldman Barrett, L. (2012). Dissociable large-scale networks anchored in the right anterior insula subserve affective experience and attention. *Neuroimage* 60, 1947–1958. doi: 10.1016/j.neuroimage.2012.02.012

Valfrè, W., Rainero, I., Bergui, M., and Pinessi, L. (2008). Voxel-based morphometry reveals gray matter abnormalities in migraine. *Headache* 48, 109–117. doi: 10.1111/j.1526-4610.2007.00723.x

Vogt, B. A. (2005). Pain and emotion interactions in subregions of the cingulate gyrus. *Nat. Rev. Neurosci*. 6, 533–544. doi: 10.1038/nrn1704

Wager, T. D., Rilling, J. K., Smith, E. E., Sokolik, A., Casey, K. L., Davidson, R. J., et al. (2004). Placebo-induced changes in FMRI in the anticipation and experience of pain. *Science* 303, 1162–1167. doi: 10.1126/science.1093065

Wang, J., Becker, B., Wang, L., Li, H., Zhao, X., and Jiang, T. (2019a). Corresponding anatomical and coactivation architecture of the human precuneus showing similar connectivity patterns with macaques. *Neuroimage* 200, 562–574.

Wang, J., Ji, Y., Li, X., He, Z., Wei, Q., Bai, T., et al. (2020a). Improved and residual functional abnormalities in major depressive disorder after electroconvulsive therapy. *Progr. Neuro-Psychopharmacol. Biol. Psychiatry* 100:109888. doi: 10.1016/j.pnpbp.2020.109888

Wang, J., Xie, S., Guo, X., Becker, B., Fox, P. T., Eickhoff, S. B., et al. (2017). Correspondent functional topography of the human left inferior parietal lobule at rest and under task revealed using resting-state fMRI and coactivation based parcellation. *Hum. Brain Mapp*. 38, 1659–1675. doi: 10.1002/hbm.23488

Wang, J., Yang, Y., Fan, L., Xu, J., Li, C., Liu, Y., et al. (2015). Convergent functional architecture of the superior parietal lobule unraveled with multimodal neuroimaging approaches. *Hum. Brain Mapp*. 36, 238–257. doi: 10.1002/hbm.22626

Wang, J., Yang, Y., Zhao, X., Zuo, Z., and Tan, L.-H. (2020b). Evolutional and developmental anatomical architecture of the left inferior frontal gyrus. *Neuroimage* 222:117268. doi: 10.1016/j.neuroimage.2020.117268

Wang, L., Xu, J., Wang, C., and Wang, J. (2018a). *Whole brain functional connectivity pattern homogeneity mapping. Front. Hum. Neurosci.* 12:164. doi: 10.3389/fnhum.2018.00164

Wang, L., Yu, L., Wu, F., Wu, H., and Wang, J. (2019b). Altered whole brain functional connectivity pattern homogeneity in medication-free major depressive disorder. *J. Affect. Disord*. 253, 18–25. doi: 10.1016/j.jad.2019.04.040

Wang, Y., Zhu, L., Zou, Q., Cui, Q., Liao, W., Duan, X., et al. (2018b). Frequency dependent hub role of the dorsal and ventral right anterior insula. *Neuroimage* 165, 112–117. doi: 10.1016/j.neuroimage.2017.10.004

Wang, Y., Zou, Q., Ao, Y., Liu, Y., Ouyang, Y., Wang, X., et al. (2020c). Frequency-dependent circuits anchored in the dorsal and ventral left anterior insula. *Sci. Rep*. 10:16394. doi: 10.1038/s41598-020-73192-z

Xue, T., Yuan, K., Cheng, P., Zhao, L., Zhao, L., Yu, D., et al. (2013). Alterations of regional spontaneous neuronal activity and corresponding brain circuit changes during resting state in migraine without aura. *NMR Biomed*. 26, 1051–1058. doi: 10.1002/nbm.2917

Yeo, B. T., Krienen, F. M., Sepulcre, J., Sabuncu, M. R., Lashkari, D., Hollinshead, M., et al. (2011). The organization of the human cerebral cortex estimated by intrinsic functional connectivity. *J. Neurophysiol*. 106, 1125–1165. doi: 10.1152/jn.00338.2011

Yu, D., Yuan, K., Zhao, L., Zhao, L., Dong, M., Liu, P., et al. (2012). Regional homogeneity abnormalities in patients with interictal migraine without aura: a resting-state study. *NMR Biomed*. 25, 806–812. doi: 10.1002/nbm.1796

Zang, Y., Jiang, T., Lu, Y., He, Y., and Tian, L. (2004). Regional homogeneity approach to fMRI data analysis. *Neuroimage* 22, 394–400. doi: 10.1016/j.neuroimage.2003.12.030

Conflict of Interest: The authors declare that the research was conducted in the absence of any commercial or financial relationships that could be construed as a potential conflict of interest.

frontiers in Neuroscience

ORIGINAL RESEARCH
published: 28 January 2021
doi: 10.3389/fnins.2020.629630

Multisite Autism Spectrum Disorder Classification Using Convolutional Neural Network Classifier and Individual Morphological Brain Networks

Jingjing Gao[1†], Mingren Chen[2†], Yuanyuan Li[3], Yachun Gao[4], Yanling Li[5], Shimin Cai[2*] and Jiaojian Wang[3,6*]*

[1] School of Information and Communication Engineering, University of Electronic Science and Technology of China, Chengdu, China, [2] School of Computer Science and Engineering, University of Electronic Science and Technology of China, Chengdu, China, [3] Key Laboratory for NeuroInformation of the Ministry of Education, School of Life Sciences and Technology, University of Electronic Science and Technology of China, Chengdu, China, [4] School of Physics, University of Electronic Science and Technology of China, Chengdu, China, [5] School of Electrical Engineering and Electronic Information, Xihua University, Chengdu, China, [6] Center for Language and Brain, Shenzhen Institute of Neuroscience, Shenzhen, China

OPEN ACCESS

Edited by:
Kai Yuan,
Xidian University, China

Reviewed by:
Xun Chen,
University of Science and Technology of China, China
Zaixu Cui,
University of Pennsylvania, United States

***Correspondence:**
Shimin Cai
shimin.cai81@gmail.com
Jiaojian Wang
jiaojianwang@uestc.edu.cn
Jingjing Gao
jingjing.gao@uestc.edu.cn

† These authors have contributed equally to this work

Specialty section:
This article was submitted to Brain Imaging Methods, a section of the journal Frontiers in Neuroscience

Received: 15 November 2020
Accepted: 29 December 2020
Published: 28 January 2021

Citation:
Gao J, Chen M, Li Y, Gao Y, Li Y, Cai S and Wang J (2021) Multisite Autism Spectrum Disorder Classification Using Convolutional Neural Network Classifier and Individual Morphological Brain Networks. Front. Neurosci. 14:629630. doi: 10.3389/fnins.2020.629630

Autism spectrum disorder (ASD) is a range of neurodevelopmental disorders with behavioral and cognitive impairment and brings huge burdens to the patients' families and the society. To accurately identify patients with ASD from typical controls is important for early detection and early intervention. However, almost all the current existing classification methods for ASD based on structural MRI (sMRI) mainly utilize the independent local morphological features and do not consider the covariance patterns of these features between regions. In this study, by combining the convolutional neural network (CNN) and individual structural covariance network, we proposed a new framework to classify ASD patients with sMRI data from the ABIDE consortium. Moreover, gradient-weighted class activation mapping (Grad-CAM) was applied to characterize the weight of features contributing to the classification. The experimental results showed that our proposed method outperforms the currently used methods for classifying ASD patients with the ABIDE data and achieves a high classification accuracy of 71.8% across different sites. Furthermore, the discriminative features were found to be mainly located in the prefrontal cortex and cerebellum, which may be the early biomarkers for the diagnosis of ASD. Our study demonstrated that CNN is an effective tool to build the framework for the diagnosis of ASD with individual structural covariance brain network.

Keywords: autism spectrum disorder, individual morphological covariance brain network, convolutional neural network, gradient-weighted class activation mapping, structural MRI

INTRODUCTION

Autism spectrum disorder (ASD) encompasses a range of neurodevelopmental disorders. The core symptoms of ASD comprise abnormal emotional regulation and social interactions, restricted interest, repetitive behaviors, and hypo-/hyperreactivity to sensory stimuli (Guze, 1995). Many individuals with autism spectrum disorder usually exhibit impairments in learning, development,

control, and interaction, as well as some daily life skills. ASD causes heavy economic burden for the patients' families and the society. It is urgent to establish an early and accurate diagnosis framework to identify ASD patients from typical controls (TC). Recently, noninvasive and *in vivo* neuroimaging techniques have become an area of intense investigation to explore the auxiliary diagnostic for ASD.

A variety of neuroimaging modalities, such as structural MRI (sMRI), diffusion MRI, functional MRI, magnetoencephalography, electroencephalography, and electrocorticography, are widely adopted to uncover patterns in both brain anatomical structure and function. Structural MRI provides abundant measures to delineate the structural properties of the brain (Wang et al., 2017, 2018, 2019; Wu et al., 2017; Xu et al., 2019). Although there were many controversial findings regarding brain structural changes in individuals with autism (Chen et al., 2011), to identify ASD based on sMRI still received a great deal of attention from researchers. Wang et al. (2016) linearly projected gray matter (GM) and white matter (WM) features extracted from sMRI onto a canonical space to maximize their correlations. With the projected GM and WM as features, they achieved the classification accuracy of 75.4% with the data scanned at New York University (NYU) Langone Medical Center from ABIDE. Recently, the classification accuracy for ASD is up to 90.39%, which is obtained with sMRI constrained to the same single-site dataset (Kong et al., 2019). Although previous studies achieved high classification accuracy, almost all these results were obtained from a single site, and reproducibility and generation in a multisite remain uncertain (Button et al., 2013).

It is well accepted that multisite datasets can represent greater variance of disease and control samples to establish more stable generalization models for replication across different sites, participants, imaging parameters, and analysis methods (Nielsen et al., 2013). Thus, there are some studies focused on larger sample sizes from a multisite. However, the classification accuracy drops significantly due to the complexity and heterogeneity of ASD (Nielsen et al., 2013). In a study by Zheng et al. (2018), the elastic network was utilized to quantify corticocortical similarity based on seven morphological features on 132 selected subjects from four independent sites of the ABIDE dataset. Although the classification performance of this study was 78.63%, the samples used in this study only cover a small portion of the ABIDE dataset. Additionally, there are few other studies that use larger datasets from ABIDE but with low accuracy. For instance, Haar et al. (2016) used linear and quadratic (nonlinear) discriminant analyses to classify ASD and control subjects based on structural measures of the quality-controlled samples from ABIDE, but the accuracies were only 56 and 60% when using subcortical volumes or cortical thickness measures. Katuwal et al. (2015) used random forest (RF), support vector machine (SVM), and gradient boosting machine (GBM) to classify 373 ASD from 361 TC male subjects from the ABIDE database and obtained 60% classification accuracy. The accuracy was further improved to 67% when IQ and age information were added to morphometric features. Although the existing approaches can obtain high classification accuracy based on sMRI measures in a single site or with a small number of subjects, an acceptable method to achieve high classification accuracy across different sites with different scanning paradigms is still needed.

The low classification accuracy for different sites may mainly result from the following reasons. First, the data collected from different sites expand the variances of structural measures, which increases the difficulty in learning high accuracy classifiers with such data. Second, the brain is an integrative and dynamic system for information processing between brain regions (Vértes and Bullmore, 2014), yet most of the existing methods only extract independent local morphological features of different brain areas with sMRI and did not consider the interregional morphological covariant relationships. Third, although some deep neural network classifiers were used in ASD/TC classification by transforming the features to a one-dimensional vector followed by features selection algorithm, the classification results are hard to interpret in the absence of the contributions of the classification features leading to lack of clinical significance. In view of the abovementioned problems, to further explore an efficient classification method is essential to establish the ASD diagnosis model. Here, we combine a deep learning classifier and gradient-weighted class activation mapping (Grad-CAM) (Selvaraju et al., 2020) based on morphological covariance brain networks to identify ASD patients from TC with all the ABIDE dataset. We first constructed the individual-level morphological covariance brain networks, and the interregional morphological covariance values were used as the input feature for the classifier. Next, the convolutional neural network (CNN) classifier with Grad-CAM is applied to differentiate ASD from TC and to identify features contributing the largest for the classification in our framework.

MATERIALS AND METHODS

The ABIDE Dataset

Data used in this study are accessed from a large open access data repository, Autism Brain Imaging Data Exchange I (ABIDE[1]), which came from 17 international sites with no prior coordination (Di Martino et al., 2014). ABIDE includes structural MRI, corresponding rs-fMRI, and phenotype information for individuals with ASD and TC and allows for replication, secondary analyses, and discovery efforts. Although all data in ABIDE were collected with 3 T scanners, the sequence parameters as well as the type of scanner varied across sites. In this paper, we used the structural MR images of 518 ASD patients and 567 age-matched normal controls (ages 7–64 years, median 14.7 years across groups) aggregated from all 17 international sites. The key phenotypical information is summarized in **Table 1**. As seen from **Table 1**, the variation in age range across samples varied greatly, and most of the ASD subjects are male with 25% of the sites excluding females by design.

[1]http://fcon_1000.projects.nitrc.org/indi/abide

TABLE 1 | Demographic information of subjects with autism spectrum disorder (ASD) and typical controls (TC).

Site	Autism spectrum disorder (ASD)			Typical controls (TC)	
	Number of subjects	Age (years)	ADOS	Number of subjects	Age (years)
CALTECH	19 (15 M/4 F)	27.4	13.1	18 (14 M/4 F)	28
CMU	14 (11 M/3 F)	26.4	13.1	13 (10 M/3 F)	26.8
KKI	20 (16 M/4 F)	10.0	12.5	28 (20 M/8 F)	10
LEUVEN	29 (26 M/3 F)	17.8	*	34 (29 M/5 F)	18.2
MAX MUN	24 (21 M/3 F)	26.1	9.5	28 (27 M/1 F)	24.6
NYU	75 (65 M/10 F)	14.7	11.4	100 (74 M/26 F)	15.7
OHSU	12 (12 M/0 F)	11.4	9.2	14 (14 M/0 F)	10.1
OLIN	19 (16 M/3 F)	16.5	14.1	15 (13 M/2 F)	16.7
PITT	29 (25 M/4 F)	19.0	12.4	27 (23 M/4 F)	18.9
SBL	15 (15 M/0 F)	35.0	9.2	15 (15 M/0 F)	33.7
SDSU	14 (13 M/1 F)	14.7	11.2	22 (16 M/6 F)	14.2
STANFORD	19 (15 M/4 F)	10.0	11.7	20 (16 M/4 F)	10
TRINITY	22 (22 M/0 F)	16.8	10.8	25 (25 M/0 F)	17.1
UCLA	54 (48 M/6 F)	13.0	10.9	44 (38 M/6 F)	13.0
UM	66 (57 M/9 F)	13.2	*	74 (56 M/18 F)	14.8
USM	46 (46 M/0 F)	23.5	13.0	25 (25 M/0 F)	21.3
YALE	28 (20 M/8 F)	12.7	11.0	28 (20 M/8 F)	12.7

Data Preprocessing

All structural MR images used in our work were preprocessed by the deformable medical image registration toolbox—DRAMMS (Ou et al., 2011). DRAMMS is a software package designed for 2D-to-2D and 3D-to-3D deformable medical image registration tasks. The preprocessing procedures in our study include cross-subject registration, motion correction, intensity normalization, and skull stripping. Especially, T1W MRI images in different sites were registered to the SRI24 atlas (Rohlfing et al., 2010) for the morphological covariance brain network mapping.

Individual-Level Morphological Covariance Brain Networks

The morphological features of the human brain have long been characterized by structural MRI. In our study, the individual-level morphological covariance brain network (Wang et al., 2016) is used to estimate interregional structural connectivity to characterize the interregional morphological relationship. The detailed construction procedures were described below. First, after preprocessing, the structural T1 images were segmented into cerebrospinal fluid (CSF), WM, and GM by the multiplicative intrinsic component optimization (MICO) method (Li et al., 2014). Next, a GM volume map was obtained for each participant in template space. Second, the large-scale morphological covariance brain network for each participant was constructed based on their GM volume images according to a previous study (Wang et al., 2016). A brain network is usually comprised of a collection of nodes and edges, wherein the network nodes are defined as different regions in SRI24 atlases and the edge is defined as the interregional similarity in the distribution of the regional GM volume. The SRI24 atlas (Rohlfing et al., 2010) parcellates the whole brain into 116 subregions and 58 subregions in each hemisphere. Because of low signal-to-noise ratio and blank values of gray matter volume in Vermis during network analysis, we excluded eight areas in the Vermis (the cerebellar Vermis labeled from 109 to 116) to ensure the reliability of our study. Finally, a 108×108 matrix was obtained for each subject for further analyses. To be specific, the edge of the individual network is calculated as follows: the kernel density estimation (KDE) (Rosenblatt, 1956) is firstly used to estimate the probability density function (PDF) of the extracted GM volume values as Eq. (1).

$$P(i) = \frac{f_h(i)}{\sum_{j=1}^{N} f_h(j)} \tag{1}$$

where $P(i)$ is the PDF of the i-th brain area, N is the total number of regions, and $f_h(i)$ is the kernel density of the i-th area defined as (Wang et al., 2016):

$$f_h(i) = \frac{1}{nh} \sum_{j=1}^{N} K\left(\frac{v(i) - v(j)}{h}\right) \tag{2}$$

where $K(.)$ is a non-negative function that integrates to one and has mean zero, $h > 0$ is a smoothing parameter called the bandwidth, and $v(i)$ is the GM volume value of the i-th ROI.

The variation of the KL divergence (KLD) is calculated subsequently from the above PDFs as Eq. (3):

$$D_{\mathrm{KL}}(P, Q) = \sum_{i=1}^{N} \left(P(i) \log \frac{P(i)}{Q(i)} + Q(i) \log \frac{Q(i)}{P(i)}\right) \tag{3}$$

where P and Q are the PDFs of different ROI. The network edge is formally defined as the structural connectivity between two regions and is quantified by a KL divergence-based similarity (KLS) measure (Kong et al., 2014) with the calculated variation of KLD. Thus, the similarity matrix can be defined as:

$$\mathrm{KLS}(P, Q) = e^{-D_{\mathrm{KL}}(P,Q)} \tag{4}$$

For more details of the calculation process, refer to the previous literature (Wang et al., 2016).

Convolutional Neural Network Classifier

Deep CNNs have led to a series of breakthroughs for image classification (Liu et al., 2017, 2018). The deep residual networks (ResNet) (He et al., 2016) have recently achieved state-of-the-art on challenging computer vision tasks, which consists of an ensemble of basic residual unit. According to the study of He et al. (2016), ResNet tries to learn both local and global features *via* skip connections combining different levels to overcome the incapability of integrating different level features found in plain networks, as seen in **Figure 1A**. Here, X is the input of the residual unit, and $F(X)$ denotes the residue mapping of the stacked convolution layers. The formulation of $F(X) + X$ can be realized by feedforward neural networks

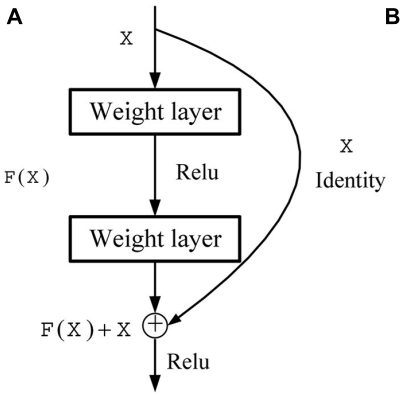

B

Layer Name	Conv_1	Conv_2	Conv_3	Conv_4	Conv_5	Full Connect
Input Size	108×108	54×54	27×27	14×14	7×7	4×4
Kernel Size	7×7, 64 3×3, *max pool* Stride 2	$\begin{bmatrix}3 \times 3, 64\\3 \times 3, 64\end{bmatrix} \times 2$ Stride 2	$\begin{bmatrix}3 \times 3, 128\\3 \times 3, 128\end{bmatrix} \times 2$ Stride 2	$\begin{bmatrix}3 \times 3, 256\\3 \times 3, 256\end{bmatrix} \times 2$ Stride 2	$\begin{bmatrix}3 \times 3, 512\\3 \times 3, 512\end{bmatrix} \times 2$ Stride 2	Average pool Full Connect Softmax
Output Size	54×54	27×27	14×14	7×7	4×4	1×2

FIGURE 1 | Residual learning and architectures for our work. **(A)** The formulation of $F(X) + X$ can be realized by feedforward neural networks with shortcut connections. **(B)** Architectures for our work. The downsampling is performed by Conv_1, Conv_2, Conv_3, Conv_4, and Conv_5 with a stride of 2.

with shortcut connections. Thus, a simple identity mapping directly connects the input and output layers by using ResNet with the skip connection. In our work, five bottlenecks are used to perform the classification, and the detailed architecture of ResNet used in our work is shown in **Figure 1B**. The binary cross-entropy (BCE) cost function is used as the loss function of our work in the residual learning, which is defined as follows:

$$L = -(y * \log(\hat{y}) + (1 - y) * \log(1 - \hat{y})) \tag{5}$$

where y is the ground-truth label, and $\hat{y}$ is the prediction result of our work.

Grad-CAM

The Grad-CAM is able to produce "visual explanations" for decisions from a large class of CNN-based models and makes them more transparent (Selvaraju et al., 2017, 2020). It uses the gradient information flowing into the last convolutional layer of CNN to assign importance values to each neuron for a particular decision of interest to avoid the model structure modification and refrainment to keep both interpretability and accuracy (Selvaraju et al., 2020). Also, the produced localization map highlights the important regions in the image for predicting the concept. It is an important tool for users to evaluate and place trust in classification systems (Selvaraju et al., 2020). In this work, we only focus on the explaining output layer decisions by identifying the contributions of the classification features to help researchers focus on the highlighted regions and trust the model. The gradient of the score y^c for class c is computed with respect to feature map activations A^k of a convolutional layer. In the study by Selvaraju et al. (2020), the neuron importance weights α_k^c are defined as:

$$\alpha_k^c = \frac{1}{Z} \sum_i \sum_j \frac{\partial y^c}{\partial A_{i,j}^k} \tag{6}$$

where $A_{i,j}^k$ is the feature map activations A^k indexed by i and j.

Then, a ReLU function is applied to a weighted combination of forward activation maps to obtain the Grad-CAM (Selvaraju et al., 2020):

$$L_{\text{Grad-CAM}}^c = \text{ReLU}(\sum_k \alpha_k^c A^k) \tag{7}$$

Finally, the heat map highlighting the regions with a positive influence on ASD/TC classification is obtained by upsampling $L_{\text{Grad-CAM}}^c$.

Implementation

An overview of the proposed ASD/TC classification framework in our work is shown in **Figure 2**. We first constructed the individual-level morphological covariance brain network according to the SRI24 atlas as the input images for the classification. Subsequently, the ResNet network is used to perform the classification. Meanwhile, the importance value to each neuron is obtained from Grad-CAM to explain model decisions. Specially, our implementation for ASD/TC classification based on the morphological covariance brain networks performs the following practice. The size of input image for ResNet is 108×108, and the crop is not needed to be sampled from an image or its horizontal flip. We adopt batch normalization (Ioffe and Szegedy, 2015) right after each convolution and before activation based on a previous study (Ioffe and Szegedy, 2015). Moreover, we do not use dropout (Hinton et al., 2012) which is the practice of a previous study (Ioffe and Szegedy, 2015). We initialized the weights randomly and trained all plain/residual nets from scratch. We use the Adam optimization method (Zhang et al., 2016) with a minibatch size of 32 to minimize the BCE in this study. Also, the learning rate is settled as $1e$-5 in our ResNet work. Furthermore, we use a 10-fold cross-validation strategy in specific implementation processes and repeat 20 times to evaluate our proposed method. Specifically, all subjects used in our work are randomly equally partitioned into 10 groups defined as $\{S_1, S_2, S_3, ..., S_{10}\}$ in each classification process. Group S_{10} is usually set as the testing set and the other nine groups are further randomly

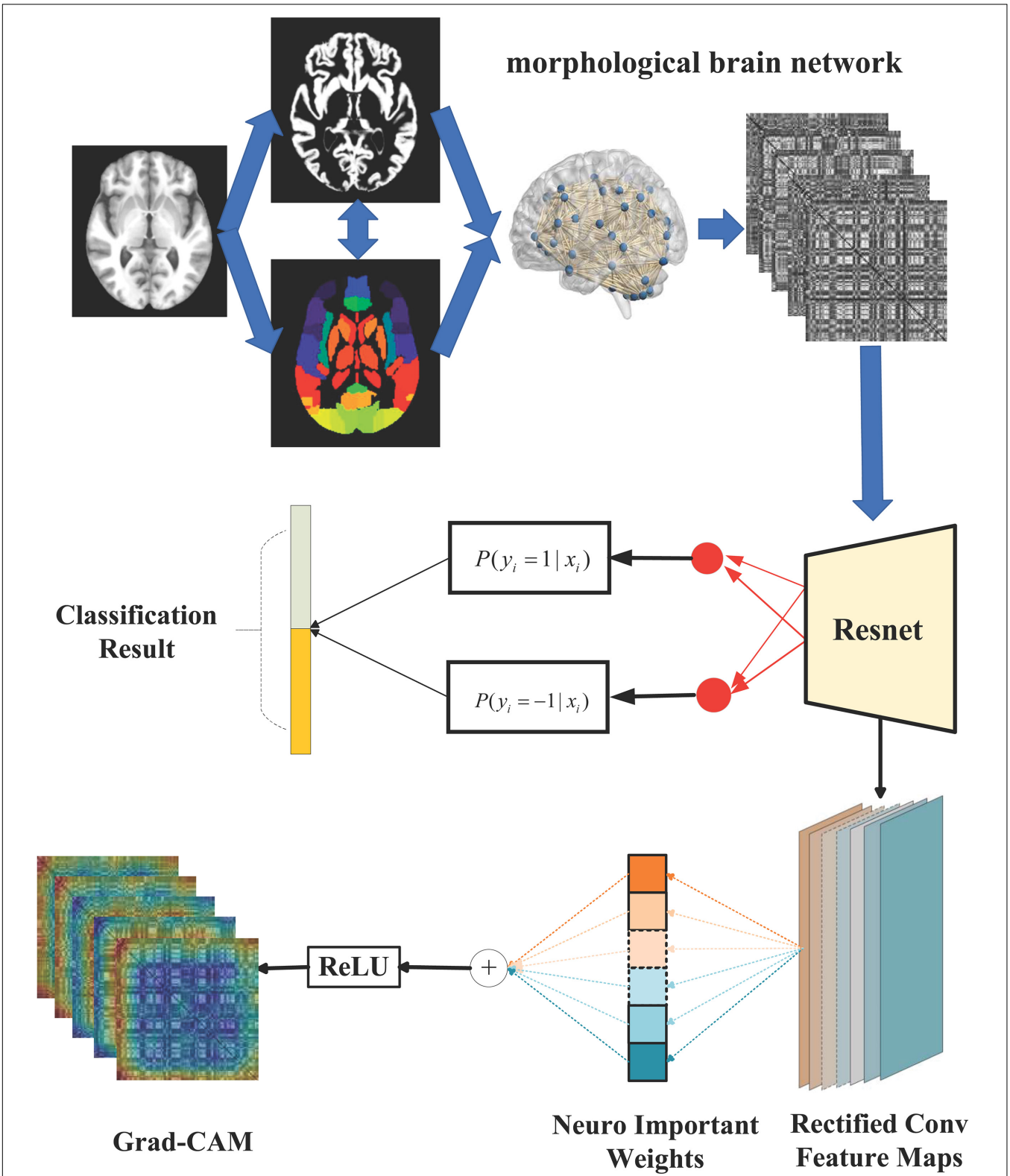

FIGURE 2 | The overall flow chart of our study. Briefly, the individual-level morphological covariance brain network is first constructed according to the SRI24 atlas and gray matter volume map of each subject, as shown in the dashed boxes. The above morphological covariance brain network is used as the input feature for the classifier. Subsequently, the ResNet network is used to perform the ASD/TC classification, as shown in the middle of this figure. Meanwhile, the Grad-CAM is combined with the ResNet-based architecture based on the rectified convolution feature maps from the ResNet to obtain the heat map for explaining model decisions, as shown at the bottom of this figure.

equally repartitioned into 10 subgroups, one of which is selected as the validation set and the other nine subgroups used as the training data.

RESULTS

Four parameters, namely accuracy (ACC), sensitivity (SEN), specificity (SPE), and F1 score, are calculated to evaluate the performance of our proposed ASD/TC classification framework. The deep convolutional neural network used in our work achieved a mean classification accuracy of 71.8%, mean sensitivity value of 81.25%, specificity value of 68.75%, and F1 score of 0.687 from cross-validation. Our results improved the mean classification accuracy of the state-of-the-art from 70 to 71.8% in the ABIDE data, and the former accuracy is obtained by DNN based on fMRI in ABIDE (Heinsfeld et al., 2018). To evaluate our results obtained with the deep convolutional neural network, the performance of our model is compared with the results of classifiers trained using RF (Vapnik, 1998), SVM (Ho, 1995), XgBoost (XGB) (Chen and Guestrin, 2016), and autoencoder (AE). With the purpose of using 2D input data for subject classification by these conventional machine learning methods, a vector of features is firstly retrieved by flattening the 2D morphological covariance brain network (i.e., collapse it in a one dimension vector). The number of resultant features is 11,664, which is computed by 108×108. Evaluation of all the models is based on a 10-fold cross-validation schema, which mixes data from all 17 sites while keeping the proportions between different sites. The results of comparing these methods are reported in **Table 2**. Furthermore, the performance of these classifiers was assessed by the area under the curve (AUC) values shown in **Figure 3**. Our proposed framework has the best performances in classifying ASD from TC with the highest ACC, SEN, F1 score, and AUC values compared with the other methods. Furthermore, the permutation test with 5,000 times is used to evaluate the significance of the prediction accuracy. During the permutation testing, 20% of the labels of the samples are changed randomly in each time. The histogram of accuracy of the permutation test is shown in **Figure 4**. The accuracy of our method (0.718) is indicated by the red dotted line. As shown in **Figure 4**, the 71.8% accuracy of our method is higher than 95% of the permutated accuracy values.

To determine the weight values of the features contributing to classification, the Grad-CAM method was adopted, and the weight of each connectivity was obtained. The individual and fused connectivities supporting the correct classification of ASD patients using Grad-CAM visualizations for our ResNet framework are shown in **Figure 5A**. In order to make the fusion of Grad-CAM more transparent and explainable, we selected the covariance connectivities with the largest contribution to classification. The largest contributions of the connectivities were determined by identifying the weights above the mean + 3SD. Finally, 63 connectivities between 12 different regions were found using the fused Grad-CAM approach. The top 12 regions correspond to the bilateral precentral gyrus (left and right), superior frontal gyrus, orbital part of the superior frontal gyrus, and cerebellum 8–10 (see **Figure 5B**).

TABLE 2 | Comparison of the classification performances between our method and other methods.

Method	Accuracy	Sensitivity	Specificity	F1 score
Our method	0.718182	0.8125	0.6875	0.686869
AE	0.672727	0.6875	0.875	0.571429
RF	0.536364	0.352941	0.694915	0.413793
SVM	0.618182	0.529412	0.694915	0.5625
XgBoost	0.609091	0.529412	0.677966	0.556701

DISCUSSION

As far as we know, the great majority of machine learning or deep learning methods used to identify ASD patients from controls are mainly based on the resting-state fMRI. Although fMRI constructs individual brain networks by estimating interregional functional connectivity, those networks are made by the graph theory analytical method, which are only efficient for imaging data with 4D time series. However, given the great individual variability of fMRI, sMRI and its derived measures with high reproducibility have been widely used for disease classification. Although some previous studies extracted local conventional morphological features, such as gray matter volume, thickness, or volume of different regions from sMRI for machine learning, the relationship between structural properties of different regions has not been explored since the coordinated patterns of the local morphological features between regions are important for cognitive development (Bullmore and Bassett, 2010; Vértes and Bullmore, 2014). Thus, the construction of a structural covariance network with sMRI to explore individual brain topological organization and to investigate its alterations or abnormalities under both healthy and pathological conditions has attracted increasing attention. The whole-brain morphological network at the individual level based on sMRI characterizes the topological organizations at both the global and nodal levels (Wang et al., 2016). Thus, the individual-level morphological brain networks can better reflect individual behavior differences in both typical and atypical populations than the group-level morphological network. Moreover, compared with the local regional measures with sMRI, the individual morphological covariance network can provide more features to meet the requirements for the number of features during deep learning training. Thus, combining the morphological covariance network and deep learning will open a new avenue for future studies with sMRI.

In recent works, deep learning algorithms improve the classification accuracy in the identification of ASD versus TC. However, they are usually treated as "black-box" methods because of the lack of understanding of their internal functions (Lipton, 2016). The black-box methods cannot explain their predictions in a way that humans can understand. To fix this problem, the Grad-CAM technique uses gradients of the target concept (identification of ASD in a classification network for our work) and produces a coarse localization map to identify the weight

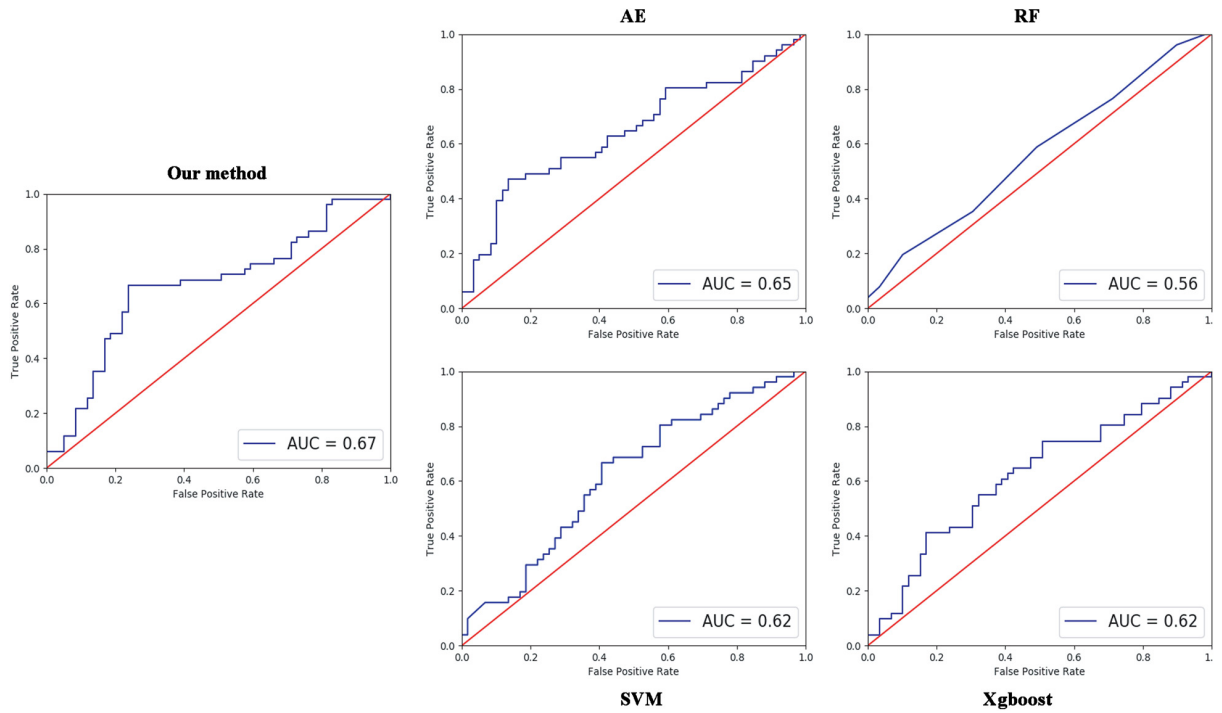

FIGURE 3 | Comparisons between our method and other methods for classification. The area under the curve (AUC) values were used to assess the classification performances for our method, AE, RF, SVM, and XgBoost.

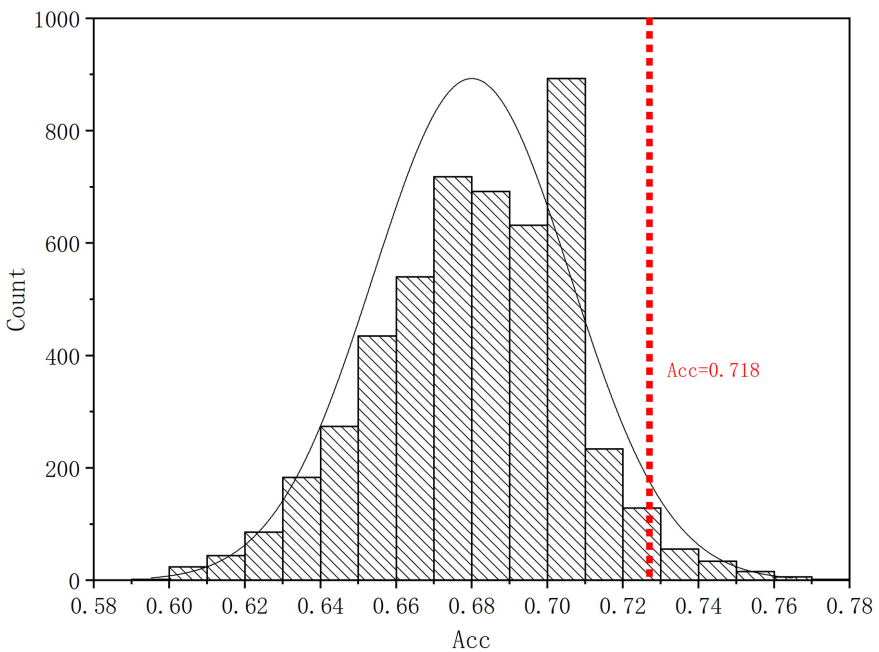

FIGURE 4 | The histogram of accuracy of the permutation test. The permutation test with 5,000 times was used to evaluate the significance of our method. The accuracy of our method (0.718) is indicated by the red dotted line. The classification accuracy is higher than 95% of the permutated accuracy values.

of each feature of the image during classification or prediction, which produces "visual explanations" for decisions from the CNN-based models and makes them to be more transparent and explainable (Selvaraju et al., 2020). Compared with other visualization techniques, Grad-CAM can highlight the important connectivities in the morphological covariance brain networks

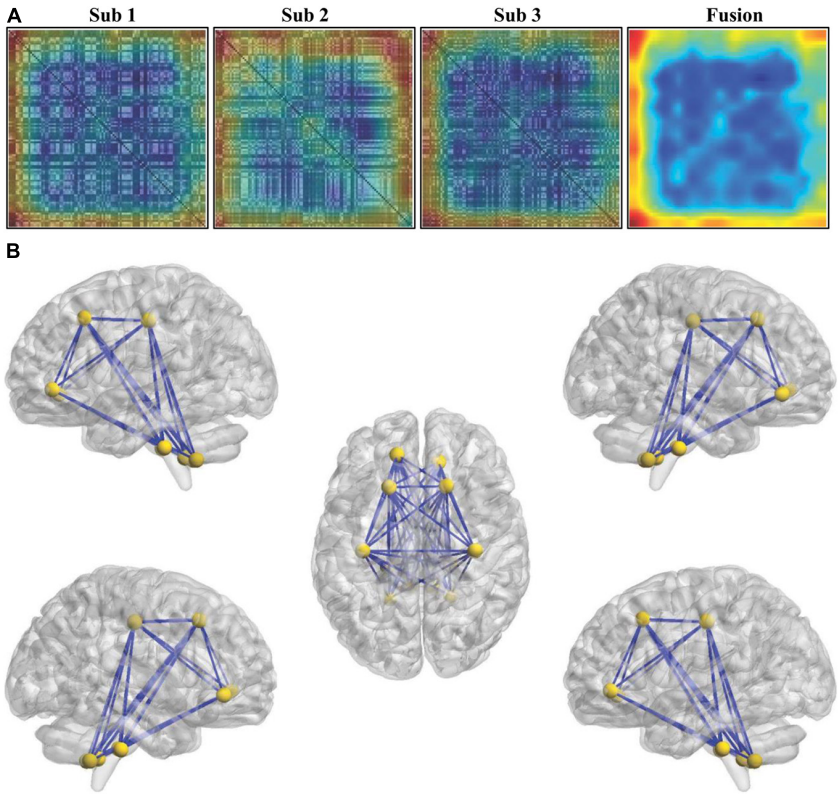

FIGURE 5 | Weights of the features for classification. **(A)** The individual and fused connectivities supporting the correct classification of ASD patients were mapped using the Grad-CAM visualizations for our ResNet framework. The red regions correspond to high score for ASD class. **(B)** The top 12 regions and the corresponding connectivities which have the largest contribution correctly classifying ASD patients were identified.

for discriminating ASD without model architectural changes or retraining. Thus, Grad-CAM combined with our classification model provides a reference for future study to determine the important features in deep learning framework.

Using the Grad-CAM method, we found that the morphological covariance between frontal and cerebellar areas has the largest contribution for classification. The frontal areas include the precentral gyrus, superior frontal gyrus, and orbital part of the superior frontal gyrus. For the cerebellum, cerebellum 8, 9, and 10 were found to contribute greatly for classification. The precentral gyrus and cerebellum have been widely demonstrated to be associated with motor processing and integration of sensory information. Thus, the structural covariance between the precentral gyrus and cerebellum suggested that they may be related to the rigid, stereotyped, and repetitive behaviors in ASD (Mei et al., 2020). Furthermore, we also found the structural covariance connectivities among the superior frontal gyrus, orbital part of the superior frontal gyrus, and cerebellum contributing largely to the classification. The cerebellum participates not only in motor functions but also in emotion, memory, language, and social cognition processing (Strick et al., 2009; Buckner, 2013). The superior frontal gyrus has been demonstrated to be involved in social cognition (Monk et al., 2009; Li et al., 2013). Thus, the superior frontal gyrus and its orbital part and the cerebellum may be related to social cognition processing in ASD. Given that rigid, stereotyped, and repetitive behaviors and impaired social cognition are the core symptoms of ASD, our findings further demonstrated the reliability and feasibility of our proposed method for ASD classification. Also, our proposed method may advance establishing the framework for early diagnosis of ASD.

CONCLUSION

In this study, we proposed a convolutional neural network framework based on the individual-level morphological covariance brain network for ASD diagnosis. We found that our proposed method outperformed other classification methods for the classification of ASD in a multisite. Moreover, using Grad-CAM, we can identify the weight of each feature for classification, which solves the black-box problems of deep learning. Our study proposes a new paradigm for ASD classification that has a good performance in multisite datasets and will facilitate establishing the diagnosis framework for ASD.

DATA AVAILABILITY STATEMENT

The raw data supporting the conclusions of this article will be made available by the authors, without undue reservation.

ETHICS STATEMENT

The studies involving human participants were reviewed and approved by the St. James's Hospital/AMNCH (ref: 2010/09/07) and the Linn Dara CAMHS Ethics Committees (ref: 2010/12/07). Written informed consent to participate in this study was provided by the participants' legal guardian/next of kin.

AUTHOR CONTRIBUTIONS

JW, SC, and JG designed this study. JG, MC, YG, and YuL performed the experiments. JG, YaL, and JW wrote the manuscript. All the authors discussed and edited this manuscript.

FUNDING

This work was funded in part by the Sichuan Science and Technology Program (2021YJ0186 and 2019YJ0193), the National Natural Science Foundation of China (61701078 and 71572152), Sichuan Key Research and Development Plan (21ZDYF3062), and the Science Promotion Programme of UESTC, China (Y03111023901014006).

REFERENCES

Buckner, R. L. (2013). The cerebellum and cognitive function: 25 years of insight from anatomy and neuroimaging. *Neuron* 80, 807–815. doi: 10.1016/j.neuron.2013.10.044

Bullmore, E., and Bassett, D. (2010). Brain graphs: graphical models of the human brain connectome. *Annu. Rev. Clin. Psychol.* 7, 113–140. doi: 10.1146/annurev-clinpsy-040510-143934

Button, K. S., Ioannidis, J. P., Mokrysz, C., Nosek, B. A., Flint, J., Robinson, E. S., et al. (2013). Power failure: why small sample size undermines the reliability of neuroscience. *Nat. Rev. Neurosci.* 14, 365–376. doi: 10.1038/nrn3475

Chen, R., Jiao, Y., and Herskovits, E. H. (2011). Structural MRI in autism spectrum disorder. *Pediatric Res.* 69(5 Pt 2), 63R–68R.

Chen, T., and Guestrin, C. (2016). XGBoost: a scalable tree boosting system. *arXiv* [Preprint] doi: 10.1145/2939672.2939785

Di Martino, A., Yan, C. G., Li, Q., Denio, E., Castellanos, F. X., Alaerts, K., et al. (2014). The autism brain imaging data exchange: towards a large-scale evaluation of the intrinsic brain architecture in autism. *Mol. Psychiatry* 19, 659–667.

Guze, S. B. (1995). Diagnostic and statistical manual of mental disorders, 4th ed. (DSM-IV). *Am. J. Psychiatry* 152, 1228–1228.

Haar, S., Berman, S., Behrmann, M., and Dinstein, I. (2016). Anatomical abnormalities in autism? *Cereb. Cortex* 26, 1440–1452. doi: 10.1093/cercor/bhu242

He, K., Zhang, X., Ren, S., and Sun, J. (2016). "Deep residual learning for image recognition," in *Proceedings of the 2016 IEEE Conference on Computer Vision and Pattern Recognition (CVPR)* (Las Vegas, NV), 770–778.

Heinsfeld, A. S., Franco, A. R., Craddock, R. C., Buchweitz, A., and Meneguzzi, F. (2018). Identification of Autism spectrum disorder using deep learning and the ABIDE dataset. *Neuroimage Clin.* 17, 16–23. doi: 10.1016/j.nicl.2017.08.017

Hinton, G., Srivastava, N., Krizhevsky, A., Sutskever, I., and Salakhutdinov, R. (2012). Improving neural networks by preventing co-adaptation of feature detectors. *arXiv* [Preprint] arXiv.1207.0580.

Ho, T. K. (1995). "Random decision forests," in *Proceedings of 3rd International Conference on Document Analysis & Recognition* (Montreal QC).

Ioffe, S., and Szegedy, C. (2015). "Batch normalization: accelerating deep network training by reducing internal covariate shift," in *Proceedings of the 32nd International Conference on Machine Learning* (France).

Katuwal, G. J., Cahill, N. D., Baum, S. A., and Michael, A. M. (2015). "The predictive power of structural MRI in Autism diagnosis," in *Proceedings of the 37th Annual International Conference of the IEEE Engineering in Medicine and Biology Society IEEE Engineering in Medicine and Biology Society Annual International Conference*, Vol. 2015 (Milan), 4270–4273.

Kong, X. Z., Wang, X., Huang, L., Pu, Y., Yang, Z., Dang, X., et al. (2014). Measuring individual morphological relationship of cortical regions. *J. Neurosci. Methods* 237, 103–107. doi: 10.1016/j.jneumeth.2014.09.003

Kong, Y., Gao, J., Xu, Y., Pan, Y., Wang, J., and Liu, J. (2019). Classification of autism spectrum disorder by combining brain connectivity and deep neural network classifier. *Neurocomputing* 324, 63–68. doi: 10.1016/j.neucom.2018.04.080

Li, C., Gore, J. C., and Davatzikos, C. (2014). Multiplicative intrinsic component optimization (MICO) for MRI bias field estimation and tissue segmentation. *Magn. Reson. Imaging* 32, 913–923. doi: 10.1016/j.mri.2014.03.010

Li, W., Qin, W., Liu, H., Fan, L., Wang, J., Jiang, T., et al. (2013). Subregions of the human superior frontal gyrus and their connections. *Neuroimage* 78, 46–58. doi: 10.1016/j.neuroimage.2013.04.011

Lipton, Z. (2016). The mythos of model interpretability. *Commun. ACM* 61:10.

Liu, Y., Chen, X., Peng, H., and Wang, Z. (2017). Multi-focus image fusion with a deep convolutional neural network. *Inf. Fusion* 36, 191–207. doi: 10.1016/j.inffus.2016.12.001

Liu, Y., Chen, X., Wang, Z., Wang, Z. J., Ward, R. K., and Wang, X. (2018). Deep learning for pixel-level image fusion: recent advances and future prospects. *Inf. Fusion* 42, 158–173. doi: 10.1016/j.inffus.2017.10.007

Mei, T., Llera, A., Floris, D. L., Forde, N. J., Tillmann, J., Durston, S., et al. (2020). Gray matter covariations and core symptoms of autism: the EU-AIMS longitudinal European Autism project. *Mol. Autism* 11:86.

Monk, C. S., Peltier, S. J., Wiggins, J. L., Weng, S. J., Carrasco, M., Risi, S., et al. (2009). Abnormalities of intrinsic functional connectivity in autism spectrum disorders. *Neuroimage* 47, 764–772. doi: 10.1016/j.neuroimage.2009.04.069

Nielsen, J. A., Zielinski, B. A., Fletcher, P. T., Alexander, A. L., Lange, N., Bigler, E. D., et al. (2013). Multisite functional connectivity MRI classification of autism: ABIDE results. *Front. Hum. Neurosci.* 7:599. doi: 10.3389/fnhum.2013.00599

Ou, Y., Sotiras, A., Paragios, N., and Davatzikos, C. (2011). DRAMMS: deformable registration via attribute matching and mutual-saliency weighting. *Med. Image Anal.* 15, 622–639. doi: 10.1016/j.media.2010.07.002

Rohlfing, T., Zahr, N. M., Sullivan, E. V., and Pfefferbaum, A. (2010). The SRI24 multichannel atlas of normal adult human brain structure. *Hum. Brain Mapp.* 31, 798–819. doi: 10.1002/hbm.20906

Rosenblatt, M. (1956). Remarks on some nonparametric estimates of a density function. *Ann. Math. Stat.* 27, 832–837. doi: 10.1214/aoms/1177728190

Selvaraju, R. R., Cogswell, M., Das, A., Vedantam, R., Parikh, D., and Batra, D. (2017). "Grad-CAM: visual explanations from deep networks via gradient-based localization," in *Proceedings of the 2017 IEEE International Conference on Computer Vision (ICCV)* (Venice), 618–626.

Selvaraju, R. R., Cogswell, M., Das, A., Vedantam, R., Parikh, D., and Batra, D. (2020). Grad-CAM: visual explanations from deep networks via gradient-based localization. *Int. J. Comput. Vis.* 128, 336–359. doi: 10.1007/s11263-019-01228-7

Strick, P. L., Dum, R. P., and Fiez, J. A. (2009). Cerebellum and nonmotor function. *Annu. Rev. Neurosci.* 32, 413–434. doi: 10.1146/annurev.neuro.31.060407.125606

Vapnik, V. (1998). "The support vector method of function estimation," in *Nonlinear Modeling: Advanced Black-Box Techniques*, eds J. A. K. Suykens and J. Vandewalle (Boston, MA: Springer US), 55–85. doi: 10.1007/978-1-4615-5703-6_3

Vértes, P., and Bullmore, E. (2014). Annual research review: growth connectomics – the organization and reorganization of brain networks

during normal and abnormal development. *J. Child Psychol. Psychiatry Allied Dis.* 56, 299–320. doi: 10.1111/jcpp.12365

Wang, H., Jin, X., Zhang, Y., and Wang, J. (2016). Single-subject morphological brain networks: connectivity mapping, topological characterization and test-retest reliability. *Brain Behav/* 6:e00448.

Wang, J., Becker, B., Wang, L., Li, H., Zhao, X., and Jiang, T. (2019). Corresponding anatomical and coactivation architecture of the human precuneus showing similar connectivity patterns with macaques. *Neuroimage* 200, 562–574.

Wang, J., Feng, X., Wu, J., Xie, S., Li, L., Xu, L., et al. (2018). Alterations of gray matter volume and white matter integrity in maternal deprivation monkeys. *Neuroscience* 384, 14–20. doi: 10.1016/j.neuroscience.2018.05.020

Wang, J., Wei, Q., Bai, T., Zhou, X., Sun, H., Becker, B., et al. (2017). Electroconvulsive therapy selectively enhanced feedforward connectivity from fusiform face area to amygdala in major depressive disorder. *Soc. Cogn. Affect. Neurosci.* 12, 1983–1992. doi: 10.1093/scan/nsx100

Wu, H., Sun, H., Wang, C., Yu, L., Li, Y., Peng, H., et al. (2017). Abnormalities in the structural covariance of emotion regulation networks in major depressive disorder. *J. Psychiatric Res.* 84, 237–242. doi: 10.1016/j.jpsychires.2016.10.001

Xu, J., Wang, J., Bai, T., Zhang, X., Li, T., Hu, Q., et al. (2019). Electroconvulsive therapy induces cortical morphological alterations in major depressive disorder revealed with surface-based morphometry analysis. *Int. J. Neural. Syst.* 29:1950005. doi: 10.1142/s0129065719500059

Zhang, K., Zuo, W., Chen, Y., Meng, D., and Zhang, L. (2016). Beyond a Gaussian Denoiser: residual learning of deep CNN for image denoising. *IEEE Trans. Image Process.* 26, 3142–3155. doi: 10.1109/tip.2017.2662206

Zheng, W., Eilamstock, T., Wu, T., Spagna, A., Chen, C., Hu, B., et al. (2018). Multi-feature based network revealing the structural abnormalities in autism spectrum disorder. *IEEE Trans. Affect. Comput.* 1949–3045. doi: 10.1109/taffc.2018.2890597

Conflict of Interest: The authors declare that the research was conducted in the absence of any commercial or financial relationships that could be construed as a potential conflict of interest.

frontiers in Human Neuroscience

REVIEW
published: 01 February 2021
doi: 10.3389/fnhum.2021.625321

A Critical Review of Cranial Electrotherapy Stimulation for Neuromodulation in Clinical and Non-clinical Samples

Tad T. Brunyé[1,2]*, *Joseph E. Patterson*[2], *Thomas Wooten*[3] *and Erika K. Hussey*[1,2]

[1] U. S. Army Combat Capabilities Development Command Soldier Center, Cognitive Science Team, Natick, MA, United States, [2] Center for Applied Brain and Cognitive Sciences, Tufts University, Medford, MA, United States, [3] Department of Psychology, Tufts University, Medford, MA, United States

OPEN ACCESS

Edited by:
Hongming Li,
University of Pennsylvania,
United States

Reviewed by:
Noah S. Philip,
Brown University, United States
Jiliang Fang,
China Academy of Chinese Medical Sciences, China

***Correspondence:**
Tad T. Brunyé
tbruny01@tufts.edu

Specialty section:
This article was submitted to Brain Imaging and Stimulation, a section of the journal Frontiers in Human Neuroscience

Received: 02 November 2020
Accepted: 07 January 2021
Published: 01 February 2021

Citation:
Brunyé TT, Patterson JE, Wooten T and Hussey EK (2021) A Critical Review of Cranial Electrotherapy Stimulation for Neuromodulation in Clinical and Non-clinical Samples. Front. Hum. Neurosci. 15:625321. doi: 10.3389/fnhum.2021.625321

Cranial electrotherapy stimulation (CES) is a neuromodulation tool used for treating several clinical disorders, including insomnia, anxiety, and depression. More recently, a limited number of studies have examined CES for altering affect, physiology, and behavior in healthy, non-clinical samples. The physiological, neurochemical, and metabolic mechanisms underlying CES effects are currently unknown. Computational modeling suggests that electrical current administered with CES at the earlobes can reach cortical and subcortical regions at very low intensities associated with subthreshold neuromodulatory effects, and studies using electroencephalography (EEG) and functional magnetic resonance imaging (fMRI) show some effects on alpha band EEG activity, and modulation of the default mode network during CES administration. One theory suggests that CES modulates brain stem (e.g., medulla), limbic (e.g., thalamus, amygdala), and cortical (e.g., prefrontal cortex) regions and increases relative parasympathetic to sympathetic drive in the autonomic nervous system. There is no direct evidence supporting this theory, but one of its assumptions is that CES may induce its effects by stimulating afferent projections of the vagus nerve, which provides parasympathetic signals to the cardiorespiratory and digestive systems. In our critical review of studies using CES in clinical and non-clinical populations, we found severe methodological concerns, including potential conflicts of interest, risk of methodological and analytic biases, issues with sham credibility, lack of blinding, and a severe heterogeneity of CES parameters selected and employed across scientists, laboratories, institutions, and studies. These limitations make it difficult to derive consistent or compelling insights from the extant literature, tempering enthusiasm for CES and its potential to alter nervous system activity or behavior in meaningful or reliable ways. The lack of compelling evidence also motivates well-designed and relatively high-powered experiments to assess how CES might modulate the physiological, affective, and cognitive responses to stress. Establishing reliable empirical links between CES administration and human performance

is critical for supporting its prospective use during occupational training, operations, or recovery, ensuring reliability and robustness of effects, characterizing if, when, and in whom such effects might arise, and ensuring that any benefits of CES outweigh the risks of adverse events.

Keywords: non-invasive brain stimulation, neuromodulation, psychiatry, human performance, electrotherapy

INTRODUCTION

Cranial electrotherapy stimulation (CES) involves delivering low-intensity (50 μA to 4 mA) electrical current via a pair of electrodes attached to bilateral anatomical positions around the head (e.g., eyelids, earlobes, mastoids, temples), with the intent of acutely modulating central and/or peripheral nervous system activity. This review describes past and present research and development efforts with this neuromodulatory technique, with emphasis on its potential for enhancing well-being in clinical contexts and optimizing or enhancing human performance in healthy, neurotypical populations.

In clinical populations, CES has been used as an adjunctive treatment for several clinical disorders including insomnia, depression, post-traumatic stress disorder, and anxiety (Gunther and Phillips, 2010; Bracciano et al., 2012; Morriss and Price, 2020). While the precise mechanisms underlying putative CES effects on clinical disorders remain elusive, proposed effects include modulation of central and peripheral nervous systems, altering resting state and limbic system activity, increasing cortical alpha-band activity, and modulating the release of neurotransmitters and downstream hormones including catecholamines and glucocorticoids (Schroeder and Barr, 2001; Feusner et al., 2012; Qiao et al., 2015; Wagenseil et al., 2018; Yennurajalingam et al., 2018; Wu et al., 2020).

In healthy populations engaged in high-stakes occupational contexts and tasks, performance enhancement can occur during learning or training, and prior to, during, and/or after occupational task performance. Indeed, neuromodulation approaches hold potential to accelerate learning and training, but also acutely modulate task performance and assist in rest, recovery, and reset phases. For example, an emergency first responder might incorporate neuromodulatory techniques to accelerate the learning of new procedural skills, modulate stress responses during high-stakes operations, or to assist emotion regulatory processes following exposure to stress. In these scenarios, CES may carry potential to help sustain or improve behavioral outcomes related to occupational performance including vigilance, perceptuomotor control, situation awareness, and emotion regulation.

To examine whether CES may carry potential to reliably alter brain activity, physiology, neurotransmitters and hormones, or behavior in clinical and non-clinical populations, we critically review extant scientific outcomes from studies examining CES, detail mechanistic models of CES effects, and reveal several methodological strengths and weaknesses of the existing literature. The report concludes with paths forward for CES research and potential application to occupational performance in healthy, neurotypical populations.

A BRIEF HISTORY OF CES

The first CES device, the Somniatron, was developed in the Soviet Union in the early 1900s and delivered 1–4 mA alternating current at 100 Hz via two electrodes attached to the eyelids (Robinovitch, 1914). The Somniatron was used to induce analgesia and sleep in patients with insomnia. In 1973, the first CES device was marketed in the United States without formal regulatory oversight, the Electrosone 50, for inducing relaxation and sleep (Kirsch et al., 2014). The Electrosone delivered alternating current at variable pulse frequency (up to 4,000 Hz) with 2 mA to 8 mA intensity; the device was portable and battery-operated, and electrodes were placed on the eyelids and mastoids.

Three years after the release of the Electrosone, the United States Food and Drug Administration (FDA) began regulating medical devices. In 1978, the Neurotone 101 became the first FDA-approved CES device, delivering up to 1.5 mA intensity at 50–100 Hz (Guleyupoglu et al., 2013) via electrodes placed on the supraorbital ridge and mastoid. The device was marketed for the treatment of anxiety, depression, and insomnia. In the years that followed, several CES devices were developed and marketed in the United States, including the Pain Suppressor, Transcranial Electrostimulator, Electrodorm, Fisher Wallace Cranial Electrical Stimulator, and the Alpha-Stim (Shekelle et al., 2018a).

The United States Food and Drug Administration (FDA) classifies medical devices into three Classes: Class I, II, and III, each with their own regulatory controls (Peña et al., 2007). The level of regulatory control increases across the three Classes, with Class I requiring general controls, Class II requiring special controls, and Class III requiring premarket approval. Class I products are generally low risk and not intended for supporting or sustaining life or preventing health-related impairment; examples include bandages, electronic toothbrushes, and stethoscopes. Class II products are generally moderate risk and have sustained contact with a patient, and general controls are not sufficient for ensuring device safety or efficacy; examples include syringes, contact lenses, and absorbable sutures. Class III products are generally high-risk and have unproven safety or efficacy, and have sustained and potentially life-supporting contact with a patient; examples include pacemakers, defibrillators, and medical implants. From the 1980's through early 2000's, many of the original CES devices were regulated as Class III devices by the United States Food and Drug Administration (FDA).

More recently, the FDA issued a final order (Docket No. FDA-2014-N-1209) to classify CES devices marketed to treat anxiety or insomnia as Class II (special controls) medical devices. A Class

II designation is given by the FDA for devices for which general controls are insufficient to provide reasonable assurance of the safety and effectiveness of the device (21CFR860.3). In contrast, CES devices marketed to treat depression are classified as Class III medical devices, requiring additional regulatory oversight due to potential unreasonable risk of illness or injury (21CFR860.3). As part of the FDA regulation of CES devices, only licensed medical practitioners can order patient use of a CES device.

Despite this regulation, about a dozen devices are currently available for consumer purchase in the United States, varying in price from ∼$300–5000USD. Technically, all available devices can only be ordered by licensed medical practitioners, or by patients who complete a low-cost telemedicine visit. Note that our research group has been able to readily procure CES devices for research purposes, specifically the Alpha-Stim M, by stating our research purpose and without demonstrating licensure. Below are some examples of currently marketed CES devices:

1. Alpha-Stim M (Electromedical Products International, Inc.)
    a. Output: Bipolar asymmetric rectangular wave at 0.5, 1.5, and 100 Hz, up to 600 μA.
    b. Electrodes: Ear clips.
    c. URL: https://www.alpha-stim.com/product/alpha-stim-m-microcurrent-cranial-electrotherapy-stimulator/.
2. Alpha-Stim 100 (Electromedical Products International, Inc.)
    a. Output: Bipolar asymmetric rectangular wave at 0.5, 1.5, and 100 Hz, up to 600 μA.
    b. Electrodes: Ear clips.
    c. URL: http://alphachoices.com/as100.html.
3. Fisher Wallace Stimulator (Fisher Wallace Laboratories, Inc.)
    a. Output: Symmetrical biphasic square wave at 15, 500, and 15k Hz, up to 4 mA.
    b. Electrodes: Sponge electrodes, mounted on temples.
    c. URL: https://www.fisherwallace.com/.
4. CES Ultra (Neuro-Fitness, LLC)
    a. Output: Modified square wave at 100 Hz, up to 1.5 mA.
    b. Electrodes: Woven electrodes with conductive gel, mounted on temples.
    c. URL: https://www.cesultra.com/.
5. Caputron MindGear (Caputron Medical Products, LLC)
    a. Output: Symmetrical biphasic square wave at 0.5 Hz, up to 1.5 mA.
    b. Electrodes: Ear clips or self-adhesive electrodes for temples.
    c. URL: https://caputron.com/collections/mindgear.
6. Neurocare NeuroMICRO (Neurocare, Inc.)
    a. Output: Modified square DC biphasic pulses at 0.3, 8, and 80 Hz, at 12V.
    b. Electrodes: Carbon electrodes with conductive gel, mounted on temples.
    c. URL: http://neurocare.com/neuromicro-cranial-electrotherapy-stimulation/.

CLINICAL APPLICATIONS OF CES

CES has predominantly been used for the relief of symptoms accompanying three clinical disorders: insomnia, anxiety, and depression. While hundreds of studies have been published examining the effects of CES on insomnia, depression, and anxiety, most are inadequately designed and show a high risk of bias according to the Cochrane criteria (Higgins et al., 2011). To mitigate these biases, in our review we primarily consider placebo-controlled randomized clinical trials with objective measures, similarly to what was done in recent reviews by the Department of Veterans Affairs (Shekelle et al., 2018a,b).

CES for Clinical Insomnia

The four sham-controlled randomized clinical trials using CES to treat insomnia reveal inconsistent results. One study involving 57 active-duty service member participants showed no significant change in hours of sleep time following a 5-day (60-min/day) CES treatment (100 μA, 0.5 Hz) relative to sham (Lande and Gragnani, 2013). This study used the Alpha-Stim SCS device with two electrodes attached to bilateral earlobes, and the sham condition involved an inactive device. No comparative (active vs. sham) assessment of cutaneous perception was reported. The authors suggested the CES treatment may not have been sufficient intensity (i.e., in microamps or duration) to induce reliable effects on sleep, though to our knowledge no follow-up study was conducted.

A second study involving 10 participants showed significant reduction of sleep latencies measured with electroencephalography (EEG) (Weiss, 1973). In this study, CES treatment involved a 24-day (15-min/day) CES treatment (500 μA, 100 Hz), delivered using the Electrodorm 1 device with an array of electrodes placed above the eyes and on the nape of the neck. The sham condition involved an initial stimulation and habituation phase, and then disabling the device. A report of cutaneous sensation was gathered to ensure that each participant felt a "tingling" sensation during the habituation phase, and post-treatment reports of persistent sensations (tingling, prickling, burning) were similar between the active and sham groups. Another study involving 19 psychiatric patients showed significant reduction of global insomnia ratings with a 14-day CES treatment vs. sham, using the Electrosone-50 device with electrodes placed over the orbital and mastoid areas (30-min/day; 100–250 μA, 50–100 Hz) (Feighner et al., 1973). Like the procedure used by Weiss (1973), the sham condition involved an initial stimulation phase followed by disabling the device; no comparative assessment (active vs. sham) of vestibular or cutaneous sensation was reported. Note that insomnia ratings only improved at the 15-day timepoint (not at days 1 or 26, and also not at 1-month follow-up).

A fourth double-blind randomized placebo-controlled study involving 40 females without sleep disorders showed no significant effect of CES ($n = 25$) vs. sham ($n = 15$) using

the Alpha-Stim 100 device with bilateral earlobe electrodes (60-min; 100 μA, 0.5 Hz) on any measures of sleep latency or quality (Wagenseil et al., 2018). In this study, the sham condition involved an inactive device, and no measures of vestibular or cutaneous sensation were reported. While there were no significant effects of CES on sleep latency or quality, there was some limited evidence for an effect in the EEG α band as measured using polysomnography. Specifically, there was a significant decline of low-frequency (8–10 Hz) α band peak frequency, though this pattern only arose at two EEG electrode sites and was not found in the high-frequency (10–11 Hz) α band. There was no alteration of α band power across any frequency range, and the authors suggested that the EEG peak frequency results warranted replication given their apparent specificity.

CES for Clinical Depression

A review of CES applications for depression revealed a severe lack of rigorous randomized placebo-controlled clinical trials, and a tendency to use non-standard instruments for diagnosing and monitoring depression symptoms (Kavirajan et al., 2014). In fact, of the 270 published reports on CES effects on depression, none of them reached the Cochrane quality criteria (Higgins et al., 2011). This was largely due to a failure to use standardized diagnostic criteria (e.g., the Beck Depression Inventory; BDI), lack of sufficient participant blinding (e.g., no cutaneous perception in sham group), high rates of comorbidity (e.g., fibromyalgia, anxiety, dementia, substance abuse, head injury), or consideration of only institutionalized patients with severe refractory depression (Kavirajan et al., 2014).

Two relatively high-quality publications are worth mentioning. In the first study, a group of 16 participants with depression received either sham or active CES using the Fisher Wallace Cranial Stimulator device with two electrodes placed over bilateral temples (2 mA, 5–15,000 Hz) for 10 days (20-min/day), in a randomized, double-blind, placebo-controlled design (McClure et al., 2015). The sham group received active stimulation until the participant reported a tingling sensation on the scalp, and then the device was disabled for the remainder of the session; no details were reported regarding potential differences in vestibular or cutaneous sensations between the control and sham groups. Results showed significant reductions in depressive symptoms for the active but not sham CES group at the end of week 2, measured using the BDI. These results should be interpreted with caution, however, given the relatively small sample size (active $n = 7$, sham $n = 9$).

In the second study with a larger sample size, a group of 30 participants with depression received either sham or active CES using the Fisher Wallace Cranial Stimulator (FW-100; 1–4 mA, 15–15,000 Hz) for 15 days (20-min/day), in a randomized, double-blind, placebo-controlled design (Mischoulon et al., 2015). According to the authors, this device was used with two bilateral electrodes placed over bilateral regions of the dorsolateral prefrontal cortex (dlPFC); however, as seen in Figure 2 of their report, it appears the electrodes were placed inferior to the bilateral temples. This is an important distinction because a CES device with electrodes places over the dlPFC would more accurately constitute transcranial alternating current stimulation (tACS) rather than CES. Sham devices were inactive, and there was no reporting of possible vestibular or cutaneous sensation differences between conditions. Results showed no significant differences in depressive symptoms for the active vs. sham CES groups at the end of week 3, measured using the Hamilton Rating Scale for depression (HAM-D-17).

CES for Clinical Anxiety

The effects of CES on anxiety are marginally more reliable than effects on depression. To date, five randomized, double-blind, placebo-controlled studies have been conducted, generally showing support for CES in reducing symptoms of anxiety (Shekelle et al., 2018a). These studies suffer the limitation of clinical disorder comorbidity, with most participants diagnosed with not only anxiety (i.e., generalized anxiety disorder) but also depression, post-traumatic stress disorder, and/or insomnia. Additional limitations include the use of antiquated devices (e.g., Neurotone 101 or Electrosone-50) that are no longer available for investigation, inconsistent electrode placement (head, ears, face), lack of standardized instruments for measuring anxiety, and very small sample sizes. A recent open consecutive cohort study demonstrated improvement in anxiety and depression symptoms of generalized anxiety order following 12 and 24 weeks of CES treatment with the Alpha-Stim AID device with bilateral earlobe electrodes (100 μA, 0.5 Hz); however, the study was not randomized or placebo-controlled, and the research group was funded by the manufacturer of the Alpha-Stim AIM device (Morriss et al., 2019; Morriss and Price, 2020).

One relatively large and well-conducted study shows compelling results for CES effectiveness in anxiety disorders (Barclay and Barclay, 2014). In this study, a group of 115 participants with a diagnosed anxiety disorder received either sham or active (100 μA, 0.5 Hz) CES for 5 weeks (60-min/day) using the Alpha-Stim 100 device with bilateral earlobe electrodes. The sham condition used inactive devices provided by the manufacturer, and no assessment of vestibular or cutaneous sensation was reported. By week 5, results demonstrated an ∼32% reduction in anxiety symptoms measured using the Hamilton Rating Scale for anxiety (HAM-A-17). No long-term follow-up was reported.

CES for Clinical Applications: Conclusions

In conclusion, about half of the relatively high-quality studies examining CES for insomnia treatment showed improvement in symptoms; these included improvement in latency to sleep onset, sleep quality, and sleep duration. It is important to note that while some studies showed no effects of CES, we did not find any studies suggesting a worsening of insomnia symptoms (Aseem and Hussain, 2019).

The lack of compelling evidence for CES effectiveness for mitigating depression symptoms likely underlies the FDA's decision to classify CES devices as Class III when marketed for the treatment of depression, given that the benefits do not clearly outweigh potential risks of adverse effects. The FDA therefore applies relatively stringent regulatory oversight for CES use in depression, in comparison to when marketed for treatment of insomnia or anxiety.

With clinical anxiety, we only identified one compelling study demonstrating beneficial effects of CES on the severity of anxiety symptoms, with most other studies showing methodological shortcomings and/or a high risk of bias. Again, while some studies showed no effects of CES on anxiety, we did not find any studies suggesting a worsening of symptoms with CES treatment.

Across all three categories of clinical application, we found very few rigorously designed experiments, with a pervasive lack of control for confounding variables (e.g., comorbidity, blinding, randomization, crossover). For example, most of the studies used an inactive sham control and did not assess possible vestibular or cutaneous sensation differences between active and sham groups that could be confounding results (Barclay and Barclay, 2014; McClure et al., 2015; Mischoulon et al., 2015; Wagenseil et al., 2018).

Even when well-controlled, experiments are generally inconclusive, showing inconsistently robust or reliable effects of CES on symptoms of insomnia, depression, or anxiety. There is also high methodological heterogeneity and lack of details, making it difficult to discern whether a study should be regarded as CES or tACS, *per se*. In our experience, CES is intended to provide relatively diffuse alternating current to the central and peripheral nervous systems by way of bilateral electrodes attached to the earlobes, temples, or orbital regions. In contrast, tACS uses electrode positions intended to target cortical regions more selectively, such as the prefrontal cortex or parietal lobe. As noted by other authors, there is generally a lack of compelling or consistent evidence for the effects of CES on clinical outcomes (Zaghi et al., 2010).

CES FOR NON-CLINICAL APPLICATIONS

With insomnia, depression, and anxiety, studies examining CES effects are conducted with clinical samples, many of whom were hospitalized, medicated, and/or show clinical comorbidities at the time of recruitment. This contrasts the potential application of CES technologies in healthy, non-clinical samples. Studies examining CES effects on healthy, neurotypical participants are relatively limited in number.

CES for Acute Stress Mitigation

Three studies were identified examining CES effects on non-clinical state anxiety and stress. The first study involved 33 healthy participants undergoing routine dental procedures, randomly assigned to receive either active (0.5 Hz, 200 μA) or sham CES using the Alpha-Stim 100 with bilateral earlobe electrodes (Winick, 1999). In a double-blind design, participants received active or sham CES during a dental procedure, and reported symptoms of anxiety using a visual analog scale (VAS). The sham condition used an inactive device, and no assessments of vestibular or cutaneous sensation were reported between the active and sham groups. Results demonstrated that active CES produced significantly lower anxiety ratings post-treatment (but not during the treatment) relative to sham. The authors note, however, that there was an unequal distribution of dental procedure severity (e.g., routine cleaning vs. root canal) across treatment groups, potentially influencing the results.

A second study similarly examined CES in a dental setting, randomly assigning 40 participants to one of three multi-day interventions: relaxation therapy alone, CES alone (0.5 Hz, 100–600 μA) using the Alpha-Stim 100 device with bilateral earlobe electrodes, or the combination of the two (Koleoso et al., 2013). A fourth group served as a no-contact control, without any intervention, and no measures of vestibular or cutaneous sensation were collected in any group. Results showed that all three interventions reduced self-reported dental anxiety relative to control, but the three interventions did not differ from each another. In other words, CES did not provide any additional advantage for anxiety reduction relative to a relaxation therapy intervention. Note that participants were not blinded to treatment condition.

Another study examined CES for preoperative anxiety in 50 healthy women, prior to undergoing surgery for thyroidectomy. CES was administered using the Alpha-Stim 100 device with bilateral earlobe electrodes, using active (0.5 Hz, 100 μA) or sham stimulation immediately prior to surgery, in a single-blind, randomized, placebo-controlled design (Lee et al., 2013). The sham condition involved an inactive device, and no assessments of vestibular or cutaneous sensation differences across groups were reported. Results showed reduced anxiety and pain ratings in the CES vs. control groups, extending for at least 4 h post-surgery. Blood sampling showed no significant change in adrenocorticotrophic hormone (ACTH), cortisol, or glucose levels immediately prior to surgery; however, diurnal changes in cortisol, individual variability, and/or a low stress response to thyroidectomy may have interfered with the ability to identify any such effects.

CES for Acute Sleep Quality Modification

A recent study examined the effects of CES on the sleep quality of 40 healthy women, in a randomized, sham-controlled (inactive device), double-blind study (Wagenseil et al., 2018). Using the Alpha-Stim 100 device with bilateral earlobe electrodes, active CES (0.5 Hz, 100 μA, for 60-min) was compared to a placebo control (device attached, but not active). Measures included polysomnography (PSG) and electroencephalography (EEG). PSG measures of sleep quality revealed no significant influence of CES. CES did induce a frequency-lowering effect in the alpha band of the EEG signal, similarly to what we will describe in the CES Effects on Electrical Brain Activity section.

CES for Acute Human Performance Modification

In the only study examining cognitive performance outcomes of CES treatment in a healthy sample, 52 participants were randomly assigned to an active CES (15–500 Hz, intensity not disclosed, for 20-min) or sham (device attached, but not active) group in a double-blind design (Southworth, 1999). Stimulation was administered using the LISS Body Stimulator Bipolar Model, with bilateral electrodes placed below the temples. Participants completed a continuous performance test (CPT) at baseline, and then again following 20-min of active or sham stimulation. Results demonstrated improved attention (higher accuracy, faster

response times) on the CPT following active vs. sham CES. No assessments of vestibular or cutaneous sensation were reported.

We found only one English-language study examining physical performance outcomes of CES treatment, involving 10 male weightlifters administered active CES (0.5 Hz, 10–500 μA, for 15-min) using the Alpha-Stim SCS device with bilateral earlobe electrodes (Cupriks et al., 2016). Before and after CES administration, muscle force output was measured during clean and press barbell lift repetitions (without the overhead phase). The authors reported that CES increased average and maximal force output. It is important to note, however, that this study was not placebo-controlled, randomized, or blinded in any manner. Furthermore, it is a very small sample size with specialized weightlifting skills.

CES for Non-clinical Applications: Conclusions

In contrast to clinical applications, relatively few studies have examined CES effects on healthy, neurotypical participants. Among these, studies have emphasized CES effects on state anxiety responses, sleep quality, as well as cognitive and motor performance. In the three studies examining CES effects on anxiety, there was consistent support for CES reducing subjective feelings of anxiety, though this was not accompanied by expected endocrine response modulation. The fact that physiological indices of stress response were unchanged suggests that at least a portion of emotional responses seen with CES may be due to participant expectations and lack of effective blinding. In fact, all the identified studies used a sham procedure with a completely inactive device, increasing the risk that vestibular or cutaneous sensation differences between active and sham groups could be partially driving group differences. While authors tend to report verbal claims of subthreshold stimulation made by device manufacturers (Winick, 1999; Wagenseil et al., 2018), we found no quantitative evidence to support such a claim.

In the human performance domain, CES produced faster and more accurate performance on the CPT, and some cursory evidence for increased motor force output during a weightlifting task. The latter study is severely limited by its design, however, and results should be considered with caution. The effect of CES on CPT outcomes (Southworth, 1999) deserves continuing attention and replication. Any effects of CES on CPT must be disentangled from potential non-specific effects of neurostimulation; specifically, neuromodulatory techniques can cause intersensory facilitation, and arousal due solely to the sensory experiences of active stimulation (Campana et al., 2002; Dräger et al., 2004).

CES SIDE EFFECTS AND ADVERSE EVENTS

The most frequently reported side effects of CES administration are vertigo, skin irritation, and headaches (Kirsch and Nichols, 2013), which are estimated to occur about 1% of the time (Kirsch et al., 2014). In user manuals and reports published by device manufacturers, the guidance is to reduce stimulation intensity to mitigate any reported side effects; of course, in a research setting this strategy is undesirable due to differences in stimulation intensity across sessions or participants.

In studies not funded or published by authors associated with a CES device manufacturer, frequency of side effects is mixed. In one study using the Alpha-Stim SCS device with bilateral earlobe electrodes (0.5 Hz, 10–500 μA, 60-min), 25% (3/12) participants self-withdrew due to discomfort with side effects of dizziness or headache (Bystritsky et al., 2008). In another study using the Fisher Wallace Cranial Stimulator using a ramp-up sham procedure, side effect rates were generally high in both the active and sham conditions (e.g., 44% of participants reported headache) (McClure et al., 2015). Finally, another study using the Fisher Wallace Cranial Stimulator found high rates of poor concentration (59%) and malaise (29%) with active CES, both significantly greater than seen in the sham group (Mischoulon et al., 2015).

An early FDA-commissioned review of the safety of CES by the National Research Council (1974) stated, "significant side effects or complications attributable" to the application of electric current of ∼1 mA or less for "therapeutic effect to the head" (i.e., cranial electrotherapy stimulation) were "virtually non-existent" (p. 42).

To examine more recent adverse events reported to the FDA by device users, we searched the FDA Manufacturer and User Facility Device Experience (MAUDE) database for records between 1990 and 2020 for the CES devices listed in the section titled A Brief History of CES. Three adverse reactions were reported during or following the use of an Alpha-Stim CES device, one in 2012 for burns experienced on earlobes, one in 2013 for onset of severe tinnitus, and one in 2019 for severe gastrointestinal distress and insomnia. Furthermore, seven adverse reactions were reported during or following the use of a Fisher Wallace CES device, including for disorientation, vestibular problems (balance, coordination, dizziness, vertigo), headaches, tinnitus, anxiety, depression, fatigue, brain hemorrhage, and death.

It is challenging to effectively dissociate side effects related to CES vs. comorbid health disorders, especially outside of the context of a controlled experiment. Given that some reported side effects may overlap with the symptoms of the disorder being treated, any worsening of symptoms should be taken seriously. For example, CES has been explored for the treatment of migraine and tension-related headaches while experimental reports of headache-related side effects of CES are also generally high (Solomon et al., 1989; Bystritsky et al., 2008; McClure et al., 2015).

MECHANISTIC EXPLANATIONS OF CES EFFECTS

Like other transcranial electrical stimulation (tES) methodologies, such as transcranial direct and alternating current stimulation (tDCS/tACS), the mechanisms underlying CES effects on brain and behavior remain elusive. This is for four primary reasons: a lack of well-controlled studies, equivocal experimental results, lack of methodological standardization,

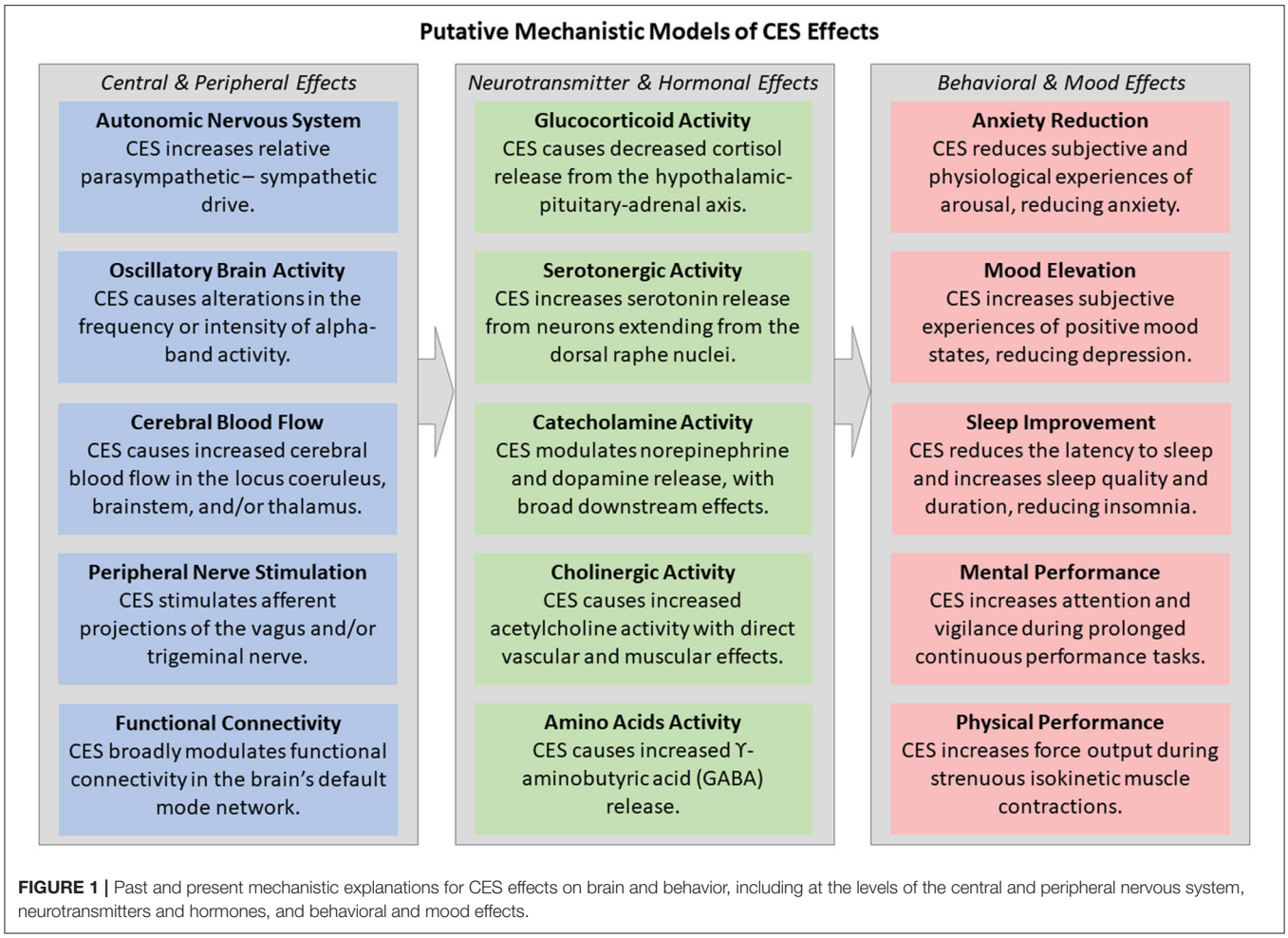

FIGURE 1 | Past and present mechanistic explanations for CES effects on brain and behavior, including at the levels of the central and peripheral nervous system, neurotransmitters and hormones, and behavioral and mood effects.

and frequent mischaracterization of study results (Edelmuth et al., 2010). **Figure 1** demonstrates the heterogeneity of past and current mechanistic explanations for CES effects on the central and peripheral nervous system, neurotransmitters and hormones, and behavior and mood. Current computational modeling efforts and experimentation do suggest a mild effect of CES on brain activity (electrical, blood flow oxygenation) and potentially neurotransmitter and hormonal responses.

Modeling CES Effects on the Central Nervous System

Computer-based modeling provides the opportunity to assess three critical questions regarding CES: does electrical current administered via CES reach cortical and/or subcortical brain regions, where are the effects of current propagation most and least pronounced, and how do morphological differences affect current flow across individuals? A few published papers explore these questions through computational modeling approaches.

The first model of CES current propagation predicted current density across four concentric anatomical spheres capturing the scalp, skull, cerebrospinal fluid, and cortical tissue (Ferdjallah et al., 1996). The authors were interested in whether applied electrical current might be dissipated over the surface of the scalp during stimulation, rendering little if any effect on underlying cortical tissue. The authors found that the maximum current density to reach relatively deep brain structures (e.g., thalamus) with a 1 mA intensity is ∼5 μA/cm2 (15 V/m). This reported V/m value is exceedingly high and likely inaccurate, pointing to the need for more modern modeling tools. However, this model did provide the first evidence that at least a portion of electrical current administered via CES reaches cortical (and perhaps subcortical) brain regions. It did not, however, provide insights into the relative spatial distribution of current over various anatomical structures, or how morphological variation might impact current flow.

A second more realistic and comprehensive model of CES current propagation used a high-resolution head model (derived from magnetic resonance imaging; MRI) that predicts not only current density across cortical and subcortical targets, but also the effects of anatomical variation in gyri/sulci (Datta et al., 2013). The models considered 1.0 mA DC administration (at 150 Hz) with five different electrode montages, including conventional ear clips, and detailed current propagation across the scalp, skull, cerebrospinal fluid, eyes, muscle, gray and white matter, and air. With ear clips, peak current density ∼0.10 V/m, with the strongest effects at the temporal regions and medulla oblongata,

with diffuse effects across the midbrain, thalamus, pons, insula, and hypothalamus. An ear-hook montage induced the highest peak current intensity, at 0.47 V/m, with a relatively superior current flow through the cortex. Interestingly, with all electrodes, the current intensities reaching subcortical regions were similar to those reaching cortical regions, suggesting that CES may induce behavioral effects suggesting subcortical modulation (e.g., fatigue, attention, anxiety, sleep, appetite).

Thus, computational modeling of CES current propagation through tissue demonstrates that CES does effectively penetrate the scalp and skull, reaching both cortical and subcortical brain regions. The intensity of current at cortical and subcortical appear to be rather weak, though the two published models gave very mixed predictions (15 V/m vs. 0.47 V/m). Most CES current intensities predicted by computational modeling approaches are up to 1,000-times lower than the intensities induced with transcranial magnetic stimulation (TMS) (Bijsterbosch et al., 2012), predicting only subthreshold, if any, modulation of neuronal populations with CES. Furthermore, the second modeling effort may have limited applicability to CES given its emphasis on DC rather than AC stimulation.

CES Effects on Electrical Brain Activity

Several studies have examined the effects of CES on electroencephalography (EEG) signals, using power spectral density analyses. EEG power spectral density refers to the frequency content of brain signals collected at the surface of the scalp. Frequency content of EEG signals is typically divided into at least four functionally distinct bands: Beta (12–40 Hz), Alpha (8–12 Hz), Theta (4–8 Hz), and Delta (1–4 Hz). The most common way to analyze activity in each frequency band is to calculate average band power, which aggregates the contribution of each frequency band to the overall power of the EEG signal (Tatum, 2014).

Power levels within each frequency band have been associated with physiological, cognitive, and affective processes (Niedermeyer and da Silva, 2005). Beta activity has been associated with motor planning, cognitive task engagement, alertness, anxiety, and rumination (Oken and Salinsky, 1992; Jacobs et al., 1996; Isotani et al., 2001). Alpha activity has been associated with idle motor behavior, eye closure, and relaxation (Niedermeyer, 1997; Feshchenko et al., 2001). Theta activity is relatively diminished in adulthood, showing most prominently in sleep-related phenomena such as near-sleep (hypnagogic state), rapid eye movement (REM) sleep, and sleep deprivation (Schacter, 1977). It has also been associated with attention, task engagement, memory, and cognitive performance (Klimesch, 1999). Delta activity has been associated with attention to internal thought processes, slow-wave sleep, homeostasis, motivation, salience detection, and subliminal perception (Harmony et al., 1996; Knyazev, 2012).

Given the associations between power in specific frequency bands and affective and cognitive functions, one might expect CES to decrease beta power, increase alpha power, and possibly decrease theta and/or delta power. Studies have found inconsistent support for these hypotheses. One study using the Alpha-Stim 100 device (0.5 or 100 Hz; 10–100 μA, 20-min) found no significant change in alpha band power with CES vs. sham, but a small shift to lower alpha frequencies overall during stimulation (Schroeder and Barr, 2001). In this study, the sham condition used an inactive device following a brief sensation thresholding procedure. However, this study used only a single EEG electrode for recording, examined only 12 male participants, and did not measure EEG after cessation of stimulation (introducing the possibility that some measured EEG effects were artifactual from CES administration). Another study described earlier in this report found a similar frequency shift in alpha band power with CES (Wagenseil et al., 2018). This latter study improved upon the earlier design, with 23-channel EEG (vs. 1-channel) recording, a larger sample size (40 vs. 12), and only measured EEG during a period in which the CES device was turned off.

A more recent study recorded EEG before and after CES administered with the Endomed 482 using bilateral earlobe electrodes at 0.5 or 100 Hz, with the sham group using an inactive device (no vestibular or cutaneous sensations were reported for either group). The authors found increased high frequency (11–13 Hz) parietal alpha band activity with 0.5 Hz stimulation, and increased low and mid-frequency temporal beta band activity with 100 Hz stimulation (Lee et al., 2019). The authors suggest these results show evidence for CES increasing "clear state of mind," attention, and concentration. However, the study used a relatively low-density EEG montage (6 electrodes), did not reveal statistical outcomes for critical comparisons, and was not double-blinded.

Another study often cited by CES manufacturers in marketing materials was sourced to a student presentation at the International Society for Neuronal Regulation (Black et al., 2004). This pilot study was not randomized, placebo-controlled, or blinded, but the authors reported increased alpha band power following a single 20-min CES session (0.5 Hz, unknown intensity).

CES Effects on Brain Hemodynamics

Two neuroimaging methods have been used to assess CES effects on brain hemodynamics, including magnetic resonance imaging (MRI) and Xenon-enhanced computed tomography (XeCT). The blood-oxygen-level-dependent (BOLD) signal is a primary measure of brain hemodynamics when using MRI, and is thought to index the extent to which blood is carrying oxygen to supply relatively active neurons (Raichle, 1998). In typical experiments, the BOLD signal is compared between multiple task conditions; for example, a cognitive task involving spatial orienting vs. inhibitory control. By comparing the spatial distribution of BOLD responses across the brain during performance of each task, researchers can derive insights into the brain regions that may underlie performance of one task vs. another.

In addition to the task-dependent BOLD response, MRI also provides measures of resting state activity across functionally connected regions of the brain. These networks of functional connectivity include the default mode network (DMN), sensorimotor network, frontoparietal network, and executive control network (Moussa et al., 2012). Activity in these and other networks has been used for a variety of clinical and neuropsychological purposes, including identifying and

characterizing disease presence and prognosis (Greicius et al., 2004; Fox and Greicius, 2010), predicting cognitive task aptitudes (Hampson et al., 2006), and understanding the influence of clinical therapies on brain functional connectivity (Flodin et al., 2015; King et al., 2016).

Only one study has used MRI to evaluate effects of CES on brain hemodynamics. Eleven healthy participants were administered CES (0.5 and 100 Hz) for brief alternating periods of active and inactive stimulation (22-s each) using the Alpha-Stim 100 device with bilateral earlobe electrodes (Feusner et al., 2012). No control condition was used, though the authors did try to ensure that stimulation was subthreshold for cutaneous sensation in both the 0.5 and 100 Hz conditions. Measures of BOLD response demonstrated broad regional brain deactivation in both 0.5 and 100 Hz conditions, except for the thalamus. Measures of resting state network activity demonstrated that the 100 Hz condition was associated with alterations of DMN activity (both increased and decreased functional connectivity across nodes of the DMN), but not sensorimotor or frontoparietal networks. The authors proposed that the therapeutic effects of CES may be derived from a downregulation of internal thought related to worry or rumination, perhaps by shifting attention to external stimuli (Hamilton et al., 2011); however, it is important to note that CES did not produce any changes on the state-trait anxiety inventory (STAI). Methodological limitations include a small sample size, lack of a control condition, and no double-blinding.

Xenon-enhanced computed tomography (XeCT) uses CT scanning coupled with xenon gas inhalation by participants. The XeCT system measures the presence of the gas as it is carried by the blood and variably diffused into brain tissue, resulting in a quantitative measure of cerebral blood flow (CBF) (Zink, 2001). Only one study has used XeCT to evaluate CBF changes as a function of CES administration (Gense de Beaufort et al., 2012), using the Anesthelec device with three electrodes (one at center of forehead, two behind bilateral mastoids) and an inactive sham condition. In this study, the authors were interested in whether CES would modulate CBF in the brainstem and thalamus, given their role in pain and anxiety control, and links to the opioid system. A total of 36 healthy participants were randomly assigned to an active or sham CES group, and received a single 120-min stimulation following a baseline XeCT measurement. The device stimulated using a complex monophasic current at 100 Hz with reported peak-to-peak intensity of 280 mA, and XeCT was measured before and after CES administration. Results demonstrated no global change in CBF, but a pronounced decrease in CBF locally in the brainstem and thalamus, suggesting a role for CES impacts on these brain regions in modulating pain response and anxiety. No assessments of vestibular or cutaneous sensation differences were reported.

CES Effects on Neurotransmitters and Hormones

Given the putative effects of CES on brain function, some studies have examined whether CES modulates salivary, urinary, cerebrospinal fluid, or blood levels of stress hormones (cortisol, alpha amylase, catecholamines, adrenocorticotropic hormone/ACTH), markers of inflammation and immune response (C-reactive protein, interleukin), and proteins reflecting the growth and survival of neurons (brain-derived neurotrophic factor/BDNF, nerve growth factor/NGF).

Some review articles claim evidence from animal models suggesting that CES can increase dopamine release in the basal ganglia in canines (Pozos et al., 1971), increase parasympathetic nervous system activation (Toriyama, 1975), or elevate β-endorphine levels in rat cerebrospinal fluid (Pert et al., 1981). However, these articles either describe a technique other than CES (e.g., electroacupuncture), or were not accessible for verification.

In humans, we found a total of five studies examining the effects of CES on neurotransmitter and/or hormone levels. In the first, 20 patients with alcoholism and affective disorders received either active (70–80 Hz, 4–7 mA) or control ($\leq$ 1 mA constant current) stimulation for 4 weeks using an undisclosed device with three electrodes (one at center of forehead, two behind bilateral mastoids), in a double-blind placebo-controlled study (Krupitsky et al., 1991). No assessments of vestibular or cutaneous sensations were reported. In comparing the groups post-treatment, the authors found increased blood levels of monoamine oxidase-B (MAO-B) and gamma aminobutyric acid (GABA), but no change in levels of serotonin, dopamine, or β-endorphins.

In a second study, 52 cancer patients received active (0.5 Hz, 0.1 mA) stimulation using the Alpha-Stim M device for 4 weeks (with bilateral earlobe electrodes, used for 60-min/day) (Yennurajalingam et al., 2018). There was no control condition, and no assessments of vestibular or cutaneous sensation were reported. When comparing baseline vs. after 4-weeks of CES, no differences were found in salivary measures of alpha amylase, cortisol, C-reactive protein, interleukin-1, or interleukin-6. These results suggest that CES treatment, at least with these methodological parameters, does not reliably modulate stress hormones or markers of inflammation and immune response.

In a third study, 36 obese females were randomly assigned to one of three groups: aerobic exercise only, aerobic exercise and CES, or control (Cho et al., 2016). Active CES was administered with the Alpha-Stim 100 device with bilateral earlobe electrodes for 20-min at 100 μA intensity and 0.5 Hz; the control group was no-contact without any sham procedure, and no measures of vestibular or cutaneous sensation were reported. While serum BDNF and NGF increased after all interventions, they did not differ between the exercise only vs. exercise and CES groups. Similar results were found with cortisol and ACTH, with no significant differences between those two groups.

In a fourth study, 15 participants (note: including the authors and colleagues) received active or sham CES for 20-min with one of two waveforms (1 mA at 15 Hz bipolar or monopolar) delivered by the LISS Cranial Stimulator with electrodes placed "transcranially" at undisclosed locations (Liss and Liss, 1996). The sham condition involved an inactive device, and no measures of vestibular or cutaneous sensation were reported. The authors found evidence that CES treatment increased ACTH, β-endorphine, and serotonin levels, and decreased

cortisol levels. It is important to note that in addition to the experimenters testing themselves, additional competing interest and methodological limitations were present, including the authors' proprietorship of a CES manufacturer, and the lack of blinding or random assignment.

Finally, a more recent and better controlled study examined 50 healthy women randomly assigned to active CES (0.5 Hz, 100 μA, 20-min/day for 8 weeks) or sham (device attached, but inactive) using the Alpha-Stim 100 device with bilateral earlobe electrodes, in an open label design (Roh and So, 2017). Blood samples were collected to assess cortisol, ACTH, BDNF, and NGF, and the profile of mood states (POMS) was administered to measure subjective anxiety. The authors found evidence that CES reduced anxiety ratings on the POMS, but did not significantly alter any blood levels of neurotrophic factors or hormones. These results were similar to those found by Lee et al. (2013), as discussed previously.

Note also that some other articles frequently cited in reviews as support for CES effects on neurotransmitters or hormones were limited in various ways; for example, using transcutaneous electrical stimulation of the legs or arms rather than cranial stimulation (Salar et al., 1981), or using a sham CES procedure that is active and a higher intensity than active CES used in other published papers (Gabis et al., 2003).

Overall, only one study suggested CES effects on neurotransmitter activity (Liss and Liss, 1996), but it suffers from high risk of bias and conflict of interest.

CES Effects on Parasympathetic Nervous System Activity

One model of CES action on the brain and behavior (Gilula, 2007) suggests very broad and diverse neuromodulatory effects across the limbic system, reticular-activating system, and thalamus and hypothalamus. This network of modulation predicts changes in sensory processing, regulation of mood states, altered arousal states, and even analgesia, perhaps through activation of the parasympathetic division of the autonomic nervous system.

Such diverse neuromodulatory effects may arise from stimulating afferent projections of peripheral nerves such as the trigeminal nerve, vagus nerve, facial nerve, and/or auditory nerve. Indeed, one proposed effect of CES is increased parasympathetic nervous system activation due to stimulation of the vagus nerve, with or without any cortical modulation (Zaghi et al., 2010; Howland, 2014; Asamoah et al., 2019). While this is a compelling possibility, there is no direct evidence for CES effects on relative parasympathetic/sympathetic activity.

METHODOLOGICAL LIMITATIONS OF CES RESEARCH

Through our review, we have identified several limitations to the extant literature examining CES effects on clinical and non-clinical participants. An overview of these limitations is below.

Potential Conflicts of Interest

Conflicts of interest (COI) occur when professional judgments or actions regarding a primary interest (e.g., sound research) are influenced by a secondary interest (e.g., financial gain) (Lo and Field, 2009). For example, a primary interest to conduct research in a sound, methodical, and honest manner may be unduly influenced by a secondary interest of financial gain, promotion, or recognition. Conflicts of interest can arise when an investigator is also a patient's physician, and/or when they stand to benefit from the success of an investigated drug or therapy.

There is a long history of potential COI in CES research. Nearly half of the published CES research we found appears to be funded by CES manufacturers or authored by the founders, owners, management, consultants, or board members of CES manufacturers or retailers. These authors stand to benefit from positive effects of CES systems, introducing the possibility that results are influenced (intentionally or unintentionally) by the potential COI. These COIs may cause authors to aggregate results in reviews or meta-analyses in a biased manner or misrepresent the design or results of primary research. Examples include omitting primary research that does not show positive benefits of CES, and citing primary research that did not examine CES specifically, examined animal models rather than humans, or was not published in a peer-reviewed journal (e.g., student poster presentations). As noted by other reviews on this topic, many reviews authored by individuals associated with CES device manufacturers "did not report any formalized search strategy, inclusion criteria or quality assessment and discussed a number of unpublished studies that remain unpublished at the time of the current review" (O'Connell et al., 2011). Together, it is our impression that a large portion of the existing CES literature has high potential for COI influencing data, theory, and application.

Risk of Bias in Clinical Trials

The Cochrane Collaboration has developed guidelines and software tools for assessing the risk of bias in clinical trials (Higgins et al., 2011; Sterne et al., 2019). Five domains of bias are identified: bias arising from the randomization process, bias due to deviations from intended interventions, bias due to missing outcome data, bias in measurement of the reported outcome, and bias in selection of the reported result. In our review of the CES literature, we found several examples of these potential biases. Many studies did not use (or did not report) random selection, had missing outcome data due to data loss or participant attrition, used non-standardized outcome measures with high subjectivity, and/or did not comprehensively report all results. For these reasons, reviews of CES effects conforming to the Cochrane guidelines are severely limited in the number of studies that can be included in a review.

For example, in a review and meta-analysis of non-invasive brain stimulation (NIBS) effects on chronic pain, applying the Cochrane guidelines resulted no single CES study being judged as having a low risk of bias (O'Connell et al., 2011). Even when including potentially biased studies, the meta-analysis demonstrated no significant advantage of CES relative to placebo. Similarly, a Cochrane review of CES for headache therapy revealed only one study that fit Cochrane criteria,

though baseline group differences limited results interpretation (Brønfort et al., 2014).

In a meta-analysis of CES effects on depression (and headache, insomnia, anxiety, and brain dysfunction) co-authored by the chairman of a CES device manufacturer (Kirsch and Gilula, 2007), we encountered major challenges interpreting results due to four primary weaknesses: first, the authors aggregated data from both open label and blinded studies; second, the analysis included studies showing very high comorbidity of disorders, including fibromyalgia, insomnia, anxiety, alcoholism, and attention disorders; third, no formal inclusion or exclusion criteria were provided for their literature search; fourth, the authors combined a highly heterogenous set of clinical ratings scales into a single percent improvement score, and did not compare it to a sham group (Kavirajan et al., 2014). Interestingly, the authors also selectively excluded a study that showed a negative influence of CES, suggesting that it was not valid due to improvement in the sham condition.

A similar monograph, including a review and informal meta-analysis, was published by an author affiliated with a different CES device manufacturer (Smith, 2007). This report suffers from similar weaknesses to the one cited above (Kavirajan et al., 2014). Interestingly, this author also offers [on a device manufacturers website; (Smith, 2013)] to analyze data and prepare manuscripts related to CES effects free of charge. While we did not find any statements disclosing Smith's relationships with CES device companies, we did find evidence that he was (and perhaps remains) the Director of Science for Electromedical Products International, Inc. (Kirsch and Smith, 2000).

Finally in a more recent, well-conducted review and meta-analysis of CES effects on depression using the Cochrane guidelines, not a single study passed the Cochrane criteria for inclusion in the meta-analysis (Kavirajan et al., 2014).

Sham Credibility and Blinding

Active CES commonly causes feelings of dizziness, cutaneous tingling or skin irritation at the electrode sites, or light-headedness (Bystritsky et al., 2008; Amr et al., 2013; Kirsch and Nichols, 2013; Wu et al., 2020). In fact, some studies use dizziness or light-headedness as a criterion for identifying the appropriate stimulation intensity for an individual participant; specifically, increasing stimulation intensity until the participant reports these symptoms, and then reducing intensity slightly from that threshold (Bystritsky et al., 2008; Kirsch and Chan, 2013). Of course, any sensory habituation achieved during this phase of a study could be changed or eliminated during subsequent phases or sessions. Most studies reviewed here, however, report a static AC frequency and intensity for active CES administration, rather than customizing CES intensity to individual tolerances; this is especially the case for non-clinical settings. In our own testing of the Alpha-Stim M, we found suprathreshold cutaneous sensation and vertigo at or above 100 μA (0.5 Hz). We are currently conducting a double-blind, cross-over study to assess cutaneous and vestibular sensations induced via CES at various intensities and frequencies. The possibility that users can readily identify when the device is active vs. inactive increases the likelihood that any attempts at participant blinding to CES conditions will be ineffective, particularly in cross-over designs (O'Connell et al., 2011).

Relatedly, in our review of the literature we found a highly mixed application of sham procedures. In most cases, the CES electrodes were attached to the participant, but the device was never turned on (Liss and Liss, 1996; Schroeder and Barr, 2001; Gense de Beaufort et al., 2012; Roh and So, 2017). In some other cases, there was either no control group (Feusner et al., 2012; Yennurajalingam et al., 2018), a no-contract control group (Cho et al., 2016), or the device was active but at a lower intensity than in the active CES condition (Krupitsky et al., 1991; Wu et al., 2020). The latter procedure is intended to produce mild cutaneous sensations in both groups, reducing the likelihood that participants can determine whether they are receiving active or sham CES. However, it should be noted that some low-intensity sham procedures use a higher intensity (e.g., 0.75 mA) stimulation than the active CES used in other studies (Gabis et al., 2003, 2009; O'Connell et al., 2011). In other words, these low-intensity sham procedures could be inducing similar effects to the active procedures used in other studies, reducing the likelihood of finding effects across treatment groups, and limiting comparability to other studies.

Parameter Heterogeneity

Across published studies, CES is administered using a variety of parameters, including the number, type, and placement of electrodes, the timing and duration of stimulation, and the amplitude, intensity, and dynamics of AC waveforms. Stimulation electrodes are typically placed on the temples, mastoids, and/or ear lobes, and vary in size between small ear lobe clips and large saline-soaked sponges (Zaghi et al., 2010; Datta et al., 2013). As reviewed by Zaghi, stimulation parameters typically vary in duration from between 5 and 30 min, and intensity between 0.1 and 4.0 mA (Zaghi et al., 2010). The timing of CES administration relative to outcome measures, and the frequency and duration of stimulation also vary dramatically across studies.

Alternating current dynamically alternates polarity over time, typically represented by sinusoidal waveform. With CES, device manufacturers typically modify the amplitude, frequency, and shape of the waveform. In terms of amplitude, we found studies using amplitudes as low as 100 μA (Lande and Gragnani, 2013; Wagenseil et al., 2018) and as high as 4 mA (Mischoulon et al., 2015), with one outlying study reporting the use of a novel Limoge waveform at 49 mA (Gense de Beaufort et al., 2012). For frequency, we found studies using AC frequencies reported as low as 0.5 Hz (Winick, 1999; Koleoso et al., 2013; Cho et al., 2016) and as high as 15,000 Hz (Southworth, 1999; McClure et al., 2015; Mischoulon et al., 2015). The shape of the waveforms also vary dramatically across studies and devices, including symmetrical or asymmetrical biphasic waveforms, unmodified and modified square waveforms, and monophasic and biphasic waveforms (O'Connell et al., 2011; Bikson et al., 2019).

The heterogeneity of stimulation methods, including electrode types and placement, stimulation timing and parameters, all influence the reproducibility, comparability, and generalizability of research outcomes in CES, making it

challenging to derive insights into its suitability for application in clinical or non-clinical domains. These issues are compounded by the fact that many of the devices used in past research are obsolete, antiquated, and otherwise unavailable for scientists to conduct replication attempts.

FUTURE RESEARCH DIRECTIONS

We propose two primary directions for continuing CES research, particularly regarding non-clinical applications. First is basic research characterizing CES effects on central and peripheral nervous system activity and behavior, with potential application to modulating stress responses and possibly mitigating adverse performance effects under conditions of stress. Second is more attention to methodological considerations in the design, analysis, and reporting of CES research. We consider these two topics, in turn.

Threats to the physical or social self, uncertainty and novelty, and the perceived uncontrollability of situations all produce transient stress states (Mason, 1968). Adaptability under conditions of stress and uncertainty is critical to sustaining cognitive performance, and maladaptive responses under these circumstances give rise to long-term negative repercussions for psychological well-being (Grupe and Nitschke, 2013). Acute stress causes reliable physiological, affective, and cognitive responses. Physiologically, stress activates the sympathetic nervous system and causes a rapid release of catecholamines, namely epinephrine and norepinephrine. A second, slower response is activation of the hypothalamic-pituitary-adrenal (HPA) axis, resulting in the release of corticotropin-releasing hormone (CRH), ACTH, and cortisol. Activating these two stress systems produces a cascade of hormonal and neural effects throughout the central and peripheral nervous systems, with downstream effects on perception, affective states, and cognition (Gagnon and Wagner, 2016).

Stress is often seen as adaptive (Charmandari et al., 2005; Grupe and Nitschke, 2013) and can help direct selective attention and increase vigilance to sensory input (Eysenck et al., 2007; Pessoa, 2009). However, stress can also induce impairments in tasks involving several brain structures sensitive to the presence of catecholamines and glucocorticoids, including the prefrontal cortex, hippocampus, striatum, and amygdala (Arnsten, 1998; Hermans et al., 2014; Kim et al., 2015). These brain regions play diverse roles in our ability to attend to, process, understand, and use information in an adaptive manner. Indeed acute stress can degrade performance on working memory tasks (Luethi et al., 2008), disrupt visuomotor task performance and top-down attentional control (Vedhara et al., 2000; Vine et al., 2016), impair memory encoding and/or retrieval (Gagnon and Wagner, 2016), and impair cognitive control and flexible, goal-directed thinking in general (Eysenck et al., 2007).

Given the diverse and reliable effects of acute stress on the brain, cognition, and behavior, candidate technologies or methodologies to temporarily reduce the intensity or duration of the stress response are of interest to the defense science community. Candidate technologies could be used during training, in real-time during stressful occupational tasks, or to help facilitate recovery post-stressor.

CES is one candidate technology that could hold potential in reducing the downstream hormonal, neural, and behavioral effects of stress by modulating central and peripheral nervous system activity. Specifically, a transient increase in relative parasympathetic activation (i.e., altering the sympathetic/parasympathetic balance), whether through cranial (vagus) nerve stimulation or *n*th order neuromodulatory effects of CES, would carry effects for several brain regions, including the thalamus, hypothalamus, amygdala, locus coeruleus, cerebellum, orbitofrontal cortex, and medulla (Chae et al., 2003). A reduction in sympathetic drive would increase relative parasympathetic dominance (Clancy et al., 2014), possibly leading to reductions in inflammatory responses (Borovikova et al., 2000; Breit et al., 2018), and altering levels of hormones, peptides and neurotransmitters such as norepinephrine, serotonin, and cortisol. Further downstream effects of vagus stimulation would include alteration of activity in at least the heart, respiratory system, stomach (including small and large intestine), liver, and pancreas (Breit et al., 2018). These possibilities point to future basic research directions with CES.

We also make five primary methodological recommendations for continuing CES research. First, we suggest using larger sample sizes to increase power and the likelihood of identifying any true effects that may exist. Many CES studies have very small sample sizes that lower power and increase the likelihood of Type I errors; small sample sizes and are unlikely to identify a true effect, hold low predictive value, and any identified effects are likely inflated (Button et al., 2013). To justify small sample sizes, some papers cite existing research also with small sample sizes but showing strong effect sizes; however, to better estimate sample size needs, authors may find value in using meta-analytic estimates of effect size, rather than single effect sizes found in studies that may also suffer from methodological challenges.

Second, assuming sample size criteria are adequately defined and met, scientists, institutions, and publishers should assign equal value to manuscripts reporting null or unexpected results (Schooler, 2011; Martin and Clarke, 2017). Publication bias toward positive findings occurs not only in original science, but also in replication attempts and contaminates theory development and the systematic aggregation of results via meta-analysis (Francis, 2012). Third, registered reports are an effective tool for reducing publication bias and increasing the transparency and reproducibility of science (Schooler, 2011). In these cases, authors propose their complete methodology and analysis plan and receive in-principle acceptance for the manuscript, regardless of whether data ultimately support their hypotheses.

Fourth, parameter standardization across studies and laboratories will help researchers and clinicians derive more reliable understandings of how CES electrode placement, stimulation frequency, waveform, intensity and duration, all influence clinical and human performance outcomes with CES. Standardizing parameter selection and manipulation will inform the most reliable and robust ways to administer CES, and also facilitate predictive modeling efforts in this

regard. Finally, while it may be appealing to reduce cost or increase research efficiencies by partnering with individuals or corporations with conflicting interests, ultimately these relationships can limit progress in research and clinical practice. Independently supported research using sound methodologies and analytical and reporting techniques will only benefit the research community and populations interested in using these tools to reduce symptoms of clinical disorders.

CONCLUSIONS

CES was developed as a tool for treating the symptoms of clinical disorders such as insomnia, anxiety, and depression. The FDA differently regulates CES devices based on their intent, with relatively stringent controls (Class III) for the treatment of depression, given a lack of data demonstrating that any benefits outweigh potential risks. Studies examining CES effectiveness in the treatment of these disorders are equivocal, and there is generally a lack of compelling evidence from well-designed studies. Notably, however, no single study showed a worsening of insomnia, anxiety, or depression symptoms during or following CES treatment. It is worth considering that any placebo effects that may be elicited by CES due to participant expectations, experimenter bias, and/or cutaneous or vestibular perception may be sufficient enough to induce behavioral and physiological effects (Enserink, 1999; Dräger et al., 2004).

Very few studies have examined CES for application to healthy, neurotypical populations. In studies examining acute stress responses in healthy participants, CES appears to reduce subjective feelings of anxiety, but these are not necessarily accompanied by any changes in endocrine responses. In two human performance-oriented studies, CES produced faster and more accurate responding on certain CPT measures (Southworth, 1999), and increased motor force output during a weightlifting task (Cupriks et al., 2016). The former outcome warrants replication and extension, whereas the latter study has considerable methodological challenges that limit interpretation. Reproducible, reliable (within and across participants), and robust demonstrations of CES effects on nervous system activity and behavior are necessary before adopting CES for use in occupational contexts, including training, job performance, and recovery contexts (Bostrom and Sandberg, 2009; Agar, 2013; Chatterjee, 2013; Colzato, 2018; Dessy et al., 2018; Blacker et al., 2019; Feltman et al., 2019; Brunyé et al., 2020).

Several studies have attempted to elucidate the mechanisms underlying CES effects on brain and behavior. Among these are studies examining: (1) computational modeling of current propagation through the skin, skull, cerebrospinal fluid, and brain, (2) CES effects on electrical brain activity and hemodynamics, and (3) CES effects on endocrine and neurotransmitter systems. In general, computational modeling efforts predict CES currents effectively penetrating the scalp and scull and reaching cortical and subcortical brain regions, however at very low current intensities at target. Brain monitoring studies have shown inconsistent support for changes in frequency band activity using EEG, but preliminary support for changes in default mode network activity and reduced activity in brain stem and limbic systems. Finally, studies examining CES effects on neurotransmitters and hormones are very mixed, with most finding no evidence that CES modulates markers of inflammation, immune response, or stress hormones.

Most existing CES research suffers from considerable methodological challenges. The primary ones identified were potential conflicts of interest, risk of bias, sham credibility and blinding, and the heterogeneity of CES parameters used (Kavirajan et al., 2014; Shekelle et al., 2018a). These limitations make it difficult to derive consistent or compelling insights from the extant literature, tempering our enthusiasm for CES and its potential to alter brain function, behavior, or endocrine responses reliably or robustly, in clinical or non-clinical settings.

The lack of compelling evidence also motivates well-designed and relatively high-powered experiments to assess how CES might modulate the physiological, affective, and cognitive responses to stress. Indeed, the challenges faced by CES research are similar to those faced by other contentious research topics in psychology and neuroscience (Earp and Trafimow, 2015; Maxwell et al., 2015), including other domains of neurostimulation (Koenigs et al., 2009; Brem et al., 2014; Horvath et al., 2014; Vannorsdall et al., 2016; Brunyé et al., 2018), and would likely benefit from similar methodological and reporting improvements. Continuing transparency and methodological improvements with CES will allow the scientific community to develop more informed and nuanced understandings of how CES can be used to modulate nervous system activity and behavior, with potentially expanded applications to both clinical and non-clinical settings.

AUTHOR CONTRIBUTIONS

This report was drafted by TB. Revised and expanded upon by JP, TW, and EH. All authors contributed to the article and approved the submitted version.

FUNDING

This report was funded by the Combat Capabilities Development Command Soldier Center (CCDC SC) under the Measuring and Advancing Soldier Tactical Readiness and Effectiveness (MASTR-E) program.

REFERENCES

Agar, N. (2013). *Truly Human Enhancement: A Philosophical Defense of Limits*. MIT Press. doi: 10.7551/mitpress/9780262026635.001.0001

Amr, M., El-Wasify, M., Elmaadawi, A. Z., Roberts, R. J., and El-Mallakh, R. S. (2013). Cranial electrotherapy stimulation for the treatment of chronically symptomatic bipolar patients. *J. ECT* 29, e31–32. doi: 10.1097/YCT.0b013e31828a344d

Arnsten, A. F. T. (1998). Catecholamine modulation of prefrontal cortical cognitive function. *Trends Cogn. Sci.* 2, 436–447. doi: 10.1016/S1364-6613(98)01240-6

Asamoah, B., Khatoun, A., and Mc Laughlin, M. (2019). TACS motor system effects can be caused by transcutaneous stimulation of peripheral nerves. *Nat. Commun.* 10:266. doi: 10.1038/s41467-018-08183-w

Aseem, A., and Hussain, M. E. (2019). Impact of cranial electrostimulation on sleep: a systematic review. *Sleep Vigilance* 3, 101–112. doi: 10.1007/s41782-019-00075-3

Barclay, T. H., and Barclay, R. D. (2014). A clinical trial of cranial electrotherapy stimulation for anxiety and comorbid depression. *J. Affect. Disord.* 164, 171–177. doi: 10.1016/j.jad.2014.04.029

Bijsterbosch, J. D., Barker, A. T., Lee, K. H., and Woodruff, P. W. R. (2012). Where does transcranial magnetic stimulation (TMS) stimulate? Modelling of induced field maps for some common cortical and cerebellar targets. *Med. Biol. Eng. Comput.* 50, 671–681. doi: 10.1007/s11517-012-0922-8

Bikson, M., Esmaeilpour, Z., Adair, D., Kronberg, G., Tyler, W. J., Antal, A., et al. (2019). Transcranial electrical stimulation nomenclature. *Brain Stimul.* 12, 1349–1366. doi: 10.1016/j.brs.2019.07.010

Black, L., Cannon, R., Hanslmayr, S., Kennerly, R., Rothove, J., Sherlin, L., et al. (2004). Student Scholarship Presentation Abstracts. *J. Neurother.* 8, 107–118. doi: 10.1300/J184v08n02_11

Blacker, K. J., Hamilton, J., Roush, G., Pettijohn, K. A., and Biggs, A. T. (2019). Cognitive training for military application: a review of the literature and practical guide. *J. Cogn. Enhanc.* 3, 30–51. doi: 10.1007/s41465-018-0076-1

Borovikova, L. V., Ivanova, S., Zhang, M., Yang, H., Botchkina, G. I., Watkins, L. R., et al. (2000). Vagus nerve stimulation attenuates the systemic inflammatory response to endotoxin. *Nature* 405, 458–462. doi: 10.1038/35013070

Bostrom, N., and Sandberg, A. (2009). Cognitive enhancement: Methods, ethics, regulatory challenges. *Sci. Eng. Ethics* 15, 311–341. doi: 10.1007/s11948-009-9142-5

Bracciano, A. G., Chang, W. P., Kokesh, S., Martinez, A., Meier, M., and Moore, K. (2012). Cranial electrotherapy stimulation in the treatment of posttraumatic stress disorder: a pilot study of two military veterans. *J. Neurother.* 16, 60–69. doi: 10.1080/10874208.2012.650100

Breit, S., Kupferberg, A., Rogler, G., and Hasler, G. (2018). Vagus nerve as modulator of the brain–gut axis in psychiatric and inflammatory disorders. *Front. Psychiatry* 9:44. doi: 10.3389/fpsyt.2018.00044

Brem, A. K., Fried, P. J., Horvath, J. C., Robertson, E. M., and Pascual-Leone, A. (2014). Is neuroenhancement by noninvasive brain stimulation a net zero-sum proposition? *Neuroimage* 85, 1058–1068. doi: 10.1016/j.neuroimage.2013.07.038

Brønfort, G., Haas, M., Evans, R. L., Goldsmith, C. H., Assendelft, W. J., and Bouter, L. M. (2014). Non-invasive physical treatments for chronic/recurrent headache. *Cochrane Database Syst. Rev.* 2014:CD001878. doi: 10.1002/14651858.CD001878.pub3

Brunyé, T. T., Brou, R., Doty, T. J., Gregory, F. D., Hussey, E. K., Lieberman, H. R., et al. (2020). A Review of US army research contributing to cognitive enhancement in military contexts. *J. Cogn. Enhanc.* 4, 453–468. doi: 10.1007/s41465-020-00167-3

Brunyé, T. T., Smith, A. M., Horner, C. B., and Thomas, A. K. (2018). Verbal long-term memory is enhanced by retrieval practice but impaired by prefrontal direct current stimulation. *Brain Cogn.* 128, 80–88. doi: 10.1016/j.bandc.2018.09.008

Button, K. S., Ioannidis, J. P. A., Mokrysz, C., Nosek, B. A., Flint, J., Robinson, E. S. J., et al. (2013). Power failure: why small sample size undermines the reliability of neuroscience. *Nat. Rev. Neurosci.* 14, 365–376. doi: 10.1038/nrn3475

Bystritsky, A., Kerwin, L., and Feusner, J. (2008). A pilot study of cranial electrotherapy stimulation for generalized anxiety disorder. *J. Clin. Psychiatry* 69, 412–417. doi: 10.4088/JCP.v69n0311

Campana, G., Cowey, A., and Walsh, V. (2002). Priming of motion direction and area V5/MT: a test of perceptual memory. *Cerebral Cortex* 12, 663–669. doi: 10.1093/cercor/12.6.663

Chae, J. H., Nahas, Z., Lomarev, M., Denslow, S., Lorberbaum, J. P., Bohning, D. E., et al. (2003). A review of functional neuroimaging studies of vagus nerve stimulation (VNS). *J. Psychiatr. Res.* 37, 443–455. doi: 10.1016/S0022-3956(03)00074-8

Charmandari, E., Tsigos, C., and Chrousos, G. (2005). Endocrinology of the stress response. *Annu. Rev. Physiol.* 67, 259–284. doi: 10.1146/annurev.physiol.67.040403.120816

Chatterjee, A. (2013). "Chapter 27—The ethics of neuroenhancement," in *Handbook of Clinical Neurology,* eds J. L. Bernat and H. R. Beresford (New York, NY: Elsevier), 323–334. doi: 10.1016/B978-0-444-53501-6.00027-5

Cho, S. Y., So, W. Y., and Roh, H. T. (2016). Effects of aerobic exercise training and cranial electrotherapy stimulation on the stress-related hormone, the neurotrophic factor, and mood states in obese middle-aged women: a pilot clinical trial. *Salud Mental* 39, 249–256. doi: 10.17711/SM.0185-3325.2016.029

Clancy, J. A., Mary, D. A., Witte, K. K., Greenwood, J. P., Deuchars, S. A., and Deuchars, J. (2014). Non-invasive vagus nerve stimulation in healthy humans reduces sympathetic nerve activity. *Brain Stimul.* 7, 871–877. doi: 10.1016/j.brs.2014.07.031

Colzato, L. S. (2018). Responsible cognitive enhancement: neuroethical considerations. *J. Cogn. Enhanc.* 2, 331–334. doi: 10.1007/s41465-018-0090-3

Cupriks, L., Vimbsons, V., Cuprika, A., and Rudzitis, A. (2016). Cranial electrical stimulation in fitness with weightlifting tools. *LASE J. Sport Sci.* 7, 21–32. doi: 10.1515/ljss-2016-0010

Datta, A., Dmochowski, J. P., Guleyupoglu, B., Bikson, M., and Fregni, F. (2013). Cranial electrotherapy stimulation and transcranial pulsed current stimulation: a computer based high-resolution modeling study. *Neuroimage* 65, 280–287. doi: 10.1016/j.neuroimage.2012.09.062

Dessy, E., Van Puyvelde, M., Mairesse, O., Neyt, X., and Pattyn, N. (2018). Cognitive performance enhancement: do biofeedback and neurofeedback work? *J. Cogn. Enhanc.* 2, 12–42. doi: 10.1007/s41465-017-0039-y

Dräger, B., Breitenstein, C., Helmke, U., Kamping, S., and Knecht, S. (2004). Specific and nonspecific effects of transcranial magnetic stimulation on picture-word verification. *Eur. J. Neurosci.* 20, 1681–1687. doi: 10.1111/j.1460-9568.2004.03623.x

Earp, B. D., and Trafimow, D. (2015). Replication, falsification, and the crisis of confidence in social psychology. *Front. Psychol.* 6:21. doi: 10.3389/fpsyg.2015.00621

Edelmuth, R. C., Nitsche, M. A., Battistella, L., and Fregni, F. (2010). Why do some promising brain-stimulation devices fail the next steps of clinical development? *Exp. Rev. Med. Dev.* 7, 67–97. doi: 10.1586/erd.09.64

Enserink, M. (1999). Can the placebo be the cure? *Science* 284, 238–240. doi: 10.1126/science.284.5412.238

Eysenck, M. W., Derakshan, N., Santos, R., and Calvo, M. G. (2007). Anxiety and cognitive performance: attentional control theory. *Emotion* 7, 336–353. doi: 10.1037/1528-3542.7.2.336

Feighner, J. P., Brown, S. L., and Olivier, J. E. (1973). Electrosleep therapy: a controlled double blind study. *J. Nerv. Ment. Dis.* 157, 121–128. doi: 10.1097/00005053-197308000-00004

Feltman, K. A., Hayes, A. M., Bernhardt, K. A., Nwala, E., and Kelley, A. M. (2019). Viability of tDCS in military environments for performance enhancement: a systematic review. *Mil. Med.* 185, e53–e60. doi: 10.1093/milmed/usz189

Ferdjallah, M., Bostick, F. X., and Barr, R. E. (1996). Potential and current density distributions of cranial electrotherapy stimulation (CES) in a four-concentric-spheres model. *IEEE Trans. Biomed. Eng.* 43, 939–943. doi: 10.1109/10.532128

Feshchenko, V. A., Reinsel, R. A., and Veselis, R. A. (2001). Multiplicity of the alpha rhythm in normal humans. *J. Clin. Neurophysiol.* 18, 331–344. doi: 10.1097/00004691-200107000-00005

Feusner, J. D., Madsen, S., Moody, T. D., Bohon, C., Hembacher, E., Bookheimer, S. Y., et al. (2012). Effects of cranial electrotherapy stimulation on resting state brain activity. *Brain Behav.* 2, 211–220. doi: 10.1002/brb3.45

Flodin, P., Martinsen, S., Mannerkorpi, K., Löfgren, M., Bileviciute-Ljungar, I., Kosek, E., et al. (2015). Normalization of aberrant resting state functional connectivity in fibromyalgia patients following a three month physical exercise therapy. *Neuroimage Clin.* 9, 134–139. doi: 10.1016/j.nicl.2015.08.004

Fox, M. D., and Greicius, M. (2010). Clinical applications of resting state functional connectivity. *Front. Syst. Neurosci.* 4:19. doi: 10.3389/fnsys.2010.00019

Francis, G. (2012). Publication bias and the failure of replication in experimental psychology. *Psychonom. Bull. Rev.* 19, 975–991. doi: 10.3758/s13423-012-0322-y

Gabis, L., Shklar, B., Baruch, Y. K., Raz, R., Gabis, E., and Geva, D. (2009). Pain reduction using transcranial electrostimulation: A double

blind "active placebo" controlled trial. *J. Rehabil. Med.* 41, 256–261. doi: 10.2340/16501977-0315

Gabis, L., Shklar, B., and Geva, D. (2003). Immediate influence of transcranial electrostimulation on pain and β-Endorphin blood levels: an active placebo-controlled study. *Am. J. Phys. Med. Rehabil.* 82, 81–85. doi: 10.1097/00002060-200302000-00001

Gagnon, S. A., and Wagner, A. D. (2016). Acute stress and episodic memory retrieval: neurobiological mechanisms and behavioral consequences. *Ann. N. Y. Acad. Sci.* 1369, 55–75. doi: 10.1111/nyas.12996

Gense de Beaufort, D., Sesay, M., Stinus, L., Thiebaut, R., Auriacombe, M., and Dousset, V. (2012). Cerebral blood flow modulation by transcutaneous cranial electrical stimulation with Limoge's current. *J. Neuroradiol.* 39, 167–175. doi: 10.1016/j.neurad.2011.06.001

Gilula, M. F. (2007). Cranial electrotherapy stimulation and fibromyalgia. *Expert Rev Med Devices* 4, 489–495. doi: 10.1586/17434440.4.4.489

Greicius, M. D., Srivastava, G., Reiss, A. L., and Menon, V. (2004). Default-mode network activity distinguishes Alzheimer's disease from healthy aging: evidence from functional MRI. *Proc. Natl. Acad. Sci. U.S.A.* 101, 4637–4642. doi: 10.1073/pnas.0308627101

Grupe, D. W., and Nitschke, J. B. (2013). Uncertainty and anticipation in anxiety: an integrated neurobiological and psychological perspective. *Nat. Rev. Neurosci.* 14, 488–501. doi: 10.1038/nrn3524

Guleyupoglu, B., Schestatsky, P., Edwards, D., Fregni, F., and Bikson, M. (2013). Classification of methods in transcranial electrical stimulation (tES) and evolving strategy from historical approaches to contemporary innovations. *J. Neurosci. Methods* 219, 297–311. doi: 10.1016/j.jneumeth.2013.07.016

Gunther, M., and Phillips, K. D. (2010). Cranial electrotherapy stimulation for the treatment of depression. *J. Psychosoc. Nurs. Ment. Health Serv.* 48, 37–42. doi: 10.3928/02793695-20100701-01

Hamilton, J. P., Furman, D. J., Chang, C., Thomason, M. E., Dennis, E., and Gotlib, I. H. (2011). Default-mode and task-positive network activity in major depressive disorder: implications for adaptive and maladaptive rumination. *Biol. Psychiatry* 70, 327–333. doi: 10.1016/j.biopsych.2011.02.003

Hampson, M., Driesen, N. R., Skudlarski, P., Gore, J. C., and Constable, R. T. (2006). Brain connectivity related to working memory performance. *J. Neurosci.* 26, 13338–13343. doi: 10.1523/JNEUROSCI.3408-06.2006

Harmony, T., Fernández, T., Silva, J., Bernal, J., Díaz-Comas, L., Reyes, A., et al. (1996). EEG delta activity: an indicator of attention to internal processing during performance of mental tasks. *Int. J. Psychophysiol.* 24, 161–171. doi: 10.1016/S0167-8760(96)00053-0

Hermans, E. J., Henckens, M. J. A. G., Joëls, M., and Fernández, G. (2014). Dynamic adaptation of large-scale brain networks in response to acute stressors. *Trends Neurosci.* 37, 304–314. doi: 10.1016/j.tins.2014.03.006

Higgins, J. P. T., Altman, D. G., Gotzsche, P. C., Juni, P., Moher, D., Oxman, A. D., et al. (2011). The cochrane collaboration's tool for assessing risk of bias in randomised trials. *BMJ* 343:d5928. doi: 10.1136/bmj.d5928

Horvath, J. C., Carter, O., and Forte, J. D. (2014). Transcranial direct current stimulation: five important issues we aren't discussing (but probably should be). *Front. Syst. Neurosci.* 8:2. doi: 10.3389/fnsys.2014.00002

Howland, R. H. (2014). Vagus nerve stimulation. *Current Behav. Neurosci. Rep.* 1, 64–73. doi: 10.1007/s40473-014-0010-5

Isotani, T., Tanaka, H., Lehmann, D., Pascual-Marqui, R. D., Kochi, K., Saito, N., et al. (2001). Source localization of EEG activity during hypnotically induced anxiety and relaxation. *Int. J. Psychophysiol.* 41, 143–153. doi: 10.1016/S0167-8760(00)00197-5

Jacobs, G. D., Benson, H., and Friedman, R. (1996). Topographic EEG mapping of the relaxation response. *Biofeedb. Self Regul.* 21, 121–129. doi: 10.1007/BF02284691

Kavirajan, H. C., Lueck, K., and Chuang, K. (2014). Alternating current cranial electrotherapy stimulation (CES) for depression. *Cochrane Database Syst. Rev.* 8:CD010521. doi: 10.1002/14651858.CD010521.pub2

Kim, E. J., Pellman, B., and Kim, J. J. (2015). Stress effects on the hippocampus: a critical review. *Learn. Mem.* 22, 411–416. doi: 10.1101/lm.037291.114

King, A. P., Block, S. R., Sripada, R. K., Rauch, S., Giardino, N., Favorite, T., et al. (2016). Altered default mode network (dmn) resting state functional connectivity following a mindfulness-based exposure therapy for posttraumatic stress disorder (ptsd) in combat veterans of Afghanistan and Iraq. *Depress. Anxiety* 33, 289–299. doi: 10.1002/da.22481

Kirsch, D. L., and Chan, S. C. (2013). *Microcurrent and Cranial Electrotherapy Stimulator for Control of Anxiety, Insomnia, Depression and Pain* (United States Patent and Trademark Office Patent No. US8612 008B2).

Kirsch, D. L., and Gilula, M. F. (2007). CES in the treatment of depression, part 2. *Pract. Pain Manag.* 6, 32–40.

Kirsch, D. L., and Nichols, F. (2013). Cranial electrotherapy stimulation for treatment of anxiety, depression, and insomnia. *Psychiatr. Clin. North Am.* 36, 169–176. doi: 10.1016/j.psc.2013.01.006

Kirsch, D. L., Price, L. R., Nichols, F., Marksberry, J. A., and Platoni, K. T. (2014). Military service member and veteran self reports of efficacy of cranial electrotherapy stimulation for anxiety, posttraumatic stress disorder, insomnia, and depression. *US. Army Med. Dep. J.* 2014:46–54.

Kirsch, D. L., and Smith, R. B. (2000). The use of cranial electrotherapy stimulation in the management of chronic pain: a review. *NeuroRehabilitation* 14, 85–94. doi: 10.3233/NRE-2000-14204

Klimesch, W. (1999). EEG alpha and theta oscillations reflect cognitive and memory performance: a review and analysis. *Brain Res. Rev.* 29, 169–195. doi: 10.1016/S0165-0173(98)00056-3

Knyazev, G. G. (2012). EEG delta oscillations as a correlate of basic homeostatic and motivational processes. *Neurosci. Biobehav. Rev.* 36, 677–695. doi: 10.1016/j.neubiorev.2011.10.002

Koenigs, M., Ukueberuwa, D., Campion, P., Grafman, J., and Wassermann, E. (2009). Bilateral frontal transcranial direct current stimulation: failure to replicate classic findings in healthy subjects. *Clin. Neurophysiol.* 120, 80–84. doi: 10.1016/j.clinph.2008.10.010

Koleoso, O. N., Osinowo, H. O., and Akhigbe, K. O. (2013). The role of relaxation therapy and cranial electrotherapy stimulation in the management of dental anxiety in Nigeria. *IOSR J. Dent. Med. Sci.* 10, 51–57. doi: 10.9790/0853-1045157

Krupitsky, E. M., Burakov, A. M., Karandashova, G. F., Katsnelson Ja, S., Lebedev, V. P., Grinenko A. Ja., et al. (1991). The administration of transcranial electric treatment for affective disturbances therapy in alcoholic patients. *Drug Alcohol Depend.* 27, 1–6. doi: 10.1016/0376-8716(91)90080-I

Lande, R. G., and Gragnani, C. (2013). Efficacy of cranial electric stimulation for the treatment of insomnia: a randomized pilot study. *Complement. Ther. Med.* 21, 8–13. doi: 10.1016/j.ctim.2012.11.007

Lee, J., Lee, H., and Park, W. (2019). Effects of cranial electrotherapy stimulation on electrocephalogram. *J. Int. Acad. Phys. Ther. Res.* 10, 1687–1694. doi: 10.20540/JIAPTR.2019.10.1.1687

Lee, S. H., Kim, W. Y., Lee, C. H., Min, T. J., Lee, Y. S., Kim, J. H., et al. (2013). Effects of cranial electrotherapy stimulation on preoperative anxiety, pain and endocrine response. *J. Int. Med. Res.* 41, 1788–1795. doi: 10.1177/0300060513500749

Liss, S., and Liss, B. (1996). Physiological and therapeutic effects of high frequency electrical pulses. *Integr. Physiol. Behav. Sci.* 31, 88–95. doi: 10.1007/BF026 99781

Lo, B., and Field, M. J. (2009). *Conflict of Interest in Medical Research, Education, and Practice*. Washington, DC: National Academies Press.

Luethi, M., Meier, B., and Sandi, C. (2008). Stress effects on working memory, explicit memory, and implicit memory for neutral and emotional stimuli in healthy men. *Front. Behav. Neurosci.* 2:5. doi: 10.3389/neuro.08.005.2008

Martin, G. N., and Clarke, R. M. (2017). Are psychology journals anti-replication? A snapshot of editorial practices. *Front. Psychol.* 8:523. doi: 10.3389/fpsyg.2017.00523

Mason, J. W. (1968). A review of psychoendocrine research on the pituitary-adrenal cortical system. *Psychosom. Med.* 30, 576–607. doi: 10.1097/00006842-196809000-00020

Maxwell, S. E., Lau, M. Y., and Howard, G. S. (2015). Is psychology suffering from a replication crisis? What does "failure to replicate" really mean? *Am. Psychol.* 70, 487–498. doi: 10.1037/a0039400

McClure, D., Greenman, S. C., Koppolu, S. S., Varvara, M., Yaseen, Z. S., and Galynker, I. I. (2015). A pilot study of safety and efficacy of cranial electrotherapy stimulation in treatment of bipolar II depression. *J. Nerv. Ment. Dis.* 203, 827–835. doi: 10.1097/NMD.0000000000000378

Mischoulon, D., De Jong, M. F., Vitolo, O. V., Cusin, C., Dording, C. M., Yeung, A. S., et al. (2015). Efficacy and safety of a form of cranial electrical stimulation (CES) as an add-on intervention for treatment-resistant major depressive

disorder: a three week double blind pilot study. *J. Psychiatr. Res.* 70, 98–105. doi: 10.1016/j.jpsychires.2015.08.016

Morriss, R., and Price, L. (2020). Differential effects of cranial electrotherapy stimulation on changes in anxiety and depression symptoms over time in patients with generalized anxiety disorder. *J. Affect. Disord.* 277, 785–788. doi: 10.1016/j.jad.2020.09.006

Morriss, R., Xydopoulos, G., Craven, M., Price, L., and Fordham, R. (2019). Clinical effectiveness and cost minimisation model of Alpha-Stim cranial electrotherapy stimulation in treatment seeking patients with moderate to severe generalised anxiety disorder. *J. Affect. Disord.* 253, 426–437. doi: 10.1016/j.jad.2019.04.020

Moussa, M. N., Steen, M. R., Laurienti, P. J., and Hayasaka, S. (2012). Consistency of Network Modules in Resting-State fMRI Connectome Data. *PLoS ONE* 7:e44428. doi: 10.1371/journal.pone.0044428

National Research Council (1974). *An Evaluation of Electroanesthesia and Electrosleep: Report of the Ad Hoc Committee on Electrical Stimulation of the Brain*. Report PB-241 305. Springfield, VA: National Technical Information Service.

Niedermeyer, E. (1997). Alpha rhythms as physiological and abnormal phenomena. *Int. J. Psychophysiol.* 26, 31–49. doi: 10.1016/S0167-8760(97)00754-X

Niedermeyer, E., and da Silva, F. H. L. (2005). *Electroencephalography: Basic Principles, Clinical Applications, and Related Fields*. Philadelphia, PA: Lippincott Williams & Wilkins.

O'Connell, N. E., Wand, B. M., Marston, L., Spencer, S., and Desouza, L. H. (2011). Non-invasive brain stimulation techniques for chronic pain. A report of a Cochrane systematic review and meta-analysis. *Eur. J. Phys. Rehabil. Med.* 47, 309–326.

Oken, B. S., and Salinsky, M. (1992). Alertness and attention: basic science and electrophysiologic correlates. *J. Clin. Neurophysiol.* 9, 480–494. doi: 10.1097/00004691-199210000-00003

Peña, C., Bowsher, K., Costello, A., De Luca, R., Doll, S., Li, K., et al. (2007). An overview of FDA medical device regulation as it relates to deep brain stimulation devices. *IEEE Trans. Neural Syst. Rehabil. Eng.* 15, 421–424. doi: 10.1109/TNSRE.2007.903973

Pert, A., Dionne, R., Ng, L., Bragin, E., Moody, T. W., and Pert, C. B. (1981). Alterations in rat central nervous system endorphins following transauricular electroacupuncture. *Brain Res.* 224, 83–93. doi: 10.1016/0006-8993(81)91118-5

Pessoa, L. (2009). How do emotion and motivation direct executive control? *Trends Cogn. Sci.* 13, 160–166. doi: 10.1016/j.tics.2009.01.006

Pozos, R. S., Richardson, A. W., and Kaplan, H. M. (1971). "Electroanesthesia: a proposed physiologic mechanism," in *Neuroelectric Research*, eds D. V. Reynolds and A. Sjodberg (Springfield, IL: Charles Thomas), 110–113.

Qiao, J., Weng, S., Wang, P., Long, J., and Wang, Z. (2015). Normalization of intrinsic neural circuits governing tourette's syndrome using cranial electrotherapy stimulation. *IEEE Trans. Biomed. Eng.* 62, 1272–1280. doi: 10.1109/TBME.2014.2385151

Raichle, M. E. (1998). Behind the scenes of functional brain imaging: a historical and physiological perspective. *Proc. Natl. Acad. Sci. U.S.A.* 95, 765–772. doi: 10.1073/pnas.95.3.765

Robinovitch, L. G. (1914). "Electrical analgesia, sleep, and resuscitation," in *Anesthesia*, ed J. T. Gwathmey (New York, NY: Appleton).

Roh, H. T., and So, W. Y. (2017). Cranial electrotherapy stimulation affects mood state but not levels of peripheral neurotrophic factors or hypothalamic- pituitary-adrenal axis regulation. *Technol. Health Care* 25, 403–412. doi: 10.3233/THC-161275

Salar, G., Job, I., Mingrino, S., Bosio, A., and Trabucchi, M. (1981). Effect of transcutaneous electrotherapy on CSF β-endorphin content in patients without pain problems. *Pain* 10, 169–172. doi: 10.1016/0304-3959(81)90192-5

Schacter, D. L. (1977). EEG theta waves and psychological phenomena: a review and analysis. *Biol. Psychol.* 5, 47–82. doi: 10.1016/0301-0511(77)90028-X

Schooler, J. (2011). Unpublished results hide the decline effect. *Nature* 470, 437–437. doi: 10.1038/470437a

Schroeder, M. J., and Barr, R. E. (2001). Quantitative analysis of the electroencephalogram during cranial electrotherapy stimulation. *Clin. Neurophysiol.* 112, 2075–2083. doi: 10.1016/S1388-2457(01)00657-5

Shekelle, P. G., Cook, I. A., Miake-Lye, I. M., Booth, M. S., Beroes, J. M., and Mak, S. (2018a). Benefits and harms of cranial electrical stimulation for chronic painful conditions, depression, anxiety, and insomnia. *Ann. Intern. Med.* 168, 414–421. doi: 10.7326/M17-1970

Shekelle, P. G., Cook, I. A., Miake-Lye, I. M., Mak, S., Booth, M. S., Shanman, R., et al. (2018b). *The Effectiveness and Risks of Cranial Electrical Stimulation for the Treatment of Pain, Depression, Anxiety, PTSD, and Insomnia: A Systematic Review (VA ESP Project #05-226)*. Washington, DC: Department of Veterans Affairs.

Smith, R. B. (2007). *Cranial Electrotherapy Stimulation: Its First Fifty Years, Plus Three: A Monograph*. Mustang, OK: Tate Publishing & Enterprises, LLC.

Smith, R. B. (2013). *CES Ultra: All Likert Scales [Retail]*. CES ULTRA. Available online at: https://www.cesultra.com/blog/all-likert-scales/

Solomon, S., Elkind, A., Freitag, F., Gallagher, R. M., Moore, K., Swerdlow, B., et al. (1989). Safety and effectiveness of cranial electrotherapy in the treatment of tension headache. *Headache* 29, 445–450. doi: 10.1111/j.1526-4610.1989.hed2907445.x

Southworth, S. (1999). A study of the effects of cranial electrical stimulation on attention and concentration. *Integr. Physiol. Behav. Sci.* 34, 43–53. doi: 10.1007/BF02688709

Sterne, J. A. C., Savović, J., Page, M. J., Elbers, R. G., Blencowe, N. S., Boutron, I., et al. (2019). RoB 2: a revised tool for assessing risk of bias in randomised trials. *BMJ* 366:l4898. doi: 10.1136/bmj.l4898

Tatum, W. O. (2014). *Handbook of EEG Interpretation.* New York, NY: Demos Medical Publishing. doi: 10.1891/9781617051807

Toriyama, M. (1975). Ear acupuncture anesthesia. *Ear Throat* 47, 497–501.

Vannorsdall, T. D., van Steenburgh, J. J., Schretlen, D. J., Jayatillake, R., Skolasky, R. L., and Gordon, B. (2016). Reproducibility of tDCS results in a randomized trial: failure to replicate findings of tDCS-induced enhancement of verbal fluency. *Cogn. Behav. Neurol.* 29, 11–17. doi: 10.1097/WNN.0000000000000086

Vedhara, K., Hyde, J., Gilchrist, I. D., Tytherleigh, M., and Plummer, S. (2000). Acute stress, memory, attention and cortisol. *Psychoneuroendocrinology* 25, 535–549. doi: 10.1016/S0306-4530(00)00008-1

Vine, S. J., Moore, L. J., and Wilson, M. R. (2016). An integrative framework of stress, attention, and visuomotor performance. *Front. Psychol.* 7:1671. doi: 10.3389/fpsyg.2016.01671

Wagenseil, B., Garcia, C., Suvorov, A. V., Fietze, I., and Penzel, T. (2018). The effect of cranial electrotherapy stimulation on sleep in healthy women. *Physiol. Meas.* 39:114007. doi: 10.1088/1361-6579/aaeafa

Weiss, M. F. (1973). The treatment of insomnia through the use of electrosleep: an EEG study. *J. Nerv. Ment. Dis.* 157, 108–120. doi: 10.1097/00005053-197308000-00003

Winick, R. L. (1999). Cranial electrotherapy stimulation (CES): a safe and effective low cost means of anxiety control in a dental practice. *Gen. Dent.* 47, 50–55.

Wu, W. J., Wang, Y., Cai, M., Chen, Y. H., Zhou, C. H., Wang, H. N., et al. (2020). A double-blind, randomized, sham-controlled study of cranial electrotherapy stimulation as an add-on treatment for tic disorders in children and adolescents. *Asian J. Psychiatr.* 51, 101992. doi: 10.1016/j.ajp.2020.101992

Yennurajalingam, S., Kang, D. H., Hwu, W. J., Padhye, N. S., Masino, C., Dibaj, S. S., et al. (2018). Cranial electrotherapy stimulation for the management of depression, anxiety, sleep disturbance, and pain in patients with advanced cancer: a preliminary study. *J. Pain Sympt. Manag.* 55, 198–206. doi: 10.1016/j.jpainsymman.2017.08.027

Zaghi, S., Acar, M., Hultgren, B., Boggio, P. S., and Fregni, F. (2010). Noninvasive brain stimulation with low-intensity electrical currents: putative mechanisms of action for direct and alternating current stimulation. *Neuroscientist* 16, 285–307. doi: 10.1177/1073858409336227

Zink, B. J. (2001). Traumatic brain injury outcome: concepts for emergency care. *Ann. Emerg. Med.* 37, 318–332. doi: 10.1067/mem.2001.113505

Conflict of Interest: The authors declare that the research was conducted in the absence of any commercial or financial relationships that could be construed as a potential conflict of interest.

frontiers in Human Neuroscience

ORIGINAL RESEARCH
published: 10 February 2021
doi: 10.3389/fnhum.2021.636472

Altered Dynamic Amplitude of Low-Frequency Fluctuations in Patients With Migraine Without Aura

*Hong Chen, Guiqiang Qi, Yingxia Zhang, Ying Huang, Shaojin Zhang, Dongjun Yang, Junwei He, Lan Mu, Lin Zhou and Min Zeng**

Department of Radiology, The Third Affiliated Hospital of Chengdu Medical College, Pidu District People's Hospital, Chengdu, China

Migraine is a chronic and idiopathic disorder leading to cognitive and affective problems. However, the neural basis of migraine without aura is still unclear. In this study, dynamic amplitude of low-frequency fluctuations (dALFF) analyses were performed in 21 patients with migraine without aura and 21 gender- and age-matched healthy controls to identify the voxel-level abnormal functional dynamics. Significantly decreased dALFF in the bilateral anterior insula, bilateral lateral orbitofrontal cortex, bilateral medial prefrontal cortex, bilateral anterior cingulate cortex, and left middle frontal cortex were found in patients with migraine without aura. The dALFF values in the anterior cingulate cortex were negatively correlated with pain intensity, i.e., visual analog scale. Finally, support vector machine was used to classify patients with migraine without aura from healthy controls and achieved an accuracy of 83.33%, sensitivity of 90.48%, and specificity of 76.19%. Our findings provide the evidence that migraine influences the brain functional activity dynamics and reveal the neural basis for migraine, which could facilitate understanding the neuropathology of migraine and future treatment.

Keywords: migraine without aura, dynamic amplitude of low-frequency fluctuations, resting-state, functional MRI, classification 3

OPEN ACCESS

Edited by:
Bochao Cheng,
Sichuan University, China

Reviewed by:
Lijie Wang,
University of Electronic Science and Technology of China, China
Jingjing Gao,
University of Electronic Science and Technology of China, China

****Correspondence:***
Min Zeng
minzengnihao@163.com

Specialty section:
This article was submitted to Brain Imaging and Stimulation, a section of the journal Frontiers in Human Neuroscience

Received: *01 December 2020*
Accepted: *07 January 2021*
Published: *10 February 2021*

Citation:
Chen H, Qi G, Zhang Y, Huang Y, Zhang S, Yang D, He J, Mu L, Zhou L and Zeng M (2021) Altered Dynamic Amplitude of Low-Frequency Fluctuations in Patients With Migraine Without Aura. Front. Hum. Neurosci. 15:636472. doi: 10.3389/fnhum.2021.636472

INTRODUCTION

Migraine is an idiopathic and chronic disorder influencing the life quality of patients (Kruit et al., 2004). The frequent migraine attacks also affect patients' mental and physical health (Tietjen, 2004; Borsook et al., 2012). The previous studies have demonstrated that long-term chronic pain leads to functional damages in sensory, cognition, and affective processing (Montero-Homs, 2009; Linton, 2013; Denkinger et al., 2014). A lot of previous studies have revealed that migraine induced brain gray matter volume and white matter integrity changes using structural and diffusion magnetic resonance imaging (MRI) (DaSilva et al., 2007; Kim et al., 2008; Schmidt-Wilcke et al., 2008; Valfrè et al., 2008). With the use of resting-state functional MRI (fMRI), altered local regional homogeneity and whole-brain functional connectivity homogeneity were found in patients with migraine (Yu et al., 2012; Zhang et al., 2020). All these findings suggest that migraine could change the brain structure and functions.

The low-frequency oscillation of the brain is mainly characterized using resting-state fMRI with blood oxygen level-dependent (BOLD) signals (Biswal et al., 1995; Fox and Raichle, 2007). Resting-state fMRI has been widely applied to study the brain functional organization (Greicius et al., 2003; Fox et al., 2006; Wang et al., 2015, 2017c; Xu et al., 2019; Gao et al., 2020), to identify the functional

abnormalities in patients with brain disorders (Greicius et al., 2007; Brier et al., 2012; Muller et al., 2013; Wu et al., 2016; Sun et al., 2018), and to reveal the neural basis of treatment response (Guo et al., 2012; Mulders et al., 2016; Wang et al., 2017b, 2018; Xu et al., 2020). To quantitatively measure low-frequency oscillation, the amplitude of low-frequency fluctuations (ALFF) is proposed (Zang et al., 2007). Using ALFF, Xue et al. (2013) found decreased ALFF values in the left rostral anterior cingulate cortex and bilateral prefrontal cortex as well as increased ALFF values in the right thalamus. Using ALFF to reveal the early abnormal functional activity is promising to explore early marker for migraine. Recently, using sliding-window approach, the dynamic ALFF (dALFF) method was developed by calculating the variance of ALFF over time (Fu et al., 2018). The dALFF has been applied to study the functional activity abnormalities in subjects under disease state and provides some new evidence (Fu et al., 2018; Ma et al., 2020; Pang et al., 2020). Thus, to reveal the dynamic changes of the low-frequency oscillation in migraine patients may provide supplementary information to understand its neural basis.

In this study, with 21 patients with migraine without aura and 21 gender- and age-matched healthy controls, a voxel-wise dALFF method was used to reveal the dynamic changes of low-frequency oscillation in migraine patients. Moreover, using the dALFF values in brain regions showing differences between patients and controls as features, support vector machine (SVM) was used to classify migraine patients from healthy controls to further validate the results.

MATERIALS AND METHODS

Participants

In this study, we recruited 21 right-handed patients with migraine without aura (female/male = 16/5; age = 31.19 ± 6.38 years) and 21 gender- and age-matched right-handed healthy controls (female/male = 13/8; age = 30.19 ± 6.3 years) at the Third Affiliated Hospital of Chengdu Medical College, Pidu District People's Hospital. The diagnosis of migraine without aura was based on the International Headache Society criteria. The inclusion criteria for patients with migraine without aura were follows: (1) no migraine precipitated during or on the day after the scan; (2) did not suffer from a migraine attack at least 72 h before the experiment; (3) for migraine patients and healthy controls, no lifetime history of seizures, head trauma, serious medical or surgical illness, substance dependence or abuse, and contraindications for MRI. The participants were excluded if structural abnormalities were detected on MRI examination, and no subject with structural deficits was found. Written informed consent was provided and obtained from all the subjects. This study was approved by the local ethics committees of the Third Affiliated Hospital of Chengdu Medical College, Pidu District People's Hospital. The detailed information for the subjects can be found in our previous study (Zhang et al., 2020).

Resting-State Functional MRI Data Acquisition

MRI data were acquired on a 3-Tesla Siemens MRI scanner in the Department of Radiology, the Third Affiliated Hospital of Chengdu Medical College, Pidu District People's Hospital of Chengdu, China. The participants were instructed to close their eyes and not fall asleep, and earplugs and foam padding were used to reduce scanner noise and head motion. Resting-state fMRI data were acquired using a gradient-echo echo-planar imaging (GRE-EPI) sequence with the following parameters: repetition time (TR) = 2,000 ms, echo time (TE) = 30 ms, flip angle (FA) = 90°, matrix = 64 × 64, field of view (FOV) = 220 × 220 mm, slice thickness = 4 mm with inter-slice gap = 0.6 mm, 32 axial slices, and 250 time points. The information can be found in our previous study (Zhang et al., 2020).

Resting-State Functional MRI Data Preprocessing

The resting-state fMRI data were preprocessed using the toolkit of DPARSF version 2.3 (Chao-Gan and Yu-Feng, 2010) (www.restfmri.net/forum/DPARSF). To exclude unstable magnetization effect, the first 10 volumes were discarded. Then, all the remaining volumes were realigned to the first volume to correct head motion. Next, all the images were normalized to standard EPI template in Montreal Neurological Institute (MNI) space and resampled to 3-mm voxel resolution. Subsequently, 6-mm Gaussian kernel was used to smooth the fMRI data; and Friston 24-parameter of head motion, white matter, cerebrospinal fluid, and global mean signals were regressed out. Finally, the resting-state data were filtered with a frequency band of 0.01–0.08 Hz for dALFF analyses. To remove head-motion effects, the subjects were excluded if the head movement exceeds 3 mm or 3°. Additionally, "scrubbing" was used to delete the bad images before 2 time points and after 1 time point exceeding the preset criteria [frame displacement (FD) < 0.5] (Power et al., 2012). We also calculated the mean FD values of healthy controls and migraine patients, and the two-sample *t*-test was used and did not find the significant difference (FD values of patients = 0.16 ± 0.29; FD values of controls = 0.15 ± 0.027; $p = 0.49$).

Dynamic Amplitude of Low-Frequency Fluctuations Calculation

The ALFF was proposed to characterize the resting-state functional activity of each voxel in brain (Zou et al., 2008). To calculate ALFF, the time series was first transformed to frequency domain, and the ALFF is computed at the power within the low-frequency range of 0.01–0.8 Hz. To calculate dALFF, a sliding window method was used. The length of sliding window is determined based on the criterion that minimum window length should be larger than $1/f_{\min}$, where $f_{\min}$ is the minimum frequency of time series (Leonardi and Van De Ville, 2015; Du et al., 2017; Li et al., 2019). Finally, a window length of 50 TR with step size of 5 TR was applied in this study. The ALFF map was computed in each window, and the variance of the ALFF maps across all the windows was computed to

TABLE 1 | Demographics and clinical characteristics of the subjects used in present study.

	Migraine ($n = 21$)	Controls ($n = 21$)	p
Gender (male/female)	16/5	13/8	0.51
Age (mean ± SD)	31.19 ± 6.38	30.19 ± 6.3	0.61
HAMA (mean ± SD)	7.95 ± 6.77		
HAMD (mean ± SD)	6.71 ± 6.25		
Duration of illness (months)	44.69 ± 61.13		
VAS (mean ± SD)	4.33 ± 1.46		

A Pearson chi-squared test was used for gender comparison. Two-sample t-tests were used for age comparisons.
VAS, visual analog scale; HAMD, Hamilton Depression Rating Scale; HAMA, Hamilton Anxiety Scale.

measure the dynamic. The dALFF maps were transformed to z-scores for statistical analyses. Two-sample t-test was performed to compare the dALFF maps between healthy controls and patients with migraine without aura. The significant level was set at $p < 0.05$ using a Gaussian random field (GRF) correction method. To further validate the results obtained with the window length of 50 TR, the window length of 30 and 70 TR were further applied.

Correlation Analyses

To explore the relationship between dALFF and clinical measures, correlation analyses were performed between the dALFF values of the areas showing differences in patients and visual analog scale (VAS), and disease duration. The significance was set at $p < 0.05$ with Bonferroni correction.

Support Vector Machine Classification

A linear SVM classifier was performed using LIBSVM software (Chang and Lin, 2011). For classification, the mean dALFF values of the areas showing differences between patients and controls were used as the features. To estimate the performance of our classifier, a leave-one-out cross-validation (LOOCV) test was used to assess the generalization ability because of our limited number of samples in the present study. The classification result was assessed using the classification accuracy, sensitivity, and specificity.

RESULTS

Clinical Characteristics

There were no significant differences in age ($p = 0.61$) and sex ($p = 0.51$) between healthy controls and patients with migraine without aura (**Table 1**).

Changed Dynamic Amplitude of Low-Frequency Fluctuations

By the analysis of dALFF in window length of 50 TR, significantly decreased dALFF in the bilateral anterior insula, bilateral lateral orbitofrontal cortex, bilateral medial prefrontal cortex, bilateral anterior cingulate cortex, and left middle frontal cortex in patients with migraine without aura compared with healthy controls (**Figure 1** and **Table 2**) was found. We also analyzed dALFF in window length of 30 and 70 TR, and similar results were found (**Figure 2**).

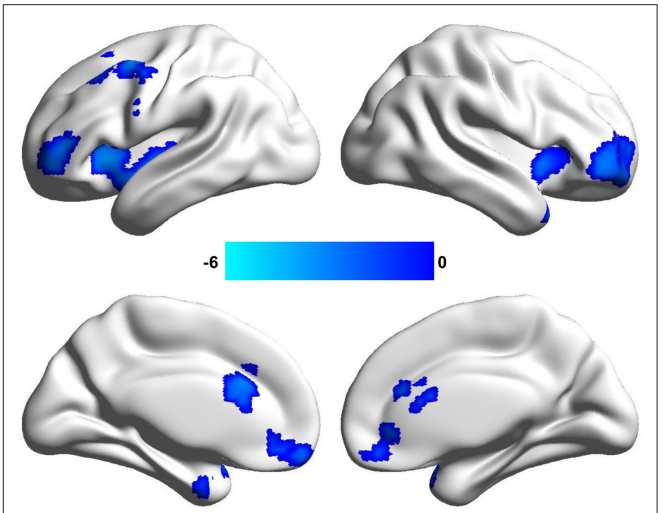

FIGURE 1 | Changed dynamic amplitude of low-frequency fluctuations (ALFF) in window length of 50 repetition time (TR) in patients with migraine without aura. Significantly decreased dynamic ALFF in the bilateral anterior insula, bilateral anterior cingulate cortex, bilateral lateral orbitofrontal cortex, and left middle frontal cortex were found in patients with migraine without aura.

Correlation Analyses

Correlation analyses identified significantly negative correlations between dALFF values in the anterior cingulate cortex and VAS scores ($r = -0.5$, $p = 0.022$) in patients with migraine without aura after multiple comparisons correction (**Figure 3**).

Classification Results

With the use of the changed dALFF values as features, experimental results showed a correct classification rate of 83.33%, sensitivity of 90.4%, and specificity of 76.19% using a leave-one-out cross-validation method (**Figure 4**).

DISCUSSION

In our study, dALFF method was applied and identified decreased dALFF in the bilateral anterior insula, bilateral orbitofrontal cortex, bilateral anterior cingulate cortex, bilateral medial prefrontal cortex, and left middle frontal cortex; and the changed dALFF in the anterior cingulate cortex was negatively correlated with VAS scores. Moreover, the changed dALFF can serve as an effective neuromarker to differentiate patients with migraine without aura from controls. Our findings revealed dynamic changes of brain functional activities in migraine patients and provide new evidence of neurophysiological abnormalities in migraine.

We found decreased dALFF in the anterior cingulate cortex and anterior insula in migraine patients without aura.

TABLE 2 | Regions with decreased dynamical amplitude of low-frequency fluctuations in patients with migraine without aura vs. healthy controls.

Brain regions	Peak MNI coordinates			t values	Cluster size
	X	Y	Z		
Anterior insula	−39	18	0	−4.71	383
Anterior insula	42	15	−9	−4.41	136
Lateral orbitofrontal cortex	−39	39	6	−4.53	185
Lateral orbitofrontal cortex	42	45	−3	−3.89	266
Middle frontal cortex	−46	0	51	−4.55	301
Medial prefrontal cortex	−3	54	−15	−3.74	118
Anterior cingulate cortex	−6	24	27	−3.87	102

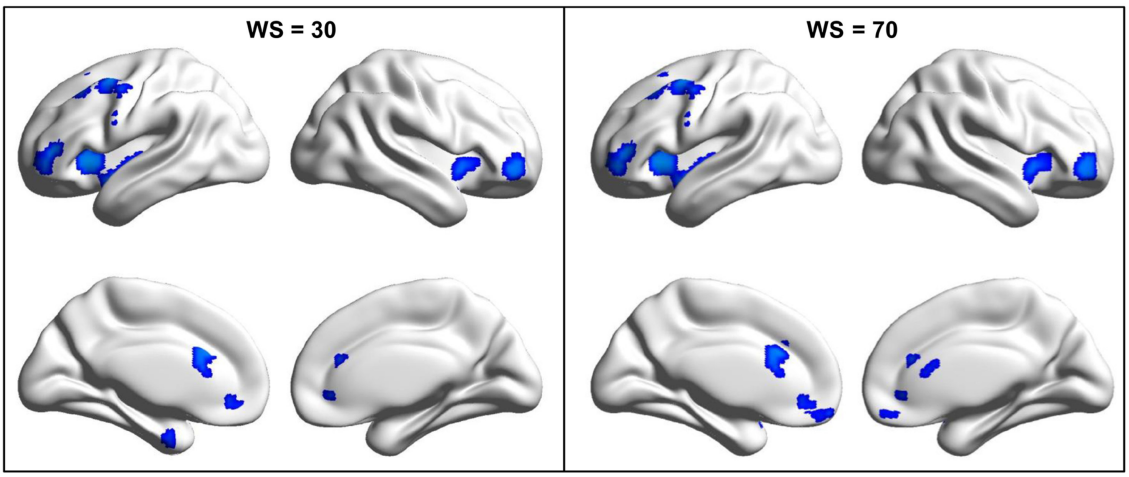

FIGURE 2 | Changed dynamic amplitude of low-frequency fluctuations (ALFF) in migraine patients was validated in window length of 30 and 70 repetition times (TRs). To validate the findings obtained with window length of 50 TR, the same procedures were performed in window length of 30 and 70 TRs and found similar results.

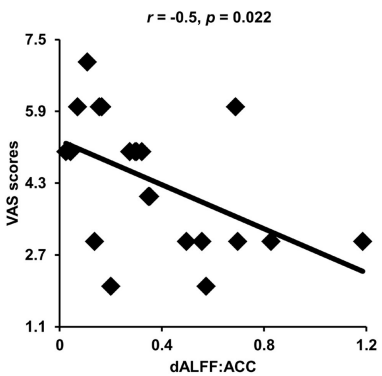

FIGURE 3 | Correlation analyses between dynamic amplitude of low-frequency fluctuations (ALFF) and clinical measures. Significant correlation was found between the dynamic ALFF in the anterior cingulate cortex and visual analog scale (VAS) scores in migraine patients.

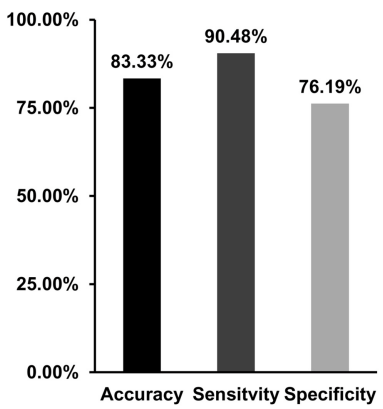

FIGURE 4 | Support vector machine (SVM) was applied to classify migraine patients and healthy controls with the dynamic amplitude of low-frequency fluctuations (ALFF) values in brain areas showing differences between patients and controls as features. SVM achieves a classification accuracy of 83.33%, sensitivity of 90.48%, and specificity of 76.19%.

The anterior insula and anterior cingulate cortex are two important nodes of salience network, which is mainly involved in coordinating the dynamic interaction between the external orient stimulus and internal self-perception (Menon and Uddin, 2010; Menon, 2011; Wang et al., 2017a, 2019b). The functional abnormality of anterior cingulate cortex and anterior insula found in our study is supported by previous functional and

structural studies (Peyron et al., 2000; Kim et al., 2008; Valfrè et al., 2008). Importantly, we found that decreased dALFF in the anterior cingulate cortex is associated with clinical pain intensity. Thus, the abnormal dynamic functional activities in the anterior cingulate cortex may be a neuromarker to predict the pain intensity.

The decreased dALFF in the medial prefrontal cortex, middle frontal cortex, and lateral orbitofrontal cortex was also observed. The medial prefrontal cortex is the core brain area of the default mode network that participates in social cognition, emotional, and self-referential processing (Gusnard et al., 2001; Amodio and Frith, 2006; Etkin et al., 2011; Wang et al., 2019a,c). The abnormal functional activities in medial prefrontal cortex have been reported in previous studies by analyses of static ALFF, local regional homogeneity, and whole-brain functional connectivity homogeneity (Yu et al., 2012; Xue et al., 2013). In addition, the middle frontal cortex and lateral orbitofrontal cortex play an important role in attention and executive control of pain-related stimuli to modulate the descending pain system (Casey, 1999; Lorenz et al., 2003; Wager et al., 2004). Thus, decreased dALFF values in the medial prefrontal cortex and middle prefrontal cortex may be related to impaired cognitive and emotion processing of pain. Moreover, we found that the changed dALFF in brain areas including the bilateral anterior insula, bilateral anterior cingulate cortex, bilateral medial prefrontal cortex, and left middle frontal cortex can well distinguish the migraine patients from controls. This finding indicates that the abnormal dynamic activities in default mode network, salience network, and executive network may be the neuropathology of migraine.

There are some limitations of our study. First, how to determine the length of sliding window is a problem for dynamic analysis. We used different window lengths to validate the findings. Second, the samples of our study are small, and the findings need to be further validated in the future studies with a larger sample.

CONCLUSION

This study revealed the abnormal dynamic low-frequency oscillation in default mode network, salience network, and executive control network in migraine patients. The decreased dALFF in these areas may be associated with disrupted emotion and cognitive functions. Our findings provide new evidence that migraine could influence the brain functions leading to functional impairments of emotion and cognitions in patients.

DATA AVAILABILITY STATEMENT

The raw data supporting the conclusions of this article will be made available by the authors, without undue reservation.

ETHICS STATEMENT

The studies involving human participants were reviewed and approved by the Third Affiliated Hospital of Chengdu Medical College, Pidu District People's Hospital. The patients/participants provided their written informed consent to participate in this study. Written informed consent was obtained from the individual(s) for the publication of any potentially identifiable images or data included in this article.

AUTHOR CONTRIBUTIONS

All authors have made a substantial contribution to this work.

REFERENCES

Amodio, D. M., and Frith, C. D. (2006). Meeting of minds: the medial frontal cortex and social cognition. *Nat. Rev. Neurosci.* 7, 268–277. doi: 10.1038/nrn1884

Biswal, B., Yetkin, F. Z., Haughton, V. M., and Hyde, J. S. (1995). Functional connectivity in the motor cortex of resting human brain using echo-planar MRI. *Magnet. Resonance Med.* 34, 537–541. doi: 10.1002/mrm.1910340409

Borsook, D., Maleki, N., Becerra, L., and McEwen, B. (2012). Understanding migraine through the lens of maladaptive stress responses: a model disease of allostatic load. *Neuron* 73, 219–234. doi: 10.1016/j.neuron.2012.01.001

Brier, M. R., Thomas, J. B., Snyder, A. Z., Benzinger, T. L., Zhang, D., Raichle, M. E., et al. (2012). Loss of intranetwork and internetwork resting state functional connections with Alzheimer's disease progression. *J. Neurosci.* 3, 8890–8899. doi: 10.1523/JNEUROSCI.5698-11.2012

Casey, K. L. (1999). Forebrain mechanisms of nociception and pain: analysis through imaging. *Proc. Natl. Acad. Sci. U.S.A.* 96, 7668–7674. doi: 10.1073/pnas.96.14.7668

Chang, C.-C., and Lin, C.-J. (2011). LIBSVM: a library for support vector machines. *ACM Trans. Intell. Syst. Technol.* 2, 1–27. doi: 10.1145/1961189.1961199

Chao-Gan, Y., and Yu-Feng, Z. (2010). DPARSF: a MATLAB toolbox for "Pipeline" data analysis of resting-state fMRI. *Front. Systems Neurosci.* 4:13. doi: 10.3389/fnsys.2010.00013

DaSilva, A. F., Granziera, C., Tuch, D. S., Snyder, J., Vincent, M., and Hadjikhani, N. (2007). Interictal alterations of the trigeminal somatosensory pathway and periaqueductal gray matter in migraine. *Neuroreport* 18, 301–305. doi: 10.1097/WNR.0b013e32801776bb

Denkinger, M. D., Lukas, A., Nikolaus, T., Peter, R., and Franke, S. (2014). Multisite pain, pain frequency and pain severity are associated with depression in older adults: results from the ActiFE Ulm study. *Age Ageing* 43, 510–514. doi: 10.1093/ageing/afu013

Du, Y., Pearlson, G. D., Lin, D., Sui, J., Chen, J., Salman, M., et al. (2017). Identifying dynamic functional connectivity biomarkers using GIG-ICA: application to schizophrenia, schizoaffective disorder, and psychotic bipolar disorder. *Human Brain Mapp.* 38, 2683–2708. doi: 10.1002/hbm.23553

Etkin, A., Egner, T., and Kalisch, R. (2011). Emotional processing in anterior cingulate and medial prefrontal cortex. *Trends Cognitive Sci.* 15, 85–93. doi: 10.1016/j.tics.2010.11.004

Fox, M. D., Corbetta, M., Snyder, A. Z., Vincent, J. L., and Raichle, M. E. (2006). Spontaneous neuronal activity distinguishes human dorsal and ventral attention systems. *Proc. Natl. Acad. Sci. U.S.A.* 103, 10046–10051. doi: 10.1073/pnas.0604187103

Fox, M. D., and Raichle, M. E. (2007). Spontaneous fluctuations in brain activity observed with functional magnetic resonance imaging. *Nat Rev. Neurosci.* 8, 700–711. doi: 10.1038/nrn2201

Fu, Z., Tu, Y., Di, X., Du, Y., Pearlson, G. D., Turner, J. A., et al. (2018). Characterizing dynamic amplitude of low-frequency fluctuation and its relationship with dynamic functional connectivity: an application to schizophrenia. *NeuroImage* 180, 619–631. doi: 10.1016/j.neuroimage.2017.09.035

Gao, Z., Guo, X., Liu, C., Mo, Y., and Wang, J. (2020). Right inferior frontal gyrus: An integrative hub in tonal bilinguals. *Human Brain Mapp.* 41, 2152–2159. doi: 10.1002/hbm.24936

Greicius, M. D., Flores, B. H., Menon, V., Glover, G. H., Solvason, H. B., Kenna, H., et al. (2007). Resting-state functional connectivity in major depression: abnormally increased contributions from subgenual cingulate cortex and thalamus. *Biol. Psychiatr.* 62, 429–437. doi: 10.1016/j.biopsych.2006.09.020

Greicius, M. D., Krasnow, B., Reiss, A. L., and Menon, V. (2003). Functional connectivity in the resting brain: a network analysis of the default mode hypothesis. *Proc. Natl. Acad. Sci. U.S.A.* 100, 253–258. doi: 10.1073/pnas.0135058100

Guo, W. B., Liu, F., Chen, J. D., Gao, K., Xue, Z. M., Xu, X. J., et al. (2012). Abnormal neural activity of brain regions in treatment-resistant and treatment-sensitive major depressive disorder: a resting-state fMRI study. *J. Psychiatric Res.* 46, 1366–1373. doi: 10.1016/j.jpsychires.2012.07.003

Gusnard, D. A., Akbudak, E., Shulman, G. L., and Raichle, M. E. (2001). Medial prefrontal cortex and self-referential mental activity: relation to a default mode of brain function. *Proc. Natl. Acad. Sci. U.S.A.* 98. 4259–4264. doi: 10.1073/pnas.071043098

Kim, J. H., Suh, S. I., Seol, H. Y., Oh, K., Seo, W. K., Yu, S. W., et al. (2008). Regional grey matter changes in patients with migraine: a voxel-based morphometry study. *Cephalalgia* 28, 598–604. doi: 10.1111/j.1468-2982.2008.01550.x

Kruit, M. C., van Buchem, M. A., Hofman, P. A. M., Bakkers, J. T. N., Terwindt, G. M., Ferrari, M. D., et al. (2004). Migraine as a risk factor for subclinical brain lesions. *JAMA* 291, 427–434. doi: 10.1001/jama.291.4.427

Leonardi, N., and Van De Ville, D. (2015). On spurious and real fluctuations of dynamic functional connectivity during rest. *NeuroImage* 104, 430–436. doi: 10.1016/j.neuroimage.2014.09.007

Li, C., Xia, L., Ma, J., Li, S., Liang, S., Ma, X., et al. (2019). Dynamic functional abnormalities in generalized anxiety disorders and their increased network segregation of a hyperarousal brain state modulated by insomnia. *J. Affect. Disord.* 246, 338–345. doi: 10.1016/j.jad.2018.12.079

Linton, S. J. (2013). A transdiagnostic approach to pain and emotion. *J. Appl. Biobehav. Res.* 18, 82–103. doi: 10.1111/jabr.12007

Lorenz, J., Minoshima, S., and Casey, K. L. (2003). Keeping pain out of mind: the role of the dorsolateral prefrontal cortex in pain modulation. *Brain* 126, 1079–1091. doi: 10.1093/brain/awg102

Ma, M., Zhang, H., Liu, R., Liu, H., Yang, X., Yin, X., et al. (2020). Static and dynamic changes of amplitude of low-frequency fluctuations in cervical discogenic pain. *Front. Neurosci.* 14:733. doi: 10.3389/fnins.2020.00733

Menon, V. (2011). Large-scale brain networks and psychopathology: a unifying triple network model. *Trends cognit. Sci.* 15, 483–506. doi: 10.1016/j.tics.2011.08.003

Menon, V., and Uddin, L. Q. (2010). Saliency, switching, attention and control: a network model of insula function. *Brain Struct. Funct.*214, 655–667. doi: 10.1007/s00429-010-0262-0

Montero-Homs, J. (2009). Nocioceptive pain, neuropathic pain and pain memory. *Neurologia* 24, 419–422.

Mulders, P. C., van Eijndhoven, P. F., Pluijmen, J., Schene, A. H., Tendolkar, I., and Beckmann, C. F. (2016). Default mode network coherence in treatment-resistant major depressive disorder during electroconvulsive therapy. *J. Affect. Disord.* 205, 130–137. doi: 10.1016/j.jad.2016.06.059

Muller, V. I., Cieslik, E. C., Laird, A. R., Fox, P. T., and Eickhoff, S. B. (2013). Dysregulated left inferior parietal activity in schizophrenia and depression: functional connectivity and characterization. *Front. Human Neurosci.* 7:268. doi: 10.3389/fnhum.2013.00268

Pang, Y., Zhang, H., Cui, Q., Yang, Q., Lu, F., Chen, H., et al. (2020). Combined static and dynamic functional connectivity signatures differentiating bipolar depression from major depressive disorder. *Australian N. Zealand J. Psychiatr.* 54, 832–842. doi: 10.1177/0004867420924089

Peyron, R., Laurent, B., and Garcia-Larrea, L. (2000). Functional imaging of brain responses to pain. A review and meta-analysis neurophysiologie clinique. *Clin. Neurophysiol.* 30, 263–288. doi: 10.1016/S0987-7053(00)00227-6

Power, J. D., Barnes, K. A., Snyder, A. Z., Schlaggar, B. L., and Petersen, S. E. (2012). Spurious but systematic correlations in functional connectivity MRI networks arise from subject motion. *NeuroImage* 59, 2142–2154. doi: 10.1016/j.neuroimage.2011.10.018

Schmidt-Wilcke, T., Gänssbauer, S., Neuner, T., Bogdahn, U., and May, A. (2008). Subtle grey matter changes between migraine patients and healthy controls. *Cephalalgia* 28, 1–4. doi: 10.1111/j.1468-2982.2007.01428.x

Sun, H., Luo, L., Yuan, X., Zhang, L., He, Y., Yao, S., et al. (2018). Regional homogeneity and functional connectivity patterns in major depressive disorder, cognitive vulnerability to depression and healthy subjects. *J. Affective Disord.* 235, 229–235. doi: 10.1016/j.jad.2018.04.061

Tietjen, G. E. (2004). Stroke and migraine linked by silent lesions. *Lancet* 3:267. doi: 10.1016/S1474-4422(04)00729-X

Valfrè, W., Rainero, I., Bergui, M., and Pinessi, L. (2008). Voxel-based morphometry reveals gray matter abnormalities in migraine. *Headache* 48, 109–117. doi: 10.1111/j.1526-4610.2007.00723.x

Wager, T. D., Rilling, J. K., Smith, E. E., Sokolik, A., Casey, K. L., Davidson, R. J., et al. (2004). Placebo-induced changes in FMRI in the anticipation and experience of pain. *Science* 303, 1162–1167. doi: 10.1126/science.1093065

Wang, C., Wu, H., Chen, F., Xu, J., Li, H., Li, H., et al. (2017a). Disrupted functional connectivity patterns of the insula subregions in drug-free major depressive disorder. *J. Affect. Disord.* 234, 297–304. doi: 10.1016/j.jad.2017.12.033

Wang, J., Becker, B., Wang, L., Li, H., Zhao, X., and Jiang, T. (2019a). Corresponding anatomical and coactivation architecture of the human precuneus showing similar connectivity patterns with macaques. *NeuroImage* 200, 562–574. doi: 10.1016/j.neuroimage.2019.07.001

Wang, J., Wei, Q., Bai, T., Zhou, X., Sun, H., Becker, B., et al. (2017b). Electroconvulsive therapy selectively enhanced feedforward connectivity from fusiform face area to amygdala in major depressive disorder. *Soc. Cognit. Affective Neurosci.* 12, 1983–1992. doi: 10.1093/scan/nsx100

Wang, J., Wei, Q., Wang, L., Zhang, H., Bai, T., Cheng, L., et al. (2018). Functional reorganization of intra- and internetwork connectivity in major depressive disorder after electroconvulsive therapy. *Human Brain Mapp.* 39, 1403–1411. doi: 10.1002/hbm.23928

Wang, J., Xie, S., Guo, X., Becker, B., Fox, P. T., Eickhoff, S. B., et al. (2017c). Correspondent functional topography of the human left inferior parietal lobule at rest and under task revealed using resting-state fmri and coactivation based parcellation. *Human Brain Mapp.* 38, 1659–1675. doi: 10.1002/hbm.23488

Wang, J., Yang, Y., Fan, L., Xu, J., Li, C., Liu, Y., et al. (2015). Convergent functional architecture of the superior parietal lobule unraveled with multimodal neuroimaging approaches. *Human Brain Mapp.* 36, 238–257. doi: 10.1002/hbm.22626

Wang, L., Wei, Q., Wang, C., Xu, J., Wang, K., Tian, Y., et al. (2019b). Altered functional connectivity patterns of insular subregions in major depressive disorder after electroconvulsive therapy. *Brain Imaging Behav.* 14, 753–761. doi: 10.1007/s11682-018-0013-z

Wang, L., Yu, L., Wu, F., Wu, H., and Wang, J. (2019c). Altered whole brain functional connectivity pattern homogeneity in medication-free major depressive disorder. *J. Affect. Disord.* 253, 18–25. doi: 10.1016/j.jad.2019.04.040

Wu, Y., Zhang, Y., Liu, Y., Liu, J., Duan, Y., Wei, X., et al. (2016). Distinct changes in functional connectivity in posteromedial cortex subregions during the progress of alzheimer's disease. *Front Neuroanat.* 10:41. doi: 10.3389/fnana.2016.00041

Xu, J., Lyu, H., Li, T., Xu, Z., Fu, X., Jia, F., et al. (2019). Delineating functional segregations of the human middle temporal gyrus with resting-state functional connectivity and coactivation patterns. *Human Brain Mapp.* 40, 5159–5171. doi: 10.1002/hbm.24763

Xu, J., Wei, Q., Bai, T., Wang, L., Li, X., He, Z., et al. (2020). Electroconvulsive therapy modulates functional interactions between submodules of the emotion regulation network in major depressive disorder. *Translational Psychiatr.* 10:271. doi: 10.1038/s41398-020-00961-9

Xue, T., Yuan, K., Cheng, P., Zhao, L., Zhao, L., Yu, D., et al. (2013). Alterations of regional spontaneous neuronal activity and corresponding brain circuit changes during resting state in migraine without aura. *NMR Biomed.* 26, 1051–1058. doi: 10.1002/nbm.2917

Yu, D., Yuan, K., Zhao, L., Zhao, L., Dong, M., Liu, P., et al. (2012). Regional homogeneity abnormalities in patients with interictal migraine without aura: a resting-state study. *NMR Biomed.* 25, 806–812. doi: 10.1002/nbm.1796

Zang, Y. F., He, Y., Zhu, C. Z., Cao, Q. J., Sui, M. Q., Liang, M., et al. (2007). Altered baseline brain activity in children with ADHD revealed by resting-state functional MRI. *Brain Dev.* 29, 83–91. doi: 10.1016/j.braindev.2006.07.002

Zhang, Y., Chen, H., Zeng, M., He, J., Qi, G., Zhang, S., et al. (2020). Abnormal whole brain functional connectivity pattern homogeneity and couplings in migraine without Aura. *Front. Human Neurosci.* 14:619839. doi: 10.3389/fnhum.2020.619839

Zou, Q. H., Zhu, C. Z., Yang, Y., Zuo, X. N., Long, X. Y., Cao, Q. J., et al. (2008). An improved approach to detection of amplitude of low-frequency fluctuation (ALFF) for resting-state fMRI: fractional ALFF. *J. Neurosci. Methods* 172, 137–141. doi: 10.1016/j.jneumeth.2008.04.012

Conflict of Interest: The authors declare that the research was conducted in the absence of any commercial or financial relationships that could be construed as a potential conflict of interest.

frontiers in Human Neuroscience

ORIGINAL RESEARCH
published: 16 February 2021
doi: 10.3389/fnhum.2021.625232

Altered Frequency-Dependent Brain Activation and White Matter Integrity Associated With Cognition in Characterizing Preclinical Alzheimer's Disease Stages

Siyu Wang[1,2], Jiang Rao[3,4], Yingying Yue[5], Chen Xue[3,6], Guanjie Hu[3], Wenzhang Qi[3,6], Wenying Ma[7], Honglin Ge[3], Fuquan Zhang[8], Xiangrong Zhang[2,8] and Jiu Chen[1,2]**

[1] Institute of Neuropsychiatry, The Affiliated Brain Hospital of Nanjing Medical University, Fourth Clinical College of Nanjing Medical University, Nanjing, China, [2] Fourth Clinical College of Nanjing Medical University, Nanjing, China, [3] Institute of Brain Functional Imaging, Nanjing Medical University, Nanjing, China, [4] Department of Rehabilitation, The Affiliated Brain Hospital of Nanjing Medical University, Nanjing, China, [5] Department of Psychosomatics and Psychiatry, The Affiliated ZhongDa Hospital, School of Medicine, Southeast University, Nanjing, China, [6] Department of Radiology, The Affiliated Brain Hospital of Nanjing Medical University, Nanjing, China, [7] Department of Neurology, The Affiliated Brain Hospital of Nanjing Medical University, Nanjing, China, [8] Department of Psychiatry, The Affiliated Brain Hospital of Nanjing Medical University, Nanjing, China, [9] Department of Geriatric Psychiatry, The Affiliated Brain Hospital of Nanjing Medical University, Nanjing, China

OPEN ACCESS

Edited by:
Jiaojian Wang,
University of Electronic Science and Technology of China, China

Reviewed by:
Liang Gong,
Chengdu Second People's Hospital, China
Rui Liu,
Capital Medical University, China

***Correspondence:**
Jiu Chen
ericcst@aliyun.com
Xiangrong Zhang
drxrz@hotmail.com

Specialty section:
This article was submitted to Brain Imaging and Stimulation, a section of the journal Frontiers in Human Neuroscience

Received: *15 December 2020*
Accepted: *06 January 2021*
Published: *16 February 2021*

Citation:
Wang S, Rao J, Yue Y, Xue C, Hu G, Qi W, Ma W, Ge H, Zhang F, Zhang X and Chen J (2021) Altered Frequency-Dependent Brain Activation and White Matter Integrity Associated With Cognition in Characterizing Preclinical Alzheimer's Disease Stages. Front. Hum. Neurosci. 15:625232. doi: 10.3389/fnhum.2021.625232

Background: Subjective cognitive decline (SCD), non-amnestic mild cognitive impairment (naMCI), and amnestic mild cognitive impairment (aMCI) are regarded to be at high risk of converting to Alzheimer's disease (AD). Amplitude of low-frequency fluctuations (ALFF) can reflect functional deterioration while diffusion tensor imaging (DTI) is capable of detecting white matter integrity. Our study aimed to investigate the structural and functional alterations to further reveal convergence and divergence among SCD, naMCI, and aMCI and how these contribute to cognitive deterioration.

Methods: We analyzed ALFF under slow-4 (0.027–0.073 Hz) and slow-5 (0.01–0.027 Hz) bands and white matter fiber integrity among normal controls (CN), SCD, naMCI, and aMCI groups. Correlation analyses were further utilized among paired DTI alteration, ALFF deterioration, and cognitive decline.

Results: For ALFF calculation, ascended ALFF values were detected in the lingual gyrus (LING) and superior frontal gyrus (SFG) within SCD and naMCI patients, respectively. Descended ALFF values were presented mainly in the LING, SFG, middle frontal gyrus, and precuneus in aMCI patients compared to CN, SCD, and naMCI groups. For DTI analyses, white matter alterations were detected within the uncinate fasciculus (UF) in aMCI patients and within the superior longitudinal fasciculus (SLF) in naMCI patients. SCD patients presented alterations in both fasciculi. Correlation analyses revealed that the majority of these structural and functional alterations were associated with complicated cognitive decline. Besides, UF alterations were correlated with ALFF deterioration in the SFG within aMCI patients.

Conclusions: SCD shares structurally and functionally deteriorative characteristics with aMCI and naMCI, and tends to convert to either of them. Furthermore, abnormalities in white matter fibers may be the structural basis of abnormal brain activation in preclinical AD stages. Combined together, it suggests that structural and functional integration may characterize the preclinical AD progression.

Keywords: amplitude of low-frequency fluctuation, diffusion tensor imaging, amnestic mild cognitive impairment, subjective cognitive decline, non-amnestic mild cognitive impairment

INTRODUCTION

Subjective cognitive decline (SCD), amnestic mild cognitive impairment (aMCI), and non-amnestic mild cognitive impairment (naMCI) are regarded to be at high risk of converting to Alzheimer's disease (AD) (Petersen et al., 2001, 2009; Jessen et al., 2014). SCD and aMCI are characterized as preclinical AD stages (Jessen et al., 2014; Rabin et al., 2017; Hao et al., 2019). While multiple research papers regard naMCI as part of the disease continuum due to diverse aspects (Yang et al., 2018; Xue C. et al., 2019), some have reservations (Vos et al., 2013, 2015; Wilcockson et al., 2019). Accordingly, the utilization of combined structural and functional neuroimaging analyses is required to further reveal convergence and divergence among normal controls (CN), SCD, naMCI, and aMCI and assist in characterizing the preclinical AD progression.

Resting-state functional magnetic resonance imaging (rs-fMRI) is applied for AD pathophysiologic measurement through blood-oxygen-level dependent (BOLD) signal alterations (Golestani et al., 2017; Kuang et al., 2019; Xue J. et al., 2019). Amplitude of low-frequency fluctuations (ALFF), defined by BOLD signal fluctuations under low frequency bands, is widely utilized in preclinical AD detection to reflect intrinsic neuronal activities (Lu et al., 2007; Hare et al., 2017). To note, the selection of specific frequency bands is critical for the precise reflection of neuronal activity (Biswal et al., 1995; Fox and Raichle, 2007; Han et al., 2011), and accurate detection of regional deterioration (Buzsaki and Draguhn, 2004). Previous studies have consistently indicated that the slow-5 band (0.01–0.027 Hz) and slow-4 band (0.027–0.073 Hz) are more sensitive in reflecting the compensation and deterioration of AD (Liu et al., 2014; Yang et al., 2018, 2019). Thus, we infer that ALFF under slow-4 and slow-5 bands may be a splendid choice for revealing preclinical AD spontaneous neuronal activities. Furthermore, diffusion tensor imaging (DTI) detects water molecule diffusion and is sensitive in white matter atrophy detection (Nir et al., 2013). DTI-based measures, e.g., fractional anisotropy (FA), mean diffusivity (MD), and relative anisotropy (RA), have been widely proven to be correlated with MCI and AD symptoms (Chandra et al., 2019; Dumont et al., 2019; Zhang et al., 2019). Therefore, utilization of DTI analyses may assist in uncovering alterative characteristics of preclinical AD stages from a structural perspective.

Numerous research papers have utilized ALFF calculation and DTI analyses separately in revealing typical characteristics of prodromal AD stages. For ALFF detection, abnormal ALFF values were widely detected in the frontal, occipital, and temporal lobes in aMCI patients and were proven to act as a sensitive biomarker for AD pathology (Han et al., 2011; Ren et al., 2016). Also, gradual disturbances among CN, SCD, aMCI, and AD were revealed through correlation analyses between ALFF alterations and neuropsychological assessments (Yang et al., 2018). DTI tractography may assist in distinguishing significantly deteriorated white matter integrity and serve as biomarkers for MCI (Teipel et al., 2019; Zhang et al., 2019). SCD suffered from more subtle alterations than MCI, indicating a potential disease progression sequence (Brueggen et al., 2019). Furthermore, white matter alterations were also revealed to be correlated with progressed cognitive decline (Power et al., 2019). Through MRI modalities, which included combined ALFF and DTI analyses, Gupta et al. created a classification tool to distinguish converting MCI (which progresses to AD) from non-converting MCI (Gupta et al., 2020). However, the mentioned research lacked consideration of the entire AD preclinical stages (i.e., SCD, naMCI, and aMCI) and analyses of the relationship with cognition. For the ALFF calculation part, separate sub-divided frequency bands were regarded to better present impairment (Buzsaki and Draguhn, 2004). Besides, comprehensive cognitive domains may reflect real cognitive conditions more accurately (Beauchet et al., 2015; Ramanan et al., 2017). A combination of structural and functional neuronal analyses may reveal alterations from a comprehensive perspective and help better understand disease pathology and progression.

This study analyzed DTI indices and ALFF to measure structural and functional alterations in preclinical AD stages. Next, correlation analyses were utilized in matched groups among cognition, white matter integrity, and ALFF values to further reveal internal associations. We speculated that convergence and divergence existed among SCD, naMCI, and aMCI. Moreover, relations between structural and functional alterations may further be revealed under AD progression.

MATERIALS AND METHODS

Subjects

Our study gained approval from the responsible Human Participants Ethics Committee of the Affiliated Nanjing Brain Hospital (Nos. 2018-KY010-01 and 2020-KY010-02) (Nanjing, China). Every participant provided written informed consent.

Data applied in this study were obtained from our in-house database: Nanjing Brain Hospital-Alzheimer's Disease Spectrum Neuroimaging Project (NBH-ADsnp) (Nanjing, China), which is constantly being updated. The details of the NBH-ADsnp-related information are provided in **Supplementary Material**. A total of 79 elderly patients were recruited initially from hospitals and communities through advertisement and broadcasting. Twelve of the participants were excluded due to no MRI data (n = 10) and excessive head motion (cumulative translation or rotation >3.0 mm or 3.0°, n = 2). A total of 67 patients were eventually included after exclusion with accordance to previous studies (Chen et al., 2016a; Dillen et al., 2017; Xue C. et al., 2019). Detailed inclusive and exclusive criteria are summarized in **Supplementary Material**.

Neuropsychological Assessments

Evaluation of the four cognitive domains (i.e., visuospatial function, executive function, information processing speed, and episodic memory) was conducted based on neuropsychological assessments according to previous studies (Chen et al., 2016b; Xue C. et al., 2019). Division and evaluation details are listed in **Supplementary Material**.

MRI Data Collection

Detailed MRI data acquisitive parameters of the NBH-ADsnp database are provided in **Supplementary Material**.

ALFF Data Analyses

For ALFF analyses, data preprocessing was performed by MATLAB2013b[1] and DPABI (Yan et al., 2016). Briefly, the preprocessing steps included slice-timing and head motion correction, nuisance covariate regression, spatial normalization, spatial smoothing with a Gaussian kernel of 6 mm × 6 mm × 6 mm (full width at half maximum, FWHM) (Chen et al., 2016b, 2020), and detrending. Participants with excessive head motion (cumulative translation or rotation >3.0 mm or 3.0°) were excluded. The details regarding preprocessing steps are provided in the **Supplementary Material**.

We used DPABI to calculate the multi-band ALFF values after the image preprocessing procedure. In brief, we used a Fast Fourier Transform (FFT) to convert the time series into the frequency domain, and obtained the power spectrum, the square root of which was calculated and averaged across frequency intervals that were pre-defined. The averaged square root obtained by the procedure was then taken as ALFF. ALFF was z-normalized as Fisher's z transformation ALFF (zALFF) after the calculation (Alonso-Solis et al., 2017). According to previous studies (Han et al., 2011; Liu et al., 2014; Yang et al., 2018, 2019), we chose the slow-4 band and slow-5 band out of the five bands, discarding the other three frequency bands (i.e., slow-2, slow-3, and slow-6) due to the reflection of high-frequency physiological noise, white matter signals, and very low frequency drift (Han et al., 2011).

[1]http://www.mathworks.com/products/matlab/

DTI Data Analyses

We applied the Pipeline for Analyzing Brain Diffusion Images toolkit (PANDA,[2]), combining the FMRIB Software Library (FSL,[3]) and Diffusion toolkit for DTI data preprocessing. The brief procedures included: (a) image conversion from DICOM to NIFTI; (b) brain extraction; (c) brain mask estimation; (d) image cropping and realignment; (e) eddy current and motion correction; (f) acquisition averaging; and (g) diffusion tensor and scalar measures (i.e., FA, MD, and RA) calculation.

Statistical Analysis

Statistical analyses were conducted by the Statistical Package for the Social Sciences (SPSS) software version 22.0 (IBM, Armonk, New York, United States). Comparison of demographic and neuropsychological data within CN, SCD, naMCI, and aMCI was done by analysis of covariance (ANCOVA) and the chi-square test (for gender). We performed two-sample T-tests for *post hoc* comparisons between any two groups (Bonferroni-corrected, $p < 0.05$).

The DPABI software was used to compare differences in ALFF indices among the four groups. Differences under slow-4 and slow-5 bands were revealed by conducting ANCOVA after controlling for age, gender, education level, and GM volume. A non-parametric permutation test (1,000 permutations) was applied to get control of the false positive rate in the cluster-level inference (Smith and Nichols, 2009). We corrected multiple comparisons of statistical maps to a significant level of $p < 0.05$, with a cluster size of over 1,350 mm^3. We used two-sample T-tests to investigate the differences between every two groups under the significant regions detected in the ANCOVA test after controlling for age, gender, education level, and GM volume. A strict TFCE-FWE was applied to correct the results to a significant level of $p < 0.05$, with a cluster size of over 270 mm^3.

In the DTI analyses, for each metric (i.e., FA, MD, and RA), we performed multiple comparisons between any two matched groups. False discovery rate (FDR) correction was utilized at a threshold of $p < 0.05$.

To note, various neurocognitive assessments were divided into four cognitive domains as mentioned above (see **Supplementary Material** for details). We obtained the composite Z scores of each domain by transforming raw scores into normalized Z scores. After extracting the ROI Series using the REST software (Song et al., 2011), the relationship among altered ALFF values, abnormal white matter integrity, and composite Z scores of each cognitive domain was examined using Pearson's correlation analysis after controlling for the effects of age, gender, and educational level.

Furthermore, all data in this study have been subjected to tests for normality. This study used the Shapiro–Wilk test to assess data normal distribution. To note, all data (age, education level, neuropsychological characteristics, altered ALFF values, and altered white matter integrity) in this study exhibited a normal/Gaussian distribution, except gender.

[2]http://www.nitrc.org/projects/panda

[3]http://fsl.fmrib.ox.ac.uk/fsl

RESULTS

Demographic and Neuropsychological Characteristics

Demographic and neuropsychological characteristics of the four groups can be found in **Table 1**. To begin, SCD scored the highest among the four groups in the SCD-Q test. In comparison with CN, aMCI presented significantly lower scores in MDRS-2, MMSE, and MoCA tests (all $p < 0.05$). The aMCI group exhibited significant deficits in visuospatial function, executive function, episodic memory, and information processing speed (all $p < 0.05$). The aMCI group also showed significantly lower scores in executive function and episodic memory in comparison with the SCD group (all $p < 0.05$). Compared to CN, naMCI displayed lower scores in executive function and information processing speed, while naMCI showed lower scores in executive function, information processing speed, and education level in comparison with SCD (all $p < 0.05$). aMCI displayed lower scores in episodic memory in comparison with naMCI (all $p < 0.05$) (see **Table 1**).

Altered ALFF Values Among CN, SCD, naMCI, and aMCI

Under the slow-4 band, the ANCOVA analysis exhibited significant differences in six brain regions among CN, SCD, naMCI, and aMCI, including the right superior parietal lobule, bilateral lingual gyrus (LING), bilateral superior frontal gyrus (SFG), and right middle frontal gyrus (cluster size $>1{,}350$ mm^3, $p < 0.05$). Compared to CN, SCD, and naMCI displayed an increase in ALFF in the right LING and left SFG, respectively. In comparison with CN, aMCI showed reduced ALFF values in the right middle frontal gyrus and left SFG. Compared to aMCI, naMCI exhibited increased ALFF values in the right LING (cluster size >270 mm^3, $p < 0.05$, TFCE-FWE corrected) (see **Table 2** and **Figure 1**).

Under the slow-5 band, the ANCOVA analysis exhibited significant differences in three brain regions among CN, SCD, naMCI, and aMCI, including the right SFG, right middle frontal gyrus, and right superior parietal lobule/left precuneus (cluster size $>1{,}350$ mm^3, $p < 0.05$). Compared to CN, SCD, and naMCI, aMCI exhibited descended ALFF values in the right SFG, right middle frontal gyrus, and right superior parietal lobule/left precuneus, respectively (cluster size >270 mm^3, $p < 0.05$, TFCE-FWE corrected) (see **Table 2** and **Figure 2**).

Deteriorated White Matter Integrity Among CN, SCD, naMCI, and aMCI

Significant results were mainly present in the superior longitudinal fasciculus (SLF) and uncinate fasciculus (UF) among paired groups. Compared to CN, SCD, and naMCI presented significantly descended FA in the SLF.R. Besides, in comparison with CN, SCD and aMCI exhibited significantly descended MD in the UF.L. Compared to CN, SCD and aMCI also presented significantly descended RA in the UF.L (all $p < 0.05$, FDR corrected) (see **Figure 3**).

Associations Between Aaltered ALFF Values, White Matter Integrity, and Cognition

Significant associations between altered ALFF values and cognition were detected with age, gender, and education level as covariates ($p < 0.05$, Bonferroni corrected). Under the slow-4 band, the ALFF values of the right superior parietal lobule were positively correlated with executive function in the groups of CN and aMCI ($r = 0.6557$, $p = 0.0002$) (see **Figure 4**). Under the slow-5 band, the ALFF values of the right superior parietal lobule/left precuneus were positively correlated with episodic memory within the groups of naMCI and aMCI ($r = 0.4734$, $p = 0.0035$). The ALFF values of the right superior parietal lobule in combination with SCD and aMCI were positively correlated with episodic memory ($r = 0.4866$, $p = 0.0034$) (see **Figure 4**).

Significant associations between altered DTI scores and cognitions were detected with age, gender, and education level as covariates ($p < 0.05$). MD values of the UF.L were positively correlated with executive function in SCD patients ($r = 0.7934$, $p = 0.0188$). RA values of the UF.L were positively correlated with executive function in SCD patients ($r = 0.7571$, $p = 0.0296$). MD values of the UF.L were positively correlated with visuospatial function in SCD patients ($r = 0.7839$, $p = 0.0213$). RA values of the UF.L were positively correlated with visuospatial function in SCD patients ($r = 0.7394$, $p = 0.0360$) (see **Figure 5**).

Significant associations between altered DTI scores and abnormal ALFF values were detected with age, gender, and education level as covariates ($p < 0.05$). Under the slow-4 band, MD values of the UF.L were positively correlated with ALFF values of the left SFG in aMCI patients ($r = 0.4295$, $p = 0.0285$). Besides, RA values of the UF.L were positively correlated with ALFF values of the left SFG in aMCI patients ($r = 0.4049$, $p = 0.0402$) (see **Figure 5**).

DISCUSSION

To the best of our knowledge, our study was the first to combine ALFF detection with DTI analyses and cognition to reveal the inner relationship of CN, SCD, naMCI, and aMCI. Our results discovered ascended ALFF values mainly in SCD and naMCI patients while descended ALFF values in aMCI patients in comparison with the other three groups. aMCI and naMCI patients reflected white matter alterations in the UF and SLF, respectively, while SCD patients exhibited alterations in both fasciculi. To note, the majority of damage was associated with decline in specific cognitive domains. On balance, these results indicate that SCD may act as the preclinical stage of naMCI or aMCI. Besides, aMCI has a divergent deteriorative pattern and degree compared to naMCI. Overall, this study indicates the complicated relationship between structural and functional deterioration and further implies that structural and functional integration may characterize the preclinical AD disease progression.

TABLE 1 | Demographic data of CN, SCD, naMCI, and aMCI.

	CN	SCD	naMCI	aMCI	*F*-values ($\chi 2$)	*P*-values
	***n* = 21**	***n* = 10**	***n* = 15**	***n* = 33**		
Age (years)	57.52 ± 8.072	63.10 ± 8.774	63.87 ± 8.568	66.03 ± 8.579[a]	4.388	0.007
Gender (male/female)	7/14	4/6	6/9	11/22	6.696	0.010
Education level (years)	12.05 ± 2.747	13.85 ± 1.827	10.60 ± 2.694[a]	11.06 ± 3.358	3.086	0.032
MMSE	28.81 ± 1.209	27.70 ± 1.160	28.27 ± 1.710	26.88 ± 2.027[a]	6.156	0.001
MDRS	141.00 ± 2.915	138.80 ± 3.393	137.07 ± 3.432	134.82 ± 7.970[a]	5.193	0.003
MoCA	26.20 ± 2.624	25.00 ± 3.432	24.14 ± 2.931	22.40 ± 3.379[a]	5.357	0.002
Composite Z score of each cognitive domain						
Episodic memory	0.49 ± 0.584	0.57 ± 0.484	0.33 ± 0.532	−0.62 ± 0.549[a,b,c]	25.373	0.000
Information processing speed	0.45 ± 0.759	0.41 ± 0.468	−0.40 ± 0.658[a,b]	−0.22 ± 0.775[a]	6.535	0.001
Executive function	0.45 ± 0.728	0.43 ± 0.504	−0.27 ± 0.489[a,b]	−0.24 ± 0.613[a,b]	7.974	0.000
Visuospatial function	0.26 ± 0.567	0.41 ± 0.446	−0.12 ± 0.681	−0.24 ± 1.011	2.790	0.046

Data are exhibited as mean ± standard deviation (SD). $p < 0.05$ meant significant differences existed among CN, SCD, naMCI, and aMCI. All p-values were achieved through ANOVA analyses except gender (chi square test). Between-group comparisons were further utilized to reveal specific alterations among matched groups ([a]: compared to CN; [b]: compared to SCD; and [c]: compared to naMCI), Bonferroni corrected, $p < 0.05$. CN, normal control; SCD, subjective cognitive decline; naMCI, non-amnestic mild cognitive impairment; aMCI, amnestic mild cognitive impairment; MMSE, Mini-Mental State Examination; MDRS, Mattis Dementia Rating Scale; MoCA, Montreal Cognitive Assessment; ANOVA, analysis of variance.

TABLE 2 | Differences in ALFF under slow-4 and slow-5 bands among CN, SCD, naMCI, and aMCI.

Brain regions (aal)		Peak MNI coordinate			*F*/*T*-values	Cluster size (mm^3)
		x	*y*	*z*		
Slow-4	**ANCOVA**					
	L lingual gyrus	−27	−72	−3	0.117	1512
	R lingual gyrus	12	−90	−15	9.087	2646
	R middle frontal gyrus	57	18	33	6.876	1539
	R superior parietal lobule	27	−66	63	0.133	1890
	L superior frontal gyrus	−12	48	42	4.646	2943
	R superior frontal gyrus	36	0	36	3.465	5859
	CN vs. SCD					
	R lingual gyrus	6	−90	−15	−4.076	324
	CN vs. naMCI					
	R superior frontal gyrus	21	−15	60	−6.766	324
	CN vs. aMCI					
	R middle frontal gyrus	51	30	30	4.418	1107
	L superior frontal gyrus	−18	48	36	3.350	432
	naMCI vs. aMCI					
	L lingual gyrus	−3	−93	−6	3.898	297
Slow-5	**ANCOVA**					
	R superior frontal gyrus	27	60	−6	6.964	3267
	R middle frontal gyrus	30	18	48	6.885	2187
	L superior parietal lobule/L precuneus	−24	−48	66	10.854	2889
	CN vs. aMCI					
	R middle frontal gyrus	36	57	6	3.409	378
	SCD vs. aMCI					
	R superior frontal gyrus	30	18	48	4.114	1404
	naMCI vs. aMCI					
	L superior parietal lobule/L precuneus	−24	−48	66	5.298	1863

All significant results were presented in control of age, gender, and educational level with $p < 0.05$. TFCE-FWE correction was applied for voxel-wised two-sample T-test. To note, cluster size was set over 1,350 mm^3 in ANCOVA analyses and over 270 mm^3 in two-sample T-tests. CN, normal control; SCD, subjective cognitive decline; naMCI, non-amnestic mild cognitive impairment; aMCI, amnestic mild cognitive impairment; ALFF, amplitude of low-frequency fluctuation; ANCOVA, analysis of covariance; AAL, anatomical automatic labeling; MNI, Montreal Neurological Institute; R, right; L, left.

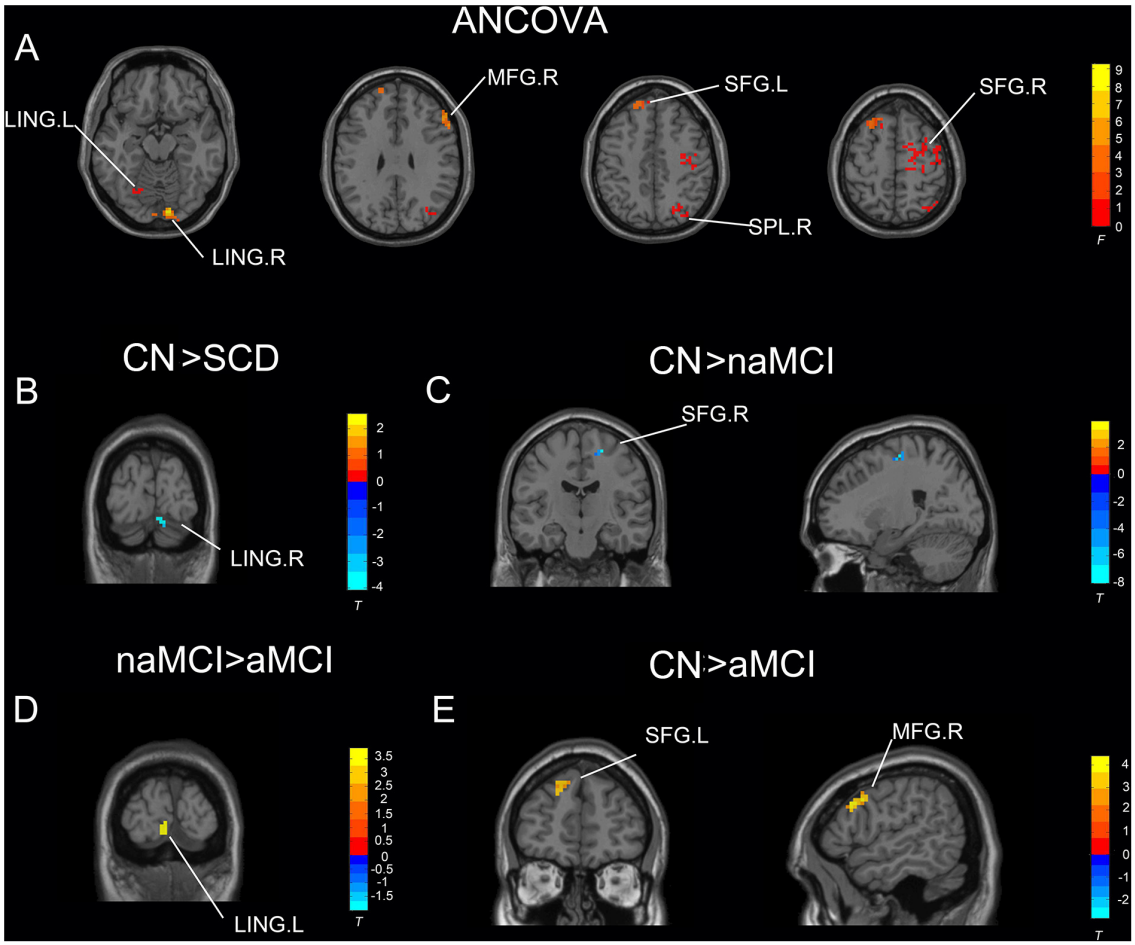

FIGURE 1 | Significant differences in ALFF under the slow-4 band among CN, SCD, naMCI, and aMCI. **(A)** Results of ANCOVA analysis among CN, SCD, naMCI, and aMCI (cluster size >1,350 mm^3, $p < 0.05$). **(B–E)** Results of voxel-wised analyzed two-sample *T*-tests (cluster size >270 mm^3, $p < 0.05$, TFCE-FWE corrected). To note, these analyses set age, gender, educational level, and GM volume as covariates. CN, normal control; SCD, subjective cognitive decline; naMCI, non-amnestic mild cognitive impairment; aMCI, amnestic mild cognitive impairment; ANCOVA, analysis of covariance; SPL, superior parietal lobe; SFG, superior frontal gyrus; LING, lingual gyrus; MFG, middle frontal gyrus. R, right hemisphere; L, left hemisphere.

Convergent Structural and Functional Alterations in SCD and aMCI Patients

As was presented, white matter integrity alterations in the UF within SCD patients were associated with deteriorated executive function and visuospatial function performance. Besides, UF white matter alterations were correlated with descended ALFF values in the SFG within aMCI patients. Descended ALFF values were also detected in the MFG within aMCI patients, which was in close association with deteriorated executive function performance. According to previous studies, the UF serves as a major white matter tract connecting the lateral orbitofrontal cortex and anterior temporal lobes bidirectionally. Due to its bidirectionality, UF alterations may result in both temporal and frontal dysfunction. Studies have discovered decision-making dysfunction and deterioration of specific learning and mnemonic acquisition associated with altered UF values (Von Der Heide et al., 2013; Hein et al., 2018). Furthermore, the MFG and SFG all belong to prefrontal brain regions which are closely connected to the UF. Lower ALFF values represent weakened spontaneous neural activity. Anatomically, white matter degeneration is associated with gray matter atrophy which is correlated with neuronal dysfunction. Our study results further imply the consistency of ALFF value deterioration and DTI alterations. Besides, the rostral area of the MFG has been revealed to be closely related with working memory and executive cognitive function (Barbey et al., 2013). MCI patients have presented executive dysfunction associated with the MFG in previous studies (Zheng et al., 2014; Xue C. et al., 2019). Combined together, it indicates that dysfunctional neuronal activities and altered white matter integrity jointly lead to executive dysfunction. The SFG is usually considered to be strongly connected with working memory (Alagapan et al., 2019). The SFG is also in association with the UF. It is reported that strong connections exist between episodic memory and UF alterations (Platel, 2005; Christidi et al., 2014). We speculate that interaction between the UF and SFG may be potential reasons

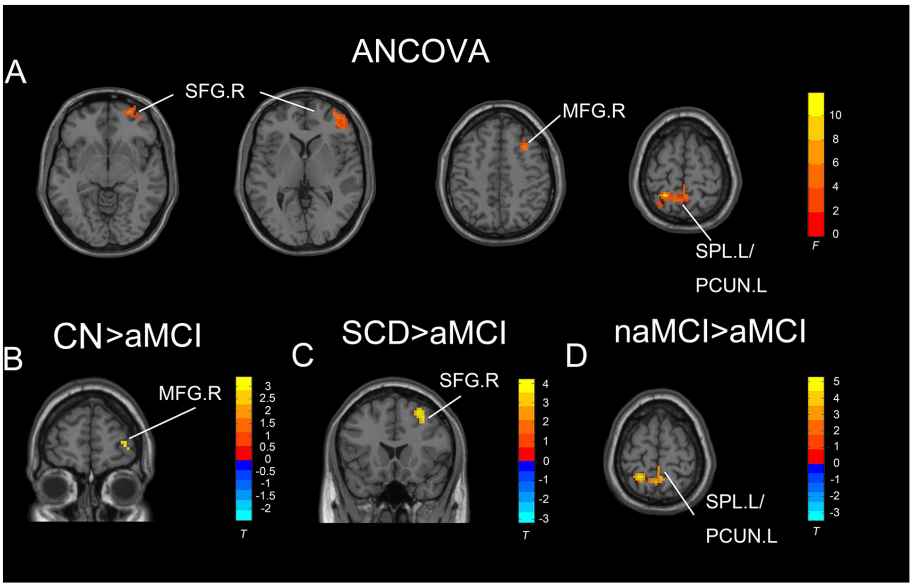

FIGURE 2 | Significant differences in ALFF under the slow-five band among CN, SCD, naMCI, and aMCI. **(A)** Results of ANCOVA analysis among CN, SCD, naMCI, and aMCI (cluster size >1,350 mm^3, $p < 0.05$). **(B–D)** Results of voxel-wised analyzed two-sample *T*-tests (cluster size >270 mm^3, $p < 0.05$, TFCE-FWE corrected). To note, these analyses set age, gender, educational level, and GM volume as covariates. CN, normal control; SCD, subjective cognitive decline; naMCI, non-amnestic mild cognitive impairment; aMCI, amnestic mild cognitive impairment; ANCOVA, analysis of covariance; SPL, superior parietal lobe; SFG, superior frontal gyrus; PCUN, precuneus; MFG, middle frontal gyrus. R, right hemisphere; L, left hemisphere.

for the presented results of dysfunction in episodic memory in the SFG. Notably, compared to SCD and aMCI exhibited a significant decrease in ALFF values in the SFG, which further demonstrates the continuous episodic memory decline from SCD to aMCI in patients.

Altogether, in accordance with these results, we may indicate that SCD and aMCI share convergence in the mechanism of UF alterations. Previous studies have revealed decreased FA values and increased MD values in AD patients (Mayo et al., 2018; Brueggen et al., 2019). Our study, however, discovered decreased MD values. We imply that this may reflect the potential compensatory mechanism. Decreased RA values were also detected in the UF. Few analyses focused on RA alterations in preclinical AD stages. In accordance with multiple sclerosis, Klawiter et al. (2011) discovered that RA alterations were related to demyelination. We speculate this mechanism also exists in preclinical AD stages. Through these UF white matter integrity alterations, which are associated with gray matter damage, prefrontal regions reflect dysfunctional conditions which further lead to comprehensive cognitive decline. Besides, in detail, both SCD and aMCI present similarly deteriorated cognition in episodic memory, indicating that SCD may act as a prodromal stage of aMCI (Li et al., 2016; Yan et al., 2018).

Convergent Structural and Functional Alterations in SCD and naMCI Patients

Significantly decreased FA values were detected in both SCD and naMCI patients in the SLF. The SLF is a major white matter tract between the temporoparietal junction and parietal lobe with the frontal lobe. According to previous studies, the SLF engages in working memory regulation and somatosensory information transference (Hecht et al., 2015; Wang et al., 2016). Our study may prove the convergent deteriorative mechanism between SCD and naMCI in fasciculi. However, no descended ALFF value was detected in SCD and naMCI patients. Several previous animal studies have indicated that white matter damage appears prior to cortical plaques (Desai et al., 2010; Horiuchi et al., 2012). However, a reversed conclusion has been raised with regard to vascular insufficiency. Still, the tight correlation between white matter atrophy and neuronal dysfunction has been confirmed (Nasrabady et al., 2018). Araque Caballero et al. (2018) discovered that regional white matter degeneration occurs years before the onset of symptoms. In accordance with our results, we speculate that in the SLF, structural abnormality may be detected earlier in these two disease stages.

Besides, the LING and SFG presented increased ALFF values in SCD and naMCI patients, respectively. Ewers et al. (2011) reported that neurodegenerative pathology leads to the stimulation of hyper-excited neurons by accumulated amyloid plaques. Increased ALFF values indicate enhanced neuronal connectivity within related brain regions (Di et al., 2013; Yang et al., 2018). Furthermore, the LING belongs to the visual network that is associated with visual processing (Bogousslavsky et al., 1987). The SFG belongs to the prefrontal cortex (PFC) which is in possession of prefrontal working memory activity (Funahashi, 2006; Riley and Constantinidis, 2015) and further predicts the performance of episodic memory (Melrose et al., 2020). Compensation and deterioration of these two regions have been widely detected in previous studies (Kirby et al., 2010;

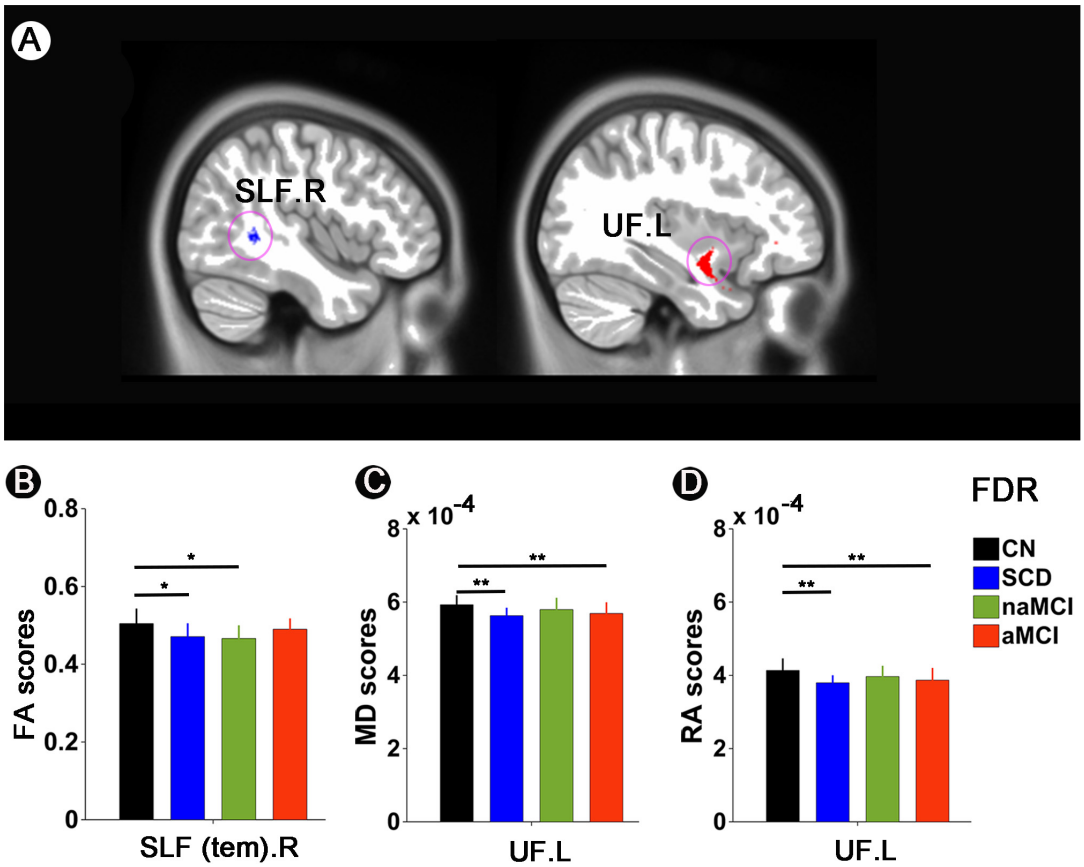

FIGURE 3 | White matter integrity alterations among CN, SCD, naMCI, and aMCI. **(A,B)** FA scores in the SLF.R among CN, SCD, naMCI, and aMCI. **(A,C)** MD scores in the UF.L among CN, SCD, naMCI, and aMCI. **(A,D)** RA scores in the UF.L among CN, SCD, naMCI, and aMCI. */** meant that significance existed between paired groups. All these significant results were corrected applying FDR correction with a threshold of $p < 0.05$ after controlling for age, gender, educational level, and GM volume. CN, normal control; SCD, subjective cognitive decline; naMCI, non-amnestic mild cognitive impairment; aMCI, amnestic mild cognitive impairment. FA, fractional anisotropy; MD, mean diffusivity; RA, relative anisotropy; SLF, superior longitudinal fasciculus; UL, uncinate fasciculus. R, right; L, left.

Kusne et al., 2017; Liu et al., 2017; Zhu et al., 2017). On balance, this phenomenon implies the neuronal plasticity of brain regions, indicating that ALFF may serve as an important role in early functional compensation detection.

Divergent Structural and Functional Alterations in naMCI and aMCI Patients

Non-amnestic mild cognitive impairment patients mainly presented decreased white matter integrity in the SLF. Furthermore, ALFF analyses discovered that naMCI patients exhibited ascended ALFF values in the SFG. These indicate the consistency of brain region requisition in both deterioration and compensation aspects from structural and functional levels, respectively. This may indicate the potential damaging progression of naMCI in the SLF and connected frontal regions according to our results.

Amnestic mild cognitive impairment patients detected deteriorated ALFF values in diverse brain regions (i.e., the MFG, SFG, PCUN, and LING). For DTI analyses, white matter alterations were mostly located in the UF. We detected associations between altered white matter integrity in the UF and ALFF deterioration in the SFG. As is mentioned, we speculate that UF alterations interact with dysfunction in the SFG and MFG. Combined together, structural and functional damage leads to a sharp decline in comprehensive cognition. Descended ALFF values in the MFG are connected with executive dysfunction. Partial MFG belongs to prefrontal regions and is in involved in executive function (Zhao et al., 2016). With the UF participating in execution, we may speculate that functional intercommunication exists between white matter and gray matter.

To note, in comparison with naMCI and aMCI presented significantly descended ALFF values in the PCUN and LING. The LING participates in the visual network. Episodic memory integrates as much sensation as auditory and visual information (Wang et al., 2018). Researchers have discovered that episodic memory performance is related to the LING (Kondo et al., 2005; Stothart et al., 2015; Oishi et al., 2018). The PCUN is the putative pivotal region of default mode network (DMN), which is considered to be associated with self-related cognitive processing (Harrison et al., 2008; Spreng et al., 2009;

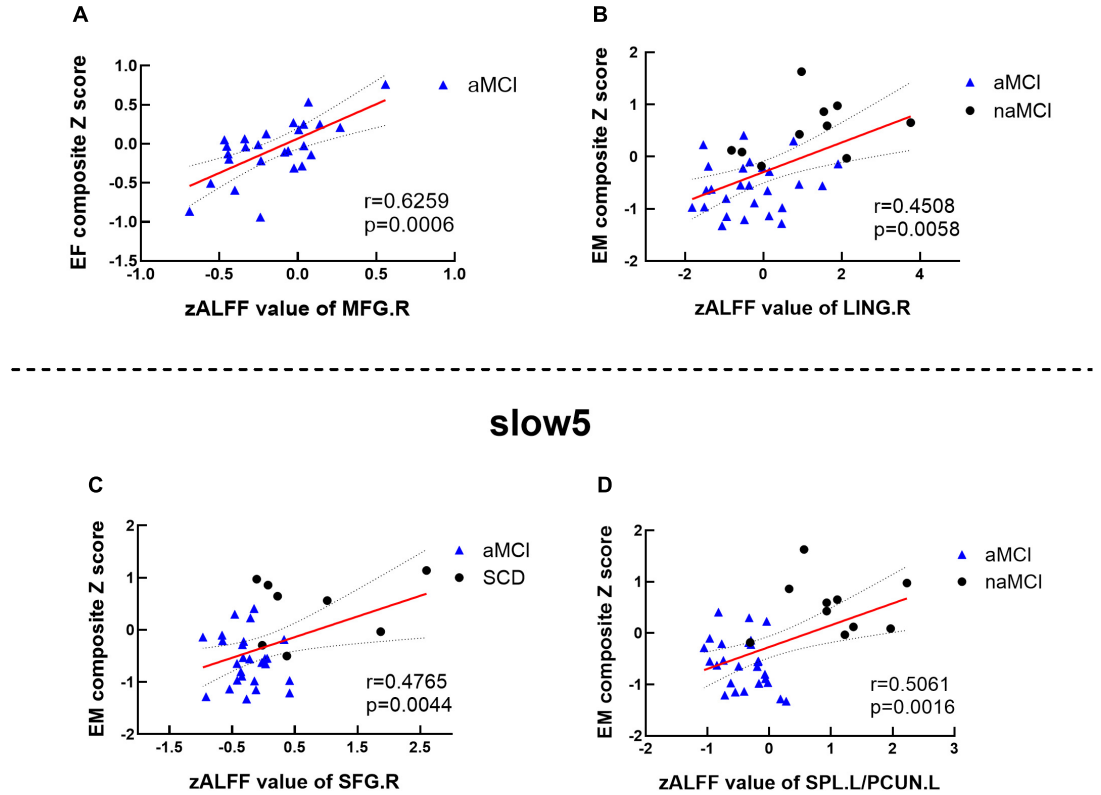

FIGURE 4 | Altered ALFF values associated with cognition. **(A,B)** Significant correlations between ALFF values and cognition among matched groups under the slow-4 band. **(C,D)** Significant correlations between ALFF values and cognition among matched groups under the slow-5 band. These analyses set age, gender, educational level, and GM volume as covariates. All presented results were corrected by utilizing Bonferroni correction with a threshold of $p < 0.05$. EM, episodic memory; EF, executive function. SCD, subjective cognitive decline; naMCI, non-amnestic mild cognitive impairment; aMCI, amnestic mild cognitive impairment. MFG, middle frontal gyrus; LING, lingual gyrus; SFG, superior frontal gyrus; SPL, superior parietal lobe; PCUN, precuneus; R, right; L, left.

Drzezga et al., 2011). This brain region is also regarded to have central roles in episodic memory that declines in early disease progression (Chen et al., 2017). Descended ALFF values have been detected in the PCUN in SCD, MCI, and AD (Liu et al., 2014; Huang et al., 2015; Yang et al., 2018). Our results reflect the association between episodic memory decline and functional deterioration in the LING and PCUN, indicating the potential neuronal network deficiency of aMCI. Furthermore, this further demonstrates that typical cognitive deterioration in aMCI tends to be episodic memory decline in comparison with naMCI. The LING and PCUN may be highly involved in the episodic memory deteriorative mechanism and serve as biomarkers for distinction between naMCI and aMCI.

Furthermore, no related atrophy in white matter with ALFF alterations was found in the PCUN and LING. We speculate that there is still a neuronal compensation mechanism in late aMCI, which can be reflected in the inapparent damage in DTI analyses. However, specific neuronal atrophy has formed. The severity of the disease leads to insufficient compensation, resulting in irreversible dysfunction. Based on this, we imply that early damage to the PCUN has not been well compensated, resulting in the clinical manifestations of decreased episodic memory in aMCI patients.

Overall, aMCI presents decreased white matter integrity in the UF and more severe ALFF alterations compared to naMCI. Therefore, this may indicate that aMCI and naMCI may not only share parallel relationships with distinctly declined cognition. aMCI may act as a more severe disease condition, which is a preclinical AD stage with enhanced research value.

LIMITATIONS

Three limitations became apparent in the study and should be mentioned. First, the sample size was small, which may cause the results to be less reliable. To improve statistical power, a non-parametric permutation test (1,000 permutations) was applied to control the false positive rate in the cluster-level inference. Furthermore, our NBH-ADsnp database continuously recruits volunteers and gets updated. Once enough volunteers are gathered, we will further verify the accuracy of the conclusion.

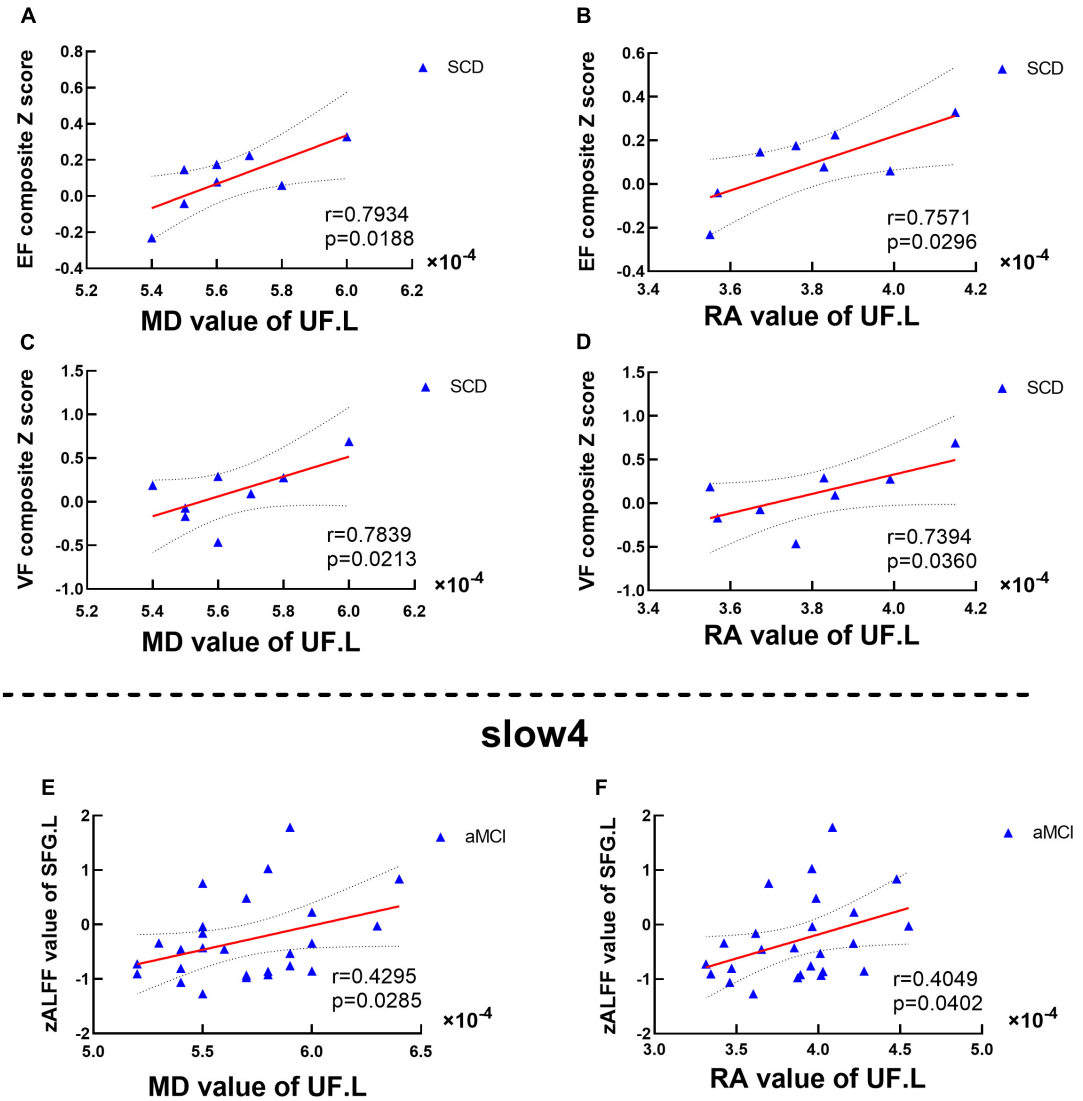

FIGURE 5 | Altered DTI scores associated with abnormal cognition and ALFF values. **(A–D)** Significant correlations between altered DTI scores and cognition. **(E,F)** Significant correlations between altered ALFF values and abnormal DTI scores. This study set age, gender, educational level, and GM volume as covariates.EF, executive function; VF, visuospatial function. SFG, superior frontal gyrus; SCD, subjective cognitive decline; aMCI, amnestic mild cognitive impairment. MD, mean diffusivity; RA, relative anisotropy; UL, uncinate fasciculus. L, left.

Second, individual differences existed in age as well as education levels among CN, SCD, naMCI, and aMCI. Although all these were used as covariates to maintain the accuracy and reliability of the study, follow-ups have been performed to further reduce this effect and confirm the conclusions reached today in the following studies. Finally, this study only used ALFF to reveal the underlying pathological mechanism of AD disease progression. Yang and colleagues have indicated that fractional fALFF (fALFF) can reduce the impact of respiration, cardiac action, or motion while other studies have suggested that ALFF has higher reliability than fALFF (Zuo et al., 2010; Yang et al., 2018). Indeed, both indicators have their strengths and weaknesses (Zuo et al., 2010). Furthermore, Han and colleagues have emphasized that both ALFF and fALFF are useful and sensitive indexes for the detection of the pathological mechanism of AD-related neurodegeneration (Han et al., 2011). Therefore, in the future, we will expand the sample to further verify the validity of our conclusions and analyze both ALFF and fALFF for an in-depth and comprehensive understanding of the underlying pathological mechanism of AD disease progression.

CONCLUSION

Subjective cognitive decline presents the joint deteriorative characteristics of aMCI and naMCI and tends to convert to either aMCI and naMCI. Besides, aMCI has a divergent deteriorative

pattern and degree compared to naMCI. Overall, this study further indicates that abnormalities in specific white matter fibers may be the structural basis of brain activation in preclinical AD stages, which may contribute to cognitive decline. Structural and functional integration can together characterize the preclinical AD disease progression.

DATA AVAILABILITY STATEMENT

The raw data supporting the conclusions of this article will be made available by the authors, without undue reservation.

ETHICS STATEMENT

The studies involving human participants were reviewed and approved by the responsible Human Participants Ethics Committee of The Affiliated Nanjing Brain Hospital. The patients/participants provided their written informed consent to participate in this study.

AUTHOR CONTRIBUTIONS

XZ and JC designed the study. SW, CX, YY, GH, WQ, WM, and JR collected the data. SW, FZ, and JC analyzed the data and prepared the manuscript. All authors contributed to the article and approved the submitted version.

FUNDING

This study was supported by the National Natural Science Foundation of China (Nos. 81701675, 2018YFC1314300, 81971255, and 81700666); the Key Project supported by Medical Science and technology development Foundation, Nanjing Department of Health (No. JQX18005); the Cooperative Research Project of Southeast University-Nanjing Medical University (No. 2018DN0031); the Key Research and Development Plan (Social Development) Project of Jiangsu Province (Nos. BE2018608 and BE2019610); the Innovation and Entrepreneurship Training Program for College Students in Jiangsu Province (Nos. 201810312061X and 201910312035Z); the Key Scientific Research Projects of Colleges and Universities in Henan Province (No. 18A190003); and the Jiangsu Provincial Natural Science Foundation-Youth Foundation Projects (BK20180370).

SUPPLEMENTARY MATERIAL

The Supplementary Material for this article can be found online at: https://www.frontiersin.org/articles/10.3389/fnhum.2021.625232/full#supplementary-material

REFERENCES

Alagapan, S., Lustenberger, C., Hadar, E., Shin, H. W., and Frhlich, F. (2019). Low-frequency direct cortical stimulation of left superior frontal gyrus enhances working memory performance. *Neuroimage* 184, 697–706. doi: 10.1016/j.neuroimage.2018.09.064

Alonso-Solis, A., Vives-Gilabert, Y., Portella, M. J., Rabella, M., Grasa, E. M., Roldan, A., et al. (2017). Altered amplitude of low frequency fluctuations in schizophrenia patients with persistent auditory verbal hallucinations. *Schizophr. Res.* 189, 97–103. doi: 10.1016/j.schres.2017.01.042

Araque Caballero, M. Á, Suárez-Calvet, M., Duering, M., Franzmeier, N., Benzinger, T., Fagan, A. M., et al. (2018). White matter diffusion alterations precede symptom onset in autosomal dominant Alzheimer's disease. *J. Neurol.* 141, 3065–3080. doi: 10.1093/brain/awy229

Barbey, A. K., Koenigs, M., and Grafman, J. (2013). Dorsolateral prefrontal contributions to human working memory. *Cortex* 49, 1195–1205. doi: 10.1016/j.cortex.2012.05.022

Beauchet, O., Launay, C. P., Fantino, B., Annweiler, C., and Allali, G. (2015). Episodic memory and executive function impairments in non-demented older adults: which are the respective and combined effects on gait performances? *Age* 37:9812. doi: 10.1007/s11357-015-9812-y

Biswal, B., Yetkin, F. Z., Haughton, V. M., and Hyde, J. S. (1995). Functional connectivity in the motor cortex of resting human brain using echo-planar MRI. *Magn. Reson. Med.* 34, 537–541. doi: 10.1002/mrm.1910340409

Bogousslavsky, J., Miklossy, J., Deruaz, J. P., Assal, G., and Regli, F. (1987). Lingual and fusiform gyri in visual processing: a clinico-pathologic study of superior altitudinal hemianopia. *J. Neurol. Neurosurg. Psychiatry* 50, 607–614. doi: 10.1136/jnnp.50.5.607

Brueggen, K., Dyrba, M., Cardenas-Blanco, A., Schneider, A., Fliessbach, K., Buerger, K., et al. (2019). Structural integrity in subjective cognitive decline, mild cognitive impairment and Alzheimer's disease based on multicenter diffusion tensor imaging. *J. Neurol.* 266, 2465–2474. doi: 10.1007/s00415-019-09429-3

Buzsaki, G., and Draguhn, A. (2004). Neuronal oscillations in cortical networks. *Science* 304, 1926–1929. doi: 10.1126/science.1099745

Chandra, A., Dervenoulas, G., Politis, M., and Alzheimer's Disease Neuroimaging Initiative (2019). Magnetic resonance imaging in Alzheimer's disease and mild cognitive impairment. *J. Neurol.* 266, 1293–1302. doi: 10.1007/s00415-018-9016-3

Chen, J., Ma, N., Hu, G., Nousayhah, A., Xue, C., Qi, W., et al. (2020). rTMS modulates precuneus-hippocampal subregion circuit in patients with subjective cognitive decline. *Aging* 13, 1314–1331. doi: 10.18632/aging.202313

Chen, J., Shu, H., Wang, Z., Liu, D., Shi, Y., Xu, L., et al. (2016a). Protective effect of APOE epsilon 2 on intrinsic functional connectivity of the entorhinal cortex is associated with better episodic memory in elderly individuals with risk factors for Alzheimer's disease. *Oncotarget* 7, 58789–58801. doi: 10.18632/oncotarget.11289

Chen, J., Shu, H., Wang, Z., Zhan, Y., Liu, D., Liao, W., et al. (2016b). Convergent and divergent intranetwork and internetwork connectivity patterns in patients with remitted late-life depression and amnestic mild cognitive impairment. *Cortex* 83, 194–211. doi: 10.1016/j.cortex.2016.08.001

Chen, Y., Liu, Z., Zhang, J., Chen, K., Yao, L., Li, X., et al. (2017). Precuneus degeneration in nondemented elderly individuals with APOE varepsilon4: evidence from structural and functional MRI analyses. *Hum. Brain Mapp.* 38, 271–282. doi: 10.1002/hbm.23359

Christidi, F., Zalonis, I., Kyriazi, S., Rentzos, M., Karavasilis, E., Wilde, E. A., et al. (2014). Uncinate fasciculus microstructure and verbal episodic memory in amyotrophic lateral sclerosis: a diffusion tensor imaging and neuropsychological study. *Brain Imaging Behav.* 8, 497–505. doi: 10.1007/s11682-013-9271-y

Desai, M. K., Mastrangelo, M. A., Ryan, D. A., Sudol, K. L., Narrow, W. C., and Bowers, W. J. (2010). Early oligodendrocyte/myelin pathology in Alzheimer's disease mice constitutes a novel therapeutic target. *Am. J. Pathol.* 177, 1422–1435. doi: 10.2353/ajpath.2010.100087

Di, X., Kim, E. H., Huang, C. C., Tsai, S. J., Lin, C. P., and Biswal, B. B. (2013). The influence of the amplitude of low-frequency fluctuations on resting-state

functional connectivity. *Front. Hum. Neurosci.* 7:118. doi: 10.3389/fnhum.2013.00118

Dillen, K. N. H., Jacobs, H. I. L., Kukolja, J., Richter, N., von Reutern, B., Onur, O. A., et al. (2017). Functional disintegration of the default mode network in prodromal Alzheimer's disease. *J. Alzheimers Dis*. 59, 169–187. doi: 10.3233/JAD-161120

Drzezga, A., Becker, J. A., Van Dijk, K. R., Sreenivasan, A., Talukdar, T., Sullivan, C., et al. (2011). Neuronal dysfunction and disconnection of cortical hubs in non-demented subjects with elevated amyloid burden. *Brain* 134, 1635–1646. doi: 10.1093/brain/awr066

Dumont, M., Roy, M., Jodoin, P. M., Morency, F. C., Houde, J. C., Xie, Z., et al. (2019). Free water in white matter differentiates MCI and AD from control subjects. *Front. Aging Neurosci*. 11:270. doi: 10.3389/fnagi.2019.00270

Ewers, M., Sperling, R. A., Klunk, W. E., Weiner, M. W., and Hampel, H. (2011). Neuroimaging markers for the prediction and early diagnosis of Alzheimer's disease dementia. *Trends Neurosci*. 34, 430–442. doi: 10.1016/j.tins.2011.05.005

Fox, M. D., and Raichle, M. E. (2007). Spontaneous fluctuations in brain activity observed with functional magnetic resonance imaging. *Nat. Rev. Neurosci*. 8, 700–711. doi: 10.1038/nrn2201

Funahashi, S. (2006). Prefrontal cortex and working memory processes. *Neuroscience* 139, 251–261. doi: 10.1016/j.neuroscience.2005.07.003

Golestani, A. M., Kwinta, J. B., Khatamian, Y. B., and Chen, J. J. (2017). The effect of low-frequency physiological correction on the reproducibility and specificity of resting-state fMRI metrics: functional connectivity, ALFF, and ReHo. *Front. Neurosci*. 11:546. doi: 10.3389/fnins.2017.00546

Gupta, Y., Kim, J. I., Kim, B. C., and Kwon, G. R. (2020). Classification and graphical analysis of Alzheimer's disease and its prodromal stage using multimodal features from structural, diffusion, and functional neuroimaging data and the APOE genotype. *Front. Aging Neurosci*. 12:238. doi: 10.3389/fnagi.2020.00238

Han, Y., Wang, J., Zhao, Z., Min, B., Lu, J., Li, K., et al. (2011). Frequency-dependent changes in the amplitude of low-frequency fluctuations in amnestic mild cognitive impairment: a resting-state fMRI study. *Neuroimage* 55, 287–295. doi: 10.1016/j.neuroimage.2010.11.059

Hao, L., Xing, Y., Li, X., Mu, B., Zhao, W., Wang, G., et al. (2019). Risk factors and neuropsychological assessments of subjective cognitive decline () in chinese memory clinic. *Front. Neurosci*. 13:846. doi: 10.3389/fnins.2019.00846

Hare, S. M., Ford, J. M., Ahmadi, A., Damaraju, E., Belger, A., Bustillo, J., et al. (2017). Modality-dependent impact of hallucinations on low-frequency fluctuations in schizophrenia. *Schizophr. Bull*. 43, 389–396. doi: 10.1093/schbul/sbw093

Harrison, B. J., Pujol, J., Lopez-Sola, M., Hernandez-Ribas, R., Deus, J., Ortiz, H., et al. (2008). Consistency and functional specialization in the default mode brain network. *Proc Natl. Acad. Sci. U.S.A*. 105, 9781–9786. doi: 10.1073/pnas.0711791105

Hecht, E. E., Gutman, D. A., Bradley, B. A., Preuss, T. M., and Stout, D. (2015). Virtual dissection and comparative connectivity of the superior longitudinal fasciculus in chimpanzees and humans. *Neuroimage* 108, 124–137. doi: 10.1016/j.neuroimage.2014.12.039

Hein, T. C., Mattson, W. I., Dotterer, H. L., Mitchell, C., Lopez-Duran, N., Thomason, M. E., et al. (2018). Amygdala habituation and uncinate fasciculus connectivity in adolescence: a multi-modal approach. *Neuroimage* 183, 617–626. doi: 10.1016/j.neuroimage.2018.08.058

Horiuchi, M., Maezawa, I., Itoh, A., Wakayama, K., Jin, L. W., Itoh, T., et al. (2012). Amyloid β1-42 oligomer inhibits myelin sheet formation in vitro. *Neurobiol. Aging* 33, 499–509. doi: 10.1016/j.neurobiolaging.2010.05.007

Huang, J., Bai, F., Yang, X., Chen, C., Bao, X., and Zhang, Y. (2015). Identifying brain functional alterations in postmenopausal women with cognitive impairment. *Maturitas* 81, 371–376. doi: 10.1016/j.maturitas.2015.04.006

Jessen, F., Amariglio, R. E., van Boxtel, M., Breteler, M., Ceccaldi, M., Chételat, G., et al. (2014). A conceptual framework for research on subjective cognitive decline in preclinical Alzheimer's disease. *Alzheimers Dement*. 10, 844–852. doi: 10.1016/j.jalz.2014.01.001

Kirby, E., Bandelow, S., and Hogervorst, E. (2010). Visual impairment in Alzheimer's disease: a critical review. *J. Alzheimers Dis*. 21, 15–34. doi: 10.3233/JAD-2010-080785

Klawiter, E. C., Schmidt, R. E., Trinkaus, K., Liang, H. F., Budde, M. D., Naismith, R. T., et al. (2011). Radial diffusivity predicts demyelination in ex vivo multiple sclerosis spinal cords. *Neuroimage* 55, 1454–1460. doi: 10.1016/j.neuroimage.2011.01.007

Kondo, Y., Suzuki, M., Mugikura, S., Abe, N., Takahashi, S., Iijima, T., et al. (2005). Changes in brain activation associated with use of a memory strategy: a functional MRI study. *Neuroimage* 24, 1154–1163. doi: 10.1016/j.neuroimage.2004.10.033

Kuang, L., Han, X., Chen, K., Caselli, R. J., Reiman, E. M., Wang, Y., et al. (2019). A concise and persistent feature to study brain resting-state network dynamics: findings from the Alzheimer's disease neuroimaging initiative. *Hum. Brain Mapp*. 40, 1062–1081. doi: 10.1002/hbm.24383

Kusne, Y., Wolf, A. B., Townley, K., Conway, M., and Peyman, G. A. (2017). Visual system manifestations of Alzheimer's disease. *Acta Ophthalmol*. 95, e668–e676. doi: 10.1111/aos.13319

Li, X. Y., Tang, Z. C., Sun, Y., Tian, J., Liu, Z. Y., and Han, Y. (2016). White matter degeneration in subjective cognitive decline: a diffusion tensor imaging study. *Oncotarget* 7, 54405–54414. doi: 10.18632/oncotarget.10091

Liu, X., Chen, W., Hou, H., Chen, X., Zhang, J., Liu, J., et al. (2017). Decreased functional connectivity between the dorsal anterior cingulate cortex and lingual gyrus in Alzheimer's disease patients with depression. *Behav. Brain Res*. 326, 132–138. doi: 10.1016/j.bbr.2017.01.037

Liu, X., Wang, S., Zhang, X., Wang, Z., Tian, X., and He, Y. (2014). Abnormal amplitude of low-frequency fluctuations of intrinsic brain activity in Alzheimer's disease. *J. Alzheimers Dis*. 40, 387–397. doi: 10.3233/JAD-131322

Lu, H., Zuo, Y., Gu, H., Waltz, J. A., Zhan, W., Scholl, C. A., et al. (2007). Synchronized delta oscillations correlate with the resting-state functional MRI signal. *Proc. Natl. Acad. Sci. U.S.A*. 104, 18265–18269. doi: 10.1073/pnas.0705791104

Mayo, C. D., Garcia-Barrera, M. A., Mazerolle, E. L., Ritchie, L. J., Fisk, J. D., and Gawryluk, J. R. (2018). Relationship between DTI metrics and cognitive function in Alzheimer's disease. *Front. Aging Neurosci*. 10:436. doi: 10.3389/fnagi.2018.00436

Melrose, R. J., Zahniser, E., Wilkins, S. S., Veliz, J., Hasratian, A. S., Sultzer, D. L., et al. (2020). Prefrontal working memory activity predicts episodic memory performance: a neuroimaging study. *Behav. Brain Res*. 379:112307. doi: 10.1016/j.bbr.2019.112307

Nasrabady, S. E., Rizvi, B., Goldman, J. E., and Brickman, A. M. (2018). White matter changes in Alzheimer's disease: a focus on myelin and oligodendrocytes. *Acta Neuropathol. Commun*. 6:22. doi: 10.1186/s40478-018-0515-3

Nir, T. M., Jahanshad, N., Villalon-Reina, J. E., Toga, A. W., Jack, C. R., Weiner, M. W., et al. (2013). Effectiveness of regional DTI measures in distinguishing Alzheimer's disease, MCI, and normal aging. *NeuroImage. Clin*. 3, 180–195. doi: 10.1016/j.nicl.2013.07.006

Oishi, Y., Imamura, T., Shimomura, T., and Suzuki, K. (2018). Visual texture agnosia in dementia with Lewy bodies and Alzheimer's disease. *Cortex* 103, 277–290. doi: 10.1016/j.cortex.2018.03.018

Petersen, R. C., Doody, R., Kurz, A., Mohs, R. C., Morris, J. C., Rabins, P. V., et al. (2001). Current concepts in mild cognitive impairment. *Arch. Neurol*. 58, 1985–1992.

Petersen, R. C., Roberts, R. O., Knopman, D. S., Boeve, B. F., Geda, Y. E., Ivnik, R. J., et al. (2009). Mild cognitive impairment: ten years later. *Arch. Neurol*. 66, 1447–1455. doi: 10.1001/archneurol.2009.266

Platel, H. (2005). Functional neuroimaging of semantic and episodic musical memory. *Ann. N. Y. Acad. Sci*. 1060, 136–147. doi: 10.1196/annals.1360.010

Power, M. C., Su, D., Wu, A., Reid, R. I., Jack, C. R., Knopman, D. S., et al. (2019). Association of white matter microstructural integrity with cognition and dementia. *Neurobiol. Aging* 83, 63–72. doi: 10.1016/j.neurobiolaging.2019.08.021

Rabin, L. A., Smart, C. M., and Amariglio, R. E. (2017). Subjective cognitive decline in preclinical Alzheimer's disease. *Ann. Rev. Clin. Psychol*. 13, 369–396. doi: 10.1146/annurev-clinpsy-032816-045136

Ramanan, S., Bertoux, M., Flanagan, E., Irish, M., Piguet, O., Hodges, J. R., et al. (2017). Longitudinal executive function and episodic memory profiles in behavioral-variant frontotemporal dementia and Alzheimer's disease. *J. Int. Neuropsychol. Soc*. 23, 34–43. doi: 10.1017/S1355617716000837

Ren, P., Lo, R. Y., Chapman, B. P., Mapstone, M., Porsteinsson, A., and Lin, F. (2016). Longitudinal alteration of intrinsic brain activity in the striatum in mild cognitive impairment. *J. Alzheimers Dis.* 54, 69–78. doi: 10.3233/JAD-160368

Riley, M. R., and Constantinidis, C. (2015). Role of prefrontal persistent activity in working memory. *Front. Syst. Neurosci.* 9:181. doi: 10.3389/fnsys.2015.00181

Smith, S. M., and Nichols, T. E. (2009). Threshold-free cluster enhancement: addressing problems of smoothing, threshold dependence and localisation in cluster inference. *Neuroimage* 44, 83–98. doi: 10.1016/j.neuroimage.2008.03.061

Song, X. W., Dong, Z. Y., Long, X. Y., Li, S. F., Zuo, X. N., Zhu, C. Z., et al. (2011). REST: a toolkit for resting-state functional magnetic resonance imaging data processing. *PLoS One* 6:e25031. doi: 10.1371/journal.pone.0025031

Spreng, R. N., Mar, R. A., and Kim, A. S. (2009). The common neural basis of autobiographical memory, prospection, navigation, theory of mind, and the default mode: a quantitative meta-analysis. *J. Cogn. Neurosci.* 21, 489–510. doi: 10.1162/jocn.2008.21029

Stothart, G., Kazanina, N., Naatanen, R., Haworth, J., and Tales, A. (2015). Early visual evoked potentials and mismatch negativity in Alzheimer's disease and mild cognitive impairment. *J. Alzheimers Dis.* 44, 397–408. doi: 10.3233/JAD-140930

Teipel, S. J., Kuper-Smith, J. O., Bartels, C., Brosseron, F., Buchmann, M., Buerger, K., et al. (2019). Multicenter tract-based analysis of microstructural lesions within the Alzheimer's disease spectrum: association with amyloid pathology and diagnostic usefulness. *J. Alzheimers Dis.* 72, 455–465. doi: 10.3233/JAD-190446

Von Der Heide, R. J., Skipper, L. M., Klobusicky, E., and Olson, I. R. (2013). Dissecting the uncinate fasciculus: disorders, controversies and a hypothesis. *J. Neurol.* 136, 1692–1707. doi: 10.1093/brain/awt094

Vos, S. J. B., van Rossum, I. A., Verhey, F., Knol, D. L., Soininen, H., Wahlund, L. O., et al. (2013). Prediction of Alzheimer disease in subjects with amnestic and nonamnestic MCI. *Neurology* 80, 1124–1132. doi: 10.1212/WNL.0b013e318288690c

Vos, S. J. B., Verhey, F., Frölich, L., Kornhuber, J., Wiltfang, J., Maier, W., et al. (2015). Prevalence and prognosis of Alzheimer's disease at the mild cognitive impairment stage. *J. Neurol.* 138, 1327–1338. doi: 10.1093/brain/awv029

Wang, D., Clouter, A., Chen, Q., Shapiro, K. L., and Hanslmayr, S. (2018). Single-trial phase entrainment of theta oscillations in sensory regions predicts human associative memory performance. *J. Neurosci.* 38, 6299–6309. doi: 10.1523/JNEUROSCI.0349-18.2018

Wang, X., Pathak, S., Stefaneanu, L., Yeh, F. C., Li, S., and Fernandez-Miranda, J. C. (2016). Subcomponents and connectivity of the superior longitudinal fasciculus in the human brain. *Brain Struct. Funct.* 221, 2075–2092. doi: 10.1007/s00429-015-1028-5

Wilcockson, T. D. W., Mardanbegi, D., Xia, B., Taylor, S., Sawyer, P., Gellersen, H. W., et al. (2019). Abnormalities of saccadic eye movements in dementia due to Alzheimer's disease and mild cognitive impairment. *Aging* 11, 5389–5398. doi: 10.18632/aging.102118

Xue, C., Yuan, B., Yue, Y., Xu, J., Wang, S., Wu, M., et al. (2019). Distinct disruptive patterns of default mode subnetwork connectivity across the spectrum of preclinical Alzheimer's disease. *Front. Aging Neurosci.* 11:307. doi: 10.3389/fnagi.2019.00307

Xue, J., Guo, H., Gao, Y., Wang, X., Cui, H., Chen, Z., et al. (2019). Altered directed functional connectivity of the hippocampus in mild cognitive impairment and Alzheimer's disease: a resting-state fMRI study. *Front. Aging Neurosci.* 11:326. doi: 10.3389/fnagi.2019.00326

Yan, C. G., Wang, X. D., Zuo, X. N., and Zang, Y. F. (2016). DPABI: data processing & analysis for (resting-state) brain imaging. *Neuroinformatics* 14, 339–351. doi: 10.1007/s12021-016-9299-4

Yan, T., Wang, W., Yang, L., Chen, K., Chen, R., and Han, Y. (2018). Rich club disturbances of the human connectome from subjective cognitive decline to Alzheimer's disease. *Theranostics* 8, 3237–3255. doi: 10.7150/thno.23772

Yang, L., Yan, Y., Li, Y., Hu, X., Lu, J., Chan, P., et al. (2019). Frequency-dependent changes in fractional amplitude of low-frequency oscillations in Alzheimer's disease: a resting-state fMRI study. *Brain Imaging Behav.* 14, 2187–2201. doi: 10.1007/s11682-019-00169-6

Yang, L., Yan, Y., Wang, Y., Hu, X., Lu, J., Chan, P., et al. (2018). Gradual disturbances of the amplitude of low-frequency fluctuations (ALFF) and fractional ALFF in Alzheimer spectrum. *Front. Neurosci.* 12:975. doi: 10.3389/fnins.2018.00975

Zhang, X., Sun, Y., Li, W., Liu, B., Wu, W., Zhao, H., et al. (2019). Characterization of white matter changes along fibers by automated fiber quantification in the early stages of Alzheimer's disease. *NeuroImage Clin.* 22:101723. doi: 10.1016/j.nicl.2019.101723

Zhao, J., Liu, J., Jiang, X., Zhou, G., Chen, G., Ding, X. P., et al. (2016). Linking resting-state networks in the prefrontal cortex to executive function: a functional near infrared spectroscopy study. *Front. Neurosci.* 10:452. doi: 10.3389/fnins.2016.00452

Zheng, D., Sun, H., Dong, X., Liu, B., Xu, Y., Chen, S., et al. (2014). Executive dysfunction and gray matter atrophy in amnestic mild cognitive impairment. *Neurobiol. Aging* 35, 548–555. doi: 10.1016/j.neurobiolaging.2013.09.007

Zhu, H., Xu, J., Li, J., Peng, H., Cai, T., Li, X., et al. (2017). Decreased functional connectivity and disrupted neural network in the prefrontal cortex of affective disorders: a resting-state fNIRS study. *J. Affect. Disord.* 221, 132–144. doi: 10.1016/j.jad.2017.06.024

Zuo, X. N., Di Martino, A., Kelly, C., Shehzad, Z. E., Gee, D. G., Klein, D. F., et al. (2010). The oscillating brain: complex and reliable. *Neuroimage* 49, 1432–1445. doi: 10.1016/j.neuroimage.2009.09.037

Conflict of Interest: The authors declare that the research was conducted in the absence of any commercial or financial relationships that could be construed as a potential conflict of interest.

frontiers in Psychiatry

BRIEF RESEARCH REPORT
published: 18 February 2021
doi: 10.3389/fpsyt.2021.626479

Intermittent Theta-Burst Stimulation Over the DorsoLateral PreFrontal Cortex (DLPFC) in Healthy Subjects Produces No Cumulative Effect on Cortical Excitability

Noomane Bouaziz[1]*, *Charles Laidi*[2], *Fanny Thomas*[1], *Palmyre Schenin-King Andrianisaina*[1], *Virginie Moulier*[1,3] and *Dominique Januel*[1]

[1] Unité de recherche clinique, Pôle 93G03, EPS de Ville Evrard, Neuilly sur Marne, France, [2] Pôle de Psychiatrie, Assistance Publique-Hôpitaux de Paris, Faculté de Médecine de Créteil, DMU IMPACT, Hôpitaux Universitaires Mondor, Créteil, France, [3] Service hospitalo-universitaire de psychiatrie adulte, CH du Rouvray, Sotteville-lès-Rouen, France

OPEN ACCESS

Edited by:
Hongming Li, University of Pennsylvania, United States

Reviewed by:
Wei-Peng Teo, Nanyang Technological University, Singapore
Angela Maria Sanna, University of Cagliari, Italy

***Correspondence:**
Noomane Bouaziz
bouaziznoomane@gmail.com

Specialty section:
This article was submitted to Neuroimaging and Stimulation, a section of the journal Frontiers in Psychiatry

Received: *05 November 2020*
Accepted: *28 January 2021*
Published: *18 February 2021*

Citation:
Bouaziz N, Laidi C, Thomas F, Schenin-King Andrianisaina P, Moulier V and Januel D (2021) Intermittent Theta-Burst Stimulation Over the DorsoLateral PreFrontal Cortex (DLPFC) in Healthy Subjects Produces No Cumulative Effect on Cortical Excitability. Front. Psychiatry 12:626479. doi: 10.3389/fpsyt.2021.626479

Background: Intermittent Theta Burst Stimulation (iTBS) is a design of repetitive Transcranial Magnetic Stimulation (rTMS) and could be a candidate to replace rTMS in the treatment of depression, thanks to its efficacy, shorter duration, and ease of use. The antidepressant mechanism of iTBS, and whether this mechanism is mediated by a modulation of cortical excitability, remains unknown.

Methods: Using a randomized double-blind, sham-controlled trial, 30 healthy volunteers received either iTBS or a sham treatment targeting the left DorsoLateral PreFrontal Cortex (L-DLPFC), twice a day over 5 consecutive days. Cortical excitability was measured before and after the 5 days of stimulation.

Results: No difference in cortical excitability was observed between active or sham iTBS.

Conclusion: Our study does not support any effect on cortical excitability of repetitive iTBS targeting the L-DLPFC.

Keywords: neuro modulation, iTBS, rTMS (repetitive transcranial magnetic stimulation), cortical excitability transcranial magnetic stimulation, neuroexcitability, depression

INTRODUCTION

Repeated Transcranial Magnetic Stimulation (rTMS) is a validated non-invasive brain stimulation technique used to treat resistant depression (1).

Intermittent Theta Burst Stimulation (iTBS) is a design of rTMS that uses a very highly modulated frequency to produce a high number of pulses in a shorter time. This increases cortical excitability in a more robust and longer lasting way than rTMS, and in a similar way to High-Frequency (HF) rTMS (2).

Several studies have reported that iTBS is non-inferior to the gold standard 10 Hz rTMS in the treatment of major depression (3, 4). Furthermore, one session of iTBS lasts only 3 min, making it more acceptable to participants than longer lasting protocols such as 10 Hz rTMS, which can last 20–40 min (5).

The exact neurobiological mechanisms of iTBS/rTMS that lead to an antidepressant effect remain unknown.

Some etiologies of depression involve an imbalance of inter-hemispheric neuroexcitability. This imbalance has been identified in the dorsolateral prefrontal cortex (DLPFC) via imaging and EEG studies. This has justified the use of high-frequency (HF) rTMS targeting the left DLPFC to treat major depressive episodes (6, 7). Other studies have identified this imbalance as hypoexcitability of the left motor cortex. Some studies relate this hypoexcitability to an increase in the left rMT in patients with depression compared to healthy subjects (7–9). Other studies report that in patients with depression, the rMT of the left motor cortex was higher than that of the contralateral motor cortex (9, 10). In 2006, Bajbouj et al. (11) reported that the rMT of the left cortex was higher than that of the right cortex in depressed patients, whereas in healthy subjects this phenomenon was reversed. This suggests that, in patients with depression, there is an overall deficit of any excitability in the left hemisphere (7). This possibility has also been supported by other authors (12). Nevertheless, as cortical excitability is specifically related to the motor cortex, there is limited evidence that the enhancement of the excitability of the DLPFC using rTMS/iTBS could result in the same effect in the ipsilateral motor cortex.

We have thus stipulated that the remission of depressive symptoms after an increase in DLPFC excitability via HF rTMS (or iTBS) could also lead to a similar increase in the excitability of the ipsilateral motor cortex. A study by Spampinato et al. (13) supports this hypothesis by reporting that the antidepressant efficacy of HF rTMS (10 HZ) targeting the ipsilateral DLPFC was associated with a decrease in the ipsilateral rMT. The same authors hypothesized that an overall pro-excitability effect of HF rtMS would be mediated by the Long-Term Potentiation (LTP) phenomenon. Triggs et al. (14) also reported a significant decrease in the left rMT in ten patients with depression after a two-week open-label trial of 20 Hz rTMS (2,000 pulses/session, 20 sessions) over the ipsilateral DLPFC. Both studies showed an increase in M1 excitability after HF rTMS targeting the ipsilateral DLPFC. Based on these studies, we hypothesized that iTBS (having the same pro neuroexcitatory profile) targeting the left DLPFC would lead to an increase in the excitability of the ipsilateral M1.

The aim of this study was to assess the effect of iTBS on cortical excitability in the motor cortex in healthy controls.

MATERIALS AND METHODS

This study is a randomized double-blind vs. placebo trial designed to assess cortical excitability in the motor cortex before and after ten sessions of iTBS over the L-DLPFC.

Participants

Thirty volunteers, who had given written consent, were randomly assigned to either an active or a sham iTBS group. Healthy subjects between 18 and 65 years old, with no known history of psychiatric illness, and who had been matched in age, gender and education level, were included. They had to be right-handed, with a BDI (Beck Depression Inventory) score of <8, and an HDRS (Hamilton Depression Rating Scale) score of <8. Healthy female subjects had to confirm that they were not pregnant, and were on oral contraception. The non-inclusion criteria consisted of: being on any psychotropic drug, having any psychiatric disorder on axis I or II of the DSM-IV-TR (Diagnostic and Statistical Manual of Mental Disorders: Revised text), suffering from epilepsy, or having any other contraindications for rTMS.

All participants gave written consent, and the study was approved by the local ethical committee (CPP Ile de France VIII, number 101078, ID-RCB 2010A01032-37).

Cortical Excitability Assessment Procedures

Surface electromyograms were taken from abductor pollicis brevis muscles (APB) via electromyographic (EMG) self-adhesive electrodes, with solid gel coated disposable Ag/AgCl electrodes placed on the belly and tendons of the APB muscles.

To assess cortical excitability, TMS was performed using a standard 70 mm figure-of-eight coil (MCF-B65 Butterfly Coil) attached to a Medtronic MagOption stimulator. The coil was attached to the head with the handle pointing backwards and laterally, at an angle of 45° to the sagittal plane.

EMG activity was amplified 10,000-fold using a Matrix Light amplifier (Micromed, Mâcon, France) through filters set at 20 Hz and 2 kHz with a sampling rate of 16 kHz. The activity was then recorded by a computer using SystemPlus EVOLUTION software (version 1.04, Micromed, Mâcon, France).

Cortical Excitability Parameters Assessment Paradigm

The cortical excitability of each subject was assessed at baseline and 48 h after the end of the treatment. The following features of the left and right cortices were assessed: resting motor threshold (rMT), motor evoked potentials (MEPs), and intracortical facilitation (ICF).

The rMT was defined as the lowest TMS intensity required to induce an MEP with an amplitude of at least 50 microVolts (μV) in at least five out of ten trials (15).

Motor evoked potentials were defined as the overall reaction of a peripheral muscle, as measured by electromyography (EMG), that were induced via TMS of the contralateral motor cortex (16). The peak-to-peak amplitude of MEPs produced from a single TMS pulse provides an objective measure of corticospinal excitability (16). Our standard MEP or "test stimulus" was obtained after a single pulse delivered at 120% of the rMT.

Intracortical facilitation (ICF) was performed using two stimuli with an inter-stimulus interval (ISI) of 15 ms (melliseconds) Intracortical facilitation is believed to be mediated by excitatory inputs from glutamatergic pathways (17). In our study, the intensity of the test pulse was at a suprathreshold of 120% of the rMT and the intensity of the conditioned pulse was at a subthreshold of 80% of the rMT.

For all these excitability parameters, five trials were recorded with an interval of at least 5 s between each trial. For the rMT and MEPs, results were expressed using the mean and standard deviation of the five trials. For the ICF, results were expressed as

the ratio of the average of the five MEPs obtained via the ICF paradigm to the average of the standard MEPs (13).

iTBS Procedure

iTBS was applied using parameters described by Huang et al. (2), except for the intensity of the stimulation, which was at 80% of the rMT in our study compared to 80% of the active motor threshold (aMT) initially used by Huang and colleagues in 2005 (2).

Using an intensity at 80% of the rMT instead of 80% of the active motor threshold (aMT) allows for higher stimulation power. Two of the most cited studies that have used iTBS in the treatment of resistant depression, namely Blumberger et al. (4) and Cole et al. (18) used stimulation intensity at 120 and 90% of the rMT respectively, and reported very good tolerance. The use of the rMT instead of aMT is also methodologically easier, since TMS interferes with the ability to maintain steady muscle contraction with stable background EMG activity of 10–20% of maximal contraction (6). Furthermore, the use of aMT could result in the spontaneous pre-activation of target muscles, which may alter the aftereffects of iTBS (18).

Three 50 Hz stimuli were repeated at a frequency of 200 ms for 2 s, which constituted a stimulation train. This train was then repeated every 10 s with a total stimulation duration of 190 s, and a total number of stimuli at 600.

A Magstim Super Rapid stimulator (Magstim, Wales) was used with a 70 mm double air film coil. For the control group, a sham coil providing the same acoustic sensation and visual impact as the active coil was used. The sham coil stimulated the skin and subcutaneous tissue of the scalp, giving the subjects the sensation of magnetic stimulation. The coil was positioned over the left DLPFC using Brainsight, an MRI-guided neuronavigation software (Rogue Research Inc., Canada).

MRI scans were performed on a 3 Tesla scanner (Siemens Healthcare, Erlangen, Germany). A 3D T1-weighted sequence was acquired with the following parameters: 176 contiguous slices, slice thickness = 1.0 mm, repetition time (TR) = 2,300 ms, echo time (TE) = 2.98 ms, field of view = 256*256.

The rTMS coil was applied over the L-DLPFC, which was targeted using established spatial coordinates for this area (Montreal Neurological Institute (MNI) coordinates: x = −50, y = 30, z = 36) (19). To do this, one spherical region of interest (ROI) of a 5 mm radius and centered at these MNI coordinates was generated using the MarsBaR toolbox (http://marsbar.sourceforge.net/) (20). The ROI was de-normalized from the MNI space to the individual space on each patient using the inverse transformation obtained from the VBM8 toolbox. The rTMS coil was positioned tangential to the scalp location overlying the L-DLPFC using an MRI-based frameless stereotactic neuronavigation system (Brainsight, Rogue Research Inc., Montreal, Canada).

Statistical Analysis

Differences between subjects in active and sham arms for sociodemographic characteristics were compared with a Student's *t*-test.

We computed the delta (baseline - after stimulation) for each measurement (rMT, MEPs, ICF) and for each group (active or sham).

We compared the delta in the active and sham group.

The Gaussian Distribution of each variable was evaluated by the Shapiro-Wilk test.

Some of the variables did not meet the assumptions for parametric statistics (Gaussian distribution for t-test, normal distribution for the residuals of the ANOVA) and is why we chose non-parametric statistical tests (Mann–Whitney U) for some. For the normally distributed variables, we performed t-test instead of ANCOVA because our groups were matched for age and gender, thus there was no confound that we could take into account. All statistical analyses were conducted using Python Statsmodels, an open-source library (21).

RESULTS

There were no significant differences in age or gender ratio between active and placebo groups at baseline (**Table 1**).

The impact of iTBS and sham stimulation on all endpoint parameters is reported in **Table 2** and in **Figures 1–3**.

No difference was found between active and placebo stimulation in the rMT, MEPs and ICF in the right and the left cortex. There was also no trend suggesting a difference between the active and the sham arm.

DISCUSSION

We found no difference in all cortical excitability measurements between active and placebo stimulation in the left or right hemisphere. This negative result was contrary to our expectations.

The DLPFC has various anatomical projections on M1. These two regions are believed to work closely together to form fundamental circuitry involved in motor tasks of varying complexity (22). It is also widely believed that the impact of rTMS occurs if sessions of rTMS are repeated over a period of several days, leading to a "build-up" effect (23).

We therefore hypothesized that repeated sessions of iTBS over the L-DLPFC would result in increased excitability of the ipsilateral M1.

Studies assessing iTBS on cortical excitability are scarce, but can be divided into three types: (i) studies exploring TBS impact on cortical excitability after only one session of stimulation targeting the M1, (ii) studies exploring iTBS impact on cortical excitability after repeated sessions targeting the M1, (iii) studies exploring iTBS impact on cortical excitability targeting the DLPFC (a protocol template for treating depression).

Regarding (i), Chung et al. (16) replicated the findings of Huang et al. (2), being that one session of iTBS over the M1 in healthy subjects results in an increase in excitability by enhancing MEP amplitude, and that continuous Theta Burst Stimulation (cTBS) results in the opposite effect.

Regarding (ii), Perellón-Alfonso et al. (24) reported that over a 5-day "treatment" protocol, cumulative active iTBS over the M1

in 20 healthy volunteers was not superior to sham stimulation at inducing long-lasting facilitation of corticospinal excitability.

To date (iii), only Cao et al. (25) has assessed the effects of iTBS over the DLPFC on M1 cortical excitability. These authors reported that one iTBS session over the DLPFC, in 15 healthy right-handed participants, decreased the MEP amplitude in the M1, whereas the cTBS session resulted in the opposite effect. The authors explained their results by the Zero-Sum Enhancement theory. According to this theory, the increase in the excitability of the DLPFC is necessarily accompanied by a decrease in the excitability of the M1 at the other end of the network (26).

Triggs et al. (14) and Spampinato et al. (13) reported the opposite results after several sessions of HF rTMS (thought to have the same excitatory properties as iTBS) over the L-DLPFC. They reported a decrease in the rMT of the ipsilateral motor cortex.

Brown et al. (22) found no effect on M1 excitability after stimulation of the ipsilateral DLPFC using the TMS Conditioning-Test Approach. This is a method to evaluate the impact of a TMS conditioning stimulus (CS) applied over the frontal cortex on MEPs elicited by the TMS test stimulus (TS) over the M1 (22).

Our study is the first to evaluate the effect of iTBS over the L-DLPFC on cumulative cortical excitability in healthy subjects, using a "depression stimulation protocol." Our results do not

TABLE 1 | Sociodemographic characteristics in iTBS and sham groups.

Variables	Active iTBS arm	Sham iTBS arm	*p* value
Number	14	16	
Age (mean, SD)	24.57 (6.65)	25.75 (6.19)	0.61
Gender ratio (M/F)	1	1	-
Handedness (mean, SD)	87 (9.66)	87 (15)	1
Level of education (mean, SD)	15.35 (1.69)	14.5 (1.63)	0.16

SD, standard deviation; M, male; F, female; iTBS, intermittent theta burst stimulation.

TABLE 2 | Difference (before and after stimulation) in the placebo and the active arm in resting motor threshold, motor evoked potentials and intracortical facilitation of both cortices before and after stimulation.

Excitability parameters	Target	Active baseline	Active post iTBS	Active delta	Sham baseline	Sham post iTBS	sham delta	Comparison between active delta and sham delta	*p*-value
rMT** Mean (sd)	R DLPFC	52.15 (6.96)	52.81 (8.49)	0.63 (2.97)	51.4 (8.39)	51.93 (7.79)	0.5 (4.5)	MW stat. = 79.5	0.44
	L DLPFC	53.61 (7.8)	55.08 (8.83)	1.16 (3.37)	51.33 (9.18)	50.46 (8.31)	−0.86 (4.88)	*T*-test stat. = 1.22	0.23
MEP* Mean (sd)	R DLPFC	1.51 (1.16)	1.26 (1.06)	−0.25 (1.24)	1.43 (0.95)	1.59 (1.29)	0.09 (1.42)	*T*-test stat. = 0.68	0.5
	L DLPFC	1.86 (1.03)	1.64 (1.05)	−0.22 (0.94)	1.71 (1.22)	2.30 (2.25)	0.58 (1.96)	*T*-test stat. = 1.34	0.18
Ratio ICF* Mean (sd)	R DLPFC	121.21 (72.41)	131.17 (87.49)	7 (116)	136.88 (133.17)	201.20 (195.25)	72.53 (250)	*T*-test stat. = 1.22	0.23
	L DLPFC	125 (58)	102.64 (39)	−23.25 (136.69)	169.94 (181)	151.92 (106.47)	−23 (58)	MW stat. = 94	0.33

***2 missing values; *one missing value, rMT, resting motor threshold (% of maximal output); MEP, motor evoked potential (120% of rMT in μV); Ratio ICF, Intracortical facilitation ration; t-test, the Student's t-test; MWt, Mann–Whitney U test; R-DLPFC, right dorsolateral prefrontal cortex; L-DLPFC, left dorsolateral prefrontal cortex; SD, standard deviation.*

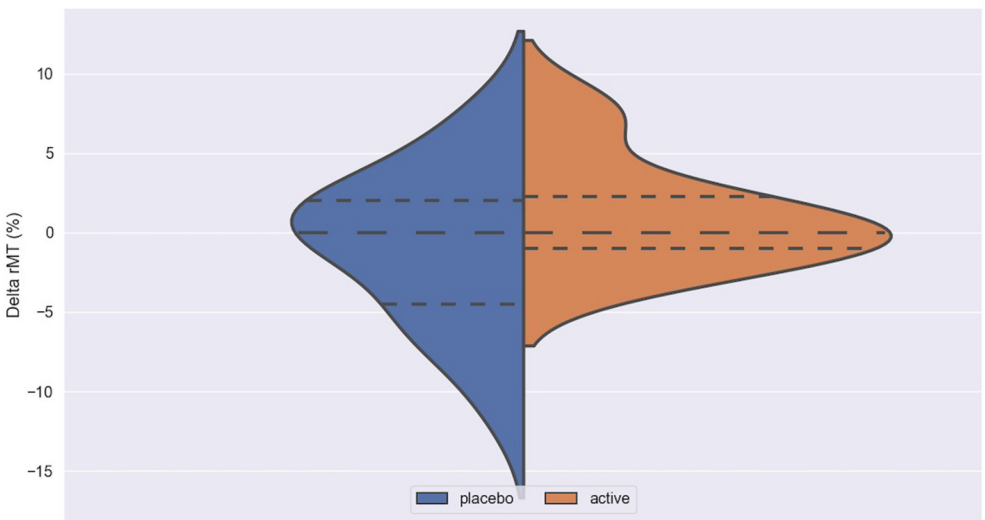

FIGURE 1 | Delta rMT in active and placebo groups in left cortex. rMT, resting motor threshold; Delta rMT, difference in rMT before and after iTBS.

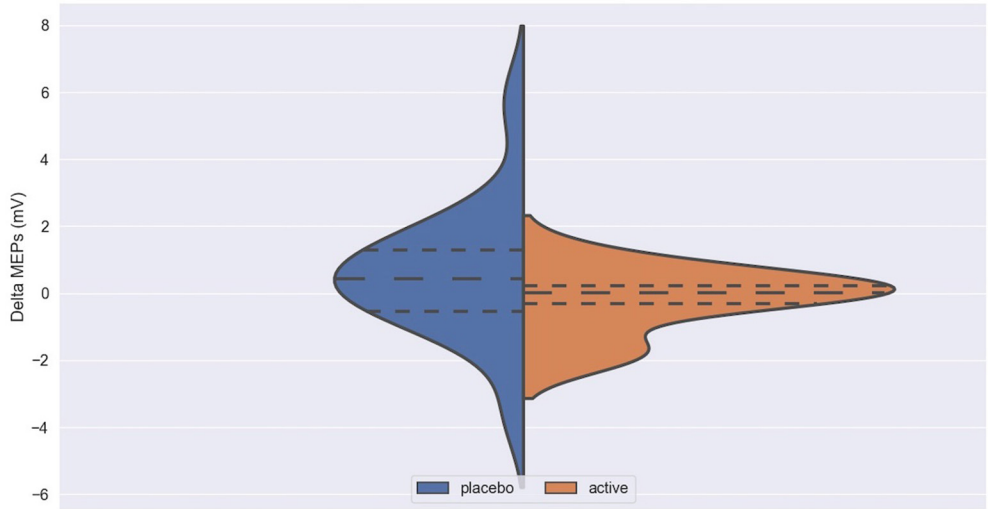

FIGURE 2 | Delta MEPs in active and placebo groups in left cortex. MEPs, Motor Evoked Potentials at 120% of rMT; Delta MEPs, difference in MEPs before and after iTBS.

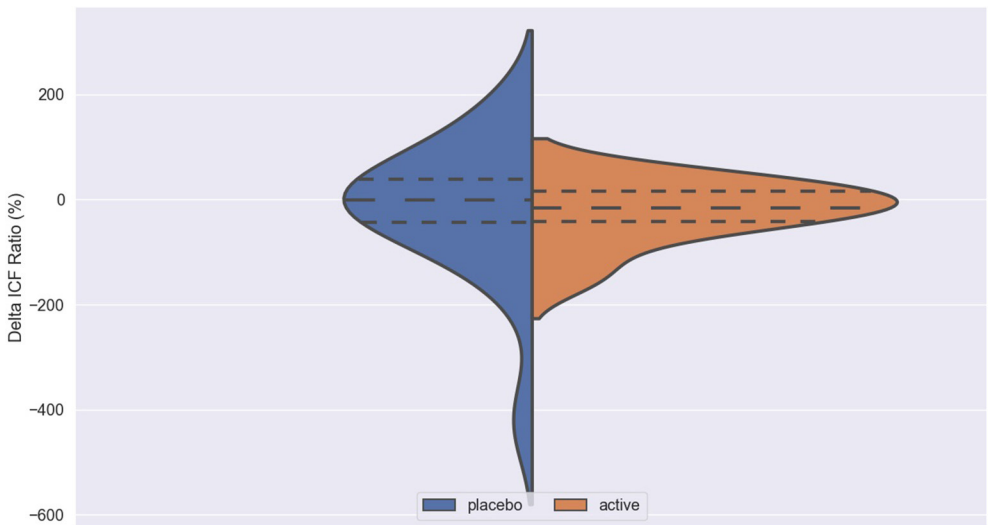

FIGURE 3 | Delta ICF in active and placebo groups in left cortex. ICF, intracortical facilitation; Delta ICF, difference in ICF before and after iTBS. Delta: difference in the resting Motor Threshold (rMT, **Figure 1**) after minus before active or sham stimulation, the Motor Evoked Potentials (MEPs, **Figure 2**) and Intracortical Facilitation (ICF) before and after intermittent Theta Burst Stimulation (iTBS) in the placebo (blue) and the active (orange) arm. Hashed lines delineate quartile of the distribution; to central hashed lines refer to the mean of the distribution. We choose the violin plots to provide information about the distribution of the variables, which is not possible with box plots and/or scatter plots. We believe that this representation of the results gives additional information to the reader. The x axis represents both the placebo (blue) and active (orange) group.

support any impact of repeated iTBS sessions applied over the L-DLPFC on the excitability of the M1.

The result of our study, especially in view of the scarcity of studies on the subject and their contradictory results, is difficult to explain. Nevertheless, some hypotheses are possible.

First, although a DLPFC-M1 connection has been widely reported (22, 25, 26), it may not be direct, and may be influenced by postsynaptic connections with other brain regions (basal ganglia, thalamus) (22).

Secondly, the stimulated target and coil orientation were probably not optimal to test our hypothesis. Indeed, we targeted an area traditionally used for the treatment of depression, whereas it could have been preferable to vary the target area from patient to patient, to identify a specific area more likely to induce excitability in M1.

Thirdly, the hypothesis linking the antidepressant effect of rTMS/iTBS to a change in cortical excitability may not be accurate. This is because the antidepressant action may be

mediated by other neurobiological mechanisms that are distinct from a simple modulation of cortical excitability, such as modulation in dopamine and/or glutamate, connectivity between non-motor brain regions, modulation of gene expression, de novo expression of proteins, morphological changes, and/or changes in intrinsic firing patterns of diverse neocortical neurons or intrinsic membrane properties (27).

The conclusion of our study, which does not support any impact of repeated iTBS sessions applied over L-DLPFC on the excitability of the M1 should be taken with caution. Despite its original design, our study suffers from several limitations: first, the relatively small sample size may have resulted in Type 2 errors. Secondly, our methodology for collecting cortical excitability parameters is probably not optimal. In fact, we conducted five trials of each variable, but more trials would be preferable. Using Transcranial Magnetic Stimulation (TMS) to assess cortical excitability (single pulse TMS for corticospinal processes, rMT and MEPs and paired pulses for intracortical processes) can be considerably affected by interpersonal, intrapersonal and intersessional variability, which reduces the sensitivity and reproducibility of this method. Our results showed a significant interpersonal and intrapersonal variability in cortical excitability between the different sessions that was partly due to the choice of conducting an average of only five trials for each parameter. Biabani et al. (28) reported that the optimal number of TMS trials needed for reproducible measurements of corticospinal excitability and intracortical inhibition was 26. Conducting 30 trials resulted in a significant improvement in the reproducibility of ICF in a single session, but only moderately improved the reproducibility between different sessions. Goldsworthy et al. (29) reported that 20–30 TMS trials are optimal to ensure a stable measure of MEP amplitude with high within- and between-session reliability. Chang et al. (30) reported that the optimal number of neuronavigated trials required to improve the reliability of the evaluation of the amplitude of MEP, latency of MEP, ICF and Short-Interval Intracortical Inhibition (SICI), are 21, 23, 20, and 25 respectively. However, these three authors used 5 out of 10 trials to determine the participants' rMT, as we did.

To the best of our knowledge, the majority of studies using TMS or iTBS in physiology or in therapeutic trials use at least five out of ten positive trials (motor response and/or induction of an EMP with amplitude $\geq$50 μV) to determine the motor threshold. However, the updated IFCN guidelines Rossini et al. (6) suggest using 10 MEPs out of 20 trials to improve the accuracy of these measurements. In view of this, we suggest that despite it being probably time-consuming, an increase in the number of trials, potentially coupled with a neuronavigation of MEPs, to evaluate the different assessments of cortical excitability parameters, might ultimately increase the consistency of this method of investigation. Thirdly, the reassessment of cortical excitability 48 h after the last iTBS session may be too late, as the brain has probably regained its baseline excitability state through the subsequent homeostatic synaptic plasticity phenomena (27). Our choice to evaluate the effect of repeated iTBS sessions on excitability after 48 h after the last stimulation session was motivated by the search for a possible persistent build-up of cumulative effects on neuroplasticity. Indeed, if iTBS draws its potential antidepressant effect from its modulation of cortical excitability, it would be expected that this effect would persist beyond the stimulation sessions alone. Evaluating immediately or close after the last stimulation session may results in the assessment of only the immediate effect of this last session.

Studies evaluating the cumulative effects of iTBS (or rTMS) on cortical excitability are rare.

Bäumer et al. (31) reported that while the effects of rTMS on ICF after 1Hz rTMS remains 30 min, the effect lasts up to 2 h when the stimulation was made on two consecutive days suggesting build up excitatory effect. Indeed, the evaluation of excitability before each session, 30 min after each session, or before the first session, 30 min after the first session and 30 min after the last session, in addition to the 48-h assessment, could have provided us with more information on the effects of iTBS on cortical excitability in the short- and medium- term.

Another limitation is the fact that in our study we did not control the timing of inclusion, stimulation and assessment of excitability in relation to the phase of the menstrual cycle, which could be a limitation of our study. Given the potential influence of female hormones on cortical excitability, one could speculate that rMT and other indices of cortical excitability may vary with different phases of the menstrual cycle. Indeed, and despite heterogeneous studies, female hormones probably impact cortical excitability. Smith et al. (32) described an excitatory neuronal effect associated with estradiol, and an inhibition effect associated with progesterone. Inghilleri et al. (33) reported similar results, with cortical excitability during the follicular period increasing in conjunction with an increase in estrogen levels. Recently, Schloemer et al. (34) reported that the fluctuation in estrogen (but not progesterone) levels modulates cortical excitability in non-motor (somatosensory and visual) cortices. However, Chagas et al. (35) did not find any variation in rMT according to the phases of the menstrual cycle. Nevertheless, they reported an increase in rMT in women with amenorrhea compared to those at the beginning of their menstrual cycle. In this study our female volunteers were only included if they were taking hormonal contraceptives, which may have minimized the possible influence of hormonal variations caused by the menstrual cycle on cortical excitability. Gender differences were not assessed too. Few studies have evaluated the hypothetical difference in cortical excitability between women and men. Cantone et al. (36) who assessed a large Italian cohort, found some differences between males and females in TMS-induced MEPs of the lower limbs, but not of the upper limbs. Either way, data from the studies cited above strongly suggest that the hormonal status of the women participating in the cortical excitability studies is probably a confounding factor, and should be considered in future studies.

Despite these limitations, we believe that our study has strengths, and that its original design would benefit from being replicated and improved.

To the best of our knowledge, this randomized double-blind controlled study is the first to evaluate the effect of iTBS over

the L-DLPFC on cortical excitability in healthy subjects, using a "depression stimulation" protocol with repetitive sessions. Furthermore, this is the largest trial assessing TBS impact on cortical excitability in healthy volunteers. Our study corroborates the safety and the good tolerability of repeated sessions of iTBS.

Even with a higher intensity than that initially used by Huang et al. (2) (80% of rMT instead of 80% of aMT), we observed no serious adverse effects: only a few cases of mild headache that did not persist.

DATA AVAILABILITY STATEMENT

The raw data supporting the conclusions of this article will be made available by the authors, without undue reservation.

ETHICS STATEMENT

The studies involving human participants were reviewed and approved by CPP Ile de France VIII, number 101078, ID-RCB 2010A01032-37. The patients/participants provided their written informed consent to participate in this study. Written informed consent was obtained from the individual(s) for the publication of any potentially identifiable images or data included in this article.

AUTHOR CONTRIBUTIONS

NB: wrote the article, contributed to the conception and design of the study, carried the statistical analysis, and contributed to the carrying out of cortical excitability procedures. CL: contributed to the writing of the article and the carrying out of the statistical tests. FT: contributed to the carrying out of cortical excitability procedures. PS-K: contributed to magnetic stimulation, participant monitoring and to the carrying out of cortical excitability procedures. VM: contributed to the design of the study and the methodological follow-up. DJ: contributed to the conception and design of the study, as well as the writing of the article. All authors contributed to the article and approved the submitted version.

REFERENCES

1. Milev RV, Giacobbe P, Kennedy SH, Blumberger DM, Daskalakis ZJ, Downar J, et al. Canadian network for mood and anxiety treatments (CANMAT) 2016 clinical guidelines for the management of adults with major depressive disorder: section 4. *Neurostimulation Treatm Can J Psychiatry*. (2016) 61:561–75. doi: 10.1177/0706743716660033
2. Huang Y-Z, Edwards MJ, Rounis E, Bhatia KP, Rothwell JC. Theta burst stimulation of the human motor cortex. *Neuron*. (2005) 45:201–6. doi: 10.1016/j.neuron.2004.12033
3. Bakker N, Shahab S, Giacobbe P, Blumberger DM, Daskalakis ZJ, Kennedy SH, et al. rTMS of the dorsomedial prefrontal cortex for major depression: safety, tolerability, effectiveness, and outcome predictors for 10 Hz versus intermittent theta-burst stimulation. *Brain Stimul*. (2015) 8:208–15. doi: 10.1016/j.brs.2014.11002
4. Blumberger DM, Vila-Rodriguez F, Thorpe KE, Feffer K, Noda Y, Giacobbe P, et al. Effectiveness of theta burst versus high-frequency repetitive transcranial magnetic stimulation in patients with depression (THREE-D): a randomised non-inferiority trial. *Lancet*. (2018) 391:1683–92. doi: 10.1016/S0140-6736(18)30295-2
5. Suppa A, Huang Y-Z, Funke K, Ridding MC, Cheeran B, Di Lazzaro V, et al. Ten years of theta burst stimulation in humans: established knowledge, unknowns and prospects. *Brain Stimul*. (2016) 9:323–35. doi: 10.1016/j.brs.2016.01006
6. Rossini PM, Burke D, Chen R, Cohen LG, Daskalakis Z, Di Iorio R, et al. Non-invasive electrical and magnetic stimulation of the brain, spinal cord, roots and peripheral nerves: Basic principles and procedures for routine clinical and research application. An updated report from an IFCN committee. *Clin Neurophysiol*. (2015) 126:1071–107. doi: 10.1016/j.clinph.2015.02001
7. Khedr EM, Elserogy Y, Fawzy M, Elnoaman M, Galal AM. Global cortical hypoexcitability of the dominant hemisphere in major depressive disorder: a transcranial magnetic stimulation study. *Neurophysiol Clin*. (2020) 50:175–83. doi: 10.1016/j.neucli.2020.02005
8. Lefaucheur JP, Lucas B, Andraud F, Hogrel JY, Bellivier F, Del Cul A, et al. Inter-hemispheric asymmetry of motor corticospinal excitability in major depression studied by transcranial magnetic stimulation. *J Psychiatr Res*. (2008) 42:389–98. doi: 10.1016/j.jpsychires.2007.03001
9. Concerto C, Lanza G, Cantone M, Pennisi M, Giordano D, Spampinato C, et al. Different patterns of cortical excitability in major depression and vascular depression: a transcranial magnetic stimulation study. *BMC Psychiatry*. (2013) 13:300. doi: 10.1186/1471-244X-13-300
10. Maeda F, Keenan JP, Pascual-Leone A. Interhemispheric asymmetry of motor cortical excitability in major depression as measured by transcranial magnetic stimulation. *Br J Psychiatry*. (2000) 177:169–73. doi: 10.1192/bjp.177.2169
11. Bajbouj M, Lisanby SH, Lang UE, Danker-Hopfe H, Heuser I, Neu P. Evidence for impaired cortical inhibition in patients with unipolar major depression. *Biol Psychiatry*. (2006) 59:395–400. doi: 10.1016/j.biopsych.2005.07036
12. Kinjo M, Wada M, Nakajima S, Tsugawa S, Nakahara T, Blumberger DM, et al. Transcranial magnetic stimulation neurophysiology of patients with major depressive disorder: a systematic review and meta-analysis. *Psychol Med*. (2020) 1–10. doi: 10.1017/S0033291720004729
13. Spampinato C, Aguglia E, Concerto C, Pennisi M, Lanza G, Bella R, et al. Transcranial magnetic stimulation in the assessment of motor cortex excitability and treatment of drug-resistant major depression. *IEEE Trans Neural Syst Rehabil Eng*. (2013) 21:391–403. doi: 10.1109/TNSRE.20132256432
14. Triggs WJ, McCoy KJ, Greer R, Rossi F, Bowers D, Kortenkamp S, et al. Effects of left frontal transcranial magnetic stimulation on depressed mood, cognition, and corticomotor threshold. *Biol Psychiatry*. (1999) 45:1440–6. doi: 10.1016/S0006-3223(99)00031-1
15. Bunse T, Wobrock T, Strube W, Padberg F, Palm U, Falkai P, et al. Motor cortical excitability assessed by transcranial magnetic stimulation in psychiatric disorders: a systematic review. *Brain Stimul*. (2014) 7:158–69. doi: 10.1016/j.brs.2013.08009
16. Chung SW, Hill AT, Rogasch NC, Hoy KE, Fitzgerald PB. Use of theta-burst stimulation in changing excitability of motor cortex: a systematic review and meta-analysis. *Neurosci Biobehav Rev*. (2016) 63:43–64. doi: 10.1016/j.neubiorev.2016.01008
17. Radhu N, de Jesus DR, Ravindran LN, Zanjani A, Fitzgerald PB, Daskalakis ZJ. A meta-analysis of cortical inhibition and excitability using transcranial magnetic stimulation in psychiatric disorders. *Clin Neurophysiol*. (2013) 124:1309–20. doi: 10.1016/j.clinph.2013.01014
18. Cole EJ, Stimpson KH, Bentzley BS, Gulser M, Cherian K, Tischler C, et al. Stanford accelerated intelligent neuromodulation therapy for treatment-resistant depression. *Am J Psychiatry*. (2020) 177:716–26. doi: 10.1176/appi.ajp.2019.19070720
19. Rusjan PM, Barr MS, Farzan F, Arenovich T, Maller JJ, Fitzgerald PB, et al. Optimal transcranial magnetic stimulation coil placement for targeting the dorsolateral prefrontal cortex using novel magnetic resonance image-guided neuronavigation. *Hum. Brain Mapp*. (2010) 31:1643–52. doi: 10.1002/hbm20964

20. Brett M, Anton J-L, Valabregue R, Poline J-B. Region of interest analysis using an SPM toolbox [Abstract]. *Neuroimage*. (2002). 16. doi: 10.1016/S1053-8119(02)90013-3
21. Seabold S, Perktold J. Statsmodels: econometric and statistical modeling with python. In: van der Walt S, Millman J, editors. *Proceedings of the 9th Python in Science Conference*. Austin, TX: Millman; Jarod (2010). p. 92–96. doi: 10.25080/Majora-92bf1922-011
22. Brown MJN, Goldenkoff ER, Chen R, Gunraj C, Vesia M. Using dual-site transcranial magnetic stimulation to probe connectivity between the dorsolateral prefrontal cortex and ipsilateral primary motor cortex in humans. *Brain Sci*. (2019) 9:177. doi: 10.3390/brainsci9080177
23. Lefaucheur J-P, André-Obadia N, Antal A, Ayache SS, Baeken C, Benninger DH, et al. Evidence-based guidelines on the therapeutic use of repetitive transcranial magnetic stimulation (rTMS). *Clin Neurophysiol*. (2014) 125:2150–206. doi: 10.1016/j.clinph.2014.05021
24. Perellón-Alfonso R, Kralik M, Pileckyte I, Princic M, Bon J, Matzhold C, et al. Similar effect of intermittent theta burst and sham stimulation on corticospinal excitability: A 5-day repeated sessions study. *Eur J Neurosci*. (2018) 48:1990–2000. doi: 10.1111/ejn14077
25. Cao N, Pi Y, Liu K, Meng H, Wang Y, Zhang J, et al. Inhibitory and facilitatory connections from dorsolateral prefrontal to primary motor cortex in healthy humans at rest-An rTMS study. *Neurosci Lett*. (2018) 687:82–7. doi: 10.1016/j.neulet.2018.09032
26. Pascual-Leone A, Horvath JC, Robertson EM. Enhancement of normal cognitive abilities through noninvasive brain stimulation. In: Chen R, Rothwell JC, editors. *Cortical Connectivity: Brain Stimulation for Assessing and Modulating Cortical Connectivity and Function*. Berlin, Heidelberg: Springer (2012). p. 207–49. doi: 10.1007/978-3-662-45797-9_11
27. Cirillo G, Pino GD, Capone F, Ranieri F, Florio L, Todisco V, et al. Neurobiological after-effects of non-invasive brain stimulation. *Brain Stimul*. (2017) 10:1–18. doi: 10.1016/j.brs.2016.11009
28. Biabani M, Farrell M, Zoghi M, Egan G, Jaberzadeh S. The minimal number of TMS trials required for the reliable assessment of corticospinal excitability, short interval intracortical inhibition, and intracortical facilitation. *Neurosci Lett*. (2018) 674:94–100. doi: 10.1016/j.neulet.2018.03026
29. Goldsworthy MR, Hordacre B, Ridding MC. Minimum number of trials required for within- and between-session reliability of TMS measures of corticospinal excitability. *Neuroscience*. (2016) 320:205–9. doi: 10.1016/j.neuroscience.2016.02012
30. Chang WH, Fried PJ, Saxena S, Jannati A, Gomes-Osman J, Kim Y-H, et al. Optimal number of pulses as outcome measures of neuronavigated transcranial magnetic stimulation. *Clin Neurophysiol*. (2016) 127:2892–7. doi: 10.1016/j.clinph.2016.04001
31. Bäumer T, Lange R, Liepert J, Weiller C, Siebner HR, Rothwell JC, et al. Repeated premotor rTMS leads to cumulative plastic changes of motor cortex excitability in humans. *Neuroimage*. (2003) 20:550–60. doi: 10.1016/S1053-8119(03)00310-0
32. Smith MJ, Adams LF, Schmidt PJ, Rubinow DR, Wassermann EM. Effects of ovarian hormones on human cortical excitability. *Ann Neurol*. (2002) 51:599–603. doi: 10.1002/ana10180
33. Inghilleri M, Conte A, Currà A, Frasca V, Lorenzano C, Berardelli A. Ovarian hormones and cortical excitability. An rTMS study in humans. *Clin Neurophysiol*. (2004) 115:1063–8. doi: 10.1016/j.clinph.2003.12003
34. Schloemer N, Lenz M, Tegenthoff M, Dinse HR, Höffken O. Parallel modulation of intracortical excitability of somatosensory and visual cortex by the gonadal hormones estradiol and progesterone. *Sci Rep*. (2020) 10:22237. doi: 10.1038/s41598-020-79389-6
35. Chagas AP, Monteiro M, Mazer V, Baltar A, Marques D, Carneiro M, et al. Cortical excitability variability: Insights into biological and behavioral characteristics of healthy individuals. *J Neurol Sci*. (2018) 390:172–7. doi: 10.1016/j.jns.2018.04036
36. Cantone M, Lanza G, Vinciguerra L, Puglisi V, Ricceri R, Fisicaro F, et al. Age, height, and sex on motor evoked potentials: translational data from a large italian cohort in a clinical environment. *Front Hum Neurosci*. (2019) 13:185. doi: 10.3389/fnhum.201900185

Conflict of Interest: The authors declare that the research was conducted in the absence of any commercial or financial relationships that could be construed as a potential conflict of interest.

frontiers in Human Neuroscience

MINI REVIEW
published: 26 March 2021
doi: 10.3389/fnhum.2021.622313

Phase–Amplitude Coupling, Mental Health and Cognition: Implications for Adolescence

Dashiell D. Sacks, Paul E. Schwenn, Larisa T. McLoughlin, Jim Lagopoulos and Daniel F. Hermens*

Thompson Institute, University of the Sunshine Coast, Sunshine Coast, QLD, Australia

Identifying biomarkers of developing mental disorder is crucial to improving early identification and treatment—a key strategy for reducing the burden of mental disorders. Cross-frequency coupling between two different frequencies of neural oscillations is one such promising measure, believed to reflect synchronization between local and global networks in the brain. Specifically, in adults phase–amplitude coupling (PAC) has been shown to be involved in a range of cognitive processes, including working and long-term memory, attention, language, and fluid intelligence. Evidence suggests that increased PAC mediates both temporary and lasting improvements in working memory elicited by transcranial direct-current stimulation and reductions in depressive symptoms after transcranial magnetic stimulation. Moreover, research has shown that abnormal patterns of PAC are associated with depression and schizophrenia in adults. PAC is believed to be closely related to cortico-cortico white matter (WM) microstructure, which is well established in the literature as a structural mechanism underlying mental health. Some cognitive findings have been replicated in adolescents and abnormal patterns of PAC have also been linked to ADHD in young people. However, currently most research has focused on cross-sectional adult samples. Whereas initial hypotheses suggested that PAC was a state-based measure due to an early focus on cognitive, task-based research, current evidence suggests that PAC has both state-based and stable components. Future longitudinal research focusing on PAC throughout adolescent development could further our understanding of the relationship between mental health and cognition and facilitate the development of new methods for the identification and treatment of youth mental health.

Keywords: EEG, cross-frequency coupling, PAC, mental disorder, cognition, youth mental health, neurostimulation, DTI

OPEN ACCESS

Edited by:
Hongming Li,
University of Pennsylvania,
United States

Reviewed by:
Yifeng Wang,
Sichuan Normal University, China
Justin Riddle,
University of North Carolina at Chapel Hill, United States

****Correspondence:***
Dashiell D. Sacks
dsacks@usc.edu.au

Specialty section:
This article was submitted to Brain Imaging and Stimulation, a section of the journal Frontiers in Human Neuroscience

Received: *28 October 2020*
Accepted: *02 March 2021*
Published: *26 March 2021*

Citation:
Sacks DD, Schwenn PE, McLoughlin LT, Lagopoulos J and Hermens DF (2021) Phase–Amplitude Coupling, Mental Health and Cognition: Implications for Adolescence. Front. Hum. Neurosci. 15:622313. doi: 10.3389/fnhum.2021.622313

INTRODUCTION

In Australia, mental disorders were estimated to have a direct economic cost of up to $51 billion and a further $130 billion cost as a result of diminished well-being during the 2018–2019 period (Productivity Commission, 2019). Mental health research and reform is currently focusing on adolescence as it is recognized as a critical period for the development of mental disorder (Paus, 2005; Hickie et al., 2013). More than 50% of mental disorders develop before 14 years of age

and more than 75% before 24 years of age (Kessler et al., 2005). In Australia, 14% of those aged 4–17 years are evaluated as having a mental disorder in the prior 12 months (Lawrence et al., 2015). Young people frequently present with subthreshold, non-specific symptoms that are associated with significant, ongoing socio-occupational impairment (Lee et al., 2013; Iorfino et al., 2018) and an increased chance of developing discrete disorders (Fergusson et al., 2005; Iorfino et al., 2019). The rapid differential structural brain changes that occur during adolescence result in an increased risk of developing mental disorders during this period, as well as risk-taking behavior that can introduce various other risk factors for mental health (Andersen, 2003; Paus, 2005; Casey et al., 2010, 2011).

Traditional psychiatric approaches that focus on the identification and treatment of established mental disorders have limited application for developing psychopathology (Hickie et al., 2013). Thus, using neuroscience to investigate biomarkers related to youth mental health is critical to improving our understanding of emerging psychopathology and developing new methods of early identification and treatment. Phase–amplitude coupling (PAC), a type of cross-frequency coupling (CFC) between different frequencies of neural oscillation is a promising biomarker that may improve our understanding of mental health and cognition in adolescence. In this review article, we provide a brief overview of (1) CFC, specifically PAC in EEG research, (2) PAC in cognition/information processing, including memory, attention, language, and fluid intelligence, (3) PAC's implications for neurostimulation and mental health, (4) PAC and structural connectivity, and (5) PAC developmentally. Finally, future directions for research are discussed.

EEG AND PAC

The EEG has been used to analyze the rhythmic, oscillatory activity of the human brain for nearly 100 years since Berger (1929) performed the first human EEG studies and discovered the alpha wave. Subsequently, an abundance of research has focused on delineating the properties and functions of individual frequency bands of various neural oscillations. The five most well-established frequency bands are: delta, theta, alpha, beta, and gamma, which have been implicated across a range of cognitive functions that vary according to context and associated region. For an overview, see Herrmann et al. (2016). Analysis of different frequencies independently aligns with the traditional perspective that the brain is comprised of phylogenetically distinct networks that operate at different frequencies. However, recent EEG research, in conjunction with electrocorticography (ECoG) and magnetoencephalography (MEG), suggests that there is a dynamic interplay between neural frequencies that reflects the integrative nature of cortical networks.

Cross-frequency coupling between two different frequencies of neural oscillations is hypothesized to facilitate communication between meso and microscales within regions, and synchronization and interaction between local and global networks in the brain inter-regionally (Canolty and Knight, 2010). Through use of source localization techniques and concurrent fMRI, studies are now able to provide greater spatial resolution to complement EEG analyses. A now common perspective is that oscillatory activity is hierarchical—the phase of slower oscillations modulates the amplitude, frequency, or phase of faster oscillations (Jerath et al., 2019). Recent efforts have focused on coupling between the phase of slower oscillatory activity and the amplitude of faster oscillatory activity (i.e., PAC). Importantly, it is now understood that PAC provides additional explanatory power beyond simple "neuronal communication through neuronal coherence" (Fries, 2005), with evidence suggesting that PAC may facilitate separate, spatially distributed cortical networks operating in parallel (van der Meij et al., 2012). Findings suggest that PAC is a fundamental neurological process that can potentially help us better understand information processing and mental health in the brain.

PAC AND COGNITION

PAC and Memory

One of the most researched areas in the context of PAC is memory. Numerous adult EEG studies have implicated theta–gamma PAC as a neural substrate of visual and auditory working memory (Axmacher et al., 2010; Kaminski et al., 2019). Theta–gamma PAC (one of the most prominent types of PAC) has been recorded within multiple brain regions, but specifically in the hippocampal region and prefrontal cortex during working memory tasks. These results have been replicated in adolescents. Theta–gamma PAC within frontal and temporal regions, as well as interregionally between frontal and posterior regions has also been implicated in the encoding and retrieval of items in long-term, declarative memory in adults (Friese et al., 2013; Lara et al., 2018; Köster et al., 2019).

One popular model of working memory suggests that individual gamma waves represent memory items, which are "nested" in theta, enabling the retention of multiple items. See Sauseng et al. (2019) for a review of evidence—pertinently, researchers were able to elicit temporary improvements in visual and verbal working memory using transcranial alternating current stimulation (tACS) to slow theta waves, theoretically enabling the nesting of an additional gamma wave (Vosskuhl et al., 2015; Wolinski et al., 2018).

PAC, Language, Attention, and Intelligence

Other complex areas of cognition that have been associated with PAC in adults include language, attention, and fluid intelligence. PAC has been associated with linguistic processes such as verb generation (Doesburg et al., 2012), linguistic structure composition (Brennan and Martin, 2020), and language prediction (Wang et al., 2018). An oscillatory model of language is described by Murphy et al. across a series of studies (Murphy, 2016, 2018; Benítez-Burraco and Murphy, 2019).

Phase–amplitude coupling is also implicated in selective attention in adults (e.g., Doesburg et al., 2012; Saalmann et al., 2012). Gonzalez-Trejo et al. (2019) demonstrated differences between "car drivers" and "co-pilots" in PAC within the

prefrontal cortex, frontal eye fields, primary motor cortex, and visual cortex during a simulated driving task. Mento et al. (2018) demonstrated that theta–beta coupling at Cz is associated with the temporal orienting of attention in 8–12-years-olds.

Chuderski (2016) criticized the methods used by previous research that reported a relationship between PAC and fluid intelligence (Pahor and Jaušovec, 2014) but highlighted that measures of intelligence are strongly correlated with working memory and thus likely associated with PAC. Gągol et al. (2018) identified that greater beta–gamma PAC coupling at rest and during a reasoning task was associated with increased fluid intelligence at individual sites across the brain, with greater strength at medial, frontal, and parietal electrodes. See Hyafil et al. (2015) for further discussion about the cognitive mechanisms of PAC. Further research is required to determine how findings in adults translate into adolescents. It is now well established that cognition and mental health are closely intertwined; consistent cognitive deficits are present across mental disorders in youth and relate directly to functioning and illness trajectory (Lee et al., 2013, 2018). Evidence increasingly suggests that PAC is a fundamental process underlying information processing.

PAC, NEUROSTIMULATION, AND MENTAL HEALTH

Neurostimulation

One of the most interesting developments in the PAC literature is that both temporary and lasting changes can be elicited by contemporary treatment modalities such as tACS (mentioned above), transcranial direct current stimulation (tDCS), and transcranial magnetic stimulation (TMS). Jones et al. (2020) demonstrated that combining tDCS with working memory training over 4 days resulted in significantly greater working memory improvements than working memory training alone in adults, which were mediated by greater inter-regional theta–gamma PAC strength between the prefrontal cortex and temporo-parietal regions. This is not only relevant to cognition, but also mental health.

Noda et al. (2017) analyzed resting-state PAC before and after a typical 2-week course (10 sessions) of repetitive TMS (rTMS) targeting the dorsolateral prefrontal cortex in adult patients with depression; rTMS was associated with improved scores on the Hamilton Rating Scale for Depression, Beck Depression Inventory and increased PAC at the C3 (left temporal) and T3 electrode site at rest. These findings suggest that decreased resting-state theta–gamma PAC may be a biomarker of poorer mental health (specifically depression) and that lasting changes in PAC may be a mechanism underlying TMS treatment. Notably, cross-frequency theta–gamma tACS protocols have been demonstrated to influence memory (Alekseichuk et al., 2016; Lara et al., 2018), cognitive control (Turi et al., 2020), and emotional-action control (Bramson et al., 2020). Alekseichuk et al. (2016) reported that theta–gamma tACS has a greater effect on working memory than theta tACS. If PAC is disrupted in mental disorder, then cross-frequency tACS may be a promising prospective treatment.

Mental Disorder

Currently, research investigating the links between mental health and PAC is emerging. A number of studies have investigated the relationship between PAC and psychotic disorders. Barr et al. (2017) compared PAC between adults diagnosed with schizophrenia and healthy controls. Theta–gamma coupling within the prefrontal cortex was significantly reduced during a working memory task in the patient group compared to controls. Whereas increased theta–gamma coupling was associated with correct responses on a working memory task in the controls, there was no association between coupling and accuracy in the patient group. Theta–gamma coupling within the occipital region decreased with working memory load in controls, but there was no pattern in patients. Other studies (Won et al., 2018; Lee et al., 2019) have compared PAC at rest in healthy controls to young adults (*mean* age = 23.2 and *SD* = 4.9) with first-episode psychosis and adults with neuroleptic-naïve schizophrenia, respectively. Both studies identified increased theta–gamma PAC at rest within regions known to be associated with the default mode network (DMN) in patient groups compared to controls. These results suggest people with psychosis have dysfunctional hyperactivation of resting-state theta–gamma PAC within DMN-related brain regions, which may be a result of compensatory reallocation of cognitive resources due to dysfunction in the prefrontal cortex. Won et al. (2018) also reported that PAC better predicts patients with schizophrenia (with a classification accuracy of 92.5%) compared to power spectra analysis (which had 62.2% accuracy), suggesting that it is a promising neurophysiological marker of schizophrenia.

Another study compared theta–gamma PAC between young people with ADHD and healthy controls. The ADHD group demonstrated significantly reduced PAC within diffuse regions across the cortex during an arithmetic task compared to the controls. Deficits in PAC were associated with reduced performance on the arithmetic task. The authors hypothesized that reductions in PAC reflected deactivation of the DMN during the task, but failure to shift to attentional networks (Kim et al., 2016). Although further PAC research is required across a range of disorders, these early results suggest that PAC is associated with functional aspects of various mental disorders. Further detailed research is likely to provide a greater understanding of its mechanisms across cognition and mental health.

PAC AND STRUCTURAL CONNECTIVITY

Currently, the exact mechanisms that underpin CFC are unknown. The EEG signal is believed to be predominantly generated by pyramidal cells in the cortex (for a full explanation of the EEG signal generation process, see Steriade et al., 1990; Kirschstein and Köhling, 2009). EEG functional connectivity is believed to be strongly influenced by white matter (WM) in myelinated axons—specifically cortico-cortical axons (Nunez et al., 2015). Through *in vivo* analysis of WM using

contemporary MRI techniques such as diffusion tensor imaging (DTI) abnormalities in WM microstructure have been established across a range of mental disorders (Kanaan et al., 2005; Sexton et al., 2009; Heng et al., 2010). Although DTI resolution is too limited to create comprehensive maps of axon connectivity (Nunez et al., 2015), combining EEG and DTI may improve our understanding of how anatomical connectivity shapes functional connectivity (Cohen, 2011). Early research into alternative measures (cross-correlation and coherence) of EEG functional connectivity has identified associations with structural connectivity (Chu et al., 2015).

We are unaware of any studies to date that have implemented concurrent EEG and DTI to investigate how PAC is related to brain structure. Hawasli et al. (2016) hypothesized that WM and gray matter (GM) lesions in humans undergoing resection surgery for epilepsy or brain tumors would result in disruption to PAC. Contrary to their hypothesis, they reported that PAC was maintained after WM lesions, and GM lesions resulted in increased beta–gamma PAC in the resected area. Using concurrent DTI and EEG analyses may provide further insight into how the relationship between WM microstructure and PAC both within regions and across cortical networks affects information processing. Specifically, such research during adolescent brain development may help us better understand healthy and pathological neural development trajectories and thus lead to new methods of identification and treatment for mental disorder in youths.

PAC AND THE DEVELOPING ADOLESCENT BRAIN

The majority of PAC research to date has focused on cross-sectional adult samples. Although some recent studies investigating younger age groups have been completed (i.e., in memory, attention, and ADHD), there does not appear to have been any large-scale studies that have investigated PAC longitudinally, from a developmental perspective. As adolescence is known to be a critical period for the development of mental disorders, recent evidence that PAC is associated with mental health demonstrates a clear requirement for PAC research throughout this period. Understanding the emergence of pathology is critical for understanding the biological basis of mental illness. Because initial PAC research focused on task-based cognitive studies, some initial perspectives suggested that PAC is a transient, state-based measure, whereas other forms of CFC may be more steady and suited to longitudinal research. For example, amplitude–amplitude coupling (AAC) between lower frequency oscillations was suggested to be particularly suited to longitudinal research as it demonstrated trait like properties associated with motivational and emotional processes, as well as anxiety (Schutter and Knyazev, 2012). Knyazev et al. (2019) investigated AAC annually in 7–10-year-olds, finding that AAC appears to have non-linear growth trajectories with strong test–retest reliability and that higher AAC in cortical areas related to emotion, attention, and social cognition was related to introversion.

However, little is known about AAC as it has received relatively little attention in the literature compared to PAC. Recent evidence demonstrating that PAC is associated with mental health and cognition, including at rest and pre-post intervention, illustrates that PAC clearly has persistent, stable components equally suited to longitudinal research. This emerging research suggesting that PAC may be an important biomarker of mental health highlights the importance of longitudinal research investigating PAC throughout the rapid differential structural brain changes that occur during adolescence. Longitudinal research to determine whether PAC demonstrates similar non-linear growth trajectories to AAC and how these are associated with adolescent cognitive development and mental health may be crucial to better understanding how PAC research can contribute to better understanding mental health.

LIMITATIONS

It is important to also acknowledge potential confounds in PAC research. Specifically, the susceptibility of PAC measures to spurious identification of PAC has recently been highlighted (Aru et al., 2015). Numerous measures have been developed, each with strengths and weaknesses (Hülsemann et al., 2019). In particular higher harmonics from non-sinusoidal cortical activity can result in PAC that does not reflect true neuronal activity. This potential for spurious PAC does not preclude the significance of true PAC, rather it highlights the importance of deliberate methods and analyses in future research to ensure that PAC findings reflect true neural phenomena. Aru et al. (2015) and Jensen et al. (2017) outline key recommendations and considerations for avoiding confounds, including critically the presence of oscillations with clear peaks in a time-resolved power spectrum. A number of advanced signal-processing tools are being developed, including the Extended Modulation Index Toolbox by Jurkiewicz et al. (2020) designed specifically to address these issues.

CONCLUSION AND FUTURE DIRECTIONS

Research increasingly suggests that PAC is a fundamental component of human information processing, involved across a range of cognitive processes. Recently, PAC has been implicated in mental health as well, with a number of studies identifying abnormalities in PAC as features of psychotic disorders and ADHD. Decreased symptoms of depression after TMS were also associated with an increase in PAC. More in-depth research is required to fully understand PAC's role in these disorders, as well as similar research investigating whether abnormalities in PAC are implicated across a range of other mental disorders. However, PAC is believed to be closely associated with neuroplasticity and thus likely critical across mental disorder and treatment. Current findings suggest that better understanding PAC could potentially lead to a better understanding of mental health. While our knowledge regarding PAC is growing, the majority of research to

date has focused on cross-sectional adult samples. As much of the initial PAC literature focused on task-based cognitive research, some initial perspectives suggested that PAC is useful only as a transient, state-based measure. However, it is now evident that PAC has both state-based and stable components, considering current evidence demonstrating PAC's association with mental health at rest and changes over time pre- and post-TMS treatment.

Further research is required to understand PAC during adolescence—a critical period for mental health in which early identification and treatment has been identified as a key strategy for reducing the burden of mental disorder. Longitudinal research focusing on PAC throughout adolescence could help pinpoint the development of psychopathology and the links between cognition and mental health during this period. Combining EEG PAC analysis with DTI for concurrent assessment of structural and functional connectivity may provide the first insights into the relationship between WM microstructure and PAC. For example, coupling between the phase of theta oscillations in prefrontal cortex to the amplitude of gamma oscillations in posterior visual cortex may correspond to increased structural connectivity between these regions. Such research may lead to a greater understanding of the relationship between structural and functional mechanisms underlying information processing and mental health throughout adolescent development. Considering the recently discovered association between PAC and contemporary treatment methods such as TMS, such research has the potential to facilitate a better understanding of the mechanisms underlying such treatment and lead to improved application of these treatments for mental health disorders in the future.

AUTHOR CONTRIBUTIONS

All authors listed have made a substantial, direct and intellectual contribution to the work, and approved it for publication.

FUNDING

DS was supported by an Australian Government Research Training Program (RTP) Scholarship.

REFERENCES

Alekseichuk, I., Turi, Z., Amador de Lara, G., Antal, A., and Paulus, W. (2016). Spatial working memory in humans depends on theta and high gamma synchronization in the prefrontal cortex. *Curr. Biol.* 26, 1513–1521. doi: 10.1016/j.cub.2016.04.035

Andersen, S. L. (2003). Trajectories of brain development: point of vulnerability or window of opportunity? *Neurosci. Biobehav. Rev.* 27, 3–18. doi: 10.1016/s0149-7634(03)00005-8

Aru, J., Aru, J., Priesemann, V., Wibral, M., Lana, L., Pipa, G., et al. (2015). Untangling cross-frequency coupling in neuroscience. *Curr. Opin. Neurobiol.* 31, 51–61. doi: 10.1016/j.conb.2014.08.002

Axmacher, N., Henseler, M. M., Jensen, O., Weinreich, I., Elger, C. E., and Fell, J. (2010). Cross-frequency coupling supports multi-item working memory in the human hippocampus. *Proc. Natl. Acad. Sci.* 107, 3228–3233. doi: 10.1073/pnas.0911531107

Barr, M. S., Rajji, T. K., Zomorrodi, R., Radhu, N., George, T. P., Blumberger, D. M., et al. (2017). Impaired theta-gamma coupling during working memory performance in schizophrenia. *Schizophrenia Res.* 189, 104–110. doi: 10.1016/j.schres.2017.01.044

Benítez-Burraco, A., and Murphy, E. (2019). Why brain oscillations are improving our understanding of language. *Front. Behav. Neurosci.* 13:190. doi: 10.3389/fnbeh.2019.00190

Berger, H. (1929). Über das elektrenkephalogramm des menschen. *Archiv für Psychiatrie und Nervenkrankheiten.* 87, 527–570. doi: 10.1007/BF01797193

Bramson, B., den Ouden, H. E. M., Toni, I., and Roelofs, K. (2020). Improving emotional-action control by targeting long-range phase-amplitude neuronal coupling. *eLife* 9:e59600. doi: 10.7554/eLife.59600

Brennan, J. R., and Martin, A. E. (2020). Phase synchronization varies systematically with linguistic structure composition. *Philos. Trans. R. Soc. Lond B Biol. Sci.* 375:20190305. doi: 10.1098/rstb.2019.0305

Canolty, R. T., and Knight, R. T. (2010). The functional role of cross-frequency coupling. *Trends Cogn. Sci.* 14, 506–515. doi: 10.1016/j.tics.2010.09.001

Casey, B., Jones, R. M., and Somerville, L. H. (2011). Braking and accelerating of the adolescent brain. *J. Res. Adolesc.* 21, 21–33. doi: 10.1111/j.1532-7795.2010.00712.x

Casey, B. J., Jones, R. M., Levita, L., Libby, V., Pattwell, S. S., Ruberry, E. J., et al. (2010). The storm and stress of adolescence: insights from human imaging and mouse genetics. *Dev. Psychobiol.* 52, 225–235. doi: 10.1002/dev.20447

Chu, C. J., Tanaka, N., Diaz, J., Edlow, B. L., Wu, O., Hämäläinen, M., et al. (2015). EEG functional connectivity is partially predicted by underlying white matter connectivity. *NeuroImage.* 108, 23–33. doi: 10.1016/j.neuroimage.2014.12.033

Chuderski, A. (2016). Fluid intelligence and the cross-frequency coupling of neuronal oscillations. *Spanish J. Psychol.* 19:E91. doi: 10.1017/sjp.2016.86

Cohen, M. X. (2011). It's about time. *Front. Hum. Neurosci.* 5:2. doi: 10.3389/fnhum.2011.00002

Doesburg, S., Vinette, S., Cheung, M., and Pang, E. (2012). Theta-modulated gamma-band synchronization among activated regions during a verb generation task. *Front. Psychol.* 3:195. doi: 10.3389/fpsyg.2012.00195

Doesburg, S. M., Green, J. J., McDonald, J. J., and Ward, L. M. (2012). Theta modulation of inter-regional gamma synchronization during auditory attention control. *Brain Res.* 1431, 77–85. doi: 10.1016/j.brainres.2011.11.005

Fergusson, D. M., Horwood, L. J., Ridder, E. M., and Beautrais, A. L. (2005). Subthreshold depression in adolescence and mental health outcomes in adulthood. *Arch. Gen. Psychiatry.* 62, 66–72. doi: 10.1001/archpsyc.62.1.66

Fries, P. (2005). A mechanism for cognitive dynamics: neuronal communication through neuronal coherence. *Trends Cogn. Sci.* 9, 474–480. doi: 10.1016/j.tics.2005.08.011

Friese, U., Köster, M., Hassler, U., Martens, U., Trujillo-Barreto, N., and Gruber, T. (2013). Successful memory encoding is associated with increased cross-frequency coupling between frontal theta and posterior gamma oscillations in human scalp-recorded EEG. *NeuroImage.* 66, 642–647. doi: 10.1016/j.neuroimage.2012.11.002

Gagol, A., Magnuski, M., Kroczek, B., Kałamała, P., Ociepka, M., Santarnecchi, E., et al. (2018). Delta-gamma coupling as a potential neurophysiological mechanism of fluid intelligence. *Intelligence.* 66, 54–63. doi: 10.1016/j.intell.2017.11.003

Gonzalez-Trejo, E., Mögele, H., Pfleger, N., Hannemann, R., and Strauss, D. J. (2019). Electroencephalographic phase-amplitude coupling in simulated driving with varying modality-specific attentional demand. *IEEE Trans. Hum. Machine Syst.* 49, 589–598. doi: 10.1109/THMS.2019.2931011

Hawasli, A. H., Kim, D., Ledbetter, N. M., Dahiya, S., Barbour, D. L., and Leuthardt, E. C. (2016). Influence of white and gray matter connections on endogenous human cortical oscillations. *Front. Hum. Neurosci.* 10:330. doi: 10.3389/fnhum.2016.00330

Heng, S., Song, A. W., and Sim, K. (2010). White matter abnormalities in bipolar disorder: insights from diffusion tensor imaging studies. *J. Neural. Trans.* 117, 639–654. doi: 10.1007/s00702-010-0368-9

Herrmann, C. S., Strüber, D., Helfrich, R. F., and Engel, A. K. (2016). EEG oscillations: from correlation to causality. *Int. J. Psychophysiol.* 103, 12–21. doi: 10.1016/j.ijpsycho.2015.02.003

Hickie, I. B., Scott, J., Hermens, D. F., Scott, E. M., Naismith, S. L., Guastella, A. J., et al. (2013). Clinical classification in mental health at the cross-roads: which direction next? *BMC Med.* 11:125. doi: 10.1186/1741-7015-11-125

Hülsemann, M. J., Naumann, E., and Rasch, B. (2019). Quantification of phase-amplitude coupling in neuronal oscillations: comparison of phase-locking value, mean vector length, modulation index, and generalized-linear-modeling-cross-frequency-coupling. *Front. Neurosci.* 13:573. doi: 10.3389/fnins.2019.00573

Hyafil, A., Giraud, A. L., Fontolan, L., and Gutkin, B. (2015). Neural cross-frequency coupling: connecting architectures, mechanisms, and functions. *Trends Neurosci.* 38, 725–740. doi: 10.1016/j.tins.2015.09.001

Iorfino, F., Hermens, D. F., Cross, S. P., Zmicerevska, N., Nichles, A., Badcock, C.-A., et al. (2018). Delineating the trajectories of social and occupational functioning of young people attending early intervention mental health services in australia: a longitudinal study. *BMJ Open* 8:e020678. doi: 10.1136/bmjopen-2017-020678

Iorfino, F., Scott, E. M., Carpenter, J. S., Cross, S. P., Hermens, D. F., Killedar, M., et al. (2019). Clinical stage transitions in persons aged 12 to 25 years presenting to early intervention mental health services with anxiety, mood, and psychotic disorders. *JAMA Psychiatry* 76, 1167–1175. doi: 10.1001/jamapsychiatry.2019.2360

Jensen, O., Spaak, E., and Park, H. (2017). Discriminating valid from spurious indices of phase-amplitude coupling. 3:ENEURO.0334–0316.2016. doi: 10.1523/ENEURO.0334-16.2016

Jerath, R., Beveridge, C., and Jensen, M. (2019). On the hierarchical organization of oscillatory assemblies: layered superimposition and a global bioelectric framework. *Front. Hum. Neurosci.* 13:426. doi: 10.3389/fnhum.2019.00426

Jones, K. T., Johnson, E. L., and Berryhill, M. E. (2020). Frontoparietal theta-gamma interactions track working memory enhancement with training and tDCS. *NeuroImage.* 211:116615. doi: 10.1016/j.neuroimage.2020.116615

Jurkiewicz, G. J., Hunt, M. J., and Żygierewicz, J. (2020). Addressing pitfalls in phase-amplitude coupling analysis with an extended modulation index toolbox. *Neuroinformatics.* doi: 10.1007/s12021-020-09487-3 [Epub ahead of print].

Kaminski, M., Brzezicka, A., Kaminski, J., and Blinowska, K. J. (2019). Coupling between brain structures during visual and auditory working memory tasks. *Int. J. Neural. Syst.* 29:3. doi: 10.1142/S0129065718500466

Kanaan, R. A. A., Kim, J.-S., Kaufmann, W. E., Pearlson, G. D., Barker, G. J., and McGuire, P. K. (2005). Diffusion tensor imaging in schizophrenia. *Biol. Psychiatry.* 58, 921–929. doi: 10.1016/j.biopsych.2005.05.015

Kessler, R. C., Berglund, P., Demler, O., Jin, R., Merikangas, K. R., and Walters, E. E. (2005). Lifetime prevalence and age-of-onset distributions of DSM-IV disorders in the national comorbidity survey replication. *Arch. Gen. Psychiatry* 62, 593–602. doi: 10.1001/archpsyc.62.6.593

Kim, J. W., Kim, B.-N., Lee, J., Na, C., Kee, B. S., Min, K. J., et al. (2016). Desynchronization of theta-phase gamma-amplitude coupling during a mental arithmetic task in children with attention deficit/hyperactivity disorder. *PLoS One* 11:e0145288. doi: 10.1371/journal.pone.0145288

Kirschstein, T., and Köhling, R. (2009). What is the source of the EEG? *Clin. EEG Neurosci.* 40, 146–149.

Knyazev, G. G., Savostyanov, A. N., Bocharov, A. V., Tamozhnikov, S. S., Kozlova, E. A., Leto, I. V., et al. (2019). Cross-frequency coupling in developmental perspective. *Front. Hum. Neurosci.* 13:158. doi: 10.3389/fnhum.2019.00158

Köster, M., Martens, U., and Gruber, T. (2019). Memory entrainment by visually evoked theta-gamma coupling. *NeuroImage.* 188, 181–187. doi: 10.1016/j.neuroimage.2018.12.002

Lara, G. A. D., Alekseichuk, I., Turi, Z., Lehr, A., Antal, A., and Paulus, W. (2018). Perturbation of theta-gamma coupling at the temporal lobe hinders verbal declarative memory. *Brain Stimulation* 11, 509–517. doi: 10.1016/j.brs.2017.12.007

Lawrence, D., Johnson, S. E., Hafekost, J., Boterhoven de Haan, K., Sawyer, M., Ainley, J., et al. (2015). *The Mental Health of Children and Adolescents. Report on the second Australian Child and Adolescent Survey of Mental Health and Wellbeing*. Australia: Australian Goverment.

Lee, R. S., Hermens, D. F., Redoblado-Hodge, M. A., Naismith, S. L., Porter, M. A., Kaur, M., et al. (2013). Neuropsychological and socio-occupational functioning in young psychiatric outpatients: a longitudinal investigation. *PLoS One.* 8:e58176. doi: 10.1371/journal.pone.0058176

Lee, R. S. C., Hermens, D. F., Naismith, S. L., Kaur, M., Guastella, A. J., Glozier, N., et al. (2018). Clinical, neurocognitive and demographic factors associated with functional impairment in the australian brain and mind youth cohort study (2008–2016). *BMJ Open* 8:e022659. doi: 10.1136/bmjopen-2018-022659

Lee, T. H., Kim, M., Hwang, W. J., Kim, T., Kwak, Y. B., and Kwon, J. S. (2019). Relationship between resting-state theta phase-gamma amplitude coupling and neurocognitive functioning in patients with first-episode psychosis. *Schizophrenia Res.* 216, 154–160. doi: 10.1016/j.schres.2019.12.010

Mento, G., Astle, D. E., and Scerif, G. (2018). Cross-frequency phase–amplitude coupling as a mechanism for temporal orienting of attention in childhood. *J. Cogn. Neurosci.* 30, 594–602. doi: 10.1162/jocn_a_01223

Murphy, E. (2016). The human oscillome and its explanatory potential. *Biolinguistics.* 10, 006–020.

Murphy, E. (2018). "Interfaces (travelling oscillations)+ recursion (delta-theta code)= language," in *The Talking Species: Perspectives on the Evolutionary, Neuronal and Cultural Foundations of Language*, eds E. Luef and M. Manuela (Graz: Unipress Graz Verlag), 251–269.

Noda, Y., Zomorrodi, R., Saeki, T., Rajji, T. K., Blumberger, D. M., Daskalakis, Z. J., et al. (2017). Resting-state EEG gamma power and theta–gamma coupling enhancement following high-frequency left dorsolateral prefrontal rTMS in patients with depression. *Clin. Neurophysiol.* 128, 424–432. doi: 10.1016/j.clinph.2016.12.023

Nunez, P. L., Srinivasan, R., and Fields, R. D. (2015). EEG functional connectivity, axon delays and white matter disease. *Clin. Neurophysiol.* 126, 110–120. doi: 10.1016/j.clinph.2014.04.003

Pahor, A., and Jaušovec, N. (2014). Theta–gamma cross-frequency coupling relates to the level of human intelligence. *Intelligence.* 46, 283–290. doi: 10.1016/j.intell.2014.06.007

Paus, T. (2005). Mapping brain maturation and cognitive development during adolescence. *Trends Cogn. Sci.* 9, 60–68. doi: 10.1016/j.tics.2004.12.008

Productivity Commission. (2019). *Mental Health, Report no. 95*. Canberra: Productivity Commission.

Saalmann, Y. B., Pinsk, M. A., Wang, L., Li, X., and Kastner, S. (2012). The pulvinar regulates information transmission between cortical areas based on attention demands. *Science* 337, 753–756. doi: 10.1126/science.1223082

Sauseng, P., Peylo, C., Biel, A. L., Friedrich, E. V. C., and Romberg-Taylor, C. (2019). Does cross-frequency phase coupling of oscillatory brain activity contribute to a better understanding of visual working memory? *Br. J. Psychol.* 110, 245–255. doi: 10.1111/bjop.12340

Schutter, D. J. L. G., and Knyazev, G. G. (2012). Cross-frequency coupling of brain oscillations in studying motivation and emotion. *Motiv. Emotion* 36, 46–54. doi: 10.1007/s11031-011-9237-6

Sexton, C. E., Mackay, C. E., and Ebmeier, K. P. (2009). A systematic review of diffusion tensor imaging studies in affective disorders. *Biol. Psychiatry* 66, 814–823. doi: 10.1016/j.biopsych.2009.05.024

Steriade, M., Gloor, P., Llinás, R. R., Lopes da Silva, F. H., and Mesulam, M. M. (1990). Basic mechanisms of cerebral rhythmic activities. *Electroencephal. Clin. Neurophysiol.* 76, 481–508. doi: 10.1016/0013-4694(90)90001-Z

Turi, Z., Mittner, M., Lehr, A., Bürger, H., Antal, A., and Paulus, W. (2020). θ-γ Cross-frequency transcranial alternating current stimulation over the trough impairs cognitive control. *eNeuro* 7:5. doi: 10.1523/ENEURO.0126-20.2020

van der Meij, R., Kahana, M., and Maris, E. (2012). Phase–amplitude coupling in human electrocorticography is spatially distributed and phase diverse. *J. Neurosci.* 32, 111–123. doi: 10.1523/JNEUROSCI.4816-11.2012

Vosskuhl, J., Huster, R. J., and Herrmann, C. S. (2015). Increase in short-term memory capacity induced by down-regulating individual theta frequency via transcranial alternating current stimulation. *Front. Hum. Neurosci.* 9:257. doi: 10.3389/fnhum.2015.00257

Wang, L., Hagoort, P., and Jensen, O. (2018). Language prediction is reflected by coupling between frontal gamma and posterior alpha oscillations. *J. Cogn. Neurosci.* 30, 432–447.

Wolinski, N., Cooper, N. R., Sauseng, P., and Romei, V. (2018). The speed of parietal theta frequency drives visuospatial working memory capacity. *plos Biol.* 16:e2005348. doi: 10.1371/journal.pbio.2005348

Won, G. H., Kim, J. W., Choi, T. Y., Lee, Y. S., Min, K. J., and Seol, K. H. (2018). Theta-phase gamma-amplitude coupling as a neurophysiological marker in neuroleptic-naïve schizophrenia. *Psychiatry Res.* 260, 406–411. doi: 10.1016/j.psychres.2017.12.021

Conflict of Interest: The authors declare that the research was conducted in the absence of any commercial or financial relationships that could be construed as a potential conflict of interest.

frontiers in Neuroscience

ORIGINAL RESEARCH
published: 26 March 2021
doi: 10.3389/fnins.2021.645936

Functional and Structural Connectivity Between the Left Dorsolateral Prefrontal Cortex and Insula Could Predict the Antidepressant Effects of Repetitive Transcranial Magnetic Stimulation

*Yixiao Fu[1†], Zhiliang Long[2†], Qinghua Luo[1], Zhen Xu[1], Yisijia Xiang[1], Wanyi Du[1], Yuanyuan Cao[1], Xiaoli Cheng[1] and Lian Du[1]**

[1] Department of Psychiatry, The First Affiliated Hospital of Chongqing Medical University, Chongqing, China, [2] Sleep and NeuroImaging Center, Faculty of Psychology, Southwest University, Chongqing, China

Background: The efficacy of repetitive transcranial magnetic stimulation (rTMS) in depression is nonuniform across patients. This study aims to determine whether baseline neuroimaging characters can provide a pretreatment predictive effect for rTMS.

Methods: Twenty-seven treatment-naive patients with major depressive disorder (MDD) were enrolled and scanned with resting-state functional magnetic resonance imaging (fMRI) and diffusion tensor imaging. Clinical symptoms were assessed pre- and post-rTMS. Functional and structural connectivity between the left dorsolateral prefrontal cortex (DLPFC) and bilateral insula were measured, and the connectivity strength in each modality was then correlated to the clinical efficacy of rTMS.

Results: When the coordinates of left DLPFC were located as a node in the central executive network, the clinical efficacy of rTMS was significantly correlated with the functional connectivity strength between left DLPFC and bilateral insula (left insula: r = 0.66; right insula: r = 0.65). The structural connectivity strength between the left DLPFC and left insular cortex also had a significantly positive correlation with symptom improvement (r_S = 0.458).

Conclusion: This study provides implications that rTMS might act more effectively when the pretreatment functional and structural connectivity between the insula and left DLPFC is stronger.

Keywords: repetitive transcranial magnetic stimulation, resting-state functional magnetic resonance imaging, diffusion tensor imaging, dorsolateral prefrontal cortex, insula

OPEN ACCESS

Edited by:
Jiaojian Wang,
University of Electronic Science and Technology of China, China

Reviewed by:
Jijun Wang,
Shanghai Jiao Tong University, China
Dahua Yu,
Inner Mongolia University of Science and Technology, China

***Correspondence:**
Lian Du
fmridul@126.com

† These authors have contributed equally to this work and share first authorship

Specialty section:
This article was submitted to Brain Imaging Methods, a section of the journal Frontiers in Neuroscience

Received: *24 December 2020*
Accepted: *25 February 2021*
Published: *26 March 2021*

Citation:
Fu Y, Long Z, Luo Q, Xu Z, Xiang Y, Du W, Cao Y, Cheng X and Du L (2021) Functional and Structural Connectivity Between the Left Dorsolateral Prefrontal Cortex and Insula Could Predict the Antidepressant Effects of Repetitive Transcranial Magnetic Stimulation. Front. Neurosci. 15:645936. doi: 10.3389/fnins.2021.645936

INTRODUCTION

The pathophysiology of depression involves dysfunction in both limbic and cortical regions (Mayberg, 2007). Among these regions, the left DLPFC (Koenigs and Grafman, 2009) and insula (Sliz and Hayley, 2012) have been extensively studied given their high rate of involvement in depression-related abnormalities. The DLPFC is a key region of executive control network (CEN), mediating cognitive functions. Functional imaging studies have revealed hypoactivity in the left DLPFC during the progression of depression and hyperactivity during the recovery phase (Koenigs and Grafman, 2009). Lesion studies in patients have shown that relative to nonfrontal lesions, bilateral dorsal PFC lesions were associated with substantially higher levels of depression (Koenigs and Grafman, 2009). The insula has distributed connectivity with the prefrontal, temporal, parietal, and limbic regions (Sliz and Hayley, 2012), which has been putatively implicated as an integration center between the external environment and internal processing and regulating regions in the brain (Sliz and Hayley, 2012). Tracer studies in primates have shown direct white matter connections between the anterior insula and prefrontal regions (Mesulam and Mufson, 1982). The anterior insula has been reported to be associated with the cognitive–affective dimension (Peltz et al., 2011) and further reported to be a part of a "salience network" (SN) (Sridharan et al., 2008). A growing body of literature has identified insula dysfunction in adolescents at-risk for (Gotlib et al., 2010) and with depression (Tahmasian et al., 2013; Jacobs et al., 2016; Yin et al., 2018). Changes in insula activity have been thought to be associated with antidepressant treatments (Fu et al., 2013).

Some previous findings have shown aberrant connectivity between insular and dorsal lateral frontal regions connectivity in sub-threshold depression patients (Hwang et al., 2015), as well as between SN and CEN in depression (Manoliu et al., 2014). Sevdalina et al. further showed that patients had significant reduced strength of the connection from the anterior insula to the DLPFC in depression (Kandilarova et al., 2018). Moreover, Hyett et al. (2015) found that melancholic patients demonstrated weaker effective connectivity between the right frontoparietal and insula networks. This suggests the possibility that a disrupted connectivity between the DLPFC and the insula in depression.

Repetitive transcranial magnetic stimulation (rTMS) is regarded as a promising treatment option for depression (Hallett, 2007), has been approved by the US Food and Drug Administration (FDA), and is covered by many public and private insurers in the USA and other countries (Perera et al., 2016). However, rTMS treatment for depression usually takes 4-6 weeks, and only a portion of patients can benefit from rTMS, while others could not (O'Reardon et al., 2007). Therefore, it is of critical importance to obtain a measurement that can provide predictive value on the treatment efficacy of rTMS in depression. The left DLPFC was one of regions targeted most often in treating depression with rTMS. Notably, TMS can not only directly affect regions at the cortical surface but also propagate beyond the site of stimulation, impacting a distributed network of brain regions (Ferreri et al., 2011; Fox et al., 2012b) including the insula (Kito et al., 2011). Thus, we hypothesized that rTMS took effects through the connectivity between left DLPFC (directly stimulated region) and insula. To elucidate these issues, the present study used resting-state functional connectivity magnetic resonance imaging (MRI) (Van Dijk et al., 2010) and diffusion tensor imaging (DTI) to determine whether resting-state functional and structural connectivity between the left DLPFC and bilateral insula can provide a pretreatment predictive measure for the antidepressant effect of rTMS.

MATERIALS AND METHODS

Participants

A total of 27 right-handed outpatients (18 females, 9 males; age: 40 $\pm$ 13.8 years), with a single episode or recurrent depressive episodes and who were medication-free (not treated in the previous month and had been previously medicated for less than a week) were recruited for this study. The diagnosis of MDD was confirmed by the Structured Clinical Interview for the Diagnostic and Statistical Manual of Mental Disorders IV (SCID-I/P, Chinese version). Patients were excluded if they had a history of current or past psychotic disorders, alcohol or drug abuse, any current clinically significant neurological disorder or other serious physical diseases, morphological abnormalities in the brain, less than 18 years of age, and any electronic or metal implants. The therapeutic schedule for the MDD patients was decided by their clinicians; we only observed and recorded the relevant situations. At the beginning of this study, patients were screened by the researchers to assess if they met the above inclusion/exclusion criteria. All the patients were assessed for clinical severity using the 17-item Hamilton Depression Scale (HAMD) both at baseline and at the end of rTMS treatment. This study was reviewed and approved by the Local Medical Ethics Committee of the First Affiliated Hospital of Chongqing Medical University. All participants provided written informed consent before participating in this work.

rTMS Protocol

rTMS was delivered in sessions by a YRD CCY-I magnetic simulator (YIRUIDE Inc., Wuhan, China). The patients received a total of 10 sessions of rTMS (five sessions per week for 2 weeks). The stimulation parameters were within the safe range requirements (George and Belmaker, 2007): 100% magnetic field strength relative to the patient's observed resting motor threshold, at 10 pulses per second for 3 s, with an interval of 21 s. Treatment sessions lasted for 20 min (50 trains) and consisted of 1,500 pulses. The stimulation position for the left DLPFC was located using the "5 cm" method (Johnson et al., 2013) (with the left DLPFC target as a point located 5 cm in front of the "hand motor hotspot" in the parasaggital plane pointing anteriorwards).

MRI Scan Acquisition

The 27 patients were scanned by MRI at baseline. Data were acquired on a 3.0 Tesla MRI system (GE Medical Systems, Waukesha, WI, United States) at the First Affiliated Hospital of Chongqing Medical University. The participants were asked to remain motionless, keep their eyes closed, and not think

of anything. Functional images were obtained by using an echo-planar imaging sequence with the following parameters: TR/TE = 2000/30 ms, 33 axial slices, field of view = 240 × 240 mm^2, matrix size = 64 × 64, voxel size = 3.75 × 3.75 × 5 mm^3, flip angle = 90°, and a total of 240 volumes. The T1 structural images were acquired using the following parameters: TR/TE = 8.35/3.27 ms, slice thickness = 1 mm, flip angle = 12°, matrix size = 256 × 256, and 156 sagittal slices. The parameters for the DTI scanning were as follows: TR/TE = 15000/88.3 ms, slice thickness = 2 mm, flip angle = 90°, 56 axial slices, matrix size = 256 × 256, 30 noncollinear diffusion weighting gradient directions [b = 1000 s/mm^2], and four additional images without diffusion weighting [b = 0 s/mm^2].

Functional Data Preprocessing and Functional Connectivity Analysis

The preprocessing of the resting-state MRI data was performed using the SPM12 software toolbox[1]. The first 10 time points were discarded due to the adaptation of the participants to the scanning environment and magnetization stabilization. The images were then corrected for the time-delay between slices and the motion movement between volumes. The participants with their x, y, or z directions larger than 3 mm or rotation around each axis larger than 3° were excluded. All subjects met the criterion. The resulting images were normalized by using a unified segmentation of anatomical images and resampled into a 3 × 3 × 3 mm^3 voxel size. A multiple regression model was employed to remove the effect of covariates of no interest, including 24 motion parameters, mean white matter signal and mean CSF signal. The resulting images were finally linearly detrended and filtered in the range of 0.01 to 0.08 Hz.

Given that resting-state functional connectivity (FC) is sensitive to minor head movements (Power et al., 2012, 2014, 2015; Satterthwaite et al., 2013), we computed the framewise displacement (FD) (Power et al., 2012) at time point *i*, which is defined as follows:

$$FD_i = |\Delta d_{ix}| + |\Delta d_{iy}| + |\Delta d_{iz}| + r|\Delta\alpha_i| + r|\Delta\beta_i| + r|\Delta\gamma_i|$$

where the $\Delta d_{ix} = d_{(i-1)x} - d_{ix}$ and is similar for the other parameters Δd_{iy}, Δd_{iz}, $\Delta\alpha_i$, $\Delta\beta_i$, and $\Delta\gamma_i$. The radius *r* is 50 mm, which is the approximate mean distance from the cortex to the center of the head. The "bad" time points as well as their 1-back and 2-forward time points were removed from the time series by employing a "scrubbing" method (Power et al., 2012) with an FD threshold of 0.5 mm. The participants retaining more than 80% of the original signals after scrubbing were included in further analyses.

The spherical regions of interest (ROI) of the left DLPFC were obtained with the center of -36 27 29 and radius of 8 mm (de Kwaasteniet et al., 2015), according to the coordinates of a node in CEN, and multiplied by a mask of the automated anatomical labeling (AAL) atlas (Tzourio-Mazoyer et al., 2002) to exclude none gray matter voxels. The ROIs of the bilateral insular cortex were selected based on the AAL atlas.

Seed-based functional connectivity (FC) analysis was conducted between the averaged time course of the left DLPFC and the time series of all voxels across the insular cortex for each subject by using Pearson's correlations. The correlation values were subsequently *r*-to-*z* transformed. A two-tailed one-sample *t*-test was then employed to test whether the FC value was different from zero. Voxels with $p < 0.05$ were saved as a mask for the following multiple regression analysis.

Considering the small sample size in the current study, multiple regression analysis was conducted between FC maps and the HAMD score reductions by employing Statistical Non-Parametric Mapping (SNPM version 13)[2] with 5000 permutations (Nichols and Holmes, 2001). The multiple comparisons were corrected by using the cluster-size-based familywise error of $p < 0.05$ with a cluster-forming threshold of $p < 0.005$.

It has been suggested that resting-state functional connectivity is sensitive to head movement. So we computed mean FD for each subject, and included it as a covariate, in order to see if head movement has influence on the statistical results.

Considering the different coordinates of the left DLPFC according to different methods, we further used another two methods to locate the left DLPFC, the center of BA9 (−36 39 43) and the center of BA46 (−44 40 29), and then separately repeated the above steps.

Diffusion Tensor Image Analysis

The preprocessing of DTI images was carried out using the following procedures. Briefly, each individual T1-weighted image was first coregistered to the B0 image in the native diffusion space by using a linear transformation. The coregistered structural images were then mapped to the MNI T1-template. The derived transformation parameters were inverted and used to warp the ROIs of the left DLPFC and bilateral insular cortex from the MNI space to the native diffusion space. For the structural connectivity analysis, we selected BA9 plus BA46 as the ROI of the left DLPFC. These procedures were conducted using SPM12 software.

For each subject, diffusion-weighted images were corrected for the eddy-current-induced distortions and head movements using FSL[3]. Diffusion tensor models were estimated by the linear least-squares fitting method at each voxel using the Diffusion Toolkit (Wang et al., 2007). Whole-brain fiber tracking was performed in native diffusion space by employing the Fiber Assignment by Continuous Tracking (FACT) algorithm. All the tracks in the data were computed by seeding voxels with fractional anisotropy (FA) larger than 0.2 (Mori et al., 2002). Path tracing continued until either a voxel with FA less than 0.2 was reached or the angle between the current and the previous path segment exceeded 45 degrees (Shu et al., 2011).

We calculated the mean FA values of connected fibers between the left DLPFC and insular cortex. The FA value is an important index to evaluate fiber integrity (Beaulieu, 2002) and can detect local subtle brain lesions (Lim and Helpern, 2002). Furthermore, nonparametric Spearman correlation analysis was performed to

[1]https://www.fil.ion.ucl.ac.uk/spm/

[2]http://warwick.ac.uk/snpm

[3]https://www.fmrib.ox.ac.uk/fsl

investigate the relationship between the nonzero FA values and the corresponding HAMD score reductions. A statistical level of $p < 0.05$ was considered significant.

RESULTS

Clinical Outcomes

The demographic and clinical features of the MDD patients are summarized in **Table 1**. After 2 weeks of rTMS treatment, the total scores on the HAMD were significantly decreased ($t = 5.97$, $p < 0.001$; **Figure 1**), with the HAMD reductive rate of 0.29 ± 0.24 (mean ± std).

Correlation of Functional Connectivity at Baseline With Clinical Efficacy

When the coordinates of the left DLPFC were located according to the coordinates of a node in the CEN, a one-sample *t*-test revealed that the left DLPFC had positive functional connectivity with the bilateral insular cortex (**Figure 2**). In addition, functional connectivity between the left DLPFC and bilateral anterior insular cortex was significantly correlated ($r = 0.66$, $p < 0.001$, for left insula; $r = 0.65$, $p < 0.001$, for the right insula; **Figure 3**).

Whether included mean FD as a covariate or not in the statistical analysis, we both found significantly positive correlation between left DLPFC-left insula FC and clinical efficacy of rTMS.

When the coordinates of the left DLPFC were located at the center of BA9 and BA46, we did not observe any significant correlations between the connectivity of the left DLPFC with the insula and the clinical efficacy of rTMS (**Supplementary Figures 1**, **2**).

Correlation of Structural Connectivity at Baseline With Clinical Efficacy

We observed that fiber tracks existed only between the left DLPFC and left insula but not between the left DLPFC and right insula. Analysis of the diffusion tensor images revealed that the mean FA values of structural connectivity between the left DLPFC and left insula cortex had a significantly positive correlation with the rTMS-induced HAMD score reductions ($r_s = 0.458$, $p = 0.028$) (**Figure 4**).

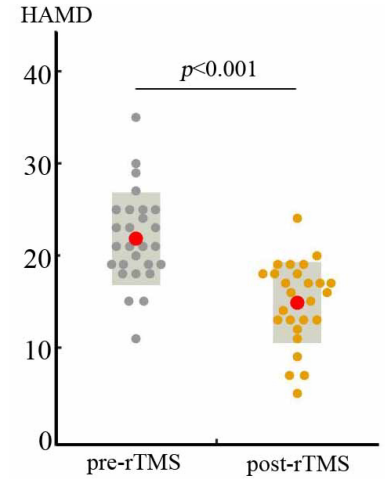

FIGURE 1 | Two weeks of rTMS induced significant decreases in HAMD scores ($t = 5.97$, $p < 0.001$).

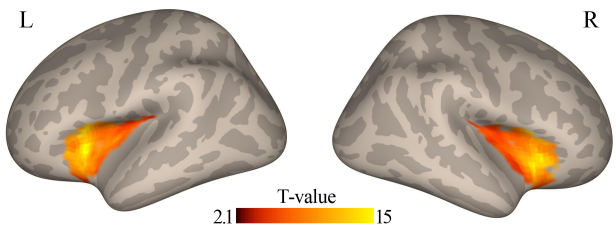

FIGURE 2 | Positive functional connectivity between the left DLPFC and bilateral insular cortex was observed using a one-sample *t*-test ($p < 0.05$). DLPFC, dorsal lateral prefrontal cortex.

TABLE 1 | Demographics and clinical characters of MDD patients.

Demographics	MDD ($n = 27$)	*p*-value	*T*-value
Age (years)	40.04 ± 13.79	/	/
Sex (male/female)	9/18	/	/
Episode (first/recurrent)	15/12	/	/
Education (years)	12.00 ± 3.95	/	/
Age of onset (years)	34.44 ± 13.33	/	/
HAMD scores: Pre-rTMS	21.81 ± 5.04	$p < 0.0001$[a]	5.97
Post-rTMS	14.89 ± 4.41		
HAMD reduction rate	0.29 ± 0.24		

The values are illustrated as mean ± SD.
MDD, major depressive disorder;
HAMD, Hamilton Depression Scale.
[a] *paired t-test.*

DISCUSSION

In the current article, we used a connectivity analysis to gain insight into why rTMS using the same '5 cm method' to locate the left DLPFC on the surface of the skull has different clinical effects in depressed patients. We identified a positive correlation between the clinical efficacy of rTMS and functional connectivity (left DLPFC–bilateral insula) in the pre-rTMS state as well as structural connectivity (left DLPFC–left insula). This makes it plausible that different levels of connectivity between the left DLPFC and insula across patients can predict the different effect sizes of rTMS. Interestingly, the predictive effect only occurs when the seed of the left DLPFC was selected as a node in the CEN, rather than the traditional BA9 or BA46. We first combined a functional and structural connectivity approach to illustrate the correlations of the superficial region (left DLPFC) with the deeper brain areas (insula) and found that their connectivity strength could predict the antidepressant effects of rTMS, which suggests

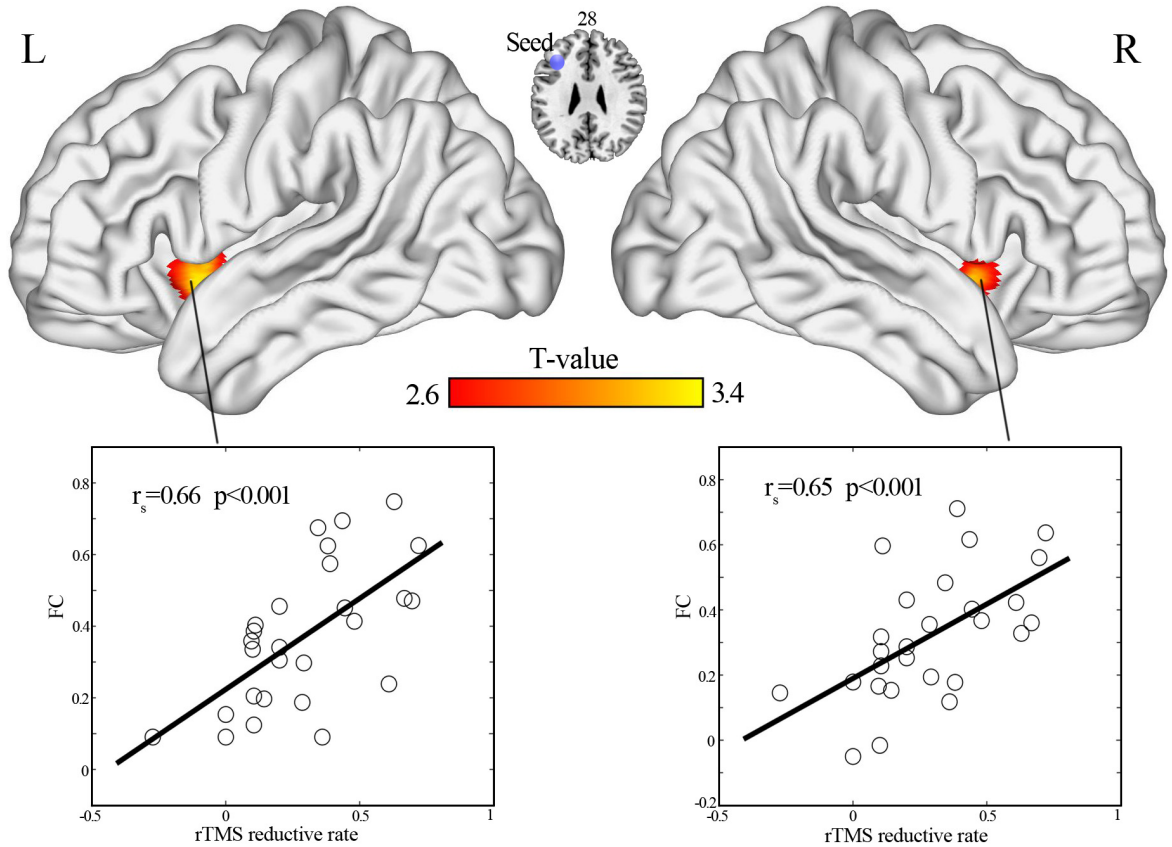

FIGURE 3 | Positive correlation of HAMD scores reduction with functional connectivity between the left DLPFC and bilateral anterior insular cortex (cluster-wise and family-wise error correction with voxel $p < 0.005$ and cluster $p < 0.05$). DLPFC, dorsal lateral prefrontal cortex.

that frontal-insular connectivity plays an important role on the predictive mechanism of rTMS in MDD.

The possible mechanisms for the differential effects of rTMS on depression warrant discussion. We examined the predictive neuroimaging mechanisms of rTMS with respect to both functional and structural connectivity of the superficial left DLPFC with deep brain areas that correlate to clinical efficacy. Fox et al. (2012a) found that the antidepressant efficacy of different left DLPFC TMS sites was related to the anticorrelation extent of each site with the subgenual cingulate, but the measures of clinical efficacy in that article were based on previously published data. Moreover, one idea about the mechanisms of rTMS that have been aggressively pursued was the propagation of TMS effects through anatomical connections to deeper limbic regions (Padberg and George, 2009). However, the anticorrelation between subgenual ACC and DLPFC is thought unlikely to be the result of direct inhibitory connections. A growing number of cross-sectional studies have used DTI to investigate the white matter (WM) microstructure in patients with MDD. Despite different methodological approaches, most investigations have reported MDD-related reductions in fractional anisotropy (FA), which is used as an index of WM integrity. A number of previous reviews have pointed to smaller FA values in WM regions associated with frontal, limbic and striatal lobes in patients with MDD, which meant altered regional patterns of WM structural connectivity in those areas (Korgaonkar et al., 2011; Cole et al., 2012). Electroconvulsive treatment (ECT) was thought to modulate the WM microstructure in pathways connecting the frontal and limbic areas in patients with MDD and relate to its therapeutic response (Lyden et al., 2014). Thus, this study combined resting-state fMRI and DTI to calculate the functional correlations and FA values and then explored whether functional and structural connectivity between left DLPFC and insula predicted the clinical efficacy of rTMS.

The current study found that insula (mainly anterior insula) and DLPFC are intrinsically positively correlated in the resting state. There are several implications of this result. First, primary hypoactivity in the left DLPFC might result in secondary hypoactivity of the insula. Second, focal excitation/inhibition in one region could be expected to enhance/suppress activity in the other region. Third, the stronger the correlation between the activities of the two regions, the more likely that rTMS will be fully effective. Lastly, the DTI analysis showed that there were fiber connections between the insula and left DLPFC. This supports the feasibility that rTMS could affect the function of the left insula following direct stimulation of the left DLPFC through their fiber connections.

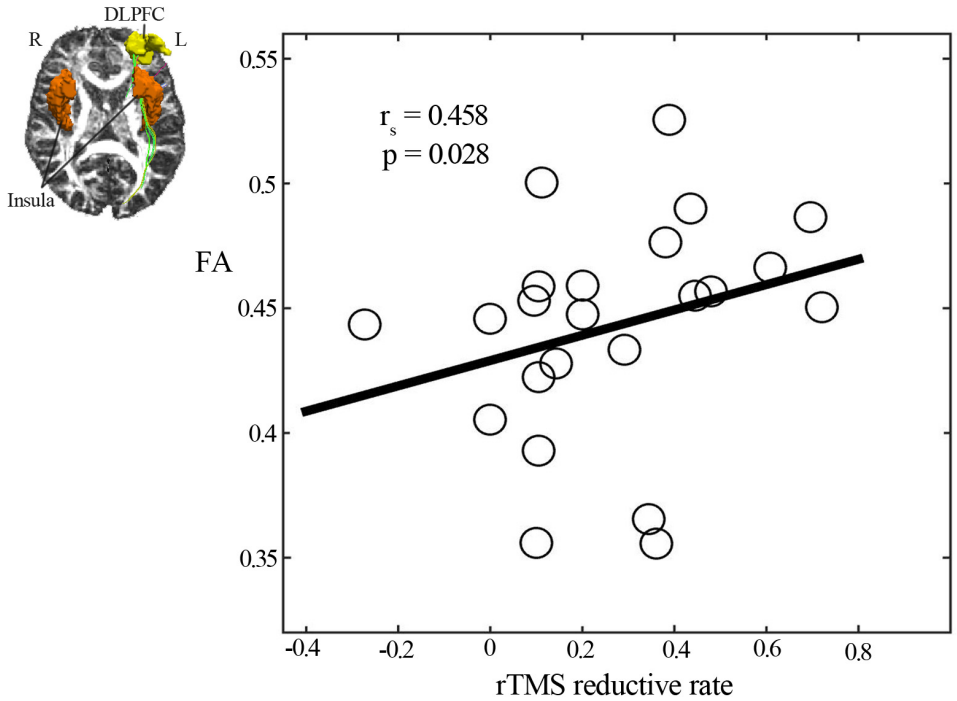

FIGURE 4 | Spearman correlation analysis showed a positive correlation of clinical efficacy with the mean FA value of structural connectivity between the left DLPFC and left insular cortex. DLPFC, dorsal lateral prefrontal cortex; FA, fractional anisotropy.

Moreover, the functional connectivity between the left DLPFC and insula could predict the antidepressant effect of rTMS only when the coordinate of left DLPFC was selected in the node of CEN. If we used other methods, such as the center of BA9 or BA46 as the seed site, the prediction effect was not significant. This emphasized the importance of CEN in the action of rTMS, which could be understood and explained by previous studies about large-scale networks in MDD. Recent studies have shown that depression is characterized by abnormal functional integration of brain networks at rest (Alexopoulos et al., 2012; Liao et al., 2018), mainly including the following three neural networks: the DMN, CEN, and SN (Seeley et al., 2007; Alexopoulos et al., 2012; Kaiser et al., 2015; Liao et al., 2018). In addition, previous study showed that functional connectivity patterns of brain regions between and within networks appeared to play an important role in identifying a favorable response for a drug treatment for MDD (Liston et al., 2014). These neural circuit impairments in depression are involved in the processing of both positive and negative emotional information, attribution of salience, and both cognitive and emotional control (Kaiser et al., 2015). The CEN, which plays a key role in executive function and emotion regulation, includes the DLPFC and lateral posterior parietal regions (Seeley et al., 2007). Meta-analyses have noted consistent patterns of resting-state hypoconnectivity within the executive control network for MDD (Kaiser et al., 2015). The SN is involved in detecting, integrating and processing internal and external salient information, and it includes the dorsal anterior cingulate cortex (dACC), anterior insula, amygdala, and ventral striatum (Seeley et al., 2007). The left DLPFC and anterior insula are the key nodes of the CEN and SN, respectively. To some extent, the strength of connectivity between the left DLPFC and insula reflects the degree of correlation of the CEN and SN. Thus, we speculate the reason why more relevancy predicted better antidepressant effect might be that, rTMS adjusts the function of CEN through stimulating left DLPFC, and then affects the function of SN through connectivity between left DLPFC and insula, and might also affect DMN through the connectivity between CEN and DMN as well as between SN and DMN. The antidepressants effects might be produced through the modulation of the function of the above networks. However, these are only hypotheses and further research is needed to verify the alteration of brain networks induced by rTMS. In summary, the current findings suggest that the antidepressant effect of rTMS might be optimized when the placement location of left DLPFC is according to the CEN. However, the position is lateral or medial, anterior or posterior might not be so important.

While the above discussion focused on the insula and the DLPFC, sgACC is an area of interest in the field of rTMS in depression. Liston et al. (2014) pointed out that rTMS acted by reducing sgACC-to-DMN connectivity and inducing anticorrelated connectivity between the DLPFC and DMN. Fox et al. (2012a) implicated left DLPFC-sgACC functional connectivity in the action of rTMS. However, one of our previous studies in depression found that compared to those not improved, early improvers did not exhibit significant differences in left DLPFC–sgACC functional connectivity strength (Du et al., 2018). Therefore, we speculate that the strength of the connection

between left DLPFC and insula might also be a predictor of the rTMS efficacy.

Limitations

The current work is limited in several respects, and these limitations suggest important avenues for future research. First, the sample size is small. Only 27 patients were included in the analysis. Second, we failed to detect the effect of a sham control group versus active rTMS, which would have made it more convincing that these neuroimaging features could predict the clinical efficacy of rTMS.

CONCLUSION

This study explored the predictive neuroimaging mechanisms of rTMS in patients with MDD. Based on the role of DLPFC and insula in depression, as well as the fact that the left DLPFC is one of the common targets of rTMS, we measured the functional and structural connectivity between the left DLPFC and insula using rs-fMRI and DTI, and analyzed the correlation of connectivity strength with clinical efficacy of rTMS. We found that the functional and structural connectivity between the two regions could positively predict the antidepressant effects; the stronger the connection strength was, the better the clinical efficacy. In addition, we found that only when the position of the left DLPFC was located as a node of CEN, other than located according to previous studies (e.g., the center of BA9 or BA46), the significant positive predictive effects were obtained. These findings provided implications that CEN might be important to rTMS, which could produce therapeutic effects through the connectivity between insula and left DLPFC by directly stimulating the latter region. However, how rTMS takes effects and influences large-scale brain networks through the left DLPFC-insula connectivity is beyond the scope of this article and remains to be investigated in the future.

DATA AVAILABILITY STATEMENT

The raw data supporting the conclusions of this article will be made available by the authors, without undue reservation.

ETHICS STATEMENT

The studies involving human participants were reviewed and approved by the Local Medical Ethics Committee of The First Affiliated Hospital of Chongqing Medical University. The patients/participants provided their written informed consent to participate in this study. Written informed consent was obtained from the individual(s) for the publication of any potentially identifiable images or data included in this article.

AUTHOR CONTRIBUTIONS

LD conceived and designed the experiments. ZX, YX, YC, and XC prepared the samples and performed fMRI for patients. WD and QL performed rTMS in MDD patients. LD, YF, and ZL contributed to the data analysis and wrote the manuscript. All authors contributed to the article and approved the submitted version.

FUNDING

This work was supported by the National Key R&D Program of China (2018YFC1314600), the National Natural Science Foundation of China (81801362, 81901725), the Medical Research Project of Chongqing Health and Family Planning Commission (2017MSXM024), and the Key Medical Research Projects of Chongqing Health and Family Planning Commission (2016ZDXM003).

SUPPLEMENTARY MATERIAL

The Supplementary Material for this article can be found online at: https://www.frontiersin.org/articles/10.3389/fnins.2021.645936/full#supplementary-material

Supplementary Figure 1 | When the coordinates of the left DLPFC were located at the center of BA9, **(A)** one sample *t*-test showed positive functional connectivity between left DLPFC and bilateral insula. **(B)** The correlations between the connectivity and the clinical efficacy of rTMS were not significant.

Supplementary Figure 2 | When the coordinates of the left DLPFC were located at the center of BA46, **(A)** one sample *t*-test showed positive functional connectivity between left DLPFC and bilateral insula. **(B)** The correlations between the connectivity and the clinical efficacy of rTMS were not significant.

REFERENCES

Alexopoulos, G. S., Hoptman, M. J., Kanellopoulos, D., Murphy, C. F., Lim, K. O., and Gunning, F. M. (2012). Functional connectivity in the cognitive control network and the default mode network in late-life depression. *J. Affect. Disord.* 139, 56–65. doi: 10.1016/j.jad.2011.12.002

Beaulieu, C. (2002). The basis of anisotropic water diffusion in the nervous system - a technical review. *NMR Biomed.* 15, 435–455. doi: 10.1002/nbm.782

Cole, J., Chaddock, C. A., Farmer, A. E., Aitchison, K. J., Simmons, A., McGuffin, P., et al. (2012). White matter abnormalities and illness severity in major depressive disorder. *Br. J. Psychiatry* 201, 33–39.

de Kwaasteniet, B. P., Rive, M. M., Ruhé, H. G., Schene, A. H., Veltman, D. J., Fellinger, L., et al. (2015). Decreased resting-state connectivity between neurocognitive networks in treatment resistant depression. *Front. Psychiatry* 6:28. doi: 10.3389/fpsyt.2015.00028

Du, L., Liu, H., Du, W., Chao, F., Zhang, L., Wang, K., et al. (2018). Stimulated left DLPFC-nucleus accumbens functional connectivity predicts the anti-depression and anti-anxiety effects of rTMS for depression. *Transl. Psychiatry* 7:3.

Ferreri, F., Pasqualetti, P., Määttä, S., Ponzo, D., Ferrarelli, F., Tononi, G., et al. (2011). Human brain connectivity during single and paired pulse transcranial magnetic stimulation. *Neuroimage* 54, 90–102. doi: 10.1016/j.neuroimage.2010.07.056

Fox, M. D., Buckner, R. L., White, M. P., Greicius, M. D., and Pascual-Leone, A. (2012a). Efficacy of transcranial magnetic stimulation targets for depression is related to intrinsic functional connectivity with the subgenual cingulate. *Biol. Psychiatry* 72, 595–603. doi: 10.1016/j.biopsych.2012.04.028

Fox, M. D., Halko, M. A., Eldaief, M. C., and Pascual-Leone, A. (2012b). Measuring and manipulating brain connectivity with resting state functional connectivity magnetic resonance imaging (fcMRI) and transcranial magnetic stimulation (TMS). *Neuroimage* 62, 2232–2243. doi: 10.1016/j.neuroimage.2012.03.035

Fu, C. H., Steiner, H., and Costafreda, S. G. (2013). Predictive neural biomarkers of clinical response in depression: a meta-analysis of functional and structural neuroimaging studies of pharmacological and psychological therapies. *Neurobiol. Dis.* 52, 75–83. doi: 10.1016/j.nbd.2012.05.008

George, M. S., and Belmaker, R. H. (2007). *Transcranial Magnetic Stimulation in Clinical Psychiatry*, 1st Edn. (Washington, DC: American Psychiatric Publishing, Inc), 20–23.

Gotlib, I. H., Hamilton, J. P., Cooney, R. E., Singh, M. K., Henry, M. L., and Joormann, J. (2010). Neural processing of reward and loss in girls at risk for major depression. *Arch. Gen. Psychiatry* 67, 380–387. doi: 10.1001/archgenpsychiatry.2010.13

Hallett, M. (2007). Transcranial magnetic stimulation: a primer. *Neuron* 55, 187–199. doi: 10.1016/j.neuron.2007.06.026

Hwang, J. W., Egorova, N., Yang, X. Q., Zhang, W. Y., Chen, J., Yang, X. Y., et al. (2015). Subthreshold depression is associated with impaired resting-state functional connectivity of the cognitive control network. *Transl. Psychiatry* 5:e683. doi: 10.1038/tp.2015.174

Hyett, M. P., Breakspear, M. J., Friston, K. J., Guo, C. C., and Parker, G. B. (2015). Disrupted effective connectivity of cortical systems supporting attention and interoception in melancholia. *JAMA Psychiatry* 72, 350–358. doi: 10.1001/jamapsychiatry.2014.2490

Jacobs, R. H., Barba, A., Gowins, J. R., Klumpp, H., Jenkins, L. M., Mickey, B. J., et al. (2016). Decoupling of the amygdala to other salience network regions in adolescent-onset recurrent major depressive disorder. *Psychol. Med.* 46, 1055–1067. doi: 10.1017/s0033291715002615

Johnson, K. A., Baig, M., Ramsey, D., Lisanby, S. H., Avery, D., McDonald, W. M., et al. (2013). Prefrontal rTMS for treating depression: location and intensity results from the OPT-TMS multi-site clinical trial. *Brain Stimul.* 6, 108–117. doi: 10.1016/j.brs.2012.02.003

Kaiser, R. H., Andrews-Hanna, J. R., Wager, T. D., and Pizzagalli, D. A. (2015). Large-scale network dysfunction in major depressive disorder: a meta-analysis of resting-state functional connectivity. *JAMA Psychiatry* 72, 603–611. doi: 10.1001/jamapsychiatry.2015.0071

Kandilarova, S., Stoyanov, D., Kostianev, S., and Specht, K. (2018). Altered resting state effective connectivity of anterior insula in depression. *Front. Psychiatry* 9:83. doi: 10.3389/fpsyt.2018.00083

Kito, S., Hasegawa, T., and Koga, Y. (2011). Neuroanatomical correlates of therapeutic efficacy of low-frequency right prefrontal transcranial magnetic stimulation in treatment-resistant depression. *Psychiatry Clin. Neurosci.* 65, 175–182. doi: 10.1111/j.1440-1819.2010.02183.x

Koenigs, M., and Grafman, J. (2009). The functional neuroanatomy of depression: distinct roles for ventromedial and dorsolateral prefrontal cortex. *Behav. Brain Res.* 201, 239–243. doi: 10.1016/j.bbr.2009.03.004

Korgaonkar, M. S., Grieve, S. M., Koslow, S. H., Gabrieli, J. D., Gordon, E., and Williams, L. M. (2011). Loss of white matter integrity in major depressive disorder: evidence using tract-based spatial statistical analysis of diffusion tensor imaging. *Hum. Brain Mapp.* 32, 2161–2171. doi: 10.1002/hbm.21178

Liao, W., Li, J., Duan, X., Cui, Q., Chen, H., and Chen, H. (2018). Static and dynamic connectomics differentiate between depressed patients with and without suicidal ideation. *Hum. Brain Mapp.* 39, 4105–4118. doi: 10.1002/hbm.24235

Lim, K. O., and Helpern, J. A. (2002). Neuropsychiatric applications of DTI - a review. *NMR Biomed.* 15, 587–593. doi: 10.1002/nbm.789

Liston, C., Chen, A. C., Zebley, B. D., Drysdale, A. T., Gordon, R., Leuchter, B., et al. (2014). Default mode network mechanisms of transcranial magnetic stimulation in depression. *Biol. Psychiatry* 76, 517–526. doi: 10.1016/j.biopsych.2014.01.023

Lyden, H., Espinoza, R. T., Pirnia, T., Clark, K., Joshi, S. H., Leaver, A. M., et al. (2014). Electroconvulsive therapy mediates neuroplasticity of white matter microstructure in major depression. *Transl. Psychiatry* 4:e380. doi: 10.1038/tp.2014.21

Manoliu, A., Meng, C., Brandl, F., Doll, A., Tahmasian, M., Scherr, M., et al. (2014). Insular dysfunction within the salience network is associated with severity of symptoms and aberrant inter-network connectivity in major depressive disorder. *Front. Hum. Neurosci.* 7:930. doi: 10.3389/fnhum.2013.00930

Mayberg, H. S. (2007). Defining the neural circuitry of depression: toward a new nosology with the rapeutic implications. *Biol. Psychiatry* 61, 729–730. doi: 10.1016/j.biopsych.2007.01.013

Mesulam, M. M., and Mufson, E. J. (1982). Insula of the old world monkey. III: efferent cortical output and comments on function. *J. Comp. Neurol.* 212, 38–52. doi: 10.1002/cne.902120104

Mori, S., Kaufmann, W. E., Davatzikos, C., Stieltjes, B., Amodei, L., Fredericksen, K., et al. (2002). Imaging cortical association tracts in the human brain using diffusion-tensor-based axonal tracking. *Magn. Reson. Med.* 47, 215–223. doi: 10.1002/mrm.10074

Nichols, T. E., and Holmes, A. P. (2001). Nonparametric permutation tests for functional neuroimaging- a primer with examples. *Hum. Brain Mapp.* 15, 1–25. doi: 10.1002/hbm.1058

O'Reardon, J. P., Solvason, H. B., Janicak, P. G., Sampson, S., Isenberg, K. E., Nahas, Z., et al. (2007). Efficacy and safety of transcranial magnetic stimulation in the acute treatment of major depression: a multisite randomized controlled trial. *Biol. Psychiatry* 62, 1208–1216. doi: 10.1016/j.biopsych.2007.01.018

Padberg, F., and George, M. S. (2009). Repetitive transcranial magnetic stimulation of the prefrontal cortex in depression. *Exp. Neurol.* 219, 2–13. doi: 10.1016/j.expneurol.2009.04.020

Peltz, E., Seifert, F., DeCol, R., Dörfler, A., Schwab, S., and Maihöfner, C. (2011). Functional connectivity of the human insular cortex during noxious and innocuous thermal stimulation. *Neuroimage* 54, 1324–1335. doi: 10.1016/j.neuroimage.2010.09.012

Perera, T., George, M. S., Grammer, G., Janicak, P. G., Pascual-Leone, A., and Wirecki, T. S. (2016). The Clinical TMS Society ConsensusReview and treatment recommendations for tms therapy for majordepressive disorder. *Brain Stimul.* 9, 336–346. doi: 10.1016/j.brs.2016.03.010

Power, J. D., Barnes, K. A., Snyder, A. Z., Schlaggar, B. L., and Petersen, S. E. (2012). Spurious but systematic correlations in functional connectivity MRI networks arise from subject motion. *Neuroimage* 59, 2142–2154. doi: 10.1016/j.neuroimage.2011.10.018

Power, J. D., Mitra, A., Laumann, T. O., Snyder, A. Z., Schlaggar, B. L., and Petersen, S. E. (2014). Methods to detect, characterize, and remove motion artifact in resting state fMRI. *Neuroimage* 84, 320–341. doi: 10.1016/j.neuroimage.2013.08.048

Power, J. D., Schlaggar, B. L., and Petersen, S. E. (2015). Recent progress and outstanding issues in motion correction in resting state fMRI. *Neuroimage* 105, 536–551. doi: 10.1016/j.neuroimage.2014.10.044

Satterthwaite, T. D., Elliott, M. A., Gerraty, R. T., Ruparel, K., Loughead, J., Calkins, M. E., et al. (2013). An improved framework for confound regression and filtering for control of motion artifact in the preprocessing of resting-state functional connectivity data. *Neuroimage* 64, 240–256. doi: 10.1016/j.neuroimage.2012.08.052

Seeley, W. W., Menon, V., Schatzberg, A. F., Keller, J., Glover, G. H., Kenna, H., et al. (2007). Dissociable intrinsic connectivity networks for salience processing and executive control. *J. Neurosci.* 27, 2349–2356. doi: 10.1523/jneurosci.5587-06.2007

Shu, N., Liu, Y., Li, K., Duan, Y., Wang, J., Yu, C., et al. (2011). Diffusion tensor tractography reveals disrupted topological efficiency in white matter structural networks in multiple sclerosis. *Cereb. Cortex* 21, 2565–2577. doi: 10.1093/cercor/bhr039

Sliz, D., and Hayley, S. (2012). Major depressive disorder and alterations in insular cortical activity: a review of current functional magnetic imaging research. *Front. Hum. Neurosci.* 6:323. doi: 10.3389/fnhum.2012.00323

Sridharan, D., Levitin, D. J., and Menon, V. (2008). A critical role for the right fronto-insular cortex in switching between central-executive and default-mode networks. *Proc. Natl. Acad. Sci. U.S.A.* 105, 12569–12574. doi: 10.1073/pnas.0800005105

Tahmasian, M., Knight, D. C., Manoliu, A., Schwerthöffer, D., Scherr, M., Meng, C., et al. (2013). Aberrant intrinsic connectivity of hippocampus and amygdala overlap in the fronto-insular and dorsomedial-prefrontal cortex in major depressive disorder. *Front. Hum. Neurosci.* 7:639. doi: 10.3389/fnhum.2013.00639

Tzourio-Mazoyer, N., Landeau, B., Papathanassiou, D., Crivello, F., Etard, O., Delcroix, N., et al. (2002). Automated anatomical labeling of activations in SPM using a macroscopic anatomical parcellation of the MNI MRI single-subject brain. *Neuroimage* 15, 273–289. doi: 10.1006/nimg.2001.0978

Van Dijk, K. R., Hedden, T., Venkataraman, A., Evans, K. C., Lazar, S. W., and Buckner, R. L. (2010). Intrinsic functional connectivity as a tool for human connectomics: theory, properties, and optimization. *J. Neurophysiol.* 103, 297–321. doi: 10.1152/jn.00783.2009

Wang, R., Benner, T., and Sorensen, A. G. (2007). Diffusion toolkit- a software package for diffusion imaging data processing and tractography. *Proc. Intl. Soc. Mag. Reson. Med.* 15:3720.

Yin, Z., Chang, M., Wei, S., Jiang, X., Zhou, Y., Cui, L., et al. (2018). Decreased functional connectivity in insular subregions in depressive episodes of bipolar disorder and major depressive disorder. *Front. Neurosci.* 12:842. doi: 10.3389/fnins.2018.00842

Conflict of Interest: The authors declare that the research was conducted in the absence of any commercial or financial relationships that could be construed as a potential conflict of interest.

frontiers in Neuroscience

ORIGINAL RESEARCH
published: 14 April 2021
doi: 10.3389/fnins.2021.671280

Abnormal Intrinsic Functional Interactions Within Pain Network in Cervical Discogenic Pain

Hong Zhang[1†], Dongqin Xia[2†], Xiaoping Wu[1], Run Liu[1], Hongsheng Liu[1], Xiangchun Yang[1], Xiaohui Yin[1], Song Chen[3] and Mingyue Ma[1]*

[1] Department of Radiology, The Affiliated Xi'an Central Hospital, Xi'an Jiaotong University, Xi'an, China, [2] Department of Ultrasound, The Affiliated Xi'an Central Hospital, Xi'an Jiaotong University, Xi'an, China, [3] Department of Radiology, The Affiliated Xi'an XD Group Hospital, Shaanxi University of Traditional Chinese Medicine, Xi'an, China

Cervical discogenic pain (CDP) is mainly induced by cervical disc degeneration. However, how CDP modulates the functional interactions within the pain network remains unclear. In the current study, we studied the changed resting-state functional connectivities of pain network with 40 CDP patients and 40 age-, gender-matched healthy controls. We first defined the pain network with the seeds of the posterior insula (PI). Then, whole brain and seed-to-target functional connectivity analyses were performed to identify the differences in functional connectivity between CDP and healthy controls. Finally, correlation analyses were applied to reveal the associations between functional connectivities and clinical measures. Whole-brain functional connectivity analyses of PI identified increased functional connectivity between PI and thalamus (THA) and decreased functional connectivity between PI and middle cingulate cortex (MCC) in CDP patients. Functional connectivity analyses within the pain network further revealed increased functional connectivities between bilateral PI and bilateral THA, and decreased functional connectivities between left PI and MCC, between left postcentral gyrus (PoCG) and MCC in CDP patients. Moreover, we found that the functional connectivities between right PI and left THA, between left PoCG and MCC were negatively and positively correlated with the visual analog scale, respectively. Our findings provide direct evidence of how CDP modulates the pain network, which may facilitate understanding of the neural basis of CDP.

Keywords: cervical discogenic pain, pain network, resting-state, functional connectivity, fMRI

OPEN ACCESS

Edited by:
Bochao Cheng,
Sichuan University, China

Reviewed by:
Lijie Wang,
University of Electronic Science and Technology of China, China
Jinping Xu,
Chinese Academy of Sciences (CAS), China

****Correspondence:***
Mingyue Ma
mmy_2005@163.com

[†] These authors have contributed equally to this work

Specialty section:
This article was submitted to Brain Imaging Methods, a section of the journal Frontiers in Neuroscience

Received: *23 February 2021*
Accepted: *22 March 2021*
Published: *14 April 2021*

Citation:
Zhang H, Xia D, Wu X, Liu R, Liu H, Yang X, Yin X, Chen S and Ma M (2021) Abnormal Intrinsic Functional Interactions Within Pain Network in Cervical Discogenic Pain. Front. Neurosci. 15:671280. doi: 10.3389/fnins.2021.671280

INTRODUCTION

Cervical discogenic pain (CDP) is a chronic pain with clinical manifestations of pain in the head, neck, shoulder, and upper limbs, as well as pain associated with numbness. CDP is a common source of neck pain with a reported prevalence between 16% and 41% (Peng and DePalma, 2018). Cervical discs have an amount of nerve fibers that are prone to structural disruption and inflammatory reactions that make them susceptible to pain. CDP seriously affects physical and mental health as well as the life quality of patients (Tracy and Bartleson, 2010; Thoomes et al., 2012). Long-term CDP leads to functional abnormalities in sensorimotor processing, emotion, cognition, and memory

(Montero-Homs, 2009; Linton, 2013; Denkinger et al., 2014). Despite such high prevalence, the neuropathology of CDP is still unclear.

The term "pain matrix" which is constituted of a set of brain areas mainly including the insula, cingulate cortex, parietal opercular and so on, is thought to be primarily involved in nociceptive processing (Isnard et al., 2011; Mouraux et al., 2011; Favilla et al., 2014). The insular cortex serves as an interface between internal and external stimuli for integrating multimodal information with rich connections to cortical and subcortical brain areas, and thus it is considered to be a core brain area of the pain network (Craig et al., 2000; Craig, 2002, 2003; Deen et al., 2011; Favilla et al., 2014). The posterior insula (PI) is a part of the lateral pain matrix and is considered a key area for pain perception and generation (Craig et al., 2000; Tracey, 2005; Favilla et al., 2014). Therefore, uncovering changes in functional interactions within the pain network may provide new insights into the neuropathology of CDP.

Resting-state fMRI is a non-invasive method of studying brain functional activities with blood oxygen level-dependent (BOLD) signals (Biswal et al., 1995; Fox and Raichle, 2007). Resting-state fMRI has been widely used to identify the intrinsic functional topography and networks of the brain (Cohen et al., 2008; Yeo et al., 2011; Wang et al., 2015, 2017, 2019a; Gao et al., 2020). Moreover, compared to task-fMRI, resting-state fMRI is an easier approach for detecting the intrinsic functional organization of the brain without complex task design and individual differences in finishing the task. Thus, resting-state has been widely applied to study the intrinsic functional abnormalities and treatment mechanisms for depression (Chen et al., 1997; Wu H. et al., 2016; Drysdale et al., 2017; Wang et al., 2018, 2019b,c, 2020), Alzheimer's disease (Greicius et al., 2004; Liu et al., 2014; Wu Y. et al., 2016; Zhan et al., 2016), schizophrenia (Anticevic et al., 2014; Du et al., 2017; Fu et al., 2018), and so on.

In this study, 40 CDP patients and 40 age- and gender-matched healthy controls (HC) were used to identify the abnormalities of functional interactions within the pain network to reveal its neuropathology. First, the center coordinates of bilateral PI were used to define the pain network. Next, the pair-wise functional connections within the pain network were calculated and compared between CDP and HC to identify changed functional connectivities. Finally, correlation analyses were performed to identify the relationships between functional connections and clinical characteristics.

MATERIALS AND METHODS

Participants

The current study included 40 right-handed CDP patients (F/M = 22/18; mean age = 53.6 ± 6.9 years) and 40 age- and gender-matched healthy controls (F/M = 22/18; mean age = 52.8 ± 7.6 years). CDP patients were diagnosed by one experienced orthopedist using physical and imaging examination. For CDP patients, the lesioned disc showed obvious reduced weighted T2 signals compared to the neighboring normal disc. Furthermore, only the pain caused by intervertebral disc disorder, not by segmental nerve disorder or radiation pain was considered to be CDP. The patients with disc degeneration and stenosis, cervical disc herniation, cervical spondylosis, hypertension, mental illness, diabetes, intracranial infection, craniocerebral trauma, MRI contraindication, and a history of chronic pain were excluded. 40 right-handed healthy controls without any hypertension, mental illness, intracranial infection, diabetes, craniocerebral trauma, and a history of chronic pain were included. The pain intensity was assessed with the visual analog scale (VAS) test, cognitive functions were assessed with the Montreal cognitive assessment scale (MoCA), and emotional states were assessed using the Hamilton depression scale (HAMD) and Hamilton anxiety scale (HAMA). Written informed consent was obtained from all the subjects, and this study was approved by the ethics committee of the affiliated Xi'an central hospital of Xi'an Jiaotong University and was in accordance with the Helsinki declaration and its later amendments or comparable ethical standards.

Resting-State fMRI Data Acquisition

The resting-state fMRI data were acquired with a Philips 3.0T MRI scanner. All the subjects were asked to keep their eyes closed, not to move, and fall asleep. Foam pads and headphones were used to reduce head movement and scanner noise. The resting-state fMRI data was scanned using echo plane imaging (EPI) with the following parameters: repetition time (TR) = 2000 ms, echo time (TE) = 30 ms, flip angle = 90°, field of view = 230 × 230, acquisition matrix size = 64 × 64, 38 slices with 0.6 mm gap, the voxel size = 3.6 mm × 3.6 mm × 3.6 mm, 240 volumes.

Resting-State fMRI Data Preprocessing

The resting-state fMRI data were preprocessed with the following steps: (1) the first 10 volumes were discarded to facilitate magnetization equilibrium effects; (2) the remaining images were realigned to the first volume to correct head motion; (3) all the images were normalized to standard EPI template and resampled to 3 mm^3 isotropic voxels; (4) all the data were smoothed with 6 mm Gaussian kernel; (5) Friston 24-parameter of head motion, white matter, cerebrospinal fluid, and whole brain mean signals were regressed out; (6) the fMRI images were filtered by the frequency band of 0.01–0.08 Hz. To exclude head motion effects, a scrubbing approach was used to cut the bad images before 2 time points and after 1 time point exceeding the pre-set criteria of frame displacement (FD) > 0.5 (Power et al., 2012). All the subjects' information, resting-state fMRI data acquisition and preprocessing can be found in our previous study (Ma et al., 2020).

Definition of the Posterior Insula

The posterior insula (PI) is considered to be a core brain area of the pain network (Apkarian et al., 2005; Isnard et al., 2011). To define the pain network, whole brain functional connectivity analyses of bilateral PIs were employed to identify the functionally connected brain areas with PI. The PI seed areas were defined with the MNI center coordinates by drawing spheres with 6mm radius for whole brain resting-state functional

connectivity analyses. The MNI center coordinate for left PI is [−39 −11 6], and the MNI center coordinate for right PI is [40 −6 10] (**Figure 1**) (Favilla et al., 2014).

Seed-Based Functional Connectivity Analysis

First, seed-based functional connectivity analyses of bilateral PIs were performed to identify functional connectivity differences between CDP patients and healthy controls. Resting-state functional connectivity strength was measured using Pearson's correlation coefficients. After whole brain functional connectivity maps were obtained, Fisher z transformations were used to transform functional connectivity maps to Z-maps to improve normality. Finally, two-sample t-tests with MoCA, HAMD, and HAMA as covariates were performed to identify the functional connectivity differences with bilateral PIs between CDP and healthy controls. The significant level was determined using a Gaussian random field (GRF) correction method with $p < 0.05$.

Determination of Pain Network

To define the pain network, whole brain resting-state functional connectivity analyses of bilateral PIs were performed in healthy controls. After obtaining the whole brain functional connectivity maps for left and right PIs, one-sample *t*-tests and family wise error (FWE) correction with $p < 0.05$ and cluster size ≥ 100 were used to identify the brain regions which functionally connected to bilateral PIs. Finally, the peak MNI coordinates of these brain areas were obtained and used to draw 6 mm radius spheres for seed to target functional connectivity analyses.

Functional Connectivity Analyses of Pain Network

After obtaining the pain network, seed to targets resting-state functional connectivity between each pair of brain regions belonging to the pain network were calculated. A Fisher z transformation was used to change the correlation coefficient to z value to improve normality. To identify the significant changes of functional connectivities within the pain network in CDP patients, two-sample t-tests were performed and the significance level was set at $p < 0.05$ with Bonferroni correction.

Correlation Analyses

To explore the relationship between functional connectivities and clinical measurements, correlation analyses were performed between functional connectivities showing differences between CDP and healthy controls and VAS, MoCA, HAMD, HAMA, and duration of disease in CDP patients. The significance was set at $p < 0.05$ with Bonferroni correction.

RESULTS

Clinical Characteristics

The well matched age ($p = 0.78$) and gender ($p = 1$) between CDP patients and healthy controls were shown in **Table 1**. Significantly decreased MoCA ($p < 0.001$) and significantly increased HAMD ($p < 0.001$), HAMA ($p < 0.001$) scores in CDP patients compared to healthy controls were found (**Table 1**).

Changed Whole Brain Functional Connectivity of Bilateral PIs

Whole brain functional connectivity analyses of bilateral PIs found bilateral PIs had significantly increased functional connectivities with bilateral thalamus (THA) and left PI additionally had decreased functional connectivity with the middle cingulate cortex (MCC)/supplementary motor area (**Figure 2**).

Determining the Pain Network

With bilateral PIs as seed regions, whole brain functional connectivity analyses in healthy controls identified five other brain regions showing significant functional connectivities. The five brain regions are MCC, left and right THA, left postcentral gyrus (PoCG), and right cerebellum (Cereb). In total, seven different regions consisted of the pain network and were used for seed to target functional connectivity analyses (**Figure 3** and **Table 2**).

Changed Functional Connectivities Within Pain Network

Seed to target functional connectivity analyses found a significant increase in functional connectivities between bilateral PIs and

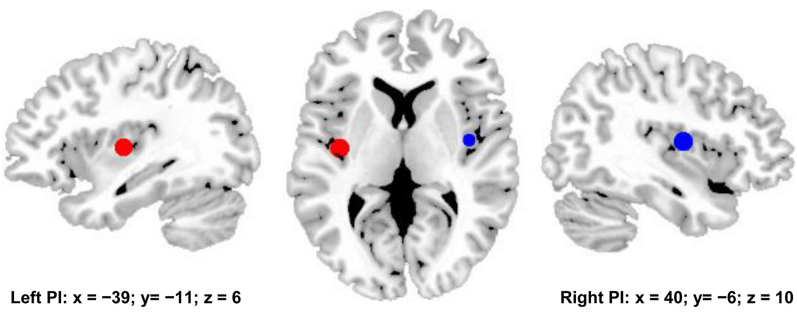

FIGURE 1 | Bilateral posterior insula (PI) were used to define pain matrix. The center MNI coordinates were used to draw spheres with 6 mm radius for functional connectivity analyses. The center MNI coordinate for left PI is [–39, –11, 6], and the center MNI coordinates for right PI is [40, –6, 10].

TABLE 1 | Demographic characteristics of cervical discogenic pain (CDP) and healthy controls (HC).

Characteristic	CDP (40, 22F/18M)	HC (40, 22F/18M)	*p* value
Age (Mean ± SD years)	53.6 ± 6.9	52.8 ± 7.6	0.78
VAS	6.73 ± 1.65		NA
MoCA	17.03 ± 1.83	26.38 ± 3.67	< 0.001
HAMD	4.94 ± 3.95	0.91 ± 0.73	< 0.001
HAMA	5.27 ± 3.78	0.77 ± 0.59	< 0.001
Duration of pain (years)	3.25 ± 1.46		NA

F, female; M, male; VAS, visual analog scale; MoCA, Montreal Cognitive Assessment; HAMD, Hamilton Depression Rating Scale; HAMA, Hamilton Anxiety Scale; NS, not significant; NA, not available.

bilateral THA in CDP patients as compared to healthy controls (**Figure 4**). Significantly reduced functional connectivities between MCC and left PI, PoCG.L were also identified in CDP patients (**Figure 4**).

Correlation Analyses

Correlation analyses identified a negative correlation between the functional connectivities of PoCG.L to MCC and VAS scores after multiple comparison corrections ($r = -0.59$, $p = 0.0001$). The positive correlation between the functional connectivities of THA.L to PI.R and VAS scores in CDP patients was found but not significant after multiple comparison correction ($r = 0.4$, $p = 0.011$) (**Figure 5**).

DISCUSSION

In this study, we identified different changing patterns within the pain network, including increased functional connections between bilateral PIs and bilateral THA and decreased functional connections between MCC and left PI, left PoCG in CDP patients. Moreover, the changed functional connections within the pain network were closely associated with pain intensity, i.e., VAS, scores. Our findings revealed changed patterns in the pain network of CDP patients, which may provide the neurophysiological basis and facilitate understanding of the neuropathology of CDP.

We found increased functional connectivities between bilateral posterior insula and thalamus in CDP patients. The posterior insula functionally connected with primary and secondary somatomotor cortices and medial thalamus is important for processing touch, pain, and thermal stimulation (Dosenbach et al., 2007; Thielscher and Pessoa, 2007; Deen et al., 2011; Kelly et al., 2012). The posterior insula is also a critical site for interoception and triggers the pain matrix network for subjective pain experience (Taylor et al., 2009; Isnard et al., 2011; Favilla et al., 2014). The thalamus is a relay for information exchanges between cortical and subcortical areas and plays a key role in the regulation of consciousness (Steriade and Llinas, 1988; Hwang et al., 2017; Lipiec and Wisniewska, 2019; Redinbaugh et al., 2020; Tang et al., 2020). The thalamus, which receives projections from multiple ascending pain pathways for modulating nociceptive information, is mainly involved in the sensory discriminative and affective motivational components of pain (Ab Aziz and Ahmad, 2006). A study using magnetic resonance imaging found that people with neuropathic pain showed reduced GABA in the thalamus (Henderson et al., 2013). The abnormal static and dynamic amplitude of low frequency fluctuations in CDP were also found in our previous study (Ma et al., 2020). All the evidence indicated that the abnormal functional activities or couplings of the insula and thalamus may be a neuromarker for CDP. Moreover, the functional connectivities between the posterior insula and thalamus were positively correlated with pain severity, suggesting that increased functional connectivities may be related to over sensitivity to pain stimuli in CDP patients.

The decreased functional connectivities between the middle cingulate cortex and left posterior insula, and left postcentral gyrus were found in CDP patients. Our finding was supported by previous studies which found changed structures and functions in these areas in cervical spondylosis and chronic knee osteoarthritis (Liao et al., 2018; Woodworth et al., 2019; Ma et al., 2020). The

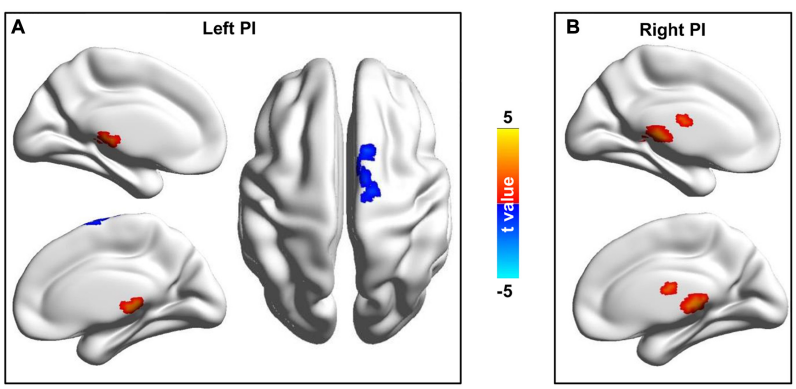

FIGURE 2 | Changed resting-state functional connectivities of the bilateral posterior insula (PI) in CDP patients. **(A)** Left PI showed increased functional connectivities with the thalamus and decreased functional connectivities with the middle cingulate cortex/supplementary motor area in CDP patients compared to healthy controls. **(B)** Right PI showed increased functional connectivities with thalamus in CDP patients compared to healthy controls.

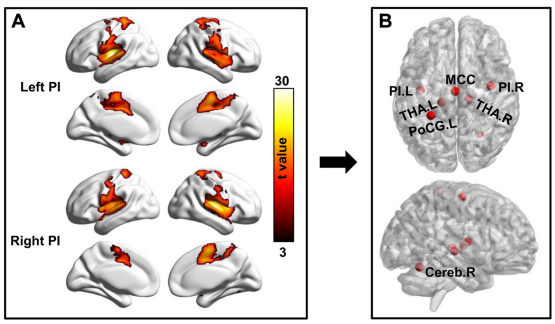

FIGURE 3 | Definition of pain network. **(A)** Whole brain resting-state functional connectivity analyses of the bilateral posterior insula (PI) were performed and corrected using family wise error (FWE) correction method with $p < 0.05$ to identify the brain regions functionally connected to bilateral PIs. **(B)** Several brain areas including bilateral PI, bilateral thalamus (THA.L, THA.R), middle cingulate cortex (MCC), left postcentral gyrus (PoCG.L), and right cerebellum (Cereb.R) were identified and defined as pain network.

TABLE 2 | The MNI peak coordinates of the pain network related brain regions, obtained with whole brain functional connectivity analyses of the bilateral posterior insula in healthy controls.

Brain regions	L/R	Abbreviation	Peak MNI coordinates		
			X	Y	Z
Posterior insula	L	PI	−39	−11	6
Posterior insula	R	PI	40	−6	10
Thalamus	L	THA	−15	−24	3
Thalamus	R	THA	15	−21	0
Postcentral gyrus	L	PoCG	−27	−39	66
Middle cingulate cortex	L/R	MCC	0	−12	60
Cerebellum	R	Cereb	27	−60	−18

MNI, Montreal Neurological Institute; L, left hemisphere; R, right hemisphere.

middle cingulate cortex has been reported in pain processing and is considered to be a key region in the pain matrix (Peyron et al., 2000; Favilla et al., 2014). The middle cingulate

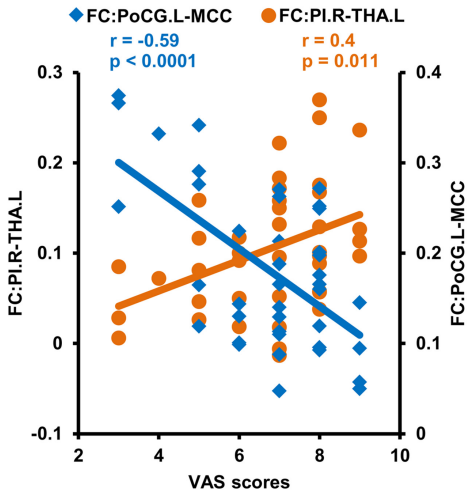

FIGURE 5 | Correlation analyses between functional connectivities and clinical measures. Correlation analyses identified a significantly positive correlation between VAS scores and functional connectivities of the right posterior insula (PI.R) with left thalamus (THA.L), and negative correlations between VAS scores and the functional connectivities of the middle cingulate cortex (MCC) to left postcentral gyrus (PoCG.L) in CDP patients.

cortex is a part of the medial pain subsystem and is mainly involved in the effective and/or cognitive dimensions of pain processing (Frot et al., 2008). The postcentral gyrus is a part of the sensorimotor network involved in processing changing pain intensity and discrimination of the sensory components of pain perception (Kanda et al., 2000; Peyron et al., 2000). Thus, the decreased functional connectivity between middle cingulate cortex and postcentral gyrus, the posterior insula may be related to damaged cognitive and attention processing as well as disrupted pain modulating in CDP patients.

This study has some limitations. First, the selection of the sliding window length remains a topic of debate and the optimal length for obtaining the dynamics of brain activity is unclear.

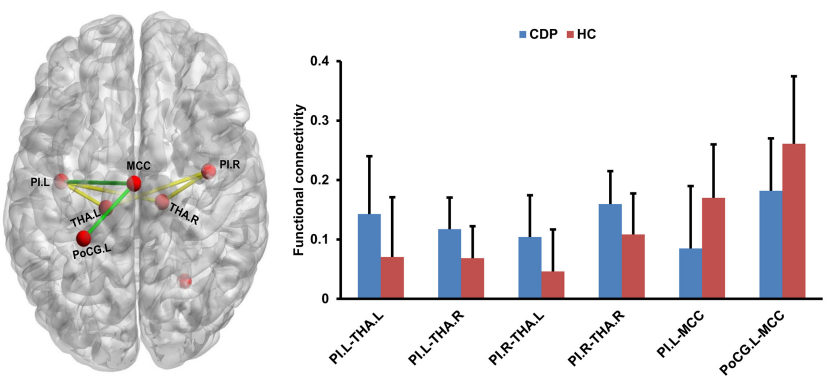

FIGURE 4 | Changed resting-state functional connectivities within pain network. CDP patients exhibited increased functional connectivities between bilateral posterior insula (PI) and bilateral thalamus (THA.L and THA.R) compared to healthy controls. Moreover, decreased functional connectivities between the middle cingulate cortex (MCC) and left postcentral gyrus (PoCG.L), left PI were also found in CDP patients.

We selected 50 TR as the window length based on the criteria that the minimum length should be larger than 1/fmin, which was proposed in previous studies (Leonardi and Van De Ville, 2015; Li et al., 2019). The results of different sliding window lengths were similar to the main results of 50 TR, demonstrating that our findings of dALFF variability were relatively stable. Second, given the high comorbidity of anxiety and depression, excluding individuals with depressive disorder from future studies could decrease the generalizability of our findings. More comorbid samples are required to replicate and complement these findings. Third, seed based functional connectivity analysis of the posterior insula was used to define the pain network, and whether all the pain related brain areas were recruited needs further validation, which may bias the current findings. Finally, all the CDP patients were still under medication, which may affect the current findings.

CONCLUSION

The current study revealed the changed intrinsic couplings within the pain network in CDP patients. We found increased functional couplings between the bilateral posterior insula and bilateral thalamus and decreased functional couplings between the middle cingulate cortex and postcentral gyrus, posterior insula in CDP patients. These increased functional connections may reflect over sensitivity to pain stimuli, whereas the decreased functional connections may be related to impaired pain modulating in cognition and emotion. Our findings provide initial evidence for the neural basis of CDP and could facilitate future understanding of the neuropathology of CDP.

DATA AVAILABILITY STATEMENT

The raw data supporting The conclusions of this article will be made available by the authors, without undue reservation.

ETHICS STATEMENT

The studies involving human participants were reviewed and approved by The Affiliated Xi'an Central Hospital of Xi'an Jiaotong University. The patients/participants provided their written informed consent to participate in this study.

AUTHOR CONTRIBUTIONS

MM and SC designed this study. HZ, DX, XW, and RL analyzed the data and wrote the manuscript. HL, XYa, and XYi collected the data. All authors discussed and edited the manuscript.

FUNDING

This work was supported by grants from the Shaanxi Key Science and Technology Project of Social Development (No. 2016SF-129) and Shaanxi Provincial Key Research and Development Program (No. 2020SF-139).

REFERENCES

Ab Aziz, C. B., and Ahmad, A. H. (2006). The role of the thalamus in modulating pain. *Malays. J. Med. Sci.* 13, 11–18.

Anticevic, A., Cole, M. W., Repovs, G., Murray, J. D., Brumbaugh, M. S., Winkler, A. M., et al. (2014). Characterizing thalamo-cortical disturbances in schizophrenia and bipolar illness. *Cereb. Cortex* 24, 3116–3130. doi: 10.1093/cercor/bht165

Apkarian, A. V., Bushnell, M. C., Treede, R. D., and Zubieta, J. K. (2005). Human brain mechanisms of pain perception and regulation in health and disease. *Eur. J. Pain* 9, 463–484. doi: 10.1016/j.ejpain.2004.11.001

Biswal, B., Yetkin, F. Z., Haughton, V. M., and Hyde, J. S. (1995). Functional connectivity in the motor cortex of resting human brain using echo-planar MRI. *Magn. Reson. Med.* 34, 537–541. doi: 10.1002/mrm.1910340409

Chen, R., Classen, J., Gerloff, C., Celnik, P., Wassermann, E. M., Hallett, M., et al. (1997). Depression of motor cortex excitability by low-frequency transcranial magnetic stimulation. *Neurology* 48, 1398–1403. doi: 10.1212/wnl.48.5.1398

Cohen, A. L., Fair, D. A., Dosenbach, N. U., Miezin, F. M., Dierker, D., Van Essen, D. C., et al. (2008). Defining functional areas in individual human brains using resting functional connectivity MRI. *Neuroimage* 41, 45–57. doi: 10.1016/j.neuroimage.2008.01.066

Craig, A. D. (2002). How do you feel? interoception: the sense of the physiological condition of the body. *Nat. Rev. Neurosci.* 3, 655–666. doi: 10.1038/nrn894

Craig, A. D. (2003). Interoception: the sense of the physiological condition of the body. *Curr. Opin. Neurobiol.* 13, 500–505. doi: 10.1016/s0959-4388(03)00090-4

Craig, A. D., Chen, K., Bandy, D., and Reiman, E. M. (2000). Thermosensory activation of insular cortex. *Nat. Neurosci.* 3, 184–190. doi: 10.1038/72131

Deen, B., Pitskel, N. B., and Pelphrey, K. A. (2011). Three systems of insular functional connectivity identified with cluster analysis. *Cereb. Cortex* 21, 1498–1506. doi: 10.1093/cercor/bhq186

Denkinger, M. D., Lukas, A., Nikolaus, T., Peter, R., and Franke, S. (2014). Multisite pain, pain frequency and pain severity are associated with depression in older adults: results from the ActiFE Ulm study. *Age. Ageing* 43, 510–514. doi: 10.1093/ageing/afu013

Dosenbach, N. U., Fair, D. A., Miezin, F. M., Cohen, A. L., Wenger, K. K., Dosenbach, R. A., et al. (2007). Distinct brain networks for adaptive and stable task control in humans. *Proc. Natl. Acad. Sci. U S A.* 104, 11073–11078. doi: 10.1073/pnas.0704320104

Drysdale, A. T., Grosenick, L., Downar, J., Dunlop, K., Mansouri, F., Meng, Y., et al. (2017). Resting-state connectivity biomarkers define neurophysiological subtypes of depression. *Nat. Med.* 23, 28–38. doi: 10.1038/nm.4246

Du, Y., Pearlson, G. D., Lin, D., Sui, J., Chen, J., Salman, M., et al. (2017). Identifying dynamic functional connectivity biomarkers using GIG-ICA: application to schizophrenia, schizoaffective disorder, and psychotic bipolar disorder. *Hum. Brain Mapp.* 38, 2683–2708. doi: 10.1002/hbm.23553

Favilla, S., Huber, A., Pagnoni, G., Lui, F., Facchin, P., Cocchi, M., et al. (2014). Ranking brain areas encoding the perceived level of pain from fMRI data. *Neuroimage* 90, 153–162. doi: 10.1016/j.neuroimage.2014.01.001

Fox, M. D., and Raichle, M. E. (2007). Spontaneous fluctuations in brain activity observed with functional magnetic resonance imaging. *Nat. Rev. Neurosci.* 8, 700–711. doi: 10.1038/nrn2201

Frot, M., Mauguiere, F., Magnin, M., and Garcia-Larrea, L. (2008). Parallel processing of nociceptive A-delta inputs in SII and midcingulate cortex in humans. *J. Neurosci.* 28, 944–952. doi: 10.1523/jneurosci.2934-07.2008

Fu, Z., Tu, Y., Di, X., Du, Y., Pearlson, G. D., Turner, J. A., et al. (2018). Characterizing dynamic amplitude of low-frequency fluctuation and its relationship with dynamic functional connectivity: an application to schizophrenia. *Neuroimage* 180, 619–631. doi: 10.1016/j.neuroimage.2017.09.035

Gao, Z., Guo, X., Liu, C., Mo, Y., and Wang, J. (2020). Right inferior frontal gyrus: an integrative hub in tonal bilinguals. *Hum. Brain Mapp.* 41, 2152–2159. doi: 10.1002/hbm.24936

Greicius, M. D., Srivastava, G., Reiss, A. L., and Menon, V. (2004). Default-mode network activity distinguishes Alzheimer's disease from healthy aging:

evidence from functional MRI. *Proc. Natl. Acad. Sci. U S A.* 101, 4637–4642. doi: 10.1073/pnas.0308627101

Henderson, L. A., Peck, C. C., Petersen, E. T., Rae, C. D., Youssef, A. M., Reeves, J. M., et al. (2013). Chronic pain: lost inhibition? *J. Neurosci.* 33, 7574–7582.

Hwang, K., Bertolero, M. A., Liu, W. B., and D'Esposito, M. (2017). The human thalamus is an integrative hub for functional brain networks. *J. Neurosci.* 37, 5594–5607. doi: 10.1523/jneurosci.0067-17.2017

Isnard, J., Magnin, M., Jung, J., Mauguière, F., and Garcia-Larrea, L. (2011). Does the insula tell our brain that we are in pain? *PAIN* 152, 946–951. doi: 10.1016/j.pain.2010.12.025

Kanda, M., Nagamine, T., Ikeda, A., Ohara, S., Kunieda, T., Fujiwara, N., et al. (2000). Primary somatosensory cortex is actively involved in pain processing in human. *Brain Res.* 853, 282–289. doi: 10.1016/s0006-8993(99)02274-x

Kelly, C., Toro, R., Di Martino, A., Cox, C. L., Bellec, P., Castellanos, F. X., et al. (2012). A convergent functional architecture of the insula emerges across imaging modalities. *Neuroimage* 61, 1129–1142. doi: 10.1016/j.neuroimage.2012.03.021

Leonardi, N., and Van De Ville, D. (2015). On spurious and real fluctuations of dynamic functional connectivity during rest. *NeuroImage* 104, 430–436. doi: 10.1016/j.neuroimage.2014.09.007

Li, C., Xia, L., Ma, J., Li, S., Liang, S., Ma, X., et al. (2019). Dynamic functional abnormalities in generalized anxiety disorders and their increased network segregation of a hyperarousal brain state modulated by insomnia. *J. Affect. Disord.* 246, 338–345. doi: 10.1016/j.jad.2018.12.079

Liao, X., Mao, C., Wang, Y., Zhang, Q., Cao, D., Seminowicz, D. A., et al. (2018). Brain gray matter alterations in Chinese patients with chronic knee osteoarthritis pain based on voxel-based morphometry. *Medicine (Baltimore)* 97:e0145. doi: 10.1097/md.0000000000010145

Linton, S. J. (2013). A transdiagnostic approach to pain and emotion. *J. Appl. Biobehav. Res.* 18, 82–103. doi: 10.1111/jabr.12007

Lipiec, M. A., and Wisniewska, M. B. (2019). We have to find a way - growth and guidance of thalamocortical axons. *Postepy Biochem.* 65, 135–142.

Liu, Y., Yu, C., Zhang, X., Liu, J., Duan, Y., Alexander-Bloch, A. F., et al. (2014). Impaired long distance functional connectivity and weighted network architecture in Alzheimer's disease. *Cereb. Cortex* 24, 1422–1435. doi: 10.1093/cercor/bhs410

Ma, M., Zhang, H., Liu, R., Liu, H., Yang, X., Yin, X., et al. (2020). Static and dynamic changes of amplitude of low-frequency fluctuations in cervical discogenic pain. *Front. Neurosci.* 14:733. doi: 10.3389/fnins.2020.00733

Montero-Homs, J. (2009). [Nocioceptive pain, neuropathic pain and pain memory]. *Neurologia* 24, 419–422.

Mouraux, A., Diukova, A., Lee, M. C., Wise, R. G., and Iannetti, G. D. (2011). A multisensory investigation of the functional significance of the "pain matrix". *Neuroimage* 54, 2237–2249. doi: 10.1016/j.neuroimage.2010.09.084

Peng, B., and DePalma, M. J. (2018). Cervical disc degeneration and neck pain. *J. Pain Res.* 11, 2853–2857. doi: 10.2147/jpr.s180018

Peyron, R., Laurent, B., and Garcia-Larrea, L. (2000). Functional imaging of brain responses to pain. a review and meta-analysis (2000). *Neurophysiol. Clin.* 30, 263–288. doi: 10.1016/s0987-7053(00)00227-6

Power, J. D., Barnes, K. A., Snyder, A. Z., Schlaggar, B. L., and Petersen, S. E. (2012). Spurious but systematic correlations in functional connectivity MRI networks arise from subject motion. *Neuroimage* 59, 2142–2154. doi: 10.1016/j.neuroimage.2011.10.018

Redinbaugh, M. J., Phillips, J. M., Kambi, N. A., Mohanta, S., Andryk, S., Dooley, G. L., et al. (2020). Thalamus modulates consciousness via layer-specific control of cortex. *Neuron* 106, 66–75e12.

Steriade, M., and Llinas, R. R. (1988). The functional states of the thalamus and the associated neuronal interplay. *Physiol. Rev.* 68, 649–742. doi: 10.1152/physrev.1988.68.3.649

Tang, Y., Wang, M., Zheng, T., Yuan, F., Yang, H., Han, F., et al. (2020). Grey matter volume alterations in trigeminal neuralgia: a systematic review and meta-analysis of voxel-based morphometry studies. *Prog. Neuropsychopharmacol. Biol. Psychiatry* 98:109821. doi: 10.1016/j.pnpbp.2019.109821

Taylor, K. S., Seminowicz, D. A., and Davis, K. D. (2009). Two systems of resting state connectivity between the insula and cingulate cortex. *Hum. Brain Mapp.* 30, 2731–2745. doi: 10.1002/hbm.20705

Thielscher, A., and Pessoa, L. (2007). Neural correlates of perceptual choice and decision making during fear-disgust discrimination. *J. Neurosci.* 27, 2908–2917. doi: 10.1523/jneurosci.3024-06.2007

Thoomes, E. J., Scholten-Peeters, G. G., de Boer, A. J., Olsthoorn, R. A., Verkerk, K., Lin, C., et al. (2012). Lack of uniform diagnostic criteria for cervical radiculopathy in conservative intervention studies: a systematic review. *Eur. Spine J.* 21, 1459–1470. doi: 10.1007/s00586-012-2297-9

Tracey, I. (2005). Nociceptive processing in the human brain. *Curr. Opin. Neurobiol.* 15, 478–487. doi: 10.1016/j.conb.2005.06.010

Tracy, J. A., and Bartleson, J. D. (2010). Cervical spondylotic myelopathy. *Neurologist* 16, 176–187.

Wang, J., Becker, B., Wang, L., Li, H., Zhao, X., and Jiang, T. (2019a). Corresponding anatomical and coactivation architecture of the human precuneus showing similar connectivity patterns with macaques. *Neuroimage* 200, 562–574. doi: 10.1016/j.neuroimage.2019.07.001

Wang, L., Wei, Q., Wang, C., Xu, J., Wang, K., Tian, Y., et al. (2019b). Altered functional connectivity patterns of insular subregions in major depressive disorder after electroconvulsive therapy. *Brain Imag. Behav.* 14, 753–761. doi: 10.1007/s11682-018-0013-z

Wang, L., Yu, L., Wu, F., Wu, H., and Wang, J. (2019c). Altered whole brain functional connectivity pattern homogeneity in medication-free major depressive disorder. *J. Affect. Disord.* 253, 18–25. doi: 10.1016/j.jad.2019.04.040

Wang, J., Ji, Y., Li, X., He, Z., Wei, Q., Bai, T., et al. (2020). Improved and residual functional abnormalities in major depressive disorder after electroconvulsive therapy. *Prog. Neuro-Psychopharmacol. Biol. Psychiatry* 100:109888. doi: 10.1016/j.pnpbp.2020.109888

Wang, J., Wei, Q., Wang, L., Zhang, H., Bai, T., Cheng, L., et al. (2018). Functional reorganization of intra- and internetwork connectivity in major depressive disorder after electroconvulsive therapy. *Hum. Brain Mapp.* 39, 1403–1411. doi: 10.1002/hbm.23928

Wang, J., Xie, S., Guo, X., Becker, B., Fox, P. T., Eickhoff, S. B., et al. (2017). Correspondent functional topography of the human left inferior parietal lobule at rest and under task revealed using resting-state fMRI and coactivation based parcellation. *Hum. Brain Mapp.* 38, 1659–1675. doi: 10.1002/hbm.23488

Wang, J., Yang, Y., Fan, L., Xu, J., Li, C., Liu, Y., et al. (2015). Convergent functional architecture of the superior parietal lobule unraveled with multimodal neuroimaging approaches. *Hum. Brain Mapp.* 36, 238–257. doi: 10.1002/hbm.22626

Woodworth, D. C., Holly, L. T., Mayer, E. A., Salamon, N., and Ellingson, B. M. (2019). Alterations in cortical thickness and subcortical volume are associated with neurological symptoms and neck pain in patients with cervical spondylosis. *Neurosurgery* 84, 588–598. doi: 10.1093/neuros/nyy066

Wu, H., Sun, H., Xu, J., Wu, Y., Wang, C., Xiao, J., et al. (2016). Changed hub and corresponding functional connectivity of subgenual anterior cingulate cortex in major depressive disorder. *Front. Neuroanat.* 10:120. doi: 10.3389/fnana.2016.00120

Wu, Y., Zhang, Y., Liu, Y., Liu, J., Duan, Y., Wei, X., et al. (2016). Distinct changes in functional connectivity in posteromedial cortex subregions during the progress of Alzheimer's Disease. *Front. Neuroanat.* 10:41. doi: 10.3389/fnana.2016.00041

Yeo, B. T., Krienen, F. M., Sepulcre, J., Sabuncu, M. R., Lashkari, D., Hollinshead, M., et al. (2011). The organization of the human cerebral cortex estimated by intrinsic functional connectivity. *J. Neurophysiol.* 106, 1125–1165. doi: 10.1152/jn.00338.2011

Zhan, Y., Ma, J., Alexander-Bloch, A. F., Xu, K., Cui, Y., Feng, Q., et al. (2016). Longitudinal study of impaired intra- and inter-network brain connectivity in subjects at high risk for Alzheimer's Disease. *J. Alzheimers. Dis.* 52, 913–927. doi: 10.3233/jad-160008

Conflict of Interest: The authors declare that the research was conducted in the absence of any commercial or financial relationships that could be construed as a potential conflict of interest.

frontiers in Neuroscience

ORIGINAL RESEARCH
published: 21 May 2021
doi: 10.3389/fnins.2021.678465

The Abnormal Functional Connectivity in the Locus Coeruleus-Norepinephrine System Associated With Anxiety Symptom in Chronic Insomnia Disorder

Liang Gong[1†], Min Shi[2†], Jian Wang[1], Ronghua Xu[1], Siyi Yu[3], Duan Liu[1], Xin Ding[1], Bei Zhang[1], Xingping Zhang[4] and Chunhua Xi[2]*

[1] Department of Neurology, Chengdu Second People's Hospital, Chengdu, Sichuan, China, [2] Department of Neurology, The Third Affiliated Hospital of Anhui Medical University, Heifei, China, [3] Department of Acupuncture and Tuina, Chengdu University of Traditional Chinese Medicine, Chengdu, China, [4] Department of General Practice, Chengdu Second People's Hospital, Chengdu, China

OPEN ACCESS

Edited by:
Jiaojian Wang,
University of Electronic Science and Technology of China, China

Reviewed by:
Junchao Li,
Guangdong Polytechnic Normal University, China
Qing Ye,
Nanjing Drum Tower Hospital, China

***Correspondence:**
Chunhua Xi
xch3149@126.com

[†] These authors have contributed equally to this work

Specialty section:
This article was submitted to Brain Imaging Methods, a section of the journal Frontiers in Neuroscience

Received: 09 March 2021
Accepted: 13 April 2021
Published: 21 May 2021

Citation:
Gong L, Shi M, Wang J, Xu R, Yu S, Liu D, Ding X, Zhang B, Zhang X and Xi C (2021) The Abnormal Functional Connectivity in the Locus Coeruleus-Norepinephrine System Associated With Anxiety Symptom in Chronic Insomnia Disorder. Front. Neurosci. 15:678465. doi: 10.3389/fnins.2021.678465

Background: Mental syndromes such as anxiety and depression are common comorbidities in patients with chronic insomnia disorder (CID). The locus coeruleus noradrenergic (LC-NE) system is considered to be crucial for modulation of emotion and sleep/wake cycle. LC-NE system is also a critical mediator of the stress-induced anxiety. However, whether the LC-NE system contributes to the underlying mechanism linking insomnia and these comorbidities remain unclear. This study aimed to investigate the LC-NE system alterations in patients with insomnia and its relationship with depression and anxiety symptoms.

Materials and Methods: Seventy patients with CID and 63 matched good sleep control (GSC) subjects were recruited and underwent resting-state functional MRI scan. LC-NE functional network was constructed by using seed-based functional connectivity (FC) analysis. The alterations in LC-NE FC network in patients with CID and their clinical significance was explored.

Results: Compared with GSC group, the CID group showed decreased left LC-NE FC in the left inferior frontal gyrus, while they had increased LC-NE FC in the left supramarginal gyrus and the left middle occipital gyrus (MOG). For the right LC-NE FC network, decreased FC was found in left dorsal anterior cingulate cortex (dACC). Interesting, the increased LC-NE FC was located in sensory cortex, while decreased LC-NE FC was located in frontal control cortex. In addition, the FC between the left LC and left MOG was associated with the duration of the disease, while abnormal FC between right LC and left dACC was associated with the anxiety scores in patients with CID.

Conclusion: The present study found abnormal LC-NE functional network in patients with CID, and the altered LC-NE function in dACC was associated with anxiety symptoms in CID. The present study substantially extended our understanding of the neuropathological basis of CID and provided the potential treatment target for CID patients who also had anxiety.

Keywords: insomnia, locus ceruleus-norepinephrine, anxiety, functional connectivity, anterior cingulate cortex

INTRODUCTION

Insomnia is a prevalent and limiting condition affecting daytime functioning. The chronic insomnia disorder (CID) affects an estimated 10% of the population; in particular during the global lockdown due to the COVID-19 outbreak, insomnia prevalence has doubled to tripled (Kokou-Kpolou et al., 2020; Shi et al., 2020). Insomnia is also highly comorbid with other mental health disorders, especially depression and anxiety (Blake et al., 2018). However, the neuropathological basis of these comorbidities is still unclear.

Numerous groups have used various neuroimaging approaches and demonstrated specific brain structural and functional alterations in patients with CID (Huang et al., 2012; Joo et al., 2013; Li et al., 2018; Yu et al., 2018a,b; Gong et al., 2020c). However, these studies have yielded diverse findings, e.g., the altered brain structural regions included orbitofrontal cortex, hippocampus, amygdala, precuneus, and anterior cingulate cortex (ACC) (Altena et al., 2010; Winkelman et al., 2013), while the abnormal functional networks included default mode network, salience network, frontostriatal network, and reward networks (Chen et al., 2014; Huang et al., 2017). Recently, Tahmasian et al. (2018) performed activation likelihood estimation to identify consistent patterns of abnormal brain alterations in insomnia disorder and found no significant convergent evidence across previous studies. The diverse finding of brain alterations in patients with insomnia could be possibly explained by the heterogeneous neuroimaging approaches (Liu et al., 2018). In addition, the heterogeneous clinical features of insomnia should be considered, especially the high comorbidity symptoms like depression and anxiety (Sivertsen et al., 2012; Blake et al., 2018; Bragantini et al., 2019; Gong et al., 2020a,b; Sweetman et al., 2020). Thus, investigation of the brain mechanism underlying CID and mental symptom comorbidities is essential for comprehensive understanding of insomnia.

The locus coeruleus (LC) is a pontine nucleus belonging to the ascending reticular activating system (Moruzzi and Magoun, 1949), which produces the majority of brain norepinephrine (NE). The locus coeruleus noradrenergic (LC-NE) system is considered to be the crucial system involved in the regulation of physiological functions, including waking, arousal and attention (Ambrosini et al., 2013; Szabadi, 2013; Lovett-Barron et al., 2017). Previous studies indicated that excessive activity in the LC-NE system was incompatible with sleep and may contribute to insomnia (Berridge et al., 2012). The 24-h plasma NE level was lower in insomnia patients than in good sleepers, and the decreased NE level was associated with poorer sleep quality in the insomnia group (Grimaldi et al., 2020). Hyperarousal and sleep reactivity are the key components in the pathophysiology model of CID (Kalmbach et al., 2018). In addition, LC-NE system is a critical mediator of the stress-induced anxiety and a potential intervention target for stress-related depressive and anxiety disorders (McCall et al., 2015). Previous neuroimaging studies have indicated that the resting-state functional connectivity (FC) analysis of LC was feasible to detect LC-NE function in human brain (Zhang et al., 2016; Song et al., 2017). Recently, using LC FC analysis approach, the disrupted LC FC have been found in healthy adults with parental history of Alzheimer's disease (Del Cerro et al., 2020b) and patients with late-life depressive disorder (Del Cerro et al., 2020a). However, whether the LC-NE system contributes to the underlying mechanisms linking insomnia and these comorbidities remains unclear.

We aimed to investigate the LC-NE system alteration in patients with insomnia and its relationship with the depression and anxiety symptoms. To this end, we analyzed the LC-NE FC network in a group of patients with CID using resting-state functional MRI (rs-fMRI) data. Due to the role of LC in the regulation of behavioral state, we hypothesized that both increased and decreased brain regions could be found in the LC-NE network. Furthermore, we hypothesized that the altered LC-NE system would be associated with mental symptoms in patients with CID.

MATERIALS AND METHODS

Participants

Seventy patients with CID and 63 matched good sleep control (GSC) subjects were recruited in the present study. The study was approved by the local ethical committee (the Institutional Review Board of the third affiliated hospital of Anhui Medical University). All participants were of Chinese Han descent and right handed, and written informed consent was provided. Two patients with CID and three healthy participants were excluded due to excessive head motion artifacts (exceeding 1.5 mm or 1.5° of angular motion relative to the first volume). Therefore, 68 patients with CID and 60 GSCs were included in the final analysis.

For inclusion in the CID group, patients were required to meet the diagnostic criteria for CID outlined in the International Classification of Sleep Disorders, third version (Sateia, 2014). Additional inclusion criteria for the CID group were as follows: (1) had not taken any hypnotic and antidepressant medication 2 weeks before neuropsychological test and MRI scan; and (2) aged 18–55 years with age at onset under 50 years. The

exclusion criteria were: (1) a history of other neuropsychiatric disorders; (2) a history of substance abuse (caffeine, nicotine, and alcohol); and (3) contraindications to MRI. GSC subjects were required to meet the following criteria: (1) good sleep and mood and normal cognitive function; (2) no history of neurological and psychiatric disease, seizures, head injury, stroke, or transient ischemic attack; (3) no caffeine, drug, or alcohol abuse; and (4) no brain lesions found by a regular T2-weighted MRI scan.

Behavioral Assessments

Pittsburgh Sleep Quality Index (PSQI) was used to assess the subjective sleep quality in CID group (Buysse et al., 1989; Backhaus et al., 2002) and to measure the insomnia severity. The self-rating depression scale (SDS) was used for the depression evaluation, while the Zung's self-rating anxiety scale (SAS) was used for the anxiety evaluation (Zung et al., 1965; Zung, 1971).

Imaging Acquisition and Preprocessing

Imaging was performed at the Third Affiliated Hospital of Anhui Medical University using a Siemens Verio 3.0-Tesla scanner (Siemens, Erlangen, Germany). MRI data acquisition was carried out between 4 p.m. and 6 p.m. in all participants. Structural images were acquired using a high-resolution spoiled gradient-recalled echo sequence with the following parameters: repetition time/echo time (TR/TE) = 1,900/2.48 ms; flip angle (FA) = 9°; acquisition matrix = 256 × 256; field-of-view = 240 × 240 mm; thickness = 1.0 mm; gap = 0 mm; number of slices = 176; number of excitations = 1.0. The rs-fMRI datasets were obtained using an 8-min gradient-recalled echo-planar imaging pulse sequence with the following parameters: TR/TE = 2,000/35 ms; FA = 90°; acquisition matrix = 64 × 64; thickness = 3.5 mm; number of slices = 36. Other parameters were the same as those utilized for structural images. During scanning, all participants were instructed to relax and keep their eyes closed, and stabilizers were used to immobilize the head. Wakefulness was assessed following scanning, and all participants claimed to be awake during the study.

The rs-fMRI data were preprocessed using SPM12[1] and the DPABI 4.3 (Data Processing & Analysis of Brain Imaging[2]) implemented in MATLAB 8.0 (The MathWorks, Inc., Natick, MA, United States) (Yan et al., 2016). We removed the first five initial volumes to account for the magnetization equilibrium and adaptation to the experimental environment. The remaining 235 images were then slice-time corrected, reoriented, realigned, and coregistered to the T1-weighted structural images, which were segmented using DARTEL (Ashburner, 2007). The participants with excessive head motion above 1.5 mm or 1.5° of angular motion relative to the first volume were removed for next analyses. There was no significant difference in mean framewise displace between groups (CID group: 0.071 ± 0.045, GSC group: 0.082 ± 0.061; $p = 0.42$). The correlation between FD and behavioral information were calculated in the CID group. Images from all participants were normalized into standard stereotactic Montreal Neurological Institute space and smoothed using a Gaussian kernel (full width at half-maximum = 6 mm). Voxel time series were further detrended and temporally filtered (0.01–0.1 Hz). We normalized the variance of each time series to control for fluctuations in signal intensity. Noise associated with white matter/cerebrospinal fluid signals and 24 head motion-related covariates were regressed out. The global signal was not regressed out given the controversy regarding its application to rs-fMRI data (Murphy et al., 2009; Chai et al., 2012).

LC-NE Functional Network Construction

Bilateral, LC-based, voxel-wise FC analysis was conducted using the DPABI 4.3. Bilateral LC was selected as the seed region to construct the LC-NE functional network, separately. To avoid the localization error of LC by "in-house" approach, the bilateral LC seed regions were extracted from the automated anatomical labeling atlas 3 (AAL3) (Rolls et al., 2020). The average time course in each LC region, defined as the seed time course, was correlated with the time course in all brain voxels using Pearson's cross correlation. A Fisher's Z-transformation was applied to improve the correlation coefficients (CC) so that they approached normal distribution [$Z = 0.5\ln(1 + CC)/(1 - CC)$] (Lowe et al., 1998; Liu et al., 2017). Thus, a map of each individual pattern in LC FC network was separately obtained.

Statistical Analysis

First, two independent t tests and chi-square tests (only for the gender) were performed for the demographic and behavior data comparison between the two groups (SPSS 24.0; SPSSInc., Chicago, Ill). Pearson correlation analysis was employed to detect the clinical features (PSQI, SDS, SAS, and duration of disease) associations in the CID group. Statistical significance was set at p values < 0.05.

Second, a voxel-wise, two independent t test was used to obtain the group difference of LC-NE networks after removal of the effects of covariates including gender and age. The voxel-level significance threshold was set at a p value < 0.001, corrected for multiple comparisons at the cluster level using the 3dClustSim program in AFNI_18.3.03 (gray matter mask correction: 67,541 voxels, estimated smoothness is 14.53 mm of statistic image, voxel-level p value < 0.001, cluster level α value < 0.001, $\kappa > 35$, cluster size > 945 mm^3)[3]. The peak Z value in the region of interest was reported by xjview[4]. As the gender difference of LC-NE FC network was reported in a previous study (Zhang et al., 2016), we also explore the gender difference of LC-NE network in patients with CID.

Third, to further explore the clinical significance of the altered LC-NE FC in CID patients, a partial correlation analysis was used to investigate the association between the altered LC-NE and PSQI, SAS, and SDS scores, controlling for the effects of age, gender, and disease duration. Significance was set at a p value < 0.05 after correction for multiple comparisons using false-discovery rate (FDR) correction.

[1] http://www.fil.ion.ucl.ac.uk/spm

[2] http://rfmri.org/dpabi

[3] https://afni.nimh.nih.gov/pub/dist/doc/program_help/3dClustSim.html

[4] https://www.alivelearn.net/xjview/

RESULTS

Demographic and Behavioral Information

Demographic data and behavior performance in two groups are shown in **Table 1**. No significant differences in gender, age, and education were found between GSC subjects and CID patients. The mean score of PSQI (severity of insomnia) in CID group was 14.6, ranging from 11 to 19; the mean duration of insomnia was 4.45 years, ranging from 0.25 to 16.67 years. The mean depression and anxiety scores were 52.35 (range: 18–68) and 53.88 (range: 36–65), respectively. According to cut-off value of Chinese version of SDS and SAS scales (53 for SDS and 50 for anxiety), 23 CID patients presented depressive symptom and 49 CID patients displayed anxiety symptoms. The Pearson correlation analyses revealed that the SAS was positively associated with PSQI scores in the CID group (r = 0.344, p = 0.005). No other significant correlation was found between clinical features. No significant correlation was found between FD and clinical features (all $p > 0.05$).

Altered LC-NE Functional Network in CID

As illustrated in **Table 2** and **Figure 1** for the left LC-NE FC network, compared with the GSC group, CID patients showed decreased FC in the left inferior frontal gyrus (IFG), while they had increased FC in the left supramarginal gyrus (SMG) and left middle occipital gyrus (MOG). For the right LC-NE FC network, CID patients had decreased FC in the dorsal anterior cingulate cortex (dACC). Taken together, the altered regions in the LC-NE network were all located in the efferent pathway, and the areas with increased FC were located in the sensory cortex, while those with decreased FC were found in the prefrontal cortex.

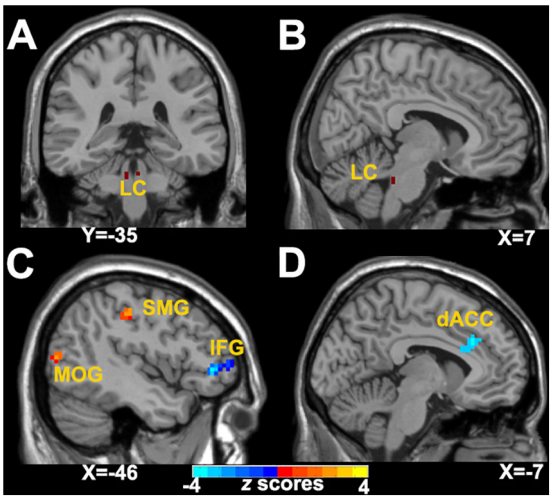

FIGURE 1 | Abnormal LC-NE functional network in patients with CID. **(A,B)** LC seed selected from AAL 3 atlas. **(C)** Altered brain regions in the left LC-NE functional network in patients with CID are found in the left IFG, IPL, and MOG. **(D)** Altered brain regions in the right LC-NE functional network in patients with CID are found in the left dACC. LC-NE, locus coeruleus-norepinephrine; CID, chronic insomnia disorder; IFG, inferior frontal gyrus; MOG, middle occipital gyrus; SMG, supramarginal gyrus; dACC, dorsal anterior cingulate cortex; AAL, automated anatomical atlas.

TABLE 1 | Demographic and clinical traits for all participants.

Characteristic	CID (n = 68)	GSC (n = 60)	T/X^2	p value
Age	39.85 ± 11.18	39.47 ± 10.40	0.20	0.43
Gender (M/F)	32/36	25/35	0.37	0.54
Education (years)	11.26 ± 2.77	11.90 ± 4.20	1.02	0.31
PSQI	14.06 ± 1.96	–	–	–
SDS	52.35 ± 7.65	–	–	–
SAS	53.88 ± 5.00	–	–	–
Duration (Years)	4.45 ± 0.4.50	–	–	–

CID, chronic insomnia disorder; GSC, good sleep controls; PSQI, Pittsburgh sleep quality index; SDS, Zung self-depression scale; SAS, Zung self-anxiety scale.

TABLE 2 | Group differences in bilateral LC-NE FC network.

Brain region	BA	Voxel size	MNI coordinates (RAI)			Peak Z score
			x	y	Z	
Left LC-NE FC network						
Left IFG	47	50	−45	39	0	−4.33
Left MOG	19	202	−42	−81	9	4.65
Left SMG	40	56	−39	−30	39	4.46
Right LC-NE FC network						
Left dACC	24	57	−3	24	18	−3.86

LC-NE FC, locus coeruleus-norepinephrine functional connectivity; BA, Brodmann's area; MNI, Montreal Neurologic Institute; RAI, the right anterior and inferior direction is positive value; IFG, inferior frontal gyrus; MOG, middle occipital gyrus; SMG, supramarginal gyrus; dACC, dorsal anterior cingulate cortex.

Gender Difference of the Altered LC-NE Functional Network in the CID Group

As shown in **Figure 2** and **Table 3**, in the right LC-NE functional network, the LC-NE FC in the left amygdala and the right middle frontal gyrus (MFG) was greater in male when compared with female in the CID group. No significant gender difference was found in the left LC-NE functional network.

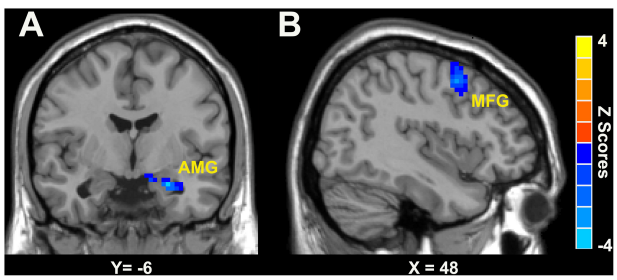

FIGURE 2 | Gender differences of LC-NE functional network in patients with CID was located in AMG **(A)** and MFG **(B)**. The blue color bar means the LC-NE FC in female is lower than that in male. AMG, amygdala; MFG, middle frontal gyrus.

TABLE 3 | Gender differences in bilateral LC-NE FC network in CID group.

Brain region	BA	Voxel size	MNI coordinates (RAI)			Peak *Z* score
			X	*y*	*z*	
Left LC-NE FC network						
None						
Right LC-NE FC network						
Left AMG	36	59	−24	−6	−21	−4.51
Right MFG	6	112	48	12	48	−3.95

LC-NE FC, locus coeruleus-norepinephrine functional connectivity; BA, Brodmann's area; MNI, Montreal Neurologic Institute; RAI, the right anterior and inferior direction is positive value; AMG, amygdala; MFG, middle frontal gyrus.

Clinical Significance of the Altered LC-NE Functional Network

A partial correlation analysis was conducted to investigate the relationship between abnormal LC-NE FC and clinical features in patients with CID. As shown in **Figure 3**, after FDR correction, FC between the left LC and left MOG was positively correlated with the duration of disease in patients with CID, after controlling for the effects of gender and age (r = 0.342, p = 0.005, pFDR = 0.042). In addition, FC between right LC and left dACC was negatively correlated with the SAS scores in patients with CID, after controlling for the effects of gender and age (r = −0.364, p = 0.003, pFDR = 0.036). No other significant correlation was found after FDR correction (pFDR > 0.05 in all cases).

DISCUSSION

Our study demonstrated that patients with CID presented both increased and decreased regions in LC-NE functional network when compared with GSC subjects. The areas with increased FC were located in the posterior sensory cortex of the LC-NE functional network, while those with decreased FC were found in the prefrontal cortex of the LC-NE functional network. Importantly, the altered LC-NE function in dACC was associated with anxiety symptoms in patients with CID. These findings indicated that there was a dysfunctional LC-NE system in patients with CID, and that this abnormal LC-NE functional network would contribute to the combined anxiety symptoms in these patients. The present study substantially extended our understanding of the neuropathological basis of CID and provided the potential treatment target for CID patients who had anxiety.

As expected, areas with both increased and decreased LC-NE FC were found in patients with CID. Anatomically, the ascending pathway of LC-NE system is projected to the limbic system, thalamus, basal forebrain, and the entire neocortex (Szabadi, 2013); the areas with abnormal LC-NE FC network in patients with CID were found in the neocortex. We found that in patients with CID, areas with increased LC-NE FC were located in SMG and MOG. The SMG is part of somatosensory association cortex, which is involved in tactile sensory, and space and limb location perception (Leichnetz, 2011), whereas the MOG is involved in visual and spatial information processing (Renier et al., 2010). Interestingly, the areas with increased LC-NE FC were located in the posterior sensory cortex. These findings could elucidate that CID patients suffer from the hypersensitivity in sensory perception of tactile, visual, and auditory stimuli. The present findings supported the notion of the hyperarousal state of the posterior sensory cortex in the LC-NE ascending pathway in patients with CID.

Areas with decreased LC-NE FC were found in the left dACC and IFG in patients with CID. The dACC is the important region for decision making in executive control network (Bush et al., 2002) and is also involved in behavioral adaptation (Logiaco et al., 2015). The decreased LC-NE network might indicate decreased

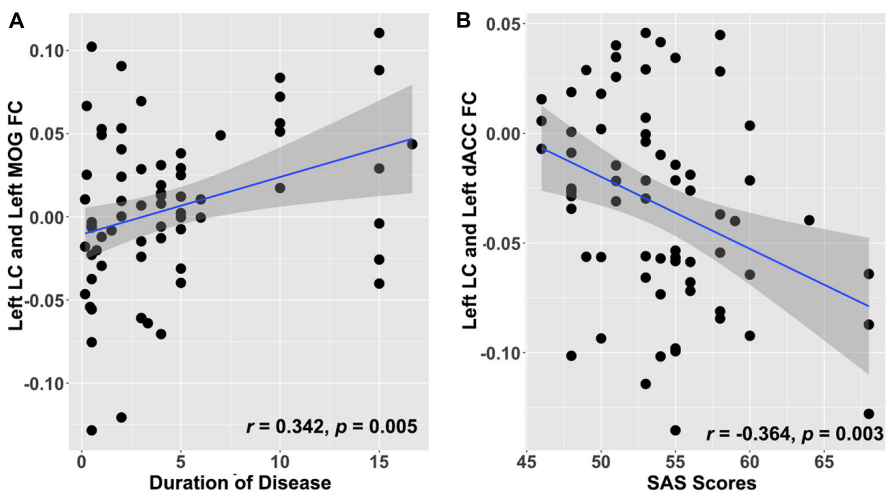

FIGURE 3 | Clinical significance of altered LC-NE functional network in patients with CID. **(A)** Increased LC-NE FC in left MOG is positively associated with duration of insomnia. **(B)** Decreased LC-NE FC in the left dACC is negatively associated with anxiety symptom in patients with CID. LC-NE, locus coeruleus-norepinephrine; CID, chronic insomnia disorder; MOG, middle occipital gyrus; dACC, dorsal anterior cingulate cortex.

self-control and adaptation of the arousal in the CID patients. The IFG is also an important region in prefrontal cortex and a core node in executive control network. Recent neuroimaging studies also found lower degree centrality, amplitude of low-frequency fluctuations, and functional connectivity between IFG and orbital frontal cortex in the IFG in patients with insomnia than in healthy controls (Li et al., 2016; Yan et al., 2018; Xie et al., 2020). In addition, the FC in IFG was associated with the duration of the disease, anxiety, and insomnia symptoms in patients with CID (Xie et al., 2020). Our findings support the "locus coeruleus neural fatigue" brain mechanism of the chronic insomnia disorder (Van Dort, 2016). Taken together, the decreased LC-NE functional network in prefrontal control network indicated the decreased cognitive control ability in patients with CID.

Previous studies have found gender difference in LC functional connectivity network in healthy control participants. For instance, Zhang et al. (2016) found that men show greater LC FC in the left hippocampus/parahippocampus and the left middle temporal gyrus than women. The results of the present study displayed that males show greater functional connectivity between LC and left amygdala and right MFG than women. As the amygdala and the MFG are important for the emotion and cognitive control process (McDougle et al., 1995; Szabadi, 2013), the gender difference might indicate different emotion and cognitive regulation strategies for insomnia. Further study might investigate the gender detail in the CID patients.

Interestingly, although posterior and frontal abnormalities in the LC-NE ascending pathway were found in patients in the CID group, such alterations were associated with different clinical manifestations. The posterior sensory cortex pathway (MOG) of the LC-NE system was associated with the duration of disease, while that of the frontal cognitive control pathway (dACC) was associated with anxiety symptoms. The prefrontal cortex is the main ascending projections in LC-NE system (Szabadi, 2013) involved in attentional and cognitive control. Recent retrograde tract-tracing experiments and optogenetic techniques also revealed target-specific projections in the LC-prefrontal cortex pathway (Chandler et al., 2014; Bari et al., 2020). The lower functional connectivity between LC and ACC have also found that in patients with late-life major depressive disorder, the LC-ACC FC was correlated with depressive severity (Del Cerro et al., 2020a). Our findings showing the LC-dACC pathway were associated with anxiety symptoms in CID patients, supporting the role of dorsal ACC in the anxiety in these patients. It should be recognized that the amygdala is the core region for emotional processing mediating fear and anxiety response in LC-NE system (McDougle et al., 1995; Szabadi, 2013); however, we did not find abnormal LC-amygdala FC in the CID group. Future studies need to verify this result. The occipital cortex is the main LC-visual cortex pathway projection involved in the modulation of visual sensory processing (McBurney-Lin et al., 2019), the increased fractional amplitude of low-frequency fluctuations (fALFF) in bilateral MOG was reported in participants with insomnia (Liu et al., 2016). Thus, the association of insomnia duration and LC-MOG pathway might indicate a mechanism that involves the hyperarousal state of the visual cortex in CID patients. Taken together, the clinical significance of the altered LC-NE system in CID patients suggests that different neural mechanisms underlie insomnia and emotional symptoms in CID and may help develop more targeted treatment strategies for CID patients with anxiety.

LIMITATIONS

The present preliminary study has some limitations. First, the LC is also involved in another neurotransmitter system, which is beyond its primary definition as a NE-producing nucleus, e.g., the GABAergic circuit (Breton-Provencher and Sur, 2019). In addition, NE interacts with the serotonin and dopamine systems, which also make an important contribution to the mood regulation (Guiard et al., 2008). Thus, further study could explore the alterations in other neurotransmitter brain functional systems and their interaction in the insomnia. Second, we did not evaluate the cognition performance in the CID group; however, there is a large body of evidence which suggests that the LC-NE system is engaged in many cognitive processes, including attention and memory retrieval and consolidation, as well as decision making (Sara, 2009). Third, this study was a cross-sectional study; thus, the abnormal LC-NE-associated anxiety symptoms could not be explained as a causal relationship. Further longitudinal studies are required to verify our speculation. Lastly, as the anxiety disorder has also been associated with insomnia symptoms, further studies are required to reveal the potential LC-NE system relationship between insomnia symptoms in anxiety disorder population.

CONCLUSION

Our study found increased FC in the LC-sensory cortex and decreased FC in the LC-prefrontal cortex in patients with CID. In addition, the altered LC-NE function in dACC was associated with anxiety symptoms in patients with CID. Our study provided evidence for abnormal LC-NE functional network in patients with CID. The present study substantially extended our understanding of the neuropathological basis of CID and provided a potential treatment target for CID patients with anxiety.

DATA AVAILABILITY STATEMENT

The original contributions presented in the study are included in the article/supplementary material, further inquiries can be directed to the corresponding author.

ETHICS STATEMENT

The studies involving human participants were reviewed and approved by Institutional Review Board of The Third Affiliated Hospital of Anhui Medical University. The patients/participants provided their written informed consent to participate in this study.

AUTHOR CONTRIBUTIONS

LG and CX designed the experiments. LG and MS wrote the manuscript. JW, RX, XD, and SY conducted the statistical analysis. BZ, DL, and XZ contributed to the manuscript revision. MS and CX collected the data. All authors contributed to the article and approved the submitted version.

FUNDING

This study was funded by the Sichuan Provincial Science and Technology Department project in China (Nos. 2020YJ0197, 2020YJ0176, and 2021YJ0176), the National Natural Science Foundation of China (Nos. 82001803 and 82004488), Chengdu University of Traditional Chinese Medicine Xinglin Scholar Discipline Talent Research and Improvement Plan (No. BSH2019011), the project of Hefei Municipal Health Commission and Collaborative Innovation Center for Neuropsychiatric Disorders and Mental Health (NDMHCI-19-01), and the Department of Science and Technology of Anhui Province (202004j07020006).

ACKNOWLEDGMENTS

We would like to thank Editage (www.editage.cn) for English language editing.

REFERENCES

Altena, E., Vrenken, H., Van Der Werf, Y. D., Van Den Heuvel, O. A., and Van Someren, E. J. (2010). Reduced orbitofrontal and parietal gray matter in chronic insomnia: a voxel-based morphometric study. *Biol. Psychiatry* 67, 182–185. doi: 10.1016/j.biopsych.2009.08.003

Ambrosini, E., Vastano, R., Montefinese, M., and Ciavarro, M. (2013). Functional specificity of the locus coeruleus-norepinephrine system in the attentional networks. *Front. Behav. Neurosci.* 7:201. doi: 10.3389/fnbeh.2013.00201

Ashburner, J. (2007). A fast diffeomorphic image registration algorithm. *Neuroimage* 38, 95–113. doi: 10.1016/j.neuroimage.2007.07.007

Backhaus, J., Junghanns, K., Broocks, A., Riemann, D., and Hohagen, F. (2002). Test-retest reliability and validity of the Pittsburgh Sleep Quality Index in primary insomnia. *J. Psychosom. Res.* 53, 737–740. doi: 10.1016/s0022-3999(02)00330-6

Bari, A., Xu, S., Pignatelli, M., Takeuchi, D., Feng, J., Li, Y., et al. (2020). Differential attentional control mechanisms by two distinct noradrenergic coeruleo-frontal cortical pathways. *Proc. Natl. Acad. Sci. U. S. A.* 117, 29080–29089. doi: 10.1073/pnas.2015635117

Berridge, C. W., Schmeichel, B. E., and España, R. A. (2012). Noradrenergic modulation of wakefulness/arousal. *Sleep Med. Rev.* 16, 187–197. doi: 10.1016/j.smrv.2011.12.003

Blake, M. J., Trinder, J. A., and Allen, N. B. (2018). Mechanisms underlying the association between insomnia, anxiety, and depression in adolescence: implications for behavioral sleep interventions. *Clin. Psychol. Rev.* 63, 25–40. doi: 10.1016/j.cpr.2018.05.006

Bragantini, D., Sivertsen, B., Gehrman, P., Lydersen, S., and Güzey, I. C. (2019). Differences in anxiety levels among symptoms of insomnia. The HUNT study. *Sleep Health* 5, 370–375. doi: 10.1016/j.sleh.2019.01.002

Breton-Provencher, V., and Sur, M. (2019). Active control of arousal by a locus coeruleus GABAergic circuit. *Nat. Neurosci.* 22, 218–228. doi: 10.1038/s41593-018-0305-z

Bush, G., Vogt, B. A., Holmes, J., Dale, A. M., Greve, D., Jenike, M. A., et al. (2002). Dorsal anterior cingulate cortex: a role in reward-based decision making. *Proc. Natl. Acad. Sci. U. S. A.* 99, 523–528. doi: 10.1073/pnas.012470999

Buysse, D. J., Reynolds, C. F. III., Monk, T. H., Berman, S. R., and Kupfer, D. J. (1989). The Pittsburgh Sleep Quality Index: a new instrument for psychiatric practice and research. *Psychiatry Res.* 28, 193–213. doi: 10.1016/0165-1781(89)90047-4

Chai, X. J., Castañón, A. N., Öngür, D., and Whitfield-Gabrieli, S. (2012). Anticorrelations in resting state networks without global signal regression. *Neuroimage* 59, 1420–1428. doi: 10.1016/j.neuroimage.2011.08.048

Chandler, D. J., Gao, W.-J., and Waterhouse, B. D. (2014). Heterogeneous organization of the locus coeruleus projections to prefrontal and motor cortices. *Proc. Natl. Acad. Sci. U. S. A.* 111, 6816–6821. doi: 10.1073/pnas.1320827111

Chen, M. C., Chang, C., Glover, G. H., and Gotlib, I. H. (2014). Increased insula coactivation with salience networks in insomnia. *Biol. Psychol.* 97, 1–8. doi: 10.1016/j.biopsycho.2013.12.016

Del Cerro, I., Martínez-Zalacaín, I., Guinea-Izquierdo, A., Gascón-Bayarri, J., Viñas-Diez, V., Urretavizcaya, M., et al. (2020a). Locus coeruleus connectivity alterations in late-life major depressive disorder during a visual oddball task. *Neuroimage Clin.* 28:102482. doi: 10.1016/j.nicl.2020.102482

Del Cerro, I., Villarreal, M. F., Abulafia, C., Duarte-Abritta, B., Sánchez, S. M., Castro, M. N., et al. (2020b). Disrupted functional connectivity of the locus coeruleus in healthy adults with parental history of Alzheimer's disease. *J. Psychiatr. Res.* 123, 81–88. doi: 10.1016/j.jpsychires.2020.01.018

Gong, L., Xu, R., Liu, D., Zhang, C., Huang, Q., Zhang, B., et al. (2020a). Abnormal functional connectivity density in patients with major depressive disorder with comorbid insomnia. *J. Affect. Disord.* 266, 417–423. doi: 10.1016/j.jad.2020.01.088

Gong, L., Xu, R., Qin, M., Liu, D., Zhang, B., Bi, Y., et al. (2020b). New potential stimulation targets for noninvasive brain stimulation treatment of chronic insomnia. *Sleep Med.* 75, 380–387. doi: 10.1016/j.sleep.2020.08.021

Gong, L., Yu, S., Xu, R., Liu, D., Dai, X., Wang, Z., et al. (2020c). The abnormal reward network associated with insomnia severity and depression in chronic insomnia disorder. *Brain Imaging Behav.* 15, 1033–1042. doi: 10.1007/s11682-020-00310-w

Grimaldi, D., Reid, K. J., Papalambros, N. A., Braun, R. I., Malkani, R. G., Abbott, S. M., et al. (2020). Autonomic dysregulation and sleep homeostasis in insomnia. *Sleep* zsaa274. [Epub online ahead of print].

Guiard, B. P., El Mansari, M., and Blier, P. (2008). Cross-talk between dopaminergic and noradrenergic systems in the rat ventral tegmental area, locus ceruleus, and dorsal hippocampus. *Mol. Pharmacol.* 74, 1463–1475. doi: 10.1124/mol.108.048033

Huang, S., Zhou, F., Jiang, J., Huang, M., Zeng, X., Ding, S., et al. (2017). Regional impairment of intrinsic functional connectivity strength in patients with chronic primary insomnia. *Neuropsychiatr. Dis. Treat.* 13, 1449–1462. doi: 10.2147/ndt.s137292

Huang, Z., Liang, P., Jia, X., Zhan, S., Li, N., Ding, Y., et al. (2012). Abnormal amygdala connectivity in patients with primary insomnia: evidence from resting state fMRI. *Eur. J. Radiol.* 81, 1288–1295. doi: 10.1016/j.ejrad.2011.03.029

Joo, E. Y., Noh, H. J., Kim, J. S., Koo, D. L., Kim, D., Hwang, K. J., et al. (2013). Brain Gray Matter Deficits in Patients with Chronic Primary Insomnia. *Sleep* 36, 999–1007. doi: 10.5665/sleep.2796

Kalmbach, D. A., Cuamatzi-Castelan, A. S., Tonnu, C. V., Tran, K. M., Anderson, J. R., Roth, T., et al. (2018). Hyperarousal and sleep reactivity in insomnia: current insights. *Nat. Sci. Sleep* 10, 193–201. doi: 10.2147/nss.s138823

Kokou-Kpolou, C. K., Megalakaki, O., Laimou, D., and Kousouri, M. (2020). Insomnia during COVID-19 pandemic and lockdown: prevalence, severity, and associated risk factors in French population. *Psychiatry Res.* 290:113128. doi: 10.1016/j.psychres.2020.113128

Leichnetz, G. R. (2011). "Supramarginal Gyrus," in *Encyclopedia of Clinical Neuropsychology*, eds J. S. Kreutzer, J. Deluca, and B. Caplan (New York, NY: Springer), 2439–2440. doi: 10.1007/978-0-387-79948-3_369

Li, C., Ma, X., Dong, M., Yin, Y., Hua, K., Li, M., et al. (2016). Abnormal spontaneous regional brain activity in primary insomnia: a resting-state

functional magnetic resonance imaging study. *Neuropsychiatr. Dis. Treat.* 12, 1371–1378. doi: 10.2147/ndt.s109633

Li, M., Yan, J., Li, S., Wang, T., Wen, H., Yin, Y., et al. (2018). Altered gray matter volume in primary insomnia patients: a DARTEL-VBM study. *Brain Imaging Behav.* 12, 1759–1767. doi: 10.1007/s11682-018-9844-x

Liu, C. H., Liu, C. Z., Zhang, J., Yuan, Z., Tang, L. R., Tie, C. L., et al. (2016). Reduced spontaneous neuronal activity in the insular cortex and thalamus in healthy adults with insomnia symptoms. *Brain Res.* 1648, 317–324. doi: 10.1016/j.brainres.2016.07.024

Liu, F., Wang, Y., Li, M., Wang, W., Li, R., Zhang, Z., et al. (2017). Dynamic functional network connectivity in idiopathic generalized epilepsy with generalized tonic–clonic seizure. *Hum. Brain Mapp.* 38, 957–973. doi: 10.1002/hbm.23430

Liu, H., Shi, H., and Pan, P. (2018). Brain structural and functional alterations in insomnia disorder: more "homogeneous" research is needed. *Sleep Med. Rev.* 42, 234–235. doi: 10.1016/j.smrv.2018.08.005

Logiaco, L., Quilodran, R., Procyk, E., and Arleo, A. (2015). Spatiotemporal Spike Coding of Behavioral Adaptation in the Dorsal Anterior Cingulate Cortex. *PLoS Biol.* 13:e1002222. doi: 10.1371/journal.pbio.1002222

Lovett-Barron, M., Andalman, A. S., Allen, W. E., Vesuna, S., Kauvar, I., Burns, V. M., et al. (2017). Ancestral circuits for the coordinated modulation of brain state. *Cell* 171, 1411–1423.e17.

Lowe, M. J., Mock, B. J., and Sorenson, J. A. (1998). Functional connectivity in single and multislice echoplanar imaging using resting-state fluctuations. *Neuroimage* 7, 119–132. doi: 10.1006/nimg.1997.0315

McBurney-Lin, J., Lu, J., Zuo, Y., and Yang, H. (2019). Locus coeruleus-norepinephrine modulation of sensory processing and perception: a focused review. *Neurosci. Biobehav. Rev.* 105, 190–199. doi: 10.1016/j.neubiorev.2019.06.009

McCall, J. G., Al-Hasani, R., Siuda, E. R., Hong, D. Y., Norris, A. J., Ford, C. P., et al. (2015). CRH Engagement of the Locus Coeruleus Noradrenergic System Mediates Stress-Induced Anxiety. *Neuron* 87, 605–620. doi: 10.1016/j.neuron.2015.07.002

McDougle, C. J., Krystal, J. H., Price, L. H., Heninger, G. R., and Charney, D. S. (1995). Noradrenergic response to acute ethanol administration in healthy subjects: comparison with intravenous yohimbine. *Psychopharmacology* 118, 127–135. doi: 10.1007/bf02245830

Moruzzi, G., and Magoun, H. W. (1949). Brain stem reticular formation and activation of the EEG. *Electroencephalogr. Clin. Neurophysiol.* 1, 455–473. doi: 10.1016/0013-4694(49)90219-9

Murphy, K., Birn, R. M., Handwerker, D. A., Jones, T. B., and Bandettini, P. A. (2009). The impact of global signal regression on resting state correlations: are anti-correlated networks introduced? *Neuroimage* 44, 893–905. doi: 10.1016/j.neuroimage.2008.09.036

Renier, L. A., Anurova, I., De Volder, A. G., Carlson, S., Vanmeter, J., and Rauschecker, J. P. (2010). Preserved functional specialization for spatial processing in the middle occipital gyrus of the early blind. *Neuron* 68, 138–148. doi: 10.1016/j.neuron.2010.09.021

Rolls, E. T., Huang, C. C., Lin, C. P., Feng, J., and Joliot, M. (2020). Automated anatomical labelling atlas 3. *Neuroimage* 206:116189. doi: 10.1016/j.neuroimage.2019.116189

Sara, S. J. (2009). The locus coeruleus and noradrenergic modulation of cognition. *Nat. Rev. Neurosci.* 10, 211–223. doi: 10.1038/nrn2573

Sateia, M. J. (2014). International classification of sleep disorders-third edition: highlights and modifications. *Chest* 146, 1387–1394. doi: 10.1378/chest.14-0970

Shi, L., Lu, Z. A., Que, J. Y., Huang, X. L., Liu, L., Ran, M. S., et al. (2020). Prevalence of and Risk Factors Associated With Mental Health Symptoms Among the General Population in China During the Coronavirus Disease 2019 Pandemic. *JAMA Netw. Open* 3:e2014053. doi: 10.1001/jamanetworkopen.2020.14053

Sivertsen, B., Salo, P., Mykletun, A., Hysing, M., Pallesen, S., Krokstad, S., et al. (2012). The bidirectional association between depression and insomnia: the HUNT study. *Psychosom. Med.* 74, 758–765. doi: 10.1097/psy.0b013e3182648619

Song, A. H., Kucyi, A., Napadow, V., Brown, E. N., Loggia, M. L., and Akeju, O. (2017). Pharmacological Modulation of Noradrenergic Arousal Circuitry Disrupts Functional Connectivity of the Locus Ceruleus in Humans. *J. Neurosci.* 37, 6938–6945. doi: 10.1523/jneurosci.0446-17.2017

Sweetman, A., Lovato, N., Micic, G., Scott, H., Bickley, K., Haycock, J., et al. (2020). Do symptoms of depression, anxiety or stress impair the effectiveness of cognitive behavioural therapy for insomnia? A chart-review of 455 patients with chronic insomnia. *Sleep Med.* 75, 401–410. doi: 10.1016/j.sleep.2020.08.023

Szabadi, E. (2013). Functional neuroanatomy of the central noradrenergic system. *J. Psychopharmacol.* 27, 659–693. doi: 10.1177/0269881113490326

Tahmasian, M., Noori, K., Samea, F., Zarei, M., Spiegelhalder, K., Eickhoff, S. B., et al. (2018). A lack of consistent brain alterations in insomnia disorder: an activation likelihood estimation meta-analysis. *Sleep Med. Rev.* 42, 111–118. doi: 10.1016/j.smrv.2018.07.004

Van Dort, C. J. (2016). Locus Coeruleus Neural Fatigue: a Potential Mechanism for Cognitive Impairment during Sleep Deprivation. *Sleep* 39, 11–12. doi: 10.5665/sleep.5302

Winkelman, J. W., Plante, D. T., Schoerning, L., Benson, K., Buxton, O. M., O'connor, S. P., et al. (2013). Increased Rostral Anterior Cingulate Cortex Volume in Chronic Primary Insomnia. *Sleep* 36, 991–998. doi: 10.5665/sleep.2794

Xie, D., Qin, H., Dong, F., Wang, X., Liu, C., Xue, T., et al. (2020). Functional Connectivity Abnormalities of Brain Regions With Structural Deficits in Primary Insomnia Patients. *Front. Neurosci.* 14:566. doi: 10.3389/fnins.2020.00566

Yan, C.-G., Wang, X.-D., Zuo, X.-N., and Zang, Y.-F. (2016). DPABI: data Processing & Analysis for (Resting-State) Brain Imaging. *Neuroinformatics* 14, 339–351. doi: 10.1007/s12021-016-9299-4

Yan, C. Q., Wang, X., Huo, J. W., Zhou, P., Li, J. L., Wang, Z. Y., et al. (2018). Abnormal Global Brain Functional Connectivity in Primary Insomnia Patients: a Resting-State Functional MRI Study. *Front. Neurol.* 9:856. doi: 10.3389/fneur.2018.00856

Yu, S., Feng, F., Zhang, Q., Shen, Z., Wang, Z., Hu, Y., et al. (2018a). Gray matter hypertrophy in primary insomnia: a surface-based morphometric study. *Brain Imaging Behav.* 14, 1309–1317. doi: 10.1007/s11682-018-9992-z

Yu, S., Shen, Z., Lai, R., Feng, F., Guo, B., Wang, Z., et al. (2018b). The orbitofrontal cortex gray matter is associated with the interaction between insomnia and depression. *Front. Psychiatry* 9:651. doi: 10.3389/fpsyt.2018.00651

Zhang, S., Hu, S., Chao, H. H., and Li, C. S. (2016). Resting-State Functional Connectivity of the Locus Coeruleus in Humans: in Comparison with the Ventral Tegmental Area/Substantia Nigra Pars Compacta and the Effects of Age. *Cereb. Cortex* 26, 3413–3427. doi: 10.1093/cercor/bhv172

Zung, W. W. (1971). A rating instrument for anxiety disorders. *Psychosomatics* 12, 371–379. doi: 10.1016/s0033-3182(71)71479-0

Zung, W. W., Richards, C. B., and Short, M. J. (1965). Self-rating depression scale in an outpatient clinic. Further validation of the SDS. Arch. Gen. Psychiatry 13, 508–515. doi: 10.1001/archpsyc.1965.01730060026004

Conflict of Interest: The authors declare that the research was conducted in the absence of any commercial or financial relationships that could be construed as a potential conflict of interest.

frontiers in Psychiatry

SYSTEMATIC REVIEW
published: 07 June 2021
doi: 10.3389/fpsyt.2021.646569

The Effects of Transcranial Electrical Stimulation of the Brain on Sleep: A Systematic Review

Clément Dondé[1,2,3]*, *Jerome Brunelin*[4,5,6], *Jean-Arthur Micoulaud-Franchi*[7,8], *Julia Maruani*[9,10,11], *Michel Lejoyeux*[12,13], *Mircea Polosan*[1,2,3] and *Pierre A. Geoffroy*[12,13,14]

[1] University Grenoble Alpes, Grenoble, France, [2] U1216 INSERM, Grenoble Institut of Neuroscience, La Tronche, France, [3] Psychiatry Department, CHU Grenoble Alpes, Grenoble, France, [4] INSERM U1028, CNRS UMR5292, Lyon Neuroscience Research Center, PSY-R2 Team, Lyon, France, [5] Lyon University, Lyon, France, [6] Centre Hospitalier le Vinatier, Batiment 416, Bron, France, [7] University Sleep Clinic, Services of Functional Exploration of the Nervous System, University Hospital of Bordeaux, Bordeaux, France, [8] USR CNRS 3413 SANPSY, University Hospital Pellegrin, University of Bordeaux, Bordeaux, France, [9] Département de Psychiatrie et de Médecine Addictologique, Hôpital Fernand Widal, Assistance Publique des Hôpitaux de Paris (APHP), Paris, France, [10] Université de Paris, Paris, France, [11] INSERM U1144, Optimisation Thérapeutique en Neuropsychopharmacologie, Paris, France, [12] Paris Diderot University-Paris VII, 5 Rue Thomas Mann, Paris, France, [13] University Hospital Bichat-Claude Bernard, 46 rue Henri Huchard, Paris, France, [14] Université de Paris, NeuroDiderot, Inserm, Paris, France

Transcranial Electrical Stimulation (tES) is a promising non-invasive brain modulation tool. Over the past years, there have been several attempts to modulate sleep with tES-based approaches in both the healthy and pathological brains. However, data about the impact on measurable aspects of sleep remain scattered between studies, which prevent us from drawing firm conclusions. We conducted a systematic review of studies that explored the impact of tES on neurophysiological sleep oscillations, sleep patterns measured objectively with polysomnography, and subjective psychometric assessments of sleep in both healthy and clinical samples. We searched four main electronic databases to identify studies until February 2020. Forty studies were selected including 511 healthy participants and 452 patients. tES can modify endogenous brain oscillations during sleep. Results concerning changes in sleep patterns are conflicting, whereas subjective assessments show clear improvements after tES. Possible stimulation-induced mechanisms within specific cortico-subcortical sleep structures and networks are discussed. Although these findings cannot be directly transferred to the clinical practice and sleep-enhancing devices development for healthy populations, they might help to pave the way for future researches in these areas. PROSPERO registration number 178910.

Keywords: sleep, transcranial electrical stimulation, sleep oscillations, sleep pattern, subjective sleep, systematic review

OPEN ACCESS

Edited by:
Kai Wang,
Anhui Medical University, China

Reviewed by:
Wolnei Caumo,
Clinical Hospital of Porto Alegre (HCPA), Brazil
Ki-Young Jung,
Seoul National University, South Korea

***Correspondence:**
Clément Dondé
clement.dondé@univ-grenoble-alpes.fr
orcid.org/0000-0002-5121-8769

Specialty section:
This article was submitted to Neuroimaging and Stimulation, a section of the journal Frontiers in Psychiatry

Received: *27 December 2020*
Accepted: *19 April 2021*
Published: *07 June 2021*

Citation:
Dondé C, Brunelin J, Micoulaud-Franchi J-A, Maruani J, Lejoyeux M, Polosan M and Geoffroy PA (2021) The Effects of Transcranial Electrical Stimulation of the Brain on Sleep: A Systematic Review. Front. Psychiatry 12:646569. doi: 10.3389/fpsyt.2021.646569

INTRODUCTION

Sleep plays a vital role in well-being and good health throughout life. It is essential for many brain processes including the consolidation of memories (1, 2), alertness, processing speed, and decision-making (3). Healthy regulation of these processes by sleep has a significant relationship with scores of quality of life and global functioning (4). Sleep disorders, as medically defined, have significant public health implications, with insomnia complaints reported by nearly one third of the general

population, and excessive daytime sleepiness affecting up to one fourth (5). In addition, it has been demonstrated that alteration of sleep is a marker of risk for numerous physical and mental disorders (6, 7). Abnormal fluctuations in sleep duration and efficiency (8–10), regularity of sleep cycle (11), subjective sleep quality (12), attentive wakefulness (13), and timing of sleep (14) are associated with greater risk of adverse general health outcomes including death. More specifically, sleep disruptions are associated with higher risk of diabetes, stroke, coronary heart disease and heart attack (10, 15), obesity (16), as well as mental disorders (7). Moreover, sleep complaints are often integral and important parts of a large range of diagnosed chronic medical conditions (17, 18).

Several tools have been developed to measure and assess objective and subjective aspects of sleep. Electroencephalography (EEG) studies have provided numerous indicators of the sleep course and quality. For instance, slow-wave oscillations have been demonstrated as accurate indexes of sleep homeostasis (19). In parallel, sleep patterns including architecture, timing, and stages differentiation can be measured with standardized polysomnography. Finally, several psychometric rating scales and brief interviews have been validated to assess subjective aspects of sleep and are widely used in clinical trials as main outcomes (20).

The functioning of brain areas and networks can be modified by applying electrical currents over the scalp. To modulate brain activity and eventually restore altered functions, transcranial Electrical Stimulation (tES) has recently emerged as a non-invasive painless brain modulation tool that involves the application of a weak (0.5–2 mA) current via two scalp electrodes (a cathode and an anode) overlying targeted cortical areas (21, 22). The electrical current flowing between the electrodes induces changes in neuronal excitability and activity through specific molecular mechanisms that mediate synaptic plasticity (23). tES studies have traditionally used direct current modalities for stimulation (tDCS: transcranial direct stimulation), where a constant unidirectional low current flows inward under the anode and outward under the cathode. Besides, other stimulation modalities have been developed for tES involving random noise frequencies (tRNS) or alternating (tACS) patterns of the current (24, 25). In healthy samples, an increasing number of studies have reported that tES can enhance various cognitive functions including memory, learning and attention, especially during learning of the task (26–28). In parallel, tDCS has shown promising results in treating psychiatric disorders such as major depressive disorder (29), various clinical symptoms and cognitive impairments in bipolar disorder (30, 31), auditory hallucinations (32), and negative symptoms (33) in schizophrenia, as well as numerous others (34).

Abbreviations: ADHD, Attention Deficit/Hyperactivity Disorder; EEG, electroencephalography; ESS, Epworth Sleepiness Scale; MeSH, Medical Subject Heading; MADRS, Montgomery-Asberg Depression Rating Scale; NREM, Non-Rapid Eye Movement (sleep); PRISMA, Preferred Reporting Items for Systematic Reviews and Meta-analysis; PROSPERO, International prospective register of systematic reviews; PSQI, The Pittsburgh Sleep Quality Index; REM, Rapid-Eye Movement (sleep); QualSyst, Standard Quality Assessment; SWS, Slow Wave Sleep; tACS, transcranial Alternating Current Stimulation; tDCS, transcranial Direct Current Stimulation; tES, transcranial Electrical Stimulation; tRNS, transcranial Random Noise Stimulation.

Arousal and sleep are physiologically modulated by "top-down" cortico-subcortical loops (35) that are known to be altered in some sleep disorders such as insomnia (36). The "top-down" concept raises the idea of modulating sleep with external stimulation of the neocortex. Given that tES has primarily cortical direct effects, this approach appears thus as a relevant therapeutic strategy. Over the past years, there have been several attempts to modulate sleep with tES-based approaches targeting "top-down" networks in both the healthy and pathological brains. However, in addition to heterogeneous and inconsistent results, studies strongly differ in terms of the number of samples, tES protocols, and type of measures. Furthermore, despite a growing interest in sleep modulations with electric current, data about the impact of tES in sleep remain scattered between studies and have not been systematically reviewed, which prevent from drawing definitive conclusions on the effect of tES on measurable aspects of sleep.

To gather knowledge about the specific effects of brain tES on core measurable aspects of sleep, we conducted a systematic review of studies that explored the impact of such procedure on neurophysiological sleep oscillations, sleep patterns measured objectively with polysomnography and subjective psychometric assessments of sleep. Here, we focus on the specific impact of tES on these sleep-related outcomes in both healthy and clinical populations; for details about the effect of tES during sleep on wake cognitive processes, we refer the interested reader to the exhaustive review recently published by Barham et al. (37). Results presented in our review will contribute to the understanding of underlying mechanisms of tES on sleep and improvement of sleep health, sleep complaints, and sleep disorders with tES. In parallel, this review may lend insight for further enhancement of sleep induction/stability, as well as physiological effects of sleep (e.g., memory strengthening) with innovative techniques of neuromodulation in healthy people.

METHODS

Eligibility

Recommendations of the PRISMA guidelines for systematic review and meta-analysis were followed (38). The protocol was prospectively registered at the PROSPERO register (ID: 178910) (39).

The criteria for inclusion were as follows: (i) English language studies published in peer-review journals, (ii) participants' age from 10–80 years. (iii) oscillatory data measured with electroencephalography and/or sleep pattern data reported from polysomnographic (or actigraphy) recordings and/or subjective sleep data assessed with validated rating scale, and (iv) measures collected pre-to-post and/or during the tES procedure. If two publications reported findings from the same dataset, the authors were contacted to identify the most appropriate data to review.

Literature Search Strategy

We searched the MEDLINE, Embase, ScienceDirect, and Clinical Trials databases using the following Medical Subject Heading (MeSH) terms in reference title, abstract, or keywords with no limitation of date until February 2020:

- (i) *Sleep*: "sleep," "insomnia," "hypersomnia," "sleepiness," "sleep apnea," "somnolence," "snoring," "restless legs syndrome," "periodic limb movements disorder," "REM sleep behavior disorder," "obstructive sleep apnea," "sleep-wake disruption," "parasomnia," "bruxism," "circadian rhythm sleep disorder."
- (ii) *tES*: "Transcranial stimulation," "tES," "Transcranial Electrical Stimulation," "tDCS," "Transcranial Direct Current Stimulation," "tRNS," "Transcranial Random Noise Stimulation," "tACS," "Transcranial Alternating Current Stimulation."

After excluding duplicate references, two reviewers (CD and PAG) independently screened the title and abstract of each study identified by the search and applied the inclusion criteria. Following this first screen, we applied the same procedure to the full text of eligible studies. Discrepancies between reviewers were resolved by discussion with a third member of the authorship. The "similar articles" findings in MEDLINE and Reference lists in identified studies were also reviewed for additional studies, although none were identified in this manner. The literature search strategy is detailed in the flow chart diagram (**Figure 1**).

Data Extraction

Two reviewers (CD and PAG) independently extracted the following data when present: (i) population data (sample size, gender ratio, disorder, or healthy status), (ii) study design (parallel or crossover groups, controlled or uncontrolled), (iii) tES protocol (anode and cathode placement; electrode size; current density and intensity; number, frequency, and duration of sessions; period and condition of stimulation), (iv) neurophysiological outcomes as measured with electroencephalography and/or sleep pattern outcomes as measured with polysomnographic (or actigraphy) recordings and/or subjective sleep outcomes as assessed with validated rating scale, and (v) adverse effects of the tES procedure.

Quality Assessment

To measure the overall quality of the included references, a global rating score was calculated for each study using the Standard Quality Assessment [QualSyst tool (40)].

RESULTS

Literature Search

As shown in **Figure 1**, the initial search returned 459 references after duplicate removal. Following preliminary screening of the titles and/or abstracts, 215 were excluded accordingly. Among the 59 references that were reviewed in detail, 40 studies were selected for systematic review including 511 healthy participants and 452 patients. The age of the participants varied from 12.3 to 73.4 years. Only 8 studies out of 40 reported transient adverse effects associated to the tES procedure (41–48). Overall, the quality assessment was satisfactory (mean: 22.1 ± 3.99). Total scores and details of the assessment are given in the

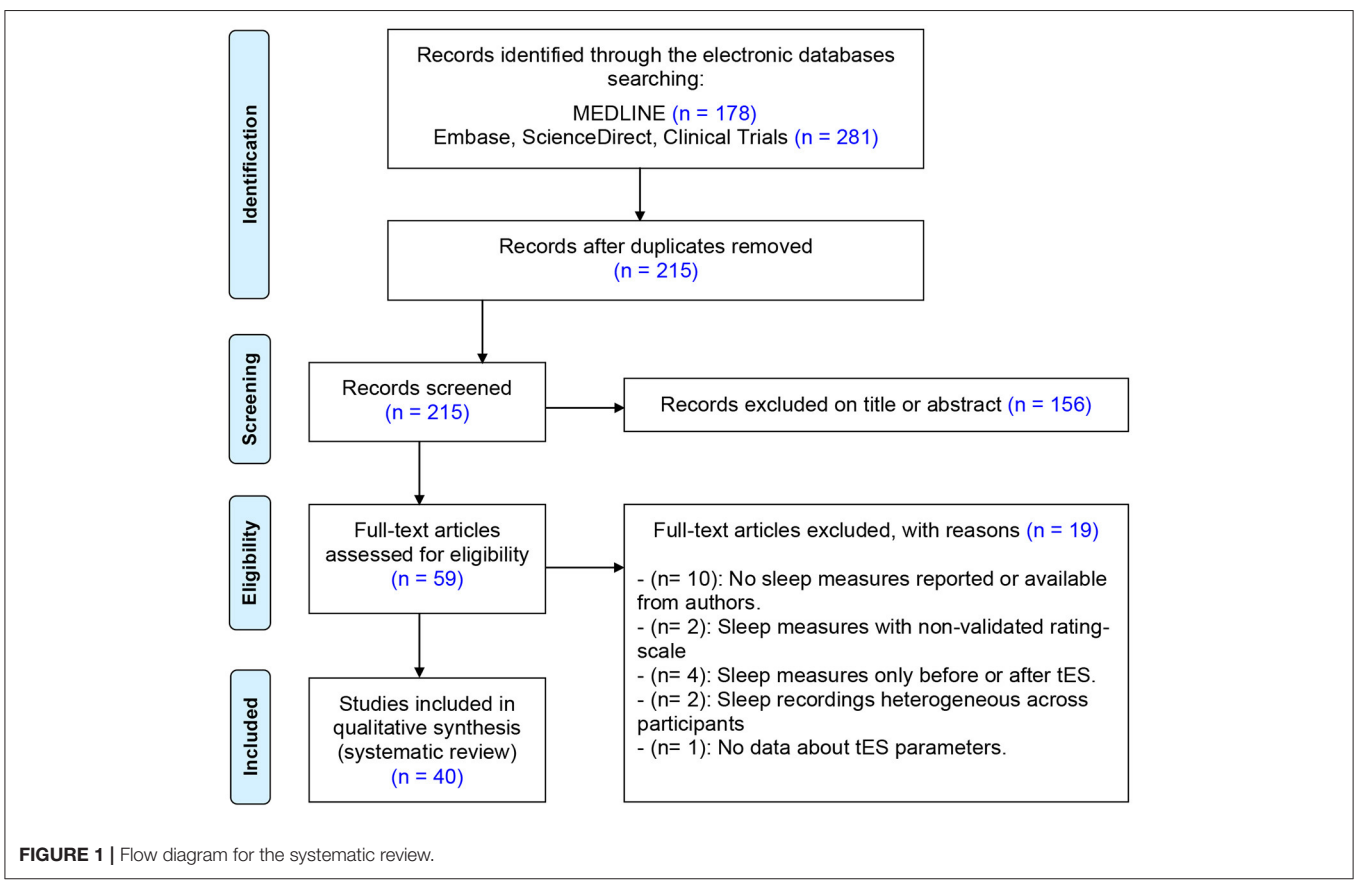

FIGURE 1 | Flow diagram for the systematic review.

Supplementary Table 1. Highlights of major significant effects of tES on sleep are pictured in **Figure 2** and detailed in **Supplementary Table 2**.

Oscillatory Aspects of Sleep

Study Designs and Characteristics

Twenty-four studies investigated the impact of tES on oscillatory aspects of sleep in healthy populations (45, 47, 49–64) and clinical populations (65–70). All used a crossover sham-controlled design with days-to-week washout periods between conditions, with the exception of two studies that included parallel arms of participants (60, 69). Study details are described in **Table 1**.

Results From Studies in Healthy Populations

Most research groups aimed for "top-down" effects and gave a single tES session targeting bilateral frontal areas with returning electrodes overlying the mastoids or the vertex. In these studies, the stimulation applied cycles of slow alternating current (around 0.75 Hz, interspersed by stimulation-free intervals) that were triggered during early stages NREM sleep (47, 49, 51, 55–57, 59, 61, 64, 67, 68). This specific design was employed after Marshall et al. original study to test if the prefrontal slow oscillations enhancement by tES during NREM is associated with increased hippocampal–neocortical-dependent declarative memory consolidation. This hypothesis is based on evidence that slow oscillations are the hallmark of neurophysiological activity during NREM being associated with neutral declarative memory (58). A subsequent enhancement of slow oscillations PSD by direct (58) and slow alternating (50, 56, 59, 64) tES vs. sham was repeatedly observed during stimulation-free intervals at the stimulated areas. In addition, increased spindle waves PSD (56, 59) and decreased delta/theta PSD (51, 53) were reported during these intervals. Another study from Marshall's group that involved higher-frequency alternating current (5 Hz) observed

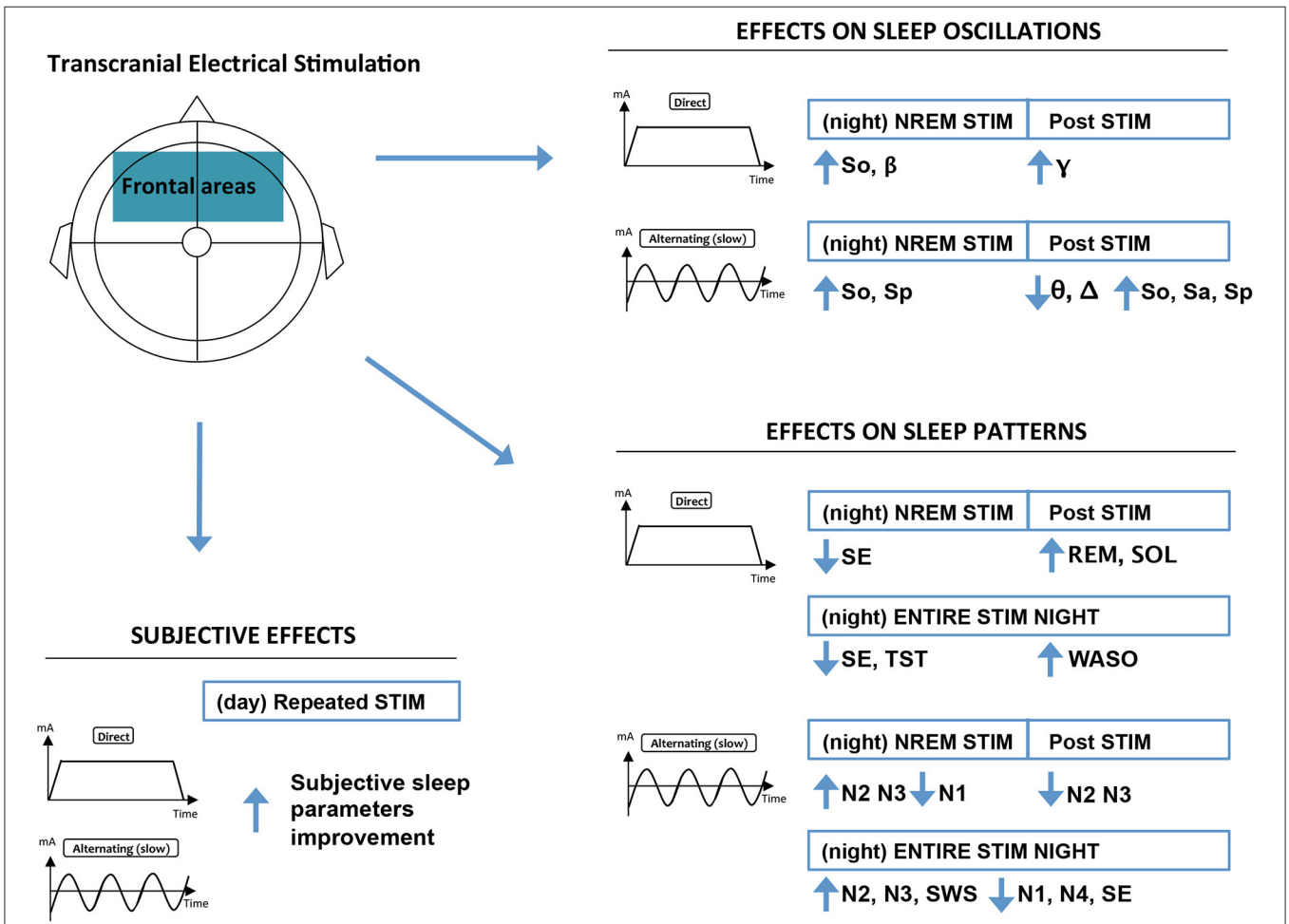

FIGURE 2 | Highlights of major significant effects of frontal tES on sleep. Results regarding non-frontal tES, tES during REM, and fast alternating tES were scarce, and thus omitted from the figure. Effect on sleep patterns: NREM, non-rapid eye movement sleep; N1–4, NREM sleep stages relative duration; REM, rapid eye movement sleep; SE, sleep efficiency; SWS, slow wave sleep relative duration; SOL, sleep onset latency; WASO, wake after sleep onset. Effects on sleep oscillations: β, beta power (15–25 Hz); Δ, delta power (1–4 Hz); γ, gamma power (>25 Hz); θ, theta power (4–8 Hz); NREM, non-rapid eyes movement sleep; So, slow oscillations power (0.5–1 Hz); Sa, slow activity power (0.5–4 Hz); Sp, spindle power (10–15 Hz).

TABLE 1 | Impact of transcranial electrical stimulation on oscillatory aspects of sleep.

References	Design	tES montage	tES sessions	Outcomes	Significant findings	Side effects
Placebo-controlled parallel-arms						
Garside et al. (53)	8 healthy (21.0 ± 0.93) 1 active arm, 1 sham arm	*Electrodes*: 5 cm^2 *Anodes*: 2 anterior–posterior to the left DLPFC (C3), 2 contralateral *Cathode*: 2 anterior–posterior to the left mastoid, 2 contralateral *Intensity*: 0.55 mA *Current*: alternating (0.75 Hz)	*Number*: 1 *Duration*: 30 min (5-min cycles with 1-min free intervals) *Period*: daytime nap N2 or N3	*Waves:* slow oscillations (0.7–0.8 Hz), delta (1–4 Hz), theta (4–8 Hz), alpha (9–12 Hz), fast spindle (12–14 Hz) *Parameters:* PSD	*Stimulation-free intervals:* decreased (reduced normal increase) delta power at Fz, C3, C4 by active vs. sham *1-min post-stimulation interval:* no significant changes	NA
Roizenblatt et al. (69)	*Frontal-active arm:* 11 fibromyalgia (47.3 ± 11.0 age, 11F) *Motor-active arm:* 11 fibromyalgia (54.8 ± 9.3 age, 11F) *Sham arm*: 10 fibromyalgia (50.8 ± 10.2 age, 10F)	*Electrodes*: 25 cm^2 *Active frontal arm: Anode*: right primary motor area (C3), *Cathode:* left supraorbital area (Fp2) *Active motor arm: Anode*: left DLPFC (C3), *Cathode:* right supraorbital area (Fp1) *Intensity*: 2 mA *Type*: direct	*Number*: 5 *Frequency:* daily *Duration*: 20 min *Period*: daytime before night sleep	*Waves:* delta (1–4 Hz), alpha (8–12 Hz) *Parameters:* PSD	*N1–N4 night sleep after stimulation procedure:* increased alpha and decreased delta at all electrodes by frontal-active vs. sham; increased delta by motor-active vs. sham.	None reported
Antonenko et al. (49)	15 healthy (23.4 ± 1.9 age, 7F) 1 active arm, 1 sham arm 4-week washout	*Electrodes*: 0.8 cm^2 *Anodes*: 2, DLPFC (F3, F4) *Cathodes:* 2 extra-cerebral (bilateral mastoids) *Intensity*: 0.32 mA/cm^2 *Current*: alternating (0.75 Hz squared)	*Number*: 1 *Duration*: 30 min (4-min cycles with 1-min free intervals) *Period*: 4 min after night N2 or N3 onset	*Waves:* slow activity (0.5–4 Hz), slow spindle (9–12 Hz), fast spindle (12–15 Hz), beta (15–25 Hz) *Parameters:* PSD, PAC	*Stimulation-free intervals:* no significant results *Stimulation intervals*: coupling of slow activity up-phases with spindle waves at Pz by active vs. sham.	NA
Cellini et al. (50)	17 healthy (32.2 ± 8.1 age, 6F) 1 active arm, 1 sham arm 1-week washout	*Electrodes*: 40 cm^2 *Anodes*: 2 anterior–posterior to the left DLPFC (C3), 2 contralateral *Cathode*: 2 anterior–posterior to the left mastoid, 2 contralateral *Intensity*: 2 mA *Current*: alternating (0.75 Hz)	*Number*: 1 *Duration*: 4-s cycles 5 s after endogenous slow-oscillations *Period*: daytime nap N2 or N3	*Waves:* slow oscillations (0.75 Hz), fast spindle (12–15 Hz), slow spindle (9–12 Hz) *Parameters:* PSD	*Stimulation-free intervals:* increased slow oscillations at Fz, Fp1, FP2, F7, FC1 by active vs. sham.	NA
Del Felice et al. (65)	12 with temporal lobe epilepsia (34.2 ± 15.4 age, 8F) 1 active arm, 1 sham arm 1-week washout	*Electrodes*: 0.8 cm^2 *Anodes*: affected temporal lobe (F7-T3 or F8-T8) *Cathode*: ipsilateral mastoid *Intensity*: 0.25 mA *Current*: alternating (0.75 Hz)	*Number*: 1 *Duration*: 30 min (5-min cycles with 1-min free intervals) *Period*: daytime before nap	*Waves:* slow spindle (10–12 Hz), fast spindle (12–14 Hz) *Parameters:* PSD	*Entire post-stimulation sleep period:* increased slow spindle power at all electrodes by active vs. sham.	NA
Eggert et al. (51)	23 healthy (69.3 ± 8.0 years; 14F) 1 active arm, 1 sham arm 1-week washout	*Electrodes*: NA *Anodes*: 2, DLPFC (F3, F4) *Cathodes:* 2 extra-cerebral (bilateral mastoids) *Intensity*: 0.33 mA/cm^2 *Current*: alternating (0.75 Hz)	*Number*: 1 *Duration*: five 5/16-min cycles with 1-min free intervals *Period*: after night N3 onset	*Waves*: slow oscillation (0.5–1 Hz), delta (1–4 Hz), theta (4–8 Hz), alpha (8–11 Hz), slow spindle (11–13 Hz), fast spindle (13–15 Hz), beta (15–25 Hz) *Parameters:* PSD	*Stimulation-free intervals:* decreased delta power at F7 and T3 electrodes by active vs. sham *60-min post-stimulation interval*: no significant results *Entire night*: no significant results	NA

(Continued)

TABLE 1 | Continued

References	Design	tES montage	tES sessions	Outcomes	Significant findings	Side effects
Frase et al. (52)	19 healthy (53.7 ± 6.9 age, 13F) 1 anodal-active arm; 1 cathodal-active arm; 1 sham arm 1-week washout	*Electrodes*: 35 cm^2 (anode), 100 cm^2 (cathode) *Anodal-active arm:* *Anode*: 2 supraorbital areas (Fp1, Fp2) *Cathode*: 2 parietal (P3, P4) *Cathodal-active arm:* *Cathode*: 2 supraorbital areas (Fp1, Fp2) *Anode*: 2 parietal (P3, P4) *Intensity*: 2 mA *Current*: direct	*Number*: 2 with 20-min inter-stimulation interval *Duration*: 13 min (anodal), 9 min (cathodal) *Period*: daytime before night sleep	*Waves*: delta (0.1–3.5 Hz), theta (3.5–8 Hz), alpha (8–12 Hz), sigma (12–16 Hz), beta (16–24 Hz), gamma (24–50 Hz) *Parameters:* PSD	*NREM night sleep*: increased beta power at C3-A2 electrodes by active cathodal (vs. anodal and sham) during first quarter of the night. *5-min interval after stimulation night*: increased gamma power at C3-A2 electrodes by anodal (vs. cathodal), decrease gamma power at C3-A2 electrodes after cathodal (vs. sham and anodal) *5-min interval 24 h after stimulation night*: increased gamma power C3-A2 electrodes by anodal (vs. cathodal).	NA
Frase et al. (66)	19 insomnia disorder (43.8 ± 15.1 age, 13F) 1 anodal-active arm; 1 cathodal-active arm; 1 sham arm 1-week washout				*N1-N4 night sleep*: decreased delta power at Fz electrodes by anodal vs. sham and cathodal vs. sham. *5-min interval after stimulation night*: no significant changes *5-min interval 24 h after stimulation night*: no significant changes	NA
Johnson and Durrant (45)	15 healthy (20.7 ± 0.3 age, 10F) 1 5 Hz active arm; 1 0.75 Hz active arm; 1 sham arm 2-day washout	*Electrodes*: 2.5 cm^2 (cathode), 24 cm^2 (anode) *Cathode*: right DLPFC F4 *Anode*: extra-cranial *Intensity*: 0.4-mA *Current:* alternating (5 Hz or 0.75 Hz)	*Number*: 1 *Duration*: 25 min *Period*: 4 min after night REM sleep onset	*Waves*: slow activity (0.5–2 Hz), theta (4–8 Hz) *Parameters:* PSD	*Slow wave and REM night sleep:* no significant changes.	NA
Ketz et al. (54)	16 healthy (22.3 ± 5.0 age, 3F) 1 active arm, 1 sham arm 1-week washout	*Electrodes*: NA *Anodes*: 2, DLPFC (F3, F4) *Cathodes:* 2 extra-cerebral (bilateral mastoids) *Intensity*: 1.5 mA *Current*: alternating (0.5–1.2 Hz)	*Number*: 1 *Duration*: periods of 5 slow-wave cycles throughout the night *Period*: 4 min after N2 sleep onset, during slow oscillations	*Waves:* slow oscillations (0.5–1.2 Hz) *Parameters:* PSD, PAC	*10-s post-stimulation interval:* increased (+3–4 s) then decreased (+4–10 s) slow oscillation power, and increased coupling with spindle amplitude of slow oscillations at all electrodes by active vs. sham	NA
Koo et al. (55)	25 healthy (22.4 ± 2.1 15F) 1 active arm, 1 sham arm, 1-week washout	*Electrodes*: 0.5 cm^2 *Anodes*: 2, DLPFC (F3, F4) *Cathodes:* 2 extra-cerebral (bilateral mastoids) *Intensity*: NA *Type*: alternating 0.84 Hz	*Number*: 1 *Duration*: 30 min (5-min cycles with 1-min free intervals) *Period*: during N2	*Waves:* slow oscillation (0.5–1.5 Hz), delta (1.5–4 Hz), theta (4–8 Hz), slow spindle (9–12 Hz), fast spindle (12–15 Hz). *Parameters:* PSD, length	*Stimulation-free intervals:* no significant differences *150-min post-stimulation interval*: increased fast spindle PSD and length at C and P electrodes by active vs. sham	NA

(Continued)

TABLE 1 | Continued

References	Design	tES montage	tES sessions	Outcomes	Significant findings	Side effects
Ladenbauer et al. (67)	16 mild cognitive impairment (70.6 ± 8.9 age, 7F) 1 active arm, 1 sham arm, 2-week washout	*Electrodes*: 0.5 cm^2 *Anodes*: 2, DLPFC (F3, F4) *Cathodes:* 2 extra-cerebral (bilateral mastoids) *Intensity*: 0.52 mA/cm^2 *Type*: alternating 84 Hz	*Number*: 1 *Duration*: 30 min (5-min cycles with 100-s free intervals) *Period*: during N2	*Waves:* slow oscillation (0.5–1.5 Hz), slow spindle (8–12 Hz), fast spindle (12–15 Hz). *Parameters:* PSD	*Stimulation-free intervals:* increased slow oscillation and fast spindle at C and P electrode by active vs. sham. *Stimulation intervals*: coupling of slow oscillation up-phases with fast spindle at F, C, and P electrodes by active vs. sham.	NA
Lustenberger et al. (47)	15 healthy males 1 active arm, 1 sham arm	*Electrodes*: 35 cm^2 *Anode*: 1 left DLPFC (F3) *Cathode*: 1 right DLPFC (F4) *Intensity*: 0.16 mA/cm^2 *Current:* alternating 12 Hz	*Number*: 1 *Duration*: cycles of a few seconds only when spindle activity (11–16 Hz) is prevailing *Period*: night N2/N3	*Waves*: delta (1–4 Hz), theta (4–8 Hz), fast spindle (11–16 Hz) *Parameters:* PSD	*Stimulation-free intervals:* increased spindle power, decreased delta and theta power at all electrodes by active vs. sham	1 in the active group (first-degree burn)
Marshall et al. (58)	18 healthy (19–28 age) 1 active arm, 1 sham arm 1-week washout	*Electrodes*: 0.5 cm^2 *Anodes*: 2 anterior–posterior to the left DLPFC (C3), 2 contralateral *Cathode*: 2 anterior–posterior to the left mastoid, 2 contralateral *Intensity*: 0.26 mA/cm^2 *Current*: direct	*Number*: 1 *Duration*: 30 min (sixty 15-s stimulation alternating with sixty 15-s free intervals) *Period*: 30 s after night N3 or N4 onset	*Waves:* slow oscillation (0.5–1 Hz), delta (1–4 Hz), theta (4–8 Hz), alpha (8–12 Hz), fast spindle (12–15 Hz), beta (20–25 Hz) *Parameters:* PSD	*Stimulation-free intervals:* increased slow-oscillations at P electrode and delta at F and P electrodes by active vs. sham *N2:* no significant changes *N3-N4*: decreased theta, alpha, and beta at C, F, and P by active vs. sham	NA
Marshall et al. (56)	13 healthy 1 active arm, 1 sham arm 10 week washout	*Electrodes*: 0.5 cm^2 *Anodes*: 2 anterior–posterior to the left DLPFC (C3), 2 contralateral *Cathode*: 2 anterior–posterior to the left mastoid, 2 contralateral *Intensity*: 0.52 mA/cm^2 *Current*: alternating (0.75 Hz)	*Number*: 1 *Duration*: 30 min (5-min cycles with 1-min free intervals) *Period*: 4 min after night N2 onset	*Waves:* slow oscillation (0.5–1 Hz), delta (1–4 Hz), slow spindle (8–12 Hz), fast spindle (12–15 Hz) *Parameters:* PSD	*Stimulation-free intervals:* increased slow oscillations (power) and slow spindle PSD at Fz by active vs. sham	NA
Marshall et al. (57)	25 healthy (18–35 age) 1 N2-active arm, 1 REM-active arm, 1 sham arm 10-day washout	*Electrodes*: 0.5 cm^2 *Anodes*: 2 anterior–posterior to the left DLPFC (C3), 2 contralateral *Cathode*: 2 anterior–posterior to the left mastoid, 2 contralateral *Intensity*: 0.52 mA/cm^2 *Current*: alternating (5 Hz)	*Number*: 1 *Duration*: 30 min (5-min cycles with 1-min free intervals) *Period*: 4 min after night N2 or REM onset	*Waves:* slow oscillation (0.5–1 Hz), delta (1–4 Hz), theta (4–8 Hz), slow spindle (8–12 Hz), fast spindle (12–15 Hz), beta (12–25 Hz), gamma (25–45 Hz) *Parameters:* PSD	*Stimulation-free intervals:* decreased slow oscillations and delta power at C, F, and P electrodes, and decreased slow spindles power at Fz by N2-active vs. sham; increased gamma power at C, F, and P during REM-active vs. sham *First 30-min post-stimulation interval:* increased slow oscillations power at C, F, and P and increased slow spindles power at Fz electrode during by N2 active vs. sham; *Second 30-min post-stimulation interval*: no significant results	NA

(Continued)

TABLE 1 | Continued

References	Design	tES montage	tES sessions	Outcomes	Significant findings	Side effects
Munz et al. (68)	14 ADHD (12.3 ± 1.4 age) 1 active arm, 1 sham arm, 1-week washout	*Electrodes*: 0.5 cm^2 *Anodes*: 2, DLPFC (F3, F4) *Cathodes:* 2 extra-cerebral (bilateral mastoids) *Intensity*: 0.52 mA/cm^2 *Type*: alternating 0.75 Hz	*Number*: 1 *Duration*: 30 min (5-min cycles with 1-min free intervals) *Period*: 4 min after N2 onset	*Waves*: slow oscillations *Parameters:* PSD	*Stimulation-free intervals:* increased slow oscillations power at all electrodes by active vs. sham. *60-min post-stimulation interval*: no significant results	NA
Passman et al. (59)	21 healthy (65.0 ± 1.0 age, 10F) 1 active arm, 1 sham arm, 2/3-week washout	*Electrodes*: 0.5 cm^2 *Anodes*: 2, DLPFC (F3, F4) *Cathodes:* 2 extra-cerebral (bilateral mastoids) *Intensity*: 0.52 mA/cm^2 *Type*: alternating 0.75 Hz	*Number*: 1 *Duration*: 30 min (5-min cycles with 1-min free intervals) *Period*: 4 min after N2 onset	*Waves*: slow oscillation (0.5–1 Hz), slow spindle (8–12 Hz), fast spindle (12–15 Hz) *Parameters:* PSD	*Stimulation-free intervals:* increased slow oscillations and slow spindle power at F electrodes; increased fast spindle power at C and P electrodes by active vs. sham. *1 min after 60-min post-stimulation interval*: increased slow oscillations power at F electrodes,	NA
Reato et al. (60)	*Active arm*: 13 healthy, *Sham arm*: 10 healthy	*Electrodes*: NA *Anodes*: 2, DLPFC (F3, F4) *Cathodes:* 2 extra-cerebral (bilateral mastoids) *Intensity*: 0.26 mA *Current*: alternating (0.75 Hz)	*Number*: 1 *Duration*: 30 min (5-min cycles with 1-min free intervals) *Period*: night N2 or N3	*Waves:* slow oscillations (0.5–1 Hz), slow activity (0.5–4 Hz) *Parameters:* PSD, spatial coherence	*Entire post-stimulation sleep period*: increased (reduced normal decrease) slow oscillations and slow activity (PSD and spatial coherence) at all electrodes by active vs. sham	NA
Saebipour et al. (70)	6 insomnia (34 ± 7 age, 2F) 1 active arm, 1 sham arm, 1-day washout	*Electrodes*: 0.5 cm^2 *Anodes*: 2, DLPFC (F3, F4) *Cathodes:* 2 extra-cerebral (bilateral mastoids) *Intensity*: NA *Type*: alternating 0.75 Hz	*Number*: 1 *Duration*: 30 min (5-min cycles with 1-min free intervals) *Period*: 4 min after N2 onset	*Waves*: slow oscillation (0.1–1 Hz) *Parameters:* PSD	*Stimulation-free intervals:* increased slow oscillation at C3 by active vs. sham Post-stimulation interval: increased probability of transition from N2 to N3, decreased probability of transition from N3 to wakefulness	NA
Sahlem et al. (61)	12 healthy (25.0 age, 9F) 1 active arm, 1 sham arm 1-day washout	*Electrodes*: 1.13 cm^2 *Anodes*: 2, DLPFC (F3, F4) *Cathodes:* 2 extra-cerebral (bilateral mastoids) *Intensity*: 0.6 mA *Current*: alternating (0.75 Hz squared)	*Number*: 1 *Duration*: 30 min (5-min cycles with 1-min free intervals) *Period:* 4 min after night N2 or N3 onset	*Waves*: slow oscillation (0.5–1 Hz), delta (1–4 Hz), theta (4–8 Hz) slow spindle (8–12 Hz), fast spindle (12–15 Hz), beta (15–25 Hz) *Parameters:* PSD	*Stimulation-free intervals:* no significant results *60-min post-stimulation interval*: no significant results	NA

(Continued)

TABLE 1 | Continued

References	Design	tES montage	tES sessions	Outcomes	Significant findings	Side effects
Venugopal et al. (62)	12 healthy (29.8 ± 6.2 age, 12M), 1 active-N2 arm, 1 active-REM arm 1-day washout	*Electrodes*: 4 cm^2 *Anodes*: 2, DLPFC (F3, F4) *Cathodes:* 2 extra-cerebral (bilateral mastoids) *Intensity*: 0.2 mA *Current*: alternating (0.75 Hz for active-N2, 40 Hz for active-REM protocol)	*Number*: 1 *Duration*: 15 min (four 30-s cycles with 3-min free intervals) *Period*: 1 min after night N2 or REM onset	EEG power before/after stimulation *Waves:* slow activity (0.5–4 Hz), theta (4–8 Hz), alpha (8–12 Hz), beta (12–30 Hz) *Parameters:* PSD	*30-s post-stimulation interval*: no significant changes	NA
Voss et al. (63)	27 healthy (18–26 age, 15F) 7 active and 7 corresponding sham conditions counter-balanced across 4 consecutive nights	*Electrodes*: 14 cm^2 *Anodes*: 2, DLPFC (F3, F4) *Cathodes:* 2 extra-cerebral (bilateral mastoids) *Intensity*: 0.25 mA *Current*: alternating (2, 6, 12, 25, 40, 70, or 100 Hz)	*Number*: 1 *Duration*: 30 s *Period*: 2 min after REM sleep onset	*Waves:* from 0 to 100 Hz *Parameters:* PSD	*Stimulation intervals:* no significant changes	NA
Westerberg et al. (64)	19 healthy (73.4 age, 16F) 1 active arm, 1 sham arm 1-week washout	*Electrodes*: 0.50-cm^2 *Anodes*: 2, DLPFC (F7, F8) *Cathodes:* 2 extra-cerebral (bilateral mastoids) *Intensity*: NA *Current*: alternating (0.75 Hz)	*Number*: 1 *Duration*: 30 min (5-min cycles with 1-min free intervals) *Period:* 4 min after daytime nap N2 or N3 onset	*Waves*: slow oscillation (0.5–1 Hz), delta (1–4.5 Hz), slow spindle (8.5–13.5 Hz), fast spindle (13.5–15.5 Hz) *Parameters:* PSD	*Stimulation-free intervals:* increased slow oscillations PSD at F electrodes; decreased fast spindle PSD at F electrodes by active vs. sham *60-min post-stimulation interval*: no significant results	NA

DLPFC, dorsolateral prefrontal cortex; NA, not available; NREM 1–4, Non-Rapid Eye Movement Sleep (four stages of non-rapid eye movement sleep, each progressively going into deeper sleep); REM, Rapid Eye Movement Sleep (unique stage of sleep characterized by random rapid movement of the eyes, low muscle tone throughout the body and propensity of the sleeper to dream vividly).

Sleep oscillations parameters: PAC (PAC), measure of the coupling between the phase of low-frequency rhythms and the amplitude of higher-frequency oscillations; Power Spectral Density (PSD), measure of frequency content (energy per unit time) vs. frequency; Length, reflects the full extension (ms) of the time-frequency bin on the time axis; Spatial coherence, correlation (or predictable relationship) between waves at different points in space.

opposite patterns of changes, i.e., decreased slow oscillations, delta, and slow spindle power by tES (57). In contrast, one experiment using a slow spindle-like alternating current (12 Hz) observed an increase of power after tES in this specific frequency range (47).

An increase in slow oscillations and spindle waves power by active tES against sham was mainly demonstrated by several studies during long intervals after both slow-wave (0.75 Hz) and theta (5 Hz) alternating NREM stimulation (46, 57, 59, 60). However, recordings during post-stimulation periods were highly heterogeneous in terms of intervals where oscillations were measured and averaged. Regarding per-stimulation recordings, a single study using specific filtering procedures demonstrated a significant coupling between NREM slow oscillations up-phases and spindle waves at parietal electrodes concomitant to active tES vs. sham (49). No significant changes in sleep oscillations were observed when taking into consideration the entire stimulation night (51). In parallel, some research groups stimulated the brain with slow alternating current during REM (rapid-eye movement sleep). An increase in gamma power during stimulation-free intervals was demonstrated (57), but no significant changes were reported during stimulation intervals and entire sleep periods (45, 63).

Two studies used a bifrontal tES montage involving direct stimulating current (52, 58). It was observed that direct cathodal stimulation during daytime before sleep increased beta power at central sites during the first NREM night sleep cycle vs. both anodal and sham stimulation. By contrast, anodal stimulation induced an increase in gamma band power after the stimulation night compared with the other stimulation conditions (52). In parallel, Marshall and colleagues demonstrated that direct tES concomitant to NREM increases delta power in stimulation-free intervals and decreases higher-frequency band power during post-stimulation periods of slow wave sleep (58). No long-term effects were investigated across studies.

Results From Studies in Clinical Populations

Six studies investigated the effect of a single brain tES session on oscillatory aspects of sleep in clinical populations. All were sham-controlled crossover trials. Two studies involved patients with insomnia disorder. Decreased NREM delta power after a single frontal anodal direct stimulation during daytime (66) and increased slow oscillation power during NREM stimulation-free intervals by alternating slow current vs. sham were observed in this population (70). In parallel, an increase of slow oscillation power during NREM stimulation-free intervals by alternating slow current vs. sham was reported in a group of patients with ADHD (Attention Deficit/Hyperactivity Disorder) (68). A similar tES montage also increased slow oscillations in patients with mild cognitive impairment, along with increased spindle power during NREM stimulation-free intervals (67). A three-arm study involving patients with fibromyalgia reported an increased alpha and decreased delta power after five sessions of frontal stimulation vs. sham and an increased delta power after five sessions of motor stimulation vs. sham (69). Finally, stimulation of the affected temporal lobe of patients with temporal lobe epilepsy before a nap induced an increase of slow spindle wave power (65).

Sleep Patterns

Study Designs and Characteristics

Twenty studies investigated the impact of tES on sleep patterns in healthy (45, 47, 49–52, 55–61, 63, 64) and clinical (65–70) populations. Studies explored tES-induced changes in patterns of sleep including continuity (e.g., total sleep time, sleep efficiency, wake after sleep onset, and sleep onset latency) and architecture (i.e., sleep stages relative duration—expressed as percentage of total sleep time—and latency). Study details are described in **Table 2**.

Results From Studies in Healthy Populations

Fourteen studies investigated the effect of a single brain tES session on sleep patterns in healthy samples (45, 47, 49–52, 55–61, 63, 64). All used a crossover sham-controlled design with days-to-week washout periods between conditions.

Most studies used the Marshall's bifrontal montage (58) with alternating current (49–51, 56–58, 64). Only a minority of studies reported significant results, and these were highly heterogeneous. Over the entire stimulation night, two reports demonstrated an increase in the relative duration of late NREM stages (N3, N4) by active stimulation vs. sham (50, 56). However, a study Passmann et al. found the opposite (59). One study observed a decreased relative duration of stage N1 (50). During stimulation-free intervals, an increased relative duration of stage N2 and wake after sleep onset was found, while later NREM stages were decreased (51, 57). During post-stimulation periods, two studies reported a decrease of N2 and N3 relative duration by active vs. sham (57, 61). A research group that explored the effect of the same montage during REM sleep—in order to trigger conscious awareness in dreams—reported no effect on sleep architecture (63). In parallel, a protocol using bifrontal tES reported a significant decrease of sleep efficiency over the entire stimulation night by alternating stimulation (0.75 Hz) as compared to sham and faster stimulation (5.0 Hz) during REM (45).

Regarding non-bifrontal montages, a single study studied the effect of direct current tES before sleep using fronto-parietal electrode placements (52). These authors reported decreased total sleep time and sleep efficiency when anodes were placed over the frontal cortex and cathodes over the parietal areas, in comparison to the reverse and sham montages. By contrast, REM relative duration was increased by frontal cathodal stimulation in comparison to anodal (52). Finally, a single session of tES during early NREM with the anode overlying the left prefrontal cortex and a contralateral cathode induced no significant changes in sleep architecture parameters of a healthy sample (47).

Results From Studies in Clinical Populations

Six studies investigated the effect of a single brain tES session on sleep patterns in clinical samples (65–70). Two crossover sham-controlled studies involved individuals with insomnia disorder. The first demonstrated that a single session of active bifrontal alternating current during early NREM decreases N1 and increases N3 relative duration in the post-stimulation

TABLE 2 | Impact of transcranial electrical stimulation on pattern aspects of sleep.

References	Sample and design	tES montage	tES sessions	Outcomes	Significant findings	Adverse effects
Placebo-controlled parallel-arms						
Roizenblatt et al. (69)	*Active frontal arm:* 11 fibromyalgia (47.3 ± 11.0 age, 11F) *Active motor arm:* 11 fibromyalgia (54.8 ± 9.3 age, 11F) *Sham arm*: 10 fibromyalgia (50.8 ± 10.2 age, 10F)	*Electrodes*: 25 cm^2 *Active frontal arm: Anode*: right primary motor area (C3), *Cathode:* left supraorbital area (Fp2) *Active motor arm: Anode*: left DLPFC (C3), *Cathode:* right supraorbital area (Fp1) *Intensity*: 2 mA *Type*: direct	*Number*: 5 *Frequency:* daily *Duration*: 20 min *Period*: 1 week	*Sleep continuity:* AI, SE, SOL, and TST *Sleep architecture:* N1, N2, N3, N4, REM relative duration	*Entire night after stimulation procedure:* decreased SE, increased SOL and increased REM relative duration by frontal-active vs. sham; increased SE, decreases arousals by motor-active vs. sham.	None reported
Lustenberger et al. (47)	16 healthy males 1 active arm, 1 sham arm	*Electrodes*: 35 cm^2 *Anode*: 1 left DLPFC (F3) *Cathode*: 1 right DLPFC (F4) *Intensity*: 4 mA *Current:* alternating 12 Hz	*Number*: 1 *Period*: during night N2 (spindle activity 11–16 Hz)	*Sleep continuity:* SE, SOL, TST, WASO *Sleep architecture:* N1, N2, N3, REM relative duration	*Entire night:* no significant changes.	NA
Placebo-controlled crossover						
Cellini et al. (50)	17 healthy (32.2 ± 8.1 age, 6F) 1 active arm, 1 sham arm 1-week washout	*Electrodes*: 0.8 cm^2 *Anodes*: 2 anterior–posterior to the left DLPFC (C3), 2 contralateral *Cathode*: 2 anterior–posterior to the left mastoid, 2 contralateral *Intensity*: 2 mA *Current*: alternating (0.75 Hz)	*Number*: 1 *Duration*: 4-s cycles 5 s after endogenous slow oscillations *Period*: night N2 or N3	*Sleep continuity:* SE, SOL, TST, WASO *Sleep architecture:* N1, N2, SWS (N3), REM relative duration	*Entire stimulation night*: increased N3 relative duration and decreased N1 relative duration by active vs. sham	NA
Del Felice et al. (65)	12 with temporal lobe epilepsia (34.2 ± 15.4 age, 8F) 1 active arm, 1 sham arm 1-week washout	*Electrodes*: 0.8 cm^2 *Anodes*: affected temporal lobe (F7-T3 or F8-T8) *Cathode*: ipsilateral mastoid *Intensity*: 0.25 mA *Current*: alternating (0.75 Hz)	*Number*: 1 *Duration*: 30 min (5-min cycles with 1-min free intervals) *Period*: daytime before nap	*Sleep continuity:* SOL, TST *Sleep architecture:* N1, N2, N3, REM relative duration	*Entire post-stimulation nap:* increased TST and decreased SOL by active vs. sham.	NA
Voss et al. (63)	27 healthy (18–26 age, 15F) 7 active and 7 corresponding sham conditions counter-balanced across 4 consecutive nights	*Electrodes*: 14 cm^2 *Anodes*: 2, DLPFC (F3, F4) *Cathodes:* 2 extra-cerebral (bilateral mastoids) *Intensity*: 0.25 mA *Current*: alternating (2, 6, 12, 25, 40, 70, or 100 Hz)	*Number*: 1 *Duration*: 30 s *Period*: 2 min after REM sleep onset	*Sleep continuity:* SE, SOL, TST, WASO *Sleep architecture:* N1, N2, SWS (N3), REM relative duration	*Entire stimulation night*: no significant changes.	NA
Marshall et al. (58)	18 healthy (19–28 age) 1 active arm, 1 sham arm 1-week washout	*Electrodes*: 0.5 cm^2 *Anodes*: 2 anterior–posterior to the left DLPFC (C3), 2 contralateral *Cathode*: 2 anterior–posterior to the left mastoid, 2 contralateral *Intensity*: 0.26 mA/cm^2 *Current*: direct	*Number*: 1 *Duration*: 30 min (sixty 15-s stimulation alternating with sixty 15-s free intervals) *Period*: 30-s after night N3 or N4 onset	*Sleep continuity:* TST, WASO *Sleep architecture:* N1, N2, SWS (N3+N4), REM relative duration; N2 and SWS latency	*Entire stimulation night*: no significant changes.	NA

(Continued)

TABLE 2 | Continued

References	Sample and design	tES montage	tES sessions	Outcomes	Significant findings	Adverse effects
Marshall et al. (56)	13 healthy 1 active arm, 1 sham arm 1-week washout	*Electrodes*: 0.5 cm^2 *Anodes*: 2 anterior–posterior to the left DLPFC (C3), 2 contralateral *Cathode*: 2 anterior–posterior to the left mastoid, 2 contralateral *Intensity*: 0.52 mA/cm^2 *Current*: alternating (0.75 Hz)	*Number*: 1 *Duration*: 30 min (5-min cycles with 1-min free intervals) *Period*: 4-min after night N2 onset	*Sleep continuity:* WASO *Sleep architecture:* N1, N2, SWS (N3+N4) relative duration	*Entire stimulation night*: increased SWS relative duration by 0.75-Hz active vs. sham.	NA
Marshall et al. (57)	25 healthy (18–35 age) 1 N2-active arm, 1 REM-active arm, 1 sham arm 10-day washout	*Electrodes*: 0.5 cm^2 *Anodes*: 2 anterior–posterior to the left DLPFC (C3), 2 contralateral *Cathode*: 2 anterior–posterior to the left mastoid, 2 contralateral *Intensity*: 0.52 mA/cm^2 *Current*: alternating (5 Hz)	*Number*: 1 *Duration*: 30 min (5-min cycles with 1-min free intervals) *Period*: 4 min after night N2 or REM onset	*Sleep continuity:* SOL, TST, WASO *Sleep architecture:* N1, N2, SWS (N3+N4), REM relative duration; SWS and REM latency	*Entire stimulation night*: increased SWS latency by N2-active vs. sham *Stimulation free intervals*: increased N2 relative duration, decreased SWS relative duration by N2-active vs. sham *30-min post-stimulation*: decreased N2 relative duration by N2-active vs. sham	NA
Antonenko et al. (49)	15 healthy (23.4 ± 1.9 age, 7F) 1 active arm, 1 sham arm 4-week washout	*Electrodes*: 0.8 cm^2 *Anodes*: 2, DLPFC (F3, F4) *Cathodes:* 2 extra-cerebral (bilateral mastoids) *Intensity*: 0.32 mA/cm^2 *Current*: alternating (0.75 Hz squared)	*Number*: 1 *Duration*: 30 min (4-min cycles with 1-min free intervals) *Period*: 4 min after night N2 or N3 onset	*Sleep continuity:* AI, SE, SOL, TST, WASO *Sleep architecture:* N1, N2, N3, N4, REM relative duration	*Entire stimulation night*: no significant changes	NA
Westerberg et al. (64)	19 healthy (73.4 age, 16F) 1 active arm, 1 sham arm 1-week washout	*Electrodes*: 0.50 cm^2 *Anodes*: 2, DLPFC (F7, F8) *Cathodes:* 2 extra-cerebral (bilateral mastoids) *Intensity*: NA *Current*: alternating (0.75 Hz)	*Number*: 1 *Duration*: 30 min (5-min cycles with 1-min free intervals) *Period:* 4 min after nap N2 or N3 onset	*Sleep continuity:* SE, SOL, WASO *Sleep architecture:* N1, N2, REM, SWS (N3+N4) relative duration	*Entire stimulation night*: no significant changes	NA
Eggert et al. (51)	23 healthy (69.3 ± 8.0 years; 14F) 1 active arm, 1 sham arm 1-week washout	*Electrodes*: NA *Anodes*: 2, DLPFC (F3, F4) *Cathodes:* 2 extra-cerebral (bilateral mastoids) *Intensity*: 0.33 mA/cm^2 *Current*: alternating (0.75 Hz)	*Number*: 1 *Duration*: five 5/16-min cycles with 1-min free intervals *Period*: early night N3	*Sleep continuity:* WASO *Sleep architecture:* N1, N2, SWS (N3+N4), REM relative duration	*Entire stimulation night*: no significant changes *Stimulation-free intervals*: increased WASO relative duration and decreased N3 relative duration by active vs. sham *60-min post-stimulation*: no significant changes	NA

(Continued)

TABLE 2 | Continued

References	Sample and design	tES montage	tES sessions	Outcomes	Significant findings	Adverse effects
Frase et al. (52)	19 healthy (53.7 ± 6.9 age, 13F) 1 anodal-active arm; 1 cathodal-active arm; 1 sham arm 1-week washout	*Electrodes*: 35 cm^2 (anode), 100 cm^2 (cathode) *Anodal-active arm: Anode*: 2 supraorbital areas (Fp1, Fp2), *Cathode*: 2 parietal (P3, P4) *Cathodal-active arm: Cathode*: 2 supraorbital areas (Fp1, Fp2), *Anode*: 2 parietal (P3, P4) *Intensity*: 2 mA *Current*: direct	*Number*: 2 with 20-min inter-stimulation interval *Duration*: 10 min *Period*: day before night sleep	*Sleep continuity:* AI, SE, SOL, TST, WASO *Sleep architecture:* N2, SWS (N3), REM relative duration; REM latency, REM cycles,	*Entire stimulation night*: decreased SE and TST; increased WASO relative duration by anodal-active (vs. cathodal-active and sham); increased REM relative duration by cathodal-active (vs. sham)	NA
Johnson and Durrnt (45)	15 healthy (20.7 ± 0.3 age, 10F) 1.5 Hz active arm; 1 0.75 Hz active arm; 1 sham arm 2-day washout	*Electrodes*: 2.5 cm^2 (cathode), 24 cm^2 (anode) *Cathode*: right DLPFC F4 *Anode*: extra-cranial *Intensity*: 0.4 mA *Current:* alternating (5 Hz or 0.75 Hz)	*Number*: 1 *Duration*: 25 min *Period*: 4 min after night REM sleep onset	*Sleep continuity:* SE, TST *Sleep architecture:* N1, N2, SWS, REM relative duration	*Entire stimulation night:* decreased SE by 0.75 Hz active (vs. 5 Hz active and sham)	None reported
Sahlem et al. (61)	12 healthy (25.0 age, 9F) 1 active arm, 1 sham arm 1-week washout	*Electrodes*: 1.13 cm^2 *Anodes*: 2, DLPFC (F3, F4) *Cathodes:* 2 extra-cerebral (bilateral mastoids) *Intensity*: 0.6 mA *Current*: alternating (0.75 Hz squared)	*Number*: 1 *Duration*: 30 min (5-min cycles with 1-min free intervals) *Period:* 4 min after N2 or N3 onset	*Sleep continuity:* SE, TST *Sleep architecture:* N1, N2, SWS (N3+N4), REM relative duration	*Entire stimulation night:* no significant results *60-min post-stimulation:* decreased N2, N3 by active vs. sham	NA
Passmann et al. (59)	21 healthy (65.0 ± 1.0 age, 10F) 1 active arm, 1 sham arm, 2/3-week washout	*Electrodes*: 0.5 cm^2 *Anodes*: 2, DLPFC (F3, F4) *Cathodes:* 2 extra-cerebral (bilateral mastoids) *Intensity*: 0.52 mA/cm^2 *Type*: alternating 0.75 Hz	*Number*: 1 *Duration*: 30 min (5-min cycles with 1-min free intervals) *Period*: 4 min after N2 onset	*Sleep continuity:* WASO *Sleep architecture:* N1, N2, SWS (N3+N4), REM relative duration	*Entire stimulation night*: decreased N4 by active vs. sham *Stimulation-free intervals*: no significant changes *60-min post-stimulation*: no significant changes	NA
Koo et al. (55)	25 healthy (22.4 ± 2.1 15F) 1 active arm, 1 sham arm, 1-week washout	*Electrodes*: 0.5 cm^2 *Anodes*: 2, DLPFC (F3, F4) *Cathodes:* 2 extra-cerebral (bilateral mastoids) *Intensity*: NA *Type*: alternating 84 Hz	*Number*: 1 *Duration*: 30 min (5-min cycles with 1-min free intervals) *Period*: during N2	*Sleep continuity:* SE, SOL, TST, TMT, WASO *Sleep architecture:* N1, N2, N3, REM relative duration; REM latency	*Entire stimulation night*: no significant changes	NA
Koo et al. (67)	6 mild cognitive impairment (71.9 ± 9.0 age, 7F) 1 active arm, 1 sham arm, 2-week washout	*Electrodes*: 0.5 cm^2 *Anodes*: 2, DLPFC (F3, F4) *Cathodes:* 2 extra-cerebral (bilateral mastoids) *Intensity*: 0.52 mA/cm^2 *Type*: alternating 84 Hz	*Number*: 1 *Duration*: 30 min (5-min cycles with 100-s free intervals) *Period*: during N2	*Sleep continuity:* WASO *Sleep architecture:* N1, N2, N3, N4, REM relative duration	*Entire stimulation night*: no significant changes *Stimulation-free intervals*: Increased N2 by active vs. sham	NA

(Continued)

TABLE 2 | Continued

References	Sample and design	tES montage	tES sessions	Outcomes	Significant findings	Adverse effects
Saebipour et al. (70)	6 insomnia (34 ± 7 age, 2F) 1 active arm, 1 sham arm, 1-day washout	*Electrodes*: 0.5 cm^2 *Anodes*: 2, DLPFC (F3, F4) *Cathodes:* 2 extra-cerebral (bilateral mastoids) *Intensity*: NA *Intensity*: alternating 0.75 Hz	*Number*: 1 *Duration*: 30 min (5-min cycles with 1-min free intervals) *Period*: 4 min after N2 onset	*Sleep continuity:* SOL, TST, WASO *Sleep architecture:* N1, N2, N3, REM relative duration	*Entire night after stimulation:* increased probability of transition from N2 to N3, decreased probability of transition from N3 to wakefulness *90-min post-stimulation*: decreased N1 and increased N3 by active vs. sham	
Munz et al. (68)	14 ADHD (12.3 ± 1.4 age) 1 active arm, 1 sham arm, 1-week washout	*Electrodes*: 0.5 cm^2 *Anodes*: 2, DLPFC (F3, F4) *Cathodes:* 2 extra-cerebral (bilateral mastoids) *Intensity*: 0.52 mA/cm^2 *Type*: alternating 0.75 Hz	*Number*: 1 *Duration*: 30 min (5-min cycles with 1-min free intervals) *Period*: 4 min after N2 onset	*Sleep continuity:* SE, TST, *Sleep architecture:* N1, N2, SWS (N3+N4), REM relative duration	*Entire night:* no significant changes	NA
Frase et al. (66)	19 insomnia disorder (43.8 ± 15.1 age, 13F) 1 anodal-active arm; 1 cathodal-active arm; 1 sham arm 1-week washout	*Electrodes*: 35 cm^2 (anode), 100 cm^2 (cathode) *Anodal-active arm: Anode*: 2 supraorbital areas (Fp1, Fp2), *Cathode*: 2 parietal (P3, P4) *Cathodal-active arm: Cathode*: 2 supraorbital areas (Fp1, Fp2), *Anode*: 2 parietal (P3, P4) *Intensity*: 2 mA *Current*: direct	*Number*: 2 with 20-min inter-stimulation interval *Duration*: 25 min *Period*: day before night sleep	*Sleep continuity:* Arousal Index, SE, SOL, TST, WASO *Sleep architecture:* N2, SWS (N3), REM relative duration; REM latency, REM cycles,	*Entire stimulation night:* no significant changes	NA

DLPFC, dorsolateral prefrontal cortex.

Sleep architecture: NREM 1–4, Non-Rapid Eye Movement Sleep (four stages of non-rapid eye movement sleep, each progressively going into deeper sleep); REM, Rapid Eye Movement Sleep (unique stage of sleep characterized by random rapid movement of the eyes, low muscle tone throughout the body and propensity of the sleeper to dream vividly).

Sleep architecture (stages) parameters: relative duration, sleep stage proportion during total sleep time (%); latency, time taken for sleep stage onset (minutes); cycles, number of sleep stage occurrence during total sleep time (number count).

Sleep continuity: AI, Arousal Index (number of arousals and awakenings per hour of sleep, in number count); SE, Sleep Efficiency (total time in bed divided by total sleep time in %); SOL, Sleep Onset Latency (time taken for sleep onset in minutes); SWS, Slow Wave Sleep (consists of NREM 3 or NREM 3+4); TST, Total Sleep Time (total time spent asleep in minutes); WASO, Wave After Sleep Onset (time spent awake after sleep onset per night in minutes).

periods as compared to sham (70). The second study showed no significant changes in sleep patterns across the entire night after two fronto-parietal direct current tES sessions during daytime (66). In parallel, a crossover sham-controlled study that gave a single session of bifrontal active alternating current in subjects with ADHD failed to demonstrate significant changes across the entire stimulation night (68). By contrast, a research group that used the same protocol in six elder subjects with mild cognitive impairment found an increase of N2 relative duration during stimulation-free intervals (67). A three-arm study involving participants with fibromyalgia observed a significant sham-controlled effect of five consecutive direct current tES sessions that was specific to the stimulation site, such as anodal stimulation of the left primary motor area increased sleep efficiency and decreased number of arousals, whereas anodal stimulation of the left prefrontal cortex was associated with an increase of sleep latency and REM relative duration, and a decrease in sleep efficiency (69). Finally, a protocol stimulating the affected temporal lobe of patients with temporal lobe epilepsy before a nap demonstrated a significant increase of total sleep time and decrease of sleep onset latency by active vs. sham stimulation (65).

Subjective Assessments of Sleep

Study Designs and Characteristics

Fifteen studies investigated the impact of tES on subjective aspects of sleep in healthy (45, 52, 71–73) and clinical samples (41–44, 46, 48, 66, 74–81). Most used parallel arms (45, 52, 66, 72) or crossover-controlled designs (41–43, 46, 71, 73, 74, 78, 80, 81). The others were uncontrolled series or case reports. Studies details are described in **Table 3**.

Results From Studies in Healthy Population

Five studies investigated the impact of a single tES session during wake periods on the subjective sleep parameters in healthy groups. One that used high-definition direct current tES targeting the left prefrontal cortex in elders observed an increase in subjective sleep duration and sleep efficiency in the active group vs. a waiting list group (73). Similarly, a crossover study that tested slow alternating tES during sleep found higher sleep quality and efficiency after active vs. sham stimulation (72). A study that specifically investigated frontal stimulation in athletes observed a global improvement in subjective sleep after two consecutive active stimulation sessions in comparison to a group that received sham stimulations (71). Finally, no significant changes were observed in sleepiness scales neither after two frontal tES sessions during daytime (52) nor during REM sleep (45).

Results From Studies in Clinical Populations

All studies used direct current tES (tDCS). Parkinson's disease was the most represented neuropsychiatric disorder. A crossover placebo-controlled trial investigated the effect of 10 consecutive days of tDCS treatment on non-motor symptoms (80). No significant differences between groups were seen in the Epworth Sleepiness Scale (ESS) at week 2 and week 14 following treatment. Similarly, a sham-controlled study that gave eight bifrontal tES sessions reported no significant changes in the Epworth Sleepiness Scale both after the procedure and at long term (74). An uncontrolled study reported an absence of significant effects on the PROMIS^{TM} sleep assessment after 10 sessions of bifrontal tDCS (transcranial direct current stimulation) (44). By contrast, another study observed a significant improvement of the Pittsburgh Sleep Quality Index (PSQI) sleep latency subscore and total score after 10 sessions of a tDCS montage involving two anodes placed between the primary motor area and the prefrontal cortex, and two cathodes placed over the supraorbital areas (77).

In parallel, a single placebo-controlled trial in individuals with post-polio syndrome observed a significant PSQI improvement after 15 consecutive sessions of tDCS with two anodes targeting primary motor areas (41). Besides, studies exploring the impact of tDCS targeting the inferior frontal cortex in HIV patients (43) and targeting the motor areas in patients with restless legs syndrome (46) and chronic pain associated with insomnia (78) yielded negative results.

Regarding mood disorders, a non-controlled tDCS protocol placing the anode over the prefrontal cortex and the cathode over the cerebellum significantly improved sleep quality with 46% improvement of the PSQI in a sample of euthymic patients with bipolar disorder (79). In contrast, no effect of bifrontal tDCS was observed on the sleep item of the Montgomery–Asberg Depression Rating Scale (MADRS) in a randomized controlled trial involving participants with depression (42).

No significant changes were reported for subjective parameters including tiredness and alertness in a crossover study involving two bifrontal tES sessions in patients with insomnia disorder (66). By contrast, a recent randomized placebo-controlled trial demonstrated that 20 daily consecutive sessions of frontal tES with alternating current significantly improved PSQI both after the procedure and at 2 months follow-up (81).

A case series of idiopathic hypersomnia showed that 4 weeks of bifrontal tDCS can reduce excessive daytime sleepiness, as assessed by the ESS (76). Finally, case reports observed daytime vigilance and sleep quality improvement using specific rating scales in organic hypersomnia (75) and after-stroke condition (48), respectively.

DISCUSSION

Through this systematic literature review, we observe that tES can modify endogenous brain oscillations during sleep and that subjective assessments show clear improvements after tES, while relationships with concomitant changes in sleep architecture warrant validations (see **Figure 2** and **Supplementary Table 2** for a summary of main results). Tolerability profile of tES appears good with few non-severe side effects reported across studies.

tES During Sleep Can Be Effective at Modulating Endogenous Oscillations

The main neurophysiological finding of our systematic review is that anodal tES of the frontal areas with a slow alternating or direct current during NREM sleep can immediately enhance the

TABLE 3 | Impact of transcranial electrical stimulation on subjective aspects of sleep.

References	Design	tES montage	tES sessions	Outcomes	Significant findings	Adverse effects
Placebo-controlled crossover						
Robinson et al. (72)	21 healthy (20.1, 7F) 1 active anodal arm; 1 sham arm 1-week washout	*Electrodes*: 4 cm^2 *Anode*: F10 (wake), F3 or F4 (N2/N3 sleep) *Cathode*: extra-cerebral *Intensity*: 2 mA *Current*: alternating	*Number*: 2 (1 wake, 1 sleep) *Duration*: 30 min *Period*: 1 day	KSD	KSD sleep efficiency and sleep quality improvement by active vs. sham at day 1	NA
Johnson and Durrant (45)	15 healthy (20.7 ± 0.3 age, 10F) Active 5-Hz arm Active 0.75-Hz arm Sham arm	*Electrodes*: 2.5 cm^2 (cathode), 24 cm^2 (anode) *Cathode*: right DLPFC F4 *Anode*: extra-cranial *Intensity*: 0.4 mA *Current:* alternating (5 Hz or 0.75 Hz)	*Number*: 2 with 20-min inter-stimulation interval *Duration*: 25 min *Period*: during REM sleep	SSS	No significant changes at day 1	1 in the active group (first-degree burn)
Frase et al. (52, 66)	19 healthy (53.7 ± 6.9 age, 13F) 1 active anodal arm; 1 active cathodal arm; 1 sham arm 1-week washout	*Electrodes*: 35 cm^2 (anode), 100 cm^2 (cathode) *Active anodal arm:* *Anode*: 2 supraorbital areas (Fp1, Fp2) *Cathode*: 2 parietal (P3, P4) *Active cathodal arm:* *Cathode*: 2 supraorbital areas (Fp1, Fp2) *Anode*: 2 parietal (P3, P4) *Intensity*: 2 mA *Current*: direct	*Number*: 2 with 20-min inter-stimulation interval *Duration*: 20 min *Period*: day before sleep	Subjective sleep parameters/tiredness (VIS-M) and alertness (TAP).	No significant changes at day 3	NA
	19 insomnia disorder (43.8 ± 15.1 age, 13F) 1 active anodal arm; 1 active cathodal arm; 1 sham arm 1-week washout					
Placebo-controlled parallel-arms						
Wang et al. (81)	*Active arm:* 31 insomnia disorder (52.5 ± 10.7 age, 24F) *Sham arm:* 31 insomnia disorder (55.3 ± 8.0 age, 23F)	*Electrodes*: anode (42.4 cm^2), cathode (12.1 cm^2) *Anode*: Fpz *Cathode*: 2, mastoids *Intensity*: 15 mA *Current:* alternating (77.5 Hz)	*Number*: 20 *Frequency:* daily *Duration*: 40 min *Period*: 4 weeks	PSQI	PSQI improvement by active vs. sham at both week 4 and week 8 Daily disturbance improvement by active vs. sham at week 8	None reported
Charest et al. (71)	*Active arm:* 15 healthy athletes (22.1 ± 1.8 age, 7F) *Sham arm:* 15 healthy athletes (20.1 ± 2.0 age, 8F)	*Electrodes*: 35 cm^2 *Anode*: (FPz) *Cathode*: (Pz) *Intensity*: 2 mA *Current*: direct	*Number*: 2 *Frequency:* daily *Duration*: 20 min *Period*: 2 days	PSQI ESS ISI ASSQ	PSQI, ISI, and ASSQ improvement by active vs. sham at week 2	NA
Sheng et al. (73)	*Active arm:* 16 healthy (67.6 ± 4.7 age, 9F) *Waiting-list*: 15 healthy (65.8 ± 5.2 age, 10F)	*Electrodes*: High definition *Anode*: left DLPFC (F3) *Cathode*: 4 at 7-cm radius *Intensity*: 1.5 mA *Current*: direct	*Number*: 10 *Frequency:* daily *Duration*: 25 min *Period*: 2 weeks	PSQI	PSQI sleep duration and PSQI sleep efficiency improvement by active vs. sham at week 2	NA

(Continued)

TABLE 3 | Continued

References	Design	tES montage	tES sessions	Outcomes	Significant findings	Adverse effects
Cody et al. (43)	*Active arm:* 17 HIV (56.0 ± 3.2 age, 6F) *Sham arm*: 16 HIV (55.6 ± 5.4 age, 5F)	*Electrodes*: 4 cm^2 *Anode*: 1 inferior frontal cortex (F10) *Cathode*: 1 extra-cranial *Intensity*: 2 mA *Current*: direct	*Number*: 15 *Frequency:* every 2–3 days *Duration*: 20 min *Period*: 5 weeks	PSQI	No significant changes at week 5	1 in the active group (first-degree burn)
Acler et al. (41)	*Active arm:* 16 post-polio syndrome *Sham arm*: 16 post-polio syndrome	*Electrodes*: 35 cm^2 *Anodes*: 1 right premotor cortex (C4), 1 left premotor cortex (C3) *Cathode*: 1 extra-cranial *Intensity*: 1.5 mA *Current*: direct	*Number*: 15 *Frequency:* daily *Duration*: 15 min *Period*: 3 weeks	PSQI	PSQI total improvement by active vs. sham at week 3	1 in the active group (dizziness)
Forogh et al. (74)	*Active arm:* 12 Parkinson disease (61.3 age, 7F) *Sham arm*: 11 Parkinson disease (64.8 age, 7F) 14	*Electrodes*: 35 cm^2 *Anode*: 1 left DLPFC (F3) *Cathode*: 1 right DLPFC (F4) *Intensity*: 4 mA *Current*: direct	*Number*: 8 *Frequency:* every 1–2 days *Duration*: NA *Period*: 2-weeks	ESS	No significant changes at week 5 and month 3	NA
Harvey et al. (78)	*Active arm:* 6 insomnia disorder (71.0 ± 7.0 age, 11F) *Sham arm*: 8 insomnia disorder (71.0 ± 8.0 age, 6F)	*Electrodes*: 35-cm^2 *Anode*: primary motor area contralateral to the most painful site (C3/C4) *Cathode*: supraorbital area contralateral to the anode *Intensity*: 2 mA *Current*: direct	*Number*: 5 *Frequency:* daily *Duration*: 20 min *Period*: 1 week	PSQI	No significant changes at week 1 and week 2	None reported
Koo et al. (46)	*Active cathodal arm:* 10 restless legs syndrome (47.3 ± 11.0 age) *Active anodal arm:* 10 restless legs syndrome (44.1 ± 13.4 age) *Sham arm*: 11 restless legs syndrome (46.0 ± 10.1 age)	*Electrodes*: 25 cm^2 *Active anodal arm: anode*: primary motor area (Cz), *cathode*: extra-cerebral *Active cathodal arm: anode*: extra-cerebral, *cathode*: primary motor area (Cz) *Intensity*: 2 mA *Current*: direct	*Number*: 5 *Frequency:* daily *Duration*: 20 min *Period*: 1 week	PSQI	No significant changes at week 1 and week 2	13 transient but no significant differences between groups
Shill et al. (80)	*Active arm:* 12 Parkinson disease *Sham arm*: 11 Parkinson disease	*Electrodes*: NA *Anodes*: 2 prefrontal areas *Cathodes*: 2 mastoids *Intensity*: 1.5 mA *Current*: direct	*Number*: 10 *Frequency:* daily *Duration*: 45 min *Period*: 2 weeks	ESS	No significant changes at weeks 2, 6, 10 and 14	None
Brunoni et al. (42)	*Sham-tDCS/placebo-pill arm:* 30 depression (46.4 ± 14.0 age, 20F) *Sham-tDCS/sertraline arm:* 30 depression (41.0 ± 12.0 age, 17F *Active-tDCS/placebo-pill arm:* 30 depression (41.0 ± 12.0 age, 21F) *Sertraline-pill arm:* 30 depression (41.0 ± 13.0 age, 24F)	*Electrodes*: anode 42 cm^2, cathode 12 cm^2 *Anode*: left DLPFC (F3) *Cathode*: right DLPFC (F4) *Intensity*: 2 mA *Current*: direct	*Number*: 10 *Frequency:* daily + 2 fortnight *Duration*: 30 min *Period*: 6 weeks	MADRS (Sleep item)	No significant changes at week 2	Skin redness rates were higher in the active vs. sham group (25% vs. 8%, $p = 0.03$),

(Continued)

TABLE 3 | Continued

References	Design	tES montage	tES sessions	Outcomes	Significant findings	Adverse effects
Uncontrolled						
Dobbs et al. (44)	12 Parkinson disease (66.9 ± 5.4 age, 4F) Add-on cognitive training	*Electrodes*: 25 cm^2 *Anode*: left DLPFC (F3) *Cathode*: right DLPFC (F4) *Intensity*: 2 mA *Current*: direct	*Number*: 10 *Frequency:* daily *Duration*: 20 min *Period*: 2 weeks	PROMIS sleep	No significant changes at week 2	Around 50% had mild side effects that resolved after sessions
Hadoush et al. (77)	21 Parkinson disease (62.5 age, 6F)	*Electrodes*: 25 cm^2 *Anodes*: 1 right primary motor area + DLPFC (FC1) + 1 left (FC2) *Cathode*: 1 right orbitofrontal area (Fp2) + 1 left (Fp1) *Intensity*: 1 mA *Current*: direct	*Number*: 10 *Frequency:* daily *Duration*: 20 min *Period*: 2 weeks	PSQI	PSQI-total and PSQI-sleep latency improvement at week 2	None reported
Minichino et al., (79)	25 bipolar disorder in euthymic state (41.9 ± 12.6 age, 17F)	*Electrodes*: 25 cm^2 *Anode*: left DLPFC (F3) *Cathode*: right cerebellar cortex *Intensity*: 2 mA *Current*: direct	*Number*: 15 *Frequency:* daily *Duration*: 20 min *Period*: 3 weeks	PSQI	PSQI-total and items (-sleep latency, -sleep quality, -sleep duration, -sleep disturbance, -daytime dysfunction) improvement at week 2	NA
Galbiati et al. (76)	8 idiopathic hypersomnia (35.0 ± 15.5 age, 5F)	*Electrodes*: 25 cm^2 *Anode*: left DLPFC (F3) *Cathode*: right supraorbital area (Fp2) *Intensity*: 2 mA	*Number*: 12 *Frequency:* three per week *Duration*: 20 min *Period*: 4 weeks	ESS	ESS improvement at week 4 and week 6. No improvement at week 8	NA
Case reports						
Frase et al. (75)	1 organic hypersomnia following reanimation (52.0 age, male)	*Electrodes*: 35 cm^2 (anodes), 100 cm^2 (cathodes), *Anodes*: 2 Fp1-Fp2 *Cathodes*: 2 P3-P4 *Intensity*: 2 mA *Current*: direct	*Number*: 6 alternated (3 active, 3 sham) *Frequency:* daily *Duration*: 13 min *Period*: 1 week	PVT psychomotor vigilance task	Pre-to-post improvement in response speed by active in comparison to sham at week 1	None
			Number: 6 (2 blocks of three active with 4 weeks interval) *Frequency:* daily *Duration*: 1 min *Period*: 4 weeks	VAS subjective vigilance	Significant increase in subjective vigilance and reduction of daytime sleep at week 4	
Sanchez-Kuhn et al. (48)	1 chronic after-stroke dysphagia (64.0 age, male)	*Electrodes*: 35 cm^2 *Anode*: left M1 (TP-T7) *Cathode*: extra-cerebral *Intensity*: 1 mA *Current*: direct	*Number*: 16 *Frequency:* daily (4 days/w) *Duration*: 20 min *Period*: 4 weeks	SWAL-QoL sleep item	Enhancement in sleep at week 4	Mild itching sensations during the stimulation

ASSQ, Athlete Sleep Screening Questionnaire; DLPFC, dorsolateral prefrontal cortex; ESS, Epworth Sleepiness Scale; GSAQ, Global Sleep Assessment Questionnaire; ISI, Insomnia Severity Infex; KSD, Karolinska Drowsiness Scale; MADRS, Montgomery–Åsberg Depression Rating Scale; NA, not available; PSQI, Pittsburgh Sleep Quality Index; PVT, Psychomotor Vigilance Task; SE, Sleep Efficiency; SOL, Sleep Onset Latency; SSS, Stanford Sleepiness Scale; SWAL-QoL, Swallowing Quality of Life questionnaire; TAP, Testbatterie zur Aufmerksamkeitsleistung; TST, Total Sleep Time; VAS, Visual Analog Scale.

power spectral density (PSD) of endogenous slow oscillations at the stimulated areas (50, 56, 58, 59, 64). Slow oscillatory activity originates in the centro-frontal neocortex and coordinates widespread firing synchrony across other brain regions, including adjacent cortices and subcortical structures such as the thalamus and brainstem nuclei (82–84). This crosstalk is essential for the generation of oscillatory cycles that orchestrate brain activity during sleep (85). Regarding our results, although tES has primarily cortical direct effects, it is likely that external stimulation of the neocortex spreads to the entire cortico-subcortical network through top-down mechanisms to facilitate slow oscillatory activity. This rationale is supported by preclinical results demonstrating that the modulatory effects of electrical stimulation of centro-frontal cortices extend to subcortical arousal networks (86, 87). Moreover, it has been reported that stimulating the prefrontal region can reach deeper structures and lead to subcortical dopamine release in the ventral striatum (88). In parallel, slow alternating stimulation during NREM sleep has been shown to facilitate corticocortical network activity, which can explain the observed enhancement of sleep-dependent restorative processes of tES with respect to declarative memory in healthy participants (45, 47, 50), as well as behavioral inhibition and executive functions in patients with ADHD (68). For more details about the effect of tES during sleep on memory processes, we refer the interested reader to this exhaustive review (37). At the cellular level, it is likely that enhancement of slow oscillatory activity is related to tES-induced anodal polarization, which corroborates previous demonstrations that endogenous negative potentials arising during late stages of NREM sleep and facilitating specific shifts in extracellular ionic concentration play a supportive role in the generation of slow oscillations (84, 89, 90).

In parallel, it was shown that slow oscillation PSD immediately following tES is negatively correlated with measures of slow oscillation spectral power and coherence immediately preceding stimulation, suggesting that tES may be more effective when applied during less synchronized and more "quiet" periods of brain activity (50). This put forward the importance of the baseline cortical activation state on the impact of tES (91). As observed during magnetic stimulation of the brain (92), these findings imply that tES effect interacts with the ongoing activity of the sleeping brain at the time of stimulation.

In addition to modulating corresponding spectral ranges, it was shown that slow oscillatory frontal tES induces collateral modulation and enhancement of spindle waves (47, 49, 56, 59). These observations support the conclusion that slow alternating tES enhances physiologically normal conditions in which slow alternating activity drives the generation of spindle, which implies that spindle activity is maximal during late stages of NREM sleep (i.e., transition to slow wave sleep) (93–95). These neurophysiological changes were also observed during post-stimulation intervals (46, 57, 59, 60), suggesting short-term plasticity effect induced with regard to putative synaptic mechanism consequences described above. Spike timing-dependent plasticity has been proposed for the observed after-effects of tES. According to this form of brain plasticity, when the frequency of an externally induced driving force (i.e., tES) is matched with a neural circuit resonance frequency, spike timing-dependent plasticity can strengthen synapses in this circuit (96). However, changes were not replicated when taking into consideration the entire stimulation night (51), which could be attributed to the decreasing levels of slow oscillations typically observed across a sleep period (97). Regarding lower-frequency ranges, significant delta modulations induced by frontal slow alternating or direct tES during NREM sleep suggest potential cross-frequency coupling mechanisms (51, 53, 58).

tES Is Mainly Ineffective on Sleep Patterns

Only a minority of studies reported significant changes in sleep architecture, namely, increased sleep stage NREM2 and decreased further slow wave sleep stages relative duration (51, 57, 67), indicating a potential sleep-stabilizing effect of slow oscillatory tES (single session) during NREM sleep. In parallel, an absence of tES beneficial effects on polysomnographic measures of sleep was repeatedly observed across studies conducted in both clinical and healthy samples. It is likely that potential improvement of sleep continuity has been missed due to a ceiling effect in good sleepers. A few studies observed tES-induced sleep continuity disruption, which may be related to potential increase of external disturbance or unwanted modulation of vigilance control circuits (45, 57, 66). Thus, when performing tES especially in the clinical population, stimulation sessions upon awakening should be recommended in order to avoid adverse effects on sleep continuity. Interestingly, a study observed a relative stronger decrease of sleep continuity in healthy controls following tES, but not in patients with insomnia disorder. It is proposed that this differential effect of tES is related to persistent hyperarousal in this clinical population, preventing the arousal-inducing effect of anodal active tES in healthy controls (66).

tES Can Significantly Improve Subjective Aspects of Sleep

A significant number of studies observed significant improvements of subjective sleep after tES in both healthy (71–73) and a large range of neuropsychiatric diseases (41, 48, 75–77, 79, 81). The positive results were observed across various rating instruments, suggesting large impact of tES on subjective components of sleep. Notably, all studies showing significant improvements used tES montages that stimulated frontal and/or motor areas. This is not surprising since neuroimaging methods identified that cortical topography of slow waves during sleep are primarily associated with activity in a core set of cortical areas that are mainly located in the prefrontal cortex and motor regions (98, 99). Although conventional tES current may spread to other regions than the targeted area (100), studies showing a subjective improvement of sleep after tES used comprehensive stimulation protocols assuring activation of the major cortical areas involved in sleep regulation which, in turn, reflected on subjective sleep measures. It is reported that complementary biological mechanisms of subjective sleep improvement by tES can involve stimulation of the reticular formation (41), which plays a central role in states of consciousness like sleep. In addition, sleep promotion induced by decoupling functional connectivity between wakeful-active

default mode network and subcortical structures (73) and activation of non-motor function of the cerebellum such as sleep regulation (101) may underlie subjective sleep improvement by tES.

These results hold promises for the use of tES to target sleep symptoms in various clinical populations with neuropsychiatric disorders. Furthermore, significant correlations were observed between subjective sleep parameters and non-sleep parameters, such as depressive symptoms (77) and attention performance (76). Further investigations are well-warranted to identify if other clinical dimensions are improved through improvement of sleep.

Negative Results and Limitations

The main limitation of comparisons across reviewed studies relies on the high heterogeneity of results and the important rate of negative results. A main shortcoming that may explain this limitation is the very high heterogeneity of stimulation protocol parameters that could influence the effect on sleep and sleep measures, such as the device type, duration of stimulation on/offsets, electrode impedance, and electrode placement across studies. Slight methodological variations regarding the stimulation signal (direct vs. alternating) and the applied current density may also impact observations. For instance, current ramping at the beginning and at the end of each stimulation interval is likely to influence short-lasting stimulation-dependent entrainments of the specific oscillatory activity (51, 58). In addition, heterogeneity of samples sizes, sleep variations according to age and gender (102, 103), and the considerable interindividual and intraindividual differences commonly observed in sleep recordings may have accounted for the conflicting results. Another potential explanation for inconsistent effects of tES on endogenous oscillations and sleep patterns, which are derived from physiological recordings, is the difficulty in collecting high-quality stable long-term measurements during sleep due to a number of issues such as movement artifacts (rapid eye movements, tossing, turning, etc.) and slippage in the placement of electrodes through the night. As pointed out in a few recent studies (104, 105), the effects of tES on endogenous oscillations can systematically vary through the course of the night due to refractory effects—so future studies need to track stimulation-induced biomarkers for the outcomes of interest during sleep. Finally, no quantitative meta-analyses were applicable due to the high heterogeneity of studies included in this systematic review.

Regarding changes in sleep oscillations, a potential "endogenous" explanation is that the stimulation was likely given in different sleep stages across studies, especially since not all studies controlled stimulation-free intervals of neurophysiological measurement for ongoing sleep stage. Given the interindividual variability of sleep architecture and fragmentation and the fact that oscillatory stimulation effects are strongly dependent on ongoing brain state and network activity, this may have accounted for heterogeneity (106).

Some discrepancies were observed between healthy and clinical samples. It might be that the latter may have different responses to tES with different response/activation threshold, as for instance in insomnia vs. healthy subjects, who met hyperarousal symptoms (66). It is also possible that subjective sleep alterations are secondary to other symptoms such as pain (78), whose neurobiological bases are not directly targeted by tES in sleep-oriented studies. In addition, the strong placebo response observed in neuropsychiatric disorders might have hampered the observation of sleep improvement under active stimulation (80).

Finally, it should be noted that the vast majority of studies included in this systematic review involve frontal stimulation, which prevents us from concluding on a general effect of tES on sleep. A review focusing only on studies stimulating frontal areas could have indeed led to a more homogeneous picture. Nevertheless, we a priori defined the aim of our study to conduct an exhaustive systematic review of tES on sleep with the objective to account for all the existing literature and all possible stimulation areas.

CONCLUSION

tES-based approaches have a significant impact on oscillatory neurophysiological parameters of sleep. Furthermore, studies suggest their enhancement as physiological restorative processes that could serve as a potential therapeutic target in neuropsychiatric disorders. While the conflicting effects of tES on sleep patterns shed some doubt on its potential utility to improve sleep continuity, the significance of subjective aspects of sleep in various populations invites further development of non-invasive stimulation treatments for sleep conditions that are among the most prevalent health problems worldwide. Given the important heterogeneity of stimulation protocols and samples, future studies should examine the impact of these variables on the effect of tES on sleep measures. Furthermore, several major questions should be investigated to define optimal application of tES for sleep improvement, in terms of stimulation parameters (e.g., current type, duration, sessions), stimulation location, and type of brain state (e.g., wake/sleep, sleep stage) during stimulation.

DATA AVAILABILITY STATEMENT

The original contributions presented in the study are included in the article/**Supplementary Material**, further inquiries can be directed to the corresponding author/s.

AUTHOR CONTRIBUTIONS

CD designed the study, performed the literature review, and wrote the first draft of the manuscript. PG supervised the study. JB, J-AM-F, JM, ML, and MP provided critical inputs to the manuscript. All authors reviewed and approved the manuscript in its final form.

SUPPLEMENTARY MATERIAL

The Supplementary Material for this article can be found online at: https://www.frontiersin.org/articles/10.3389/fpsyt.2021.646569/full#supplementary-material

REFERENCES

1. Pennartz CM, Uylings HB, Barnes CA, McNaughton BL. Memory reactivation and consolidation during sleep: from cellular mechanisms to human performance. *Prog Brain Res.* (2002) 138:143–66. doi: 10.1016/S0079-6123(02)38076-2
2. Walker MP. The role of slow wave sleep in memory processing. *J Clin Sleep Med.* (2009) 5:S20–6. doi: 10.5664/jcsm.5.2S.S20
3. Dorrian J, Dinges DF. *Psychomotor Vigilance Performance: Neurocognitive Assay Sensitive to Sleep Loss*. New York, NY: Marcel Dekker (2005). doi: 10.1201/b14100-5
4. Verster J, Pandi-Perumal SR, Streiner DL. *Sleep and Quality of Life in Clinical Medicine*. Totowa, NJ: Humana Press (2008). doi: 10.1007/978-1-60327-343-5
5. Ohayon MM. Epidemiological Overview of sleep Disorders in the General Population. *Sleep Med Res.* (2011) 1:1–9. doi: 10.17241/smr.2011.2.1.1
6. Buysse DJ. Sleep health: can we define it? Does it matter? *Sleep.* (2014) 37:9–17. doi: 10.5665/sleep.3298
7. Geoffroy PA, Tebeka S, Blanco C, Dubertret C, Le Strat Y. Shorter and longer durations of sleep are associated with an increased twelve-month prevalence of psychiatric and substance use disorders: Findings from a nationally representative survey of US adults (NESARC-III). *J Psychiatr Res.* (2020) 124:34–41. doi: 10.1016/j.jpsychires.2020.02.018
8. Cappuccio FP, D'Elia L, Strazzullo P, Miller MA. Sleep duration and all-cause mortality: a systematic review and meta-analysis of prospective studies. *Sleep.* (2010) 33:585–92. doi: 10.1093/sleep/33.5.585
9. Medic G, Wille M, Hemels ME. Short- and long-term health consequences of sleep disruption. *Nat Sci Sleep.* (2017) 9:151–61. doi: 10.2147/NSS.S134864
10. Yin J, Jin X, Shan Z, Li S, Huang H, Li P, et al. Relationship of sleep duration with all-cause mortality and cardiovascular events: a systematic review and dose-response meta-analysis of prospective cohort studies. *J Am Heart Assoc.* (2017) 6:e005947. doi: 10.1161/JAHA.117.005947
11. Lunsford-Avery JR, Engelhard MM, Navar AM, Kollins SH. Validation of the sleep regularity index in older adults and associations with cardiometabolic risk. *Sci Rep.* (2018) 8:14158. doi: 10.1038/s41598-018-32402-5
12. Hoevenaar-Blom MP, Spijkerman AM, Kromhout D, van den Berg JF, Verschuren WM. Sleep duration and sleep quality in relation to 12-year cardiovascular disease incidence: the MORGEN study. *Sleep.* (2011) 34:1487–92. doi: 10.5665/sleep.1382
13. Newman AB, Spiekerman CF, Enright P, Lefkowitz D, Manolio T, Reynolds CF, et al. Daytime sleepiness predicts mortality and cardiovascular disease in older adults. The Cardiovascular Health Study Research Group. *J Am Geriatr Soc.* (2000) 48:115–23. doi: 10.1111/j.1532-5415.2000.tb03901.x
14. Knutsson A. Health disorders of shift workers. *Occup Med.* (2003) 53:103–8. doi: 10.1093/occmed/kqg048
15. Nuyujukian DS, Anton-Culver H, Manson SM, Jiang L. Associations of sleep duration with cardiometabolic outcomes in American Indians and Alaska Natives and other race/ethnicities: results from the BRFSS. *Sleep Health.* (2019) 5:344–51. doi: 10.1016/j.sleh.2019.02.003
16. Li L, Zhang S, Huang Y, Chen K. Sleep duration and obesity in children: a systematic review and meta-analysis of prospective cohort studies. *J Paediatr Child Health.* (2017) 53:378–85. doi: 10.1111/jpc.13434
17. Spiegelhalder K, Regen W, Nanovska S, Baglioni C, Riemann D. Comorbid sleep disorders in neuropsychiatric disorders across the life cycle. *Curr Psychiatry Rep.* (2013) 15:364. doi: 10.1007/s11920-013-0364-5
18. Taylor DJ, Mallory LJ, Lichstein KL, Durrence HH, Riedel BW, Bush AJ. Comorbidity of chronic insomnia with medical problems. *Sleep.* (2007) 30:213–8. doi: 10.1093/sleep/30.2.213
19. Dijk DJ. EEG slow waves and sleep spindles: windows on the sleeping brain. *Behav Brain Res.* (1995) 69:109–16. doi: 10.1016/0166-4328(95)00007-G
20. Devine EB, Hakim Z, Green J. A systematic review of patient-reported outcome instruments measuring sleep dysfunction in adults. *Pharmacoeconomics.* (2005) 23:889–912. doi: 10.2165/00019053-200523090-00003
21. Nitsche MA, Cohen LG, Wassermann EM, Priori A, Lang N, Antal A, et al. Transcranial direct current stimulation: state of the art 2008. *Brain Stimul.* (2008) 1:206–23. doi: 10.1016/j.brs.2008.06.004
22. Nitsche MA, Paulus W. Excitability changes induced in the human motor cortex by weak transcranial direct current stimulation. *J Physiol.* (2000) 3:633–9. doi: 10.1111/j.1469-7793.2000.t01-1-00633.x
23. Rroji O, van Kuyck K, Nuttin B, Wenderoth N. Anodal tDCS over the primary motor cortex facilitates long-term memory formation reflecting use-dependent plasticity. *PLoS ONE.* (2015) 10:e0127270. doi: 10.1371/journal.pone.0127270
24. Donde C, Brevet-Aeby C, Poulet E, Mondino M, Brunelin J. Potential impact of bifrontal transcranial random noise stimulation (tRNS) on the semantic Stroop effect and its resting-state EEG correlates. *Neurophysiol Clin.* (2019) 49:243–8. doi: 10.1016/j.neucli.2019.03.002
25. Yavari F, Nitsche MA, Ekhtiari H. Transcranial electric stimulation for precision medicine: a spatiomechanistic framework. *Front Hum Neurosci.* (2017) 11:159. doi: 10.3389/fnhum.2017.00159
26. Coffman BA, Clark VP, Parasuraman R. Battery powered thought: enhancement of attention, learning, and memory in healthy adults using transcranial direct current stimulation. *Neuroimage.* (2014) 85:895–908. doi: 10.1016/j.neuroimage.2013.07.083
27. Dayan E, Censor N, Buch ER, Sandrini M, Cohen LG. Noninvasive brain stimulation: from physiology to network dynamics and back. *Nat Neurosci.* (2013) 16:838–44. doi: 10.1038/nn.3422
28. Levasseur-Moreau J, Brunelin J, Fecteau S. Non-invasive brain stimulation can induce paradoxical facilitation. Are these neuroenhancements transferable and meaningful to security services? *Front Hum Neurosci.* (2013) 7:449. doi: 10.3389/fnhum.2013.00449
29. Moffa AH, Martin D, Alonzo A, Bennabi D, Blumberger DM, Bensenor IM, et al. Efficacy and acceptability of transcranial direct current stimulation (tDCS) for major depressive disorder: An individual patient data meta-analysis. *Prog Neuropsychopharmacol Biol Psychiatry.* (2020) 99:109836. doi: 10.1016/j.pnpbp.2019.109836
30. Donde C, Amad A, Nieto I, Brunoni AR, Neufeld NH, Bellivier F, et al. Transcranial direct-current stimulation (tDCS) for bipolar depression: a systematic review and meta-analysis. *Prog Neuropsychopharmacol Biol Psychiatry.* (2017) 78:123–31. doi: 10.1016/j.pnpbp.2017.05.021
31. Donde C, Neufeld NH, Geoffroy PA. The Impact of Transcranial Direct Current Stimulation (tDCS) on bipolar depression, mania, and euthymia: a systematic review of preliminary data. *Psychiatr Q.* (2018) 89:855–67. doi: 10.1007/s11126-018-9584-5
32. Mondino M, Sauvanaud F, Brunelin J. A review of the effects of transcranial direct current stimulation for the treatment of hallucinations in patients with schizophrenia. *J ECT.* (2018) 34:164–71. doi: 10.1097/YCT.0000000000000525
33. Valiengo L, Goerigk S, Gordon PC, Padberg F, Serpa MH, Koebe S, et al. Efficacy and safety of transcranial direct current stimulation for treating negative symptoms in schizophrenia: a randomized clinical trial. *JAMA Psychiatry.* (2019) 77:121–9. doi: 10.1001/jamapsychiatry.2019.3199
34. Lefaucheur JP, Antal A, Ayache SS, Benninger DH, Brunelin J, Cogiamanian F, et al. Evidence-based guidelines on the therapeutic use of transcranial direct current stimulation (tDCS). *Clin Neurophysiol.* (2017) 128:56–92. doi: 10.1016/j.clinph.2016.10.087
35. Krone L, Frase L, Piosczyk H, Selhausen P, Zittel S, Jahn F, et al. Top-down control of arousal and sleep: Fundamentals and clinical implications. *Sleep Med Rev.* (2017) 31:17–24. doi: 10.1016/j.smrv.2015.12.005
36. Riemann D, Nissen C, Palagini L, Otte A, Perlis ML, Spiegelhalder K. The neurobiology, investigation, and treatment of chronic insomnia. *Lancet Neurol.* (2015) 14:547–58. doi: 10.1016/S1474-4422(15)00021-6
37. Barham MP, Enticott PG, Conduit R, Lum JA. Transcranial electrical stimulation during sleep enhances declarative (but not procedural) memory consolidation: Evidence from a meta-analysis. *Neurosci Biobehav Rev.* (2016) 63:65–77. doi: 10.1016/j.neubiorev.2016.01.009
38. Moher D, Shamseer L, Clarke M, Ghersi D, Liberati A, Petticrew M, et al. Preferred reporting items for systematic review and meta-analysis protocols (PRISMA-P) 2015 statement. *Syst Rev.* (2015) 4:1. doi: 10.1186/2046-4053-4-1
39. Chien PF, Khan KS, Siassakos D. Registration of systematic reviews: PROSPERO. *BJOG.* (2012) 119:903–5. doi: 10.1111/j.1471-0528.2011.03242.x

40. Kmet L, Lee R, Cook L. *Standard Quality Assessment Criteria For Evaluating Primary Research Papers From a Variety of Fields*, Edmonton, AB: Alberta Heritage Foundation for Medical Research Suite (2004).
41. Acler M, Bocci T, Valenti D, Turri M, Priori A, Bertolasi L. Transcranial direct current stimulation (tDCS) for sleep disturbances and fatigue in patients with post-polio syndrome. *Restor Neurol Neurosci.* (2013) 31:661–8. doi: 10.3233/RNN-130321
42. Brunoni AR, Junior RF, Kemp AH, Lotufo PA, Bensenor IM, Fregni F. Differential improvement in depressive symptoms for tDCS alone and combined with pharmacotherapy: an exploratory analysis from the Sertraline vs. Electrical current therapy for treating depression clinical study. *Int J Neuropsychopharmacol.* (2014) 17:53–61. doi: 10.1017/S1461145713001065
43. Cody SL, Fazeli PL, Crowe M, Kempf MC, Moneyham L, Stavrinos D, et al. Effects of speed of processing training and transcranial direct current stimulation on global sleep quality and speed of processing in older adults with and without HIV: A pilot study. *Appl Neuropsychol Adult.* (2019) 27:267–78. doi: 10.1080/23279095.2018.1534736
44. Dobbs B, Pawlak N, Biagioni M, Agarwal S, Shaw M, Pilloni G, et al. Generalizing remotely supervised transcranial direct current stimulation (tDCS): feasibility and benefit in Parkinson's disease. *J Neuroeng Rehabil.* (2018) 15:114. doi: 10.1186/s12984-018-0457-9
45. Johnson JM, Durrant SJ. The effect of cathodal transcranial direct current stimulation during rapid eye-movement sleep on neutral and emotional memory. *R Soc Open Sci.* (2018) 5:172353. doi: 10.1098/rsos.172353
46. Koo YS, Kim SM, Lee C, Lee BU, Moon YJ, Cho YW, et al. Transcranial direct current stimulation on primary sensorimotor area has no effect in patients with drug-naive restless legs syndrome: a proof-of-concept clinical trial. *Sleep Med.* (2015) 16:280–7. doi: 10.1016/j.sleep.2014.07.032
47. Lustenberger C, Boyle MR, Alagapan S, Mellin JM, Vaughn BV, Frohlich F. Feedback-controlled transcranial alternating current stimulation reveals a functional role of sleep spindles in motor memory consolidation. *Curr Biol.* (2016) 26:2127–36. doi: 10.1016/j.cub.2016.06.044
48. Sanchez-Kuhn A, Medina Y, Garcia-Perez M, De Haro P, Flores P, Sanchez-Santed F. Transcranial direct current stimulation treatment in chronic after-stroke dysphagia: A clinical case. *Psicothema.* (2019) 31:179–83. doi: 10.7334/psicothema2018.310
49. Antonenko D, Diekelmann S, Olsen C, Born J, Molle M. Napping to renew learning capacity: enhanced encoding after stimulation of sleep slow oscillations. *Eur J Neurosci.* (2013) 37:1142–51. doi: 10.1111/ejn.12118
50. Cellini N, Shimizu RE, Connolly PM, Armstrong DM, Hernandez LT, Polakiewicz AG, et al. Short duration repetitive transcranial electrical stimulation during sleep enhances declarative memory of facts. *Front Hum Neurosci.* (2019) 13:123. doi: 10.3389/fnhum.2019.00123
51. Eggert T, Dorn H, Sauter C, Nitsche MA, Bajbouj M, Danker-Hopfe H. No effects of slow oscillatory transcranial direct current stimulation (tDCS) on sleep-dependent memory consolidation in healthy elderly subjects. *Brain Stimul.* (2013) 6:938–45. doi: 10.1016/j.brs.2013.05.006
52. Frase L, Piosczyk H, Zittel S, Jahn F, Selhausen P, Krone L, et al. Modulation of Total Sleep Time by Transcranial Direct Current Stimulation (tDCS). *Neuropsychopharmacology.* (2016) 41:2577–86. doi: 10.1038/npp.2016.65
53. Garside P, Arizpe J, Lau CI, Goh C, Walsh V. Cross-hemispheric alternating current stimulation during a nap disrupts slow wave activity and associated memory consolidation. *Brain Stimul.* (2015) 8:520–7. doi: 10.1016/j.brs.2014.12.010
54. Ketz N, Jones AP, Bryant NB, Clark VP, Pilly PK. Closed-loop slow-wave tACS improves sleep-dependent long-term memory generalization by modulating endogenous oscillations. *J Neurosci.* (2018) 38:7314–26. doi: 10.1523/JNEUROSCI.0273-18.2018
55. Koo PC, Molle M, Marshall L. Efficacy of slow oscillatory-transcranial direct current stimulation on EEG and memory - contribution of an inter-individual factor. *Eur J Neurosci.* (2018) 47:812–23. doi: 10.1111/ejn.13877
56. Marshall L, Helgadottir H, Molle M, Born J. Boosting slow oscillations during sleep potentiates memory. *Nature.* (2006) 444:610–3. doi: 10.1038/nature05278
57. Marshall L, Kirov R, Brade J, Molle M, Born J. Transcranial electrical currents to probe EEG brain rhythms and memory consolidation during sleep in humans. *PLoS ONE.* (2011) 6:e16905. doi: 10.1371/journal.pone.0016905
58. Marshall L, Molle M, Hallschmid M, Born J. Transcranial direct current stimulation during sleep improves declarative memory. *J Neurosci.* (2004) 24:9985–92. doi: 10.1523/JNEUROSCI.2725-04.2004
59. Passmann S, Kulzow N, Ladenbauer J, Antonenko D, Grittner U, Tamm S, et al. Boosting slow oscillatory activity using tDCS during early nocturnal slow wave sleep does not improve memory consolidation in healthy older adults. *Brain Stimul.* (2016) 9:730–9. doi: 10.1016/j.brs.2016.04.016
60. Reato D, Gasca F, Datta A, Bikson M, Marshall L, Parra LC. Transcranial electrical stimulation accelerates human sleep homeostasis. *PLoS Comput Biol.* (2013) 9:e1002898. doi: 10.1371/journal.pcbi.1002898
61. Sahlem GL, Badran BW, Halford JJ, Williams NR, Korte JE, Leslie K, et al. Oscillating square wave transcranial direct current stimulation (tDCS) delivered during slow wave sleep does not improve declarative memory more than sham: a randomized sham controlled crossover study. *Brain Stimul.* (2015) 8:528–34. doi: 10.1016/j.brs.2015.01.414
62. Venugopal R, Sasidharan A, Marigowda V, Kumar G, Nair AK, Sharma S, et al. Beyond hypnograms: assessing sleep stability using acoustic and electrical stimulation. *Neuromodulation.* (2019) 22:911–5. doi: 10.1111/ner.12847
63. Voss U, Holzmann R, Hobson A, Paulus W, Koppehele-Gossel J, Klimke A, et al. Induction of self awareness in dreams through frontal low current stimulation of gamma activity. *Nat Neurosci.* (2014) 17:810–2. doi: 10.1038/nn.3719
64. Westerberg CE, Florczak SM, Weintraub S, Mesulam MM, Marshall L, Zee PC, et al. Memory improvement via slow-oscillatory stimulation during sleep in older adults. *Neurobiol Aging.* (2015) 36:2577–86. doi: 10.1016/j.neurobiolaging.2015.05.014
65. Del Felice A, Magalini A, Masiero S. Slow-oscillatory transcranial direct current stimulation modulates memory in temporal lobe epilepsy by altering sleep spindle generators: a possible rehabilitation tool. *Brain Stimul.* (2015) 8:567–73. doi: 10.1016/j.brs.2015.01.410
66. Frase L, Selhausen P, Krone L, Tsodor S, Jahn F, Feige B, et al. Differential effects of bifrontal tDCS on arousal and sleep duration in insomnia patients and healthy controls. *Brain Stimul.* (2019) 12:674–83. doi: 10.1016/j.brs.2019.01.001
67. Ladenbauer J, Ladenbauer J, Kulzow N, de Boor R, Avramova E, Grittner U, et al. Promoting sleep oscillations and their functional coupling by transcranial stimulation enhances memory consolidation in mild cognitive impairment. *J Neurosci.* (2017) 37:7111–24. doi: 10.1523/JNEUROSCI.0260-17.2017
68. Munz MT, Prehn-Kristensen A, Thielking F, Molle M, Goder R, Baving L. Slow oscillating transcranial direct current stimulation during non-rapid eye movement sleep improves behavioral inhibition in attention-deficit/hyperactivity disorder. *Front Cell Neurosci.* (2015) 9:307. doi: 10.3389/fncel.2015.00307
69. Roizenblatt S, Fregni F, Gimenez R, Wetzel T, Rigonatti SP, Tufik S, et al. Site-specific effects of transcranial direct current stimulation on sleep and pain in fibromyalgia: a randomized, sham-controlled study. *Pain Pract.* (2007) 7:297–306. doi: 10.1111/j.1533-2500.2007.00152.x
70. Saebipour MR, Joghataei MT, Yoonessi A, Sadeghniiat-Haghighi K, Khalighinejad N, Khademi S. Slow oscillating transcranial direct current stimulation during sleep has a sleep-stabilizing effect in chronic insomnia: a pilot study. *J Sleep Res.* (2015) 24:518–25. doi: 10.1111/jsr.12301
71. Charest J, Marois A, Bastien CH. Can a tDCS treatment enhance subjective and objective sleep among student-athletes? *J Am Coll Health.* (2019) 14:1–12. doi: 10.1080/07448481.2019.1679152
72. Robinson CSH, Bryant NB, Maxwell JW, Jones AP, Robert B, Lamphere M, et al. The benefits of closed-loop transcranial alternating current stimulation on subjective sleep quality. *Brain Sci.* (2018) 8:204. doi: 10.3390/brainsci8120204
73. Sheng J, Xie C, Fan DQ, Lei X, Yu J. High definition-transcranial direct current stimulation changes older adults' subjective sleep and corresponding resting-state functional connectivity. *Int J Psychophysiol.* (2018) 129:1–8. doi: 10.1016/j.ijpsycho.2018.05.002
74. Forogh B, Rafiei M, Arbabi A, Motamed MR, Madani SP, Sajadi S. Repeated sessions of transcranial direct current stimulation evaluation on fatigue

and daytime sleepiness in Parkinson's disease. *Neurol Sci.* (2017) 38:249–54. doi: 10.1007/s10072-016-2748-x
75. Frase L, Maier JG, Zittel S, Freyer T, Riemann D, Normann C, et al. Bifrontal anodal transcranial direct current stimulation (tDCS) improves daytime vigilance and sleepiness in a patient with organic hypersomnia following reanimation. *Brain Stimul.* (2015) 8:844–6. doi: 10.1016/j.brs.2015.05.009
76. Galbiati A, Abutalebi J, Iannaccone S, Borsa VM, Musteata S, Zucconi M, et al. The effects of transcranial direct current stimulation (tDCS) on idiopathic hypersomnia: a pilot study. *Arch Ital Biol.* (2016) 154:1–5. doi: 10.12871/00039829201611
77. Hadoush H, Al-Sharman A, Khalil H, Banihani SA, Al-Jarrah M. Sleep quality, depression, and quality of life after bilateral anodal transcranial direct current stimulation in patients with Parkinson's disease. *Med Sci Monit Basic Res.* (2018) 24:198–205. doi: 10.12659/MSMBR.911411
78. Harvey MP, Lorrain D, Martel M, Bergeron-Vezina K, Houde F, Seguin M, et al. Can we improve pain and sleep in elderly individuals with transcranial direct current stimulation? - Results from a randomized controlled pilot study. *Clin Interv Aging.* (2017) 12:937–47. doi: 10.2147/CIA.S133423
79. Minichino A, Bersani FS, Spagnoli F, Corrado A, De Michele F, Calo WK, et al. Prefronto-cerebellar transcranial direct current stimulation improves sleep quality in euthymic bipolar patients: a brief report. *Behav Neurol.* (2014) 2014:876521. doi: 10.1155/2014/876521
80. Shill HA, Obradov S, Katsnelson Y, Pizinger R. A randomized, double-blind trial of transcranial electrostimulation in early Parkinson's disease. *Mov Disord.* (2011) 26:1477–80. doi: 10.1002/mds.23591
81. Wang HX, Wang L, Zhang WR, Xue Q, Peng M, Sun ZC, et al. Effect of transcranial alternating current stimulation for the treatment of chronic insomnia: a randomized, double-blind, parallel-group, placebo-controlled clinical trial. *Psychother Psychosom.* (2020) 89:38–47. doi: 10.1159/000504609
82. Crunelli V, Hughes SW. The slow (<1 Hz) rhythm of non-REM sleep: a dialogue between three cardinal oscillators. *Nat Neurosci.* (2010) 13:9–17. doi: 10.1038/nn.2445
83. Leger D, Debellemaniere E, Rabat A, Bayon V, Benchenane K, Chennaoui M. Slow-wave sleep: from the cell to the clinic. *Sleep Med Rev.* (2018) 41:113–32. doi: 10.1016/j.smrv.2018.01.008
84. Neske GT. The slow oscillation in cortical and thalamic networks: mechanisms and functions. *Front Neural Circuits.* (2015) 9:88. doi: 10.3389/fncir.2015.00088
85. Krueger JM, Rector DM, Roy S, Van Dongen HP, Belenky G, Panksepp J. Sleep as a fundamental property of neuronal assemblies. *Nat Rev Neurosci.* (2008) 9:910–9. doi: 10.1038/nrn2521
86. Chauvette S, Volgushev M, Timofeev I. Origin of active states in local neocortical networks during slow sleep oscillation. *Cereb Cortex.* (2010) 20:2660–74. doi: 10.1093/cercor/bhq009
87. Steriade M, Contreras D, Curro Dossi R, Nunez A. The slow (< 1 Hz) oscillation in reticular thalamic and thalamocortical neurons: scenario of sleep rhythm generation in interacting thalamic and neocortical networks. *J Neurosci.* (1993) 13:3284–99. doi: 10.1523/JNEUROSCI.13-08-03284.1993
88. Fonteneau C, Redoute J, Haesebaert F, Le Bars D, Costes N, Suaud-Chagny MF, et al. Frontal transcranial direct current stimulation induces dopamine release in the ventral striatum in human. *Cereb Cortex.* (2018) 28:2636–46. doi: 10.1093/cercor/bhy093
89. Amzica F, Steriade M. Neuronal and glial membrane potentials during sleep and paroxysmal oscillations in the neocortex. *J Neurosci.* (2000) 20:6648–65. doi: 10.1523/JNEUROSCI.20-17-06648.2000
90. Bazhenov M, Timofeev I, Steriade M, Sejnowski TJ. Model of thalamocortical slow-wave sleep oscillations and transitions to activated States. *J Neurosci.* (2002) 22:8691–704. doi: 10.1523/JNEUROSCI.22-19-08691.2002
91. Hsu TY, Juan CH, Tseng P. Individual differences and state-dependent responses in transcranial direct current stimulation. *Front Hum Neurosci.* (2016) 10:643. doi: 10.3389/fnhum.2016.00643
92. Silvanto J, Pascual-Leone A. State-dependency of transcranial magnetic stimulation. *Brain Topogr.* (2008) 21:1–10. doi: 10.1007/s10548-008-0067-0
93. Molle M, Marshall L, Gais S, Born J. Grouping of spindle activity during slow oscillations in human non-rapid eye movement sleep. *J Neurosci.* (2002) 22:10941–7. doi: 10.1523/JNEUROSCI.22-24-10941.2002
94. Niethard N, Ngo HV, Ehrlich I, Born J. Cortical circuit activity underlying sleep slow oscillations and spindles. *Proc Natl Acad Sci USA.* (2018) 115:E9220–9. doi: 10.1073/pnas.1805517115
95. Steriade M, Timofeev I. Neuronal plasticity in thalamocortical networks during sleep and waking oscillations. *Neuron.* (2003) 37:563–76. doi: 10.1016/S0896-6273(03)00065-5
96. Zaehle T, Rach S, Herrmann CS. Transcranial alternating current stimulation enhances individual alpha activity in human EEG. *PLoS ONE.* (2010) 5:e13766. doi: 10.1371/journal.pone.0013766
97. Bliwise DL. Sleep in normal aging and dementia. *Sleep.* (1993) 16:40–81. doi: 10.1093/sleep/16.1.40
98. Murphy M, Huber R, Esser S, Riedner BA, Massimini M, Ferrarelli F, et al. The cortical topography of local sleep. *Curr Top Med Chem.* (2011) 11:2438–46. doi: 10.2174/156802611797470303
99. Murphy M, Riedner BA, Huber R, Massimini M, Ferrarelli F, Tononi G. Source modeling sleep slow waves. *Proc Natl Acad Sci USA.* (2009) 106:1608–13. doi: 10.1073/pnas.0807933106
100. Romero Lauro LJ, Rosanova M, Mattavelli G, Convento S, Pisoni A, Opitz A, et al. TDCS increases cortical excitability: direct evidence from TMS-EEG. *Cortex.* (2014) 58:99–111. doi: 10.1016/j.cortex.2014.05.003
101. DelRosso LM, Hoque R. The cerebellum and sleep. *Neurol Clin.* (2014) 32:893–900. doi: 10.1016/j.ncl.2014.07.003
102. Mander BA, Winer JR, Walker MP. Sleep and Human Aging. *Neuron.* (2017) 94:19–36. doi: 10.1016/j.neuron.2017.02.004
103. Mong JA, Cusmano DM. Sex differences in sleep: impact of biological sex and sex steroids. *Philos Trans R Soc Lond B Biol Sci.* (2016) 371:20150110. doi: 10.1098/rstb.2015.0110
104. Jones AP, Choe J, Bryant NB, Robinson CSH, Ketz NA, Skorheim SW, et al. Dose-dependent effects of closed-loop tACS delivered during slow-wave oscillations on memory consolidation. *Front Neurosci.* (2018) 12:867. doi: 10.3389/fnins.2018.00867
105. Ngo HV, Miedema A, Faude I, Martinetz T, Molle M, Born J. Driving sleep slow oscillations by auditory closed-loop stimulation-a self-limiting process. *J Neurosci.* (2015) 35:6630–8. doi: 10.1523/JNEUROSCI.3133-14.2015
106. Kirov R, Weiss C, Siebner HR, Born J, Marshall L. Slow oscillation electrical brain stimulation during waking promotes EEG theta activity and memory encoding. *Proc Natl Acad Sci USA.* (2009) 106:15460–5. doi: 10.1073/pnas.0904438106

Conflict of Interest: The authors declare that the research was conducted in the absence of any commercial or financial relationships that could be construed as a potential conflict of interest.

frontiers in Psychiatry

ORIGINAL RESEARCH
published: 09 June 2021
doi: 10.3389/fpsyt.2021.660642

Physical Activity Reduces Clinical Symptoms and Restores Neuroplasticity in Major Depression

*Wanja Brüchle[1], Caroline Schwarzer[2], Christina Berns[1], Sebastian Scho[1], Jessica Schneefeld[1], Dirk Koester[2,3], Thomas Schack[2], Udo Schneider[1] and Karin Rosenkranz[1]**

[1] Faculty of Medicine, University Clinic of Psychiatry and Psychotherapie Luebbecke, Ruhr University Bochum, Bochum, Germany, [2] Neurocognition and Action Group, Faculty of Psychology and Sports Sciences, Bielefeld University, Bielefeld, Germany, [3] Department of Business Psychology, Faculty Business and Management, BSP Business School Berlin, Berlin, Germany

Major depressive disorder (MDD) is the most common mental disorder and deficits in neuroplasticity are discussed as one pathophysiological mechanism. Physical activity (PA) enhances neuroplasticity in healthy subjects and improves clinical symptoms of MDD. However, it is unclear whether this clinical effect of PA is due to restoring deficient neuroplasticity in MDD. We investigated the effect of a 3-week PA program applied on clinical symptoms, motor excitability and plasticity, and on cognition in patients with MDD ($N = 23$), in comparison to a control intervention (CI; $N = 18$). Before and after the interventions, the clinical symptom severity was tested using self- (BDI-II) and investigator- (HAMD-17) rated scales, transcranial magnetic stimulation (TMS) protocols were used to test motor excitability and paired-associative stimulation (PAS) to test long-term-potentiation (LTP)-like plasticity. Additionally, cognitive functions such as attention, working memory and executive functions were tested. After the interventions, the BDI-II and HAMD-17 decreased significantly in both groups, but the decrease in HAMD-17 was significantly stronger in the PA group. Cognition did not change notably in either group. Motor excitability did not differ between the groups and remained unchanged by either intervention. Baseline levels of LTP-like plasticity in the motor cortex were low in both groups (PA: 113.40 ± 2.55%; CI: 116.83 ± 3.70%) and increased significantly after PA (155.06 ± 10.48%) but not after CI (122.01 ± 4.1%). Higher baseline BDI-II scores were correlated with lower levels of neuroplasticity. Importantly, the more the BDI-II score decreased during the interventions, the stronger did neuroplasticity increase. The latter effect was particularly strong after PA ($r = -0.835$; $p < 0.001$). The level of neuroplasticity related specifically to the psychological/affective items, which are tested predominantly in the BDI-II. However, the significant clinical difference in the intervention effects was shown in the HAMD-17 which focuses more on somatic/neurovegetative items known to improve earlier in the course of MDD. In summary, PA improved symptoms of MDD and restored the deficient neuroplasticity. Importantly, both changes were strongly

OPEN ACCESS

Edited by:
Kai Wang,
Anhui Medical University, China

Reviewed by:
Jennifer L. Vande Voort,
Mayo Clinic, United States
Ming-Kuei Lu,
China Medical University, Taiwan

***Correspondence:**
Karin Rosenkranz
rosenkranz.karin@gmx.de

Specialty section:
This article was submitted to Neuroimaging and Stimulation, a section of the journal Frontiers in Psychiatry

Received: *29 January 2021*
Accepted: *18 May 2021*
Published: *09 June 2021*

Citation:
Brüchle W, Schwarzer C, Berns C, Scho S, Schneefeld J, Koester D, Schack T, Schneider U and Rosenkranz K (2021) Physical Activity Reduces Clinical Symptoms and Restores Neuroplasticity in Major Depression. Front. Psychiatry 12:660642. doi: 10.3389/fpsyt.2021.660642

related on the individual patients' level, highlighting the key role of neuroplasticity in the pathophysiology and the clinical relevance of neuroplasticity-enhancing interventions for the treatment of MDD.

Keywords: neuroplasticity and exercise, major depression, paired associative stimulation, transcranial magnetic stimulation, physical activity

INTRODUCTION

Major depressive disorder (MDD) is a common illness worldwide, with more than 264 million people affected (1). The pathophysiology of MDD is complex and likely due to different, possibly interacting mechanisms. Several preclinical and clinical studies described altered neuroplasticity in MDD (2–4), such as lower synaptic density in the brain which is associated with the severity of depressive symptoms (5).

Reduced LTP-like plasticity in the motor cortex has been described in MDD in studies using paired associative stimulation (PAS) as a specific transcranial magnetic stimulation (TMS) protocol (2, 6), which tests synaptic plasticity in the human brain (7). As this reduction showed some association with the symptom severity measured in clinical scales, developing interventions that aim at enhancing synaptic plasticity might be of crucial relevance in the treatment of MDD.

Physical activity (PA) is associated with higher levels of neuroplasticity in healthy subjects (8, 9), and has been identified as a protective factor against the onset of depression (10–13). The effect of PA or sports programs have been widely studied in MDD and the clinical benefit and therapeutic relevance has been shown (14–17) even of short-term interventions (18–22). Furthermore, PA seems to influence cognitive symptoms in MDD, such as deficits in attention, concentration, memory and executive functions (23, 24).

Most of these studies focused on measuring the effect of PA interventions using clinical outcome parameters, such as self- or investigator-rated depression scores, and did not investigate which neurobiological parameters, e.g., neuronal excitability or plasticity in the brain, might be associated with these clinical changes.

Our study investigated the effect of a PA program applied over a period of 3 weeks on clinical symptoms, neural excitability and PAS-induced plasticity in the motor cortex, as well as on cognitive performance in in-patients with an acute episode of MDD during their stay on the psychiatric ward. As most patients followed a more sedentary lifestyle before admission to hospital, we designed the PA program to be of moderate intensity, including elements of endurance, strength and coordination exercises that required interaction and teamwork of the participants, in order to avoid competition and the risk of perceived performance failure (25, 26). The effect of the PA program was compared to a control intervention (CI) administered over the same period of time that controlled for investigator-related effects, experience of group cohesion and social interaction, while the patients abstained from additional physical activity.

We expected—similar to previous studies—the level of PAS-induced plasticity to be low in MDD, and PA to lead to an improvement of clinical symptoms—at least of those known to be first indicators of symptom reduction, such as psychomotor retardation or loss of energy. Leading on from that, we asked (i) whether measures of PAS-induced plasticity and clinical symptoms are related on an individual subject's level, (ii) whether PA reverses neuroplasticity deficits in MDD, and (iii) whether PAS-induced plasticity could act as a marker to predict the clinical outcome of neuroplasticity enhancing interventions, such as PA.

MATERIALS AND METHODS

The study was approved by the Ethics committee of the Ruhr University Bochum, medical faculty in Bad Oeynhausen (Germany) and conducted in accordance with the Declaration of Helsinki.

Subjects

After giving written informed consent, 50 in-patients meeting the clinical criteria of MDD as defined by the international classification of disease (ICD-10: F32, F33) were recruited (see **Table 1** for details). The inclusion criteria were: (i) Age between 18 and 65 years, (ii) current depressive episode (BDI-II score $\geq$ 10 points; Hamilton depression score (HAMD-17) $\geq$ nine points), (iii) no concurrent brain stimulation treatment, (iv) no severe cardiovascular disease and body mass index $<$30 kg/m^2, (v) no structural brain alteration as shown in brain imaging, and (vi) in case of concurrent medication: no major changes to antidepressant medication during the study; no medication with anticonvulsive medication or lithium; medication with benzodiazepine $<$1 mg/day lorazepam equivalent; no medication with antipsychotics in dosages known to alter brain excitability (27). Medication (e.g., with antidepressants) was continued as long as it complied with the inclusion criteria (see above) and left unchanged during the interventions.

Study Design

The study was performed within the setting of a primary care psychiatric university hospital on in-patients and ran for 18 months in total. Patients were screened according to the above mentioned criteria. In case of consent, they were recruited for participation in the study around 7–14 days after their admission to hospital, in order to allow for completion of diagnostics and for amelioration of severe symptoms of depression, such as suicidal ideation or agitation. They were informed that the purpose of the study was to compare the effect of two different interventions on their mood, their cognition and on neurophysiological parameters without implying a superior effect of one intervention to the other. As the recruitment rate of patients who fulfilled

TABLE 1 | Patients' characteristics.

	PA	CI	*t*-test
N	23	18	
Age (years ± SEM)	33.3 ± 3.06	40.11 ± 3.63	p=0.157
Age range (years)	18 – 63	18 – 65	
Sex	12 male: 11 female	11 male: 7 female	
Handedness	2 left: 21 right	1 left: 17 right	
Body mass index (kg/m²)	24.33 ± 0.93	25.69 ± 0.90	p=0.306
HAMD-17 (mean ± SEM) at M1	19.17 ± 0.78	17.83 ± 0.75	p=0.230
Severity (N)			
mild (9–16 points)	7	8	
moderate (17–24 points)	13	10	
severe (≥ 25 points)	2	0	
BDI-II (mean ± SEM) at M1	27.74 ± 1.44	26.11 ± 1.77	p=0.475
Severity (N)			
mild (10–19 points)	3	2	
moderate (20–29 points)	12	11	
severe (≥ 30 points)	8	5	

the inclusion criteria was expected to be low, the patients were successively recruited (rather than randomly assigned) in one of the two intervention groups and the investigators were not blinded. The first 25 patients were recruited into the PA group, and the succeeding 25 patients into the CI group. This approach ensured that 6–8 patients were participating at a time, which enabled interaction amongst participants during the sessions. Each patient participated for 3 weeks in one of the interventions. As neither the PA nor the CI sessions build up on each other, participants could join at any date.

Before the start (measurement 1; M1) and within 2–3 days after the end of the intervention period (measurement 2; M2) neurophysiological and cognitive parameters were tested (see **Figure 1**: experimental design), and clinical assessments by use of self- and investigator-related scales were performed.

Interventions and Assessment of Physiological Parameters

Each intervention ran for 3 weeks. For each intervention the total duration was 180 min/week; thus the total intervention time was 540 min in 3 weeks.

The PA was performed on 3 days a week (Monday, Wednesday, Friday) and was guided by an instructor. Each session lasted 60 min (without breaks) and focused on one out of three exercise types once a week, either coordination, endurance or strength training. These three exercise sessions were repeated every week. The PA program aimed to increase motivation for and to induce a positive affective response towards physical and sportive activity. It mainly consisted of interactive games, which the patients had to perform within the group or with one patient as partner. This approach reduced competitiveness among participants which could trigger a sense of underachievement or failure, or could invoke negative prior experiences (e.g., with PA at school). In addition, each PA session started with a 10-min warm-up which combined physical and cognitive tasks, by coding certain movements (e.g., circling of arms, lifting knees up) with colors (colored cards held up by the instructor). During the warm-up participants walked briskly through the room and had to perform the required movement (once) when the instructor showed the respective colored card. The color-movement associations were changed randomly in every PA session.

The CI consisted of two sessions of 90 min each per week and was guided by an instructor. While the participants remained seated on chairs, they performed different games (logical puzzles, "black stories," card games), which required them to interact and to cooperate with each other. In the logical puzzles pieces of information were given and required the participants to put them into a matrix and find out the missing pieces of information by deduction (e.g., *Who owned the zebra?*). The "black stories" were mysterious stories that required the participants to reconstruct what has happened by asking and guessing. The card games prompted the participants to cooperate and to exchange cards in order to play and win together against the rule of the game (e.g., *The Game—Spiel… solange Du kannst!*).

The CI controlled for the presence of and attention given by an instructor and the feeling of group cohesion. The participants were cognitively engaged (solving logical problems, memorizing facts, and forming strategies). Importantly, the participants of the CI group were not included in other PA programs of the psychiatric clinic, and were instructed not to engage in any physical or sportive activity beyond their routine activity (such as walking in the hospital and hospital garden). The clinical and nursing staff was informed about the study participation and monitored the participants activity accordingly.

During the PA and CI sessions the heart rate was measured using a pulse tracker fixed to the upper arm with an elastic band (OH1, Polar Electro Oy, Kempele, Finland). The mean heart rate at rest (before the start of the session) and during the session were calculated for each participant.

Clinical Assessment

The Becks Depression Inventory II (BDI-II) was used for patients' self-assessment (28) and the Hamilton depression scale with 17 items (HAMD-17) was used for investigator-based assessment of clinical symptoms (29–31) once before and after the 3 weeks intervention period.

Neurophysiology

Transcranial Magnetic Stimulation (TMS)

TMS was performed using a Magstim 200 stimulator connected to a figure-of-eight-shaped coil with an internal wing diameter of 70 mm (Magstim Company Ltd, Whitland, UK). At the start of the experimental sessions M1 and M2 the motor "hot spot" of the abductor pollicis brevis (ABP) muscle was determined. The coil was held with the handle pointing backwards and laterally 45° to the interhemispheric line to evoke anteriorly directed current in the brain and was optimally positioned to obtain motor evoked potentials (MEP) in the APB of the dominant hand ("hot spot"). The subjects were wearing a tight fitting cotton wool cap on which the coil position was marked using a soft tip pen in order

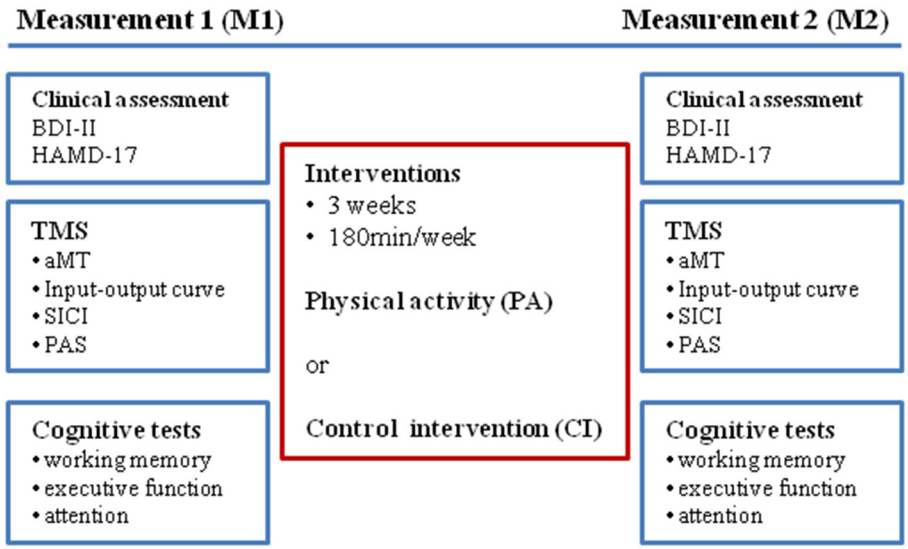

FIGURE 1 | Experimental design.

to ensure that the coil was held in a constant position during the experimental session.

Stimulation intensities are quoted as percentage of maximal stimulator output (mean ± SEM).

EMG Recording

Surface electromyographic (EMG) recordings in a belly-to-tendon montage were made from the APB and the first dorsal interosseus (FDI) muscles of the dominant hand. The raw signal was amplified and filtered with a bandpass filter of 30 Hz to 1 kHz (Digitimer D360; Welwyn Garden City, UK). Signals were digitized at 2 kHz (CED Power1401, Cambridge Electronic Design, UK) and stored on a laboratory computer for offline analysis. Online EMG was used to control for muscle relaxation during data recording and trials showing voluntary muscle activation were discarded from the analysis (<1% of trials). The recordings of the FDI were only displayed on screen during the experiments in order to support the experimenter in holding the coil in a constant position and were not analyzed further.

Motor Excitability

At the start of each measurement (M1 and M2), the active motor threshold (aMT) and the stimulus intensity (SI) needed to evoke a MEP of ∼1 mV peak-to-peak amplitude (SI_{1mV}) were defined in the APB. To determine the aMT, the EMG pattern (rectified amplitude) under maximum voluntary contraction (MVC) was displayed on the screen and a marker line was set to determine 30% of this amplitude. The subjects were instructed to activate their APB (pressing the thumb down while their hand lies in a pronated position on a cushion placed on their lap) so that the EMG amplitude was as close to that marker line as possible. The TMS measurements were always performed by two experimenters. In the measurement of the aMT, one experimenter controlled the participants APB activation level to be constant and of defined strength. The aMT was defined as the minimum intensity needed to evoke a MEP of ≥200 μV in five out of 10 trials.

The SI_{1mV} was determined while the subjects were at rest with their hand muscles relaxed (as controlled by online EMG). Single TMS pulses were given (interstimulus interval 7 s) to determine the SI that gives a MEP of 1 mV peak-to-peak amplitude in five consecutive trials.

The input-output relationship of MEP amplitude to SI (IOcurve) was measured. For each SI of the IOcurve [50, 70, 80, 90, 100 (equal to SI_{1mV}), 110, 120 130, and 150% of SI_{1mV}] five consecutive TMS single pulses were applied with an interstimulus interval of 7 s and the MEPs recorded. The mean MEP amplitude per SI was calculated for each subject. Furthermore, the steepness of the IOcurve slopes defined as the steepness of the linear regression line through the given data points between 80 and 120% of SI_{1mV} (IOslope) were calculated.

Short Interval Intracortical Inhibition (SICI)

The short-interval intracortical inhibition [SICI curve; (32, 33)] was measured using subthreshold conditioning stimulus intensities of 70, 80, and 90% of active motor threshold (aMT) and two magnetic stimulators (MagStim 200) connected *via* a BiStim module (Magstim Company Ltd, Whitland, UK). The conditioning stimulus preceded the suprathreshold test stimulus (intensity set at SI_{1mV}) by 3 ms (34).

Three blocks consisting of 30 trials each were performed. Each block examined one conditioning pulse intensity and consisted of 15 MEPs elicited by the test stimulus alone (test MEPs) and 15 conditioned MEPs presented in pseudorandom order (intertrial interval 7 s). The peak-to-peak amplitude of the conditioned and test MEPs was measured for each single trial to calculate the mean amplitude and percentage SICI (conditioned MEP/ test MEP; in %) for the three different conditioning stimulus intensities. This

approach allowed us to measure the level of SICI at a single conditioning intensity as well as the recruitment of SICI (SICI curve) defined as the increase of SICI with increasing intensities of the conditioning stimulus.

Plasticity in the Motor Cortex as Assessed by Paired-Associative Stimulation (PAS)

PAS consisted of 200 electrical stimuli of the median nerve at the wrist of the relaxed dominant hand paired with a single TMS pulse (at SI_{1mV}) over the contralateral hand motor cortex with a rate of 0.25 Hz. TMS single pulses were delivered through a figure-of-eight shaped coil (diameter of each wing 70 mm) connected to a Magstim 200 stimulator and was held in the same position as described above. Electrical stimulation (Digitimer DS7A) was applied through a bipolar electrode (cathode proximal), using square-wave pulses (duration 0.2 ms) at an intensity of three times the perceptual threshold.

The electrical stimuli preceded the TMS pulses by 25 ms (PAS25). PAS25 has been shown previously to induce a long-lasting MEP increase (7, 35, 36). Subjects were instructed to look at their stimulated hand and count the peripheral electrical stimuli they perceived; they were asked the actual count by the experimenter about three to four times during the application of PAS (37). During PAS, the MEPs evoked in the APB and FDI were displayed on-line on the computer screen to control for the correct coil position and stored for off-line analysis.

Before and 10 min after the end of the PAS-intervention 20 TMS pulses were delivered (intertrial interval 7 s) using SI_{1mV} and the MEPs recorded. Their mean amplitude was calculated. The effect of PAS was defined in each subject as change of the MEP amplitude in the APB (PASeffect = MEP after PAS / MEP before PAS; in %). In addition, PASchange refers to the change of PASeffects (PASchange = PASeffect after / before the intervention; in %).

Cognition

A PC-based test battery (Vienna test system, Schuhfried®, Austria) was used to measure different aspects of cognitive performance and executive function. Attention was tested using the work performance series which required subjects to perform additions and subtractions of single-digit numbers as fast and accurate as possible for 7 min. The Trail making test (part A and B) was used to assess the visuomotor processing speed and cognitive flexibility (38). The Response Inhibition (RI) task was used to assess voluntary control over responses within a changing context and required subjects to press a button as quickly as possible in reaction to a "Go" - signal (triangles) and to inhibit this reaction to an intermittently presented "NoGo" - signal (circle) (39, 40).

The Tower of London (TOL) assessed the planning abilities on the basis of clear rules and required the subjects to rearrange colored balls in a minimum number of moves (41, 42).

The STROOP interference test (color/word interference) was used to investigate the subjects' ability to control cognitive interference (43, 44).

Working memory performance was tested with the N-back verbal test [NBV; (45, 46)], a continuous performance measure (47, 48). A series of consonants was presented successively and subjects were required to press a button when the consonant displayed was identical to the one shown two places back (2-back paradigm) (49). To minimize the effect of familiarity, parallel versions of the tests were used in M2.

Data Analysis and Statistics

All data was tested for normal distribution by use of the Kolmogorov-Smirnov test. In case of not normally distributed data, non-parametric tests were used. All ANOVAs were tested for sphericity using Mauchly's test. In case of non-sphericity, Greenhouse-Geisser corrections were performed. Effect sizes (η^2; r) were calculated for significant interactions. All data are given as mean ± SEM. Significance levels for the statistical tests are set to $p \leq 0.05$; in case of multiple comparisons (results of cognitive tests) the significance level was adjusted to $p \leq 0.01$.

The TMS parameters (aMT and SI_{1mV}) of M1 and M2 were compared within groups by paired t-tests and between groups by unpaired t-tests. The IOcurve and SICI data were analyzed using ANOVA with the factor *group* (PA/CI) and the within-group factors *intervention* (before/after), *stimulus intensity* (IOcurve) or *conditioning pulse intensity* (SICI). The MEPs measured in M1 and M2 before PAS were compared by means of paired t-tests (within group) and unpaired t-tests (between groups) in order to control for correct adjustment of MEP size to 1 mV peak-to-peak amplitude. ANOVAs were performed on the raw data of MEPs with the factors *group*, *intervention* and *MEP amplitude before/after PAS*. For further analysis, the MEP raw data were normalized and expressed as percentage of MEPs (MEPs after PAS/ MEPs before PAS; PASeffect).

Correlations between neurophysiological data and clinical outcome (BDI-II and HAMD-17 scores) were calculated and significant results are reported giving Pearson's r for normally distributed and Kendall's tau for non-normally distributed data.

The raw data of cognitive tests was transformed into T-scores (mean = 50; SD = 10); with T-scores >50 indicating higher, and T-scores <50 indicating lower performance in comparison to a representative population (matched for age, sex and level of education) as given by the Vienna Test System (Schufried®, Austria). Similar to the analysis of the neurophysiological data, ANOVAs were performed with the between group factor *group* and the factors *intervention* as within-group factor. *Post-hoc* tests were performed when necessary and the significance level was adjusted to correct for multiple comparisons (see above).

RESULTS

Subjects' and Clinical Data

Out of 50 recruited patients, 23 (of 25) in the PA group and 18 (of 25) in the CI group finished the study. Two patients of the PA group and three patients of the CI group were discharged from hospital before the M2 measurements could be taken. In addition, in the CI group two patients required emergency treatment and two patients discontinued their participation. Only results of patients who participated in both measurements (M1 and M2) and in all intervention sessions during the 3 weeks intervention period are reported. The patients in the PA and CI groups were

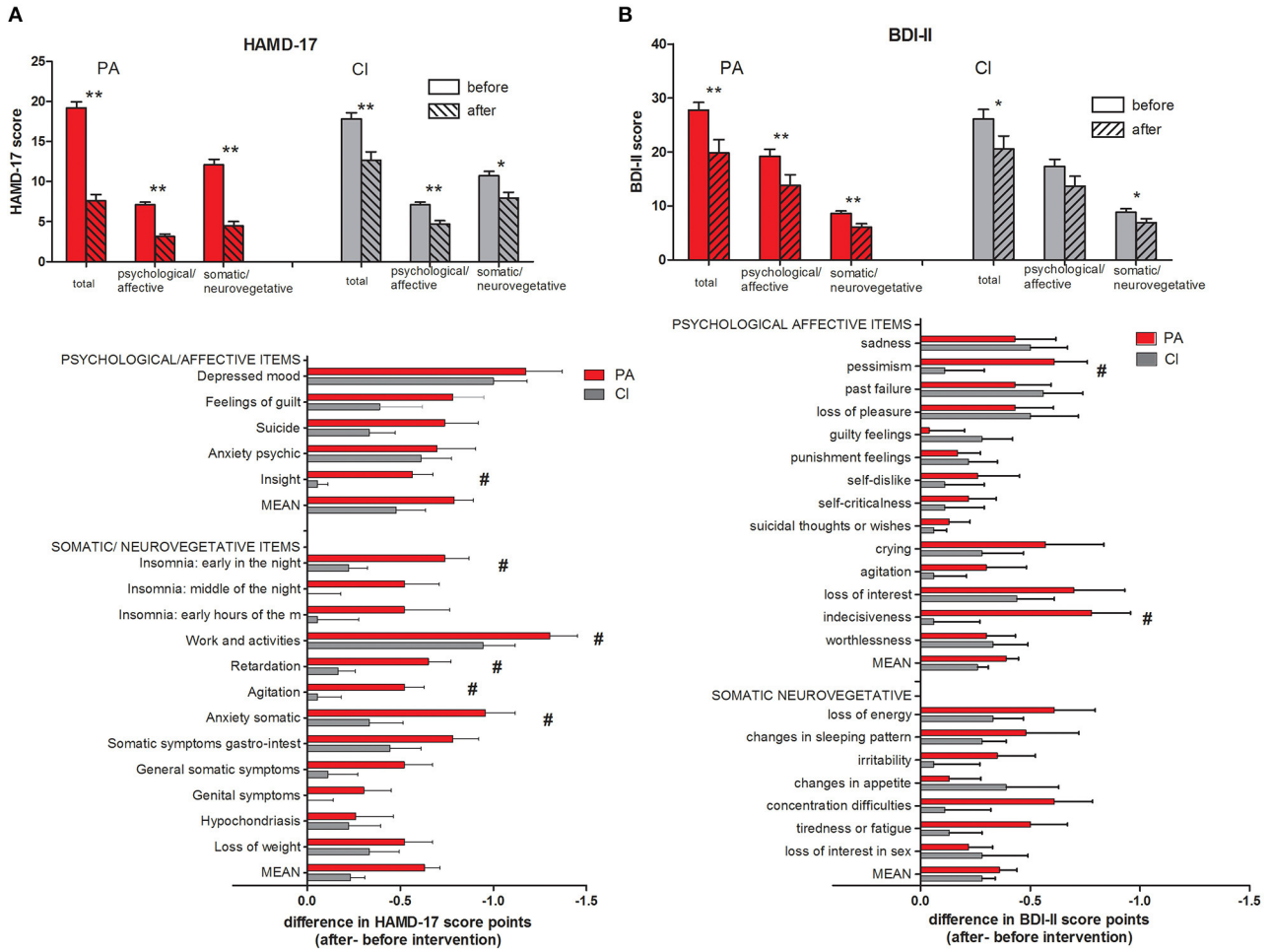

FIGURE 2 | HAMD-17 **(A)** and BDI-II **(B)** scores with subscales. The mean scores of all items (total) as well as subscores for psychological/affective and somatic/neurovegetative items are given (mean ± SEM; *t*-test: $^{**}p < 0.001$; $^{*}p < 0.01$). Below the score change (after – before intervention) is given for each single item of the questionnaire (*t*-test; $^{\#}p < 0.05$).

comparable with regard to age, body mass index, BDI-II and HAMD-17 scores at M1 (see **Table 1** for details).

Clinical Assessment

The subjects in the PA and CI groups did not differ in their BDI-II and HAMD-17 scores before the start of the intervention (unpaired *t*-tests, n.s.; see **Table 1** and **Figure 2**). After the intervention, the BDI-II and HAMD-17 scores decreased significantly in both groups (paired *t*-tests; $p < 0.009$; see **Figure 2**) while the decrease in HAMD-17 score (HAMD-17 after—before intervention) was significantly stronger in the PA group (unpaired *t*-test; $p < 0.001$), there was no between-group difference in the decrease of the BDI-II score. A two-way ANOVA with the factors *group* (PA/CI) and *intervention* (before/after) showed for the HAMD-17 scores a significant interaction [ANOVA; $F_{(1,39)} = 16.52$; $p < 0.001$], and significant main effects of the factor *group* [ANOVA; $F_{(1,39)} = 4.41$; $p = 0.042$] and the factor *intervention* [ANOVA; $F_{(1,39)} = 112.94$; $p < 0.001$]. For the BDI-II score data, there was no significant interaction, but a main effect of *intervention* [ANOVA; $F_{(1,39)} = 27.19$; $p < 0.001$].

A detailed analysis of the single items of the HAMD-17 scores (see **Figure 2A**) showed that the decrease in the items "insight," "insomnia: early in the night," "work and activities," "retardation," "agitation," and "anxiety somatic" was significantly stronger in the PA group than in the CI group. For the BDI-II scores (see **Figure 2B**), the score for the items "pessimism" and "indecisiveness" decreased significantly stronger in the PA group than in the CI group.

The BDI-II and HAMD-17 scores measured before and after the interventions did not show a significant correlation in either the PA or the CI group.

Physiological Parameters

Before and during the interventions, the subjects' heart rate was continuously monitored. At rest, the mean heart rates were not different in the PA [69.00 ± 2.03 beats per minute (bpm)] and the CI group (71.39 ± 3.19 bpm; *t*-test: n.s.). During PA, the

TABLE 2 | TMS and PAS parameters and MEP amplitudes.

	PA		CI	
TMS parameters (% stimulator output)	**Mean**	**SEM**	**Mean**	**SEM**
aMT M1	34.96	± 1.22	33.17	± 1.09
aMT M2	34.78	± 0.84	35.50	± 1.12
SI_{1mV} M1	51.87	± 1.75	51.89	± 2.12
SI_{1mV} M2	51.74	± 1.59	53.89	± 1.79
PAS parameters				
Sensory threshold M1 (mA)	0.28	± 0.02	0.36	± 0.02
Sensory threshold M2 (mA)	0.27	± 0.06	0.36	± 0.02
Sensory stimuli counted M1 (N)	201.05	± 0.40	199.06	± 0.76
Sensory stimuli counted M2 (N)	200.52	± 0.63	199.22	± 0.68
MEP amplitudes (mV)				
IOcurve MEP (SI_{1mV}) M1	0.93	± 0.15	0.92	± 0.09
IOcurve MEP (SI_{1mV}) M2	1.03	± 0.17	1.04	± 0.12
SICI test MEP M1	1.01	± 0.14	1.02	± 0.15
SICI test MEP M2	0.99	± 0.15	0.99	± 0.13
MEP before PAS M1	1.15	± 0.15	0.93	± 0.09
MEP after PAS M1	1.29	± 0.16	1.09	± 0.11
MEP before PAS M2	0.99	± 0.10	1.08	± 0.12
MEP after PAS M2	1.45	± 0.16	1.34	± 0.17

mean heart rate increased to 126.84 ± 2.83 bpm, showing that the patients were exercising with moderate intensity. In the CI group, the heart rate increased slightly to 83.02 ± 3.08, but this increase was not significantly different from their baseline mean heart rate (paired *t*-test; n.s.). The mean heart rates were not correlated to any neurophysiological or clinical parameters in either group.

Motor Cortical Excitability and Short-Interval Intracortical Inhibition

The aMT and SI_{1mV} were not different between the two groups (see **Table 2**). The IOcurves (see **Figures 3A,B**) showed an increase of MEP amplitudes with increasing TMS intensity. The IOcurves measured before and after the interventions were not different in either the PA or the CI group (ANOVA, main effect of *stimulus intensity* $p < 0.001$; no effect of *intervention*). Furthermore, there were no group differences between the IOcurves (ANOVA; main effect *group*: $p = 0.96$; no significant interaction). The SICI (see **Figures 3C,D**) was stronger with increasing conditioning stimulus intensities. Again, there was no difference in SICI before and after the intervention within each group (ANOVAs; main effect of *conditioning stimulus intensity*: $p < 0.001$; effect of *intervention*: n.s.), nor was there any difference between the groups (ANOVA, main effect of factor *group*: $p = 0.775$; no significant interactions).

Motor Cortical Plasticity - PAS

The mean MEP amplitudes measured before PAS were not different within each group when tested either before or after the intervention (paired *t*-tests, n.s.), and not different between the groups (unpaired *t*-tests: n.s.); thus ensuring comparability between the groups. In the PA group, PAS induced a significant increase (paired *t*-tests; $p < 0.001$) of the mean MEP amplitude before and after the intervention. The PASeffect (MEP after/before PAS, in %) was significantly stronger after PA (before: 113.40 ± 2.55%; after: 155.06 ± 10.48; paired *t*-test; $p < 0.001$; see **Figure 4A**).

In the CI group, PAS also significantly increased the mean MEP amplitude before and after the intervention (paired *t*-tests; $p < 0.001$). However, there was no difference in the PASeffects measured before and after the CI (before: 116.83 ± 3.70%; after: 122.01 ± 4.91%; paired *t*-test; n.s.; see **Figure 4A**).

The interaction of the factor *intervention* (before/after) and *group* (PA/CI) was significant [ANOVA; $F_{(1, 39)} = 9.09$; $p = 0.005$; $\eta^2 = 0.40$; $r = 0.63$], as were the main effects of *intervention* [$F_{(1, 39)} = 14.98$; $p < 0.001$] and *group* [ANOVA; $F_{(1, 39)} = 4.15$; $p = 0.048$]. The PASchange was significantly higher in the PA than in the CI group (unpaired *t*-test; $p = 0.004$).

The PASeffects measured before and after the intervention were only weakly correlated in each group (PA: Pearson's $r = 0.337$, $p = 0.116$; CI: Pearson's $r = 0.328$, $p = 0.183$; see **Figures 4B,C**). While the PASeffect at baseline and the PASchange showed no correlation in the PA group (Pearons's $r = 0.087$, $p = 0.693$, see **Figure 4D**), there was a weak but non-significant correlation in the control group (Pearson's $r = -0.443$, $p = 0.065$; see **Figure 4E**). Thus, the baseline PASeffect did neither predict the PASeffect after the intervention, nor PASchange.

Correlations Between Clinical Scales and PAS

In both groups, there was a significant negative correlation between the BDI-II scores and the PASeffect measured before the interventions (see **Figures 5A,B**; PA: Pearson's $r = -0.71$, $p < 0.001$; CI: Pearson's $r = -0.68$, $p = 0.002$; for both groups together: Pearson's $r = -0.695$, $p < 0.001$): with increasing BDI-II scores the PASeffect was less strong. Furthermore, the change of the BDI-II scores and the change of the PASeffect by the intervention were significantly correlated in each groups (see **Figures 5E,F**; PA: Pearson's $r = -0.835$; $p < 0.001$; CI: -0.663, $p = 0.003$): the stronger the BDI-II score decreased, the stronger did the PASeffect increase. The latter effect was more prominent in the PA group (see **Figure 5E**).

The BDI-II scores at baseline were not correlated to the PASchange in either of the groups (**Figures 5C,D**; PA: $r = -0.19$; $p = 0.384$; CI: $r = 0.252$; $p = 0.312$); thus, the baseline BDI-II did not predict the PASchange. Furthermore, the change of BDI-II scores were not correlated to the PASeffect at M1 in either group (**Figures 5G,H**; PA: $r = -0.268$; $p = 0.216$; CI: $r = 0.136$; $p = 0.59$), showing that the PASeffect at baseline did not predict the clinical effect of the interventions as shown in reduction of BDI-II scores.

There were no correlations between the HAMD-17 scores and the PAS data in either group; and no correlations between clinical scales and other neurophysiological parameters.

Cognition

Table 3 shows the results of the cognitive test performed before and after the intervention in each group (mean T-scores ± SEM). After the intervention, there was a significant increase of T-scores of some parameters within groups that indicated an

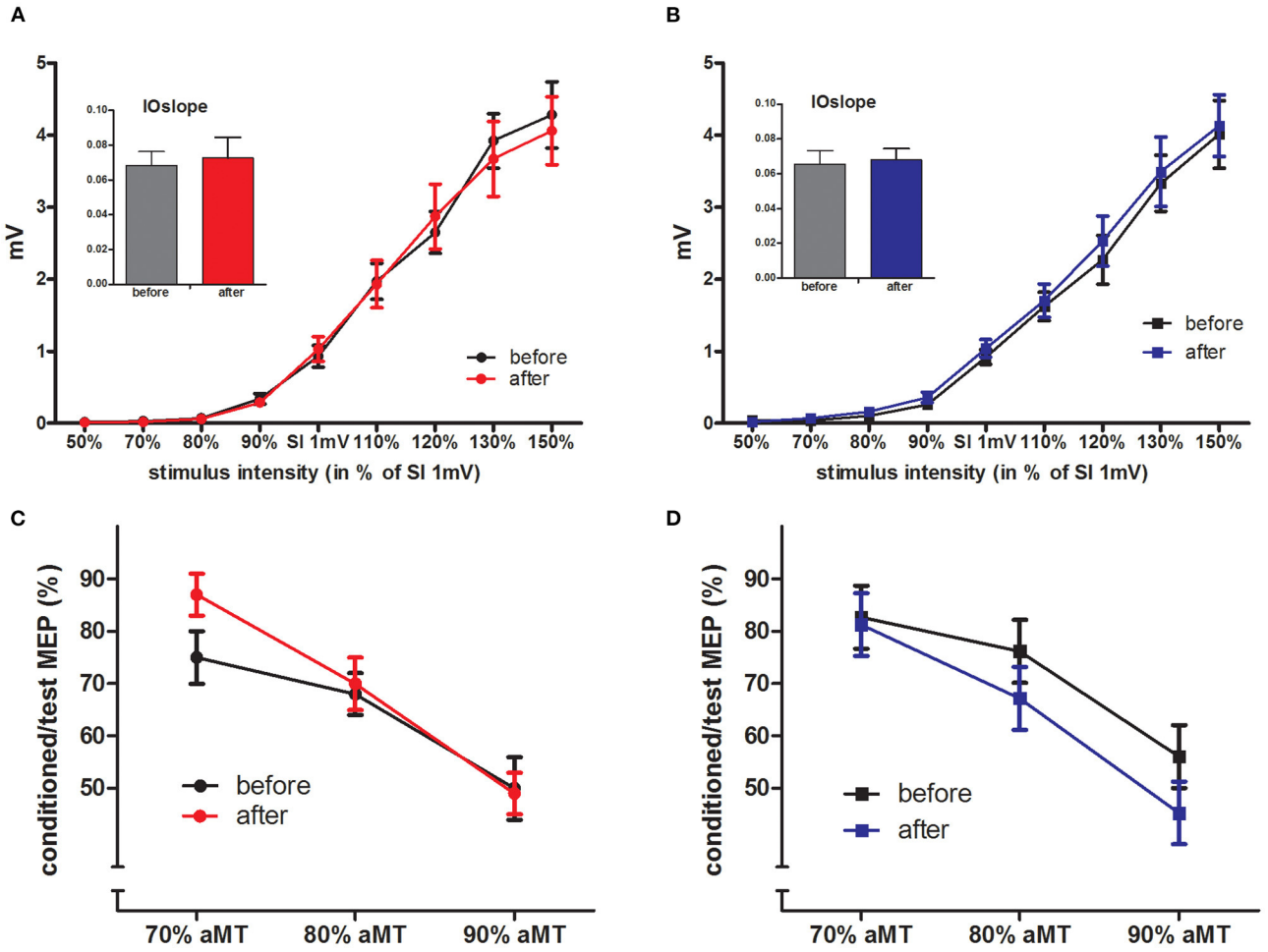

FIGURE 3 | IOcurves and SICI. **(A,B)** displays the IOcurves measured in PA **(A)** and CI **(B)** groups before and after the intervention, with the IOslope given in the inserted diagram (mean ± SEM). IOcurves and IOslopes were not changed by the interventions within the groups, and there were no between-group differences. **(C,D)** displays the SICI results for PA **(C)** and CI **(D)** groups, again there were no differences within the groups (before/after intervention) nor between the groups.

improved performance (see results of paired *t*-tests in **Table 3**). There were no between-group differences in cognitive test before or after intervention, apart from a significant difference in the STROOP test (Δ after-before: baseline reading), which is of minor relevance in the absence of differences in the interference conditions.

Although there were no significant differences on how the performance was influenced by the intervention between the two groups, T-scores tended to increase stronger in the PA group: here the stronger increase of T-scores in Trail making and N-back tasks might indicate a stronger improvement of attention/working speed and of working memory, respectively.

DISCUSSION

Our study investigated the effect of PA—in comparison to a CI—on neuronal excitability and plasticity, as well as on clinical and cognitive symptoms in MDD. Confirming previous studies, we showed that (i) PA had a beneficial clinical effect as such as it reduced the severity of symptoms, such as psychomotor retardation and loss of energy as assessed by HAMD-17 and known to improve early in the course of MDD; and that (ii) the baseline level of motor cortical LTP-like plasticity is low in MDD.

Our study now crucially expands these findings by showing, that (iii) the severity of psychological/affective symptoms of MDD, as monitored with the BDI-II is highly correlated to the amount of LTP-like plasticity, and (iv) that PA as intervention can normalize deficient neuroplasticity which—in turn—is correlated to the reduction of clinical symptoms. In addition, (v) working memory performance (N-back verbal test), executive functions (Response Inhibition) and cognitive working speed (Trail making test) tended to improve stronger after PA than after the CI.

The reduction of PAS-induced LTP-like plasticity in the motor cortex in MDD before the interventions confirms findings of previous studies (2, 6), and different mechanisms may account

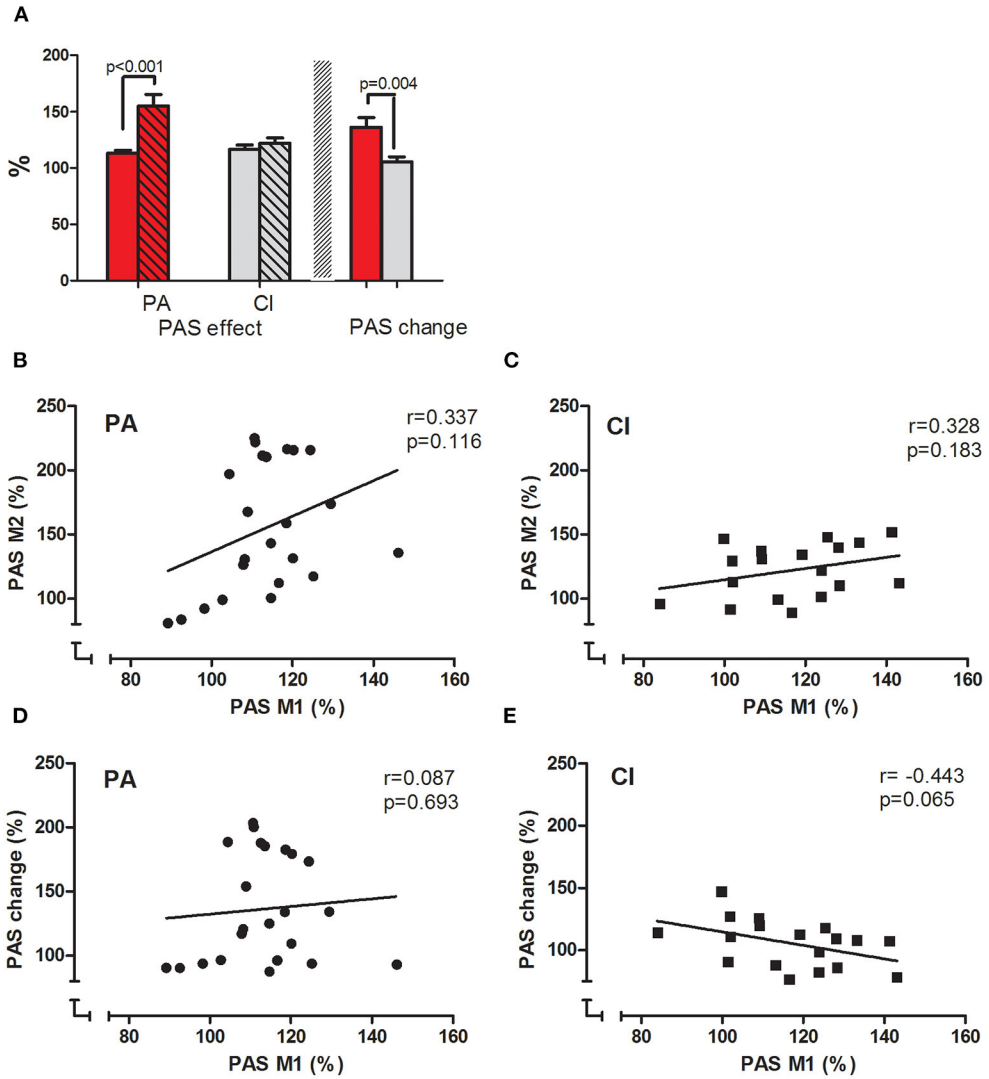

FIGURE 4 | PASeffect and correlations. **(A)** Displays the PASeffects measured before (clear bars) and after (hatched bars) the interventions in PA (red bars) and CI (gray bars) groups. The PASeffect increased significantly after the intervention in the PA group, but not in the CI group (*t*-test results are given). **(B,C)** display the correlation between the PASeffects measured before and after the intervention in PA **(B)** and CI **(C)** groups; **(D,E)** display the correlation between the PASeffect measured before the intervention and PASchange for each group [PA: **(D)** and CI: **(E)**]. The results of Pearson's correlation are given.

for this. First, changes in structural and functional synaptic plasticity, such as reduced synaptic density in dorsolateral prefrontal cortex (DLPFC), the anterior corpus callosum (ACC), and the hippocampus (5, 50, 51) are described in MDD, likely leading to reduced functional connectivity within and between networks underlying mood and cognition. The motor cortex is an important node in the brain and processes information from various inputs (52, 53) as it is strongly interconnected with numerous brain areas. Several key structures of the cognitive network, such as the DLPFC (54), the posterior parietal cortex (55), as well as frontal areas (56) have been shown to be connected to the motor cortex, as several double-pulse TMS studies (57–60) as well as cortico-cortical paired associative stimulation studies have shown (61–64). Therefore, the PASeffect measured in the motor cortex represents a valid surrogate marker for plasticity in the networks that play a key role in the pathophysiology of MDD.

Second, the induction of LTP-like plasticity depends on postsynaptic activation of NMDA-receptors (35), and the alterations in the glutamatergic system described in MDD (65) are likely to contribute to a reduction of PASeffects.

Lastly, the presence of hallmark symptoms of MDD, such as anhedonia, loss of interest and of motivation, and psychomotor retardation, might further contribute to a reduction of synaptic plasticity. A lack of physical (66) and cognitive activity, and of social interaction, deprives the brain of important stimuli, which consequently might contribute to the downscaling or loss of synapses, which are necessary to keep the brain susceptible to plastic changes (67). Enhancing neuroplasticity is therefore a

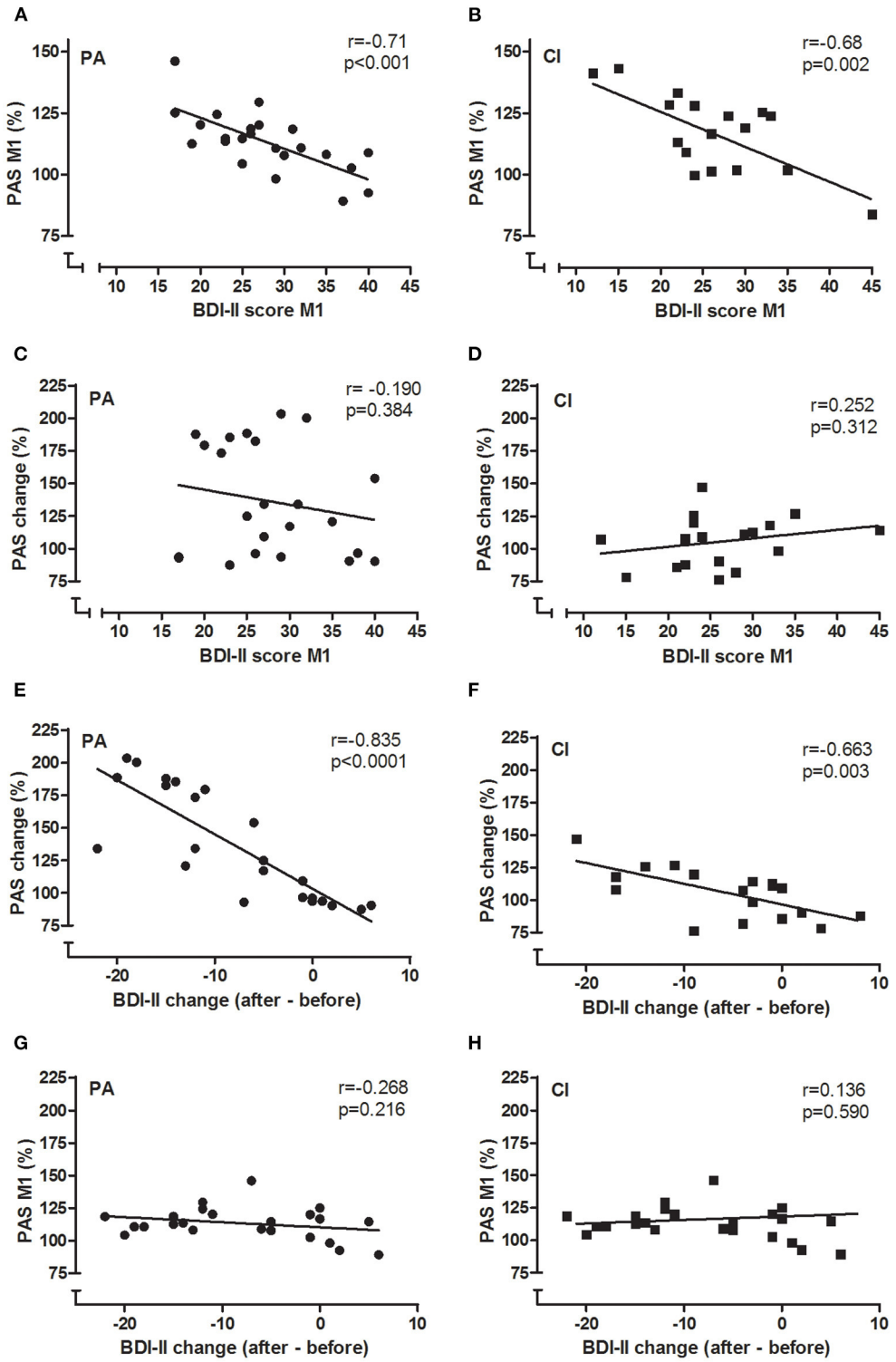

FIGURE 5 | Correlations between BDI-II and PAS. The correlations of BDI-II and PAS are given for PA **(A,C,E,G)** and CI **(B,D,F,H)** groups. Pearson's *r* and *p*-values are given in each figure. BDI-II and PASeffect measured before the intervention (M1) were negatively correlated in each group **(A,B)**: the higher the BDI-II score, the smaller was the PASeffect. Similarly, the change of BDI-II and PASeffects by the intervention were negatively correlated in each group **(E,F)**. The BDI-II at baseline did not predict the amount of PASchange that could be induced by the interventions **(C,D)**, neither did the PASeffect at baseline (M1) predict the amount of BDI-II change **(G,H)**.

TABLE 3 | Results of cognitive tests (T-scores).

		PA					CI			
Attention and working speed		**Mean**		**SEM**	**Paired *t*-test**		**Mean**		**SEM**	**Paired *t*-test**
Work performance series										
Numbers worked	Before	48.96	±	1.73		Before	52.89	±	3.03	
	After	53.35	±	1.72	$p < 0.001$	After	54.78	±	2.43	n.s.
	Δafter-before	4.39	±	0.59		Δafter-before	1.89	±	1.63	
Errors	Before	51.83	±	2.22		Before	42.89	±	3.03	
	After	52.26	±	2.21	n.s.	After	50.00	±	1.57	$p < 0.05$
	Δafter-before	0.43	±	1.99		Δafter-before	7.11	±	3.00	
Trail making test										
Part A	Before	49.61	±	0.95		Before	51.28	±	1.54	
	After	54.39	±	1.41	$p < 0.001$	After	54.78	±	2.50	n.s.
	Δafter-before	4.78	±	1.08		Δafter-before	3.47	±	1.79	
Part B	Before	52.83	±	1.27		Before	50.39	±	2.13	
	After	58.87	±	1.65	$p < 0.001$	After	54.83	±	2.31	$p < 0.001$
	Δafter-before	6.04	±	1.27		Δafter-before	4.44	±	1.03	
Executive function		**Mean**		**SEM**	**Paired *t*-test**		**Mean**		**SEM**	**Paired *t*-test**
STROOP										
Baseline reading	Before	52.13	±	1.54		Before	51.50	±	2.02	
	After	57.57	±	1.74	$p < 0.001$	After	52.50	±	2.11	n.s.
	Δafter-before	5.43	±	0.93		Δafter-before	1.00	±	1.13	
Baseline naming	Before	52.00	±	1.79		Before	50.28	±	2.34	
	After	55.57	±	1.91	$p < 0.001$	After	51.83	±	1.95	n.s.
	Δafter-before	3.57	±	0.88		Δafter-before	1.56	±	1.91	
Interference reading	Before	49.96	±	1.51		Before	45.50	±	2.96	
	After	50.48	±	1.80	n.s.	After	46.44	±	2.02	n.s.
	Δafter-before	0.52	±	1.94		Δafter-before	0.94	±	2.64	
Interference naming	Before	51.48	±	2.06		Before	52.89	±	2.67	
	After	50.22	±	1.80	n.s.	After	48.33	±	1.65	n.s.
	Δafter-before	−1.26	±	1.77		Δafter-before	−4.56	±	2.73	
Response Inhibition										
Commission errors	Before	48.61	±	1.96		Before	49.06	±	2.60	
	After	52.26	±	2.17	$p < 0.05$	After	51.33	±	2.76	n.s.
	Δafter-before	3.65	±	1.40		Δafter-before	2.28	±	2.16	
Omission errors	Before	44.78	±	1.97		Before	45.89	±	2.19	
	After	49.39	±	1.82	$p < 0.05$	After	48.72	±	2.25	n.s.
	Δafter-before	4.61	±	1.80		Δafter-before	2.83	±	1.96	
Sensitivity index	Before	46.74	±	2.25		Before	47.78	±	3.01	
	After	52.13	±	2.20	$p < 0.01$	After	50.28	±	2.60	n.s.
	Δafter-before	5.39	±	1.57		Δafter-before	2.50	±	2.09	
Tower of London										
	Before	55.83	±	2.00		before	54.22	±	1.61	
	After	57.87	±	1.35	n.s.	after	55.56	±	2.51	n.s.
	Δafter-before	2.04	±	1.85		Δafter-before	1.33	±	2.59	
Working memory	**Mean**	**SEM**	**Paired *t*-test**			**Mean**		**SEM**	**Paired *t*-test**	
N-back-verbal										
Correct answers	Before	55.65	±	3.94		Before	54.61	±	3.95	
	After	73.22	±	2.76	$p < 0.001$	After	67.00	±	4.03	$p < 0.01$
	Δafter-before	17.57	±	4.49		Δafter-before	12.39	±	3.76	

promising treatment approach, and using PA as an intervention has been proven to be clinically beneficial in MDD.

There is good evidence that PA modifies structural and functional brain plasticity (68–70). PAS-induced plasticity is higher in physically active healthy subjects compared to those with a sedentary lifestyle (8, 71). PA has been shown to increase metabolism and oxygenation, to modulate neurotransmitters and the release of neurochemical and neurotropic factors in the brain (72–77), and by these mechanisms likely contributes to the enhancement of plasticity.

After the 3 weeks of intervention, the PASeffect increased stronger in patients of the PA than of the CI group. Since parameters of neural excitability, the IOcurve and SICI, did not change, this is likely to be due to enhanced LTP-like plasticity after PA, rather than stronger motorneuronal recruitment or a reduction of GABAergic inhibition. Importantly, the PASeffect measured before the interventions was not related to PASchange, which precludes a saturation effect ("ceiling effect").

We monitored the intensity of the PA program by measuring the heart rate, and its rise to moderate levels during the PA session indicated a moderate level of physical strain for the patients; while there was no notable change of heart rate in patients of the CI group. Given the moderate intensity and short duration of the PA program, the strength of its effect on PAS-induced plasticity in MDD was surprising. In the context of synaptic density and activity being reduced in MDD (5), it might point toward enhanced susceptibility to undergo LTP-like plasticity induction, in terms of a homeostatic mechanism. Similar to increased plasticity after sensory deprivation (78), the PA program might have re-activated synaptic connections and consequently "boosted" the efficiency of the PAS protocol to induce LTP-like plasticity (79).

Previous studies using PAS (6) and measures of synaptic density (5) have described an association between the severity of depressive symptoms and neuroplasticity in MDD. We extended these findings in our study by showing that the amount of LTP-like plasticity strongly correlates with the BDI-II scores in both groups at baseline; and further, that the amount of BDI-II score reduction and the increase of PAS plasticity seen after the interventions were correlated in both groups, though stronger in the PA. However, as the baseline PASeffect was not correlated to the BDI-II score change, and the baseline BDI-II was not correlated to the PASchange, the value of the PASeffect or the BDI-II score measured before the interventions is limited with regard to predicting either the clinical outcome or the amount of neuroplastic change.

There were no such correlations of the HAMD-17 and PASeffects, nor of the HAMD-17 and BDI-II scores. However, the difference in clinical outcome was shown in the HAMD-17, which decreased significantly stronger in the PA than in the CI group.

Several studies in MDD have already shown that self- and observer-rated scales are only moderately correlated, if at all (80, 81). Compared to the BDI-II (82), the HAMD-17 (83) has a higher sensitivity to depict changes (81, 84). The scores are quite different with regard to their item structure. The BDI-II focuses more on psychological/affective and the HAMD-17 more on somatic/neurovegetative items. As a self-rated score, the BDI is dependent on the patients' self-perception which—in turn—is often compromised by the symptoms of depression themselves. As it is focussing more on cognitive symptoms, the BDI-II is likely to be less sensitive to change because cognitive symptoms are more persistent than somatic symptoms in the course of treatment (85–87). Thus, the BDI-II has probably not been sensitive enough to depict early symptom changes that might have evolved during the 3 weeks observational period. The HAMD-17 is investigator-rated, focuses stronger on somatic/neurovegetative symptoms that are more likely to remit at an earlier phase in the course of treatment, and therefore is more perceptive to change over shorter observation periods (81). Furthermore, an observer could be more likely to see improvement in depressive symptoms than a patient affected by a cognitive bias (86, 87).

Thus, if there are first signs of symptom remittance, they are more likely to present as a reduction in HAMD-17 than in BDI-II; as was the case for the patients of the PA group. The correlation of the BDI-II and PAS-induced neuroplasticity might indicate, that factors like loss of interest, indecisiveness and pessimism, which were most strongly reduced in the PA group, might be more closely associated to deficient neuroplasticity and therefore sensitive to plasticity enhancing interventions.

The patients' attention, working memory and executive functions as tested by the cognitive test battery were not notably different from the age- and education-matched healthy control group (implemented in the test battery). Similar to other studies our findings might indicate that patients with MDD achieve this level of performance by a compensatory higher level of brain network activation, and thus their cognitive capacity is compromised by recruiting more brain resources as healthy controls (88).

Though there were no statistically significant differences, the cognitive performance tended to increase more in the PA than CI groups after the interventions, hinting toward an increased cognitive capacity by PA, as similarly described in physically active healthy subjects (89–91).

The study was performed on patients during their stay on the psychiatric ward and thus the duration of the interventions was limited to 3 weeks which might have been too short a period to induce differentiated effects on cognitive symptoms. Furthermore, we tested neuroplasticity, clinical and cognitive symptoms directly after the end of the interventions. Future studies need to address how long the PA-induced changes might last for and how they might be used to facilitate standard treatment of MDD.

In summary, we showed that a PA intervention supports the remission of clinical symptoms and normalizes deficient LTP-induced neuroplasticity in MDD, and that these two observations are highly correlated. Our study therefore further highlights the role of neuroplasticity in the pathophysiology of MDD and of PA in its treatment by showing that this intervention directly targets the deficient neuroplasticity as an underlying pathophysiological mechanism. Further research is needed to explore whether the effect of therapeutic interventions, might be predicted by clinical

or neurophysiological parameters, as this would support the development of individualized treatments strategies.

DATA AVAILABILITY STATEMENT

The original contributions presented in the study are included in the article/supplementary material, further inquiries can be directed to the corresponding author/s.

ETHICS STATEMENT

The studies involving human participants were reviewed and approved by Ethics committee of the Ruhr University Bochum in Bad Oeynhausen/ Germany. The patients/participants provided their written informed consent to participate in this study.

AUTHOR CONTRIBUTIONS

WB, DK, and KR contributed to the experimental design. WB, CS, CB, SS, JS, and KR performed the experiments and contributed to the data acquisition. WB and KR analyzed and interpreted the data and wrote the manuscript. DK, CS, TS, and US contributed to the interpretation of the results. All authors gave their final approval of the version to be published.

FUNDING

This project was supported by a project grant from the Ruhr University Bochum awarded to the University Clinic of Psychiatry and Psychotherapy, Lübbecke, and to Bielefeld University, Faculty of Psychology and Sport Science, Neurocognition and Action Group (Forschungsfond für den Aufbau transdisziplinärer, medizinrelevanter Forschungskooperationen in der Region OWL).

ACKNOWLEDGMENTS

We thank the patients for their participation in the study. We thank Mrs Ulrike Bökenheide for her support in the laboratory, and Dr. Elisabeth Wilking and Dr. Angelika Böhm for their support with the recruitment of patients.

REFERENCES

1. James SL, Abate D, Abate KH, Abay SM, Abbafati C, Abbasi N, et al. Global, regional, and national incidence, prevalence, and years lived with disability for 354 diseases and injuries for 195 countries and territories, 1990–2017: a systematic analysis for the Global Burden of Disease Study 2017. *Lancet.* (2018) 392:1789–858. doi: 10.1016/S0140-6736(18)32279-7
2. Player MJ, Taylor JL, Weickert CS, Alonzo A, Sachdev P, Martin D, et al. Neuroplasticity in depressed individuals compared with healthy controls. *Neuropsychopharmacology.* (2013) 38:2101–8. doi: 10.1038/npp.2013.126
3. Malykhin NV, Coupland NJ. Hippocampal neuroplasticity in major depressive disorder. *Neuroscience.* (2015) 309:200–13. doi: 10.1016/j.neuroscience.2015.04.047
4. Noda Y, Zomorrodi R, Vila-Rodriguez F, Downar J, Farzan F, Cash RF, et al. Impaired neuroplasticity in the prefrontal cortex in depression indexed through paired associative stimulation. *Depress Anxiety.* (2018) 35:448–56. doi: 10.1002/da.22738
5. Holmes SE, Scheinost D, Finnema SJ, Naganawa M, Davis MT, DellaGioia N, et al. Lower synaptic density is associated with depression severity and network alterations. *Nat Commun.* (2019) 10:1529. doi: 10.1038/s41467-019-09562-7
6. Kuhn M, Mainberger F, Feige B, Maier JG, Mall V, Jung NH, et al. State-dependent partial occlusion of cortical LTP-like plasticity in major depression. *Neuropsychopharmacology.* (2016) 41:2794. doi: 10.1038/npp.2016.97
7. Stefan K, Kunesch E, Cohen LG, Benecke R, Classen J. Induction of plasticity in the human motor cortex by paired associative stimulation. *Brain.* (2000) 123:572–84. doi: 10.1093/brain/123.3.572
8. Ridding MC, Ziemann U. Determinants of the induction of cortical plasticity by non-invasive brain stimulation in healthy subjects. *J Physiol.* (2010) 588:2291–304. doi: 10.1113/jphysiol.2010.190314
9. Mellow ML, Goldsworthy MR, Coussens S, Smith AE. Acute aerobic exercise and neuroplasticity of the motor cortex: a systematic review. *J Sci Med Sport.* (2020) 23:408–14. doi: 10.1016/j.jsams.2019.10.015
10. Teychenne M, Ball K, Salmon J. Physical activity and likelihood of depression in adults: a review. *Prev Med.* (2008) 46:397–411. doi: 10.1016/j.ypmed.2008.01.009
11. Mammen G, Faulkner G. Physical activity and the prevention of depression: a systematic review of prospective studies. *Am J Prev Med.* (2013) 45:649–57. doi: 10.1016/j.amepre.2013.08.001
12. Choi KW, Chen C-Y, Stein MB, Klimentidis YC, Wang M-J, Koenen KC, et al. Assessment of bidirectional relationships between physical activity and depression among adults: a 2-sample Mendelian randomization study. *JAMA Psychiatry.* (2019) 76:399–408. doi: 10.1001/jamapsychiatry.2018.4175
13. Kim S-Y, Park J-H, Lee MY, Oh K-S, Shin D-W, Shin Y-C. Physical activity and the prevention of depression: a cohort study. *General Hospital Psychiatry.* (2019) 60:90–7. doi: 10.1016/j.genhosppsych.2019.07.010
14. Kvam S, Kleppe CL, Nordhus IH, Hovland A. Exercise as a treatment for depression: a meta-analysis. *J Affect Disord.* (2016) 202:67–86. doi: 10.1016/j.jad.2016.03.063
15. Schuch FB, Vancampfort D, Richards J, Rosenbaum S, Ward PB, Stubbs B. Exercise as a treatment for depression: a meta-analysis adjusting for publication bias. *J Psychiatr Res.* (2016) 77:42–51. doi: 10.1016/j.jpsychires.2016.02.023
16. Schuch FB, Vancampfort D, Firth J, Rosenbaum S, Ward PB, Silva ES, et al. Physical activity and incident depression: a meta-analysis of prospective cohort studies. *Am J Psychiatry.* (2018) 175:631–48. doi: 10.1176/appi.ajp.2018.17111194
17. Ledochowski L, Stark R, Ruedl G, Kopp M. Körperliche Aktivität als therapeutische Intervention bei Depression. *Nervenarzt.* (2017) 88:765–78. doi: 10.1007/s00115-016-0222-x
18. Martinsen EW, Medhus A, Sandvik L. Effects of aerobic exercise on depression: a controlled study. *Br Med J.* (1985) 291:109. doi: 10.1136/bmj.291.6488.109
19. Knubben K, Reischies FM, Adli M, Schlattmann P, Bauer M, Dimeo F. A randomised, controlled study on the effects of a short-term endurance training programme in patients with major depression. *Br J Sports Med.* (2007) 41:29–33. doi: 10.1136/bjsm.2006.030130
20. Schuch FB, Vasconcelos-Moreno MP, Borowsky C, Fleck MP. Exercise and severe depression: preliminary results of an add-on study. *J Affect Disord.* (2011) 133:615–8. doi: 10.1016/j.jad.2011.04.030
21. Schuch FB, Vasconcelos-Moreno MP, Borowsky C, Zimmermann AB, Rocha NS, Fleck MP. Exercise and severe major depression: effect on symptom severity and quality of life at discharge in an inpatient cohort. *J Psychiatr Res.* (2015) 61:25–32. doi: 10.1016/j.jpsychires.2014.11.005
22. Ho CW, Chan SC, Wong JS, Cheung WT, Chung DW, Lau TF. Effect of aerobic exercise training on Chinese population with mild to moderate depression in Hong Kong. *Rehabil Res Pract.* (2014) 2014:627376. doi: 10.1155/2014/627376

23. McDermott LM, Ebmeier KP. A meta-analysis of depression severity and cognitive function. *J Affect Disord.* (2009) 119:1–8. doi: 10.1016/j.jad.2009.04.022
24. McClintock SM, Husain MM, Greer TL, Cullum CM. Association between depression severity and neurocognitive function in major depressive disorder: a review and synthesis. *Neuropsychology.* (2010) 24:9–34. doi: 10.1037/a0017336
25. Rhodes RE, Kates A. Can the affective response to exercise predict future motives and physical activity behavior? a systematic review of published evidence. *Ann Behav Med.* (2015) 49:715–31. doi: 10.1007/s12160-015-9704-5
26. Williams DM, Dunsiger S, Ciccolo JT, Lewis BA, Albrecht AE, Marcus BH. Acute affective response to a moderate-intensity exercise stimulus predicts physical activity participation 6 and 12 months later. *Psychol Sport Exerc.* (2008) 9:231–45. doi: 10.1016/j.psychsport.2007.04.002
27. Ziemann U, Reis J, Schwenkreis P, Rosanova M, Strafella A, Badawy R, et al. TMS and drugs revisited 2014. *Clin Neurophysiol.* (2015) 126:1847–68. doi: 10.1016/j.clinph.2014.08.028
28. Beck AT, Steer RA, Brown GK. *Manual for Beck Depression Inventory II (BDI-II)*. San Antonio, TX: Psychological Corp (1996). doi: 10.1037/t00742-000
29. Hamilton M. A rating scale for depression. *J Neurol Neurosurg Psychiatry.* (1960) 23:56–62. doi: 10.1136/jnnp.23.1.56
30. Hamilton M. Development of a rating scale for primary depressive illness. *Br J Soc Clin Psychol.* (1967) 6:278–96. doi: 10.1111/j.2044-8260.1967.tb00530.x
31. Williams JB. Standardizing the Hamilton depression rating scale: past, present, and future. *Eur Archiv Psychiatry Clin Neurosci.* (2001) 251(Suppl.2):II6–12. doi: 10.1007/BF03035120
32. Orth M, Snijders A, Rothwell J. The variability of intracortical inhibition and facilitation. *Clin Neurophysiol.* (2003) 114:2362–9. doi: 10.1016/S1388-2457(03)00243-8
33. Rosenkranz K, Williamon A, Rothwell JC. Motorcortical excitability and synaptic plasticity is enhanced in professional musicians. *J Neurosci.* (2007) 27:5200–6. doi: 10.1523/JNEUROSCI.0836-07.2007
34. Kujirai T, Caramia MD, Rothwell JC, Day BL, Thompson PD, Ferbert A, et al. Corticocortical inhibition in human motor cortex. *J Physiol.* (1993) 471:501–19. doi: 10.1113/jphysiol.1993.sp019912
35. Stefan K, Kunesch E, Benecke R, Cohen LG, Classen J. Mechanisms of enhancement of human motor cortex excitability induced by interventional paired associative stimulation. *J Physiol.* (2002) 543:699–708. doi: 10.1113/jphysiol.2002.023317
36. Ziemann U, Ilić TV, Iliać TV, Pauli C, Meintzschel F, Ruge D. Learning modifies subsequent induction of long-term potentiation-like and long-term depression-like plasticity in human motor cortex. *J Neurosci.* (2004) 24:1666–72. doi: 10.1523/JNEUROSCI.5016-03.2004
37. Stefan K, Wycislo M, Classen J. Modulation of associative human motor cortical plasticity by attention. *J Neurophysiol.* (2004) 92:66–72. doi: 10.1152/jn.00383.2003
38. Rodewald K, Weisbrod M, Aschenbrenner S. *Trail Making Test - Langensteinbacher Version*. Mödling: Schuhfried GmbH (2012). p. 36.
39. Kaiser S, Mundt C, Weisbrod M. Exekutive Kontrollfunktionen und neuropsychiatrische Erkrankungen - Perspektiven für Forschung und Klinik. *Fortschr Neurol Psychiatr.* (2005) 73:438–50. doi: 10.1055/s-2004-830303
40. Kaiser S, Aschenbrenner S, Pfüller U, Roesch-Ely D, Weisbrod M. *Response Inhibiton*. Mödling: Schuhfried GmbH (2010).
41. Shallice T. Specific impairments of planning. *Philos Trans R Soc Lond B, Biol Sci.* (1982) 298:199–209. doi: 10.1098/rstb.1982.0082
42. Kaller CP, Unterrainer JM, Kaiser S, Weisbrod M, Aschenbrenner S. *Tower of London - Freiburger Version*. Mödling: Schuhfried GmbH (2011).
43. Stroop JR. Studies of interference in serial verbal reactions. *J Exp Psychol.* (1935) 18:643–62. doi: 10.1037/h0054651
44. Schuhfried. *Interferenztest nach Stroop*. Mödling: Schuhfried GmbH (1999). p. 29.
45. Gevins AS, Custillo BC. Neuroelectric evidence for distributed processing in human working memory. *Electroencephalogr Clin Neurophysiol.* (1993) 87:128–43. doi: 10.1016/0013-4694(93)90119-G
46. Cohen JD, Perlstein WM, Braver TS, Nystrom LE, Noll DC, Jonides J, et al. Temporal dynamics of brain activation during a working memory task. *Nature.* (1997) 386:604–8. doi: 10.1038/386604a0
47. Kirchner WK. Age differences in short-term retention of rapidly changing information. *J Exp Psychol.* (1958) 55:352–8. doi: 10.1037/h0043688
48. Soveri A, Antfolk J, Karlsson L, Salo B, Laine M. Working memory training revisited: a multi-level meta-analysis of n-back training studies. *Psychon Bull Rev.* (2017) 24:1077–96. doi: 10.3758/s13423-016-1217-0
49. Schellig D, Schuri U. *N-back verbal*. Mödling: Schuhfried GmbH (2009). p. 45.
50. Czéh B, Lucassen PJ. What causes the hippocampal volume decrease in depression? Are neurogenesis, glial changes and apoptosis implicated? *Eur Archiv Psychiatry Clin Neurosci.* (2007) 257:250–60. doi: 10.1007/s00406-007-0728-0
51. Bennett MR. The prefrontal-limbic network in depression: a core pathology of synapse regression. *Progr Neurobiol.* (2011) 93:457–67. doi: 10.1016/j.pneurobio.2011.01.001
52. Tomasi D, Volkow ND. Association between functional connectivity hubs and brain networks. *Cereb Cortex.* (2011) 21:2003–13. doi: 10.1093/cercor/bhq268
53. Berns C, Brüchle W, Scho S, Schneefeld J, Schneider U, Rosenkranz K. Intensity dependent effect of cognitive training on motor cortical plasticity and cognitive performance in humans. *Exp Brain Res.* (2020) 238:2805–18. doi: 10.1007/s00221-020-05933-5
54. Takeuchi H, Taki Y, Nouchi R, Hashizume H, Sekiguchi A, Kotozaki Y, et al. Effects of multitasking-training on gray matter structure and resting state neural mechanisms. *Hum Brain Mapp.* (2014) 35:3646–60. doi: 10.1002/hbm.22427
55. Draganski B, May A. Training-induced structural changes in the adult human brain. *Behav Brain Res.* (2008) 192:137–42. doi: 10.1016/j.bbr.2008.02.015
56. Ceccarelli A, Rocca MA, Pagani E, Falini A, Comi G, Filippi M. Cognitive learning is associated with gray matter changes in healthy human individuals: a tensor-based morphometry study. *Neuroimage.* (2009) 48:585–9. doi: 10.1016/j.neuroimage.2009.07.009
57. Civardi C, Cantello R, Asselman P, Rothwell JC. Transcranial magnetic stimulation can be used to test connections to primary motor areas from frontal and medial cortex in humans. *Neuroimage.* (2001) 14:1444–53. doi: 10.1006/nimg.2001.0918
58. Koch G, Fernandez Del Olmo M, Cheeran B, Ruge D, Schippling S, Caltagirone C, et al. Focal stimulation of the posterior parietal cortex increases the excitability of the ipsilateral motor cortex. *J Neurosci.* (2007) 27:6815–22. doi: 10.1523/JNEUROSCI.0598-07.2007
59. Davare M, Lemon R, Olivier E. Selective modulation of interactions between ventral premotor cortex and primary motor cortex during precision grasping in humans. *J Physiol.* (2008) 586:2735–42. doi: 10.1113/jphysiol.2008.152603
60. Hasan A, Galea JM, Casula EP, Falkai P, Bestmann S, Rothwell JC. Muscle and timing-specific functional connectivity between the dorsolateral prefrontal cortex and the primary motor cortex. *J Cogn Neurosci.* (2013) 25:558–70. doi: 10.1162/jocn_a_00338
61. Koch G, Ponzo V, Di Lorenzo F, Caltagirone C, Veniero D. Hebbian and anti-Hebbian spike-timing-dependent plasticity of human cortico-cortical connections. *J Neurosci.* (2013) 33:9725–33. doi: 10.1523/JNEUROSCI.4988-12.2013
62. Veniero D, Ponzo V, Koch G. Paired associative stimulation enforces the communication between interconnected areas. *J Neurosci.* (2013) 33:13773–83. doi: 10.1523/JNEUROSCI.1777-13.2013
63. Chao C-C, Karabanov AN, Paine R, Carolina de Campos A, Kukke SN, Wu T, et al. Induction of motor associative plasticity in the posterior parietal cortex-primary motor network. *Cereb Cortex.* (2015) 25:365–73. doi: 10.1093/cercor/bht230
64. Kohl S, Hannah R, Rocchi L, Nord CL, Rothwell J, Voon V. Cortical paired associative stimulation influences response inhibition: cortico-cortical and cortico-subcortical networks. *Biol Psychiatry.* (2019) 85:355–63. doi: 10.1016/j.biopsych.2018.03.009
65. Sanacora G, Zarate CA, Krystal JH, Manji HK. Targeting the glutamatergic system to develop novel, improved therapeutics for mood disorders. *Nat Rev Drug Discov.* (2008) 7:426–37. doi: 10.1038/nrd2462
66. Difrancesco S, Lamers F, Riese H, Merikangas KR, Beekman AT, van Hemert AM, et al. Sleep, circadian rhythm, and physical activity patterns in depressive and anxiety disorders: a 2-week ambulatory assessment study. *Depress Anxiety.* (2019) 36:975–86. doi: 10.1002/da.22949

67. Raichlen DA, Alexander GE. Adaptive capacity: an evolutionary neuroscience model linking exercise, cognition, and brain health. *Trends Neurosci.* (2017) 40:408–21. doi: 10.1016/j.tins.2017.05.001
68. Hötting K, Röder B. Beneficial effects of physical exercise on neuroplasticity and cognition. *Neurosci Biobehav Rev.* (2013) 37:2243–57. doi: 10.1016/j.neubiorev.2013.04.005
69. Voelcker-Rehage C, Niemann C. Structural and functional brain changes related to different types of physical activity across the life span. *Neurosci Biobehav Rev.* (2013) 37:2268–95. doi: 10.1016/j.neubiorev.2013.01.028
70. Kramer AF, Erickson KI. Capitalizing on cortical plasticity: influence of physical activity on cognition and brain function. *Trends Cogn Sci.* (2007) 11:342–8. doi: 10.1016/j.tics.2007.06.009
71. Cirillo J, Lavender AP, Ridding MC, Semmler JG. Motor cortex plasticity induced by paired associative stimulation is enhanced in physically active individuals. *J Physiol.* (2009) 587:5831–42. doi: 10.1113/jphysiol.2009.181834
72. Sparling PB, Giuffrida A, Piomelli D, Rosskopf L, Dietrich A. Exercise activates the endocannabinoid system. *Neuroreport.* (2003) 14:2209–11. doi: 10.1097/00001756-200312020-00015
73. Dietrich A, McDaniel WF. Endocannabinoids and exercise. *Br J Sports Med.* (2004) 38:536–41. doi: 10.1136/bjsm.2004.011718
74. Duman RS, Monteggia LM. A neurotrophic model for stress-related mood disorders. *Biol Psychiatry.* (2006) 59:1116–27. doi: 10.1016/j.biopsych.2006.02.013
75. Dishman RK, Berthoud H-R, Booth FW, Cotman CW, Edgerton VR, Fleshner MR, et al. Neurobiology of exercise. *Obesity.* (2006) 14:345–56. doi: 10.1038/oby.2006.46
76. Sarbadhikari SN, Saha AK. Moderate exercise and chronic stress produce counteractive effects on different areas of the brain by acting through various neurotransmitter receptor subtypes: a hypothesis. *Theoret Biol Med Model.* (2006) 3:33. doi: 10.1186/1742-4682-3-33
77. Deslandes A, Moraes H, Ferreira C, Veiga H, Silveira H, Mouta R, et al. Exercise and mental health: many reasons to move. *Neuropsychobiology.* (2009) 59:191–8. doi: 10.1159/000223730
78. Orczyk JJ, Garraghty PE. Reconciling homeostatic and use-dependent plasticity in the context of somatosensory deprivation. *Neural Plast.* (2015) 2015:290819. doi: 10.1155/2015/290819
79. Desai NS. Homeostatic plasticity in the CNS: synaptic and intrinsic forms. *J Physiol Paris.* (2003) 97:391–402. doi: 10.1016/j.jphysparis.2004.01.005
80. Carter JD, Frampton CM, Mulder RT, Luty SE, Joyce PR. The relationship of demographic, clinical, cognitive and personality variables to the discrepancy between self and clinician rated depression. *J Affect Disord.* (2010) 124:202–6. doi: 10.1016/j.jad.2009.11.011
81. Schneibel R, Brakemeier E-L, Wilbertz G, Dykierek P, Zobel I, Schramm E. Sensitivity to detect change and the correlation of clinical factors with the Hamilton Depression Rating Scale and the Beck Depression Inventory in depressed inpatients. *Psychiatry Res.* (2012) 198:62–7. doi: 10.1016/j.psychres.2011.11.014
82. Edwards BC, Lambert MJ, Moran PW, McCully T, Smith KC, Ellingson AG. A meta-analytic comparison of the Beck Depression Inventory and the Hamilton Rating Scale for Depression as measures of treatment outcome. *Br J Clin Psychol.* (1984) 23:93–9. doi: 10.1111/j.2044-8260.1984.tb00632.x
83. Lambert MJ, Hatch DR, Kingston MD, Edwards BC. Zung, Beck, and Hamilton Rating Scales as measures of treatment outcome: a meta-analytic comparison. *J Consult Clin Psychol.* (1986) 54:54–9. doi: 10.1037/0022-006X.54.1.54
84. Sayer NA, Sackeim HA, Moeller JR, Prudic J, Devanand DP, Coleman EA, et al. The relations between observer-rating and self-report of depressive symptomatology. *Psychol Assess.* (1993) 5:350–60. doi: 10.1037/1040-3590.5.3.350
85. Prusoff BA, Klerman GL, Paykel ES. Concordance between clinical assessments and patients' self-report in depression. *Arch Gen Psychiatry.* (1972) 26:546–52. doi: 10.1001/archpsyc.1972.01750240058009
86. Rush AJ, Hiser W, Giles DE. A comparison of self-reported versus clinician-related symptoms in depression. *J Clin Psychiatry.* (1987) 48:246–8.
87. Rush AJ, Trivedi MH, Carmody TJ, Ibrahim HM, Markowitz JC, Keitner GI, et al. Self-reported depressive symptom measures: sensitivity to detecting change in a randomized, controlled trial of chronically depressed, nonpsychotic outpatients. *Neuropsychopharmacology.* (2005) 30:405–16. doi: 10.1038/sj.npp.1300614
88. Harvey P-O, Fossati P, Pochon J-B, Levy R, Lebastard G, Lehéricy S, et al. Cognitive control and brain resources in major depression: an fMRI study using the n-back task. *Neuroimage.* (2005) 26:860–9. doi: 10.1016/j.neuroimage.2005.02.048
89. Dregan A, Gulliford MC. Leisure-time physical activity over the life course and cognitive functioning in late mid-adult years: a cohort-based investigation. *Psychol Med.* (2013) 43:2447–58. doi: 10.1017/S0033291713000305
90. Cox EP, O'Dwyer N, Cook R, Vetter M, Cheng HL, Rooney K, et al. Relationship between physical activity and cognitive functison in apparently healthy young to middle-aged adults: a systematic review. *J Sci Med Sport.* (2016) 19:616–28. doi: 10.1016/j.jsams.2015.09.003
91. Gaertner B, Buttery AK, Finger JD, Wolfsgruber S, Wagner M, Busch MA. Physical exercise and cognitive function across the life span: results of a nationwide population-based study. *J Sci Med Sport.* (2018) 21:489–94. doi: 10.1016/j.jsams.2017.08.022

Conflict of Interest: The authors declare that the research was conducted in the absence of any commercial or financial relationships that could be construed as a potential conflict of interest.

frontiers in Psychiatry

ORIGINAL RESEARCH
published: 23 August 2021
doi: 10.3389/fpsyt.2021.715898

fMRI Neurofeedback-Enhanced Cognitive Reappraisal Training in Depression: A Double-Blind Comparison of Left and Right vlPFC Regulation

Micha Keller[1], Jana Zweerings[1], Martin Klasen[1,2], Mikhail Zvyagintsev[1], Jorge Iglesias[3], Raul Mendoza Quiñones[3] and Klaus Mathiak[1,4]*

[1] Department of Psychiatry, Psychotherapy and Psychosomatics, School of Medicine, RWTH Aachen University, Aachen, Germany, [2] Interdisciplinary Training Centre for Medical Education and Patient Safety—AIXTRA, Medical Faculty, RWTH Aachen University, Aachen, Germany, [3] Department of Cognitive Neuroscience, Cuban Center for Neuroscience, Havana, Cuba, [4] JARA-Brain, Research Center Jülich, Jülich, Germany

OPEN ACCESS

Edited by:
Hongming Li, University of Pennsylvania, United States

Reviewed by:
Dandan Zhang, Shenzhen University, China
Jennifer Barredo, Providence VA Medical Center, United States

***Correspondence:**
Micha Keller
mkeller@ukaachen.de;
kmathiak@ukaachen.de

Specialty section:
This article was submitted to Neuroimaging and Stimulation, a section of the journal Frontiers in Psychiatry

Received: *27 May 2021*
Accepted: *29 July 2021*
Published: *23 August 2021*

Citation:
Keller M, Zweerings J, Klasen M, Zvyagintsev M, Iglesias J, Mendoza Quiñones R and Mathiak K (2021) fMRI Neurofeedback-Enhanced Cognitive Reappraisal Training in Depression: A Double-Blind Comparison of Left and Right vlPFC Regulation. Front. Psychiatry 12:715898. doi: 10.3389/fpsyt.2021.715898

Affective disorders are associated with maladaptive emotion regulation strategies. In particular, the left more than the right ventrolateral prefrontal cortex (vlPFC) may insufficiently regulate emotion processing, e.g., in the amygdala. A double-blind cross-over study investigated NF-supported cognitive reappraisal training in major depression ($n = 42$) and age- and gender-matched controls ($n = 39$). In a randomized order, participants trained to upregulate either the left or the right vlPFC during cognitive reappraisal of negative images on two separate days. We wanted to confirm regional specific NF effects with improved learning for left compared to right vlPFC (ClinicalTrials.gov NCT03183947). Brain responses and connectivity were studied with respect to training progress, gender, and clinical outcomes in a 4-week follow-up. Increase of vlPFC activity was stronger after NF training from the left- than the right-hemispheric ROI. This regional-specific NF effect during cognitive reappraisal was present across patients with depression and controls and supports a central role of the left vlPFC for cognitive reappraisal. Further, the activity in the left target region was associated with increased use of cognitive reappraisal strategies ($r = 0.48$). In the 4-week follow-up, 75% of patients with depression reported a successful application of learned strategies in everyday life and 55% a clinically meaningful symptom improvement suggesting clinical usability.

Keywords: real-time fMRI neurofeedback, depression, emotion regulation, cognitive reappraisal, lateral PFC

INTRODUCTION

In everyday life we are frequently challenged by situations that evoke negative emotions. As part of an adaptive response to these encounters we may change the experience and expression of our emotions by using emotion regulation (1). However, the success of our emotional response modulation may depend on our mental condition. For instance, emotion dysregulation is a characteristic symptom of major depressive disorder (MDD). Increased selective attention and

processing of negative mood-congruent stimuli as well as maladaptive emotional responses may propel the development and recurrence of depressive episodes (2–4). A recent meta-analysis indicates that patients with depression show abnormal recruitment of the emotion regulation brain network during cognitive reappraisal of negative images (5). Furthermore, patients with depression often find it difficult to spontaneously utilize these strategies in everyday situations (6, 7) and methods are needed to bridge the gap between theory and everyday life application. A recent study by (8) has shown that even a single session of real-time functional magnetic imaging neurofeedback (rtfMRI-NF) could enhance the transfer of skills learned by patients with depression during CBT to real-world situations. RtfMRI-NF is a novel technique by which individuals with psychiatric disorders can learn to voluntarily self-regulate their brain signal in areas amongst others involved in the neural circuitry of emotion regulation and thereby induce changes in neural plasticity (9–13). Therefore, providing NF can inform neuroscience-based interventions for emotion dysregulation and may offer a more specific clinical tool for augmenting self-regulation in patients with depression by strengthening the monitoring within the emotion regulation process (7, 14).

Cognitive reappraisal is essential for psychological functioning and well-being and has been linked to lower levels of psychopathology (15). This strategy is focused on lowering the valence of negative situations by reinterpreting its meaning in a more positive way (1). This process is associated with a decrease in negative and an increase in positive affect (16). It mediates the relationship between stress and depressive symptoms (17) and may be beneficial on the long run by decreasing the impact of recurrent negative stimuli (18). Yet, patients with depression tend to overuse maladaptive emotion regulation strategies such as rumination as well as suppression of emotional experiences (19–21) which adds to the negativity bias of attention, information processing and memory formation (22–24). Emotion dysregulation may facilitate the development and recurrence of symptoms of depression (25, 26). As cognitive reappraisal strategies are not frequently used by patients with depression (20, 27–29), training reappraisal ability is an established component of cognitive behavioral therapy (CBT) (30, 31). CBT modulates the neural circuitry of emotions (32). Furthermore, self-reported reappraisal success following CBT in patients with social anxiety disorder predicted symptom reductions (33). Despite of promising effects, patients often struggle to transfer these cognitive strategies from theoretical to real-world applications (34). This can be supported by web-based interventions that train cognitive reappraisal on a regular basis by receiving feedback from peers (35) or instead by rtfMRI NF training (8).

On the neurobiological level, the downregulation of emotional reactivity in healthy participants is associated with a widespread network including frontal, parietal as well as subcortical regions (36–38). In this network, the vlPFC seems to play a pivotal role for the process of emotion regulation due to its dense structural and functional connections to other prefrontal, somatosensory, motor and language areas and its link to response selection and inhibition (37). Furthermore, gray matter volume reductions in the vlPFC have been found in patients with depression (39). Especially reinterpretation (compared to distancing) of negative affective content has been related to peak activation in the left vlPFC and the left STG (40). The vlPFC relays the need to regulate to a fronto-parietal cognitive control network (dlPFC, pre-SMA, STG, posterior parietal cortex) which is subsequently involved in the execution of regulation (37). Cognitive reappraisal or related emotion regulation strategies that are applied in response to emotional provocation, modulate the semantic representation of an emotional stimulus and the emotional responding through subcortical pathways (36, 41). Interestingly, gender differences in cognitive regulation such as more rumination and catastrophizing in females (42) and alcohol for coping in men (43) have also been observed on the neural level (44). Meta-analyses have investigated differences during emotion regulation between healthy controls and individuals with depression (5, 40). Hyperactivity in the amygdala during downregulation of negative stimuli has consistently been reported to be specific for affective disorders which indicates increased bottom-up responding or ineffective modulatory capacity of regulatory networks during emotion appraisals (5). Furthermore, the vlPFC and dlPFC (5) as well as the left STG (40) show less activation in patients with mood disorders which may be related to a dysfunctional management of attentional and inhibitory resources and make these areas potential targets for NF training.

Neuromodulation approaches of emotion regulation networks not only underline the causal role of the lPFC for cognitive reappraisal but also show promise for improving depressive symptomatology. For instance, repetitive transcranical magnetic stimulation (rTMS) over the lPFC is an evidence-based treatment for depression which is successfully applied in treatment refractory depression (45, 46). In a meta-analysis of therapeutic responses to brain stimulation in depression (47), excitatory rTMS seemed to perform better at the left than the right lPFC (odds ratio: 1.89) and the reversed pattern was observed after inhibitory stimulation (OR: 3.29). These comparisons, however, did not encompass direct comparison within studies and failed to show a statistically significant difference. The causal role of the vlPFC in specific is supported by experimental TMS studies that demonstrated a facilitation of reappraisal after vlPFC stimulation (48, 49). In a similar vein, transcranial direct current stimulation (tDCS) of the vlPFC may influence emotion regulation. For instance, excitatory tDCS stimulation of the vlPFC facilitated the downregulation of negative emotions using cognitive reappraisal compared to dlPFC or sham stimulation (50–52). Taken together, these findings further support a key role of the lPFC for mood disorders and show that especially the vlPFC is a suitable target for NF-supported emotion regulation training.

EEG and fMRI studies indicate that the laterality of neural activation may be indicative of affective style. According to the frontal asymmetry model, relatively higher right frontal alpha power (more left PFC neural activity) suggests approach-related emotions while higher left frontal alpha power (more right PFC neural activity) may relate to withdrawal-related emotions (53, 54). Furthermore, electrophysiological studies have suggested that left-sided frontal alpha asymmetry (FAA; higher alpha

power in the left compared to right frontal channels) may be a biomarker of depression [e.g., (55)]. Even though the relation of FAA and depression may be only of small magnitude and use of FAA as a biomarker of depression seems too farfetched (56), frontal EEG asymmetry may be used as index of emotion regulation capability (57). For instance, a shift toward left asymmetry induced by mindfulness training was associated with improved responses during emotional challenges (58). In an EEG emotion regulation paradigm, individuals with higher capacity for reappraisal showed more left-lateralized (ventro) lateral PFC activation (59). Consequently, recruitment of left-lateralized PFC areas was associated with creating alternative appraisals of negative situations. Furthermore, in an fMRI investigation of laterality, less activation of the left relative to right IFG was associated with poor performance on an emotion perception task (60). Lastly, in a combined rtfMRI-EEG-NF paradigm, patients with depression achieved a shift toward left frontal activation as well as simultaneous changes in amygdala neural activity laterality, indicating an enhancement of approach motivation (61). These studies indicate that training left relative to right hemispheric IFG activity may be beneficial for patients with depression. Nevertheless, the right vlPFC seems to exhibit similar effects as the left hemispheric cognate in social perception (48, 50).

So far, several rtfMRI NF studies training self-regulation of emotion processing areas suggest this method may have an added benefit for the treatment of depression (62, 63). A reduction of depressive symptomatology has been achieved by training upregulation of the amygdala (64, 65) and of areas responsive to positive mental imagery (66, 67). To date, only one NF study trained patients with depression to downregulate brain activity in response to negative stimuli. Hamilton et al. (68) observed that providing patients with real [salience network (SN) node] compared to yoked feedback during an emotion regulation task led to decreased SN responses and greater reduction of emotional responses to negative stimuli. Successful downregulation of subcortical emotional processing areas such as the amygdala has also been shown in healthy individuals (69). Furthermore, limbic activity can indirectly be influenced by increasing top-down regulation. For instance, Sarkheil et al. (70) showed that attenuation of amygdala responses during emotion regulation training in healthy individuals could be enhanced by receiving feedback from the lateral PFC. In a similar NF-supported emotion regulation paradigm, Zweerings et al. (71) found reduced amygdala responses when receiving NF vs. not receiving NF in patients with posttraumatic stress disorder. Furthermore, the level of amygdala attenuation could be associated with improved symptomatology and negative affect 4 weeks later. In a preliminary report by Takamura et al. (72), rtfMRI NF of the left dlPFC was associated with clinical measures of depression. Patients with depression show deficient top-down regulation and may profit from NF-guided cognitive reappraisal training which may ease the transition from laboratory settings to the application in daily life. Emotion regulation strategies such as cognitive reappraisal are difficult to apply in emotionally demanding (high stress) situations and ways to train cognitive reappraisal more effectively may be beneficial. RtfMRI NF provides an objective neural indicator of regulation success that may improve identification of successful regulation strategies and strengthen experienced self-efficacy.

In the current study, we investigated the feasibility of a NF-guided cognitive reappraisal training in patients with depression using a double-blind cross-over design. On two separate NF training days, participants upregulated either the left or right vlPFC in response to negative pictures by applying strategies of cognitive reappraisal. Based on the reviewed fMRI and EEG literature, we hypothesized that the left compared to right vlPFC may be more important for the emotion regulation process. Therefore, the right vlPFC was chosen as active control condition as it is known to be involved in cognitive reappraisal, however, it is less consistently observed and activation levels tend to be lower (37, 70, 71). An active control condition can circumvent the problem of causing frustration as regulation is expected to be possible in both conditions. Accordingly, motivation levels between conditions are likely comparable. Following this line of interpretation, we hypothesized that (1) learning of regulation would be enhanced by feedback from the left compared to the right vlPFC. This hypothesis reflected the double-blind randomization condition and was registered a-priori as primary outcome (NCT03183947). To further explore effects of the training, we (2) investigated neurofeedback effects on the whole-brain level as well as (3) task-dependent changes in connectivity patterns. Lastly, we (4) hypothesized that successful regulation during NF would be accompanied by changes in measures of mood, emotion regulation and depressive symptomatology.

METHOD

Participants

Forty-two patients with major depressive disorder (MDD) and 39 age and gender matched healthy individuals completed the rt-fMRI NF training. All participants had adequate knowledge of the German language, normal or corrected to normal vision and were right-handed. Exclusion criteria were contraindications to MRI, traumatic brain injury, neurological illness, serious suicidal ideation, or inability for informed consent. Furthermore, healthy participants were not included if they had a history of psychiatric illness assessed with the screening questions of the German version of the Structured Clinical Interview for assessment of DSM-IV-TR criteria [SCID-I; (73)]. All patients fulfilled the formal criteria of a diagnosis of an acute MDD such as established by a psychiatrist. We included patients meeting criteria for comorbid disorders in addition to MDD. The diagnosis was confirmed according to the Diagnostic and Statistical Manual of Mental Disorders (DSM-IV-TR; American Psychiatric Association) (73) criteria by an experienced psychologist. Average number of MDEs was 4.5 ($\pm$ 5.7) and average duration of illness was 8.4 years ($\pm$ 8.0). Patients had a stable level of medication for at least 1 week prior to inclusion and during the time of the study. For the analysis, three patients were excluded due to remission at the time of NF training and two control participants were excluded due to excessive head movement during measurements and lost data (technical problems in real-time processing). Accordingly, the analyzed

sample consisted of 39 patients (35.2 ± 2.2 years; 17 female) and 37 healthy controls (32.3 ± 2.1 years; 15 female). Groups did not differ with respect to age [$t_{(74)} = -0.96$, $p = 0.34$] and years of education [$t_{(74)} = 0.78$, $p = 0.44$] (**Table 1** for more information). The study was pre-registered at clinicaltrials.gov (NCT7171). Due to constraints in recruitment procedures the subsample of patients with schizophrenia has not been completed until now. The study was approved by the local Ethics Committee of the RWTH Aachen (EK 050/17) and all participants provided written informed consent.

Experimental Procedure

In a randomized, double-blind cross-over design (see **Figure 1A**), participants were trained to upregulate their brain activation in the anatomically defined region of interest (ROI) (left or right ventrolateral prefrontal cortex, vlPFC). At the first *visit*, patients underwent the SCID interview and were assessed on the items of the Hamilton Rating Scale for Depression (HAM-D) (74). Furthermore, all participants completed questionnaires and received a standardized cognitive reappraisal training and instructions about the NF training. The second *visit* entailed two baseline cognitive reappraisal runs without NF (1st run: decrease negative feelings in response to aversive pictures; 2nd run: increase positive feelings in response to pleasant pictures) as well as anatomical recordings. However, second day data is not part of the current analyses. The NF training was completed on the *third and fourth visit* with random allocation to the order of left vs. right vlPFC regulation. This was done in a double-blind manner as investigators saw the time-courses of both left and right vlPFC ROIs during the NF training, however, were blind to which ROI was used for feedback computation. Trainings were separated by at least 1 week. On each NF day, participants completed four NF runs (∼7 min each), each comprised of 9 regulation blocks. Participants received intermittent numerical feedback, signaling the increase in brain activation within the target ROI. Each NF training was preceded and followed by a resting state (RS) fMRI measurement. In a *follow-up* telephone interview 4 weeks after completing the last NF training, the change of symptomatology, affect, and emotion regulation strategy use were assessed.

Cognitive Reappraisal Training for Emotion Regulation

A 30-min training entailed instructions and information about the NF procedure and training on the content and application of reappraisal strategies. Participants were told that the goal of the NF training was to temporarily enhance activation in a region of the brain that has been associated with the regulation of emotions. Emotional reactions to negative stimuli were discussed and participants learned to apply reappraisal strategies. In specific, participants saw negative stimuli and were instructed to use reappraisal strategies to reduce their negative affect. Suggested strategies were to think (1) the situation will change in the future, (2) the situation is not as bad as it looks. Participants could also imagine that the situation is not real or change their perspective (e.g., professional). Lastly, it was explained that a more successful cognitive reappraisal could be associated with increased activation in the target region and higher NF scores.

NF Task

The NF task was adapted from our previous study in patients with PTSD (71) and consisted of 18 blocks of picture presentation (12 s each; see **Figure 1B**). The task was either to passively view a picture and to allow spontaneous thoughts and emotions to occur ("view" condition) or to upregulate the BOLD signal in the respective target region by using a cognitive reappraisal strategy to reduce negative feelings associated with the presented picture ("reappraise" condition). The condition was indicated by a fixation cross ("x" = view; "+" = reappraise). Each picture presentation (12 s) was followed by a 4 s rest period (display of "x" or "+") and 4 s presentation of either a numerical feedback value (1–99) after "reappraise" condition or a placeholder ("%%") after the "view" condition, respectively. During the "reappraise" condition participants were free to try strategies related to cognitive reappraisal. They were, however, asked to stick to the same strategy during a regulation block. Prior to and following each NF run, participants indicated their emotional state using a Self-Assessment Manikin (SAM) from 1 to 9 (valence and arousal).

Stimuli

For the NF training, 72 pictures with negative valence were selected from the International Affective Picture System (IAPS). The IAPS contains pictures validated on valence (1–9; 1 = extremely negative) and arousal (1–9; 1 = no arousal) (75). From these 72 pictures (see **Appendix A**), two sets of 36 pictures were selected which were matched for overall valence and arousal (Set1: MeanValence = 2.55 ± 0.31, MeanArousal = 5.82 ± 0.53; Set2: MeanValence = 2.54 ± 0.36, MeanArousal = 5.81 ± 0.48) and the two semi-randomized versions of these sets were randomized over days. Each complete set consisted of two subsets of 18 pictures. One subset was used for Run 1 and 3 whereas the other was used for Run 2 and 4. The order of "view" and "reappraise" was switched within each subset for each repetition. Within subsets "view" and "reappraise" pictures were also matched for valence and arousal. All chosen pictures were related to one of four categories ("accident," "assault," "sadness," "other") and each "view-reappraise" cycle showed two pictures of the same category.

Questionnaires and Neuropsychological Assessment

Symptom severity was assessed at different time points using well-established measures of depression and related features. At baseline, the patients completed the German version of the 21-item Hamilton Rating Scale for Depression (74) as well as the Becks Depression Inventory (BDI-II) (76), the Hospital Anxiety and Depression Scale (HADS) (77), the Chapman Anhedonia Scale (78), the Emotion Regulation Questionnaire (ERQ) (73), and the Heidelberg Form for Emotion Regulation Strategies (HFERST) (79). The BDI-II as well as the ERQ and HFERST were repeated on the day of the first MRI measurement if the time between baseline and first fMRI measurement was >1 week

TABLE 1 | Demographic and clinical data.

	MDD ($n = 39$)		HC ($n = 37$)			Comparison	
	Mean	**SD**	**Mean**	**SD**	***Df***	***t***	***p***
Age (years)	35.2	13.6	32.3	12.8	74	−0.96	0.34
Education (years)	14.3	2.5	14.8	2.6	74	0.78	0.44
Parental education (years)	13.7	2.7	13.6	3.2	67	−0.16	0.88
Socioeconomic status (monthly income in Euro)	1,372	1,191	1,115	1,034	72	−0.99	0.33
Clinical characteristics							
ERQ[a] -							
Reappraisal	3.8	1.3	5.0	0.8	71	4.7	**<0.001**
Suppression	4.3	1.3	3.6	1.1	71	−2.4	**<0.05**
HFERST[b] -							
Reappraisal	2.7	0.8	3.7	0.6	71	5.7	**<0.001**
Acceptance	2.8	1.1	3.8	0.7	71	5.0	**<0.001**
Problem solving	3.7	1.0	4.3	0.5	71	3.2	**<0.01**
Social support	2.4	1.2	3.4	1.0	71	3.8	**<0.001**
Rumination	4.0	0.7	3.1	0.7	71	−5.1	**<0.001**
Avoidance	3.5	1.2	2.8	0.8	71	−2.9	**<0.01**
Experience suppression	2.8	0.7	2.4	0.6	71	−2.7	**<0.05**
Expressive suppression	3.4	1.0	3.0	0.7	71	−1.8	0.08
Verbal IQ (WST[c])	31.0	5.0	31.9	5.4	74	0.73	0.47
Digit span	15.2	4.3	15.2	3.8	74	0.04	0.97
Digit symbol test	55.3	13.9	58.1	11.4	72	0.96	0.34
Anhedonia (Chapman)	16.2	5.4	10.6	5.8	74	−4.3	**<0.001**
HADS[d] - Anxiety	10.9	3.2	4.7	4.6	74	−6.9	**<0.001**
HADS - Depression	10.9	3.9	2.8	3.6	74	−9.5	**<0.001**
HAM-D[e]	16.5	7.5					
BDI-II[f] baseline	26.8	11.5	3.8	4.2	73	−10.8	**<0.001**
Average number of MDEs	4.5	5.7					
Duration of illness	8.5	8.0					
Antidepressants[g] ($N = 35$)	198.0	137.7					
Antipsychotics[g] ($N = 5$)	48.0	68.9					
Comorbidities *N* (%)							
Dysthimia	1 (2.56)						
Anxiety Disorders	24 (61.5)						
Eating Disorders	2 (5.13)						

ERQ[a], emotion regulation questionnaire; HFERST[b], heidelberg Form for emotion regulation strategies; WST[c], wortschatztest; HADS[d], hospital anxiety and depression scale; HAM-D[e], hamilton depression rating scale; BDI-II[f], beck depression inventory-II; [g], medication is reported as percentage of the defined daily dose. Bold values indicate significant difference between healthy individuals and patients with depression.

and were completed again before the first and second NF training and at follow-up. All questionnaires (excluding HAM-D) were also completed by healthy individuals. Mood as measured by the Positive and Negative Affect Schedule (PANAS) (80) was assessed at baseline, before and after each fMRI measurement and at follow-up. Furthermore, to assess meta-cognitive awareness of regulation success a short interview was completed before and after each rtfMRI NF measurement. Before each NF training (Pre-NF interview), participants were asked (1) whether they think they generally have control over their brain activity ("yes" or "no") as well as the level of perceived control (0 = no control; 10 = a lot of control), (2) whether they think they will be able to regulate their brain signal during the NF training ("yes" or "no") and the expected level of control (0 = not at all; 10 = very much) and (3) how successful they expect to be in using the strategy of cognitive reappraisal during the NF training (0 = not at all; 10 = very successful). Following each NF training (Post-NF interview), participants were asked (1) whether they thought they were able to regulate their brain signal during the training ("yes" or "no") and about the level of perceived control (0–10), (2) how well the application of the cognitive reappraisal strategy worked (0 = not at all; 10 = very good) and (3) to rank how often they used the suggested (or other) strategies. Further, a selection of negative pictures viewed and reappraised during the

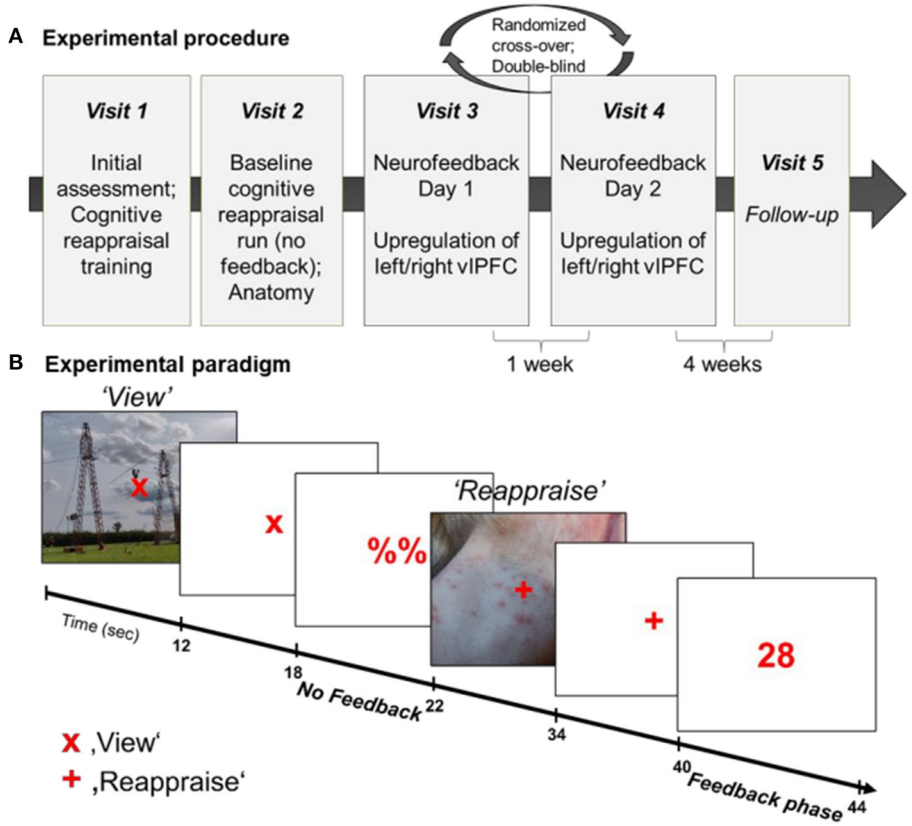

FIGURE 1 | (A) Experimental procedure. The NF training entailed 5 visits to the lab, starting with initial assessment and cognitive reappraisal training (Visit 1), followed by baseline cognitive reappraisal runs and anatomical recordings (Visit 2), two NF training days (Visit 3 and 4) and a follow-up assessment (Visit 5). **(B)** Experimental paradigm during NF training. All participants completed 4 NF runs on each of the two NF days. Each NF run entailed 9 view-regulate cycles. During "view" trials ("x"), participants passively viewed the picture and could allow spontaneous thoughts and emotions. On "regulate" trials ("+") participants reappraised the picture to reduce the negative affect and upregulate the BOLD signal in the target area. Each picture was presented for 12 s, followed by a 6-s fixation cross and 4-s (pseudo-) neurofeedback interval.

NF training were rated on valence and arousal after each training day and the applied regulation strategies were noted. To assess cognitive performance, a verbal intelligence test (Wortschatztest – WST) (81), a working memory test measuring the capacity to store numbers (digit-span task) as well as the Digit Symbol Substitution Test were administered.

fMRI Data Acquisition

A 3.0 T whole body scanner (Magnetom TRIO, Siemens Medical Systems, Erlangen, Germany) with a standard 20-channel head coil was used to acquire the fMRI data. For baseline cognitive reappraisal runs as well as NF runs, 230 T2*- weighted whole-brain functional images were recorded using echo-planar imaging (TR = 2,000 ms, TE = 28 ms, flip angle = 77°, voxel size = 3 × 3 × 3 mm, matric size = 64 × 64, ascending interleaved acquisition of 34 transverse slices, 3 mm slice thickness, 0.75 mm gap). Furthermore, high resolution T1-weighted images were acquired using a MPRAGE sequence (TE = 3.03 ms, inversion time TI = 900 ms, TR = 2,000 ms, flip angle = 9°, FOV = 256 × 256 mm2, 1 mm isotropic voxels, 0.5 mm gap, 176 sagittal slices).

Online Real-Time fMRI Analysis

Online analysis of functional data during real-time fMRI was performed using Turbo-BrainVoyagerTM (TBV) Version 3.2 (Brain Innovation, Maastricht, NL) as elsewhere described in more detail (82). Online preprocessing included 3D motion detection and correction as well as intra session alignment for subsequent NF runs (alignment to reference volume of the first run), linear trend removal, spatial smoothing with 3 mm Gaussian smoothing kernel and temporal filtering (drift removal). Statistics were computed incrementally using a general linear model (GLM) based on the predefined stimulation protocol. The BOLD percentage signal change within the ROI was calculated using the "reappraise > view" contrast and fed back as a positive number between 1 and 99 reflecting 0–1% BOLD signal change. Feedback was computed and presented with custom scripts running under Matlab R2014a (The MathWorks Inc., Natick, MA).

ROI Definition

Predefined anatomical ROIs, namely the left and right vlPFC, were used for NF training. The chosen ROIs are major hubs

of the cognitive reappraisal network and were based on peak coordinates provided by a meta-analysis about the neural correlates of cognitive reappraisal in healthy individuals (37). The lateral PFC has been shown to be consistently recruited during cognitive reappraisal of negative stimuli and activation in the vlPFC is altered in depression (5). For a comparable selection of left and right vlPFC, the mirrored center of the MNI coordinates of left and right vlPFC (left vlPFC: −42,22, −6; right vlPFC: 50,30, −8) (37) were selected as respective ROIs (± 46, 26, −7) and transformed to Tailarach space (± 44, 22, 3) using the "mni2tal" web application (https://bioimagesuiteweb.github.io/webapp/mni2tal.html). Based on these coordinates, ROIs (10 × 10× 10 mm) were created for the left and right vlPFC using BrainVoyager QX 2.8 (Brain Innovation, Maastricht, NL). These standardized ROIs were applied using coregistration of individual anatomical scans to the Tailarach template.

TBV Based ROI Analysis

To test our primary hypothesis concerning a learning effect of self-control over the neuronal activity within the target ROIs we examined the feedback data recorded during NF trainings. Investigation of the learning effect is in line with the consensus paper by Ros et al. (83). To avoid confounds such as order effects, only the first day of NF training was used for this analysis. The ROI data created by TBV during online processing was exported to and analyzed in Matlab R2018. Similar to the online FB calculation, differences between regulation and view blocks were calculated for each regulation trial (4 runs each with 9 reappraise-view trials) to investigate the learning effect within runs. Learning within runs was defined as a linear increase as suggested by the "consensus" (83), computed as linear regression slope across trials for each NF run. Separate independent *t*-tests investigated differences in learning in the left and right ROI between groups and between receiving left vs. right feedback. Associations between learning success (average learning slope in vlPFC ROI) with changes in self-rating of depressive severity [BDI-II Total score (Post NF1) – BDI-II Total score (baseline)] and cognitive reappraisal [ERQ-CR Total score (Post NF1) – ERQ-CR Total score (baseline)] were calculated. Accordingly, improvement of depressive symptomatology was indicated by a negative change score whereas improvement on cognitive reappraisal use was linked to a positive change score. One-tailed testing was chosen based on the assumption of a negative relation between learning and symptoms of depression and a positive relation between learning and cognitive reappraisal use.

Offline Data Processing and Analysis

Quality Assurance of MRI Data

To ensure high quality functional and structural MRI data, all data sets were examined within 48 h following recording using a standardized quality assurance pipeline developed and used by the Psychiatric Imaging Network Germany (PING; ping-rwth-aachen.de). Quality of structural data was assured by the quality parameters of the Computational Anatomy Toolbox (CAT) (84). Further, the procedure entailed the assessment of functional data within the Automated Quality Assurance toolbox (AQuA) (85). All fMRI data used for further analyses had (on average) percent signal change values below 5%. Three participants (MDD: $n = 1$) had single runs exceeding this threshold. However, the first level fMRI results of these participants did not show significant motion Artifacts upon visual inspection and were therefore included. Average PSC values did not differ between groups (HC: 2.48 ± 0.7; MDD: 2.48 ± 0.5; $t_{(74)} = -0.02$, $p > 0.05$) and indicate adequate data quality. Movement parameters did not exceed 3 mm within any NF run.

Preprocessing

fMRI data was preprocessed in Matlab R2018b (Mathworks Inc., Natick, MA) using the Statistical Parametric Mapping 12 toolbox (SPM12; https://www.fil.ion.ucl.ac.uk/spm/software/spm12/). To minimize T1-saturation effects, the first five volumes of each NF run were discarded for data analysis. Functional fMRI data were realigned to the first volume (6 movement parameters). Furthermore, fMRI data was co-registered to the participant's structural T1 image, smoothed with an 8 mm FWHM Gaussian kernel and normalized to the T1-weighted ICBM152 brain template of the Montreal Neurological Institute (MNI). Data from all participants was visually inspected after preprocessing to ensure adequate coregistration and normalization.

Whole Brain Analysis

Brain mapping analyses were performed using SPM12. On the first level, the six movement parameters were added as covariates of no interest. The main contrast of interest (reappraise > view) from the first level analysis was used in a 2 × 2 × 2 × 4 full factorial model [group (HC, MDD) × gender (female, male) × condition (Left, Right), run (NF1, NF2, NF3, NF4)]. Results were evaluated after application of a voxel-wise threshold of $p < 0.001$ and family-wise error (FWE) correction of $p\text{FWE} < 0.05$ at voxel level.

Generalized Psychophysiological Interaction

A generalized psychophysiological interaction (gPPI) was computed using the functional connectivity toolbox CONN (www.nitrc.org/projects/conn, RRID:SCR_009550). Signal variance that correlated with the seed region during the regulation compared to view condition ("reappraise – view") was investigated. The bilateral vlPFC was chosen as a seed and was created based on the target regions. Second-level results were evaluated at $p < 0.001$ uncorrected voxel level and with $p < 0.05$ FDR-correction at the cluster level.

Statistical Analyses

Statistical analyses were performed in IBM SPSS Statistics (version 26). Independent samples *t*-tests were computed to investigate differences in baseline questionnaires (e.g., BDI-II, ERQ, neuropsychological tests, PANAS) as well as demographic measures (age, educational level) between groups. To investigate changes in symptom severity (BDI-II) and use of cognitive reappraisal strategies from baseline to follow-up measurement, two 2 × 2 × 2 [Time (NF1, NF2) × Group (MDD, controls) × Condition (L-R, R-L)] repeated measures ANOVAs were computed. Furthermore, 2 × 2 × 2 repeated measures ANOVAS [Time × Condition × Group] were calculated separately for SAM valence and arousal ratings. Lastly, to investigate the

subjective experience during NF trainings, three 2 × 2 × 2 repeated measures ANOVAs (Time x Condition × Group) of metacognitive parameters of self-control (perceived intensity of general control, perceived intensity to control brain signal, perceived success to use cognitive reappraisal strategies) were computed. *Post-hoc t*-tests were performed whenever suitable. A p-value of < 0.05 was considered statistically significant.

RESULTS

Demographic and Clinical Data

Groups did not significantly differ regarding age, (parental) education, socioeconomic status, or basic cognitive functioning such as working memory, verbal IQ, and attention (all $p > 0.2$, see **Table 1**) as well as in gender ratio [$\chi^2_{(1,76)} = 0.07$, $p > 0.2$]. However, there were significantly more smokers in the patient group [HC: 6, MDD: 18, $\chi^2_{(1,74)} = 8.9$, $p < 0.01$]. As expected, patients with depression showed elevated baseline scores on depression [BDI-II: $t_{(73)} = -10.8$, $p < 0.001$; HADS-depression: $t_{(74)} = -9.5$, $p < 0.001$] as well as HADS-anxiety scores [$t_{(74)} = -6.9$, $p < 0.001$] compared to HCs (see **Table 1**). On the 21-item HAM-D, patients had average scores of 16.5 (± 7.5) indicating mild to moderate depressive symptoms. Prior to the first fMRI measurement, patients showed higher negative affect [MDD: 20.0 ± 9.2, HC: 12.4 ± 4.3; $t_{(74)} = -4.6$, $p < 0.001$] and lower positive affect [MDD: 26.9 ± 6.6, HC: 32.5 ± 7.4; $t_{(74)} = 3.5$, $p = 0.001$] than healthy individuals assessed through the PANAS. Furthermore, HCs indicated to use more cognitive reappraisal strategies [$t_{(71)} = 4.7$, $p < 0.001$] and less suppression [$t_{(71)} = -2.4$, $p < 0.05$] than patients with MDD (ERQ). The HFERST subscales further supported the clinical picture with lower scores of patients on reappraisal, acceptance, problem solving (all $p < 0.001$), and social support ($p < 0.01$) and higher scores on rumination ($p < 0.001$), avoidance ($p < 0.01$), experience suppression ($p < 0.05$), and expressive suppression ($p = 0.08$) compared to HCs.

Two separate 2 × 2 × 2 repeated measures ANOVAs (Time × Group × Condition) investigated mean SAM valence and arousal ratings across NF days, conditions, and groups (**Table 2**). The average SAM valence ratings were similar across NF days [$F_{(1,72)} = 0.05$, $p > 0.2$) and conditions [$F_{(1,72)} = 0.1$, $p > 0.2$], however, significantly different between groups [$F_{(1,72)} = 24.9$, $p < 0.001$] with higher (more positive) valence ratings for healthy individuals (6.7 ± 1.3) than patients with depression (5.4 ± 1.25). Furthermore, there was a significant group x condition interaction [$F_{(1,72)} = 6.4$, $p < 0.05$] and *post-hoc* tests indicated that HCs showed a significant difference between conditions on the second [$t_{(35)} = -2.1$, $p < 0.05$] but not first day of NF [$t_{(35)} = -1.1$, $p = 0.30$] whereas patients with depression showed a significant difference between conditions on day 1 [$t_{(37)} = 2.1$, $p < 0.05$] but not on day 2 [$t_{(37)} = -1.1$, $p = 0.14$] of NF training. A repeated measures ANOVA of mean arousal ratings showed no significant difference between NF days [$F_{(1,72)} = 1.6$, $p > 0.2$], between conditions [$F_{(1,72)} = 0.2$, $p > 0.2$] or groups [$F_{(1,72)} = 2.5$, $p = 0.12$] indicating similar arousal throughout NF trainings, across groups and conditions.

Different metacognitive parameters of self-control were assessed before and after each NF session (also see **Appendix B**). Before each NF training, participants were asked whether they think they are *generally able to control their brain activity* (yes/no) and asked for the intensity of control. On the first day, more healthy individuals than patients with MDD indicated that they generally have control over their brain activity [HC: 90%, MDD: 53%; $\chi^2_{(1,67)} = 11.2$, $p = 0.001$] whereas this difference was not significant anymore at the second training [HC: 90%, MDD: 71%; $\chi^2_{(1,67)} = 3.5$, $p = 0.06$]. A 2 × 2 × 2 repeated measures ANOVA [Time (NF1, NF2) × Condition (Left, Right) × Group (MDD, control); **Table 2**] of perceived intensity of general control (1–10) revealed a significant main effect of time [Day1: 4.99 ± 2.1, Day2: 5.61 ± 1.9; $F_{(1,62)} = 7.7$, $p = 0.007$] as well as a significant group difference [MDD: 4.71 ± 1.7, HC: 6.03 ± 1.7; $F_{(1,62)} = 9.97$, $p = 0.002$]. The increase of patients' positive evaluations of the ability to control one's brain activity combined with increasing perceived intensity of control indicates an increase of self-efficacy across NF days.

NF Effects

To test whether learning success was specific to the left vs. right vlPFC NF condition, ROI data of the first NF day was investigated. Within run learning slopes were steeper when receiving left as compared to right ROI feedback for both vlPFC ROIs [left vlPFC: $t_{(74)} = 2.55$, $p = 0.01$; right vlPFC: $t_{(74)} = 3.73$, $p < 0.001$]. This confirmed the primary hypothesis of a regional specific NF effect meaning that receiving feedback from the left ROI was advantageous over feedback from the right ROI. MDD and controls did not differ at either ROI [left vlPFC: $t_{(74)} = 0.51$, $p > 0.2$; right vlPFC: $t_{(74)} = 0.96$, $p > 0.2$]. Learning slopes within NF runs were significantly correlated with the change in self-reported cognitive reappraisal use from baseline to after the first NF training when receiving feedback from the left vlPFC (bilateral vlPFC ROI: $r = 0.484$, $p = 0.002$) but not from the right vlPFC (bilateral vlPFC ROI: $r = 0.170$, $p = 0.150$; **Figure 2**). However, there was no association between learning slopes on the first day and change of severity of symptoms of depression (left feedback: $r = 0.09$, $p = 0.33$; right feedback: $r = 0.04$, $p = 0.41$). This indicates that receiving feedback from the left as compared to the right vlPFC did not have a detectable effect on depressive symptomatology, however, left over right vlPFC feedback showed an advantage for increasing the subjective use of cognitive reappraisal strategies. Values fed back to participants during NF training are shown in **Appendix C**.

Offline Analysis

Whole-Brain Analysis

Whole-brain activations related to NF training with cognitive reappraisal were investigated with a 2 × 2 × 2 × 4 full factorial model [Group (MDD, control) × Gender (Female, Male) × Condition (L-R, R-L) × Run (NF1, NF2, NF3, NF4)] which revealed a main effect of group showing involvement of a dorsal fronto-parietal network during NF training (**Figure 3A**; top; **Table 3**). Healthy controls exhibited more activation in the right (and to some extent left) opercular and triangular part of the inferior frontal gyrus (IFG), the right middle temporal gyrus,

TABLE 2 | Repeated-measures ANOVAs of change from baseline to follow-up (BDI-II and ERQ) and change of general perceived control across neurofeedback trainings.

Parameter	Source	*F*	*p*
Mean SAM valence ratings at neurofeedback day 1 and 2	Time	0.05	0.83
	Group	24.9	**<0.001**
	Condition	0.01	0.92
	Time × Group	0.05	0.83
	Time × Condition	3.2	0.08
	Group × Condition	6.4	**<0.05**
	Time × Group × Condition	0.22	0.64
Mean SAM arousal ratings at neurofeedback day 1 and 2	Time	1.6	0.21
	Group	2.5	0.12
	Condition	0.21	0.65
	Time × Group	1.5	0.22
	Time × Condition	0.04	0.84
	Group × Condition	0.06	0.80
	Time × Group × Condition	2.3	0.14
Perceived level of general control (scale of 1–10)	Time	7.7	**<0.01**
	Group	9.97	**<0.01**
	Condition	0.18	0.68
	Time × Group	2.4	0.13
	Time × Condition	0.98	0.33
	Group × Condition	0.17	0.68
	Time × Group × Condition	0.05	0.82
Change of symptoms of depression (BDI-II) from baseline to follow-up	Time	23.7	**<0.001**
	Group	100.3	**<0.001**
	Condition	0.12	0.73
	Time × Group	15.0	**<0.001**
	Time × Condition	1.1	0.29
	Group × Condition	0.39	0.53
	Time × Group × Condition	0.50	0.48
Change of cognitive reappraisal (ERQ-CR) from baseline to follow-up	Time	2.2	0.14
	Group	14.3	**<0.001**
	Condition	0.85	0.36
	Time × Group	5.9	0.02
	Time × Condition	0.93	0.34
	Group × Condition	0.29	0.59
	Time × Group × Condition	0.004	0.95
Change of suppression (ERQ-suppression) from baseline to follow-up	Time	0.82	0.37
	Group	3.9	**0.05**
	Condition	0.45	0.50
	Time × Group	0.0	0.99
	Time × Condition	0.58	0.45
	Group × Condition	0.22	0.64
	Time × Group × Condition	1.6	0.21

SAM, self-assessment manikin; BDI-II, beck depression inventory-II; ERQ, emotion regulation questionnaire. Bold values highlight significance of tests.

and left superior temporal gyrus (STG) (**Figure 3A**; middle; **Table 3**), whereas patients with MDD recruited more cingulate areas (clusters extending from anterior to posterior cingulate cortex), bilateral precuneus, bilateral pre- and postcentral gyri as well as the medial segment of the right IFG pars triangularis (see **Figure 3A**; bottom; **Table 3**). Furthermore, the main effect of condition was not significant indicating that the effect of the online TBV ROI analysis could not be detected on the whole-brain level. There was a strong main effect of gender with male participants showing more activation in the bilateral IFG, supplementary motor area (SMA), dorsomedial PFC (dmPFC), bilateral precentral gyrus, bilateral thalamus and

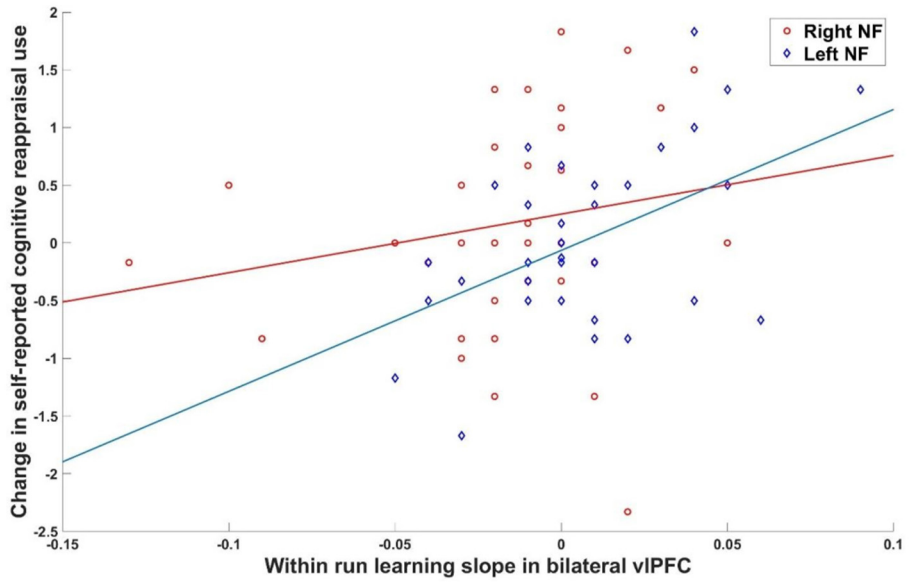

FIGURE 2 | Brain behavior relationship. Association between within run learning during the first NF day and change in cognitive reappraisal use was significant for left ($r = 0.484$, $p = 0.002$) but not right ($r = 0.170$, $p = 0.150$) vlPFC feedback.

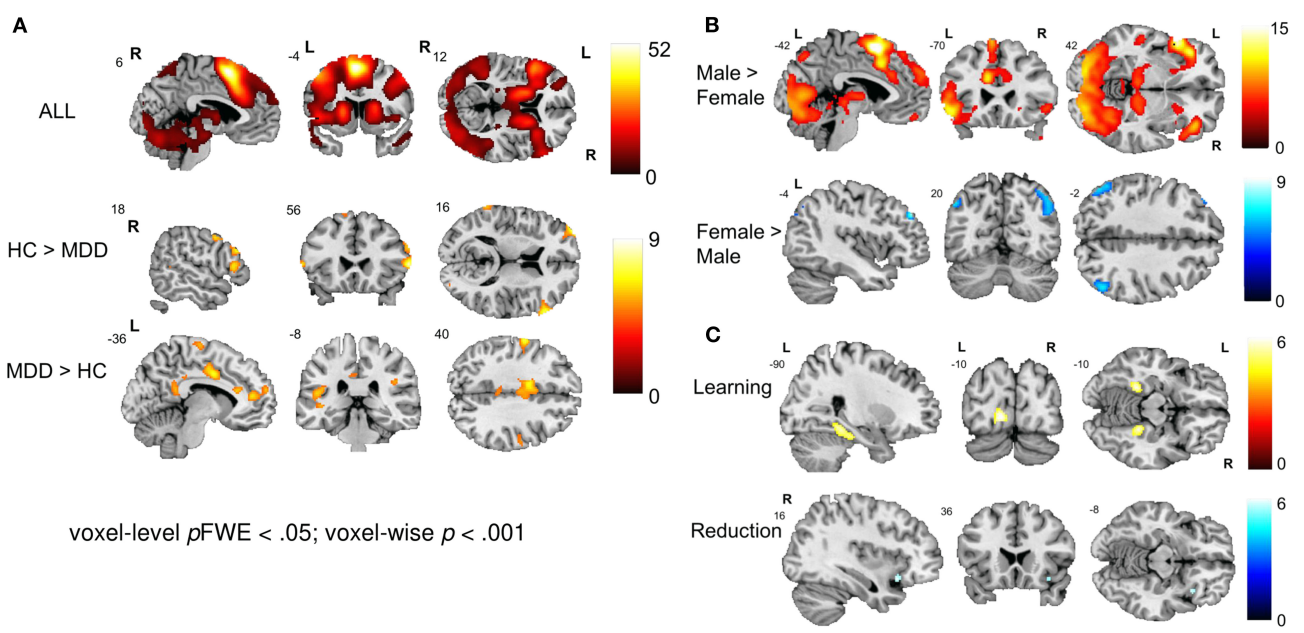

FIGURE 3 | Neural correlates of emotion regulation. **(A)** The main effect of group revealed a widespread network active during NF including the bilateral prefrontal cortex, precentral gyrus, SMA, MCC, bilateral occipital and superior parietal areas, thalamus, and cerebellum. Healthy individuals showed a stronger engagement of prefrontal areas while patients showed more activation in cingulate areas. **(B)** The main effect of gender revealed engagement of an extensive network during emotion regulation in males including the bilateral prefrontal cortex, SMA, dmPFC, bilateral precentral and occipital gyrus and bilateral thalamus. Female participants showed stronger activation in the bilateral angular gyrus. **(C)** Learning and reduction across NF runs 1 to 4. Overall, participants showed an increase in the bilateral fusiform gyrus and occipital lobe as well as a decrease of activation in the right insula and the MCC.

bilateral occipital lobe (**Figure 3B**; top; **Table 3**) and female participants showing more activation in the bilateral angular gyrus (**Figure 3B**; bottom; **Table 3**). Across NF runs there was an increase in bilateral fusiform gyrus and occipital lobe as well as a decrease of activation in the right insula (**Figure 3C**; **Table 3**).

TABLE 3 | Activation peaks associated with NF-guided cognitive reappraisal.

Cluster	Brain region	MNI coordinates			T	k_E
		x	y	z		
All (regulate > view)						
1	Bilateral IFG, dorsal ACC, MCC, dmPFC, SMA, SFG, STG, angular gyrus, thalamus, striatum, occipital gyrus, pre-/postcentral gyrus, cerebellum, superior parietal lobe	−4	6	62	52.84	67,733
Healthy controls > MDD (regulate > view)						
1	Left MFG	−36	56	20	9.07	124
2	Right IFG	62	20	10	8.76	321
3	Right MFG	36	2	44	8.14	393
4	Right SFG	10	60	34	8.04	102
5	Left superior occipital gyrus	−24	−92	30	7.60	223
6	Right MTG	44	−42	4	6.81	82
7	Left SMA	−18	12	68	6.76	202
8	Right superior occipital gyrus	22	0.94	28	6.19	82
MDD > Healthy controls (regulate > view)						
1	Left anterior insula extending into frontal operculum	−34	28	10	9.02	181
2	Right pre-/postcentral gyrus	62	2	22	8.06	506
3	Left pre-/postcentral gyrus	−60	−8	42	7.45	486
4	MCC	−8	−4	42	7.05	893
5	ACC	10	38	22	6.79	441
6	Supplementary motor cortex	−6	−20	74	5.79	116
7	PCC	−12	−50	32	5.77	124
Male > Female (regulate > view)						
1	Bilateral IFG, pre-/postcentral gyrus, SMA, dmPFC, SFG, thalamus, striatum, occipital gyrus, left STG	−4	6	62	52.84	78,444
Female > Male (regulate > view)						
1	Right angular gyrus	44	−62	56	9.41	1,632
2	Left angular gyrus	−48	−70	44	6.50	386
3	ACC extending into left MFG	−12	38	−4	5.78	1,122
Learning over time (regulate > view)						
1	Left superior occipital gyrus	−12	−90	2	6.32	121
2	Left fusiform gyrus	−26	−44	−8	6.31	173
3	Right fusiform gyrus	24	−40	−12	5.96	249
Reduction over time (regulate > view)						
1	Right anterior insula	20	30	14	5.20	97

$p < 0.001$ voxel threshold and $p < 0.05$ FWE-corrected at voxel level.

Connectivity Analysis

Task-dependent changes in functional connectivity of the bilateral vlPFC during neurofeedback was studied with a generalized Psychophysiological Interaction analysis in the contrast reappraise vs. view. In healthy controls, coupling increased with the left ($x = -58$, $y = -52$, $z = 46$, $T = 4.64$) and right superior parietal cortex ($x = 60$, $y = -42$, $z = 32$, $T = 4.68$) and decreased with the ACC ($x = 12$, $y = 18$, $z = 0$, $T = -6.69$), precuneus/PCC ($x = 4$, $y = -38$, $z = 8$, $T = -5.27$), right superior frontal gyrus ($x = 24$, $y = 30$, $z = 44$, $T = -4.81$). In the patients, neurofeedback enhanced coupling with the left ($x = 10$, $y = -102$, $z = 2$, $T = 5.14$) and right inferior occipital gyrus ($x = -34$, $y = -94$, $z = 0$, $T = 5.03$; $x = 44$, $y = -82$, $z = 10$, $T = 4.56$). Direct group comparison revealed significantly lower functional connectivity during NF in the left superior parietal cortex in patients compared with healthy controls ($x = -46$, $y = -48$, $z = 34$, $T = -6.69$) (**Figure 4**). In a *post-hoc* analysis, baseline BDI scores were negative linear predictors for the connectivity measure at this location [$T_{(72)} = -2.99$, $p = 0.004$].

Follow-Up Assessments

Four weeks after the last NF training, all participants were contacted to fill out questionnaires on their current depressive symptomatology, their state of affect, their use of emotion

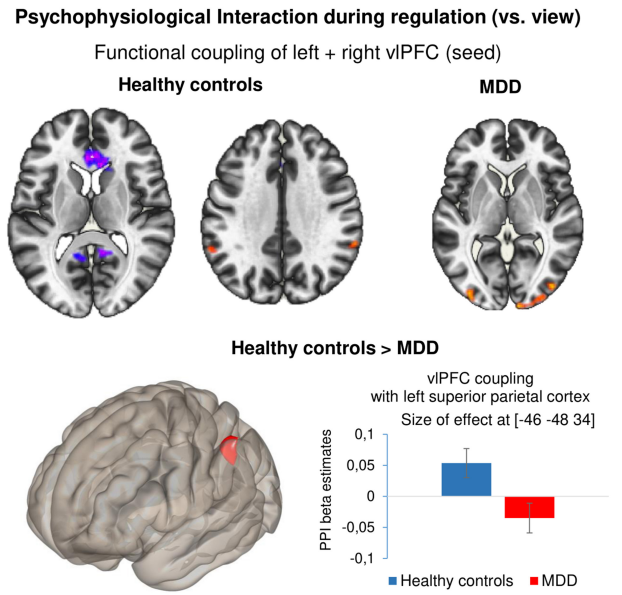

FIGURE 4 | Psychophysiological interaction during regulation. Results of the generalized psychophysiological interaction analysis for the contrast 'regulate – view' with bilateral vlPFC as seed. Healthy controls showed increased coupling between the seed region and bilateral superior parietal cortex and negative coupling between the seed and ACC as well as PCC. Patients showed positive coupling between the seed and bilateral occipital cortex. Compared with healthy controls, patients with depression showed significantly reduced coupling between the bilateral vlPFC and left superior parietal cortex. All results are reported at $p < 0.001$ voxel threshold and $p < 0.05$ FDR-corrected at cluster level. Bar plots indicate size of effect (beta values) at the voxel showing the maximum coupling effect.

regulation strategies and experience with the NF training as well as applications of learned strategies in everyday life. Not all participants could be recontacted for follow-up assessments (MDD: 32, HC: 35) and the following analyses are based on the available subset of data. Please see **Table 2** for detailed results.

Symptom Change

A 2 × 2 × 2 [Time (Baseline, Follow-up) × Group (HC, MDD) × Condition (L-R, R-L)] repeated measures ANOVA of depressive symptom severity (BDI-II) showed a significant main effect of time [$F_{(1,60)} = 23.7$, $p < 0.001$], a significant effect of group [$F_{(1,60)} = 100.3$, $p < 0.001$] whereas the main effect of condition did not reach significance [$F_{(1,60)} = .12$, $p = 0.73$]. Furthermore, the time*group interaction was significant [$F_{(1,60)} = 15.0$, $p < 0.001$] while the time*condition interaction did not show significance [$F_{(1,60)} = 1.1$, $p = 0.29$]. *Post-hoc* paired *t*-tests showed that the reduction of symptom severity from baseline to follow-up was significant for patients [9.2 ± 11.8; $t_{(28)} = 4.2$, $p < 0.001$, $d = 0.77$; **Figure 5A**] but not for HCs [1.0 ± 3.3; $t_{(34)} = 1.9$, $p = 0.07$, $d = 0.24$]. Previous studies have shown that the minimal clinically important difference (MCID) of BDI-II scores should be a change of at least 5 points (86) or 17.5% (87) depending on the baseline severity of depression. The mean change of 9.2 points (27.7% reduction) in our sample indicates that patients on average showed a meaningful reduction of BDI-II scores from baseline to follow-up. Furthermore, investigation of MCID on an individual level indicated a clinically meaningful change (change ≥5 or 17.5%) in 55% of patients who completed the follow-up interview.

Change of Emotion Regulation (ERQ)

A 2 × 2 × 2 [Time (Baseline, Follow-up) ×Group (HC, MDD) × Condition (L-R, R-L)] repeated measures ANOVA of cognitive reappraisal use at baseline and follow-up showed non-significant main effects of time [$F_{(1,59)} = 2.2$, $p = 0.14$] and condition [$F_{(1,59)} = 0.85$, $p = 0.36$], but a significant main effect of group [$F_{(1,59)} = 14.3$, $p < 0.001$] as well as significant time*group interaction [$F_{(1,59)} = 5.9$, $p = 0.02$]. *Post-hoc* tests (see **Figure 5B**) indicated that patients had a significant increase in cognitive reappraisal use [$t_{(30)} = -2.5$, $p = 0.02$, $d = 0.43$] from baseline to follow-up, whereas healthy individuals showed a stable use of cognitive reappraisal [$t_{(31)} = 0.80$, $p > 0.2$]. The difference between groups remained significant at follow-up [$t_{(64)} = 2.1$, $p < 0.05$]. A similar repeated measures ANOVA of self-reported suppression revealed only a marginally significant main effect of group [$F_{(1,59)} = 3.9$, $p = 0.05$]. *Post-hoc* tests indicated that the difference between groups for suppression that was significant at baseline [$t_{(71)} = 2.1$, $p = 0.02$] was not significant at follow-up [$t_{(64)} = -1.4$, $p > 0.1$], indicating that use of suppression in patients equalized with that of healthy individuals. Interestingly, male participants used more suppression compared to female participants at baseline [$t_{(71)} = -2.6$, $p < 0.01$] and follow-up [$t_{(64)} = -2.3$, $p = 0.02$] whereas there were no gender differences for cognitive reappraisal use at baseline [$t_{(71)} = 0.72$, $p > 0.2$] or follow-up [$t_{(64)} = 0.14$, $p > 0.2$].

Subjective Experience

At follow-up, the application of learned strategies in everyday life was assessed. Seventy-five percentage of patients with MDD and 57% of healthy individuals indicated that they had used the strategies over the past month. Of these, all patients and 89% of controls experienced the applied strategies as helpful. Patients reported that reappraisal strategies made them feel less frustrated, more relaxed, more optimistic, more aware of the situation, and led to improved mood which indicates that generalization of the training to negative situations in everyday life was high. Furthermore, 89% of controls and 91% of patients were willing to repeat such a NF training which indicates high acceptance of the NF training.

DISCUSSION

In this double-blind cross-over rtfMRI study we tested the feasibility and clinical efficacy of NF-supported cognitive reappraisal training in patients with depression and a matched group of healthy individuals. In specific, we investigated whether left- or right hemispheric ventrolateral prefrontal cortex (vlPFC) NF would be a neurologically and clinically more suitable region for NF during cognitive reappraisal. During 2 days of NF training, participants trained to regulate their brain signal in the vlPFC using reappraisal strategies in response to

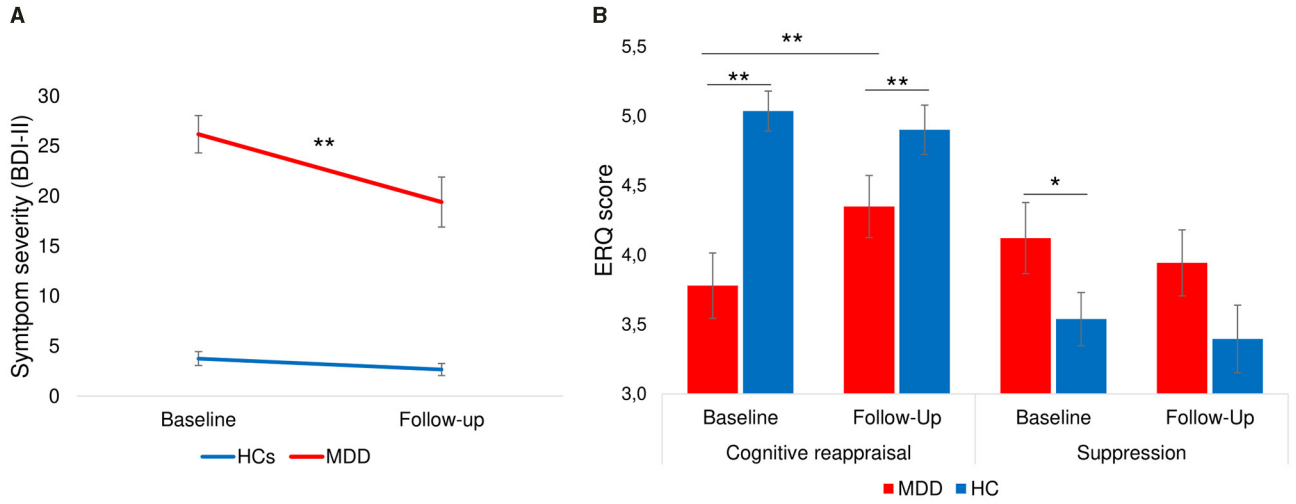

FIGURE 5 | Change of severity of depression and emotion regulation ability from baseline to follow-up. **(A)** Symptom severity measured by BDI-II showing a significant decrease of symptom scores from baseline to follow-up only in patients with depression [9.2 ± 11.8; $t_{(28)} = 4.2$, $p < 0.001$]. **(B)** Patients showed a significant increase of cognitive reappraisal and a stable level of suppression strategies. Healthy individuals had stable levels of cognitive reappraisal and suppression. Error bars indicate standard errors. $^{**}p < 0.001$, $^{*}p < 0.05$.

negative pictures and guided by intermittent NF ("reappraise > view"). This paradigm has already been applied successfully in healthy individuals (70) and patients with post-traumatic stress disorder (PTSD) (71). Overall, the cognitive reappraisal evoked predicted responses within the emotion regulation network such as activations in prefrontal, motor, and subcortical areas. Furthermore, our ROI analysis revealed that NF of left compared to right vlPFC activity specifically enhanced bilateral prefrontal activation during reappraisal in patients with depression as well as in age and gender matched healthy individuals. Such laterality effect did not survive the correction for multiple testing in the whole-brain analysis. First, it has to be taken into account that the size of lateralization effects is usually limited, e.g., about 30% lower responses at the non-dominant hemisphere to speech stimuli (88). Secondly, recent data show a relevant contribution of the right vlPFC [e.g., (50)]. However, a larger learning effect in response to left vs. right vlPFC feedback in the ROI analysis suggests a regional specificity of our rt-fMRI-based NF paradigm and may further support a central causal role of this region for cognitive reappraisal (41, 52, 89).

NF learning on the first day of training was related to improvements in self-rated reappraisal use only when receiving NF from the left rather than right vlPFC but was not associated with change of depressive symptomatology. Nevertheless, 55% of patients showed a clinically meaningful change in depression scores (BDI-II) from baseline to follow-up and 75% of patients reported that they had successfully applied the learned cognitive strategy in everyday life. Our study supports a positive effect of rt-fMRI NF for the enhancement of emotion regulation for patients with depression (90). The combination of specific NF effects, reappraisal skill learning, reduction of depressive symptomatology and a high acceptance of training yield the (especially left) vlPFC a promising target for future NF-guided rt-fMRI studies.

Behaviorally, patients with depression can achieve downregulation of negative emotions by applying reappraisal strategies within clear laboratory boundaries. However, Zilverstand et al. (5) have shown that patients with depression may – despite similar behavioral regulation success – display dysfunctions in a cognitive control network for negative emotions of which the vlPFC offers a promising NF target. Our findings from the first NF day suggest a beneficial effect of receiving left compared to right vlPFC feedback reflected by enhanced bilateral vlPFC activation and a significant increase in reappraisal strategy use specific for left vlPFC feedback. The vlPFC has repeatedly been found to support the selection of appropriate reappraisals (37, 38) and left vlPFC activity during reappraisal differentiates healthy individuals from patients with depression (5, 40). Furthermore, more evidence for a superior role of the left compared to right vlPFC for cognitive reappraisal has been provided by previous studies (52, 59).

Further investigation on the whole-brain level showed that healthy individuals and patients with depression recruited different regions of the emotion regulation network during NF-supported reappraisal training. The effect of interest showed extensive activation in the bilateral vlPFC, dlPFC, dACC, (pre-) SMA, dmPFC, SFG, MFG, STG, angular gyrus, thalamus, striatum, occipital gyrus, pre- and postcentral gyrus, cerebellum and superior parietal lobe during cognitive reappraisal. This is consistent with the emotion regulation network areas commonly recruited during reappraisal (36–38). Furthermore, in the group comparison, healthy individuals displayed more recruitment of cortical areas including the right IFG, left SMA, bilateral middle frontal gyrus, right superior frontal gyrus, right middle temporal gyrus and the bilateral superior occipital gyrus. Deficient

recruitment of prefrontal areas (vlPFC, dlPFC) (5) and the STG (40) as seen in patients with depression is in line with dysfunctional attentional and inhibitory capacities. Interestingly, we did not find any effects in the amygdala and therefore could neither replicate the attenuation of amygdala response during reappraisal training found in previous studies (70, 71) nor the group difference in terms of increased amygdala response during reappraisal (5). Accordingly, findings in the current cohort may support a direct pathway hypothesis postulating that reappraisal primarily impacts cortical systems involved in cognitive appraisals and emotional evaluation and only has a minimal impact on subcortical systems (41). Whether distinct regulation pathways during NF-guided cognitive reappraisal reflect specific diagnoses or symptom clusters, must be determined in further investigations. Across NF runs, the analysis revealed a significant increase within the bilateral fusiform gyrus as well as occipital lobe which may indicate increased processing of visual stimuli over time. Additionally, we observed a decrease of a cluster extending from the ACC to the right anterior insula which may be related to either a habituation to emotional stimuli and accordingly reduced salience of the displayed negative pictures or a reduction of salience due to more effective reappraisal application.

Patients with depression, showed more activation within midline areas (ACC, MCC, PCC, precuneus), pre- and postcentral gyrus, Supplementary motor cortex as well as the left anterior insula compared with control participants. Increased activation within the left anterior insula and the precentral gyrus in patients may be related to increased emotional experience (40). This pattern may suggest amplified physiological and motor responses resulting from increased processing of perceptual information of negative stimuli. In particular, the anterior insula is involved in the integration of external environment and interoceptive physiological signals received from the posterior insula (91, 92). Furthermore, increased activation of the precentral gyrus may stem from more intense emotion experience [e.g., (93)]. Additionally, the ACC has been related to the appraisal and expression of negative emotions (94), upregulation of this area by fMRI NF has been shown to modulate emotion perception (95) and has been related to increased rumination (96). On the other hand, higher activation levels of the MCC, PCC, and SMA in patients compared to healthy individuals may indicate a compensatory mechanism (97, 98).

During emotion regulation, the (anterior) MCC has been suggested to play an integratory role mediating between emotion appraisal in subcortical and initiation of reappraisal in prefrontal regions and relaying the need to regulate from the vlPFC to the dlPFC (37). As a hub of the default-mode network (DMN), the PCC is involved in inward attention and self-reflective thinking (99, 100). The PCC is critically involved in reappraisal (37, 38) and higher involvement of this area during NF in patients with depression was unexpected. However, it is possible that increased activation of MCC and PCC reflect a compensatory mechanism that counteracts deficiencies of the fronto-parietal attention network. For instance, PCC activation has been related to effortful cognitive control (101). In a similar vein, we found compensatory engagement of prefrontal regions during self-control of brain activation in a previous neurofeedback study in PTSD (13). Alternatively, it is conceivable that patients used more self- compared to situation-focused reappraisal strategies and therefore evoked more activation in self-monitoring brain state [e.g., (102, 103)]. The increased activation in the SMA, a region involved in the execution of regulation (37), may signal increased effort of reappraisal in patients. From a network perspective, these results suggest dysfunction in the cortical cognitive control network responsible for negative emotions with exaggerated brain responses related to increased emotional experience. Furthermore, Morawetz et al. (104) identified four large scale networks involved in emotion processing and regulation. One of the suggested networks comprised of the bilateral postcentral gyrus, left insula and PCC as well as periaqueductal gray and left superior parietal lobe shows large overlap with the pattern of activation seen in patients with depression. Further, the authors propose that this network may serve as an emotion regulation hub which integrates information from a ventral and dorsal prefronto-parietal regulation and a subcortical emotion generation network.

The task-based connectivity analysis during NF revealed enhanced coupling in healthy individuals between the seed (bilateral vlPFC) and the bilateral superior parietal cortex as well as an inhibitory effect on ACC, PCC, precuneus and the right superior frontal gyrus. Patients showed an increased coupling with the bilateral occipital lobe which may indicate increased attention toward negative emotional stimuli (105). Importantly, in a group comparison, patients with depression showed lower functional connectivity of the bilateral vlPFC and the left superior parietal cortex. Reduced connectivity between these regions has been associated with less recruitment of the regulatory fronto-parietal network involved in reappraisal and subsequent inefficient cognitive transfer of information from frontal to parietal areas (40, 106). Furthermore, weaker connectivity within a fronto-parietal attention network in depression has been related to poorer goal-directed attention (107) and seems to be a general impairment of attention that has implications for different sensory domains (108, 109). Lastly, baseline depression severity (BDI-II) was an inverse predictor of functional connectivity at this location indicating that individuals suffering from more severe symptoms showed particularly prominent decoupling in this network.

Interestingly, we observed strong gender differences in brain activation related to reappraisal. Investigation of gender differences has frequently yielded mixed findings in the literature (43). Our whole brain analysis showed that whereas females displayed enhanced activation in the bilateral superior parietal cortex, males showed a widespread pattern of activation within bilateral IFG, SMA, dmPFC, bilateral precentral gyrus, thalamus, and occipital lobe during reappraisal. On the behavioral level, these differences are underpinned by more everyday life suppression strategy use in males in both groups – patients with depression and healthy individuals. Interestingly, several studies show that males and females display different neural responses during reappraisal tasks despite comparable decreases of negative affect (44, 110). However, contrary to our findings, McRae et

al. (110) showed less increase in prefrontal regions in males compared to females during a reappraisal task. Furthermore, increased effective fronto-limbic connectivity in males compared to females during negative emotion processing indicates that men show more evaluative rather than affective processing of negative emotional stimuli (111). Whereas, males have also been shown to use more automatic, non-conscious emotion regulation, females are more likely to focus on and analyze their negative emotions (112). Furthermore, disturbed perception of appraisals has been observed in female patients with depression (113). Our findings suggest that males and females recruit different neural pathways during reappraisal. Alternatively, Whittle et al. (44) highlight females are more neurally reactive to disgust, anger and fear related negative emotional stimuli. This could imply that the observed gender differences may reflect differences in our higher-level baseline (viewing condition) which may have differentially affected the differences between reappraisal and viewing blocks in males and females. Even though the origin of the observed differences in gender-specific neural responses remains speculative at this point, our results underscore the importance of the investigation of gender effects in the context of emotion regulation.

In the current NF study, patients with depression reported a positive effect of reappraisal use such as less frustration, more relaxed handling of emotions, more awareness of negative situations as well as improved mood during the 4-week period following NF training. Our study extends the findings of our previous studies using NF supported reappraisal training for downregulation of negative emotions in healthy individuals (70) and patients with PTSD (71) and implies a possible pathway for neural enhancement-based treatment strategies in patients with depression even after short training periods. Cognitive reappraisal strategies during the 4 weeks following NF training were utilized by 75% of both patients with depression and PTSD (71). Furthermore, we could show a similar clinically meaningful effect size of depressive symptomatology change from baseline to follow-up ($d = 0.77$) as in patients with PTSD ($d = 0.64$) (71) suggesting a potential of the NF training across diagnostic categories. As NF learning was accompanied by an overall increase in perceived intensity of control over brain activation, the improvement of depressive symptomatology may possibly be related to an increase of self-efficacy beliefs associated with a non-specific reward experience of self-regulation (67). Mastery experiences build strong self-efficacy beliefs (114) and may help to overcome learned helplessness which is a common experience of patients with depression (115). As MacDuffie et al. (8) have stated, a lack of experience of the beneficial effects of newly learned cognitive skills for patients with depression may complicate their transfer to complex day to day situations. The direct objective visual feedback on neural effects of strategy use during NF may have enhanced the credibility of strategy use and motivated application in real-life.

Importantly, the observed clinical improvements in the current study, cannot be directly attributed to specific NF effects due to the nature of the cross-over design; in particular, we cannot differentiate effects of left and right vlPFC NF, the reappraisal training, placebo [see (67)] as well as time passed (116). It has to be noted that even in the direct comparison of left vs. right feedback ROI data, only moderate *t*-values were achieved (2.55 and 3.69), suggesting a small to moderate effect size only. In consequence the finding did not emerge in the brain mapping analysis with correction for multiple testing across voxels. On the other hand, considering that both the left and right vlPFC are involved in the process of reappraisal [e.g., (37)] finding a difference between regulation conditions is rather impressive. However, to allow a systematic investigation of reappraisal enhancing effects of vlPFC NF, future studies should use a between-subjects design comparing this target region with a control feedback condition. For example, the implementation of a different control condition such as a region that is not involved in reappraisal but of which participants can achieve similar control may be advantageous [e.g., (64)]. Furthermore, to disentangle effects of NF training and use of emotion regulation strategies as such, a third control group without neurofeedback is essential. Another important aspect concerns the observation that clinical symptoms continue to improve for weeks after treatment (117). To understand the trajectory of NF effects on cognitive strategy use, more frequent follow-up assessments and longer follow-up intervals should be implemented. Furthermore, objective evaluation of treatment success at follow-up such as a reappraisal transfer run may avoid a possible bias of retrospective self-report questionnaires and interview.

CONCLUSION

Our findings support a central role of the left vlPFC for the process of cognitive reappraisal. Left compared to right vlPFC NF was associated with increased bilateral frontal self-regulation and improved emotion regulation. Further, we showed differences in the specific recruitment of emotion regulation areas between patients with depression and healthy individuals as well as between females and males during cognitive reappraisal. Inefficient execution of emotion regulation in patients with depression was further supported by weaker task-based connectivity in the fronto-parietal attention network that was associated with symptom severity at baseline. Our findings suggest a good tolerability of our rtfMRI-NF-guided cognitive reappraisal training and potential for clinical use in patients with depression. Randomized clinical trials with longer follow-up intervals and additional control groups are needed to validate this potential.

DATA AVAILABILITY STATEMENT

Data used in this study is not available due to legal restrictions. Requests to access the datasets should be directed to kmathiak@ukaachen.de.

ETHICS STATEMENT

The studies involving human participants were reviewed and approved by local Ethics Committee of the RWTH Aachen. The

patients/participants provided their written informed consent to participate in this study.

AUTHOR CONTRIBUTIONS

MKe, JZ, MKl, MZ, and KM contributed to conception and design of the study. MKe, RM, and JI were involved in the investigation. MKe and KM performed the statistical analysis. MKe wrote the manuscript. All authors corrected the manuscript and approved the submitted version.

FUNDING

This study was supported by the German Ministry for Education and Research (BMBF; APIC: 01EE1405A, B, and C; TRAM: 01DN18026); German Research Foundation (DFG; IRTG 2150, MA 2631/6-1).

ACKNOWLEDGMENTS

We thank Sarah Bleich, Arndt Brandl and Manouela Kosmadaki for their assistance with participant recruitment and data collection. Furthermore, this work was supported by the Brain Imaging Facility of the Interdisciplinary Center for Clinical Research (IZKF) Aachen within the Faculty of Medicine at RWTH Aachen University.

SUPPLEMENTARY MATERIAL

The Supplementary Material for this article can be found online at: https://www.frontiersin.org/articles/10.3389/fpsyt.2021.715898/full#supplementary-material

REFERENCES

1. Gross JJ. Antecedent-and response-focused emotion regulation: divergent consequences for experience, expression, and physiology. *J Pers Soc Psychol.* (1998) 74:224. doi: 10.1037/0022-3514.74.1.224
2. Gotlib IH, Joormann J. Cognition and depression: current status and future directions. *Annu Rev Clin Psychol.* (2010) 6:285–312. doi: 10.1146/annurev.clinpsy.121208.131305
3. Joormann J, Gotlib IH. Selective attention to emotional faces following recovery from depression. *J Abnorm Psychol.* (2007) 116:80–5. doi: 10.1037/0021-843X.116.1.80
4. Joormann J, Quinn ME. Cognitive processes and emotion regulation in depression. *Depress Anxiety.* (2014) 31:308–15. doi: 10.1002/da.22264
5. Zilverstand A, Parvaz MA, Goldstein RZ. Neuroimaging cognitive reappraisal in clinical populations to define neural targets for enhancing emotion regulation. A systematic review. *Neuroimage.* (2017) 151:105–16. doi: 10.1016/j.neuroimage.2016.06.009
6. Ehring T, Tuschen-Caffier B, Schnülle J, Fischer S, Gross JJ. Emotion regulation and vulnerability to depression: spontaneous versus instructed use of emotion suppression and reappraisal. *Emotion.* (2010) 10:563. doi: 10.1037/a0019010
7. McRae K, Gross JJ. Emotion regulation. *Emotion.* (2020) 20:1–9. doi: 10.1037/emo0000703
8. MacDuffie KE, MacInnes J, Dickerson KC, Eddington KM, Strauman TJ, Adcock RA. Single session real-time fMRI neurofeedback has a lasting impact on cognitive behavioral therapy strategies. *Neuro Image Clin.* (2018) 19:868–75. doi: 10.1016/j.nicl.2018.06.009
9. Cordes JS, Mathiak KA, Dyck M, Alawi EM, Gaber TJ, Zepf FD, et al. Cognitive and neural strategies during control of the anterior cingulate cortex by fMRI neurofeedback in patients with schizophrenia. *Front Behav Neurosci.* (2015) 9:169. doi: 10.3389/fnbeh.2015.00169
10. Dyck MS, Mathiak KA, Bergert S, Sarkheil P, Koush Y, Alawi EM, et al. Targeting treatment-resistant auditory verbal hallucinations in schizophrenia with fMRI-based neurofeedback–exploring different cases of schizophrenia. *Front Psychiatry.* (2016) 7:37. doi: 10.3389/fpsyt.2016.00037
11. Weiskopf N, Scharnowski F, Veit R, Goebel R, Birbaumer N, Mathiak K. Self-regulation of local brain activity using real-time functional magnetic resonance imaging (fMRI). *J Physiol Paris.* (2004) 98:357–73. doi: 10.1016/j.jphysparis.2005.09.019
12. Zweerings J, Hummel B, Keller M, Zvyagintsev M, Schneider F, Klasen M, et al. Neurofeedback of core language network nodes modulates connectivity with the default-mode network: a double-blind fMRI neurofeedback study on auditory verbal hallucinations. *Neuroimage.* (2019) 189:533–42. doi: 10.1016/j.neuroimage.2019.01.058
13. Zweerings J, Pflieger EM, Mathiak KA, Zvyagintsev M, Kacela A, Flatten G, et al. Impaired voluntary control in PTSD: probing self-regulation of the ACC with real-time fMRI. *Front Psychiatry.* (2018) 9:219. doi: 10.3389/fpsyt.2018.00219
14. Paret C, Hendler T. Live from the "regulating brain": harnessing the brain to change emotion. *Emotion.* (2020) 20:126. doi: 10.1037/emo0000674
15. Dryman MT, Heimberg RG. Emotion regulation in social anxiety and depression: a systematic review of expressive suppression and cognitive reappraisal. *Clin Psychol Rev.* (2018) 65:17–42. doi: 10.1016/j.cpr.2018.07.1004
16. Gross JJ, John OP. Individual differences in two emotion regulation processes: implications for affect, relationships, and well-being. *J Pers Soc Psychol.* (2003) 85:348–62. doi: 10.1037/0022-3514.85.2.348
17. Troy AS, Wilhelm FH, Shallcross AJ, Mauss IB. Seeing the silver lining: cognitive reappraisal ability moderates the relationship between stress and depressive symptoms. *Emotion.* (2010) 10:783. doi: 10.1037/a0020262
18. Thiruchselvam R, Blechert J, Sheppes G, Rydstrom A, Gross JJ. The temporal dynamics of emotion regulation: an EEG study of distraction and reappraisal. *Biol Psychol.* (2011) 87:84–92. doi: 10.1016/j.biopsycho.2011.02.009
19. Aldao A, Nolen-Hoeksema S, Schweizer S. Emotion-regulation strategies across psychopathology: a meta-analytic review. *Clin Psychol Rev.* (2010) 30:217–37. doi: 10.1016/j.cpr.2009.11.004
20. Campbell-Sills L, Barlow DH, Brown TA, Hofmann SG. Acceptability and suppression of negative emotion in anxiety and mood disorders. *Emotion.* (2006) 6:587–95. doi: 10.1037/1528-3542.6.4.587
21. Compas BE, Jaser SS, Bettis AH, Watson KH, Gruhn MA, Dunbar JP, et al. Coping, emotion regulation, and psychopathology in childhood and adolescence: a meta-analysis and narrative review. *Psychol Bull.* (2017) 143:939–91. doi: 10.1037/bul0000110
22. Gotlib IH, Krasnoperova E, Yue DN, Joormann J. Attentional biases for negative interpersonal stimuli in clinical depression. *J Abnorm Psychol.* (2004) 113:121–35. doi: 10.1037/0021-843X.113.1.121
23. Leppanen JM. Emotional information processing in mood disorders: a review of behavioral and neuroimaging findings. *Curr Opin Psychiatry.* (2006) 19:34–9. doi: 10.1097/01.yco.0000191500.46411.00
24. Mennen AC, Norman KA, Turk-Browne NB. Attentional bias in depression: understanding mechanisms to improve training and treatment. *Curr Opin Psychol.* (2019) 29:266–73. doi: 10.1016/j.copsyc.2019.07.036
25. Berking M, Wirtz CM, Svaldi J, Hofmann SG. Emotion regulation predicts symptoms of depression over five years. *Behav Res Ther.* (2014) 57:13–20. doi: 10.1016/j.brat.2014.03.003
26. Just N, Alloy LB. The response styles theory of depression: tests and an extension of the theory. *J Abnorm Psychol.* (1997) 106:221–9. doi: 10.1037/0021-843X.106.2.221

27. Kovacs M, Joormann J, Gotlib IH. Emotion (Dys)regulation and links to depressive disorders. *Child Dev Perspect.* (2008) 2:149–55. doi: 10.1111/j.1750-8606.2008.00057.x
28. Visted E, Vollestad J, Nielsen MB, Schanche E. Emotion regulation in current and remitted depression: a systematic review and meta-analysis. *Front Psychol.* (2018) 9:756. doi: 10.3389/fpsyg.2018.00756
29. Webb TL, Miles E, Sheeran P. Dealing with feeling: a meta-analysis of the effectiveness of strategies derived from the process model of emotion regulation. *Psychol Bull.* (2012) 138:775–808. doi: 10.1037/a0027600
30. Beck AT, Dozois DJ. Cognitive therapy: current status and future directions. *Annu Rev Med.* (2011) 62:397–409. doi: 10.1146/annurev-med-052209-100032
31. Kazantzis N, Luong HK, Usatoff AS, Impala T, Yew RY, Hofmann SG. The processes of cognitive behavioral therapy: a review of meta-analyses. *Cog Ther Res.* (2018) 42:349–57. doi: 10.1007/s10608-018-9920-y
32. Rubin-Falcone H, Weber J, Kishon R, Ochsner K, Delaparte L, Dore B, et al. Neural predictors and effects of cognitive behavioral therapy for depression: the role of emotional reactivity and regulation. *Psychol Med.* (2020) 50:146–60. doi: 10.1017/S0033291718004154
33. Goldin PR, Lee I, Ziv M, Jazaieri H, Heimberg RG, Gross JJ. Trajectories of change in emotion regulation and social anxiety during cognitive-behavioral therapy for social anxiety disorder. *Behav Res Ther.* (2014) 56:7–15. doi: 10.1016/j.brat.2014.02.005
34. Denny BT. Getting better over time: a framework for examining the impact of emotion regulation training. *Emotion.* (2020) 20:110–4. doi: 10.1037/emo0000641
35. Morris RR, Schueller SM, Picard RW. Efficacy of a Web-based, crowdsourced peer-to-peer cognitive reappraisal platform for depression: randomized controlled trial. *J Med Internet Res.* (2015) 17:e72. doi: 10.2196/jmir.4167
36. Buhle JT, Silvers JA, Wager TD, Lopez R, Onyemekwu C, Kober H, et al. Cognitive reappraisal of emotion: a meta-analysis of human neuroimaging studies. *Cereb Cortex.* (2014) 24:2981–90. doi: 10.1093/cercor/bht154
37. Kohn N, Eickhoff SB, Scheller M, Laird AR, Fox PT, Habel U. Neural network of cognitive emotion regulation–an ALE meta-analysis and MACM analysis. *Neuroimage.* (2014) 87:345–55. doi: 10.1016/j.neuroimage.2013.11.001
38. Morawetz C, Bode S, Derntl B, Heekeren HR. The effect of strategies, goals and stimulus material on the neural mechanisms of emotion regulation: a meta-analysis of fMRI studies. *Neurosci Biobehav Rev.* (2017) 72:111–28. doi: 10.1016/j.neubiorev.2016.11.014
39. Drevets WC, Price JL, Furey ML. Brain structural and functional abnormalities in mood disorders: implications for neurocircuitry models of depression. *Brain Struct Funct.* (2008) 213:93–118. doi: 10.1007/s00429-008-0189-x
40. Pico-Perez M, Radua J, Steward T, Menchon JM, Soriano-Mas C. Emotion regulation in mood and anxiety disorders: a meta-analysis of fMRI cognitive reappraisal studies. *Prog Neuropsychopharmacol Biol Psychiatry.* (2017) 79(Pt B):96–104. doi: 10.1016/j.pnpbp.2017.06.001
41. Wager TD, Davidson ML, Hughes BL, Lindquist MA, Ochsner KN. Prefrontal-subcortical pathways mediating successful emotion regulation. *Neuron.* (2008) 59:1037–50. doi: 10.1016/j.neuron.2008.09.006
42. Tamres LK, Janicki D, Helgeson VS. Sex differences in coping behavior: a meta-analytic review and an examination of relative coping. *Pers Soc Psychol Rev.* (2002) 6:2–30. doi: 10.1207/S15327957PSPR0601_1
43. Nolen-Hoeksema S. Emotion regulation and psychopathology: the role of gender. *Annu Rev Clin Psychol.* (2012) 8:161–87. doi: 10.1146/annurev-clinpsy-032511-143109
44. Whittle S, Yucel M, Yap MB, Allen NB. Sex differences in the neural correlates of emotion: evidence from neuroimaging. *Biol Psychol.* (2011) 87:319–33. doi: 10.1016/j.biopsycho.2011.05.003
45. Lefaucheur, J.-P., André-Obadia N, Antal A, Ayache SS, Baeken C, et al. Evidence-based guidelines on the therapeutic use of repetitive transcranial magnetic stimulation (rTMS). *Clin Neurophysiol.* (2014) 125:2150–206. doi: 10.1016/j.clinph.2014.05.021
46. McClintock SM, Reti IM, Carpenter LL, McDonald WM, Dubin M, Taylor SF, et al. Consensus recommendations for the clinical application of repetitive transcranial magnetic stimulation (rTMS) in the treatment of depression. *J Clin Psychiatry*. (2017) 78.
47. Mutz J, Vipulananthan V, Carter B, Hurlemann R, Fu CH, Young AH. Comparative efficacy and acceptability of non-surgical brain stimulation for the acute treatment of major depressive episodes in adults: systematic review and network meta-analysis. *BMJ.* (2019) 364:l1079. doi: 10.1136/bmj.l1079
48. He Z, Zhao J, Shen J, Muhlert N, Elliott R, Zhang D. The right VLPFC and downregulation of social pain: a TMS study. *Hum Brain Mapp.* (2020) 41:1362–71. doi: 10.1002/hbm.24881
49. Zhao J, Mo L, Bi R, He Z, Chen Y, Xu F, et al. The VLPFC versus the DLPFC in downregulating social pain using reappraisal and distraction strategies. *J Neurosci.* (2021) 41:1331–9. doi: 10.1523/JNEUROSCI.1906-20.2020
50. He Z, Lin Y, Xia L, Liu Z, Zhang D, Elliott R. Critical role of the right VLPFC in emotional regulation of social exclusion: a tDCS study. *Soc Cogn Affect Neurosci.* (2018) 13:357–66. doi: 10.1093/scan/nsy026
51. He Z, Liu Z, Zhao J, Elliott R, Zhang D. Improving emotion regulation of social exclusion in depression-prone individuals: a tDCS study targeting right VLPFC. *Psychol Med*. (2020) 50:2768–79.
52. Marques LM, Morello LY, Boggio PS. Ventrolateral but not dorsolateral prefrontal cortex tDCS effectively impact emotion reappraisal–effects on emotional experience and interbeat interval. *Sci Rep*. (2018) 8:1–12. doi: 10.1038/s41598-018-33711-5
53. Davidson RJ. *Affect, Cognition, and Hemispheric Specialization Emotion, Cognition, and Behavior*. New York, NY: Cambridge University Press (1988). p. 320–65.
54. Palmiero M, Piccardi L. Frontal EEG asymmetry of mood: a mini-review. *Front Behav Neurosci.* (2017) 11:224. doi: 10.3389/fnbeh.2017.00224
55. Van Der Vinne N, Vollebregt MA, Van Putten MJ, Arns M. Frontal alpha asymmetry as a diagnostic marker in depression: fact or fiction? A meta-analysis. *Neuroimage Clin.* (2017) 16:79–87 doi: 10.1016/j.nicl.2017.07.006
56. Kołodziej A, Magnuski M, Ruban A, Brzezicka A. No relationship between frontal alpha asymmetry and depressive disorders in a multiverse analysis of five studies. *Elife.* (2021) 10:e60595. doi: 10.7554/eLife.60595.sa2
57. Deng X, Yang M, An S. Differences in frontal EEG asymmetry during emotion regulation between high and low mindfulness adolescents. *Biol Psychol.* (2021) 158:107990. doi: 10.1016/j.biopsycho.2020.107990
58. Zhou R, Liu L. Eight-week mindfulness training enhances left frontal EEG asymmetry during emotional challenge: a randomized controlled trial. *Mindfulness.* (2017) 8:181–9. doi: 10.1007/s12671-016-0591-z
59. Papousek I, Weiss EM, Perchtold CM, Weber H, de Assunção VL, Schulter G, et al. The capacity for generating cognitive reappraisals is reflected in asymmetric activation of frontal brain regions. *Brain Imag Behav.* (2017) 11:577–90. doi: 10.1007/s11682-016-9537-2
60. Briceño EM, Weisenbach SL, Rapport LJ, Hazlett KE, Bieliauskas LA, Haase BD, et al. Shifted inferior frontal laterality in women with major depressive disorder is related to emotion-processing deficits. *Psychol Med.* (2013) 43:1433–45. doi: 10.1017/S0033291712002176
61. Zotev V, Bodurka J. Effects of simultaneous real-time fMRI and EEG neurofeedback in major depressive disorder evaluated with brain electromagnetic tomography. *NeuroImage Clin.* (2020) 28:102459. doi: 10.1016/j.nicl.2020.102459
62. Mathiak K, Keller M. Clinical application of real-time fMRI-based neurofeedback for depression. In: Kim Y-K, editor. *Major Depressive Disorder: Rethinking and Understanding Recent Discoveries*, vol. 1305. Singapore: Springer (2021). p. 275–293.
63. Melnikov MY. The current evidence levels for biofeedback and neurofeedback interventions in treating depression: a narrative review. *Neural Plasticity*. (2021) 2021:1–31. doi: 10.1155/2021/8878857
64. Young KD, Misaki M, Harmer CJ, Victor T, Zotev V, Phillips R, et al. Real-time fMRI amygdala neurofeedback changes positive information processing in major depressive disorder. *Biol Psychiatry*. (2017) 82:578. doi: 10.1016/j.biopsych.2017.03.013
65. Young KD, Zotev V, Phillips R, Misaki M, Yuan H, Drevets WC, et al. Real-time FMRI neurofeedback training of amygdala activity in patients with major depressive disorder. *PLoS ONE.* (2014) 9:e88785. doi: 10.1371/journal.pone.0088785
66. Linden DE, Habes I, Johnston SJ, Linden S, Tatineni R, Subramanian L, et al. Real-time self-regulation of emotion networks in patients with

depression. *PLoS ONE.* (2012) 7:e38115. doi: 10.1371/journal.pone.0038115
67. Mehler DMA, Sokunbi MO, Habes I, Barawi K, Subramanian L, Range M, et al. Targeting the affective brain-a randomized controlled trial of real-time fMRI neurofeedback in patients with depression. *Neuropsychopharmacology*. (2018) 43:2578–85. doi: 10.1038/s41386-018-0126-5
68. Hamilton JP, Glover GH, Bagarinao E, Chang C, Mackey S, Sacchet MD, et al. Effects of salience-network-node neurofeedback training on affective biases in major depressive disorder. *Psychiatry Res Neuroimag.* (2016) 249:91–6. doi: 10.1016/j.pscychresns.2016.01.016
69. Herwig U, Lutz J, Scherpiet S, Scheerer H, Kohlberg J, Opialla S, et al. Training emotion regulation through real-time fMRI neurofeedback of amygdala activity. *Neuroimage.* (2019) 184:687–96. doi: 10.1016/j.neuroimage.2018.09.068
70. Sarkheil P, Zilverstand A, Kilian-Hütten N, Schneider F, Goebel R, Mathiak K. fMRI feedback enhances emotion regulation as evidenced by a reduced amygdala response. *Behav Brain Res.* (2015) 281:326–32. doi: 10.1016/j.bbr.2014.11.027
71. Zweerings J, Sarkheil P, Keller M, Dyck M, Klasen M, Becker B, et al. Rt-fMRI neurofeedback-guided cognitive reappraisal training modulates amygdala responsivity in posttraumatic stress disorder. *NeuroImage Clin*. (2020) 28:102483.
72. Takamura M, Okamoto Y, Shibasaki C, Yoshino A, Okada G, Ichikawa N, et al. Antidepressive effect of left dorsolateral prefrontal cortex neurofeedback in patients with major depressive disorder: a preliminary report. *J Affect Disord*. (2020) 271:224–7.
73. Abler B, Kessler H. Emotion regulation questionnaire–Eine deutschsprachige fassung des ERQ von gross und john. *Diagnostica.* (2009) 55:144–52. doi: 10.1026/0012-1924.55.3.144
74. Hamilton M. The Hamilton rating scale for depression. In *Assessment of Depression*. Springer (1986). p. 143–52.
75. Lang P, Bradley M, Cuthbert B. *International Affective Picture System (IAPS): Affective Ratings of Pictures and Instruction Manual*. Gainesville: University of Florida (2008).
76. Beck AT, Steer RA, Brown GK. *Beck Depression Inventory, 2nd Edn. Manual*. San Antonio, TX: The Psychological Corporation (1996).
77. Herrmann C, Buss U, Snaith R. *Hospital Anxiety and Depression Scale (HADS-D) - Deutsche Version [Gerrman version]*. Bern: Huber (1995).
78. Burgdörfer G, Hautzinger M. Physische und soziale anhedonie Die evaluation eines forschungsinstruments zur messung einer psychopathologischen basisstörung. *Eur Arch Psychiatry Neurol Sci.* (1987) 236:223–9. doi: 10.1007/BF00383852
79. Izadpanah S, Barnow S, Neubauer AB, Holl J. Development and validation of the heidelberg form for emotion regulation strategies (HFERST): factor structure, reliability, and validity. *Assessment.* (2019) 26:880–906. doi: 10.1177/1073191117720283
80. Krohne HW, Egloff B, Kohlmann C-W, Tausch A. Untersuchungen mit einer deutschen version der "positive and negative affect schedule"(PANAS). *Diag Gottin.* (1996) 42:139–56. doi: 10.1037/t49650-000
81. Schmidt M. *Wortschatztest (WST)*. Weinheim: Beltz Test GmbH (1992).
82. Goebel R. Cortex-based real-time fMRI. *Neuroimage.* (2001) 6:129. doi: 10.1016/S1053-8119(01)91472-7
83. Ros T, Enriquez-Geppert S, Zotev V, Young KD, Wood G, Whitfield-Gabrieli S, et al. Consensus on the reporting and experimental design of clinical and cognitive-behavioural neurofeedback studies (CRED-nf checklist). *Brain*. (2020). 143:1674–85. doi: 10.1093/brain/awaa009
84. Gaser C, Dahnke R. CAT-a computational anatomy toolbox for the analysis of structural MRI data. *HBM*. (2016) 2016:336–48. Available online at: http://www.neuro.uni-jena.de/hbm2016/GaserHBM2016.pdf
85. Stocker T, Schneider F, Klein M, Habel U, Kellermann T, Zilles K, et al. Automated quality assurance routines for fMRI data applied to a multicenter study. *Hum Brain Mapp*. (2005) 25:237–46. doi: 10.1002/hbm.20096
86. Hiroe T, Kojima M, Yamamoto I, Nojima S, Kinoshita Y, Hashimoto N, et al. Gradations of clinical severity and sensitivity to change assessed with the beck depression inventory-II in Japanese patients with depression. *Psychiatry Res.* (2005) 135:229–35. doi: 10.1016/j.psychres.2004.03.014
87. Button K, Kounali D, Thomas L, Wiles N, Peters T, Welton N, et al. Minimal clinically important difference on the beck depression inventory-II according to the patient's perspective. *Psychol Med.* (2015) 45:3269–79. doi: 10.1017/S0033291715001270
88. Mathiak K, Hertrich I, Lutzenberger W, Ackermann H. Preattentive processing of consonant vowel syllables at the level of the supratemporal plane: a whole-head magnetencephalography study. *Cogn Brain Res.* (1999) 8:251–7. doi: 10.1016/S0926-6410(99)00027-0
89. Mehler DMA, and Kording KP. The lure of causal statements: rampant mis-inference of causality in estimated connectivity. *arXiv [Preprint]*. (2018). Available online at: https://arxiv.org/abs/1812.03363
90. Linhartova P, Latalova A, Kosa B, Kasparek T, Schmahl C, Paret C. fMRI neurofeedback in emotion regulation: a literature review. *Neuroimage.* (2019) 193:75–92. doi: 10.1016/j.neuroimage.2019.03.011
91. Craig AD. Interoception: the sense of the physiological condition of the body. *Curr Opin Neurobiol.* (2003) 13:500–5. doi: 10.1016/S0959-4388(03)00090-4
92. Keller M, Pelz H, Perlitz V, Zweerings J, Rocher E, Baqapuri HI, et al. Neural correlates of fluctuations in the intermediate band for heart rate and respiration are related to interoceptive perception. *Psychophysiology*. (2020) 57:e13594. doi: 10.1111/psyp.13594
93. Hajcak G, Molnar C, George MS, Bolger K, Koola J, Nahas Z. Emotion facilitates action: a transcranial magnetic stimulation study of motor cortex excitability during picture viewing. *Psychophysiology.* (2007) 44:91–7. doi: 10.1111/j.1469-8986.2006.00487.x
94. Etkin A, Egner T, Kalisch R. Emotional processing in anterior cingulate and medial prefrontal cortex. *Trends Cogn Sci.* (2011) 15:85–93. doi: 10.1016/j.tics.2010.11.004
95. Gröne M, Dyck M, Koush Y, Bergert S, Mathiak K, Alawi E, et al. Upregulation of the rostral anterior cingulate cortex can alter the perception of emotions: fMRI-based neurofeedback at 3 and 7 T. *Brain Topogr.* (2015) 28:197–207. doi: 10.1007/s10548-014-0384-4
96. Ray RD, Ochsner KN, Cooper JC, Robertson ER, Gabrieli JD, Gross JJ. Individual differences in trait rumination and the neural systems supporting cognitive reappraisal. *Cogn Affect Behav Neurosci.* (2005) 5:156–68. doi: 10.3758/CABN.5.2.156
97. Fitzgerald PB, Srithiran A, Benitez J, Daskalakis ZZ, Oxley TJ, Kulkarni J, et al. An fMRI study of prefrontal brain activation during multiple tasks in patients with major depressive disorder. *Hum Brain Mapp.* (2008) 29:490–501. doi: 10.1002/hbm.20414
98. Matsuo K, Glahn DC, Peluso MA, Hatch JP, Monkul ES, Najt P, et al. Prefrontal hyperactivation during working memory task in untreated individuals with major depressive disorder. *Mol Psychiatry.* (2007) 12:158–66. doi: 10.1038/sj.mp.4001894
99. Buckner RL, Andrews-Hanna JR, Schacter DL. The brain's default network: anatomy, function, and relevance to disease. *Ann N Y Acad Sci.* (2008) 1124:1–38. doi: 10.1196/annals.1440.011
100. Raichle ME. The brain's default mode network. *Annu Rev Neurosci.* (2015) 38:433–47. doi: 10.1146/annurev-neuro-071013-014030
101. Garrison K, Santoyo J, Davis J, Thornhill T, Kerr C, Brewer J. Effortless awareness: using real time neurofeedback to investigate correlates of posterior cingulate cortex activity in meditators' self-report. *Front Human Neurosci.* (2013) 7:440. doi: 10.3389/fnhum.2013.00440
102. Ochsner KN, Ray RD, Cooper JC, Robertson ER, Chopra S, Gabrieli JD, et al. For better or for worse: neural systems supporting the cognitive down- and up-regulation of negative emotion. *Neuroimage.* (2004) 23:483–99. doi: 10.1016/j.neuroimage.2004.06.030
103. Sarkheil P, Klasen M, Schneider F, Goebel R, Mathiak K. Amygdala response and functional connectivity during cognitive emotion regulation of aversive image sequences. *Eur Arch Psychiatry Clin Neurosci.* (2019) 269:803–11. doi: 10.1007/s00406-018-0920-4
104. Morawetz C, Riedel MC, Salo T, Berboth S, Eickhoff S, Laird AR, et al. Multiple large-scale neural networks underlying emotion regulation. *Neurosci Biobehav Rev.* (2020) 116:382–95. doi: 10.1016/j.neubiorev.2020.07.001
105. Wiggins JL, Adleman NE, Kim P, Oakes AH, Hsu D, Reynolds RC, et al. Developmental differences in the neural mechanisms of

facial emotion labeling. *Soc Cogn Affect Neurosci.* (2016) 11:172–81. doi: 10.1093/scan/nsv101
106. Brzezicka A. Integrative deficits in depression and in negative mood states as a result of fronto-parietal network dysfunctions. *Acta Neurobiol Exp.* (2013) 73:313–25.
107. Keller AS, Leikauf JE, Holt-Gosselin B, Staveland BR, Williams LM. Paying attention to attention in depression. *Transl Psychiatry.* (2019) 9:279. doi: 10.1038/s41398-019-0616-1
108. Keller AS, Ball TM, Williams LM. Deep phenotyping of attention impairments and the 'inattention biotype'in major depressive disorder. *Psychol Med*. (2020) 50:2203–12. doi: 10.1017/S0033291719002290
109. Zweerings J, Zvyagintsev M, Turetsky BI, Klasen M, Konig AA, Roecher E, et al. Fronto-parietal and temporal brain dysfunction in depression: a fMRI investigation of auditory mismatch processing. *Hum Brain Mapp*. (2019) 40:3657–3668. doi: 10.1002/hbm.24623
110. McRae K, Ochsner KN, Mauss IB, Gabrieli JJD, Gross JJ. Gender differences in emotion regulation: an fMRI study of cognitive reappraisal. *Group Process Intergroup Relat.* (2008) 11:143–62. doi: 10.1177/1368430207088035
111. Lungu O, Potvin S, Tikasz A, Mendrek A. Sex differences in effective fronto-limbic connectivity during negative emotion processing. *Psychoneuroendocrinology.* (2015) 62:180–8. doi: 10.1016/j.psyneuen.2015.08.012
112. Butler LD, Nolen-Hoeksema S. Gender differences in responses to depressed mood in a college sample. *Sex roles.* (1994) 30:331–46. doi: 10.1007/BF01420597
113. Van den Bossche C, Wolf D, Rekittke LM, Mittelberg I, Mathiak K. Judgmental perception of co-speech gestures in MDD. *J Affect Dis.* (2021) 291:46–56. doi: 10.1016/j.jad.2021.04.085
114. Bandura A. Self-Efficacy. In *The Corsini Encyclopedia of Psychology*. John Wiley & Sons, Inc. (2010). doi: 10.1002/9780470479216.corpsy0836
115. Maier SF, Seligman ME. Learned helplessness at fifty: insights from neuroscience. *Psychol Rev.* (2016) 123:349. doi: 10.1037/rev0000033
116. Posternak MA, Miller I. Untreated short-term course of major depression: a meta-analysis of outcomes from studies using wait-list control groups. *J Affect Dis.* (2001) 66:139–46. doi: 10.1016/S0165-0327(00)00304-9
117. Rance M, Walsh C, Sukhodolsky DG, Pittman B, Qiu M, Kichuk SA, et al. Time course of clinical change following neurofeedback. *Neuroimage.* (2018) 181:807–13. doi: 10.1016/j.neuroimage.2018.05.001

Conflict of Interest: The authors declare that the research was conducted in the absence of any commercial or financial relationships that could be construed as a potential conflict of interest.

Publisher's Note: All claims expressed in this article are solely those of the authors and do not necessarily represent those of their affiliated organizations, or those of the publisher, the editors and the reviewers. Any product that may be evaluated in this article, or claim that may be made by its manufacturer, is not guaranteed or endorsed by the publisher.

frontiers in Psychiatry

STUDY PROTOCOL
published: 30 August 2021
doi: 10.3389/fpsyt.2021.680525

Repeated Sessions of Transcranial Direct Current Stimulation on Adolescents With Autism Spectrum Disorder: Study Protocol for a Randomized, Double-Blind, and Sham-Controlled Clinical Trial

Karin Prillinger[1], Stefan T. Radev[1,2], Gabriel Amador de Lara[1], Manfred Klöbl[3], Rupert Lanzenberger[3], Paul L. Plener[1,4], Luise Poustka[5] and Lilian Konicar[1]*

[1] Department of Child and Adolescent Psychiatry, Medical University of Vienna, Vienna, Austria, [2] Institute of Psychology, University of Heidelberg, Heidelberg, Germany, [3] Department of Psychiatry and Psychotherapy, Medical University of Vienna, Vienna, Austria, [4] Department of Child and Adolescent Psychiatry and Psychotherapy, University of Ulm, Ulm, Germany, [5] Department of Child and Adolescent Psychiatry and Psychotherapy, University Medical Center Göttingen, Göttingen, Germany

OPEN ACCESS

Edited by:
Yanghua Tian,
First Affiliated Hospital of Anhui Medical University, China

Reviewed by:
Deniz Doruk,
Mayo Clinic, United States
Lindsay M. Oberman,
National Institute of Mental Health, National Institutes of Health (NIH), United States

****Correspondence:***
Karin Prillinger
karin.prillinger@meduniwien.ac.at

Specialty section:
This article was submitted to Neuroimaging and Stimulation, a section of the journal Frontiers in Psychiatry

Received: *14 March 2021*
Accepted: *26 July 2021*
Published: *30 August 2021*

Citation:
Prillinger K, Radev ST, Amador de Lara G, Klöbl M, Lanzenberger R, Plener PL, Poustka L and Konicar L (2021) Repeated Sessions of Transcranial Direct Current Stimulation on Adolescents With Autism Spectrum Disorder: Study Protocol for a Randomized, Double-Blind, and Sham-Controlled Clinical Trial. Front. Psychiatry 12:680525. doi: 10.3389/fpsyt.2021.680525

Background: Social–emotional difficulties are a core symptom of autism spectrum disorder (ASD). Accordingly, individuals with ASD have problems with social cognition such as recognizing emotions from other peoples' faces. Various results from functional magnetic resonance imaging and electroencephalography studies as well as eye-tracking data reveal a neurophysiological basis of these deficits by linking them to abnormal brain activity. Thus, an intervention targeting the neural origin of ASD impairments seems warranted. A safe method able to influence neural activity is transcranial direct current stimulation (tDCS). This non-invasive brain stimulation method has already demonstrated promising results in several neuropsychiatric disorders in adults and children. The aim of this project is to investigate the effects of tDCS on ASD symptoms and their neural correlates in children and adolescents with ASD.

Method: This study is designed as a double-blind, randomized, and sham-controlled trial with a target sample size of 20 male participants (aged 12–17 years) diagnosed with ASD. Before randomization, the participants will be stratified into comorbid depression, comorbid ADHS/conduct disorder, or no-comorbidity groups. The intervention phase comprises 10 sessions of anodal or sham tDCS applied over the left prefrontal cortex within 2 consecutive weeks. To engage the targeted brain regions, participants will perform a social cognition training during the stimulation. TDCS-induced effects on ASD symptoms and involved neural circuits will be investigated through psychological, neurophysiological, imaging, and behavioral data at pre- and post-measurements. Tolerability will be evaluated using a standardized questionnaire. Follow-up assessments 1 and 6 months after the intervention will examine long-lasting effects.

Discussion: The results of this study will provide insights into the changeability of social impairments in ASD by investigating social and emotional abilities on different modalities following repeated sessions of anodal tDCS with an intra-simulation training. Furthermore, this trial will elucidate the tolerability and the potential of tDCS as a new treatment approach for ASD in adolescents.

Clinical Trial Registration: The study is ongoing and has been registered in the German Registry of Clinical Trials (DRKS00017505) on 02/07/2019.

Keywords: autism spectrum disorder, transcranial DC stimulation, clinical trial, social cognition, neuromodulation

INTRODUCTION

One out of 54 children fulfills the diagnostic criteria for autism spectrum disorder (ASD) (1), with boys being affected three to four times as often as girls (2). ASD is a neurodevelopmental disorder characterized by social and communicative deficits and repetitive, stereotyped behaviors, ranging over a wide spectrum with different degrees of impairment [International Classification of Diseases ICD-10; (3)].

As there is currently no cure for ASD, psychosocial and pharmacological treatments share the aim to ameliorate the core symptoms and enable a life as independent as possible (4). Psychosocial interventions show positive effects on intellectual and adaptive functioning (5), but suffer from limited support from randomized controlled trials (RCTs). Strongest evidence exists for the effectiveness of interventions that focus on early parent–child interactions (6, 7). Furthermore, there is no pharmacological treatment for the core symptoms of ASD and medication is mainly used for the therapy of commonly co-occurring disorders such as attention-deficit/hyperactivity disorder (ADHD) or depression (6). The need for efficient and affordable new treatment methods also becomes evident when assessing quality of life, employment, independency, social relationships, and mental and physical health in adults with ASD, which were found to be poor despite average cognitive functioning (8, 9). Thus, specifically targeting the mechanisms underlying the social–emotional dysfunctions in ASD can form the basis of new and viable treatment methods.

Social–emotional difficulties include pronounced impairments in empathy, a central prerequisite for social interactions. To be able to understand what others are feeling and to react appropriately to their emotions, it is often necessary to recognize the expressed emotion from others' faces. The ability to discriminate the six basic emotions (happy, sad, fear, anger, disgust, and surprise) is usually acquired in the first year of life (10), whereas the ability to discriminate more complex emotions improves until adulthood (11). It has been repeatedly shown that people with ASD have a deficit in the ability to recognize the emotions of others (12, 13). Moreover, results from neurological and electrophysiological studies show clear differences in automatic emotion recognition processes between ASD and typically developing children (14).

Another factor influencing social interactions is the direction of gaze (15). Eye-tracking reveals that children with ASD show aberrant patterns of gaze and fixation times when seeing human faces (16, 17) and eye gaze abnormalities have even been proposed as a robust biomarker for ASD (16). Moreover, dysfunctions in several brain regions including the dorsolateral prefrontal cortex (DLPFC) are involved in the development of this aberrant gaze behavior. In typically developing individuals, direct gaze leads to an enhanced response in brain areas important for empathic processes like theory of mind (ToM). In contrast, individuals with ASD show the same response when the gaze is averted and respond to direct gaze with an abnormal activation of the ToM network [medial prefrontal cortex (MPFC), temporoparietal junction, posterior superior temporal sulcus region, and amygdala] (15). These regions are also part of the social brain network (SBN) (18, 19).

Research regarding the neural underpinnings of behavioral social problems in ASD found evidence for alterations within the SBN in structural and functional magnetic resonance imaging (MRI) studies (20). Furthermore, structural MRI studies showed abnormalities in gray matter volume and white matter structure in short-distance tracts in the SBN, as well as an association between these abnormalities and social malfunctioning in ASD (21–24). Task-related fMRI studies in individuals with ASD revealed atypical activity and connectivity in social brain regions during the processing of social stimuli (25). For instance, processing of emotional facial expressions was associated with reduced activity in several brain regions important for interpersonal interactions, including the amygdala, MPFC, ventrolateral prefrontal cortex, and superior temporal sulcus region in individuals with ASD compared with typically developing individuals (26). Neuroimaging results show that the most consistently activated brain regions in ToM tasks are the medial prefrontal and orbitofrontal cortices (27). Within the ToM network, reduced functional connectivity in persons with ASD was detected (15). In detail, the functional connectivity between the MPFC and the posterior cingulate cortex (PCC) has repeatedly been shown to be lower in individuals with ASD (28, 29). A weaker connectivity between these regions is correlated with more serious social impairments [see (29)]. Both the MPFC and the PCC are part of the default mode network (DMN), which is involved in complex emotional and social processes such as ToM and self-referential thoughts (30, 31). Functional connectivity of DMN regions has been shown to be altered at rest and reduced in several social tasks such as face processing in adolescents and adults with ASD (28, 32). While the functional

connectivity between the DMN nodes normally increases with age, the development of long-distance functional connectivity in the DMN cannot be observed in adolescents with ASD (28, 33). Also, brain regions important for social interactions outside the DMN exhibit reduced activity and functional connectivity during resting state (20). Individuals with ASD showed, compared with typically developing individuals, a weaker functional connectivity between the amygdala and the ventromedial prefrontal cortex (34) and a reduced connectivity within the lateral occipital cortex, which was associated with symptom severity (35). Thus, it appears that neurophysiologically based interventions should target the MPFC as a potential mediator for the reduction of ASD symptoms.

Contrary to fMRI, electroencephalography (EEG) allows for calculating the functional connectivity of the brain based on absolutely quantifiable rather than relative measures. In ASD, resting-state EEG studies suggest a reduced long-range connectivity between frontal lobe and other cortical regions and short-range overconnectivity (36, 37). Regarding frequency bands, decreased power in alpha is the most consistent finding (36, 38), which is thought to be associated with inhibitory control deficits in ASD (36).

Neuromodulation constitutes, alongside psychosocial interventions and psychopharmacology, the third pillar of therapeutic interventions in psychiatry. Transcranial direct current stimulation (tDCS) in particular is a non-invasive neurophysiological method, which has the potential to modify brain function by affecting neuronal resting membrane potentials (39, 40). It affects neuronal excitability on a sub-threshold level without eliciting action potentials (40–42). Depending on the goal of the intervention, anodal or cathodal stimulation can be used to either enhance or reduce neuronal excitability and thereby modulate processes related to the target brain region in the desired direction (43). The effects of direct current stimulation elicits a polarity-dependent facilitation or inhibition of the spontaneous neuronal firing rate (40, 43, 44). Post-stimulation effects of tDCS are contingent on the duration of the stimulation and last from several minutes up to some hours (40, 45). Studies investigating the effects of tDCS on neural activity showed that direct current can modulate cortical connectivity in the brain (46) and induce changes in the alpha frequency band during and after the stimulation (47–49). Moreover, fMRI studies found changes in brain connectivity in both task-related and resting-state networks after the application of tDCS (50–53). Brain stimulation is more effective and causes more long-lasting plastic changes in already activated neural circuits (54). Additionally, aftereffects of tDCS were shown to depend on the emotional and physiological state during stimulation (41). Given these findings, intra-stimulation engagement tasks are used to enhance the effects of tDCS [e.g., (55, 56)].

Therapeutically, tDCS is used to alter local neuronal excitability that is assumed to be in a dysfunctional hypo- or hyperactive state (45). Effects of the stimulation expand by changes in the neural network into more distant regions and lead to reorganization of neuronal circuits (45, 57). Due to encouraging results in the treatment of various neuropsychiatric disorders in adults (58–61), tDCS has gained attention in the treatment of childhood and adolescent neuropsychiatric disorders over the past years (45, 62–64).

Regarding the use of tDCS in children with ASD, 12 articles have been published to date (65–76). Among these, four are randomized, double-blind, sham-controlled studies; the remaining articles comprise experimental, quasi-experimental, and pilot studies, a case series, and a case study. Outcome measurements, number and details of stimulation sessions, and control conditions vary across the studies [for reviews see (77, 78)]. Therefore, the current evidence is sparse and methodologically incomparable (79). Nevertheless, these studies point toward positive effects of tDCS in the treatment of ASD showing an improvement in ASD symptoms such as socialization, sensory awareness, repetitive behaviors, and behavioral problems (65, 68, 70, 76) as well as in cognitive abilities often impaired in individuals with ASD (71, 74). The available results not only provide indications for significant symptom reductions maintained for 6 months (68) but also emphasize the necessity of further research (70, 79). The potential of tDCS to counteract ASD-specific aberrant brain activity was highlighted by studies showing modulation of long-distance connectivity (66), an increase in functional connectivity in the alpha band (68, 80), increasing connectivity between the hemispheres within alpha and induced neuroplastic changes (75). Moreover, studies report a reduction in ASD symptoms that were associated with an increase in the peak alpha frequency band in resting-state EEG (76) and increasing EEG complexity (72) after tDCS stimulation. These studies as well as the majority of the present tDCS studies in children and adolescents with ASD report reduced ASD symptoms after anodal stimulation with the anode placed over the DLPFC (77). However, none of the studies used a simulation-based approach to evaluate the peak magnitudes of the electric fields and to define the stimulation target. TDCS applied over this commonly used stimulation site is able to increase the functional connectivity between the MPFC and the PCC in healthy adults (51) as well as in individuals with ASD (81). Taken together, both theoretical considerations and empirical findings regarding the pathophysiological signature of ASD lead to the proposition that tDCS can be used to alter dysfunctional patterns of brain activity.

The goal of the present study is to investigate the clinical and scientific significance of tDCS for improving social cognition abilities in ASD with a clear neurobiological rationale. Therefore, the planned study will (1) examine tDCS-related changes on reported symptomatic changes, behavior, brain activity, and connectivity; and (2) explore the long-term effects of tDCS in ASD and thereby evaluate tDCS as a cost-effective, time-efficient treatment option for children and adolescents with ASD.

METHODS AND ANALYSIS

The study is designed as a randomized, double-blind, sham-controlled clinical trial with two follow-up measurements 1 and 6 months after the last stimulation session, respectively.

Participants

Measurements and interventions will be carried out at the Department of Child and Adolescent Psychiatry at the Medical University of Vienna, Austria. The participants will be recruited from the outpatient clinic and from local institutes for individuals with ASD.

Sample Size Calculations

Power analysis was done with G*Power version 3.1.9.2 (82) to detect a difference in the primary outcome [SRS, (83)] calculating repeated measures ANOVA considering an effect size f of 0.25, a power of 80%, and an α of 0.05. Previous studies in children with ASD have shown larger effect sizes for tDCS (63). A sample size of 20 participants ($N = 20$) will be necessary to report medium effect sizes on the primary outcome. Analyses of secondary outcomes were not included in the power analysis and therefore considered underpowered.

Randomization

A total of 20 male participants will be included. To balance the experimental and control group with respect to comorbidities, all participants will be stratified into one of three subgroups based on their clinical presentation: subgroup A for participants without comorbidity, subgroup B for participants with depression as primary comorbidity, and subgroup C for participants with ADHD and/or conduct disorder as primary comorbidity. After subgroup stratification, the participants will be randomly allocated to the active condition or the sham condition by assigning a code to each participant. To ensure a quick study start for the participants after enrollment, a block randomization design will be used.

Blinding

The study mode of the stimulation device encodes sham and active stimulation using preprogramed codes so that the participant and investigators will be blind to the type of stimulation. The stimulation parameters (duration, fade-in, fade-out time, and current intensity) are set and saved on the device to avoid accidental modification of the parameters. To investigate the success of the subject-blinding, participants will be asked about their beliefs of the received stimulation type at the last stimulation session. After completing the 6-month follow-up measurement or after dropping out of the study, participants, and their caregiver will be informed about group allocation. Participants in the sham condition will not receive active stimulation after the end of the trial. Premature unblinding using prepared envelopes can be performed when knowledge of the actual group allocation becomes necessary for the safety of the patient. The blinding, code storage, and preparation of code-break envelopes will be done by a staff member not directly involved in the intervention and the day-to-day management of the study.

Inclusion Criteria

Participants eligible for the trial must comply with all of the following:

- Male
- Fulfilling ICD-10 criteria for ASD and diagnosed with ASD from a trained professional using the Autism Diagnostic Interview-Revised [ADI-R; (84)] and/or the Autism Diagnostic Observation Schedule [ADOS 2; (85)]
- Age between 12 and 18 years
- Right-handed
- IQ $\geq$ 70 assed using standardized instruments
- Treatment-naive to neurostimulation
- Signed written informed consent of the participant and primary caregiver.

Exclusion Criteria

- Contraindications for tDCS such as cardiac pacemakers, defibrillator, cochlear implant, intracranial/cranial stimulators, and other metals in the head
- Contraindications for MRI
- Epilepsy or related seizure disorders
- Other severe neurologic or psychiatric disorders or medical conditions (e.g., skull defect and craniotomy)
- Concomitant psychopharmacological medication.

Ongoing concomitant social or psychotherapeutic long-term interventions must be held constant during the course of the intervention.

Intervention

The intervention phase comprises 10 sessions of tDCS or sham stimulation within two consecutive weeks, with a 2-day break after the fifth session (see **Figure 1** for study overview). If feasible for the participant, all stimulation sessions will be held at the same time of the day. In each session, prior to the stimulation, the participant will complete a brief questionnaire about general well-being, attention, motivation, and experiences before the session. Afterwards, two rubber electrodes with conductive paste will be attached to the head of the participant. To decide on the optimal stimulation parameters, an MRI-based finite-element model approach was utilized, which simulates the intensity, distribution, and focality of the electric field induced by tDCS. To this aim, SimNIBS 3.1 (86) and structural T1 images of adolescents with ASD from a previous clinical trial executed by our research group were used. The parameters under comparison comprised an intensity of 2 mA, three different electrode sizes (3 $\times$ 3, 5 $\times$ 5, and 5 $\times$ 7 cm rectangular rubber electrodes) and two different conductors (NaCl solution and Ten20 paste).

Simulations demonstrated peak intensity of electric fields showing stronger fields with smaller electrodes (3 $\times$ 3 cm) and conductive Ten20 paste. Here, stimulating anodal tDCS over the left DLPFC would lead to peak magnitudes at the MPFC (see **Figure 2**), which match with the targeted neural circuit. This stimulation setup is in line with the recommendations suggested in a recent systematic review and meta-analysis on the existing literature of tDCS in ASD (77) and with other studies demonstrating effects of tDCS on reducing ASD symptoms. Therefore, an electrode montage with the anode over the left DLPFC (F3 according to the international 10-20 system for EEG) and the cathode over the right supraorbital region will be used in the current trial.

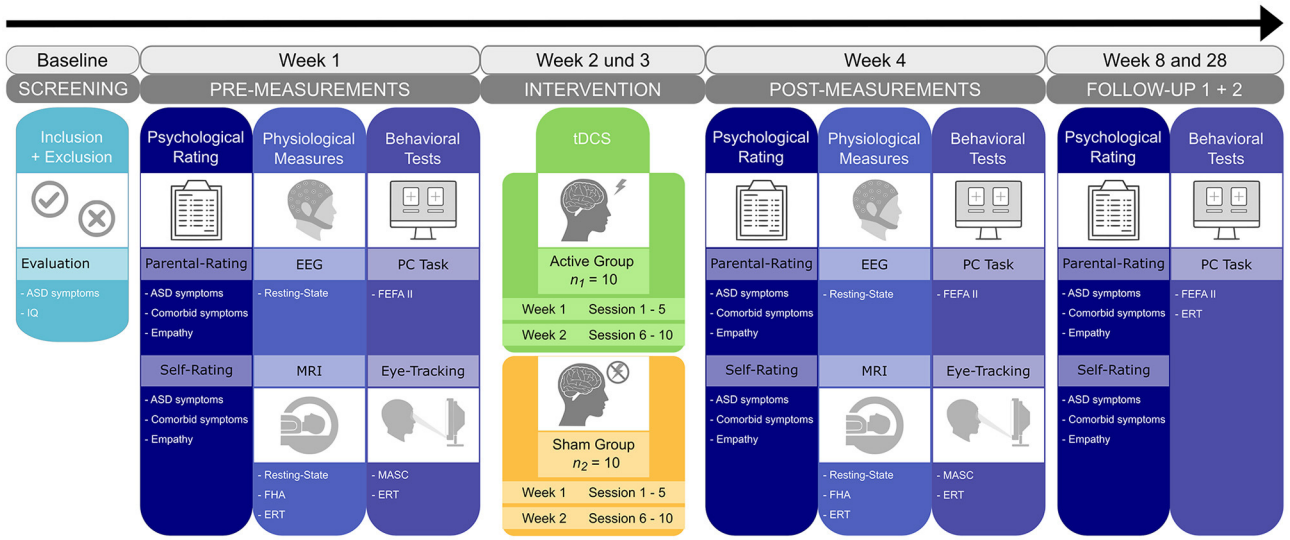

FIGURE 1 | Study timeline and overview. After enrollment, participants will undergo a set of psychological, behavioral, and physiological baseline measures in the first week. Following randomization, 10 sessions of either active or sham tDCS will be conducted within a 2-week interval. Post-treatment measures are repeated on the subsequent week. Two follow-up measures are planned 1 and 6 months after the end of the tDCS intervention. ERT, emotion recognition task; FEFA II, frankfurter test and training for recognizing facial affect; FHA, frith-happé animations; MASC, movie for the assessment of social cognition.

To localize the electrode site F3, the Beam F3 system (87) will be used. Anodal tDCS will be administered through an Eldith-DC Stimulator (NeuroConn GmbH, Germany) at 2 mA current strength for 20 min with a fade-in and fade-out of 30 s at the start and end of the stimulation. During the sham stimulation, a fade-in phase of 30 s, followed by 40 s of 2 mA stimulation and a fade-out phase of 30 s will be applied. The participants will experience the typical skin sensation usually produced at the beginning of an active tDCS stimulation and are therefore expected to remain unaware of the real condition (88).

Safety and Adverse Events

As for potential risks of tDCS, guidelines report no serious adverse events in over 18,000 sessions of low-intensity transcranial electrical stimulation in pediatric and adult patients, as well as in healthy subjects (89). Current data also specifically emphasize the feasibility, tolerability, and safety of tDCS in children and adolescents (45, 63, 90). Adverse effects of tDCS in children and adolescents were described as mild and transient, including tingling (11.5%), itching (5.8%), redness (4.7%), and scalp discomfort (3.1%) (91). Thus, when guidelines are followed, tDCS is a safe modality for children and adolescents with various neurological conditions (92). The proposed parameters of this study (including electrode size, current strength, and duration) were previously tested for their safety in children younger than the participants in this study (93, 94). The brain stimulation device will be operated by experienced psychologists, neuroscientists, and research assistants trained in the application. Therefore, no serious adverse events or serious health risks for the participants of this study are expected. In the case of a serious adverse event, the participant will be excluded from the trial and the adverse event will be reported to the ethics committee of the Medical University of Vienna and to the Austrian Agency for Health and Food Safety (AGES). To protocol adverse effects, the German version of the questionnaire of sensations related to transcranial electrical stimulation will be used at the last stimulation session (accessible at: http://neurologie.uni-goettingen.de/downloads.html).

Instruments

In accordance with the complexity of the disorder, the effects of the tDCS intervention will be investigated at three different levels:

1. Psychological ratings to detect changes in ASD symptoms as well as in comorbid symptoms;
2. Neurophysiological measures to detect changes in brain responses to emotional stimuli;
3. Behavioral tests to detect changes in responses and gaze behavior.

Psychological Ratings

Clinical information *via* questionnaires will be collected from participants and caregivers following a multi-perspective approach. The Social Responsiveness Scale [SRS; (83)] reliably indicates the presence and severity of social impairment in ASD and correlates with real-world dysfunctional behaviors. Five subscales (social awareness, social cognition, social communication, social motivation, restricted interests and repetitive behavior) and a total score will be calculated. Additionally, various instruments targeting different aspects of ASD symptoms [Autism Treatment Evaluation Checklist—ATEC (95); Social Communication Questionnaire—SCQ (96)] will be used for pre-, post-, and follow-up assessments.

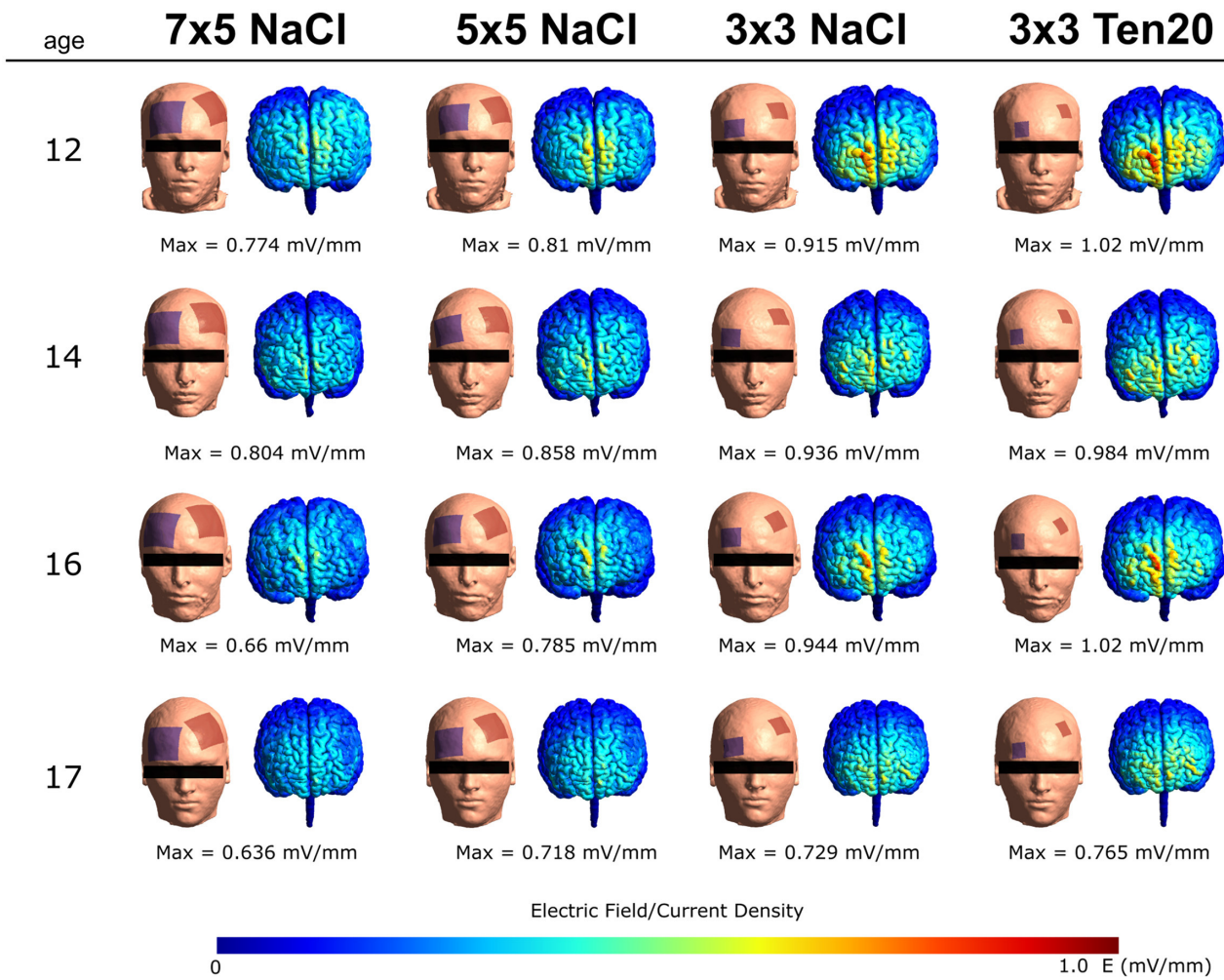

FIGURE 2 | Four examples of the simulations of our tDCS protocol in adolescents using SimNIBS and previously acquired T1-weighted MRI scans of a comparable population. The electric field was simulated using bilateral montages (anode at F3 and cathode Fp2-supraorbital), an intensity of 2 mA, and three different electrode sizes. Each row represents one participant and each column represents one montage. Peak magnitudes of the intracranially generated electric fields are listed below each simulated configuration.

Furthermore, affective and cognitive components of empathy and emotion regulation abilities will be measured *via* self-reports [Emotion Regulation Questionnaire—ERQ (97); Index of Empathy for Children and Adolescents—IECA (98); Basic Empathy Scale—BES (99)] and parental questionnaires [Griffith Empathy Measure—GEM (100); Emotion Regulation Checklist—ERC (101)]. For subgroup stratification and the investigation of comorbid symptoms of ASD such as attention deficit, anxiety, aggression, and depression, the Diagnostic System for Mental Disorders in Childhood and Adolescence for ADHD, Depression, Anxiety, and Conduct Disorder [DISYPS III ADHS, DEP, ANG, SSV—self- and parental rating versions; (102)] will be used.

Behavioral Tests

Frankfurter test and training for recognizing facial affect (FEFA II): This computer-based program was developed to train and reliably test the recognition of facial affect in individuals with high-functioning ASD (103). Participants are asked to identify the six basic emotions and neutral expressions presented in 50 black-and-white photographs of faces. The stimuli used are based on Ekman's conceptualization of basic emotions (104). Correct classification and reaction times are measured.

Movie for the assessment of social cognition (MASC): The German version of the MASC (105) is a reliable and sensitive naturalistic measure of social cognition and gaze behavior in adolescents with ASD (106). The MASC consists of a film showing two females and two males having a dinner party. The film lasts about 15 min and is paused 43 times to ask questions about the actors' emotions, thoughts, and intentions. The revised MASC score is a measure of the degree of social cognition adopted for adolescents and will be calculated from the correct responses (106). Additionally, eye-tracking data of the participants' gaze behavior will be recorded during the

presentation of the movie using the Tobii Pro eye-tracker (Tobii Group, Danderyd, Schweden) and Tobii Studio 3.4.5 (107).

Emotion recognition task (ERT): This self-developed task uses videos of faces and social scenes depicting different emotional states to investigate emotion recognition skills. The task involves three parts (see **Figure 3** for a graphical illustration) addressing different emotion recognition competencies: (a) shows videos of one person expressing a basic or complex emotion; (b) is more challenging and presents a more naturalistic scenario in which two or more people engage in an emotional and dynamic social scene; (c) consists of morphing videos (displaying a face transitioning from a neutral expression to a basic emotion) and participants will be instructed to interrupt the morphing process as soon as they recognize the displayed emotion. Afterwards, participants will be asked to classify the emotion that was displayed in the video. The emotional stimuli represent all age groups and genders equally and are taken from validated databases. Parts (a) and (b) use stimuli form the EU Emotion Stimuli Set (108, 109), while part (c) uses stimuli from the FACES Database (110, 111). This task was implemented in Python (version 3.6.7) using the PyQt (version 5.15.2) graphics library. The ERT will be employed in pre- and post-measurements to examine changes in correct classifications and response times and to investigate pre–post changes in gaze behavior using the Tobii Pro eye-tracker (Tobii Group, Danderyd, Schweden).

Pre-stimulation task: Prior to each stimulation session, the participants will be measured on accuracy of performance and response time on the ERT. This pre-stimulation task without tDCS functions as a reference to compare with the intra-stimulation task, which is presented during tDCS. This comparison will provide information about the acute effects of tDCS on emotion recognition abilities.

Intra-stimulation training: During the 20 min of active or sham tDCS, all participants will undergo a structured training that aims to further stimulate the engagement of the targeted circuits during the active and sham tDCS sessions. At the first 5 min of the stimulation, the child-friendly movie *Inside Out* (112), which focuses on emotions and was developed with scientific consultants studying emotions, will be presented. The movie will be interrupted various times to ask questions about the mental state and emotions of the characters. Next, the ERT will be completed by the participants to further stimulate the engagement of the targeted circuits. Afterwards, the next part of the movie, again interrupted with questions, will be presented. This approach will ensure that all participants will be dealing with the same material and therefore are assumed to engage similar brain regions during the stimulation. Furthermore, this repeated examination of emotion recognition performance with the ERT will provide important information about learning curves and session-by-session changes, which may reveal insights into the optimal number of stimulation sessions.

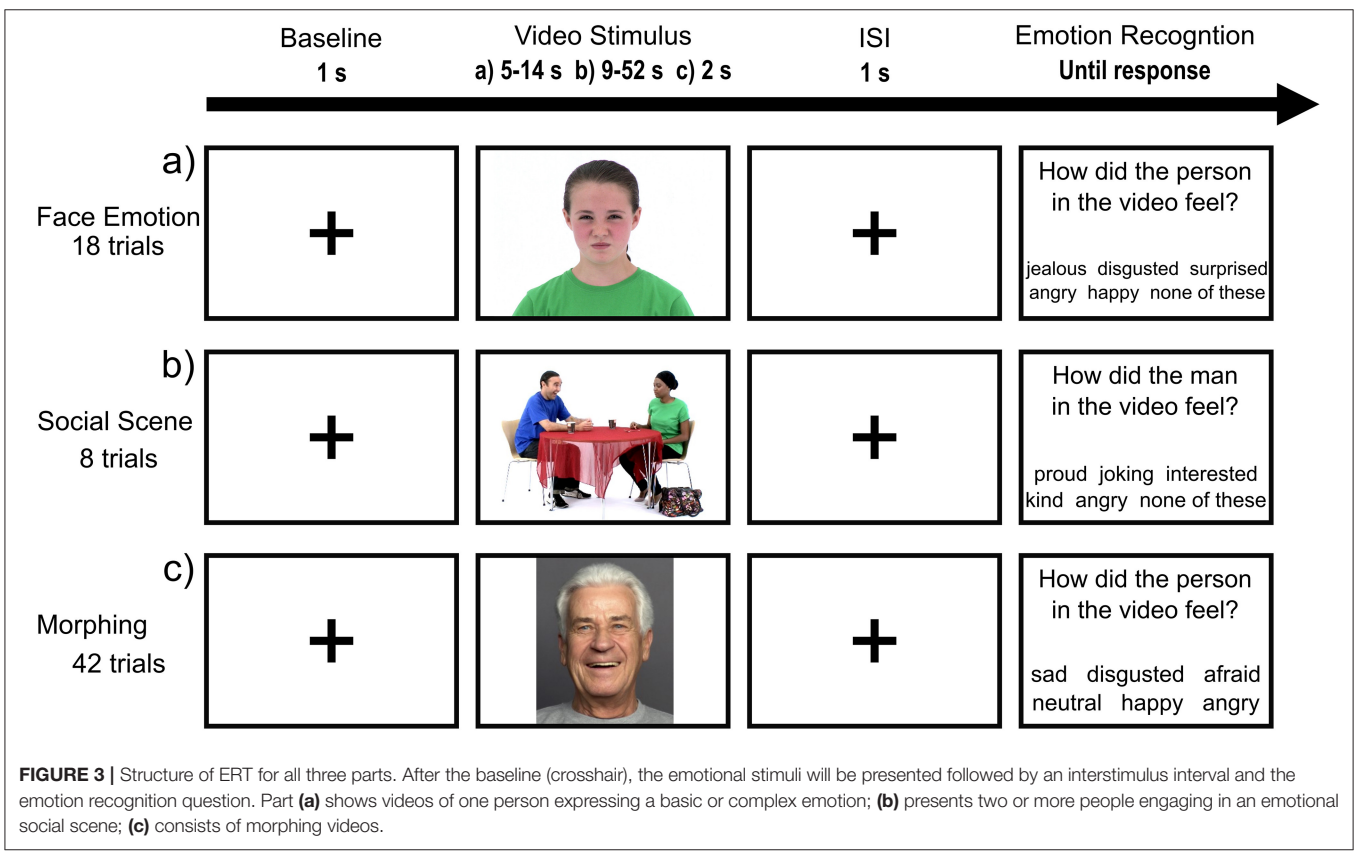

FIGURE 3 | Structure of ERT for all three parts. After the baseline (crosshair), the emotional stimuli will be presented followed by an interstimulus interval and the emotion recognition question. Part **(a)** shows videos of one person expressing a basic or complex emotion; **(b)** presents two or more people engaging in an emotional social scene; **(c)** consists of morphing videos.

Neurophysiological Measures

EEG data acquisition: EEG data will be collected from 19 cortical sites (Fp1, Fp2, F3, F4, F7, F8, Fz, FCz, C3, C4, Cz, T5, T6, P3, P4, Pz, O1, O2, and Oz) positioned according to the international 10-20 system using Ag/AgCl electrodes and the Thera Prax Q-EEG System (NeuroConn, Illmenau, Germany). Electrode-skin impedance will be kept below 3 kΩ.

Resting-state EEG: Neural oscillations will be recorded in eight 1-min trials, four with eyes-closed (C) and four with eyes-open (O). A guideline-based counterbalanced order (COCO-pause-OCOC) will be used considering disorder-specific characteristics such as a discomfort with longer eyes-closed intervals and minimizing the risk of participants falling asleep in the eyes-closed condition (113, 114).

MRI data acquisition: Functional and structural whole-brain imaging will be conducted using a 3-T Siemens MAGNETOM Prisma MR Scanner (Siemens, Erlangen, Germany) equipped with a 64-channel head coil.

Resting-state fMRI: RS data will be acquired for 7 min using an echo-planar imaging sequence with the following parameters: TE/TR = 35/728 ms, field of view (FoV) = 192 × 192 × 144 mm, matrix size = 96 × 96, 72 slices, multiband factor = 8, resulting in an isotropic voxel size of 2 mm, flip angle = 55° (optimized Ernst angle), and bandwidth = 3,365 Hz/Px [sequence optimized according to (115)]. To reduce head motion and participant drowsiness, the movie *Inscapes* (116) will be shown during resting-state recordings. This non-social movie features abstract shapes and was developed for the use with children and clinical populations to increase compliance while minimizing cognitive demand (116).

ToM-task: frith-happé animations (FHA): To investigate changes in the ability to infer people's thoughts and feelings, a validated ToM-task, the FHA, will be used (117–119). Participants will be instructed to categorize 12 video clips depicting two animated triangles as showing either no interaction/random movements, physical interaction/goal-directed behavior, or emotional interaction/ToM after each video. Additionally, after the four ToM trials only, they need to state how each of the triangles felt at the end of the video using visual analog scales (VAS). VAS are used instead of the original good/neutral/bad decision to allow for more fine-grained inferences. For each decision (i.e., the video category and emotional state of each triangle), subjects are given 5 s, before the paradigm continues, even when no answer was given. One trial contains up to three baseline (BL) periods: (1) Before the videos, BLs are uniformly jittered between 7 and 13 s. (2) Before the category choice, the BL is between 2 and 4 s. (3) In case a ToM video was shown, the BL before the VAS is 6 s minus the duration for 2.

Emotion recognition task: Parts (a) and (c) of the ERT (see **Figure 3**) will be presented during MRI using a jittered and randomized baseline duration between (a) 9–15 s and (c) 5–10 s. Imaging is conducted using the same parameters as for the resting-state recordings.

Structural MRI: These measures will be performed to exclude previously unknown alterations in brain anatomy using the following parameters: T1: TE/TR/TI = 2.29/2,300/900 ms, FoV = 165.44 × 240 × 240 mm, matrix size = 256 × 256, 176 slices, 0.94 × 0.94 × 0.94 mm voxel size (rounded), flip angle = 8°, bandwidth = 200 Hz/Px; T2: TE/TR = 408/3,200 ms, FoV = 172.8 × 230 × 230 mm, matrix size = 256 × 256, 192 slices, 0.9 × 0.9 × 0.9 mm voxel size (rounded), flip angle = 120°, bandwidth = 725 Hz/Px. During the structural scans, cartoons will be shown to the participants.

Outcomes

The primary outcome will be a reduction in ASD symptoms from baseline in the experimental group compared to the sham group. ASD symptoms will be quantified by the raw score of the German version of the SRS (83) assessed by the primary caregiver.

The secondary outcomes will be increased social cognition and emotion recognition quantified by the raw scores of the MASC (105) as well as correct classifications in the ERT and the FEFA 2 (120). Regarding gaze behavior, longer fixation duration on the eyes and increased pupil dilation will be the outcomes on the MASC and ERT. Outcomes on participants and caregiver ratings will be a decrease in ASD symptoms measured with the ATEC (95) and SCQ (96) and an increase in empathy and emotion regulation abilities measured with the ERQ (97), IECA (98), BES (99), GEM (100), and ERC (101). Neurophysiological activity will be measured at baseline and after the intervention using resting-state EEG and fMRI to measure changes in functional connectivity and electrical activity in the brain. We expect an increased resting-state alpha-power, a decrease in the other frequency bands, and an increased connectivity within the ToM network and DMN. An increased regional activation in key areas of the SBN will be the outcomes during the FHA and ERT.

The exploratory outcomes will include participant and caregiver ratings on comorbid symptoms of ASD using the DISYPS III (102). The brain activation in regions involved in emotion recognition processes and cognitive empathy during emotion recognition with the ERT during fMRI will also be examined exploratorily.

Statistical Analysis

For the statistical analyses, repeated measures analysis of variance (ANOVA) and hierarchical linear models (HLMs) will be used. A 4 × 2 mixed ANOVA (primary outcome as dependent variable) with *Time* (pre vs. post vs. follow-up 1 vs. follow-up 2) as the within-subjects factor and *Group* (experimental vs. control group) as the between-subject factor will be conducted to investigate an interaction between time and group. In order to test specific effects, *post-hoc* tests will be employed. A HLM will be formulated to investigate time-dependent changes and group differences in task performance across stimulation sessions. A $p < 0.05$ will be considered statistically significant. Analysis will be conducted in *R* (121).

For the eye-tracking data, analysis of fixation duration and pupil dilation will be done in Tobii Studio 3.4.5 (107) following the preprocessing pipeline of other studies using eye-tracking to investigate emotion recognition and social cognition in adolescents with ASD [for the ERT (17) and for the MASC

(106)]. These results in a fixation duration on the specified area of interest (AOI) and a measure of average pupil dilation per video. Further analysis regarding pre–post comparisons of AOIs and pupil dilation will be done in *R* (121) using linear models.

For the EEG data, we will employ the *MNE* library (122) written in *Python* (123) to execute data pre-processing, segmentation, and frequency and connectivity analyses. The raw EEG data of each participant will be segmented into epochs of 2 s. A multi-taper method with adaptive weights will be applied to each epoch to obtain power spectral density (PSD) values in each frequency band of interest. Frequency bands of interest will be delta (0.5–4 Hz), theta (4–8 Hz), and alpha (8–12 Hz). Subsequently, PSD values in each frequency band will be averaged across epochs separately for each participant, measurement occasion, and experimental condition.

Basic fMRI processing will be conducted according to (124) using Statistical Parametric Mapping [SPM; (125)]. To counteract the expected high level of in-scanner motion, PESTICA/SLOMOCO (126, 127) and the BrainWavelet toolbox (128) will be used for additional movement and artifact correction. Spatial normalization will be performed to a custom template created using the CerebroMatic toolbox (129) to avoid implausible deformation to match the usual standard adult brain. Subject-level analysis will be conducted using the general linear model in SPM. The FHA task will be modeled according to (118, 130). The ERTs will be modeled as block designs with a single condition. For the morphing variant, the reaction times will be included as a parametric modulator to uncover the possible influence of the subjective strength of the perceived emotion. The RS data will be analyzed by means of seed-based functional connectivity. Since the ERTs constitute newly implemented paradigms, interesting regions of their baseline activation will be used as seeds here. Nuisance regressors for the linear models will be derived *via* the CompCor (131) and Friston-24 (132) approaches with an additional bandpass applied to the RS data. Group-level analyses of fMRI data will be conducted using the Flexible Factorial module in SPM. The time-by-treatment interaction effects will be tested at $p < 0.05$ family-wise error corrected at the peak level and with a primary threshold of $p < 0.001$ uncorrected at the cluster level.

DISCUSSION

This study protocol presents the design of an RCT investigating the therapeutic effects of repeated sessions of anodal tDCS over the left DLPFC using a combined approach of EEG, fMRI, and eye-tracking data as well as clinically relevant scores from participants and caregivers. Therefore, the results of this study will elucidate the changeability of aberrant activity through neurostimulation on multiple levels.

An important determinant of stimulation effectiveness is the placement and size of the electrodes (133, 134). Accordingly, and in contrast to previous tDCS studies in children and adolescents with ASD, our study utilizes a parameter configuration based on computational modeling using MRI scans from adolescents with ASD for the simulations.

Another contrast to previous investigations is the use of an intra-stimulation training aiming specifically at improving social cognition and emotion recognition. The training is designed to not only motivate the participants and standardize what they are doing during the stimulation, but also to evoke activity in the target regions of the stimulation. To account for different levels of skills among the participants and to increase ecological validity, the task involves emotion recognition at different levels of difficulty using basic and complex emotions that will be presented isolated or in a dynamic social scene. Moreover, the repeated examination of emotion recognition performance will provide important information about learning curves and session-by-session changes. This may guide future projects in deciding about the ideal number of stimulation sessions, as studies investigating the cumulative effects of tDCS over several days are sparse. Furthermore, there is not much evidence available about the long-term effects of this treatment method. By including two follow-up measures, this study will provide information about the persistence of treatment effects regarding the clinical symptomatology up to 6 months after the end of the intervention.

Within this project, it will also be monitored how the participants react to the stimulation using the questionnaire of sensations related to transcranial electrical stimulation. Even though the safety of tDCS in pediatric populations has been demonstrated repeatedly (92), information about how this patient group perceives and tolerates the mild adverse events of tDCS seems warranted. Individuals with ASD often suffer from sensory hypersensitivity (135) and may thus respond differently to the stimulation.

In this trial, a standard bipolar tDCS montage will be used with the anode placed over the DLPFC targeting the MPFC. However, other montages or stimulation methods such as multi-electrode tDCS or repetitive transcranial magnetic stimulation (rTMS) are also of interest for this population. Here, this established bipolar direct current protocol was chosen as it has milder side effects, has no history of reported serious adverse effects, and is noiseless compared to rTMS (91, 92, 136, 137). Therefore, it might be better tolerated in individuals with ASD, and participants will not be distracted from the intra-stimulation training by potentially painful sensations or sound. Regarding the usage of tDCS as a clinical treatment, a bipolar tDCS has the advantage of being more affordable, portable, and easy to administer, and it opens the possibility for home use in the future. A comparison of the effects of different stimulation protocols as well as stimulation sites is an essential element for future studies.

During the intervention, participants will have daily contact with the study team and undergo the intra-stimulation training. Although these factors could have a beneficial effect on ASD symptoms and emotion recognition skills, the double-blind design and randomization to either active or sham tDCS treatment should mitigate this potential bias.

In conclusion, children and adolescents with ASD are in need of an effective treatment, and modulating brain activity could be a first step toward a new efficient intervention. This

neurophysiologically based approach benefits from being non-invasive, being easy to administer, and having only mild and transient side effects (92, 138). TDCS further aims to overcome shortcomings of traditional interventions, such as often long and expensive treatment periods (5). Taken together, this study will provide information about the efficacy of tDCS and the potential to establish it as an affordable alternative or additive treatment for individuals with ASD in the long run.

TRIAL STATUS

The described trial is ongoing, and recruitment commenced in July 2019. Recruitment and interventions had to be paused due to COVID-19 restrictions from March 13, 2020 to June 15, 2020. The data collection will continue until 20 participants completed all 10 intervention sessions and the corresponding pre- and post-measurements. Follow-ups will be conducted 1 and 6 months after the stimulation sessions to investigative long-lasting effects.

ETHICS STATEMENT

The study was approved by the ethics committee of the Medical University of Vienna and the Austrian Agency for Health and Food Safety (AGES) and will be conducted according to the Declaration of Helsinki. Both participants and caregivers receive information sheets and consent forms about the study to take home. Participants and caregivers must agree to take part in the study and return their signed informed consent forms, before being included in the study. Consent can be withdrawn by the participants or caregivers at any time without any effect on their standard clinical treatment.

AUTHOR CONTRIBUTIONS

KP, LK, LP, and PP designed the trial. KP and SR developed, programmed, and piloted the ERT paradigm. GA, KP, and LK designed the stimulation model and defined the stimulation parameters. MK, RL, SR, and KP planned the data analysis. KP and LK coordinate the recruitment of the participants. KP and MK are responsible for the data collection during the study. KP, SR, GA, MK, RL, PP, LP, and LK wrote, edited, and revised the paper. All authors approved the final manuscript.

FUNDING

KP, SR, GA, MK, and LK are partly supported by the Austrian Science Fund (FWF): KLI600B27. SR was supported by the German Research Foundation (DFG): GRK2277.

ACKNOWLEDGMENTS

The authors would like to acknowledge Franz Benninger, Kamer Doganay, Nina Ebner, Mercedes Huscsava, Susanne Ohmann, Julia Philipp, Thomas Straß, Christine Vesely, and Sonja Werneck-Rohrer (in alphabetical order) for assisting in the recruiting process and IT.

REFERENCES

1. Maenner MJ, Shaw KA, Baio J, Washington A, Patrick M, DiRienzo M, et al. Prevalence of autism spectrum disorder among children aged 8 Years - Autism and developmental disabilities monitoring network, 11 Sites, United States, 2016. *MMWR Surveill Summar.* (2020) 69:1–12. doi: 10.15585/mmwr.ss6904a1
2. Loomes R, Hull L, Mandy WPL. What is the male-to-female ratio in autism spectrum disorder? A systematic review and meta-analysis. *J Am Acad Child Adolesc Psychiatry.* (2017) 56:466–74. doi: 10.1016/j.jaac.2017.03.013
3. WHO (2016). *Internationale Klassifikation psychischer Störungen: ICD-10.* Göttingen: Hogrefe.
4. Medavarapu, S., Marella, L. L., Sangem, A., and Kairam, R. (2019). Where is the evidence? A narrative literature review of the treatment modalities for autism spectrum disorders. *Cureus.* 11:e3901. doi: 10.7759/cureus.3901
5. DeFilippis M, Wagner KD. Treatment of autism spectrum disorder in children and adolescents. *Psychopharmacol Bull.* (2016) 46:18–41.
6. Fuentes J, Hervás A, Howlin P. ESCAP practice guidance for autism: a summary of evidence-based recommendations for diagnosis and treatment. *Eur Child Adolesc Psychiatry*. (2020) 30:961–84. doi: 10.1007/s00787-020-01587-4
7. Sandbank M, Bottema-Beutel K, Crowley S, Cassidy M, Dunham K, Feldmann JI, et al. Project AIM: autism intervention meta-analysis for studies of young children. *Psychol Bull.* (2020) 146:1–29. doi: 10.1037/bul0000215
8. Howlin P, Magiati I. Autism spectrum disorder: outcomes in adulthood. *Curr Opin Psychiatry.* (2017) 30:69–76. doi: 10.1097/YCO.0000000000000308
9. Howlin P, Moss P. Adults with autism spectrum disorders. *Can J Psychiatry.* (2012) 57:275–83. doi: 10.1177/070674371205700502
10. Barrera ME, Maurer D. The perception of facial expressions by the three-month-old. *Child Dev.* (1981) 52:203–6. doi: 10.2307/1129231
11. Meinhardt-Injac B, Kurbel D, and Meinhardt G. The coupling between face and emotion recognition from early adolescence to young adulthood. *Cogn. Dev.* (2020) 53:100851. doi: 10.1016/j.cogdev.2020.100851
12. Rueda P, Fernández-Berrocal P, Baron-Cohen S. Dissociation between cognitive and affective empathy in youth with Asperger Syndrome. *Eur J Dev Psychol.* (2015) 12:85–98. doi: 10.1080/17405629.2014.950221
13. Uljarevic M, Hamilton A. Recognition of emotions in autism: a formal meta-analysis. *J Aut.* (2013) 43:1517–26. doi: 10.1007/s10803-012-1695-5
14. Sivaratnam CS, Newman LK, Tonge BJ, Rinehart NJ. Attachment and emotion processing in children with autism spectrum attachment and emotion processing in children with autism spectrum disorders : neurobiological, neuroendocrine, and neurocognitive considerations. *Rev J Autism Dev Disord.* (2015) 2:222–42. doi: 10.1007/s40489-015-0048-7
15. Von Dem Hagen EAH, Stoyanova RS, Rowe JB, Baron-Cohen S, Calder AJ. Direct gaze elicits atypical activation of the theory-of-mind network in Autism spectrum conditions. *Cereb Cortex.* (2014) 24:1485–92. doi: 10.1093/cercor/bht003
16. Papagiannopoulou EA, Chitty KM, Hermens DF, Hickie IB, Papagiannopoulou EA, Chitty KM, et al. A systematic review and meta-analysis of eye-tracking studies in children with autism spectrum disorders. *Soc Neurosci.* (2014) 9:37–41. doi: 10.1080/17470919.2014.934966
17. Reisinger DL, Shaffer RC, Horn PS, Hong MP, Pedapati EV, Dominick KC, et al. Atypical social attention and emotional face processing in autism spectrum disorder: insights from face scanning and pupillometry. *Front Integr Neurosci.* (2020) 13:76. doi: 10.3389/fnint.2019.00076
18. Blakemore SJ. The social brain in adolescence. *Nat Rev Neurosci.* (2008) 9:267–77. doi: 10.1038/nrn2353
19. Mills KL, Lalonde F, Clasen LS, Giedd JN, Blakemore SJ. Developmental changes in the structure of the social brain in late childhood and adolescence. *Soc Cogn Affect Neurosci.* (2014) 9:123–31. doi: 10.1093/scan/nss113

20. Sato W, Uono S. The atypical social brain network in autism: advances in structural and functional MRI studies. *Curr Opin Neurol.* (2019) 32:617–21. doi: 10.1097/WCO.0000000000000713
21. D'Albis MA, Guevara P, Guevara M, Laidi C, Boisgontier J, Sarrazin S, et al. Local structural connectivity is associated with social cognition in autism spectrum disorder. *Brain.* (2018) 141:3472–81. doi: 10.1093/brain/awy275
22. Pereira AM, Campos BM, Coan AC, Pegoraro LF, de Rezende TJR, Obeso I, et al. Differences in cortical structure and functional MRI connectivity in high functioning autism. *Front. Neurol.* (2018) 9:539. doi: 10.3389/fneur.2018.00539
23. Sato W, Uono S, Kochiyama T, Yoshimura S, Sawada R, Kubota Y, et al. Structural correlates of reading the mind in the eyes in autism spectrum disorder. *Front Hum Neurosci.* (2017) 11:361. doi: 10.3389/fnhum.2017.00361
24. Yang X, Si T, Gong Q, Qiu L, Jia Z, Zhou M, et al. Brain gray matter alterations and associated demographic profiles in adults with autism spectrum disorder: a meta-analysis of voxel-based morphometry studies. *Austr N Z J Psychiatry.* (2016) 50:741–53. doi: 10.1177/0004867415623858
25. Müller R-A, Fishman I. Brain connectivity and neuroimaging of social networks in autism. *Trends Cogn Sci.* (2018) 22:1103–16. doi: 10.1016/j.tics.2018.09.008
26. Ciaramidaro A, Bölte S, Schlitt S, Hainz D, Poustka F, Weber B, et al. Transdiagnostic deviant facial recognition for implicit negative emotion in autism and schizophrenia. *Eur Neuropsychopharmacol.* (2018) 28:264–75. doi: 10.1016/j.euroneuro.2017.12.005
27. Carrington SJ, Bailey AJ. Are there theory of mind regions in the brain? A review of the neuroimaging literature. *Hum Brain Mapp.* (2009) 30:2313–35. doi: 10.1002/hbm.20671
28. Doyle-Thomas KAR, Lee W, Foster NEV, Tryfon A, Ouimet T, Hyde KL, et al. Atypical functional brain connectivity during rest in autism spectrum disorders. *Ann Neurol.* (2015) 77:866–76. doi: 10.1002/ana.24391
29. Yerys BE, Gordon EM, Abrams DN, Satterthwaite TD, Weinblatt R, Jankowski KF, et al. Default mode network segregation and social deficits in autism spectrum disorder: evidence from non-medicated children DMN in children with ASD. *NeuroImage.* (2015) 9:223–32. doi: 10.1016/j.nicl.2015.07.018
30. Buckner RL, DiNicola LM. The brain's default network: updated anatomy, physiology and evolving insights. *Nat Rev Neurosci.* (2019) 20:593–608. doi: 10.1038/s41583-019-0212-7
31. Minshew NJ, Keller TA. The nature of brain dysfunction in autism: functional brain imaging studies. *Curr Opin Neurol.* (2010) 23:124–30. doi: 10.1097/WCO.0b013e32833782d4
32. Kleinhans NM, Richards T, Sterling L, Stegbauer KC, Mahurin R, Johnson LC, et al. Abnormal functional connectivity in autism spectrum disorders during face processing. *Brain.* (2008). 131(Pt 1):1000–12. doi: 10.1093/brain/awm334
33. Washington SD, Gordon EM, Brar J, Warburton S, Sawyer AT, Wolfe A, et al. Dysmaturation of the default mode network in autism. *Hum Brain Mapp.* (2014) 35:1284–96. doi: 10.1002/hbm.22252
34. Odriozola P, Dajani DR, Burrows CA, Gabard-Durnam LJ, Goodman E, Baez AC, et al. Atypical frontoamygdala functional connectivity in youth with autism. *Dev Cogn Neurosci.* (2019) 37:100603. doi: 10.1016/j.dcn.2018.12.001
35. Jung M, Tu Y, Lang CA, Ortiz A, Park J, Jorgenson K, et al. Decreased structural connectivity and resting-state brain activity in the lateral occipital cortex is associated with social communication deficits in boys with autism spectrum disorder. *Neuroimage.* (2019) 190:205–12. doi: 10.1016/j.neuroimage.2017.09.031
36. Wang J, Barstein J, Ethridge LE, Mosconi MW, Takarae Y, Sweeney JA. Resting state EEG abnormalities in autism spectrum disorders. *J Neurodev Disord.* (2013) 5:24. doi: 10.1186/1866-1955-5-24
37. Zhou T, Kang J, Cong F, Li DX. Early childhood developmental functional connectivity of autistic brains with non-negative matrix factorization. *NeuroImage.* (2020) 26:102251. doi: 10.1016/j.nicl.2020.102251
38. Mash LE, Keehn B, Linke AC, Liu TT, Helm JL, Haist F, et al. Atypical relationships between spontaneous EEG and fMRI activity in Autism. *Brain Connect.* (2020) 10:18–28. doi: 10.1089/brain.2019.0693
39. Brunoni AR, Nitsche MA, Bolognini N, Bikson M, Wagner T, Merabet L, et al. Clinical research with transcranial direct current stimulation (tDCS): challenges and future directions. *Brain Stimul.* (2012) 5:175–95. doi: 10.1016/j.brs.2011.03.002
40. Nitsche MA, Paulus W. Excitability changes induced in the human motor cortex by weak transcranial direct current stimulation. *J Physiol.* (2000) 633–9. doi: 10.1111/j.1469-7793.2000.t01-1-00633.x
41. Antal A, Terney D, Poreisz C, Paulus W. Towards unravelling task-related modulations of neuroplastic changes induced in the human motor cortex. *Eur J Neurosci.* (2007) 26:2687–91. doi: 10.1111/j.1460-9568.2007.05896.x
42. Stagg CJ, Antal A, Nitsche MA. Physiology of transcranial direct current stimulation. *JECT.* (2018) 34:144–52. doi: 10.1097/YCT.0000000000000510
43. Krause B, Cohen Kadosh R. Can transcranial electrical stimulation improve learning difficulties in atypical brain development? A future possibility for cognitive training. *Dev Cogn Neurosci.* (2013) 6:176–94. doi: 10.1016/j.dcn.2013.04.001
44. Nitsche M, Liebetanz D, Lang N, Antal A, Tergau F, Paulus W, et al. Safety criteria for transcranial direct current stimulation (tDCS) in humans [1] (multiple letters). *Clin Neurophysiol.* (2003) 114:2220–3. doi: 10.1016/S1388-2457(03)00235-9
45. Palm U, Segmiller FM, Epple AN, Freisleder F-J, Koutsouleris N, Schulte-Körne G, et al. Transcranial direct current stimulation in children and adolescents: a comprehensive review. *J Neural Transm.* (2016) 123:1219–34. doi: 10.1007/s00702-016-1572-z
46. Vecchio F, Di Iorio R, Miraglia F, Granata G, Romanello R, Bramanti P, et al. Transcranial direct current stimulation generates a transient increase of small-world in brain connectivity: an EEG graph theoretical analysis. *Exp Brain Res.* (2018) 236:1117–27. doi: 10.1007/s00221-018-5200-z
47. Balconi M, Vitaloni S. The tDCS effect on alpha brain oscillation for correct vs. incorrect object use the contribution of the left DLPFC. *Neurosci Lett.* (2012) 517:25–9. doi: 10.1016/j.neulet.2012.04.010
48. Mangia AL, Pirini M, Cappello A. Transcranial direct current stimulation and power spectral parameters: a tDCS/EEG co-registration study. *Front Hum Neurosci.* (2014) 8:601. doi: 10.3389/fnhum.2014.00601
49. Spitoni GF, Cimmino RL, Bozzacchi C, Pizzamiglio L, Di Russo F. Modulation of spontaneous alpha brain rhythms using low-intensity transcranial direct-current stimulation. *Front Hum Neurosci.* (2013) 7:529. doi: 10.3389/fnhum.2013.00529
50. Antonenko XD, Schubert F, Bohm XF, Ittermann B, Aydin S, Hayek D, et al. tDCS-Induced modulation of GABA levels and resting-state functional connectivity in older adults. *J. Neurosci.* (2017) 37:4065–73. doi: 10.1523/JNEUROSCI.0079-17.2017
51. Keeser D, Meindl T, Bor J, Palm U, Pogarell O, Mulert C, et al. Prefrontal transcranial direct current stimulation changes connectivity of resting-state networks during fMRI. *J Neurosci.* (2011) 31:15284–93. doi: 10.1523/JNEUROSCI.0542-11.2011
52. Neeb L, Bayer A, Bayer K, Farmer A, Fiebach JB, Siegmund B, et al. Transcranial direct current stimulation in inflammatory bowel disease patients modifies resting-state functional connectivity: a RCT. *Brain Stimul.* (2019) 12:978–80. doi: 10.1016/j.brs.2019.03.001
53. Weber MJ, Messing SB, Rao H, Detre JA, Thompson-Schill SL. Prefrontal transcranial direct current stimulation alters activation and connectivity in cortical and subcortical reward systems: a tDCS-fMRI study. *Hum Brain Mapp.* (2014) 35:3673–86. doi: 10.1002/hbm.22429
54. Deng Z, De Luber B, Balderston NL, Velez Afanador M, Noh MM, Thomas J, et al. Device-based modulation of neurocircuits as a therapeutic for psychiatric disorders. *Annu Rev Pharmacol Toxicol.* (2020) 60:591–614. doi: 10.1146/annurev-pharmtox-010919-023253
55. Ke Y, Wang N, Du J, Kong L, Liu S, Xu M, et al. The effects of transcranial direct current stimulation (tDCS) on working memory training in healthy young adults. *Front Hum Neurosci.* (2019) 13:19. doi: 10.3389/fnhum.2019.00019
56. Martin DM, Teng JZ, Lo TY, Alonzo A, Goh T, Iacoviello BM, et al. Clinical pilot study of transcranial direct current stimulation combined with Cognitive Emotional Training for medication resistant depression. *J Affect Disord.* (2018) 232:89–95. doi: 10.1016/j.jad.2018.02.021
57. Chan MMY, Han YMY. (2020). Effects of transcranial direct current stimulation (tdcs) in the normalization of brain activation in patients with neuropsychiatric disorders: a systematic review of

neurophysiological and neuroimaging studies. *Neural Plast.* (2020) 2020:8854412. doi: 10.1155/2020/8854412
58. Adeyemo BO, Simis M, Macea DD, Fregni F. Systematic review of parameters of stimulation, clinical trial design characteristics, and motor outcomes in non-invasive brain stimulation in stroke. *Front Psychiatry.* (2012) 3:88. doi: 10.3389/fpsyt.2012.00088
59. Biou E, Cassoudesalle H, Cogné M, Sibon I, De Gabory I, Dehail P, et al. Transcranial direct current stimulation in post-stroke aphasia rehabilitation: a systematic review. *Ann Phys Rehabil Med.* (2019) 62:104–21. doi: 10.1016/j.rehab.2019.01.003
60. Dondé C, Amad A, Nieto I, Brunoni AR, Neufeld NH, Bellivier F, et al. Transcranial direct-current stimulation (tDCS) for bipolar depression: a systematic review and meta-analysis. *Prog Neuro-Psychopharmacol Biol Psychiatry.* (2017) 78:123–31. doi: 10.1016/j.pnpbp.2017.05.021
61. Kostova R, Cecere R, Thut G, Uhlhaas PJ. Targeting cognition in schizophrenia through transcranial direct current stimulation: a systematic review and perspective. *Schizophr Res.* (2020) 220:300–10. doi: 10.1016/j.schres.2020.03.002
62. Kenney-Jung DL, Blacker CJ, Camsari DD, Lee JC, Lewis CP. Transcranial direct current stimulation. *Child Adolesc Psychiatr Clin N Am.* (2019) 28:53–60. doi: 10.1016/j.chc.2018.07.008
63. Muszkat D, Polanczyk GV, Dias TGC, Brunoni AR. Transcranial direct current stimulation in child and adolescent psychiatry. *J Child Adolesc Psychopharmacol.* (2016) 26:590–7. doi: 10.1089/cap.2015.0172
64. Salehinejad MA, Wischnewski M, Nejati V, Vicario CM, Nitsche MA. Transcranial direct current stimulation in attention-deficit hyperactivity disorder: a meta-analysis of neuropsychological deficits. *PLoS ONE.* (2019) 14:e221613. doi: 10.1371/journal.pone.0221613
65. Amatachaya A, Auvichayapat N, Patjanasoontorn N, Suphakunpinyo C, Ngernyam N, Aree-Uea B, et al. Effect of anodal transcranial direct current stimulation on autism: a randomized double-blind crossover trial. *Behav Neurol.* (2014) 2014:173073. doi: 10.1155/2014/173073
66. Auvichayapat N, Patjanasoontorn N, Phuttharak W, Suphakunpinyo C, Keeratitanont K, Tunkamnerdthai O, et al. Brain metabolite changes after anodal transcranial direct current stimulation in autism spectrum disorder. *Front Mol Neurosci.* (2020) 13:70. doi: 10.3389/fnmol.2020.00070
67. Costanzo F, Menghini D, Casula L, Amendola A, Mazzone L, Valeri G, et al. Transcranial direct current stimulation treatment in an adolescent with autism and drug-resistant catatonia. *Brain Stimul.* (2015) 8:1233–5. doi: 10.1016/j.brs.2015.08.009
68. Gómez L, Vidal B, Maragoto C, Morales LM, Berrillo S, Cuesta HV, et al. Non-invasive brain stimulation for children with autism spectrum disorders : a short-term outcome study. *Behav Sci.* (2017) 7:1–12. doi: 10.3390/bs7030063
69. Hadoush H, Alafeef M, Abdulhay E. Brain complexity in children with mild and severe autism spectrum disorders: analysis of multiscale entropy in EEG. *Brain Topogr.* (2019) 32:914–21. doi: 10.1007/s10548-019-00711-1
70. Hadoush H, Nazzal M, Almasri NA, Khalil H, Alafeef M. Therapeutic effects of bilateral anodal transcranial direct current stimulation on prefrontal and motor cortical areas in children with autism spectrum disorders: a pilot study. *Autism Res.* (2020) 13:828–36. doi: 10.1002/aur.2290
71. Hupfeld K, Ketcham C. Behavioral effects of transcranial direct current stimulation on motor and language planning in minimally verbal children with Autism Spectrum Disorder (ASD): feasibility, limitations and future directions. *J Childh Dev Disord.* (2016) 2:1–12. doi: 10.4172/2472-1786.100029
72. Kang J, Cai E, Han J, Tong Z, Li X, Sokhadze EM, et al. Transcranial direct current stimulation (tDCS) can modulate EEG complexity of children with autism spectrum disorder. *Front Neurosci.* (2018) 12:201. doi: 10.3389/fnins.2018.00201
73. Mahmoodifar E, Sotoodeh MS. Combined transcranial direct current stimulation and selective motor training enhances balance in children with autism spectrum disorder. *Percept Mot Skills.* (2020) 127:113–25. doi: 10.1177/0031512519888072
74. Schneider HD, Hopp JP. The use of the Bilingual Aphasia Test for assessment and transcranial direct current stimulation to modulate language acquisition in minimally verbal children with autism. *Clin Linguist Phonet.* (2011) 25:640–54. doi: 10.3109/02699206.2011.570852
75. Zhou T, Kang J, Li Z, Chen H, Li X. Transcranial direct current stimulation modulates brain functional connectivity in autism. *NeuroImage.* (2020) 28:102500. doi: 10.1016/j.nicl.2020.102500
76. Amatachaya A, Jensen MP, Patjanasoontorn N, Auvichayapat N, Suphakunpinyo C, Janjarasjitt S, et al. The short-term effects of transcranial direct current stimulation on electroencephalography in children with autism: A randomized crossover controlled trial. *Behav Neurol.* (2015) 2015:928631. doi: 10.1155/2015/928631
77. García-González S, Lugo-Marín J, Setien-Ramos I, Gisbert-Gustemps L, Arteaga-Henríquez G, Díez-Villoria E, et al. Transcranial direct current stimulation in Autism Spectrum Disorder: a systematic review and meta-analysis. *Eur Neuropsychopharmacol.* (2021) 48:89–109. doi: 10.1016/j.euroneuro.2021.02.017
78. Khaleghi A, Zarafshan H, Vand SR, Mohammadi MR. Effects of non-invasive neurostimulation on autism spectrum disorder: a systematic review. *Clin Psychopharmacol Neurosci.* (2020) 18:527–52. doi: 10.9758/cpn.2020.18.4.527
79. Caldas Osório AA, Brunoni AR. Transcranial direct current stimulation in children with autism spectrum disorder : a systematic scoping review. *Dev Med Child Neurol.* (2019) 61:298–304. doi: 10.1111/dmcn.14104
80. Gómez-Fernández L, Vidal-Martínez B, Maragoto-Rizo C, Morales-Chacón L, Berrillo-Batista S, Vera-Cuesta H, et al. Safety and effectiveness of non-invasive brain stimulation in autism spectrum disorder: results from a proof of concept study. *Rev Mexicana Neuroci.* (2018) 19:8–20.
81. van Steenburgh JJ, Varvaris M, Vannorsdall TD, Schretlen D, Gordon B. Transcranial direct current stimulation enhances functional connectivity in high-functioning individuals with autism. In: *43rd Annual Meeting of the Child-Neurology-Society*. Vol. 76. Baltimore, MD (2014).
82. Erdfelder E, Faul F, Buchner A, Lang AG. Statistical power analyses using G*Power 3.1: tests for correlation and regression analyses. *Behav Res Methods.* (2009) 41:1149–60. doi: 10.3758/BRM.41.4.1149
83. Poustka F, Bölte S. *Skala zur Erfassung sozial Reaktivität (SRS)*. Bern: Huber (2008).
84. Bölte S, Rühl D, Schmötzer G, Poustka F. *Diagnostisches Interview für Autismus-Revidiert (ADI-R)*. Bern: Huber (2006).
85. Poustka L, Rühl D, Feineis-Matthews S, Poustka F, Hartung M, Bölte S. *ADOS-2. Diagnostische Beobachtungsskala für Autistische Störungen - 2. Deutschsprachige Fassung der Autism Diagnostic Observation Schedule*. Mannheim: Huber (2015).
86. Saturnino GB, Siebner HR, Thielscher A, Madsen KH. Accessibility of cortical regions to focal TES: dependence on spatial position, safety, and practical constraints. *Neuroimage.* (2019) 203:116183. doi: 10.1016/j.neuroimage.2019.116183
87. Beam W, Borckardt JJ, Reeves ST, George MS. An efficient and accurate new method for locating the F3 position for prefrontal TMS applications. *Brain Stimul.* (2009) 2:50–4. doi: 10.1016/j.brs.2008.09.006
88. Ambrus GG, Al-Moyed H, Chaieb L, Sarp L, Antal A, Paulus W. The fade-in - short stimulation - fade out approach to sham tDCS - reliable at 1 mA for naïve and experienced subjects, but not investigators. *Brain Stimul.* (2012) 5:499–504. doi: 10.1016/j.brs.2011.12.001
89. Lefaucheur J-P, Antal A, Ayache SS, Benninger DH, Brunelin J, Cogiamanian F, et al. Evidence-based guidelines on the therapeutic use of transcranial direct current stimulation (tDCS). *Clin Neurophysiol.* (2017) 128:56–92. doi: 10.1016/j.clinph.2016.10.087
90. Buchanan DM, Bogdanowicz T, Khanna N, Lockman-Dufour G, Robaey P, D'Angiulli A. Systematic review on the safety and tolerability of transcranial direct current stimulation in children and adolescents. *Brain Sci.* (2021) 11:1–21. doi: 10.3390/brainsci11020212
91. Krishnan C, Santos L, Peterson MD, Ehinger M. Safety of noninvasive brain stimulation in children and adolescents. *Brain Stimul.* (2015) 8:76–87. doi: 10.1016/j.brs.2014.10.012
92. Antal A, Alekseichuk I, Bikson M, Brockmöller J, Brunoni AR, Chen R, et al. Low intensity transcranial electric stimulation: safety, ethical, legal regulatory and application guidelines. *Clin Neurophysiol.* (2017) 128:1774–809. doi: 10.1016/j.clinph.2017.06.001

93. Andrade AC, Magnavita GM, Allegro JVBN, Neto CEBP, de Cássia Saldanha Lucena R, Fregni F, et al. Feasibility of transcranial direct current stimulation use in children aged 5 to 12 years. *J Child Neurol.* (2014) 29:1360–5. doi: 10.1177/0883073813503710
94. Bandeira ID, Guimarães RSQ, Jagersbacher JG, Barretto TL, de Jesus-Silva JR, Santos SN, et al. Transcranial direct current stimulation in children and adolescents with attention-deficit/hyperactivity disorder (ADHD). *J Child Neurol.* (2016) 31:918–24. doi: 10.1177/0883073816630083
95. Accardo P, Bostwick H. Zebras in the living room: the changing faces of autism. *J Pediatr.* (1999) 135:533–5. doi: 10.1016/S0022-3476(99)70045-4
96. Bölte S, Poustka F. *Fragebogen zur Sozialen Kommunikation - Austismus Screening (FSK)*. Bern: Huber (2006).
97. Abler B, Kessler H. Emotion regulation questionnaire - eine deutschsprachige fassung des ERQ von Gross und John. *Diagnostica.* (2009) 55:144–52. doi: 10.1026/0012-1924.55.3.144
98. Bryant BK. An index of empathy for children and adolescents. *Child Dev.* (1982) 53:413. doi: 10.2307/1128984
99. Heynen EJE, Van der Helm GHP, Stams GJJM, Korebrits AM. Measuring empathy in a german youth prison: a validation of the german version of the basic empathy scale (BES) in a sample of incarcerated juvenile offenders. *J Forensic Psychol Pract.* (2016) 16:336–46. doi: 10.1080/15228932.2016.1219217
100. Dadds MR, Hunter K, Hawes DJ, Frost ADJ, Vassallo S, Bunn P, et al. A measure of cognitive and affective empathy in children using parent ratings. *Child Psychiatry Hum Dev.* (2008) 39:111–122. doi: 10.1007/s10578-007-0075-4
101. Shields A, Cicchetti D. Emotion regulation among school age children: the development and validation of a new criterion q-sort scale. *Dev Psychol.* (1997) 33:906–16. doi: 10.1037/0012-1649.33.6.906
102. Döpfner M, Görtz-Dorten A. *DISYPS-III. Diagnostik-System für Psychische Störungen Nach ICD-10 und DSM-5 für Kinder und Jugendliche - III.* Bern: Hogrefe (2017).
103. Bölte S, Feineis-Matthews S, Leber S, Dierks T, Hubl D, Poustka F. The development and evaluation of a computer-based program to test and to teach the recognition of facial affect. *Int J Circump Health.* (2002) 61(Suppl. 2):61–8. doi: 10.3402/ijch.v61i0.17503
104. Ekman P, Friesen WV. Constants across cultures in the face and emotion. *J Pers Soc Psychol.* (1971) 17:124–9. doi: 10.1037/h0030377
105. Dziobek I, Fleck S, Kalbe E, Rogers K, Hassenstab J, Brand M, et al. Introducing MASC: a movie for the assessment of social cognition. *J Autism Dev Disord.* (2006) 36:623–36. doi: 10.1007/s10803-006-0107-0
106. Müller N, Baumeister S, Dziobek I, Banaschewski T, Poustka L. Validation of the movie for the assessment of social cognition in adolescents with ASD: fixation duration and pupil dilation as predictors of performance. *J Autism Dev Disord.* (2016) 46:2831–44. doi: 10.1007/s10803-016-2828-z
107. Tobii Pro AB. *Tobii Studio (Version 3.4.5)*. Danderyd: Tobii Pro AB (2016).
108. O'Reilly H, Lundqvist D, Pigat D, Baron K, Fridenson S, Tal S, et al. *The EU-Emotion Stimulus Set*. Cambridge: Autism Research Centre; University of Cambridge (2012).
109. O'Reilly H, Pigat D, Fridenson S, Berggren S, Tal S, Golan O, et al. The EU-emotion stimulus set : a validation study. *Behav Res Methods.* (2016) 48:567–76. doi: 10.3758/s13428-015-0601-4
110. Ebner N, Riediger M, Lindenberger U. FACES - A database of facial expressions in young. middle-aged, and older women and men. *Behav Res Methods.* (2010) 42:351–62. doi: 10.3758/BRM.42.1.351
111. Holland CAC, Ebner NC, Lin T, Samanez-Larkin GR. Emotion identification across adulthood using the Dynamic FACES database of emotional expressions in younger, middle aged, and older adults. *Cogn Emot.* (2018) 33:245–57. doi: 10.1080/02699931.2018.1445981
112. Docter P, and Del Carmen R. *Inside Out*. Walt Disney Studios Motion Pictures (2015).
113. Jia H, Yu D. Aberrant intrinsic brain activity in patients with autism spectrum disorder: insights from eeg microstates. *Brain Topogr.* (2019) 32:295–303. doi: 10.1007/s10548-018-0685-0
114. Jobert M, Wilson FJ, Ruigt GSF, Brunovsky M, Prichep LS, Drinkenburg. Guidelines for the recording and evaluation of pharmaco-EEG data in man: the international pharmaco-EEG society (IPEG). *Neuropsychobiology.* (2012) 66:201–20. doi: 10.1159/000343478
115. Smith SM, Andersson J, Auerbach EJ, Beckmann CF, Bijsterbosch J, Douaud G, et al. Resting-state fMRI in the human connectome project. *Neuroimage.* (2013) 80:144–68. doi: 10.1016/j.neuroimage.2013.05.039
116. Vanderwal T, Kelly C, Eilbott J, Mayes LC, Castellanos FX. Inscapes: a movie paradigm to improve compliance in functional magnetic resonance imaging. *Neuroimage.* (2015) 122:222–32. doi: 10.1016/j.neuroimage.2015.07.069
117. Abell F, Happe F, Frith U. Do triangles play tricks? Attribution of mental states to animated shapes in normal and abnormal development. *J Cogn Dev.* (2000) 15:1–20. doi: 10.1016/S0885-2014(00)00014-9
118. Moessnang C, Schäfer A, Bilek E, Roux P, Otto K, Baumeister S, et al. Specificity, reliability and sensitivity of social brain responses during spontaneous mentalizing. *Soc Cogn Affect Neurosci.* (2016) 1687–97. doi: 10.1093/scan/nsw098
119. White SJ, Coniston D, Rogers R, Frith U. Developing the frith-happe animations: a quick and objective test of theory of mind for adults with autism. *Autism Res.* (2011) 4:149–54. doi: 10.1002/aur.174
120. Bölte S, Feineis-Matthews S, Poustka F. *Frankfurter Test und Training des Erkennens von fazialem Affekt (FEFA)*. Klinik für Psychiatrie und Psychotherapie des Kindes- und Jugendalter, Klinikum der J.W.G.-Universität. (2003).
121. R Core Team. *R: A Language and Environment for Statistical Computing*. Vienna: R Core Team (2020).
122. Gramfort A, Luessi M, Larson E, Engemann DA, Strohmeier D, Brodbeck C, et al. MEG and EEG data analysis with MNE-Python. *Front. Neurosci.* (2013) 7:267. doi: 10.3389/fnins.2013.00267
123. Gramfort A, Luessi M, Larson E, Engemann D, Strohmeier D, Brodbeck C, et al. MNE software for processing MEG and EEG data. *Neuroimage.* (2014) 86:446–60. doi: 10.1016/j.neuroimage.2013.10.027
124. Poldrack RA, Mumford JA, Nichols TE. *Handbook of Functional MRI Data Analysis*. Cambridge: Cambridge University Press (2011).
125. Friston K, Ashburner J, Kiebel S, Nichols T, Penny W. (editors.). *Statistical Parametric Mapping. The Analysis of Functional Brain Images*. London: Academic Press (2007).
126. Beall EB, Lowe MJ. Isolating physiologic noise sources with independently determined spatial measures. *Neuroimage.* (2007) 37:1286–300. doi: 10.1016/j.neuroimage.2007.07.004
127. Beall EB, Lowe MJ. SimPACE: Generating simulated motion corrupted BOLD data with synthetic-navigated acquisition for the development and evaluation of SLOMOCO: a new, highly effective slicewise motion correction. *Neuroimage.* (2014) 101:21–34. doi: 10.1016/j.neuroimage.2014.06.038
128. Patel AX, Kundu P, Rubinov M, Jones PS, Vértes PE, Ersche KD, et al. A wavelet method for modeling and despiking motion artifacts from resting-state fMRI time series. *Neuroimage.* (2014) 95:287–304. doi: 10.1016/j.neuroimage.2014.03.012
129. Wilke M, Altaye M, Holland SK, The CMIND Authorship Consortium. CerebroMatic: a versatile toolbox for spline-based MRI template creation. *Front Comput Neurosci.* (2017) 11:5. doi: 10.3389/fncom.2017.00005
130. Moessnang C, Baumeister S, Tillmann J, Goyard D, Charman T, Ambrosino S, et al. Social brain activation during mentalizing in a large autism cohort: the Longitudinal European Autism Project. *Mol Autism.* (2020) 11:1–17. doi: 10.1186/s13229-020-0317-x
131. Behzadi Y, Restom K, Liau J, Liu TT. A component based noise correction method (CompCor) for BOLD and perfusion based fMRI. *Neuroimage.* (2007) 37:90–101. doi: 10.1016/j.neuroimage.2007.04.042
132. Friston KJ, Williams S, Howard R, Frackowiak RS, Turner R. Movement-related effects in fMRI time-series. *Magn Reson Med.* (1996) 35:346–55. doi: 10.1002/mrm.1910350312
133. Medeiros LF, de Souza ICC, Vidor LP, de Souza A, Deitos A, Volz MS, et al. Neurobiological effects of transcranial direct current stimulation: a review. *Front Psychiatry.* (2012) 3:110. doi: 10.3389/fpsyt.2012.00110
134. Woods AJ, Antal A, Bikson M, Boggio PS, Brunoni AR, Celnik P, et al. A technical guide to tDCS, and related non-invasive brain stimulation tools. *Clin Neurophysiol.* (2016) 127:1031–48. doi: 10.1016/j.clinph.2015.11.012
135. Jussila K, Junttila M, Kielinen M, Ebeling H, Joskitt L, Moilanen I, et al. Sensory abnormality and quantitative autism traits in children with and without autism spectrum disorder in an epidemiological population. *J Autism Dev Disord.* (2020) 50:180–8. doi: 10.1007/s10803-019-04237-0

136. Dhamne SC, Kothare RS, Yu C, Hsieh TH, Anastasio EM, Oberman L, et al. A measure of acoustic noise generated from transcranial magnetic stimulation coils. *Brain Stimul.* (2014) 7:432–4. doi: 10.1016/j.brs.2014.01.056
137. Taylor R, Galvez V, Loo C. Transcranial magnetic stimulation (TMS) safety: a practical guide for psychiatrists. *Austr Psychiatry.* (2018) 26:189–92. doi: 10.1177/1039856217748249
138. Brunoni AR, Boggio PS, Ferrucci R, Priori A, Fregni F. Transcranial direct current stimulation: Challenges, opportunities, and impact on psychiatry and neurorehabilitation. *Front Psychiatry.* (2013) 4:19. doi: 10.3389/fpsyt.2013.00019

Conflict of Interest: RL received travel grants and/or conference speaker honoraria within the last 3 years from Bruker BioSpin MR and Heel and has served as a consultant for Ono Pharmaceutical. He received investigator-initiated research funding from Siemens Healthcare regarding clinical research using PET/MR. He is a shareholder of the start-up company BM Health GmbH since 2019.

The remaining authors declare that the research was conducted in the absence of any commercial or financial relationships that could be construed as a potential conflict of interest.

Publisher's Note: All claims expressed in this article are solely those of the authors and do not necessarily represent those of their affiliated organizations, or those of the publisher, the editors and the reviewers. Any product that may be evaluated in this article, or claim that may be made by its manufacturer, is not guaranteed or endorsed by the publisher.

frontiers in Neuroscience

ORIGINAL RESEARCH
published: 01 September 2021
doi: 10.3389/fnins.2021.722894

rTMS Induces Brain Functional and Structural Alternations in Schizophrenia Patient With Auditory Verbal Hallucination

Yuanjun Xie[1], Muzhen Guan[2], Zhongheng Wang[3], Zhujing Ma[4], Huaning Wang[3], Peng Fang[5] and Hong Yin[1]**

[1] Department of Radiology, Xijing Hospital, Fourth Military Medical University, Xi'an, China, [2] Department of Mental Health, Xi'an Medical University, Xi'an, China, [3] Department of Psychiatry, Xijing Hospital, Fourth Military Medical University, Xi'an, China, [4] Department of Clinical Psychology, School of Medical Psychology, Fourth Military Medical University, Xi'an, China, [5] Department of Military Medical Psychology, School of Medical Psychology, Fourth Military Medical University, Xi'an, China

OPEN ACCESS

Edited by:
Jiaojian Wang, University of Electronic Science and Technology of China, China

Reviewed by:
Ruiyang Ge, University of British Columbia, Canada
Arun Sasidharan, National Institute of Mental Health and Neurosciences, India

***Correspondence:**
Peng Fang
fangpeng@fmmu.edu.cn
Hong Yin
yinhong@fmmu.edu.cn

Specialty section:
This article was submitted to Brain Imaging Methods, a section of the journal Frontiers in Neuroscience

Received: *09 June 2021*
Accepted: *12 August 2021*
Published: *01 September 2021*

Citation:
Xie YJ, Guan MZ, Wang ZH, Ma ZJ, Wang HN, Fang P and Yin H (2021) rTMS Induces Brain Functional and Structural Alternations in Schizophrenia Patient With Auditory Verbal Hallucination. Front. Neurosci. 15:722894. doi: 10.3389/fnins.2021.722894

Background: Low-frequency transcranial magnetic stimulation (rTMS) over the left temporoparietal cortex reduces the auditory verbal hallucination (AVH) in schizophrenia. However, the underlying neural basis of the rTMS treatment effect for schizophrenia remains not well understood. This study investigates the rTMS induced brain functional and structural alternations and their associations with clinical as well as neurocognitive profiles in schizophrenia patients with AVH.

Methods: Thirty schizophrenia patients with AVH and thirty-three matched healthy controls were enrolled. The patients were administered by 15 days of 1 Hz rTMS delivering to the left temporoparietal junction (TPJ) area. Clinical symptoms and neurocognitive measurements were assessed at pre- and post-rTMS treatment. The functional (amplitude of low-frequency fluctuation, ALFF) and structural (gray matter volume, GMV) alternations were compared, and they were then used to related to the clinical and neurocognitive measurements after rTMS treatment.

Results: The results showed that the positive symptoms, including AVH, were relieved, and certain neurocognitive measurements, including visual learning (VisLearn) and verbal learning (VerbLearn), were improved after the rTMS treatment in the patient group. Furthermore, the rTMS treatment induced brain functional and structural alternations in patients, such as enhanced ALFF in the left superior frontal gyrus and larger GMV in the right inferior temporal cortex. The baseline ALFF and GMV values in certain brain areas (e.g., the inferior parietal lobule and superior temporal gyrus) could be associated with the clinical symptoms (e.g., positive symptoms) and neurocognitive performances (e.g., VerbLearn and VisLearn) after rTMS treatment in patients.

Conclusion: The low-frequency rTMS over the left TPJ area is an efficacious treatment for schizophrenia patients with AVH and could selectively modulate the neural basis underlying psychiatric symptoms and neurocognitive domains in schizophrenia.

Keywords: schizophrenia, auditory verbal hallucination, transcranial magnetic stimulation, MCCB, amplitude of low-frequency fluctuation, voxel-based morphometry

INTRODUCTION

Schizophrenia is a severe and chronic mental disorder that is characterized by diverse psychopathology, including positive symptoms, negative symptoms, and cognitive impairments (Os and Kapur, 2009). Auditory verbal hallucinations (AVH), erroneous perceptions of voices in the absence of external stimuli, are among the main symptoms of schizophrenia reported by 50–70% of patients with schizophrenia (Llorca et al., 2016). Neuroimaging studies have demonstrated that AVH is associated with increased activity in brain regions involving speech perception, including left and right superior temporal cortex (Lennox et al., 2000; Shergill et al., 2000a), left temporoparietal cortex (Silbersweig et al., 1995), and Broca area (McGuire et al., 1993), which reflect abnormal activation of normal auditory pathways. It has been demonstrated that low-frequency (e.g., 1 Hz) repetitive transcranial magnetic stimulation (rTMS) produces a sustained reduction in brain activation that directly stimulated and other relevant brain areas (Boroojerdi et al., 2000; Rossi et al., 2000) and suggests the decreased excitability of pyramidal neurons and long-term depression-like neuroplasticity changes (Touge et al., 2001; Hoffman and Cavus, 2002).

Consequently, low-frequency rTMS delivering to brain regions critical to auditory speech perception may reduce the severity of AVH in schizophrenia. The left temporoparietal junction (TPJ) area appears the most optimal target region for low-frequency rTMS treatment in schizophrenia. Many studies have investigated the efficacy of this setup and have indicated that low-frequency rTMS patterns over the left TPJ area significantly decreased the AVH severity of schizophrenia (Tranulis et al., 2008; Demeulemeester et al., 2012; Otani et al., 2015). Meanwhile, cognitive impairments, such as deficits in working memory (WM), attention, executive function, and processing speed, are core features of schizophrenia (Bora, 2015; Lystad et al., 2017), occurring in a different stage of this disease. Although high-frequency rTMS has been evidence for reducing cognitive impairments (Barr et al., 2013; Jiang et al., 2019; Xiu et al., 2020), low-frequency rTMS also significantly improves certain cognitive functions in schizophrenia (Brunelin et al., 2006; Hoffman et al., 2013). However, the previous studies have shown that the effect of low-frequency rTMS on AVH and cognition in schizophrenia was mixed (Schneider et al., 2008; Lage et al., 2016; Marzouk et al., 2020).

Hence, it is necessary to understand the underlying neural substrate of the rTMS treatment effect to decide whether it is a productive approach for treating schizophrenia. Recently, resting-state functional magnetic resonance imaging (fMRI) has become a promising tool for exploring brain activity and enhancing our understanding of the pathophysiology of schizophrenia (Bassett et al., 2012; Rubinov and Bullmore, 2013). Both functional and structural abnormalities have been reported in schizophrenia by resting-state fMRI data. In the functional domain, the abnormal amplitude of low-frequency fluctuation (ALFF) has been observed in the temporal, occipital, cingulate cortex, and subcortical structures (e.g., hippocampus and thalamus; Alonso-Solis et al., 2017; Hare et al., 2017). For instance, schizophrenia patients with AVH showed increased ALFF in the bilateral temporal role and parahippocampus gyrus, while decreased ALFF in the parietal, occipital, and cingulate cortex. In the structural domain, smaller gray matter volume (GMV) with AVH in schizophrenia patients, as measured with voxel-based morphometry (VBM), have been identified in a wide range of brain regions, including the prefrontal, parietal, temporal, and occipital cortex (Dean et al., 2020; Zhuo et al., 2020).

Few studies have investigated the impact of rTMS treatment on brain activation for schizophrenia patients with AVH. In a first preliminary study, Fitzgerald et al. (2007) reported increased task-related activation in brain areas involved in speech processing circuity (e.g., left inferior frontal gyrus and angular gyrus) in schizophrenia patients with refractory hallucinations after rTMS treatment. In a PET and low-resolution brain electromagnetic tomography (LORETA) study, Horacek et al. (2007) found that schizophrenia patients with auditory hallucinations showed decreased brain metabolism in the left superior temporal gyrus and increased metabolism in the contralateral cortex when low-frequency rTMS was applied to the left temporoparietal cortex. A similar PET study indicated that rTMS-treatment schizophrenia patients with AVH had reduced neuronal activity in language-related regions (e.g., primary auditory and left Broca area; Kindler et al., 2013). Recently, using an inner speech task, Bais et al. (2017) evaluated the effect of rTMS treatment on task-related brain networks in patients with schizophrenia and AVH. They observed that rTMS over the left TPJ area resulted in deactivation of the left supramarginal gyrus and bilateral frontotemporal network, reducing the likelihood of speech intrusion. These results suggest that rTMS over the left TPJ area may affect neural activation in relevant regions for schizophrenia patients.

Although low-frequency rTMS has been applied to treat schizophrenia patients, the underlying neural mechanisms through which rTMS exert such therapeutic effect remain inadequately understood. The present study investigated the effect of 1 Hz rTMS stimulation over the left TPJ area in schizophrenia patients with AVH and identified functional (ALFF) and structural (GMV) alternations using resting-state (fMRI) data. A battery of clinical and neuropsychological assessments was collected and used to evaluate whether the brain alternations were associated with clinical and neurocognitive profiles following the rTMS treatment in patients.

MATERIALS AND METHODS

Subjects

Patients met diagnostic criteria for schizophrenia using the Structural Clinical Interview for DSM-V (Stein et al., 2010). The main inclusion criteria were medication-resistant auditory hallucinations for at least one conventional and one classical antipsychotic and at least five episodes of auditory hallucinations per day during the past month. All patients were on stable

antipsychotic medication for at least 3 weeks before and throughout the rTMS treatment. Exclusion criteria included significant neurological illness or head trauma, unstable medical condition, current alcohol or drug abuse, pregnancy, or MRI contraindication. A total of 32 patients was enrolled in the study. In the meantime, 35 matched healthy controls were recruited; their inclusive criteria were without any history of Axis I disorders or a first-degree relative with a psychotic illness. All participants provided their informed consent before this study. The study trial was registered in the Chinese Clinical Trial Register[1] (registration number: ChiCTR2100041876) and approved by the Medical Ethics Committee of Xijing Hospital.

rTMS Protocol

rTMS treatment was provided for 15 min per day on 15 successive days. The treatment was administered at 1 Hz and 110% of the resting motor threshold (RMT). RMT was determined before the stimulation session according to the standard method (Hoffman et al., 2003), which produced a motor evoked potential of no less than 50 mV in ten trials delivered. The stimulation site was targeted at the TPJ area referenced to the TP3 according to the International 10–20 EEG electrode position system. The stimulus pulse was delivered in sessions by YRD CCY-I magnetic stimulator (YIRUIDE Inc., Wuhan, China) with the figure of 8 coil, at one pulse per second for 10 s, with 5 s interval, consisted of 600 pluses with 60 trains.

Clinical and Neurocognitive Investigation

The clinical symptoms were assessed with the Positive and Negative Scale (PANSS; Kay et al., 1987) and the Auditory Hallucination Rating Scale (AHRS; Hoffman et al., 2005). Neurocognitive assessments were completed using the Chinese version of MATRICS consensus cognitive battery (MCCB; Shi et al., 2015). The Chinese version of MCCB includes nine standardized subtests which reflect seven cognitive domains, including speed of processing (SOP), attention and vigilance (AV), WM, VerbLearn, VisLearn, reasoning and problem-solving (RPS), and social cognition (SC). Experienced psychiatrists executed all assessments at baseline and the end of the rTMS treatment.

Imaging Data Acquire and Preprocessing

The patients underwent scanning within 48 h before the commencement of rTMS treatment and on the day following the end of the treatment course. The healthy controls were only scanned at baseline. Imaging data were acquired on a 3.0 Tesla MRI system with a standard 8-channel head coil (GE Medical Systems, Milwaukee, WI, United States). Earplugs and foam pads were used to minimize scanner noise and head motion. Participants were instructed to close their eyes and remain awake during the scan state. Functional images were acquired using a gradient echo-planar imaging (EPI) sequence (repetition time, 2,000 ms; echo time, 40 ms; field of view, 240 mm × 240 mm flip angle, 90°; matrix, 64 × 64; slice thickness, 3.5 mm; 45 axial slices no gap. A total of 210 volumes were collected for a total scan time of 420 s. Subsequently, high-resolution 3D T1-weighted anatomical images were acquired with an MPRAGE sequence (repetition time, 8.1 ms; echo time, 3.2 ms; field of view, 240 mm × 240 mm; flip angle, 10°; matrix, 256 × 256; slice thickness, 1 mm; and 176 slices sagittal slices).

All images were visually inspected for major artifacts prior to preprocessing. Functional Image data preprocessing was performed using Data Processing Assistant for Resting-State fMRI (DPABI; Yan et al., 2016). The initial ten scan volumes were discarded for steady-state magnetization, and subsequent images were corrected for temporal differences by slice timing and head motion by alignment. The resulting functional images were spatially normalized to the standard space of the Montreal Neurological Institute (MNI) using an optimum affine transformation and non-linear deformations (Ashburner and Friston, 1999), and then resampled to 3 mm × 3 mm × 3 mm isotropic voxels. Nuisance signals, including those from Friston motion parameters, white matter signals, cerebrospinal fluid signals, and mean global signals, were regressed out. Then all the functional images were smoothed with a 6-mm full-width at half-maximum (FWHM) Gaussian filter. Time series linear detrending was conducted to remove low-frequency drifts and high-frequency physiological noise.

Preprocessing of T1-weighted was used by SPM 8 (Statistical Parametric Mapping, Institute of Neurology, London, United Kingdom) accessed through the VBM 8 toolbox.[2] Images were bias-corrected and tissue-classified into gray matter, white matter, and cerebrospinal fluid with the volume probability maps. The gray matter images were registered through the DARTEL approach and normalized to MNI space. The resulting images were modulated and smoothed using an 8 mm FWHM Gaussian filter.

ALFF and VBM Analysis

The ALFF analysis was carried out using the DPABI toolkit. ALFF was calculated by obtaining the square root of the signal across

[1] http://www.chictr.org.cn

[2] http://dbm.neuro.uni-jena.de/vbm/

TABLE 1 | Demographic and clinical characteristics for participants.

Variable	Patients (n = 30)		Controls (n = 33)	t (χ^2)	p
	Baseline	Post-rTMS			
Age (year)	30.30 ± 4.46	–	32.03 ± 7.31	0.954	0.345
Sex (female/male)	17 (13)	–	20 (13)	0.101	0.751
Education (year)	13.20 ± 2.67	–	12.09 ± 2.04	1.708	0.094
Duration of illness (months)	21.36 ± 4.89	–	–	–	–
CPED (mg/day)[a]	584.8 ± 152.39	–	–	–	–

[a] *CPED, Chlorpromazine equivalent doses (Woods, 2003).*

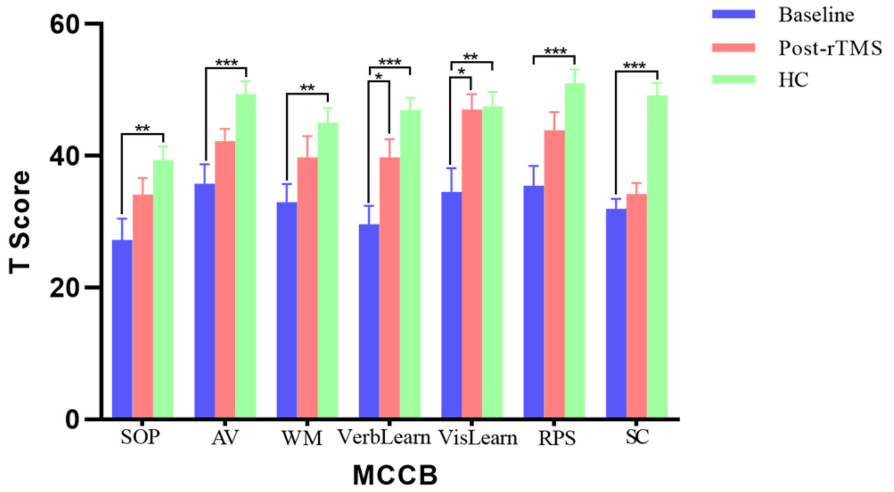

FIGURE 1 | The results of MATRICS consensus cognitive battery (MCCB) comparisons between patients (baseline and post treatment) and controls. $^{*}p < 0.05$, $^{**}p < 0.01$, and $^{***}p < 0.001$.

TABLE 2 | Amplitude of low-frequency fluctuation differences between the patient and control group at baseline.

Brain region	Broadmann	MNI coordinate			Cluster size	*T*
		x	*y*	*z*		
Left superior frontal gyrus (medial)	10	−9	60	9	106	−8.34
Right inferior parietal lobule	40	54	−57	48	51	8.49
Right precuneus	27	12	−39	0	85	12.68

0.01–0.1 Hz for each voxel of the whole brain. For standardization purposes and reducing the influence of individual variation across participants, ALFF was further normalized by dividing the mean within the brain ALFF value for each participant. This created a standardized whole-brain ALFF map. VBM analysis was performed by SPM 8 package,[3] the modulated and smoothed gray matter imagines were entered into the second level module to compare the GMV differences between the patient and control group.

Statistical Analysis

Demographic, clinical, and neurocognitive results were processed in SPSS 20.0 (IBM, Armonk, New York, United States). Two-sample *t*-test and chi-square tests were used to examine group differences for continuous and categorical variables. In addition, independent sample *t*-tests were used to compare ALFF and GMV differences at baseline between patient group and control groups, and paired sample *t*-tests were used to compare ALFF and GMV alternations between baseline and post-rTMS treatment in the patient group. In addition, multiple linear regression analysis was used to explore whether the baseline ALFF and GMV values could be associated with the clinical symptoms and neurocognitive measurements after rTMS treatment in patients.

[3]http://www.fil.ion.ucl.ac.uk/spm/software/spm8/

RESULTS

Demographic, Clinical, and Neurocognitive Outcomes

The demographic and clinical characteristics that were available for participants are displayed in **Table 1**. Two patients and two controls were excluded because of excessive head motion artifacts (head motion exceeded 3 mm or rotation that exceeded 2.5°). The remaining 30 patients and 33 controls were included in the further analysis. The average age of patients included in the present study was 30.30 years old (SD = 4.46, ranging from 18 to 47 years). Seventeen patients (56.76%) were male. The average illness duration was 21.36 months (SD = 4.89, ranged from 10 to 38 months). There were no significant differences between patients and controls in age ($t = 0.954$, $p = 0.345$), sex ($\chi^2 = 0.101$, $p = 0.751$), and education ($t = 1.708$, $p = 0.094$).

After rTMS treatment, the total scores (79.85 ± 10.55 vs. 67.50 ± 7.98), positive symptom scores (19.65 ± 4.59 vs. 14.45 ± 2.80), and general symptom scores (40.35 ± 6.65 vs. 35.20 ± 5.54) in PANSS, and AHRS scores (27.45 ± 6.14 vs. 13.75 ± 7.07) significantly decreased relative to pre-treatment in patients (all $p < 0.01$).

In addition, the patients showed neurocognitive impairments in all seven cognitive domains of MCCB compared to the health controls (all $p < 0.01$) with the multiple comparison corrections using the false discover rate (FDR) approach (**Figure 1**). Moreover, after the rTMS treatment, there were significant improvements in several cognitive domains (FDR correction, $p < 0.05$) in patients, including verbal learning (29.60 ± 12.60

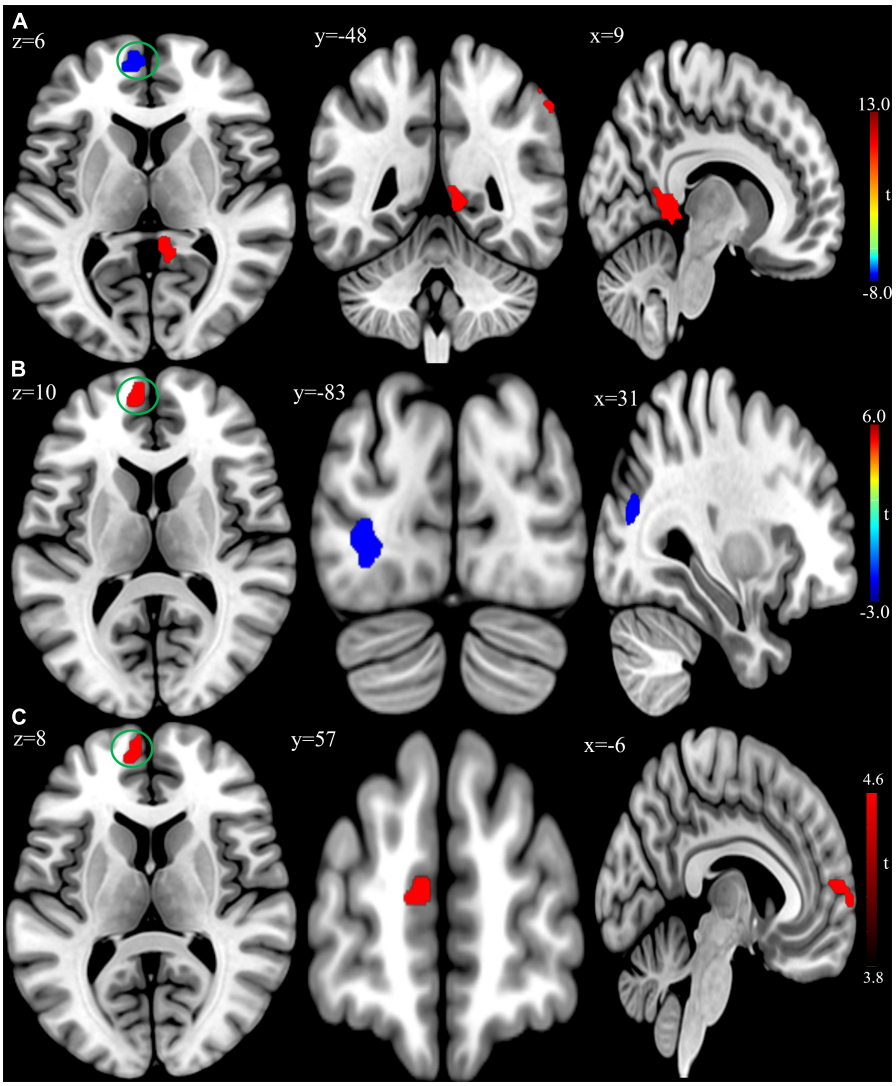

FIGURE 2 | (A) Brain regions showing significant differences of amplitude of low-frequency fluctuation (ALFF) between patient group and healthy control group at baseline. **(B)** Brain regions showing significant differences of ALFF between the posttreatment and baseline in the patient group. **(C)** Conjunction analysis maps of ALFF differences [(baseline vs. controls) ∩ (posttreatment vs. baseline)]. The warm color denoted the region where ALFF is higher, and the cool color denotes the region where ALFF is lower. The color circle denoted the overlapped region of ALFF differences.

vs. 39.60 ± 12.24, $p = 0.035$) and visual learning (34.55 ± 15.95 vs. 47.00 ± 10.54, $p = 0.031$).

Neuroimaging Comparisons at Baseline Between the Patients and Controls

At the baseline, ALFF analysis showed that patients had lower ALFF in the left superior frontal gyrus and higher ALFF in the right inferior parietal lobule and right precuneus compared to the controls (**Table 2** and **Figure 2A**). The cluster threshold was set at $p < 0.05$ and voxel-level at $p < 0.01$ (size > 30) with FDR correction.

In addition, VBM analysis showed that the GMV of the bilateral superior temporal gyrus was significantly larger, while the GMV of the left posterior cingulate gyrus and parahippocampus gyrus were significantly smaller in the patient group relative to the control group at baseline (**Table 3** and **Figure 3A**; FDR correction, cluster-level $p < 0.05$, voxel-level $p < 0.01$, size > 30).

Neuroimaging Comparisons Between Posttreatments and Baseline in Patients

Compared to baseline, the patients with rTMS treatment showed higher ALFF in the left superior frontal gyrus, while lower ALFF in the left inferior occipital gyrus and right middle occipital gyrus (FDR correction, cluster-level $p < 0.05$, voxel-level $p < 0.01$, size > 30; **Table 4** and **Figure 2B**). Additionally, conjunction analysis (Nichols et al., 2005) was used to identity whether there are areas presenting jointly

TABLE 3 | Gray matter volume differences between patient and control group at baseline.

Brain region	Broadmann	MNI coordinates			Cluster size	*T*
		x	*y*	*z*		
Left inferior temporal gyrus	38	−48	−3	−35	217	−11.85
Right inferior temporal gyrus	38	35	−14	−41	372	−13.08
Left inferior frontal gyrus	47	−24	36	2	231	−14.97
Left posterior cingulate cortex	26	−3	−38	15	250	−16.41
Left thalamus	–	−17	−8	8	182	−15.71

significant differences of ALFF for both the baseline and post-treatment comparisons. The ALFF of the left superior frontal gyrus was found to be jointly and significantly higher in posttreatment compared to baseline in patient group (**Figure 2C**).

After rTMS treatment, the patient group had larger GMV in the bilateral inferior temporal cortex, left inferior parietal lobule, and superior occipital cortex relative to baseline (FDR correction, cluster-level $p < 0.05$, voxel-level $p < 0.01$, size > 30; **Table 5** and **Figure 3B**). Also, the conjunction analysis revealed that the GMV of the right inferior temporal gyrus was jointly larger in patients with rTMS than baseline (**Figure 3C**).

Linear Regression Analysis in Patient Group

For the patient group, multiple linear regression analyses were performed with the baseline ALFF and GMV values of the significant brain regions as independent variables and clinical as well as neurocognitive scores after rTMS treatment as dependent variables, obtaining the relationship between the brain metrices

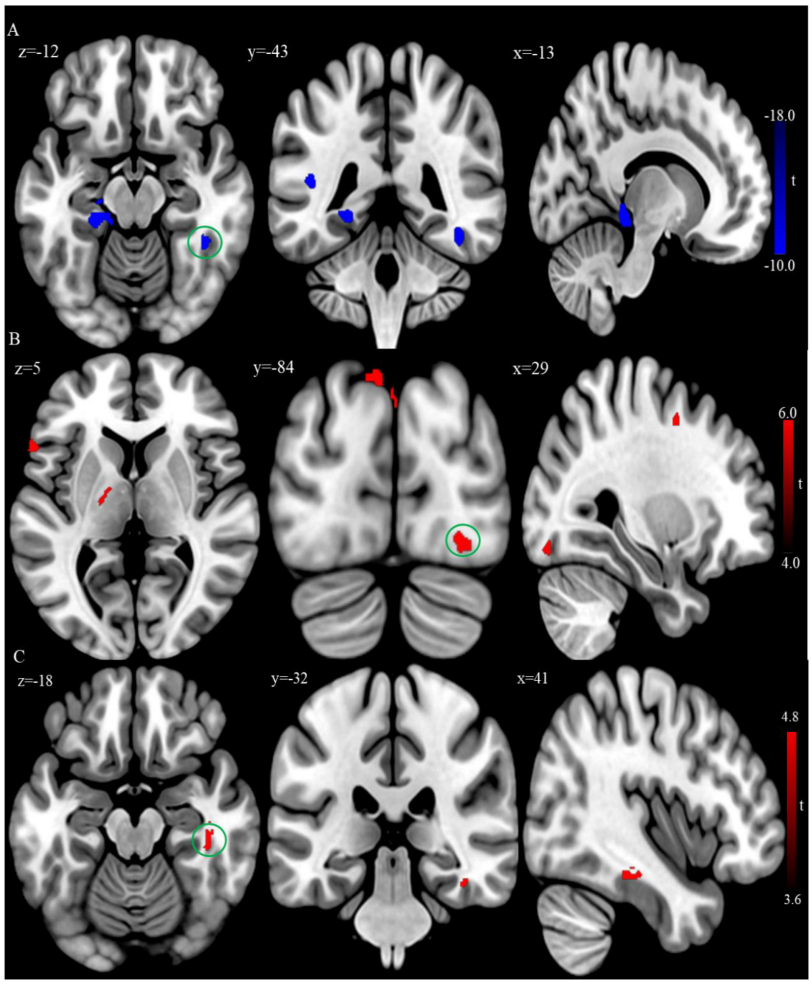

FIGURE 3 | (A) Brain regions showing significant differences of gray matter volume (GMV) between the patient group and healthy control group at baseline. **(B)** Brain regions showing significant difference of GMV between the posttreatment and baseline in the patient group. **(C)** Conjunction analysis maps of GMV differences [(baseline vs. controls) ∩ (posttreatment vs. baseline)]. The warm color denotes the region where the GMV is larger, and the cool color denotes the region where the GMV is smaller. The color circle denoted the overlapped region of GMV differences.

TABLE 4 | Amplitude of low-frequency fluctuation differences between the post treatment and baseline in the patient group.

Brain region	Broadmann	MNI coordinates			Cluster size	*T*
		x	*y*	*z*		
Left superior frontal gyrus (medial)	8	−9	57	12	75	5.08
Left middle occipital gyrus	19	−27	−84	3	134	−3.94
Right middle occipital gyrus	19	30	−75	18	105	−5.39

TABLE 5 | Gray matter volume differences between the posttreatment and baseline in the patient group.

Brain region	Broadmann	MNI coordinate			Cluster size	*T*
		x	*y*	*z*		
Left inferior frontal gyrus	47	−60	20	3	53	4.84
Right inferior frontal gyrus	47	45	51	−21	67	4.42
Right inferior temporal gyrus	20	50	−30	−20	199	5.50
Left middle occipital gyrus	18	−29	−87	45	553	5.70
Right middle occipital gyrus	19	−14	−89	47	65	5.04
Left thalamus	–	−18	−11	6	150	4.16

and clinical symptoms or neurocognitive performances (age, sex, education, and illness of disease as covariates; **Table 6**). The regression analysis revealed a significant positive association between baseline ALFF value of the right inferior parietal lobule and the severity of positive symptoms after rTMS treatment ($B = 0.507$, $p = 0.043$). In addition, the multiple regression showed that the baseline GMV values of the left and right superior temporal gyrus were associated with the verbal learning performance ($B = 0.748$, $p = 0.035$; $B = 0.837$, $p = 0.025$) and visual learning performance ($B = 0.738$, $p = 0.036$; $B = 0.731$, $p = 0.045$) after rTMS treatment.

DISCUSSION

The present study investigated the effect of low-frequency rTMS over the left TPJ area for treating schizophrenia patients with AVH and the following brain functional and structural changes (e.g., ALFF and GMV). The results showed that the positive symptoms, including AVH, were reduced, and certain neurocognitive functions were improved after the rTMS treatment in patients. The results were consistent with the previous report (Aleman et al., 2007) and confirmed that low-frequency rTMS was efficacious in treating schizophrenia patients with AVH. Moreover, rTMS treatment induced ALFF and GMV changes in certain brain regions, and the baseline brain metrics were associated with the positive symptoms as well as neurocognitive performances after rTMS treatment in patient group.

After rTMS treatment, some brain functional and structural changes were observed by resting-state fMRI data analysis in patients. Among these results, the following seem to be interesting. Firstly, ALFF was jointly higher in the left superior frontal gyrus (medial part, BA10) after rTMS treatment. ALFF is thought to reflect spontaneous low-frequency fluctuation of neural activity in a particular voxel. The medial part of superior frontal gyrus (MSFG) is a subdivision of superior frontal cortex (Li et al., 2013) and implicated in the pathophysiology of schizophrenia (Pomarol-Clotet et al., 2010). The MSFG has been described to be a major hub of the default mode network, which is typically more active at rest (Buckner et al., 2008). While this area is hypoactive during the resting state in schizophrenia and associated with the severity of clinical symptoms (Williams et al., 2004; Park et al., 2009; Berger et al., 2018). Then it was possible to observe lower spontaneous activity (e.g., ALFF) of this area in the schizophrenia patients with AVH. Besides, the left MSFG has been suggested to be a part of the complex cortical network related to language processing (Li et al., 2009; Rapp and Steinhäuser, 2013). Patients with schizophrenia have significantly lower signal variations of this cortex compared to controls and could represent an underlying neural basis for impaired language communication and comprehension (Dollfus et al., 2008; Razafimandimby et al., 2016). And the MSFG receives projections from various cortical regions within the lobe (e.g., the superior temporal gyrus and temporal pole; Bachevalier et al., 1997) and could constitute an auditory language network (Reyes-Aguilar et al., 2018). Therefore, abnormality in the MSFG could be reversed through resetting local AVH-related circuits via rTMS treatment and manifested as higher AFLL of this area in patients.

It was worth that the patients had higher baseline ALFF of the right inferior parietal lobule compared to the healthy controls, which met the previous studies (Li et al., 2016; Liang et al., 2019), and were associated with the severity of positive symptoms after rTMS treatment. The inferior parietal lobule is an important part of the frontal-limbic-temporal-parietal network implicated in the schizophrenia disease process (Torrey, 2007), and its overactivity is associated with the presence of positive symptoms in schizophrenia patients (Yildiz et al., 2011). Hence the functional abnormality of the inferior parietal lobule seems to be involved in the clinical symptoms of psychosis.

Secondly, the baseline GMV of the temporal regions was jointly significantly larger in patients after rTMS treatment. AVH arises from a defective self-monitoring of inner speech (Seal et al., 2004; Ditman and Kuperberg, 2005). Self-monitoring of inner speech is associated with activations in the temporal cortex (Frith and Done, 1988). Schizophrenia patients with AVH have attenuated activation in regions implicated in the routine monitoring of inner speech (e.g., temporal cortex; McGuire et al., 1995; Shergill et al., 2000b). The structural abnormalities of the temporal cortex (e.g., reduced GMV) are also frequently reported in schizophrenia patients with AVH (Rajarethinam et al., 2000; Job et al., 2002; Onitsuka et al., 2004). One possible explanation for larger GMV in the right inferior temporal gyrus post-treatment is that rTMS directly stimulating

TABLE 6 | Results of regression analysis at baseline brain metrics on responses to repetitive transcranial magnetic stimulation in the patient group.

	AHRS		Positive symptoms		Verbal learning		Visual learning	
	B	*p*	*B*	*p*	*B*	*p*	*B*	*p*
ALFF								
L SFGmed	−0.036	0.899	0.027	0.924	0.244	0.581	−0.326	0.460
R IPL	−0.171	0.472	0.507	0.043*	0.435	0.242	−0.521	0.163
R PCUN	0.104	0.709	0.234	0.398	0.100	0.815	0.054	0.898
GMV								
L STG	−0.053	0.804	−0.374	0.087	0.748	0.035*	0.738	0.036*
R STG	−0.226	0.318	−0.130	0.555	0.837	0.025*	0.731	0.045*
L IFG	0.051	0.824	−0.152	0.500	−0.278	0.431	0.769	0.040*
L PCC	−0.090	0.747	−0.122	0.656	−0.330	0.444	0.381	0.375
L Thala	0.293	0.209	−0.025	0.917	−0.063	0.792	−0.035	0.882

*$p < 0.05$. *L, left; R, right; SFG, superior frontal gyrus; Med, medial; IPL, inferior parietal lobule; PCUN, precuneus; STG, superior temporal gyrus; IFG, inferior frontal gyrus; PCC, posterior cingulate cortex; Thala, thalamus.*

over the left TPJ area causes brain structural changes on adjacent regions such as the inferior temporal gyrus because of intrinsic connections within these regions (Scheinost et al., 2012).

Another interesting finding was that ALFF was lower in the middle occipital gyrus after the rTMS treatment in patients. Results on ALFF changes in the middle occipital gyrus for schizophrenia were mixed (Gong et al., 2020). Some studies reported a decreased ALFF of the middle occipital gyrus in schizophrenia patients compared to healthy controls (Yu et al., 2014), while others indicated an increased ALFF in the same area (Ren et al., 2013). Although we did not see any change of ALFF in the area at baseline, we speculated that low-frequency rTMS might produce an inhibitory effect on underlying neuronal populations involved in the target site (e.g., TPJ area). The left TPJ area is implicated in cognitive control (Mayer et al., 2004) and connected with the right middle occipital gyrus (Wu et al., 2015), so the inhibition of low-frequency rTMS over the left TPJ would induce connectivity-mediated brain hemodynamic changes and result in the deactivation of the relevant brain areas (e.g., the right middle occipital cortex).

Additionally, this study demonstrated that widespread cognitive impairments existed in schizophrenia patients with AVH in all seven cognitive domains of MCCB and agreed with the previously published studies, which reported that patients with schizophrenia had widespread cognitive deficits (Schuepbach et al., 2002; Chen et al., 2021). Furthermore, we found that certain cognitive domains, such as verbal learning and visual learning, were improved after the rTMS treatment for patients. The results suggest that low-frequency rTMS could contribute to improvements of certain cognitive domains, similar to the high-frequency rTMS protocol applied in schizophrenia (Mogg et al., 2007; Demirtas-Tatlidede et al., 2010; Oh and Kim, 2011), which reported better performance in verbal learning and visual learning in rTMS group.

Specifically, the smaller volume has been identified in the superior temporal gyrus in patients with schizophrenia (Bandeira et al., 2020) and is not due to the effect of medication (Takahashi et al., 2010), which represents a vulnerability marker of psychosis (Borgwardt et al., 2007). In addition to manifesting in psychotic symptoms such as hallucinations (Barta et al., 1990), the superior temporal gyrus is implicated in cognitive functions such as verbal memory (Grasby et al., 1993). Lesion of this cortex impairs verbal memory performance (Takayama et al., 2004). In addition, the superior temporal gyrus is involved in visuospatial processing (e.g., visual search and spatial perception; Karnath et al., 2001; Ellison et al., 2004; Gharabaghi et al., 2006). Therefore, we observed that the baseline GMV of the superior temporal gyrus could be associated with certain cognitive functions after rTMS treatment in patient group, including verbal learning and visual learning, and suggested that the brain structural metric of this cortex is related to cognitive performance (Achiron et al., 2013). The GMV of the left inferior frontal gyrus could be correlated with the patients' the visual learning performance after rTMS treatment, which was consistent with the previous report that this cortex is involved in visual learning and memory (Grèzes and Decety, 2002; Manjaly et al., 2005), and damage to this cortex results in impairment of visual task performance (Husain and Kennard, 1996). These results suggested the GMV of the superior temporal cortex and the inferior frontal cortex were important markers of cognitive impairments in schizophrenia and specifically related to verbal learning and visual learning, as these brain areas are known to be associated with speech comprehension and visuospatial processing.

Some limitations of the present study should be considered. One major limitation of this study is the lack of placebo sham-stimulation control for low-frequency rTMS, which checked our conclusion on the efficacy of the stimulation paradigm. Future research should use the sham-stimulation control to reduce the possible placebo effect. Another potential limitation includes the control participants were only scanned once, which

produced possible confusion on the generality of the results. Future research should preferably use the standard protocol to improve the reliability of the results.

CONCLUSION

The present study investigated the alternations in brain function and structure induced by low-frequency rTMS over the left TPJ area in schizophrenia patients with AVH using resting-state fMRI data. Our findings showed that the rTMS treatment was efficacious for reducing positive symptoms and improving cognitive functions in patients. And the rTMS treatment could lead to specific brain functional and structural alternations. The baseline functional fluctuation (e.g., ALFF) and structural integrity (e.g., GMV) at certain brain areas could be associated with the positive symptoms and neurocognitive functions in patients with rTMS treatment.

DATA AVAILABILITY STATEMENT

The raw data supporting the conclusion of this article will be made available by the authors, without undue reservation.

ETHICS STATEMENT

The studies involving human participants were reviewed and approved by the Medical Ethics Committee of Xijing Hospital, Fourth Military Medical University. The patients/participants provided their written informed consent to participate in this study.

AUTHOR CONTRIBUTIONS

YJX and MZG: conceptualization, methodology and software, and writing. YJX, MZG, and ZHW: validation and formal analysis. YJX, ZHW, and ZJM: data curation. HNW and HY: supervision. PF, HNW, and HY: funding acquisition. All authors have read and agreed to the published version of the manuscript.

FUNDING

This work was supported by the National Natural Science Foundation of China (Grant Nos. 81974215, 61806210, and 81571651).

REFERENCES

Achiron, A., Chapman, J., Tal, S., Bercovich, E., Gil, H., and Achiron, A. (2013). Superior temporal gyrus thickness correlates with cognitive performance in multiple sclerosis. *Brain Struct. Funct.* 218, 943–950. doi: 10.1007/s00429-012-0440-3

Aleman, A., Sommer, I. E., and Kahn, R. S. (2007). Efficacy of slow repetitive transcranial magnetic stimulation in the treatment of resistant auditory hallucinations in schizophrenia: a meta-analysis. *J. Clin. Psychiatry* 68, 416–421. doi: 10.4088/jcp.v68n0310

Alonso-Solis, A., Vives-Gilabert, Y., Portella, M. J., Rabella, M., Grasa, E. M., Roldan, A., et al. (2017). Altered amplitude of low frequency fluctuations in schizophrenia patients with persistent auditory verbal hallucinations. *Schizophr. Res.* 189, 97–103. doi: 10.1016/j.schres.2017.01.042

Ashburner, J., and Friston, K. J. (1999). Nonlinear spatial normalization using basis functions. *Hum. Brain Mapp.* 7, 254–266. doi: 10.1002/(sici)1097-0193(1999)7:4<254::aid-hbm4>3.0.co;2-g

Bachevalier, J., Meunier, M., Lu, M. X., and Ungerleider, L. G. (1997). Thalamic and temporal cortex input to medial prefrontal cortex in rhesus monkeys. *Exp. Brain Res.* 115, 430–444. doi: 10.1007/PL00005713

Bais, L., Liemburg, E., Vercammen, A., Bruggeman, R., Knegtering, H., and Aleman, A. (2017). Effects of low frequency rTMS treatment on brain networks for inner speech in patients with schizophrenia and auditory verbal hallucinations. *Prog. Neuro Psychopharmacol. Biol. Psychiatry* 78, 105–113. doi: 10.1016/j.pnpbp.2017.04.017

Bandeira, I. D., Barouh, J. L., Bandeira, I. D., and Quarantini, L. (2020). Analysis of the superior temporal gyrus as a possible biomarker in schizophrenia using voxel-based morphometry of the brain magnetic resonance imaging: a comprehensive review. *CNS Spectr.* 26, 319–325. doi: 10.1017/S1092852919001810

Barr, M. S., Farzan, F., Rajji, T. K., Voineskos, A. N., Blumberger, D. M., Arenovich, T., et al. (2013). Can repetitive magnetic stimulation improve cognition in schizophrenia? Pilot data from a randomized controlled trial. *Biol. Psychiatry* 73, 510–517. doi: 10.1016/j.biopsych.2012.08.020

Barta, P. E., Pearlson, G. D., Powers, R. E., Richards, S. S., and Tune, L. E. (1990). Auditory hallucinations and smaller superior temporal gyral volume in schizophrenia. *Am. J. Psychiatry* 147, 1457–1462. doi: 10.1176/ajp.147.11.1457

Bassett, D. S., Nelson, B. G., Mueller, B. A., Camchong, J., and Lim, K. O. (2012). Altered resting state complexity in schizophrenia. *NeuroImage* 59, 2196–2207. doi: 10.1016/j.neuroimage.2011.10.002

Berger, P., Bitsch, F., Nagels, A., Straube, B., and Falkenberg, I. (2018). Frontal hypoactivation and alterations in the reward-system during humor processing in patients with schizophrenia spectrum disorders. *Schizophr. Res.* 202, 149–157. doi: 10.1016/j.schres.2018.06.053

Bora, E. (2015). Neurodevelopmental origin of cognitive impairment in schizophrenia. *Psychol. Med.* 45, 1–9. doi: 10.1017/S0033291714001263

Borgwardt, S. J., Riecher-Rössler, A., Dazzan, P., Chitnis, X., Aston, J., Drewe, M., et al. (2007). Regional gray matter volume abnormalities in the at risk mental state. *Biol. Psychiatry* 61, 1148–1156. doi: 10.1016/j.biopsych.2006.08.009

Boroojerdi, B., Prager, A., Muellbacher, W., and Cohen, L. G. (2000). Reduction of human visual cortex excitability using 1-Hz transcranial magnetic stimulation. *Neurology* 54, 1529–1533. doi: 10.1212/WNL.54.7.1529

Brunelin, J., Poulet, E., Bediou, B., Kallel, L., Dalery, J., D'Amato, T., et al. (2006). Low frequency repetitive transcranial magnetic stimulation improves source monitoring deficit in hallucinating patients with schizophrenia. *Schizophr. Res.* 81, 41–45. doi: 10.1016/j.schres.2005.10.009

Buckner, R. L., Andrews-Hanna, J. R., and Schacter, D. L. (2008). "The brain's default network: anatomy, function, and relevance to disease," in *The Year in Cognitive Neuroscience*, eds A. Kingstone and M. B. Miller (Malden, MA: Blackwell Publishing), 1–38. doi: 10.1196/annals.1440.011

Chen, S., Liu, Y., Liu, D., Zhang, G., and Wu, X. (2021). The difference of social cognitive and neurocognitive performance between patients with schizophrenia at different stages and influencing factors. *Schizophr. Res. Cogn.* 24, 1–7. doi: 10.1016/j.scog.2021.100195

Dean, D. J., Woodward, N., Walther, S., McHugo, M., Armstrong, K., and Heckers, S. (2020). Cognitive motor impairments and brain structure in schizophrenia spectrum disorder patients with a history of catatonia. *Schizophr. Res.* 222, 335–341. doi: 10.1016/j.schres.2020.05.012

Demeulemeester, M., Amad, A., Bubrovszky, M., Pins, D., Thomas, P., and Jardri, R. (2012). What is the real effect of 1-Hz repetitive transcranial magnetic stimulation on hallucinations? Controlling for publication bias in neuromodulation trials. *Biol. Psychiatry* 71, e15–e16. doi: 10.1016/j.biopsych.2011.10.010

Demirtas-Tatlidede, A., Freitas, C., Cromer, J. R., Safar, L., Ongur, D., Stone, W. S., et al. (2010). Safety and proof of principle study of cerebellar vermal theta burst stimulation in refractory schizophrenia. *Schizophr. Res.* 124, 91–100. doi: 10.1016/j.schres.2010.08.015

Ditman, T., and Kuperberg, G. R. (2005). A source-monitoring account of auditory verbal hallucinations in patients with schizophrenia. *Harv. Rev. Psychiatry* 13, 280–299. doi: 10.1080/10673220500326391

Dollfus, S., Razafimandimby, A., Maiza, O., Lebain, P., Brazo, P., Beaucousin, V., et al. (2008). Functional deficit in the medial prefrontal cortex during a language comprehension task in patients with schizophrenia. *Schizophr. Res.* 99, 304–311. doi: 10.1016/j.schres.2007.11.016

Ellison, A., Schindler, I., Pattison, L. L., and Milner, A. D. (2004). An exploration of the role of the superior temporal gyrus in visual search and spatial perception using TMS. *Brain* 127, 2307–2315. doi: 10.1093/brain/awh244

Fitzgerald, P. B., Sritharan, A., Benitez, J., Daskalakis, Z. J., Jackson, G., Kulkarni, J., et al. (2007). A preliminary fMRI study of the effects on cortical activation of the treatment of refractory auditory hallucinations with rTMS. *Psychiatry Res. Neuroimaging* 155, 83–88. doi: 10.1016/j.pscychresns.2006.12.011

Frith, C. D., and Done, D. J. (1988). Towards a neuropsychology of schizophrenia. *Br. J. Psychiatry* 153, 437–443. doi: 10.1192/bjp.153.4.437

Gharabaghi, A., Fruhmann Berger, M., Tatagiba, M., and Karnath, H.-O. (2006). The role of the right superior temporal gyrus in visual search—insights from intraoperative electrical stimulation. *Neuropsychologia* 44, 2578–2581. doi: 10.1016/j.neuropsychologia.2006.04.006

Gong, J., Wang, J., Luo, X., Chen, G., Huang, H., Huang, R., et al. (2020). Abnormalities of intrinsic regional brain activity in first-episode and chronic schizophrenia: a meta-analysis of resting-state functional MRI. *J. Psychiatry Neurosci.* 45, 55–68. doi: 10.1503/jpn.180245

Grasby, P. M., Frith, C. D., Friston, K. J., Bench, C., Frackowiak, R. S. J., and Dolan, R. J. (1993). Functional mapping of brain areas implicated in auditory—verbal memory function. *Brain* 116, 1–20. doi: 10.1093/brain/116.1.1

Grèzes, J., and Decety, J. (2002). Does visual perception of object afford action? Evidence from a neuroimaging study. *Neuropsychologia* 40, 212–222. doi: 10.1016/s0028-3932(01)00089-6

Hare, S. M., Ford, J. M., Ahmadi, A., Damaraju, E., Belger, A., Bustillo, J., et al. (2017). Modality-dependent impact of hallucinations on low-frequency fluctuations in schizophrenia. *Schizophr. Bull.* 43, 389–396. doi: 10.1093/schbul/sbw093

Hoffman, R. E., and Cavus, I. (2002). Slow transcranial magnetic stimulation, long-term depotentiation, and brain hyperexcitability disorders. *Am. J. Psychiatry* 159, 1093–1102. doi: 10.1176/appi.ajp.159.7.1093

Hoffman, R. E., Gueorguieva, R., Hawkins, K. A., Varanko, M., Boutros, N. N., Wu, Y.-T., et al. (2005). Temporoparietal transcranial magnetic stimulation for auditory hallucinations: safety, efficacy and moderators in a fifty patient sample. *Biol. Psychiatry* 58, 97–104. doi: 10.1016/j.biopsych.2005.03.041

Hoffman, R. E., Hawkins, K. A., Gueorguieva, R., Boutros, N. N., Rachid, F., Carroll, K., et al. (2003). Transcranial magnetic stimulation of left temporoparietal cortex and medication-resistant auditory hallucinations. *Arch. Gen. Psychiatry* 60, 49–56. doi: 10.1001/archpsyc.60.1.49

Hoffman, R. E., Wu, K., Pittman, B., Cahill, J. D., Hawkins, K. A., Fernandez, T., et al. (2013). Transcranial magnetic stimulation of wernicke's and right Homologous sites to curtail "Voices": a randomized trial. *Biol. Psychiatry* 73, 1008–1014. doi: 10.1016/j.biopsych.2013.01.016

Horacek, J., Brunovsky, M., Novak, T., Skrdlantova, L., Klirova, M., Bubenikova-Valesova, V., et al. (2007). Effect of low-frequency rTMS on electromagnetic tomography (LORETA) and regional brain metabolism (PET) in schizophrenia patients with auditory hallucinations. *Neuropsychobiology* 55, 132–142. doi: 10.1159/000106055

Husain, M., and Kennard, C. (1996). Visual neglect associated with frontal lobe infarction. *J. Neurol.* 243, 652–657. doi: 10.1007/BF00878662

Jiang, Y., Guo, Z., Xing, G., He, L., Peng, H., Du, F., et al. (2019). Effects of high-frequency transcranial magnetic stimulation for cognitive deficit in schizophrenia: a meta-analysis. *Front. Psychiatry* 10:135. doi: 10.3389/fpsyt.2019.00135

Job, D. E., Whalley, H. C., McConnell, S., Glabus, M., Johnstone, E. C., and Lawrie, S. M. (2002). Structural gray matter differences between first-episode schizophrenics and normal controls using voxel-based morphometry. *NeuroImage* 17, 880–889. doi: 10.1006/nimg.2002.1180

Karnath, H.-O., Ferber, S., and Himmelbach, M. (2001). Spatial awareness is a function of the temporal not the posterior parietal lobe. *Nature* 411, 950–953. doi: 10.1038/35082075

Kay, S. R., Fiszbein, A., and Opler, L. A. (1987). The positive and negative syndrome scale (PANSS) for schizophrenia. *Schizophr. Bull.* 13, 261–276. doi: 10.1093/schbul/13.2.261

Kindler, J., Homan, P., Jann, K., Federspiel, A., Flury, R., Hauf, M., et al. (2013). Reduced neuronal activity in language-related regions after transcranial magnetic stimulation therapy for auditory verbal hallucinations. *Biol. Psychiatry* 73, 518–524. doi: 10.1016/j.biopsych.2012.06.019

Lage, C., Wiles, K., Shergill, S. S., and Tracy, D. K. (2016). A systematic review of the effects of low-frequency repetitive transcranial magnetic stimulation on cognition. *J. Neural Transm.* 123, 1479–1490. doi: 10.1007/s00702-016-1592-8

Lennox, B. R., Park, S. B. G., Medley, I., Morris, P. G., and Jones, P. B. (2000). The functional anatomy of auditory hallucinations in schizophrenia. *Psychiatry Res. Neuroimaging* 100, 13–20. doi: 10.1016/s0925-4927(00)00068-8

Li, F., Lui, S., Yao, L., Hu, J., Lv, P., Huang, X., et al. (2016). Longitudinal changes in resting-state cerebral activity in patients with first-episode schizophrenia: a 1-year follow-up functional MR imaging study. *Radiology* 279, 867–875. doi: 10.1148/radiol.2015151334

Li, W., Qin, W., Liu, H., Fan, L., Wang, J., Jiang, T., et al. (2013). Subregions of the human superior frontal gyrus and their connections. *NeuroImage* 78, 46–58. doi: 10.1016/j.neuroimage.2013.04.011

Li, X., Branch, C. A., and DeLisi, L. E. (2009). Language pathway abnormalities in schizophrenia: a review of fMRI and other imaging studies. *Curr. Opin. Psychiatry* 22, 131–139. doi: 10.1097/yco.0b013e328324bc43

Liang, Y., Shao, R., Zhang, Z., Li, X., Zhou, L., and Guo, S. (2019). Amplitude of low-frequency fluctuations in childhood-onset schizophrenia with or without obsessive-compulsive symptoms: a resting-state functional magnetic resonance imaging study. *Arch. Med. Sci.* 15, 126–133. doi: 10.5114/aoms.2018.73422

Llorca, P. M., Pereira, B., Jardri, R., Chereau-Boudet, I., Brousse, G., Misdrahi, D., et al. (2016). Hallucinations in schizophrenia and Parkinson's disease: an analysis of sensory modalities involved and the repercussion on patients. *Sci. Rep.* 6:38152. doi: 10.1038/srep38152

Lystad, J. U., Falkum, E., Haaland, V. Ø., Bull, H., Evensen, S., McGurk, S. R., et al. (2017). Cognitive remediation and occupational outcome in schizophrenia spectrum disorders: a 2 year follow-up study. *Schizophr. Res.* 185, 122–129. doi: 10.1016/j.schres.2016.12.020

Manjaly, Z. M., Marshall, J. C., Stephan, K. E., Gurd, J. M., Zilles, K., and Fink, G. R. (2005). Context–dependent interactions of left posterior inferior frontal gyrus in a local visual search task unrelated to language. *Cogn. Neuropsychol.* 22, 292–305. doi: 10.1080/02643290442000149

Marzouk, T., Winkelbeiner, S., Azizi, H., Malhotra, A. K., and Homan, P. (2020). Transcranial magnetic stimulation for positive symptoms in schizophrenia: a systematic review. *Neuropsychobiology* 79, 384–396. doi: 10.1159/000502148

Mayer, A. R., Dorflinger, J. M., Rao, S. M., and Seidenberg, M. (2004). Neural networks underlying endogenous and exogenous visual–spatial orienting. *NeuroImage* 23, 534–541. doi: 10.1016/j.neuroimage.2004.06.027

McGuire, P. K., David, A. S., Murray, R. M., Frackowiak, R. S. J., Frith, C. D., Wright, I., et al. (1995). Abnormal monitoring of inner speech: a physiological basis for auditory hallucinations. *Lancet* 346, 596–600. doi: 10.1016/s0140-6736(95)91435-8

McGuire, P. K., Murray, R. M., and Shah, G. M. S. (1993). Increased blood flow in Broca's area during auditory hallucinations in schizophrenia. *Lancet* 342, 703–706. doi: 10.1016/0140-6736(93)91707-s

Mogg, A., Purvis, R., Eranti, S., Contell, F., Taylor, J. P., Nicholson, T., et al. (2007). Repetitive transcranial magnetic stimulation for negative symptoms of schizophrenia: a randomized controlled pilot study. *Schizophr. Res.* 93, 221–228. doi: 10.1016/j.schres.2007.03.016

Nichols, T., Brett, M., Andersson, J., Wager, T., and Poline, J.-B. (2005). Valid conjunction inference with the minimum statistic. *NeuroImage* 25, 653–660. doi: 10.1016/j.neuroimage.2004.12.005

Oh, S.-Y., and Kim, Y.-K. (2011). Adjunctive treatment of bimodal repetitive transcranial magnetic stimulation (rTMS) in pharmacologically non-responsive patients with schizophrenia: a preliminary study. *Prog. Neuro Psychopharmacol. Biol. Psychiatry* 35, 1938–1943. doi: 10.1016/j.pnpbp.2011.07.015

Onitsuka, T., Shenton, M. E., Salisbury, D. F., Dickey, C. C., Kasai, K., Toner, S. K., et al. (2004). Middle and inferior temporal gyrus gray matter volume

abnormalities in chronic schizophrenia: an MRI study. *Am. J. Psychiatry* 161, 1603–1611. doi: 10.1176/appi.ajp.161.9.1603

Os, J. V., and Kapur, S. (2009). Schizophrenia. *Lancet* 374, 635–645.

Otani, V. H. O., Shiozawa, P., Cordeiro, Q., and Uchida, R. R. (2015). A systematic review and meta-analysis of the use of repetitive transcranial magnetic stimulation for auditory hallucinations treatment in refractory schizophrenic patients. *Int. J. Psychiatry Clin. Pract.* 19, 228–232. doi: 10.3109/13651501.2014.980830

Park, I. H., Kim, J.-J., Chun, J., Jung, Y. C., Seok, J. H., Park, H.-J., et al. (2009). Medial prefrontal default-mode hypoactivity affecting trait physical anhedonia in schizophrenia. *Psychiatry Res. Neuroimaging* 171, 155–165. doi: 10.1016/j.pscychresns.2008.03.010

Pomarol-Clotet, E., Canales-Rodríguez, E. J., Salvador, R., Sarró, S., Gomar, J. J., Vila, F., et al. (2010). Medial prefrontal cortex pathology in schizophrenia as revealed by convergent findings from multimodal imaging. *Mol. Psychiatry* 15, 823–830. doi: 10.1038/mp.2009.146

Rajarethinam, R. P., DeQuardo, J. R., Nalepa, R., and Tandon, R. (2000). Superior temporal gyrus in schizophrenia: a volumetric magnetic resonance imaging study. *Schizophr. Res.* 41, 303–312. doi: 10.1016/s0920-9964(99)00083-3

Rapp, A. M., and Steinhäuser, A. E. (2013). Functional MRI of sentence-level language comprehension in schizophrenia: a coordinate-based analysis. *Schizophr. Res.* 150, 107–113. doi: 10.1016/j.schres.2013.07.019

Razafimandimby, A., Hervé, P.-Y., Marzloff, V., Brazo, P., Tzourio-Mazoyer, N., and Dollfus, S. (2016). Functional deficit of the medial prefrontal cortex during emotional sentence attribution in schizophrenia. *Schizophr. Res.* 178, 86–93. doi: 10.1016/j.schres.2016.09.004

Ren, W., Lui, S., Deng, W., Li, F., Li, M., Huang, X., et al. (2013). Anatomical and functional brain abnormalities in drug-naive first-episode schizophrenia. *Am. J. Psychiatry* 170, 1308–1316. doi: 10.1176/appi.ajp.2013.12091148

Reyes-Aguilar, A., Valles-Capetillo, E., and Giordano, M. (2018). A quantitative meta-analysis of neuroimaging studies of pragmatic language comprehension: in search of a universal neural substrate. *Neuroscience* 395, 60–88. doi: 10.1016/j.neuroscience.2018.10.043

Rossi, S., Pasqualetti, P., Rossini, P. M., Feige, B., Ulivelli, M., Glocker, F. X., et al. (2000). Effects of repetitive transcranial magnetic stimulation on movement-related cortical activity in humans. *Cereb. Cortex* 10, 802–808. doi: 10.1093/cercor/10.8.802

Rubinov, M., and Bullmore, E. (2013). Schizophrenia and abnormal brain network hubs. *Dialogues Clin. Neurosci.* 15, 339–349. doi: 10.31887/DCNS.2013.15.3/mrubinov

Scheinost, D., Benjamin, J., Lacadie, C. M., Vohr, B., Schneider, K. C., Ment, L. R., et al. (2012). The intrinsic connectivity distribution: a novel contrast measure reflecting voxel level functional connectivity. *NeuroImage* 62, 1510–1519. doi: 10.1016/j.neuroimage.2012.05.073

Schneider, A. L., Schneider, T. L., and Stark, H. (2008). Repetitive transcranial magnetic stimulation (rTMS) as an augmentation treatment for the negative symptoms of schizophrenia: a 4-week randomized placebo controlled study. *Brain Stimul.* 1, 106–111. doi: 10.1016/j.brs.2008.01.001

Schuepbach, D., Keshavan, M. S., Kmiec, J. A., and Sweeney, J. A. (2002). Negative symptom resolution and improvements in specific cognitive deficits after acute treatment in first-episode schizophrenia. *Schizophr. Res.* 53, 249–261. doi: 10.1016/s0920-9964(01)00195-5

Seal, M., Aleman, A., and McGuire, P. (2004). Compelling imagery, unanticipated speech and deceptive memory: neurocognitive models of auditory verbal hallucinations in schizophrenia. *Cogn. Neuropsychiatry* 9, 43–72. doi: 10.1080/13546800344000156

Shergill, S. S., Brammer, M. J., Williams, S. C. R., Murray, R. M., and McGuire, P. K. (2000a). Mapping auditory hallucinations in schizophrenia using functional magnetic resonance imaging. *Arch. Gen. Psychiatry* 57, 1033–1038. doi: 10.1001/archpsyc.57.11.1033

Shergill, S. S., Bullmore, E., Simmons, A., Murray, R., and McGuire, P. (2000b). Functional anatomy of auditory verbal imagery in schizophrenic patients with auditory hallucinations. *Am. J. Psychiatry* 157, 1691–1693. doi: 10.1176/appi.ajp.157.10.1691

Shi, C., Kang, L., Yao, S., Ma, Y., Li, T., Liang, Y., et al. (2015). The MATRICS consensus cognitive battery (MCCB): co-norming and standardization in China. *Schizophr. Res.* 169, 109–115. doi: 10.1016/j.schres.2015.09.003

Silbersweig, D. A., Stern, E., Frith, C., Cahill, C., Holmes, A., Grootoonk, S., et al. (1995). A functional neuroanatomy of hallucinations in schizophrenia. *Nature* 378, 176–179. doi: 10.1038/378176a0

Stein, D. J., Phillips, K. A., Bolton, D., Fulford, K. W. M., Sadler, J. Z., and Kendler, K. S. (2010). What is a mental/psychiatric disorder? From DSM-IV to DSM-V. *Psychol. Med.* 40, 1759–1765. doi: 10.1017/S0033291709992261

Takahashi, T., Wood, S. J., Yung, A. R., Walterfang, M., Phillips, L. J., Soulsby, B., et al. (2010). Superior temporal gyrus volume in antipsychotic-naive people at risk of psychosis. *Br. J. Psychiatry* 196, 206–211. doi: 10.1192/bjp.bp.109.069732

Takayama, Y., Kinomoto, K., and Nakamura, K. (2004). Selective impairment of the auditory-verbal short-term memory due to a lesion of the superior temporal gyrus. *Eur. Neurol.* 51, 115–117. doi: 10.1159/000076792

Torrey, E. F. (2007). Schizophrenia and the inferior parietal lobule. *Schizophr. Res.* 97, 215–225. doi: 10.1016/j.schres.2007.08.023

Touge, T., Gerschlager, W., Brown, P., and Rothwell, J. C. (2001). Are the after-effects of low-frequency rTMS on motor cortex excitability due to changes in the efficacy of cortical synapses? *Clin. Neurophysiol.* 112, 2138–2145.

Tranulis, C., Sepehry, A. A., Galinowski, A., and Stip, E. (2008). Should we treat auditory hallucinations with repetitive transcranial magnetic stimulation? a metaanalysis. *Can. J. Psychiatry* 53, 577–586. doi: 10.1177/070674370805300904

Williams, L. M., Das, P., Harris, A. W. F., Liddell, B. B., Brammer, M. J., Olivieri, G., et al. (2004). Dysregulation of arousal and amygdala-prefrontal systems in paranoid schizophrenia. *Am. J. Psychiatry* 161, 480–489. doi: 10.1176/appi.ajp.161.3.480

Woods, S. W. (2003). Chlorpromazine equivalent doses for the newer atypical antipsychotics. *J. Clin. Psychiatry* 64, 663–667. doi: 10.4088/jcp.v64n0607

Wu, Q., Chang, C.-F., Xi, S., Huang, I. W., Liu, Z., Juan, C.-H., et al. (2015). A critical role of temporoparietal junction in the integration of top-down and bottom-up attentional control. *Hum. Brain Mapp.* 36, 4317–4333. doi: 10.1002/hbm.22919

Xiu, M. H., Guan, H. Y., Zhao, J. M., Wang, K. Q., Pan, Y. F., Su, X. R., et al. (2020). Cognitive enhancing effect of high-frequency neuronavigated rTMS in chronic schizophrenia patients with predominant negative symptoms: a double-blind controlled 32-week follow-up study. *Schizophr. Bull.* 46, 1219–1230. doi: 10.1093/schbul/sbaa035

Yan, C.-G., Wang, X.-D., Zuo, X.-N., and Zang, Y.-F. (2016). DPABI: data processing and analysis for (resting-state) brain imaging. *Neuroinformatics* 14, 339–351. doi: 10.1007/s12021-016-9299-4

Yildiz, M., Borgwardt, S. J., and Berger, G. E. (2011). Parietal lobes in schizophrenia: do they matter? *Schizophr. Res. Treat.* 2011, 1–16. doi: 10.1155/2011/581686

Yu, R., Chien, Y.-L., Wang, H.-L. S., Liu, C.-M., Liu, C.-C., Hwang, T.-J., et al. (2014). Frequency-specific alternations in the amplitude of low-frequency fluctuations in schizophrenia. *Hum. Brain Mapp.* 35, 627–637.

Zhuo, C., Chen, M., Xu, Y., Jiang, D., Chen, C., Ma, X., et al. (2020). Reciprocal deterioration of visual and auditory hallucinations in schizophrenia presents V-shaped cognition impairment and widespread reduction in brain gray matter-A pilot study. *J. Clin. Neurosci.* 79, 154–159. doi: 10.1016/j.jocn.2020.07.054

Conflict of Interest: The authors declare that the research was conducted in the absence of any commercial or financial relationships that could be construed as a potential conflict of interest.

Publisher's Note: All claims expressed in this article are solely those of the authors and do not necessarily represent those of their affiliated organizations, or those of the publisher, the editors and the reviewers. Any product that may be evaluated in this article, or claim that may be made by its manufacturer, is not guaranteed or endorsed by the publisher.

frontiers | Frontiers in Neuroscience

TYPE Correction
PUBLISHED 17 January 2023
DOI 10.3389/fnins.2022.1118304

OPEN ACCESS

EDITED AND REVIEWED BY
Julia Stephen,
Mind Research Network (MRN), United States

*CORRESPONDENCE
Peng Fang
✉ fangpeng@fmmu.edu.cn
Hong Yin
✉ yinhong@fmmu.edu.cn

SPECIALTY SECTION
This article was submitted to Brain Imaging Methods, a section of the journal Frontiers in Neuroscience

RECEIVED 07 December 2022
ACCEPTED 20 December 2022
PUBLISHED 17 January 2023

CITATION
Xie Y, Guan M, Wang Z, Ma Z, Wang H, Fang P and Yin H (2023) Corrigendum: rTMS induces brain functional and structural alternations in schizophrenia patient with auditory verbal hallucination. *Front. Neurosci.* 16:1118304. doi: 10.3389/fnins.2022.1118304

Corrigendum: rTMS induces brain functional and structural alternations in schizophrenia patient with auditory verbal hallucination

Yuanjun Xie[1], Muzhen Guan[2], Zhongheng Wang[3], Zhujing Ma[4], Huaning Wang[3], Peng Fang[5]* and Hong Yin[1]*

[1]Department of Radiology, Xijing Hospital, Fourth Military Medical University, Xi'an, China, [2]Department of Mental Health, Xi'an Medical University, Xi'an, China, [3]Department of Psychiatry, Xijing Hospital, Fourth Military Medical University, Xi'an, China, [4]Department of Clinical Psychology, School of Medical Psychology, Fourth Military Medical University, Xi'an, China, [5]Department of Military Medical Psychology, School of Medical Psychology, Fourth Military Medical University, Xi'an, China

KEYWORDS

schizophrenia, auditory verbal hallucination, transcranial magnetic stimulation, MCCB, amplitude of low-frequency fluctuation, voxel-based morphometry

A corrigendum on

rTMS induces brain functional and structural alternations in schizophrenia patient with auditory verbal hallucination

by Xie, Y., Guan, M., Wang, Z., Ma, Z., Wang, H., Fang, P., and Yin, H. (2021). *Front. Neurosci.* 15:722894. doi: 10.3389/fnins.2021.722894

In the published article, there was an error in Figure 2 as published. The bottom of Figure 2 was slightly cropped. The revised Figure 2 appears below.

In the published article, there was also an error in **Materials and Methods**, *Imaging Data Acquire and Preprocessing*, Paragraph 1. The repetition time and echo time were incorrectly given as "repetition time, 1,900 ms; echo time, 2.26 ms" but should be "repetition time, 8.1 ms; echo time, 3.2 ms". The corrected paragraph appears below:

"The patients underwent scanning within 48 h before the commencement of rTMS treatment and on the day following the end of the treatment course. The healthy controls were only scanned at baseline. Imaging data were acquired on a 3.0 Tesla MRI system with a standard 8-channel head coil (GE Medical Systems, Milwaukee, WI, United States). Earplugs and foam pads were used to minimize scanner noise and head motion. Participants were instructed to close their eyes and remain awake during the scan state. Functional images were acquired using a gradient echo-planar imaging (EPI) sequence (repetition time, 2,000 ms; echo time, 40 ms; field of view, 240 mm × 240 mm; flip angle, 90°; matrix, 64 × 64; slice thickness, 3.5 mm; 45 axial slices no gap. A total of 210 volumes were collected for a total scan time of 420 s. Subsequently, high-resolution 3D T1-weighted anatomical images were acquired with an MPRAGE sequence (repetition time, 8.1 ms; echo time, 3.2 ms; field of view, 240 mm × 240 mm; flip angle, 10°; matrix, 256 × 256; slice thickness, 1 mm; and 176 slices sagittal slices)".

The authors apologize for these errors and state that this does not change the scientific conclusions of the article in any way. The original article has been updated.

Publisher's note

10.3389/fnins.2022.1118304

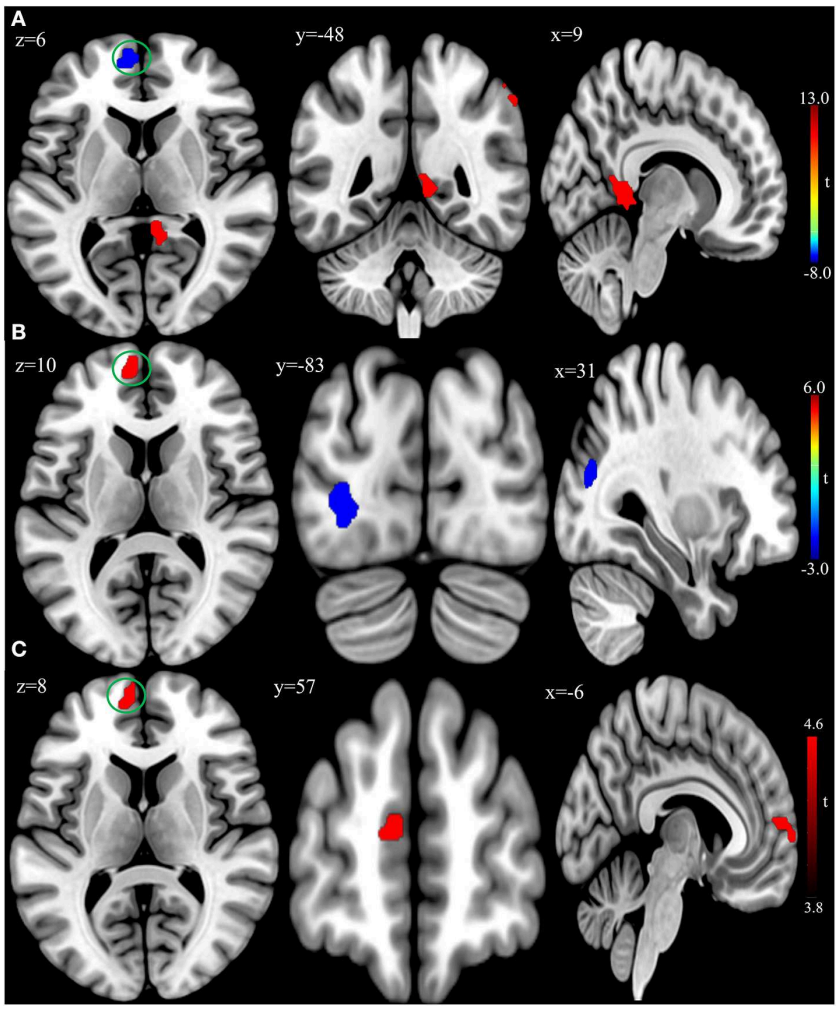

FIGURE 2
(A) Brain regions showing significant differences of amplitude of low-frequency fluctuation (ALFF) between patient group and healthy control group at baseline. **(B)** Brain regions showing significant differences of ALFF between the posttreatment and baseline in the patient group. **(C)** Conjunction analysis maps of ALFF differences [(baseline vs. controls) n (posttreatment vs. baseline)]. The warm color denoted the region where ALFF is higher, and the cool color denotes the region where ALFF is lower. The color circle denoted the overlapped region of ALFF differences.

frontiers in Neuroscience

ORIGINAL RESEARCH
published: 09 September 2021
doi: 10.3389/fnins.2021.729958

Establishment of Effective Biomarkers for Depression Diagnosis With Fusion of Multiple Resting-State Connectivity Measures

Yanling Li[1,2,3], Xin Dai[4], Huawang Wu[5] and Lijie Wang[6]**

[1] School of Electrical Engineering and Electronic Information, Xihua University, Chengdu, China, [2] Key Laboratory of Fluid and Power Machinery, Ministry of Education, Xihua University, Chengdu, China, [3] Key Laboratory of Fluid Machinery and Engineering, Sichuan Province, Xihua University, Chengdu, China, [4] School of Automation, Chongqing University, Chongqing, China, [5] The Affiliated Brain Hospital of Guangzhou Medical University (Guangzhou Huiai Hospital), Guangzhou, China, [6] School of Computer Science and Engineering, University of Electronic Science and Technology of China, Chengdu, China

Major depressive disorder (MDD) is a severe mental disorder and is lacking in biomarkers for clinical diagnosis. Previous studies have demonstrated that functional abnormalities of the unifying triple networks are the underlying basis of the neuropathology of depression. However, whether the functional properties of the triple network are effective biomarkers for the diagnosis of depression remains unclear. In our study, we used independent component analysis to define the triple networks, and resting-state functional connectivities (RSFCs), effective connectivities (EC) measured with dynamic causal modeling (DCM), and dynamic functional connectivity (dFC) measured with the sliding window method were applied to map the functional interactions between subcomponents of triple networks. Two-sample *t*-tests with $p < 0.05$ with Bonferroni correction were used to identify the significant differences between healthy controls (HCs) and MDD. Compared with HCs, the MDD showed significantly increased intrinsic FC between the left central executive network (CEN) and salience network (SAL), increased EC from the right CEN to left CEN, decreased EC from the right CEN to the default mode network (DMN), and decreased dFC between the right CEN and SAL, DMN. Moreover, by fusion of the changed RSFC, EC, and dFC as features, support vector classification could effectively distinguish the MDD from HCs. Our results demonstrated that fusion of the multiple functional connectivities measures of the triple networks is an effective way to reveal functional disruptions for MDD, which may facilitate establishing the clinical diagnosis biomarkers for depression.

Keywords: fusion, resting-state functional connectivity, effective connectivity, dynamic functional connectivity, classification

OPEN ACCESS

Edited by:
Bochao Cheng,
Sichuan University, China

Reviewed by:
Yajing Pang,
Zhengzhou University, China
Sangma Xie,
Hangzhou Dianzi University, China

****Correspondence:***
Yanling Li
153275236@qq.com
Lijie Wang
ljwang@uestc.edu.cn

Specialty section:
This article was submitted to Brain Imaging Methods, a section of the journal Frontiers in Neuroscience

Received: *24 June 2021*
Accepted: *14 July 2021*
Published: *09 September 2021*

Citation:
Li Y, Dai X, Wu H and Wang L (2021) Establishment of Effective Biomarkers for Depression Diagnosis With Fusion of Multiple Resting-State Connectivity Measures. Front. Neurosci. 15:729958. doi: 10.3389/fnins.2021.729958

INTRODUCTION

Major depressive disorder (MDD) is a severe mental illness with emotional and cognitive abnormalities, and anhedonia, reduced energy, poor attention, and concentration are core symptoms of MDD (Diener et al., 2012; Belzung et al., 2015). Recently, the triple network model, consisting of the central executive network (CEN), default mode network (DMN), and

salience network (SAL), was proposed, and dysfunctions of the three networks may underlay the cognitive and affective abnormalities in psychiatric and neurological disorders (Menon, 2011). Although the functional abnormalities of the three networks have been reported in different studies (Kaiser et al., 2015; Mulders et al., 2015; Brakowski et al., 2017; Wang et al., 2017c), it remains unclear whether/how the intrinsic functional changes and the casual influences between the sub-components of the three networks contribute to the neuropathology of depression.

Resting-state functional connectivity (RSFC), which can be used to investigate the temporal coherence of spontaneous neural activity, offers a task-free approach to detect the intrinsic functional brain networks (Yeo et al., 2011; Wang et al., 2015, 2017d; Glasser et al., 2016; Wang et al., 2019). Independent component analysis (ICA) is a model-free method to obtain a set of components that are maximally independent of each other (Calhoun et al., 2009). ICA has been widely used to define large-scale brain networks, such as DMN, CEN, SAL, and visual and motor networks, in a large number of previous studies (van den Heuvel and Hulshoff Pol, 2010; Mulders et al., 2015; Luo et al., 2021). To explore the causal effects between brain regions, effective connectivity (EC) is a valuable method to identify the information flow during functional interaction (Wang et al., 2017b; Wang et al., 2020). Dynamic causal modeling (DCM) is able to estimate the causal influences of one neuronal subpopulation over another to characterize the causal organization of the brain (Friston et al., 2013). Moreover, more and more studies applied dynamic functional connectivity (dFC) using a sliding window method to reveal the time dynamic of functional couplings between brain areas (Allen et al., 2014). Thus, using intrinsic, effective, and dynamic connectivities to explore the abnormal interactions between the sub-components of the tripe network without any assumption may provide us with new information specific to the neuropathology of MDD. In addition, fusion of the multiple functional connectivity measures may facilitate establishing more effective diagnosis biomarkers than using single connectivity measures.

In this study, we first applied ICA to define the triple network and to extract the time courses of each sub-network using the resting-state fMRI data in 27 MDD patients and 28 healthy controls (HCs). Next, the RSFC, EC, and dFC between each pair of sub-components were analyzed and compared to HC and MDD to identify the group differences. Finally, the changed connectivity measures were taken as features to set up the classification models for MDD to identify the diagnosis biomarkers.

MATERIALS AND METHODS

Subjects

In total, 27 drug-free MDD patients and 28 HC subjects were recruited, and written informed consent was provided and obtained from each subject. MDD patients were diagnosed with the Structured Clinical Interview for DSM Disorders (SCID) using DSM-IV criteria, and the severity of depressive symptoms was measured by Hamilton Depression Rating Scale (HAMD). The inclusion criteria for MDD patients were as follows: not taking any antidepressant medication during the recurrent episode; not having any other comorbid mental disorders; and no contraindications showing up on MRI scans. The HC subjects were also included, and the exclusion criteria were as follows: known personal or family history of psychiatric disorders; current or lifetime diagnosis of Axis I illness; lifetime history of substance abuse or dependence, head trauma, seizures, serious medical or surgical illness; or contraindications showing up on MRI scans. The current study was approved by the Ethics Committee of The Affiliated Brain Hospital of Guangzhou Medical University.

Resting-State fMRI Data Acquisition

Resting-state fMRI data acquisition was performed using a 3.0-Tesla Philips MR imaging system with an eight-channel SENSE head coil and echo-planar imaging (GRE-EPI) sequence. Before the scanning, all subjects were asked to relax, keep their eyes closed, and not fall asleep. The detailed scanning parameters were as follows: repetition time (TR) = 2000 ms, echo time (TE) = 30 ms, flip angle (FA) = 90^o, field of view (FOV) = 220 × 220 mm^2, matrix = 64 × 64, slice thickness = 4 mm, inter-slice gap = 0.6 mm, and volume of 240.

Resting-State fMRI Preprocessing

The resting-state fMRI data were preprocessed using SPM8 software[1] with various steps, including discarding the first 10 volumes, head motion correction, spatial normalization to the standard EPI template, and smoothing with a 6 mm Gaussian kernel. For resting-state functional and EC analyses, the time courses of each subcomponent of the triple network obtained by ICA were further detrended, despiked, and filtered with a bandpass of 0.01–0.1 Hz.

Group ICA

The spatial group ICA was used to identify the different resting-state components in all MDD patients and HCs using the GIFT toolbox[2] (Calhoun et al., 2001; Erhardt et al., 2011; Calhoun and Adali, 2012). The principal component analysis was first used to reduce the dimensions of the functional data. Next, the number of independent components was automatically estimated using the Infomax algorithm to define the most stable and reliable components by running them 100 times with the ICASSO algorithm (Bell and Sejnowski, 1995), and 28 components were finally found. Then, subject-specific time series and spatial ICs were back reconstructed and converted into *z*-maps (Calhoun et al., 2001; Erhardt et al., 2011). Finally, the sub-components of the triple network were identified by visually checking all the independent components for subsequent analyses. The detailed procedures for ICA analysis can be found in our previous study (Luo et al., 2021).

[1]https://www.fil.ion.ucl.ac.uk/spm/software/spm8/

[2]http://mialab.mrn.org/software/gift

TABLE 1 | Demographics and clinical characteristics of the used subjects.

Subjects	MDD	HC	*P*-value
Number of subjects	27	28	
Gender (male: female)	10/17	12/16	0.66
Age (mean ± SD)	29.67 ± 7.26	30.57 ± 6.68	0.63
Years of education (mean ± SD)	13.83 ± 3.70	13.89 ± 2.2	0.94
HDRS scores (mean ± SD)	33.56 ± 7.21		
Age of onset (years)	26.48 ± 7.82		
Duration of illness(months)	38.92 ± 54.96		

A Pearson chi-squared test was used for gender comparison. Two-sample t-tests were used for age and education comparisons. HDRS, Hamilton Depression Rating Scale score; MDD, major depression disorder (MDD); HC, healthy control (HC).

Functional Network Connectivity (FNC) Analysis

The RSFCs between sub-components of the triple network were calculated. Next, a Fisher r-to-z transformation was applied to convert the correlation coefficient to z values to improve normality. Finally, two-sample t-tests were performed to identify the significant alterations in FCs between MDD and HCs. The significance level was set at $p < 0.05$ with Bonferroni corrections.

DCM Analyses

To calculate the EC, the time series for each sub-component of the triple network was first obtained as state above. Then, the spectral DCM (dcm), which is developed specifically for resting-state fMRI DCM analyses, was used to investigate the causal interaction between the sub-components of the triple network in both MDD and HCs. The spDCM is an extension of the conventional DCM except, adding a stochastic term and removing the modulatory component. This means that spDCM estimates the time-invariant covariance between time series instead of estimating time-varying hidden states. Thus, spDCM only needs to estimate the covariance of the random fluctuations, a scale-free (power law) form for the state noise. The detailed procedures for spDCM can be found in a previous study (Razi et al., 2015). After obtaining the ECs for each subject, two-sample t-tests were used to compare the causal effects between MDD patients and controls. The significant level was set at $p < 0.05$ with Bonferroni correction.

dFC Analyses

The dFC was calculated using a sliding window method. Since the length of the sliding window is the absence of a standard criterion, the length of the sliding window was set at $1/f_{min}$ (f_{min} is the minimum frequency of time series), which has been proven to be able to well characterize the time dynamics (Leonardi and Van De Ville, 2015; Du et al., 2017; Li et al., 2019). Thus, a window length of 50 TR (100 s) with a step size of 5 TR (10 s) as the optimal parameter was applied to keep the balance between capturing reliable dynamics and obtain steady correlations between regions. In each window, the FC values were computed between any pair of subcomponents of triple networks, and the variance of the FC values across all the windows was used to measure the dynamic. Finally, the dFC values were normalized to z-scores for statistical analyses.

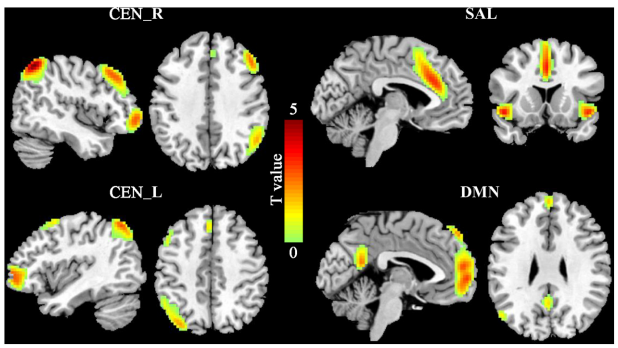

FIGURE 1 | The triple networks. The group independent component analysis (ICA) was used to define the triple networks. Four subcomponents of the triple networks were identified including default mode network (DMN), salience network (SAL), and left and right central executive network (CEN_L, CEN_R).

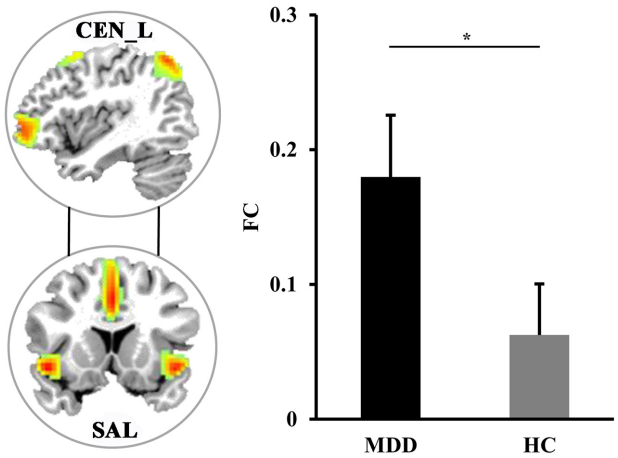

FIGURE 2 | The differences in functional network connectivities. The significantly increased functional network connectivity between the left central executive network (CEN_L) and salience network (SAL) was found in MDD patients. *Represents significant difference.

Correlation Analyses

Pearson correlation analyses were conducted between the changed FNC, EC, dFC, and HAMD scores and disease duration.

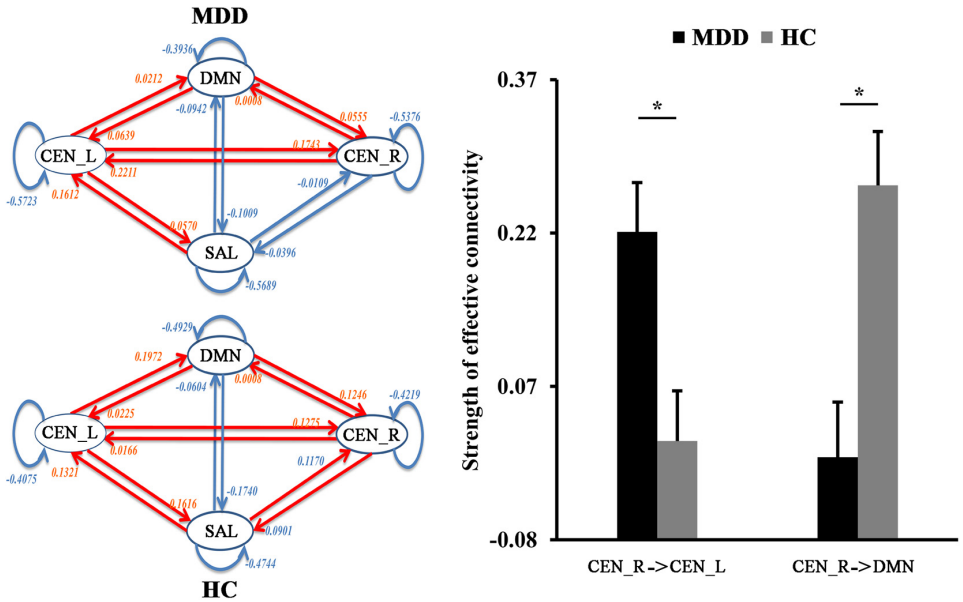

FIGURE 3 | The differences in functional network effective connectivities. Dynamic causal modeling was used to determine the differences in effective connectivities between the triple networks. The significantly increased effective connectivity from right to the left central executive network (CEN) was found in MDD patients while significantly decreased effective connectivity from right CEN to default mode network (DMN) was found in MDD patients. *Represents significant difference.

The significance was set at a threshold of $p < 0.05$. No correction was performed to show the trend of the associations because of the small samples in our study.

SVM Classification

To validate whether multiple connectivity measures could serve as effective biomarkers for depression, fusions of changed RSFC, EC, and dFC were taken as features, and a linear support vector classification (SVC) was employed to train the mode for classifying (Chang and Lin, 2011). A leave-one-out cross-validation (LOOCV) test was used to assess the generalization ability because of the limited number of samples in the present study. The classification result was assessed using the classification accuracy, sensitivity, specificity, and area under the curve (AUC) values.

RESULTS

Demographics and Clinical Characteristics

The demographics and clinical characteristics of the HCs and MDD patients are shown in **Table 1**. There are no significant differences in gender ($p = 0.66$), age ($p = 0.63$), and education level ($p = 0.94$) between MDD and HCs.

ICA Results

Four sub-components of the triple network including left and right CEN (CEN_L, CEN_R), DMN, and SAL were identified in this study (**Figure 1**). The spatial patterns of the four subcomponents of the triple network were consistent with the previous findings (Damoiseaux et al., 2006; Arbabshirani et al., 2013; Mueller et al., 2014).

Resting-State FNC Results

Pearson correlation coefficients between each pair of the four sub-components were calculated to study the changes of the large-scale FC. Compared with HCs, the MDD patients had significantly increased FC between left CEN (CEN_L) and SAL ($p = 0.0082$) (**Figure 2**).

DCM Results

The spDCM was performed to identify the changes of casual interactions between sub-components of the triple network in MDD. Compared with HCs, the significantly increased magnitude of causal interactions from right CEN (CEN_R) to CEN_L ($p = 0.0045$) and significantly decreased magnitude of causal interactions from the right CEN_R to DMN ($p = 0.00087$) were found in MDD patients (**Figure 3**).

dFC Results

The significantly decreased dFC between right CEN (CEN_R) and SAL ($p = 0.012$), DMN ($p = 0.011$) were found in MDD patients as compared to HCs (**Figure 4**).

Clinical Correlations

We found negative correlations between the ECs from CEN_R to CEN_L and HAMD scores ($r = -0.3841$, $p = 0.0479$) and disease duration ($r = -0.3950$, $p = 0.0414$) (**Figure 5**).

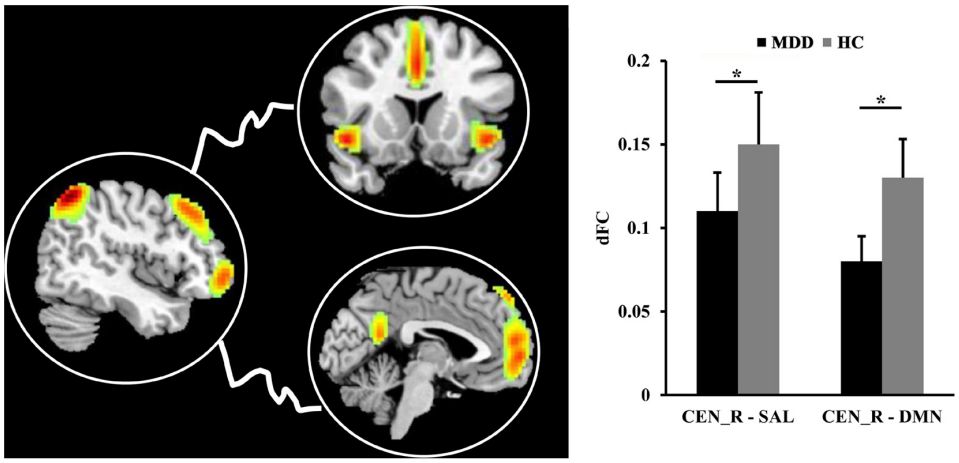

FIGURE 4 | The differences in dynamic functional connectivity (dFC). The significantly decreased dFC between right central executive network (CEN) and salience network (SAL), default mode network (DMN) was found in MDD patients compared to healthy controls. *Represents significant difference.

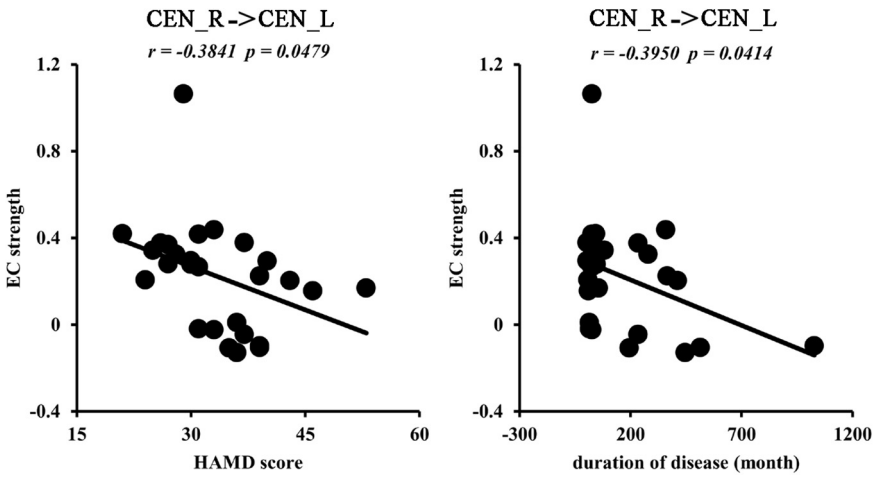

FIGURE 5 | Correlation analyses. The significantly negative correlations between effective functional connectivities from right to left central network networks (CEN) and Hamilton Depression Rating Scale (HAMD) scores, disease duration were found in MDD patients.

Classification Results

With the fusion of changed RSFC, EC, and dFC as features, SVC could distinguish MDD from HCs with an accuracy of 90.91%, a sensitivity of 92.59%, a specificity of 89.29%, and an ACU of 0.895 (**Figure 6**).

DISCUSSION

In this study, we aimed to explore the intrinsic, effective, and dynamic connectivity alterations between subcomponents of the triple networks to reveal the potential neuropathology of MDD. Compared to HCs, MDD patients showed increased intrinsic functional connectivity between CEN_L and SAL, increased EC from CEN_R to CEN_L, decreased EC from CEN_R to DMN, and decreased dFC between CEN_R and SAL, DMN. Interestingly, the increased ECs from CEN_R to CEN_L were negatively correlated with HAMD scores and disease duration in MDD patients. Furthermore, by fusion of the multiple connectivity measures, we demonstrated that changed RSFC, EC, and dFC could effectively distinguish MDD from HCs. Our findings provide evidence for how functional disorganization of the triple network in MDD patients could facilitate the development of clinical diagnosis biomarkers for depression.

We found abnormal functional interactions among CEN, SAL, and DMN in MDD patients with increased functional couplings between left CEN and SAL, decreased EC from CEN to DMN, and decreased dFC between CEN and SAL, DMN in MDD patients. Our findings were consistent with that reported in MDD patients in previous studies (Greicius et al., 2007; Zhu et al., 2012; Wang et al., 2017a, 2018). SAL plays an important role in switching information between CEN and DMN (Menon and Uddin, 2010; Menon, 2011). CEN is mainly involved in external

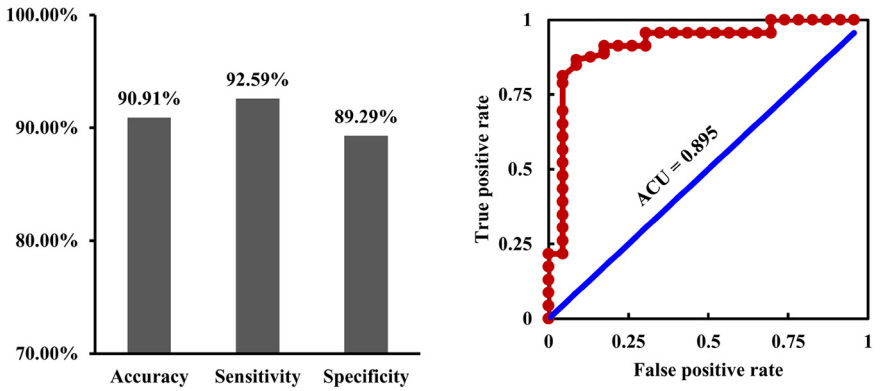

FIGURE 6 | Fusion of connectivity measures for classification. By fusion of the changed resting-state, functional connectivities, causal effective connectivities, and dynamic functional connectivities as features, support vector classification could effectively differentiate depression from healthy controls with an accuracy of 90.91%, a sensitivity of 92.59%, a specificity of 89.29%, and an ACU of 0.895.

executive and cognitive control, while DMN is mainly involved in internal attention and self-reference (Corbetta and Shulman, 2002; Hamilton et al., 2015; Wang et al., 2015, 2016; Wu et al., 2016; Wang et al., 2019). The increased functional connections between CEN and SAL may be a compensatory mechanism for the functional impairments in switching between external and internal attention in MDD patients (Barch and Sheffield, 2014). On the contrary, the decreased EC from CEN to DMN and dFC between CEN and SAL, DMN indicated disrupted switching between the internal self-reference and the demand cognitive action (Seeley et al., 2007; Scheibner et al., 2017). All the evidence suggested that functional dysfunctions of information switching among CEN, SAL, and DMN may be the neuroanatomical basis of rumination of MDD. Moreover, we found that the changed RSFC, ECs, and dFC as features could effectively distinguish the MDD patients from HCs. This finding indicated that the abnormal functional couplings of the triple network may be the underlying neuropathological mechanism of depression.

Interestingly, our study revealed increased EC from the right CEN to left CEN in MDD patients, and the effective connections were closely associated with depression symptoms and disease duration. This finding indicated that the functional balance of bilateral CEN is fundamental to maintaining the normal functions of the brain in MDD patients (Grimm et al., 2008; Triggs et al., 2010; Chen et al., 2013). Moreover, we found that the effective connections were negatively correlated with HAMD scores. This finding suggests that enhanced interaction from the right to left CEN is a compensatory mechanism and not a neuropathological change.

There are some limitations to our study. First, the sample size in our study is relative small, and a larger number of patients are needed to validate the findings in further studies. Second, although all the patients are medication-free in the current episode, some patients took antidepressant medications before. Thus, the first-episodic drug-naïve MDD patients are warranted to better identify the neural basis for MDD.

CONCLUSION

This study revealed large-scale functional network dysfunctions in MDD, including increased functional connectivity between left CEN and SAL, increased EC from right CEN to left CEN, reduced EC from right CEN to DMN, and decreased dFC between right CEN and SAL, DMN. Moreover, by fusion of the changed connectivity measures as features, our study revealed that it is able to distinguish MDD from HCs. These findings provide new evidence for the neuropathology of triple networks in MDD. Our study may facilitate developing clinical diagnosis biomarkers and the future treatment for MDD.

DATA AVAILABILITY STATEMENT

The raw data supporting the conclusions of this article will be made available by the authors, without undue reservation.

ETHICS STATEMENT

The studies involving human participants were reviewed and approved by the Ethics Committee of The Affiliated Brain Hospital of Guangzhou Medical University. The patients/participants provided their written informed consent to participate in this study.

AUTHOR CONTRIBUTIONS

All authors listed have made a substantial, direct and intellectual contribution to the work, and approved it for publication.

REFERENCES

Allen, E. A., Damaraju, E., Plis, S. M., Erhardt, E. B., Eichele, T., and Calhoun, V. D. (2014). Tracking whole-brain connectivity dynamics in the resting state. *Cereb. Cortex* 24, 663–676. doi: 10.1093/cercor/bhs352

Arbabshirani, M. R., Havlicek, M., Kiehl, K. A., Pearlson, G. D., and Calhoun, V. D. (2013). Functional network connectivity during rest and task conditions: a comparative study. *Hum. Brain Mapp.* 34, 2959–2971. doi: 10.1002/hbm.22118

Barch, D. M., and Sheffield, J. M. (2014). Cognitive impairments in psychotic disorders: common mechanisms and measurement. *World Psychiatry* 13, 224–232. doi: 10.1002/wps.20145

Bell, A. J., and Sejnowski, T. J. (1995). An information-maximization approach to blind separation and blind deconvolution. *Neural Comput.* 7, 1129–1159. doi: 10.1162/neco.1995.7.6.1129

Belzung, C., Willner, P., and Philippot, P. (2015). Depression: from psychopathology to pathophysiology. *Curr. Opin. Neurobiol.* 30, 24–30. doi: 10.1016/j.conb.2014.08.013

Brakowski, J., Spinelli, S., Dorig, N., Bosch, O. G., Manoliu, A., Holtforth, M. G., et al. (2017). Resting state brain network function in major depression – depression symptomatology, antidepressant treatment effects, future research. *J. Psychiatr. Res.* 92, 147–159. doi: 10.1016/j.jpsychires.2017.04.007

Calhoun, V. D., and Adali, T. (2012). Multisubject independent component analysis of fMRI: a decade of intrinsic networks, default mode, and neurodiagnostic discovery. *IEEE Rev. Biomed. Eng.* 5, 60–73. doi: 10.1109/rbme.2012.2211076

Calhoun, V. D., Adali, T., Pearlson, G. D., and Pekar, J. J. (2001). A method for making group inferences from functional MRI data using independent component analysis. *Hum. Brain Mapp.* 14, 140–151. doi: 10.1002/hbm.1048

Calhoun, V. D., Liu, J., and Adali, T. (2009). A review of group ICA for fMRI data and ICA for joint inference of imaging, genetic, and ERP data. *Neuroimage* 45, S163–S172.

Chang, C.-C., and Lin, C.-J. (2011). LIBSVM: a library for support vector machines. *ACM Trans. Intell. Syst. Technol.* 2, 1–27.

Chen, J., Zhou, C., Wu, B., Wang, Y., Li, Q., Wei, Y., et al. (2013). Left versus right repetitive transcranial magnetic stimulation in treating major depression: a meta-analysis of randomised controlled trials. *Psychiatry Res.* 210, 1260–1264. doi: 10.1016/j.psychres.2013.09.007

Corbetta, M., and Shulman, G. L. (2002). Control of goal-directed and stimulus-driven attention in the brain. *Nat. Rev. Neurosci.* 3, 201–215. doi: 10.1038/nrn755

Damoiseaux, J. S., Rombouts, S. A., Barkhof, F., Scheltens, P., Stam, C. J., Smith, S. M., et al. (2006). Consistent resting-state networks across healthy subjects. *Proc. Natl. Acad. Sci. U. S. A.* 103, 13848–13853. doi: 10.1073/pnas.0601417103

Diener, C., Kuehner, C., Brusniak, W., Ubl, B., Wessa, M., and Flor, H. (2012). A meta-analysis of neurofunctional imaging studies of emotion and cognition in major depression. *Neuroimage* 61, 677–685. doi: 10.1016/j.neuroimage.2012.04.005

Du, Y., Pearlson, G. D., Lin, D., Sui, J., Chen, J., Salman, M., et al. (2017). Identifying dynamic functional connectivity biomarkers using GIG-ICA: application to schizophrenia, schizoaffective disorder, and psychotic bipolar disorder. *Hum. Brain Mapp.* 38, 2683–2708. doi: 10.1002/hbm.23553

Erhardt, E. B., Rachakonda, S., Bedrick, E. J., Allen, E. A., Adali, T., and Calhoun, V. D. (2011). Comparison of multi-subject ICA methods for analysis of fMRI data. *Hum. Brain Mapp.* 32, 2075–2095. doi: 10.1002/hbm.21170

Friston, K., Moran, R., and Seth, A. K. (2013). Analysing connectivity with Granger causality and dynamic causal modelling. *Curr. Opin. Neurobiol.* 23, 172–178. doi: 10.1016/j.conb.2012.11.010

Glasser, M. F., Coalson, T. S., Robinson, E. C., Hacker, C. D., Harwell, J., Yacoub, E., et al. (2016). A multi-modal parcellation of human cerebral cortex. *Nature* 536, 171–178.

Greicius, M. D., Flores, B. H., Menon, V., Glover, G. H., Solvason, H. B., Kenna, H., et al. (2007). Resting-state functional connectivity in major depression: abnormally increased contributions from subgenual cingulate cortex and thalamus. *Biol. Psychiatry* 62, 429–437. doi: 10.1016/j.biopsych.2006.09.020

Grimm, S., Beck, J., Schuepbach, D., Hell, D., Boesiger, P., Bermpohl, F., et al. (2008). Imbalance between left and right dorsolateral prefrontal cortex in major depression is linked to negative emotional judgment: an fMRI study in severe major depressive disorder. *Biol. Psychiatry* 63, 369–376. doi: 10.1016/j.biopsych.2007.05.033

Hamilton, J. P., Farmer, M., Fogelman, P., and Gotlib, I. H. (2015). Depressive rumination, the default-mode network, and the dark matter of clinical neuroscience. *Biol. Psychiatry* 78, 224–230. doi: 10.1016/j.biopsych.2015.02.020

Kaiser, R. H., Andrews-Hanna, J. R., Wager, T. D., and Pizzagalli, D. A. (2015). Large-scale network dysfunction in major depressive disorder: a meta-analysis of resting-state functional connectivity. *JAMA Psychiatry* 72, 603–611. doi: 10.1001/jamapsychiatry.2015.0071

Leonardi, N., and Van De Ville, D. (2015). On spurious and real fluctuations of dynamic functional connectivity during rest. *Neuroimage* 104, 430–436. doi: 10.1016/j.neuroimage.2014.09.007

Li, C., Xia, L., Ma, J., Li, S., Liang, S., Ma, X., et al. (2019). Dynamic functional abnormalities in generalized anxiety disorders and their increased network segregation of a hyperarousal brain state modulated by insomnia. *J. Affect. Disord.* 246, 338–345. doi: 10.1016/j.jad.2018.12.079

Luo, L., Wu, H., Xu, J., Chen, F., Wu, F., Wang, C., et al. (2021). Abnormal large-scale resting-state functional networks in drug-free major depressive disorder. *Brain Imaging Behav.* 15, 96–106.

Menon, V. (2011). Large-scale brain networks and psychopathology: a unifying triple network model. *Trends Cogn. Sci.* 15, 483–506. doi: 10.1016/j.tics.2011.08.003

Menon, V., and Uddin, L. Q. (2010). Saliency, switching, attention and control: a network model of insula function. *Brain Struct. Funct.* 214, 655–667. doi: 10.1007/s00429-010-0262-0

Mueller, S., Costa, A., Keeser, D., Pogarell, O., Berman, A., Coates, U., et al. (2014). The effects of methylphenidate on whole brain intrinsic functional connectivity. *Hum. Brain Mapp.* 35, 5379–5388. doi: 10.1002/hbm.22557

Mulders, P. C., van Eijndhoven, P. F., Schene, A. H., Beckmann, C. F., and Tendolkar, I. (2015). Resting-state functional connectivity in major depressive disorder: a review. *Neurosci. Biobehav. Rev.* 56, 330–344. doi: 10.1016/j.neubiorev.2015.07.014

Razi, A., Kahan, J., Rees, G., and Friston, K. J. (2015). Construct validation of a DCM for resting state fMRI. *Neuroimage* 106, 1–14. doi: 10.1016/j.neuroimage.2014.11.027

Scheibner, H. J., Bogler, C., Gleich, T., Haynes, J. D., and Bermpohl, F. (2017). Internal and external attention and the default mode network. *Neuroimage* 148, 381–389. doi: 10.1016/j.neuroimage.2017.01.044

Seeley, W. W., Menon, V., Schatzberg, A. F., Keller, J., Glover, G. H., Kenna, H., et al. (2007). Dissociable intrinsic connectivity networks for salience processing and executive control. *J. Neurosci.* 27, 2349–2356. doi: 10.1523/jneurosci.5587-06.2007

Triggs, W. J., Ricciuti, N., Ward, H. E., Cheng, J., Bowers, D., Goodman, W. K., et al. (2010). Right and left dorsolateral pre-frontal rTMS treatment of refractory depression: a randomized, sham-controlled trial. *Psychiatry Res.* 178, 467–474. doi: 10.1016/j.psychres.2010.05.009

van den Heuvel, M. P., and Hulshoff Pol, H. E. (2010). Exploring the brain network: a review on resting-state fMRI functional connectivity. *Eur. Neuropsychopharmacol.* 20, 519–534. doi: 10.1016/j.euroneuro.2010.03.008

Wang, C., Wu, H., Chen, F., Xu, J., Li, H., Li, H., et al. (2017a). Disrupted functional connectivity patterns of the insula subregions in drug-free major depressive disorder. *J. Affect. Disord.* 234, 297–304. doi: 10.1016/j.jad.2017.12.033

Wang, J., Becker, B., Wang, L., Li, H., Zhao, X., and Jiang, T. (2019). Corresponding anatomical and coactivation architecture of the human precuneus showing similar connectivity patterns with macaques. *Neuroimage* 200, 562–574. doi: 10.1016/j.neuroimage.2019.07.001

Wang, J., Tian, Y., Wang, M., Cao, L., Wu, H., Zhang, Y., et al. (2016). A lateralized top-down network for visuospatial attention and neglect. *Brain Imaging Behav.* 10, 1029–1037. doi: 10.1007/s11682-015-9460-y

Wang, J., Wei, Q., Bai, T., Zhou, X., Sun, H., Becker, B., et al. (2017b). Electroconvulsive therapy selectively enhanced feedforward connectivity from fusiform face area to amygdala in major depressive disorder. *Soc. Cogn. Affect. Neurosci.* 12, 1983–1992. doi: 10.1093/scan/nsx100

Wang, J., Wei, Q., Wang, L., Zhang, H., Bai, T., Cheng, L., et al. (2018). Functional reorganization of intra- and internetwork connectivity in major depressive disorder after electroconvulsive therapy. *Hum. Brain Mapp.* 39, 1403–1411. doi: 10.1002/hbm.23928

Wang, J., Wei, Q., Yuan, X., Jiang, X., Xu, J., Zhou, X., et al. (2017c). Local functional connectivity density is closely associated with the response of electroconvulsive therapy in major depressive disorder. *J. Affect. Disord.* 225, 658–664. doi: 10.1016/j.jad.2017.09.001

Wang, J., Xie, S., Guo, X., Becker, B., Fox, P. T., Eickhoff, S. B., et al. (2017d). correspondent functional topography of the human left inferior parietal lobule at rest and under task revealed using resting-state fmri and coactivation based parcellation. *Hum. Brain Mapp.* 38, 1659–1675. doi: 10.1002/hbm.23488

Wang, J., Yang, Y., Fan, L., Xu, J., Li, C., Liu, Y., et al. (2015). Convergent functional architecture of the superior parietal lobule unraveled with multimodal neuroimaging approaches. *Hum. Brain Mapp.* 36, 238–257. doi: 10.1002/hbm.22626

Wang, L., Wei, Q., Wang, C., Xu, J., Wang, K., Tian, Y., et al. (2020). Altered functional connectivity patterns of insular subregions in major depressive disorder after electroconvulsive therapy. *Brain Imaging Behav.* 14, 753–761.

Wu, Y., Wang, J., Zhang, Y., Zheng, D., Zhang, J., Rong, M., et al. (2016). The neuroanatomical basis for posterior superior parietal lobule control lateralization of visuospatial attention. *Front. Neuroanat.* 10:32. doi: 10.3389/fnana.2016.00032

Yeo, B. T., Krienen, F. M., Sepulcre, J., Sabuncu, M. R., Lashkari, D., Hollinshead, M., et al. (2011). The organization of the human cerebral cortex estimated by intrinsic functional connectivity. *J. Neurophysiol.* 106, 1125–1165. doi: 10.1152/jn.00338.2011

Zhu, X., Wang, X., Xiao, J., Liao, J., Zhong, M., Wang, W., et al. (2012). Evidence of a dissociation pattern in resting-state default mode network connectivity in first-episode, treatment-naive major depression patients. *Biol. Psychiatry* 71, 611–617. doi: 10.1016/j.biopsych.2011.10.035

Conflict of Interest: The authors declare that the research was conducted in the absence of any commercial or financial relationships that could be construed as a potential conflict of interest.

Publisher's Note: All claims expressed in this article are solely those of the authors and do not necessarily represent those of their affiliated organizations, or those of the publisher, the editors and the reviewers. Any product that may be evaluated in this article, or claim that may be made by its manufacturer, is not guaranteed or endorsed by the publisher.

frontiers in Human Neuroscience

REVIEW
published: 28 September 2021
doi: 10.3389/fnhum.2021.749162

Transcranial Focused Ultrasound Neuromodulation: A Review of the Excitatory and Inhibitory Effects on Brain Activity in Human and Animals

Tingting Zhang[1,2], Na Pan[1,2], Yuping Wang[1,2,3], Chunyan Liu[1,2] and Shimin Hu[1,2]**

[1] Department of Neurology, Xuanwu Hospital, Capital Medical University, Beijing, China, [2] Beijing Key Laboratory of Neuromodulation, Beijing, China, [3] Center of Epilepsy, Institute of Sleep and Consciousness Disorders, Beijing Institute for Brain Disorders, Capital Medical University, Beijing, China

Non-invasive neuromodulation technology is important for the treatment of brain diseases. The effects of focused ultrasound on neuronal activity have been investigated since the 1920s. Low intensity transcranial focused ultrasound (tFUS) can exert non-destructive mechanical pressure effects on cellular membranes and ion channels and has been shown to modulate the activity of peripheral nerves, spinal reflexes, the cortex, and even deep brain nuclei, such as the thalamus. It has obvious advantages in terms of security and spatial selectivity. This technology is considered to have broad application prospects in the treatment of neurodegenerative disorders and neuropsychiatric disorders. This review synthesizes animal and human research outcomes and offers an integrated description of the excitatory and inhibitory effects of tFUS in varying experimental and disease conditions.

Keywords: transcranial focused ultrasound, neuromodulation, non-invasive brain stimulation, human, animal

OPEN ACCESS

Edited by:
Jiaojian Wang,
University of Electronic Science and Technology of China, China

Reviewed by:
Xiaojing Long,
Shenzhen Institutes of Advanced Technology, Chinese Academy of Sciences (CAS), China
Li Wang,
Beijing Institute of Technology, China

***Correspondence:**
Shimin Hu
583534035@qq.com
Chunyan Liu
lcy_e_mail@163.com

Specialty section:
This article was submitted to Brain Imaging and Stimulation, a section of the journal Frontiers in Human Neuroscience

Received: *29 July 2021*
Accepted: *06 September 2021*
Published: *28 September 2021*

Citation:
Zhang T, Pan N, Wang Y, Liu C and Hu S (2021) Transcranial Focused Ultrasound Neuromodulation: A Review of the Excitatory and Inhibitory Effects on Brain Activity in Human and Animals. Front. Hum. Neurosci. 15:749162. doi: 10.3389/fnhum.2021.749162

INTRODUCTION

Brain stimulation techniques have shown efficacy for ameliorating neurological and psychiatric disorders (Hoy and Fitzgerald, 2010). Invasive electrical brain stimulation modalities, such as vagus nerve stimulation (VNS) or deep brain stimulation (DBS), require the surgical placement of electrodes in the brain (Rahimpour et al., 2021; Wang Y. et al., 2021). The modulation effects of non-invasive strategies, such as transcranial direct current stimulation (tDCS) and repetitive transcranial magnetic stimulation (rTMS) are limited to the cortical surface (Hoy and Fitzgerald, 2010; Romanella et al., 2020). Transcranial focused ultrasound (tFUS) transmits low-intensity ultrasound into the brain non-invasively and focuses on deep brain regions. It is an emerging neuromodulation technology with the advantages of better spatial resolution and safety (Mehic et al., 2014).

The frequency of the ultrasound mechanical wave is higher than the range of human hearing (> 20 kHz). Ultrasound can be focused across solid structures and transmitted long distances with minimal power loss in soft biological tissues (Bystritsky et al., 2011). It has been the most widely used biomedical imaging modality for a long history. Ultrasound display different biological effect based on a different intensity. High-intensity (> 200 W/cm^2) focused ultrasound induces permanent lesions through coagulation of cellular proteins and thermal ablation. It has been approved by the FDA for the treatment of tremors associated with Parkinson's disease and

essential tremors. Medium intensity (100–200 W/cm^2) ultrasound has been used to break through the blood-brain barrier for drug delivery. Low-intensity (< 100 W/cm^2) focused ultrasound is considered the main form of non-invasive neuromodulation (Kubanek, 2018).

Research on the potential clinical value of focused ultrasound as a neuromodulation method started half a century ago, with interest increasing dramatically over the past decade (Fini and Tyler, 2017). Studies using various parameters have shown that tFUS can modulate neural activity in the brains of animals and humans. It has the potential to modulate brain activities indicated by sensory or motor behaviors, functional magnetic resonance imaging (fMRI), electroencephalography (EEG), and near-infrared spectroscopy (NIRS) (Krishna et al., 2018; Legon et al., 2018b). The findings of *in vitro* and *in vivo* experiments have promoted the understanding of ultrasound neuromodulation. However, the high variability in experimental conditions, different ultrasound parameters, as well as partially conflicting results, led to contradictory interpretations. To achieve clinical application, it is important to clarify the excitatory and inhibitory effects of tFUS. In this review, we summarize the current findings of the brain modulatory effects of tFUS in both animal and human studies. We discussed findings of the excitatory or inhibitory effect of tFUS in light of varying experimental and disease conditions. Finally, the proposed mechanism for ultrasound neuromodulation was discussed.

LITERATURE SEARCH

We searched the literature in the databases of the PubMed /MEDLINE/EMBASE with the following research string, in March 2021: ("Low-intensity focused ultrasound[Title/Abstract]" OR "Transcranial focused ultrasound[Title/Abstract]") AND ("Neuromodulation[Title/Abstract]" OR "Brain Stimulation [Title/Abstract]"). Non-English language studies and duplicates were excluded. Studies were also excluded according to the following criteria: (1) Study investigating the diagnostic aspect of transcranial ultrasound rather than neuromodulation effects; (2) Study investigating the application of transcranial ultrasound in ablation neurosurgery or drug delivery; (3) Study focusing on the development of new ultrasound device; (4) Study published as the conference abstract without a full text, as dissertation or those published in books or only providing surrogate biomarkers. The resulting original articles that reported the use of tFUS in animals and human subjects to modulate brain activity were included (**Tables 1**, **2**). Ultimately 41 studies were selected for discussion in this review, including 23 animals and 18 human studies.

MAIN ULTRASOUND PARAMETERS

The neuromodulation effect of ultrasound depends on the stimulation parameters used. Pulsed ultrasound is the main form of neuromodulation application to minimize the probability of tissue heating or damage. Fundamental frequency, pulse repetition frequency (PRF), duty cycle (DC), sonication duration (SD), and intensity are the five most important elements that define a sonication protocol. The fundamental frequency refers to the number of oscillatory cycles per unit time and is inversely proportional to wavelength. Fundamental frequency significantly affects the spatial targeting of brain regions. A higher fundamental frequency induces stimulation with a tighter focus (when the frequency is > 1 MHz, the diameter can be as narrow as few millimeters). But ultrasound with higher fundamental frequency has more transcranial attenuation and scattering. 200–650 kHz have been used in most human and animal studies. PRF refers to the rate of the pulses delivered. DC is the proportion of each pulse filled with ultrasound cycles, which is an important parameter that determines the direction of the neuromodulation effect. SD refers to the total time from the onset of the first pulse to the termination of the last pulse, which may determine the total intensity and tissue heating. The combination of PRF, DC, and SD may affect the inhibition or excitation of cortical neurons. The intensity of acoustic exposure is commonly characterized by two parameters: the spatial-peak temporal average (I_{spta}) and the spatial-peak pulse average (I_{sppa}). I_{spta} measures the average intensity during the entire sonication therapy and is proportional to SD. I_{sppa} measures the average intensity of a single pulse and provides estimates of short-term mechanical biological effects. The mechanical index (MI) is an indicator of the risk of potentially destructive biomechanical effects on tissues, such as inertial cavitation. It is equal to the peak negative pressure divided by the square of the fundamental frequency. Considering that thermal and mechanical effects may cause brain damage, FDA guidelines for cephalic ultrasound suggest a maximum safety value range of Ispta < 94 mW/cm^2, Isppa < 190 W/cm^2, and MI < 1.9 to avoid cavitation and heating in humans (United States Food and Drug Administration. Marketing clearance of diagnostic ultrasound systems and transducers. Draft guidance for industry and food and drug administration staff. 2019).

NEUROMODULATION EFFECTS IN ANIMALS

To use ultrasound for neuromodulation therapy, an important issue is to clarify its excitatory or inhibitory effects on the central nervous system. We reviewed the reports of the neuromodulatory effects of ultrasound in animals. Studies have been conducted in mice, rats, ovines, swine, sheep, and macaques with different ultrasound parameters, and brain targets. The reported brain targets included the motor cortex, midbrain, somatosensory cortex, hypothalamus, right anterior cortex, hippocampus, thalamus, and visual cortex. The excitatory and inhibitory effects vary with the stimulation targets and sonication parameters (**Table 1**).

EXCITATORY EFFECT

Several studies have reported excitatory effects of tFUS targeting the cortex and deep brain areas. For targeting at

TABLE 1 | tFUS neuromodulation studies in animals.

References	Animal species	Targets	Sonication parameters	Key findings	Effect
Mohammadjavadi et al. (2019)	Normal mice	Midbrain	Focused, frequency = 500 kHz, PRF = 1.5 kHz, 8 kHz	tFUS-evoked motor responses independent of the peripheral auditory system; high correlation between tFUS pulse duration and electromyography response duration	Excitatory
Yuan et al. (2020)	Normal mice	Motor cortex	Unfocused, frequency = 500 kHz, PRF = 1 kHz, SD = 400 ms, DC = 40%, Isppa = 0.8 W/cm^2	Ultrasound pulses induced motor response, neural activity, and rapid hemodynamic response selectively at the stimulation site	Excitatory
Kim et al. (2014)	Normal rats	Somatomotor area	Focused, frequency = 350 kHz and 650 Hz, DC = 30–100%, PRF = 0.1–2.8 kHz, SD = 150–400 ms, TBD = 0.25–5 ms	1–5 ms TBD, 50% DC, 300 ms SD stimulates the somatomotor area most effectively; 350 kHz frequency outperforms 650 kHz; pulsed outperforms the equivalent continuous sonication	Excitatory
Yu et al. (2016)	Normal rats	Right anterior cortex	Focused, frequency = 500 kHz, PRF = 2.0 kHz, Isppa = 0.74–4.6 mW/cm^2	Low-intensity tFUS activated neurons correlated to intensity and SD. tFUS stimulation activated the focal site and propagating to surrounding areas over time	Excitatory
Moore et al. (2015)	Normal mice	Somatosensory barrel cortex	Focused, frequency = 350 kHz, DC = 42.8%, PRF = 2.0 kHz, TBD = 0.5 ms	Ultrasound stimulation induced depolarition of pyramidal cells	Excitatory
Fisher and Gumenchuk (2018)	Normal mice	Primary somatosensory cortex	Focused, frequency = 510 kHz,PRF = 1 kHz, Isppa = 0.69 or 3.5 W/cm^2	Low-intensity FUS alters both the kinetics and spatial patterns of neural activity	Excitatory
Yoo et al. (2011)	Normal rats	Thalamus	Focused, frequency = 440–700 KHz, PRF = 100 Hz,TBD = 0.5 ms, DC = 50%, Isppa = 3.3–6 W/cm^2	Ultrasound stimulation reduced the time to emergence from ketamine/xylazine anesthesia in rats	Excitatory
Baek et al. (2018)	Stroke mice	Lateral cerebellar nucleus	Focused, frequency = 350 kHz DC = 50%, PRF = 1 kHz, TBD = 0.5 ms, SD = 300 ms, Isppa = 2.54 W/cm^2	tFUS enhanced the sensorimotor performance in mice of photothrombotic stroke	Excitatory
Lee et al. (2018)	Normal rats	Motor cortex	Focused, frequency = 600 kHz, PRF = 500 Hz,TBD = 1 ms,DC = 50%, Isppa = 8.8 W/cm^2,14.9 W/cm^2	Wearable miniature stimulator applied tFUS and elicited movements in both awake and anesthetized rats	Excitatory
Li et al. (2019)	Normal mice	Somatosensory cortex	Focused, frequency = 2 MHz,PRF = 1 kHz, DC = 30%, SD = 300 ms	Wearable ultrasound stimulator induced action potentials and evoked sonication−related movement behaviors	Excitatory
Darrow et al. (2019)	Normal rats	Thalamus	Focused,frequency = 3.2 MHz, PRF = 500 Hz, DC = 5–70%, Ispta = 0.01–36.03 W/cm^2	tFUS suppressed a primary sensory pathway, much of the suppression could be attributed to thermal neuromodulation	Inhibitory
Dallapiazza et al. (2018)	Swine	Thalamus	Focused, Frequency = 1.145 MHz,650 kHz, 220 kHz,DC = 43.7%, Isppa = 25–30 W/cm^2	Low intensity focused ultrasound inhibited sensory evoked potentials with a spatial resolution ∼2 mm.	Inhibitory
Min et al. (2011)	PTZ-injected epilepsy rats	Thalamus	Focused, frequency = 690 kH, TBD = 0.25–5 ms, PRF = 100 Hz, DC = 5%, Isppa = 130 mW/cm^2	tFUS decreased epileptic EEG bursts and the epileptic behavior, did not cause any damage to the brain tissue	Inhibitory
Yang et al. (2020)	TLE mice	Hippocampus	Focused, frequency = 500 kHz, for modulation of the neural oscillation: PRF = 1 kHz, SD = 400 ms, DC = 40%; for seizure inhibition: frequency = 500 kHz, PRF = 500 Hz, SD = 30 s, and DC = 5%	The ultrasound modulated the neural oscillation and inhibit the seizure in TLE mice	Inhibitory
Chen et al. (2020)	PTZ-injected epilepsy rats	Cortex or hippocampus area	Focused, frequency = 0.5 MHz, various sonication parameters	Pulsed FUS exposure suppressed epileptic spikes and affected the PI3K-Akt-mTOR pathway	Inhibitory
Lin et al. (2020)	Macaques model of epilepsy, tissues from patients with TLE	Right frontal lobe	Focused, frequency = 750 kHz, Isppa = 2.02 W/cm^2, PRF = 1 kHz, TBD = 0.3 ms, SD = 200 ms	tFUS reduces epileptiform activities and behavioral seizures in epileptic monkeys, inhibits the epileptiform discharges in neurons from patients, activates the inhibitory interneurons	Inhibitory
Kim et al. (2015)	Normal rats	Visual cortex	350 kHz, PRF = 100 Hz, Isppa = 1, 3, 5 W/cm^2, DC = 1, 5, 8.3%	5%DC: VEPs magnitude decreased by tFUS with 3 W/cm^2 Isppa, but not 1 W/cm^2, slightly elevated when use 5 W/cm^2 Isppa; 3 W/cm^2 Isppa: VEPs magnitude decreased by tFUS with 5% DC, but not 1% DC, slightly elevated when use 8.3% DC	Inhibitory
Yoon et al. (2019)	Ovine	Primary sensorimotor area and its thalamic projection	Focused, frequency = 250 kHz; Excitatory effects: DC = 30, 50, 70, 100%, PRF = 100–1400 Hz, TBD = 0.5–3 ms, Isppa = 15.8, 18.2 W/cm^2. Inhibitory effects: DC = 3, 5%, PRF = 30–100 Hz, TBD = 0.5, 1.0 ms, Isppa = 5.4, 11.6 W/cm^2	tFUS with 70% DC showed superior stimulation efficiency and 0.5 ms TBD resulted in the highest response rate. The modulatory effects were transient and reversible. Repeated exposure to tFUS did not damage the brain tissue	Excitatory from EMG and inhibitory from SEPs
Verhagen et al. (2019)	Macaque	SMA, FPC	Focused, frequency = 250 kHz, PRF = 10 Hz, DC = 30%, PD = 30 ms, Isppa = 24.1 W/cm^2 for SMA and 31.7 W/cm^2 for FPC	tFUS changed each area's connectional fingerprint, enhanced the connectivity activity in proximal areas, reduced coupling between the stimulated area and less closed regions. The effects were temporary and not associated with microstructural changes.	Change the connectional fingerprint

(Continued)

TABLE 1 | (Continued)

References	Animal species	Targets	Sonication parameters	Key findings	Effect
Folloni et al. (2019)	Macaque	Amygdala, ACC	Focused, frequency = 250 kHz, DC = 30%, Isppa = 64.9 W/cm^2 in the amygdala and 18.8 W/cm^2 in ACC	tFUS transiently and reversibly altered neural activity in subcortical and deep cortical areas with high spatial specificity; reduced the interconnection of the targeted areas with other regions.	Decreased network connectivity
Fouragnan et al. (2019)	Macaque	ACC	Focused, frequency = 250 kHz, PRF = 10 Hz, DC = 30%, PD = 30 ms	tFUS significantly changed ACC activity, altered strength of connectivity from ACC with 3 other regions, impaired translation of counterfactual choice values into actual behavioral change	Changed connectivity map
Wattiez et al. (2017)	Macaques	Visual cortex	Frequency = 320 kHz, Isppa = 5.6, 1.9 W/cm^2	tFUS changed 40% of neurons in the recorded region, half showed a transient increase of activity and half showed decrease of activity.	Different neurons respond differently
Yang et al. (2021)	Macaque	Somatosensory areas 3a/3b	Focused, frequency = 250 kHz, DC = 50%, PRF = 2 kHz, Isppa = 2.0 W/cm^2	tFUS suppressed tactile stimulus-evoked fMRI responses, directly activated neurons within the target at resting state	Neuron state-dependent effect

ACC, anterior cingulate cortex; DC, duty cycle; FPC, frontal polar cortex; Isppa, the intensity of spatial-peak pulse average; PRF, pulse repetition frequency; SD, sonication duration; TBD, tone-burst duration; SMA, supplementary motor area; tFUS; TLE, temporal lobe epilepsy; PTZ, Pentylenetetrazol; fMRI, functional magnetic resonance imaging; VEPs, visual evoked potentials; EEG, electroencephalography; EMG, electromyography; SEPs, somatosensory evoked potentials.

the motor cortex, unfocused ultrasound with a frequency of 500 kHz evokes motor responses, and the responses are not related to the stimulation of the peripheral auditory system, which emphasizes the direct action of motor neurons in the brain (Mohammadjavadi et al., 2019). Another study used low-intensity tFUS (500 kHz) to stimulate mouse motor cortical regions and demonstrated that tFUS induced tail movement, neural activity, and hemodynamic responses (cortical blood flow, CBF) immediately and returned to baseline at ∼5.5 s. The relationships between CBF and key ultrasound parameters showed that the CBF responses increasing with increasing intensities (Isppa = 0.2–1.1 W/cm^2, SD = 400 ms, DC = 40%) and SD (SD = 50–400 ms, Isppa = 0.8 W/cm^2, DC = 40%), while had a weak dependence on DC (DC = 10–40%, SD = 50–400 ms, Isppa = 0.8 W/cm^2) (Yuan et al., 2020). Kim et al. (2014) examined the stimulation effects of tFUS with a range of sonication parameters administrated to the somatomotor cortex of rats *in vivo*. Based on comparison experiments, the authors found that 50% of DC outperforms 30 and 70%. Operating at 50% DC, the use of TBDs in the range of 1–5 ms, serving as an effective pulsing scheme, 350 kHz fundamental frequency outperforms 650 kHz, pulsed tFUS outperforms equivalent continuous sonication stimulate the target cortex most effectively. Further, for the parameter of SD, they found that 400 ms required higher Isppa for eliciting motor activity than 300 ms, which may indicate that the longer SD might have recruited inhibitory neural circuits or neural cells. Overall, this study found non-linear neural responses to tFUS that might include the activation of motor neurons and inhibitory interneurons (Kim et al., 2014).

For other cortex regions, Yu et al. (2016) demonstrated that low intensity (Ispta < 1 Mw/cm^2) 500 kHz pulsed tFUS targeting the right anterior cortex of rats evoked time-locked activation of the brain, as correlated to intensity and SD. They also suggested electrophysiological source imaging as a useful tool to quantify tFUS effects, guide its use for neuromodulation (Yu et al., 2016). The study of Moore et al. (2015) recorded local field potential fluctuations in the motor cortex in response to ultrasound stimulation of the mouse somatosensory barrel cortex. Ultrasound stimulation at 350 kHz and 42.8% DC induced depolarization of cerebral cortical pyramidal neurons, which indicates an excitatory effect of nerve transmission (Moore et al., 2015). Fisher and Gumenchuk (2018) demonstrated that tFUS with a frequency of 510 kHz reduced the latency and concentrates the spatial patterns of neural activity in the primary somatosensory cortex. The findings suggest the using of tFUS to target and alter spatial aspects of sensory receptive fields on the cerebral cortex (Fisher and Gumenchuk, 2018). As for deep brain targets, the research of Yoo et al. (2011) revealed that pulsed FUS targeting at the thalamus significantly decreased the time to emergence from ketamine/xylazine anesthesia in rats. This study provided early evidence for the excitatory neuromodulatory potential of tFUS targeting the deep brain area (Yoo et al., 2011). The study of Baek et al. (2018) provides the first evidence in the disease model showing that tFUS-induced cerebellar modulation improved impaired sensorimotor function in stroke mice and could be a potential strategy for post stroke recovery. They hypothesized that the effectiveness could be attributable to long-term potentiation of hypoactive neural connections between the motor cortex and deep cerebellar nucleus induced by tFUS. Longer follow-up studies are necessary to fully confirm the effects of tFUS on post stroke recovery (Baek et al., 2018).

INHIBITORY EFFECT

Three studies targeting the thalamus showed inhibitory effects of tFUS. The study of Darrow et al. (2019) revealed that 3.2 MHz tFUS targeting the rat thalamus reversibly suppressed somatosensory evoked potentials (SEPs) in a spatially and intensity-dependent manner. The effect was independent of the parameters of DC, peak pressure, or modulation frequency. The ultrasound frequency used in this study is higher than most other studies, which may cause an obvious thermal effect and lead to the suppression effect (Darrow et al., 2019). The study of Dallapiazza et al. (2018) demonstrated that low-intensity focused ultrasound with frequencies of 1.1 MHz, 220 kHz,

TABLE 2 | tFUS neuromodulation studies in human.

References	Subjects/study design	Targets	Sonication parameters	indexes	Key findings	Modulate effects	Adverse effects
Lee et al. (2015)	Healthy volunteers (*n* = 1)/within-subjects, sham-controlled study	S1 (hand)	Focused, frequency = 250 kHz, PRF = 500 Hz, TBD = 1 ms, DC = 50%, SD = 300 ms, Isppa = 3 W/cm^2	EEG, fMRI, tactile sensations task	tFUS elicited transient tactile sensations accurately to one finger, evoked cortical potentials similar to the SEPs generated by MN stimulation.	Excitatory	No
Lee et al. (2016b)	Healthy volunteers (*n* = 29)/within-subjects, single-blind, sham-controlled study	V1	Focused, frequency = 270 kHz, PRF = 500 Hz, PD = 1 ms, DC = 50%, SD = 300 ms, Isppa = 3 W/cm^2	fMRI, EEG, phosphene perception task	tFUS elicited activation of V1 and other visual areas, elicited cortical evoked EEG potentials similar to classical VEPs	Excitatory	No
Lee et al. (2016a)	Healthy volunteers (*n* = 10)/within-subjects, double-blind, sham-controlled study	S1 and S2	Focused, frequency = 210 kHz, PRF = 500 Hz, PD = 1 ms,DC = 50%, SD = 500 ms, Isppa = 7.0–8.8 W/cm^2	fMRI, EEG, tactile sensory task	tFUS targeting at S1 and S2 separately or simultaneously, elicited tactile sensations from the contralateral hand/arm areas	Excitatory	No
Liu et al. (2021)	Healthy subjects (*n* = 9)/sham-controlled, crossover study	S1	Focused, frequency = 500 kHz, SD = 500 ms, PRF = 300 Hz	64-channel EEG and ESI, sensory task	tFUS improved the subjects' discrimination ability through excitatory effects	Excitatory	Not available
Gibson et al. (2018)	Healthy volunteers (*n* = 40)/between-subjects, single-blind, sham-controlled study	M1	Unfocused, Continuous, frequency = 2.32 MHz, Isppa = 34.96 W/cm^2	TMS-induced MEPs	Ultrasound increased MEPs amplitude: 33.7% at 1 min, 32.2% at 6 min post stimulation)	Excitatory	No
Ai et al. (2018)	Healthy volunteers (*n* = 6)/Pre-post interventional study	Primary sensorimotor cortex (caudate area)	Focused, frequency = 500 kHz, PRF = 1 kHz, DC = 36% in 3T MRI experiment; frequency = 860 kHz, PRF = 0.5 kHz, DC = 50% in 7T MRI experiment; SD = 500 ms, Isppa: 6 W/cm^2	fMRI scan (cortical BOLD at 3T and sub-cortical BOLD at 7T)	BOLD response was detected in the S1 in the 3T studies and in the caudate in the 7T study	Excitatory	Not available
Leo et al. (2016)	Healthy volunteers (*n* = 5)/within-subjects, sham-controlled study	M1	Focused, frequency = 500 kHz, PD = 0.36 ms; PRF = 1 kHz; DC = 36%; SD = 500 ms. Isppa: 16.95 W/cm^2	fMRI scan during finger tapping task	tFUS induced BOLD response in the targeted cortical regions (in 3 of 6 subjects)	Excitatory	No
Yu et al. (2020)	Healthy subjects (*n* = 15)/within-subjects, sham-controlled study	S1 (leg area)	Focused, frequency = 500 kHz, SD = 500 ms, PRF = 300 and 3,000 Hz, Isppa = 5.90 W/cm^2	64-channel EEG and ESI, EMP, voluntary foot tapping task	tFUS modulated MRCP source dynamics with high spatiotemporal resolutions; tFUS increased the MSPA; high ultrasound PRF enhances the MSPA outperforms low PRF.	Excitatory	Not available
Legon et al. (2014)	Healthy volunteers (*n* = 30 totally in 3 exp)/within-subjects, sham-controlled study	CP3	Focused, frequency = 500 kHz, SD = 500 ms; PRF = 1 kHz; DC = 36%, Isppa = 23.87 W/cm^2	EEG activity recorded from four electrodes surrounding CP3 (C3, CP1, CP5 and P3); SEPs induced by MN stimulation; two-point discrimination tasks	tFUS spatially attenuated the amplitudes of SEPs, modulated the spectral content of sensory-evoked brain oscillations, enhanced the somatosensory discrimination abilities.	Inhibitory	No thermal or mechanical sensations
Mueller et al. (2014)	Healthy volunteers (*n* = 25)/within-subjects, sham-controlled study	CP3 and 1 cm laterally	Focused, frequency = 500 kHz, PD = 0.36 ms; PRF = 1 kHz, DC = 36%; SD = 500 ms, Isppa = 23.87 W/cm^2	EEG data were acquired at sites C3, CP1, CP5, and P3; SEPs induced by MN stimulation	tFUS altered the phase distribution of intrinsic brain activity for beta frequencies, changed the phase rate of beta and gamma frequencies, affected phase distributions in the beta band of early SEPs	Inhibitory	Not available

(Continued)

TABLE 2 | (Continued)

References	Subjects/study design	Targets	Sonication parameters	indexes	Key findings	Modulate effects	Adverse effects
					components.		
Legon et al. (2018a)	Healthy volunteers (n = 40)/within-subjects, sham-controlled study	Unilateral sensory nuclei of thalamus	Focused, frequency = 500 kHz; PD = 0.36 ms; PRF = 1 kHz; DC = 36%; Isppa: 7.03 W/cm^2	EEG, SEPs induced by MN stimulation, two-point discrimination tasks	FUS inhibited the amplitude of the P14 SEPs, attenuated alpha and beta power, inhibited the locked gamma power, decreased the performance in tactile judgment task	Inhibitory	Not available
Legon et al. (2018b)	Healthy volunteers (n = 50)/within-subjects, sham-controlled study	M1	Focused, frequency = 500 kHz, PD = 0.36 ms; PRF = 1 kHz; DC = 36%; SD = 500 ms, Isppa = 17.12 W/cm^2	Recruitment curves, MEPs, SICI, ICF, stimulus response reaction time task	tFUS inhibited the amplitude of MEPs, attenuated ICF, reduced reaction time in a motor task.	Inhibitory	Mild and moderate neck pain, sleepiness, muscle twitches, itchiness and headache.
Fomenko et al. (2020)	Healthy subjects (n = 16)/double-blinded study	M1	Annular ultrasound, frequency = 500 kHz, PRF = 1,000 Hz, SD = 0.1–0.5 s, DC = 10/30/50%, Isp ta = 0.93/2.78/4.63 W/cm^2	TMS-induced resting peak-to-peak MEPs, visuomotor task	Ultrasound dose dependently suppressed TMS-elicited MEPs, increased GABAA-mediated SICI and decreased reaction time on visuomotor task	Inhibitory	No
Sanguinetti et al. (2020)	Healthy subjects (n = 50)/randomized, placebo-controlled, double-blind study	rIFG	Focused, frequency = 500 kHz, PD = 65 μs, PRF = 40 Hz, DC = 0.26%, SD = 30 s, Ispta = 130 mW/cm^2	Mood questionnaires and EEG, fMRI and resting-state functional connectivity	30-s tFUS induced positive mood effects for up to 30 min, 2 min of tFUS modulated functional connectivity related to the rIFG and DMN	Unknown	Not available
Hameroff et al. (2013)	Chronic pain (n = 31)/double blind, sham-controlled, crossover study	Posterior frontal cortex, contralateral to the maximal pain	Unfocused, Continuous, frequency = 8 MHz, MI = 0.7, max Intensity = 152 mW/cm^2	Heart rate, systolic and diastolic blood pressure, oxygen saturation, numerical rating scale for pain, Visual Analog Mood Scale	15 s ultrasound significantly improved mood at 10 and 40 min following stimulation	Excitatory	Transient headache exacerbation following stimulation (1 subj)
Monti et al. (2016)	Post-traumatic disorder of consciousness 19 days post-injury (n = 1)/Case report, part of an ongoing clinical trial	Thalamus	Focused frequency = 650 kHz, PD = 0.5 ms; DC = 5%, PRF = 100 Hz. Ispta = 720 mW/cm^2.	Chart review, response to command, and reliable communication (by yes/no head gesturing)	3 days of ultrasound treatment the patient demonstrated emergence from minimally conscious state. 5 days after treatment, the patient attempted to walk.	Excitatory	No
Beisteiner et al. (2020)	AD patients (n = 35)/multicenter pre-post study	AD relevant brain areas and the global brain	Single ultrashort (3 μs) ultrasound pulses, typical energy levels = 0.2–0.3 mJ/mm^2, PRF = 1–5 Hz, maximum energy flux density = 0.25 Mj/mm^2 at 4 Hz, maximum Ispta = 0.1 W/cm^2, maximum number of pulses per treatment = 6,000	EEG data recorded at CP3, SEPs, neuropsychological tests, MRI	TPS treatment significantly improved neuropsychological scores, the effects last up to 3 months and correlates with an upregulation of the memory network	Excitatory	No
Badran et al. (2020)	Healthy subjects (n = 19)/double-blind, sham-controlled, crossover study	Right anterior thalamus	Focused, frequency = 650 kHz, PD = 5 ms, PRF = 10 Hz, DC = 5%, SD = 30 s, Ispta = 719 and 995 W/cm^2	Sensory threshold, sensory, pain, and tolerance thresholds to a thermal stimulus	Thermal pain sensitivity was significantly attenuated after tFUS treatment	Inhibitory	No

AD, Alzheimer's disease; BOLD, blood oxygenation level dependent; DC, duty cycle; DMN, default mode network; EMG, electromyography; ESI, electrophysiological source imaging; Ispta, the intensity of spatial-peak temporal average; M1, primary motor cortex; MEPs, motor-evoked potential; MRCP, movement-related cortical potential; MSPA, MRCP source profile amplitude; MN, median nerve; PRF, pulse repetition frequency; rIFG, right inferior frontal gyrus; S1, left primary and secondary somatosensory cortex; S2, left secondary somatosensory cortex; SEPs, somatosensory evoked potentials; SD, sonication duration; TBD, tone-burst duration; TPS, transcranial pulse stimulation; SICI, short interval intracortical inhibition; TMS, transcranial magnetic stimulation; V1, primary visual cortex; VEPs, visual evoked potentials.

and 650 kHz inhibited sensory evoked potentials with a spatial resolution of ∼2 mm in swine, supporting its potential use in non-invasive brain mapping. Longer ultrasound pulses delivered over prolonged periods tend to result in a more substantial and sustained decrease in neural function. The physiological effects lasted for a period of several minutes without inducing tissue heating or histological damage (Dallapiazza et al., 2018). Kim et al. (2015) reported that the application of pulsed 350 kHz tFUS using a 5% DC and Isppa intensity of 3 W/cm^2 to the visual cortex area suppressed the magnitude of visual evoked potentials (VEPs) in rats. Under the same conditions, higher intensity (5 W/cm^2) or DC (8.3%) induced slight elevation in VEPs (Kim et al., 2015). Yoon et al. (2019) investigated the bimodal effects of tFUS in the modulation of the sensorimotor cortex and thalamus in an ovine model by evaluating the rate and magnitude of electrophysiological responses to a wide range of sonication parameters. The study suggests that a shorter SD ($\leq$ ∼500 ms) at a higher DC (30%) favored excitation, and a longer SD (∼1 min) at a lower DC ($\leq$ 10%) resulted in suppression. For excitation effects, the use of 15.8 W/cm^2 Isppa generated a higher response rate than the use of 18.2 W/cm^2. This study provided important evidence for the effects of varying sonication parameters on neuromodulation response (Yoon et al., 2019).

The above studies that reported excitatory and inhibitory regulation effects demonstrated the feasibility of tFUS to the clinical application of neural modulation. However, the ultrasound parameters used by different research groups are different, no two studies used consistent parameters. The rules of the neuromodulation effect corresponding to parameter changes are still unclear. Change of any one of the main ultrasound parameters may produce a change of efficacy of excitatory or inhibitory effects, with the correlation relationship is considered to be non-linear. Nevertheless, the influence of any parameters on the modulatory direction is inconclusive, and the combination of multiple parameters seems more difficult. Further research should be conducted to explore how to precisely control parameters to achieve a specific adjustment purpose.

Other evidence of inhibitory neuromodulation effects comes from research in animal models of epilepsy. An early study by Min et al. (2011) reported that low-intensity, pulsed FUS (690 kHz) sonication suppressed the number of epileptic signal bursts and severe epileptic behavior using an acute epilepsy model in animals. Yang et al. (2020) delivered pulsed closed-loop transcranial ultrasound stimulation with a frequency of 500 kHz to the hippocampus to modulate neural oscillation and effectively inhibited the seizure of a temporal lobe epilepsy (TLE) mouse. The study of Chen et al. (2020) reported that pulsed tFUS (500 kHz) effectively suppressed epileptic spikes in an acute epilepsy animal model and found that ultrasound pulsation interferes with neuronal activity. Zhengrong Lin et al. (2020) demonstrated that low-intensity pulsed FUS could improve the electrophysiological activities and behavioral outcomes in non-human primate models of epilepsy. The study also demonstrated that ultrasound suppressed abnormal epileptiform activities of neurons from human epileptic slices (Lin et al., 2020). The suppression of epileptic neuro-electric activity and the behavior of tFUS may mainly indicate inhibitory effects.

Moreover, most current animal experiments are performed using anesthetized animal models to prevent animal motion during ultrasound administration. A recently published study by Wang X. et al. (2021) demonstrated that the behavioral states, especially anesthesia, modulate the ultrasound stimulation-induced neural activity. The effect of pharmacological sedation on tFUS induced effects is not clear and may obfuscate the interpretation of the tFUS neuromodulation response (Jerusalem et al., 2019). Studies in awake and freely moving animals are needed. Lee et al. (2018) conducted the first study that using awake rats to evaluate the neuromodulatory efficacy of tFUS. They developed a miniature tFUS headgear with a frequency of 600 kHz, and the stimulation of motor cortical areas by their configuration elicited body movements from various areas in freely moving rats. Compared with the anesthetic rats, the stimulation in awake rats induced an increased response rate with reduced variability and shorter latency. However, the lack of measurement of electrophysiological signals in this study limited its information (Lee et al., 2018). Li et al. (2019) designed a miniature and lightweight head-mounted ultrasound stimulator that can be used in freely moving mice. When target at the primary somatosensory cortex barrel field, the device evoked head-turning behaviors and action potentials recorded *in situ* (Li et al., 2019). The application of stimulation in awake animals is valuable for the research on the neuromodulation effects and mechanisms of tFUS, especially for investigations that are not possible with anesthesia, such as social behavioral studies and disease models that are influenced by anesthesia (e.g., epilepsy).

NEUROMODULATION IN HUMAN SUBJECTS

The excitatory effects of tFUS were identified in healthy human subjects in 9 studies as indicated by fMRI and EEG. Six studies showed the inhibitory effects of TUS indicated by SEPs, motor induced potentials (MEPs), and intracortical facilitation (ICF). The modulated brain targets included the motor cortex, somatosensory cortex, thalamus, caudate nuclei, and visual cortex. Several studies have reported the effect of FUS stimulation on patients with chronic pain, posttraumatic disorder of consciousness, and Alzheimer's disease (AD) (**Table 2**).

EXCITATORY MODULATION

Studies provide evidence that FUS stimulation can activate the brain to produce sensory and motor nerve responses without any external stimulation. Three studies conducted by Lee et al. (2015) showed excitatory effects of tFUS on the human primary and secondary somatosensory cortex and visual cortex. tFUS targeting the human hand somatosensory cortex (S1) elicited somatosensory sensations with anatomical specificity up to a finger and evoked EEG potentials similar to the classical SEPs generated by median nerve stimulation (Lee et al., 2015). In another study, they reported that FUS targeting to the human visual cortex (V1) induced the perception of phosphine and

activated a network of regions involved in visual and higher-order cognitive processes (Lee et al., 2016b). They also reported that tFUS application to the human bilateral primary somatosensory cortex (S1) and secondary somatosensory cortex (S2) elicited various tactile sensations in the targeted hand area. This study also showed the possibility of simultaneous stimulation of the S1 and S2 (proximal to each other) with ultrasound, which has not been feasible with conventional non-invasive brain stimulation approaches such as TMS or tDCS. The ability to selectively stimulate multiple human brain areas in a spatially restricted manner may offer an unprecedented opportunity to study the causal relationships between brain activity and subsequent efferent behaviors (Lee et al., 2016a). Ai et al. (2018) combined tFUS with high-field 7T fMRI in humans and evaluated its neuromodulation effect by the BOLD response. tFUS stimulation targeted individual finger representations within M1 increased the activation volumes of the M1 thumb representation in a spatially restricted manner. These results provide a more detailed perspective on the spatial resolution of tFUS for neuromodulation of individual finger representations within a single gyrus reflected by the BOLD response (Leo et al., 2016; Ai et al., 2018).

FUS stimulation modulates the neural response induced by behavioral tasks and TMS-induced MEPs. Liu et al. (2021) evaluated the interference of tFUS stimulation at S1 on the performances in a mechanical vibration frequency discrimination task in a group of healthy human participants. The behavioral results indicated that low-intensity tFUS stimulation improved vibration frequency discrimination capability. EEG and electrophysiological source imaging (ESI) results revealed that tFUS improved sensory discrimination capability through exciting the targeted sensory cortex (Liu et al., 2021). The study by Gibson et al. (2018) used a diagnostic imaging ultrasound system to stimulate the motor cortex. Increased TMS-induced MEPs amplitude (34%) was recorded up to 6 min after stimulation but disappeared 11 min later (Gibson et al., 2018). This result contrasts with the research of Legon et al., who reported tFUS inhibited MEPs induced by TMS (Legon et al., 2018b). As discussed by the authors, the different findings may be caused by stimulation parameters and other methodological factors. Yu et al. (2020) demonstrated the neuromodulatory effects of low-intensity tFUS on human voluntary movement-related cortical potential (MRCP). Through ESI, the results showed that tFUS modulates MRCP source dynamics with high spatiotemporal resolutions and significantly increases the MRCP source profile amplitude (MSPA), and further, a high PRF enhances the MSPA outperforms a low UPRF does. This study provides the first evidence that tFUS enhances human endogenous motor cortical activities through excitatory modulation (Yu et al., 2020).

INHIBITORY MODULATION

Five studies by one research group reported the inhibitory modulation effect of tFUS targeting the primary somatosensory cortex (CP3), unilateral sensory nuclei of the thalamus, and primary motor cortex. They used similar ultrasound parameters with the 500 kHz frequency, 36% DC, 500 ms SD, and 1 kHz PRF. The first study reported that tFUS targeting CP3 significantly attenuated the amplitudes of SEPs and modulated the spectral content of brain oscillations elicited by median nerve stimulation, while enhanced the somatosensory discrimination abilities of participants. Importantly, this research also showed that the influence of tFUS on brain activity can be spatially restricted within 1 cm (Legon et al., 2014). The following study by Mueller et al. (2014) found that tFUS preferentially affected the phase distribution of the beta band and modulated the phase rate of both beta and gamma frequencies. The third study reported that tFUS targeting the thalamus attenuated the SEPs generated in the ventral-lateral nucleus and serially connected cortical regions. The study provided initial evidence that tFUS can non-invasively modulate subcortical areas of the human brain with good spatial precision and resolution (Legon et al., 2018a). The fourth study showed that tFUS inhibits the amplitude of single-pulse MEPs and attenuates intracortical facilitation, which confirms previous results that ultrasound results in effective neuronal inhibition. tFUS did not affect short interval intracortical inhibition (SICI) or reduce reaction time in a simple stimulus response task in this study (Legon et al., 2018b). The studies of Fomenko et al. (2020) reported that tFUS targeting at the motor cortex displayed inhibitory effects on cortical excitability, but the effects on SICI were inconsistent. Furthermore, other studies have reported heterogeneous effects of FUS targeting on the motor cortex, demonstrating increased cortical excitability or the amplitude of MEPs after prolonged sonication (Gibson et al., 2018; Yu et al., 2020).

Like animal studies, human studies have inconsistent conclusions about whether ultrasound modulation is exciting or inhibiting. In addition to the influence of sonication parameters, differences in detection methods also may introduce inherent variability. For example, the study of Leo et al. (2016) and Legon et al. (2018a) used similar FUS protocols (500 kHz frequency, 36% DC, and 1 kHz RPF) targeting the M1 cortex demonstrated excitatory or inhibitory effect, respectively. Leo et al. (2016) reported BOLD fMRI signals were induced by tFUS, while Legon et al. (2018a) detected reduced amplitude of MEPs and intracortical facilitation. Further prospective studies are needed to elucidate region- and neuron-specific sensitivity to focused ultrasound with a wider range of parameters.

CLINICAL APPLICATION

Preliminary research has explored the role of this technology in the treatment of human brain functional diseases. In healthy subjects, Sanguinetti et al. (2020) reported two experiments that demonstrated that tFUS targeting the right inferior frontal gyrus (rIFG) enhances mood and changed the functional connectivity in networks related to emotional regulation. These results suggest that tFUS may be useful in modulating mood and emotional regulation networks (Sanguinetti et al., 2020). Badran BW conducted a controlled, double-blind study to investigate

whether sonication targeting deep brain structures produces quantifiable antinociceptive effects in healthy adults. The study reveals that two 10-min sessions of tFUS delivered to the right anterior thalamus produced significant antinociceptive effects in thermal pain threshold ratings, suggesting that tFUS appears to be able to focally target deep brain structures and modulate pain perceptions (Badran et al., 2020).

Four studies have provided evidence for its potential in disease treatment in patients with chronic pain, a minimally conscious state, AD and epilepsy. Hameroff et al. (2013) reported a double-blind, sham-controlled crossover study applying 8 MHz unfocused transcranial ultrasound stimulation targeted to the posterior frontal cortex in 31 patients with chronic pain. They found improvement in subjective mood 10 and 40 min after stimulation, suggesting that ultrasound treatment can beneficially affect mental state. However, the study was limited in clinic time and unable to perform extensive psychological testing (Hameroff et al., 2013). Monti et al. (2016) published a clinical case report showed that thalamic tFUS stimulation improved the minimally conscious state in a patient after acute brain injury. An important study by Beisteiner et al. (2020) introduces a clinical sonication technique based on single ultrashort ultrasound pulses (3 μs) repeated every 200–300 ms transcranial pulse stimulation (TPS), which markedly differs from others. The TPS was applied to brain regions of patients with probable AD. The researchers found that the treatment significantly improved neuropsychological scores and upregulated corresponding memory network. This study provided comprehensive preclinical and clinical feasibility, safety, and efficacy data for TPS in the treatment of AD. Thus, widespread neuroscientific application and translation of the method to clinical therapy is encouraged (Beisteiner et al., 2020). An early research by Brinker et al. (2020) developed a laboratory-built experimental device platform and successfully delivered repetitive low-intensity tFUS across the hippocampus in seizure onset zones of patients with drug-resistant TLE. Further study is still ongoing for investigating the effects of tFUS therapeutic neuromodulation in the patients with TLE (Brinker et al., 2020). Overall, to move tFUS forward as a potential therapy for brain diseases, more researches in patients are needed to explore targeting, dosing, and parameter optimization modes.

EVIDENCE FOR MECHANISMS

The precise mechanisms of neuromodulation with ultrasound are unclear. Studies have explored the mechanism for the neuromodulation effect of tFUS from the perspective of brain networks, neural cells, and molecules (**Table 1**). The effect of ultrasound neuromodulation on brain network connections has been reported in researches using macaques and rats. Verhagen et al. (2019) reported that 40 s of ultrasound stimulation in macaques modulated the brain activation for more than 1 h and the ultrasound displays offline and sustained impact on the connectional fingerprint of stimulated brain regions. The study of Folloni et al. (2019) demonstrated that a tFUS protocol impacts activity in the subcortical brain structure of the amygdala and deep cortical region of the anterior cingulate cortex in macaques. The stimulation suppressed the connectivity of the targeted brain area to its network (Folloni et al., 2019). The study of Fouragnan et al. (2019) investigated how representations of counterfactual choices are held in memory and guide behavior in macaque monkeys. tFUS was used to focally alter the neural activity to examine the causal importance of the anterior cingulate cortex (ACC) for behavior. They found that tFUS significantly impaired translation of counterfactual choice values into actual behavioral change and changed the activity and connectivity maps of the ACC (Fouragnan et al., 2019). The study of Zhang et al. (2021) reported that FUS reduced the network connections of epilepsy circuits and change the structure of the brain network at the whole-brain level. The adjustment effect of tFUS on neural network connection may be the mechanism of its repeated application to improve brain diseases.

At the cellular level of neurons, two studies reported bimodal neural modulation effects of tFUS in macaques. The study of Wattiez et al. (2017) assessed the neuromodulatory effects of tFUS in awake behaving monkeys by recording discharge activity from a brain region (supplementary eye field) reciprocally connected with the stimulated region (frontal eye field). They demonstrated that stimulation in the visual cortex significantly changed the activity of 40% of neurons in the recorded region. Half of the neurons showed transiently increased activity, and the other half showed decreased activity. In this study, the ultrasonic effect was quantified based on the direct measurement of the intensity of the modulation induced on a single neuron in a freely performing animal. In particular, the study suggests that different neurons respond differently to tFUS stimuli and indicates further parametric studies should pay attention to the regulation of neural activity at the cell level (Wattiez et al., 2017). Yang et al. (2021) reported that medium amplitude tFUS (425 kPa free-field at 250 kHz) in the macaque brain modulated the activity of neurons at the target in dual directions (excitation and suppression). This simultaneous excitatory and suppressive neuromodulation may be mediated by activation of large excitatory pyramidal and small inhibitory interneurons, respectively. This study first examined the neuromodulation effects of FUS at the whole-brain level and the ability of concurrent FUS and MRI to evaluate causal interactions between functional circuits and neuron-class selectivity (Yang et al., 2021).

Several studies provided evidence for the mechanism of the neuromodulation effect at the molecular level. Recent investigations on the interactions between sound pressure waves and brain tissue suggest that ultrasound primarily exerts its modulatory effects through mechanical action on cell membranes, notably affecting ion channel gating (Kubanek et al., 2016). Liang et al. (2020) explored the efficacy and mechanisms of tFUS in treating pain caused by soft tissue injury. Low-intensity focused ultrasound relieved pain, and the mechanism could be attributed to decreasing the release of analgesic substances from the nerve and reducing local inflammatory factors (Liang et al., 2020). Na Pang et al. (2021) demonstrated that transcranial ultrasound stimulation was effective in modulating the learning behaviors of mice and the expression of apoptosis, oxidative stress, and inflammation. Xu et al. (2020) demonstrated that low-intensity ultrasound is able to stimulate DA release and

helps to regenerate dopaminergic neurons in a mouse model of Parkinson's disease (PD). Huang et al. (2019) reported that non-invasive low-intensity pulsed ultrasound stimulation improved c-fos expression and reduced the incidence rate ($p < 0.05$) and length of primary cilia ($p < 0.01$) of neurons in the rat CA1 hippocampus. Bobola et al. (2020) reported that acutely applied tFUS activated microglia to colocalize with Aβ plaques in a mouse model of AD, and 5 days of tFUS cleared almost 50% of the Aβ plaque. The study of Chen et al. (2020) suggested that pulsed tFUS exposure effectively suppresses epileptic spikes in an acute epilepsy animal model and revealed that ultrasound pulsation affects the PI3K-Akt-mTOR pathway, which might be the molecular mechanism. These studies only provide preliminary clues, and more studies are needed in the future.

SAFETY OF TRANSCRANIAL FOCUSED ULTRASOUND

Currently, ultrasound for neuromodulation in humans generally follows the guidelines of the FDA for adult cephalic applications. Legon et al. (2020) qualitatively evaluated minor adverse events in seven independent experiments using different ultrasound protocols for human neuromodulation. The intensity (Isppa) used in these studies ranged from 11.56 to 17.12 W/cm^2 that is considerably lower than FDA thresholds for ultrasound diagnostics. The parameter of Ispta, which is defined as the Isppa multiplied by the duty factor, in these studies was above FDA thresholds for diagnostics. They found that none of the participants experienced serious adverse effects, and 7/64 reported mild to moderate symptoms probably related to ultrasound treatment. The symptoms include neck pain, attention problems, muscle twitches, and anxiety. They concluded that the symptom rate and type induced by tFUS are similar to other forms of human non-invasive neuromodulation, such as TMS and tDCS, these two have been used as safe forms of human neuromodulation. Despite the causation role of ultrasound has not been defined, the findings suggest limiting the intensity used in future ultrasound experiments for neuromodulation (Legon et al., 2020). Gaur et al. (2020) examined a range of experimental parameters, including the number of focal spot locations, the number of FUS bursts applied to each spot, the timing between FUS sessions, and applied acoustic intensity, to investigate the safety of FUS neuromodulation. The *in situ* intensities were 9.5 W/cm^2 in macaques and 6.7 W/cm^2 in sheep, similar to and slightly higher than previously reported Ispta values of up to 4.4 W/cm^2 in humans. Repeated FUS neuromodulation at various intensity levels for multiple days did not cause histologic damage. The study suggesting that the neuromodulation protocols evaluated do not cause tissue damage and provide important information for the safety profiles of FUS neuromodulation (Gaur et al., 2020).

DISCUSSION

Overall, tFUS is a promising non-invasive brain stimulation technology. The current findings in both animal and human studies reported both the excitatory and inhibitory modulatory effects of tFUS on brain activity. These findings confirmed the application prospects of this technology in the treatment of brain functional diseases. However, the current research does not clarify the correlation among the roles of the stimulus parameters in excitatory or inhibitory modulatory effects. The excitatory and inhibitory effects shown in current research are mostly on a macro level, and it is not clear whether these effects are derived from inhibitory or excitatory neuronal activity. Inhibitory effects may come from the excitement of inhibitory neurons or the inhibition of excitatory neurons, and the opposite is also possible. The physiological state (active or resting) of neurons in the stimulated area and its connected areas and how these neurons interact during the modulation process could also influence the results. Like clinical trials, animal experiments have been conducted in normal animals and disease model animals, the targets include the sensory cortex, motor cortex, and deep nuclei such as the thalamus. The range of ultrasonic parameters used in animal studies were similar to that in clinical trials. Due to the differences in skull size and geometry of the brain, the parameters from tFUS used in animals are less likely to be translated to humans. Further animal studies should focus on the change law of excitation or inhibition effect with the fine change of parameters, and to further reveal the mechanism of regulation effect at the nerve conduction, cellular and molecular levels. The safety profile, effectiveness, and finer device parameters in humans in either healthy or diseased conditions need further research.

AUTHOR CONTRIBUTIONS

TZ drafted this report. SH, CL, NP, and YW revised and expanded. All authors contributed to the article and approved the submitted version.

FUNDING

We acknowledge the support by the National Natural Science Foundation of China (No. 82071483) and the Natural Science Foundation of Beijing (No. 7212048) within the funding program Open Access Publishing.

REFERENCES

Ai, L., Bansal, P., Mueller, J. K., and Legon, W. (2018). Effects of transcranial focused ultrasound on human primary motor cortex using 7T fMRI: a pilot study. *BMC Neurosci.* 19:56. doi: 10.1186/s12868-018-0456-6

Badran, B. W., Caulfield, K. A., Stomberg-Firestein, S., Summers, P. M., Dowdle, L. T., Savoca, M., et al. (2020). Sonication of the anterior thalamus with MRI-Guided transcranial focused ultrasound (tFUS) alters pain thresholds in healthy adults: a double-blind, sham-controlled study. *Brain Stimul.* 13, 1805–1812. doi: 10.1016/j.brs.2020.10.007

Baek, H., Pahk, K. J., Kim, M. J., Youn, I., and Kim, H. (2018). Modulation of cerebellar cortical plasticity using low-intensity focused ultrasound for poststroke sensorimotor function recovery. *Neurorehabil. Neural Repair* 32, 777–787. doi: 10.1177/1545968318790022

Beisteiner, R., Matt, E., Fan, C., Baldysiak, H., Schonfeld, M., Philippi Novak, T., et al. (2020). Transcranial pulse stimulation with ultrasound in Alzheimer's disease-a new navigated focal brain therapy. *Adv. Sci.* 7:1902583. doi: 10.1002/advs.201902583

Bobola, M. S., Chen, L., Ezeokeke, C. K., Olmstead, T. A., Nguyen, C., Sahota, A., et al. (2020). Transcranial focused ultrasound, pulsed at 40 Hz, activates microglia acutely and reduces Abeta load chronically, as demonstrated in vivo. *Brain Stimul.* 13, 1014–1023. doi: 10.1016/j.brs.2020.03.016

Brinker, S. T., Preiswerk, F., White, P. J., Mariano, T. Y., McDannold, N. J., and Bubrick, E. J. (2020). Focused ultrasound platform for investigating therapeutic neuromodulation across the human hippocampus. *Ultrasound Med. Biol.* 46, 1270–1274. doi: 10.1016/j.ultrasmedbio.2020.01.007

Bystritsky, A., Korb, A. S., Douglas, P. K., Cohen, M. S., Melega, W. P., Mulgaonkar, A. P., et al. (2011). A review of low-intensity focused ultrasound pulsation. *Brain Stimul.* 4, 125–136. doi: 10.1016/j.brs.2011.03.007

Chen, S. G., Tsai, C. H., Lin, C. J., Lee, C. C., Yu, H. Y., Hsieh, T. H., et al. (2020). Transcranial focused ultrasound pulsation suppresses pentylenetetrazol induced epilepsy in vivo. *Brain Stimul.* 13, 35–46. doi: 10.1016/j.brs.2019.09.011

Dallapiazza, R. F., Timbie, K. F., Holmberg, S., Gatesman, J., Lopes, M. B., Price, R. J., et al. (2018). Noninvasive neuromodulation and thalamic mapping with low-intensity focused ultrasound. *J. Neurosurg.* 128, 875–884. doi: 10.3171/2016.11.jns16976

Darrow, D. P., O'Brien, P., Richner, T. J., Netoff, T. I., and Ebbini, E. S. (2019). Reversible neuroinhibition by focused ultrasound is mediated by a thermal mechanism. *Brain Stimul.* 12, 1439–1447. doi: 10.1016/j.brs.2019.07.015

Fini, M., and Tyler, W. J. (2017). Transcranial focused ultrasound: a new tool for non-invasive neuromodulation. *Int. Rev. Psychiatry* 29, 168–177. doi: 10.1080/09540261.2017.1302924

Fisher, J. A. N., and Gumenchuk, I. (2018). Low-intensity focused ultrasound alters the latency and spatial patterns of sensory-evoked cortical responses in vivo. *J. Neural Eng.* 15:e035004. doi: 10.1088/1741-2552/aaaee1

Folloni, D., Verhagen, L., Mars, R. B., Fouragnan, E., Constans, C., Aubry, J. F., et al. (2019). Manipulation of subcortical and deep cortical activity in the primate brain using transcranial focused ultrasound stimulation. *Neuron* 101, 1109.e5–1116.e5. doi: 10.1016/j.neuron.2019.01.019

Fomenko, A., Chen, K. S., Nankoo, J. F., Saravanamuttu, J., Wang, Y., El-Baba, M., et al. (2020). Systematic examination of low-intensity ultrasound parameters on human motor cortex excitability and behavior. *eLife* 9:e54497. doi: 10.7554/eLife.54497

Fouragnan, E. F., Chau, B. K. H., Folloni, D., Kolling, N., Verhagen, L., Klein-Flugge, M., et al. (2019). The macaque anterior cingulate cortex translates counterfactual choice value into actual behavioral change. *Nat. Neurosci.* 22, 797–808. doi: 10.1038/s41593-019-0375-6

Gaur, P., Casey, K. M., Kubanek, J., Li, N., Mohammadjavadi, M., Saenz, Y., et al. (2020). Histologic safety of transcranial focused ultrasound neuromodulation and magnetic resonance acoustic radiation force imaging in rhesus macaques and sheep. *Brain Stimul.* 13, 804–814. doi: 10.1016/j.brs.2020.02.017

Gibson, B. C., Sanguinetti, J. L., Badran, B. W., Yu, A. B., Klein, E. P., Abbott, C. C., et al. (2018). Increased excitability induced in the primary motor cortex by transcranial ultrasound stimulation. *Front. Neurol.* 9:1007. doi: 10.3389/fneur.2018.01007

Hameroff, S., Trakas, M., Duffield, C., Annabi, E., Gerace, M. B., Boyle, P., et al. (2013). Transcranial ultrasound (TUS) effects on mental states: a pilot study. *Brain Stimul.* 6, 409–415. doi: 10.1016/j.brs.2012.05.002

Hoy, K. E., and Fitzgerald, P. B. (2010). Brain stimulation in psychiatry and its effects on cognition. *Nat. Rev. Neurol.* 6, 267–275. doi: 10.1038/nrneurol.2010.30

Huang, X., Lin, Z., Meng, L., Wang, K., Liu, X., Zhou, W., et al. (2019). Non-invasive low-intensity pulsed ultrasound modulates primary cilia of rat hippocampal neurons. *Ultrasound Med. Biol.* 45, 1274–1283. doi: 10.1016/j.ultrasmedbio.2018.12.012

Jerusalem, A., Al-Rekabi, Z., Chen, H., Ercole, A., Malboubi, M., Tamayo-Elizalde, M., et al. (2019). Electrophysiological-mechanical coupling in the neuronal membrane and its role in ultrasound neuromodulation and general anaesthesia. *Acta Biomater.* 97, 116–140. doi: 10.1016/j.actbio.2019.07.041

Kim, H., Chiu, A., Lee, S. D., Fischer, K., and Yoo, S. S. (2014). Focused ultrasound-mediated non-invasive brain stimulation: examination of sonication parameters. *Brain Stimul.* 7, 748–756. doi: 10.1016/j.brs.2014.06.011

Kim, H., Park, M. Y., Lee, S. D., Lee, W., Chiu, A., and Yoo, S. S. (2015). Suppression of EEG visual-evoked potentials in rats through neuromodulatory focused ultrasound. *Neuroreport* 26, 211–215. doi: 10.1097/wnr.0000000000000330

Krishna, V., Sammartino, F., and Rezai, A. (2018). A review of the current therapies, challenges, and future directions of transcranial focused ultrasound technology: advances in diagnosis and treatment. *JAMA Neurol.* 75, 246–254. doi: 10.1001/jamaneurol.2017.3129

Kubanek, J. (2018). Neuromodulation with transcranial focused ultrasound. *Neurosurg. Focus* 44:E14. doi: 10.3171/2017.11.focus17621

Kubanek, J., Shi, J., Marsh, J., Chen, D., Deng, C., and Cui, J. (2016). Ultrasound modulates ion channel currents. *Sci. Rep.* 6:24170. doi: 10.1038/srep24170

Lee, W., Kim, H. C., Jung, Y., Chung, Y. A., Song, I. U., Lee, J. H., et al. (2016b). Transcranial focused ultrasound stimulation of human primary visual cortex. *Sci. Rep.* 6:34026. doi: 10.1038/srep34026

Lee, W., Chung, Y. A., Jung, Y., Song, I. U., and Yoo, S. S. (2016a). Simultaneous stimulation of the human primary and secondary somatosensory cortices using transcranial focused ultrasound. *J. Ther. Ultras.* 4:31. doi: 10.1186/s40349-016-0076-5

Lee, W., Croce, P., Margolin, R. W., Cammalleri, A., Yoon, K., and Yoo, S. S. (2018). Transcranial focused ultrasound stimulation of motor cortical areas in freely-moving awake rats. *BMC Neurosci.* 19:57. doi: 10.1186/s12868-018-0459-3

Lee, W., Kim, H., Jung, Y., Song, I. U., Chung, Y. A., and Yoo, S. S. (2015). Image-guided transcranial focused ultrasound stimulates human primary somatosensory cortex. *Sci. Rep.* 5:8743. doi: 10.1038/srep08743

Legon, W., Adams, S., Bansal, P., Patel, P. D., Hobbs, L., Ai, L., et al. (2020). A retrospective qualitative report of symptoms and safety from transcranial focused ultrasound for neuromodulation in humans. *Sci. Rep.* 10:5573. doi: 10.1038/s41598-020-62265-8

Legon, W., Bansal, P., Tyshynsky, R., Ai, L., and Mueller, J. K. (2018b). Transcranial focused ultrasound neuromodulation of the human primary motor cortex. *Sci. Rep.* 8:10007. doi: 10.1038/s41598-018-28320-1

Legon, W., Ai, L., Bansal, P., and Mueller, J. K. (2018a). Neuromodulation with single-element transcranial focused ultrasound in human thalamus. *Hum. Brain Mapp.* 39, 1995–2006. doi: 10.1002/hbm.23981

Legon, W., Sato, T. F., Opitz, A., Mueller, J., Barbour, A., Williams, A., et al. (2014). Transcranial focused ultrasound modulates the activity of primary somatosensory cortex in humans. *Nat. Neurosci.* 17, 322–329. doi: 10.1038/nn.3620

Leo, A., Mueller, J. K., Grant, A., Eryaman, Y., and Wynn, L. (2016). Transcranial focused ultrasound for BOLD fMRI signal modulation in humans. *IEEE Eng. Med. Biol. Soc.* 2016, 1758–1761. doi: 10.1109/EMBC.2016.7591057

Li, G., Qiu, W., Zhang, Z., Jiang, Q., Su, M., Cai, R., et al. (2019). Noninvasive ultrasonic neuromodulation in freely moving mice. *IEEE Trans. Biomed. Eng.* 66, 217–224. doi: 10.1109/TBME.2018.2821201

Liang, D., Chen, J., Zhou, W., Chen, J., Chen, W., and Wang, Y. (2020). Alleviation effects and mechanisms of low-intensity focused ultrasound on pain triggered by soft tissue injury. *J. Ultrasound Med.* 39, 997–1005. doi: 10.1002/jum.15185

Lin, Z., Meng, L., Zou, J., Zhou, W., Huang, X., Xue, S., et al. (2020). Non-invasive ultrasonic neuromodulation of neuronal excitability for treatment of epilepsy. *Theranostics* 10, 5514–5526. doi: 10.7150/thno.40520

Liu, C., Yu, K., Niu, X., and He, B. (2021). Transcranial focused ultrasound enhances sensory discrimination capability through somatosensory cortical excitation. *Ultras. Med. Biol.* 47, 1356–1366. doi: 10.1016/j.ultrasmedbio.2021.01.025

Mehic, E., Xu, J. M., Caler, C. J., Coulson, N. K., Moritz, C. T., and Mourad, P. D. (2014). Increased anatomical specificity of neuromodulation via modulated focused ultrasound. *PLoS One* 9:e86939. doi: 10.1371/journal.pone.0086939

Min, B. K., Bystritsky, A., Jung, K. I., Fischer, K., Zhang, Y., Maeng, L. S., et al. (2011). Focused ultrasound-mediated suppression of chemically-induced acute epileptic EEG activity. *BMC Neurosci.* 12:23. doi: 10.1186/1471-2202-12-23

Mohammadjavadi, M., Ye, P. P., Xia, A., Brown, J., Popelka, G., and Pauly, K. B. (2019). Elimination of peripheral auditory pathway activation does not affect

motor responses from ultrasound neuromodulation. *Brain Stimul.* 12, 901–910. doi: 10.1016/j.brs.2019.03.005

Monti, M. M., Schnakers, C., Korb, A. S., Bystritsky, A., and Vespa, P. M. (2016). Non-invasive ultrasonic thalamic stimulation in disorders of consciousness after severe brain injury: a first-in-man report. *Brain Stimul.* 9, 940–941. doi: 10.1016/j.brs.2016.07.008

Moore, M. E., Loft, J. M., Clegern, W. C., and Wisor, J. P. (2015). Manipulating neuronal activity in the mouse brain with ultrasound: a comparison with optogenetic activation of the cerebral cortex. *Neurosci. Lett.* 604, 183–187. doi: 10.1016/j.neulet.2015.07.024

Mueller, J., Legon, W., Opitz, A., Sato, T. F., and Tyler, W. J. (2014). Transcranial focused ultrasound modulates intrinsic and evoked EEG dynamics. *Brain Stimul.* 7, 900–908. doi: 10.1016/j.brs.2014.08.008

Pang, N., Huang, X., Zhou, H., Xia, X., Liu, X., Wang, Y., et al. (2021). Transcranial ultrasound stimulation of hypothalamus in aging mice. *IEEE Trans. Ultrason. Ferroelectr. Freq. Control* 68, 29–37. doi: 10.1109/TUFFC.2020.2968479

Rahimpour, S., Kiyani, M., Hodges, S. E., and Turner, D. A. (2021). Deep brain stimulation and electromagnetic interference. *Clin. Neurol. Neurosurg.* 203:106577. doi: 10.1016/j.clineuro.2021.106577

Romanella, S. M., Sprugnoli, G., Ruffini, G., Seyedmadani, K., Rossi, S., and Santarnecchi, E. (2020). Noninvasive brain stimulation & space exploration: opportunities and challenges. *Neurosci. Biobehav. Rev.* 119, 294–319. doi: 10.1016/j.neubiorev.2020.09.005

Sanguinetti, J. L., Hameroff, S., Smith, E. E., Sato, T., Daft, C. M. W., Tyler, W. J., et al. (2020). Transcranial focused ultrasound to the right prefrontal cortex improves mood and alters functional connectivity in humans. *Front. Hum. Neurosci.* 14:52. doi: 10.3389/fnhum.2020.00052

Verhagen, L., Gallea, C., Folloni, D., Constans, C., Jensen, D. E., Ahnine, H., et al. (2019). Offline impact of transcranial focused ultrasound on cortical activation in primates. *eLife* 8:e40541. doi: 10.7554/eLife.40541

Wang, X., Zhang, Y., Zhang, K., and Yuan, Y. (2021). Influence of behavioral state on the neuromodulatory effect of low-intensity transcranial ultrasound stimulation on hippocampal CA1 in mouse. *Neuroimage* 241:118441. doi: 10.1016/j.neuroimage.2021.118441

Wang, Y., Zhan, G., Cai, Z., Jiao, B., Zhao, Y., Li, S., et al. (2021). Vagus nerve stimulation in brain diseases: therapeutic applications and biological mechanisms. *Neurosci. Biobehav. Rev.* 127, 37–53. doi: 10.1016/j.neubiorev.2021.04.018

Wattiez, N., Constans, C., Deffieux, T., Daye, P. M., Tanter, M., Aubry, J. F., et al. (2017). Transcranial ultrasonic stimulation modulates single-neuron discharge in macaques performing an antisaccade task. *Brain Stimul.* 10, 1024–1031. doi: 10.1016/j.brs.2017.07.007

Xu, T., Lu, X., Peng, D., Wang, G., Chen, C., Liu, W., et al. (2020). Ultrasonic stimulation of the brain to enhance the release of dopamine - A potential novel treatment for Parkinson's disease. *Ultrason. Sonochem.* 63:104955. doi: 10.1016/j.ultsonch.2019.104955

Yang, H., Yuan, Y., Wang, X., and Li, X. (2020). Closed-loop transcranial ultrasound stimulation for real-time non-invasive neuromodulation *in vivo*. *Front. Neurosci.* 14:445. doi: 10.3389/fnins.2020.00445

Yang, P. F., Phipps, M. A., Jonathan, S., Newton, A. T., Byun, N., Gore, J. C., et al. (2021). Bidirectional and state-dependent modulation of brain activity by transcranial focused ultrasound in non-human primates. *Brain Stimul.* 14, 261–272. doi: 10.1016/j.brs.2021.01.006

Yoo, S. S., Kim, H., Min, B. K., Franck, E., and Park, S. (2011). Transcranial focused ultrasound to the thalamus alters anesthesia time in rats. *Neuroreport* 22, 783–787. doi: 10.1097/WNR.0b013e32834b2957

Yoon, K., Lee, W., Lee, J. E., Xu, L., Croce, P., Foley, L., et al. (2019). Effects of sonication parameters on transcranial focused ultrasound brain stimulation in an ovine model. *PLoS One* 14:e0224311. doi: 10.1371/journal.pone.0224311

Yu, K., Liu, C., Niu, X., and He, B. (2020). Transcranial focused ultrasound neuromodulation of voluntary movement-related cortical activity in humans. *IEEE Trans. BioMed. Eng.* 68, 1923–1931. doi: 10.1109/TBME.2020.3030892

Yu, K., Sohrabpour, A., and He, B. (2016). Electrophysiological source imaging of brain networks perturbed by low-intensity transcranial focused ultrasound. *IEEE Trans. Biomed. Eng.* 63, 1787–1794. doi: 10.1109/tbme.2016.2591924

Yuan, Y., Wang, Z., Liu, M., and Shoham, S. (2020). Cortical hemodynamic responses induced by low-intensity transcranial ultrasound stimulation of mouse cortex. *Neuroimage* 211:116597. doi: 10.1016/j.neuroimage.2020.116597

Zhang, M., Li, B., Lv, X., Liu, S., Liu, Y., Tang, R., et al. (2021). Low-intensity focused ultrasound-mediated attenuation of acute seizure activity based on EEG brain functional connectivity. *Brain Sci.* 11:711. doi: 10.3390/brainsci11060711

Conflict of Interest: The authors declare that the research was conducted in the absence of any commercial or financial relationships that could be construed as a potential conflict of interest.

Publisher's Note: All claims expressed in this article are solely those of the authors and do not necessarily represent those of their affiliated organizations, or those of the publisher, the editors and the reviewers. Any product that may be evaluated in this article, or claim that may be made by its manufacturer, is not guaranteed or endorsed by the publisher.

frontiers in Neuroscience

ORIGINAL RESEARCH
published: 08 October 2021
doi: 10.3389/fnins.2021.756868

Autistic Spectrum Disorder Detection and Structural Biomarker Identification Using Self-Attention Model and Individual-Level Morphological Covariance Brain Networks

Zhengning Wang, Dawei Peng, Yongbin Shang and Jingjing Gao*

School of Information and Communication Engineering, University of Electronic Science and Technology of China, Chengdu, China

Autism spectrum disorder (ASD) is a range of neurodevelopmental disorders, which brings enormous burdens to the families of patients and society. However, due to the lack of representation of variance for diseases and the absence of biomarkers for diagnosis, the early detection and intervention of ASD are remarkably challenging. In this study, we proposed a self-attention deep learning framework based on the transformer model on structural MR images from the ABIDE consortium to classify ASD patients from normal controls and simultaneously identify the structural biomarkers. In our work, the individual structural covariance networks are used to perform ASD/NC classification *via* a self-attention deep learning framework, instead of the original structural MR data, to take full advantage of the coordination patterns of morphological features between brain regions. The self-attention deep learning framework based on the transformer model can extract both local and global information from the input data, making it more suitable for the brain network data than the CNN- structural model. Meanwhile, the potential diagnosis structural biomarkers are identified by the self-attention coefficients map. The experimental results showed that our proposed method outperforms most of the current methods for classifying ASD patients with the ABIDE data and achieves a classification accuracy of 72.5% across different sites. Furthermore, the potential diagnosis biomarkers were found mainly located in the prefrontal cortex, temporal cortex, and cerebellum, which may be treated as the early biomarkers for the ASD diagnosis. Our study demonstrated that the self-attention deep learning framework is an effective way to diagnose ASD and establish the potential biomarkers for ASD.

Keywords: autism spectrum disorder, individual morphological covariance brain networks, self-attention based neural networks, deep learning, biomarker

OPEN ACCESS

Edited by:
Bochao Cheng,
West China Second University Hospital, Sichuan University, China

Reviewed by:
Jingliang Peng,
University of Jinan, China
Yi-Fei Pu,
Sichuan University, China

****Correspondence:***
Zhengning Wang
zhengning.wang@uestc.edu.cn

Specialty section:
This article was submitted to Brain Imaging Methods, a section of the journal Frontiers in Neuroscience

Received: *11 August 2021*
Accepted: *06 September 2021*
Published: *08 October 2021*

Citation:
Wang Z, Peng D, Shang Y and Gao J (2021) Autistic Spectrum Disorder Detection and Structural Biomarker Identification Using Self-Attention Model and Individual-Level Morphological Covariance Brain Networks. Front. Neurosci. 15:756868. doi: 10.3389/fnins.2021.756868

INTRODUCTION

Autism spectrum disorder (ASD) is a developmental disability that can affect significant communications, behavior, and social interactions. The term "spectrum" in ASD is because of the variation in the type and severity of symptoms people experience. The main symptoms of ASD are abnormal emotional regulation and social interaction, limited interest, repetitive behavior,

and hypo- or hyper reactivity to sensory stimuli (Guze, 1995). Symptoms will hurt their ability to function properly in school, work, and other areas of life. ASD has caused a severe burden on patients and their families. Therefore, early diagnosis and intervention of ASD are critical. However, the current clinical diagnosis of ASD is mainly based on the doctor's subjective scale assessment and lacks objective diagnostic methods. The diagnosis based on medical images, especially MRI images, has a certain degree of objectivity, but lacks credible imaging markers. Therefore, objective imaging-based diagnosis of ASD and the provision of reliable imaging markers are significant research trends.

Existing ASD diagnosis methods on structural MRI images are mainly traditional machine learning methods. The handcrafted features in these methods are extracted from morphological structure, such as the cortical thickness of brain gray matter and other geometric features at each cerebral vertex (Ecker et al., 2010b; Sato et al., 2013; Zheng et al., 2019). Jiao et al. (2010) constructed a small-scale dataset that contains 22 ASD and 16 normal control subjects (NC), and defined voxel-based and surface-based features. Four machine-learning techniques: support vector machines (SVMs), multilayer perceptrons (MLPs), functional trees (FTs), and logistic model trees (LMTs) were employed to classify ASD. LMT achieved the best accuracy of 87.0% for surface-based classification. Ecker et al. (2010a) proposed a five-dimensional feature followed by SVM to distinguish ASD from NC. It achieved the classification accuracy of 79.0% in the left hemisphere, 65.0% in the right on a single-site dataset. Although these methods reach a satisfactory diagnosis, the handcrafted features they used mainly come primarily from experience, also are bound by the experience.

Given the drawbacks of machine learning, some deep neural networks automatically acquire effective feature representation from sMRI data (Heinsfeld et al., 2018; Lian et al., 2018). However, the conflict between a small sample size and huge model parameters will lead to overfitting or other erratic model behavior. Thus, it is necessary to outline critical features from the MRI data before being fed into the networks. The morphological brain networks measuring the intracortical similarities in the gray matter play a crucial role in investigating abnormalities in neurological diseases (He et al., 2007; Yu et al., 2018).

Kong et al. (2019) proposed a simple individual brain network to express connectivity features between each pair of regions of interest (ROIs). Then the connectivity features are ranked by F-score in descending order. Finally, 3,000 top features were selected to perform classification *via* a DNN network. It achieved an accuracy of 90.39% in a subset of 182 subjects. However, it only carried out bi-level (ASD/TC) classification, neither was a large dataset from a multi-site included, nor the biomarker considered. To fix the problems, (Gao et al., 2021) used a Res-Net and Grad-CAM on individual structural covariance networks to perform the ASD diagnosis and biomarker identification. They achieved an accuracy of 71.8% on the ABIDE dataset and confirmed the prefrontal cortex and cerebellum as the biomarkers for ASD.

Though these methods achieved remarkable performance, they still have the following drawbacks: (1) The small sample size leads to overfitting and generalization problems, not to mention a small sample size from a single site. The single-site datasets can neither represent the variance of disease and control samples, nor establish stable generalization models for replication across different sites, participants, imaging parameters, and analysis methods (Nielsen et al., 2013). (2) So far, most machine learning methods for ASD diagnosis on sMRI data have considered morphological features extracted at different ROIs independently, ignoring the integrality of brain structure, and even in Gao et al. (2021), although the individual structural covariance networks are fed into the deep learning framework, the CNN framework only extracts the local feature by the kernel, which is not suitable for the brain network data. (3) The classification results from the deep learning model are hard to interpret in the absence of the contributions of the classification features leading to a lack of clinical significance. Although some biomarkers were found in Gao et al. (2021) by Grad-CAM (Selvaraju et al., 2017), it is fit for CNN-based models to produce the decisional explanations. The residual learning in Gao et al. (2021) is not suitable for the covariance networks, which leads to the biomarkers obtained from Grad-CAM being narrowly acceptable. Furthermore, there still exist gradient saturation and false confidence problems in Grad-CAM (Wang et al., 2020).

In view of the drawbacks, to explore an efficient ASD diagnosis method, we propose a self-attention deep learning framework to diagnose ASD and identify biomarkers on a multi-site dataset. This work is divided into two steps: first, we construct the individual morphological brain network from sMRI to characterize the interregional morphological relationship, and then, the output of morphological networks, instead of sMRI, is fed into a self-attention deep learning model to classify ASD from NCs. Meanwhile, the regional biomarkers are identified by the attention weight presenting the degree of contribution of the corresponding regional feature.

In the following sections, we will present our materials and methods in section "Materials and Methods," results in section "Results," discussion in Section "Discussion," and conclusion in section "Conclusion."

MATERIALS AND METHODS

The Dataset

The ABIDE dataset (Di Martino et al., 2014), a large open access data repository, is used in this study, which is accessed from 17 international sites with no prior coordination. It includes structural MRI, corresponding rs-fMRI, and phenotype information for individuals with ASD and TC, which allows for replication, secondary analyses, and discovery efforts. Even if all data in it were collected with 3T scanners, the sequence parameters and the type of scanner varied across sites. In our work, the structural MR images we used were aggregated from all 17 international sites, which contain 518 ASD patients and 567 age-matched normal controls (ages 7–64 years, median 14.7 years across groups). In addition, the data we used contains 926 males and 159 females.

Data Preprocessing

We used DRAMMS (Ou et al., 2011) to process all structural MR images in the preprocessing step, in which the cross-subject registration, motion correction, intensity normalization, and skull stripping are included. Furthermore, all T1W MRI images were registered to the SRI24 atlas (Rohlfing et al., 2010) for subsequent analysis. Then, We used the multiplicative intrinsic component optimization (MICO) method (Li et al., 2014) to segment the T1W images into the cerebrospinal fluid (CSF), white matter (WM), and gray matter (GM).

Individual-Level Morphological Covariance Brain Networks

In our study, the individual level morphological covariance brain network (Wang et al., 2016) is used to extract interregional structural variations to characterize the interregional morphological relationship. The detailed procedures are described below. First, a GM volume map was acquired for each participant in the template space. Second, the individual-level morphological covariance brain network was constructed from their GM volume images, which refers to the literature (Wang et al., 2016). Although the SRI24 atlas parcellates the whole brain into 116 subregions, with 58 subregions in each hemisphere, due to the low signal-to-noise ratio and blank values of the gray matter volume in the Vermis, eight regions in the Vermis (the cerebellar Vermis labeled from 108 to 115) were excluded to ensure the reliability of our study. Finally, a 108 × 108 matrix was obtained according to SRI24 atlas. That is, a vector X_p for each region and a matrix X for the whole brain were obtained for each subject for further analyses.

To be specific, the variation $x_{pq}$is calculated as follows: the probability density function (PDF) of the extracted GM volume values is first estimated by the kernel density estimation (KDE) (Parzen, 1962).

Then, the variation of the KL divergence (KLD) between the region $P$and Q is calculated subsequently from the above PDFs as Eq. 1:

$$D_{KL}(P, Q) = \sum_{i=1}^{N} \left(P(i) \log \frac{P(i)}{Q(i)} + Q(i) \log \frac{Q(i)}{P(i)} \right) \quad (1)$$

where $_{P(i)}$ and $_{Q(i)}$ are the PDFs of the region $_P$ and $_Q$. $_N$ is the number of PDF sample points. The element of variation matrix is formally defined as the structural variation between two regions, which is quantified by a KL divergence-based similarity (KLS) measure (Kong et al., 2014) with the calculated variation of KLD. Thus, the variation between the region $_P$ and $_Q$ can be defined as Eq. 2:

$$x_{PQ} = KLS(P, Q) = \mathrm{e}^{-D_{KL}(P,Q)} \quad (2)$$

Finally, the structural variation feature vector for the region P can be described as Eq. 3:

$$X_p = (x_{p0}, x_{p1}, \ldots, x_{p(M-1)})^T \in R^{M\times 1} \quad (3)$$

The structural variation matrix $_X$ can be described as Eq. 4:

$$X = (x_{pq}) = (X_0, X_1, \ldots, X_{M-1}) \in R^{M\times M} \quad (4)$$

where $_M$ is the number of regions, which is set as 108 in our study.

In the classification task, the matrix $_X$ can be fed into the neural networks to replace the structural MR images.

Self-Attention Neural Network Classifier

Transformer was first applied to machine translation tasks and has achieved great success in the field of natural language processing (Vaswani et al., 2017). The tremendous success in NLP has led researchers to adapt it to computer vision, where it has achieved great performance on the tasks of image classification (Dosovitskiy et al., 2020) and general-purpose backbone for computer vision (Liu et al., 2021). Especially, the transformer is designed for sequence modeling and transduction tasks, and the self-attention mechanism is notable for modeling long-range dependencies in the data (Wang et al., 2018; Cao et al., 2019; Liu et al., 2021). As the basis for powerful architectures, the self-attention mechanism in transformer has displaced CNN and RNN across a variety of tasks (Vaswani et al., 2017; Zhao et al., 2020; Han et al., 2021; Liu et al., 2021; Radford et al., 2021; Touvron et al., 2021; Wang et al., 2021; Yuan et al., 2021).

Morphological brain network refers to the intracortical variations in gray matter morphology. It is presented as the structural variation matrix among brain regions. In our work, the information of a brain region is represented by a feature vector to characterize its variation with other regions, and we expect to extract global information from the feature vectors of brain regions for the diagnosis. Thus, an optimal arrangement of data and feature extraction method are important for our work. Gao et al. (2021) viewed all region features as a matrix and fed it into a CNN framework. However, the CNN model only utilizes the local representation property of the extracted features by the convolution kernel; neither the dependency relationships between non-local regions are considered. The self-attention mechanism is adept at handling non-local dependencies in the data, which is able to take the place of the CNN model and extract the non-local feature from the data. Thus, it is suitable for the morphological brain network.

The output vectors of a self-attention layer are the weighted sum of input vectors, and the weight assigned to each vector is computed by the similarity of two vectors.

In the classification step, the vectors $X = (X_0, X_1, \ldots, X_{M-1})$ are first fed into the self-attention layer, and the query Q_p, keys K_p and values V_p for the region P are defined as Eqs 5–7:

$$Q_p = W_Q X_p \quad (5)$$

$$K_p = W_K X_p \quad (6)$$

$$V_p = W_V X_p \quad (7)$$

where $_{X_p}$ is the variation feature vector for the region $_P$, $_{W_Q}$, $_{W_K}$, and $_{W_V}$ are the parameters to be learned.

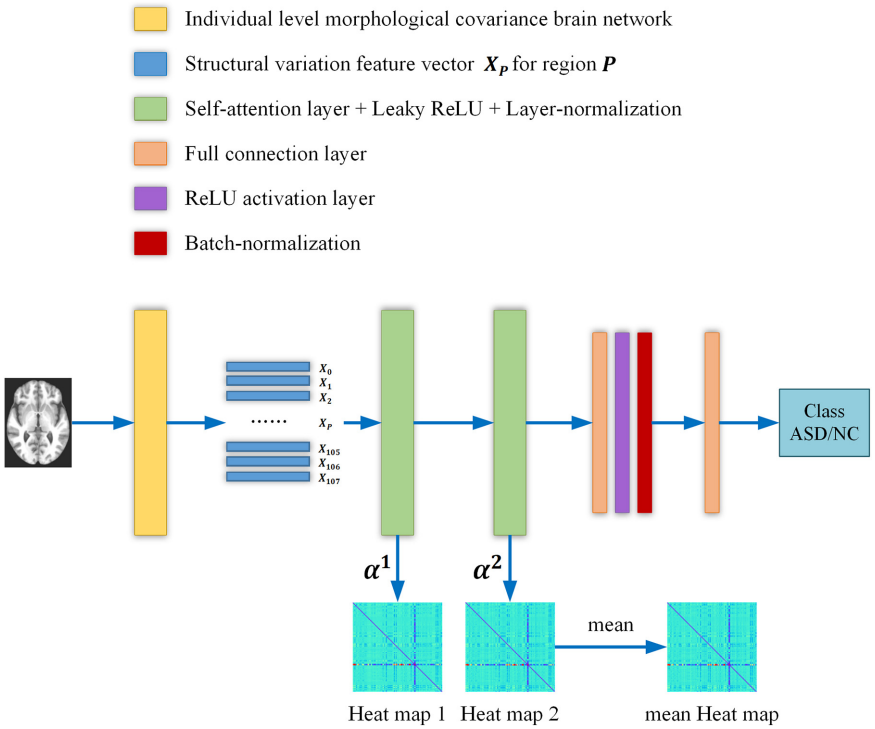

FIGURE 1 | The overall flow chart of our study. Briefly, the individual level morphological covariance brain network is first constructed according to the SRI24 atlas and gray matter volume map of each subject. The above morphological covariance brain network is used to extract interregional structural variation vectors to characterize the interregional morphological relationship. Then the vectors are fed into two self-attention layers classification neural networks. Meanwhile, the contribution of each region for classification is obtained from the self-attention coefficients map of each layer. Finally, two heat maps are averaged to obtain a mean output heat map for diagnosis biomarker identification.

TABLE 1 | Comparison of the classification performances between our method and other methods.

Method	Accuracy	Sensitivity	Specificity	F1 score
Self-attention(ous)	**0.7248**	0.7581	0.6809	**0.7581**
RF	0.6091	0.4902	0.7119	0.5376
SVM	0.5818	0.3726	0.7627	0.4524
Xgboost	0.6091	0.5294	0.6780	0.5567
AE	0.6727	0.6875	**0.8750**	0.5714
2D CNN	0.7182	**0.8125**	0.6875	0.6869
3D CNN	0.5596	0.5714	0.4545	0.7000

SVM, support vector machine; XGB, Xgboost; AE, autoencoder. The bold values indicate maximum value of each index.

Then, the self-attention coefficients α_{pq} are computed *via* dot product attention as Eq. 8:

$$\alpha_{pq} = Softmax\left(\frac{Q_p^T K_q}{\sqrt{d_K}}\right) \tag{8}$$

where d_K is the dimension of K_q .

Finally, the output vector X_p^1 of the region P after the self-attention layer is computed as Eq. 9:

$$X_p^1 = \sum_{q=0}^{M-1} \alpha_{pq} V_q \tag{9}$$

Biomarker Identification Based on Self-Attention Model

As the weight of the input feature vectors, the self-attention coefficients α can indicate the contribution of the input vector to the output. Therefore, the self-attention coefficient map can be considered as the basis for the identification of biomarkers. The larger the weight α of a feature vector is, the higher its contribution to the classification task is, and the more likely the corresponding brain region is the biomarker for ASD diagnosis.

Implementation

An overview of our proposed ASD/NC classification framework is shown in **Figure 1**, and two self-attention layers were adopted in the networks. First, we constructed an individual-level morphological covariance brain network according to the SRI24 atlas to obtain the structural variation feature vectors for each region. Then, the vectors were fed into two self-attention layers classification neural networks. In this work, the structural variation feature vector $X_{p \in R^{108\times 1}}$ covers 108 regions, and the size of the output vectors X_p^1 and X_p^2 of each self-attention layer is $R^{32\times 1}$. Meanwhile, the contribution of each region for classification was obtained from the self-attention coefficients map of each layer. After each self-attention layer, Leaky ReLU activation and layer-normalization (Ba et al., 2016) were adopted

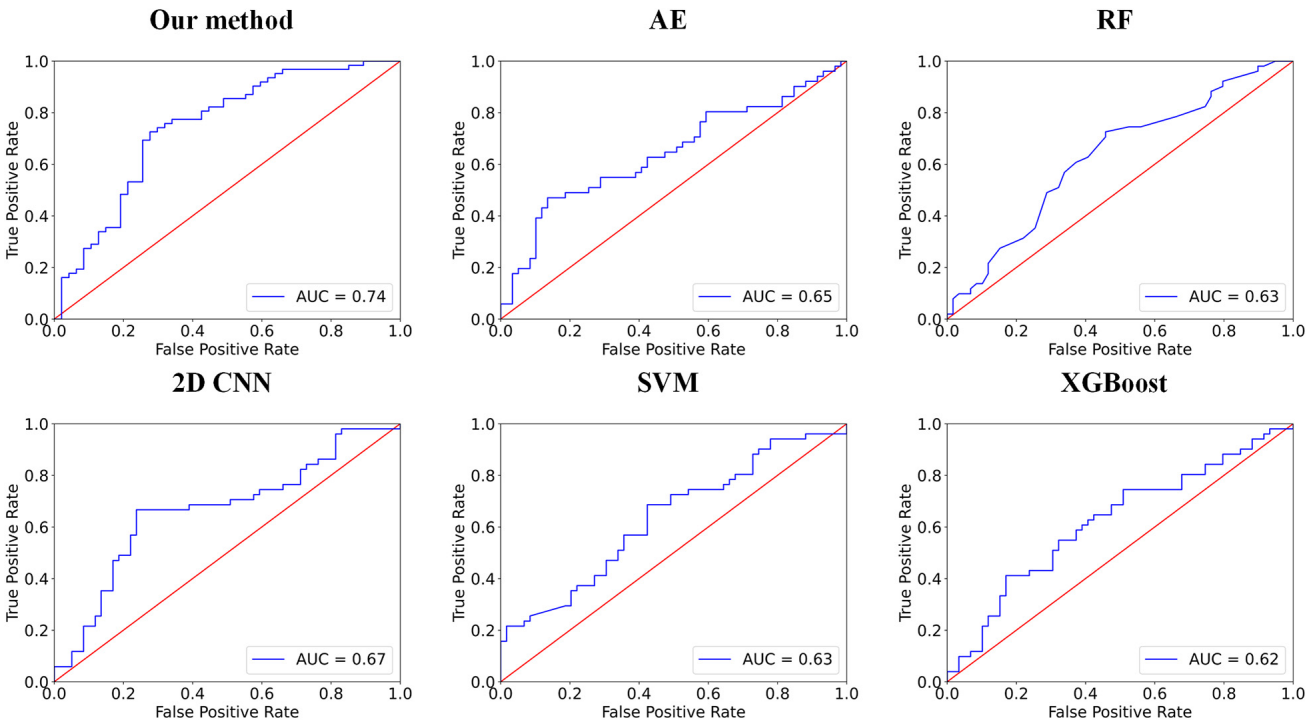

FIGURE 2 | Comparisons between our method and other methods for classification. The area under the curve (AUC) values are used to assess the classification performances for our method, 2D CNN, autoencoder (AE), RF, support vector machine (SVM), and Xgboost (XGB).

TABLE 2 | Comparison of the classification performances between the different number of heads in the self-attention layer.

Method	Accuracy	Sensitivity	Specificity	F1 score
1-Head	**0.7248**	**0.7581**	**0.6809**	**0.7581**
2-Head	0.6881	0.7549	0.6154	0.7167
4-Head	0.6789	0.7000	0.6410	0.7369
8-Head	0.6697	0.6667	0.6786	0.7500

The bold values indicate maximum value of each index.

TABLE 3 | Comparison of our networks with the different number of self-attention layers.

Number of Self-Attention Layers	Accuracy	Sensitivity	Specificity	F1 score
1	0.6697	0.6627	**0.6923**	0.7534
2	**0.7248**	**0.7581**	0.6809	**0.7581**
3	0.6606	0.6711	0.6364	0.7338
4	0.6147	0.6667	0.5435	0.6667
5	0.6055	0.7174	0.5238	0.6055

The bold values indicate maximum value of each index.

to ensure the training was stable and efficient. The negative slope of the Leaky ReLU activation layer is settled as $_{1e-2}$, and the input feature size of each linear layer is $_{R^{32\times1}}$. After the first linear layer, a ReLU activation and a batch-normalization (Ioffe and Szegedy, 2015) layer were adopted. We employed an Adam optimizer (Kingma and Ba, 2014) with the learning rate of $_{6e-6}$. A batch size of 32 and a weight decay of 0.01 are used. After initializing the weights randomly, the binary cross-entropy loss is chosen to supervise the training for the ASD/NC classification.

RESULTS

In this group of experiments, we compare our framework with six competing methods in the task of ASD *versus* NC classification. Four parameters, namely accuracy (ACC), sensitivity (SEN), specificity (SPE), and F1 score, are calculated to evaluate the performance of our proposed framework. The deep self-attention neural networks used in our work achieved a mean classification accuracy of 72.5%, mean sensitivity value of 75.8%, specificity value of 68.1%, and F1 score of 0.758. Our results improved the mean classification accuracy of the state-of-the-art (Gao et al., 2021) from 71.8 to 72.5% in the ABIDE data. To evaluate the performance of our work, the result of our framework is compared with those of conventional machine learning methods [i.e., RF (Ho, 1995), SVM (Vapnik et al., 1998), and Xgboost (XGB) (Chen and Guestrin, 2016)] and deep learning methods [i.e., autoencoder (AE), 2D CNN (Gao et al., 2021) and 3D CNN]. Note that with the purpose of using structural variation matrix $_{X\in R^{108\times108}}$ for subject classification by these conventional machine learning methods and AE, it is first collapsed in a one-dimension vector $_{Y\in R^{11664\times1}}$. Specifically, the dimension of the vector $_{Y}$ was first reduced by Principal

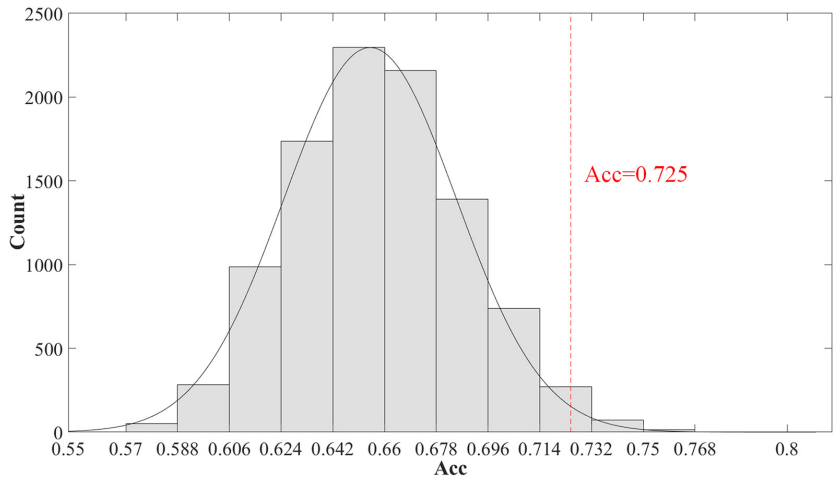

FIGURE 3 | The histogram of the accuracy of the permutation test. The permutation test with 10,000 times was used to evaluate the significance of our method. The accuracy of our method (0.725) is indicated by the red dotted line. The classification accuracy is higher than 96.4% of the permutated accuracy values.

Component Analysis (PCA) in SVM classification, and the material sMRI images were fed into 3D CNN neural networks. The comparisons are presented in **Table 1**. Furthermore, the performance assessed by the area under the curve (AUC) values of these classifiers is shown in **Figure 2**. Our proposed framework has the best performances in classifying ASD from NC with the highest ACC, F1 score, and AUC values compared with the other methods.

In our work, the self-attention layer can be set as a multi-head self-attention layer. Through comparison of the experiments in **Table 2**, we found that the network with a single-head self-attention layer achieved the best performance. There is the same number of parameters to be learned in the experiments in **Table 2**. In addition, through comparison presented in **Table 3**, we found that our model with two self-attention layers achieved the best performance.

Furthermore, we evaluated the significance of the classification accuracy by the permutation test 10,000 times. During the permutation testing, we changed 20% of the labels of the samples randomly each time. The histogram of the accuracy of the permutation test is shown in **Figure 3**. The accuracy of our method (72.5%) is indicated by the red dotted line. As shown in **Figure 3**, the 72.5% accuracy of our method is higher than 96.4% of the permutated accuracy values.

In our proposed framework, the self-attention coefficients α were obtained through the self-attention layer, which can be seen as the contribution indicator of brain regions to the ASD/NC classification. In order to make our proposed model diagnose ASD more transparent and explainable, the self-attention coefficients map is obtained according to the following step. According to Eqs 8, 9, the self-attention coefficient α_{pq} indicates the contribution of the feature vector X_q to the output feature vector X_p^1. Thus, the larger α_{pq} is, the larger the contribution of the region Q to the classification is. In our result, we found that the self-attention coefficients maps of the first and second layers are extremely similar, so we average them to obtain a mean output coefficients map. In our work, the self-attention coefficients were first ranked in descending order. Then, the top coefficients were selected to determine the biomarker of regions. Three typical individual and final fused contributions supporting the correct classification of ASD patients are shown in **Figures 4**, **5**. In these subfigures, the redder the regional color is, the more contribution the brain region affords. We selected the largest contributions of the regions by identifying the weights above the $_{\text{mean}+3\,\text{SD}}$. Finally, 53 coefficients about 42 different regions were found by the self-attention coefficients. The top 42 regions (see **Figure 6**) are significant for ASD/NC classification. Specifically, the feature vectors of these regions were selectively aggregated into the output feature vectors of two especial regions, which represent pallidum in the left and right hemispheres according to SRI24 atlas. It indicates that not only the 42 regions are significant for classification, but also the pallidum is more significant and specific. As seen in our result, the structure of pallidum has been found to be more significant than other regions for ASD, which is identical with the result in Turner et al. (2016).

DISCUSSION

In this manuscript, we propose a new framework for ASD detection and structural biomarkers identification from multi-site sMRI datasets by individual brain networks and self-attention deep neural networks. Our method has achieved state-of-the-art on ASD/NC classification task in the ABIDE data. Compared with the majority of machine learning and deep learning methods, our method has the following advantages: First, our work is stable and generalized due to the multi-site sMRI dataset with a large sample size, and the multi-site dataset is able to overcome the inherent heterogeneity in neuroimaging datasets.

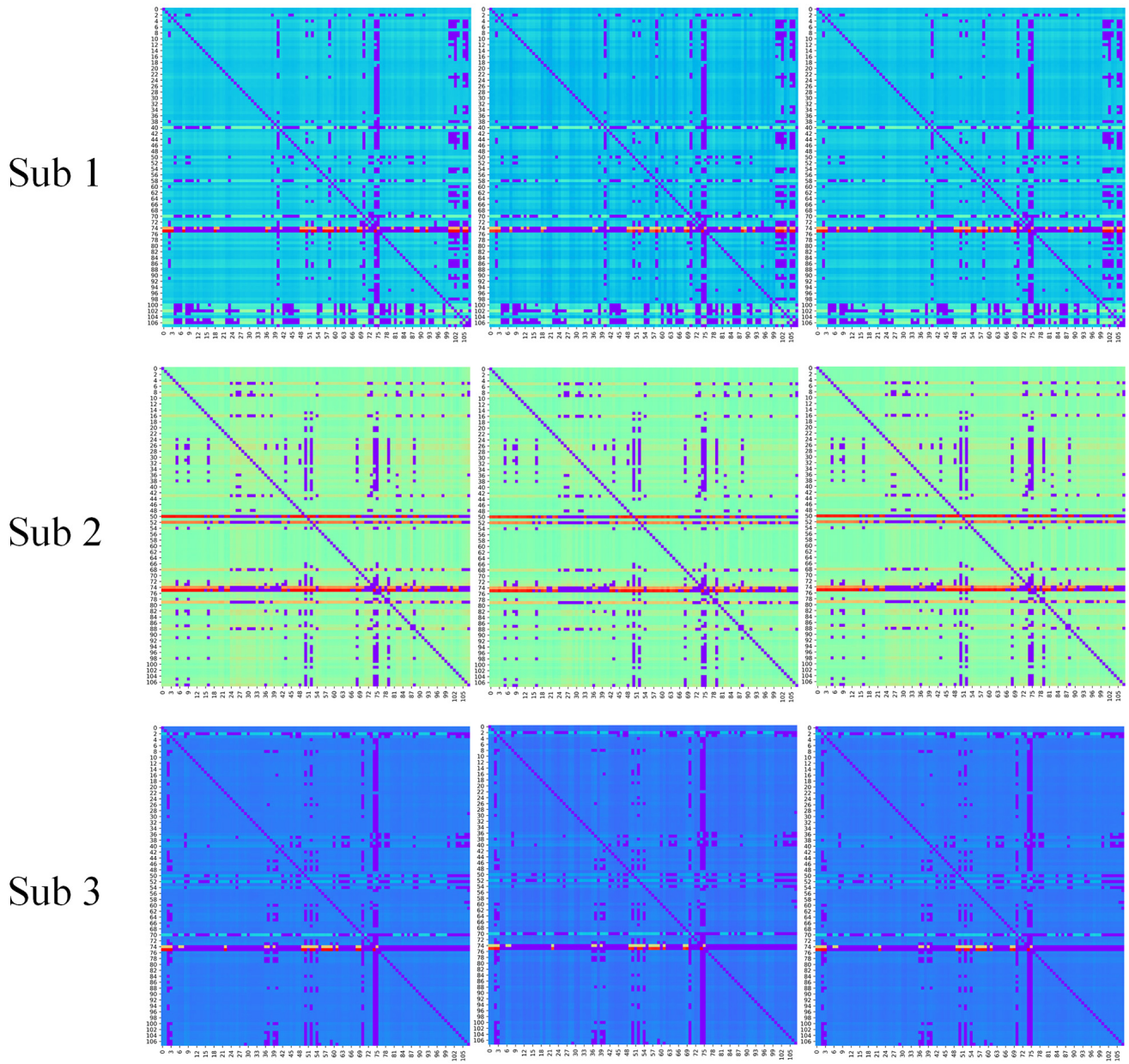

FIGURE 4 | The contribution of brain regions to the autism spectrum disorder/normal control (ASD/NC) classification. Three typical individual heat maps supporting the correct classification of ASD patients were mapped by self-attention coefficients in our framework. The redder the color is, the more contributions the brain region affords.

Second, interregional structural variations can be extracted by the individual level morphological covariance network to characterize the interregional morphological relationship of the brain. Compared with the group-level morphological network, the individual-level morphological brain networks can better reflect individual behavior differences in both typical and atypical populations (Gao et al., 2021). Furthermore, the individual level morphological covariance network provides further empirical evidence to support the theory that the human brain has evolved to support both specialized or modular processing in local regions and distributed or integrated processing over the entire brain (Bullmore and Sporns, 2012; Wang et al., 2016). Thus, it provides an alternative method for researchers to explore hubs of the brain under both healthy and pathological conditions.

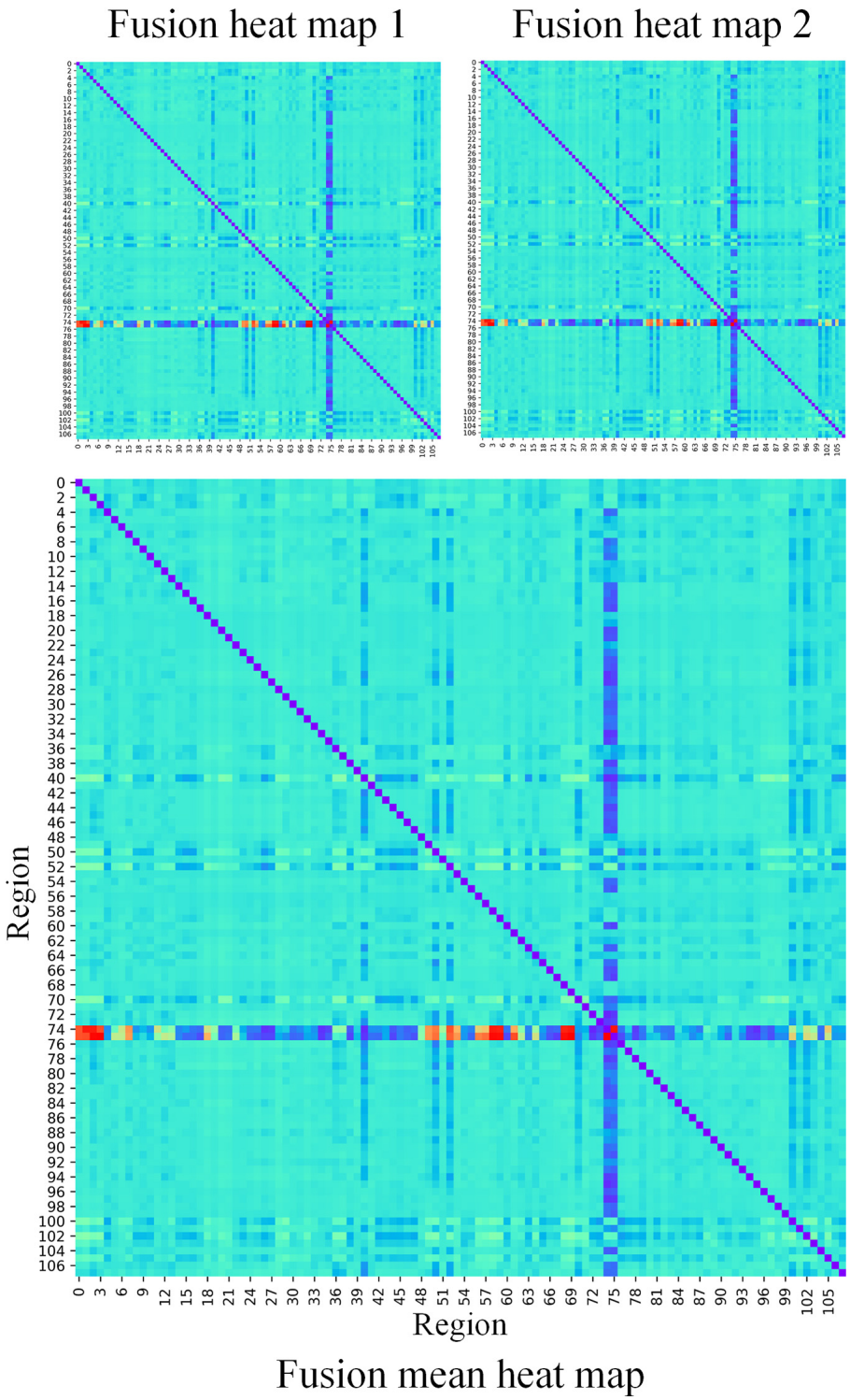

FIGURE 5 | The fusion heat maps obtained by the average heat maps of all true negative subjects. The redder the color is, the more contributions the brain region affords.

Third, the self-attention neural networks adopted in our model can aggregate not only short-range but also long-range dependencies in the data, which solves the local problem in CNN (Wang et al., 2018; Cao et al., 2019; Fu et al., 2019; Lee et al., 2019; Yin et al., 2020; Liu et al., 2021). Meanwhile, the biomarkers are obtained from self-attention

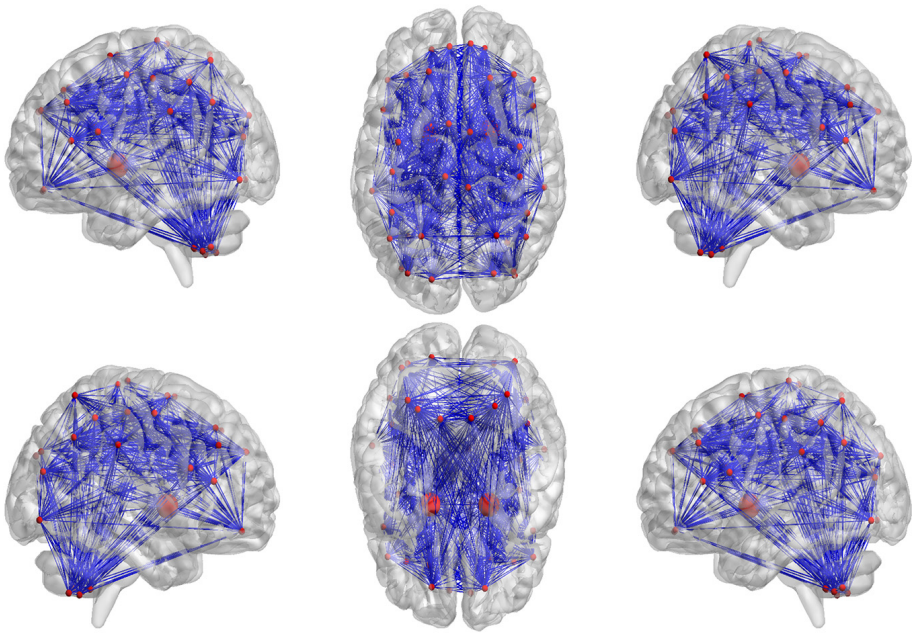

FIGURE 6 | The top 42 regions which have the largest contributions to correctly classifying ASD patients were identified. As seen in our result, the pallidum in the left and right hemispheres have been found to be more significant and specific for ASD, which are drawn larger than other regions.

coefficients without model architectural changes or retraining (Sarlin et al., 2020). Specifically, the heat maps of different layers obtained by Grad-CAM in Gao et al. (2021) have a clear hierarchical relationship, which is related to the feature extraction method of CNN. With the increase of the number of network layers, the receptive field becomes large, and the features extracted by CNN change from simple and local to complex and abstract (Wang et al., 2018). Therefore, the heat maps of different layers in Gao et al. (2021) vary greatly. However, the self-attention coefficients maps of the first and second layers in our method are extremely similar, which implies the consistency of the diagnosis. Furthermore, the diagnosis biomarker identification method based on self-attention coefficients is interpretable because the meaning of coefficients can be clearly obtained in Eqs 5–9 (Sarlin et al., 2020). In addition, due to the strong global feature extraction ability, the self-attention networks can achieve better performance than CNN with less training time and parameters in our work.

Moreover, with the self-attention explanation approach, the connectivity features of the morphological covariance network having the greatest contribution to classification were identified. The brain areas corresponding to these important connectivity features mainly include the prefrontal cortex, temporal cortex, and cerebellum. These brain areas have been reported to be implicated in ASD in previous studies indicating that the established classification model using deep learning and individual morphological covariance network may serve as a reliable tool to facilitate clinical diagnosis. For example, anatomically and functionally, there is considerable evidence that the medial prefrontal cortex is involved in basic conscious feelings, and the atypicality of it is associated with the emotional–social domain in autism (Shalom, 2009). The direct connections between the auditory association areas of the superior temporal gyrus with the medial temporal cortex have been demonstrated to underlie recognition memory for sounds (Muñoz-López et al., 2015). Furthermore, the cerebellum is not only involved in motor coordination but that it also intervenes in cognitive operations, emotion, memory, and language (Silveri and Misciagna, 2000). Thus, the prefrontal cortex, temporal cortex, and cerebellum may be related to social cognition processing in ASD.

CONCLUSION

In this work, we propose a classification neural network for ASD detection and structural biomarkers identification from multi-site sMRI datasets, which is based on self-attention neural networks and individual-level morphological covariance brain networks. Comparison by experiments, we found that our proposed method outperformed other conventional machine learning and deep learning classification methods for the classification of ASD. Moreover, the biomarker identification method based on self-attention coefficients is efficient and interpretable, which provides a new solution to the black-box problems of deep learning, and prefrontal cortex, temporal cortex, and cerebellum found by this method provide a good reference for ASD diagnosis. Meanwhile, the morphological

alterations in the pallidum in autism are worthy of the attention of researchers.

DATA AVAILABILITY STATEMENT

The datasets presented in this study can be found in online repositories. The names of the repository/repositories and accession number(s) can be found below: http://fcon_1000.projects.nitrc.org/indi/abide/abide_I.html.

ETHICS STATEMENT

The studies involving human participants were reviewed and approved by Ethical approval was obtained from the St. James's Hospital/AMNCH (ref: 2010/09/07) and the Linn Dara CAMHS Ethics Committees (ref: 2010/12/07). Written informed consent to participate in this study was provided by the participants' legal guardian/next of kin.

AUTHOR CONTRIBUTIONS

All authors contributed to the article and approved the submitted version.

FUNDING

This work is supported by the grants from the National Natural Science Foundation of China (Nos. 61701078, 61872068, and 61720106004), Science & Technology Department of Sichuan Province of China (Nos. 2021YFG0126 and 2019YJ0193), and Medical-Engineering Cross Fund of UESTC (No. ZYGX2021YGLH014).

REFERENCES

Ba, J. L., Kiros, J. R., and Hinton, G. E. (2016). Layer normalization. *arXiv* [preprint]. arXiv:06450,

Bullmore, E., and Sporns, O. (2012). The economy of brain network organization. *Nat. Rev. Neurosci.* 13, 336–349. doi: 10.1038/nrn3214

Cao, Y., Xu, J., Lin, S., Wei, F., and Hu, H. (2019). "Gcnet: non-local networks meet squeeze-excitation networks and beyond," in *Proceedings of the IEEE/CVF International Conference on Computer Vision Workshops*. doi: 10.1109/ICCVW.2019.00246

Chen, T., and Guestrin, C. (2016). "Xgboost: a scalable tree boosting system," in *Proceedings of the 22nd Acm Sigkdd International Conference on Knowledge Discovery and Data Mining*. doi: 10.1145/2939672.2939785

Di Martino, A., Yan, C.-G., Li, Q., Denio, E., Castellanos, F. X., Alaerts, K., et al. (2014). The autism brain imaging data exchange: towards a large-scale evaluation of the intrinsic brain architecture in autism. *Mol. Psychiatry* 19, 659–667. doi: 10.1038/mp.2013.78

Dosovitskiy, A., Beyer, L., Kolesnikov, A., Weissenborn, D., Zhai, X., Unterthiner, T., et al. (2020). "An image is worth 16x16 words: transformers for image recognition at scale," in *Proceeding of the International Conference on Learning Representations*.

Ecker, C., Rocha-Rego, V., Johnston, P., Mourao-Miranda, J., Marquand, A., Daly, E. M., et al. (2010b). Investigating the predictive value of whole-brain structural MR scans in autism: a pattern classification approach. *Neuroimage* 49, 44–56. doi: 10.1016/j.neuroimage.2009.08.024

Ecker, C., Marquand, A., Mourão-Miranda, J., Johnston, P., Daly, E. M., Brammer, M. J., et al. (2010a). Describing the brain in autism in five dimensions—magnetic resonance imaging-assisted diagnosis of autism spectrum disorder using a multiparameter classification approach. *J. Neurosci.* 30, 10612–10623. doi: 10.1523/JNEUROSCI.5413-09.2010

Fu, J., Liu, J., Tian, H., Li, Y., Bao, Y., Fang, Z., et al. (2019). "Dual attention network for scene segmentation," in *Proceedings of the IEEE/CVF Conference on Computer Vision and Pattern Recognition*. doi: 10.1109/CVPR.2019.00326

Gao, J., Chen, M., Li, Y., Gao, Y., Li, Y., Cai, S., et al. (2021). Multisite autism spectrum disorder classification using convolutional neural network classifier and individual morphological brain networks. *Front. Neurosci.* 14:1473.

Guze, S. B. (1995). Diagnostic and statistical manual of mental disorders, (DSM-IV). *Am. J. Psychiatry* 152, 1228–1228. doi: 10.1176/ajp.152.8.1228

Han, K., Xiao, A., Wu, E., Guo, J., Xu, C., and Wang, Y. (2021). Transformer in transformer. *arXiv* [preprint]. arXiv:00112,

He, Y., Chen, Z. J., and Evans, A. C. (2007). Small-world anatomical networks in the human brain revealed by cortical thickness from MRI. *Cerebral Cortex* 17, 2407–2419. doi: 10.1093/cercor/bhl149

Heinsfeld, A. S., Franco, A. R., Craddock, R. C., Buchweitz, A., and Meneguzzi, F. (2018). Identification of autism spectrum disorder using deep learning and the ABIDE dataset. *NeuroImage Clin.* 17, 16–23. doi: 10.1016/j.nicl.2017.08.017

Ho, T. K. (1995). "Random decision forests," in *Proceedings of 3rd International Conference on Document Analysis and Recognition*, (IEEE).

Ioffe, S., and Szegedy, C. (2015). "Batch normalization: accelerating deep network training by reducing internal covariate shift," in *proceeding of the International Conference on Machine Learning*.

Jiao, Y., Chen, R., Ke, X., Chu, K., Lu, Z., and Herskovits, E. H. (2010). Predictive models of autism spectrum disorder based on brain regional cortical thickness. *Neuroimage* 50, 589–599. doi: 10.1016/j.neuroimage.2009.12.047

Kingma, D. P., and Ba, J. (2014). Adam: a method for stochastic optimization. *arXiv* [preprint]. arXiv:1412.6980,

Kong, X.-Z., Wang, X., Huang, L., Pu, Y., Yang, Z., Dang, X., et al. (2014). Measuring individual morphological relationship of cortical regions. *J. Neurosci. Methods* 237, 103–107. doi: 10.1016/j.jneumeth.2014.09.003

Kong, Y., Gao, J., Xu, Y., Pan, Y., Wang, J., and Liu, J. (2019). Classification of autism spectrum disorder by combining brain connectivity and deep neural network classifier. *Neurocomputing* 324, 63–68. doi: 10.1016/j.neucom.2018.04.080

Lee, J., Lee, Y., Kim, J., Kosiorek, A., Choi, S., and Teh, Y. W. (2019). "Set transformer: a framework for attention-based permutation-invariant neural networks," in *Proceeding of the International Conference on Machine Learning*.

Li, C., Gore, J. C., and Davatzikos, C. (2014). Multiplicative intrinsic component optimization (MICO) for MRI bias field estimation and tissue segmentation. *Magnetic Resonance Imaging* 32, 913–923. doi: 10.1016/j.mri.2014.03.010

Lian, C., Liu, M., Zhang, J., and Shen, D. (2018). Hierarchical fully convolutional network for joint atrophy localization and Alzheimer's disease diagnosis using structural MRI. *IEEE Trans. Pattern Analy. Mach. Intelli.* 42, 880–893. doi: 10.1109/TPAMI.2018.2889096

Liu, Z., Lin, Y., Cao, Y., Hu, H., Wei, Y., Zhang, Z., et al. (2021). Swin transformer: hierarchical vision transformer using shifted windows. *arXiv* [preprint]. arXiv:14030,

Muñoz-López, M., Insausti, R., Mohedano-Moriano, A., Mishkin, M., and Saunders, R. (2015). Anatomical pathways for auditory memory II: information from rostral superior temporal gyrus to dorsolateral temporal pole and medial temporal cortex. *Front. Neurosci.* 9:158. doi: 10.3389/fnins.2015.00158

Nielsen, J. A., Zielinski, B. A., Fletcher, P. T., Alexander, A. L., Lange, N., Bigler, E. D., et al. (2013). Multisite functional connectivity MRI classification of autism: ABIDE results. *Front. Hum. Neurosci.* 7:599. doi: 10.3389/fnhum.2013.00599

Ou, Y., Sotiras, A., Paragios, N., and Davatzikos, C. (2011). DRAMMS: deformable registration *via* attribute matching and mutual-saliency weighting. *Med. Image Analy.* 15, 622–639. doi: 10.1016/j.media.2010.07.002

Parzen, E. (1962). On estimation of a probability density function and mode. *Ann. Math. Statist.* 33, 1065–1076. doi: 10.1214/aoms/1177704472

Radford, A., Kim, J. W., Hallacy, C., Ramesh, A., Goh, G., Agarwal, S., et al. (2021). Learning transferable visual models from natural language supervision. *arXiv* [preprint]. arXiv:00020,

Rohlfing, T., Zahr, N. M., Sullivan, E. V., and Pfefferbaum, A. (2010). The SRI24 multichannel atlas of normal adult human brain structure. *Hum. Brain Mapp.* 31, 798–819. doi: 10.1002/hbm.20906

Sarlin, P.-E., DeTone, D., Malisiewicz, T., and Rabinovich, A. (2020). "Superglue: learning feature matching with graph neural networks," in *Proceedings of the IEEE/CVF Conference on Computer Vision and Pattern Recognition*. doi: 10.1109/CVPR42600.2020.00499

Sato, J. R., Hoexter, M. Q., de Magalhães Oliveira, P. P. Jr., Brammer, M. J., Murphy, D., Ecker, C., et al. (2013). Inter-regional cortical thickness correlations are associated with autistic symptoms: a machine-learning approach. *J. Psychiatric Res.* 47, 453–459. doi: 10.1016/j.jpsychires.2012.11.017

Selvaraju, R. R., Cogswell, M., Das, A., Vedantam, R., Parikh, D., and Batra, D. (2017). "Grad-cam: visual explanations from deep networks *via* gradient-based localization," in *Proceedings of the IEEE International Conference on Computer Vision*.

Shalom, D. B. (2009). The medial prefrontal cortex and integration in autism. *Neuroscientist* 15, 589–598. doi: 10.1177/1073858409336371

Silveri, M. C., and Misciagna, S. (2000). Language, memory, and the cerebellum. *J. Neurolinguistics* 13, 129–143. doi: 10.1016/S0911-6044(00)00008-7

Touvron, H., Cord, M., Douze, M., Massa, F., Sablayrolles, A., and Jégou, H. (2021). "Training data-efficient image transformers & distillation through attention," in *Proceeding of the International Conference on Machine Learning*.

Turner, A. H., Greenspan, K. S., and van Erp, T. G. (2016). Pallidum and lateral ventricle volume enlargement in autism spectrum disorder. *Psychiatry Res. Neuroimag.* 252, 40–45. doi: 10.1016/j.pscychresns.2016.04.003

Vapnik, V., Suykens, J. A. K., and Vandewalle, J. (eds) (1998). "The support vector method of function estimation," in *Nonlinear Modeling*, (Boston, MA: Springer), 55–85. doi: 10.1007/978-1-4615-5703-6_3

Vaswani, A., Shazeer, N., Parmar, N., Uszkoreit, J., Jones, L., Gomez, A. N., et al. (2017). "Attention is all you need," in *Proceedings of the Advances in Neural Information Processing Systems.First 12 Conferences*.

Wang, H., Jin, X., Zhang, Y., and Wang, J. (2016). Single-subject morphological brain networks: connectivity mapping, topological characterization and test–retest reliability. *Brain Behav.* 6:e00448. doi: 10.1002/brb3.448

Wang, H., Wang, Z., Du, M., Yang, F., Zhang, Z., Ding, S., et al. (2020). "Score-CAM: score-weighted visual explanations for convolutional neural networks," in *Proceedings of the IEEE/CVF Conference on Computer Vision and Pattern Recognition Workshops*. doi: 10.1109/CVPRW50498.2020.00020

Wang, W., Xie, E., Li, X., Fan, D.-P., Song, K., Liang, D., et al. (2021). Pyramid vision transformer: a versatile backbone for dense prediction without convolutions. *arXiv* [preprint]. arXiv:12122,

Wang, X., Girshick, R., Gupta, A., and He, K. (2018). "Non-local neural networks," in *Proceedings of the IEEE Conference on Computer Vision and Pattern Recognition*. doi: 10.1109/CVPR.2018.00813

Yin, M., Yao, Z., Cao, Y., Li, X., Zhang, Z., Lin, S., et al. (2020). "Disentangled non-local neural networks," in *European Conference on Computer Vision*, eds A. Vedaldi, H. Bischof, T. Brox, and J. M. Frahm (Cham: Springer). doi: 10.1007/978-3-030-58555-6_12

Yu, K., Wang, X., Li, Q., Zhang, X., Li, X., and Li, S. (2018). Individual morphological brain network construction based on multivariate euclidean distances between brain regions. *Front. Hum. Neurosci.* 12:204. doi: 10.3389/fnhum.2018.00204

Yuan, L., Chen, Y., Wang, T., Yu, W., Shi, Y., Jiang, Z., et al. (2021). Tokens-to-token vit: training vision transformers from scratch on imagenet. *arXiv* [preprint]. arXiv:11986,

Zhao, H., Jia, J., and Koltun, V. (2020). "Exploring self-attention for image recognition," in *Proceedings of the IEEE/CVF Conference on Computer Vision and Pattern Recognition*. doi: 10.1109/CVPR42600.2020.01009

Zheng, W., Eilamstock, T., Wu, T., Spagna, A., Chen, C., Hu, B., et al. (2019). *Multi-Feature Based Network Revealing the Structural Abnormalities in Autism Spectrum Disorder*. Piscataway: IEEE Transactions on Affective Computing.

Conflict of Interest: The authors declare that the research was conducted in the absence of any commercial or financial relationships that could be construed as a potential conflict of interest.

Publisher's Note: All claims expressed in this article are solely those of the authors and do not necessarily represent those of their affiliated organizations, or those of the publisher, the editors and the reviewers. Any product that may be evaluated in this article, or claim that may be made by its manufacturer, is not guaranteed or endorsed by the publisher.

frontiers in Psychiatry

ORIGINAL RESEARCH
published: 13 October 2021
doi: 10.3389/fpsyt.2021.758978

Dysfunction of Resting-State Functional Connectivity of Amygdala Subregions in Drug-Naïve Patients With Generalized Anxiety Disorder

Mei Wang[1†], Lingxiao Cao[2,3†], Hailong Li[2,3], Hongqi Xiao[1], Yao Ma[1], Shiyu Liu[1], Hongru Zhu[1], Minlan Yuan[1], Changjian Qiu[1] and Xiaoqi Huang[2,3]*

[1] Mental Health Center and Psychiatric Laboratory, West China Hospital of Sichuan University, Chengdu, China, [2] Huaxi MR Research Center (HMRRC), Functional and Molecular Imaging Key Laboratory of Sichuan Province, Department of Radiology, West China Hospital, Sichuan University, Chengdu, China, [3] Psychoradiology Research Unit of the Chinese Academy of Medical Sciences, West China Hospital of Sichuan University, Chengdu, China

OPEN ACCESS

Edited by:
Jiaojian Wang,
University of Electronic Science and Technology of China, China

Reviewed by:
Lihua Qiu,
Second People's Hospital of Yibin, China
Xiuli Wang,
Chengdu No.4 People's Hospital, China

***Correspondence:**
Changjian Qiu
qiuchangjian18@126.com

[†] These authors have contributed equally to this work

Specialty section:
This article was submitted to Neuroimaging and Stimulation, a section of the journal Frontiers in Psychiatry

Received: 15 August 2021
Accepted: 03 September 2021
Published: 13 October 2021

Citation:
Wang M, Cao L, Li H, Xiao H, Ma Y, Liu S, Zhu H, Yuan M, Qiu C and Huang X (2021) Dysfunction of Resting-State Functional Connectivity of Amygdala Subregions in Drug-Naïve Patients With Generalized Anxiety Disorder. Front. Psychiatry 12:758978. doi: 10.3389/fpsyt.2021.758978

Objective: Although previous studies have reported on disrupted amygdala subregional functional connectivity in generalized anxiety disorder (GAD), most of these studies were conducted in GAD patients with comorbidities or with drug treatment. Besides, whether/how the amygdala subregional functional networks were associated with state and trait anxiety is still largely unknown.

Methods: Resting-state functional connectivity of amygdala subregions, including basolateral amygdala (BLA) and centromedial amygdala (CMA) as seed, were mapped and compared between 37 drug-naïve, non-comorbidity GAD patients and 31 age- and sex-matched healthy controls (HCs). Relationships between amygdala subregional network dysfunctions and state/trait anxiety were examined using partial correlation analyses.

Results: Relative to HCs, GAD patients showed weaker functional connectivity of the left BLA with anterior cingulate/medial prefrontal cortices. Significantly increased functional connectivity of right BLA and CMA with superior temporal gyrus and insula were also identified in GAD patients. Furthermore, these functional connectivities showed correlations with state and trait anxiety scores.

Conclusions: These findings revealed abnormal functional coupling of amygdala subregions in GAD patients with regions involved in fear processing and emotion regulation, including anterior cingulate/medial prefrontal cortex and superior temporal gyrus, which provide the unique biological markers for GAD and facilitating the future accurate clinical diagnosis and target treatment.

Keywords: generalized anxiety disorder, amygdala, resting-state functional connectivity, state anxiety, trait anxiety

INTRODUCTION

Generalized anxiety disorder (GAD) is a common anxiety disorder characterized by excessive, pervasive, and uncontrollable anxiety, with a lifetime prevalence of about 5.7% (1). GAD is associated with substantial mental impairment affecting daily physical, psychological, and social functioning (2). The amygdala, as a core structure involved in fear processing and emotion regulation, is considered to be central to the pathophysiology of GAD (3). Although a lot of previous studies have reported functional abnormalities of amygdala in GAD (4–7), whether/how the intrinsic functional changes of amygdala in drug-naïve GAD are still not well-investigated, especially at the functionally heterogeneous subregional level.

The structural and functional heterogeneity of amygdala have been well-documented (8–10). The amygdala is commonly classified into the basolateral amygdala (BLA) and centromedial amygdala (CMA), which have different functions through distinct connectivity patterns (11). The BLA receives and integrates cortical input information from multiple brain systems for perception, evaluation, and memory formation of emotionally salient events. The CMA, in contrast, mainly receives modulatory inputs from the BLA and orbitofrontal cortex and projects to the brainstem, cerebellum, and hypothalamus for behavioral and physiological aspects of emotion processing and associative learning (11–14). These connectivity patterns of amygdala subregions have been proven by tractography, task-based and resting-state functional magnetic resonance imaging (9, 10, 13).

Resting-state functional connectivity (RSFC) analysis is a powerful method to examine intrinsic functional connectivity abnormalities in various mental disorders, which delineates the functional architecture of intrinsically coupled brain networks (15–20). By using RSFC analysis, disruptions of the amygdala subregional functional connectivity have been reported in patients with GAD. For example, BLA and CMA connectivity patterns were found to be significantly less distinct in adults with GAD (21). Roy et al. found that adolescents with GAD showed disrupted amygdala subregional functional networks that included regions in medial prefrontal cortex, insula, and cerebellum (22). However, these findings were concluded from a relatively small sample of GAD patients with comorbidities or with drug treatment, which need to be further validated.

Moreover, GAD patients are frequently involved in a state of anxiety, a measure of the intensity of anxiety experienced on comparatively short timescales. If state anxiety is deployed appropriately, it serves as an adaptive function priming individuals to detect and respond to danger. Compared with state anxiety, trait anxiety is derived from self-report questionnaires to measure the frequency of anxiety symptoms that are experienced by an individual or the general personality properties (23, 24). State and trait anxiety are different, and elevated levels of trait anxiety are a risk factor for the development of clinical anxiety disorders (25). Yet, the associations of amygdala subregional functional connectivity with state and trait anxiety have rarely been investigated in GAD. Thus, to depict the relationship of amygdala subregional functional connectivity patterns with state and trait anxiety in drug-naïve patients may better identify GAD neuropathological basis.

In the current study, we aimed to explore the specific amygdala subregional functional connectivity alterations in drug-naïve, non-comorbidity patients with GAD compared with age- and sex-matched healthy controls (HCs). Then, we evaluated the associations of amygdala subregional connectivity dysfunctions with different anxiety types. Based on the above mentioned findings, we hypothesized that GAD patients showed weaker connectivity between BLA and prefrontal regions, such as the medial prefrontal and anterior cingulate cortices and hyperconnectivity between the CMA and insula.

MATERIALS AND METHODS

Participants

This study was approved by the Ethics Committee of West China Hospital, Sichuan University. A total of 38 patients with GAD and 31 age- and sex-matched HCs participated in the present study after giving their written informed consent. All participants were right-handed. GAD patients were recruited from the Mental Health Center, West China Hospital of Sichuan University. Psychiatric diagnoses were determined using the Mini International Neuropsychiatric Interview (MINI), Chinese version, by two experienced psychiatrists. Exclusion criteria were (1) age <18 years or over 65 years; (2) psychiatric comorbidity assessed using the MINI; (3) any history of cardiovascular diseases, major physical illness, or neurological disorder; (4) substance abuse or dependence; and (5) pregnancy. The Hamilton Anxiety Scale (HAMA) and the Generalized Anxiety Disorder 7-item Scale (GAD-7) were used to assess symptom severity. GAD patients and HCs also completed the State-Trait Anxiety Inventory (STAI).

MRI Data Acquisition

MRI data were acquired via a 3-Tesla Siemens MRI system with an eight-channel phase-array head coil. Head motion was controlled using foam pads. Prior to scanning, participants were instructed to lie still with their eyes closed and not to fall asleep. The resting-state fMRI images were obtained using a gradient-echo echo-planar imaging sequence with the following parameters: repetition time = 2,000 ms, echo time = 30 ms, flip angle = 90°, slice thickness = 5 mm with no slice gap, field of view = 240 × 240 mm^2, 30 axial slices, and 205 volumes in each run. High-resolution T1-weighted data were acquired using the following scan parameters: TR = 1,900 ms, TE = 2.28 ms, flip angle = 9°, 176 sagittal slices with slice thickness = 1.0 mm, field of view = 240 × 240 mm^2, data matrix = 256 × 256.

Resting-State fMRI Data Preprocessing

Resting-state data were preprocessed using the Data Processing and Analysis for Brain Imaging toolkit (DPABI, http://www.rfmri.org/dpabi). The first 10 volumes were removed to allow for signal equilibration effects. Slice timing and realignment were then performed. The Friston 24-parameter model of head motion and other sources of spurious variance (white matter and cerebrospinal fluid signals) were removed from the data

to reduce the effects of non-neuronal BOLD fluctuations. Next, the images were spatially normalized to the standard Montreal Neurological Institute (MNI) space and resampled to a voxel size of $3 \times 3 \times 3$ mm^3. Spatial smoothing with an isotropic Gaussian kernel with a full width at half maximum of 8 mm was then applied. Subsequently, linear trend removal and temporal band-pass filtering (0.01–0.08 Hz) were performed to decrease the effects of high-frequency physiological noise and low-frequency drift. To further exclude head motion effects, scrubbing was performed with the threshold for frame-wise displacement (FD > 0.5) (26). In addition, the MRI data was ruled out in the following analysis if (1) spatial movement in any direction >2 mm or 2°, (2) mean FD >0.3 mm, and (3) the scrubbed data <5 min. According to this threshold, one GAD patient was excluded in the further analysis. Additionally, there was no significant difference in head motion (mean FD) between GAD patients and HCs.

Amygdala Subregion Definition

The amygdala subregions of BLA and CMA in each hemisphere were obtained by calculating the maximum probability maps defined by cytoarchitecture through the SPM Anatomy Toolbox (27). The obtained BLA and CMA masks were then downsampled to 3-mm cubic voxel for functional connectivity analyses.

Functional Connectivity Analysis

Seed-based whole-brain functional connectivity analysis was used to map the functional connectivity pattern for each amygdala subregion. First, the mean time series of each individual amygdala subregion was calculated. Then, voxel-wise correlation between each seed and each voxel of the rest of the brain were computed. Finally, the correlation coefficients were changed to z-score using Fisher's r-to-z transformation yielding individual level whole-brain FC map for each amygdala subregion.

Using SPM 12, the FC maps of each seed from the individual level analyses were then entered into a second-level group analysis that treated subjects as a random variable in a 2-by-2-by-2 full factorial analyses of variance, with subregion (BLA vs. CMA) and hemisphere (left vs. right) as within-subject factors and group (GAD vs. HC) as a between-subject factor.

As our main aim is to identify the functional connectivity difference of each amygdala subregion between GAD patients and HCs, the second stage of analysis was performed using two-sample *t*-tests with age, sex, education, and head motion as covariates. The significance threshold was set to $p < 0.005$ (uncorrected) at the voxel level and the family-wise error (FWE) correction ($p < 0.05$) at the cluster level for multiple comparisons.

To explore whether amygdala subregional FC abnormalities were associated with illness duration and symptom severity in GAD patients, we conducted partial correlation analyses between FC strength extracted from each region showing significant group differences and illness duration, HAMA, and GAD-7 (adjusted for age, sex, education, and head motion). Furthermore, associations between these FC and personality traits as assessed by STAI were examined both in the sample as a whole and separately in the GAD patients and HCs.

TABLE 1 | Subject demographics.

	GAD ($n = 37$)	HC ($n = 31$)	*p*-Values
Age (years)	39.78 (9.38)	36.16 (9.23)	0.133
Sex (M/F)	10/27	7/24	0.673
Education (years)	11.35 (4.04)	14.00 (3.41)	0.006*
Duration (months)	39.65 (45.85)	–	–
HAMA	25.49 (6.51)	0.29 (0.64)	0.001*
HAMD	16.11 (5.75)	0.10 (0.30)	0.001*
GAD-7	12.26 (5.39)	1.61 (2.77)	0.001*
SAI	51.86 (13.52)	31.55 (8.73)	0.001*
TAI	53.25 (10.80)	33.00 (8.45)	0.001*
Mean FD	0.127 (0.060)	0.127 (0.060)	0.996

FD, frame-wise displacement; F, female; M, male; GAD-7, Generalized Anxiety Disorder (7-item); HAMA, Hamilton Anxiety Scale; HAMD, Hamilton Depressive Scale; SAI, State Anxiety Inventory; TAI, Trait Anxiety Inventory.
**Represents significant differences.*

RESULTS

Demographic and Clinical Characteristic

As shown in **Table 1**, GAD patients and HC groups do not differ in age and sex. As expected, the scores of the clinical rating scale identified more severe anxiety and depressive symptoms in GAD patients than in HCs. Education level in GAD patients was significantly lower than that in HCs.

Amygdala Subregional Functional Connectivity

Full factorial analysis of variance did not identify any significant clusters. Compared with HCs, GAD patients showed weaker functional connectivity between the left BLA and left anterior cingulate/medial prefrontal cortices (**Figure 1**) and stronger FC between the right BLA and left superior temporal gyrus/insula, and between the right CMA and left superior temporal gyrus (**Figure 2**).

The FC values between the left BLA and anterior cingulate/medial prefrontal cortices correlated negatively with both state ($r = -0.388$, $p = 0.002$) and trait ($r = -0.396$, $p = 0.001$) anxiety in the whole sample group. The FC values between the right BLA and left superior temporal gyrus/insula showed positive correlation with state ($r = 0.293$, $p = 0.02$) and trait ($r = 0.275$, $p = 0.029$) anxiety. The FC values between the right CMA and left superior temporal gyrus positively correlated with state ($r = 0.374$, $p = 0.003$) and trait ($r = 0.388$, $p = 0.002$) anxiety. Additionally, positive correlations between FC of CMA with the left superior temporal gyrus/insula and trait anxiety were found in the GAD group ($r = 0.355$, $p = 0.046$) (**Supplementary Figure 1**).

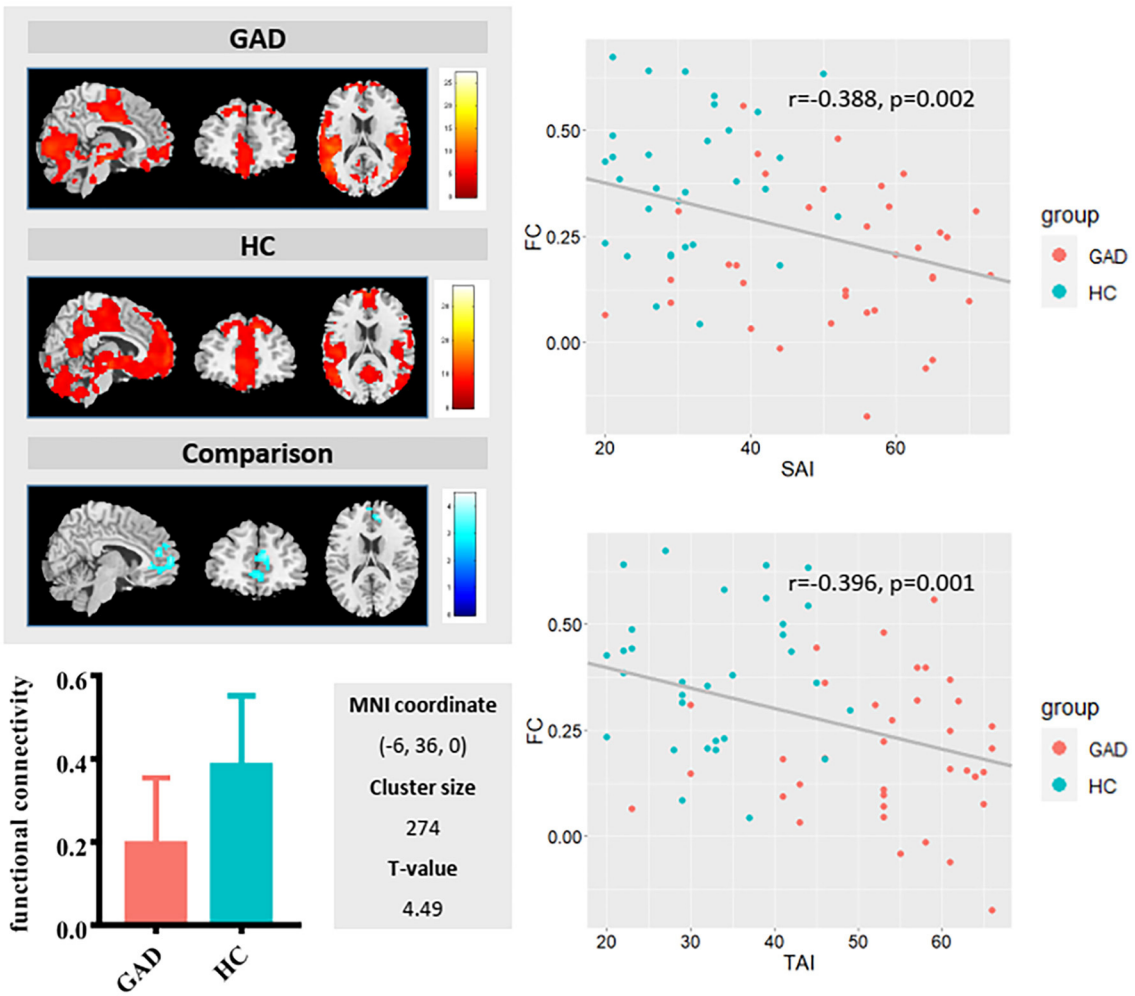

FIGURE 1 | Left basolateral amygdala (BLA) functional connectivity (upper left panel) in generalized anxiety disorder (GAD) patients (first row) and in healthy controls (HCs; second row), and group differences shown in the third row. Compared with HCs, GAD patients showed weaker functional connectivity between the left BLA and anterior cingulate/medial prefrontal cortices (see bar graph in lower left panel). As shown in the scatterplot (right panel), a weaker FC between the left BLA and anterior cingulate/medial prefrontal cortices is associated with a higher-state anxiety and trait anxiety score in the sample as a whole.

DISCUSSION

In the current study, we revealed disrupted amygdala subregional functional connectivity in a group of drug-naive and non-comorbidity GAD patients. We found that GAD patients showed weaker functional connectivity of the left BLA with the anterior cingulate/medial prefrontal cortices and stronger FC of the right BLA and CMA with the superior temporal gyrus and insula. In addition, these functional connectivities associated with both state and trait anxiety, suggesting that amygdala subregional functional coupling may reflect the neural correlates of current fear or anxiety state and trait vulnerability for excessive fear responses.

Our finding of decreased functional connectivity between left BLA and anterior cingulate/medial prefrontal cortices in GAD supports top–down emotional dysregulation model hypothesis for the pathological mechanism of GAD (28, 29). The top–down modulation of prefrontal cortex to amygdala and related limbic structures is the neural basis of emotion regulation, and anxiety individuals experience excessive negative emotions indicating potential dysfunction of downregulation of negative emotions (28, 30). The amygdala is mainly involved in expression of emotion (31), and the prefrontal cortex is mainly associated with emotional regulation (32, 33). Besides, the anterior cingulate cortex and medial prefrontal cortex is also related to detection of emotional salience, cognition, emotion–cognition interaction, and self-consciousness and self-related mental processes (34, 35). Therefore, the amygdala–anterior cingulate cortex and amygdala–medial prefrontal cortex circuits are closely related to the occurrence and development of

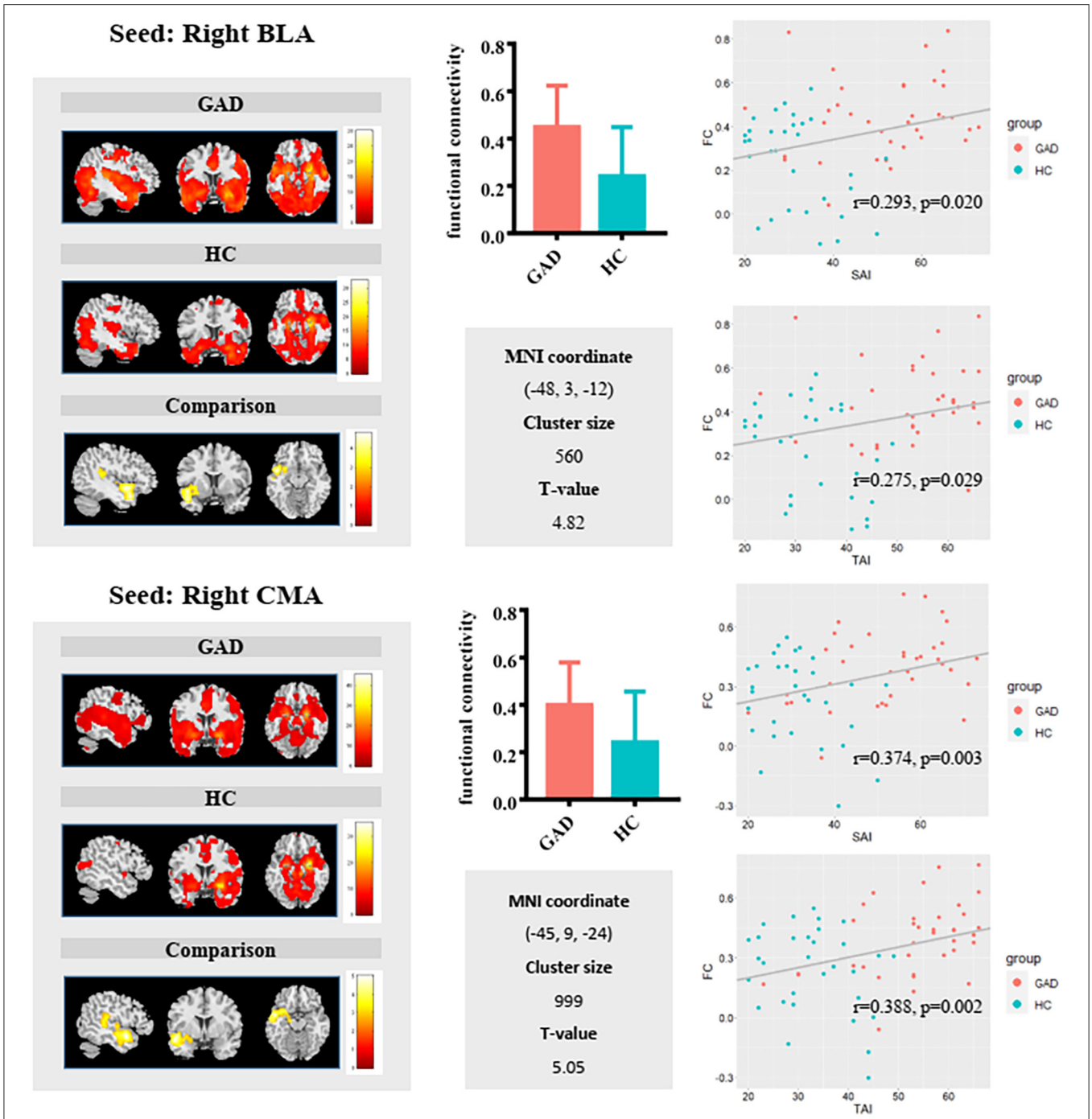

FIGURE 2 | Group comparisons in FC of the right basolateral amygdala (BLA) (upper panel) and right centromedial amygdala (CMA) (lower panel) revealed relatively similar results. GAD patients exhibited significantly increased right BLA/CMA functional connectivity with a cluster including the superior temporal gyrus and insula. Additionally, the scatterplot showed positive associations between FC and State Anxiety Inventory (SAI)/Trait Anxiety Inventory (TAI) in the sample as a whole.

emotion, especially the anterior cingulate–amygdala circuit. In addition, the BLA nucleus of the amygdala–anterior cingulate cortex loop mediated associative learning process, conditioned fear, anxiety, and anticipatory anxiety (36–38). In addition, we identified negative correlation between amygdala–anterior cingulate cortex/prefrontal cortex functional connectivity and trait anxiety levels, which is consistent with previous findings that lower functional connectivity between the amygdala and anterior cingulate cortex/prefrontal cortex was associated with higher trait and state anxiety in psychiatrically healthy

individuals (39–41). All the evidence indicated that the weakening of functional links between BLA and anterior cingulate cortex/medial prefrontal cortex may be the neural mechanism of disrupted top–down emotion regulation in GAD (21, 42).

The increased functional connectivity between the right BLA and CMA with the superior temporal gyrus and insula in GAD patients demonstrated that besides the high vigilance theory, GAD is also characterized by fear of threats (43, 44). A previous study found that functional connectivity between the amygdala and STG and insula was positively correlated with anxiety severity level in the GAD group (22). The superior temporal gyrus is related to the high-level cognitive process of fear experience and regulation of amygdala activity (45). Both insula and superior temporal gyrus play an important role in the nervous regulation of visceral organs to physiological conditions caused by anxiety response, such as temperature, pain, and exercise (46). Moreover, functional connectivity of the amygdala–superior temporal gyrus/insula was found to be positively correlated with trait anxiety levels suggesting that functional connectivity of the amygdala–superior temporal gyrus/insula is able to predict levels of anxiety (47–49). Therefore, we speculated that increased functional connectivity between BLA, CMA, and superior temporal gyrus/insula may be related to high worry about affairs and overreaction to sensation in GAD patients, which may be the neural basis of the abnormal physical performance of GAD patients.

Given the novelty of the current study, it also bears several limitations. First, in our study, although the non-comorbidity GAD patients were recruited to identify GAD-specific alterations, it may also lead to reducing the generalizability of our results to normal clinical setting. Second, the GAD samples are still small, and the findings need to be further validated. Finally, longitudinal studies with multimodal MRI data are warranted to better reveal the neuropathology of the GAD. Further researches are needed to clarify and extend our findings.

In conclusion, our study found disrupted left BLA–prefrontal and right BLA/CMA-temporal/insular circuits in GAD patients. More importantly, we found a negative correlation between connectivity of the amygdala–prefrontal cortex/anterior cingulate cortex circuit and positive correlation between the connectivity of the amygdala–superior temporal gyrus/insula circuit and trait anxiety levels. These findings highlight the important roles of the amygdala–frontal and amygdala–temporal circuits in the neuropathology of anxiety. This abnormal functional connectivity may underlie disrupted cognitive and affective processes in GAD patients.

DATA AVAILABILITY STATEMENT

The data that support the findings of this study are available from the corresponding author upon reasonable request.

ETHICS STATEMENT

This study was approved by the Ethics Committee of West China Hospital, Sichuan University, and written informed consent was obtained from each participant.

AUTHOR CONTRIBUTIONS

MW, LC, CQ, and XH formulated the research questions. CQ and XH designed the study. HL, HX, and YM acquired the data. MW, LC, and SL analyzed the data. MW, LC, CQ, and XH wrote the article or revised it. HZ and MY reviewed the article. All authors approved the final version to be published.

FUNDING

This study was supported by the National Nature Science Foundation (Grant Nos. 81671669, 81871061, and 81701328), the Science and Technology Project of Sichuan Province (Grant Nos. 2017JQ0001, 2018SZ0131, 2020YFS0231, and 2020YFS0582), the 1·3·5 Project for Disciplines of Excellence, West China Hospital, Sichuan University (Grant Nos. ZYJC21041 and ZYJC21083), a grant from the Postdoctoral Foundation of West China Hospital (Grant No. 2020HXBH041), and the Science and Technology Project of Chengdu City (Grant No. 2019-YF05-00509-SN).

SUPPLEMENTARY MATERIAL

The Supplementary Material for this article can be found online at: https://www.frontiersin.org/articles/10.3389/fpsyt.2021.758978/full#supplementary-material

REFERENCES

1. Weisberg RB. Overview of generalized anxiety disorder: epidemiology, presentation, and course. *J Clin Psychiatry.* (2009) 70(Suppl. 2):4–9. doi: 10.4088/JCP.s.7002.01
2. Slee A, Nazareth I, Bondaronek P, Liu Y, Cheng Z, Freemantle N. Pharmacological treatments for generalised anxiety disorder: a systematic review and network meta-analysis. *Lancet.* (2019) 393:768–77. doi: 10.1016/S0140-6736(18)31793-8
3. Etkin A, Wager TD. Functional neuroimaging of anxiety: a meta-analysis of emotional processing in PTSD. Social anxiety disorder, specific phobia. *Am J Psychiatry.* (2007) 164:1476–88. doi: 10.1176/appi.ajp.2007.07030504
4. De Bellis MD, Casey BJ, Dahl RE, Birmaher B, Williamson DE, Thomas KM, et al. A pilot study of amygdala volumes in pediatric generalized anxiety disorder. *Biol Psychiatry.* (2000) 48:51–7. doi: 10.1016/S0006-3223(00)00835-0
5. Martin EI, Ressler KJ, Binder E, Nemeroff CB. The neurobiology of anxiety disorders: brain imaging, genetics, and psychoneuroendocrinology. *Psychiatr Clin N Am.* (2009) 32:549–75. doi: 10.1016/j.psc.2009.05.004
6. Dong M, Xia L, Lu M, Li C, Xu K, Zhang L. A failed top-down control from the prefrontal cortex to the amygdala in generalized anxiety disorder: evidence from resting-state fMRI with Granger causality analysis. *Neurosci Lett.* (2019) 707:134314. doi: 10.1016/j.neulet.2019.134314
7. Kolesar TA, Bilevicius E, Wilson AD, Kornelsen J. Systematic review and meta-analyses of neural structural and functional differences in generalized

anxiety disorder and healthy controls using magnetic resonance imaging. *Neuroimage Clin.* (2019) 24:102016. doi: 10.1016/j.nicl.2019.102016
8. Amunts K, Kedo O, Kindler M, Pieperhoff P, Mohlberg H, Shah NJ, et al. Cytoarchitectonic mapping of the human amygdala, hippocampal region and entorhinal cortex: intersubject variability and probability maps. *Anat Embryol.* (2005) 210:343–52. doi: 10.1007/s00429-005-0025-5
9. Bach DR, Behrens TE, Garrido L, Weiskopf N, Dolan RJ. Deep and superficial amygdala nuclei projections revealed *in vivo* by probabilistic tractography. *J Neurosci.* (2011) 31:618–23. doi: 10.1523/JNEUROSCI.2744-10.2011
10. Bzdok D, Laird AR, Zilles K, Fox PT, Eickhoff SB. An investigation of the structural, connectional, and functional subspecialization in the human amygdala. *Hum Brain Mapp.* (2013) 34:3247–66. doi: 10.1002/hbm.22138
11. LeDoux J. The amygdala. *Curr Biol.* (2007) 17:R868–74. doi: 10.1016/j.cub.2007.08.005
12. Ghashghaei HT, Barbas H. Pathways for emotion: interactions of prefrontal and anterior temporal pathways in the amygdala of the rhesus monkey. *Neuroscience.* (2002) 115:1261–79. doi: 10.1016/S0306-4522(02)00446-3
13. Sah P, Faber ESL, Lopez De Armentia M, Power J. The amygdaloid complex: anatomy and physiology. *Physiol Rev.* (2003) 83:803–34. doi: 10.1152/physrev.00002.2003
14. Moul C, Killcross S, Dadds MR. A model of differential amygdala activation in psychopathy. *Psychol Rev.* (2012) 119:789–806. doi: 10.1037/a0029342
15. Greicius MD, Srivastava G, Reiss AL, Menon V. Default-mode network activity distinguishes Alzheimer's disease from healthy aging: evidence from functional MRI. *Proc Natl Acad Sci USA.* (2004) 101:4637–42. doi: 10.1073/pnas.0308627101
16. Fox MD, Raichle ME. Spontaneous fluctuations in brain activity observed with functional magnetic resonance imaging. *Nat Rev Neurosci.* (2007) 8:700–11. doi: 10.1038/nrn2201
17. Greicius MD, Flores BH, Menon V, Glover GH, Solvason HB, Kenna H, et al. Resting-state functional connectivity in major depression: abnormally increased contributions from subgenual cingulate cortex and thalamus. *Biol Psychiatry.* (2007) 62:429–37. doi: 10.1016/j.biopsych.2006.09.020
18. Wang J, Wei Q, Wang L, Zhang H, Bai T, Cheng L, et al. Functional reorganization of intra- and internetwork connectivity in major depressive disorder after electroconvulsive therapy. *Hum Brain Mapp.* (2018) 39:1403–11. doi: 10.1002/hbm.23928
19. Wang L, Wei Q, Wang C, Xu J, Wang K, Tian Y, et al. Altered functional connectivity patterns of insular subregions in major depressive disorder after electroconvulsive therapy. *Brain Imaging Behav.* (2019) 14:753–61. doi: 10.1007/s11682-018-0013-z
20. Wang L, Yu L, Wu F, Wu H, Wang J. Altered whole brain functional connectivity pattern homogeneity in medication-free major depressive disorder. *J Affect Disord.* (2019) 253:18–25. doi: 10.1016/j.jad.2019.04.040
21. Etkin A, Prater KE, Schatzberg AF, Menon V, Greicius MD. Disrupted amygdalar subregion functional connectivity and evidence of a compensatory network in generalized anxiety disorder. *Arch Gen Psychiatry.* (2009) 66:1361–72. doi: 10.1001/archgenpsychiatry.2009.104
22. Roy AK, Fudge JL, Kelly C, Perry JS, Daniele T, Carlisi C, et al. Intrinsic functional connectivity of amygdala-based networks in adolescent generalized anxiety disorder. *J Am Acad Child Adolesc Psychiatry.* (2013) 52:290–9 e292. doi: 10.1016/j.jaac.2012.12.010
23. Spielberger CD, Gorsuch RL, Lushene RE. *State-trait Anxiety Inventory*. Palo Alto, CA: Consulting Psychologists Press (1970).
24. Saviola F, Pappaianni E, Monti A, Grecucci A, Jovicich J, De Pisapia N. Trait and state anxiety are mapped differently in the human brain. *Sci Rep.* (2020) 10:11112. doi: 10.1038/s41598-020-68008-z
25. Raymond JG, Steele JD, Seriès P. Modeling trait anxiety: from computational processes to personality. *Front Psychiatry.* (2017) 8:1. doi: 10.3389/fpsyt.2017.00001
26. Power JD, Barnes KA, Snyder AZ, Schlaggar BL, Petersen SE. Spurious but systematic correlations in functional connectivity MRI networks arise from subject motion. *Neuroimage.* (2012) 59:2142–54. doi: 10.1016/j.neuroimage.2011.10.018
27. Eickhoff SB, Stephan KE, Mohlberg H, Grefkes C, Fink GR, Amunts K, et al. A new SPM toolbox for combining probabilistic cytoarchitectonic maps and functional imaging data. *Neuroimage.* (2005) 25:1325–35. doi: 10.1016/j.neuroimage.2004.12.034
28. Ball TM, Ramsawh HJ, Campbell-Sills L, Paulus MP, Stein MB. Prefrontal dysfunction during emotion regulation in generalized anxiety and panic disorders. *Psychol Med.* (2013) 43:1475–86. doi: 10.1017/S0033291712002383
29. Mochcovitch MD, da Rocha RC, Freire Garcia RF, Nardi AE. A systematic review of fMRI studies in generalized anxiety disorder: evaluating its neural and cognitive basis. *J Affect Disord.* (2014) 167:336–42. doi: 10.1016/j.jad.2014.06.041
30. Campbell-Sills L, Simmons AN, Lovero KL, Rochlin AA, Paulus MP, Stein MB. Functioning of neural systems supporting emotion regulation in anxiety-prone individuals. *Neuroimage.* (2011) 54:689–96. doi: 10.1016/j.neuroimage.2010.07.041
31. Salzman CD, Fusi S. Emotion, cognition, and mental state representation in amygdala and prefrontal cortex. *Annu Rev Neurosci.* (2010) 33:173–202. doi: 10.1146/annurev.neuro.051508.135256
32. Critchley HD, Mathias CJ, Dolan RJ. Neural activity in the human brain relating to uncertainty and arousal during anticipation. *Neuron.* (2001) 29:537–45. doi: 10.1016/S0896-6273(01)00225-2
33. Etkin A, Egner T, Kalisch R. Emotional processing in anterior cingulate and medial prefrontal cortex. *Trends Cogn Sci.* (2011) 15:85–93. doi: 10.1016/j.tics.2010.11.004
34. Allman JM, Hakeem A, Erwin JM, Nimchinsky E, Hof P. The anterior cingulate cortex. The evolution of an interface between emotion and cognition. *Ann N Y Acad Sci.* (2001) 935:107–17. doi: 10.1111/j.1749-6632.2001.tb03476.x
35. Stevens FL, Hurley RA, Taber KH. Anterior cingulate cortex: unique role in cognition and emotion. *J Neuropsychiatry Clin Neurosci.* (2011) 23:121–5. doi: 10.1176/jnp.23.2.jnp121
36. Hoehn-Saric R, Schlund MW, Wong SH. Effects of citalopram on worry and brain activation in patients with generalized anxiety disorder. *Psychiatry Res.* (2004) 131:11–21. doi: 10.1016/j.pscychresns.2004.02.003
37. Paulesu E, Sambugaro E, Torti T, Danelli L, Ferri F, Scialfa G, et al. Neural correlates of worry in generalized anxiety disorder and in normal controls: a functional MRI study. *Psychol Med.* (2010) 40:117–24. doi: 10.1017/S0033291709005649
38. Weinberg A, Hajcak G. Electrocortical evidence for vigilance-avoidance in generalized anxiety disorder. *Psychophysiology.* (2011) 48:842–51. doi: 10.1111/j.1469-8986.2010.01149.x
39. Kim MJ, Loucks RA, Palmer AL, Brown AC, Solomon KM, Marchante AN, et al. The structural and functional connectivity of the amygdala: from normal emotion to pathological anxiety. *Behav Brain Res.* (2011) 223:403–10. doi: 10.1016/j.bbr.2011.04.025
40. Gold AL, Shechner T, Farber MJ, Spiro CN, Leibenluft E, Pine DS, et al. Amygdala-cortical connectivity: associations with anxiety, development, and threat. *Depress Anxiety.* (2016) 33:917–26. doi: 10.1002/da.22470
41. Weger M, Sandi C. High anxiety trait: a vulnerable phenotype for stress-induced depression. *Neurosci Biobehav Rev.* (2018) 87:27–37. doi: 10.1016/j.neubiorev.2018.01.012
42. Roy AK, Shehzad Z, Margulies DS, Kelly AM, Uddin LQ, Gotimer K, et al. Functional connectivity of the human amygdala using resting state fMRI. *Neuroimage.* (2009) 45:614–26. doi: 10.1016/j.neuroimage.2008.11.030
43. Aikins DE, Craske MG. Cognitive theories of generalized anxiety disorder. *Psychiatric Clin N Am.* (2001) 24:57–74. doi: 10.1016/S0193-953X(05)70206-9
44. Lissek S, Kaczkurkin AN, Rabin S, Geraci M, Pine DS, Grillon C. Generalized anxiety disorder is associated with overgeneralization of classically conditioned fear. *Biol Psychiatry.* (2014) 75:909–15. doi: 10.1016/j.biopsych.2013.07.025
45. Quirk GJ, Armony JL, LeDoux JE. Fear conditioning enhances different temporal components of tone-evoked spike trains in auditory cortex and lateral amygdala. *Neuron.* (1997) 19:613–24. doi: 10.1016/S0896-6273(00)80375-X
46. van Tol MJ, van der Wee NJA, van den Heuvel OA, Nielen MMA, Demenescu LR, Aleman A, et al. Regional brain volume in depression and anxiety disorders. *Arch Gen Psychiatry.* (2010) 67:1002–11. doi: 10.1001/archgenpsychiatry.2010.121
47. Baur V, Hanggi J, Langer N, Jancke L. Resting-state functional and structural connectivity within an insula-amygdala route specifically index state and

trait anxiety. *Biol Psychiatry*. (2013) 73:85–92. doi: 10.1016/j.biopsych.2012.06.003
48. Ball TM, Sullivan S, Flagan T, Hitchcock CA, Simmons A, Paulus MP, et al. Selective effects of social anxiety, anxiety sensitivity, and negative affectivity on the neural bases of emotional face processing. *Neuroimage*. (2012) 59:1879–7. doi: 10.1016/j.neuroimage.2011.08.074
49. Rosso IM, Makris N, Britton JC, Price LM, Gold AL, Zai D, et al. Anxiety sensitivity correlates with two indices of right anterior insula structure in specific animal phobia. *Depress Anxiety*. (2010) 27:1104–1110. doi: 10.1002/da.20765

Conflict of Interest: The authors declare that the research was conducted in the absence of any commercial or financial relationships that could be construed as a potential conflict of interest.

frontiers in Psychiatry

METHODS
published: 12 November 2021
doi: 10.3389/fpsyt.2021.764328

Brain Entropy Study on Obsessive-Compulsive Disorder Using Resting-State fMRI

Xi Jiang[1,2], *Xue Li*[1,2], *Haoyang Xing*[1,2]*, *Xiaoqi Huang*[1], *Xin Xu*[1] and *Jing Li*[1]

[1] Magnetic Resonance Research Center, West China Hospital, Sichuan University, Chengdu, China, [2] School of Physics, Sichuan University, Chengdu, China

Object: Brain entropy is a potential index in the diagnosis of mental diseases, but there are some differences in different brain entropy calculation, which may bring confusion and difficulties to the application of brain entropy. Based on the resting-state function magnetic resonance imaging (fMRI) we analyzed the differences of the three main brain entropy in the statistical significance, including approximate entropy (ApEn), sample entropy (SampEn) and fuzzy entropy (FuzzyEn), and studied the physiological reasons behind the difference through comparing their performance on obsessive-compulsive disorder (OCD) and the healthy control (HC).

Method: We set patients with OCD as the experimental group and healthy subjects as the control group. The brain entropy of the OCD group and the HC are calculated, respectively, by voxel and AAL region. And then we analyzed the statistical differences of the three brain entropies between the patients and the control group. To compare the sensitivity and robustness of these three kinds of entropy, we also studied their performance by using certain signal mixed with noise.

Result: Compare with the control group, almost the whole brain's ApEn and FuzzyEn of OCD are larger significantly. Besides, there are more brain regions with obvious differences when using ApEn comparing to using FuzzyEn. There was no statistical difference between the SampEn of OCD and HC.

Conclusion: Brain entropy is a numerical index related to brain function and can be used as a supplementary biological index to evaluate brain state, which may be used as a reference for the diagnosis of mental illness. According to an analysis of certain signal mixed with noise, we conclude that FuzzyEn is more accurate considering sensitivity, stability and robustness of entropy.

Keywords: brain entropy, approximate entropy, sample entropy, fuzzy entropy (FuzzyEn), fMRI, OCD

OPEN ACCESS

Edited by:
Jiaojian Wang,
University of Electronic Science and Technology of China, China

Reviewed by:
Yi Sui,
Mayo Clinic, United States
Luqi Cheng,
Guilin University of Electronic Technology, China

***Correspondence:**
Haoyang Xing
xhy@scu.edu.cn

Specialty section:
This article was submitted to Neuroimaging and Stimulation, a section of the journal Frontiers in Psychiatry

Received: *25 August 2021*
Accepted: *14 October 2021*
Published: *12 November 2021*

Citation:
Jiang X, Li X, Xing H, Huang X, Xu X and Li J (2021) Brain Entropy Study on Obsessive-Compulsive Disorder Using Resting-State fMRI. Front. Psychiatry 12:764328. doi: 10.3389/fpsyt.2021.764328

INTRODUCTION

Entropy is a physical concept proposed by the German physicist Clausius in 1865, which is used to measure the complexity, randomness, or predictability of a dynamic process. In 1948, Shannon (1) introduced entropy into information theory and used entropy to quantify the complexity of information for the first time. And then the concept and application scope of entropy were

gradually extended to cybernetics, probability theory, number theory, astrophysics, life science and other fields. Wang et al. (2) calculated the three-dimensional brain entropy map through the resting-state fMRI images of 1,049 subjects, and found that the distribution of brain entropy was consistent with the brain structure and functional partition. Saxe et al. (3) found that high intelligence would correspond to a high level of brain entropy in a sample of 892 healthy adults who participated in both resting-state fMRI and intelligence testing. Shi et al. (4) found that there was a significant positive relationship between creativity and the brain entropy values of DLPFC and DACC brain functional areas, which are responsible for cognitive flexibility and inhibitory control. Their study provides evidence of the associations of regional brain entropy with individual variations in divergent thinking and show that brain entropy is sensitive to detecting variations in important cognitive abilities in healthy subjects. Song et al. (5) found that brain entropy can be enhanced through caffeine intake, this study verifies the sensitivity of brain entropy to drug regulation, supports that brain entropy can sensitively reflect the neural effects of caffeine, and supports that brain entropy can be used as an indicator to detect changes in brain activity. Other researchers also reported changes in entropy in brain conditions such as normal aging (6–9), multiple sclerosis (10), schizophrenia (11), Alzheimer's disease (12), and Attention deficit hyperactivity disorder (13). These studies show that brain entropy can reflect information of the brain activity, and can be used as a tool for diagnosis and treatment of brain diseases, and can provide a potential way to explore complex brain function. There are three main types of brain entropy including ApEn, SampEn, and FuzzyEn, and they are certainly different among different brain entropy calculations. Up to now, the accuracy and sensitivity of the three different calculation methods in measuring the degree of brain dysfunction are not clear.

According to the Diagnostic and Statistical Manual of Mental Disorders V (DSM-V), OCD has become an independent disease with obsessive thinking and compulsive behavior as the main clinical manifestations. It is characterized by the coexistence of conscious compulsion and anti-compulsion, and some meaningless or even against one's own wishes. Impulse repeatedly invades the patient's daily life. Previous studies showed that there are Amplitude of Low Frequency Fluctuations (ALFF) abnormalities (14, 15) and Functional Connectivity (FC) abnormalities (16, 17) in the brains of OCD, and the neuron activity in the corresponding brain area [such as CSTC (18–20), DLPFC (21)] is stronger. These studies indicate that OCD may be a disease of brain abnormalities. However, for the study of abnormal brain areas and their functional status in OCD, the results of brain dysfunction areas in OCD detected by ALFF and FC are not consistent. Therefore, a more comprehensive, accurate and sensitive detection method is needed. The change of brain entropy can reflect the intensity of neuronal activity in the corresponding brain area, which can be used as a tool for the diagnosis and treatment of brain diseases. However, the relationship between abnormal neuron activity and brain entropy in OCD is still unclear.

In order to clarify the response of brain entropy to the brain function activities of OCD patients, three different brain entropies (ApEn, SampEn, and FuzzyEn) and their degree of response to OCD will be obtained in this experiment explore, and then elicit a new method of OCD diagnosis to provide experimental basis for further research on the pathogenesis of OCD.

Definition of three Entropies

Approximate Entropy

ApEn is defined by Pincus (22) according to Kolmogorov entropy (23, 24), which is the conditional probability that the similarity vector will continue to maintain its similarity when it increases from m dimension to $m+1$ dimension. Its physical meaning is the probability of the time series generating new patterns when the dimension changes. The greater the probability of the new pattern generated, the more complex the sequence is, the larger the corresponding ApEn is. It is a non-negative number which is used to quantify the regularity, unpredictability, and complexity of a time series. The calculation method is as follows:

Denote the rsfMRI data extract the time series of a voxel X= $[X_1, X_2, \ldots, X_n]$. Define the parameters m and r, where m is the pre-defined dimension, and r is a pre-specified distance threshold. Reconstruct the m-dimensional vector, $U_i = [X_i, X_{i+1}, \ldots, X_{i+m-1}]$, where if $= 1$ *to* $n - m + 1$

The distance between the two vectors $d\left(U_i, U_j\right) = max\left|U_i\left(a\right) - U_j(a)\right|$, and we get

$$C_i^m\left(r\right) = \left(n - m + 1\right)^{-1}\left[\textit{the number of}\ \mathrm{d}\left(U_i, U_j\right) < r\right] \quad (1)$$

$$\Phi^m\left(r\right) = \left(n - m + 1\right)^{-1}\sum_{i=1}^{N-m+1} C_i^m(r) \quad (2)$$

Repeat the above steps to get $\Phi^{m+1}\left(r\right)$.

$$ApEn\left(m, r\right) = \Phi^m\left(r\right) - \Phi^{m+1}\left(r\right) \quad (3)$$

Sample Entropy

SampEn (25) excludes self-matching compared to ApEn.

$$C_i^m\left(r\right) = \left(n - m - 1\right)^{-1}\left[\textit{the number of}\ \mathrm{d}\left(U_i, U_j\right) < r\right] \quad (4)$$

where j changes from 1 to n–m, and $j \neq i$.

$$\Phi^m\left(r\right) = \left(n - m\right)^{-1}\sum_{i=1}^{N-m+1} C_i^m(r) \quad (5)$$

$$SampEn\left(m, r\right) = In\Phi^{m+1}\left(r\right) - In\Phi^m\left(r\right) = -\ln\left(\frac{\Phi^m\left(r\right)}{\phi^{m+1}\left(r\right)}\right) \quad (6)$$

Fuzzy Entropy

FuzzyEn (26) introduces the fuzzy membership function $\mu(\mathrm{d})$ on the basis of the SampEn, and removes a baseline. Introduce the fuzzy membership function $u\left(d\right)$:

$$u\left(d\right) = \begin{cases} 1 & d = 0 \\ \exp\left[-ln\left(2\right)\left(\frac{d}{r}\right)^2\right] & d > 0 \end{cases} \quad (7)$$

Where d is the distance between the two vectors.

$$C_i^m(r) = \sum u(d)/(n-m+1) \quad (8)$$

$$\Phi^m(r) = (n-m+1)^{-1} \sum_{i=1}^{N-m+1} C_i^m(r) \quad (9)$$

Repeat the above steps to get $\Phi^{m+1}(r)$.

$$\text{FuzzyEn}(m,r) = \text{In}\Phi^m(r) - In\Phi^{m+1}(r). \quad (10)$$

Comparison of Three Entropies

For ApEn:

$$\begin{aligned}\text{ApEn}(\text{m},\text{r}) &= \Phi^{\text{m}}(\text{r}) - \Phi^{\text{m+1}}(\text{r}) \\ &= \sum_{\text{i=1}}^{\text{N-m+1}} \ln[\text{C}_\text{i}^{\text{m}}(\text{r})/\text{C}_\text{i}^{\text{m+1}}(\text{r})] \end{aligned} \quad (11)$$

Where pi= $C_i^m(r)/C_i^{m+1}(r)$ is the conditional probability that the time series will produce a new pattern when the dimension changes. In order to avoiding the appearance of $\ln(0)$, the ApEn has a self-comparison value in the process of comparing whether two vectors are similar. Obviously, such an algorithm is unscientific, so SampEn optimizes it and eliminates the bias caused by self-matching.

For SampEn:

$$\begin{aligned}SampEn(m,r) &= \text{In}\Phi^{\text{m}}(\text{r}) - \text{In}\Phi^{\text{m+1}}(\text{r}) \\ &= \text{In}[\sum \text{C}_\text{i}^{\text{m}}(\text{r})/\sum \text{C}_\text{i}^{\text{m+1}}(\text{r})] \end{aligned} \quad (12)$$

The calculation of SampEn is to first sum and then take the logarithm to avoid the appearance of $\ln(0)$, which does not include the comparison of its own data segments. The other steps are similar to ApEn, so SampEn theoretically has higher accuracy than ApEn. Although SampEn is an improved algorithm of ApEn, ApEn is closely related to the definition of the traditional definition of entropy whose existence helps us better understand the nature of entropy.

For ApEn and SampEn, judging whether two vectors are similar is depending on the parameter *r*. As long as the distance is within *r*, the two vectors are considered similar, which means that they will be considered dissimilar even if the distance is only slightly larger than *r*. That will let them have significant changes due to changes in the parameter *r*. For FuzzyEn, the concept of fuzzy is introduced into the calculation of entropy. The value taken in the interval [0, 1] is used to replace *t* 0 and 1. The soft continuous boundary not only guarantees the definition of the fuzzy function at small parameters, but also makes the fuzzy function change continuously. In addition, compared to ApEn and FuzzyEn, when constructing the m-dimensional similarity vector, a baseline is removed, which makes the definition of FuzzyEn more accurate than the other two (26).

MATERIALS AND METHODS

Subjects

We recruited 74 drug-naive patients diagnosed with OCD using the Structured Clinical Interview for DSM-IV Axis I Disorders (SCID) by two experienced psychiatrists from the Mental Health Center, West China Hospital, Sichuan University, and 93 healthy control subjects (HCs) matched for sex and age via poster advertisements. Only right-handed Chinese individuals between 18 and 60 years of age were included, and the exclusion criteria for both groups included (1) any history of major physical illness, cardiovascular disease, or psychiatric or neurological disorder; (2) substance abuse or dependence; (3) inability to undergo an MRI scan; and (4) pregnancy. Additionally, OCD patients with a psychiatric comorbidity assessed using the SCID were excluded. The Yale-Brown-Obsessive-Compulsive Scale (YBOCS) was used to evaluate OCD symptoms severity, and anxiety and depressive symptoms were assessed using the 14-item Hamilton Anxiety Scale (HAMA) and 17-item Hamilton Depression Scale (HAMD), respectively. This study was approved by the Ethics Committee of the West China Hospital, Sichuan University. All subjects provided an informed consent form.

rsfMRI Data Acquisition and Preprocessing

All the images were obtained using a 3T GE MRI scanner with an eight-channel phase-array head coil. The following scanning parameters were used: number of slices = 30, time repetition (TR) = 2,000 ms, time echo = 30 mms, flip angle = 90, slice thickness = 5 mm with no slice gap, field of view = 240 × 240 mm^2, and 200 volumes in each run. We also acquired a high-resolution T_1-weighted 3D sequence (TR = 8.5ms, echo time = 3.4 ms, flip angle = 12), slice thickness = 1.0mm, field of view = 240 × 240 mm^2). Imaging preprocessing was carried out using the Data Processing and Analysis of Brain Imaging (DPABI) toolbox (27) (http://rfmri.org/dpabi). Preprocessing steps included (1) discarding the first 10 images for magnetization equilibrium and (2) slice timing correction and head-motion correction for the remaining 190 images. The mean framewise displacement (FD) was calculated to evaluate the head movement of each participant. To minimize the effect of head motion, we selected a stringent criterion: excluded the participants whose maximal head movement translation exceeded 3 mm, whose mean FD was more than 0.2 mm or whose rotation was more than 2. One patient and three HCs were excluded due to excessive head motion. Next, (3) spatial normalization to standard Montreal Neurological Institute space and resampling to 3 × 3 × 3 mm^3 resolution *via* T_1-weighted anatomical images were performed. (4) The cerebrospinal fluid signal, white matter and Friston-24 motion parameters were considered nuisance covariates, and global signal regression was not used (28). Finally, (5) the data were spatially smoothed with an 8 mm full-width half-maximum (FWHM) isotropic Gaussian kernel.

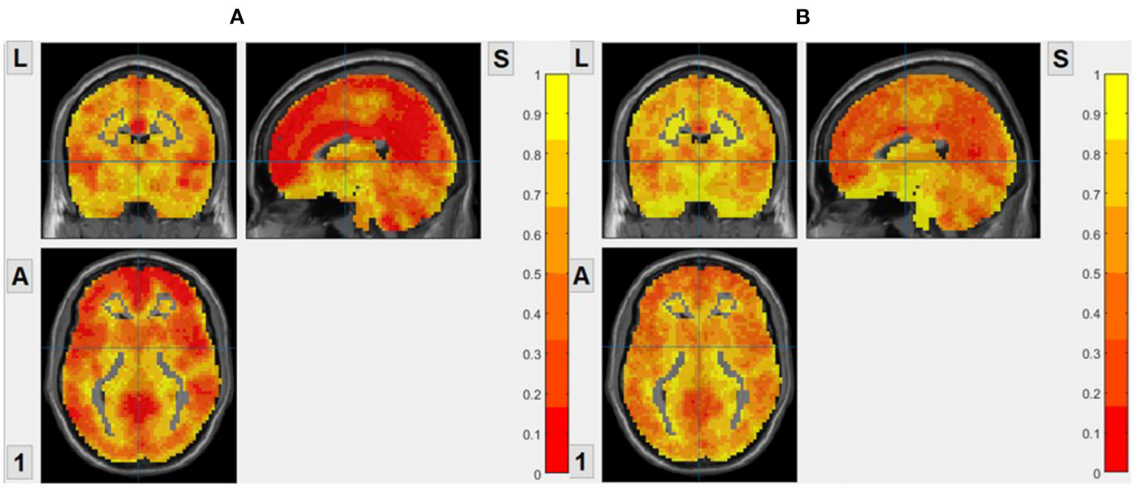

FIGURE 1 | The brain entropy distribution of a normal subject. **(A)** ApEn, based on voxel, $m = 2$, $r = 0.2$. **(B)** FuzzyEn, based on voxel, $m = 2$, $r = 0.2$.

Brain Entropy Calculation

After preprocessing, we calculated the brain entropy. Refer to 1.1 for the calculation method, and based on the literature (26), m usually is taken as 2 or 3, and r is usually taken from 0.2 to 1.2, which depends on the actual application scenario. In this experiment we take $m = 3$ and $r = 0.2$.

Statistical Analysis

Two-sample t-test was used to compare the differences in brain entropy between the two groups. The covariables contained age, gender, and head motion. And we used false discover rate (FDR) correction for the multiple comparisons and the significance level was set $p < 0.05$.

RESULT

The Distribution of Brain Entropy

As shown in **Figure 1**, We calculated the brain entropy of the entire brain area of normal people and found that the distribution of ApEn and FuzzyEn is generally consistent with the brain structure and functional partition, but SampEn isn't. So, we do not show the brain entropy distribution of SampEn.

Gender Differences of Brain Entropy

We divided the subjects in the group into two groups according to gender, and compare whether there are obvious gender differences in brain entropy. None of the three entropies show significant differences between genders.

Brain Entropy Based on Voxel

We set patients with OCD as the experimental group and healthy subjects as the control group. The brain entropy of the OCD group and the HC are calculated by voxel. And we use two-sample t-test to compare the differences in brain entropy between the two groups. The covariables contained age, gender, and head motion. And we used false discover rate (FDR) correction for multiple comparisons and the significance level was set $p < 0.05$. The result is shown in **Figure 2**, For ApEn, the result shows that the ApEn of almost the whole brain of OCD is greater than that of HC. For FuzzyEn, the result also shows that the FuzzyEn of OCD is greater than that of HC, but there are fewer brain regions with difference. For SampEn**,** there is no statistical difference between OCD and HC, so we do not show that.

Brain Entropy Based on AAL

We took the average of the time series of all voxels in the same brain area as the time series of the brain area, and then calculated the brain entropy values based on AAL. **Figure 3** shows the brain regions with a significant difference in brain entropy between OCD and HC including frontal region, Hippocampus, ParaHippocampal, and Thalamus.

DISCUSSION

From this experiment, both ApEn and FuzzyEn can reflect the abnormality of OCD brain entropy. And it is obvious that compared with FuzzyEn there are more different brain regions using ApEn. It seems that ApEn is more sensitive and can better reflect the difference between OCD and HC, which is not in accordance with the results of our previous theoretical analysis (the definition of FuzzyEn is more accurate than the other two).

In order to further evaluate the reliability of the different brain entropy analysis, we calculate the entropy of a simulated signal consisting of a certain signal and noise to investigate their robustness. Details and results are as follows.

To test the sensitivity of the three entropies, we extract a voxel time series of cerebrospinal fluid as noise, add sine waves of different amplitudes as certain signals, and then measure the brain entropy of the mixed signal. From **Figure 4**, we can see that the entropy decreases with the amplitude of the sine

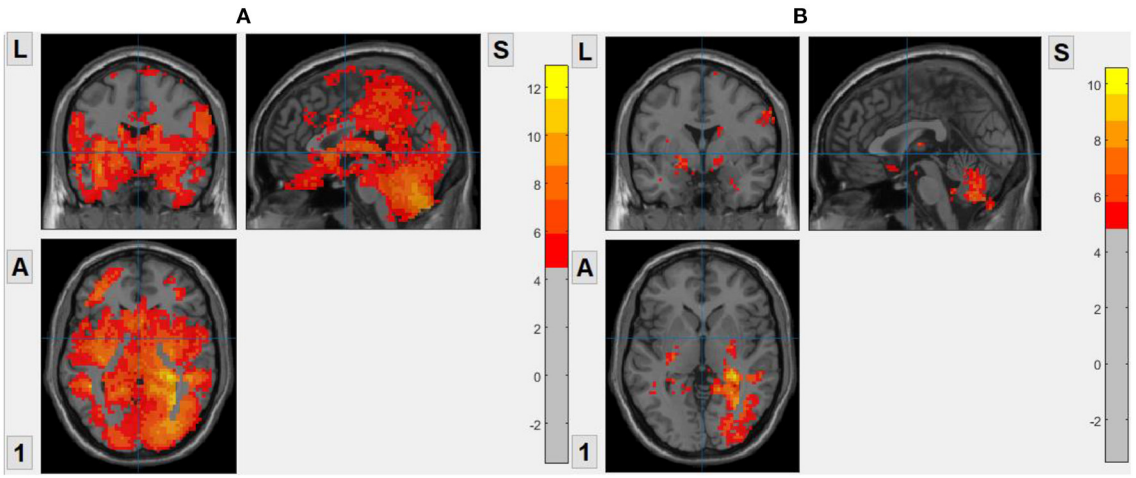

FIGURE 2 | Brain regions with statistical differences between OCD and HC. Warm color means OCD has a higher value. **(A)** ApEn, based on voxel, $m = 2$, $r = 0.2$. **(B)** FuzzyEn, based on voxel, $m = 2$, $r = 0.2$.

wave increases. When the signal amplitude is much greater than the noise, the entropy is almost a fixed value. The change of SampEn and ApEn is faster than FuzzyEn, which maybe affect the sensitivity of entropy index, but the ApEn is unstable and fluctuates irregularly.

To test the robustness to noise of the three entropies, we measure the brain entropy of the sine wave signal, which add Gaussian white noise with different intensity of noise. From **Figure 5**, it can be found that ApEn fluctuates greatly and is unstable with the change of noise intensity, which may be indicate that ApEn shows quite sensitive to the changes of noise, while FuzzyEn is the most stable to the change in noise. FuzzyEn shows the best robustness to noise, which is similar to the results of previous studies (26).

From the above two simulations, we find that although ApEn has higher sensitivity, its robustness to noise is not as good as FuzzyEn. This may be the reason why we get more brain regions with entropy difference between OCD and HC when we use ApEn. In addition, although SampEn shows good sensitivity and robustness to noise in the simulation, in the experiment, it does not show the difference between OCD and HC. This may be because the above two simple simulations cannot fully evaluate these three entropies, and it may also be related to the selection of parameters r. When we take similarity $r = 0.6$, there is a significant difference between OCD and HC. So, we integrated theory, experiment, and simulation to conclude that FuzzyEn is the most accurate.

There are studies finding that the onset of OCD is probably due to the abnormality of the Cortico-striate-thalami-cortical (CSTC) (18), especially the orbit frontal cortex (OFC), anterior cingulate cortex (ACC), striatum and thalamus (20). In addition, studies have pointed out that the brain default network (29), the prominent network and the limbic system of OCD patients are also abnormal to a certain extent. And, in this article, compare with the control group, almost the whole brain's entropies of OCD are larger significantly. Among them the entropy of the default network (default mode network, DMN), left and right OFC, thalamus, and ACC increase the most. OFC is a classic brain area in the CSTC loop. Previous studies have shown that it has abnormalities in structure, function, and metabolism. ACC is involved in the regulation of selective attention; OFC is involved in the regulation of impulsive behavior. Entropy represents the irregularity and information processing ability of a system, and the increase of entropy indicates the increase of the randomness and complexity of a system, which means that OCD patients perform an increased neuronal activity in the above brain areas in the resting state. And this is also consistent with the clinical manifestations of OCD obsessive thinking and compulsive behavior. The abnormality of CTSC and DMN function was verified from the perspective of entropy, which is similar to the results of previous studies.

In this study, the FuzzyEn of the left dorsolateral prefrontal cortex (DLPFC) of patients with OCD in the resting state is significantly higher. DLPFC participates in anxiety and other negative emotion regulation (30, 31) and goal-oriented planning, cognitive re-evaluation, and other cognitive executive functions (32), which is consistent with our brain entropy research results. The hippocampus is an important emotion regulation center, and has always been an important nucleus of depression research. And the paraHippocampal gyrus is an important structure for the hippocampus to function. Damage to its structure can cause abnormalities in emotion and cognitive behavior. This study found that the fuzzy entropy of the above two brain regions of OCD patients was significantly greater than that of HC.

There are still a few limitations in this study. The sample size is generally small, and the conclusions are not very representative. Secondly the fMRI data has the characteristics of

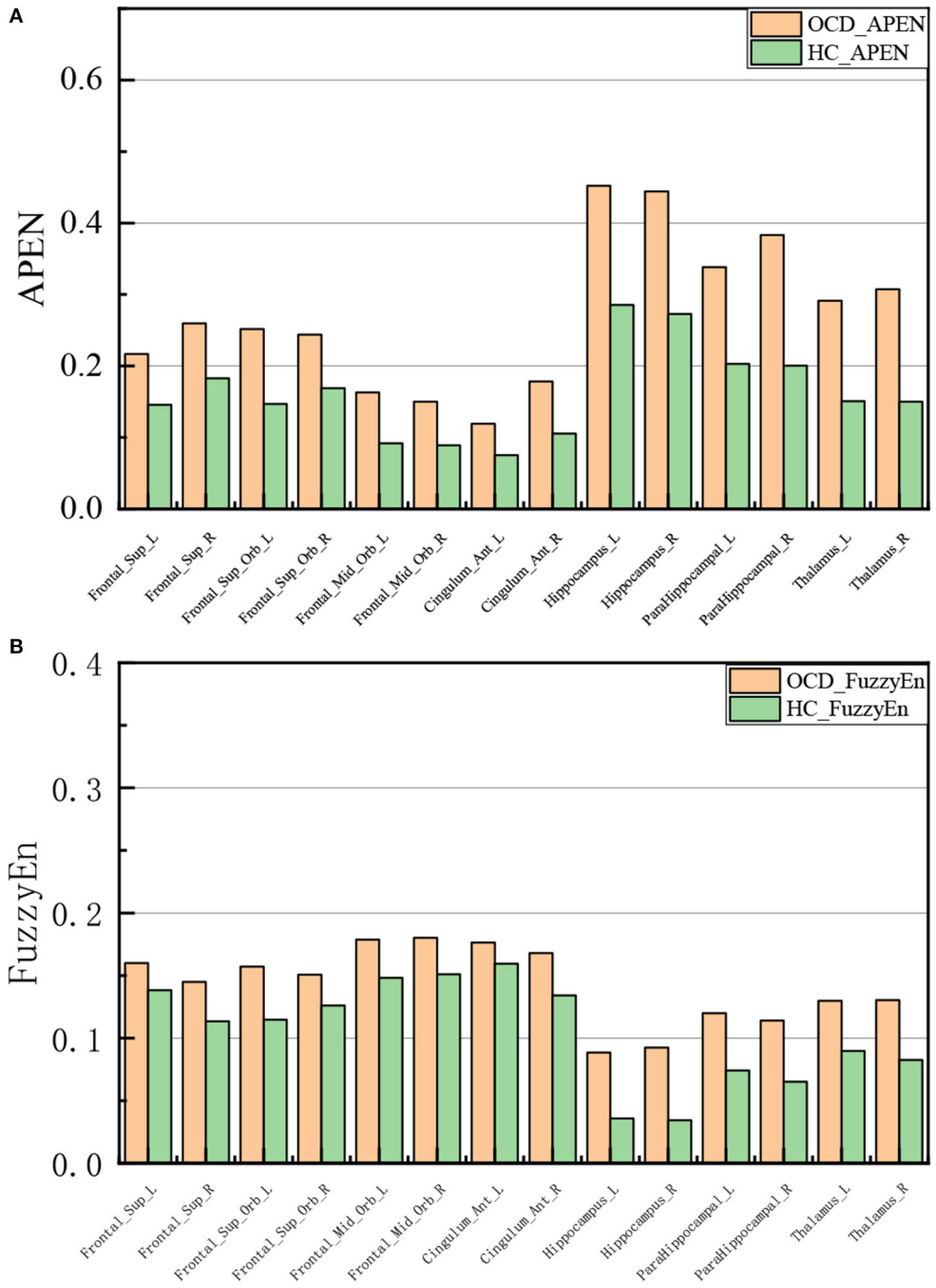

FIGURE 3 | Brain regions with statistical differences between OCD and HC. **(A)** ApEn **(B)** FuzzyEn.

low signal-to-noise ratio. And we did not consider the influence of the characteristic symptoms of OCD patients on neuronal activity during the statistical analysis. The above two simple simulations cannot fully evaluate these three entropies. Our future research plans to further increase the sample size, refine the characteristic symptoms, eliminate the noise, and simulate the real BOLD signal as much as possible to study the brain conditions of OCD.

CONCLUSION

Brain entropy can quantitatively describe non-linear time series and provide new ideas for describing brain characteristics. From a theoretical point of view, the core of these three types of entropy is the conditional probability that the similarity vector continues to maintain its similarity when it increases from m-dimension to m + 1-dimension. The optimization of SampEn relative to ApEn

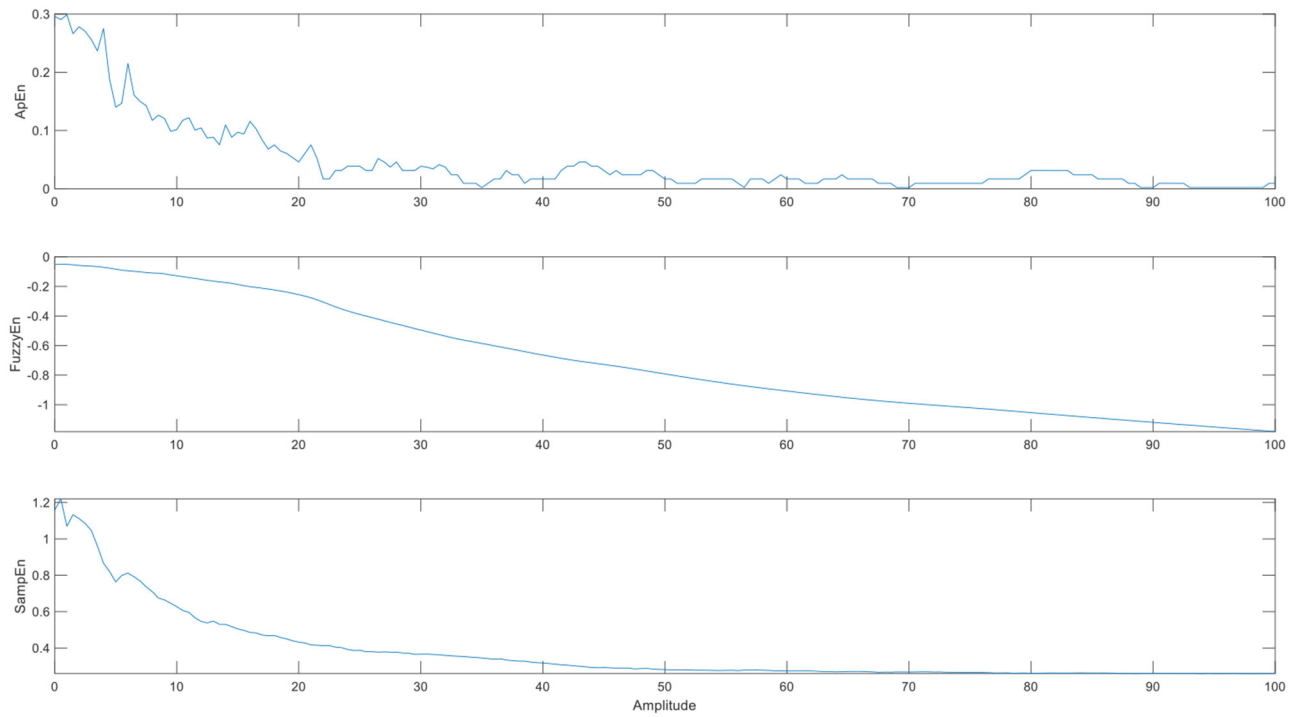

FIGURE 4 | The brain entropy adding different amplitudes of sine waves to a voxel time series of cerebrospinal fluid. (The abscissa is the amplitude of the sine wave, and its value is a multiple of the maximum noise).

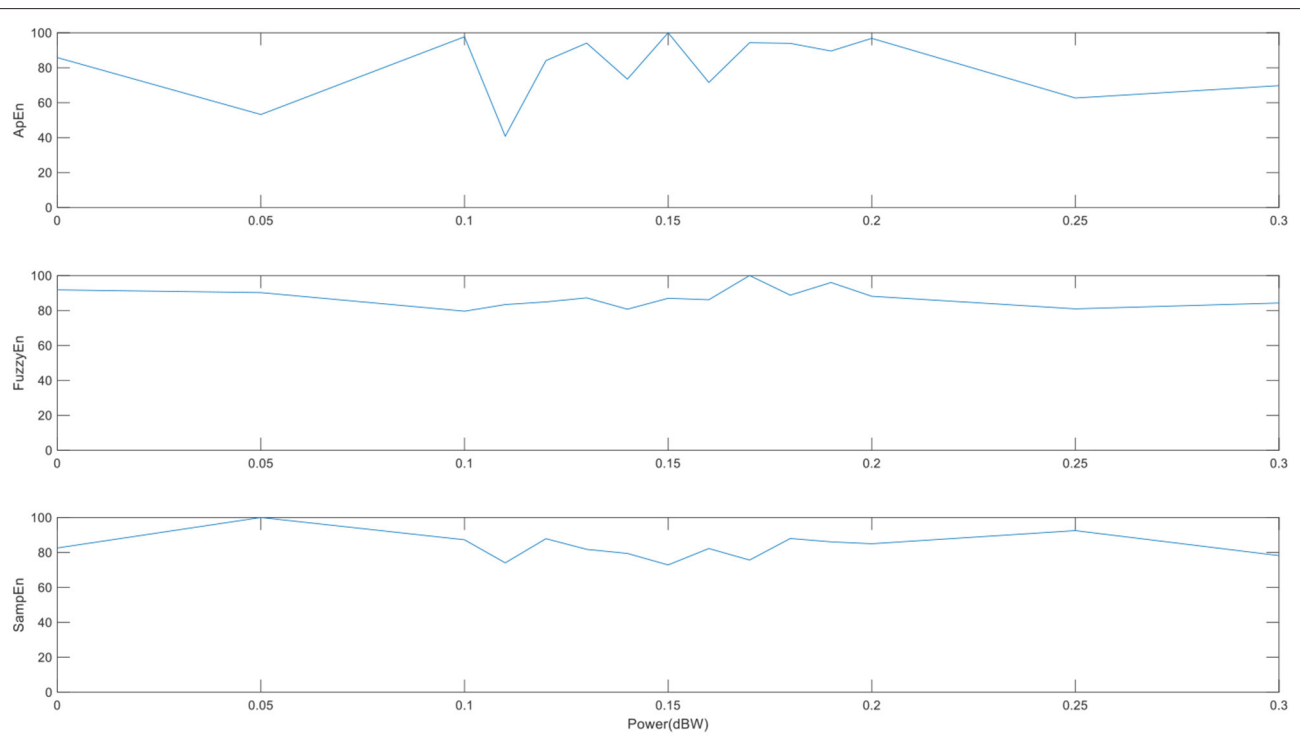

FIGURE 5 | The performances of the three entropies adding different noise level. (The abscissa is the intensity of the specified output noise in the unit).

is to exclude the influence of self-matching. The optimization of FuzzyEn lies in the introduction of a fuzzy boundary, which makes it less sensitive to the distance threshold *r*, and a slight change in *r* will not change the result greatly.

From the experimental results, although ApEn has higher sensitivity, its robustness to noise is not as good as FuzzyEn. And the SampEn does not show the difference between OCD and HC. we conclude that FuzzyEn is more accurate considering sensitivity, stability and robustness of entropy.

In conclusion, the brain is a complex system, and brain entropy can measure the complexity of the human brain. It provides us with different aspect for researching brain activity, and helps us understand our brains in a different direction. In addition, among the three kinds of entropy mentioned in the article, both theoretically and experimentally, it seems that using FuzzyEn is more accurate.

DATA AVAILABILITY STATEMENT

The original contributions presented in the study are included in the article/supplementary material, further inquiries can be directed to the corresponding author/s.

ETHICS STATEMENT

The studies involving human participants were reviewed and approved by the Ethics Committee of the West China Hospital, Sichuan University. The patients/participants provided their written informed consent to participate in this study.

AUTHOR CONTRIBUTIONS

XJ: conceptualization, formal analysis, methodology, software, visualization, writing—original draft, writing—review and editing. XL: conceptualization, data curation, formal analysis, methodology, validation, writing—review and editing. HX and XH: writing—review and editing, funding acquisition, project administration, and supervision. XX and JL: writing—review and editing. All authors contributed to the article and approved the submitted version.

FUNDING

This study was supported by the National Key Technologies R&D Program of China (Grant No. 82027808), the Key Research Project of Sichuan Science and Technology Department (Grant No. 2020YFS0048), and the Science Specialty Program of Sichuan University (Grant No. 2020SCUNL210).

ACKNOWLEDGMENTS

We thank HX and XH for comments on early versions of this manuscript.

REFERENCES

1. Shannon C. A mathematical theory of communication. *Mobile Comput Commun Rev.* (2001) 5:3–55. doi: 10.1145/584091.584093
2. Wang Z, Li Y, Childress A, Detre J. Brain entropy mapping using fMRI. *PLoS ONE.* (2014) 9:E89948. doi: 10.1371/journal.pone.0089948
3. Saxe G, Calderone D, Morales L. Brain entropy and human intelligence: a resting-state fMRI study. *PLoS ONE.* (2018) 13:E0191582. doi: 10.1371/journal.pone.0191582
4. Shi L, Beaty R, Chen Q, Sun J, Wei D, Yang W, et al. Brain entropy is associated with divergent thinking. *Cereb Cortex.* (2020) 30:708–17. doi: 10.1093/cercor/bhz120
5. Chang D, Song D, Zhang J, Shang Y, Ge Q, Wang Z. Caffeine caused a widespread increase of resting brain entropy. *Sci Rep.* (2018) 8:2700–7. doi: 10.1038/s41598-018-21008-6
6. Yang A, Huang C, Yeh H, Liu M, Hong C, Tu P, et al. Complexity of spontaneous BOLD activity in default mode network is correlated with cognitive function in normal male elderly: a multiscale entropy analysis. *Neurobiol Aging.* (2013) 34:428–38. doi: 10.1016/j.neurobiolaging.2012.05.004
7. Yao Y, Lu W, Xu B, Li C, Lin C, Waxman D, et al. The increase of the functional entropy of the human brain with age. *Sci Rep.* (2013) 3:2853. doi: 10.1038/srep02853
8. Smith R, Yan L, Wang D. Multiple time scale complexity analysis of resting state FMRI. *Brain Imaging Behav.* (2014) 8:284–91. doi: 10.1007/s11682-013-9276-6
9. Li T, Yao Y, Cheng Y, Xu B, Cao X, Waxman D, et al. Cognitive training can reduce the rate of cognitive aging: a neuroimaging cohort study. *BMC Geriatr.* (2016) 16:12. doi: 10.1186/s12877-016-0194-5
10. Zhou F, Zhuang Y, Gong H, Zhan J, Grossman M, Wang Z. Resting state brain entropy alterations in relapsing remitting multiple sclerosis. *PLoS ONE.* (2016) 11:E0146080. doi: 10.1371/journal.pone.0146080
11. Sokunbi M, Gradin V, Waiter G, Cameron G, Ahearn T, Murray A, et al. Nonlinear complexity analysis of brain FMRI signals in schizophrenia. *PLoS ONE.* (2014) 9:E95146. doi: 10.1371/journal.pone.0095146
12. Liu C, Krishnan A, Yan L, Smith R, Kilroy E, Alger J, et al. Complexity and synchronicity of resting state blood oxygenation level-dependent (BOLD) functional MRI in normal aging and cognitive decline. *J Magnet Reson Imaging.* (2013) 38:36–45. doi: 10.1002/jmri.23961
13. Sato J, Takahashi D, Hoexter M, Massirer K, Fujita A. Measuring network's entropy in ADHD: a new approach to investigate neuropsychiatric disorders. *NeuroImage.* (2013) 77:44–51. doi: 10.1016/j.neuroimage.2013.03.035
14. Qiu L, Fu X, Wang S, Tang Q, Chen X, Cheng L, et al. Abnormal regional spontaneous neuronal activity associated with symptom severity in treatment-naive patients with obsessive-compulsive disorder revealed by resting-state functional MRI. *Neurosci Lett.* (2017) 640:99–104. doi: 10.1016/j.neulet.2017.01.024
15. Fan J, Zhong M, Gan J, Liu W, Niu C, Liao H, et al. Spontaneous neural activity in the right superior temporal gyrus and left middle temporal gyrus is associated with insight level in obsessive-compulsive disorder. *J Affect Disord.* (2016) 207:203–11. doi: 10.1016/j.jad.2016.08.027
16. Niu Q, Yang L, Song X, Chu C, Liu H, Zhang L, et al. Abnormal resting-state brain activities in patients with first-episode obsessive-compulsive disorder. *Neuropsychiatr Dis Treatment.* (2017) 13:507–13. doi: 10.2147/NDT.S117510
17. Sun T, Song Z, Tian Y, Tian W, Zhu C, Ji G, et al. Basolateral amygdala input to the medial prefrontal cortex controls obsessive-compulsive disorder-like checking behavior. *Proc Natl Acad Sci.* (2019) 116:3799–804. doi: 10.1073/pnas.1814292116
18. Jang J, Kim J, Jung W, Choi J, Jung M, Lee J, et al. Functional connectivity in fronto-subcortical circuitry during the resting state in obsessive-compulsive disorder. *Neurosci Lett.* (2010) 474:158–62. doi: 10.1016/j.neulet.2010.03.031
19. Nakamae T, Sakai Y, Abe Y, Nishida S, Fukui K, Yamada K, et al. Altered fronto-striatal fiber topography and connectivity in obsessive-compulsive disorder. *PLoS ONE.* (2014) 9:E112075. doi: 10.1371/journal.pone.0112075

20. Posner J, Marsh R, Maia T, Peterson B, Gruber A, Simpson H. Reduced functional connectivity within the limbic cortico-striato-thalamo-cortical loop in unmedicated adults with obsessive-compulsive disorder. *Hum Brain Mapp.* (2014) 35:2852–60. doi: 10.1002/hbm.22371
21. Göttlich M, Krämer U, Kordon A, Hohagen F, Zurowski B. Decreased limbic and increased fronto-parietal connectivity in unmedicated patients with obsessive-compulsive disorder. *Hum Brain Mapp.* (2014) 35:5617–32. doi: 10.1002/hbm.22574
22. Pincus S. Approximate entropy as a measure of system complexity. *Proc Natl Acad Sci.* (1991) 88:2297–301. doi: 10.1073/pnas.88.6.2297
23. Aftanas L, Lotova N, Koshkarov V, Pokrovskaja V, Popov S, Makhnev V. Non-linear analysis of emotion EEG: calculation of Kolmogorov entropy and the principal Lyapunov exponent. *Neurosci Lett.* (1997) 226:13–6. doi: 10.1016/S0304-3940(97)00232-2
24. Gao L, Wang J, Chen L. Event-related desynchronization and synchronization quantification in motor-related EEG by Kolmogorov entropy. *J Neural Eng.* (2013) 10:036023. doi: 10.1088/1741-2560/10/3/036023
25. Richman J, Moorman J. Physiological time-series analysis using approximate entropy and sample entropy. *Am J Physiol Heart Circulat Physiol.* (2000) 278:2039–49. doi: 10.1152/ajpheart.2000.278.6.H2039
26. Chen W, Zhuang J, Yu W, Wang Z. Measuring complexity using FuzzyEn, ApEn, and SampEn. *Med Eng Physics.* (2008) 31:61–8. doi: 10.1016/j.medengphy.2008.04.005
27. Chao-Gan Y, Yu-Feng Z. DPARSF: a MATLAB toolbox for "Pipeline" data analysis of resting-state fMRI. *Front Syst Neurosci.* (2010) 4:13. doi: 10.3389/fnsys.2010.00013
28. Saad Z, Gotts S, Murphy K, Chen G, Jo H, Martin A, Cox R. Trouble at rest: How correlation patterns and group differences become distorted after global signal regression. *Brain Connectivity.* (2012) 2:25.
29. Stern E, Fitzgerald K, Welsh R, Abelson J, Taylor S. Resting-state functional connectivity between fronto-parietal and default mode networks in obsessive-compulsive disorder. *PLoS ONE.* (2012) 7:E36356. doi: 10.1371/journal.pone.0036356
30. Han H, Jung W, Yun J, Park J, Cho K, Hur J, et al. Disruption of effective connectivity from the dorsolateral prefrontal cortex to the orbitofrontal cortex by negative emotional distraction in obsessive–compulsive disorder. *Psychol Med.* (2016) 46:921–32. doi: 10.1017/S0033291715002391
31. De Wit S, Van der Werf Y, Mataix-Cols D, Trujillo J, Van Oppen P, Veltman D, et al. Emotion regulation before and after transcranial magnetic stimulation in obsessive compulsive disorder. *Psychol Med.* (2015) 45:3059–73. doi: 10.1017/S0033291715001026
32. Vaghi M, Vértes P, Kitzbichler M, Apergis-Schoute A, Van der Flier F, Fineberg N, et al. Specific frontostriatal circuits for impaired cognitive flexibility and goal-directed planning in obsessive-compulsive disorder: evidence from resting-state functional connectivity. *Biol Psychiatry (1969).* (2016) 81:708–17. doi: 10.1016/j.biopsych.2016.08.009

Conflict of Interest: The authors declare that the research was conducted in the absence of any commercial or financial relationships that could be construed as a potential conflict of interest.

frontiers in Human Neuroscience

ORIGINAL RESEARCH
published: 15 November 2021
doi: 10.3389/fnhum.2021.777762

Altered Brain Structure and Spontaneous Functional Activity in Children With Concomitant Strabismus

*Xiaohui Yin[1], Lingjun Chen[2], Mingyue Ma[1], Hong Zhang[1], Ming Gao[1], Xiaoping Wu[1] and Yongqiang Li[3]**

[1]Department of Radiology, The Affiliated Xi'an Central Hospital of Xi'an Jiaotong University, Xi'an, China, [2]Department of Radiology, Gaoling District Hospital, Xi'an, China, [3]Department of CT and MRI, Weinan Hospital of Traditional Chinese Medicine, Weinan, China

Strabismus occurs in about 2% of children and may result in amblyopia or lazy eyes and loss of depth perception. However, whether/how long-term strabismus shapes the brain structure and functions in children with concomitant strabismus (CS) is still unclear. In this study, a total of 26 patients with CS and 28 age-, sex-, and education-matched healthy controls (HCs) underwent structural and resting-state functional magnetic resonance imaging examination. The cortical thickness and amplitude of low-frequency fluctuation (ALFF) were calculated to assess the structural and functional plasticity in children with CS. Compared with HCs group, patients with CS showed increased cortical thickness in the precentral gyrus and angular gyrus while decreased cortical thickness in the left intraparietal sulcus, parieto-occipital sulcus, superior and middle temporal gyrus, right ventral premotor cortex, anterior insula, orbitofrontal cortex, and paracentral lobule. Meanwhile, CS patients exhibited increased ALFF in the prefrontal cortex and superior temporal gyrus, and decreased ALFF in the caudate and hippocampus. These results show that children with CS have abnormal structure and function in brain regions subserving eye movement, controls, and high-order cognitive functions. Our findings revealed the structural and functional abnormalities induced by CS and may provide new insight into the underlying neural mechanisms for CS.

Keywords: concomitant strabismus, cortical thickness, ALFF, structural MRI, resting-state fMRI

OPEN ACCESS

Edited by:
Bochao Cheng,
Sichuan University, China

Reviewed by:
Lijie Wang,
University of Electronic Science and Technology of China, China
Jingjing Gao,
University of Electronic Science and Technology of China, China

****Correspondence:***
Yongqiang Li
wnlyq8688@163.com

Specialty section:
This article was submitted to Brain Imaging and Stimulation, a section of the journal Frontiers in Human Neuroscience

Received: *15 September 2021*
Accepted: *25 October 2021*
Published: *15 November 2021*

Citation:
Yin X, Chen L, Ma M, Zhang H, Gao M, Wu X and Li Y (2021) Altered Brain Structure and Spontaneous Functional Activity in Children With Concomitant Strabismus. Front. Hum. Neurosci. 15:777762. doi: 10.3389/fnhum.2021.777762

INTRODUCTION

Concomitant strabismus (CS) is the most common type of strabismus and is characterized by an equal angle of ocular misalignment in all fields of gaze, regardless of which eye is used for fixation ocular motility disorders (Robaei et al., 2006). CS develops most commonly in early childhood and presents with abnormal eye position and poor stereopsis (Oystreck and Lyons, 2012). Alternatively, children with CS often suffer from several psychosocial and emotional consequences, for example, negative social bias, increased social anxiety, and poor interpersonal relationship (Archer et al., 2005). Nevertheless, beyond the clinical data, the pathological mechanisms underlying CS remain unclear. Accordingly, it is urgently needed to deepen the current understanding of the etiology of CS, which may provide new clues of the planning of the surgery.

Magnetic resonance imaging (MRI) techniques have developed rapidly to provide a non-invasive neuroimaging method that can characterize the structural and functional changes in the brain (Singh et al., 2013; Pirnia et al., 2016; Wang et al., 2017, 2019; Xu et al., 2019b). Using structural MRI, decreased gray matter volume (GMV) and white matter volume (WMV) in the middle temporal gyrus, cerebellum posterior lobe, posterior cingulate cortex, and premotor cortex were found in CS patients, and the decreased GMV and WMV were negatively correlated with duration (Ouyang et al., 2017). In addition, patients with CS also exhibited abnormal fractional anisotropy and mean diffusivity vales in the prefrontal cortex (PFC), superior temporal gyrus, globus pallidus/brainstem, precuneus, anterior cingulate, and cerebellum posterior lobe (Huang et al., 2016a). Measuring the spontaneous brain activity, resting-state functional MRI study reported abnormal amplitude of low-frequency fluctuation (ALFF) values in the medial PFC, angular gyrus, and cerebellum posterior lobe, and the changed ALFF values in these areas were correlated with the degree of depression in adults with CS (Tan et al., 2016). The increased regional homogeneity values in the inferior temporal cortex, fusiform gyrus, cerebellum anterior lobe, lingual gyrus, and cingulate gyrus were also reported in adults with CS (Huang et al., 2016b). Moreover, CS patients had increased functional connectivity between the posterior primary visual cortex and other oculomotor regions (Yan et al., 2019). These findings suggest significant brain abnormalities in CS, which may underlie the pathologic mechanisms of fusion defects and ocular motility disorders in patients with CS. However, the above mentioned studies were focused on adults with CS, whether/how the structure and function change in children with CS remains unclear.

In the present study, the cortical thickness and ALFF were calculated in order to measure the brain structure and intrinsic activity in children with CS. Based on previous literature, we hypothesized that children with CS would exhibit abnormal cortical thickness and ALFF in brain regions subserving eye movement, cognition, and emotion.

MATERIALS AND METHODS

Participants

A total of 26 patients with CS (16 males and 12 females) were recruited from the affiliated Xi'an Central Hospital of Xi'an Jiaotong University. All patients were diagnosed by two experienced ophthalmologists according to the diagnostic criteria of the Chinese Medical Association. The inclusion criteria of CS were: (1) age with 8–15 years; (2) Naked or corrected visual acuity $\geq$0.8, and (3) children with no anisometropia, ocular and systemic organic diseases. The exclusion criteria were: (1) amblyopia, (2) patients with a history of previous ocular surgery, including intraocular and extraocular surgery, and (3) mental illness, brain trauma, and major neurological disorders. Twenty-eight healthy controls (HCs) who were closely matched in age, gender, and education level with patients with CS were recruited through advertisements. In all participants, the current severity of anxiety and depression was evaluated using the Hamilton Anxiety Scale (HAMA) and 17 items Hamilton Depression Rating Scale (HAMD), and cognitive function was assessed using the Montreal Cognitive Assessment scale (MoCA). The written informed consent was obtained from all participants before experimentation. This study was approved by the research ethics committee of the affiliated Xi'an Central Hospital of Xi'an Jiaotong University and is in accordance with the latest revision of the Declaration of Helsinki.

MRI Acquisition

The data of all participants were collected using a Philips 3.0 T MRI scanner. Head movement and scanner noise were controlled using foam pads and headphones. Participants were instructed to keep their eyes closed, not think of anything, not fall asleep, and keep their head motionless during scanning. The T1 structural image was scanned using the following parameters: repetition time/echo time = 8.2/3.7 ms, inversion time = 1,100 ms, flip angle = 7°, acquisition matrix = 256 × 256, field of view = 256 × 256 mm^2, voxel size = 1 × 1 × 1 mm^3 and no gap. Resting-state fMRI data were obtained using an echo-planar imaging sequence with the following parameters: repetition time/echo time = 2,000/30 ms, matrix size = 64 × 64, field of view = 230 × 230 mm^2, voxel size = 3.6 × 3.6 × 3.6 mm^3, flip angle = 90°, 38 slices, gap = 0.6 mm, and 240 volumes.

Structural MRI Preprocessing

The T1-weighted images were processed using the recon-all command in Freesurfer package 6.0.0 to generate the cortical surface and cortical thickness of the whole brain. The detailed pipeline has been described elsewhere (Dale and Sereno, 1993; Dale et al., 1999). For each subject, the preprocessing stream included motion correction, removal of non-brain tissue, transformation to Talairach space, segmentation of gray/white matter tissue, reconstructing the pial surface and surface of the gray/white junction, inflation of the folding surface plane, and topology correction (Fischl et al., 1999, 2002). Then, all surface data were visually inspected and inaccuracies were manually corrected. The thickness was defined as the shortest distance between the gray/white junction and the pial surfaces at each vertex across the cortical mantle. In order to arrive at the accurate matching of thickness measurement locations among participants, the cortical thickness maps were mapped to an average surface and were smoothed using a Gaussian kernel with a full width at half maximum (FWHM) of 10 mm prior to statistical analysis.

fMRI Preprocessing

Image preprocessing was performed using the DPARSF toolbox[1] based on SPM12[2]. The first 10 volumes were discarded before subsequent processing. The remaining 230 volumes were slice-timing and head motion correction. All participants were retained under the head motion criteria of translation <1.5 mm or rotation <1.5° in any direction. The data were then spatially normalized to the standard Montreal Neurological Institute

[1]http://rfmri.org/dpabi

[2]http://www.fil.ion.ucl.ac.uk/spm/software/spm12/

(MNI) space with a voxel size of $2 \times 2 \times 2$ mm^3. Nuisance covariates included white matter, cerebrospinal fluid, and the Friston-24 parameters of head motion were regressed out from each voxel's time course. The data were then smoothened with FWHM = 6 mm. The linear detrend and filtering (0.01–0.08 Hz) were performed to reduce the influence of low-frequency drift and high-frequency physiological noise. Subsequently, the filtered time series of each voxel was converted to the frequency domain using a Fast Fourier Transform and the power spectrum was then obtained. The averaged square root of the power spectrum was termed as ALFF. Lastly, the ALFF maps were standardized through division by the global mean of ALFF values.

Statistical Analysis

The group differences of whole-brain cortical thickness between CS and HCs groups were conducted based on GLM models with MoCA, HAMD, and HAMA as covariates in Freesurfer, and the surface-based findings were corrected using family-wise error rate (FWE) with $p < 0.05$.

The ALFF distribution in the CS and HCs groups was obtained by averaging ALFF values at each voxel across subjects of each group. A two-sample *t*-test was performed to assess the group differences in ALFF between the CS and HCs groups with MoCA, HAMD, and HAMA as covariates. The result was multiple corrected using Gaussian random field (GRF) theory with cluster corrected $p < 0.05$ and a voxel height of $p < 0.001$.

Correlation Analysis

Pearson correlation analyses were performed to evaluate the relationship between altered cortical thickness and ALFF of those identified regions and clinical performance, e.g., disease duration, HAMD, HAMA, and MoCA scores. The statistical significance was set at $p < 0.05$.

RESULTS

Demographics and Clinical Characteristics

The demographic and clinical information of the HCs and patients with CS are presented in **Table 1**. There were no differences in age ($p = 0.95$), gender ($p = 0.97$), and years of education ($p = 0.68$) between two groups. However, the patients with CS showed higher HAMA ($p = 0.026$) and HAMD ($p = 0.018$) scores, whereas lower MoCA scores ($p = 0.003$) than HCs.

Cortical Thickness Changes in CS Patients

In contrast to HCs, patients with CS showed increased cortical thickness in the left precentral gyrus and right angular gyrus, while decreased cortical thickness in the left intraparietal sulcus, parieto-occipital sulcus, superior and middle temporal gyrus, right ventral premotor cortex, anterior insula, orbitofrontal cortex, and paracentral lobule (**Figure 1**).

ALFF Changes in CS Patients

Contrast to HCs, the patients with CS showed increased ALFF in the increased ALFF in the prefrontal cortex and superior temporal gyrus, and decreased ALFF in the caudate and hippocampus (**Figure 2** and **Table 2**).

Correlation Results

There were no significant correlations between altered cortical thickness, ALFF values, and disease duration, HAMA, HAMD, and MoCA scores.

DISCUSSION

This is the first study to investigate the change of structure and function of brain regions in children with CS. In contrast to HCs, CS patients showed increased cortical thickness in the precentral gyrus and angular gyrus, decreased cortical thickness in the frontal, parietal, occipital, and temporal cortex regions. Meanwhile, CS patients exhibited increased ALFF in the frontal and temporal cortex regions and decreased ALFF in the subcortical regions. These results provided novel evidence to deepen our understanding of the pathological mechanism underlying children with CS.

Children with CS showed abnormal cortical thickness in brain regions subserving visual information processing and eye movement. The occipitotemporal sulcus has been called a visual word form area (Mano et al., 2013), with the posterior part structurally connected to the intraparietal sulcus and involved in visual feature extraction; and the anterior part structurally connected to the angular gyrus and involved in integrating information with the language network (Wang et al., 2012, 2015b; Lerma-Usabiaga et al., 2018). Parieto-occipital sulcus acts as an interface between the dorsal and ventral streams of visual processing in disparity-defined near and far space processing (Wang et al., 2016, 2019). The precentral gyrus is a part of the primary motor cortex which is involved in ocular movement (Halsband et al., 1994). The

TABLE 1 | Characteristics of demographic and clinical variables.

Variables	CS (n = 26)	HC (n = 28)	P value
Age (years)	10.77 ± 3.63	12.07 ± 3.69	0.95[a]
Gender (Male/Female)	15/11	16/12	0.97[b]
Education (years)	9.97 ± 4.18	9.66 ± 3.65	0.68[a]
Duration (years)	2.05 ± 1.22		
MoCA	21.27 ± 4.72	27.33 ± 2.63	0.003[a]
HAMA	5.72 ± 2.89	0.97 ± 0.86	0.026[a]
HAMD	6.04 ± 3.30	1.32 ± 0.14	0.018[a]

Values are mean ± standard deviation. MoCA, Montreal Cognitive Assessment scale; HAMA, Hamilton Anxiety Scale; HAMD, Hamilton depression scale, HS, healthy control; CS, concomitant strabismus. [a]Two-sample t-test (two-tailed). [b]Chi-square t-test.

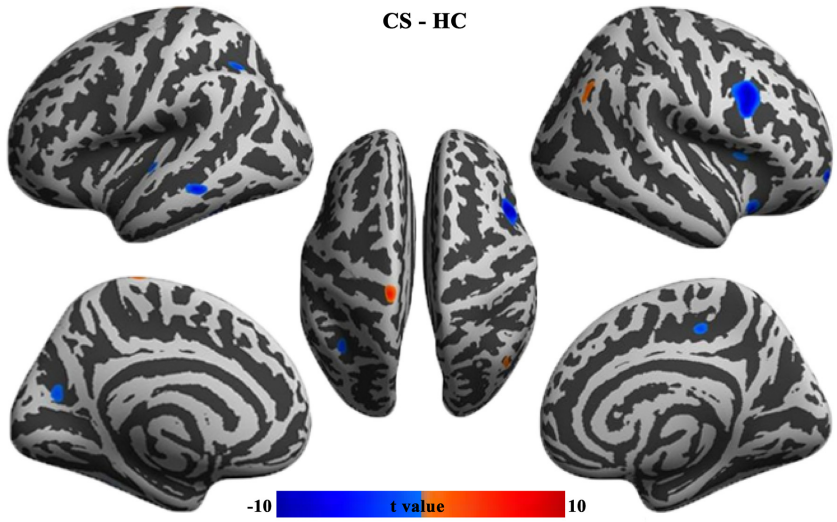

FIGURE 1 | Group differences in cortical thickness between CS patients and HCs (FWE corrected, $p < 0.05$). CS, concomitant strabismus; HC, healthy control; FWE, family-wise error rate.

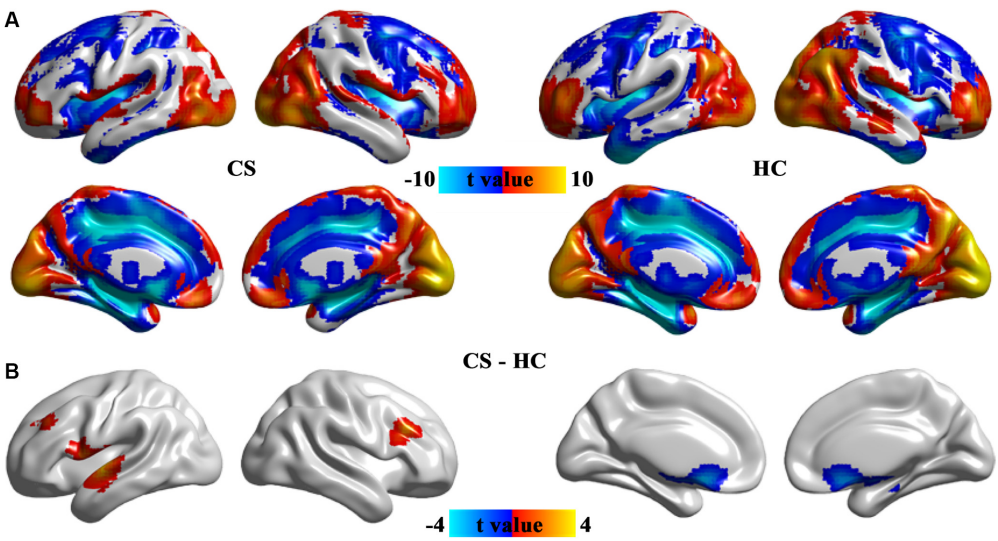

FIGURE 2 | The pattern of ALFF in the CS and HC groups **(A)** and brain regions with significant group differences in ALFF **(B)**. Group differences in ALFF between the CS and HC groups were identified using a two-sample t-test. The statistical significance level was set at $p < 0.05$, GRF corrected. ALFF, the amplitude of low-frequency fluctuation; CS, concomitant strabismus; HC, healthy control.

frontal eye field (FEF) controls saccade modulation (Ohayon et al., 2013) and triggers the generation of saccade movements (Keller et al., 2008). The middle temporal gyrus is responsible for three-dimensional surface orientation and retinal image velocities (Nguyenkim and DeAngelis, 2003; Xu et al., 2015, 2019a). The lesions of these regions lead to ocular movement disorders. Significantly decreased GMV and WMV in the premotor cortex and middle temporal gyrus in adults with CS (Ouyang et al., 2017), and increased GMV in the FEF in adult strabismus (Chan et al., 2004) were previously reported. Strabismic amblyopia showed abnormal mean diffusion in the occipital tracts and the association tracts connecting the visual cortex to the frontal and temporal lobes (Duan et al., 2015). Moreover, strabismic amblyopia patients showed lower degree centrality value in the angular gyrus (Wu et al., 2020), and increased ReHo values in the cingulate gyrus (Huang et al., 2016b). Our results together with previous findings implied that CS may lead to the aberrant structure

TABLE 2 | Group differences in ALFF between CS patients and HCs.

	Brain regions	L/R	Peak MNI coordinates			Cluster size (voxels)	*t* value
			x	*y*	*z*		
CS > HC	Rolandic operculum	L	−60	9	3	209	3.82
	Middle frontal gyrus	L	−42	36	39	44	3.30
	Superior temporal gyrus	L	−51	−12	−3	209	4.44
	Inferior frontal gyrus	R	48	27	30	47	3.59
CS < HC	Caudate	L	−6	−15	−18	284	−3.19
	Caudate	R	3	9	−15	284	−3.76
	Hippocampus	R	18	−15	−18	284	−3.26

ALFF, amplitude of low-frequency fluctuation.

of visual cortex regions for impaired oculomotor in the CS patients.

More interestingly, CS patients reported decreased cortical thickness and increased ALFF in the high-order cognitive regions. PFC is interconnected with visual cortical areas and influences visual representations in sensory areas through attentional demands (Yeterian et al., 2012). The frontomarginal gyrus is a part of the orbitofrontal cortex which plays a central role in visuo-affective prediction (Chaumon et al., 2014). Lateral PFC modulates high-order attention control and provides a substrate for discriminating between perceptual and mnemonic representations of visual features (Wu et al., 2016; Mendoza-Halliday and Martinez-Trujillo, 2017). The superior temporal gyrus is involved in the comprehension of language (Kovelman et al., 2015; Wang et al., 2015a) and auditory-visual processing (Reale et al., 2007). Insula and rolandic operculum are involved in a multisensory integration center for spatial orientation and ocular motor function (Dieterich et al., 1998; Nagai et al., 2007; Wang et al., 2018, 2020). The abnormal structure and function of these high-order cognition regions were previously reported to be associated with strabismus. Abnormal fractional anisotropy and mean diffusivity values in the superior temporal gyrus and lateral PFC regions were reported in CS adults (Huang et al., 2016a). Moreover, increased degree centrality values in the superior temporal gyrus and decreased values in the lateral PFC in adults with comitant exotropia strabismus (Tan et al., 2018). Decreased long-range functional connectivity density in the insula, rolandic operculum, and lateral PFC were found in children with anisometropic amblyopia (Wang et al., 2014). Consistent with previous studies, our result further revealed the altered structure and function in high-order cortical regions in children with CS and highlighted the neural basis underlying abnormal top-down control visual attention in patients.

CS patients also exhibited decreased ALFF in the caudate and hippocampus. The caudate and hippocampus are a part of the visual loop, which is involved in eye movement control and visual working memory, in particular selecting or gating which visual representations should be maintained and processed in working memory (Seger, 2013). The caudate is implicated in dynamic visual information processing, saccade control, and eye movement (Nagypál et al., 2015), while the hippocampus is implicated in visual discrimination of complex spatial scene stimuli (Lee et al., 2012). A voxel-mirrored homotopic connectivity study reported increased interhemispheric functional connectivity in the caudate and hippocampus in patients with strabismic amblyopia (Zhang et al., 2021). In the present study, we speculated that the dysfunction of subcortical regions perhaps contributed to the dysfunction of eye movement and visual working memory in children with CS.

There are still some limitations in our study. First, this is a cross-study and longitudinal studies are warranted to better reveal the neuropathology of CS. Second, only cortical thickness was studied in this study. How cortical area and complexity changes in CS are deserved to be investigated since the three indices reflect different genetic information. Third, the sample size of this study is small. The expiations of these results should be cautious and the results need to be further validated in future studies.

CONCLUSION

In this study, we reported abnormal structure and function in children with CS for the first time. CS patients exhibited not only abnormal oculomotor control but also impaired high-order cognitive and affective functions, which provides a neural basis for understanding the pathophysiology of CS. These findings suggest the importance of investigating the brain alteration to improve our understanding of CS. Future research is needed to further explore the neural basis of CS using the brain connectivity method.

DATA AVAILABILITY STATEMENT

The raw data supporting the conclusions of this article will be made available by the authors, without undue reservation.

ETHICS STATEMENT

The studies involving human participants were reviewed and approved by affiliated Xi'an Central Hospital of Xi'an Jiaotong University. The patients/participants provided their written informed consent to participate in this study.

AUTHOR CONTRIBUTIONS

All the authors have made substantial contribution to this work. All authors contributed to the article and approved the submitted version.

REFERENCES

Archer, S. M., Musch, D. C., Wren, P. A., Guire, K. E., and Del Monte, M. A. (2005). Social and emotional impact of strabismus surgery on quality of life in children. *J. Am. Assoc. Pediatric Ophthalmol. Strabismus* 9, 148–151. doi: 10.1016/j.jaapos.2004.12.006

Chan, S.-T., Tang, K.-W., Lam, K.-C., Chan, L.-K., Mendola, J. D., and Kwong, K. K. (2004). Neuroanatomy of adult strabismus: a voxel-based morphometric analysis of magnetic resonance structural scans. *Neuroimage* 22, 986–994. doi: 10.1016/j.neuroimage.2004.02.021

Chaumon, M., Kveraga, K., Barrett, L. F., and Bar, M. (2014). Visual predictions in the orbitofrontal cortex rely on associative content. *Cereb. Cortex* 24, 2899–2907. doi: 10.1093/cercor/bht146

Dale, A. M., Fischl, B., and Sereno, M. I. (1999). . Cortical surface-based analysis: I. Segmentation and surface reconstruction. *Neuroimage* 9, 179–194. doi: 10.1006/nimg.1998.0395

Dale, A. M., and Sereno, M. I. (1993). Improved localizadon of cortical activity by combining EEG and MEG with MRI cortical surface reconstruction: a linear approach. *J. Cogn. Neurosci.* 5, 162–176. doi: 10.1162/jocn.1993.5.2.162

Dieterich, M., Bucher, S. F., Seelos, K. C., and Brandt, T. (1998). Horizontal or vertical optokinetic stimulation activates visual motion-sensitive, ocular motor and vestibular cortex areas with right hemispheric dominance. An fMRI study. *Brain* 121, 1479–1495. doi: 10.1093/brain/121.8.1479

Duan, Y., Norcia, A. M., Yeatman, J. D., and Mezer, A. (2015). The structural properties of major white matter tracts in strabismic amblyopia. *Invest. Ophthalmol. Vis. Sci.* 56, 5152–5160. doi: 10.1167/iovs.15-17097

Fischl, B., Salat, D. H., Busa, E., Albert, M., Dieterich, M., Haselgrove, C., et al. (2002). Whole brain segmentation: automated labeling of neuroanatomical structures in the human brain. *Neuron* 33, 341–355. doi: 10.1016/s0896-6273(02)00569-x

Fischl, B., Sereno, M. I., and Dale, A. M. (1999). Cortical surface-based analysis - II: Inflation, flattening and a surface-based coordinate system. *Neuroimage* 9, 195–207. doi: 10.1006/nimg.1998.0396

Halsband, U., Matsuzaka, Y., and Tanji, J. (1994). Neuronal activity in the primate supplementary, pre-supplementary and premotor cortex during externally and internally instructed sequential movements. *Neurosci. Res.* 20, 149–155. doi: 10.1016/0168-0102(94)90032-9

Huang, X., Li, H.-J., Zhang, Y., Peng, D.-C., Hu, P.-H., Zhong, Y.-L., et al. (2016a). Microstructural changes of the whole brain in patients with comitant strabismus: evidence from a diffusion tensor imaging study. *Neuropsychiatr. Dis. Treat.* 12, 2007–2014. doi: 10.2147/NDT.S108834

Huang, X., Li, S.-H., Zhou, F.-Q., Zhang, Y., Zhong, Y.-L., Cai, F.-Q., et al. (2016b). Altered intrinsic regional brain spontaneous activity in patients with comitant strabismus: a resting-state functional MRI study. *Neuropsychiatr. Dis. Treat.* 12, 1303–1308. doi: 10.2147/NDT.S105478

Keller, E. L., Lee, B.-T., and Lee, K.-M. (2008). Frontal eye field signals that may trigger the brainstem saccade generator. *Prog. Brain Res.* 171, 107–114. doi: 10.1016/S0079-6123(08)00614-6

Kovelman, I., Wagley, N., Hay, J. S., Ugolini, M., Bowyer, S. M., Lajiness-O'Neill, R., et al. (2015). Multimodal imaging of temporal processing in typical and atypical language development. *Ann. N. Y. Acad. Sci.* 1337, 7–15. doi: 10.1111/nyas.12688

Lee, A. C., Yeung, L.-K., and Barense, M. D. (2012). The hippocampus and visual perception. *Front. Hum. Neurosci.* 6:91. doi: 10.3389/fnhum.2012.00091

Lerma-Usabiaga, G., Carreiras, M., and Paz-Alonso, P. M. (2018). Converging evidence for functional and structural segregation within the left ventral occipitotemporal cortex in reading. *Proc. Natl. Acad. Sci.* 115, E9981–E9990. doi: 10.1073/pnas.1803003115

Mano, Q. R., Humphries, C., Desai, R. H., Seidenberg, M. S., Osmon, D. C., Stengel, B. C., et al. (2013). The role of left occipitotemporal cortex in reading: reconciling stimulus, task and lexicality effects. *Cereb. Cortex* 23, 988–1001. doi: 10.1093/cercor/bhs093

Mendoza-Halliday, D., and Martinez-Trujillo, J. C. (2017). Neuronal population coding of perceived and memorized visual features in the lateral prefrontal cortex. *Nat. Commun.* 8:15471. doi: 10.1038/ncomms15471

Nagai, M., Kishi, K., and Kato, S. (2007). Insular cortex and neuropsychiatric disorders: a review of recent literature. *Eur. Psychiatry* 22, 387–394. doi: 10.1016/j.eurpsy.2007.02.006

Nagypál, T., Gombkötö, P., Barkóczi, B., Benedek, G., and Nagy, A. (2015). Activity of caudate nucleus neurons in a visual fixation paradigm in behaving cats. *PLoS One* 10:e0142526. doi: 10.1371/journal.pone.0142526

Nguyenkim, J. D., and DeAngelis, G. C. (2003). Disparity-based coding of three-dimensional surface orientation by macaque middle temporal neurons. *J. Neurosci.* 23, 7117–7128. doi: 10.1523/JNEUROSCI.23-18-07117.2003

Ohayon, S., Grimaldi, P., Schweers, N., and Tsao, D. Y. (2013). Saccade modulation by optical and electrical stimulation in the macaque frontal eye field. *J. Neurosci.* 33, 16684–16697. doi: 10.1523/JNEUROSCI.2675-13.2013

Ouyang, J., Yang, L., Huang, X., Zhong, Y.-L., Hu, P.-H., Zhang, Y., et al. (2017). The atrophy of white and gray matter volume in patients with comitant strabismus: Evidence from a voxel-based morphometry study. *Mol. Med. Rep.* 16, 3276–3282. doi: 10.3892/mmr.2017.7006

Oystreck, D. T., and Lyons, C. J. (2012). Comitant strabismus: perspectives, present and future. *Saudi J. Ophthalmol.* 26, 265–270. doi: 10.1016/j.sjopt.2012.05.002

Pirnia, T., Joshi, S. H., Leaver, A. M., Vasavada, M., Njau, S., Woods, R. P., et al. (2016). Electroconvulsive therapy and structural neuroplasticity in neocortical, limbic and paralimbic cortex. *Transl. Psychiatry* 6:e832. doi: 10.1038/tp.2016.102

Reale, R., Calvert, G., Thesen, T., Jenison, R., Kawasaki, H., Oya, H., et al. (2007). Auditory-visual processing represented in the human superior temporal gyrus. *Neuroscience* 145, 162–184. doi: 10.1016/j.neuroscience.2006.11.036

Robaei, D., Rose, K. A., Kifley, A., Cosstick, M., Ip, J. M., and Mitchell, P. (2006). Factors associated with childhood strabismus: findings from a population-based study. *Ophthalmology* 113, 1146–1153. doi: 10.1016/j.ophtha.2006.02.019

Seger, C. A. (2013). The visual corticostriatal loop through the tail of the caudate: circuitry and function. *Front. Syst. Neurosci.* 7:104. doi: 10.3389/fnsys.2013.00104

Singh, M. K., Kesler, S. R., Hadi Hosseini, S. M., Kelley, R. G., Amatya, D., Hamilton, J. P., et al. (2013). Anomalous gray matter structural networks in major depressive disorder. *Biol. Psychiatry* 74, 777–785. doi: 10.1016/j.biopsych.2013.03.005

Tan, G., Dan, Z.-R., Zhang, Y., Huang, X., Zhong, Y.-L., Ye, L.-H., et al. (2018). Altered brain network centrality in patients with adult comitant exotropia strabismus: a resting-state fMRI study. *Int. J. Med. Res.* 46, 392–402. doi: 10.1177/0300060517715340

Tan, G., Huang, X., Zhang, Y., Wu, A.-H., Zhong, Y.-L., Wu, K., et al. (2016). A functional MRI study of altered spontaneous brain activity pattern in patients with congenital comitant strabismus using amplitude of low-frequency fluctuation. *Neuropsychiatr. Dis. Treat.* 12, 1243–1250. doi: 10.2147/NDT.S104756

Wang, J., Becker, B., Wang, L., Li, H., Zhao, X., and Jiang, T. (2019). Corresponding anatomical and coactivation architecture of the human precuneus showing similar connectivity patterns with macaques. *Neuroimage* 200, 562–574. doi: 10.1016/j.neuroimage.2019.07.001

Wang, J., Fan, L., Wang, Y., Xu, W., Jiang, T., Fox, P. T., et al. (2015a). Determination of the posterior boundary of wernicke's area based on multimodal connectivity profiles. *Hum. Brain Mapp.* 36, 1908–1924. doi: 10.1002/hbm.22745

Wang, J., Yang, Y., Fan, L., Xu, J., Li, C., Liu, Y., et al. (2015b). Convergent functional architecture of the superior parietal lobule unraveled with multimodal neuroimaging approaches. *Hum. Brain Mapp.* 36, 238–257. doi: 10.1002/hbm.22626

Wang, J., Fan, L., Zhang, Y., Liu, Y., Jiang, D., Zhang, Y., et al. (2012). Tractography-based parcellation of the human left inferior parietal lobule. *Neuroimage* 63, 641–652. doi: 10.1016/j.neuroimage.2012.07.045

Wang, T., Li, Q., Guo, M., Peng, Y., Li, Q., Qin, W., et al. (2014). Abnormal functional connectivity density in children with anisometropic amblyopia at resting-state. *Brain Res.* 1563, 41–51. doi: 10.1016/j.brainres.2014.03.015

Wang, A., Li, Y., Zhang, M., and Chen, Q. (2016). The role of parieto-occipital junction in the interaction between dorsal and ventral streams in disparity-defined near and far space processing. *PLoS One* 11:e0151838. doi: 10.1371/journal.pone.0151838

Wang, J., Wei, Q., Bai, T., Zhou, X., Sun, H., Becker, B., et al. (2017). Electroconvulsive therapy selectively enhanced feedforward connectivity from fusiform face area to amygdala in major depressive disorder. *Soc. Cogn .Affect Neurosci.* 12, 1983–1992. doi: 10.1093/scan/nsx100

Wang, L., Wei, Q., Wang, C., Xu, J., Wang, K., Tian, Y., et al. (2020). Altered functional connectivity patterns of insular subregions in major depressive disorder after electroconvulsive therapy. *Brain Imaging Behav.* 14, 753–761. doi: 10.1007/s11682-018-0013-z

Wang, C., Wu, H., Chen, F., Xu, J., Li, H., Li, H., et al. (2018). Disrupted functional connectivity patterns of the insula subregions in drug-free major depressive disorder. *J. Affect. Disord.* 234, 297–304. doi: 10.1016/j.jad.2017.12.033

Wu, Y., Wang, J., Zhang, Y., Zheng, D., Zhang, J., Rong, M., et al. (2016). The neuroanatomical basis for posterior superior parietal lobule control lateralization of visuospatial attention. *Front. Neuroanat.* 10:32. doi: 10.3389/fnana.2016.00032

Wu, K.-R., Yu, Y.-J., Tang, L.-Y., Chen, S.-Y., Zhang, M.-Y., Sun, T., et al. (2020). Altered brain network centrality in patients with adult strabismus with amblyopia: a resting-state functional magnetic resonance imaging (fMRI) study. *Med. Sci. Monit.* 26:e925856. doi: 10.12659/MSM.925856

Xu, J., Lyu, H., Li, T., Xu, Z., Fu, X., Jia, F., et al. (2019a). Delineating functional segregations of the human middle temporal gyrus with resting-state functional connectivity and coactivation patterns. *Hum. Brain Mapp.* 40, 5159–5171. doi: 10.1002/hbm.24763

Xu, J., Wang, J., Bai, T., Zhang, X., Li, T., Hu, Q., et al. (2019b). Electroconvulsive therapy induces cortical morphological alterations in major depressive disorder revealed with surface-based morphometry analysis. *Int. J. Neural Syst.* 29:1950005. doi: 10.1142/S0129065719500059

Xu, J., Wang, J., Fan, L., Li, H., Zhang, W., Hu, Q., et al. (2015). Tractography-based parcellation of the human middle temporal gyrus. *Sci. Rep.* 5:18883. doi: 10.1038/srep18883

Yan, X., Wang, Y., Xu, L., Liu, Y., Song, S., Ding, K., et al. (2019). Altered functional connectivity of the primary visual cortex in adult comitant strabismus: a resting-state functional MRI study. *Curr. Eye Res.* 44, 316–323. doi: 10.1080/02713683.2018.1540642

Yeterian, E. H., Pandya, D. N., Tomaiuolo, F., and Petrides, M. (2012). The cortical connectivity of the prefrontal cortex in the monkey brain. *Cortex* 48, 58–81. doi: 10.1016/j.cortex.2011.03.004

Zhang, S., Gao, G.-P., Shi, W.-Q., Li, B., Lin, Q., Shu, H.-Y., et al. (2021). Abnormal interhemispheric functional connectivity in patients with strabismic amblyopia: a resting-state fMRI study using voxel-mirrored homotopic connectivity. *BMC Ophthalmol.* 21:255. doi: 10.1186/s12886-021-02015-0

Conflict of Interest: The authors declare that the research was conducted in the absence of any commercial or financial relationships that could be construed as a potential conflict of interest.

Publisher's Note: All claims expressed in this article are solely those of the authors and do not necessarily represent those of their affiliated organizations, or those of the publisher, the editors and the reviewers. Any product that may be evaluated in this article, or claim that may be made by its manufacturer, is not guaranteed or endorsed by the publisher.

frontiers in Psychiatry

ORIGINAL RESEARCH
published: 15 November 2021
doi: 10.3389/fpsyt.2021.777447

The Deficits of Individual Morphological Covariance Network Architecture in Schizophrenia Patients With and Without Violence

Danlin Shen[1], Qing Li[1], Jianmei Liu[2], Yi Liao[3], Yuanyuan Li[1], Qiyong Gong[4], Xiaoqi Huang[4], Tao Li[1,5], Jing Li[1], Changjian Qiu[1] and Junmei Hu[6]**

[1] Mental Health Center, West China Hospital, Sichuan University, Chengdu, China, [2] Qingyang Yalun Clinic, Chengdu, China, [3] Department of Radiology, West China Second University Hospital, Sichuan University, Chengdu, China, [4] Huaxi MR Research Center (HMRRC), West China Hospital, Sichuan University, Chengdu, China, [5] Affiliated Mental Health Center, School of Medicine, Zhejiang University, Hangzhou, China, [6] School of Basic Science and Forensic Medicine, Sichuan University, Chengdu, China

OPEN ACCESS

Edited by:
Jiaojian Wang,
University of Electronic Science and Technology of China, China

Reviewed by:
Fengmei Lu,
Chengdu No.4 People's Hospital, China
Limei Song,
Weifang Medical University, China

***Correspondence:**
Changjian Qiu
qiuchangjian18@126.com
Junmei Hu
hujunmei@scu.edu.cn

Specialty section:
This article was submitted to Neuroimaging and Stimulation, a section of the journal Frontiers in Psychiatry

Received: 15 September 2021
Accepted: 18 October 2021
Published: 15 November 2021

Citation:
Shen D, Li Q, Liu J, Liao Y, Li Y, Gong Q, Huang X, Li T, Li J, Qiu C and Hu J (2021) The Deficits of Individual Morphological Covariance Network Architecture in Schizophrenia Patients With and Without Violence. Front. Psychiatry 12:777447. doi: 10.3389/fpsyt.2021.777447

Background: Schizophrenia is associated with a significant increase in the risk of violence, which constitutes a public health concern and contributes to stigma associated with mental illness. Although previous studies revealed structural and functional abnormalities in individuals with violent schizophrenia (VSZ), the neural basis of psychotic violence remains controversial.

Methods: In this study, high-resolution structural magnetic resonance imaging (MRI) data were acquired from 18 individuals with VSZ, 23 individuals with non-VSZ (NSZ), and 22 age- and sex-matched healthy controls (HCs). Whole-brain voxel-based morphology and individual morphological covariance networks were analysed to reveal differences in gray matter volume (GMV) and individual morphological covariance network topology. Relationships among abnormal GMV, network topology, and clinical assessments were examined using correlation analyses.

Results: GMV in the hypothalamus gradually decreased from HCs and NSZ to VSZ and showed significant differences between all pairs of groups. Graph theory analyses revealed that morphological covariance networks of HCs, NSZ, and VSZ exhibited small worldness. Significant differences in network topology measures, including global efficiency, shortest path length, and nodal degree, were found. Furthermore, changes in GMV and network topology were closely related to clinical performance in the NSZ and VSZ groups.

Conclusions: These findings revealed the important role of local structural abnormalities of the hypothalamus and global network topological impairments in the neuropathology of NSZ and VSZ, providing new insight into the neural basis of and markers for VSZ and NSZ to facilitate future accurate clinical diagnosis and targeted treatment.

Keywords: individual morphological covariance network, graph theory, schizophrenia, violent, gray matter volume

INTRODUCTION

Schizophrenia (SZ) is a serious mental disorder affecting 1% of the world's population in terms of thinking, feeling, and behaviors that cause abnormal perceptions of reality (1). The link between SZ and violent offending has long been the subject of research with a significant impact on mental health policy. Patients with SZ have an elevated risk for aggression and violent behavior, which leads to fear and contributes to the major stigma of this disease (2). Although previous studies have reported that environmental factors, such as low socio-economic status and childhood trauma, may lead to violence in SZ (3–5), increasing evidence indicates that neurobiological factors may also play a key role in the increased risk of violence in individuals with SZ (6, 7). The origins of violent behavior in people with SZ are not yet sufficiently understood (8). Moreover, the management of aggression in SZ patients is a challenging clinical dilemma given that violence or aggressive behavior is heterogeneous in origin (8–10). Therefore, delineating the underlying neurobiological basis of violence in SZ may facilitate its management and effective therapy.

Non-invasive magnetic resonance imaging (MRI) provides the opportunity to study brain structure and function *in vivo*. Widely used structural MRI (sMRI), diffusion MRI, and functional MRI enable investigations of brain morphology, white matter (WM) microstructure, and functional activities, respectively (11–17). In recent decades, mounting studies have demonstrated that brain function is not only fulfilled by a single area but also involves interactions across multiple distributed systems to form a complex brain network (18–22). Traditionally, brain networks were mapped using diffusion MRI for axonal connections or functional MRI for functional connectivities (23–28). Recently, using sMRI to map whole-brain morphological connectivity patterns by characterizing interregional morphological similarities was proposed due to its advantages of easy access, high signal-to-noise ratio, and robustness to artifacts (29–31). Unlike four-dimensional functional MRI, sMRI only contains three-dimensional location information. Early studies thus constructed the morphological covariance network at the population level by taking each individual subject as a time point to model time series of functional MRI (30, 32). A group of subjects can only obtain one connectivity matrix to reflect the group-level morphological covariance, ignoring individual variability. Recently, Wang et al. (33) developed an individual morphological covariance network method used for brain disease research (34, 35). Thus, individual morphological covariance networks with graph theory analysis may provide new insight into brain network organization patterns and improve the understanding of the neurobiological underpinnings of violent SZ (VSZ) patients.

In the current study, we aimed to explore structural and topological differences in gray matter volume (GMV) and individual morphological covariance networks among healthy controls (HCs) and individuals with non-VSZ (NSZ) and VSZ. In addition, we evaluated the associations of changes in GMV and network topology with clinical variables.

MATERIALS AND METHODS

Participants

This study was approved by the Ethics Committee of West China Hospital, Sichuan University. A total of 18 VSZ, 23 NSZ, and 22 HCs participated in the present study. All the subjects were male and were matched based on age and education level among the three groups. All participants were right-handed, and written informed consent was provided and obtained. All subjects were recruited from the forensic psychiatry department of Preclinical Science and Forensic Medicine College of Sichuan University, Chengdu, Sichuan. Psychiatric diagnoses were determined by two experienced psychiatrists using the Structured Clinical Interview for *Diagnostic and Statistical Manual of Mental Disorders*, Fourth Edition (DSM-IV) (SCID-I/P), Chinese version. The inclusion criteria for VSZ were murder, attempted murder, and severe physical assault toward other people (including sexual assaults) based on the MacArthur criteria (36). These individuals committed serious violence with at least one fatal or near-fatal act of violence against their victims and were referred to forensic psychiatric examination for legal competence before court decisions. All participants were diagnosed with SZ before receiving any medical treatment. The exclusion criteria were (1) age <18 years or over 65 years; (2) other psychiatric co-morbidities; (3) any history of cardiovascular diseases, major physical illness, or neurological disorder; and (4) substance abuse or dependence. Brain MRI performed under the supervision of an experienced neuroradiologist showed no gross abnormalities.

Clinical Assessments and Criminal Information

Psychopathology was assessed using the Chinese version of the Positive and Negative Syndrome Scale (PANSS) (37), which provides a total score and positive, negative, and general symptoms, and supplement scores. The Chinese version of the PANSS consists of the original PANSS plus three supplementary excitability items, including anger, difficulty in delay gratification, and affective liability, to measure the excitement dimension. The supplement scores were not added to the PANSS total score. The assessments were conducted by clinical psychiatrists who were professionally trained to conduct the PANSS interview and employ rating methods. Individual incidents of aggression were recorded using self-reporting criminology-characterized tables and modified overt aggression scale (MOAS) (38). The tables characterized by self-reported criminology include types of cases, attack targets, preparation of crime, criminal motivation, and self-protection. All of the information was collected based on criminal case files.

Structural MRI Data Acquisition

sMRI data were acquired using a 3-Tesla Siemens MRI system with an eight-channel phase-array head coil. Head motion was controlled using foam pads. Prior to scanning, participants were instructed to lie still with their eyes closed and not to fall asleep. High-resolution T1-weighted data were acquired using the following scan parameters: repetition time (TR) = 1,900 ms, echo time (TE) = 2.28 ms, flip angle = 9°, 176 sagittal slices with

slice thickness = 1.0 mm, field of view = 240 × 240 mm^2, and data matrix = 256 × 256.

Voxel-Based Morphometry Analyses

The sMRI images were processed using the CAT12 toolbox in SPM12 software (http://dbm.neuro.uni-jena.de/wordpress/vbm/download/). Voxel-based morphometry (VBM) analysis included the following steps. MRI images were first assessed to exclude artifacts or gross anatomical abnormalities and were reoriented to the anterior commissure. Then, the structural images were segmented into GM, WM, and cerebrospinal fluid (CSF). Next, GM images were normalized to the Montreal Neurological Institute (MNI) space using the Diffeomorphic Anatomical Registration using Exponentiated Lie algebra (DARTEL) normalization approach and were modulated to account for volume changes. Finally, the GM images were smoothed using a Gaussian kernel of 8-mm full-width at half maximum (FWHM) (32, 39), and whole-brain voxelwise one-way ANOVA with PANSS and disease duration as covariates was performed to identify differences in GMV among HCs, NSZ, and VSZ. The significance level was set as $p < 0.05$ using false discovery rate (FDR) correction and a minimum cluster size of >30. After identification of GMV differences, the mean GMV in brain areas with altered GMV in the HC, NSZ, and VSZ groups was calculated. *Post-hoc* two-sample *t*-tests were further used to identify between-group differences, and the significance was set at $p < 0.05$ with Bonferroni correction.

Individual Morphological Covariance Network Analysis

Defining Network Nodes

To explore brain network topology changes across different groups, individual morphological covariance networks were studied with GM images in the template space for each subject. The brain network includes network nodes and network edges. In this study, network nodes were defined with automated anatomical labeling (AAL) atlases (40). Each cortical and subcortical subregion served as a node in the morphological covariance network.

Defining Network Edges

After the nodes of the morphological network were defined, the edge was defined as the interregional similarity in the distribution of the regional GMV. The edge of the individual morphological covariance network was calculated as follows: kernel density estimation (KDE) was first used to estimate the probability density function of the extracted GMV values of each subregion in the AAL atlas, and the variation in the Kullback–Leibler (KL) divergence (KLD) was calculated to define the similarity of GM values between each pair of subregions. The similarities were taken as the edges of the morphological covariance network (33). Given that the AAL atlas segments the cortex and subcortex into 90 subregions, a 90 × 90 matrix was obtained for each subject. Finally, a binary network was generated for each subject for further analyses.

Graph Theory-Based Network Analyses

To explore network topology parameter differences among HCs, NSZ, and VSZ, graph theory-based network analyses were performed with sparsity values from 0.05 to 0.39 using steps of 0.02. First, small worldness was assessed for each morphological covariance network. If each morphological covariance network met the small-world property (normalized clustering coefficient >> 1, normalized characteristic path length ≈ 1, and small worldness > 1), the global and nodal topological parameters, including clustering coefficient (Cp), global efficiency (Eg), local efficiency (Eloc), shortest path length (Lp), assortativity, modularity, nodal degree, and nodal betweenness, were calculated. One-way ANOVA with PANSS and disease duration as covariates was first used to identify differences in network parameters among HCs, NSZ, and VSZ; and the significance level was set at $p < 0.05$. *Post-hoc* two-sample *t*-tests were further used to determine between-group differences corrected with the Bonferroni method with $p < 0.05$.

Correlation Analyses

To explore whether GMV and network topology abnormalities were associated with illness duration, PANSS, and aggression, correlation analyses were conducted in NSZ and VSZ patients. The significance level was set at $p < 0.05$ corrected using the FDR method.

RESULTS

Demographic and Clinical Information

No significant differences in age ($p = 0.53$) or education ($p = 0.38$) were noted among the HC, NSZ, and VSZ groups as shown in **Table 1**. Patients with VSZ had longer disease duration ($p = 0.0063$), higher PANSS ($p < 0.001$), and higher aggression scores ($p < 0.001$) than NSZ patients (**Table 1**).

Abnormal Gray Matter Volume

Abnormal GMV in the right hypothalamus (peak coordinate, x = 3, y = −11, z = −6) was noted among the HC, NSZ, and VSZ groups. *Post-hoc* two-sample *t*-tests found significantly lower GMVs in SZ patients compared with HCs and significantly lower GMVs in VSZ patients compared with NSZ patients (**Figure 1**).

Abnormal Network Topology

All the morphological covariance networks of HCs, NSZ, and VSZ showed small-worldness properties at sparsity values ranging from 0.05 to 0.39 (**Figure 2**). Abnormal network topological parameters, including Eg, Lp, and nodal degree, were found among the HC, NSZ, and VSZ groups (**Figure 3**). Both NSZ and VSZ patients showed significantly higher Eg than HCs; and VSZ individuals had significantly higher Eg than NSZ individuals. For Lp, both NSZ and VSZ patients exhibited significantly lower Lp than HCs, and VSZ exhibited significantly lower Lp than NSZ. The mean nodal degree in NSZ individuals was significantly greater than that observed in HCs and VSZ, but no significant difference was noted between HCs and VSZ. For other network topological parameters, including small worldness (Gamma, Lambda, and Sigma),

TABLE 1 | Subject demographics.

	HC ($n = 22$)	NSZ ($n = 23$)	VSZ ($n = 18$)	*F*/*t* values	*p*-values
Age (years)	32.36 (4.93)	31.22 (6.54)	33.61 (8.62)	0.64	0.53
Sex (M/F)	22/0	23/0	18/0	NA	NA
Education (years)	12.48 (2.61)	12.78 (2.98)	11.56 (2.97)	0.98	0.38
Duration (months)	NA	16.1 (28.88)	59.89 (65.25)	2.89	0.0063*
PANSS	NA	86.3 (16.49)	112 (7.4)	6.13	<0.001*
MOAS	NA	14.96 (3.99)	29 (3.33)	12	<0.001*

HCs, healthy controls; NSZ, nonviolent schizophrenia; VSZ, violent schizophrenia; M, male; F, female; PANSS, Positive and Negative Syndrome Scale; MOAS, modified overt aggression scale.
**Significant differences.*

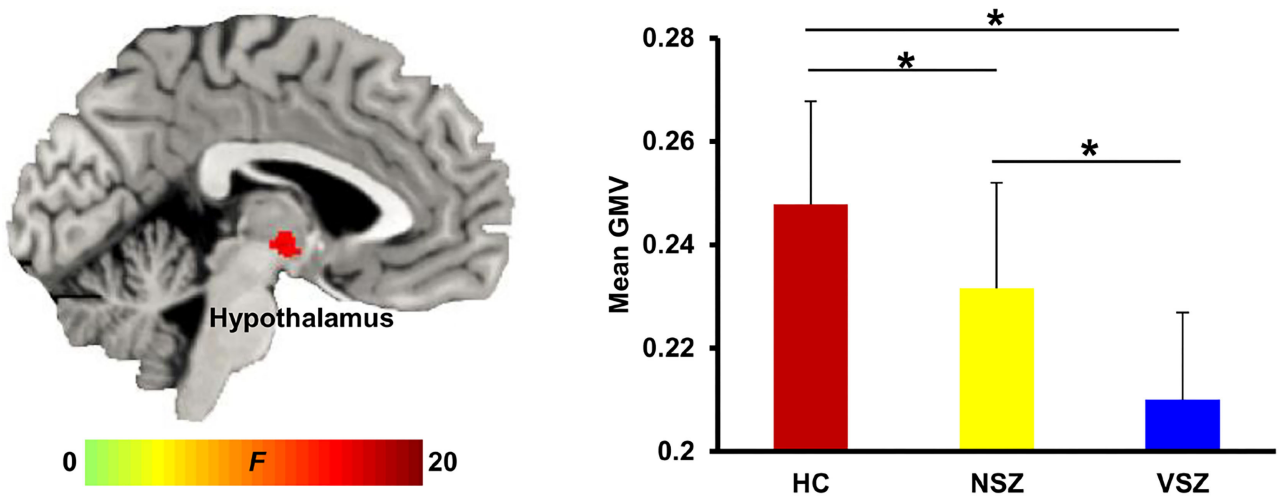

FIGURE 1 | Abnormal gray matter (GM) volume in the hypothalamus was found among healthy controls (HCs), nonviolent schizophrenia (NSZ) patients, and violent schizophrenia (VSZ) patients. A gradient decrease in GM volume from HCs to NSZ and VSZ was observed. *Significant difference with $p < 0.05$.

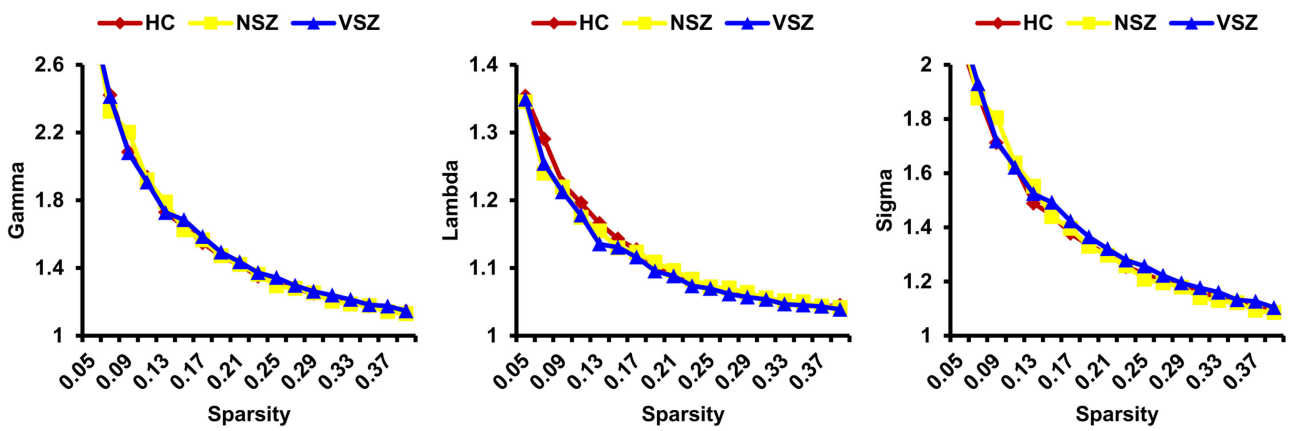

FIGURE 2 | All the HC, NSZ, and VSZ groups showed small-worldness properties of the individual morphological covariance network at sparsity values ranging from 0.05 to 0.39. HC, healthy control; NSZ, nonviolent schizophrenia; VSZ, violent schizophrenia.

Eloc, assortativity, modularity, Cp, and nodal betweenness, no significant differences were noted among HCs, NSZ, and VSZ (**Supplementary Figure 1**).

Correlation Analysis Results

As shown in **Figure 4**, after correction for multiple comparisons, GMV of the hypothalamus and nodal degree showed

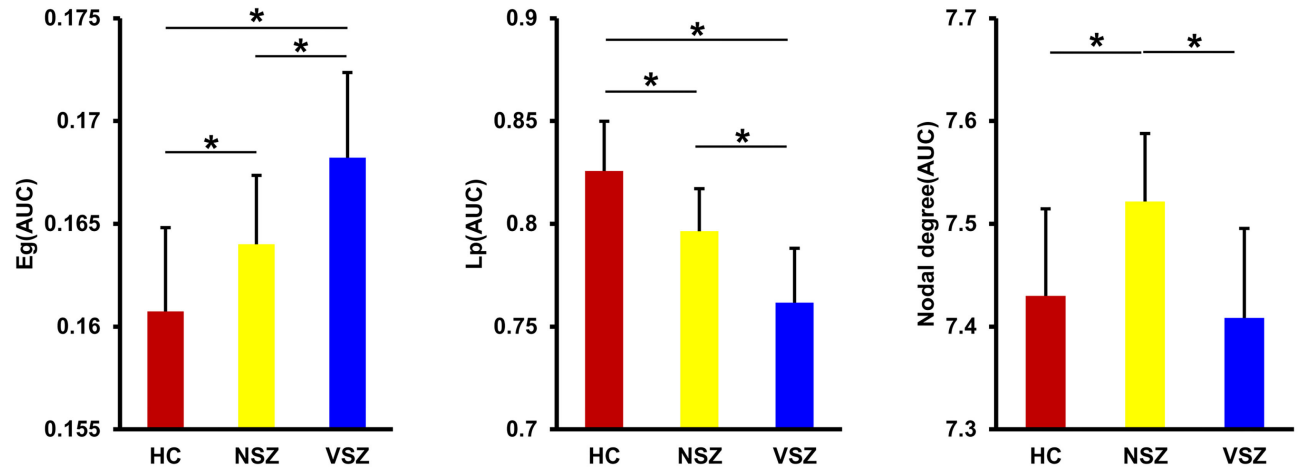

FIGURE 3 | Significant differences in global efficiency (Eg), shortest path length (Lp), and nodal degree were found among the HC, NSZ, and VSZ groups. A gradient increase in Eg and a gradient decrease in Lp from HCs to NSZ and VSZ were found. NSZ had a significantly higher nodal degree than both HCs and VSZ. * Significant difference with $p < 0.05$. HC, healthy control; NSZ, nonviolent schizophrenia; VSZ, violent schizophrenia.

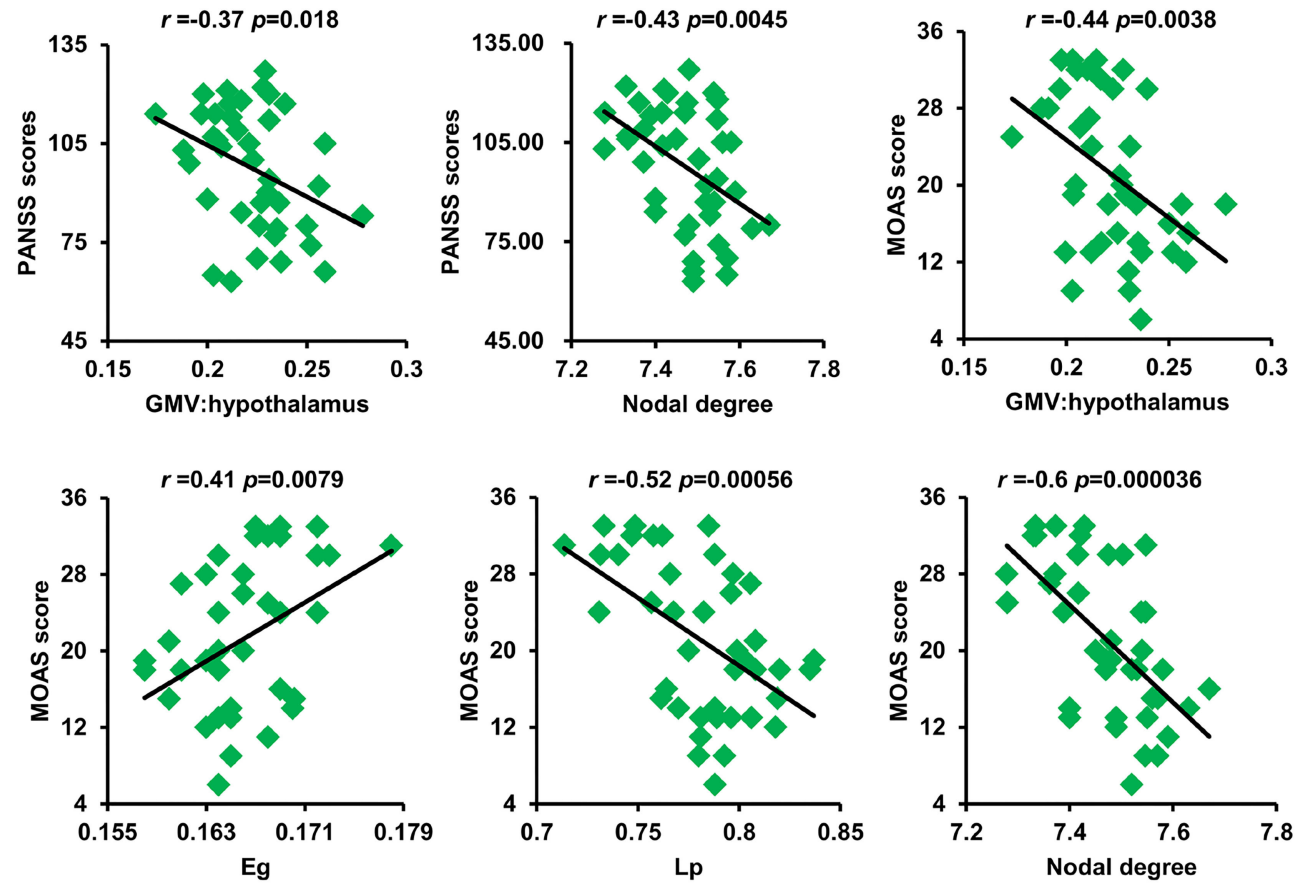

FIGURE 4 | Significant correlations between GM volume of the hypothalamus and nodal degree and PANSS scores as well as between GM volume of the hypothalamus and Eg, Lp, nodal degree, and MOAS scores were found. GM, gray matter; PANSS, Positive and Negative Syndrome Scale; Eg, global efficiency; Lp, shortest path length; MOAS, modified overt aggression scale.

significantly negative correlations with PANSS scores. The GMV of the hypothalamus, Lp, and nodal degree showed significantly negative correlations with aggression scores, whereas Eg exhibited a significantly positive correlation with aggression scores.

DISCUSSION

In the current study, we revealed alterations in GMV and disrupted network topology in SZ patients with and without violence using voxel-based morphology and novel individual morphological covariance network analyses. Significantly decreased GMV in the hypothalamus and significantly disrupted global efficiency, short path length, and nodal degree were found in the NSZ and VSZ groups. Moreover, these changed GMVs and network topologies were significantly associated with clinical characteristics. These findings highlighted the important role of the hypothalamus in SZ patients with and without violence and deepened our understanding of the neuropathology of SZ and violence in SZ from a network perspective.

The hypothalamus is the control center for many autonomic functions of the peripheral nervous system and plays a vital role in maintaining homeostasis (41–43). As a part of the limbic system, the hypothalamus also influences various emotional responses (44). Many recent studies have demonstrated that the hypothalamus is important for circadian control aggression in both humans and animals (45–47). Decreased hypothalamus volume has been reported in patients with SZ (48–50). The decreased GMV in the hypothalamus supported our finding of decreased GMV in NSZ patients compared with HCs. However, few studies have reported abnormal GMV in the hypothalamus in SZ patients with aggression. Only one study by Schiffer et al. (51) found increased GMV in the hypothalamus in patients with SZ with conduct disorder, which is associated with violent behavior. In our study, we found decreased GMV in individuals with VSZ. The difference may result from different subtypes of VSZ, suggesting that different subtypes of VSZ may have distinct neural circuits. Moreover, we found that the GMV gradually decreased from HCs to NSZ and VSZ and was significantly correlated with PANSS and aggression scores in patients. These findings indicate that abnormal GMV of the hypothalamus may be an intrinsic biomarker to distinguish individuals with SZ from healthy individuals and to differentiate individuals with VSZ and NSZ.

The human brain is conceptualized as a complex network structured to optimize the interplay between segregation and integration of functionally specialized subsystems (19, 52). Many previous studies have utilized diffusion MRI or functional MRI to map anatomical or functional brain networks to explore network topological abnormalities in SZ (53–57). By measuring across-subject covariance in morphological measures, such as cortical thickness (29), gyrification (58), and GMVs (31, 59), structural network topological attributes were also studied in SZ. Although the GMV covariance network has been analyzed in SZ, all previous studies use population-level data to construct only one single connectivity network across all subjects, which cannot account for individual network topology. To the best of our knowledge, this is the first study to map the individual morphological covariance network to investigate abnormal network topology in VSZ and NSZ. We found gradually increased global efficiency and gradually decreased shortest path length from HCs to NSZ and VSZ. We also found an increased mean nodal degree in NSZ individuals compared with both HC and VSZ individuals. The findings in our study were supported by previous complex brain network analyses in SZ (54, 56, 60). All the evidence suggested higher information processing efficiency in NSZ and VSZ individuals compared with HCs. Our results together with previous findings may support the "hyperconnectivity" hypothesis of SZ (61–63). In addition, abnormal global efficiency, shortest path length, and nodal degree were significantly correlated with PANSS and aggression scores. Thus, global efficiency and shortest path length may serve as biomarkers to distinguish individuals with VSZ and NSZ, whereas nodal degree may be a specific neurobiomarker for NSZ.

The current study also has several limitations. First, in our study, the sample size was limited, and all the subjects were male. These results need to be interpreted with caution; thus, the findings in our study also require further validation. Second, longitudinal studies are warranted to better reveal the neuropathology of NSZ and VSZ using multimodal MRI data and to extend the findings in further studies.

In conclusion, our study found a gradual decrease in GMV in the hypothalamus and disrupted global topological properties, including global efficiency, shortest path length, and nodal degree, in individuals with VSZ and NSZ. In addition, we found that abnormal GMV and network topological properties were significant clinical measures. These findings highlight the important roles of the hypothalamus in individuals with VSZ and NSZ and provide neural biomarkers to distinguish SZ from healthy subjects and to differentiate subtypes of SZ.

DATA AVAILABILITY STATEMENT

The raw data supporting the conclusions of this article will be made available by the authors, without undue reservation.

ETHICS STATEMENT

The studies involving human participants were reviewed and approved by Ethics Committee of West China Hospital, Sichuan University. The patients/participants provided their written informed consent to participate in this study.

AUTHOR CONTRIBUTIONS

All authors listed have made a substantial, direct and intellectual contribution to the work, and approved it for publication.

SUPPLEMENTARY MATERIAL

The Supplementary Material for this article can be found online at: https://www.frontiersin.org/articles/10.3389/fpsyt.2021.777447/full#supplementary-material

REFERENCES

1. Tang J, Liao Y, Zhou B, Tan C, Liu W, Wang D, et al. Decrease in temporal gyrus gray matter volume in first-episode, early onset schizophrenia: an MRI study. *PLoS ONE.* (2012) 7:e40247. doi: 10.1371/journal.pone.0040247
2. Fazel S, Gulati G, Linsell L, Geddes JR, Grann M. Schizophrenia and violence: systematic review and meta-analysis. *PLoS Med.* (2009) 6:e1000120. doi: 10.1371/journal.pmed.1000120
3. Weiss EM. Neuroimaging and neurocognitive correlates of aggression and violence in schizophrenia. *Scientifica.* (2012) 2012:158646. doi: 10.6064/2012/158646
4. Fazel S, Långström N, Hjern A, Grann M, Lichtenstein P. Schizophrenia, substance abuse, and violent crime. *JAMA.* (2009) 301:2016–23. doi: 10.1001/jama.2009.675
5. van Dongen J, Buck N, Van Marle H. Unravelling offending in schizophrenia: factors characterising subgroups of offenders. *Crim Behav Ment Health.* (2015) 25:88–98. doi: 10.1002/cbm.1910
6. Rosell DR, Siever LJ. The neurobiology of aggression and violence. *CNS Spectr.* (2015) 20:254–79. doi: 10.1017/S109285291500019X
7. Fleischman A, Werbeloff N, Yoffe R, Davidson M, Weiser M. Schizophrenia and violent crime: a population-based study. *Psychol Med.* (2014) 44:3051–7. doi: 10.1017/S0033291714000695
8. Sonnweber M, Lau S, Kirchebner J. Violent and non-violent offending in patients with schizophrenia: Exploring influences and differences via machine learning. *Compr Psychiatry.* (2021) 107:152238. doi: 10.1016/j.comppsych.2021.152238
9. Volavka J, Citrome L. Pathways to aggression in schizophrenia affect results of treatment. *Schizophr Bull.* (2011) 37:921–9. doi: 10.1093/schbul/sbr041
10. Rubinov M, Bullmore E. Schizophrenia and abnormal brain network hubs. *Dialogues Clin Neurosci.* (2013) 15:339–49. doi: 10.31887/DCNS.2013.15.3/mrubinov
11. Fox MD, Raichle ME. Spontaneous fluctuations in brain activity observed with functional magnetic resonance imaging. *Nat Rev Neurosci.* (2007) 8:700–11. doi: 10.1038/nrn2201
12. Symms M, Jäger HR, Schmierer K, Yousry TA, A. review of structural magnetic resonance neuroimaging. *J Neurol Neurosurg Psychiatry.* (2004) 75:1235–44. doi: 10.1136/jnnp.2003.032714
13. Mori S, Zhang J. Principles of diffusion tensor imaging and its applications to basic neuroscience research. *Neuron.* (2006) 51:527–39. doi: 10.1016/j.neuron.2006.08.012
14. Wang J, Feng X, Wu J, Xie S, Li L, Xu L, et al. Alterations of gray matter volume and white matter integrity in maternal deprivation monkeys. *Neuroscience.* (2018) 384:14–20. doi: 10.1016/j.neuroscience.2018.05.020
15. Wang J, Becker B, Wang L, Li H, Zhao X, Jiang T. Corresponding anatomical and coactivation architecture of the human precuneus showing similar connectivity patterns with macaques. *Neuroimage.* (2019) 200:562–74. doi: 10.1016/j.neuroimage.2019.07.001
16. Wang J, Yang Y, Zhao X, Zuo Z, Tan L-H. Evolutional and developmental anatomical architecture of the left inferior frontal gyrus. *NeuroImage.* (2020) 20:117268. doi: 10.1016/j.neuroimage.2020.117268
17. Wang J, Fan L, Zhang Y, Liu Y, Jiang D, Zhang Y, et al. Tractography-based parcellation of the human left inferior parietal lobule. *Neuroimage.* (2012) 63:641–52. doi: 10.1016/j.neuroimage.2012.07.045
18. Sporns O, Tononi G, Kotter R. The human connectome: a structural description of the human brain. *PLoS Comput Biol.* (2005) 1:e42. doi: 10.1371/journal.pcbi.0010042
19. Bassett DS, Bullmore E. Small-world brain networks. *Neuroscientist.* (2006) 12:512–23. doi: 10.1177/1073858406293182
20. Bullmore E, Sporns O. Complex brain networks: graph theoretical analysis of structural and functional systems. *Nat Rev Neurosci.* (2009) 10:186–98. doi: 10.1038/nrn2575
21. Wang J, Xie S, Guo X, Becker B, Fox PT, Eickhoff SB, et al. correspondent functional topography of the human left inferior parietal lobule at rest and under task revealed using resting-state fmri and coactivation based parcellation. *Hum Brain Mapp.* (2017) 38:1659–75. doi: 10.1002/hbm.23488
22. Wang J, Yang Y, Fan L, Xu J, Li C, Liu Y, et al. Convergent functional architecture of the superior parietal lobule unraveled with multimodal neuroimaging approaches. *Hum Brain Mapp.* (2015) 36:238–57. doi: 10.1002/hbm.22626
23. Gong G, He Y, Concha L, Lebel C, Gross DW, Evans AC, et al. Mapping anatomical connectivity patterns of human cerebral cortex using in vivo diffusion tensor imaging tractography. *Cerebral cortex.* (2009) 19:524–36. doi: 10.1093/cercor/bhn102
24. Gong G, Rosa-Neto P, Carbonell F, Chen ZJ, He Y, Evans AC. Age- and gender-related differences in the cortical anatomical network. *J Neurosci.* (2009) 29:15684–93. doi: 10.1523/JNEUROSCI.2308-09.2009
25. Hagmann P, Cammoun L, Gigandet X, Meuli R, Honey CJ, Wedeen VJ, et al. Mapping the structural core of human cerebral cortex. *PLoS Biol.* (2008) 6:e159. doi: 10.1371/journal.pbio.0060159
26. Achard S, Bullmore E. Efficiency and cost of economical brain functional networks. *PLoS Comput Biol.* (2007) 3:e17. doi: 10.1371/journal.pcbi.0030017
27. Wang J, Wang Z, Zhang H, Feng S, Lu Y, Wang S, et al. White matter structural and network topological changes underlying the behavioral phenotype of MECP2 mutant monkeys. *Cerebral cortex.* (2021) 11:66. doi: 10.1093/cercor/bhab166
28. Wang J, Zuo Z, Xie S, Miao Y, Ma Y, Zhao X, et al. Parcellation of macaque cortex with anatomical connectivity profiles. *Brain Topogr.* (2018) 31:161–73. doi: 10.1007/s10548-017-0576-9
29. Zhang Y, Lin L, Lin CP, Zhou Y, Chou KH, Lo CY, et al. Abnormal topological organization of structural brain networks in schizophrenia. *Schizophr Res.* (2012) 141:109–18. doi: 10.1016/j.schres.2012.08.021
30. He Y, Chen ZJ, Evans AC. Small-world anatomical networks in the human brain revealed by cortical thickness from MRI. *Cerebral cortex.* (2007) 17:2407–19. doi: 10.1093/cercor/bhl149
31. Bassett DS, Bullmore E, Verchinski BA, Mattay VS, Weinberger DR, Meyer-Lindenberg A. Hierarchical organization of human cortical networks in health and schizophrenia. *J Neurosci.* (2008) 28:9239–48. doi: 10.1523/JNEUROSCI.1929-08.2008
32. Wu H, Sun H, Wang C, Yu L, Li Y, Peng H, et al. Abnormalities in the structural covariance of emotion regulation networks in major depressive disorder. *J Psychiatr Res.* (2017) 84:237–42. doi: 10.1016/j.jpsychires.2016.10.001
33. Wang H, Jin X, Zhang Y, Wang J. Single-subject morphological brain networks: connectivity mapping, topological characterization and test–retest reliability. *Brain Behav.* (2016) 6:e00448. doi: 10.1002/brb3.448
34. Gao J, Chen M, Li Y, Gao Y, Li Y, Cai S, et al. Multisite autism spectrum disorder classification using convolutional neural network classifier and individual morphological brain networks. *Front Neurosci.* (2021) 14:629630. doi: 10.3389/fnins.2020.629630
35. Li X, Lei D, Niu R, Li L, Suo X, Li W, et al. Disruption of gray matter morphological networks in patients with paroxysmal kinesigenic dyskinesia. *Hum Brain Mapp.* (2021) 42:398–411. doi: 10.1002/hbm.25230
36. Monahan J, Steadman HJ, Appelbaum PS, Robbins PC, Mulvey EP, Silver E, et al. Developing a clinically useful actuarial tool for assessing violence risk. *Br J Psychiatry.* (2000) 176:312–9. doi: 10.1192/bjp.176.4.312
37. Nelson HE, A. modified card sorting test sensitive to frontal lobe defects. *Cortex.* (1976) 12:313–24. doi: 10.1016/S0010-9452(76)80035-4
38. Yudofsky SC, Silver JM, Jackson W, Endicott J, Williams D. The overt aggression scale for the objective rating of verbal and physical aggression. *Am J Psychiatry.* (1986) 143:35–9. doi: 10.1176/ajp.143.1.35
39. Wang J, Wei Q, Bai T, Zhou X, Sun H, Becker B, et al. Electroconvulsive therapy selectively enhanced feedforward connectivity from fusiform face area to amygdala in major depressive disorder. *Soc Cogn Affect Neurosci.* (2017) 12:1983–92. doi: 10.1093/scan/nsx100
40. Tzourio-Mazoyer N, Landeau B, Papathanassiou D, Crivello F, Etard O, Delcroix N, et al. Automated anatomical labeling of activations in SPM using a macroscopic anatomical parcellation of the MNI MRI single-subject brain. *Neuroimage.* (2002) 15:273–89. doi: 10.1006/nimg.2001.0978
41. Pop MG, Crivii C, Opincariu I. *Anatomy and Function of the Hypothalamus: Hypothalamus in Health and Diseases* (2018).
42. Toni R, Malaguti A, Benfenati F, Martini L. The human hypothalamus: a morpho-functional perspective. *J Endocrinol Investigat.* (2004) 27(6 Suppl):73–94.
43. Lechan RM, Toni R. "functional anatomy of the hypothalamus and pituitary," In: Feingold KR, Anawalt B, Boyce A, Chrousos G, de Herder WW, Dhatariya

K, et al., editors. *Endotext*. South Dartmouth MA: © 2000-2021, MDText.com, Inc. (2000).
44. Kullmann S, Heni M, Linder K, Zipfel S, Häring HU, Veit R, et al. Resting-state functional connectivity of the human hypothalamus. *Hum Brain Mapp.* (2014) 35:6088–96. doi: 10.1002/hbm.22607
45. Todd WD, Fenselau H, Wang JL, Zhang R, Machado NL, Venner A, et al. A hypothalamic circuit for the circadian control of aggression. *Nat Neurosci.* (2018) 21:717–24.
46. Hashikawa Y, Hashikawa K, Falkner AL, Lin D. Ventromedial hypothalamus and the generation of aggression. *Front Syst Neurosci.* (2017) 11:94. doi: 10.3389/fnsys.2017.00094
47. Gouveia FV, Hamani C, Fonoff ET, Brentani H, Alho EJL, de Morais RMCB, et al. Amygdala and hypothalamus: historical overview with focus on aggression. *Neurosurgery.* (2019) 85:11–30. doi: 10.1093/neuros/nyy635
48. Tognin S, Rambaldelli G, Perlini C, Bellani M, Marinelli V, Zoccatelli G, et al. Enlarged hypothalamic volumes in schizophrenia. *Psychiatry Res.* (2012) 204:75–81. doi: 10.1016/j.pscychresns.2012.10.006
49. Goldstein JM, Seidman LJ, Makris N, Ahern T, O'Brien LM, Caviness VS, et al. Hypothalamic abnormalities in schizophrenia: sex effects and genetic vulnerability. *Biological Psychiatry.* (2007) 61:935–45. doi: 10.1016/j.biopsych.2006.06.027
50. Koolschijn PCMP, van Haren NEM, Hulshoff Pol HE, Kahn RS. Hypothalamus volume in twin pairs discordant for schizophrenia. *Euro Neuropsychopharmacol.* (2008) 18:312–5. doi: 10.1016/j.euroneuro.2007.12.004
51. Schiffer B, Leygraf N, Müller BW, Scherbaum N, Forsting M, Wiltfang J, et al. Structural brain alterations associated with schizophrenia preceded by conduct disorder: a common and distinct subtype of schizophrenia? *Schizophr Bull.* (2013) 39:1115–28. doi: 10.1093/schbul/sbs115
52. Tononi G, Sporns O, Edelman GM, A. measure for brain complexity: relating functional segregation and integration in the nervous system. *Proc Natl Acad Sci U S A.* (1994) 91:5033–7. doi: 10.1073/pnas.91.11.5033
53. Shon S-H, Yoon W, Kim H, Joo SW, Kim Y, Lee J. Deterioration in global organization of structural brain networks in schizophrenia: a diffusion MRI tractography study. *Front Psychiatry*. (2018) 9(272). doi: 10.3389/fpsyt.2018.00272
54. Lynall ME, Bassett DS, Kerwin R, McKenna PJ, Kitzbichler M, Muller U, et al. Functional connectivity and brain networks in schizophrenia. *J Neurosci.* (2010) 30:9477–87. doi: 10.1523/JNEUROSCI.0333-10.2010
55. van den Heuvel MP, Fornito A. Brain networks in schizophrenia. *Neuropsychol Rev.* (2014) 24:32–48. doi: 10.1007/s11065-014-9248-7
56. Liu Y, Liang M, Zhou Y, He Y, Hao Y, Song M, et al. Disrupted small-world networks in schizophrenia. *Brain : J Neurol.* (2008) 131(Pt 4):945–61. doi: 10.1093/brain/awn018
57. Wang Q, Su TP, Zhou Y, Chou KH, Chen IY, Jiang T, et al. Anatomical insights into disrupted small-world networks in schizophrenia. *Neuroimage.* (2012) 59:1085–93. doi: 10.1016/j.neuroimage.2011.09.035
58. Palaniyappan L, Park B, Balain V, Dangi R, Liddle P. Abnormalities in structural covariance of cortical gyrification in schizophrenia. *Brain Struct Funct.* (2015) 220:2059–71. doi: 10.1007/s00429-014-0772-2
59. Zhou HY, Shi LJ, Shen YM, Fang YM, He YQ, Li HB, et al. Altered topographical organization of grey matter structural network in early-onset schizophrenia. *Psychiatry Res Neuroimaging.* (2021) 316:111344. doi: 10.1016/j.pscychresns.2021.111344
60. Lo CY, Su TW, Huang CC, Hung CC, Chen WL, Lan TH, et al. Randomization and resilience of brain functional networks as systems-level endophenotypes of schizophrenia. *Proc Natl Acad Sci U S A.* (2015) 112:9123–8. doi: 10.1073/pnas.1502052112
61. Anticevic A, Hu X, Xiao Y, Hu J, Li F, Bi F, et al. Early-course unmedicated schizophrenia patients exhibit elevated prefrontal connectivity associated with longitudinal change. *J. Neurosci.* (2015) 35:267–86. doi: 10.1523/JNEUROSCI.2310-14.2015
62. Marsman A, van den Heuvel MP, Klomp DW, Kahn RS, Luijten PR, Hulshoff Pol HE. Glutamate in schizophrenia: a focused review and meta-analysis of H-MRS studies. *Schizophr Bull.* (2013) 39:120–9. doi: 10.1093/schbul/sbr069
63. Cao H, Ingvar M, Hultman CM, Cannon T. Evidence for cerebello-thalamo-cortical hyperconnectivity as a heritable trait for schizophrenia. *Transl Psychiatry.* (2019) 9:192. doi: 10.1038/s41398-018-0353-x

Conflict of Interest: The authors declare that the research was conducted in the absence of any commercial or financial relationships that could be construed as a potential conflict of interest.

Publisher's Note: All claims expressed in this article are solely those of the authors and do not necessarily represent those of their affiliated organizations, or those of the publisher, the editors and the reviewers. Any product that may be evaluated in this article, or claim that may be made by its manufacturer, is not guaranteed or endorsed by the publisher.

frontiers in Psychiatry

REVIEW
published: 23 November 2021
doi: 10.3389/fpsyt.2021.751215

A Review on P300 in Obsessive-Compulsive Disorder

Alberto Raggi[1], *Giuseppe Lanza*[2,3]* *and Raffaele Ferri*[3]

[1] Unit of Neurology, G.B. Morgagni – L. Pierantoni Hospital, Forlì, Italy, [2] Department of Surgery and Medical-Surgical Specialties, University of Catania, Catania, Italy, [3] Clinical Neurophysiology Research Unit, Oasi Research Institute - Istituto di Ricerca e Cura a Cattarere Scientifico (IRCCS), Troina, Italy

Neuropsychological studies indicate the presence of cognitive changes in patients with obsessive-compulsive disorder (OCD). Indeed, OCD may be included among the dysfunctions of the frontal lobes and their connections with the limbic system, associative cortex, and basal ganglia. P300 is a positive component of the human event-related potential (ERP); it is associated with processes of encoding, identification, and categorization constituting, as a whole, the superior cortical function of information processing. Thus, P300 explores several areas that are implicated in OCD pathophysiology. Our aim is to review all relevant studies on the P300 component of the human ERP in order to recognize any significant central nervous system (CNS) correlate of cognitive dysfunction in OCD. A PubMed-based literature search resulted in 35 articles assessing P300 in OCD and reporting neurophysiological correlates of response inhibition, cortical hyperarousal, and over-focused attention. A decreased P300 amplitude was reported in both adult and pediatric patients, with a trend toward normalization after pharmacological treatment. Source localization studies disclosed an association between P300 abnormalities and the functioning of brain regions involved in the pathophysiology of OCD. Moreover, studies converge on the evidence of neurophysiological dysfunction in the frontal areas with impairment of the normal inhibitory processes in OCD. At least some of these electrophysiological correlates might reflect the obsessive thoughts and compulsions that characterize this disorder. These findings may also support cognitive-behavioral therapy (CBT) approaches on over-focused attention and inflexibility of compulsive behaviors, which should be associated to pharmacological treatment in these patients.

Keywords: cortical hyperarousal, information processing, obsessive-compulsive disorder, over-focused attention, p300, translational neuroscience

OPEN ACCESS

Edited by:
Yanghua Tian,
First Affiliated Hospital of Anhui Medical University, China

Reviewed by:
Yasuo Terao,
Kyorin University, Japan
Martin Desseilles,
University of Namur, Belgium

***Correspondence:**
Giuseppe Lanza
glanza@oasi.en.it

Specialty section:
This article was submitted to Neuroimaging and Stimulation, a section of the journal Frontiers in Psychiatry

Received: *31 July 2021*
Accepted: *01 November 2021*
Published: *23 November 2021*

Citation:
Raggi A, Lanza G and Ferri R (2021) A Review on P300 in Obsessive-Compulsive Disorder. Front. Psychiatry 12:751215. doi: 10.3389/fpsyt.2021.751215

INTRODUCTION

Obsessive-compulsive disorder (OCD) affects approximately 2–3% of people at some point of their life (1). In the Diagnostic and Statistical Manual of Mental Disorders— Fifth Edition (2), OCD was moved from the group of anxiety disorders to a new category, named Obsessive-Compulsive and Related Disorders (1). Obsessive-compulsive disorder usually first appears during adolescence or in early adults, although treatment may not be sought until the middle age. The two sexes are equally affected. The onset of OCD is typically gradual and cannot be accurately dated, although, in some cases, it is triggered by a particular event in the patient's life. In most instances, OCD is

engrafted into a personality in which rigidity and lack of adaptability are prominent. These traits are manifest in the individual's punctuality and in his/her dependability in the activities of everyday life. Additionally, there is always a prevailing undercurrent sense of insecurity (3–6). Clinically, the main symptoms of OCD are intrusive thoughts or images (obsessions), which increase anxiety, and repetitive and ritualistic actions (compulsions), which typically decrease anxiety (7, 8). In all of these obsessions and compulsions, patients suffer from a feeling of insufficiency in being unable to reject their troublesome thoughts (7, 8). This insight into the psychopathological experience and the struggle against it distinguish obsessions from delusions. Therefore, the majority of OCD patients are tense, irritable, and apprehensive. They may complain of anxiety attacks and become depressed with fatigue and lack of interest (7, 8). Education and pharmacotherapy with selective serotonin reuptake inhibitors (SSRIs) are first-line treatments, along with behavior therapy (7).

Neuropsychological studies indicate that patients with OCD may present some cognitive changes mainly involving executive functioning, information coding, organization strategy, set-shifting, motor and cognitive inhibition, visual-constructive and controlled fluency, verbal memory, and processing speed (9–11). Because of its neurobiological features, OCD may be included within the wide spectrum of dysfunctions of the frontal lobes and their connections with the limbic system, the associative cortex, and the basal ganglia which, in turn, influence the ability of abstract decisions needed to create more efficient and controlled behavioral judgment or action (12). In a previous study of patients who developed elements of obsessiveness and compulsive behavior after focal brain lesions, the authors found changes in the cingulate, frontal, and temporal cortices, as well as in the basal ganglia (13). On the other hand, the surgical disconnection of the orbito-frontal regions from limbic, thalamic, and striatal structures in severely affected patients improves symptoms of OCD (14). Moreover, neuroimaging studies in OCD demonstrate the involvement of the cortico-striato-thalamo-cortical loop, anterior cingulate cortex, prefrontal cortex, cerebellum, and hippocampus (15–18).

Based on this theoretical background, in this review we aimed to assess the utility of the P300 in the identification of any central nervous system (CNS) alteration, possibly correlated with cognitive dysfunction, in OCD patients. In particular, we focused on the electrophysiological correlates of some behaviors of individuals with OCD, such as the tendency of these patients to become aroused and exhibit strong defensive reactions to minimal stimulation (19, 20). Another aim was to assess the possible contribution of the P300 to the characterization of different OCD expressions, e.g., structural vs. functional brain abnormalities, within the clinical spectrum of a disease with a likely multifactorial basis.

As known, P300 is a positive component of the human event-related potential (ERP). It is associated with processes of encoding, identification, and categorization, that constitute, as a whole, the superior cortical function of information processing, and it is influenced by the effects of natural (i.e., circadian, ultradian, seasonal) and environmental state variables, such as fatigue (21–25). P300 is generated along a widely distributed network, rather than by a specific region, including the hippocampus and the medial temporal lobe, the temporo-parietal junction, and parietal areas, although the inferior and middle frontal, the orbito-frontal, and the cingulate cortices also contribute to it (26). For this reason, P300 involves several areas that seem to be implicated in the OCD pathophysiology (12–18).

P300 is most commonly elicited with an oddball paradigm in which a subject detects an occasional target stimulus within a regular train of standard stimuli (23, 25). Another paradigm to elicit P300 is the so-called "Go/No-Go" task, in which subjects are required to respond to one of the choices but must withhold a response to the other alternative (27). The test is passed only when the "Go" condition is met and the "No-Go" condition fails (25, 27). In psychophysiology, Go/No-Go tests are used to measure the participant's capacity to sustain attention and to control responses during the electroencephalographic (EEG) recording and the acquisition of ERP waves for each answer (25, 27, 28). For instance, a "Go/No-Go" test can require a participant to perform an action given certain stimuli (e.g., press a button: "Go") and to inhibit the same action under a different set of stimuli (e.g., not press the same button: "No-Go") (25, 27).

P300, also referred to as P3b, is better recorded with a maximum peak over the Pz scalp location (according to the EEG international 10–20 system) if the subject is actively engaged in the task of detecting the target (25, 29). Otherwise, a distractor tone (novelty) usually elicits a P3a wave, that has a frontal/central maximum amplitude distribution and frontal sources (30, 31). The P3b amplitude is a function of some psychological variables, such as attention, expectation of the event, and attribution to the event of a significance and complexity of the task (22, 23). Wave latency provides an indirect measure of the duration of the processes involved in stimulus discrimination, and ranges approximately from 300 ms (for simple dual tone discrimination tasks) to 750 ms (for much more complex processes) (22).

The P300 has already been applied in depicting, better than neuropsychological tests, even subtle cognitive deficits in some neuropsychiatric diseases, both in adults and children, such as sporadic amyotrophic lateral sclerosis without dementia, narcolepsy, obstructive sleep apnoea syndrome, and migraine (32–36). Evoked potentials occurring after stimulus presentation and preceding (e.g., P100, N100, P200, N200) or following (slow wave) the P300 wave are all components reflecting the time course of task-related neural information-processing (25, 37–40). In detail, N200 is elicited by both expected and ignored rare stimuli; it is followed by P300 when the subject is engaged in a particular stimulus of recognition (40). N200 seems to be an automatic process independent of control; it is similar to P300 in terms of sensitivity to attention and stimulus infrequency, and its latency correlates with reaction time (37). Finally, it is worth reminding that P300 is not seen in the raw EEG recording and can only be detected by averaging (41).

In summary, P300 seems to be a tool to investigate possible and different information processing changes in patients with OCD. The number of studies published on this topic deserves a timely re-examination of the available literature. The conclusion arising from this review may lead to further insights into

the research agenda of OCD and, translationally, into clinical applications in other psychiatric and neuropsychiatric disorders, in terms of diagnostic work-up, follow-up assessment, and pharmacological and/or behavioral treatment index of response.

METHODS

This review included all relevant original articles published in peer-reviewed journals, indexed in the National Institutes of Health—National Library of Medicine (PubMed) literature search system, from database inception to July 2021. Search terms were "obsessive-compulsive disorder" and "P300." The main inclusion criterion required that all the original research articles measured the P300 wave in humans; conversely, all the studies that did not explicitly report data concerning the evaluation of P300 in OCD were excluded. Non-English written articles, book chapters, monographs, commentaries, reviews, case studies, dissertations, abstracts, and letters to editor were also excluded, as well as any other article that did not fit the primary goal of the present review. Titles and abstracts of the retrieved studies were independently reviewed by two authors (G.L. and R.F.) based on the inclusion and exclusion criteria. Additional articles in the reference list of the papers identified by the search were also evaluated for inclusion in the review.

RESULTS

The PubMed-based search originally produced a group of 34 studies. Three of them were excluded because they were not written in English; another article was excluded because it was a review. Five additional papers were retrieved from the reference list of the selected articles. Therefore, a final group of 35 studies (summarized in **Table 1**) investigating P300 in patients with OCD was included in this review (19, 20, 28, 42–73). **Figure 1** shows the flow of information through the different phases of the review process.

Since the studies eventually included in this review deal with different aspects and methods, we will analyze their content in the following separate paragraphs.

P300 Amplitude

Brain volume changes have been reported in OCD by neuroimaging (17). Therefore, we first consider here the studies reporting a decreased P300 amplitude, such as in neurodegenerative disorders (74, 75) or schizophrenia (76). In these conditions, a reduced amplitude of P300 is considered as a somewhat robust finding, possibly suggesting a genetic endophenotype (75, 76).

Overall, studies reporting a P300 amplitude reduction in OCD are thirteen (20, 28, 45, 51, 54, 55, 59, 64, 65, 67, 68, 70, 72), including the result of a P300 alteration at the F7 location in patients with functional constipation within a probable OCD (65). Conversely, we counted eight studies reporting enhanced P300 amplitude in OCD patients compared to normal controls (50, 52, 58, 61–63, 66, 69), a finding that was considered as an electrophysiological correlate of an OCD trait and indicating an increased propensity to be aroused (50, 77). Finally, one article reported that future responders to treatment had significantly enhanced P300 amplitude, compared to future non-responders; this finding is an example of the possible prognostic value of psychophysiological measures (47).

Clinical observations, neuropsychological testing, and pioneering neurophysiological investigations suggest deficits in set-shifting, impaired early-filtering selective attention, loss of normal inhibitory processes, and altered motor and cognitive inhibition in individuals with OCD (1, 7, 10, 11, 19, 20, 41). Accordingly, the "Go/No-Go" is a task in which subjects with impaired frontal lobe abilities are known to fail (78). Indeed, all the five studies adopting a "Go/No-Go" visual task in OCD highlighted a frontal dysfunction pattern (28, 53, 57, 65, 73), including a study in adolescent patients (73) and one in subjects with functional constipation and probable OCD (65). Therefore, the No-Go-N200 seems to be an accurate response inhibition measurement for patients affected by OCD.

A significant relationship between ERP abnormalities and severity of OCD symptoms was found in 13 studies (44, 46–53, 55, 57, 59, 64, 68–70, 72). Thus, ERP abnormalities might be considered as a sensitive tool for measuring the biological substrate of OCD severity. However, P300 characteristics were not associated with symptom severity in 11 studies on patients with OCD (19, 48, 51, 52, 54, 58, 61–63, 66, 67), thus allowing to hypothesize that P300 abnormalities in patients with OCD might constitute a trait, rather than a state, feature.

P300 Latency

The shortening in P300 latency may reflect the trait of obsessionals to increase the response speed to task-dependent processes in a context of enhanced cortical responsiveness, probably due to a low level of inhibitory activity (20, 47). Studies reporting a decreased P300 latency in OCD are nine (20, 42–49, 52, 55). For instance, some authors using a two-tone auditory paradigm (55) described a shorter P300 duration in obsessional patients, compared to normal controls, calculated as the time difference between the N200 peak and the beginning of the slow wave. As stated, N200 is similar to P300 in terms of sensitivity to attention and stimulus infrequency, and its latency correlates with the reaction time (37). There are also several articles reporting N200 latency reduction (19, 42–44, 47, 48). Regarding the effect of treatment, one study only reported a longer P300 latency at baseline in drug-free OCD patients compared to controls, along with no modification at follow-up (51).

Source Localization

A detailed knowledge of P300 generators is crucial for an appropriate understanding of its cognitive significance and clinical utility (79). However, this remains a challenging issue, especially when translating it to a practical level (e.g., the high number of EEG electrodes to be used) and when considering that a very large number of different generator assemblies can produce the same potential field on the scalp (80). As such, the localization of a limited number of equivalent dipoles is the most typical approach (81, 82) also used in OCD research.

A preliminary study was set up in order to perform a dipole source analysis for the discrimination between P3a and

TABLE 1 | Studies investigating P300 in patients with obsessive-compulsive disorder and P300 parameters at Pz (usually the lead with the largest peak).

References	Groups (*n*)	OCD group age, years mean ± SD (range)	Study design, paradigm, main findings, and significance	P 300 amplitude, μV		P 300 latency, ms	
				OCD	Controls	OCD	Controls
Ciesielski et al. (19)	8 unmedicated OCD (4 medicated), 8 HC	36.5, SD and range N/A	Cross sectional Visual oddball paradigm OCD patients showed P100 reduced amplitude and N200 decreased latency than the HC group; N.S. differences for the P300 OCD patients have a special potential for becoming aroused and exhibiting strong defensive reactions to minimal stimulation	N/A for Pz; 11.1 ± 4.9 (at P3 – DT); 10.8 ± 4.6 (at P4 – DT)	N/A for Pz; 16.0 ± 2.4 (at P3 – DT); 14.0 ± 2.8	N/A for Pz; 335 ± 23.5 (at P3 – DT); 333 ± 20.9 (at P4 – DT); (at P4 – DT)	N/A for Pz; 345 ± 10.5 (at P3 – DT); 349 ± 8.0 (at P4 – DT)
Beech et al. (20)	8 OCD (3 patients stopped antidepressant medication 48 h before testing), 8 HC	40, SD, and range N/A	Cross sectional Visual oddball paradigm OCD patients showed P300 reduced amplitude and decreased latency than the HC group OCD patients have a special potential for becoming aroused and exhibiting strong defensive reactions to minimal stimulation	N/A; 8.5 ± 2.5 (at P3 – ET); **7.1 ± 2.8** (at P3 – DT); 8.6 ± 3.0 (at P4 – ET); **7.0 ± 2.0** (at P4 – DT)	N/A; 10.8 ± 1.7 (at P3 – ET); **12.0 ± 2.0** (at P3 – DT); 10.2 ± 2.1 (at P4 – ET); **12.4 ± 2.9** (at P4 – DT)	N/A; **327 ± 37.4** (at P3 – ET); **318 ± 39.1** (at P3 – DT); **328 ± 37.0** (at P4 – ET); **319 ± 38.7** (at P4 – DT)	N/A; **356 ± 21.0** (at P3 – ET); **365 ± 26.5** (at P3 – DT); **357 ± 27.4** (at P4 – ET); **368 ± 23.1 7** (at P4 – DT)
Malloy et al. (28)	18 OCD (9 medicated), 18 HC	34 ± 12.8, range N/A	Cross sectional Go/No-Go visual test Topographic ERP mapping revealed significantly smaller P300 magnitudes in orbital frontal areas in the OCD patients Frontal dysfunction	26.2 ± 9.6 (Go); 25.9 ± 8.0 (No-Go); 10.9 ± 12.6 (Go at Fz); **14.3 ± 12.8** (No-Go at Fz)	29.9 ± 13.07 (Go); 33.0 ± 12.5 (No-Go); 12.2 ± 14.9 (Go at Fz); **22.4 ± 18.3** (No-Go at Fz)	N/A	N/A
Towey et al. (42)	10 unmedicated OCD, 10 HC	mean ± SD N/A (18–55)	Cross sectional Two-tone auditory oddball paradigm The OCD group showed significantly shorter P300 latencies and shorter N200 latencies for target stimuli with increasing task difficulty than the HC group; for both levels of task difficulty, OCD patients showed greater negativity than HC group in the N200 over the left hemisphere Cortical hyperarousal in OCD with a laterality pattern	N/A	N/A	N/A	N/A
Drake et al. (43)	20 unmedicated (10) or after a washout period of 1 week (10) GTS, 10 of whom had ADHD and 6 OCD	mean ± SD N/A (8–20)	Cross sectional Two-tone auditory oddball GTS patients with OCD had shorter N200 and P300 latencies Cortical hyperarousal in GTS patients with OCD as it happens in pure OCD patients	N/A	N/A	N/A; **272.0 ± 41.3** (at Cz – GTS+OCD)	N/A; **358 ± 13.7** (at Cz – GTS only)

(Continued)

TABLE 1 | Continued

References	Groups (*n*)	OCD group age, years mean ± SD (range)	Study design, paradigm, main findings, and significance	P 300 amplitude, μV		P 300 latency, ms	
				OCD	Controls	OCD	Controls
Towey et al. (44)	17 unmedicated OCD, 16 HC	mean ± SD N/A (18–55)	Cross sectional Two-tone auditory oddball paradigm The OCD group showed significantly shorter P300 latencies and shorter N200 latencies for target stimuli with increasing task difficulty than the HC group; for both levels of task difficulty, OCD patients showed greater negativity than HC group in the N200 over the left hemisphere Cortical hyperarousal in OCD	N/A	N/A	408 (easy task); **402** (DT); SD N/A	395 (easy task); **456** (DT); SD N/A
Towey et al. (45)	17 unmedicated OCD, 16 HC	30 ± 9.1, range N/A	Cross sectional Two-tone auditory left and right presentation oddball paradigm The OCD group showed significantly larger attention-related PN than HC group; P300 amplitudes for attended targets were smaller for OCD patient than HCs, but the reverse was true for P300 for unattended non-targets Hyper activation of the frontal lobes	N/A	N/A	N/A	N/A
de Groot et al. (46)	18 unmedicated OCD, 18 HC	30.5 ± 6.9 (19–59)	Cross sectional Two-tone auditory oddball While not reaching significance, P300 latencies tended to be shorter for the OCD group; increased N200 negative amplitude and decreased latencies of the SW components; the more chronic the OCD symptoms, the more attenuated the integrated amplitude between 140 and 170 msec Cortical hyperarousal in OCD	N/A	N/A	325 ± 31	344 ± 39
Morault et al. (47)	13 unmedicated (1-week washout period with 5 responders and 8 non-responders) OCD, 13 HC	35 ± 8 (21–60)	Comparative study Verbal auditory oddball paradigm OCD patients showed longer latencies of the N100 and P200, shorter latency of the P300 and reduced amplitude of the N200; future responders to treatment had significantly reduced N200 and enhanced P300 amplitudes relative to future nonresponders. OCD patients stress the speed of task-dependent processes; ERPs might provide psychophysiological profiles in OCD patients with clinical and pharmacological implications	8.37 ± 4.29 (responders); 4.72 ± 6.28 (nonresponders)	N/A	**442.0 ± 60**	**534.0 ± 32.1**

(Continued)

TABLE 1 | Continued

References	Groups (*n*)	OCD group age, years mean ± SD (range)	Study design, paradigm, main findings, and significance	P 300 amplitude, μV		P 300 latency, ms	
				OCD	Controls	OCD	Controls
Miyata et al. (48)	23 unmedicated OCD, 12 unmedicated SP, 18 HC	24.7 ± 5.0, range N/A	Cross sectional Two-tone auditory oddball paradigm The OCD group showed significantly shorter P300 latencies and shorter N200 latencies for target stimuli than the SP and the HC groups; there were no significant relationships between these ERP abnormalities in OCD patients and the type or severity of their OCD symptoms Shorter N200 and P300 latencies in OCD patients may be an OCD-associated phenomenon that is more closely related to the biological basis for OCD (cortical hyperarousal), rather than the characteristics of their OCD symptoms	13.5 ± 5.3	15.1 ± 6.1	**302.5 ± 29.9**	**341.9 ± 23.8**
Morault et al. (49)	21 unmedicated (1-week washout period) OCD, 21 HC	37.3 ± 10.9 (21–60)	Comparative and replication study Verbal auditory oddball paradigm OCD patients who were to respond favorably to treatment had significantly reduced N200 amplitude and shorter N200 and P300 latencies compared to non-responders and control subjects Some impairments of pre-treatment ERPs could be associated with future treatment outcome	N/A 3.5 ± 4.9 (G-mean) (responders); 1.9 ± 4.7 (non-responders)	N/A 2.2 ± 5.9 (G-mean)	N/A **466 ± 72** (G-mean) (responders); 579 ± 6.0 (non-responders)	N/A **562 ± 43** (G-mean)
Di Russo et al. (50)	8 unmedicated OCD, 12 HC	29.7 ± 6.3, range N/A	Cross sectional Discriminative response test OCD patients had greater P300 amplitude than HCs for the target stimuli, but not for non-target stimuli; spline map topography confirmed that P300 hyperactivation is localized principally on the frontal lobes Cortical hyperarousal in OCD as frontal lobe dysfunction	5.3 ± 0.7	N/A	N/A	N/A
Sanz et al. (51)	19 OCD, 19 HC	25.8, SD and range N/A	Cross sectional plus pharmacological follow-up study Two-tone auditory oddball paradigm P300 had lower baseline amplitude and longer latency in drug-free OCD patients when compared to HCs; P300 amplitude in OCD increased after treatment (clomipramine in 250-300 mg doses), although this was supported only by a statistical trend; there was no modification in P300 latency after treatment	**6.6** (SD N/A, drug free OCD)	**11.01** (SD N/A)	**308** (SD N/A)	**288** (SD N/A)

(Continued)

TABLE 1 | Continued

References	Groups (*n*)	OCD group age, years mean ± SD (range)	Study design, paradigm, main findings, and significance	P 300 amplitude, μV		P 300 latency, ms	
				OCD	Controls	OCD	Controls
			The effect of treatment suggest that the cognitive function in OCD patients improved with pharmacological treatment possibly because of a better serotonin function, and this was reflected in a P300 amplitude close to that of normal people				
Mavrogiorgou et al. (52)	21 unmedicated OCD, 21 HC	33.9 ± 12.0 (17–57)	Cross sectional Two-tone auditory oddball paradigm OCD patients showed a larger P3b amplitude and a shorter P3b latency (only right hemisphere) as well as a shorter reaction time to target tones as the HCs The P3b abnormalities found in OCD patients could be an electrophysiological correlate of overfocussed attention and faster cognitive processes in OCD, possibly due to higher arousal	N/A	N/A	N/A	N/A
Herrmann et al. (53)	12 medicated OCD, 12 HC	41.2 ± 15.7, range N/A	Cross sectional Go/No-Go visual test Reduced frontal activity during the No-Go condition in OCD, which was condensed in a reduced anteriorization of the brain electrical field Frontal dysfunction	N/A	N/A	N/A	N/A
Kim et al. (54)	19 OCD (2 medicated), 22 SPR, 21 HC	26.74 ± 6.89, range N/A	Cross sectional Two-tone auditory oddball and NPS testing P300 amplitudes on all 15 electrode sites were significantly smaller in SPR and OCD patients than in HC subjects; P300 amplitude was related to the Trail Making Test (Part B) response time Frontal dysfunction	N/A	N/A	N/A	N/A
Kivircik et al. (55)	31 unmedicated OCD, 30 HC	27 ± 9.8 (18–55)	Cross sectional Two-tone auditory oddball paradigm The OCD group showed shorter P300 duration (calculated as the time difference between N200 peak and the beginning of the SW) compared to HCs; in NPS tests, no significant differences were found between the two groups Acceleration in the P300 process	7.40 ± 4.88	7.63 ± 4.33	N/A	N/A

(Continued)

TABLE 1 | Continued

References	Groups (*n*)	OCD group age, years mean ± SD (range)	Study design, paradigm, main findings, and significance	P 300 amplitude, μV		P 300 latency, ms	
				OCD	Controls	OCD	Controls
Papageorgiou et al. (56)	18 OCD, 20 AHA, 20 HC	29 ± 10.3, range N/A	Comparative study Auditory working memory test AHA and OCD groups showed a reduction of the P300 amplitudes, located at the right frontal area as compared to HCs; the AHA exhibited a significantly lower P300 amplitude at central frontal areas relative to the other two groups; the OCD patients manifested a significant prolongation of P300 located at the central prefrontal area, relative to AHAs and HCs Both OCD and AHAs may share a common impairment of working memory and/or attention involving the right prefrontal areas.	14.9 ± 7.0	13.6 ± 5.8; 9.3 ± 5.5 (AHA)	331 ± 60; **326 ± 67** (at Fz)	302 ± 57; 309 ± 71 (AHA); **275 ± 73** (at Fz); **295 ± 36** (AHA at Fz)
Kim et al. (57)	15 OCD (11 medicated, 4 unmedicated), 15 HC	25.73 ± 4.83, range N/A	Cross sectional Go/No-Go visual test The OCD patients manifested reduced No-Go-N200 and Go-N200 amplitudes at the frontocentral electrode sites compared to the HCs; the No-Go-N200 amplitudes and latencies measured at the central sites were also negatively correlated with the severity of symptoms; the OCD and HC groups were comparable with regard to Go-P300 and No-Go-P300 amplitude and latencies Dysfunctions in frontal regions mediating response inhibition in OCD detectable more by means of N200 than P300	10.76 ± 1.03 (Go); 5.86 ± 0.92 (No-Go)	8.72 ± 1.03 (Go); 6.67 ± 0.92 (No-Go)	413.00 ± 10.39 (Go); 415.87 ± 10.41 (No-Go)	419.13 ± 10.39 (Go); 410.60 ± 10.41 (No-Go)
Gohle et al. (58)	63 unmedicated OCD, 63 HC	33.71 ± 10.17, range N/A	Cross sectional Two-tone auditory oddball to elicit P300, which was separated with dipole source analysis into temporo-superior dipole (P3a) and temporo-basal dipole (P3b) OCD patients had significantly larger amplitudes of P3b than the HCs Study suggesting disturbances also in temporo-parietal and hippocampal regions in OCD	N/A 3.94 ± 2.3 (P3a); **7.05 ± 2.42** (P3b)	N/A 3.75 ± 1.75 (P3a); **5.87 ± 1.82** (P3b)	N/A 306.1 ± 25.8 (P3a); 320.6 ± 127.2 (P3b)	N/A 308.0 ± 23.7 (P3a); 316.8 ± 25.5 (P3b)

(Continued)

TABLE 1 | Continued

References	Groups (*n*)	OCD group age, years mean ± SD (range)	Study design, paradigm, main findings, and significance	P 300 amplitude, μV		P 300 latency, ms	
				OCD	Controls	OCD	Controls
Thibault et al. (59)	15 medicated OCD, 14 GTS, 12 GTS+OCD, 14 HC	37 ± 13, range N/A	Cross sectional Visual counting oddball paradigm The P300 was reduced in participants in both OCD and GTS+OCD groups in the anterior region; the P300 oddball effect was significantly larger in participants of the GTS group compared to all other groups, mostly in the parietal region GTS is characterized by enhanced working memory updating processes and the superimposition of OCD could lead to a reduction of these processes	N/A	N/A	N/A	N/A
Pallanti et al. (60)	16 OCD, 11 schizo-OCD, 14 SPR, 12 HC	29.7 ± 6.3 (18–65)	Cross sectional Discriminative response test Schizo-OCD patients showed a distinct ERP pattern, with abnormally increased target activation (akin to OCD, but unlike the pattern observed in SPR) and reduced P300 amplitudes (akin to SPR, but unlike OCD); similar to HC; schizo-OCD patients showed larger amplitudes in the non-target condition than in the target condition Schizo-OCD may not only be a distinct clinical entity from pure OCD and SPR, but it may also be characterized by a distinguishable neurophysiologic pattern	6.30 ± 0.4	N/A	N/A	N/A
Ischebeck et al. (61)	20 OCD (10 medicated), 20 HC	32.8 ± 9.9, range N/A	Cross sectional Visual recognition test during which irrelevant repeated standard sounds and unitary novel sounds were interspersed Novelty P300 amplitude increased in OCD; scalp distribution of the novelty P300 was less lateralized in patients than in controls A physiological indicator of an enhanced cortical orienting response implicating stronger involuntary shifts of attention	N/A	N/A	N/A	N/A

(Continued)

TABLE 1 | Continued

References	Groups (*n*)	OCD group age, years mean ± SD (range)	Study design, paradigm, main findings, and significance	P 300 amplitude, μV		P 300 latency, ms	
				OCD	Controls	OCD	Controls
Andreou et al. (62)	71 unmedicated OCD, 71 HC	34.68 ± 10.83 (18–62)	Cross sectional plus pharmacological follow-up study Two-tone auditory oddball with source localization analysis Increased P300-related activity was observed predominantly in the left orbitofrontal cortex, but also in left prefrontal, parietal and temporal areas, in patients compared to controls at baseline; after treatment, reduction of left middle frontal cortex hyperactivity was observed in patients Association between P300 abnormalities and activity in brain regions postulated to be involved in the pathophysiology of OCD	**7.43 ± 2.89**	**6.47 ± 2.63**	327 ± 52.2	340 ± 57.3
Endrass et al. (63)	25 OCD (8 medicated), 25 HC	33.4 ± 9.4, range N/A	Cross sectional A four-choice object reversal learning test measuring FRN and P300 Active task that required recurrent feedback-based behavioral adjustment in response to changing reward contingencies Higher error rates of OCD patients in response to negative feedback (FRN was reduced for negative feedback); the P300 was larger on all positive feedback events and on second exploration negative than on reversal negative feedback FRN reduction suggests attenuated monitoring of feedback during the learning process in OCD	N/A	N/A	N/A	N/A
Yamamuro et al. (64)	20 OCD, 20 HC	12.8 ± 2.5, range N/A	Cross sectional Two-tone auditory oddball paradigm The amplitudes of the P300 components in the Fz, Cz, Pz, C3, and C4 regions were significantly smaller in the OCD group compared to the HC group; there was significant correlation between illness severity and amplitude values at Cz, Pz, C3 P300 amplitudes are sensitive tools for measuring the biological aspects of OCD severity	**17.9 ± 7.2**	**22.6 ± 7.3**	315.5 ± 26.6	329.7 ± 17.8

(Continued)

TABLE 1 | Continued

References	Groups (*n*)	OCD group age, years mean ± SD (range)	Study design, paradigm, main findings, and significance	P 300 amplitude, μV		P 300 latency, ms	
				OCD	Controls	OCD	Controls
Li et al. (65)	35 FC, 24 HC	mean ± SD N/A (18–70)	Observational study Go/No-Go visual test There was reduced P300 amplitude at F7 between FC and HC groups Cognitive dysfunction of implicit processing might be involved in the abnormality of visual communication and information processing	5.64 ± 3.74 (FC group)	4.75 ± 3.48	437.86 ± 127.84 (FC group)	477.09 ± 129.58
Ozcan et al. (66)	33 OCD, 18 sibling, 21 HC	35.3 ± 11.9, range N/A	Cross sectional Two-tone auditory oddball paradigm P300 amplitude was sorted as patients<siblings<controls; the logistic regression analysis showed that, higher P300 amplitude, better performance on block design test and faster completion of Stroop test would predict being in the control group, whereas higher P200 amplitude would predict being in the case (patient and sibling) groups Identification of potential NPS and ERP endophenotypes of OCD	**10.02 ± 4.08**	**13.81 ± 3.77**; **10.78 ± 4.82** (siblings)	**315.37 ± 26.67**	**334.88 ± 30.4**; **312.77 ± 29.04** (siblings)
Yamamuro et al. (67)	14 OCD, 10 HC	33.20 ± 9.84, range N/A	Longitudinal study of 1 year Two-tone auditory oddball paradigm OCD had decreased P300 amplitude at the baseline which was significantly increased at Fz, Cz, C3, and C4, indicating normalization, after 1 year of treatment P300 may be a useful tool for evaluating therapy in OCD patients	14.59 ± 1.25 at baseline; 17.34 ± 1.62 after 1 year	18.52 ± 1.37 at baseline	321.33.77 ± 7.61 at baseline; 332.77 ± 7.61 after 1 year	312.40 ± 10.93 at baseline
Yamamuro et al. (68)	12 OCD, 12 HC	13.50 ± 3.26, range N/A	Longitudinal study of 3 years Two-tone auditory oddball paradigm OCD had decreased P300 amplitude at Fz – Cz – Pz– C3 – C4, which increased partly at Fz and C4 in association with symptomatic improvements Utility of SSRIs in pediatric OCD and of ERPs for evaluating pharmacological effects in treatment-naïve pediatric OCD patients	**18.10 ± 2.3**	**25.87 ± 2.02**	332.92 ± 15.19	331.08 ± 18.76
Dayan-Riva et al. (69)	38 unmedicated OCD, 38 HC	23.82 ± 1.56, range N/A	Cross sectional Visual oddball paradigm OCD patients demonstrated significantly enhanced P300 amplitude over bilateral parietal areas in response to neutral stimuli; emotional valence reduced this effect such that OCD patients did not differ from HCs in P300 amplitude under the angry stimuli condition	N/A	N/A	N/A	N/A

(Continued)

TABLE 1 | Continued

References	Groups (*n*)	OCD group age, years mean ± SD (range)	Study design, paradigm, main findings, and significance	P 300 amplitude, μV		P 300 latency, ms	
				OCD	Controls	OCD	Controls
			Results may represent distracted primary cognitive processes in OCD, possibly serving as a basic source for compulsion initiation				
Okazaki et al. (70)	15 unmedicated OCD, 15 HC	11.53 ± 2.90, range N/A	Cross sectional Two-tone auditory oddball paradigm P300 amplitude was significantly attenuated in the OCD group at Fz, C3, and C4, compared to HCs; OCD had altered reaction time P300 reduction as an index of brain dysfunction in OCD	16.30 ± 1.68; **7.95 ± 0.85** (at Fz); **10.55 ± 1.28** (at C3); **9.38 ± 1.17** (at C4)	17.48 ± 1.18; **11.80 ± 1.46** (at Fz); **14.78 ± 1.47** (at C3); **14.36 ± 1.57** (at C4)	319.07 ± 7.05; 327.08 ± 5.78 (at Fz); 322.27 ± 6.24 (at C3); 322.21 ± 5.47 (at C4)	327.20 ± 9.41; 324.53 ± 10.46 (at Fz); 327.33 ± 8.84 (at C3); 324.33 ± 9.64 (at C4)
Wojcik et al. (71)	30 psychiatric patients including 2 OCD	mean ± SD and range N/A	Containerization study Visual oddball paradigm with source localization analysis The most active Brodmann Areas for the few OCD patients were the frontal areas Hyper activation of the frontal lobes	N/A	N/A	N/A	N/A
Kloft et al. (72)	21 tic-free OCD (5 medicated), 12 tic-related OCD (5 medicated), 21 HC	34.0 ± 8.3 (tic-free OCD), 33.6 ± 8.8 (tic-related OCD), range N/A	Comparative study Visual/auditory stop-signal paradigm P300 amplitude was larger in tic-free compared to tic-related OCD and HCs Hyperactivity in the evaluation of the outcome of the inhibition process in OCD patients	N/A; **28.9 ± 11.3** (at Cz – StC – tic-free OCD); **22.2 ± 9.2** (at Cz – StC – tic-related OCD); **28.1 ± 10.9** (at Cz – StF – tic-free OCD); **19.8 ± 8.5** (at Cz – StF – tic-related OCD)	N/A; **22 ± 6.7** (at Cz – StC); **19.4 ± 8.4** (at Cz – StF)	N/A; 302 ± 32 (at Cz – StC – tic-free OCD); 326 ± 29. (at Cz – StC – tic-related OCD); 322 ± 21 (at Cz – StF – tic-free OCD); 340 ± 48 (at Cz – StF – tic-related OCD)	N/A; 306 ± 40 (at Cz – StC); 321 ± 24 (at Cz – StF)
Wolff et al. (73)	27 OCD (2 medicated, 11 with neuropsychiatric comorbidities), 27 HC	13.8 ± 2.34, range N/A	Cross sectional Go/No-Go visual test P300 amplitudes revealed a significant main effect of condition indicating significantly increased (more positive) P300 amplitudes during Go vs. No/Go-trials; a significant main effect of congruency was observed indicating significantly increased (more positive) P300 amplitudes during incongruent vs. congruent trials Pathological fronto-striatal hyperactivity and loss of a situation-specific modulation of response selection mechanisms in OCD	**32.4 ± 2.24** (Go); **23.58 ± 0.12** (No/Go); **29.11 ± 2.18** (incongruent trials); **26.89 ± 1.97** (congruent trials)	N/A	N/A	N/A

ADHD, attention deficit hyperactivity disorder; AHA, abstinent heroin addicts; DT, difficult task; ERP, event-related potential; ET, easy task; FC, functional constipation; FRN, feedback-related negativity; G-mean, grand mean values across tasks and leads (Fz-Pz); GTS, Gilles de la Tourette syndrome; HC, healthy controls; N/A, not available; N.S., not significant; NPS, neuropsychological; OCD, obsessive-compulsive disorder; PN, processing negativity; SP, social phobia; SPR, schizophrenia; SSRI, serotonin reuptake inhibitor; StC, stop correct; StF, stop fail; SW, slow wave. Data are shown as mean ± standard deviation; statistically significant different values are in bold.

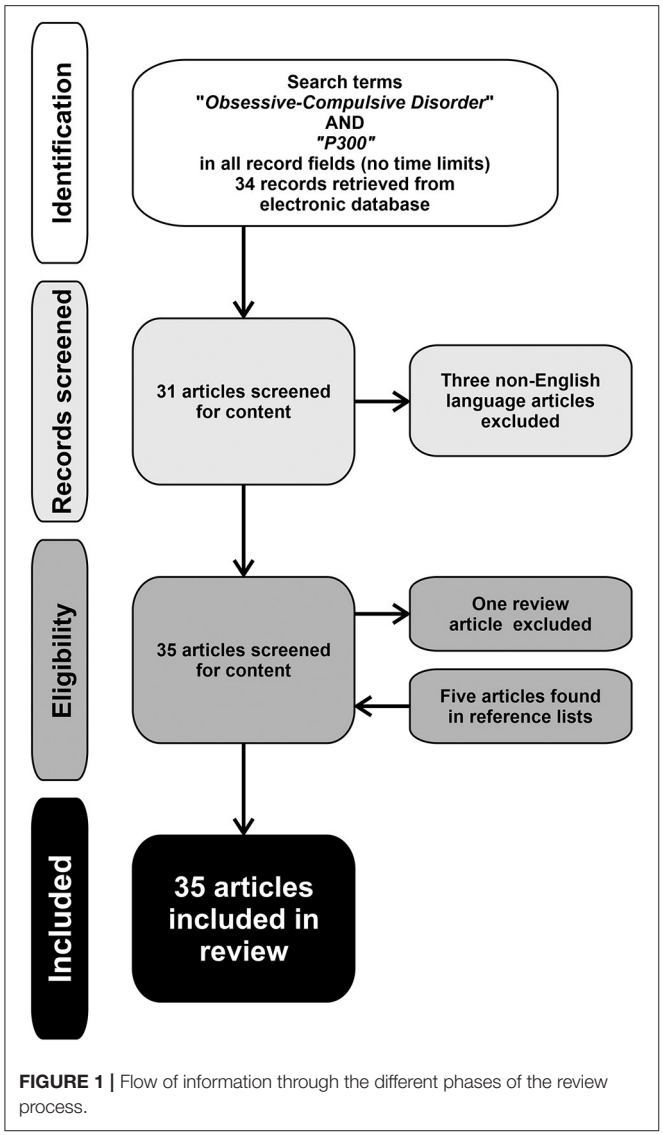

FIGURE 1 | Flow of information through the different phases of the review process.

P3b subcomponents elicited by an auditory oddball paradigm. Obsessive-compulsive disorder patients showed a larger P3b amplitude and a shorter P3b latency, as well as a shorter reaction time to target tones, compared to healthy controls. The P3b abnormalities found in these patients might be viewed as the electrophysiological correlate of overfocussed attention and faster cognitive processes, possibly due to a higher arousal (52). However, it cannot be excluded that the abnormalities in P3b amplitude and latency may reflect structural or functional disturbances in temporo-parietal or temporo-basal areas of OCD patients. This view is supported by neuroimaging research showing hyperperfusion or activation in the medial temporal lobe of subjects with OCD (83). Larger amplitude and shorter latency of the P3a subcomponent, which mainly reflects the frontal hyperactivity (42, 45, 54), were not confirmed in this study, probably because the authors found no difference in the P3a between patients and controls. It is worth to note that this apparent negative finding may also shows some limits of the technique.

The orbito-frontal cortex, the activity of which was found to be impaired in OCD patients (17, 84), is located deeply in the ventromedial anterior part of the brain. Given that neuronal activity of the orbito-frontal cortex cannot probably be recorded by scalp electrodes, the temporo-superior dipole (P3a), which is calculated for the scalp data, was unable to reflect activity from this brain area. Subsequently, other authors confirmed the previous findings on the P3b (58), whereas a more recent study on 30 psychiatric patients (but only two with OCD) was carried out with a visual oddball paradigm followed by a source localization analysis using a 256-channel EEG dense array (71). The inferior frontal gyrus was found to be the most active brain area in the few OCD patients (71). Two additional studies (62, 69) involving a higher number of subjects supported the concept that P300 is generated along a widely distributed network involving several brain areas implicated in OCD, as recently confirmed by some neuroimaging research (17, 18), with both pharmacological treatment (62) and emotional drive (60) able to attenuate these functional changes.

Moreover, topographic ERP mapping revealed significantly smaller P300 magnitude in the rostral frontal areas during the "No-Go" condition in individuals with OCD (28, 53). In a subsequent study (57), patients manifested reduced No-Go-N200 and Go-N200 amplitudes at the frontocentral electrode sites, compared to healthy controls, although the two groups were comparable with regard to Go-P300 and No-Go-P300 amplitudes and latencies.

Novelty P3a

The P3a originates from stimulus-driven frontal attention mechanisms during task processing (30). To obtain this evoked response, novel stimuli are presented infrequently within a background of frequently occurring standard stimuli and infrequently occurring distractor stimuli, while the subject is not required to respond mentally or physically to any stimulus (31). In an *ad hoc* study, novelty P3a amplitude was found to be increased in OCD patients compared to healthy controls, thus possibly representing a physiological index of enhanced cortical orienting response and implicating a facilitation of involuntary shifts of attention occurring in this condition (61).

Laterality Pattern

A re-examination of positron emission tomography (PET), EEG, and single case studies previously performed by Flor-Henry (85) suggests that a lateralized dysregulation of the left fronto-caudate network is the major cerebral determinant of the obsessive-compulsive state. The concept is even more interesting when considering the recognition of features of OCD in patients with schizophrenia (86) and the hypothesized hemispheric imbalance in psychosis (87). The laterality pattern proposed by Flor-Henry (85) was partially confirmed by some N200/P300 studies and topographical mapping in OCD (20, 42, 44, 47, 49, 62, 65). Indeed, in a dipole source analysis, patients with OCD showed P300 impairment only in the right hemisphere (52). Moreover, both abstinent heroin addicts and individuals with OCD show a

P300 amplitude reduction over the right frontal area, compared to healthy subjects (56).

P300 and Treatment

We found six articles on the relationship between P300 and treatment in OCD (47, 49, 51, 62, 67, 68), one of them (68) was a pediatric survey. One study, and its replication with additional patients, showed that future responders to 1-year treatment (fluoxetine, fluvoxamine, clomipramine) had significantly reduced N200 and enhanced P300 amplitude compared to future non-responders (47, 49). Patients were considered non-responders if they failed to to respond to separate treatments lasting for at least 8 weeks in total, and at the maximum antidepressant dose for at least 5 weeks. The authors suggested that ERPs might constitute psychophysiological profiles in individuals with OCD, thus implying potential clinical and pharmacological implications (47, 49). Another article reported that P300 had a lower baseline amplitude and a longer latency in drug-free OCD patients compared to healthy controls; subsequently, P300 exhibited a trend toward an amplitude increase after treatment (clomipramine), without modification in latency (51). A few patients were treated when included in the study and initially recorded; they stopped taking medication, and after at least 1 month, when the acute symptomatology appeared again, they underwent the second interview and the ERP study. This allowed to minimize the learning effect on P300 obtained under treatment.

Some results by other authors (62) have already been described in the paragraph on source localization; the same authors also aimed to assess the effects of 10 ± 1 weeks of treatment with sertraline on P300 brain activity patterns. In the patients retested after treatment, a reduction of P300, in both amplitude and latency, was observed which, however, did not reach statistical significance, as also found by other researchers (51). On the contrary, another investigation demonstrated that individuals with OCD had decreased P300 amplitude at baseline, which significantly increased at Fz, Cz, C3, and C4, indicating normalization, after 1 year of behavioral and pharmacological treatment (fluvoxamine, paroxetine, sertraline, clomipramine); the same group achieved similar results on the utility of SSRIs in pediatric OCD patients (68). Compared to controls, P300 amplitudes were smaller in the OCD group at Fz, Cz, Pz, C3, and C4. Approximately 3 years after the start of SSRI treatment (unspecified molecules), P300 amplitude significantly increased at Fz and C4, along with clinical improvement.

P300 in OCD Overlapping With Other Disorders

Since OCD can affect patients with other conditions, we also found some studies on OCD overlapping with other diseases, such as schizophrenia (60), Tourette syndrome (43, 59), functional constipation (65), mild depressive disorder, chronic motor or vocal tic disorder, social anxiety disorder of childhood, adjustment disorder, attention deficit-hyperactivity disorder (ADHD), social phobia, and expressive language disorder (73).

Comorbid schizophrenia-OCD (schizo-OCD) is characterized by the concurrent presentation of psychotic and obsessive-compulsive symptoms (86, 88–90), that may require high antipsychotic dosages for its acute exacerbations and for the maintenance of reduction of the severity of psychosis (91). Schizo-OCD sufferers show a distinct ERP pattern, with abnormally increased target activation similar to that described in OCD (20) but different from that usually observed in schizophrenia (76). These patients were reported to have also reduced P300 amplitude, similarly to schizophrenia (76, 92), but different from other results in individuals with OCD (50, 52, 58, 61–63, 66, 69). Therefore, schizo-OCD may be not only a clinical entity different from pure OCD and schizophrenia, but also a relatively distinct neurophysiologic condition (60).

Tourette syndrome is a neurodevelopmental disorder mainly characterized by tics, although most patients also experience sensory disturbances, especially in terms of premonitory urges and sensory hypersensitivity, which may account for comorbid OCD, ADHD, and autism spectrum disorder, with a possible partially common pathophysiology underlying them (93). One study described that patients with Tourette syndrome and OCD had shorter N200 and P300 latencies (43), thus confirming the above-mentioned common cortical hyperarousal state hypothesized for both conditions (93). Another article seems to be also in line with neuroimaging findings (18, 94) when describing a P300 amplitude reduction in the anterior scalp regions in both OCD and Tourette syndrome with OCD patients (59).

A study in patients with functional constipation found that they were also obsessive, anxious, and depressed, with reduced P300 amplitude at F7 compared to controls (65). The authors speculate that, in patients with functional constipation, asymmetric forebrain abnormal activities in the two hemispheres might initiate some implicit automatic processing, such as somatization and OCD, in order to cope with painful experiences caused by anxiety and depression.

Cognitive dysfunction of implicit processing might also be involved in impaired visual communication and information processing. One of the above-listed studies (73) did not consider comorbidities separately due to the low number of overlapping psychiatric conditions. The most active brain regions in the few OCD patients included were the frontal areas.

P300 in OCD Compared to Other Conditions

Shorter N200 and P300 latencies in OCD compared to social phobia and normal controls were believed to be an OCD-associated phenomenon (speeding of cognitive processing) (48). In two studies, P300 amplitudes were significantly smaller in schizophrenia and OCD patients than in healthy subjects (54, 60), a finding which is in line with the hypothesis of brain volume changes in both psychiatric illnesses (18, 76, 92).

One group of researchers assessed working memory and attentional capacities in OCD and opioid addicted: the abstinent group showed a notable delay of the P300 latency compared to controls and OCD only over the right occipital region, while OCD patients exhibited a significant prolongation of the P300 recorded over the central prefrontal area compared to

addicts and healthy controls (56). Although this was a rather complex study, the results of which were not fully in line with previous data on the P300 latency in OCD, it focused on the peculiar phenomenological aspect that addicts are quite similar to obsessionals when craving for drugs becomes irresistible, such as an obsession (95, 96).

P300 was reduced in participants with both OCD and Tourette syndrome and OCD over the anterior scalp regions, whereas the P300 oddball effect was significantly larger in participants with Tourette syndrome compared to all other groups (59). Therefore, the authors speculated that Tourette syndrome may be characterized by an enhanced working memory that updates processes and the superimposition of OCD might lead to a reduction of these processes (59). In one study only, P300 amplitude was found to be smaller in patients than in their siblings and also smaller in siblings than in controls; a logistic regression analysis showed that higher P300 amplitude and better performance at neuropsychological tests of the frontal cortex function were predictors for control subjects, whereas higher P200 amplitude predicted both patients and their siblings (66). The authors concluded that this pattern might be an endophenotype of OCD.

Pediatric Studies

We found five articles on P300 in pediatric OCD patients (43, 64, 68, 70, 73). Some investigators emphasized that pediatric patients have reduced P300 amplitude (64, 68, 70), altered response time (70), and partial increase of P300 amplitude after SSRI treatment (68). The replicated finding of decreased P300 amplitude in OCD children and adolescents and the correlation between illness severity and P300 amplitude led the authors to suggest that this psychophysiological feature might be considered as a sensitive tool for measuring the biological aspects of OCD severity (64, 68).

Another study investigated the auditory information processing in children and adolescents with Tourette syndrome overlapping with ADHD or OCD (43). Tourette syndrome patients with OCD had shorter N200 and P300 latencies, indicating cortical hyperarousal, similarly to pure OCD patients (20, 42, 44, 47–49, 52, 55). This pivotal concept, i.e., the fact that OCD patients may have a distinctive tendency to be aroused and to exhibit strong defensive reactions to minimal stimulation, as already highlighted by some authors (19, 20) for adults with OCD, seems to be present also in young patients. Pediatric OCD patients showed higher P300 amplitudes during "Go" vs. "No/Go" trials and during incongruent vs. congruent trials, thus confirming abnormal frontal hyperactivity also in young OCD patients (73).

DISCUSSION

This review included 35 studies with different paradigms (e.g., classical visual or auditory oddball, novelty, Go/No-Go), which have different recording modes (from only a few to 256 electrodes) and several objectives (e.g., localization of dysfunctional brain areas and treatment response) in adults, adolescents, and children. This heterogeneity did not allow us to perform any meta-analytic calculation, although the most relevant findings about P300 in OCD have been addressed in this review and summarized in **Table 2**.

Neuroimaging-based multimodal approaches have led to the conclusion that subtle brain structural changes and functional abnormality are present in OCD (15, 17, 18), with PET studies showing hypermetabolism in the orbital frontal cortex of these patients (85, 97). In the context of structural changes in OCD, the value of a decreased amplitude of P300 becomes evident, as reported by several studies (28, 45, 51, 54, 55, 64–68, 70, 72), similarly to those performed in schizophrenia (77). The finding of attenuated P300 amplitude has also been considered to be a pattern of genetic endophenotype in OCD (75, 76), which has also been confirmed in pediatric studies (64, 68, 70). Moreover, it was found to correlate with illness severity, suggesting that the reduction in P300 amplitude may be a sensitive tool for measuring some biological aspects of OCD severity (64, 68), also based on the evidence that P300 is generated along a widely distributed network that includes several brain areas implicated in the pathophysiology of OCD (12–18, 26). Of note, one study in schizo-OCD patients showed a pattern of alteration, i.e., a reduced P300 amplitude as in schizophrenia (60), which suggests the occurrence of brain structural abnormalities also in this peculiar clinical psychosis with relevant obsessional symptoms (88–90).

Nevertheless, there are also studies, depending on the type of paradigm used but suggesting the possible existence of different expressions of OCD within its clinical spectrum, reporting enhanced P300 amplitude in patients with OCD, compared to healthy controls (50, 52, 58, 61–63, 66, 69). Most of these studies considered this result as the electrophysiological correlate of an OCD trait consisting in a special tendency to get aroused (50, 77). Notably, only one of these studies (69) revealed that there was a weak relationship between ERP abnormalities and symptoms severity in OCD; more specifically, the authors reported only a weak correlation between compulsion estimation and the P300 valence effect (69). Based on the enhanced P300 amplitude, a pattern of cortical hyperarousal and over-focused attention in OCD has been hypothesized (19, 20, 42–44, 46–50), as also supported by the findings on processing negativity, which were interpreted as an indication of the existence of a hyperactivation of the frontal cortical mechanisms (12, 16, 19, 20, 85).

The decreased N200 latency in OCD (19, 42–44, 47, 48) and P300 (20, 42–44, 47–49, 52, 55) further emphasizes the concept of dysfunctional speed of information processing, possibly leading to some clinical features, such as intrusive thoughts that increase anxiety. The loss of normal inhibitory processes (28, 53, 57, 65, 73) would then serve as a basic source for the initiation of compulsion, with the to decrease anxiety.

The pattern of different amplitude seems to suggest the presence of different expressions (structural abnormalities vs. brain dysfunction) within the clinical spectrum of OCD. For instance, patients with a severe symptomatology can be seen (64, 68), including those with schizo-OCD (60), as belonging to the first group (structural abnormalities), whose abnormalities mainly concern the frontal brain areas (85, 97). The dysfunction of the frontal lobes has been implicated in OCD (12, 85). Flor-Henry suggested that OCD may be secondary to a

TABLE 2 | Summary of the relevant data found in obsessive-compulsive disorder regarding the event-related potential components considered in this review.

Feature	Finding	Main translational implication
P300 amplitude	↑ or ↓	Possible different expressions (structural vs. functional brain abnormalities) within the OCD clinical spectrum
P300 latency	↓	Cortical hyperarousal
N200 latency	↓	Cortical hyperarousal with overfocused attention
Sources	Frontal and temporo-basal areas	Support neuroimaging findings of the involvement of cortico-striato-thalamo-cortical loop, anterior cingulate cortex, prefrontal cortex, and temporal areas
Novelty (P3a amplitude)	↑	Enhanced cortical orienting response implicating stronger involuntary shifts of attention
No-Go-N200 amplitude	↓	Frontal dysfunction pattern
ERP Laterality	R<L more frequently R>L less frequently N/A for many studies	The hypothesis of a lateralized dysregulation of the left fronto-caudate network is only partially supported by this data re-examination
Effects of SSRI on P300 amplitude	↑	Partial improvement that seems to be mainly attributable to the effect of serotonin on ERPs
Effects of behavioral therapy on P300	N/A	Necessity for this investigation in future research agenda
Overlap syndromes	ADHD, FC, SPR	Shared patterns of frontal damage or dysfunction has been related to other psychiatric disorders in addition to OCD
Matching conditions	AHA, GTS, SP, SPR	Frontal dysfunctional patterns similar to that of OCD for SP and somewhat different regarding the other disorders
Symptom severity and P300 amplitude	↑ or ↓	ERP abnormalities as a sensitive tool for OCD biological feature of frontal damage vs. ERP abnormalities as per OCD dysfunctional trait
Pediatric studies (P300 amplitude)	↓	Suggesting frontal damage
Pediatric studies (P300 latency)	= or ↓	Not relevant vs. speeding of cognitive processing

ADHD, attention deficit and hyperactivity disorder; AHA, abstinent heroin addicts; ERP, event-related potential; L, left; N/A, not applicable; FC, functional constipation; GTS, Gilles de la Tourette syndrome; OCD, obsessive-compulsive disorder; R, right; SP, social phobia; SPR, schizophrenia; ↑, increased; ↓, decreased; =, unchanged.

prominent frontal lobe dysfunction, along with a loss of the physiological inhibitory processes (98). Other studies confirmed the involvement of the cortico-striato-thalamo-cortical loop, the anterior cingulate cortex, and the prefrontal cortex in OCD (9–18, 85, 97). However, frontal damage or dysfunction has been found in a number of psychiatric disorders in addition to OCD, and particularly schizophrenia. Some neuroimaging studies indicate that OCD symptoms are associated with altered activity in the orbito-frontal cortex (12, 99, 100), being this finding likely due to the dominant role of the frontal lobe in executive functioning and self-regulatory behaviors (12, 100, 101), which are both altered in several psychiatric illnesses. Therefore, the frontal abnormality may reflect a final common pathway for abnormal behavior (12, 28). Alternatively, different disorders may result from the dysfunction of different frontal subsystems (12, 28). For instance, the dorsolateral frontal region has been found to be impaired in schizophrenia, whereas the orbito-frontal areas have been implicated in OCD (12, 102).

Nevertheless, the above-mentioned features may not fully explain the inconsistency between the enhanced and reduced P300 in OCD, thus making the interpretation of these results challenging. Furthrmore, the fact that several data have been published by the same research group needs be taken into account (64, 67, 68, 70). However, it should be noted that most OCD individuals show a peculiar propensity to get aroused and typically exhibit strong defensive reactions even to minimal stimulation (19, 20, 42–46, 48, 50, 55, 71, 72). Translationally, these are the patients who can benefit from a targeted cognitive-behavioral rehabilitation, associated with drug therapy. On the contrary, pediatric subjects, schizo-OCD patients, and severe OCD cases frequently show low-amplitude P300 (28, 45, 51, 54, 55, 64, 65, 67, 68, 70, 72), a finding in line with the brain imaging data reported by different authors (15–18). Based on the P300 parameters, follow-up studies after drug and rehabilitation therapy are warranted in order to gain further insights on the disease severity and the possibility of clinical and cognitive improvement (64, 103). In this scenario, it is worth to highlight that Morault et al. (49) have already suggested that some pre-treatment features of ERPs might be associated with a more favorable outcome after treatment.

The laterality pattern, i.e., left<right, proposed by Flor-Henry (85), was partially confirmed by some N200/P300 studies and topographic mapping in OCD (20, 42, 44, 47, 49, 62, 65), whereas the partial recovery of P300 changes, in parallel with the clinical improvement (47, 49, 51, 62, 67, 68), seems to be mainly attributable to the effect of serotonin on ERP amplitude (68).

Regarding the effect of treatment, only one study (67) used psychotherapy combined with drugs. In this context, two studies have provided useful psychophysiological profiles in individuals with OCD with clinical and pharmacological implications, thus suggesting that the outcome of cognitive-behavioral therapy (CBT) combined to SSRI should be studied along with ERPs

(47, 49). In addition, there were also a few reports of P300 amplitude with partial recovery after adequate pharmacological treatment (51, 67, 68, 70).

CONCLUSIONS AND FUTURE DIRECTIONS

Notwithstanding the limitations of the studies and their heterogeneous methodology, the findings reviewed here seem to support that the different P300 patterns observed might suggest the presence of different expressions (structural vs. functional brain abnormalities) within the clinical spectrum of OCD. Event-related potentials may also be used as a treatment monitoring marker at the individual level, especially for both pharmacological treatment and/or CBT (104). In particular, the development of novel P3a paradigms in combination with P3b tasks seems to be promising for a more extensive application and reliability of ERPs (103). Moreover, similarly to patients with migraine, who can be re-tested during treatment and follow-up in order to detect an improvement of P300 habituation (35), also OCD patients might be serially evaluated over time to identify any possible change in their neurophysiological correlates of cortical hyperarousal, over-focused attention, and response inhibition. The same holds true for children and adolescents with decreased P300 amplitude at baseline, who might be re-evaluated during or after treatment in order to assess whether P300 changes reflect pharmacological and/or psychotherapeutic effects (67, 68).

Nevertheless, the majority of the articles reviewed here included very small cohorts of patients, thus emphasizing again the importance of objective evaluations in neuropsychiatric and psychological disorders, as well as the need for a systematic examination and the application of standardized procedures to obtain more realiable guidelines in the near future. For instance, it would be intriguing to apply the three-oddball paradigm (31) to record N100, MMN, and P3a with the same conscruct. Their abnormality would suggest a frontal dysfunction and might help the differentiation between OCD individuals, severe cases, and schizo-OCD. Other studies may deal with the lack of P300 habituation by using two or three blocks of stimuli, as already done in patients with migraine (35, 105). Finally, further data using multidimensional measurement techniques (e.g., behavioral, electrophysiological, structural, metabolic) will be also necessary before the relationship between brain (mainly frontal) dysfunction and OCD psychopathology can be conclusively clarified.

AUTHOR CONTRIBUTIONS

AR, GL, and RF designed research, performed literature review, analyzed data, wrote the paper, and revised the text. All authors contributed to this manuscript and agree with its content.

REFERENCES

1. Goodman WK, Grice DE, Lapidus KA, Coffey BJ. Obsessive-compulsive disorder. *Psychiatr Clin North Am.* (2014) 37:257–67. doi: 10.1016/j.psc.2014.06.004
2. American Psychiatric Association. *Diagnostic and Statistical Manual of Mental Disorders. 5th ed*. Arlington, VA: American Psychiatric Publishing (2013).
3. Pitres A, Régis E. *Les Obsessions et les Impulsions*. Paris: Octave Doin. (1902).
4. Sandler J, Hazari A. The 'obsessional': on the psychological classification of obsessional character traits and symptoms. *Br J Med Psychol.* (1960) 33:113–22. doi: 10.1111/j.2044-8341.1960.tb01232.x
5. Ingram IM. The obsessional personality and obsessional illness. *Am J Psychiatry.* (1961) 117:1016–9. doi: 10.1176/ajp.117.11.1016
6. Pancheri, P. (1992). *Ossessioni, Compulsioni E Continuum Ossessivo*. Rome: Il Pensiero Scientifico Editore.
7. Black JL. Obsessive compulsive disorder: a clinical update. *Mayo Clin Proc.* (1992) 67:266–75. doi: 10.1016/s0025-6196(12)60104-9
8. Baup N. Reconnaitre un trouble obsessionnel compulsif. *Rev Prat.* (2007) 57:27–36.
9. Boldrini M, Del Pace L, Placidi GP, Keilp J, Ellis SP, Signori S, et al. Selective cognitive deficits in obsessive-compulsive disorder compared to panic disorder with agoraphobia. *Acta Psychiatr Scand.* (2005) 111:150–8. doi: 10.1111/j.1600-0447.2004.00247.x
10. Cetinay Aydin P, Gulec Oyekcin D. Obsesif kompulsif bozuklukta bilissel islevler. *Turk Psikiyatri Derg.* (2013) 24:266–74.
11. Shin NY, Lee TY, Kim E, Kwon JS. Cognitive functioning in obsessive-compulsive disorder: a meta-analysis. *Psychol Med.* (2014) 44:1121–30. doi: 10.1017/S0033291713001803
12. Pirau, L, Lui, F. Frontal lobe syndrome. In: *StatPearls*. Treasure Island, FL: StatPearls Publishing (2020).
13. Berthier ML, Kulisevsky J, Gironell A, Heras JA. Obsessive-compulsive disorder associated with brain lesions: clinical phenomenology, cognitive function, and anatomic correlates. *Neurology.* (1996) 47:353–61. doi: 10.1212/wnl.47.2.353
14. Mindus P, Rasmussen SA, Lindquist C. Neurosurgical treatment for refractory obsessive-compulsive disorder: implications for understanding frontal lobe function. *J Neuropsychiatry Clin Neurosci.* (1994) 6:467–77. doi: 10.1176/jnp.6.4.467
15. Saxena S, Brody AL, Schwartz JM, Baxter LR. Neuroimaging and frontal-subcortical circuitry in obsessive-compulsive disorder. *Br J Psychiatry Suppl.* (1998) 35:26–37.
16. Brem S, Grunblatt E, Drechsler R, Riederer P, Walitza S. The neurobiological link between OCD and ADHD. *Atten Defic Hyperact Disord.* (2014) 6:175–202. doi: 10.1007/s12402-014-0146-x
17. Hazari N, Narayanaswamy JC, Venkatasubramanian G. Neuroimaging findings in obsessive-compulsive disorder: a narrative review to elucidate neurobiological underpinnings. *Indian J Psychiatry.* 61(Suppl 1) (2019) S9–29. doi: 10.4103/psychiatry.IndianJPsychiatry_525_18
18. Park SE, Kim BC, Yang JC, Jeong GW. MRI-based multimodal approach to the assessment of clinical symptom severity of obsessive-compulsive disorder. *Psychiatry Investig.* (2020) 17:777–85. doi: 10.30773/pi.2020.0124
19. Ciesielski KT, Beech HR, Gordon PK. Some electrophysiological observations in obsessional states. *Br J Psychiatry.* (1981) 138:479–84. doi: 10.1192/bjp.138.6.479
20. Beech HR, Ciesielski KT, Gordon PK. Further observations of evoked potentials in obsessional patients. *Br J Psychiatry.* (1983) 142:605–9. doi: 10.1192/bjp.142.6.605
21. Sutton S, Braren M, Zubin J, John ER. Evoked-potential correlates of stimulus uncertainty. *Science.* (1965) 150:1187–8. doi: 10.1126/science.150.3700.1187
22. Pritchard WS. Psychophysiology of P300. *Psychol Bull.* (1981) 89:506–40.
23. Picton TW. The P300 wave of the human event-related potential. *J Clin Neurophysiol.* (1992) 9:456–79. doi: 10.1097/00004691-199210000-00002
24. Polich J, Kok A. Cognitive and biological determinants of P300: an integrative review. *Biol Psychol.* (1995) 41:103–46. doi: 10.1016/0301-0511(95)05130-9

25. de Tommaso M, Betti V, Bocci T, Bolognini N, Di Russo F, Fattapposta F, et al. Pearls and pitfalls in brain functional analysis by event-related potentials: a narrative review by the Italian Psychophysiology and Cognitive Neuroscience Society on methodological limits and clinical reliability-part I. *Neurol Sci.* (2020) 41:2711–35. doi: 10.1007/s10072-020-04420-7
26. Linden DE, Prvulovic D, Formisano E, Vollinger M, Zanella FE, Goebel R, et al. The functional neuroanatomy of target detection: an fMRI study of visual and auditory oddball tasks. *Cereb Cortex.* (1999) 9:815–23. doi: 10.1093/cercor/9.8.815
27. Verbruggen F, Logan GD. Automatic and controlled response inhibition: associative learning in the go/no-go and stop-signal paradigms. *J Exp Psychol Gen.* (2008) 137:649–72. doi: 10.1037/a0013170
28. Malloy P, Rasmussen S, Braden W, Haier RJ. Topographic evoked potential mapping in obsessive-compulsive disorder: evidence of frontal lobe dysfunction. *Psychiatry Res.* (1989) 28:63–71. doi: 10.1016/0165-1781(89)90198-4
29. Polich J, Criado JR. Neuropsychology and neuropharmacology of P3a and P3b. *Int J Psychophysiol.* (2006) 60:172–85. doi: 10.1016/j.ijpsycho.2005.12.012
30. Polich J. Updating P300: an integrative theory of P3a and P3b. *Clin Neurophysiol.* (2007) 118:2128–48. doi: 10.1016/j.clinph.2007.04.019
31. Raggi A, Tasca D, Rundo F, Ferri R. Stability of auditory discrimination and novelty processing in physiological aging. *Behav Neurol.* (2013) 27:193–200. doi: 10.3233/BEN-120261
32. Raggi A, Iannaccone S, Cappa SF. Event-related brain potentials in amyotrophic lateral sclerosis: a review of the international literature. *Amyotroph Lateral Scler.* (2010) 11:16–26. doi: 10.3109/17482960902912399
33. Raggi A, Plazzi G, Pennisi G, Tasca D, Ferri R. Cognitive evoked potentials in narcolepsy: a review of the literature. *Neurosci Biobehav Rev.* (2011) 35:1144–53. doi: 10.1016/j.neubiorev.2010.12.001
34. Raggi A, Ferri R. Cognitive evoked potentials in obstructive sleep apnea syndrome: a review of the literature. *Rev Neurosci.* (2012) 23:311–23. doi: 10.1515/revneuro-2012-0027
35. Raggi A, Ferri R. Information processing in migraine: a review of studies on P300. *Appl Psychophysiol Biofeedback.* (2020) 45:131–44. doi: 10.1007/s10484-020-09469-w
36. Raggi A, Lanza G, Ferri R. Auditory mismatch negativity in bipolar disorder: a focused review. *Rev Neurosci.* (2021). doi: 10.1515/revneuro-2021-0010
37. Ritter W, Simson R, Vaughan HGJr. Event-related potential correlates of two stages of information processing in physical and semantic discrimination tasks. *Psychophysiology.* (1983) 20:168–79. doi: 10.1111/j.1469-8986.1983.tb03283.x
38. Perrault N, Picton TW. Event-related potentials recorded from the scalp and nasopharynx I N1 and P2. *Electroencephalogr Clin Neurophysiol.* (1984) 59:177–94. doi: 10.1016/0168-5597(84)90058-3
39. Cantone M, Lanza G, Ranieri F, Opie GM, Terranova C. Editorial: non-invasive brain stimulation in the study and modulation of metaplasticity in neurological disorders. *Front Neurol.* (2021) 12:721906. doi: 10.3389/fneur.2021.721906
40. Perrault N, Picton TW. Event-related potentials recorded from the scalp and nasopharynx. II. N2, P3 and slow wave. *Electroencephalogr Clin Neurophysiol.* (1984) 59:261–78. doi: 10.1016/0168-5597(84)90044-3
41. Dawson GD. A summation technique for the detection of small evoked potentials. *Electroencephalogr Clin Neurophysiol.* (1954) 6:65–84. doi: 10.1016/0013-4694(54)90007-3
42. Towey J, Bruder G, Hollander E, Friedman D, Erhan H, Liebowitz M, et al. Endogenous event-related potentials in obsessive-compulsive disorder. *Biol Psychiatry.* (1990) 28:92–8. doi: 10.1016/0006-3223(90)90626-d
43. Drake MEJr, Hietter SA, Padamadan H, Bogner JE, Andrews JM, Weate S. Auditory evoked potentials in Gilles de la Tourette syndrome. *Clin Electroencephalogr.* (1992) 23:19–23. doi: 10.1177/155005949202300106
44. Towey J, Bruder G, Tenke C, Leite P, DeCaria C, Friedman D, et al. Event-related potential and clinical correlates of neurodysfunction in obsessive-compulsive disorder. *Psychiatry Res.* (1993) 49:167–81. doi: 10.1016/0165-1781(93)90103-n
45. Towey JP, Tenke CE, Bruder GE, Leite P, Friedman D, Liebowitz M, et al. Brain event-related potential correlates of overfocused attention in obsessive-compulsive disorder. *Psychophysiology.* (1994) 31:535–43. doi: 10.1111/j.1469-8986.1994.tb02346.x
46. de Groot CM, Torello MW, Boutros NN, Allen R. Auditory event-related potentials and statistical probability mapping in obsessive-compulsive disorder. *Clin Electroencephalogr.* (1997) 28:148–54. doi: 10.1177/155005949702800306
47. Morault PM, Bourgeois M, Laville J, Bensch C, Paty J. Psychophysiological and clinical value of event-related potentials in obsessive-compulsive disorder. *Biol Psychiatry.* (1997) 42:46–56. doi: 10.1016/S0006-3223(96)00228-4
48. Miyata A, Matsunaga H, Kiriike N, Iwasaki Y, Takei Y, Yamagami S. Event-related potentials in patients with obsessive-compulsive disorder. *Psychiatry Clin Neurosci.* (1998) 52:513–8. doi: 10.1046/j.1440-1819.1998.00427.x
49. Morault P, Guillem F, Bourgeois M, Paty J. Improvement predictors in obsessive-compulsive disorder. An event-related potential study. *Psychiatry Res.* (1998) 81:87–96. doi: 10.1016/s0165-1781(98)00091-2
50. Di Russo F, Zaccara G, Ragazzoni A, Pallanti S. Abnormal visual event-related potentials in obsessive-compulsive disorder without panic disorder or depression comorbidity. *J Psychiatr Res.* (2000) 34:75–82. doi: 10.1016/s0022-3956(99)00030-8
51. Sanz M, Molina V, Martin-Loeches M, Calcedo A, Rubia FJ. Auditory P300 event related potential and serotonin reuptake inhibitor treatment in obsessive-compulsive disorder patients. *Psychiatry Res.* (2001) 101:75–81. doi: 10.1016/s0165-1781(00)00250-x
52. Mavrogiorgou P, Juckel G, Frodl T, Gallinat J, Hauke W, Zaudig M, et al. P300 subcomponents in obsessive-compulsive disorder. *J Psychiatr Res.* (2002) 36:399–406. doi: 10.1016/s0022-3956(02)00055-9
53. Herrmann MJ, Jacob C, Unterecker S, Fallgatter AJ. Reduced response-inhibition in obsessive-compulsive disorder measured with topographic evoked potential mapping. *Psychiatry Res.* (2003) 120:265–71. doi: 10.1016/s0165-1781(03)00188-4
54. Kim MS, Kang SS, Youn T, Kang DH, Kim JJ, Kwon JS. Neuropsychological correlates of P300 abnormalities in patients with schizophrenia and obsessive-compulsive disorder. *Psychiatry Res.* (2003) 123:109–23. doi: 10.1016/s0925-4927(03)00045-3
55. Kivircik BB, Yener GG, Alptekin K, Aydin H. Event-related potentials and neuropsychological tests in obsessive-compulsive disorder. *Prog Neuropsychopharmacol Biol Psychiatry.* (2003) 27:601–6. doi: 10.1016/S0278-5846(03)00047-2
56. Papageorgiou C, Rabavilas A, Liappas I, Stefanis C. Do obsessive-compulsive patients and abstinent heroin addicts share a common psychophysiological mechanism? *Neuropsychobiology.* (2003) 47:1–11. doi: 10.1159/000068868
57. Kim MS, Kim YY, Yoo SY, Kwon JS. Electrophysiological correlates of behavioral response inhibition in patients with obsessive-compulsive disorder. *Depress Anxiety.* (2007) 24:22–31. doi: 10.1002/da.20195
58. Gohle D, Juckel G, Mavrogiorgou P, Pogarell O, Mulert C, Rujescu D, et al. Electrophysiological evidence for cortical abnormalities in obsessive-compulsive disorder - a replication study using auditory event-related P300 subcomponents. *J Psychiatr Res.* (2008) 42:297–303. doi: 10.1016/j.jpsychires.2007.01.003
59. Thibault G, Felezeu M, O'Connor KP, Todorov C, Stip E, Lavoie ME. Influence of comorbid obsessive-compulsive symptoms on brain event-related potentials in Gilles de la Tourette syndrome. *Prog Neuropsychopharmacol Biol Psychiatry.* (2008) 32:803–15. doi: 10.1016/j.pnpbp.2007.12.016
60. Pallanti S, Castellini G, Chamberlain SR, Quercioli L, Zaccara G, Fineberg NA. Cognitive event-related potentials differentiate schizophrenia with obsessive-compulsive disorder (schizo-OCD) from OCD and schizophrenia without OC symptoms. *Psychiatry Res.* (2009) 170:52–60. doi: 10.1016/j.psychres.2008.11.002
61. Ischebeck M, Endrass T, Simon D, Kathmann N. Auditory novelty processing is enhanced in obsessive-compulsive disorder. *Depress Anxiety.* (2011) 28:915–23. doi: 10.1002/da.20886
62. Andreou C, Leicht G, Popescu V, Pogarell O, Mavrogiorgou P, Rujescu D, et al. P300 in obsessive-compulsive disorder: source localization and the effects of treatment. *J Psychiatr Res.* (2013) 47:1975–83. doi: 10.1016/j.jpsychires.2013.09.003

63. Endrass T, Koehne S, Riesel A, Kathmann N. Neural correlates of feedback processing in obsessive-compulsive disorder. *J Abnorm Psychol.* (2013) 122:387–96. doi: 10.1037/a0031496
64. Yamamuro K, Ota T, Nakanishi Y, Matsuura H, Okazaki K, Kishimoto N, et al. Event-related potentials in drug-naive pediatric patients with obsessive-compulsive disorder. *Psychiatry Res.* (2015) 230:394–9. doi: 10.1016/j.psychres.2015.09.026
65. Li X, Feng R, Wu H, Zhang L, Zhao L, Dai N, et al. Psychological characteristics and GoNogo research of patients with functional constipation. *Medicine (Baltimore).* (2016) 95:e5685. doi: 10.1097/MD.0000000000005685
66. Ozcan H, Ozer S, Yagcioglu S. Neuropsychological, electrophysiological and neurological impairments in patients with obsessive compulsive disorder, their healthy siblings and healthy controls: Identifying potential endophenotype(s). *Psychiatry Res.* (2016) 240:110–7. doi: 10.1016/j.psychres.2016.04.013
67. Yamamuro K, Okada K, Kishimoto N, Ota T, Iida J, Kishimoto T. A longitudinal, event-related potential pilot study of adult obsessive-compulsive disorder with 1-year follow-up. *Neuropsychiatr Dis Treat.* (2016) 12:2463–71. doi: 10.2147/NDT.S117100
68. Yamamuro K, Ota T, Iida J, Kishimoto N, Nakanishi Y, Matsuura H, et al. A longitudinal event-related potential study of selective serotonin reuptake inhibitor therapy in treatment-naive pediatric obsessive compulsive disorder patients. *Psychiatry Res.* (2016) 245:217–23. doi: 10.1016/j.psychres.2016.07.031
69. Dayan-Riva A, Berger A, Anholt GE. Early cognitive processes in OCD: An ERP study. *J Affect Disord.* (2019) 246:429–36. doi: 10.1016/j.jad.2018.12.109
70. Okazaki K, Yamamuro K, Iida J, Ota T, Nakanishi Y, Matsuura H, et al. Intra-individual variability across cognitive task in drug-naive pediatric patients with obsessive compulsive disorder. *Psychiatry Res.* (2018) 264:421–6. doi: 10.1016/j.psychres.2018.04.024
71. Wojcik GM, Masiak J, Kawiak A, Schneider P, Kwasniewicz L, Polak N, et al. New protocol for quantitative analysis of brain cortex electroencephalographic activity in patients with psychiatric disorders. *Front Neuroinform.* (2018) 12:27. doi: 10.3389/fninf.2018.00027
72. Kloft L, Riesel A, Kathmann N. Inhibition-related differences between tic-free and tic-related obsessive-compulsive disorder: evidence from the N2 and P3. *Exp Brain Res.* (2019) 237:3449–59. doi: 10.1007/s00221-019-05688-8
73. Wolff N, Chmielewski W, Buse J, Roessner V, Beste C. Paradoxical response inhibition advantages in adolescent obsessive compulsive disorder result from the interplay of automatic and controlled processes. *Neuroimage Clin.* (2019) 23:101893. doi: 10.1016/j.nicl.2019.101893
74. Polich J, Ladish C, Bloom FE. P300 assessment of early Alzheimer's disease. *Electroencephalogr Clin Neurophysiol.* (1990) 77:179–89. doi: 10.1016/0168-5597(90)90036-d
75. Hunerli D, Emek-Savas DD, Cavusoglu B, Donmez Colakoglu B, Ada E, Yener GG. Mild cognitive impairment in Parkinson's disease is associated with decreased P300 amplitude and reduced putamen volume. *Clin Neurophysiol.* (2019) 130:1208–17. doi: 10.1016/j.clinph.2019.04.314
76. Turetsky BI, Dress EM, Braff DL, Calkins ME, Green MF, Greenwood TA, et al. The utility of P300 as a schizophrenia endophenotype and predictive biomarker: clinical and socio-demographic modulators in COGS-2. *Schizophr Res.* (2015) 163:53–62. doi: 10.1016/j.schres.2014.09.024
77. Beech HR. Ritualistic activity in obsessional patients. *J Psychosom Res.* (1971) 15:417–22. doi: 10.1016/0022-3999(71)90022-5
78. Drewe EA. Go - no go learning after frontal lobe lesions in humans. *Cortex.* (1975) 11:8–16. doi: 10.1016/s0010-9452(75)80015-3
79. Linden DE. The p300: where in the brain is it produced and what does it tell us? *Neuroscientist.* (2005) 11:563–76. doi: 10.1177/1073858405280524
80. Nunez PL, Srinivasan R. *Electric Fields of the Brain: The Neurophysics of EEG. 2nd ed*. New York: Oxford University Press (2006).
81. Kavanagh RN, Darcey TM, Lehmann D, Fender DH. Evaluation of methods for three-dimensional localization of electrical sources in the human brain. *IEEE Trans Biomed Eng.* (1978) 25:421–9. doi: 10.1109/TBME.1978.326339
82. Michel CM, Brunet D. EEG source imaging: a practical review of the analysis steps. *Front Neurol.* (2019) 10:325. doi: 10.3389/fneur.2019.00325
83. Rauch SL, Jenike MA, Alpert NM, Baer L, Breiter HC, Savage CR, et al. Regional cerebral blood flow measured during symptom provocation in obsessive-compulsive disorder using oxygen 15-labeled carbon dioxide and positron emission tomography. *Arch Gen Psychiatry.* (1994) 51:62–70. doi: 10.1001/archpsyc.1994.03950010062008
84. Pujol J, Blanco-Hinojo L, Macia D, Alonso P, Harrison BJ, Martinez-Vilavella G, et al. Mapping alterations of the functional structure of the cerebral cortex in obsessive-compulsive disorder. *Cereb Cortex.* (2019) 29:4753–62. doi: 10.1093/cercor/bhz008
85. Flor-Henry, P. (1990). Le syndrome obsessionnel-compulsif: reflet d'un defaut de regulation fronto-caudee de l'hemisphere gauche? *Encephale 16 Spec No* 325–329.
86. Ohta M, Kokai M, Morita Y. Features of obsessive-compulsive disorder in patients primarily diagnosed with schizophrenia. *Psychiatry Clin Neurosci.* (2003) 57:67–74. doi: 10.1046/j.1440-1819.2003.01081.x
87. Gruzelier JH. Hemispheric imbalances in schizophrenia. *Int J Psychophysiol.* (1984) 1:227–40. doi: 10.1016/0167-8760(84)90043-6
88. Poyurovsky M, Hramenkov S, Isakov V, Rauchverger B, Modai I, Schneidman M, et al. Obsessive-compulsive disorder in hospitalized patients with chronic schizophrenia. *Psychiatry Res.* (2001) 102:49–57. doi: 10.1016/s0165-1781(01)00238-4
89. Kayahan B, Ozturk O, Veznedaroglu B, Eraslan D. Obsessive-compulsive symptoms in schizophrenia: prevalance and clinical correlates. *Psychiatry Clin Neurosci.* (2005) 59:291–5. doi: 10.1111/j.1440-1819.2005.01373.x
90. Owashi T, Ota A, Otsubo T, Susa Y, Kamijima K. Obsessive-compulsive disorder and obsessive-compulsive symptoms in Japanese inpatients with chronic schizophrenia - a possible schizophrenic subtype. *Psychiatry Res.* (2010) 179:241–6. doi: 10.1016/j.psychres.2009.08.003
91. Baytunca B, Kalyoncu T, Ozel I, Erermis S, Kayahan B, Ongur D. Early onset schizophrenia associated with obsessive-compulsive disorder: clinical features and correlates. *Clin Neuropharmacol.* (2017) 40:243–5. doi: 10.1097/WNF.0000000000000248
92. Ford JM. Schizophrenia: the broken P300 and beyond. *Psychophysiology.* (1999) 36:667–82.
93. Isaacs D, Riordan H. Sensory hypersensitivity in Tourette syndrome: a review. *Brain Dev.* (2020) 42:627–38. doi: 10.1016/j.braindev.2020.06.003
94. Hsu CJ, Wong LC, Wang HP, Lee WT. The multimodality neuroimage findings in individuals with Tourette syndrome. *Pediatr Neonatol.* (2020) 61:467–74. doi: 10.1016/j.pedneo.2020.03.007
95. Goldstein WN. Obsessive-compulsive behavior, DSM-III, and a psychodynamic classification of psychopathology. *Am J Psychother.* (1985) 39:346–59. doi: 10.1176/appi.psychotherapy.1985.39.3.346
96. Pitman RK. A cybernetic model of obsessive-compulsive psychopathology. *Compr Psychiatry.* (1987) 28:334–43. doi: 10.1016/0010-440x(87)90070-8
97. Baxter LRJr. Positron emission tomography studies of cerebral glucose metabolism in obsessive compulsive disorder. *J Clin Psychiatry 55 Suppl.* (1994) 54–9.
98. Flor-Henry P. *Cerebral Basis of Psychopathology*. Boston, MA: John Wright. (1983).
99. Levin S. Frontal lobe dysfunctions in schizophrenia–II. Impairments of psychological and brain functions. *J Psychiatr Res.* (1984) 18:57–72. doi: 10.1016/0022-3956(84)90047-5
100. Stuss DT, Benson DF. Neuropsychological studies of the frontal lobes. *Psychol Bull.* (1984) 95:3–28.
101. Faglioni, P. Il lobo frontale. Denes G, Pizzamiglio L, editors. In: *Manuale di Neuropsicologia. 2nd ed.* (Bologna: Zanichelli) (1996) 701–750.
102. Weinberger DR. Schizophrenia and the frontal lobe. *Trends Neurosci.* (1988) 11:367–70. doi: 10.1016/0166-2236(88)90060-4
103. Polich J. Clinical application of the P300 event-related brain potential. *Phys Med Rehabil Clin N Am.* (2004) 15:133–61. doi: 10.1016/s1047-9651(03)00109-8
104. McKay D, Sookman D, Neziroglu F, Wilhelm S, Stein DJ, Kyrios M, et al. Efficacy of cognitive-behavioral therapy for obsessive-compulsive disorder. *Psychiatry Res.* (2015) 225:236–46. doi: 10.1016/j.psychres.2014.11.058

105. Evers S, Bauer B, Suhr B, Husstedt IW, Grotemeyer KH. Cognitive processing in primary headache: a study on event-related potentials. *Neurology.* (1997) 48:108–13. doi: 10.1212/wnl.48.1.108

Conflict of Interest: The authors declare that the research was conducted in the absence of any commercial or financial relationships that could be construed as a potential conflict of interest.

Publisher's Note: All claims expressed in this article are solely those of the authors and do not necessarily represent those of their affiliated organizations, or those of the publisher, the editors and the reviewers. Any product that may be evaluated in this article, or claim that may be made by its manufacturer, is not guaranteed or endorsed by the publisher.

frontiers in Human Neuroscience

ORIGINAL RESEARCH
published: 29 November 2021
doi: 10.3389/fnhum.2021.783355

Structural and Functional Abnormalities in Knee Osteoarthritis Pain Revealed With Multimodal Magnetic Resonance Imaging

Hua Guo[1], Yuqing Wang[2], Lihua Qiu[3], Xiaoqi Huang[4], Chengqi He[1], Junran Zhang[5]* and Qiyong Gong[4]**

[1] Department of Rehabilitative Medicine, West China Hospital, Sichuan University, Chengdu, China, [2] Tsinghua University, Beijing, China, [3] Radiology Department, The Second People's Hospital of Yibin, Yibin, China, [4] Huaxi MR Research Center (HMRRC), Department of Radiology, West China Hospital of Sichuan University, Chengdu, China, [5] School of Electrical Engineering, Sichuan University, Chengdu, China

OPEN ACCESS

Edited by:
Jiaojian Wang,
University of Electronic Science and Technology of China, China

Reviewed by:
Haiming Wang,
First Affiliated Hospital of Zhengzhou University, China
Zhen Yuan,
University of Macau, China

***Correspondence:**
Chengqi He
chengqihe1998@sina.com
Junran Zhang
zhangjunran@126.com
Qiyong Gong
qiyonggong@hmrrc.org.cn

Specialty section:
This article was submitted to Brain Imaging and Stimulation, a section of the journal Frontiers in Human Neuroscience

Received: *26 September 2021*
Accepted: *28 October 2021*
Published: *29 November 2021*

Citation:
Guo H, Wang Y, Qiu L, Huang X, He C, Zhang J and Gong Q (2021) Structural and Functional Abnormalities in Knee Osteoarthritis Pain Revealed With Multimodal Magnetic Resonance Imaging. Front. Hum. Neurosci. 15:783355. doi: 10.3389/fnhum.2021.783355

The knee osteoarthritis (KOA) pain is the most common form of arthritis pain affecting millions of people worldwide. Long-term KOA pain causes motor impairment and affects affective and cognitive functions. However, little is known about the structural and functional abnormalities induced by long-term KOA pain. In this work, high-resolution structural magnetic resonance imaging (sMRI) and resting-state functional MRI (rs-fMRI) data were acquired in patients with KOA and age-, sex-matched healthy controls (HC). Gray matter volume (GMV) and fractional amplitude of low-frequency fluctuation (fALFF) were used to study the structural and functional abnormalities in patients with KOA. Compared with HC, patients with KOA showed reduced GMV in bilateral insula and bilateral hippocampus, and reduced fALFF in left cerebellum, precentral gyrus, and the right superior occipital gyrus. Patients with KOA also showed increased fALFF in left insula and bilateral hippocampus. In addition, the abnormal GMV in left insula and fALFF in left fusiform were closely correlated with the pain severity or disease duration. These results indicated that long KOA pain leads to brain structural and functional impairments in motor, visual, cognitive, and affective functions that related to brain areas. Our findings may facilitate to understand the neural basis of KOA pain and the future therapy to relieve disease symptoms.

Keywords: knee osteoarthritis pain, structural MRI, resting-state fMRI, GMV, ALFF

INTRODUCTION

Osteoarthritis is a degenerative joint disease with high incidence and mainly occurs in the elderly population. The knee osteoarthritis (KOA) is one of the most common osteoarthritis which affects millions of people worldwide. Knee pain is a main symptom of KOA which results in decreasing mobility to make the quality of life of the patients worse (Kloppenburg and Berenbaum, 2020). KOA pain is a ubiquitous and chronic pain which leads to restricted movement, sleep disturbance, and psychosocial disability (Ferket et al., 2017; Zhaoyang et al., 2020). Typically, KOA pain is worsened with activities, such as walking or climbing steps, and relieved with rest (Losina et al., 2016).

Kaplan et al. (2019) disclosed that the degree of pain does not always predict the extent of joint damage or the presence of active inflammation, which suggests the spread of central sensitizations as the underlying primary mechanisms involved in KOA pain.

The pathogenic mechanisms of pain in KOA may be related to central sensitization mechanisms (Kaplan et al., 2019). KOA can lead to persistent chronic pain affecting nervous system structure and function (Gollub et al., 2018; Zhang et al., 2020). With the development of magnetic resonance imaging (MRI), it is able to non-invasively investigate the brain structure and function and to map the brain connectivity and network *in vivo* (Xu et al., 2019, 2020; Becq et al., 2020; Li et al., 2021; Wang et al., 2021). The high-resolution sMRI is mainly used to characterize the brain morphological properties (Wang et al., 2019). The rs-fMRI allows us to study the intrinsic functional activity pattern of brain. Derived from rs-fMRI, many measures including functional connectivity (Biswal et al., 1995), regional homogeneity (Zang et al., 2004), functional connectivity pattern homogeneity (Wang et al., 2018), functional connectivity density (Tomasi and Volkow, 2010), and amplitude of low-frequency fluctuation (ALFF) (Zou et al., 2008) were proposed and applied to characterize the brain functional couplings, integration, or activity (Zou et al., 2016; Sun et al., 2018; Wang et al., 2018). In all of these measures, ALFF is a widely used index to reflect the functional activity level. The ALFF has been widely used to study the functional activities in both healthy and diseased brain (Fu et al., 2018; Wang et al., 2020). However, whether/how long-term KOA induces brain structural and functional changes is still an open problem.

To reveal the structural and functional abnormalities in patients with KOA, structural and rs-fMRI data were acquired from 13 individuals with KOA and 13 age-, sex-, and education-matched healthy controls (HC). Voxel-based morphological analysis of GMV and voxel-wise analysis of ALFF were performed. We hypnotized that patients with KOA may show structural or functional abnormalities in sensorimotor, emotion, and cognition related brain areas.

MATERIALS AND METHODS

Participants

Thirteen right-handed women patients with chronic KOA pain (mean age = 55.5 years, standard deviation = 5.5 years) were recruited from the West China Hospital, Sichuan University, Chengdu, China. Thirteen age- and sex-matched HC were also included (mean age = 53.9 years, standard deviation = 5.6 years) (**Table 1**). The inclusion criteria for KOA were as follows: (1) without neurological or psychiatric disorders; (2) without a history of medication (within 1 month) or alcohol abuse (within 1 year); (3) with typical KOA symptoms as diagnosed by X-ray; (4) without contraindications for MRI; and (5) without conflicting medications. The inclusion criteria for HC were as follows: (1) no chronic medications and no history of chronic pain; (2) no neurological or psychiatric disorders; (3) no alcohol abuse within one year; and (4) no contraindications to MRI. The written informed consent of each subject was obtained, and this work was approved by the local ethical committee of West China Hospital of Sichuan University and in accordance with the Declaration of Helsinki.

TABLE 1 | Characteristics of demographic and clinical variables.

	KOA (n = 13)	HC (n = 13)	p-value
Age (years)	55.5 ± 5.5	53.9 ± 5.6	0.95
Gender (male/female)	0/13	0/13	0.97
Education (years)	9.97 ± 4.18	9.66 ± 3.65	0.68
Duration (years)	4.73 ± 4.23	0	<0.01
VAS: left knee	26 ± 19.85	0	<0.01
right knee	63.08 ± 9.25	0	<0.01
HSS: left knee	91.23 ± 7.42	100	<0.01
right knee	73.62 ± 4.11	100	<0.01

Values are mean ± standard deviation; VAS, visual analog scale; HSS, Hospital for Special Surgery scale (HSS); KOA, knee osteoarthritis; HC, healthy controls.

Hospital for Special Surgery Scale and Visual Analog Scale Assessment

The clinical symptoms were assessed using visual analog scale (VAS) and Hospital for Special Surgery scale (HSS) (Tian et al., 2020) by two experienced physicians when the subjects were loading (standing). The loading was defined as the self-standup balance between the two legs, that is, the subjects are standing on their own. According to the standard of HSS knee function score (very good: ≥85, good: 70–84, in general: 60–69, poor: ≤59), all patients were divided into four levels. The difference in HSS between the right and left knee (D_{HSS}) was compared. The VAS was used to assess the pain severity of knees for all the subjects (scale ranges from 0 to 100; 0 = no pain; 100 = worst imaginable pain) (Király et al., 2020). Subjects were evaluated when they had stable pain, and the difference in the VAS scores between the right and left knee was also compared.

Magnetic Resonance Imaging Acquisition

Magnetic resonance imaging data was scanned on a 3T whole-body MRI scanner (Siemens Trio system, Erlangen, German) at the MRI Research Center of West China Hospital of Sichuan University. Before scanning, all the subjects were asked to keep their eyes closed with clear thoughts and not to fall asleep. The rs-fMRI data were acquired with a T2* weighted single-shot echo-planar imaging (EPI) sequence using an eight-channel head coil. The acquisition parameters were as follows: repetition time (TR) = 2000 ms, echo time (TE) = 30 ms, flip angle = 90°, field of view (FOV) = 24 cm^2 × 24 cm^2, matrix = 64 × 64, 30 transverse slices covering the whole head, slice thickness = 5.0 mm, voxel size = 3.75 mm^3 × 3.75 mm^3 × 5 mm^3, and 180 volumes. A high-resolution 3D T1-weighted image was also acquired using a spoiled gradient recalled (SPGR) sequence with the following parameters: TR = 8.5 ms, TE = 3.4 ms, flip angle = 12°, FOV = 24 × 24 cm^2, scan matrix = 256 × 256, 156 slices, voxel dimensions = 0.94 × 0.94 × 1 mm^3.

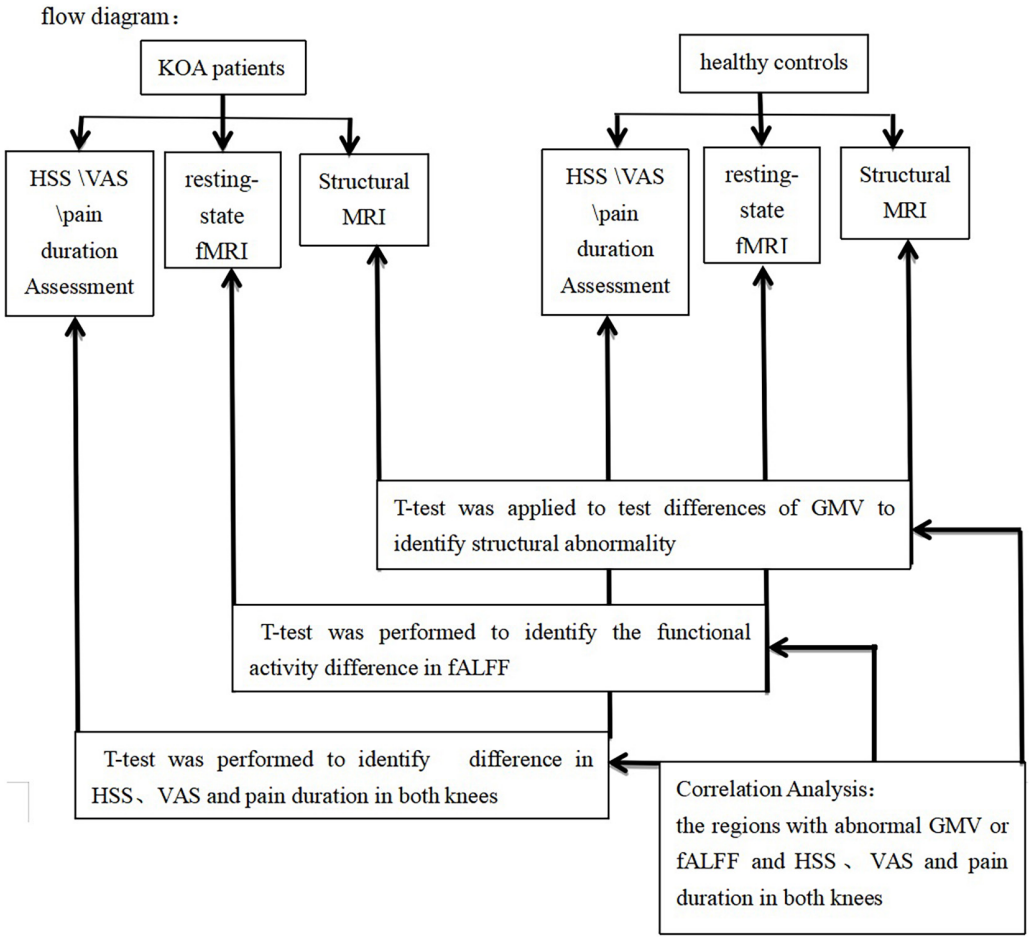

FIGURE 1 | Flow diagram.

Voxel-Based Morphometry Analysis

The high-resolution 3D anatomical images of all subjects were processed using VBM8 and SPM8 toolkits.[1] The sMRI image was first segmented into gray matter, white matter, and cerebrospinal fluid. Then, all the segmented images were registered into MNI space using DARTEL method (Ota et al., 2015; Igata et al., 2017; Wang et al., 2017, 2018; Wu et al., 2017; Gao et al., 2020). Modulated GMV for each subject was obtained and was smoothed using Gaussian kernel with FWHM = 10 mm. To identify structural abnormality in patients with KOA, two-sample *t*-test was applied to test the differences in GMV and corrected with modified Alphasim correction method with $p < 0.05$ (voxel $p < 0.001$).

Resting-State Functional Magnetic Resonance Imaging Pre-processing

Resting-state fMRI data pre-processing was carried out using DPARSF software. The first five volumes were discarded to ensure magnetization equilibrium. The remaining 175 volumes were realigned to the first volume to correct the effect of head motion. Then, the fMRI images were warped into the MNI space with a resolution of $3 \times 3 \times 3$ mm^3 with T1 images and were spatially smoothed by Gaussian kernel with FWHM = 4 mm. The smoothed volumes were detrended and finally were used to calculate the fALFF.

Functional Activity Analysis

The brain functional activity was characterized using fALFF in this work. The fALFF score was the ratio between the power of low-frequency components (0.01–0.08 Hz) and the power of all-frequency components, which described the contribution of the low-frequency components to the all-frequency bands. For statistical analyses, fALFF was normalized by divided the whole brain of ALFF in each subject. The whole brain voxel-wise statistical analysis with two-sample *t*-test was performed to identify the functional activity difference in fALFF between patients with KOA and HC, and the statistical result was corrected using modified Alphasim correction method with $p < 0.05$ (voxel $p < 0.001$).

[1] http://www.fil.ion.ucl.ac.uk/spm

TABLE 2 | Reduce volume of gray matter in patients with KOA pain.

Regions	MNI (Peak)	*t* value (Peak)	*p*- value (Peak)
Left insula	−45, −5, −6	−4.63	5.3e-5
Right insula	53, 6, −8	−5.03	1.9e-5
Left hippocampus	−21, 8, −30	−4.44	8.6e-5
Right hippocampus	29, -6, −30	-5.19	1.3e-5

TABLE 3 | Comparison of fALFF measurements in patients with KOA and control subjects.

Regions	Coordinate	*t* value	*p*-value
Left insula	−39, 6, −3	3.17	0.002
Hippocampus	15, −12, −24	4.11	0.0002
Left cerebellum	−42, −45, −24	−4.17	0.0002
Left precentral gyrus	−39, −9, 45	−5.5	0.000005
Right superior occipital gyrus	33, −84, 33	−4.45	0.00008

Correlation Analysis

After obtaining the regions with abnormal GMV or fALFF, the regional average of GMV or fALFF was calculated for each subject and used to explore the relationship with clinical symptoms. To investigate the relationship between structural and functional abnormalities with pain intensity, joint function, and disease duration, correlation analyses were performed using Pearson's correlation. The significant level was set at $p < 0.05$ uncorrected.

Flow diagram was shown in **Figure 1**.

RESULTS

As shown in **Table 1**, no significant differences in age and sex were found between patients with KOA and HC. In patients with KOA, the VAS scores were significantly different between their left knees and right knees ($p < 0.01$). The level of HSS was also significantly different between their left knees and right knees ($p < 0.01$).

Changed Gray Matter Volume

Compared with the HC, the patients with KOA exhibited reduced GMV in the bilateral insula and bilateral hippocampus (**Figure 2** and **Table 2**).

Abnormal Fractional Amplitude of Low-Frequency Fluctuation in Knee Osteoarthritis

As shown in **Figure 3** and **Table 3**, patients with KOA exhibited higher fALFF values in the left insula and bilateral hippocampus while lower fALFF values in the left cerebellum, left precentral gyrus, and right superior occipital gyrus compared with the control group (**Figure 3** and **Table 3**).

Clinical Correlation Analyses

As shown in **Figure 4**, GMVs in the left insula showed a significantly negative correlation with the VAS for the right knee ($r = -0.68$, $p = 0.011$). A significant positive correlation was found between VAS scores in the right knees and fALFF in left fusiform gyrus ($r = 0.79$, $p = 0.0007$). A significant positive correlation was also found between pain duration and fALFF in the left fusiform gyrus ($r = 0.61$, $p = 0.014$). No other significant correlations were found.

DISCUSSION

This work had three significant findings: (1) patients with chronic KOA pain exhibited reduced GMVs in the bilateral insula and hippocampus; (2) compared with the control group, the patient with KOA showed increased fALFF values in the left insula and bilateral hippocampus whereas decreased fALFF values in the left cerebellum, left precentral gyrus, and right superior occipital gyrus; and (3) the GMV in left insula and the fALFF value in left fusiform gyrus showed significant correlation with pain intensity, and the fALFF of left fusiform gyrus also showed significant correlation with disease duration in patients with KOA. These findings indicate that the left insula may be important for pain processing. More importantly, our findings highlight the key role of left fusiform gyrus in neuropathology of KOA.

The work of spontaneous fluctuations in the brain of patients with KOA reported that the involved networks in the central nervous system are associated with negative emotions and memories of pain perceptions and movement. KOA can lead to persistent chronic pain affecting nervous system function and resulting in secondary changes in brain activity which can be detected by electrophysiological or imaging techniques (Gollub et al., 2018).

Moreover, the orbitofrontal cortex in pain patients have exhibited abnormal activity during a cognitive task, which suggests that pain disturbs the normal functioning of orbitofrontal cortex during emotional modulation (Petrovic et al., 2000). In this work, the orbitofrontal cortex was activated during the anticipation of pain stimulus, which has been reported as representative pain-related expectation regions (Ushio et al., 2020). Furthermore, cognitive control can reduce pain and in part has been attributed to a brain network which comprises prefrontal regions including orbitofrontal cortex, the anterior insula, anterior cingulate cortex (ACC), and brainstem regions (Seminowicz and Moayedi, 2017).

Hippocampus and Insula in Knee Osteoarthritis Pain

The hippocampus is one of the major areas that links affective states, memory processing, pain processing, memory of pain stimulation, and the development of fear-initiated avoidance (Price and Inyang, 2015; Schmidt et al., 2019). Abnormal hippocampal structure and function that occur in chronic pain has been widely reported. Osteoarthritis was reported to be associated with a faster decline in hippocampal volumes in cognitively normal older people (Li et al., 2020). Abnormal hippocampal function in chronic pain might reorganize with neuropathic pain (Jacobs et al., 2020). Strong activation during a pricking pain condition was found in the hippocampal formation, which is related to the aspects of nociceptive

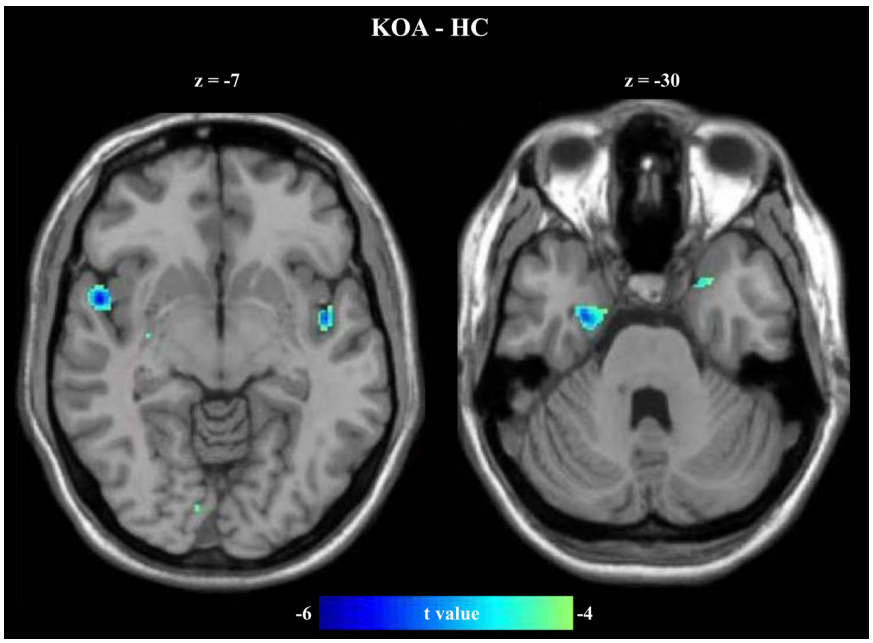

FIGURE 2 | Reduced GMVs in patients with KOA. Compared with HC, the patients with KOA pain showed lower GMV in the bilateral insula and hippocampus.

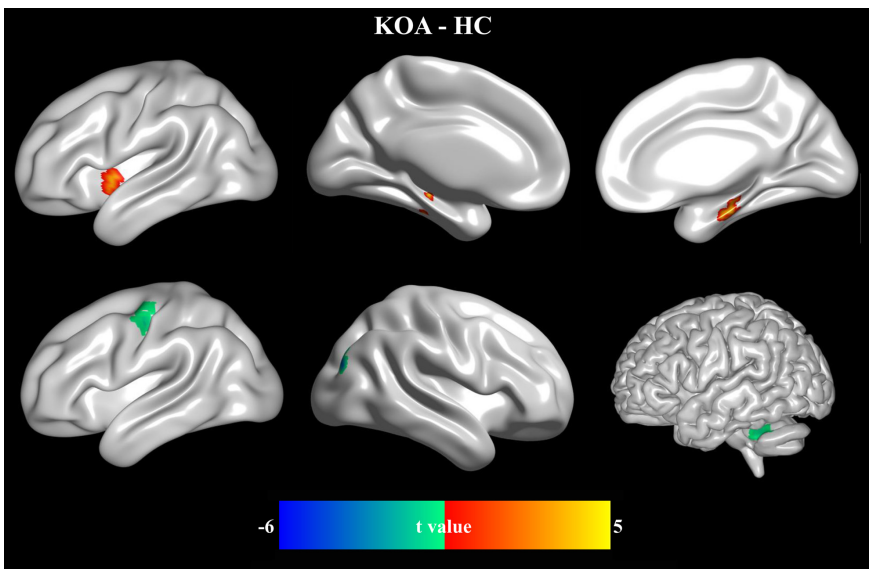

FIGURE 3 | Abnormal resting-state functional activities in patients with KOA. Comparing with HC, the patients with KOA showed higher fALFF in left insula and bilateral hippocampus while lower fALFF in left precentral gyrus, left cerebellum, and right superior occipital gyrus.

processing (Veldhuijzen et al., 2009). The enhanced spontaneous fluctuation of hippocampus in patient with KOA might originate from long-term memory formation and deepening of chronic KOA pain (Wang et al., 2011). Fasick et al. (2015) found that an inflammatory response in the hippocampus might contribute to the enhancement of pain sensitivity. Using positron emission tomography and computed tomography (PET-CT), Yang et al. (2012) found that migraine patients exhibited reduced metabolism in the hippocampus following traditional acupuncture therapy suggested that pain-related emotions and memories faded and disappeared as migraine remission occurs. These results collectedly demonstrated that abnormal GMV and fALFF in hippocampus found in our work may be associated with pain-related emotions and memory deficits (Ezzati et al., 2014).

The patients with chronic KOA pain also exhibited reduced GMVs in the insula. Our findings were consistent with a recent

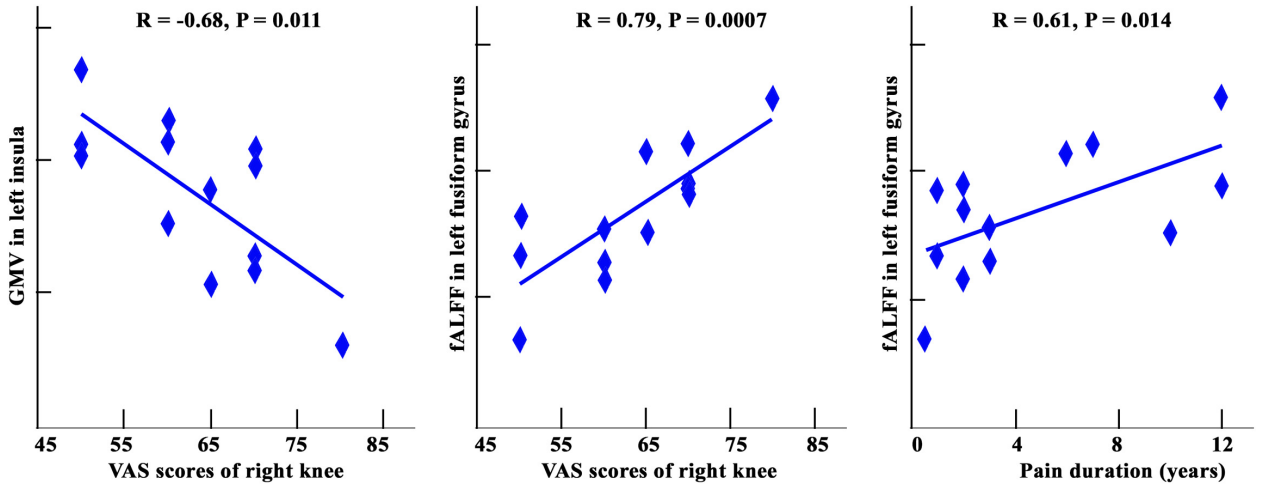

FIGURE 4 | A: Correlation analysis among GMV, fALFF, and clinical assessments in patients with KOA. Significantly negative correlation between GMV of left insula and VAS scores of right knees was found. The significantly positive correlations between fALFF values in left fusiform gyrus and VAS score and pain duration were also found.

work which showed reduced GMV in insular cortex in patients with persistent subacute back pain (Yang and Chang, 2019). Altered connectivity of the right anterior insula driving the pain connectome changes in chronic knee osteoarthritis was also observed (Cottam et al., 2016). The posterior insula was a part of the lateral pain system, which was critical for the perception, encoding, modulation, and chronification of pain and also the formation of pain experiences and the emotional aspects of pain (Lu et al., 2016; Cottam et al., 2018). Thus, the reductions in the GMV of the insula might be associated with sustained abnormal activity in the insula that was evoked by continuous KOA pain. In addition, the GMV in insula was negatively correlated with KOA pain severity. Given that insula anatomically connected with thalamus and supplementary motor area (Mertens et al., 2015), the correlation results further confirmed that insula may be associated with abnormal movement or motor preparation triggered by limb pain (Brown et al., 2014; Wang et al., 2015).

Fusiform Gyrus in Knee Osteoarthritis Pain

Fusiform gyrus located in the ventral of temporal cortex was found to show that activation increases in specific phobias probably due to increased processing of the cue and expectation of behaviorally relevant sensory input (Landgrebe et al., 2008). Ruscheweyh et al. (2018) studied the relationship between GMV and pressure pain thresholds, self-rated pain sensitivity, and found that pain sensitivity questionnaire scores were positively correlated with GMV in fusiform gyrus. Ma et al. (2018) found that migraineurs with comorbid depression had different developmental trajectories in the right fusiform, which were associated with recognizing, transmitting, controlling, and remembering pain and emotion. In this work, we found that the fALFF values in the left fusiform of patients with KOA were significantly positively related to both KOA pain duration and pain intensity in right knees, which indicates that the fusiform gyrus might be a characteristic brain area allowing for the diagnostic imaging of neural mechanism for KOA pain. In conclusion, based on the results of correlation analyses and spontaneous activity, we proposed that the fusiform gyrus should be regarded as a critical area for assessing the mechanism of central nervous system sensitivity to KOA chronic pain.

Other Brain Areas in Knee Osteoarthritis Pain

Abnormal functional activities in left cerebellum, left precentral gyrus, and right superior occipital gyrus were found. The cerebellum is involved in autonomic control, cognition, and affect, as well as in sensorimotor control (Adamaszek et al., 2017). It appears to play a crossmodal modulatory role in relation to pain with noxious stimuli impacting the processing of generalized aversions and sensorimotor adaptations to pain (Mehnert et al., 2017). Cerebellar activity changes during noxious stimuli have been considered to represent offensive motor responses. Left precentral gyrus is important not only in executive functions but also in pain process of antinociceptive effects due to its connections with other subcortical areas for the modulation of pain and inducing pain chronification (Ong et al., 2019). The decreased fALFF value in left precentral gyrus may imply that the long-term disability in the right knee would alter the intrinsic patterns of contralateral movement control among the patients with KOA. In addition, the superior occipital lobe that showed decreased fALFF in patients with KOA plays a critical role in the allocation of visuospatial attention (Sengupta et al., 2018). The decreased fALFF value in this area indicates the impaired reallocation of visuospatial attention for self-regulation in patients with KOA.

Limitations

The sample size was small due to the exclusion of the patients with KOA who had received standard therapy and patients

who had reported higher pain intensity in the left than in the right knee. Moreover, our work was conducted without the treatment for a month making it more challenging to find suitable subjects. Larger sample sizes are required to generalize our findings in this work.

CONCLUSION

Regional structural and functional abnormalities have been found in women with KOA using structural and rs-fMRI compared with that in healthy volunteers. The GMV analysis revealed abnormal pain perception and memory in patients with KOA. The spontaneous brain activity analyses revealed that patients with KOA exhibited two different patterns, a pain-related pattern with higher fALFF and a movement control-related pattern with lower fALFF. The function alternation of fusiform gyrus can be used as a potential biomarker for KOA severity.

DATA AVAILABILITY STATEMENT

The raw data supporting the conclusions of this article will be made available by the authors, without undue reservation.

ETHICS STATEMENT

The studies involving human participants were reviewed and approved by West China Hospital of Sichuan University. The patients/participants provided their written informed consent to participate in this study.

AUTHOR CONTRIBUTIONS

All authors listed have made a substantial, direct, and intellectual contribution to the work, and approved it for publication.

FUNDING

This work was supported by National Natural Science Foundation (Grant No. 81973917) and Sichuan University-Zigong City Cooperation Project (Grant No. 2018CDZG-19-SCU).

ACKNOWLEDGMENTS

We would like to thank Michael Boska for his writing suggestions.

REFERENCES

Adamaszek, M., D'Agata, F., Ferrucci, R., Habas, C., Keulen, S., Kirkby, K. C., et al. (2017). Consensus paper: cerebellum and emotion. *Cerebellum* 16, 552–576.

Becq, G. J. P. C., Habet, T., Collomb, N., Faucher, M., Delon-Martin, C., Coizet, V., et al. (2020). Functional connectivity is preserved but reorganized across several anesthetic regimes. *Neuroimage* 219:116945. doi: 10.1016/j.neuroimage.2020.116945

Biswal, B., Yetkin, F. Z., Haughton, V. M., and Hyde, J. S. (1995). Functional connectivity in the motor cortex of resting human brain using echo-planar MRI. *Magn. Reson. Med.* 34, 537–541. doi: 10.1002/mrm.1910340409

Brown, C. A., El-Deredy, W., and Jones, A. K. (2014). When the brain expects pain: common neural responses to pain anticipation are related to clinical pain and distress in fibromyalgia and osteoarthritis. *Eur. J. Neurosci.* 39, 663–672. doi: 10.1111/ejn.12420

Cottam, W. J., Condon, L., Alshuft, H., Reckziegel, D., and Auer, D. P. (2016). Associations of limbic-affective brain activity and severity of ongoing chronic arthritis pain are explained by trait anxiety. *Neuroimage Clin.* 12, 269–276. doi: 10.1016/j.nicl.2016.06.022

Cottam, W. J., Iwabuchi, S. J., Drabek, M. M., Reckziegel, D., and Auer, D. P. (2018). Altered connectivity of the right anterior insula drives the pain connectome changes in chronic knee osteoarthritis. *Pain* 159, 929–938. doi: 10.1097/j.pain.0000000000001209

Ezzati, A., Zimmerman, M. E., Katz, M. J., Sundermann, E. E., Smith, J. L., Lipton, M. L., et al. (2014). Hippocampal subfields differentially correlate with chronic pain in older adults. *Brain Res.* 1573, 54–62. doi: 10.1016/j.brainres.2014.05.025

Fasick, V., Spengler, R. N., Samankan, S., Nader, N. D., and Ignatowski, T. A. (2015). The hippocampus and TNF: common links between chronic pain and depression. *Neurosci. Biobehav. Rev.* 53, 139–159. doi: 10.1016/j.neubiorev.2015.03.014

Ferket, B. S., Feldman, Z., Zhou, J., Oei, E. H., Bierma-Zeinstra, S. M., and Mazumdar, M. (2017). Impact of total knee replacement practice: cost effectiveness analysis of data from the osteoarthritis initiative. *BMJ* 356:j1131. doi: 10.1136/bmj.j1131

Fu, Z., Tu, Y., Di, X., Du, Y., Pearlson, G. D., Turner, J. A., et al. (2018). Characterizing dynamic amplitude of low-frequency fluctuation and its relationship with dynamic functional connectivity: an application to schizophrenia. *Neuroimage* 180, 619–631. doi: 10.1016/j.neuroimage.2017.09.035

Gao, Z., Guo, X., Liu, C., Mo, Y., and Wang, J. (2020). Right inferior frontal gyrus: an integrative hub in tonal bilinguals. *Hum. Brain Mapp.* 41, 2152–2159. doi: 10.1002/hbm.24936

Gollub, R. L., Kirsch, I., Maleki, N., Wasan, A. D., Edwards, R. R., Tu, Y., et al. (2018). A functional neuroimaging study of expectancy effects on pain response in patients with knee osteoarthritis. *J. Pain* 19, 515–527. doi: 10.1016/j.jpain.2017.12.260

Igata, R., Katsuki, A., Kakeda, S., Watanabe, K., Igata, N., Hori, H., et al. (2017). PCLO rs2522833-mediated gray matter volume reduction in patients with drug-naive, first-episode major depressive disorder. *Transl. Psychiatry* 7:e1140. doi: 10.1038/tp.2017.100

Jacobs, C. A., Vranceanu, A. M., Thompson, K. L., and Lattermann, C. (2020). Rapid progression of knee pain and osteoarthritis biomarkers greatest for patients with combined obesity and depression: data from the osteoarthritis initiative. *Cartilage* 11, 38–46. doi: 10.1177/1947603518777577

Kaplan, C., Minc, A., Basu, N., and Schrepf, A. (2019). Inflammation and the central nervous system in inflammatory rheumatic disease. *Curr. Rheumatol. Rep.* 21:67.

Király, M., Kővári, E., Hodosi, K., Bálint, P. V., and Bender, T. (2020). The effects of Tiszasüly and Kolop mud pack therapy on knee osteoarthritis: a double-blind, randomised, non-inferiority controlled study. *Int. J. Biometeorol.* 64, 943–950. doi: 10.1007/s00484-019-01764-4

Kloppenburg, M., and Berenbaum, F. (2020). Osteoarthritis year in review 2019: epidemiology and therapy. *Osteoarthr. Cartil.* 28, 242–248. doi: 10.1016/j.joca.2020.01.002

Landgrebe, M., Barta, W., Rosengarth, K., Frick, U., Hauser, S., Langguth, B., et al. (2008). Neuronal correlates of symptom formation in functional somatic syndromes: a fMRI study. *Neuroimage* 41, 1336–1344. doi: 10.1016/j.neuroimage.2008.04.171

Li, X., Lei, D., Niu, R., Li, L., Suo, X., Li, W., et al. (2021). Disruption of gray matter morphological networks in patients with paroxysmal kinesigenic dyskinesia. *Hum. Brain Mapp.* 42, 398–411. doi: 10.1002/hbm.25230

Li, Y., Zhang, T., Li, W., Zhang, J., Jin, Z., and Li, L. (2020). Linking brain structure and activation in anterior insula cortex to explain the trait empathy for pain. *Hum. Brain Mapp.* 41, 1030–1042. doi: 10.1002/hbm.24858

Losina, E., Michl, G., Collins, J. E., Hunter, D. J., Jordan, J. M., Yelin, E., et al. (2016). Model-based evaluation of cost-effectiveness of nerve growth factor inhibitors in knee osteoarthritis: impact of drug cost, toxicity, and means of administration. *Osteoarthr. Cartil.* 24, 776–785. doi: 10.1016/j.joca.2015.12.011

Lu, C., Yang, T., Zhao, H., Zhang, M., Meng, F., Fu, H., et al. (2016). Insular cortex is critical for the perception, modulation, and chronification of pain. *Neurosci. Bull.* 32, 191–201. doi: 10.1007/s12264-016-0016-y

Ma, M., Zhang, J., Chen, N., Guo, J., Zhang, Y., and He, L. (2018). Exploration of intrinsic brain activity in migraine with and without comorbid depression. *J. Headache Pain* 19:48. doi: 10.1186/s10194-018-0876-9

Mehnert, J., Schulte, L., Timmann, D., and May, A. (2017). Activity and connectivity of the cerebellum in trigeminal nociception. *Neuroimage* 150, 112–118. doi: 10.1016/j.neuroimage.2017.02.023

Mertens, P., Blond, S., David, R., and Rigoard, P. (2015). Anatomy, physiology and neurobiology of the nociception: a focus on low back pain (part A). *Neuro Chirurgie* 61(Suppl. 1), S22–S34. doi: 10.1016/j.neuchi.2014.09.001

Ong, W. Y., Stohler, C. S., and Herr, D. R. (2019). Role of the prefrontal cortex in pain processing. *Mol. Neurobiol.* 56, 1137–1166. doi: 10.1007/s12035-018-1130-9

Ota, M., Noda, T., Sato, N., Okazaki, M., Ishikawa, M., Hattori, K., et al. (2015). Effect of electroconvulsive therapy on gray matter volume in major depressive disorder. *J. Affect. Disord.* 186, 186–191.

Petrovic, P., Petersson, K. M., Ghatan, P. H., Stone-Elander, S., and Ingvar, M. (2000). Pain-related cerebral activation is altered by a distracting cognitive task. *Pain* 85, 19–30. doi: 10.1016/s0304-3959(99)00232-8

Price, T. J., and Inyang, K. E. (2015). Commonalities between pain and memory mechanisms and their meaning for understanding chronic pain. *Prog. Mol. Biol. Transl. Sci.* 131, 409–434. doi: 10.1016/bs.pmbts.2014.11.010

Ruscheweyh, R., Wersching, H., Kugel, H., Sundermann, B., and Teuber, A. (2018). Gray matter correlates of pressure pain thresholds and self-rated pain sensitivity: a voxel-based morphometry study. *Pain* 159, 1359–1365. doi: 10.1097/j.pain.0000000000001219

Schmidt, K., Forkmann, K., Schultz, H., Gratz, M., Bitz, A., Wiech, K., et al. (2019). Enhanced neural reinstatement for evoked facial pain compared with evoked hand pain. *J. Pain* 20, 1057–1069. doi: 10.1016/j.jpain.2019.03.003

Seminowicz, D. A., and Moayedi, M. (2017). The dorsolateral prefrontal cortex in acute and chronic pain. *J. Pain* 18, 1027–1035. doi: 10.1016/j.jpain.2017.03.008

Sengupta, S., Fritz, F. J., Harms, R. L., Hildebrand, S., Tse, D. H. Y., Poser, B. A., et al. (2018). High resolution anatomical and quantitative MRI of the entire human occipital lobe ex vivo at 9.4T. *Neuroimage* 168, 162–171. doi: 10.1016/j.neuroimage.2017.03.039

Sun, H., Luo, L., Yuan, X., Zhang, L., He, Y., Yao, S., et al. (2018). Regional homogeneity and functional connectivity patterns in major depressive disorder, cognitive vulnerability to depression and healthy subjects. *J. Affect. Disord.* 235, 229–235. doi: 10.1016/j.jad.2018.04.061

Tian, X., Han, C., Wang, J., Tan, Y., Zhu, G., Lei, M., et al. (2020). Distal tibial tuberosity high tibial osteotomy using an image enhancement technique for orthopedic scans in the treatment of medial compartment knee osteoarthritis. *Comput. Methods Programs Biomed.* 191:105349.

Tomasi, D., and Volkow, N. D. (2010). Functional connectivity density mapping. *Proc. Natl. Acad. Sci. U S.A.* 107, 9885–9890.

Ushio, K., Nakanishi, K., Mikami, Y., Yoshino, A., Takamura, M., Hirata, K., et al. (2020). Altered resting-state connectivity with pain-related expectation regions in female patients with severe knee osteoarthritis. *J. Pain Res.* 13, 3227–3234. doi: 10.2147/JPR.S268529

Veldhuijzen, D. S., Nemenov, M. I., Keaser, M., Zhuo, J., Gullapalli, R. P., and Greenspan, J. D. (2009). Differential brain activation associated with laser-evoked burning and pricking pain: an event-related fMRI study. *Pain* 141, 104–113. doi: 10.1016/j.pain.2008.10.027

Wang, J., Wang, Z., Zhang, H., Feng, S., Lu, Y., Wang, S., et al. (2021). White matter structural and network topological changes underlying the behavioral phenotype of MECP2 mutant monkeys. *Cereb. Cortex* 31, 5396–5410. doi: 10.1093/cercor/bhab166

Wang, J., Wei, Q., Bai, T., Zhou, X., Sun, H., Becker, B., et al. (2017). Electroconvulsive therapy selectively enhanced feedforward connectivity from fusiform face area to amygdala in major depressive disorder. *Soc. Cogn. Affect. Neurosci.* 12, 1983–1992. doi: 10.1093/scan/nsx100

Wang, J., Wei, Q., Wang, L., Zhang, H., Bai, T., Cheng, L., et al. (2018). Functional reorganization of intra- and internetwork connectivity in major depressive disorder after electroconvulsive therapy. *Hum. Brain Mapp.* 39, 1403–1411. doi: 10.1002/hbm.23928

Wang, J., Yang, Y., Zhao, X., Zuo, Z., and Tan, L.-H. (2020). Evolutional and developmental anatomical architecture of the left inferior frontal gyrus. *Neuroimage* 222:117268. doi: 10.1016/j.neuroimage.2020.117268

Wang, L., Yu, L., Wu, F., Wu, H., and Wang, J. (2019). Altered whole brain functional connectivity pattern homogeneity in medication-free major depressive disorder. *J. Affect. Disord.* 253, 18–25. doi: 10.1016/j.jad.2019.04.040

Wang, Y., Chen, H., Gao, Q., Yang, Y., Gong, Q., and Gao, F. (2015). Evaluation of net causal influences in the circuit responding to premotor control during the movement-readiness state using conditional granger causality. *Brain Res.* 1595, 110–119. doi: 10.1016/j.brainres.2014.08.004

Wang, Z., Bradesi, S., Charles, J. R., Pang, R. D., Maarek, J. I., Mayer, E. A., et al. (2011). Functional brain activation during retrieval of visceral pain-conditioned passive avoidance in the rat. *Pain* 152, 2746–2756. doi: 10.1016/j.pain.2011.08.022

Wu, H., Sun, H., Wang, C., Yu, L., Li, Y., Peng, H., et al. (2017). Abnormalities in the structural covariance of emotion regulation networks in major depressive disorder. *J. Psychiatr. Res.* 84, 237–242. doi: 10.1016/j.jpsychires.2016.10.001

Xu, J., Lyu, H., Li, T., Xu, Z., Fu, X., Jia, F., et al. (2019). Delineating functional segregations of the human middle temporal gyrus with resting-state functional connectivity and coactivation patterns. *Hum. Brain Mapp.* 40, 5159–5171. doi: 10.1002/hbm.24763

Xu, J., Wei, Q., Bai, T., Wang, L., Li, X., He, Z., et al. (2020). Electroconvulsive therapy modulates functional interactions between submodules of the emotion regulation network in major depressive disorder. *Transl. Psychiatry* 10:271. doi: 10.1038/s41398-020-00961-9

Yang, J., Zeng, F., Feng, Y., Fang, L., Qin, W., Liu, X., et al. (2012). A PET-CT study on the specificity of acupoints through acupuncture treatment in migraine patients. *BMC Complement. Altern. Med.* 12:123. doi: 10.1186/1472-6882-12-123

Yang, S., and Chang, M. C. (2019). Chronic pain: structural and functional changes in brain structures and associated negative affective states. *Int. J. Mol. Sci.* 20:3130. doi: 10.3390/ijms20133130

Zang, Y., Jiang, T., Lu, Y., He, Y., and Tian, L. (2004). Regional homogeneity approach to fMRI data analysis. *Neuroimage* 22, 394–400. doi: 10.1016/j.neuroimage.2003.12.030

Zhang, Y., Cao, S., Yuan, J., Song, G., Yu, T., and Liang, X. (2020). Functional and structural changes in postherpetic neuralgia brain before and six months after pain relieving. *J. Pain Res.* 13, 909–918. doi: 10.2147/JPR.S246745

Zhaoyang, R., Martire, L. M., and Darnall, B. D. (2020). Daily pain catastrophizing predicts less physical activity and more sedentary behavior in older adults with osteoarthritis. *Pain* 161, 2603–2610. doi: 10.1097/j.pain.0000000000001959

Zou, K., Gao, Q., Long, Z., Xu, F., Sun, X., Chen, H., et al. (2016). Abnormal functional connectivity density in first-episode, drug-naive adult patients with major depressive disorder. *J. Affect. Disord.* 194, 153–158. doi: 10.1016/j.jad.2015.12.081

Zou, Q. H., Zhu, C. Z., Yang, Y., Zuo, X. N., Long, X. Y., Cao, Q. J., et al. (2008). An improved approach to detection of amplitude of low-frequency fluctuation (ALFF) for resting-state fMRI: fractional ALFF. *J. Neurosci. Methods* 172, 137–141. doi: 10.1016/j.jneumeth.2008.04.012

Conflict of Interest: The authors declare that the research was conducted in the absence of any commercial or financial relationships that could be construed as a potential conflict of interest.

Publisher's Note: All claims expressed in this article are solely those of the authors and do not necessarily represent those of their affiliated organizations, or those of the publisher, the editors and the reviewers. Any product that may be evaluated in this article, or claim that may be made by its manufacturer, is not guaranteed or endorsed by the publisher.

frontiers in Neuroscience

ORIGINAL RESEARCH
published: 03 January 2022
doi: 10.3389/fnins.2021.800436

High Gamma and Beta Temporal Interference Stimulation in the Human Motor Cortex Improves Motor Functions

Ru Ma[1†], Xinzhao Xia[2†], Wei Zhang[1], Zhuo Lu[2], Qianying Wu[1,3], Jiangtian Cui[2,4], Hongwen Song[1], Chuan Fan[2], Xueli Chen[1], Rujing Zha[1], Junjie Wei[5], Gong-Jun Ji[5], Xiaoxiao Wang[2], Bensheng Qiu[2*] and Xiaochu Zhang[1,2,6,7*]*

[1] Hefei National Laboratory for Physical Sciences at the Microscale, Division of Life Science and Medicine, Department of Radiology, The First Affiliated Hospital of USTC, School of Life Science, University of Science and Technology of China, Hefei, China, [2] Centers for Biomedical Engineering, School of Information Science and Technology, University of Science and Technology of China, Hefei, China, [3] Division of the Humanities and Social Sciences, California Institute of Technology, Pasadena, CA, United States, [4] School of Optometry and Vision Sciences, Cardiff University, Cardiff, United Kingdom, [5] Department of Neurology, The First Affiliated Hospital of Anhui Medical University, Hefei, China, [6] Department of Psychology, School of Humanities and Social Science, University of Science and Technology of China, Hefei, China, [7] Biomedical Sciences and Health Laboratory of Anhui Province, University of Science and Technology of China, Hefei, China

OPEN ACCESS

Edited by:
Jiaojian Wang,
University of Electronic Science and Technology of China, China

Reviewed by:
Kai Yuan,
Xidian University, China
Yan-Xue Xue,
Peking University, China

***Correspondence:**
Xiaoxiao Wang
Wang506@ustc.edu.cn
Bensheng Qiu
bqiu@ustc.edu.cn
Xiaochu Zhang
zxcustc@ustc.edu.cn

[†] These authors have contributed equally to this work and share first authorship

Specialty section:
This article was submitted to Brain Imaging Methods, a section of the journal Frontiers in Neuroscience

Received: 23 October 2021
Accepted: 29 November 2021
Published: 03 January 2022

Citation:
Ma R, Xia X, Zhang W, Lu Z, Wu Q, Cui J, Song H, Fan C, Chen X, Zha R, Wei J, Ji G-J, Wang X, Qiu B and Zhang X (2022) High Gamma and Beta Temporal Interference Stimulation in the Human Motor Cortex Improves Motor Functions. Front. Neurosci. 15:800436. doi: 10.3389/fnins.2021.800436

Background: Temporal interference (TI) stimulation is a new technique of non-invasive brain stimulation. Envelope-modulated waveforms with two high-frequency carriers can activate neurons in target brain regions without stimulating the overlying cortex, which has been validated in mouse brains. However, whether TI stimulation can work on the human brain has not been elucidated.

Objective: To assess the effectiveness of the envelope-modulated waveform of TI stimulation on the human primary motor cortex (M1).

Methods: Participants attended three sessions of 30-min TI stimulation during a random reaction time task (RRTT) or a serial reaction time task (SRTT). Motor cortex excitability was measured before and after TI stimulation.

Results: In the RRTT experiment, only 70 Hz TI stimulation had a promoting effect on the reaction time (RT) performance and excitability of the motor cortex compared to sham stimulation. Meanwhile, compared with the sham condition, only 20 Hz TI stimulation significantly facilitated motor learning in the SRTT experiment, which was significantly positively correlated with the increase in motor evoked potential.

Conclusion: These results indicate that the envelope-modulated waveform of TI stimulation has a significant promoting effect on human motor functions, experimentally suggesting the effectiveness of TI stimulation in humans for the first time and paving the way for further explorations.

Keywords: temporal interference stimulation, non-invasive brain stimulation, brain oscillation, motor function, motor cortex excitability

INTRODUCTION

Electrical stimulation is the most direct way to regulate neuroplasticity and electrically oscillating neural activities (Doty, 1969). Two kinds of electrical stimulation techniques have been extensively used. The first is deep brain stimulation (DBS), which has been proven to be an effective treatment for treating Parkinson's disease (Benabid, 2003; Tinkhauser et al., 2017). The delivery of DBS requires invasive surgery, thus presenting the potential for surgical complications (Ramirez-Zamora et al., 2018). Another method is transcranial electrical stimulation (tES) (Paulus, 2011; Bestmann and Walsh, 2017), which can modulate brain activities in non-invasive ways (Keeser et al., 2011; Yang et al., 2014, 2017, 2020; Liu et al., 2018). Transcranial electrical stimulation applied with alternating current, i.e., transcranial alternating current stimulation (tACS), has been used to facilitate oscillation activity within specific frequency ranges (Herrmann et al., 2013; Vossen et al., 2015). Many studies have shown that tACS can modulate motor-related oscillation brain activities, which could result in changes in cortical excitability and motor function improvement (Feurra et al., 2011, 2013; Joundi et al., 2012; Pollok et al., 2015). However, currents of tES applied over the scalp were found to be significantly attenuated when traveling through the skin, subcutaneous soft tissue and skull (Vöröslakos et al., 2018). Thus, the depth of stimulation is limited. Although simulation and experimental results show that conventional tES could also generate an electric field with enough strength to influence neural activity in some regions deep in the brain (Huang and Parra, 2019; Louviot et al., 2021). But the intensity of the electric field in the brain regions that cover the deep target would be larger (Lee et al., 2020), which might cause off-target effects and make the results difficult to explain.

To overcome the limitations of these two electrical brain stimulation techniques, temporal interference (TI) stimulation has been recently proposed (Grossman et al., 2017), which has caused considerable excitement in the research community (Dmochowski et al., 2017; Lozano, 2017; Opitz and Tyler, 2017; Grossman, 2018; Grossman et al., 2018; Halpern et al., 2018). This new technique can be applied by delivering two electric fields at frequencies that are too high ($\geq$1 kHz) to entrain neural electrical activity (Hutcheon and Yarom, 2000). The frequency difference between these two electric fields is within the range of brain oscillations (e.g., 20 Hz, 70 Hz, etc.), which could result in a prominent envelope modulated electric field in a targeted brain region. TI stimulation has been proven to be effective in driving the firing patterns of hippocampal neurons without recruiting neurons in the overlying brain cortex and evoking different motor behaviors when targeting different areas of the motor cortex in mice (Grossman et al., 2017).

Based on the concept of TI stimulation, several modeling and computation studies have been performed to explore the feasibility of TI stimulation in the human brain (Lafon et al., 2017; Fariba et al., 2019; Rampersad et al., 2019; Cao and Grover, 2020; Huang et al., 2020; Lee et al., 2020; Mirzakhalili et al., 2020). However, no data about the actual effect of TI stimulation on human brains have been reported thus far. The stimulation waveform of TI stimulation is an envelope-modulated waveform produced by the superposition of two sine waves, which is much more complex than conventional tACS. Whether such TI stimulation has a comparable effect with conventional tACS on the human brain is unknown.

In this study, we implemented TI stimulation targeting the left primary motor cortex (M1) of healthy participants to validate the effectiveness of TI stimulation on the human brain. The primary motor cortex (M1) is a common target in many pioneering experiments in non-invasive brain stimulation (NIBS) technique (Barker et al., 1985; Priori et al., 1998; Antal et al., 2008; Terney et al., 2008). High gamma and beta brain oscillations play important roles in human motor cortex. Previous studies have found that high gamma brain oscillations (e.g., 70 Hz) are transiently increased during movement and they have a promoting effect on movement initiation (Cheyne et al., 2008; Muthukumaraswamy, 2010; Gaetz et al., 2013). Meanwhile, beta activities (e.g., 20 Hz) in the motor cortex are considered an important component of motor learning (Espenhahn et al., 2019, 2020; Haar and Faisal, 2020).

Considering the prior investigations of oscillations related to M1, we designed two stimulation conditions with envelope frequencies of 20 Hz (beta) and 70 Hz (high gamma). A sham condition was used as a control. To explore the influence of TI stimulation on different levels of motor functions, two motor tasks were employed in two independent experiments, including a random reaction time task (RRTT) and a serial reaction time task (SRTT). RRTT is a single reaction time task, and the order of the reactions is totally randomized. SRTT contains repeatedly recurring response sequences, which can be learned by participants (Robertson, 2007). Based on the distinct functions of high gamma and beta oscillations in the human motor cortex we stated above, we hypothesized a promotion of reaction speed induced by 70 Hz TI stimulation in RRTT and a more significant effect of 20 Hz TI stimulation than sham stimulation on motor learning in SRTT. We also measured motor cortex excitability before and after TI stimulation (Chen, 2000; Rossini et al., 2015), which was hypothesized to be facilitated by TI stimulation based on previous findings (Moliadze et al., 2010; Feurra et al., 2011, 2013; Guerra et al., 2020).

MATERIALS AND METHODS

Participants

We recruited 27 healthy adult volunteers in the RRTT experiment, and 6 participants were removed from the analysis because of technical issues (a decrease in current due to poor contact and current crosstalk due to the flow of conductive paste). Data from the remaining 21 participants were included in the analysis (6 females, mean age $\pm$ SD: 22.429 $\pm$ 2.249 years, mean education level $\pm$ SD: 15.762 $\pm$ 2.166 years, mean handedness score $\pm$ SD: 86.667 $\pm$ 17.127). Another 33 healthy adults volunteered to participate in the SRTT experiment, but 1 participant was removed due to the sliding of electrodes, 1 participant was rejected because he switched his performing hand, and 2 participants' data were removed because of technical issues (current crosstalk due to the

flow of conductive paste). Therefore, data of 29 participants remained to be analyzed in the SRTT experiment (15 females, mean age ± SD: 22.103 ± 2.024 years, mean education level ± SD:15.966 ± 1.991 years, mean handedness score ± SD: 77.672 ± 23.792).

All participants reported no history of craniotomy or injury to the head, no personal or family history of neurological or psychiatric disease, no metal implants or implanted electronic devices, no skin sensitivity and no use of medicine during the experiment. For safety reasons, any participant who was pregnant or could be pregnant was rejected. All participants were right-handed as assessed using the Edinburgh handedness inventory (Oldfield, 1971) and had normal or corrected-to-normal vision. Informed consent was obtained prior to any involvement in the study. This study was approved by the Human Ethics Committee of the University of Science and Technology of China (IRB Number: 2020KY161).

Sample size was calculated by G*Power 3.1 (Faul et al., 2009). According to previous studies (Joundi et al., 2012; Pollok et al., 2015), we expected an effect size a little higher than medium level (Cohen's $d = 0.6$) for the paired t test between stimulation conditions (20 Hz / 70 Hz) and sham condition. With α error probability of 0.05 and power (1-β error probability) of 0.8, the resulting sample size was 24. Considering potential dropouts, we recruited a bit more participants.

Experimental Design

Three conditions, 20 Hz, 70 Hz and sham were applied in a single-blind, cross-over design (**Figure 1A**) in both the RRTT and the SRTT experiment. Participants visited the laboratory three times, at least 3 days apart, to avoid any influence of the carry-over effects of stimulation. The order of the stimulation condition (20 Hz/70 Hz/sham) was counterbalanced across participants. At the beginning of the procedures, individual M1 location was identified by single pulse TMS, and baseline motor cortex excitability was measured. Before stimulation, the participants were asked to perform a practice task with 24 random button presses. Formal experimental tasks (RRTT or SRTT) started 10 min after the beginning of TI stimulation. After the 30-min stimulation, motor cortex excitability was measured again to detect the change in excitability of M1.

TMS and MEP

Single pulse TMS was delivered manually using a figure-eight coil (AirFile Coil) connected to a Magstim Rapid^2 stimulator (The Magstim Company Ltd., Whitland, United Kingdom). Peak magnetic field of the coil is 0.8 T. To ensure the position of the coil to be consistent during the experiment, a Brainsight navigation system (Rogue Research Inc., Montreal, QC, Canada) was used. Electromyogram (EMG) of the right FDI was recorded by a pair of disposable self-adhesive electrodes in a belly tendon montage using the EMG module of the navigation system. The two electrodes were located over the muscle body of the right FDI and the first phalanx of the right index finger, respectively. Another electrode was attached at the underside of the right forearm as the ground electrode. EMG was recorded with a sample rate of 3 kHz and bandpass filtered at 16–470 Hz in Brainsight v2.3.8 software.

FDI hotspot was defined as the coil location steadily eliciting MEPs with the lowest stimulation intensity. The search for the FDI hotspot begun at the scalp location corresponding to C3 in the electroencephalography (EEG) 10–20 system. The initial TMS output intensity was set at 40% of the maximum stimulator output. The coil was placed tangentially over the scalp, and the handle of the coil was pointing posterolaterally 45° from the midline (Sakai et al., 1997; Opitz et al., 2013). Single-pulse TMS stimulation was manually triggered while we gradually moved the coil around the initial position. The search procedure was repeated with the stimulator output intensity increased in a 5% step until the TMS pulse could elicit any detectable MEP. In order to restrict the hotspot area, the TMS intensity was decreased by a staircase approach to diminish the current spread of the stimulation after the location that could the highest MEPs robustly be elicited was found (Raco et al., 2017). The FDI hotspot was then marked on a medical elastic bandage on the participants' heads after the search process. The resting motor threshold (RMT) was defined as the lowest stimulus intensity that could elicit a MEP in the resting muscle with an amplitude of 50 μV (peak-to-peak) or greater in at least 5 out of 10 recordings (Boroojerdi et al., 2001; Rossini et al., 2015).

In the RRTT experiment, we applied 15 pulses over the FDI hotspot with an interval of 7 s at stimulation intensities of 120, 100, 130, 110, and 140% of RMT before and after TI stimulation (Kleim et al., 2007). We measured 30 MEPs at a stimulation intensity of 120% of the RMT in the SRTT experiment. Only 120% RMT was used because this intensity corresponds to the linear increase range of the IO curve and is sensitive to the change in M1 excitability (Rossini et al., 2015).

Motor Tasks

The motor tasks were both modified from a SRTT task, which was previously involved in tACS experiments (Pollok et al., 2015; Krause et al., 2016). Participants were instructed to press one of four buttons (V, B, N, M) on the keyboard as fast as possible, according to the position of the light rectangles shown on the screen (**Figure 1B**). The stimulus remained on the screen until the correct response was made. After 500 ms, a new stimulus was displayed. Eight blocks were included, with 120 trials in each block. The locations corresponding to the light rectangles were pseudorandomly distributed in all 8 blocks (R) in RRTT (**Figure 1C**). The only difference between SRTT and RRTT was that the reactions were not randomized in some SRTT blocks (**Figure 1D**). The first block and the sixth block were R blocks. In the remaining blocks, the locations of the light rectangles were repeated in a 12-item sequential manner ten times in each block (S). Same to the previous studies (Curran, 1997; Schendan et al., 2003), there were three 12-item second-order predictive sequences (bnmvnbmnvbvm, nvnmbvmnbmvb, mvbmnbnvmbvn) with comparable difficulty assigned to each experimental session in a counterbalanced way across participants. All of the information about the order of the locations was unknown to the participant, which allowed them to acquire the sequence in an implicit manner. The

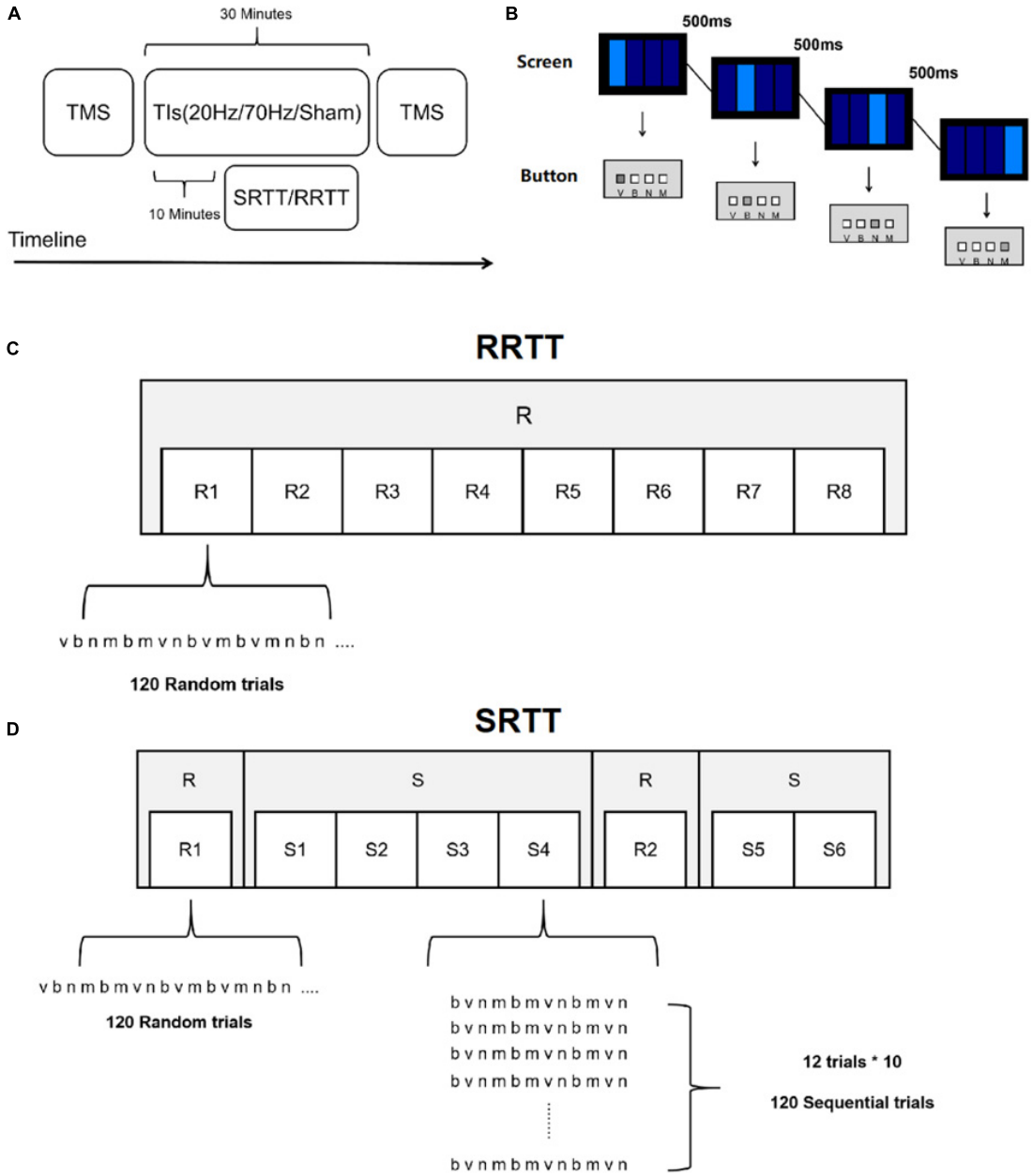

FIGURE 1 | Experimental design and motor tasks. **(A)** The experimental procedures. **(B)** Motor task implemented in our experiments. **(C)** RRTT. **(D)** SRTT. In R blocks, there were three 12-item (bnmvnbmnvbvm, nvnmbvmnbmvb, mvbmnbnvmbvn) sequences with comparable difficulty for each experimental session in a counterbalanced way.

task presentation and the recording of the reaction times (RT) were conducted using E-Prime 2.0 (Psychology Software Tools, Sharpsburg, MD, United States).

Temporal Interference Stimulation

The TI stimulation was applied by a customized battery-driven stimulator. The instrument performance (the current characterization and the characterization of channel isolation) of this TI stimulator was comparable with that of Grossman et al. (2017) (**Supplementary Figure 1** and **Supplementary Material 2.1**). For safety concerns, currents of all the four output ports were monitored by protecting circuits to ensure security. Once the amplitude of current at one single output port exceeded the safety threshold, the four output ports would all be cut down by relays. The device is powered by batteries and isolated from mains electricity.

The TI stimulation protocol was designed based on simulation analysis using finite element method (FEM) (**Supplementary Figure 2** and **Supplementary Material 2.2**). We used five Ag-AgCl electrodes with a radius of 1 cm (Pistim electrode,

Neuroelectrics, Barcelona, Spain), four of which were stimulating electrodes and one was the ground electrode located on the mastoid behind the participant's left ear to avoid current accumulations due to safety considerations. The stimulation electrodes were located 30 mm away from the FDI hotspot along the axis of the Fpz-Oz and T3-T4 in the EEG 10–20 system (**Figure 2**). Electrodes were fixed by a medical elastic bandage (Hebei Shengyu Medical Equipment, Hengshui, China) and filled with conductive gel (Quick-Gel, Compumedics USA Inc., Charlotte, CA, United States) to make the impedance of each electrode below 10 kΩ. The stimulation intensity was peak-to-peak 2 mA in a single channel (totally peak-to-peak 4 mA for two channels). Stimulation (20 Hz or 70 Hz) lasted continuously for 30 min. After a 10-min rest since the beginning of stimulation, participant started to perform the motor task, which lasted for 15–20 min (depending on the reaction speed of participants). Participants were asked to rest again until the end of the stimulation. There was a 30 s linearly ramp up and ramp down period at the beginning and the end of the stimulation. For the sham condition, TI stimulation (20 Hz or 70 Hz) only lasted for approximately 60 s (30 s ramp up and 30 s ramp down) at the beginning of this procedure.

Safety Aspects

After the TI stimulation, we asked the participants to complete a subjective questionnaire (Brunoni et al., 2011; Fertonani et al., 2015), which asked them to rate their sensations including itching, headache, burning, warmth/heat, tingling, metallic/iron taste, fatigue, vertigo, nausea and phosphene during the stimulation and on what extent do they think these feelings were relevant with the stimulation. Participants were asked to rate the extent of these sensations that they experienced, from 0 to 4, representing none, mild, moderate, considerable and strong, respectively. Similarly, the relevance to the stimulation was also rated from 0 to 4, representing none, remote, possible, probable and definite, respectively. Only sensations with a score larger than 1 were taken into consideration.

Data Analysis

All analyses were performed on MATLAB 2018a (MathWorks, Natick, MA, United States). The mean RT of the correct trials of each block in RRTT or SRTT was calculated. Accuracy was not considered a primary measure because of the ceiling effect (**Supplementary Figure 3**). Because the calculation of behavior measures needed to integrate the RT of different blocks, any session containing RT of any block beyond 2SD from all participants' mean RT was removed. The mean RT of all blocks was considered the behavior measure in the RRTT experiment. Motor learning performance (first implicit learning, FIL, Eq. 1; second implicit learning, SIL, Eq. 2) was measured as the RT reduction between S blocks and R blocks in the SRTT experiment.

$$\mathrm{FIL} = RT_{R1} - (RT_{S1} + RT_{S2} + RT_{S3} + RT_{S4})/4 \quad (1)$$

$$\mathrm{SIL} = RT_{R2} - (RT_{S5} + RT_{S6})/2 \quad (2)$$

IO curves linearly fitted using the amplitude of MEPs elicited by 100, 110, 120, 130, and 140% RMT were involved in each stimulation condition in the RRTT experiment, and the slope of the IO curve was extracted. Mean MEP amplitudes before and after TI stimulation in each condition were calculated in the SRTT experiment.

Differences in the behavior measures between the stimulation conditions and the control condition (20 Hz vs. sham, 70 Hz vs. sham) were assessed by two-tailed paired *t*-tests. Two 2 (condition: 20 Hz vs. sham/70 Hz vs. sham) × 2 (testing time: before TI stimulation vs. after TI stimulation) repeated measures ANOVA was performed on the slopes of the IO curve and MEP amplitudes. We set age, education level and handedness score as covariables to control their potential influence to the motor cortex excitability (Eisen et al., 1991; De Gennaro et al., 2004; Thomas, 2012). Since there were significant promoting effects found in the behavior measures, slopes of the IO curve and MEP amplitude before and after TI stimulation were compared by one-tailed paired *t*-tests with the hypothesis that MEPs would also be facilitated by TI stimulation. Correlations between the behavior measures and increases in the IO slopes or MEP amplitudes in each condition were tested by two-tailed partial correlations, with age, education level and handedness score controlled as covariables. Bonferroni correction was used to correct for multiple comparisons.

RESULTS

Temporal Interference Stimulation at 70 Hz Promoted the Reaction Time and M1 Excitability

In the RRTT experiment, the stimulation condition of 70 Hz showed the lowest mean RT, which was significantly different from the sham condition ($t = -2.953$, $p_{corrected} = 0.019$, Cohen's $d = 0.716$) (**Figure 3A**). There was no significant difference in the comparison between the 20 Hz and sham groups ($t = -1.199$, $p_{corrected} = 0.498$).

For the slope of the IO curve, we found no significant results either in the main effects of condition or the main effects of testing time or the interaction of the comparison between 70 and 20 Hz with sham (all $ps > 0.05$). Paired *t*-tests revealed a significant increase in the IO slope after TI stimulation at 70 Hz (70 Hz: $t = 2.395$, $p_{corrected} = 0.040$, Cohen's $d = 0.523$, one-tailed) but not at 20 Hz or in the sham condition (20 Hz: $t = -1.075$, $p_{corrected} = 0.443$, one-tailed; sham: $t = 1.597$, $p_{corrected} = 0.189$, one-tailed) (**Figure 3B**).

Temporal Interference Stimulation at 20 Hz Improved Implicit Motor Learning and MEP Amplitude

In the SRTT experiment, TI stimulation at 20 Hz showed the highest RT reduction in FIL, which was significantly different from the sham condition, while another comparison did not show significance (20 Hz vs. sham: $t = 2.577$, $p_{corrected} = 0.041$, Cohen's $d = 0.625$; 70 Hz vs. sham: $t = 0.197$, $p_{corrected} = 1$) (**Figure 4A**). No

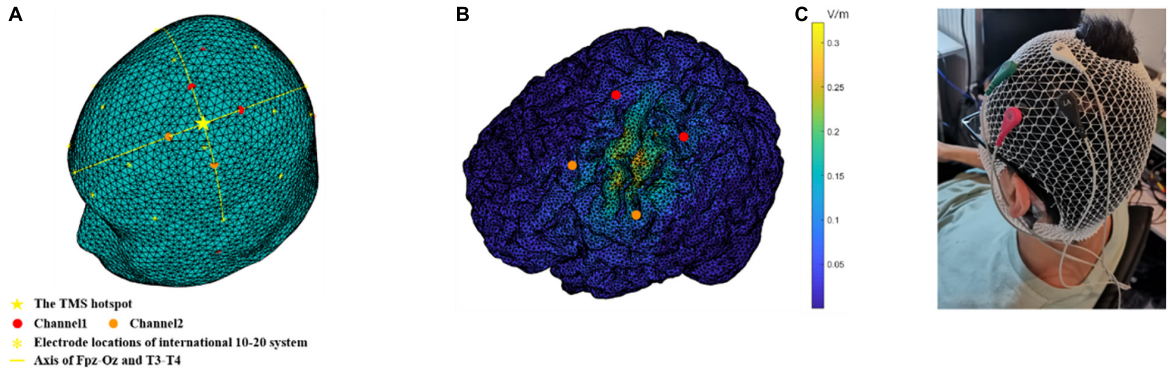

FIGURE 2 | Montage of TI stimulation and the generated electric field on a human head model. **(A)** The stimulation electrodes were located 30 mm away from the TMS hotspot, along the axis of the Fpz-Oz and T3-T4 in the EEG international 10–20 system. **(B)** The distribution of the envelope amplitude along the chosen direction (pointing posterolaterally at a 45° from the mid-line) in the brain. **(C)** An actual scene of electrode placement. The electrodes in red and green constitute channel1 and the electrodes in black and white constitute channel2. The ground electrode (brown) located on the mastoid behind the participant's left ear to avoid current accumulations due to safety considerations.

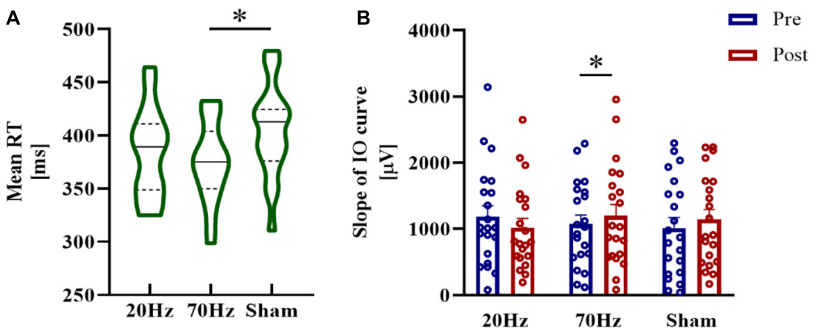

FIGURE 3 | Results of the RRTT experiment. **(A)** The mean RT of the 70 Hz condition was significantly smaller than that of the sham condition. **(B)** Significant increases in the IO slope after TI stimulation were found only in the 70 Hz condition. Error bars represent SEM; *significant at $p_{corrected} < 0.05$.

significant differences were found in SIL between the stimulation conditions and sham conditions (20 Hz vs. sham: $t = 0.5116$, $p_{corrected} = 1$; 70 Hz vs. sham: $t = 1.5716$, $p_{corrected} = 0.269$).

For MEP amplitude, when comparing the 20 Hz condition and sham condition, repeated measures analysis of variance (ANOVA) revealed a significant main effect of testing time ($F = 4.230$, $p = 0.050$, $\eta^2 = 0.145$), while the main effect of condition ($F = 1.463$, $p = 0.238$) and the interaction ($F = 0.345$, $p = 0.563$) were not significant. There was also a significant main effect of testing time ($F = 6.523$, $p = 0.017$, $\eta^2 = 0.207$) in the comparison between 70 Hz and sham, and no significant result was found in the main effect of condition ($F = 2.028$, $p = 0.167$) or in the interaction ($F = 0.942$, $p = 0.341$). MEP amplitudes increased after 20 Hz TI stimulation compared with MEP measured before stimulation at a marginally significant level ($t = 2.137$, $p_{corrected} = 0.062$, Cohen's $d = 0.397$, one-tailed) (**Figure 4B**). The increase in MEP amplitudes in the 70 Hz and sham conditions was not significant (70 Hz: $t = 1.570$, $p_{corrected} = 0.192$; sham: $t = 1.254$, $p_{corrected} = 0.330$).

The significant reduction in RT during FIL in the 20 Hz condition was positively correlated with the MEP increase ($r = 0.580$, $p_{corrected} = 0.027$) (**Figure 4C**), while RT reductions in the other two conditions showed no significant correlations with the MEP increase (70 Hz: $r = 0.073$, $p_{corrected} = 1$; sham: $r = -0.360$, $p_{corrected} = 0.426$).

Temporal Interference Stimulation Caused Minor Side Effects on Participants

Side effects occurring during TI stimulation were minor and tolerable according to the participants' descriptions and our observations. In the RRTT experiment, there were 2 sessions that participants reported moderate and larger discomforts (2.38% in active sessions (20 and 70 Hz), 4.76% in sham sessions, $\chi^2 = 0.258$, $p = 0.611$). While in the SRTT experiment, there were 4 sessions that participants reported moderate and larger discomforts (5.17% in active sessions, 3.45% in sham sessions, $\chi^2 = 0.131$, $p = 0.717$). More details are given in **Tables 1**, **2**. Notably, all discomforts during the sham sessions occurred in the middle of the session or at the end of the session, which could imply that sham stimulation did not directly cause the sensations. Our subsequent investigations of the participants also reported no other side effects after the experiments.

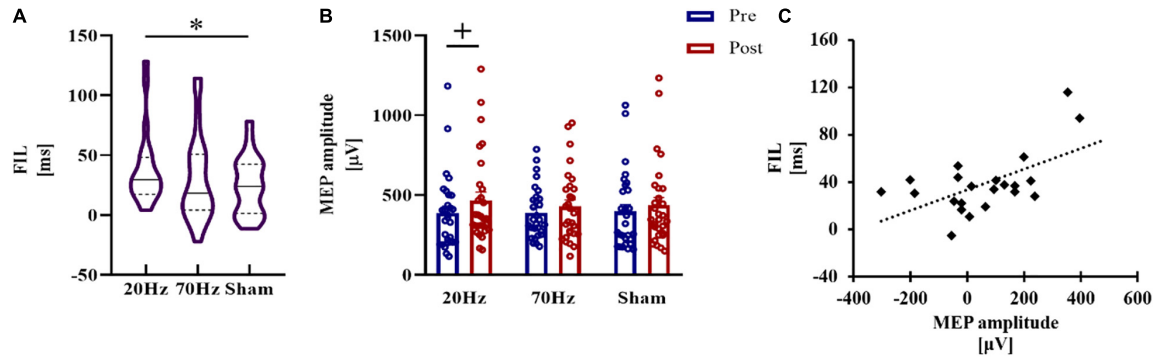

FIGURE 4 | Results of the SRTT experiment. **(A)** Implicit motor learning during FIL in SRTT. A significant RT reduction was only obtained in the 20 Hz condition. **(B)** Marginally significant increases in MEP amplitude after TI stimulation at 20 Hz. **(C)** RT reduction of FIL and the MEP increase in the 20 Hz condition was significantly positively correlated in the 20 Hz condition. Error bars represent SEM; + marginally significant at $0.05 < p_{corrected} < 0.1$, *significant at $p_{corrected} < 0.05$.

DISCUSSION

In this study, we applied TI stimulation to healthy human participants to explore the modulatory effects of TI stimulation. We investigated the changes in motor performance resulting from TI stimulation applied over M1 in two experiments involving different motor tasks. TI stimulation with an envelope frequency of 70 Hz promoted the RT performance of the motor task compared with the sham condition in the RRTT experiment. TI stimulation with an envelope frequency of 20 Hz applied over M1 enhanced the FIL performance compared with sham stimulation, and the performance was positively correlated with the MEP increase in the SRTT experiment.

Temporal Interference Stimulation Is Effective in the Human Motor Cortex

Our study, for the first time, suggests that the idea of TI stimulation is plausible, not only in computational models and experiments on mice (Grossman et al., 2017; Fariba et al., 2019; Huang and Parra, 2019; Rampersad et al., 2019; Huang et al., 2020; Lee et al., 2020), but also in actual experiments performed on healthy human participants. Since the idea of TI stimulation has been raised, the only *in vivo* investigations have been performed on mouse brains (Grossman et al., 2017). The human brain is much larger, and the layers around the brain in humans are thicker, which causes up to 100 times weaker electric fields in the human brain than in the mouse brain at the same stimulation intensity (Alekseichuk et al., 2019). The stimulation waveform of TI stimulation is an envelope-modulated waveform produced by the superposition of two sine waves, which has not been previously tested on humans. Envelope-tACS using only envelope waveforms of speech without carrier waves have been used to improve speech perception and processing (Riecke et al., 2018; Wilsch et al., 2018; Kadir et al., 2020), but the effects are still controversial (Asamoah et al., 2019; Erkens et al., 2020; Kosem et al., 2020). Amplitude-modulated tACS (AM-tACS) was proposed as a promising way to allow for effective magnetoencephalography (MEG) or EEG signal reconstruction during electrical stimulation (Witkowski et al., 2016; Kasten et al., 2018; Negahbani et al., 2018; Haslacher et al., 2021). However, similar to TI stimulation, studies on AM-tACS have also mostly focused on simulations, and no systematic experimental test to validate the effectiveness of AM-tACS on humans has been performed. Whether envelope modulated waveforms have comparable effects to conventional tACS is unknown.

To solve these problems, we applied TI stimulation to the human M1 area and found some significant effects. In the RRTT experiment, only 70 Hz TI stimulation promoted RT performance and motor cortical excitability. In the SRTT experiment, only 20 Hz TI stimulation increased the first implicit motor learning and MEP amplitudes. We found significant main effects of testing time in the analysis of MEP amplitude, which might indicate a training effect of the motor learning task (Classen et al., 1998; Fattinger et al., 2017). But only the correlation between FIL and MEP increase in 20 Hz condition was significant, indicating the increase of motor cortex excitability related with TI stimulation only occurred in 20 Hz TI stimulation. This can be supported by a meta-analysis, which shows that exogenously applied electric fields in beta frequency range can increase motor cortex excitability (Wischnewski et al., 2019). The time delay between the end of TI stimulation and the following MEP measurement was about 5–10 min, within the time window of the aftereffect

TABLE 1 | Discomforts in RRTT.

Sensations	Active sessions (N/42)	Sham sessions (N/21)
None	41	20
Fatigue and Vertigo	0	1
Headache	1	0

TABLE 2 | Discomforts in SRTT.

Sensations	Active sessions (N/58)	Sham sessions (N/29)
None	55	28
Fatigue	3	1

of conventional tES (Kuo et al., 2013; Kasten et al., 2016). Future studies could explore the duration of the aftereffect with parameterized time intervals between the end of the TI stimulation and the following measurements.

However, the effect of TI stimulation shown in this study is not as phenomenal as that in the mice study. Future studies could explore the mechanisms of TI stimulation at the level of brain regions and networks by corresponding neuroimaging techniques, e.g., functional magnetic resonance imaging (fMRI), and try to build a more effective TI stimulation system for human with a better understanding of it.

High Gamma and Beta Oscillations May Represent Different Motor Functions in M1

Distinct effects of 20 and 70 Hz TI stimulation may indicate different functions of these two motor cortical oscillations. High gamma and beta are considered vital neural rhythms corresponding to the activation of M1 (Cheyne et al., 2008; Muthukumaraswamy, 2010; Gaetz et al., 2013; Espenhahn et al., 2019, 2020; Haar and Faisal, 2020). TACS (70 Hz) has been reported to increase motor velocity and motor acceleration during stimulation in visually guided motor tasks (Joundi et al., 2012; Moisa et al., 2016). Meanwhile, tACS at 20 Hz has been reported to improve the performance of implicit learning of SRTT in previous studies (Pollok et al., 2015; Krause et al., 2016). These findings could imply that beta and high-gamma neural rhythms predominate in different motor functions in M1. Our results duplicate the functional separation between brain oscillations at 20 and 70 Hz. The functional separation between 70 Hz (2,000 and 2,070 Hz) and 20 Hz (2,000 and 2,020 Hz) TI stimulation also supports the hypothesis that electric fields of high-frequency carriers (2,000 Hz) may have little contribution to the results because of the intrinsic feature of the neural membrane that filters electrical signals in a low-pass manner (Hutcheon and Yarom, 2000; Esmaeilpour et al., 2020). Additional studies could explore the effects of carrier frequency and envelope frequency more deeply. For instance, future studies could stimulation deep brain regions and monitor if there is some influence of the stimulation on the superficial brain regions. So that whether the single high-frequency stimulation could influence the neural activity of the human brain can be explored.

The Application Potential of Temporal Interference Stimulation as a Non-invasive Brain Stimulation Technique

We assessed the side effects of TI stimulation by subjective reporting of the participants. In most sessions (>95%), participants reported no obvious side effects. No sensations related to the skin, such as tingling, itching and burning, were reported, and no burns or reddening of the skin were observed by the experimenters. Only fatigue, vertigo and headache were reported in several sessions, including two sham sessions. The side effects reported by participants in this study were far less than those reported for conventional tES (Brunoni et al., 2011; Fertonani et al., 2015; Matsumoto and Ugawa, 2017), which indicates that TI stimulation may have advantages over conventional tES in safety, user-friendliness and blinding performance.

Our study indicates that TI stimulation can be used as a new technique to modulate human neural activities in a non-invasive way. The TI stimulation was aimed to stimulate deep brain regions. However, we only explored the effects of TI stimulation on human M1 in the present study. Previous studies have suggested that to achieve effect comparable with DBS, the stimulation protocol might need to be modified to improve the stimulation strength and focality (Rampersad et al., 2019). Stimulation effects on other deeper brain regions with more sophisticated functions rely on a better understanding of the working mechanisms and prospects of TI stimulation in humans, which needs to be explored in additional research utilizing combinations of neuron models, finite element modeling simulations and experiments (Rampersad et al., 2019). There are a lot of technical problems unresolved. Therefore, before exploring the effectiveness of TI stimulation in deep brain regions, we should firstly test whether this new stimulation technique could influence human brain activity of the superficial cortex. Otherwise if TI stimulation doesn't show effects in deep brain regions, we could not explain the reason, e.g., the physical property of stimulation or other technical issues. Anyway, future studies should explore the effect of TI stimulation in deep brain regions and promote the applications of TI stimulation in clinical practice.

CONCLUSION

Our study reveals the promoting effect of TI stimulation on human motor functions and motor cortex excitability. TI stimulation with different envelope frequencies showed separate promoting effects on different motor tasks, which implied that TI stimulation may work through a low-frequency envelope. Future investigations of TI stimulation in humans could explore stimulation effects in deeper brain regions under the guidance of modeling works. In summary, TI stimulation could be a promising new technique for non-invasive brain stimulation in humans with clinical application potentials.

DATA AVAILABILITY STATEMENT

The datasets presented in this study can be found in online repositories. The names of the repository/repositories and accession number(s) can be found below: cnp.ustc.edu.cn.

ETHICS STATEMENT

The studies involving human participants were reviewed and approved by the Human Ethics Committee of the University of Science and Technology of China. The patients/participants provided their written informed consent to participate in this study.

AUTHOR CONTRIBUTIONS

RM: project administration, methodology, software, formal analysis, investigation, data curation, writing – original draft, and visualization. XX: methodology, hardware testing, formal analysis, investigation, data curation, writing – original draft, and visualization. WZ and HS: methodology, software, writing, review, and editing. ZL: methodology, hardware design and implementation, and hardware testing. QW: formal analysis, investigation, and data curation. JC: methodology, validation, and hardware testing. CF, XC, and RZ: writing, review, and editing. JW and G-JJ: methodology and techniques of TMS. XW and BQ: methodology, hardware, and supervision. XZ: conceptualization, funding acquisition, methodology, writing, review, editing, and supervision. All authors contributed to the article and approved the submitted version.

FUNDING

This work was supported by grants from the National Key Basic Research Program (2018YFC0831101), the National Natural Science Foundation of China (32171080, 31771221, 71942003, 61773360, 31800927, 31900766, and 71874170), Major Project of Philosophy and Social Science Research, Ministry of Education of China (19JZD010), CAS-VPST Silk Road Science Fund 2021 (GLHZ202128), and Collaborative Innovation Program of Hefei Science Center, CAS (2020HSC-CIP001).

ACKNOWLEDGMENTS

We would like to thank Bettina Pollok for her kindly help with programming of the experimental tasks. We would also like to thank Wei Lu for his help with circuit testing.

SUPPLEMENTARY MATERIAL

The Supplementary Material for this article can be found online at: https://www.frontiersin.org/articles/10.3389/fnins.2021.800436/full#supplementary-material

REFERENCES

Alekseichuk, I., Mantell, K., Shirinpour, S., and Opitz, A. (2019). Comparative modeling of transcranial magnetic and electric stimulation in mouse, monkey, and human. *NeuroImage* 194, 136–148. doi: 10.1016/j.neuroimage.2019.03.044

Antal, A., Boros, K., Poreisz, C., Chaieb, L., Terney, D., and Paulus, W. (2008). Comparatively weak after-effects of transcranial alternating current stimulation (tACS) on cortical excitability in humans. *Brain Stimulation* 1, 97–105. doi: 10.1016/j.brs.2007.10.001

Asamoah, B., Khatoun, A., and Mc Laughlin, M. (2019). Analytical bias accounts for some of the reported effects of tACS on auditory perception. *Brain Stimulation* 12, 1001–1009. doi: 10.1016/j.brs.2019.03.011

Barker, A. T., Jalinous, R., and Freeston, I. L. (1985). Non-invasive magnetic stimulation of human motor cortex. *Lancet* 325, 1106–1107. doi: 10.1016/s0140-6736(85)92413-4

Benabid, A. L. (2003). Deep brain stimulation for Parkinson's disease. *Curr. Opin. Neurobiol.* 13, 696–706. doi: 10.1016/j.conb.2003.11.001

Bestmann, S., and Walsh, V. (2017). Transcranial electrical stimulation. *Curr. Biol.* 27, R1258–R1262. doi: 10.1016/j.cub.2017.11.001

Boroojerdi, B., Battaglia, F., Muellbacher, W., and Cohen, L. G. (2001). Mechanisms influencing stimulus-response properties of the human corticospinal system. *Clin. Neurophysiol.* 112, 931–937. doi: 10.1016/S1388-2457(01)00523-5

Brunoni, A. R., Amadera, J., Berbel, B., Volz, M. S., Rizzerio, B. G., and Fregni, F. (2011). A systematic review on reporting and assessment of adverse effects associated with transcranial direct current stimulation. *Int. J. Neuropsychopharmacol* 14, 1133–1145. doi: 10.1017/s1461145710001690

Cao, J., and Grover, P. (2020). STIMULUS: noninvasive dynamic patterns of neurostimulation using spatio-temporal interference. *IEEE Trans. Biomed. Eng.* 67, 726–737. doi: 10.1109/TBME.2019.2919912

Chen, R. (2000). Studies of human motor physiology with transcranial magnetic stimulation. *Muscle Nerve* 23, S26–S32. doi: 10.1002/1097-45982000999:9<::AID-MUS6<3.0.CO;2-I

Cheyne, D., Bells, S., Ferrari, P., Gaetz, W., and Bostan, A. C. (2008). Self-paced movements induce high-frequency gamma oscillations in primary motor cortex. *NeuroImage* 42, 332–342. doi: 10.1016/j.neuroimage.2008.04.178

Classen, J., Liepert, J., Wise, S. P., Hallett, M., and Cohen, L. G. (1998). Rapid plasticity of human cortical movement representation induced by practice. *J. Neurophysiol.* 79, 1117–1123. doi: 10.1152/jn.1998.79.2.1117

Curran, T. (1997). Higher-order associative learning in amnesia: evidence from the serial reaction time task. *J. Cogn. Neurosci.* 9, 522–533. doi: 10.1162/jocn.1997.9.4.522

De Gennaro, L., Cristiani, R., Bertini, M., Curcio, G., Ferrara, M., Fratello, F., et al. (2004). Handedness is mainly associated with an asymmetry of corticospinal excitability and not of transcallosal inhibition. *Clin. Neurophysiol.* 115, 1305–1312. doi: 10.1016/j.clinph.2004.01.014

Dmochowski, J. P., Koessler, L., Norcia, A. M., Bikson, M., and Parra, L. C. (2017). Optimal use of EEG recordings to target active brain areas with transcranial electrical stimulation. *NeuroImage* 157, 69–80. doi: 10.1016/j.neuroimage.2017.05.059

Doty, R. W. (1969). Electrical stimulation of the brain in behavioral context. *Ann. Rev. Psychol.* 20, 289–320. doi: 10.1146/annurev.ps.20.020169.001445

Eisen, A., Siejka, S., Schulzer, M., and Calne, D. (1991). Age-dependent decline in motor evoked potential (MEP) amplitude: with a comment on changes in Parkinson's disease. *Electroencephalogr. Clin. Neurophysiol. Evoked Potentials Section* 81, 209–215. doi: 10.1016/0168-5597(91)90074-8

Erkens, J., Schulte, M., Vormann, M., and Herrmann, C. S. (2020). Lacking effects of envelope transcranial alternating current stimulation indicate the need to revise envelope transcranial alternating current stimulation methods. *Neurosci. Insights* 15:2633105520936623. doi: 10.1177/2633105520936623

Esmaeilpour, Z., Jackson, M., Kronberg, G., Zhang, T., Esteller, R., Hershey, B., et al. (2020). Limited sensitivity of hippocampal synaptic function or network oscillations to unmodulated kilohertz electric fields. *eNeuro* 7:ENEURO.0368-0320.2020. doi: 10.1523/ENEURO.0368-20.2020

Espenhahn, S., Rossiter, H. E., van Wijk, B. C. M., Redman, N., Rondina, J. M., Diedrichsen, J., et al. (2020). Sensorimotor cortex beta oscillations reflect motor skill learning ability after stroke. *Brain Commun.* 2:fcaa161. doi: 10.1093/braincomms/fcaa161

Espenhahn, S., van Wijk, B. C. M., Rossiter, H. E., de Berker, A. O., Redman, N. D., Rondina, J., et al. (2019). Cortical beta oscillations are associated with motor performance following visuomotor learning. *NeuroImage* 195, 340–353. doi: 10.1016/j.neuroimage.2019.03.079

Fariba, K., Ahmadreza, A., Rassoul, A., and Abolghasem Zeidaabadi, N. (2019). Computational analysis of non-invasive deep brain stimulation based on interfering electric fields. *Physics Med. Biol.* 64:235010. doi: 10.1088/1361-6560/ab5229

Fattinger, S., de Beukelaar, T. T., Ruddy, K. L., Volk, C., Heyse, N. C., Herbst, J. A., et al. (2017). Deep sleep maintains learning efficiency of the human brain. *Nat. Commun.* 8:15405. doi: 10.1038/ncomms15405

Faul, F., Erdfelder, E., Buchner, A., and Lang, A.-G. (2009). Statistical power analyses using G* power 3.1: tests for correlation and regression analyses. *Behav. Res. Methods* 41, 1149–1160. doi: 10.3758/BRM.41.4.1149

Fertonani, A., Ferrari, C., and Miniussi, C. (2015). What do you feel if i apply transcranial electric stimulation? Safety, sensations and secondary induced effects. *Clin. Neurophysiol.* 126, 2181–2188. doi: 10.1016/j.clinph.2015.03.015

Feurra, M., Bianco, G., Santarnecchi, E., Del Testa, M., Rossi, A., and Rossi, S. (2011). Frequency-dependent tuning of the human motor system induced by transcranial oscillatory potentials. *J. Neurosci.* 31, 12165–12170. doi: 10.1523/jneurosci.0978-11.2011

Feurra, M., Pasqualetti, P., Bianco, G., Santarnecchi, E., Rossi, A., and Rossi, S. (2013). State-dependent effects of transcranial oscillatory currents on the motor system: what you think matters. *J. Neurosci.* 33, 17483–17489. doi: 10.1523/jneurosci.1414-13.2013

Gaetz, W., Liu, C., Zhu, H., Bloy, L., and Roberts, T. P. L. (2013). Evidence for a motor gamma-band network governing response interference. *NeuroImage* 74, 245–253. doi: 10.1016/j.neuroimage.2013.02.013

Grossman, N. (2018). Modulation without surgical intervention Noninvasive deep brain stimulation can be achieved via temporally interfering electric fields. *Science* 361, 461–462. doi: 10.1126/science.aau4915

Grossman, N., Bono, D., Dedic, N., Kodandaramaiah, S. B., Rudenko, A., Suk, H.-J., et al. (2017). Noninvasive deep brain stimulation via temporally interfering electric fields. *Cell* 169, 1029–1041.e1016. doi: 10.1016/j.cell.2017.05.024

Grossman, N., Okun, M. S., and Boyden, E. S. (2018). Translating temporal interference brain stimulation to treat neurological and psychiatric conditions. *JAMA Neurol.* 75, 1307–1308. doi: 10.1001/jamaneurol.2018.2760

Guerra, A., Asci, F., D'Onofrio, V., Sveva, V., Bologna, M., Fabbrini, G., et al. (2020). Enhancing gamma oscillations restores primary motor cortex plasticity in Parkinson's disease. *J. Neurosci.* 40, 4788–4796. doi: 10.1523/jneurosci.0357-20.2020

Haar, S., and Faisal, A. A. (2020). Brain activity reveals multiple motor-learning mechanisms in a real-world task. *Front. Hum. Neurosci.* 14:354. doi: 10.3389/fnhum.2020.00354

Halpern, C. H., Miller, K. J., Wu, H., and Tass, P. A. (2018). Letter: electric beats open new frontiers for deep brain stimulation. *Neurosurgery* 82, E19–E20. doi: 10.1093/neuros/nyx482

Haslacher, D., Nasr, K., Robinson, S. E., Braun, C., and Soekadar, S. R. (2021). Stimulation artifact source separation (SASS) for assessing electric brain oscillations during transcranial alternating current stimulation (tACS). *Neuroimage* 228:117571. doi: 10.1016/j.neuroimage.2020.117571

Herrmann, C. S., Rach, S., Neuling, T., and Strueber, D. (2013). Transcranial alternating current stimulation: a review of the underlying mechanisms and modulation of cognitive processes. *Front. Hum. Neurosci.* 7:279. doi: 10.3389/fnhum.2013.00279

Huang, Y., Datta, A., and Parra, L. C. (2020). Optimization of interferential stimulation of the human brain with electrode arrays. *J. Neural Eng.* 17:036023. doi: 10.1088/1741-2552/ab92b3

Huang, Y., and Parra, L. C. (2019). Can transcranial electric stimulation with multiple electrodes reach deep targets? *Brain Stimul.* 12, 30–40. doi: 10.1016/j.brs.2018.09.010

Hutcheon, B., and Yarom, Y. (2000). Resonance, oscillation and the intrinsic frequency preferences of neurons. *Trends Neurosci.* 23, 216–222. doi: 10.1016/S0166-2236(00)01547-2

Joundi, R. A., Jenkinson, N., Brittain, J. S., Aziz, T. Z., and Brown, P. (2012). Driving oscillatory activity in the human cortex enhances motor performance. *Curr. Biol.* 22, 403–407. doi: 10.1016/j.cub.2012.01.024

Kadir, S., Kaza, C., Weissbart, H., and Reichenbach, T. (2020). Modulation of speech-in-noise comprehension through transcranial current stimulation with the phase-shifted speech envelope. *IEEE Trans. Neural. Syst. Rehabil. Eng.* 28, 23–31. doi: 10.1109/tnsre.2019.2939671

Kasten, F. H., Dowsett, J., and Herrmann, C. S. (2016). Sustained aftereffect of alpha-tACS lasts up to 70 min after stimulation. *Front. Hum. Neurosci.* 10:245. doi: 10.3389/fnhum.2016.00245

Kasten, F. H., Negahbani, E., Frohlich, F., and Herrmann, C. S. (2018). Non-linear transfer characteristics of stimulation and recording hardware account for spurious low-frequency artifacts during amplitude modulated transcranial alternating current stimulation (AM-tACS). *NeuroImage* 179, 134–143. doi: 10.1016/j.neuroimage.2018.05.068

Keeser, D., Meindl, T., Bor, J., Palm, U., Pogarell, O., Mulert, C., et al. (2011). Prefrontal transcranial direct current stimulation changes connectivity of resting-state networks during fMRI. *J. Neurosci.* 31, 15284–15293. doi: 10.1523/jneurosci.0542-11.2011

Kleim, J. A., Kleim, E. D., and Cramer, S. C. (2007). Systematic assessment of training-induced changes in corticospinal output to hand using frameless stereotaxic transcranial magnetic stimulation. *Nat. Protoc.* 2, 1675–1684. doi: 10.1038/nprot.2007.206

Kosem, A., Bosker, H. R., Jensen, O., Hagoort, P., and Riecke, L. (2020). Biasing the perception of spoken words with transcranial alternating current stimulation. *J. Cogn. Neurosci.* 32, 1428–1437. doi: 10.1162/jocn_a_01579

Krause, V., Meier, A., Dinkelbach, L., and Pollok, B. (2016). Beta band transcranial alternating (tACS) and direct current stimulation (tDCS) applied after initial learning facilitate retrieval of a motor sequence. *Front. Behav. Neurosci.* 10:4. doi: 10.3389/fnbeh.2016.00004

Kuo, H.-I., Bikson, M., Datta, A., Minhas, P., Paulus, W., Kuo, M.-F., et al. (2013). Comparing cortical plasticity induced by conventional and high-definition 4 x 1 ring tDCS: a neurophysiological study. *Brain Stimul.* 6, 644–648. doi: 10.1016/j.brs.2012.09.010

Lafon, B., Henin, S., Huang, Y., Friedman, D., Melloni, L., Thesen, T., et al. (2017). Low frequency transcranial electrical stimulation does not entrain sleep rhythms measured by human intracranial recordings. *Nat. Commun.* 8:1199. doi: 10.1038/s41467-017-01045-x

Lee, S., Lee, C., Park, J., and Im, C.-H. (2020). Individually customized transcranial temporal interference stimulation for focused modulation of deep brain structures: a simulation study with different head models. *Sci. Rep.* 10:11730. doi: 10.1038/s41598-020-68660-5

Liu, A., Voroslakos, M., Kronberg, G., Henin, S., Krause, M. R., Huang, Y., et al. (2018). Immediate neurophysiological effects of transcranial electrical stimulation. *Nat. Commun.* 9:5092. doi: 10.1038/s41467-018-07233-7

Louviot, S., Tyvaert, L., Maillard, L. G., Colnat-Coulbois, S., Dmochowski, J., and Koessler, L. (2021). Transcranial electrical stimulation generates electric fields in deep human brain structures. *Brain Stimul.* 15, 1–12. doi: 10.1016/j.brs.2021.11.001

Lozano, A. M. (2017). Waving hello to noninvasive deep-brain stimulation. *New Eng. J. Med.* 377, 1096–1098. doi: 10.1056/NEJMcibr1707165

Matsumoto, H., and Ugawa, Y. (2017). Adverse events of tDCS and tACS: a review. *Clin. Neurophysiol. Practice* 2, 19–25. doi: 10.1016/j.cnp.2016.12.003

Mirzakhalili, E., Barra, B., Capogrosso, M., and Lempka, S. F. (2020). Biophysics of temporal interference stimulation. *Cell Syst.* 11, 557–572.e5. doi: 10.1016/j.cels.2020.10.004

Moisa, M., Polania, R., Grueschow, M., and Ruff, C. C. (2016). Brain network mechanisms underlying motor enhancement by transcranial entrainment of gamma oscillations. *J. Neurosci.* 36:12053. doi: 10.1523/JNEUROSCI.2044-16.2016

Moliadze, V., Antal, A., and Paulus, W. (2010). Boosting brain excitability by transcranial high frequency stimulation in the ripple range. *J. Physiol. London* 588, 4891–4904. doi: 10.1113/jphysiol.2010.196998

Muthukumaraswamy, S. D. (2010). Functional properties of human primary motor cortex gamma oscillations. *J. Neurophysiol.* 104, 2873–2885. doi: 10.1152/jn.00607.2010

Negahbani, E., Kasten, F. H., Herrmann, C. S., and Fröhlich, F. (2018). Targeting alpha-band oscillations in a cortical model with amplitude-modulated high-frequency transcranial electric stimulation. *Neuroimage* 173, 3–12. doi: 10.1016/j.neuroimage.2018.02.005

Oldfield, R. C. (1971). The assessment and analysis of handedness: the Edinburgh inventory. *Neuropsychologia* 9, 97–113. doi: 10.1016/0028-3932(71)90067-4

Opitz, A., Legon, W., Rowlands, A., Bickel, W. K., Paulus, W., and Tyler, W. J. (2013). Physiological observations validate finite element models for estimating subject-specific electric field distributions induced by transcranial magnetic stimulation of the human motor cortex. *NeuroImage* 81, 253–264. doi: 10.1016/j.neuroimage.2013.04.067

Opitz, A., and Tyler, W. J. (2017). No implant needed. *Nat. Biomed. Eng.* 1, 632–633. doi: 10.1038/s41551-017-0120-y

Paulus, W. (2011). Transcranial electrical stimulation (tES - tDCS; tRNS, tACS) methods. *Neuropsychol. Rehabil.* 21, 602–617. doi: 10.1080/09602011.2011.557292

Pollok, B., Boysen, A.-C., and Krause, V. (2015). The effect of transcranial alternating current stimulation (tACS) at alpha and beta frequency on motor learning. *Behav. Brain Res.* 293, 234–240. doi: 10.1016/j.bbr.2015.07.049

Priori, A., Berardelli, A., Rona, S., Accornero, N., and Manfredi, M. (1998). Polarization of the human motor cortex through the scalp. *Neuroreport* 9, 2257–2260. doi: 10.1097/00001756-199807130-00020

Raco, V., Bauer, R., Norim, S., and Gharabaghi, A. (2017). Cumulative effects of single TMS pulses during beta-tACS are stimulation intensity-dependent. *Brain Stimul.* 10, 1055–1060. doi: 10.1016/j.brs.2017.07.009

Ramirez-Zamora, A., Giordano, J. J., Gunduz, A., Brown, P., Sanchez, J. C., Foote, K. D., et al. (2018). Evolving applications, technological challenges and future opportunities in neuromodulation: proceedings of the fifth annual deep brain stimulation think tank. *Front. Neurosci.* 11:734. doi: 10.3389/fnins.2017.00734

Rampersad, S., Roig-Solvas, B., Yarossi, M., Kulkarni, P. P., Santarnecchi, E., Dorval, A. D., et al. (2019). Prospects for transcranial temporal interference stimulation in humans: a computational study. *NeuroImage* 202:116124. doi: 10.1016/j.neuroimage.2019.116124

Riecke, L., Formisano, E., Sorger, B., Başkent, D., and Gaudrain, E. (2018).). Neural entrainment to speech modulates speech intelligibility. *Curr. Biol.* 28, 161–169.e165. doi: 10.1016/j.cub.2017.11.033

Robertson, E. M. (2007). The serial reaction time task: implicit motor skill learning? *J. Neurosci.* 27:10073. doi: 10.1523/JNEUROSCI.2747-07.2007

Rossini, P. M., Burke, D., Chen, R., Cohen, L. G., Daskalakis, Z., Di Iorio, R., et al. (2015). Non-invasive electrical and magnetic stimulation of the brain, spinal cord, roots and peripheral nerves: basic principles and procedures for routine clinical and research application. an updated report from an I.F.C.N. committee. *Clin. Neurophysiol.* 126, 1071–1107. doi: 10.1016/j.clinph.2015.02.001

Sakai, K., Ugawa, Y., Terao, Y., Hanajima, R., Furubayashi, T., and Kanazawa, I. (1997). Preferential activation of different I waves by transcranial magnetic stimulation with a figure-of-eight-shaped coil. *Exp. Brain Res.* 113, 24–32. doi: 10.1007/BF02454139

Schendan, H. E., Searl, M. M., Melrose, R. J., and Stern, C. E. (2003). An FMRI study of the role of the medial temporal lobe in implicit and explicit sequence learning. *Neuron* 37, 1013–1025. doi: 10.1016/s0896-6273(03)00123-5

Terney, D., Chaieb, L., Moliadze, V., Antal, A., and Paulus, W. (2008). Increasing human brain excitability by transcranial high-frequency random noise stimulation. *J. Neurosci.* 28, 14147–14155. doi: 10.1523/JNEUROSCI.4248-08.2008

Thomas, M. S. (2012). "Brain plasticity and education," in *BJEP Monograph Series II, Number 8-Educational Neuroscience*, eds D. B. Berch, D. C. Geary, and K. M. Koepke 143–156.

Tinkhauser, G., Pogosyan, A., Little, S., Beudel, M., Herz, D. M., Tan, H., et al. (2017). The modulatory effect of adaptive deep brain stimulation on beta bursts in Parkinson's disease. *Brain* 140, 1053–1067. doi: 10.1093/brain/awx010

Vöröslakos, M., Takeuchi, Y., Brinyiczki, K., Zombori, T., Oliva, A., Fernández-Ruiz, A., et al. (2018). Direct effects of transcranial electric stimulation on brain circuits in rats and humans. *Nat. Commun.* 9:483. doi: 10.1038/s41467-018-02928-3

Vossen, A., Gross, J., and Thut, G. (2015). Alpha power increase after transcranial alternating current stimulation at alpha frequency (alpha-tACS) reflects plastic changes rather than entrainment. *Brain Stimul.* 8, 499–508. doi: 10.1016/j.brs.2014.12.004

Wilsch, A., Neuling, T., Obleser, J., and Herrmann, C. S. (2018). Transcranial alternating current stimulation with speech envelopes modulates speech comprehension. *Neuroimage* 172, 766–774. doi: 10.1016/j.neuroimage.2018.01.038

Wischnewski, M., Schutter, D. J. L. G., and Nitsche, M. A. (2019). Effects of beta-tACS on corticospinal excitability: a meta-analysis. *Brain Stimul.* 12, 1381–1389. doi: 10.1016/j.brs.2019.07.023

Witkowski, M., Garcia-Cossio, E., Chander, B. S., Braun, C., Birbaumer, N., Robinson, S. E., et al. (2016). Mapping entrained brain oscillations during transcranial alternating current stimulation (tACS). *Neuroimage* 140, 89–98. doi: 10.1016/j.neuroimage.2015.10.024

Yang, L. Z., Shi, B., Li, H., Zhang, W., Liu, Y., Wang, H. Z., et al. (2017). Electrical stimulation reduces smokers' craving by modulating the coupling between dorsal lateral prefrontal cortex and parahippocampal gyrus. *Social Cogn. Affect. Neurosci.* 12, 1296–1302. doi: 10.1093/scan/nsx055

Yang, L. Z., Zhang, W., Shi, B., Yang, Z. Y., Wei, Z. D., Gu, F., et al. (2014). Electrical stimulation over bilateral occipito-temporal regions reduces N170 in the right hemisphere and the composite face effect. *PLoS One* 9:e115772. doi: 10.1371/journal.pone.0115772

Yang, L. Z., Zhang, W., Wang, W. J., Yang, Z. Y., Wang, H. Z., Deng, Z. D., et al. (2020). Neural and psychological predictors of cognitive enhancement and impairment from neurostimulation. *Adv. Sci.* 7:1902863. doi: 10.1002/advs.201902863

Conflict of Interest: The authors declare that the research was conducted in the absence of any commercial or financial relationships that could be construed as a potential conflict of interest.

Publisher's Note: All claims expressed in this article are solely those of the authors and do not necessarily represent those of their affiliated organizations, or those of the publisher, the editors and the reviewers. Any product that may be evaluated in this article, or claim that may be made by its manufacturer, is not guaranteed or endorsed by the publisher.

frontiers in Psychiatry

ORIGINAL RESEARCH
published: 14 January 2022
doi: 10.3389/fpsyt.2021.797898

Family Conflict Associated With Intrinsic Hippocampal-OFC Connectivity in Adolescent Depressive Disorder

Ruohan Feng[1,2†], Weijie Bao[1†], Lihua Zhuo[2†], Yingxue Gao[1], Hongchao Yao[2], Yang Li[3], Lijun Liang[3], Kaili Liang[1], Ming Zhou[2], Lianqing Zhang[1], Guoping Huang[3] and Xiaoqi Huang[1,4]*

[1] Department of Radiology, Huaxi Magnetic Resonance Research Center, Functional and Molecular Imaging Key Laboratory of Sichuan Province, West China Hospital, Sichuan University, Chengdu, China, [2] Department of Radiology, Sichuan Mental Health Center, The Third Hospital of Mianyang, Mianyang, China, [3] Department of Psychiatry, Sichuan Mental Health Center, The Third Hospital of Mianyang, Mianyang, China, [4] Research Unit of Psychoradiology, Chinese Academy of Medical Sciences, Chengdu, China

OPEN ACCESS

Edited by:
Jiaojian Wang,
University of Electronic Science and Technology of China, China

Reviewed by:
Chao Wang,
Shenzhen University, China
Minghao Dong,
Xidian University, China

***Correspondence:**
Xiaoqi Huang
julianahuang@163.com

[†] These authors have contributed equally to this work

Specialty section:
This article was submitted to Neuroimaging and Stimulation, a section of the journal Frontiers in Psychiatry

Received: 19 October 2021
Accepted: 30 November 2021
Published: 14 January 2022

Citation:
Feng R, Bao W, Zhuo L, Gao Y, Yao H, Li Y, Liang L, Liang K, Zhou M, Zhang L, Huang G and Huang X (2022) Family Conflict Associated With Intrinsic Hippocampal-OFC Connectivity in Adolescent Depressive Disorder. Front. Psychiatry 12:797898. doi: 10.3389/fpsyt.2021.797898

Background: Family environment and life events have long been suggested to be associated with adolescent depression. The hippocampus plays a crucial role in the neural mechanism of major depressive disorder (MDD) through memory during stressful events. However, few studies have explored the exact neural mechanisms underlying these associations. Thus, the current study aimed to explore alterations in hippocampal functional connectivity (FC) in adolescent MDD based on resting-state functional magnetic resonance imaging and further investigate the relationship between hippocampal FC, environmental factors, and clinical symptom severity.

Methods: Hippocampal FC was calculated using the seed-based approach with the bilateral hippocampus as the seed for 111 adolescents with and without MDD; comparisons were made between participants with MDD and controls. We applied the Chinese version of the Family Environment Scale (FES-CV) and Adolescents Self-Rating Life Events Checklist (ASLEC) to evaluate family environment and life stress. Their relationship with hippocampal FC alterations was also investigated.

Results: We found that compared to controls, adolescents with MDD showed decreased connectivity between the left hippocampus and bilateral orbital frontal cortex (OFC) and right inferior temporal gyrus. In addition, the hippocampal-OFC connectivity was negatively correlated with conflict scores of the FES-CV in the MDD group and mediated the association between family conflict and depressive and anxiety symptoms.

Conclusion: Our findings are novel in the field and demonstrate how family conflict contributes to MDD symptomatology through hippocampal-OFC connectivity; these findings may provide potential targets for personalized treatment strategies.

Keywords: major depressive disorder, functional connectivity, hippocampus, adolescent, family conflict

INTRODUCTION

Adolescence is a critical period of brain development and neurological and cognitive maturation (1) and is regarded as a time of "storm and stress" (2). The brain is more susceptible to the effects of environmental stress at this particular stage (3, 4). There is a notable incidence of major depressive disorder (MDD) during adolescence, which may lead to chronicity throughout life with high recurrence rates (5, 6). MDD leads to serious social and educational impairments and is closely associated with suicide (7). The developmental trajectory of depression appears to start with some environmental risk factors, such as early-life adversities, and occurs as a result of abnormalities in the brain (8).

Family environment and life stress events are both risk factors for adolescent MDD (9–12) and may also affect brain development structurally and functionally (13–15), particularly the hippocampus (16–18). For example, smaller hippocampal volume partially mediated the effect of early-life adversity on depressive episodes from a longitudinal study (19). The hippocampal network can modulate the feeling of stress (20) and play an important role in memory (21, 22). And stress can influence memory performance through hippocampal functional connectivity (FC) on a systems level (23). In recent years, several studies explored the resting-state FC (RSFC) alterations in adult MDD with bilateral hippocampus and hippocampal subfields as selected seeds, showing a significantly decreased RSFC between the bilateral hippocampal and prefrontal regions, insula, bilateral limbic system, subcortical areas, temporal lobe, and cerebellum (24–31).

Although many studies have detected altered hippocampal FC in adult MDD, only two studies with small sample sizes have investigated hippocampal FC changes in adolescent MDD. One study reported decreased intrinsic connectivity between the right hippocampus and the right insula and right middle frontal gyrus (32) in adolescents with depression comorbid with obsessive-compulsive disorder and other anxiety disorders. Another study showed significant hypoconnectivity between the bilateral hippocampus and prefrontal cortex (PFC) regions based on the region of interest (ROI)-to-ROI technique and excluded the exploration of hippocampal connectivity in other brain regions (33). However, no study has explored the relationship between hippocampal FC and stress events and depressive symptoms.

Thus, in the current study, we aimed to investigate the alteration of hippocampal FC on the whole brain base and further explore its relationship with family environment and life events in adolescent MDD by recruiting a relatively large sample of drug-naïve patients with no comorbidities to exclude the confounding effects of medication and comorbidities in the current study. We hypothesized that there are abnormalities in the intrinsic hippocampal function in emotional-related networks in adolescents with depression, and these abnormalities are related to the risk factors and symptom severity of adolescent MDD.

METHODS

Participants

Sixty-eight first-episode and medication-naïve patients with MDD were recruited from The Third People's Hospital of Mianyang, Sichuan, China. All patients were diagnosed by two professional child and adolescent psychiatrists (Y. Li and G. Huang). The inclusion criteria were as follows: (1) age between 12 and 18 years; (2) Hamilton Depression Scale (HAMD) score $\geq$8; (3) no history of drug therapy and psychotherapy; and (4) no comorbid psychosis disorder (e.g., bipolar disorder, attention-deficit/hyperactivity disorder, autism, and eating disorder) and family history of psychosis disorders.

Forty-four healthy adolescent volunteers in the same age range were also recruited through poster advertisements from the same social demographic environment. Healthy subjects were screened using the non-patient edition of SCID to exclude any DSM-5 disorders. We also excluded healthy subjects if they had any physical disease or neurological disease, psychosis disorder, or family history of psychosis disorders. Additional exclusion for all individuals included the following: had any substance abuse and dependence and any contraindications for undergoing a magnetic resonance imaging (MRI) scan.

This study was approved by the Ethics Committee of the Third People's Hospital of Mianyang. All subjects were informed of the purpose and method of this experiment, and written informed consent was obtained from all adolescents and their patients or guardians.

Clinical Measures

The 24-item HAMD (HAMD-24) (34) and 14-item Hamilton Anxiety Scale (35) (HAMA-14) were used to assess the severity of symptoms of depression and anxiety in all subjects. The higher the HAMD or HAMA scores, the more severe the symptoms.

The family environment was assessed using the Chinese version of the Family Environment Scale (FES-CV) (36), which includes 10 dimensions (cohesion, emotional expression, conflict, independence, achievement orientation, intellectual–cultural orientation, active–recreational orientation, moral–religious emphasis, organization, and control) with nine items for each dimension.

In addition, the frequency of stressful life events and stress response intensity was measured using the Adolescents Self-Rating Life Events Checklist (ASLEC) (37). This scale consists of six dimensions, namely, interpersonal relationships, study pressure, punishment, sense of loss, healthy adaptation, and other factors. A higher score indicates greater stress.

MRI Data Acquisition

All subjects were scanned using a 3.0-T MRI system (Skyra, Siemens) with a 20-channel phased-array head coil. During the entire scanning procedure, subjects were instructed to relax with their eyes closed without falling asleep and without directed thoughts. T1-weighted anatomical images were scanned with the following scanning parameters: 176 slices, slice thickness = 1 mm, flip angle = 9°, matrix size = 256 × 256, TR = 1,900 ms, TE = 2.25 ms, voxel size = 1 mm × 1 mm × 1 mm.

Whole-brain resting-state functional MRI (rs-fMRI) data depicting blood oxygen level-dependent contrast were obtained using a gradient-echo echo-planar imaging sequence with the following parameters: 35 axial slices, slice thickness = 4 mm, slice gap = 0.2 mm, repetition time (TR) = 2,000 ms, echo time (TE) = 30 ms, flip angle = 90°, matrix size = 64 × 64, voxel size = 3.75 × 3.75 × 4 mm^3, field of view (FOV) = 240 × 240 mm^2. The rs-fMRI lasted 8 min in total, and 255 volumes were obtained for each participant.

Data Preprocessing

The rs-fMRI data were preprocessed and analyzed using the Data Processing and Analysis for Brain Imaging toolkit (http://www.restfmri.net) (38) and the SPM12 (The Wellcome Department of Cognitive Neurology, London, UK, http://www.fifil.ion.ucl.ac.uk/spm/software/spm12, v6225) based on MATLAB R2018b. Specifically, the first 10 functional volumes were discarded for signal stabilization and adaptation of the subjects to the scanning surroundings. The remaining images were corrected for acquisition time intervals between slices. The images were then realigned to the first volume for motion correction. After corrections, these images were spatially normalized into the standard Montreal Neurological Institute (MNI) space, and each voxel was 3 × 3 × 3 mm^3. We smoothed these images with an 8-mm full width at half maximum Gaussian kernel. The effects of drift or trends in fMRI were removed by a detrending analysis. We also regressed out white matter signals and cerebrospinal fluid (CSF) signals to reduce the effects of physiological noise (i.e., cardiac and respiratory fluctuations). Finally, band-pass filtering (0.01–0.08 Hz) was utilized.

To reduce the head motion effects of the functional data, we used a higher-level Friston 24-parameter model, which includes six head motion parameters, one previous time point of six head motion parameters, and 12 corresponding squared items. The mean framewise displacement (FD) was also calculated as a measure of the microscale head motion of each subject. The mean FD of each participant should be <0.2 mm; according to this criterion, one healthy control (HC) was excluded.

Seed-Based FC Analysis

The bilateral hippocampal regions defined from the automated anatomical labeling atlas were selected as seeds. Seed-based RSFC analysis was performed using the RESTPlus software (http://restfmri.net/forum/index.php?q=rest). First, we extracted the time series for each seed. Subsequently, voxel-wise correlation analysis was conducted between each seed and all other voxels of the brain to acquire FC maps. Third, Pearson's correlation coefficients between each seed and all other voxels were converted to *z*-value images using the Fisher *r*-to-*z* transformation.

TABLE 1 | Demographic and clinical variables in patients with MDD and HC subjects.

Clinical data	MDD (n = 68)	HC (n = 43)	Statistics	P-value
Age (years)	14.634 ± 1.52	14.67 ± 1.86	−0.130	0.897
Gender (F/M)	50/18	25/18	2.847	0.092
Handedness (R/L)	67/1	41/2	1.013	0.314
Education (years)	8.51 ± 1.50	8.81 ± 1.88	−0.881	0.381
HAMD-24 total score	23.41 ± 7.02	2.07 ± 1.81	23.852	< 0.001
HAMA-14 total score	18.99 ± 6.02	1.30 ± 1.57	23.034	< 0.001
ASLEC				
Interpersonal relationship	15.72 ± 4.14	7.09 ± 4.09	10.740	< 0.001
Study pressure	13.90 ± 3.88	7.93 ± 4.74	7.238	< 0.001
Punishment	15.79 ± 6.28	5.00 ± 4.27	10.776	< 0.001
Sense of loss	5.85 ± 2.98	2.70 ± 2.80	5.528	< 0.001
Health adaptation	8.35 ± 2.70	2.58 ± 2.75	10.900	< 0.001
FES-CV				
Cohesion	5.32 ± 3.23	5.14 ± 2.37	0.345	0.730
Emotional expression	4.25 ± 2.15	4.30 ± 1.81	−0.132	0.895
Conflict	5.07 ± 2.30	3.33 ± 1.88	4.172	< 0.001
Independence	4.24 ± 1.76	4.26 ± 1.66	−0.061	0.951
Achievement orientation	6.19 ± 2.62	4.98 ± 1.64	3.002	0.003
Intellectual–cultural orientation	4.01 ± 2.51	4.72 ± 1.72	−1.758	0.082
Active–recreational orientation	4.31 ± 2.30	4.95 ± 1.91	−1.529	0.129
Moral–religious emphasis	5.09 ± 2.14	4.95 ± 1.83	0.341	0.734
Organization	5.35 ± 2.69	4.65 ± 1.63	1.710	0.090
Control	4.15 ± 2.31	3.95 ± 1.66	0.512	0.610

MDD, major depressive disorder; HC, healthy controls; HAMD, Hamilton Depression Rating Scale; HAMA, Hamilton Anxiety Rating Scale.

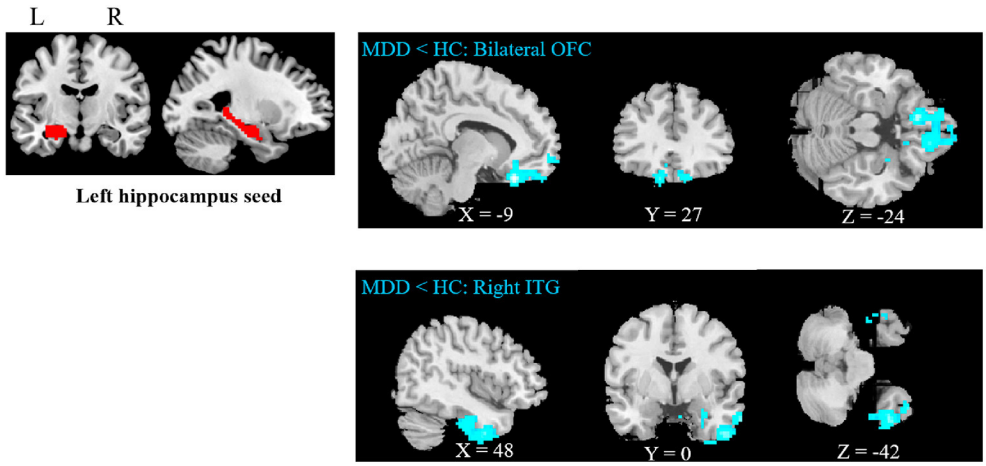

FIGURE 1 | Abnormal resting-state FC between hippocampus and regions. The OFC and ITG regions showed decreased FC in the adolescent depression group. The results were obtained using a seed-based analysis method with the left hippocampus as the seed (OFC, orbital frontal cortex; ITG, inferior temporal gyrus; HC, healthy control; MDD, major depressive disorder).

Statistical Analysis

Group Comparison

The demographic and clinical differences between patients with MDD and HCs were calculated using two independent-sample *t*-tests and chi-square tests based on SPSS software, with a threshold at the $p < 0.05$ level.

Group comparison of the FC maps between MDD and HC was performed using the two-sample *t*-test in SPM12, with age, gender, and head motion as covariates [$p < 0.005$ at the voxel level and false discovery rate (FDR)-corrected $p < 0.05$ at the cluster level].

Correlation Analysis

We conducted partial correlation analysis to explore the association between hippocampal FC and scores of clinical symptom severity scales, including total scores of the HAMD and HAMA and environmental factors including scores of ASLEC and FES-CV with age and gender as covariates.

Exploratory Mediation Analysis

We further investigated the association of environmental risk factors with clinical symptoms in the whole group, considering the potential mediation effect of hippocampal connectivity identified above.

In addition, an exploratory mediation analysis was performed to investigate whether the hippocampal FC detected between groups would mediate the relationship between potential risk factors and depressive symptom severity using the simple mediation model (i.e., Model 4) of the PROCESS v3.3 macro in SPSS (39). In the mediation model, hippocampal FC was defined as the mediator variable, environmental factors as the dependent variable, and the HAMD or HAMA total score as the independent variable with age and gender being treated as nuisance variables. A bootstrapping approach with 5,000 iterations was performed to test the significance of the mediating effect. Effects with a bootstrapped 95% confidence interval (CI) that did not include zero were regarded as significant.

RESULTS

Demographics and Clinical Characteristics

The demographic and clinical characteristics of all subjects are presented in **Table 1**. Compared to the HC group, the MDD group showed significantly higher HAMD and HAMA scores, conflict scores, and achievement orientation scores ($p < 0.05$). The ASLEC scores were also significantly higher in the MDD group than in the HC group ($p < 0.05$).

Hippocampal RSFC Pattern

Compared to HCs, adolescent MDD patients showed decreased FC between the left hippocampus and the bilateral OFC as well as between the left hippocampus and the right inferior temporal gyrus (ITG) (**Figure 1** and **Table 2**). No significant increase in hippocampal FC was observed in the MDD group compared to the HC group. There were no significant group differences between the MDD and HC groups in the right hippocampal FC.

Correlation Analysis

There was a negative correlation between hippocampal-OFC connectivity and family conflict scores of FES-CV in the MDD group ($p = 0.021$) after controlling for the effects of sex and age (**Figure 2**). No significant association between cerebral connectivity and other factors of FES-CV and ASLEC scores and clinical severity (i.e., HAMA and HAMD) were detected.

Exploratory Mediation Analysis

The correlations between the family conflict score and HAMD/HAMA total scores were significant in all subjects. The mediation analysis revealed that the hippocampal-OFC FC significantly mediated the association between family conflict and symptoms of depression (indirect effect = 0.0846, 95% CI

TABLE 2 | Region of abnormal resting-state FC between the hippocampus and regions.

Seed	Regions	Peak (MNI)			Voxels	*T*-value	*P*-value (FDR-corrected)
		x	y	z			
HC > MDD							
Left	OFC	−9	27	−24	406	4.68	0.009
Hippocampus	Right ITG	48	0	−42	548	4.00	0.002

MDD, major depressive disorder; HC, healthy controls; MNI, Montreal Neurological Institute; FDR, false discovery rate; ITG, inferior temporal gyrus; OFC, orbital frontal cortex.

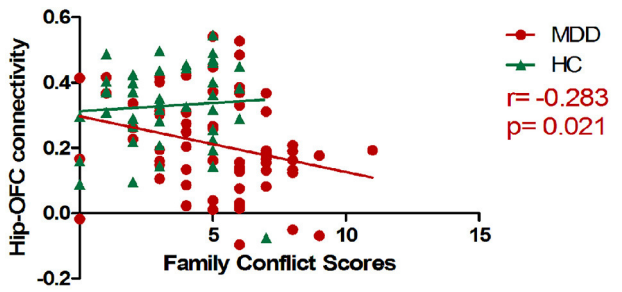

FIGURE 2 | The scatter plots of the correlations between mean hippocampal-OFC functional connectivity and family conflict scores. The RSFC between the left hippocampus and bilateral OFC was negatively associated with the conflict scores of FES-CV in the MDD group (OFC, orbital frontal cortex; FES-CV, Chinese version of the Family Environment Scale; Hip, Hippocampal; HC, healthy control; MDD, major depressive disorder).

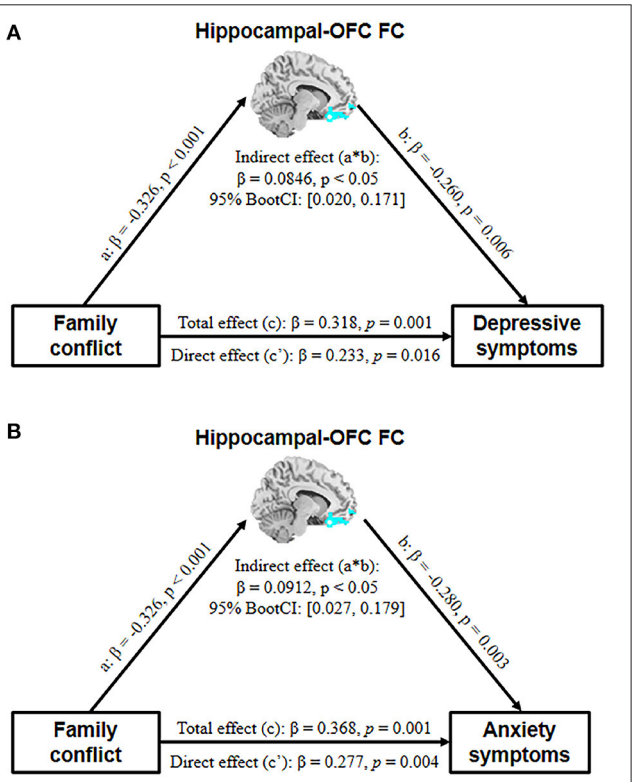

FIGURE 3 | The mediation model depicts the relationship between family conflict, adolescent depressive **(A)** and anxiety **(B)** symptoms, and hippocampal-OFC FC with age and gender as covariates (OFC, orbital frontal cortex; FC, functional connectivity).

= [0.020, 0.171], $p < 0.05$) and anxiety (indirect effect = 0.0912, 95% CI = [0.027, 0.179], $p < 0.05$) (**Figure 3**).

DISCUSSION

To the best of our knowledge, this is the first study to explore the relationship between hippocampal FC and environmental risk factors in adolescents with depression. Compared to HCs, adolescent MDD demonstrated significantly decreased hippocampal FC with bilateral OFC and right ITG. In addition, we found that depressed adolescents were associated with higher levels of stressful events and family conflict. However, only family conflict scores were negatively correlated with the hippocampal-OFC connectivity. More importantly, hippocampal-OFC connectivity mediated the association between family conflict and both depressive and anxiety symptoms. Our results suggest that family conflict may contribute to depressive symptoms in adolescents through changes in hippocampal-OFC connectivity.

Family conflict refers to active opposition between family members and can take a wide variety of forms, including verbal, physical, sexual, financial, and psychological. Conflicts may involve different combinations of family members: conflict within the couple or between parents and children or, again, between siblings (40). It can cause maladjustment by an adolescents' increasing emotional insecurity about the family system (41, 42) and affect children's levels of resilience, such as low self-esteem, mental fatigue, anxiety, poor school performance, introvertism, depression, and self-criticism (43). The higher family conflict scores of FES-CV in adolescent MDD suggest that family members express their anger, aggression, and contradiction toward each other more openly (44).

Many studies have shown that children and adolescents with depression express higher levels of family conflict than do HCs (45–48). Children with a family history of depression are at an increased risk of developing depressive symptoms in response to family conflicts (49). More importantly, it can be a stressful event for adolescents and increase the risk of depression (50–52). We speculate that irritability, a core symptom of adolescent depression, may be related to a high-family-conflict environment. A developmental model of depression based on

vulnerability diathesis and stressful life showed that early adverse events foster negative attitudes and biases about the self, which can be activated by later adverse events impinging on the specific cognitive vulnerability and lead to depression (53).

Many researchers have demonstrated that the hippocampus and OFC work together to mediate responses to stressful experiences (54, 55) and are associated with impaired cognition in depression (56, 57). Hippocampus and OFC both have been proposed to encode parallel but interactive "cognitive maps" that capture complicated relationships between various kinds of information from the environment (58). Cognitive maps provide useful scaffolds for planning complex behaviors and thus can promote model-based learning and behavior (59). A previous task-based fMRI study (60) suggested that increased hippocampal-OFC connectivity could facilitate model-based interference. Therefore, the decreased hippocampal-OFC observed in this study might be linked to abnormalities in processing of information from the external environment and inferring future outcomes, thus leading to cognitive impairments in adolescents with MDD.

In addition, family conflict can also serve as childhood early-life stress, which may independently predict adulthood MDD diagnosis and be associated with smaller volumes of the OFC and left hippocampus (52). Previous research has shown diminished connectivity between the hippocampus and OFC during conflict resolution, a way of presenting family conflict, based on theta band coherence (61). Our finding of the mediation effect of hippocampal-OFC connectivity provides solid evidence for the involvement of these two structures in depression neuropathology. It delineated how environmental risk factors, such as family conflict, lead to depressive symptoms.

We also found that hippocampal-OFC connectivity could mediate the association between family conflict and anxiety symptoms. Stressful family environments play an important role in developing anxiety symptoms (62, 63). Hippocampal connectivity can predict the subjective feeling of stress (20). OFC dysfunction is related to failure of inappropriate fear and anxiety response inhibition (64). Taken together, our findings suggest that the interaction between the hippocampus and OFC plays a critical role in affective symptom development.

In addition, we found decreased connectivity between the left hippocampus and the right ITG in adolescent MDD. Previous studies focused on Sjogren's syndrome (65) and subcortical vascular mild cognitive impairment with depression symptoms (66) have revealed decreased connectivity between the hippocampus and ITG, which is related to cognitive impairment (such as visual memory) and depression symptoms. The interaction between the hippocampus and ITG contributes to visual memory and associative memory (67–69). Therefore, the decreased FC of the left hippocampus and right ITG in adolescent MDD may be related to impaired visual memory in this population. However, this hypothesis has yet to be elucidated in further research.

Despite this being a large, well-characterized sample, this study also has some limitations. Although our study found a close association between family conflict, hippocampal-OFC connectivity, and depressive symptoms, the result could not survive FDR correction for multiple comparisons and was limited by the cross-sectional design. Future studies should verify this result from a longitudinal perspective to identify the developmental effects of family conflict exposure on the hippocampus and OFC and further uncover the mechanisms underlying the development of depression. In addition, other environmental stress factors (e.g., child maltreatment, homelessness, and poverty) that were not included in this study were also reported to be associated with depression (8). The relationship between these environmental factors and biological markers in adolescent depression should be further investigated to facilitate the detection of individuals at risk of developing depression.

In summary, we are the first to report that family conflict may contribute to depressive symptoms in adolescents through abnormal hippocampal-OFC FC. These results provide a pathogenesis mechanism for depressive disorder in adolescents and environmental factors that may be targets for future preventive strategies.

DATA AVAILABILITY STATEMENT

The raw data supporting the conclusions of this article will be made available by the authors, without undue reservation.

ETHICS STATEMENT

The studies involving human participants were reviewed and approved by the Ethics Committee of the Third People's Hospital of Mianyang. Written informed consent to participate in this study was provided by the participants' legal guardian/next of kin.

AUTHOR CONTRIBUTIONS

RF, MZ, LZha, and XH designed the study. RF, YL, LL, HY, LZhu, and GH participated in the patient recruitment. WB performed the MRI preprocessing and quality assessment. RF, WB, YG, and KL performed the data analyses and statistics. RF and WB wrote the article. XH, YG, and KL revised it critically for important intellectual content. All authors approved the final version to be published.

FUNDING

This study was supported by grants from National Natural Science Foundation of China (No. 81671669), Sichuan Provincial Youth Grant (No. 2017JQ0001), 1.3.5 project for disciplines of excellence, West China Hospital, Sichuan University (No. ZYJC21041), and Clinical and Translational Research Fund of Chinese Academy of Medical Sciences (No. 2021-I2M-C&T-B-097).

REFERENCES

1. Steinberg L, Dahl R, Keating D, Kupfer DJ, Masten AS, Pine DS. The study of developmental psychopathology in adolescence: integrating affective neuroscience with the study of context. *Dev Psychopathol.* (2015) 2:710–41. doi: 10.1002/9780470939390.ch18
2. Casey BJ, Jones RM, Levita L, Libby V, Pattwell SS, Ruberry EJ, et al. The storm and stress of adolescence: insights from human imaging and mouse genetics. *Dev Psychobiol.* (2010) 52:225–35. doi: 10.1002/dev.20447
3. Andersen SL, Teicher MH. Stress, sensitive periods and maturational events in adolescent depression. *Trends Neurosci.* (2008) 31:183–91. doi: 10.1016/j.tins.2008.01.004
4. Lupien SJ, McEwen BS, Gunnar MR, Heim C. Effects of stress throughout the lifespan on the brain, behaviour and cognition. *Nat Rev Neurosci.* (2009) 10:434–45. doi: 10.1038/nrn2639
5. Bernaras E, Jaureguizar J, Garaigordobil M. Child and adolescent depression: a review of theories, evaluation instruments, prevention programs, and treatments. *Front Psychol.* (2019) 10:543. doi: 10.3389/fpsyg.2019.00543
6. Thapar A, Collishaw S, Pine DS, Thapar AK. Depression in adolescence. *Lancet.* (2012) 379:1056–67. doi: 10.1016/S0140-6736(11)60871-4
7. Kann L, McManus T, Harris WA, Shanklin SL, Flint KH, Hawkins J, et al. Youth risk behavior surveillance - United States, 2015. *Morbid Mortal Weekly Rep Surveill Summaries.* (2016) 65:1–174. doi: 10.15585/mmwr.ss6506a1
8. Zajkowska Z, Walsh A, Zonca V, Gullett N, Pedersen GA, Kieling C, et al. A systematic review of the association between biological markers and environmental stress risk factors for adolescent depression. *J Psychiatr Res.* (2021) 138:163–75. doi: 10.1016/j.jpsychires.2021.04.003
9. Goldstein BL, Kessel EM, Kujawa A, Finsaas MC, Davila J, Hajcak G, et al. Stressful life events moderate the effect of neural reward responsiveness in childhood on depressive symptoms in adolescence. *Psychol Med.* (2020) 50:1548–55. doi: 10.1017/S0033291719001557
10. Malhi GS, Mann JJ. Depression. *Lancet.* (2018) 392:2299–312. doi: 10.1016/S0140-6736(18)31948-2
11. Otte C, Gold SM, Penninx BW, Pariante CM, Etkin A, Fava M, et al. Major depressive disorder. *Nat Rev Dis Primers.* (2016) 2:16065. doi: 10.1038/nrdp.2016.65
12. Yu Y, Yang X, Yang Y, Chen L, Qiu X, Qiao Z, et al. The role of family environment in depressive symptoms among University students: a large sample survey in China. *PloS ONE.* (2015) 10:e0143612. doi: 10.1371/journal.pone.0143612
13. Bick J, Nelson CA. Early adverse experiences and the developing brain. *Neuropsychopharmacology.* (2016) 41:177–96. doi: 10.1038/npp.2015.252
14. Miguel PM, Pereira LO, Silveira PP, Meaney MJ. Early environmental influences on the development of children's brain structure and function. *Dev Med Child Neurol.* (2019) 61:1127–33. doi: 10.1111/dmcn.14182
15. Whittle S, Simmons JG, Dennison M, Vijayakumar N, Schwartz O, Yap MB, et al. Positive parenting predicts the development of adolescent brain structure: a longitudinal study. *Dev Cogn Neurosci.* (2014) 8:7–17. doi: 10.1016/j.dcn.2013.10.006
16. McCormick CM, Green MR. From the stressed adolescent to the anxious and depressed adult: investigations in rodent models. *Neuroscience.* (2013) 249:242–57. doi: 10.1016/j.neuroscience.2012.08.063
17. Rao H, Betancourt L, Giannetta JM, Brodsky NL, Korczykowski M, Avants BB, et al. Early parental care is important for hippocampal maturation: evidence from brain morphology in humans. *Neuroimage.* (2010) 49:1144–50. doi: 10.1016/j.neuroimage.2009.07.003
18. Little K, Olsson CA, Youssef GJ, Whittle S, Simmons JG, Yücel M, et al. Linking the serotonin transporter gene, family environments, hippocampal volume and depression onset: a prospective imaging gene × environment analysis. *J Abnormal Psychol.* (2015) 124:834–49. doi: 10.1037/abn0000101
19. Rao U, Chen LA, Bidesi AS, Shad MU, Thomas MA, Hammen CL. Hippocampal changes associated with early-life adversity and vulnerability to depression. *Biol Psychiatry.* (2010) 67:357–64. doi: 10.1016/j.biopsych.2009.10.017
20. Goldfarb EV, Rosenberg MD, Seo D, Constable RT, Sinha R. Hippocampal seed connectome-based modeling predicts the feeling of stress. *Nat Commun.* (2020) 11:2650. doi: 10.1038/s41467-020-16492-2
21. Riggins T, Geng F, Blankenship SL, Redcay E. Hippocampal functional connectivity and episodic memory in early childhood. *Dev Cogn Neurosci.* (2016) 19:58–69. doi: 10.1016/j.dcn.2016.02.002
22. Frank LE, Bowman CR, Zeithamova D. Differential functional connectivity along the long axis of the hippocampus aligns with differential role in memory specificity and generalization. *J Cogn Neurosci.* (2019) 31:1958–75. doi: 10.1162/jocn_a_01457
23. Kim EJ, Pellman B, Kim JJ. Stress effects on the hippocampus: a critical review. *Learn Mem.* (2015) 22:411–6. doi: 10.1101/lm.037291.114
24. Cao X, Liu Z, Xu C, Li J, Gao Q, Sun N, et al. Disrupted resting-state functional connectivity of the hippocampus in medication-naïve patients with major depressive disorder. *J Affect Disord.* (2012) 141:194–203. doi: 10.1016/j.jad.2012.03.002
25. Chen L, Wang Y, Niu C, Zhong S, Hu H, Chen P, et al. Common and distinct abnormal frontal-limbic system structural and functional patterns in patients with major depression and bipolar disorder. *Neuroimage Clin.* (2018) 20:42–50. doi: 10.1016/j.nicl.2018.07.002
26. Fateh AA, Long Z, Duan X, Cui Q, Pang Y, Farooq MU, et al. Hippocampal functional connectivity-based discrimination between bipolar and major depressive disorders. *Psychiatry Res Neuroimaging.* (2019) 284:53–60. doi: 10.1016/j.pscychresns.2019.01.004
27. Ge R, Torres I, Brown JJ, Gregory E, McLellan E, Downar JH, et al. Functional disconnectivity of the hippocampal network and neural correlates of memory impairment in treatment-resistant depression. *J Affect Disord.* (2019) 253:248–56. doi: 10.1016/j.jad.2019.04.096
28. Hao ZY, Zhong Y, Ma ZJ, Xu HZ, Kong JY, Wu Z, et al. Abnormal resting-state functional connectivity of hippocampal subfields in patients with major depressive disorder. *BMC Psychiatry.* (2020) 20:71. doi: 10.1186/s12888-020-02490-7
29. He Z, Lu F, Sheng W, Han S, Long Z, Chen Y, et al. Functional dysconnectivity within the emotion-regulating system is associated with affective symptoms in major depressive disorder: a resting-state fMRI study. *Australian New Zeal J Psychiatry.* (2019) 53:528–39. doi: 10.1177/0004867419832106
30. Liu C, Pu W, Wu G, Zhao J, Xue Z. Abnormal resting-state cerebral-limbic functional connectivity in bipolar depression and unipolar depression. *BMC Neurosci.* (2019) 20:30. doi: 10.1186/s12868-019-0508-6
31. Tahmasian M, Knight DC, Manoliu A, Schwerthöffer D, Scherr M, Meng C, et al. Aberrant intrinsic connectivity of hippocampus and amygdala overlap in the fronto-insular and dorsomedial-prefrontal cortex in major depressive disorder. *Front Hum Neurosci.* (2013) 7:639. doi: 10.3389/fnhum.2013.00639
32. Lee J, Pavuluri MN, Kim JH, Suh S, Kim I, Lee MS. Resting-state functional connectivity in medication-naïve adolescents with major depressive disorder. *Psychiatry Res Neuroimaging.* (2019) 288:37–43. doi: 10.1016/j.pscychresns.2019.04.008
33. Geng H, Wu F, Kong L, Tang Y, Zhou Q, Chang M, et al. Disrupted structural and functional connectivity in prefrontal-hippocampus circuitry in first-episode medication-naïve adolescent depression. *PloS ONE.* (2016) 11:e0148345. doi: 10.1371/journal.pone.0148345
34. Hamilton M. Development of a rating scale for primary depressive illness. *Br J Soc Clin Psychol.* (1967) 6:278–96. doi: 10.1111/j.2044-8260.1967.tb00530.x
35. Hamilton M. The assessment of anxiety states by rating. *Br J Med Psychol.* (1959) 32:50–5. doi: 10.1111/j.2044-8341.1959.tb00467.x
36. Wang XD, Wang XL, Ma H. *Rating Scales for Mental Health*. Beijing: Chinese Mental Health Journal Press (1999).
37. Liu XC, Liu LQ, Yang J, Chai FX, Sun LM. Development and psychometric reliability and validity of adolescent self-rating life events checklist (Chinese). *Shandong Arch Psychiatry*. (1997) 10:15–19.
38. Yan CG, Wang XD, Zuo XN, Zang YF. DPABI: data processing & analysis for (resting-state) brain imaging. *Neuroinformatics.* (2016) 14:339–51. doi: 10.1007/s12021-016-9299-4
39. Hayes AF. *Introduction to Mediation, Moderation, and Conditional Process Analysis: A Regression-Based Approach*. 2nd ed. New York, NY: Guilford Press (2018).
40. Marta E, Alfieri S. Family conflicts. In: Michalos AC, editor. *Encyclopedia of Quality of Life and Well-Being Research*. Dordrecht: Springer Netherlands (2014). p. 2164–7.
41. Cummings EM, Koss KJ, Davies PT. Prospective relations between family conflict and adolescent maladjustment: security in the family system

as a mediating process. *J Abnormal Child Psychol.* (2015) 43:503–15. doi: 10.1007/s10802-014-9926-1
42. Cummings EM, Schatz JN. Family conflict, emotional security, and child development: translating research findings into a prevention program for community families. *Clin Child Fam Psychol Rev.* (2012) 15:14–27. doi: 10.1007/s10567-012-0112-0
43. Cotoranu D. Romania: The Effects of Intra-family Conflicts on Children's Resilience (2021). doi: 10.13140/RG.2.2.14728.96009
44. Phillips MR. Family Environment Scale - Chinese Version (FES-CV). *Chin J Ment Health.* (1999) 13:134–42.
45. Fosco GM, Van Ryzin MJ, Connell AM, Stormshak EA. Preventing adolescent depression with the family check-up: examining family conflict as a mechanism of change. *J Fam Psychol.* (2016) 30:82–92. doi: 10.1037/fam0000147
46. Ogburn KM, Sanches M, Williamson DE, Caetano SC, Olvera RL, Pliszka S, et al. Family environment and pediatric major depressive disorder. *Psychopathology.* (2010) 43:312–8. doi: 10.1159/000319400
47. Rothenberg WA, Hussong AM, Chassin L. Intergenerational continuity in high-conflict family environments: investigating a mediating depressive pathway. *Dev Psychol.* (2018) 54:385–96. doi: 10.1037/dev0000419
48. Sander JB, McCarty CA. Youth depression in the family context: familial risk factors and models of treatment. *Clin Child Fam Psychol Rev.* (2005) 8:203–19. doi: 10.1007/s10567-005-6666-3
49. Rice F, Harold GT, Shelton KH, Thapar A. Family conflict interacts with genetic liability in predicting childhood and adolescent depression. *J Am Acad Child Adolesc Psychiatry.* (2006) 45:841–8. doi: 10.1097/01.chi.0000219834.08602.44
50. Birmaher B, Ryan ND, Williamson DE, Brent DA, Kaufman J, Dahl RE, et al. Childhood and adolescent depression: a review of the past 10 years. Part I. *J Am Acad Child Adolesc Psychiatry.* (1996) 35:1427–39. doi: 10.1097/00004583-199611000-00011
51. Herrenkohl TI, Kosterman R, Hawkins JD, Mason WA. Effects of growth in family conflict in adolescence on adult depressive symptoms: mediating and moderating effects of stress and school bonding. *J Adolesc Health.* (2009) 44:146–52. doi: 10.1016/j.jadohealth.2008.07.005
52. Saleh A, Potter GG, McQuoid DR, Boyd B, Turner R, MacFall JR, et al. Effects of early life stress on depression, cognitive performance and brain morphology. *Psychol Med.* (2017) 47:171–81. doi: 10.1017/S0033291716002403
53. Beck AT. The evolution of the cognitive model of depression and its neurobiological correlates. *Am J Psychiatry.* (2008) 165:969–77. doi: 10.1176/appi.ajp.2008.08050721
54. McEwen BS. Physiology and neurobiology of stress and adaptation: central role of the brain. *Physiol Rev.* (2007) 87:873–904. doi: 10.1152/physrev.00041.2006
55. Mychasiuk R, Muhammad A, Kolb B. Chronic stress induces persistent changes in global DNA methylation and gene expression in the medial prefrontal cortex, orbitofrontal cortex, and hippocampus. *Neuroscience.* (2016) 322:489–99. doi: 10.1016/j.neuroscience.2016.02.053
56. Rock PL, Roiser JP, Riedel WJ, Blackwell AD. Cognitive impairment in depression: a systematic review and meta-analysis. *Psychol Med.* (2014) 44:2029–40. doi: 10.1017/S0033291713002535
57. Snyder HR. Major depressive disorder is associated with broad impairments on neuropsychological measures of executive function: a meta-analysis and review. *Psychol Bull.* (2013) 139:81–132. doi: 10.1037/a0028727
58. Wikenheiser AM, Schoenbaum G. Over the river, through the woods: cognitive maps in the hippocampus and orbitofrontal cortex. *Nat Rev Neurosci.* (2016) 17:513–23. doi: 10.1038/nrn.2016.56
59. Johnson A, Crowe D A. Revisiting Tolman, his theories and cognitive maps. *Cogn Crit.* (2009) 1:43–72. Available online at: http://www.cogcrit.umn.edu/docs/Johnson_Crowe_10.shtml
60. Wang F, Schoenbaum G, Kahnt T. Interactions between human orbitofrontal cortex and hippocampus support model-based inference. *PLoS Biol.* (2020) 18:e3000578. doi: 10.1371/journal.pbio.3000578
61. Tang AM, Chen KH, Del Campo-Vera RM, Sebastian R, Gogia AS, Nune G, et al. Hippocampal and orbitofrontal theta band coherence diminishes during conflict resolution. *World Neurosurg.* (2021) 152:e32–44. doi: 10.1016/j.wneu.2021.04.023
62. Hettema JM, Neale MC, Kendler KS. A review and meta-analysis of the genetic epidemiology of anxiety disorders. *Am J Psychiatry.* (2001) 158:1568–78. doi: 10.1176/appi.ajp.158.10.1568
63. Norton AR, Abbott MJ. The role of environmental factors in the aetiology of social anxiety disorder: a review of the theoretical and empirical literature. *Behav Change.* (2017) 34:76–97. doi: 10.1017/bec.2017.7
64. Milad MR, Rauch SL. The role of the orbitofrontal cortex in anxiety disorders. *Ann N Y Acad Sci.* (2007) 1121:546–61. doi: 10.1196/annals.1401.006
65. Zhang XD, Zhao LR, Zhou JM, Su YY, Ke J, Cheng Y, et al. Altered hippocampal functional connectivity in primary Sjögren syndrome: a resting-state fMRI study. *Lupus.* (2020) 29:446–54. doi: 10.1177/0961203320908936
66. Xu J, Wang J, Lyu H, Pu X, Xu Z, Hu Y, et al. Different patterns of functional and structural alterations of hippocampal sub-regions in subcortical vascular mild cognitive impairment with and without depression symptoms. *Brain Imaging Behav.* (2021) 15:1211–21. doi: 10.1007/s11682-020-00321-7
67. Ranganath C, Cohen MX, Dam C, D'Esposito M. Inferior temporal, prefrontal, and hippocampal contributions to visual working memory maintenance and associative memory retrieval. *J Neurosci.* (2004) 24:3917–25. doi: 10.1523/JNEUROSCI.5053-03.2004
68. Riches IP, Wilson FA, Brown MW. The effects of visual stimulation and memory on neurons of the hippocampal formation and the neighboring parahippocampal gyrus and inferior temporal cortex of the primate. *J Neurosci.* (1991) 11:1763–79. doi: 10.1523/JNEUROSCI.11-06-01763.1991
69. Rissman J, Gazzaley A, D'Esposito M. Dynamic adjustments in prefrontal, hippocampal, and inferior temporal interactions with increasing visual working memory load. *Cereb Cortex.* (2008) 18:1618–29. doi: 10.1093/cercor/bhm195

Conflict of Interest: The authors declare that the research was conducted in the absence of any commercial or financial relationships that could be construed as a potential conflict of interest.

frontiers in Psychiatry

SYSTEMATIC REVIEW
published: 18 January 2022
doi: 10.3389/fpsyt.2021.764183

Efficacy of Transcranial Magnetic Stimulation for Reducing Suicidal Ideation in Depression: A Meta-Analysis

Yanan Cui[1], Haijian Fang[1], Cui Bao[2], Wanyue Geng[2], Fengqiong Yu[3] and Xiaoming Li[3]**

[1] School of Mental Health and Psychological Sciences, Anhui Medical University, Hefei, China, [2] School of the First College for Clinical Medicine, Anhui Medical University, Hefei, China, [3] Anhui Province Key Laboratory of Cognition and Neuropsychiatric Disorders, Department of Mental Health and Psychological Science, The Second Affiliated Hospital of Anhui Medical University, Anhui Medical University, Hefei, China

Objectives: This study aimed to systematically review the efficacy of transcranial magnetic stimulation treatment in reducing suicidal ideation in depression.

Methods: PubMed, Web of Science, CBMdisc, WanFang, Chongqing VIP, and CNKI databases were electronically searched for randomized controlled trials of transcranial magnetic stimulation (TMS) intervention in the management of suicidal ideation from inception to February 24, 2021. Two reviewers independently screened studies, extracted data, and assessed the quality of included studies. Meta-analysis was then performed using STATA 15.1 software.

Results: A total of eight articles involving 566 patients were included. The meta-analysis results showed that the suicidal ideation scores of the group who received TMS treatment were significantly lower [standardized mean difference (SMD) = −0.415, 95% confidence interval (CI): −0.741 to −0.090, $P = 0.012$] than those of the control group. Subgroup analysis showed that age, TMS pattern, frequency of intervention, and stimulation threshold altered the TMS efficacy.

Conclusions: Evidence showed that TMS achieved superior results in reducing suicidal ideation. Because of the limited quality and quantity of the included studies, more high-quality studies are required to verify the conclusions.

Systematic Review Registration: https://inplasy.com/, identifier: INPLASY202180065.

Keywords: transcranial magnetic stimulation, suicidal ideation, meta-analysis, depression, TMS

OPEN ACCESS

Edited by:
Hongming Li,
University of Pennsylvania,
United States

Reviewed by:
Mohamed A. Abdelnaim,
Universität Regensburg, Germany
Melanie L. Bozzay,
Warren Alpert Medical School of Brown University, United States

****Correspondence:***
Fengqiong Yu
yufengqin1@163.com
Xiaoming Li
psyxiaoming@126.com

Specialty section:
This article was submitted to Neuroimaging and Stimulation, a section of the journal Frontiers in Psychiatry

Received: *25 August 2021*
Accepted: *20 December 2021*
Published: *18 January 2022*

Citation:
Cui Y, Fang H, Bao C, Geng W, Yu F and Li X (2022) Efficacy of Transcranial Magnetic Stimulation for Reducing Suicidal Ideation in Depression: A Meta-Analysis. Front. Psychiatry 12:764183. doi: 10.3389/fpsyt.2021.764183

INTRODUCTION

Major depressive disorder (MDD) is a serious, worldwide mental issue, influencing millions of individuals (1). More than 50% of Chinese patients with MDD have suicidal ideation (2). Suicide is not only a major health problem but also a social problem (3). According to global data released by the World Health Organization in 2012, more than 800,000 people die by suicide every year, accounting for 1.4% of the world's death toll and making it the 15th leading cause of death (4, 5). The lifetime prevalence of suicide ideation is approximately 9.2% on a global scale (6). Suicidal ideation is defined as thinking about, considering, or planning suicide (6). In a review of the ECT intervention literature, Fink et al. found that ECT

was effective for individuals with major depression and suicide, and for follow-up (7). Cipriani et al. found that the Li intervention group reduced suicide deaths by at least 60% compared to the control group (8). Accessible psychological and pharmacological interventions have meant that advancements have been made in reducing suicide (9); however, these are not without side effects, which influences their effectiveness and may further negatively affect those already at high risk of suicide (10). Hence inventive treatment procedures to prevent suicide, for use alongside existing treatments, are fundamentally required.

There is a growing interest in the use of non-invasive brain incitement techniques to decrease suicidal intent and behavior. Transcranial magnetic stimulation (TMS) is a non-invasive magnetic stimulation technology in which a pulsed magnetic field acts on the central nervous system (mainly the brain) to change the membrane potential of cortical nerve cells to produce induced current, which affects brain metabolism and nerve electrical activity, and causes a series of physiological and biochemical reactions (11). A form of TMS, intermittent TBS (iTBS), actuates a long-term potentiation (LTP)-like impact by expanding the postsynaptic concentration of calcium particles (12). Both TBS and traditional patterned TMS can induce plastic changes in a parameter-dependent manner (e.g., inhibit or excite as a function of frequency). The physiological and therapeutic antidepressant magnitude of the effect seem to be similar. Physiological studies have shown that the duration of the physiological modulation on the motor cortex may be longer for TBS than patterned TMS. It is not clear that this translates to clinical efficacy though (in fact, the antidepressant benefits may be shorter) (13–16). TBS has been shown to be safe and well-tolerated, and to have antidepressant properties (17). A recent study (18) suggests that TBS is efficacious in suicide.

Other studies have discussed that rTMS can affect the emotional and cognitive state of patients (19), and that patients with suicidal ideation and behavior often have damage to areas of the brain that are involved in cognitive and emotional control functions (20, 21), and that the targets of TMS happen to be implicated in these brain areas (22), which lends support to the idea that TMS would be expected to be an effective treatment for suicide and its potential use as a treatment for suicidal ideation.

Some studies (23) have not demonstrated a significant difference in the reduction of suicide scores between active TMS stimulation and sham stimulation. By comparing the effects of epilepsy treatment and non-invasive brain stimulation on suicide, Chen et al. supported the effect of ECT on acute suicidal ideation, but they could not suggest the same for MST, rTMS, or tDCS (24). Bozzay et al. review (25) supports the ongoing use of TMS as a new medium to reduce suicide risk; Serafini et al. analyzed the relationship between rTMS interventions and suicidal behavior, one of multiple suicidal dimensions (e.g., suicidal ideation, intensity of suicidal thoughts, suicidal behavior, and suicidal intent), in a systematic study (26). A Meta-analysis (27) concluded that the efficacy and efficiency of high frequency was higher than that of the sham stimulation group; Brunoni et al. (28) included nearly 100 studies and showed that low frequency stimulation was the most effective, while high frequency stimulation was the least effective, bilateral stimulation was intermediate, and bilateral stimulation and low frequency stimulation were the most acceptable of the stimulation modes; Dell'Osso et al. (29) showed that high-frequency stimulation and low-frequency stimulation were similarly effective. The treatment is also effective in special populations, especially adolescents, but the follow-up and delayed effects of the treatment are also of concern in adolescents who are not fully neurologically mature. However, few meta-analyses support the use of TMS for suicidal ideation (one of multiple suicidal dimensions) interventions or provide insight into how best to develop and utilize such interventions. To fill this knowledge gap, we conducted a meta-analysis on the efficacy of TMS in the treatment of suicidal ideation, with subgroup analyses of TMS patterns, age, stimulation frequency and intensity.

METHODS

The study has been registered on INPLASY website. The registration number of this meta-analyses protocol is INPLASY202180065.

Search Strategy

Six electronic databases were searched for relevant studies: PubMed, Web of Science, WanFang, Chinese National Knowledge Infrastructure, Chongqing VIP, and CBMdisc, from their establishment to February 24, 2021, with no restrictions on the publication year. The word "suicide" was combined with "transcranial magnetic stimulation" and the search strategy of combining subject words with free words was adopted (**Supplementary Materials**). Studies were assessed by the inclusion and exclusion criteria below and sorted first by examination of title, then abstract, then the full text. The final search of each database was performed independently and separately by two reviewers.

Inclusion Criteria

The selected studies were those that met the following eligibility criteria: (1) randomized controlled trials published in English or Chinese; (2) the age of participants ranged from 13- to 80-years-old; (3) the study group was treated with TMS or a physical intervention with a definite treatment plan, including a different sequence and frequency of neurophysical stimulation; (4) the control group had no restrictions in the treatment they received (except other physical treatments such as ECT,TDCS, etc.), including conventional treatment, placebo treatment, and waiting for treatment; and (5) the evaluation results were of suicidal ideation and suicidal behavior.

Data Extraction

Information was extracted independently by two reviewers in a standardized manner. Any disagreements were discussed with another reviewer, to reach consensus. Engauge Digitizer 12.1 was used to obtain more information [Only one study (30) in the included studies did not give the data we needed, but we extracted them from the figure by means of the tool]. The following data were extracted for each study: first author's name, year of publication, location, sample size, psychometric instruments

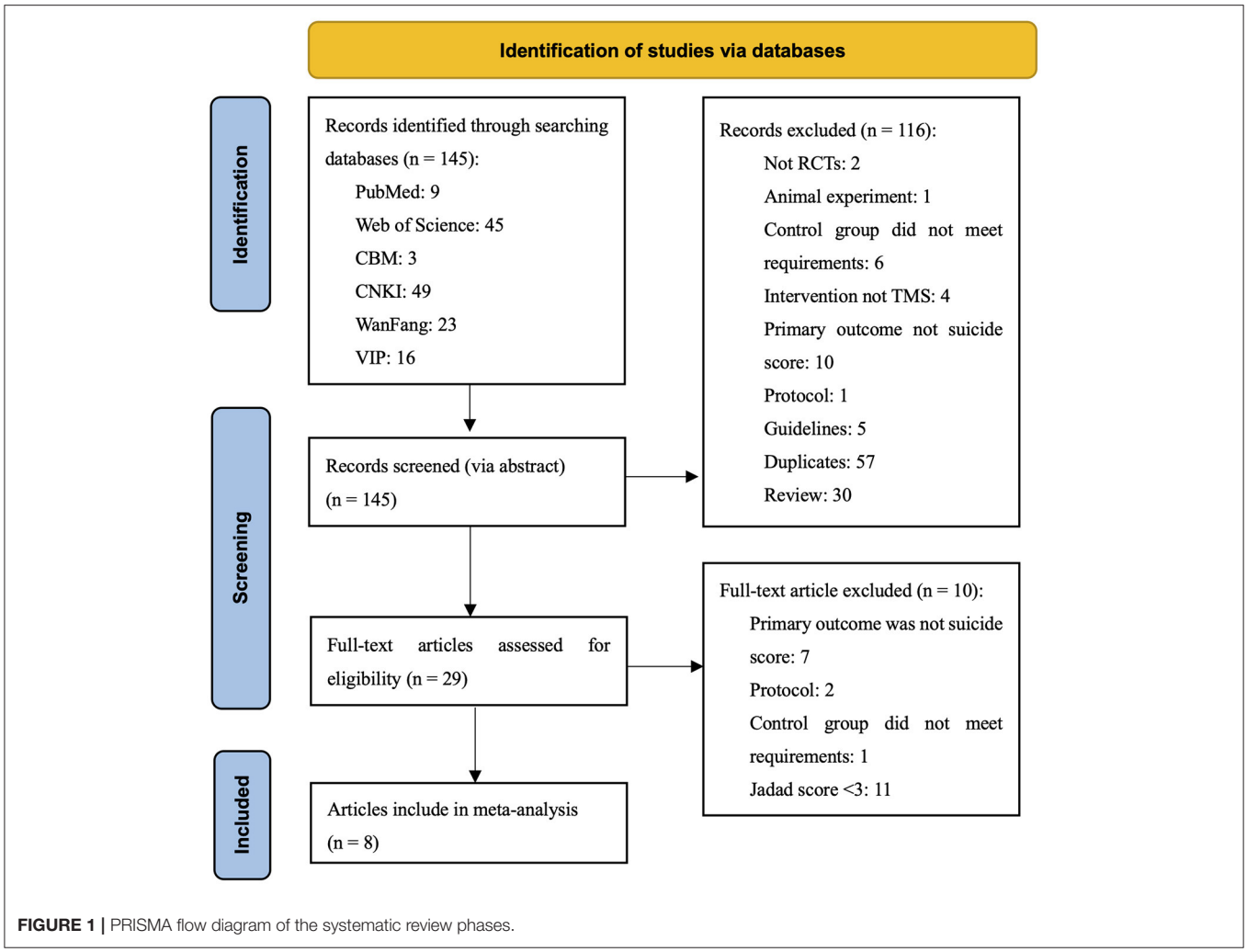

FIGURE 1 | PRISMA flow diagram of the systematic review phases.

and mean and standard deviation of suicide ideation score. We also extracted information on sample size, age, type of TMS, intervention frequency, and intensity threshold, in order to estimate TMS efficacy for suicidal ideation by subgroups.

Quality Assessment

Cochrane risk of bias assessment (31) was used to evaluate the study quality according to the following criteria: random sequence generation, allocation concealment, blinding, incomplete outcome data, selective reporting, and other sources of bias. Each area was ranked for high, low, or unknown bias risk. We also calculated the Jadad score for each of the included studies (32). In calculating the Jadad score, each study was evaluated according to the quality of randomization, blinding procedures, and description of withdrawals and dropouts. Jadad scores ranged from 0 to 5, with trials scoring 3 or greater considered good quality trials.

Statistical Analysis

WPS Office 3.0.2 software was used to organize the incorporated literature and data, and statistical analysis was completed using STATA version 15.1 software. The Q test was used to explore the variation between studies. The I^2 statistic reflected the proportion of heterogeneity in the total variation of effect. If the heterogeneity test results were $P > 0.1$ and $I^2 < 50\%$, the homogeneity of the included studies was considered to be good, and a fixed effects model was used; otherwise, a random effects model was used. Publication bias was assessed by a funnel plot and Egger's test. Subgroup analysis was conducted to explore the potential heterogeneity between studies and the efficacy of TMS intervention for suicidal ideation according to different characteristics.

RESULTS

Characteristics of Eligible Studies

Through searching, 145 potentially related articles were found. After the title and abstract were screened, a remaining 29 documents were screened for full text. Finally, eight articles met the inclusion criteria for meta-analysis. Two studies within one article met the inclusion criteria, making a total of nine studies for meta-analysis. The document screening process and results are shown in **Figure 1**.

The baseline information from the included studies is presented in **Table 1**. Nine sham-controlled clinical trials, including a total of 566 patients, 7 rTMS-controlled clinical trial including a total of 490 patients, 2 iTBS-controlled clinical trial including a total of 76 patients were included in the present systematic review. Clinical samples included predominantly patients with suicidal ideation and one of the following psychiatric diagnoses: MDD, treatment resistant depression (TRD). Subjects in all studies were taking antidepressants during treatment, except for Stefanie et al. Chris et al. (Only habitual benzodiazepine agents were allowed), two studies went through a drug washout period.The control group in all studies was given a sham stimulation treatment, i.e., the same coil also emits a tapping sound on the surface of the patient's scalp, but without pulses. The Jadad score for all the included studies was $\geq$3. The results of the bias risk assessment are shown in **Table 2**.

Overall Efficacy of TMS

Suicidal Ideation

The efficacy of TMS intervention for reducing suicidal ideation was calculated for each study, as shown in **Figure 2**. The results of the meta-analysis showed that the suicidal ideation scores of the group who received TMS treatment for suicidal ideation were statistically significantly lower [standardized mean difference (SMD) = −0.415, 95% confidence interval (CI): −0.741 to −0.090, P = 0.012] than those of the control group. The heterogeneity of the studies was high [heterogeneity chi-squared (χ^2) = 26.90, P = 0.001; I^2 = 70.3%]. The funnel plot shown in **Figure 3** reflects the publication bias by visual inspection. The results of Egger's test revealed no potential risk of publication bias (t = −1.25, P = 0.252).

Depression

Seven studies provided scores for depression after the intervention. As shown in **Figure 4**, the meta-analysis results showed that the depression scores of the TMS group were statistically significantly lower than those of the control group (SMD = −0.885, 95% CI: −1.361 to −0.409, P = 0.012). The heterogeneity of the studies was high (heterogeneity χ^2 = 35.67, P < 0.001; I^2 = 83.2%).

Subgroup Analysis

TMS Pattern

Meta-analysis using a random effects model showed that compared with iTBS (SMD = −0.207, 95% CI: −1.041 to 0.627, P = 0.627), the scores for suicidal ideation in patients who received rTMS intervention (SMD = −0.47, 95% CI: −0.849 to −0.091, P = 0.015) were significantly lower than those in the control group (**Table 3**).

Age

Meta-analysis using a random effects model showed that compared with age $\geq$50 years (SMD = −0.213, 95% CI −0.460 to 0.035, P = 0.092), suicidal ideation scores in the group aged <50 years who received the intervention (SMD = −0.498, 95% CI: −0.972 to −0.025, P = 0.039) were statistically significantly lower than those in the control group (**Table 3**).

Intensity Threshold

In three subgroups of intensity threshold 120%, 110%, and $\leq$100%, the efficacy of TMS intervention for suicidal ideation was represented by SMDs of −0.087 (95% CI: −0.371 to 0.198, P = 0.551), −0.207 (95% CI: −1.041 to 0.627, P = 0.627), and −0.681 (95% CI: −1.191 to −0.171, P = 0.009), respectively (**Table 3**).

Frequency

Meta-analysis using a random effects model showed that compared with the high frequency group (SMD = −0.382, 95% CI: −0.782 to 0.018, P = 0.061), the scores for suicidal ideation in the group who received a low frequency of rTMS (SMD = −0.516, 95% CI: −0.958 to −0.074, P = 0.022) were statistically significantly lower than those in the control group (**Table 3**).

Cumulative Meta-Analysis

No obvious time trend was observed when applying the "initial vs. follow-up" strategy (P = 0.087) and regression strategy analysis (regression coefficient = −0.05585, P < 0.001). These results remained robust when the first study was removed and the results recalculated (regression coefficient = −0.04770, P < 0.001; **Figure 5**).

Sensitivity Analysis

Sensitivity analysis of the included studies showed that the point effect values fell within the 95% CI of the final effect values, which were stable and had no significant effect on the final conclusions (**Figure 6**).

DISCUSSION

The present study systematically reviewed the efficacy of TMS in reducing suicidal ideation in depression. The results showed that compared with the control group, the suicidal ideation scores of the group receiving TMS treatment were statistically significantly lower. The results showed that TMS was also significantly effective in alleviating depression. In summary, our survey of the existing research demonstrated that the use of TMS in managing suicide risk was promising, providing new evidence of the effectiveness and safety of TMS for alleviating suicidal ideation.

Our results showed moderate heterogeneity among the included studies. To explore possible influences on the effectiveness of TMS for reducing suicidal ideation, we performed subgroup analyses according to TMS pattern, age, threshold output rate, and frequency. The results show that these variables are indeed also a source of heterogeneity in this study. Heterogeneity was high (I^2 = 70.3%), and the funnel plot showed that the outliers appeared to be from the same source (**Figure 3**). We found the article (38) that was the main source of heterogeneity and used it to draw a Galbraith star plot (**Figure 7**), and the SMD after excluding it was −0.252 (95% CI: −0.439 to −0.066, P = 0.008), with lower heterogeneity

TABLE 1 | Characteristics of eligible studies included in the meta-analysis.

References	Participants	Sample size (T/C)	Age	TMS pattern	Target	Frequency	Intensity (% MT)	Sessions/day	Number of Pulses per session	Total number of TMS sessions	Control group	Psychometric instruments
Mark et al. (30)	Depressed Adults hospitalized for suicidality with PTSD and/or mild TBI	20/21	<50	rTMS	L DLPFC	high	120%	3 sessions/day	6,000	9 sessions	Sham stimulation and TAU	SSI
Stefanie et al. (33)	MDD unipola, antidepressant-free patients	14/18	<50	iTBS	L DLPFC	high	110%	5 sessions/day	1,620	20 sessions	Sham stimulation	BSI
Chris et al. (34)	TRD, antidepressant-free patients	18/26	<50	iTBS	L DLPFC	high	110%	5 sessions/day	1,620	20 sessions	Sham stimulation and TAU	SSI
Jerome et al. (23)	inpatients with TRD, taking antidepressants.	73/77	≥50	rTMS	L DLPFC	high	120%	2–6 sessions/day	4,000	20–30 sessions	Sham stimulation and TAU	BSI
Qi (35)	MDD, taking antidepressants.	30/30	<50	rTMS	L DLPFC	high	100%	1 sessions/day	1,500	10 sessions	Sham stimulation and TAU	SSI
Qi (35)	MDD, taking antidepressants.	32/30	<50	rTMS	R DLPFC	Low	100%	1 sessions/day	1,500	10 sessions	Sham stimulation and TAU	SSI
Junbo (36)	adolescents with depression, taking antidepressants	16/16	<50	rTMS	R DLPFC	Low	80%	1 sessions/day	1,000	10 sessions	Sham stimulation	BSI
Lilei et al. (37)	elderly patients with depression and suicidal ideation, taking antidepressants	48/55	≥50	rTMS	L DLPFC	high	100%	1 sessions/day	800	20 sessions	Sham stimulation and TAU	SIOSS
Fen et al. (38)	MDD, taking antidepressants	21/21	<50	rTMS	L DLPFC	high	100%	1 sessions/day	6,000	7 sessions	Sham stimulation	BSI

rTMS, repetitive transcranial magnetic stimulation; iTBS, intermittent Theta Burst Stimulation; SIOSS, self-rating idea of suicide scale; BSI/SSI, Beck Scale for Suicide Ideation; DLPFC, Dorsolateral prefrontal cortex; L, Left; R, Righ; MDD, major depressive disorder; TRD, Treatment-Resistant Depression; TAU, Treatment As Usual.

TABLE 2 | Quality assessment of included studies.

References	Random sequence generation	Blinding	Allocation concealment	Incomplete outcome data	Selective reporting	Other sources of bias
Fen et al. (38)	Low risk	Low risk	Unclear	Low risk	Low risk	Low risk
Jerome et al. (23)	Low risk	Low risk	Low risk	Low risk	Low risk	Low risk
Lilei et al. (37)	High risk	Low risk	Unclear	Low risk	Low risk	Low risk
Junbo (36)	Low risk	Low risk	Unclear	Low risk	Low risk	Low risk
Qi (35)	Low risk	Unclear	Unclear	Low risk	Low risk	Low risk
Chris et al. (34)	High risk	Low risk	High risk	Low risk	Low risk	Low risk
Stefanie et al. (33)	High risk	Low risk	High risk	Low risk	Low risk	Low risk
Mark et al. (30)	High risk	Low risk	Low risk	Low risk	Low risk	Low risk

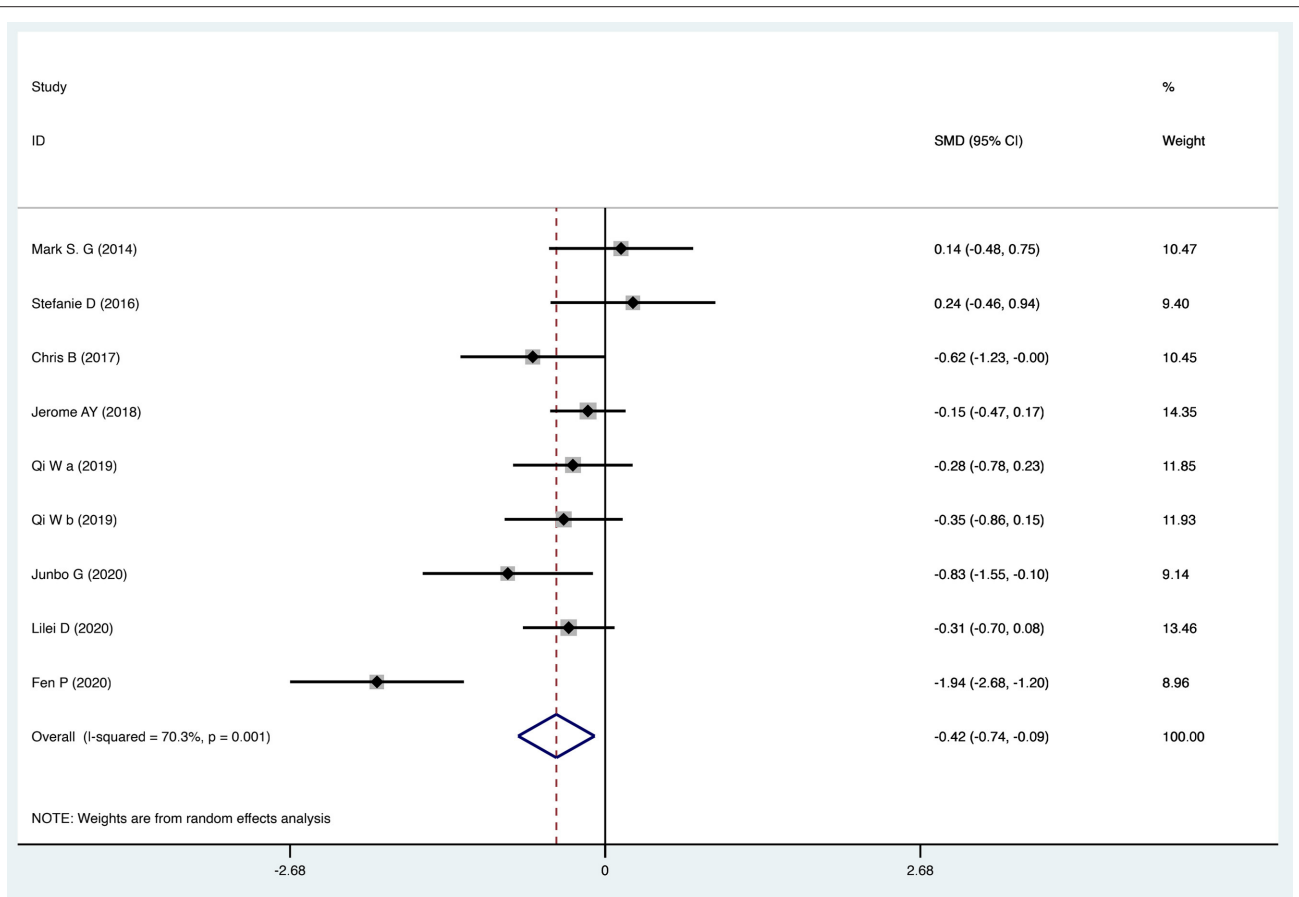

FIGURE 2 | Forest plot of transcranial magnetic stimulation intervention for suicidal ideation.

(I^2 = 10.6%). A possible explanation for this might be that a novel neuro-navigation technique was used in that study to determine the coil location for TMS treatment, rather than using the traditional 5 cm method. This did not have an impact on the overall effect.

Although subgroup analyses were performed in our study, due to the limitations of the study size (non-significant groups are always small). Unfortunately, the results of subgroup analyses are likely to be unreliable in terms of bias. Of concern, this also suggests that future studies of TMS research interventions for suicide should pay more attention to the age of the subjects, different intervention modalities, and different parameter settings.

Cumulative analyses were performed in our study according to the time sequence of the studies, and meta-analysis repeated for each study added, reflecting dynamic trends in study results over time. The intervention effect was shown to be robust, and sensitivity analysis also indicated good

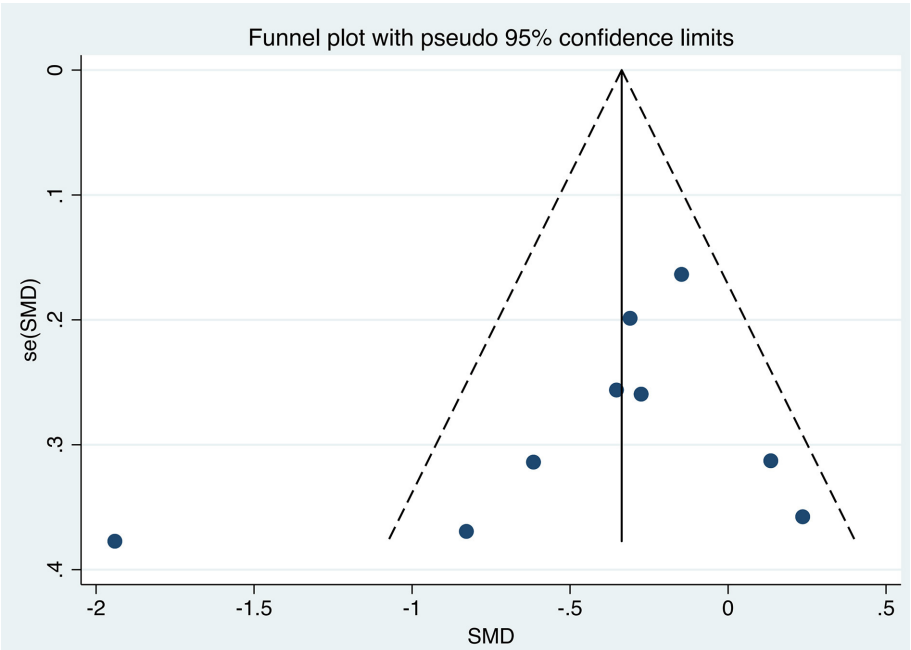

FIGURE 3 | Funnel plot. SMD, Standard Mean Difference.

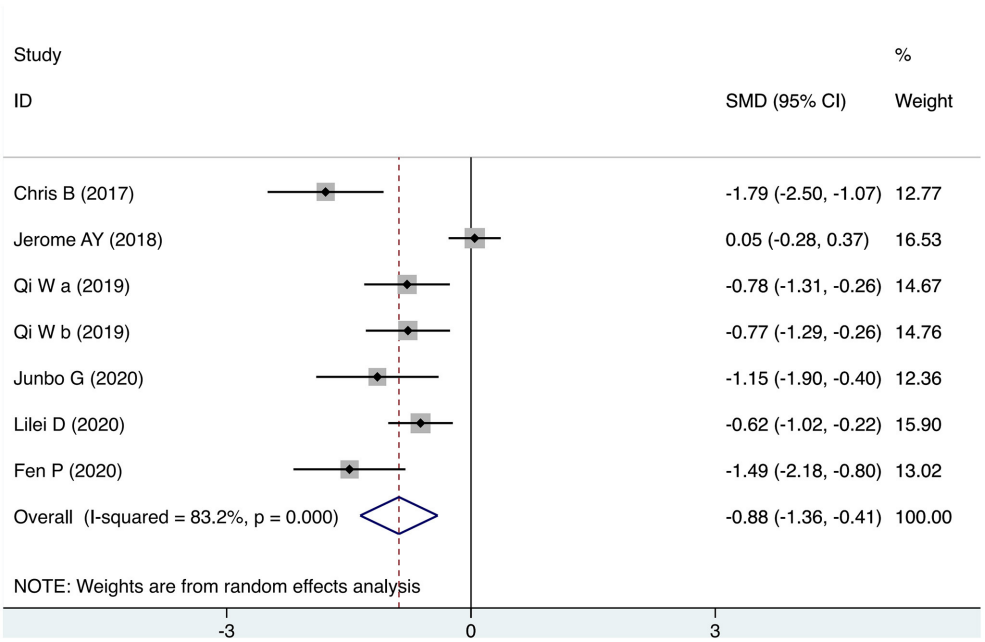

FIGURE 4 | Forest plot of transcranial magnetic stimulation intervention for depression.

stability (Sensitivity analyses were conducted by sequentially excluding studies with multiple daily sessions, and the results were that the apparent efficacy of TMS on suicidal ideation did not vary with the number of daily sessions and was robust).

TBS is a form of rTMS and these stimulation paradigms have been found to be safe in normal subjects and capable of producing consistent, rapid, and controllable electrophysiological, and behavioral changes (16, 39). However, no studies have shown that iTBS was a more effective intervention than rTMS in reducing

TABLE 3 | Subgroup analysis of included studies.

Subgroup		No. of studies	Meta-analysis		Heterogeneity	
			SMD (95% CI)	*P*	I^2 (%)	*P*
TMS pattern	rTMS	7	−0.47 (−0.849, −0.091)	*0.015*	74.50%	*0.001*
	iTBS	2	−0.207 (−1.041, 0.627)	0.627	68.80%	0.073
Age	<50	7	−0.498 (−0.972, −0.025)	*0.039*	75.70%	*<0.001*
	≥50	2	−0.213 (−0.460, 0.035)	0.092	0.00%	0.527
Intensity (% MT)	≤100%	5	−0.681 (−1.191, −0.171)	*0.009*	76.90%	*0.002*
	110%	2	−0.207 (−1.041, 0.627)	0.627	68.80%	0.073
	120%	2	−0.087 (−0.371, 0.198)	0.551	0.00%	0.424
Frequency	High	7	−0.382 (−0.782, 0.018)	0.061	76.00%	*<0.001*
	Low	2	−0.516 (−0.958, −0.074)	*0.022*	10.50%	0.291

SMD, Standard Mean Difference. Italic values represent statistically significant results.

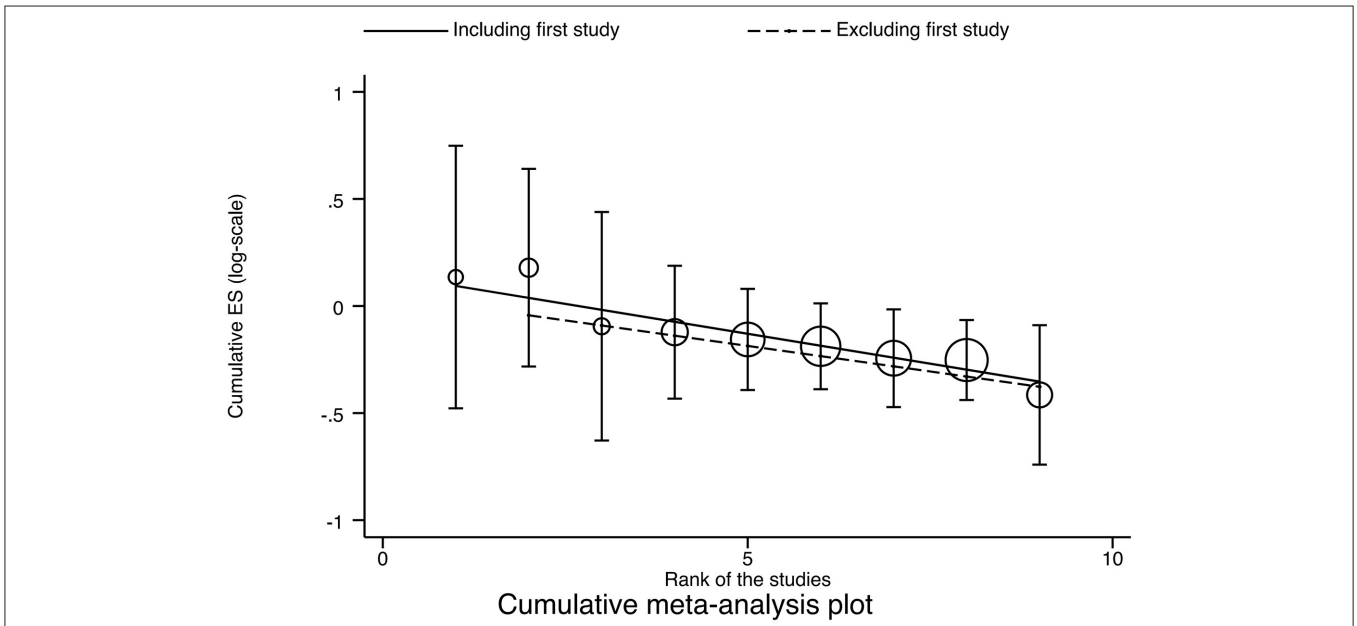

FIGURE 5 | Cumulative meta-analysis plot. ES, Effect Size.

suicidal ideation. Qin et al. who found that rTMS could achieve effective outcomes for older adults with depression, but that treatment outcomes were not as good as in young and middle-aged patients. In the study by wall et al., three adolescents had suicidal ideation and improved during TMS treatment (40). Stimulus intensity also influences the effectiveness of TMS interventions, as demonstrated by previous studies (41, 42). The rTMS may actuate, inhibit, or somehow otherwise interfere with the action of neuronal cortical networks, depending on stimulus frequency and intensity, and brain-induced electric field setup (43). But the relationship between the frequency and intensity of stimulation and the induced excitability change has not been extensively explored. In our study, the low frequency target was always on the right DLPFC, while the high frequency treatment target was always on the left DLPFC and low frequency treatment was more beneficial in reducing suicidal ideation scores in depressed patients than the higher frequencies. The effects of different stimulation frequencies on the cortex are not clear. It is commonly assumed that high frequency stimulation increases neuronal activity and cortical excitability in brain regions (44), and that low frequency stimulation decreases them (45). However, no consistent conclusions have been drawn about the therapeutic effects of different stimulation frequencies, and our conclusions on this were similar to those described by Chen et al. (46) and Lana et al. (47).

Compared to other physical interventions, such as ECT interventions, TMS interventions do not seem to be very effective (48). The most encouraging results supporting transcranial magnetic stimulation are those of studies (49–51). In a further study, DTMS was used in patients with severe TRD, via a new "H1" coil daily for 4 weeks. DTMS was associated with improvements in suicidal behavior (ideation and behavior),

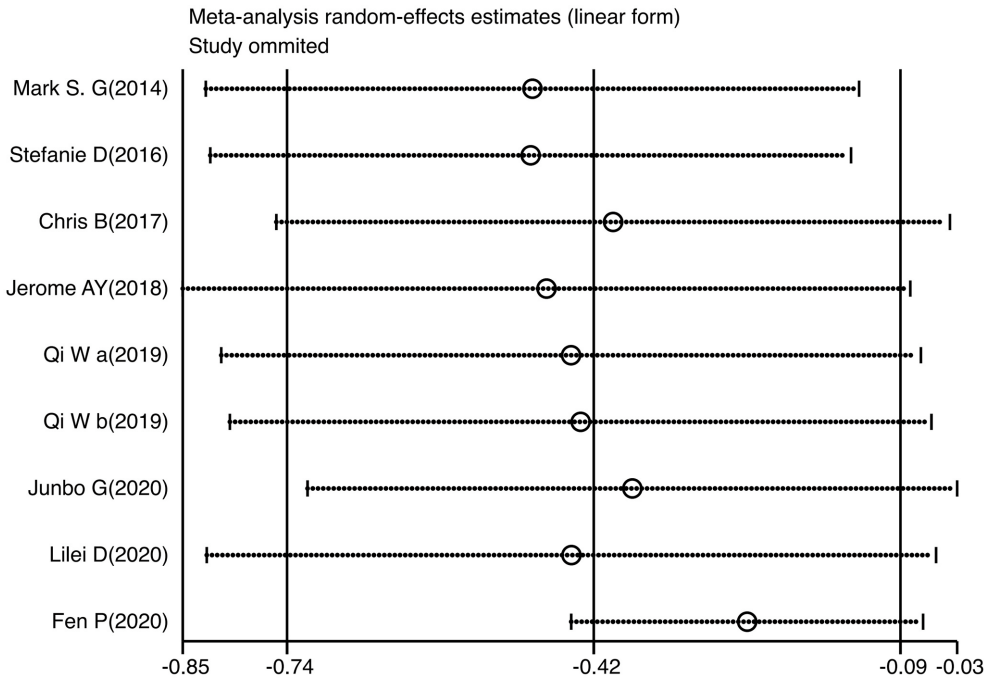

FIGURE 6 | Influence analysis of individual studies.

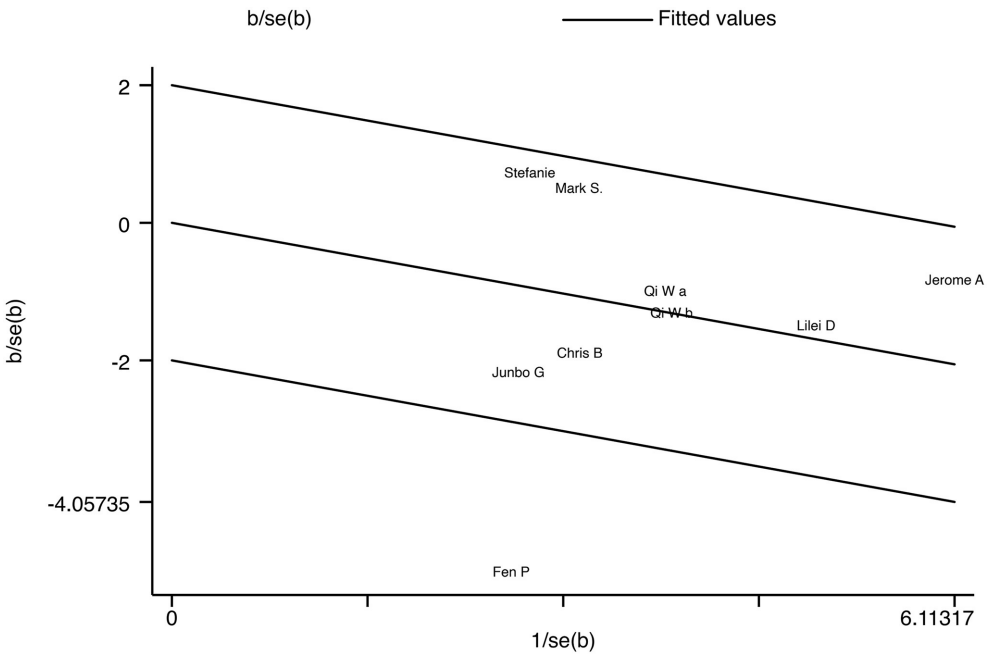

FIGURE 7 | Galbraith star plot.

depression and related anxiety symptoms. The clinical safety of DTMS was also confirmed (52). Subjects in all included studies were depressed, and patients in two studies (33, 34) (iTBS) received physical interventions without medication. Combined with the results of the subgroup analysis of the TMS model, this seems to imply that the TMS intervention is promising as an adjunctive treatment. In one study, improvements were found in both suicidal ideation (especially in the first week of

treatment) and depressive symptoms (50). An improvement in depressive symptoms was also shown in our meta-analysis of the results in depression (**Figure 4**). In a previous study, a reduction in suicide risk was found to be mediated by improvements in depressive symptoms (49). While in another study, changes in suicidal ideation were found to be unrelated to improvements in depression (33), Weissman et al. concluded that the correlation between depression and changes in suicidal ideation was 0.38 and suggested that suicidal ideation could be a specific target symptom construct for rTMS (53).

This study was designed to determine the effect of TMS treatment for reducing suicidal ideation in depression. Based on the above discussion, as well as the outcome indicators after our quantitative analysis, we believe that transcranial magnetic stimulation is promising in reducing suicidal ideation. The findings suggested that future research should focus more on low-intensity, low-frequency TMS interventions for suicidal ideation in middle-aged youth. However, due to the limitations of this study, this conclusion may warrant a serious warning, except to say that this study adds to the evidence for TMS interventions for suicidal ideation and provides a promising direction for future research on TMS interventions in large samples.

There were many limitations to this study. The unpublished literature was not searched, smaller sample subgroup analysis and the funnel plot suggested that publication bias may have resulted in an exaggeration of positive results. This study focused on suicidal ideation rather than suicidal behavior or attempts, and although SI is important, it is not the only factor that contributes to suicide. It is hoped that more future research will focus on the effects of TMS interventions on suicidal behavior or attempts. Finally, many studies have primarily included targeted treatment-resistant depression, and it is unclear whether SI in patients without TRD will show similar results. Despite its limitations, this is, to our knowledge, the first meta-analysis to quantitatively analyze the efficacy of transcranial magnetic stimulation on suicidal, which is arguably a strength of this study. And the study certainly added to our understanding of the efficacy of TMS intervention in reducing suicidal ideation in depression and provided valuable advice and direction for clinical treatment.

DATA AVAILABILITY STATEMENT

The original contributions presented in the study are included in the article/**Supplementary Material**, further inquiries can be directed to the corresponding author/s.

AUTHOR CONTRIBUTIONS

YC wrote the first draft of this manuscript and edited the subsequent versions. YC, HF, and XL are responsible for the data collection and analysis. CB, WG, XL, and FY gave critical revision for the manuscript. All authors contributed to the article and approved the submitted version.

FUNDING

This work was supported by the National Natural Science Foundation of China (31771222) and the Natural Science Foundation of Anhui Province (KJ2016A355).

SUPPLEMENTARY MATERIAL

The Supplementary Material for this article can be found online at: https://www.frontiersin.org/articles/10.3389/fpsyt.2021.764183/full#supplementary-material

REFERENCES

1. Ferrari AJ, Charlson FJ, Norman RE, Patten SB, Whiteford HA. Burden of depressive disorders by country, sex, age, and year: findings from the global burden of disease study 2010. *PLoS Med.* (2013) 10:e1001547. doi: 10.1371/journal.pmed.1001547
2. Fang X, Zhang C, Wu Z, Peng D, Xia W, Xu J, et al. Prevalence, risk factors and clinical characteristics of suicidal ideation in Chinese patients with depression. *J Affect Disord.* (2018) 235:135–41. doi: 10.1016/j.jad.2018.04.027
3. Junfeng H, Guo L, Baihui G, Yuanyuan Z, Xumei W. Research progress of suicide risk assessment scale abroad. *Int J Psychiatry.* (2015) 042:135–8.
4. Fleischmann A, De Leo D. The World Health Organization's report on suicide: a fundamental step in worldwide suicide prevention. *Crisis*. (2014) 35:289–91. doi: 10.1027/0227-5910/a000293
5. WHO. *First WHO Report On Suicide Prevention*. (2014). Available online at: http://www.who.int/mediacentre/news/releases/2014/suicide-prevention-report/en/. (accessed March 15, 2021).
6. Klonsky ED, May AM, Saffer BY. Suicide, suicide attempts, and suicidal ideation. *Ann Rev Clin Psychol.* (2016) 12:307–30. doi: 10.1146/annurev-clinpsy-021815-093204
7. Fink M, Kellner CH, McCall WV. The role of ECT in suicide prevention. *J Ect.* (2014) 30:5–9. doi: 10.1097/YCT.0b013e3182a6ad0d
8. Cipriani A, Hawton K, Stockton S, Geddes JR. Lithium in the prevention of suicide in mood disorders: updated systematic review and meta-analysis. *BMJ.* (2013) 346:f3646. doi: 10.1136/bmj.f3646
9. Zalsman G, Hawton K, Wasserman D, Heeringen KV, Zohar J. Suicide prevention strategies revisited: 10-year systematic review. *Lancet Psychiatry.* (2016) 3:646–59. doi: 10.1016/S2215-0366(16)30030-X
10. Brown GK, Karlin BE, Trockel M, Gordienko M, Yesavage J, Taylor CB. Effectiveness of cognitive behavioral therapy for veterans with depression and suicidal ideation. *Arch Suicide Res Offi J Int Acad Suicide Res.* (2016) 20:677–82. doi: 10.1080/13811118.2016.1162238
11. Lefaucheur JP, Aleman A, Baeken C, Benninger DH, Ziemann U. Evidence-based guidelines on the therapeutic use of repetitive transcranial magnetic stimulation (rTMS): an update (2014–2018). *Clin Neurophysiol.* (2020) 131:474–528. doi: 10.1016/j.clinph.2019.11.002
12. Oberman L, Edwards D, Eldaief M, Pascual-Leone A. Safety of theta burst transcranial magnetic stimulation: a systematic review of the literature. *J Clin Neurophysiol.* (2011) 28:67–74. doi: 10.1097/WNP.0b013e318205135f
13. Di Lazzaro V, Dileone M, Pilato F, Capone F, Musumeci G, Ranieri F, et al. Modulation of motor cortex neuronal networks by rTMS: comparison of local and remote effects of six different protocols of stimulation. *J Neurophysiol.* (2011) 105:2150–6. doi: 10.1152/jn.00781.2010
14. Chung SW, Hoy KE, Fitzgerald PB. Theta-burst stimulation: a new form of TMS treatment for depression? *Depress Anxiety.* (2015) 32:182–92.
15. Prasser J, Schecklmann M, Poeppl TB, Frank E, Kreuzer PM, Hajak G, et al. Bilateral prefrontal rTMS and theta burst TMS as an add-on treatment for depression: a randomized placebo controlled trial. *World J Biol Psychiatry.* (2015) 16:57–65. doi: 10.3109/15622975.2014.964768

16. Lazzaro VD, Pilato F, Dileone M, Profice P, Rothwell JC. The physiological basis of the effects of intermittent theta burst stimulation of the human motor cortex. *J Physiol.* (2010) 586:3871–9. doi: 10.1113/jphysiol.2008.152736
17. Li CT, Chen MH, Juan CH, Huang HH, Chen LF, Hsieh JC, et al. Efficacy of prefrontal theta-burst stimulation in refractory depression: a randomized sham-controlled study. *Brain.* (2014) 137:2088–98. doi: 10.1093/brain/awu109
18. Tien Y, Huang CW, Chan CH. Rapid antisuicidal effects of prolonged iTBS on treatment-resistant depression: a case report. *Psychiatry Res.* (2021) 305:114264. doi: 10.1016/j.psychres.2021.114264
19. Sher L, Mindes J, Novakovic V. Transcranial magnetic stimulation and the treatment of suicidality. *Exp Rev Neurother.* (2010) 10:1781–4. doi: 10.1586/ern.10.166
20. Bredemeier K, Miller IW. Executive function and suicidality: a systematic qualitative review. *Clin Psychol Rev.* (2015) 40:170–83. doi: 10.1016/j.cpr.2015.06.005
21. Allen K, Bozzay ML, Edenbaum ER. Neurocognition and suicide risk in adults. *Curr Behav Neurosci Rep.* (2019) 6:151–65. doi: 10.1007/s40473-019-00189-y
22. Luber B, Lisanby SH. Enhancement of human cognitive performance using transcranial magnetic stimulation (TMS). *Neuroimage.* (2014) 85:961–70. doi: 10.1016/j.neuroimage.2013.06.007
23. Yesavage JA, Fairchild JK, Mi Z, Biswas K, Davis-Karim A, Phibbs CS, et al. Effect of repetitive transcranial magnetic stimulation on treatment-resistant major depression in US veterans: a randomized clinical trial. *JAMA Psychiatry.* (2018) 75:884–93. doi: 10.1001/jamapsychiatry.2018.1483
24. Chen Y, Magnin C, Brunelin J, Leaune E, Fang Y, Poulet E. Can seizure therapies and noninvasive brain stimulations prevent suicidality? A systematic review. *Brain Behav.* (2021) 11:e02144. doi: 10.1002/brb3.2144
25. Bozzay ML, Primack J, Barredo J, Philip NS. Transcranial magnetic stimulation to reduce suicidality – a review and naturalistic outcomes. *J Psychiatric Res.* (2020) 125:106–12. doi: 10.1016/j.jpsychires.2020.03.016
26. Serafini G, Canepa G, Aguglia A, Amerio A, Bianchi D, Magnani L, et al. Effects of repetitive transcranial magnetic stimulation on suicidal behavior: a systematic review. *Prog Neuropsychopharmacol Biol Psychiatry.* (2021) 105:109981. doi: 10.1016/j.pnpbp.2020.109981
27. Berlim MT, van den Eynde F, Tovar-Perdomo S, Daskalakis ZJ. Response, remission and drop-out rates following high-frequency repetitive transcranial magnetic stimulation (rTMS) for treating major depression: a systematic review and meta-analysis of randomized, double-blind and sham-controlled trials. *Psychol Med.* (2014) 44:225–39. doi: 10.1017/S0033291713000512
28. Brunoni AR, Chaimani A, Moffa AH, Razza LB, Gattaz WF, Daskalakis ZJ, et al. Repetitive transcranial magnetic stimulation for the acute treatment of major depressive episodes: a systematic review with network meta-analysis. *JAMA Psychiatry.* (2017) 74:143–52. doi: 10.1001/jamapsychiatry.2016.3644
29. Dell'Osso B, Oldani L, Camuri G, Dobrea C, Cremaschi L, Benatti B, et al. Augmentative repetitive transcranial magnetic stimulation (rTMS) in the acute treatment of poor responder depressed patients: a comparison study between high and low frequency stimulation. *Eur Psychiatry.* (2015) 30:271–6. doi: 10.1016/j.eurpsy.2014.12.001
30. George MS, Raman R, Benedek DM, Pelic CG, Grammer GG, Stokes KT, et al. A two-site pilot randomized 3 day trial of high dose left prefrontal repetitive transcranial magnetic stimulation (rTMS) for suicidal inpatients. *Brain Stimulation.* (2014) 7:421–31. doi: 10.1016/j.brs.2014.03.006
31. Higgins J, Thompson SG, Deeks JJ, Altman DG. Cochrane handbook for systematic reviews of interventions version 5.1.0. the cochrane collaboration. *Naunyn-Schmiedebergs Archiv fexperimentelle Pathologie und Pharmakologie* (2008) 5:S38.
32. Jadad A. Assessing the quality of reports of randomized clinical trials: is blinding necessary? *Control Clin Trials.* (1996) 17:1–12. doi: 10.1016/0197-2456(95)00134-4
33. Desmyter S, Duprat R, Baeken C, Van Autreve S, Audenaert K, van Heeringen K. Accelerated intermittent theta burst stimulation for suicide risk in therapy-resistant depressed patients: a randomized, sham-controlled trial. *Front Hum Neurosci.* (2016) 10:480. doi: 10.3389/fnhum.2016.00480
34. Baeken C, Duprat R, Wu GR, De Raedt R, van Heeringen K. Subgenual anterior cingulate-medial orbitofrontal functional connectivity in medication-resistant major depression: a neurobiological marker for accelerated intermittent theta burst stimulation treatment? *Biol Psychiatry Cogn Neurosci Neuroimaging.* (2017) 2:556–65. doi: 10.1016/j.bpsc.2017.01.001
35. Qi W. *The Effect of High and Low Frequency Repetitive Transcranial Magnetic Stimulation on Clinical Symptoms and Suicidal Ideation in Patients With Depression*. Hebei: Hebei University (2019).
36. JunBo G. *Effect of Repetitive Transcranial Magnetic Stimulation on Self Harm of Adolescent Depression: A Study on the Efficacy of Low Frequency Stimulation of Right Dorsolateral Prefrontal Lobe*. Chengdu: University of Electronic Science and Technology (2020).
37. Dai L, Wang P, Zhang P, Guo Q, Du H, Li F, et al. The therapeutic effect of repetitive transcranial magnetic stimulation in elderly depression patients. *Medicine.* (2020) 99:e21493. doi: 10.1097/MD.0000000000021493
38. Pan F, Shen Z, Jiao J, Chen J, Li S, Lu J, et al. Neuronavigation-Guided rTMS for the treatment of depressive patients with suicidal ideation: a double-blind, randomized, sham-controlled trial. *Clin Pharmacol Ther.* (2020) 108:826–32. doi: 10.1002/cpt.1858
39. Huang YZ, Ed Wards MJ, Rounis E, Bhatia KP, Rothwell JC. Theta burst stimulation of the human motor cortex. *Neuron.* (2005) 45:201–6. doi: 10.1016/j.neuron.2004.12.033
40. Wall CA, Croarkin PE, Sim LA, Husain MM, Janicak PG, Kozel FA, et al. Adjunctive use of repetitive transcranial magnetic stimulation in depressed adolescents: a prospective, open pilot study. *J Clin Psychiatry.* (2011) 72:1263–9. doi: 10.4088/JCP.11m07003
41. Todd, G. Low-intensity repetitive transcranial magnetic stimulation decreases motor cortical excitability in humans. *J Appl Physiol.* (2006) 101:500–5. doi: 10.1152/japplphysiol.01399.2005
42. Lang N, Harms J, Weyh T, Lemon RN, Paulus W, Rothwell JC, et al. Stimulus intensity and coil characteristics influence the efficacy of rTMS to suppress cortical excitability. *Clin Neurophysiol.* (2006) 117:2292–301. doi: 10.1016/j.clinph.2006.05.030
43. Lefaucheur JP. Transcranial magnetic stimulation. *Handbook Clin Neurol.* (2019) 160:559–80. doi: 10.1016/B978-0-444-64032-1.00037-0
44. Dockx R, Baeken C, Duprat R, Vos FD, Saunders JH, Polis I, et al. Changes in canine cerebral perfusion after accelerated high frequency repetitive transcranial magnetic stimulation (HF-rTMS): a proof of concept study. *Vet J.* (2018) 66:66–71. doi: 10.1016/j.tvjl.2018.02.004
45. Milev RV, Giacobbe P, Kennedy SH, Blumberger DM, Daskalakis ZJ, Downar J, et al. Canadian network for mood and anxiety treatments (CANMAT) 2016 clinical guidelines for the management of adults with major depressive disorder: section 4. Neurostimulation treatments. *Can J Psychiatry.* (2016) 61:561–75. doi: 10.1177/0706743716660033
46. Chen J, Zhou C, Wu B, Wang Y, Li Q, Wei Y, et al. Left versus right repetitive transcranial magnetic stimulation in treating major depression: a meta-analysis of randomised controlled trials. *Psychiatry Res.* (2013) 210:1260–4. doi: 10.1016/j.psychres.2013.09.007
47. Donse L, Padberg F, Sack AT, Rush AJ, Arns M. Simultaneous rTMS and psychotherapy in major depressive disorder: clinical outcomes and predictors from a large naturalistic study. *Brain Stimul.* (2018) 11:337–45. doi: 10.1016/j.brs.2017.11.004
48. Keshtkar M, Ghanizadeh A, Firoozabadi A. Repetitive transcranial magnetic stimulation versus electroconvulsive therapy for the treatment of major depressive disorder, a randomized controlled clinical trial. *J Ect.* (2011) 27:310–4. doi: 10.1097/YCT.0b013e318221b31c
49. Croarkin PE, Nakonezny PA, Deng ZD, Romanowicz M, Voort JLV, Camsari DD, et al. High-frequency repetitive TMS for suicidal ideation in adolescents with depression. *J Affect Disord.* (2018) 239:282–90. doi: 10.1016/j.jad.2018.06.048
50. Hadley D, Anderson BS, Borckardt JJ, Arana A, Li X, Nahas Z, et al. Safety, tolerability, and effectiveness of high doses of adjunctive daily left prefrontal repetitive transcranial magnetic stimulation for treatment-resistant depression in a clinical setting. *J Ect.* (2011) 27:18–25. doi: 10.1097/YCT.0b013e3181ce1a8c
51. Abdelnaim MA, Langguth B, Deppe M, Mohonko A, Kreuzer PM, Poeppl TB, et al. Anti-suicidal efficacy of repetitive transcranial magnetic stimulation in

depressive patients: a retrospective analysis of a large sample. *Front Psychiatry.* (2019) 10:929. doi: 10.3389/fpsyt.2019.00929
52. Berlim MT, Van den Eynde F, Tovar-Perdomo S, Chachamovich E, Zangen A, Turecki G. Augmenting antidepressants with deep transcranial magnetic stimulation (DTMS) in treatment-resistant major depression. *World J Biol Psychiatry.* (2014) 15:570–8. doi: 10.3109/15622975.2014.925141
53. Weissman CR, Blumberger DM, Brown PE, Isserles M, Rajji TK, Downar J, et al. Bilateral repetitive transcranial magnetic stimulation decreases suicidal ideation in depression. *J Clin Psychiatry.* (2018) 79. doi: 10.4088/JCP.17m11692

Conflict of Interest: The authors declare that the research was conducted in the absence of any commercial or financial relationships that could be construed as a potential conflict of interest.

frontiers in Psychiatry

ORIGINAL RESEARCH
published: 25 January 2022
doi: 10.3389/fpsyt.2021.747386

Subcortical Brain Volumes Relate to Neurocognition in First-Episode Schizophrenia, Bipolar Disorder, Major Depression Disorder, and Healthy Controls

Jing Shi[1†], Hua Guo[2†], Sijia Liu[1], Wei Xue[3], Fengmei Fan[1], Hui Li[1], Hongzhen Fan[1], Huimei An[1], Zhiren Wang[1], Shuping Tan[1*], Fude Yang[1] and Yunlong Tan[1]*

[1] Beijing Huilongguan Hospital, Peking University HuiLongGuan Clinical Medical School, Beijing, China, [2] The Psychiatric Hospital of Zhumadian, Zhumadian, China, [3] Department of Clinical Pharmacology, Beijing Hospital of the Ministry of Health, Beijing, China

OPEN ACCESS

Edited by:
Kai Wang,
Anhui Medical University, China

Reviewed by:
Ryan Muetzel,
Erasmus Medical Center, Netherlands
Pedro Gomes Penteado Rosa,
Universidade de São Paulo, Brazil

***Correspondence:**
Zhiren Wang
zhiren75@163.com
Shuping Tan
shupingtan@126.com

[†]These authors have contributed equally to this work

Specialty section:
This article was submitted to Neuroimaging and Stimulation, a section of the journal Frontiers in Psychiatry

Received: 26 July 2021
Accepted: 30 November 2021
Published: 25 January 2022

Citation:
Shi J, Guo H, Liu S, Xue W, Fan F, Li H, Fan H, An H, Wang Z, Tan S, Yang F and Tan Y (2022) Subcortical Brain Volumes Relate to Neurocognition in First-Episode Schizophrenia, Bipolar Disorder, Major Depression Disorder, and Healthy Controls. Front. Psychiatry 12:747386. doi: 10.3389/fpsyt.2021.747386

Objective: To explore differences and similarities in relationships between subcortical structure volumes and neurocognition among the four subject groups, including first-episode schizophrenia (FES), bipolar disorder (BD), major depression disorder (MDD), and healthy controls (HCs).

Methods: We presented findings from subcortical volumes and neurocognitive analyses of 244 subjects (109 patients with FES; 63 patients with BD, 30 patients with MDD, and 42 HCs). Using the FreeSurfer software, volumes of 16 selected subcortical structures were automatically segmented and analyzed for relationships with results from seven neurocognitive tests from the MATRICS (Measurement and Treatment Research to Improve Cognition in Schizophrenia) Cognitive Consensus Battery (MCCB).

Results: Larger left lateral ventricle volumes in FES and BD, reduced bilateral hippocampus and amygdala volumes in FES, and lower bilateral amygdala volumes in BD and MDD were presented compared with HCs, and both FES and BD had a lower bilateral amygdala volume than MDD; there were seven cognitive dimension, five cognitive dimension, and two cognitive dimension impairments in FES, BD, and MDD, respectively; significant relationships were found between subcortical volumes and neurocognition in FES and BD but not in MDD and HCs; besides age and years of education, some subcortical volumes can predict neurocognitive performances variance.

Conclusion: The different degrees of subcortical volume lessening may contribute to the differences in cognitive impairment among the three psychiatric disorders.

Keywords: subcortical, cognitive, MRI, first episode, bipolar disorder, major depression disorder

INTRODUCTIONS

Schizophrenia (Sch), bipolar disorder (BD), and major depression disorder (MDD) are severe psychiatric disorders with complex etiology and pathophysiology that are far from being established. These disorders affect millions of people worldwide and are associated with great human and economic costs (stigma, limited activity, decreased life expectancy, and raised

healthcare costs). In general, most clinical symptoms of psychiatric disorders, such as delusions, anxiety, irritability, or insomnia, can be effectively treated by current psychopharmacological treatments. Nevertheless, cognitive deficits, which represent core deficits across severe mental disorders, do not improve and can even worsen over time. In Sch, widespread deficits across multiple cognitive domains are well documented (1, 2). Cognitive deficits in BD have been found to be mainly concentrated in attention, verbal learning/memory, and executive function domains (3, 4). Some studies reported that cognitive deficits were particularly related to executive function in MDD (5). Traditional views in neuroscience support the notion that cognitive functioning relies on the neocortical parts of the brain (6), whereas current views suggest that there are associations between cognitive dysfunction and neural distributed networks, including subcortical structures that work in parallel circuits (7).

Subcortical deficits, whether directly or combined with cortical areas, may underline cognitive impairment in normal people and patients with Sch, BD, and MDD (8, 9). Fan et al. demonstrated that the reasoning/problem-solving function was significantly correlated with the volume of the amygdala in first-episode Sch (8). Hartberg et al. (9) reported that bilateral putamen volumes were related to poorer verbal learning, executive functioning, and working memory performance in Sch, and larger left ventricular volumes were related to poorer motor speed and executive functioning in BD.

Meanwhile, previous scientific research has confirmed that subcortical structural abnormalities co-occur with widespread cortical volume reduction even in large-scale studies from the ENIGMA working groups for Sch, BD, and MDD (10–12). The most consistent findings are enlarged lateral ventricles and reduced hippocampal and amygdala volumes in these disorders. However, no studies have so far compared the subcortical structures among these three disorders, despite there being a few studies between Sch and BD or between BD and MDD. Based on previous pieces of evidence of overlapping abnormalities of subcortical structures in the disorders, all similar and different relationships are expected to occur among Sch, BD, and MDD. The purpose of the present study was to explore differences and similarities in relationships between subcortical structure volumes and neurocognition among the four subject groups, including first-episode Sch (FES), BD, MDD, and healthy controls (HCs). We hypothesized that the different degrees of cognitive function impairment in the three disorders were caused by the different degrees of subcortical structure lessening. It meant that the worse the performance of the diagnostic group in cognitive tasks, the smaller the subcortical volume might be.

MATERIALS AND METHODS

Participants

This study included a total of 109 patients with FES (43 men and 66 women), 63 patients with BD (38 men and 24 women), 30 patients with MDD (14 men and 16 women), and 42 HCs (22 men and 20 women). Patients were inpatients and outpatients from the Psychiatric Hospital of Zhumadian (a Zhumadian city-owned psychiatric hospital, Henan Province, China). HCs were also recruited from the local community from Zhumadian with good physical health, and none of them had any positive personal or family history of (or demonstrated) any clinical psychiatric disorders. All subjects were Han Chinese. More details of demographic characteristics for all subjects, as well as clinical and medical information for the patients, are summarized in **Table 1**.

The inclusion criteria of FES included the following: (1) Sch diagnosis according to the Diagnostic and Statistical Manual for Mental Disorders—Fourth Edition (DSM-IV) based on the Structured Clinical Interview; (2) male or female patients aged 16 years and older; (3) first outpatient treatment or hospitalization less than 2 weeks; (4) education for at least 6 years; and (5) right-handed confirmation based on the short version of the Edinburgh Handedness Scale. Exclusion criteria were as follows: (1) claustrophobia; (2) a history of head trauma; (3) brain organic disease confirmed by T2 magnetic resonance imaging (MRI); (4) substance dependence or drug abuse now or before; (5) learning disability or mental delay; and (6) other contraindications to MRI.

The inclusion criteria of BD included the following: (1) BD diagnosis and no history of any other Axis I disorder based on the DSM-IV; (2) scores of the Young Mania Rating Scale (YMRS) greater than 13 or scores of the 17-item Hamilton Depression Scale (HAMD-17) greater than 17; (3) male or female patients aged 16 years and older; (4) prescription drugs discontinued at least 2 months before seeking medical advice; (5) education for at least 6 years; and (6) right-handed confirmation based on the short version of the Edinburgh Handedness Scale. Exclusion criteria were the same as those for FES earlier.

Inclusion criteria for patients with MDD were as follows: (1) MDD diagnosis based on the DSM-IV; (2) scores of HAMD-17 greater than 17; and (3) number of depression episodes greater than 2. Other inclusion and exclusion criteria were the same as earlier.

All subjects gave written informed consent and were approved by the Institutional Review Board of the Psychiatric Hospital of Zhumadian. Researchers conducted a detailed questionnaire on each subject, including sociodemographic characteristics, general information, and medical and psychological conditions. More information was collected from available medical records.

Clinical Procedures

Whether the participants were inpatient or outpatient, they started their treatment without delay. YMRS, HAMD-17, HAS, and the Positive and Negative Syndrome Scale (PANSS) were used to assess the severity of patients' symptoms. Two trained physicians and clinical psychiatrists performed all clinical assessments. The intra-class correlation coefficient (ICC) on these scales between psychiatrists was greater than 0.91. If patients met the inclusion criteria mentioned earlier and the physician considered that the patient was stable enough to participate in an MRI, the patients were asked if they would like to attempt a scan. A complete case report form was filled in after providing written informed consent. An MRI was then

TABLE 1 | Demographic and clinical characteristics of patients with FES, BD, MDD, and HCs.

	FES ($n = 109$)	BD ($n = 63$)	MDD ($n = 30$)	HCs ($n = 42$)	χ^2/F	*P*	*Post-hoc*[a]
DEMOGRAPHIC INFORMATION							
Gender(M/F)	43/66	38/24	14/16	22/20	6.61	0.158	
Age (years)	24.4 ± 4.7	27.1 ± 6.4	30.2 ± 5.9	31.9 ± 6.5	16.39	**0.001**	FES>HCs, BD>HCs, FES>MDD
Edu (years)	10.3 ± 2.6	10.1 ± 2.9	9.4 ± 2.3	14.3 ± 2.9	20.88	**0.000**	HCs>FES, BD, MDD
Onset age (years)[b]	23.3 ± 4.7	-	-	-			
Illness duration (years)[c]	0.9 ± 1.2	-	-	-			
Number of manic episodes	-	3.0 ± 1.6	0	-			
Number of depression episodes	-	1.2 ± 0.8	1.8 ± 1.2	-			
SYMPTOMS							
YMRS	-	22.5 ± 12.3	3.2 ± 2.9	-			
HAMD	-	9.4 ± 9.6	21.9 ± 6.6	-			
HAMA	-	5.7 ± 7.0	20.2 ± 11.1	-			
PANSS-positive	23.8 ± 7.6	10.4 ± 3.8	-	-			
PANSS-negative	19.4 ± 7.3	7.0 ± 0.0	-	-			
PANSS-general	38.3 ± 9.8	27.8 ± 13.0	-	-			
PANSS total	81.5 ± 21.0	45.2 ± 14.5	-	-			

FES, first episode schizophrenia; BD, bipolar disorder; MDD, major depression disorder; HCs, healthy controls; M, male; F, female; YMRS, the Young Mania Rating Scale; HAMD, Hamilton Depression Scale; HAMA, Hamilton Anxiety Scale; PANSS, Positive and Negative Syndrome Scale.

[a]*Bonferroni post-hoc tests.*

[b]*Onset age was defined as the time when the patient him/herself or his/her family noticed first symptoms of the disease.*

Bold font indicates that the p value is less than 0.05.

scheduled. All patients completed the MRI scan within 2 weeks after starting their medication treatment.

Image Acquisition

All MRIs were carried out on a GE Signa HDxT 3.0T MRI scanner (GE Medical Systems, LLC, USA). Subjects were placed in a birdcage head coil and individually fitted to a bite bar partially composed of a dental impression compound attached to the coil to reduce head motion. T1-weighted images were acquired by covering the whole brain with a sagittal 3D-MPRAGE (magnetization prepared rapid acquisition gradient echo) sequence: repetition time (TR) = 6.77 ms, echo time (TE) = 2.488 ms, inversion time (TI) = 1,100 ms, field of view (FOV) = 256 × 256 mm^2, matrix size = 256 × 256, flip angle = 7°, and thickness/gap = 1/0 mm.

Magnetic Resonance Imaging Data Processing

In this study, subcortical volumes were extracted using Freesurfer software version 5.3.0 (http://surfer.nmr.mgh.harvard.edu/) through a standard procedure, which included motion correction, automated topology corrections, intensity normalization, and automatic segmentation of cortical and subcortical regions, and was documented elsewhere (13, 14). Specifically, the corresponding volumes of eight regions from each hemisphere (17 in total) were chosen, and the total gray volumes were calculated for the investigations, labeled as lateral ventricle, thalamus, caudate, putamen, pallidum, hippocampus, amygdala, nucleus accumbens, and total gray volumes. For quality control, we followed the ENIGMA guideline (http://enigma.ini.usc.edu/): all regions larger than 1.5 or less than 1.5 times the quartile space were identified and visually inspected by overlaying their segmentations on the subjects' anatomical images. A blinded manual check of image quality was conducted to diagnose group identity for: motion artifacts, removal of non-brain tissue and missing brain parts after skull stripping, white matter segmentation, correction of pial surface and any surface that does not follow white/gray matter boundary, and correction of subcortical segmentation caused by ventricular enlargement. Only images whose segmentation was judged to be accurate upon visual inspection were subjected to statistical analyses.

Cognitive Measures

All subjects completed the MATRICS (Measurement and Treatment Research to Improve Cognition in Schizophrenia) Cognitive Consensus Battery (MCCB) that responds to the need for a reliable, consensus-based set of standards for measuring the change in the cognitive deficits of Sch or other disorders (15, 16) within a week of finishing MRI scanning. The MCCB includes seven cognitive domains: (1) speed of processing: symbol coding, trail making test, part A, category fluency; (2) attention and vigilance: continuous performance test; (3) working memory: spatial span, digit sequencing test; (4) verbal learning: Hopkins Verbal Learning Test; (5) visual learning: brief visuospatial memory test; (6) reasoning/problem solving: mazes; and (7) social cognition: managing emotions. Raw scores were recorded and converted to Chinese-normalized T-scores. Seven-domain T-scores and a composite T-score were calculated.

Statistical Analyses

All analyses were conducted using SPSS software (version 20.0). Continuous variables first determined the data distribution before statistical analyses. The continuous variables that conformed to the normal distribution were analyzed by variance; the other continuous variables were tested by nonparametric test. The G*Power 3.1.9.2 program (http://www.softpedia.com/get/Science-CAD/G-Power.shtml) was used to perform a *post-hoc* power calculation for all difference tests ($\alpha = 0.05$).

Group Differences in Demographic, Clinical, and Subcortical Volume Variables and Neurocognition

Demographic and clinical characteristics were compared across groups using a Student's *t*-test or one-way analysis of variance for continuous variables and chi-square analysis for categorical variables. Group comparisons of neuropsychological variables (T-scores) were made using univariate analysis with age, sex, and years of education as covariates. When subcortical volumes were compared across groups, a univariate analysis was performed, and age, sex, and total intracranial volume (ICV) were controlled. ICV was used as a covariate to account for differences in head size. However, there were two possible reasons for the change of ICV: the first was that it was driven by a smaller subset of regions, and the second was that it appeared to be a global effect that could be dramatically attenuated with adjustment. So, to show the changes of subcortical volumes more comprehensively, a similar analysis unadjusted for ICV was performed. A Bonferroni procedure (adjusted $P = \mathrm{P} \times 17$ for subcortical volume, adjusted $P = P \times 8$ for neurocognition) was performed for *post-hoc* comparisons between two groups. Uncorrected *P*-values were reported throughout and followed by an adjusted *P*-value when a test was significant. Adjusted $P < 0.05$ was deemed significant. Effect sizes were calculated using Cohen's d. Correlation analysis between subcortical volumes and neurocognition.

Only the variables that showed statistically significant differences among groups were included in the subsequent analyses. To examine the correlation between subcortical volumes and neurocognition, a correlate analysis was conducted, and Pearson product-moment correlation coefficients were used. First, the correlate analysis was performed for the combined sample, then within each group. The subcortical measures in the left and right hemispheres and T-scores of the seven neurocognitive domains were entered into the analysis with age and ICV as covariates. Adjusted $P = P \times 48$ (6 significant differences regions × 8 significant differences cognitive parameters) for Bonferroni connection.

Group Differences in Correlations Between Subcortical Volumes and Neurocognition

Next, the group differences in correlation between subcortical volumes and neurocognition were compared. The way to do this was by transforming the partial correlation coefficient values from the correlation analysis into z scores. It is also known as Fisher's r to z transformation, and its significance was calculated with an online calculator when two correlation values and different sample sizes were entered (http://www.ocpaz.org/tongji/tongji.html).

Effect of Subcortical Volumes on Neurocognition

Given that correlation analysis was the basis and premise of regression analysis, whereas regression analysis was the deepening and continuation of correlation analysis, hierarchical multiple regression analysis using age, sex, and years of education as the first step, subcortical volumes as the second step, was applied to test predictors of subcortical volume change on cognitive performance.

RESULTS

Demographic and Clinical Characteristics

The demographic and clinical characteristics are summarized in **Table 1**. Significant differences were found in age among the groups ($F = 16.39$, $P = 0.001$). *Post-hoc* tests revealed that differences between FES and HCs, between BD and HCs, and between FES and MDD were statistically significant ($P = 0.014$, 0.023, and 0.035, respectively). HCs and MDD were older than FES and BD. There was a significant difference in years of education among groups ($F = 20.88$, $P = 0.000$). *Post hoc* tests showed that HCs had greater years of education than FES, BD, and MDD ($P = 0.022$, 0.026, and 0.001, respectively). There was no significant sex difference between groups ($\chi^2 = 6.61$, $P = 0.158$).

Effect Sizes for Group Differences in Subcortical Volumes

Firstly, we assessed case–control differences between each diagnosis group and HCs across 17 brain structures (**Figure 1A**). A univariate analysis with age, sex, and ICV as covariates showed that left lateral ventricle volumes were significantly larger in FES and BD compared with HCs [Cohen's d (95% confidence interval): $d = 0.21$ (0.02, 0.39), 0.38 (0.18, 0.59), $P = 4.20 \times 10^{-4}$, 8.7×10^{-4}, respectively]. After Bonferroni correction, the results were still significant (adjusted $P = 0.007$ and 0.014, respectively). Left hippocampus/amygdala and right hippocampus/amygdala/thalamus volumes were significantly lower in FES compared with HCs [Cohen's d (95% confidence interval): $d = -0.88$ (-1.06, -0.7), -0.76 (-0.96, -0.59), -0.82 (-0.99, -0.63), -0.80 (-0.99, -0.63), -0.69 (-0.85, -0.49), $P = 5.7 \times 10^{-5}$, 6.3×10^{-4}, 1.6×10^{-3}, 3.7×10^{-4}, 2.8×10^{-5}, adjusted $P = 9.1 \times 10^{-3}$, 1.1×10^{-2}, 2.6×10^{-2}, 5.9×10^{-3}, 4.2×10^{-4}, respectively]. Bilateral amygdala and right hippocampus volumes were significantly lower in BD compared with HCs [Cohen's d (95% confidence interval): $d = -0.51$ (-0.73, -0.32), -0.58 (-0.80, -0.39), -0.69 (-1.02, -0.36), $P = 4.1 \times 10^{-4}$, 4.3×10^{-5}, 7.8×10^{-4}, adjusted $P = 6.6 \times 10^{-3}$, 6.9×10^{-4}, 1.2×10^{-2}, respectively]. When ICV was not adjusted, more significant differences were shown in FES, BD, and MDD compared with HCs. Specific details can be seen in **Supplementary Table 1**. Secondly, we performed a pairwise comparison with age, sex, and ICV in subcortical volumes among the three diagnosis groups across 17 brain structures (**Figure 1B**). The results revealed that bilateral amygdala volume and the right hippocampus volume were significantly lower in FES than in MDD [Cohen's d (95% confidence interval): $d = -0.78$ (-0.98, -0.57), -0.65 (-0.86, -0.44), -0.65 (-0.86, -0.44), $P = 5.7 \times$

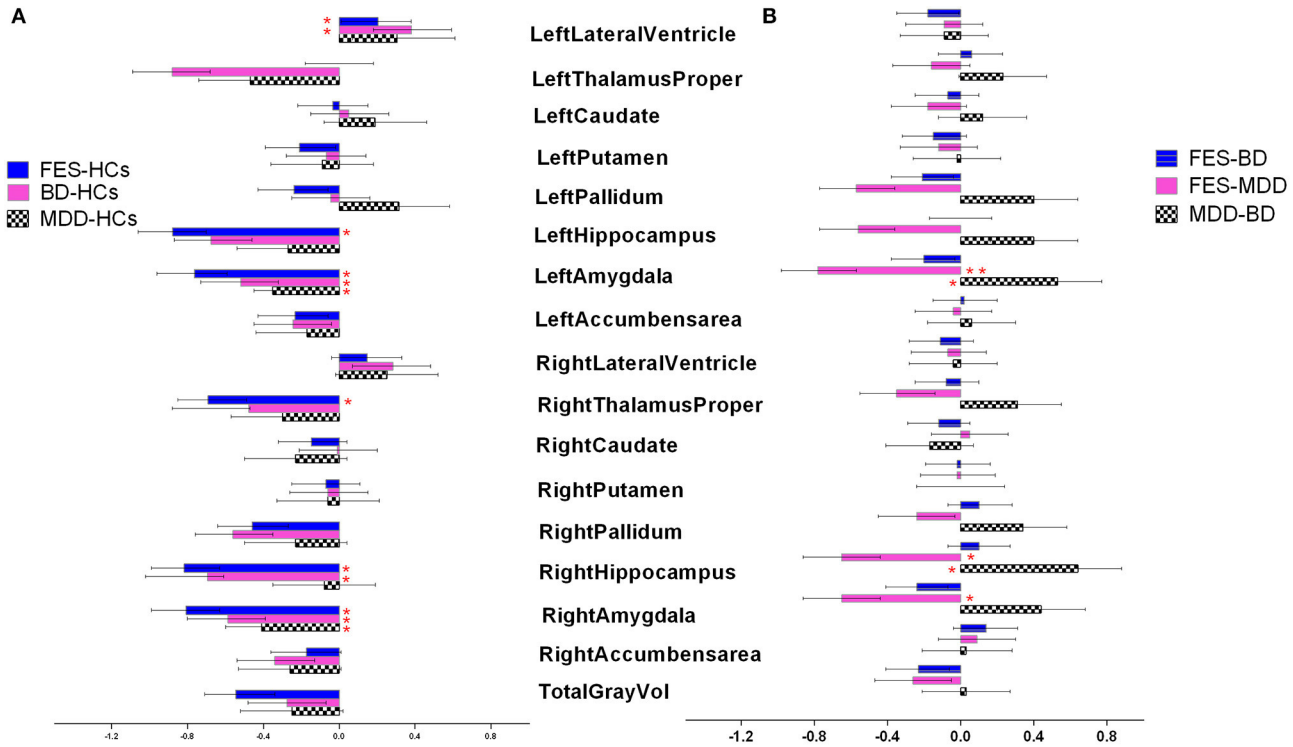

FIGURE 1 | (A,B) Cohen's d effect sizes 95% CI and for regional brain volume differences. Effect sizes for all subcortical volumes depicted were corrected for age and intracranial volume (ICV). FES, first episode schizophrenia; BD, bipolar disorder; MDD, major depression disorder; HCs, healthy controls.

10^{-4}, 2.1×10^{-3}, 1.9×10^{-3}, adjusted $P = 9.2 \times 10^{-3}$, 3.4×10^{-2}, 3.0×10^{-2}, respectively]. Both the left amygdala volume and right hippocampus volume were significantly lower in BD than in MDD [Cohen's d (95% confidence interval): $d = -0.53$ (-0.77, -0.28), -0.64 (-0.88, -0.40), $P = 2.1 \times 10^{-3}$, 5.5×10^{-4}, adjusted $P = 3.4 \times 10^{-2}$, 8.8×10^{-3}, respectively]. There was no significant difference in 17 subcortical volumes between FES and BD. When ICV was not adjusted, more significant differences were found between the three diagnostic groups (see **Supplementary Table 2**).

The statistical power for them is shown in **Supplementary Table 3**.

Group Differences in Neurocognitive Tests Among First-Episode Schizophrenia, Bipolar Disorder, Major Depression Disorder, and Healthy Controls

As shown in **Figure 2**, a univariate analysis with age, sex, and years of education as covariates revealed that group differences were significant in the T-scores of seven cognitive domains and the composite T-scores ($F = 53.8$, 68.4, 45.5, 24.0, 33.4, 55.5, 21.2, and 77.4, Cohen's $d = 0.57$, 0.61, 0.53, 0.41, 0.47, 0.57, 0.39, and 0.63, all $P < 10^{-4}$). Bonferroni *post hoc* tests revealed that the T-scores of seven cognitive domains and the composite T-scores were significantly lower in FES compared with HCs (all $P < 10^{-5}$). Patients with BD performed poorer in the speed of processing, attention and vigilance, working memory, visual learning, and reasoning/problem-solving than HCs, and composite T-scores were significantly lower in BD compared with HCs (all $P < 10^{-5}$). The T-scores of the speed of processing and reasoning/problem-solving were significantly lower in MDD compared with HCs (both $P < 10^{-4}$). The patients with FES had lower T-scores of attention and vigilance, working memory, and composite T-scores than those with MDD (both $P < 10^{-4}$). There was no significant difference between FES and BD or between BD and MDD in any test ($P > 0.05$). The statistical power and Cohen's d for group differences are shown in **Supplementary Tables 4**, **5**, respectively.

Relationships Between Subcortical Volumes and Neurocognition

The results of the relationships between subcortical volumes and neurocognition are presented in **Figure 3**. In the FES, significant relationships were found between larger left lateral ventricle volume and lower T-scores of speed of processing ($r = -0.35$, $P = 5.7 \times 10^{-4}$, adjust $P = 0.028$) and between smaller left hippocampus volume and poorer performances on working memory ($r = 0.46$, $P = 1.3 \times 10^{-4}$, adjust $P = 0.006$) and verbal learning ($r = 0.43$, $P = 4.1 \times 10^{-4}$, adjust $P = 0.020$). In BD, larger left lateral ventricle volume was significantly related to poorer speed of processing ($r = -0.31$, $P = 8.9 \times 10^{-4}$, adjust $P = 0.044$), and smaller left amygdala volume was related to reasoning/problem-solving ($r = 0.39$, $P = 7.7 \times 10^{-4}$, adjust P

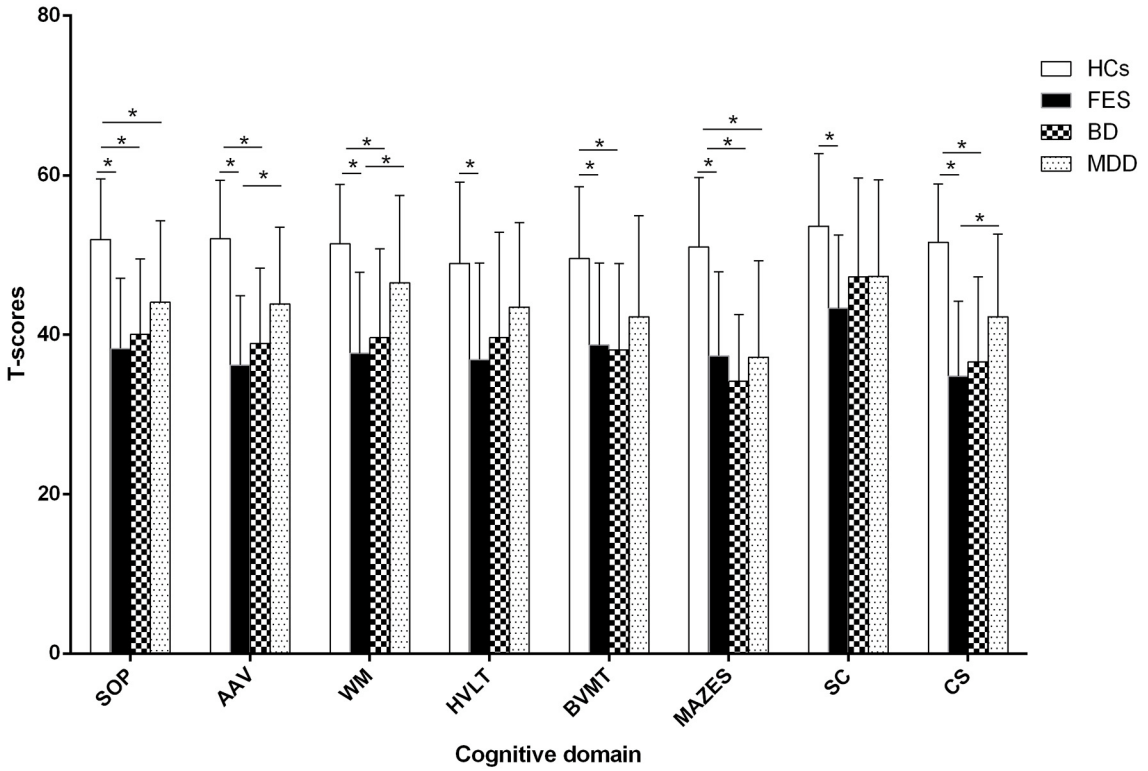

FIGURE 2 | Comparison of cognitive function among groups. * represents Bonfferoni corrected $P < 0.05/7$=0.007. SOP: speed of processing, AAV: attention and vigilance, WM: working memory, HVLT: Hopkins Verbal Learning Test, BVMT: Brief Visuospatial Memory TestM, SC: social cognition, CS: composite T-score, FES: first episode schizophrenia, BD: bipolar disorder, MDD: major depression disorder, HCs: healthy controls.

$= 0.038$) and social cognition ($r = 0.51$, $P = 2.5 \times 10^{-4}$, adjust $P = 0.012$). There were no relationships found in the combined sample, MDD, or HCs for any structures and neurocognition ($P > 0.05/7$ regions $\times$ 7 neurocognition domains $= 0.001$).

Group Differences in Correlations Between Subcortical Volumes and Neurocognition

As shown in **Table 2**, the correlations between the left hippocampus and working memory in FES were significantly different from BD and HCs ($z = 2.12, 2.72$, $P = 0.034, 0.0065$) and were similar among BD, MDD, and HCs. The correlations between the left hippocampus and verbal learning differentiated the patients with FES from BD and HCs ($z = 2.13, 2.58$, $P = 0.033, 0.0099$), whereas their correlations were similar among BD, MDD, and HCs. The correlations between the left amygdala and social cognition were also significantly different in BD compared with FES ($z = -2.16$, $P = 0.0091$), and the same pattern of relationships was observed between BD and HCs ($z = 2.39$, $P = 0.017$).

Effect of Subcortical Volumes on Neurocognition

The hierarchical multiple regression analysis indicated that within the Sch group, age and left lateral ventricle volumes were significant predictors of verbal learning performance (both $P = 0.000$), accounting for 18.3 and 17.7% of verbal learning score variance, respectively. For working memory performance, age, years of education, and right hippocampus volumes were significant predictors (all $P = 0.000$), accounting for 19.4, 11.6, and 16.8% of working memory score variance, respectively.

In the BD group, age, years of education, and left amygdala volume were significant predictors (all $P = 0.000$), accounting for 17.7, 12.2, and 14.9% of working memory score variance, respectively. No significant predictor was found in the MDD group. **Table 3** summarizes statistically significant results from the hierarchical multiple regression analysis.

The statistical power for all analyses is shown in **Supplementary Table 3**.

DISCUSSION

The major findings of this study include: (1) larger left lateral ventricle volumes in FES and BD, reduced bilateral hippocampus and amygdala volumes in FES, and lower bilateral amygdala volumes in BD and MDD were presented compared with HCs, and both FES and BD had a lower bilateral amygdala volume than MDD; (2) a comprehensive impairment in seven cognitive dimensions was found in FES, patients with BD had impairment in five cognitive dimensions, and only two cognitive dimensions deficit were shown in MDD, all measured

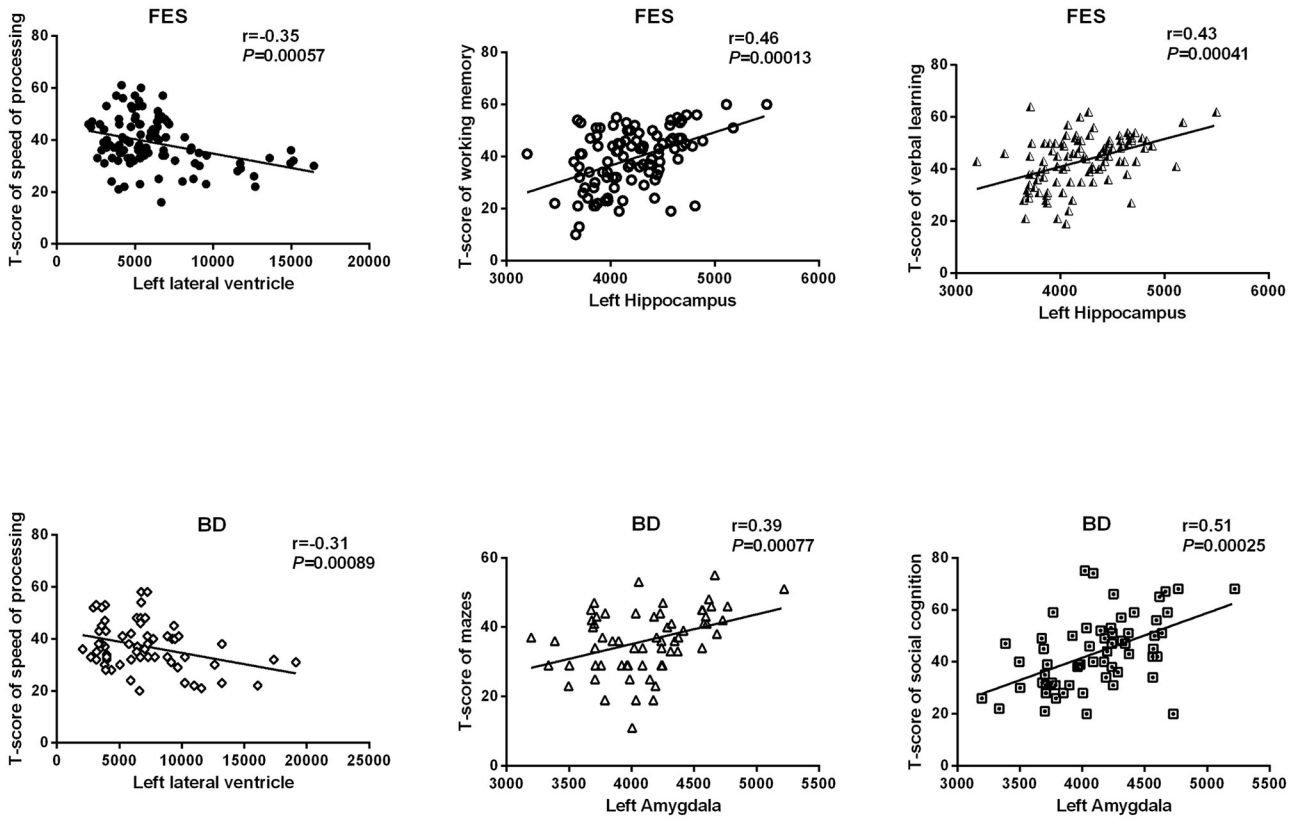

FIGURE 3 | Relationships between subcortical volumes and neurocognition. FES, first episode schizophrenia; BD, bipolar disorder.

TABLE 2 | Pairwise contrasts of correlations between subcortical volumes and neurocognitive tests.

	Group relationships				Pairwise contrasts											
	FES	BD	MDD	HCs	FES-HCs		BD-HCs		MDD-HCs		FES-BD		FES-MDD		BD-MDD	
	r				*z*	*P*	*z*	*P*	*z*	*P*	*z*	*P*	*z*	*P*	*z*	*P*
Subcortical volume/test																
Left lateral ventricle/SOP	−0.35[a]	−0.31[a]	−0.15	−0.16	−1.09	0.28	−0.77	0.44	0.04	0.96	−0.28	0.78	−0.99	0.32	−0.73	0.46
Left Hippocampus/WM	0.46[a]	0.058	0.11	0.10	2.12	**0.034**	−0.21	0.83	0.04	0.97	2.72	**0.0065**	1.79	0.07	−0.23	0.82
Left Hippocampus/VL	0.43[a]	0.043	0.24	0.06	2.13	**0.033**	−0.08	0.93	0.74	0.46	2.58	**0.0099**	1.00	0.32	−0.87	0.38
Left Amygdala/Mazes	0.23	0.39[a]	−0.039	0.05	0.98	0.32	1.76	0.078	−0.36	0.72	−1.1	0.27	1.27	0.21	1.95	0.05
Left Amygdala/SC	0.14	0.51[a]	0.19	0.07	0.38	0.71	2.39	**0.017**	0.49	0.62	−2.61	**0.0091**	−0.24	0.81	1.60	0.11

FES, first episode schizophrenia; BD, bipolar disorder; MDD, major depression disorder; HCs, healthy controls; SOP, speed of processing; WM, working memory; VL, verbal learning; SC, social cognition.

Bold font indicates that the p value is less than 0.05. [a]*P < 0.05.*

by MCCB; (3) significant relationships were found between subcortical volumes and neurocognition in FES and in BD but not in MDD and HCs; (4) besides age and years of education, some subcortical volumes can predict neurocognitive performances variance. To the best of our knowledge, this is the first study investigating the relationship between subcortical structure and cognitive function in the three disorders and HCs. In addition, the relationships were directly compared across the four groups.

Cognitive impairment is a core feature of neuropsychiatric disorders. More importantly, cognitive impairments persist after clinical remission and lead to social and occupational disability, contributing to the biggest social and economic burden of these neuropsychiatric disorders (17, 18). However, clinical treatment with replicable effects to treat cognitive deficits has not been available so far, one reason of which is that the mechanism of cognitive impairment is poorly understood. The hippocampus may play a key role in cognitive impairment and improvement

TABLE 3 | The hierarchical multiple regression analysis for neurocognition in patients with FES and BD*.

Group	Cognitive domains	Variable	B	S.E.	95%CI	β	t	Sig.	Adjusted R square(%)	*F*	*p*
FES	Verbal learning	Age	−0.34	0.09	−0.49∼-0.19	−0.46	−4.58	0.000	18.3	17.72	0.000
		Left lateral ventricle volumes	0.12	0.01	0.00∼0.12	0.43	4.19	0.000	17.7		
	Working memory	Age	−0.55	0.08	−0.87∼-0.23	−0.47	−4.65	0.000	19.4	15.48	0.000
		Years of education	0.43	0.11	0.12∼0.73	0.29	2.82	0.007	11.6		
		Right Hippocampus volume	0.38	0.00	0.14∼0.62	0.49	4.83	0.000	16.8		
BD	Working memory	Age	−0.41	0.06	−0.54∼-0.28	−0.39	−5.04	0.000	17.7	16.70	0.000
		Years of education	0.49	0.14	0.19∼0.79	0.24	2.74	0.009	12.2		
		Left amygdale volume	0.27	0.02	0.03∼0.24	0.45	4.33	0.000	14.9		

FES, first episode schizophrenia; BD, bipolar disorder.

**age, sex and years of education as the first step and subcortical volumes as the second step.*

of cognition due to its critical role in memory and learning. The present study found significantly reduced hippocampus volumes in FES consistent with most similar studies on Sch (19, 20); notably, it was demonstrated that hippocampal volume deficits were more severe in samples with a higher proportion of unmedicated patients in the large sample from the ENIGMA work team (11), indicating that reduced hippocampal volumes were not moderated by the duration of illness or medicine. In our next correlation analysis and hierarchical regression analysis, the relationship between hippocampus volumes and cognitive performance was shown. All these results suggested that the change of hippocampal volumes seemed to be a promising candidate neural marker for cognitive impairment.

It has been suggested that the changes of hippocampal volume in these disorders reflect the decrease of neural plasticity and neurogenesis, which may be downstream effects of abnormally elevated levels of cytokines and cortisol, such as interleukin-1 and tumor necrosis factor-α (21–23). A meta-analysis of blood cytokine network alteration comparison between Sch, BD, and MDD verified that levels of two cytokines (interleukin-6 and tumor necrosis factor-α), one soluble cytokine receptor (sIL-2R), and one cytokine receptor antagonist (IL-1RA) were diversely increased in acutely ill patients with Sch, bipolar mania, and MDD compared with controls (24). Actually, reduced hippocampal volumes were shown not only in FES but also in BD and even MDD in this study (see **Figure 1A**), despite the biggest effect size in FES. This further confirmed that volumetric hippocampal changes might be associated with aberrant blood cortisol and cytokine levels. In addition, the increase of hippocampal volume may be due to other mechanisms, such as dendritic sprouting or enhancement of brain-derived neurotrophic factor (BDNF) in the hippocampus (21). However, biochemical and immune studies were indeed not involved in the present study. Relevant hypotheses may be verified in further study.

Our other findings included lower bilateral amygdala volumes in all three diagnosis groups compared with HCs, with the biggest effect size in FES and the smallest in MDD. In Sch, a relative certainty was that amygdala volume was reduced compared with HCs. For example, three large-scale meta-analyses showed a statistically significant reduction in the amygdala volume in Sch despite low to moderate effect sizes ($d \approx 0.2$) (11, 25–27). However, in BD, there is considerable heterogeneity between studies about amygdala volume. More results showed less pronounced volumetric reductions than in Sch (28, 29), whereas some studies found that the amygdala in BD had more extensive shrinkage than in Sch (30). This discrepancy in findings may stem from differences in medication history, clinical severity and duration, and comorbidities. Differences in neuroimaging data acquisition, amygdala segmentation, and analysis approaches can further affect research results. Few studies have compared subcortical volume between Sch and MDD, but the subcortical comparison between unipolar and bipolar depression has found that the amygdala volume of bipolar depression is smaller than that of unipolar depression (31).

The present study demonstrated that amygdala volume was positively correlated with reasoning/problem-solving and social cognition and predicted 14.9% of working memory performance variance in BD. The amygdala is a fascinating, complex structure that is well known for its involvement in emotion processing, but it has also been documented to be involved in a surprisingly broad array of cognitions, spanning from attention, working memory to long-term memory (32–34). Firstly, the amygdala can regulate the emotional content effect in attention, working memory, and long-term memory. Its mechanism may be realized through the structural and functional connection between the amygdala with the visual cortex, hippocampus, and other brain tissues (35). Among them, the norepinephrine pathway regulates the interaction between the amygdala and hippocampus to complete the memory of emotional content (36). Secondly, the amygdala is involved in difficult working memory tasks, motivational stimulus monitoring tasks, etc. These tasks do not contain any emotional stimuli. Dopamine may play an important role in the interaction between the amygdala and working memory (37). Furthermore, the relationship between the amygdala and cognitive system is bidirectional, which depends on the limbic system and functional connectivity system of the cortical structure (38). Interestingly, hemispheric lateralization seems to appear in FES *vs.* HCs and MDD *vs.* HCs when ICV was not considered, and only effect size between each diagnosis

group and HCs was observed, as there were more subcortical structures with significant differences on the left hemisphere (see **Supplementary Table 1**). Numerous results support the existence of reduced leftward asymmetry in patients with Sch or MDD (39, 40), for example, in the premotor, occipitoparietal, and prefrontal regions for patients with FES (41) or in the cortical–striatal–pallidal–thalamic circuit for patients with MDD (40). Patients with Sch have also been noted to exhibit decreased leftward anatomical asymmetry of the planum temporale or the superior temporal gyrus (42), with some patients even showing rightward asymmetry of the planum temporale (43). Besides brain structural hemispheric lateralization, functional MRI allows the computation of functional cerebral inter-hemisphere differences reflecting the leftward or rightward dominance of activations for a specific task even in the resting state (44). The physiological mechanism of hemispheric lateralization is not well known. Some scholars propose a model in which early life stress and chronic stress not only increase the risk for psychiatric or neurodevelopmental disorders but also change structural and functional hemispheric asymmetries resulting in the aberrant lateralization patterns seen in these disorders. Therefore, pathology-related changes in hemispheric asymmetries are not a factor causing disorders but rather a different phenotype, primarily stress (45).

Several limitations should not be ignored in this study. Firstly, our sample size was not balanced among the groups, especially it was comparatively small in the MDD group, which could lead to false-positive or false-negative results due to the weak statistical power; secondly, this study was not a longitudinal observational study, so it could not provide the course of subcortical volumes with the duration of illness. Thirdly, patients with Sch enrolled in the present study were first-episode patients, whereas neither patients with BD nor MDD were. Actually, if patients with BD were first-episode patients, they had to be undergoing their first manic episode and were in a manic phase. Such a sample in the BD group was limited to the manic phase. However, patients with first-episode unipolar depression clinically showed a relatively high rate of switching to manic in the later stage, but this risk would reduce for patients with recurrent depression. Therefore, to minimize the impact of drugs on patients and consider the comparability with FES, one of our inclusion criteria for BD and MDD was that prescription drugs were discontinued at least 2 months before seeking medical advice.

Based on the results of this study, we found that the effect size was the largest in FES, second in BD, and the smallest in MDD even in the brain regions with no statistical difference between the two groups, suggesting that brain damage may be the most serious in Sch and relatively mild in MDD. We also identified that FES performed the worst in cognitive function, whereas MDD was the best. Combining the relationship between cognitive function and subcortical volumes, these results supported our inference that the difference of subcortical volumes injury may be contributed to the difference of cognitive impairment in three psychiatric disorders.

DATA AVAILABILITY STATEMENT

The original contributions presented in the study are included in the article/**Supplementary Material**, further inquiries can be directed to the corresponding authors.

ETHICS STATEMENT

The studies involving human participants were reviewed and approved by the Institutional Review Board of the Psychiatric Hospital of Zhumadian. The patients/participants provided their written informed consent to participate in this study. Written informed consent was obtained from the individual(s) for the publication of any potentially identifiable images or data included in this article.

AUTHOR CONTRIBUTIONS

JS and HG appraised potential studies and wrote and revised the draft manuscript. ZW and ST designed the study and revised the draft manuscript. SL, HL, and HA assisted with the presentation of findings and assisted with drafting and revising the manuscript. FF and HF assisted with statistical analysis. FY and YT conceived and designed the study. All authors read and approved the final manuscript.

FUNDING

This work was supported by Capital's Funds for Health Improvement and Research (2020-4-2135 and 2018-4-2133), the Beijing Natural Science Foundation (7214238 and 7162087), the Beijing Excellent Talent Traning Program (2016000021469G175), the Beijing Municipal Science and Technology Project (Z181100001518005 and Z171100001017021), the Beijing Municipal Special Foundation for High-Level Health Technology Personnel Construction (PX2016010), Beijing Municipal Science and Technology Commission grant (Z141107002514016), Beijing Municipal Administration of Hospitals Clinical Medicine Development of Special Funding (XMLX201609), and Beijing Hospital Authority Training Plan (PX2018069).

SUPPLEMENTARY MATERIAL

The Supplementary Material for this article can be found online at: https://www.frontiersin.org/articles/10.3389/fpsyt.2021.747386/full#supplementary-material

REFERENCES

1. Jones MT, Deckler E, Laurrari C, Jarskog LF, Penn DL, Pinkham AE, et al. Confidence, performance, and accuracy of self-assessment of social cognition: a comparison of schizophrenia patients and healthy controls. *Schizophrenia Res Cogn.* (2020) 19:002–2. doi: 10.1016/j.scog.2019.01.002
2. Garcia RR, Aliste F, Soto G. Social cognition in schizophrenia: cognitive and neurobiological aspects. *Rev*

Colomb Psiquiatr. (2018) 47:170–6. doi: 10.1016/j.rcpeng.2018.06.004
3. Van Rheenen TE, Lewandowski KE, Tan EJ, Ospina LH, Ongur D, Neill E, et al. Characterizing cognitive heterogeneity on the schizophrenia-bipolar disorder spectrum. *Psychol Med.* (2017) 47:1848–64. doi: 10.1017/S0033291717000307
4. Van Rheenen TE, Bryce S, Tan EJ, Neill E, Gurvich C, Louise S, et al. Does cognitive performance map to categorical diagnoses of schizophrenia, schizoaffective disorder and bipolar disorder? A discriminant functions analysis. *J Affect Disord.* (2016) 192:109–15. doi: 10.1016/j.jad.2015.12.022
5. Lee SA, Kim MK. Effect of low frequency repetitive transcranial magnetic stimulation on depression and cognition of patients with traumatic brain injury: a randomized controlled trial. *Med Sci Monit.* (2018) 24:8789–94. doi: 10.12659/MSM.911385
6. Stuss DT, Floden D, Alexander MP, Levine B, Katz D. Stroop performance in focal lesion patients: dissociation of processes and frontal lobe lesion location. *Neuropsychologia.* (2001) 39:771–86. doi: 10.1016/S0028-3932(01)00013-6
7. Middleton FA, Strick PL. Basal ganglia output and cognition: evidence from anatomical, behavioral, and clinical studies. *Brain Cogn.* (2000) 42:183–200. doi: 10.1006/brcg.1999.1099
8. Fan F, Xiang H, Tan S, Yang F, Fan H, Guo H, et al. Subcortical structures and cognitive dysfunction in first episode schizophrenia. *Psychiatry Res Neuroimaging.* (2019) 286:69–75. doi: 10.1016/j.pscychresns.2019.01.003
9. Hartberg CB, Sundet K, Rimol LM, Haukvik UK, Lange EH, Nesvag R, et al. Subcortical brain volumes relate to neurocognition in schizophrenia and bipolar disorder and healthy controls. *Prog Neuropsychopharmacol Biol Psychiatry.* (2011) 35:1122–30. doi: 10.1016/j.pnpbp.2011.03.014
10. Ho TC, Gutman B, Pozzi E, Grabe HJ, Hosten N, Wittfeld K, et al. Subcortical shape alterations in major depressive disorder: Findings from the ENIGMA major depressive disorder working group. *Hum Brain Mapp.* (2020) doi: 10.1101/534370
11. van Erp TG, Hibar DP, Rasmussen JM, Glahn DC, Pearlson GD, Andreassen OA, et al. Subcortical brain volume abnormalities in 2028 individuals with schizophrenia and 2540 healthy controls via the ENIGMA consortium. *Mol Psychiatry.* (2016) 21:585. doi: 10.1038/mp.2015.118
12. McWhinney SR, Abe C, Alda M, Benedetti F, Boen E, Del Mar Bonnin C, et al. Association between body mass index and subcortical brain volumes in bipolar disorders-ENIGMA study in 2735 individuals. *Mol Psychiatry.* (2021) 6:6806–19. doi: 10.1038/s41380-021-01098-x
13. Fischl B. FreeSurfer. *Neuroimage.* (2012) 62:774–81. doi: 10.1016/j.neuroimage.2012.01.021
14. Jovicich J, Czanner S, Greve D, Haley E, van der Kouwe A, Gollub R, et al. Reliability in multi-site structural MRI studies: effects of gradient non-linearity correction on phantom and human data. *Neuroimage.* (2006) 30:436–43. doi: 10.1016/j.neuroimage.2005.09.046
15. Nuechterlein KH, Green MF, Kern RS, Baade LE, Barch DM, Cohen JD, et al. The MATRICS Consensus Cognitive Battery, part 1: test selection, reliability, and validity. *Am J Psychiatry.* (2008) 165:203–13. doi: 10.1176/appi.ajp.2007.07010042
16. Yatham LN, Torres IJ, Malhi GS, Frangou S, Glahn DC, Bearden CE, et al. The international society for bipolar disorders-battery for assessment of neurocognition (ISBD-BANC). *Bipolar Disord.* (2010) 12:351–63. doi: 10.1111/j.1399-5618.2010.00830.x
17. Jensen JH, Knorr U, Vinberg M, Kessing LV, Miskowiak KW. Discrete neurocognitive subgroups in fully or partially remitted bipolar disorder: associations with functional abilities. *J Affect Disord.* (2016) 205:378–86. doi: 10.1016/j.jad.2016.08.018
18. Palazzo MC, Arici C, Cremaschi L, Cristoffanini M, Dobrea C, Dell'Osso B, et al. Cognitive performance in euthymic patients with bipolar disorder vs healthy controls: a neuropsychological investigation. *Clin Pract Epidemiol Ment Health.* (2017) 13:71–81. doi: 10.2174/1745017901713010071
19. Wen D, Wang J, Yao G, Liu S, Li X, Li J, et al. Abnormality of subcortical volume and resting functional connectivity in adolescents with early-onset and prodromal schizophrenia. *J Psychiatr Res.* (2021) 140:282–8. doi: 10.1016/j.jpsychires.2021.05.052
20. Heller C, Weiss T, Del Re EC, Swago S, Coman IL, Antshel KM, et al. Smaller subcortical volumes and enlarged lateral ventricles are associated with higher global functioning in young adults with 22q11.2 deletion syndrome with prodromal symptoms of schizophrenia. *Psychiatry Res.* (2021) 301:113979. doi: 10.1016/j.psychres.2021.113979
21. Miskowiak KW, Vinberg M, Macoveanu J, Ehrenreich H, Koster N, Inkster B, et al. Effects of erythropoietin on hippocampal volume and memory in mood disorders. *Biol Psychiatry.* (2015) 78:270–7. doi: 10.1016/j.biopsych.2014.12.013
22. Zhao YT, Zhang L, Yin H, Shen L, Zheng W, Zhang K, et al. Hydroxytyrosol alleviates oxidative stress and neuroinflammation and enhances hippocampal neurotrophic signaling to improve stress-induced depressive behaviors in mice. *Food Funct.* (2021) 12:5478–87. doi: 10.1039/D1FO00210D
23. Czeh B, Lucassen PJ. What causes the hippocampal volume decrease in depression? Are neurogenesis, glial changes and apoptosis implicated? *Eur Arch Psychiatry Clin Neurosci.* (2007) 257:250–60. doi: 10.1007/s00406-007-0728-0
24. Goldsmith DR, Rapaport MH, Miller BJ. A meta-analysis of blood cytokine network alterations in psychiatric patients: comparisons between schizophrenia, bipolar disorder and depression. *Mol Psychiatry.* (2016) 21:1696–709. doi: 10.1038/mp.2016.3
25. Haijma SV, Van Haren N, Cahn W, Koolschijn PC, Hulshoff Pol HE, Kahn RS. Brain volumes in schizophrenia: a meta-analysis in over 18 000 subjects. *Schizophr Bull.* (2013) 39:1129–38. doi: 10.1093/schbul/sbs118
26. Okada N, Fukunaga M, Yamashita F, Koshiyama D, Yamamori H, Ohi K, et al. Abnormal asymmetries in subcortical brain volume in schizophrenia. *Mol Psychiatry.* (2016) 21:1460–6. doi: 10.1038/mp.2015.209
27. Cohen J. *Statistical Power Analysis for the Behavioral Sciences*. Rev. ed. New York, NY: Academic Press (1977).
28. Kempton MJ, Geddes JR, Ettinger U, Williams SC, Grasby PM. Meta-analysis, database, and meta-regression of 98 structural imaging studies in bipolar disorder. *Arch Gen Psychiatry.* (2008) 65:1017–32. doi: 10.1001/archpsyc.65.9.1017
29. Hibar DP, Westlye LT, van Erp TG, Rasmussen J, Leonardo CD, Faskowitz J, et al. Subcortical volumetric abnormalities in bipolar disorder. *Mol Psychiatry.* (2016) 21:1710–6. doi: 10.1038/mp.2015.227
30. Mamah D, Alpert KI, Barch DM, Csernansky JG, Wang L. Subcortical neuromorphometry in schizophrenia spectrum and bipolar disorders. *Neuroimage Clin.* (2016) 11:276–86. doi: 10.1016/j.nicl.2016.02.011
31. Redlich R, Almeida JJ, Grotegerd D, Opel N, Kugel H, Heindel W, et al. Brain morphometric biomarkers distinguishing unipolar and bipolar depression. A voxel-based morphometry-pattern classification approach. *JAMA Psychiatry.* (2014) 71:1222–30. doi: 10.1001/jamapsychiatry.2014.1100
32. Viering T, Naaijen J, van Rooij D, Thiel C, Philipsen A, Dietrich A, et al. Amygdala reactivity and ventromedial prefrontal cortex coupling in the processing of emotional face stimuli in attention-deficit/hyperactivity disorder. *Eur Child Adolesc Psychiatry.* (2021) doi: 10.1007/s00787-021-01809-3
33. Kowalczyk OS, Pauls AM, Fuste M, Williams SCR, Hazelgrove K, Vecchio C, et al. Neurocognitive correlates of working memory and emotional processing in postpartum psychosis: an fMRI study. *Psychol Med.* (2020) 51:1724–32. doi: 10.1017/S0033291720000471
34. Basu S, Alapin JM, Dines M, Lamprecht R. Long-term memory is maintained by continuous activity of Arp2/3 in lateral amygdala. *Neurobiol Learn Mem.* (2020) 167:107115. doi: 10.1016/j.nlm.2019.107115
35. Ho NF, Li Hui Chong P, Lee DR, Chew QH, Chen G, Sim K. The amygdala in schizophrenia and bipolar disorder: a synthesis of structural MRI, diffusion tensor imaging, and resting-state functional connectivity findings. *Harv Rev Psychiatry.* (2019) 27:150–64. doi: 10.1097/HRP.0000000000000207
36. Bahtiyar S, Gulmez Karaca K, Henckens M, Roozendaal B. Norepinephrine and glucocorticoid effects on the brain mechanisms underlying memory accuracy and generalization. *Mol Cell Neurosci.* (2020) 108:103537. doi: 10.1016/j.mcn.2020.103537
37. Del Arco A, Segovia G, de Blas M, Garrido P, Acuna-Castroviejo D, Pamplona R, et al. Prefrontal cortex, caloric restriction and stress during aging: studies on dopamine and acetylcholine release, BDNF and working memory. *Behav Brain Res.* (2011) 216:136–45. doi: 10.1016/j.bbr.2010.07.024
38. Fried I, Wilson CL, Morrow JW, Cameron KA, Behnke ED, Ackerson LC, et al. Increased dopamine release in the human amygdala during performance of cognitive tasks. *Nat Neurosci.* (2001) 4:201–6. doi: 10.1038/84041

39. Shenton ME, Dickey CC, Frumin M, McCarley RW. A review of MRI findings in schizophrenia. *Schizophr Res.* (2001) 49:1–52. doi: 10.1016/S0920-9964(01)00163-3
40. Zuo Z, Ran S, Wang Y, Li C, Han Q, Tang Q, et al. Asymmetry in cortical thickness and subcortical volume in treatment-naive major depressive disorder. *Neuroimage Clin.* (2019) 21:101614. doi: 10.1016/j.nicl.2018.101614
41. Bilder RM, Wu H, Bogerts B, Degreef G, Ashtari M, Alvir JM, et al. Absence of regional hemispheric volume asymmetries in first-episode schizophrenia. *Am J Psychiatry.* (1994) 151:1437–47. doi: 10.1176/ajp.151.10.1437
42. Clark GM, Crow TJ, Barrick TR, Collinson SL, James AC, Roberts N, et al. Asymmetry loss is local rather than global in adolescent onset schizophrenia. *Schizophr Res.* (2010) 120:84–6. doi: 10.1016/j.schres.2009.12.032
43. Hasan A, Kremer L, Gruber O, Schneider-Axmann T, Guse B, Reith W, et al. Planum temporale asymmetry to the right hemisphere in first-episode schizophrenia. *Psychiatry Res.* (2011) 193:56–9. doi: 10.1016/j.pscychresns.2011.02.008
44. Zotev V, Yuan H, Misaki M, Phillips R, Young KD, Feldner MT, et al. Correlation between amygdala BOLD activity and frontal EEG asymmetry during real-time fMRI neurofeedback training in patients with depression. *Neuroimage Clin.* (2016) 11:224–38. doi: 10.1016/j.nicl.2016.02.003
45. Berretz G, Wolf OT, Gunturkun O, Ocklenburg S. Atypical lateralization in neurodevelopmental and psychiatric disorders: what is the role of stress? *Cortex.* (2020) 125:215–32. doi: 10.1016/j.cortex.2019.12.019

Conflict of Interest: The authors declare that the research was conducted in the absence of any commercial or financial relationships that could be construed as a potential conflict of interest.

frontiers in Neuroscience

ORIGINAL RESEARCH
published: 09 February 2022
doi: 10.3389/fnins.2021.749316

A Real-World Observation of Antipsychotic Effects on Brain Volumes and Intrinsic Brain Activity in Schizophrenia

Yifan Chen[1,2,3], Fay Y. Womer[4], Ruiqi Feng[1,5], Xizhe Zhang[2,6], Yanbo Zhang[7], Jia Duan[1,2,3], Miao Chang[1,5], Zhiyang Yin[1], Xiaowei Jiang[1], Shengnan Wei[1], Yange Wei[1,2,3], Yanqing Tang[1] and Fei Wang[1,2,3]**

[1] Department of Psychiatry, The First Affiliated Hospital of China Medical University, Shenyang, China, [2] Early Intervention Unit, Department of Psychiatry, Affiliated Nanjing Brain Hospital, Nanjing Medical University, Nanjing, China, [3] Department of Radiology, The First Affiliated Hospital of China Medical University, Shenyang, China, [4] Department of Psychiatry, Washington University School of Medicine, St. Louis, MO, United States, [5] School of Biomedical Engineering and Informatics, Nanjing Medical University, Nanjing, China, [6] Nanjing Brain Hospital, Nanjing Medical University, Nanjing, China, [7] Functional Brain Imaging Institute of Nanjing Medical University, Nanjing, China

OPEN ACCESS

Edited by:
Kai Wang,
Anhui Medical University, China

Reviewed by:
Jiajia Zhu,
First Affiliated Hospital of Anhui Medical University, China
Yating Lv,
Hangzhou Normal University, China

***Correspondence:**
Yanqing Tang
yanqingtang@163.com
Fei Wang
fei.wang@mail.cmu.edu.cn

Specialty section:
This article was submitted to Brain Imaging Methods, a section of the journal Frontiers in Neuroscience

Received: 29 July 2021
Accepted: 30 November 2021
Published: 09 February 2022

Citation:
Chen Y, Womer FY, Feng R, Zhang X, Zhang Y, Duan J, Chang M, Yin Z, Jiang X, Wei S, Wei Y, Tang Y and Wang F (2022) A Real-World Observation of Antipsychotic Effects on Brain Volumes and Intrinsic Brain Activity in Schizophrenia. Front. Neurosci. 15:749316. doi: 10.3389/fnins.2021.749316

Background: The confounding effects of antipsychotics that led to the inconsistencies of neuroimaging findings have long been the barriers to understanding the pathophysiology of schizophrenia (SZ). Although it is widely accepted that antipsychotics can alleviate psychotic symptoms during the early most acute phase, the longer-term effects of antipsychotics on the brain have been unclear. This study aims to look at the susceptibility of different imaging measures to longer-term medicated status through real-world observation.

Methods: We compared gray matter volume (GMV) with amplitude of low-frequency fluctuations (ALFFs) in 89 medicated-schizophrenia (med-SZ), 81 unmedicated-schizophrenia (unmed-SZ), and 235 healthy controls (HC), and the differences were explored for relationships between imaging modalities and clinical variables. We also analyzed age-related effects on GMV and ALFF values in the two patient groups (med-SZ and unmed-SZ).

Results: Med-SZ demonstrated less GMV in the prefrontal cortex, temporal lobe, cingulate gyri, and left insula than unmed-SZ and HC ($p < 0.05$, family-wise error corrected). Additionally, GMV loss correlated with psychiatric symptom relief in all SZ. However, medicated status did not influence ALFF values: all SZ showed increased ALFF in the anterior cerebrum and decreased ALFF in posterior visual cortices compared with HC ($p < 0.05$, family-wise error corrected). Age-related GMV effects were seen in all regions, which showed group-level differences except fusiform gyrus. No significant correlation was found between ALFF values and psychiatric symptoms.

Conclusion: GMV loss appeared to be pronounced to longer-term antipsychotics, whereby imbalanced alterations in regional low-frequency fluctuations persisted unaffected by antipsychotic treatment. Our findings may help to understand the disease course of SZ and potentially identify a reliable neuroimaging feature for diagnosis.

Keywords: schizophrenia, gray matter volumes, amplitude of low frequency fluctuations, antipsychotics, real-world observation

INTRODUCTION

Psychotropic medications have long confounded findings from neuroimaging studies. Their effects result in inconsistent findings and hamper efforts to understand further the pathophysiology of neuropsychiatric disorders such as schizophrenia (SZ). Mounting neuroimaging studies have indicated SZ that features structural deficits spanning the multiple brain regions such as frontal, temporal, and parietal lobes (Honea et al., 2005; Cronenwett and Csernansky, 2010; Yang et al., 2021), accompanied by functional abnormalities (Lawrie et al., 2002; Zhou et al., 2007). Despite the availability of various magnetic resonance imaging (MRI) techniques, the consistency of findings across studies remains a significant challenge. Previous studies have demonstrated gray matter volume (GMV) decreased in SZ by 2% (Wright et al., 2000; Vita et al., 2012). However, Benedicto reported no differences in GMV between SZ and healthy volunteers (Kim et al., 2000). Besides, two studies have suggested abnormally increased GMV in the orbitofrontal cortex (Hoptman et al., 2005; Lacerda et al., 2007), whereas a third study detected the opposite change in the same region (Nakamura et al., 2008). Furthermore, a recent selective meta-analysis concluded that the variability of GMV in specific areas such as the putamen and temporal lobe was significantly greater in patients (Brugger and Howes, 2017).

Scholars have emphasized more extensive brain network dysfunction. However, the specific pathological mechanism is not clear, and the high heterogeneity between the studies has also led to more controversy and discussion. For SZ with antipsychotics, there are few studies of structural imaging combined with functional imaging. One of the commonly used functional MRI techniques, such as amplitude of low-frequency fluctuations (ALFF), has been developed, which measures the intensity of spontaneous fluctuation in a particular voxel within the BOLD signal (Zang et al., 2007). The intrinsic brain activity consumes over 95% of the brain's energy and is likely to play a critical role in brain function (Zhang and Raichle, 2010). A number of recent studies have revealed synchronous changes in brain volume and ALFF values in specific disease processes, suggesting that the two brain measures are related. It is most reliable in gray matter (GM), suggesting that ALFF derives from neural activity (Vesa et al., 2003). Studies have revealed synchronous changes in brain volume and ALFF values in specific disease processes, suggesting that the two brain measures are related (Li et al., 2014; Liu et al., 2014). Notably, Qing and Gong (2016) provide direct empirical evidence of a strong association between brain size/volume and intrinsic brain activity, suggesting that brain size serves as a structural substrate for the intrinsic brain activity of the human brain.

However, studies of ALFF in SZ also have given inconsistent results. A recent meta-analysis in SZ indicated the decreased ALFF primarily in the somatosensory cortex, posterior parietal cortex, and occipital cortex and increased ALFF mainly in the bilateral medial temporal cortex and medial prefrontal cortex (Xu et al., 2015). However, some studies have contrarily reported decreased ALFF in medial prefrontal areas (Huang et al., 2010; Wenting et al., 2013). Similarly, two studies have suggested abnormally high intrinsic activity in the bilateral putamen (Huang et al., 2010; He et al., 2013); Lui did not report such high activity though (Lui et al., 2010). Altogether, although multiple factors could contribute to inconsistent findings, such as differences in sample characteristics or exact methodology, the inconsistencies across studies may, in part, reflect the effects of antipsychotics in SZ.

What the role antipsychotic treatment played on the pathophysiologic process of brain deficits in SZ remains unclear. Antipsychotics have been associated with GMV deficits in the frontotemporal cortex and the whole brain in SZ (Leung et al., 2011; Ahmed et al., 2015) but have also been associated with no change or increase in GMV (Halim et al., 2004; Ho et al., 2011). Also, a meta-analysis indicated that more significant volumetric variation in the brain structure of individuals with SZ compared with controls could suggest that antipsychotic levels may somehow be associated with greater heterogeneity in brain volume in SZ (Kuo and Pogue-Geile, 2019). However, there are still relatively limited studies regarding the influence of medications in ALFF. Six-week antipsychotic treatment has been associated with increases of ALFF in the frontal gyrus, parietal lobule, temporal gyrus, and right caudate (Lui et al., 2010). Furthermore, after 1-year treatment of antipsychotics, the majority of ALFF values did not significantly change between baseline and follow-up imaging except right inferior parietal lobule and orbitofrontal cortex and right occipital gyrus (Li et al., 2016). The earlier findings suggest that neuroimaging measures vary in their susceptibility to medication effects and that some measures more robustly reflect disease processes *versus* treatment response.

Furthermore, although experts agree on the efficacy of antipsychotics in alleviating psychotic symptoms during the early most acute phase (0–2 months), the longer-term effects of antipsychotics on the brain have long been controversial (Vita et al., 2015; van Erp et al., 2018; Liu et al., 2020). Given that evidence for the benefits of antipsychotics extends only to approximately 0–2 years, what to do in the longer term draws our attention. One recent naturalistic longitudinal study of patients with psychosis with a 3-year follow-up period reported a significantly increased rate of cortical loss compared

with healthy controls (HCs; Akudjedu et al., 2020). However, infrequent studies assessed how the brain of patients with SZ changes when treated for midterm to long term with antipsychotic medications. Moreover, views about the longer-term (>2 months) efficacy of antipsychotics often based on the results from longitudinal evaluations are subject to the risk of bias caused by dropout or statistical effectiveness reduction. For this reason, the cross-sectional studies combining structural and functional imaging based on the natural world can bring complementary information for brain changes at this stage.

Therefore, in this study, we examined GMV and ALFF using voxel-based morphometry and resting-state functional magnetic resonance imaging (fMRI) techniques in SZ based on medication status: unmedicated (medication naïve or not taking medications for at least 4 weeks before scan) and medicated (taking medications for at least 8 weeks before the scan, more than half of them for 2–4 years). We aimed for a preliminary real-world observation with no study-related and longer-term treatment changes to capture the typical conditions of neuroimaging studies to provide some basis for the identification of objective image indicators in patients with SZ. Thresholds for medication status were determined based on prior findings of antipsychotic effects on the brain as early as 1 month after treatment initiation in SZ and standards for unmedicated status by other studies in the literature (Mcclure et al., 2008; Leung et al., 2011; Kraguljac et al., 2016). We also examined associations between structural and functional metrics and clinical markers in patients with SZ.

MATERIALS AND METHODS

Subjects

The Institutional Review Board of China Medical University approved this study, and all participants provided written informed consent after a detailed description of the study. Participants in this study included 89 individuals with SZ who had been taking only atypical antipsychotics for more than 8 weeks before the time of scan (med-SZ) and 81 individuals with

TABLE 1 | Demographic and clinical characteristics of healthy controls, medicated schizophrenia, and unmedicated schizophrenia.

HC (n = 235)		SZ (n = 170)		$F/\chi^2/t$-values	P-values
		Med-SZ (n = 89)	Unmed-SZ (n = 81)		
Demographic characteristic					
Age at scan, years	28.17 (0.53)	27.65 (10.06)	25.53 (9.30)	2.740[a]	0.066
Age distribution					
−15 to 28	161 (68.51%)	53 (59.55%)	53 (65.43%)		
−29 to 42	54 (22.98%)	24 (26.97%)	22 (27.16%)		
−43 to 55	20 (8.51%)	12 (13.48%)	6 (7.40%)		
Sex (male:female)	93 (39.57%)	44 (49.44%)	32 (43.20%)	2.789[a]	0.248
Right handedness	217 (92.34%)	78 (87.64%)	68 (83.95%)	2.525[a]	0.640
Education	15.08 (3.06)	12.06 (2.98)	10.93 (3.00)	70.832	<0.001
Clinical characteristic					
First episode, yes	\	44 (49.44%)	71 (87.65%)	\	<0.001
Illness duration (months)	\	43.07 (51.01)	8.84 (17.83)	31.14[b]	<0.001
Medication use[c]	\				
Durations (months)		12.34 (13.74)	\		
-Olanzapine		21			
-Clozapine		13			
-Risperidone		41			
-Aripiprazole		19			
-Ziprasidone		4			
-Quetiapine		5			
Olanzapine equivalents		3.93 (6.15)			
BPRS-Factors	n = 159	n = 83	n = 77		
Anxiety and depression	4.28 (0.83)	6.89 (3.72)	8.90 (4.35)	5.342[b]	0.009
Lack of energy	4.03 (0.21)	6.53 (3.03)	8.14 (4.54)	11.35[b]	<0.001
Thought disorder	4 (0)	6.65 (3.77)	9.39 (4.89)	6.844[b]	0.176
Activity	3.06 (0.26)	4.29 (2.09)	4.78 (2.47)	3.267[b]	<0.001
Hostility	3.02 (0.14)	4.61 (2.78)	7.44 (4.01)	18.19[b]	<0.001
BPRS-Total score	18.39 (1.21)	28.98 (10.30)	39.03 (14.62)	9.042[b]	0.002

HC, healthy controls; med-SZ, medicated schizophrenia; unmed-SZ, unmedicated schizophrenia; BPRS, Brief Psychiatric Rating Scale. Data are n (%) or mean (SD).
[a]Examination among healthy control, medicated schizophrenia, and unmedicated schizophrenia groups.
[b]Examination between medicated schizophrenia and unmedicated schizophrenia groups.
[c]This refers to medication patients were prescribed on day of their MRI scan and not to their cumulative lifetime exposure.

SZ (unmed-SZ) who were either antipsychotics naïve (n = 31, 38.27%) or not taking antipsychotics for at least 4 weeks at the time of scan (n = 50, 61.73%) and 235 HCs aged 15–55 years. We reviewed information on the type and dosage of medication recorded at the time of the MRI scan. Med-SZ was treated with antipsychotics including clozapine, risperidone, olanzapine, aripiprazole and quetiapine, aripiprazole, and ziprasidone. The doses of antipsychotics were converted to olanzapine equivalents based on defined daily doses (Leucht et al., 2016). All participants were recruited from the outpatient clinics of the Department of Psychiatry, The First Affiliated Hospital of China Medical University, Shenyang, China, and HC participants were recruited from Shenyang, China, by advertisement. The absence or presence of Axis I disorders was independently assessed by two trained psychiatrists using the Structured Clinical Interview for Diagnostic and Statistical Manual of Mental Disorders, Fourth Edition, Axis I Disorders for participants older than 18 years and the Schedule for Affective Disorders and Schizophrenia for School-Age Children—Present and Lifetime Version (K-SADS-PL) for participants younger than 18 years. SZ participants met the Diagnostic and Statistical Manual of Mental Disorders, Fourth Edition, diagnostic criteria for SZ, schizophreniform disorder, schizoaffective disorder, and no other Axis I disorder. HC participants did not have current or lifetime Axis I disorder or history of psychotic, mood, or other Axis I disorders in first-degree relatives (as determined from detailed family history). For all participant groups, individuals were excluded for the history of substance or alcohol abuse or dependence, head injury, neurologic or concomitant major medical disorder, and any MRI contraindications for MRI symptom measures using the Brief Psychiatric Rating Scale (BPRS) in patients with SZ. **Table 1** outlines the participants' demographic and clinical status at the time of testing.

Image Acquisition

The scan was performed using a 3T MRI scanner (General Electric, Milwaukee, WI, United States) at the Image Institute of The First Affiliated Hospital of China Medical University, Shenyang, China. The three-dimensional fast spoiled gradient-echo sequence was used to obtain sagittal T1-weighted structural images of the whole brain. Scanning parameters were as follows: repetition time = 7.1 ms, echo time = 3.2 ms, field of view = 24 cm × 24 cm, voxel size = 1 mm × 1 mm × 1 mm, slice thickness = 1.0 mm without a gap, 176 slices in total, and the scan time = 8 min 6 s. Functional images were collected using a gradient echo-planar imaging sequence: repetition time = 2,000 ms, echo time = 30 ms, field of view = 240 cm × 240 cm, flip angle = 90°, matrix = 64 × 64, and slices = 35. Participants were instructed to rest with their eyes closed but remain awake during scanning.

Structural Magnetic Resonance Imaging Data Processing

Processing was performed using the DARTEL algorithm Statistical Parametric Mapping software (SPM8)[1] under the MATLAB R2010b platform (MathWorks, Sherborn, MA, United States). Briefly, the segmentation function was used to divide the regions into GM, white matter, and cerebrospinal fluid using the "new segment" tool implemented in SPM8. During spatial normalization, inter-subject registration was achieved using separate registration based on group assignment. A modulation step was used to ensure that the overall amount of tissue in a class was unaltered. The segmented images were normalized to the Montreal Neurological Institute template and were smoothed with an 8-mm full width at a half-maximum Gaussian filter. The voxel size of data acquisition was 1 mm^3, and the voxel size of normalized data was 1.5 mm^3.

Functional Magnetic Resonance Image Processing and Amplitude of Low-Frequency Fluctuation Calculation

Resting-state fMRI data preprocessing was carried out using Statistical Parametric Mapping 8 (SPM)[2]. Data Processing Assistant for Resting-State fMRI (DPARSF, V2.0_101025)[3] was based on SPM8. For each participant, the first 10 volumes of scanned data were discarded to allow for steady-state magnetization. Further data preprocessing included slice timing correction and head motion correction. Each participant's motion was assessed by means of translation/rotation and an exclusion criterion (translation >3 mm, rotation >3° in each participant). Then, spatial normalization was performed using the standard echo-planar imaging template from the Montreal Neurological Institute Spatial smoothing, which was done with a 6-mm full width at a half-maximum Gaussian filter, and linear detrending was performed to remove linear trends (Cordes et al., 2001). The filtered time series was transformed into the frequency domain with a fast Fourier transform, and the power spectrum was then obtained. ALFF was measured by obtaining the square root of the signal across 0.01–0.08 Hz for each voxel.

Statistical Analysis

Analyses of demographic and clinical characteristics were performed using analysis of variance and chi-square tests. Results were considered significant at $p < 0.05$. To compare GMV with ALFF values among the med-SZ, unmed-SZ, and HC groups, whole brain GMV and ALFF values comparisons among three groups were performed using a full-factorial design, with age and sex as covariates, using SPM8 (Wellcome Trust Centre for Neuroimaging, see text footnote 1). The GMV and ALFF value differences were considered significant at a height threshold of $p < 0.05$, family-wise error (FWE) corrected for multiple comparisons, and an extended threshold of 20 voxels (Liao et al., 2015). GMV and ALFF values were extracted from all significant regions in the three-group analysis and analyzed in *post hoc* pair-wise t-contrasts (med-SZ *vs.* unmed-SZ, med-SZ *vs.* HC, and unmed-SZ *vs.* HC) using SPSS. Duration of illness was included as a covariate of non-interest in the patient subgroup comparison. To determine age-related effects on GMV and ALFF

[1]http://www.fil.ion.ucl.ac.uk/spm/software/spm8/

[2]http://www.fil.ion.ucl.ac.uk/spm

[3]http://www.restfmri.net

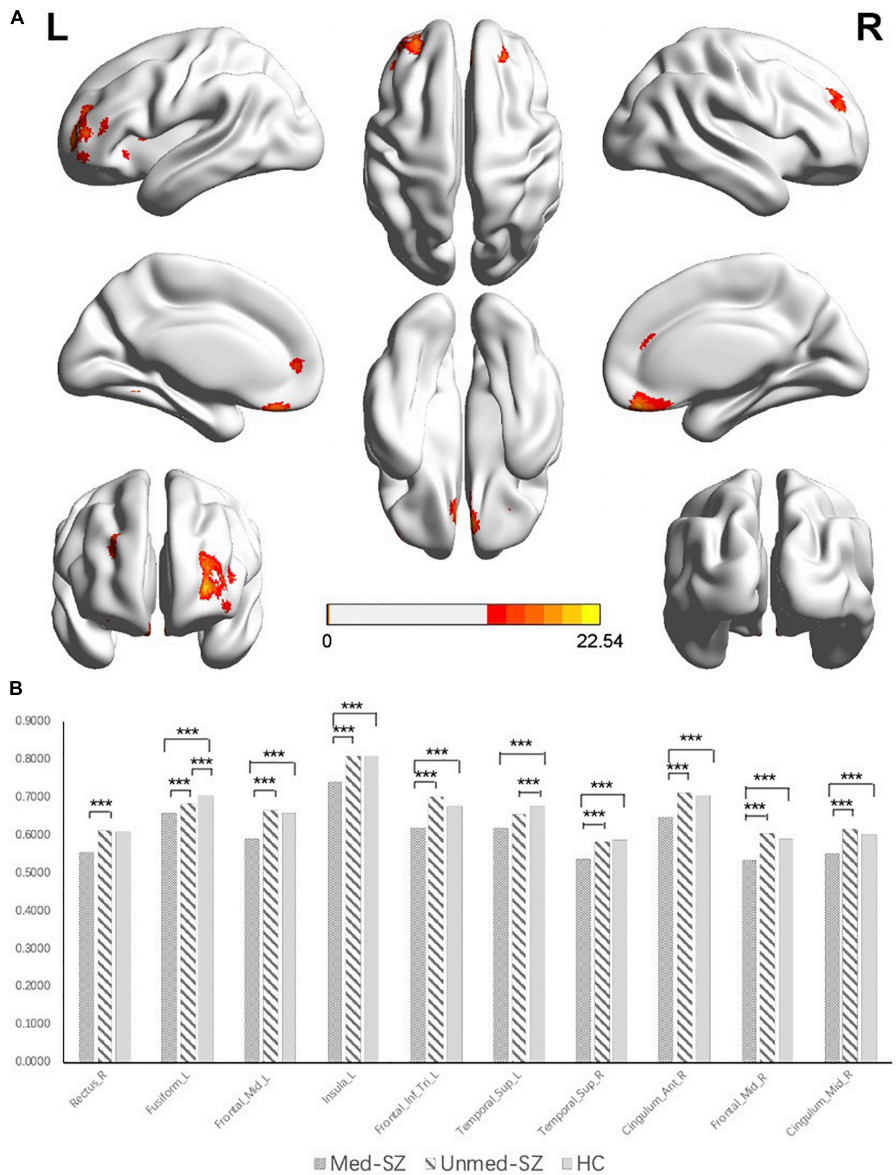

FIGURE 1 | (A) Significant differences in gray matter volumes among medicated schizophrenia, unmedicated schizophrenia, and healthy controls. ***Significant at $P < 0.05$ corrected by FWE correction. **(B)** Gray matter volumes in regions showing significant differences among medicated schizophrenia, unmedicated schizophrenia, and healthy controls. R, right; L, left; Frontal_Mid, middle frontal gyrus; Frontal_Inf_Tri, Inferior Pars Triangularis; Temporal_Sup, superior temporal cortex; Cingulum_Ant, anterior cingulate cortex; Cingulum_Mid, middle cingulate cortex.

values in the two patient groups (medicated and unmedicated), we used the mean values of GMV and ALFF in regions showing the group-level difference and ran a general linear model in SPSS. The GMV and ALFF values were considered as dependent variables. Fixed factors included age and group (med-SZ and unmed-SZ). Analyses were also performed with false discovery rate (FDR) corrected for multiple comparisons to further confirm the findings of age-related effects.

We used exploratory Pearson's correlation analyses to examine the relationship between GMV/ALFF values and BPRS scores and medication time in each patient group. Analyses were also performed with FDR corrected for multiple comparisons to further confirm the findings of correlation after FDR correction; $p < 0.005$ was considered significant in correlation analysis.

RESULTS

Demographic and Clinical Data

There was no significant difference among med-SZ, unmed-SZ, and HC groups in age ($p = 0.066$) or sex ($p = 0.248$), and handedness ($p = 0.640$). The unmed-SZ group had significantly

TABLE 2 | Regions with GM differences in demonstrating significant group differences.

Cortical regions	Cluster size	MNI coordinates			*F* values*
		X	Y	Z	
A R rectus gyrus	1,873	−2	50	3	22.5416
L superior medial frontal gyrus					
L rectus gyrus					
R superior medial frontal gyrus					
L anterior cingulum					
B L fusiform gyrus	43	−33	−53	−11	15.7687
C L middle frontal gyrus	1,011	−33	48	6	21.3453
L middle orbital frontal gyrus					
D L insula	30	−35	11	6	14.5635
E L inferior pars triangularis	79	−47	38	12	15.7309
F L superior temporal gyrus	43	−56	−14	9	17.1504
G R superior temporal gyrus	78	63	−17	12	15.953
R Rolandic operculum					
H R anterior cingulum	57	8	36	23	14.356
I R middle frontal gyrus	314	32	54	23	19.4355
R superior frontal gyrus					
J R middle cingulum	109	2	15	36	17.987
L middle cingulum					

MNI, Montreal Neurological Institute; L, Left; R, Right.
**Significant at $P < 0.05$ corrected by FWE correction.*

shorter illness duration, lower first-episode rate, and higher BPRS scores compared with the med-SZ group (see **Table 1** for details).

Gray Matter Volume Findings

Significant group differences were found in several regions consisting of the prefrontal cortex, temporal lobe, cingulate gyri, and insula ($df = 2$, $p < 0.05$, FWE corrected) (**Figure 1** and **Table 2**). Compared with unmed-SZ and HC groups, the med-SZ demonstrated decreased GMVs located in bilateral middle frontal gyrus, bilateral superior medial frontal gyrus, bilateral superior temporal gyrus, bilateral anterior cingulate gyri, bilateral middle cingulate gyri, right Rolandic operculum, right superior frontal gyrus, middle orbital frontal gyrus, left fusiform gyrus, and left insula. All clusters except the left superior temporal cortex survived when illness duration was included as a covariate in comparison between med-SZ and unmed-SZ. Significant decreases were found in the left fusiform gyrus and left superior temporal gyrus in unmed-SZ compared with HC (**Figure 1** and **Table 2**).

Amplitude of Low-Frequency Fluctuation Findings

The three-group analysis of ALFF found four clusters showing significant group differences ($df = 2$, $p < 0.05$, FWE corrected). These clusters are situated in the bilateral occipital lobe, bilateral striatum, and left parahippocampal gyrus (**Figure 2** and **Table 3**). Compared with HC, med-SZ and unmed-SZ had significant decreases of ALFF values in bilateral lingual and calcarine gyrus and significant increases mainly in bilateral caudate and putamen, as well as left parahippocampal gyrus. No differences were observed between med-SZ and unmed-SZ (**Figure 2** and **Table 3**).

Age-Related Differences in Gray Matter Volume and Amplitude of Low-Frequency Fluctuation

We examined relationships between age and GMV that differed between the two groups. More specifically, age-related GMV effects were seen in all regions, which showed group-level differences except fusiform gyrus. *Post hoc* analyses showed that the age-related decline in GMV of the bilateral middle frontal gyrus, left inferior pars triangularis, and right middle cingulum in medicated patients was significantly greater than that in unmedicated patients. Unmedicated patients showed significantly faster age-related GMV decline in the right rectus gyrus, left insula, bilateral superior temporal gyrus, and right anterior cingulum than medicated subjects. We also examined relationships between age and ALFF values that differed between the two groups but found no association after FDR correction.

Correlations With Clinical Variables and Medication Time

For both med-SZ and unmed-SZ, BPRS scores were positively correlated with GMV in bilateral middle frontal gyrus, bilateral superior medial frontal gyrus, right superior temporal gyrus, bilateral anterior cingulate gyri, bilateral middle cingulate gyri, right Rolandic operculum, right superior frontal gyrus, middle orbital frontal gyrus, and left insula. After FDR correction, most correlations survived, except the correlation between BPRS scores and the GMV in left fusiform and left superior temporal gyrus ($p < 0.05$, FDR corrected) (**Supplementary Table 1** and **Table 2**). No significant correlation was found between ALFF values and BPRS scores (**Supplementary Table 2** and **Table 3**). Besides, we did not detect any relation between medication time and GMV/ALFF values (**Supplementary Tables 1**, **2** and **Tables 2**, **3**).

DISCUSSION

In the current study, we compared the susceptibility of different imaging measures with antipsychotics. We found significant GMV decreases in the prefrontal cortex, temporal lobe, cingulate gyri, and left insula in med-SZ compared with unmed-SZ and HC. Among these regions, unmed-SZ demonstrated lower GMV in the left superior temporal cortex and left fusiform than HC additionally. We also found a significant correlation between GMV loss and decline of BPRS scores. No significant differences in ALFF were found based on medication status, and no significant correlations between ALFF and BPRS scores were observed. Both med- and unmed-SZ had significantly increased ALFF in the anterior cerebrum, including bilateral striatum and left parahippocampal, and decreased ALFF in posterior visual cortices, including the calcarine and lingual gyrus, compared with HC. Our findings indicate that GMV may be susceptible to medication effects, whereas ALFF is not in SZ.

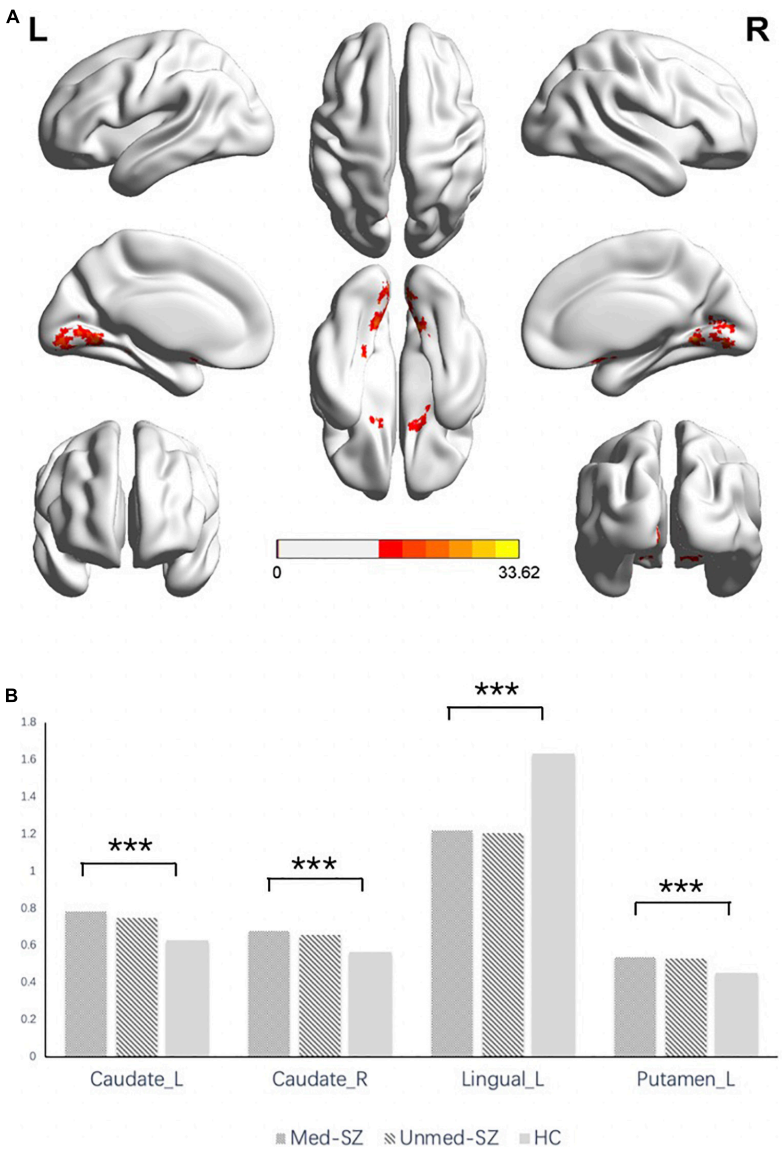

FIGURE 2 | (A) Significant differences in ALFF among medicated schizophrenia, unmedicated schizophrenia, and healthy controls. ***Significant at $P < 0.05$ corrected by FWE correction. **(B)** ALFF values in regions showing significant differences among medicated schizophrenia, unmedicated schizophrenia, and healthy controls. R, right; L, left; Caudate, caudate nucleus; Lingual, lingual gyrus.

It is widely accepted that SZ is characterized by extensive GMV abnormalities (Kubicki et al., 2002; Koolschijn et al., 2010; Pinacamacho et al., 2016); however, the contribution of medication effects to these alterations are unclear. Moreover, further investigation is needed to clarify if specific regions are more affected by neuroleptics. Our findings suggest that antipsychotic treatment may be more influential in GMV in the frontal, temporal, cingulate, and insula regions. This result is in line with evidence from substantial imaging studies indicating that antipsychotic treatment can result in GMV loss in SZ (Mccormick et al., 2005; Ho et al., 2011). Tyler et al. reported that significant cortical thinning was identified in the medicated patient group relative to the control group in prefrontal, temporal, parietal, and occipital cortices (Lesh et al., 2015). The unmedicated patient group showed no significant cortical thickness differences from the control group. Furthermore, meta-regression analyses also reported that GMV in medial frontal, anterior cingulate cortices, and left insular regions were more decreased in med-SZ (Radua et al., 2012). A study of 211 individuals with SZ over a mean 7.2-year period found that antipsychotics significantly influenced brain volumes even after accounting for illness duration, illness severity, and substance use (Ho et al., 2011). Antipsychotic dosing explained 1.7% of the decreases in total GMV (Ho et al., 2011). Animal studies also support the earlier findings that non-human primates given doses of antipsychotics similar to those given to humans showed brain

TABLE 3 | Regions with ALFF differences in demonstrating significant group differences.

Cortical regions	Cluster size	MNI coordinates			*F* values*
		X	Y	Z	
A L caudate	100	−18	21	−3	33.6157
B R caudate	137	15	12	−15	24.0428
R putamen					
C L lingual gyrus	317	−15	−63	−3	24.2724
R lingual gyrus					
L calcarine					
R calcarine					
D L putamen	22	−24	−6	9	24.3612

MNI, Montreal Neurological Institute; L, Left; R, Right.
**Significant at $P < 0.05$ corrected by FWE correction.*

volume reductions of around 10%, mostly attributable to loss of the glial cells that support and protect neurons (Cyranoski, 2011). Although substantial findings, including our results, suggest GMV loss is induced by antipsychotics (Lieberman et al., 2005; Radua et al., 2012), a few findings have identified conserved or even increased GMV in SZ with specific atypical antipsychotics (Gur et al., 1998; Molina et al., 2005), and that may be attributed to differences in sample size, the definition of medicated and unmedicated groups: in many of these studies, the sample sizes were modest (<30 subjects); the treatment duration is relatively short (mostly <6 weeks).

Gray matter volume changes in SZ do not appear entirely due to medication effects. We found significant GMV loss in the left superior temporal cortex and left fusiform in unmed-SZ, compared with HC. Previous studies have shown GMV reduction in left posterior superior temporal gyrus and left fusiform in first-episode SZ (Hirayasu et al., 1998; Lee et al., 2002, 2015). Our findings replicate prior findings of decreased left fusiform volume in treatment-naive SZ (Guo et al., 2013). Structural alterations in the left superior temporal cortex and left fusiform structural abnormalities appear less affected by illness chronicity and medication effects and hence may serve as potential biomarkers for SZ.

Gray matter volumes in prefrontal, temporal, cingulate, and insula were positively correlated with BPRS scores, consistent with previous findings (Wenting et al., 2013; Liao et al., 2015). We found GMV deficits found in frontotemporal regions that have been implicated in aggression, emotional withdrawal, blunted affect, and conceptual disorganization in SZ (Lieberman et al., 2005; Cobia et al., 2012; Fusarpoli et al., 2013). The correlation between GMV deficits and BPRS scores may reflect GMV as a marker of disease state (*versus* trait) and treatment response.

We found age-related differences in GMV between med- and unmed-SZ. More specifically, in patients with med-SZ, imaging studies found accelerated age-related GMV decline than unmed-SZ in all regions showing group-level differences except the fusiform gyrus. To our best knowledge, this is the first cross-sectional study that explores the relation between GMV and age with or without longer medication use. This finding is also consistent with previous studies suggesting that progressive brain GMV changes during the life-long course of SZ appeared in part to be related to antipsychotics (Ho et al., 2011; Lesh et al., 2015). Moreover, a recent randomized, double-blind placebo-controlled clinical trial design study found a significant treatment-group × time interaction in relation to cortical thickness with 36-week treatment (Voineskos et al., 2020). Given that medication use may bring out a detrimental effect of progressive GMV changes, which are typically interpreted in psychiatric and neurologic disorders as non-desirable, our findings could support a reconsideration of the risks and benefits of antipsychotics.

Here, we provided evidence focused on the longer-term antipsychotic treatment showing that we may underestimate the risks of longer-term antipsychotic treatment. The temporal relief of symptoms may be a compensation for GMV loss; the coverage of the worrying issue of the longer-term effects of antipsychotics on brain structure loss must not be overlooked. Recently, Correll et al. (2018) argued for a positive view of the risk–benefit ratio for long-term continuous antipsychotic treatment of SZ. However, Correll et al. (2018) too readily dismiss the evidence that prolonged antipsychotic use is associated with decreased GM and fail to cite the monkey and rodent studies in which administration of antipsychotics causes brain volume losses (Cyranoski, 2011). As we have noted, the association between cumulative dose of antipsychotics and general GMV reduction has been repeatedly reported. Moreover, the accompanying dopamine hypersensitivity psychosis and poor long-term (7–20 years) prognosis suggest the inevitable issue of its adverse effects on brain structure (Martin and Jobe, 2018). Furthermore, some studies assess whether patients with SZ improve when treated longer than 2 or 3 years with antipsychotic medications (Morgan et al., 2014; Harrow et al., 2017; Velthorst et al., 2017). Interestingly, unlike short-term studies, none of them showed positive long-term results. Although administered widely, we still do not have a clear knowledge of all of the antipsychotic effects. Further questions and studies of it would seem critical.

Our findings with ALFF suggest that ALFF is less influenced by medication and disease state. We found increased ALFF in the anterior cerebrum, including the bilateral striatum, and decreased ALFF in the posterior visual cortex, consistent with previous studies in both unmed- and med-SZ (He et al., 2013; Li et al., 2017; Chang et al., 2019). A meta-analysis also concluded that the foci with increased ALFF are mainly located in the striatum and decreased ALFF situated in the occipital cortex consistently (Xu et al., 2015). The striatum, together with other basal ganglia nuclei, regulates information flow to and from the cerebral cortex and other related subcortical regions (such as the thalamus). Our finding of altered ALFF in the bilateral striatum is consistent with prior studies implicating striatal abnormalities in the pathophysiology of SZ. Prior functional and metabolic studies have found increased striatal dopamine neurotransmission and activity in SZ (Kegeles et al., 2010; Zhuo et al., 2014), and our results may support the hypothesis that the striatum of SZ is in a state of hyper-dopamine (Abidargham, 2014).

Bilateral lingual and calcarine gyrus, which function as the primary visual cortex, have been related to visual hallucinations in most studies (González-Hernández et al., 2003;

Onitsuka et al., 2007; Hoptman et al., 2010; Lang et al., 2010), suggesting that the visual cortex alterations may be important in SZ. We found that med-SZ and unmed-SZ showed decreased ALFF values in the posterior visual cortex, including lingual gyrus and calcarine gyrus, consistent with the hypothesis that SZ is associated with low-level sensory functions (Butler et al., 2001; Butler and Javitt, 2005). For instance, the magnocellular deficits were found in SZ, which may lead to their higher-level visual processing difficulties as well (Butler and Javitt, 2005). However, a previous functional neuroimaging study reported a different result from ours. Increased ALFF was found in the bilateral prefrontal and parietal cortex, left superior temporal cortex, and right caudate nucleus after 6-week treatment of atypical antipsychotics (Lui et al., 2010), but this finding has not been replicated, and the heterogeneity of findings may be caused by sample differences such as illness chronicity. The ALFF signal is correlated with baseline cerebral blood flow and is thought to reflect spontaneous, intrinsic neuronal activity (Zhou et al., 2010). ALFF signal is mostly reliable in GM, not white matter, suggesting that ALFF derives from neural activity, although further work is needed for the exact neural substrate for ALFF (Kiviniemi et al., 2003). Our studies suggest that these abnormalities may be trait-like alterations of brain function that current antipsychotics do not effectively normalize.

No significant correlation was found between ALFF and BPRS, indicating that amplitude cannot be used as a quantitative marker for the assessment of symptoms of SZ, although it can be used in a qualitative way to help locate aberrant functional areas. Previous studies have shown that striatal ALFF was not associated with psychotic symptom severity in the first episode and medication naïve SZ (Huang et al., 2010; He et al., 2013; Wenting et al., 2013; Li et al., 2017). Anna et al. reported that SZ exhibited decreased ALFF values in the occipital pole and lingual gyrus regardless of the severity of auditory verbal hallucinations (Alonso-Solís et al., 2017). Thus, ALFF appears to be a relatively static measure that does not vary with state changes in SZ.

There are several limitations to this study. As this represented a real-world observational study, data regarding medication dose, compliance, and duration were not available or included in our analyses. Besides, the ratio of antipsychotic-naïve in the unmed-SZ was 38.3%, which may be a potential confounding effect of medication exposure in the unmed-SZ group. Furthermore, the study was cross-sectional and not longitudinal, in which the same individual was observed in medicated and unmedicated state, although the demographic data among the three groups have been matched to reduce the influence of confounding factors to a certain extent. Thus, further research is needed to confirm the generalizability of our findings.

Through real-world observation, our study suggests that GMV is a sensitive spatiotemporal marker of longer-term pharmacologic intervention in the brain, whereas ALFF is a relatively static measure reflecting more core disease traits that are less influenced by medication status and disease state (e.g., active *versus* remitted). Our study underscores the need for careful selection of neuroimaging measures based on study purpose and the focus on longer-term antipsychotics (e.g., use GMV when primary interest in treatment response and ALFF when main focus on disease trait).

DATA AVAILABILITY STATEMENT

The original contributions presented in the study are included in the article/**Supplementary Material**, further inquiries can be directed to the corresponding authors.

ETHICS STATEMENT

The studies involving human participants were reviewed and approved by the Medical Science Research Ethics Committee of The First Affiliated Hospital of China Medical University. Written informed consent to participate in this study was provided by the participants' legal guardian/next of kin.

AUTHOR CONTRIBUTIONS

FW and YT designed the experiments. YC, MC, RF, JD, ZY, YW, SW, and XJ acquired the data. YC, RF, and XZ analyzed the data. YC and FW wrote the manuscript. FYW and FW reviewed or edited the manuscript. All authors discussed the results, reviewed the manuscript, and meet the criteria for authorship to be named as authors.

FUNDING

This study was supported by the National Key R&D Program of China (grant nos. 2018YFC1311600 and 2016YFC1306900 to YT), Liaoning Revitalization Talents Program (grant #XLYC1808036 to YT), Science and Technology Plan Program of Liaoning Province (2015225018 to YT), National Science Fund for Distinguished Young Scholars (81725005 to FW), Liaoning Education Foundation (Pandeng Scholar to FW), Innovation Team Support Plan of Higher Education of Liaoning Province (LT2017007 to FW), and Major Special Construction Plan of China Medical University (3110117059 and 3110118055 to FW), and the National Natural Science Foundation of China (62176129 to XZ).

ACKNOWLEDGMENTS

We thank all the participants for their cooperation, and we are grateful for the support of Shenyang Mental Health Center, Department of Psychiatry and Radiology, The First Affiliated Hospital of China Medical University.

SUPPLEMENTARY MATERIAL

The Supplementary Material for this article can be found online at: https://www.frontiersin.org/articles/10.3389/fnins.2021.749316/full#supplementary-material

REFERENCES

Abidargham, A. (2014). Schizophrenia: overview and dopamine dysfunction. *J. Clin. Psychiatry* 75:e31. doi: 10.4088/JCP.13078tx2c

Ahmed, M., Cannon, D. M., Scanlon, C., Holleran, L., Schmidt, H., Mcfarland, J., et al. (2015). Progressive brain atrophy and cortical thinning in schizophrenia after commencing clozapine treatment. *Neuropsychopharmacology* 40, 2409–2417. doi: 10.1038/npp.2015.90

Akudjedu, T., Tronchin, G., Mcinerney, S., Scanlon, C., Kenney, J., Mcfarland, J., et al. (2020). Progression of neuroanatomical abnormalities after first-episode of psychosis: a 3-year longitudinal sMRI study. *J. Psychiatr. Res.* 130, 137–151. doi: 10.1016/j.jpsychires.2020.07.034

Alonso-Solís, A., Vives-Gilabert, Y., Portella, M. J., Rabella, M., Grasa, E. M., Roldán, A., et al. (2017). Altered amplitude of low frequency fluctuations in schizophrenia patients with persistent auditory verbal hallucinations. *Schizophr. Res.* 189, 97–103. doi: 10.1016/j.schres.2017.01.042

Brugger, S. P., and Howes, O. D. (2017). Heterogeneity and homogeneity of regional brain structure in schizophrenia: a meta-analysis. *JAMA Psychiatry* 74, 1104–1111. doi: 10.1001/jamapsychiatry.2017.2663

Butler, P. D., and Javitt, D. C. (2005). Early-stage visual processing deficits in schizophrenia. *Curr. Opin. Psychiatry* 18, 151–157. doi: 10.1097/00001504-200503000-00008

Butler, P. D., Schechter, I., Zemon, V., Schwartz, S. G., Greenstein, V. C., Gordon, J., et al. (2001). Dysfunction of early-stage visual processing in schizophrenia. *Am. J. Psychiatry* 158, 1126–1133.

Chang, M., Edmiston, E. K., Womer, F. Y., Zhou, Q., Wei, S., Jiang, X., et al. (2019). Spontaneous low-frequency fluctuations in the neural system for emotional perception in major psychiatric disorders: amplitude similarities and differences across frequency bands. *J. Psychiatry Neurosci.* 44, 132–141. doi: 10.1503/jpn.170226

Cobia, D. J., Smith, M. J., Wang, L., and Csernansky, J. G. (2012). Longitudinal progression of frontal and temporal lobe changes in schizophrenia. *Schizophr. Res.* 139, 1–6. doi: 10.1016/j.schres.2012.05.002

Cordes, D., Haughton, V. M., Arfanakis, K., Carew, J. D., Turski, P. A., Moritz, C. H., et al. (2001). Frequencies contributing to functional connectivity in the cerebral cortex in "resting-state" data. *Am. J. Neuroradiol.* 22, 1326–1333.

Correll, C. U., Rubio, J. M., and Kane, J. M. (2018). What is the risk-benefit ratio of long-term antipsychotic treatment in people with schizophrenia? *World Psychiatry* 17, 149–160. doi: 10.1002/wps.20516

Cronenwett, W. J., and Csernansky, J. (2010). Thalamic pathology in schizophrenia. *Curr. Top. Behav. Neurosci.* 4, 509–528. doi: 10.1007/7854_2010_55

Cyranoski, D. (2011). Antipsychotic drugs could shrink patients' brains. *Nature.* doi: 10.1038/news.2011.75

van Erp, T. G. M., Walton, E., Hibar, D. P., Schmaal, L., Jiang, W., Glahn, D. C., et al. (2018). Cortical Brain Abnormalities in 4474 Individuals With Schizophrenia and 5098 Control Subjects via the Enhancing Neuro Imaging Genetics Through Meta Analysis (ENIGMA) Consortium. *Biol. Psychiatry* 84, 644–654. doi: 10.1016/j.biopsych.2018.04.023

Fusarpoli, P., Smieskova, R., Kempton, M. J., Ho, B. C., Andreasen, N. C., and Borgwardt, S. (2013). Progressive brain changes in schizophrenia related to antipsychotic treatment? A meta-analysis of longitudinal MRI studies. *Neurosci. Biobehav. Rev.* 37, 1680–1691. doi: 10.1016/j.neubiorev.2013.06.001

González-Hernández, J. A., Pita-Alcorta, C., Cedeño, I., Dias-Comas, L., and Figueredo-Rodriguez, P. (2003). Abnormal functional asymmetry in occipital areas may prevent frontotemporal regions from achieving functional laterality during the WCST performance in patients with schizophrenia. *Schizophr. Res.* 61, 229–233. doi: 10.1016/s0920-9964(02)00236-0

Guo, X., Li, J., Wei, Q., Fan, X., Kennedy, D. N., Shen, Y., et al. (2013). Duration of untreated psychosis is associated with temporal and occipitotemporal volume decrease in treatment naïve schizophrenia. *PLoS One* 8:e83679. doi: 10.1371/journal.pone.0083679

Gur, R. E., Maany, V., Mozley, P. D., Swanson, C., Bilker, W., and Gur, R. C. (1998). Subcortical MRI volumes in neuroleptic-naive and treated patients with schizophrenia. *Am. J. Psychiatry* 155, 1711–1717. doi: 10.1176/ajp.155.12.1711

Halim, N. D., Weickert, C. S., Mcclintock, B. W., Weinberger, D. R., and Lipska, B. K. (2004). Effects of chronic haloperidol and clozapine treatment on neurogenesis in the adult rat hippocampus. *Neuropsychopharmacology* 29, 1063–1069. doi: 10.1038/sj.npp.1300422

Harrow, M., Jobe, T. H., Faull, R. N., and Yang, J. (2017). A 20-Year multi-followup longitudinal study assessing whether antipsychotic medications contribute to work functioning in schizophrenia. *Psychiatry Res.* 256, 267–274. doi: 10.1016/j.psychres.2017.06.069

He, Z., Deng, W., Li, M., Chen, Z., Jiang, L., Wang, Q., et al. (2013). Aberrant intrinsic brain activity and cognitive deficit in first-episode treatment-naive patients with schizophrenia. *Psychol. Med.* 43, 769–780. doi: 10.1017/S0033291712001638

Hirayasu, Y., Shenton, M. E., Salisbury, D. F., Dickey, C. C., Fischer, I. A., Mazzoni, P., et al. (1998). Lower left temporal lobe MRI volumes in patients with first-episode schizophrenia compared with psychotic patients with first-episode affective disorder and normal subjects. *Am. J. Psychiatry* 155, 1384–1391. doi: 10.1176/ajp.155.10.1384

Ho, B. C., Andreasen, N. C., Ziebell, S., Pierson, R., and Magnotta, V. (2011). Long-term antipsychotic treatment and brain volumes: a longitudinal study of first-episode schizophrenia. *Arch. Gen. Psychiatry* 68, 128–137. doi: 10.1001/archgenpsychiatry.2010.199

Honea, R., Crow, T. J., Passingham, D., and Mackay, C. E. (2005). Regional deficits in brain volume in schizophrenia: a meta-analysis of voxel-based morphometry studies. *Am. J. Psychiatry* 162, 2233–2245. doi: 10.1176/appi.ajp.162.12.2233

Hoptman, M. J., Volavka, J., Weiss, E. M., Czobor, P., Szeszko, P. R., Gerig, G., et al. (2005). Quantitative MRI measures of orbitofrontal cortex in patients with chronic schizophrenia or schizoaffective disorder. *Psychiatry Res.* 140, 133–145. doi: 10.1016/j.pscychresns.2005.07.004

Hoptman, M. J., Zuo, X. N., Butler, P. D., Javitt, D. C., D'angelo, D., Mauro, C. J., et al. (2010). Amplitude of low-frequency oscillations in schizophrenia: a resting state fMRI study. *Schizophr. Res.* 117, 13–20. doi: 10.1016/j.schres.2009.09.030

Huang, X. Q., Lui, S., Deng, W., Chan, R. C. K., Wu, Q. Z., Jiang, L. J., et al. (2010). Localization of cerebral functional deficits in treatment-naive, first-episode schizophrenia using resting-state fMRI. *Neuroimage* 49, 2901–2906. doi: 10.1016/j.neuroimage.2009.11.072

Kegeles, L. S., Abi-Dargham, A., Frankle, W. G., Gil, R., Cooper, T. B., Slifstein, M., et al. (2010). Increased synaptic dopamine function in associative regions of the striatum in schizophrenia. *Arch. Gen. Psychiatry* 67, 231–239. doi: 10.1001/archgenpsychiatry.2010.10

Kim, J. J., Crespo-Facorro, B., Andreasen, N. C., O'Leary, D. S., and Magnotta, V. (2000). Regional temporal abnormalities in schizophrenia: a quantitative gray matter volume and cortical surface size study. *Neuroimage* 11:S197. doi: 10.1016/s1053-8119(00)91130-3

Kiviniemi, V., Kantola, J. H., Jauhiainen, J., Hyvarinen, A., and Tervonen, O. (2003). Independent component analysis of nondeterministic fMRI signal sources. *Neuroimage* 19, 253–260.

Koolschijn, P. C., Van Haren, N. E., Cahn, W., Schnack, H. G., Janssen, J., Klumpers, F., et al. (2010). Hippocampal volume change in schizophrenia. *J. Clin. Psychiatry* 71, 737–744.

Kraguljac, N. V., White, D. M., Hadley, N., Hadley, J. A., Ver Hoef, L., Davis, E., et al. (2016). Aberrant hippocampal connectivity in unmedicated patients with schizophrenia and effects of antipsychotic medication: a longitudinal resting state functional MRI study. *Schizophr. Bull.* 42, 1046–1055. doi: 10.1093/schbul/sbv228

Kubicki, M., Shenton, M. E., Salisbury, D. F., Hirayasu, Y., Kasai, K., Kikinis, R., et al. (2002). Voxel-based morphometric analysis of gray matter in first episode schizophrenia. *Neuroimage* 17, 1711–1719. doi: 10.1006/nimg.2002.1296

Kuo, S. S., and Pogue-Geile, M. F. (2019). Variation in fourteen brain structure volumes in schizophrenia: a comprehensive meta-analysis of 246 studies. *Neurosci. Biobehav. Rev.* 98, 85–94.

Lacerda, A. L. T., Hardan, A. Y., Yorbik, O., Vemulapalli, M., Prasad, K. M., and Keshavan, M. S. (2007). Morphology of the orbitofrontal cortex in first-episode schizophrenia: relationship with negative symptomatology. *Prog. Neuropsychopharmacol. Biol. Psychiatry* 31, 510–516. doi: 10.1016/j.pnpbp.2006.11.022

Lang, P. J., Bradley, M. M., Fitzsimmons, J. R., Cuthbert, B. N., Scott, J. D., Moulder, B., et al. (2010). Emotional arousal and activation of the visual cortex: an fMRI analysis. *Psychophysiology* 35, 199–210. doi: 10.1111/1469-8986.3520199

Lawrie, S. M., Buechel, C., Whalley, H. C., Frith, C. D., Friston, K. J., and Johnstone, E. C. (2002). Reduced frontotemporal functional connectivity in schizophrenia associated with auditory hallucinations. *Biol. Psychiatry* 51, 1008–1011. doi: 10.1016/s0006-3223(02)01316-1

Lee, C. U., Shenton, M. E., Salisbury, D. F., Kasai, K., Onitsuka, T., Dickey, C. C., et al. (2002). Fusiform gyrus volume reduction in first-episode schizophrenia: a magnetic resonance imaging study. *Arch. Gen. Psychiatry* 59, 775–781. doi: 10.1001/archpsyc.59.9.775

Lee, S. H., Niznikiewicz, M., Asami, T., Otsuka, T., Salisbury, D. F., Shenton, M. E., et al. (2015). Initial and progressive gray matter abnormalities in insular Gyrus and temporal pole in first-episode schizophrenia contrasted with first-episode affective psychosis. *Schizophr. Bull.* 42, 790–801. doi: 10.1093/schbul/sbv177

Lesh, T. A., Tanase, C., Geib, B. R., Niendam, T. A., Yoon, J. H., Minzenberg, M. J., et al. (2015). A multimodal analysis of antipsychotic effects on brain structure and function in first-episode schizophrenia. *JAMA Psychiatry* 72, 226–234. doi: 10.1001/jamapsychiatry.2014.2178

Leucht, S., Samara, M., Heres, S., and Davis, J. M. (2016). Dose equivalents for antipsychotic drugs: the DDD Method. *Schizophr. Bull.* 42(Suppl. 1), S90–S94. doi: 10.1093/schbul/sbv167

Leung, M., Cheung, C., Yu, K., Yip, B., Sham, P., Li, Q., et al. (2011). Gray matter in first-episode schizophrenia before and after antipsychotic drug treatment. Anatomical likelihood estimation meta-analyses with sample size weighting. *Schizophr. Bull.* 37, 199–211. doi: 10.1093/schbul/sbp099

Li, F., Lui, S., Yao, L., Hu, J., Lv, P., Huang, X., et al. (2016). Longitudinal changes in resting-state cerebral activity in patients with first-episode Schizophrenia: a 1-Year Follow-up Functional MR Imaging Study. *Radiology* 279, 867–875. doi: 10.1148/radiol.2015151334

Li, X., Cao, M., Zhang, J., Chen, K., Chen, Y., Ma, C., et al. (2014). Structural and functional brain changes in the default mode network in subtypes of amnestic mild cognitive impairment. *J. Geriatr. Psychiatry Neurol.* 27, 188–198. doi: 10.1177/0891988714524629

Li, Z., Lei, W., Deng, W., Zheng, Z., Li, M., Ma, X., et al. (2017). Aberrant spontaneous neural activity and correlation with evoked-brain potentials in first-episode, treatment-naïve patients with deficit and non-deficit schizophrenia. *Psychiatry Res. Neuroimaging* 261, 9–19. doi: 10.1016/j.pscychresns.2017.01.001

Liao, J., Yan, H., Liu, Q., Yan, J., Zhang, L., Jiang, S., et al. (2015). Reduced paralimbic system gray matter volume in schizophrenia: Correlations with clinical variables, symptomatology and cognitive function. *J. Psychiatr. Res.* 65, 80–86. doi: 10.1016/j.jpsychires.2015.04.008

Lieberman, J. A., Tollefson, G. D., Charles, C., Zipursky, R., Sharma, T., Kahn, R. S., et al. (2005). Antipsychotic drug effects on brain morphology in first-episode psychosis. *Arch. Gen. Psychiatry* 62, 361–370. doi: 10.1001/archpsyc.62.4.361

Liu, N., Xiao, Y., Zhang, W., Tang, B., Zeng, J., Hu, N., et al. (2020). Characteristics of gray matter alterations in never-treated and treated chronic schizophrenia patients. *Transl. Psychiatry* 10:136. doi: 10.1038/s41398-020-0828-4

Liu, X., Wang, S., Zhang, X., Wang, Z., Tian, X., and He, Y. (2014). Abnormal amplitude of low-frequency fluctuations of intrinsic brain activity in Alzheimer's disease. *J. Alzheimers Dis.* 40, 387–397. doi: 10.3233/JAD-131322

Lui, S., Li, T., Deng, W., Jiang, L., Wu, Q., Tang, H., et al. (2010). Short-term effects of antipsychotic treatment on cerebral function in drug-naive first-episode schizophrenia revealed by "resting state" functional magnetic resonance imaging. *Arch. Gen. Psychiatry* 67, 783–792. doi: 10.1001/archgenpsychiatry.2010.84

Martin, H., and Jobe, T. H. (2018). Long-term antipsychotic treatment of schizophrenia: Does it help or hurt over a 20-year period? *World Psychiatry* 17, 162–163. doi: 10.1002/wps.20518

Mcclure, R. K., Carew, K., Greeter, S., Maushauer, E., Steen, G., and Weinberger, D. R. (2008). Absence of regional brain volume change in schizophrenia associated with short-term atypical antipsychotic treatment. *Schizophr. Res.* 98, 29–39. doi: 10.1016/j.schres.2007.05.012

Mccormick, L., Decker, L., Nopoulos, P., Ho, B. C., and Andreasen, N. (2005). Effects of atypical and typical neuroleptics on anterior cingulate volume in schizophrenia. *Schizophr. Res.* 80, 73–84. doi: 10.1016/j.schres.2005.06.022

Molina, V., Reig, S., Sanz, J., Palomo, T., Benito, C., Sánchez, J., et al. (2005). Increase in gray matter and decrease in white matter volumes in the cortex during treatment with atypical neuroleptics in schizophrenia. *Schizophr. Res.* 80, 61–71. doi: 10.1016/j.schres.2005.07.031

Morgan, C., Lappin, J., Heslin, M., Donoghue, K., Lomas, B., Reininghaus, U., et al. (2014). Reappraising the long-term course and outcome of psychotic disorders: the AESOP-10 study. *Psychol. Med.* 44, 2713–2726. doi: 10.1017/s0033291714000282

Nakamura, M., Nestor, P. G., Levitt, J. J., Cohen, A. S., Kawashima, T., Shenton, M. E., et al. (2008). Orbitofrontal volume deficit in schizophrenia and thought disorder. *Brain* 131, 180–195. doi: 10.1093/brain/awm265

Onitsuka, T., Mccarley, R. W., Kuroki, N., Dickey, C. C., Kubicki, M., Demeo, S. S., et al. (2007). Occipital lobe gray matter volume in male patients with chronic schizophrenia: a quantitative MRI Study. *Schizophr. Res.* 92, 197–206. doi: 10.1016/j.schres.2007.01.027

Pinacamacho, L., Reymejías, ÁD., Janssen, J., Bioque, M., Gonzálezpinto, A., Arango, C., et al. (2016). Age at first episode modulates diagnosis-related structural brain abnormalities in psychosis. *Schizophr. Bull.* 42, 344–357. doi: 10.1093/schbul/sbv128

Qing, Z., and Gong, G. (2016). Size matters to function: brain volume correlates with intrinsic brain activity across healthy individuals. *Neuroimage* 139, 271–278. doi: 10.1016/j.neuroimage.2016.06.046

Radua, J., Borgwardt, S., Crescini, A., Mataix-Cols, D., Meyer-Lindenberg, A., Mcguire, P. K., et al. (2012). Multimodal meta-analysis of structural and functional brain changes in first episode psychosis and the effects of antipsychotic medication. *Neurosci. Biobehav. Rev.* 36, 2325–2333. doi: 10.1016/j.neubiorev.2012.07.012

Velthorst, E., Fett, A. J., Reichenberg, A., Perlman, G., Van Os, J., Bromet, E. J., et al. (2017). The 20-year longitudinal trajectories of social functioning in individuals with psychotic disorders. *Am. J. Psychiatry* 174, 1075–1085.

Vesa, K., Juha-Heikki, K., Jukka, J., Aapo, H. R., and Osmo, T. (2003). Independent component analysis of nondeterministic fMRI signal sources. *Neuroimage* 19, 253–260.

Vita, A., De Peri, L., Deste, G., Barlati, S., and Sacchetti, E. (2015). The effect of antipsychotic treatment on cortical gray matter changes in Schizophrenia: Does the Class Matter? A Meta-analysis and Meta-regression of Longitudinal Magnetic Resonance Imaging Studies. *Biol. Psychiatry* 78, 403–412.

Vita, A., De Peri, L., Deste, G., and Sacchetti, E. (2012). Progressive loss of cortical gray matter in schizophrenia: a meta-analysis and meta-regression of longitudinal MRI studies. *Transl. Psychiatry* 2:e190.

Voineskos, A. N., Mulsant, B. H., Dickie, E. W., Neufeld, N. H., Rothschild, A. J., Whyte, E. M., et al. (2020). Effects of antipsychotic medication on brain structure in patients with major depressive disorder and psychotic features: neuroimaging findings in the context of a randomized placebo-controlled clinical trial. *JAMA Psychiatry* 77, 674–683.

Wenting, R., Su, L., Wei, D., Fei, L., Mingli, L., Xiaoqi, H., et al. (2013). Anatomical and functional brain abnormalities in drug-naive first-episode schizophrenia. *Am. J. Psychiatry* 170, 1308–1316.

Wright, I. C., Rabe-Hesketh, S., Woodruff, P. W., David, A. S., Murray, R. M., and Bullmore, E. T. (2000). Meta-analysis of regional brain volumes in schizophrenia. *Am. J. Psychiatry* 157, 16–25.

Xu, Y., Zhuo, C., Qin, W., Zhu, J., and Yu, C. (2015). Altered spontaneous brain activity in schizophrenia: a meta-analysis and a large-sample study. *Biomed Res. Int.* 2015:204628.

Yang, C., Tang, J., Liu, N., Yao, L., Xu, M., Sun, H., et al. (2021). The effects of antipsychotic treatment on the brain of patients with first-episode schizophrenia: a selective review of longitudinal

MRI Studies. *Front. Psychiatry* 12:593703. doi: 10.3389/fpsyt.2021.593703

Zang, Y. F., He, Y., Zhu, C. Z., Cao, Q. J., Sui, M. Q., Liang, M., et al. (2007). Altered baseline brain activity in children with ADHD revealed by resting-state functional MRI. *Brain Dev.* 29, 83–91.

Zhang, D., and Raichle, M. (2010). Disease and the brain's dark energy. *Nat. Rev. Neurol.* 6, 15–28.

Zhou, Y., Liang, M., Jiang, T., Tian, L., Liu, Y., Liu, Z., et al. (2007). Functional dysconnectivity of the dorsolateral prefrontal cortex in first-episode schizophrenia using resting-state fMRI. *Neurosci. Lett.* 417, 297–302.

Zhou, Y., Wang, K., Liu, Y., Song, M., Song, S. W., and Jiang, T. (2010). Spontaneous brain activity observed with functional magnetic resonance imaging as a potential biomarker in neuropsychiatric disorders. *Cogn. Neurodyn.* 4, 275–294.

Zhuo, C., Zhu, J., Qin, W., Qu, H., Ma, X., Tian, H., et al. (2014). Functional connectivity density alterations in schizophrenia. *Front. Behav. Neurosci.* 8:404. doi: 10.3389/fnbeh.2014.00404

Conflict of Interest: The authors declare that the research was conducted in the absence of any commercial or financial relationships that could be construed as a potential conflict of interest.

frontiers in Psychiatry

ORIGINAL RESEARCH
published: 10 February 2022
doi: 10.3389/fpsyt.2022.798105

Associations of Neurocognition and Social Cognition With Brain Structure and Function in Early-Onset Schizophrenia

Pengfei Guo[1], *Shuwen Hu*[1], *Xiaolu Jiang*[1], *Hongyu Zheng*[1], *Daming Mo*[2], *Xiaomei Cao*[2], *Jiajia Zhu*[3] *and Hui Zhong*[1,2]*

[1] Department of Child and Adolescent Mental Disorder, Affiliated Psychological Hospital of Anhui Medical University, Hefei, China, [2] Department of Child and Adolescent Mental Disorder, Anhui Mental Health Center, Hefei, China, [3] Department of Radiology, First Affiliated Hospital of Anhui Medical University, Hefei, China

Background: Cognitive impairment is a core feature of schizophrenia that is more serious in patients with early-onset schizophrenia (EOS). However, the neuroimaging basis of cognitive functions, including neurocognition and social cognition, remains unclear in patients with EOS.

Methods: Forty-three patients with EOS underwent structural and resting state functional magnetic resonance imaging scans. Brain structure and function were evaluated through the analysis of brain gray matter volume (GMV) and amplitude of low-frequency fluctuations (ALFF). They underwent comprehensive assessments for neurocognition (verbal memory, verbal expression, attention, and executive function) and social cognition (theory of mind and attributional bias). Correlation analyses were conducted to detect the potential link between cognitive function indices and brain imaging parameters.

Results: First, neurocognition was linked to brain structure characterized by higher immediate recall scores associated with increased GMV in the left temporal pole, higher verbal fluency scores associated with increased GMV in the left temporal pole: middle temporal gyrus, and higher Stroop-word scores associated with increased GMV in the right middle frontal gyrus. Second, social cognition was related to brain function characterized by lower sense of reality scores associated with increased ALFF in the left precentral gyrus, higher scores of accidental hostility bias associated with increased ALFF in the right middle temporal gyrus, and higher scores of accidental aggression bias associated with increased ALFF in the left precentral gyrus.

Conclusion: These findings may add to the existing knowledge about the cognitive function-brain relationship. They may have clinical significance for studying the mechanism of neurocognitive and social cognitive impairment in patients with EOS and providing potential neural targets for their treatment and intervention.

Keywords: early-onset schizophrenia, neurocognition, social cognition, gray matter volume, amplitude of low-frequency fluctuation

OPEN ACCESS

Edited by:
Yanghua Tian,
First Affiliated Hospital of Anhui Medical University, China

Reviewed by:
Gaelle Eve Doucet,
Boys Town National Research Hospital, United States
Takefumi Ueno,
Hizen Psychiatric Center (NHO), Japan

***Correspondence:**
Hui Zhong
313956777@qq.com

Specialty section:
This article was submitted to Neuroimaging and Stimulation, a section of the journal Frontiers in Psychiatry

Received: *19 October 2021*
Accepted: *18 January 2022*
Published: *10 February 2022*

Citation:
Guo P, Hu S, Jiang X, Zheng H, Mo D, Cao X, Zhu J and Zhong H (2022) Associations of Neurocognition and Social Cognition With Brain Structure and Function in Early-Onset Schizophrenia. Front. Psychiatry 13:798105. doi: 10.3389/fpsyt.2022.798105

INTRODUCTION

Schizophrenia is a chronic and declining psychiatric disorder that affects nearly 1% of the world's population, and commonly occurs in late adolescence or early adulthood (1). Approximately 11% of patients had onset of schizophrenia before the age of 18 (2), which is defined as early-onset schizophrenia (EOS) (3). Compared with adult-onset schizophrenia, adolescents with EOS have significantly worse symptoms and social outcomes characterized by a chronic illness course, insidious onset, and long treatment delays (4, 5). Cognitive dysfunction is a core feature of schizophrenia and can predict functional outcomes (6, 7). Furthermore, after standard treatment with antipsychotic drugs, the cognitive function of patients with schizophrenia cannot be completely improved and may require adjuvant treatments (8, 9). The refractoriness of antipsychotics may be closely related to the early onset of psychotic symptoms. Data from a prospective trial have shown that EOS is more likely to be refractory than adult-onset schizophrenia and have more severe cognitive impairment (10). The results of a longitudinal study have indicated a neurodevelopmental pathway of EOS with subnormal cognitive development specific to adolescence (11). Therefore, a full understanding of the neurobiological basis of cognitive impairment in patients with EOS may have important clinical significance.

In the past, many efforts have been made to explore the mechanisms of cognitive impairment in schizophrenia. It has been reported that cognitive dysfunction in schizophrenia can be improved by stimulating the glycine regulatory site of the N-methyl-d-aspartate-type glutamate receptor (12, 13). Fachim et al. further pointed out that changes in GRIN2B promoter methylation may lead to glutamatergic dysfunction in psychosis and are related to reduced cognitive performance in patients with first-episode schizophrenia (14). Data from electroencephalogram studies revealed that sleep spindle deficits in patients with schizophrenia can predict lower cognitive performance; this includes patients with EOS (15). A previous study suggested that sleep spindle deficits may be caused by dysfunction of the thalamic cortical network (16). A neuroimaging study using diffusion tensor imaging and tractography methods also found that lower fractional anisotropy of the left inferior fronto-occipital fasciculus and left inferior longitudinal fasciculus can predict worse neurocognitive performance in EOS (17). Although these findings contribute to the understanding of the mechanism of cognitive impairment in EOS, the complex association between them still needs further elucidation.

A safe, non-invasive, and easily reproducible neuroimaging approach has been provided for *in vivo* human brain exploration through advances in magnetic resonance imaging (MRI) techniques (18, 19). Voxel-based morphometry (VBM) can be used to analyze the gray matter volume (GMV) in structural MRI (20). The amplitude of low-frequency fluctuation (ALFF) measures the low-frequency oscillation intensity of blood-oxygen-level-dependent (BOLD) time courses in resting-state functional MRI and reflects local neural activity strength (21). Using these methods, some studies have revealed changes in brain structure and function in patients with EOS (22–24). Nevertheless, there is a paucity of structural and functional MRI studies exploring the neural mechanisms of cognitive impairment in patients with EOS. Only a few related studies have reported that the pathophysiological mechanism of widespread cognitive impairment in EOS may be linked to abnormal changes in the GMV (25). For example, Kadriu et al. found that the development of early cognitive deficits in EOS may occur either concomitantly or closely with changes in the hippocampal volume (26). Shi et al. indicated that structural changes and disturbed resting-state functional connectivity in the core empathy network may correlate with the social cognitive deficits in patients with EOS (27). However, these previous studies have been largely limited to a portion of the cognitive functions of patients; they have paid less attention to the global cognitive functions, including neurocognition and social cognition.

A growing body of research showed that cognitive impairment in schizophrenia involves two dimensions: neurocognition and social cognition. Similar to adult-onset cases, EOS patients had neurocognitive and social cognitive impairments (28). Neurocognition is the basic function of the central nervous system, which includes attention and working memory, verbal memory, executive function, thought disorder, and processing speed. Social cognition refers to the ability to recognize and explain the emotions or intentions of others, and the ability to use these social signals to guide conclusions or behaviors, including theory of mind, attribution bias, emotional processing, social knowledge, and social perception (29–32). These dimensions are different but highly correlated (33). Bell et al. suggested that neurocognition leads to different rehabilitation outcomes by affecting social cognition (30).

In this study, neuropsychological tools were used to evaluate the neurocognitive and social cognitive functions of patients with EOS. These included verbal memory and expression, attention and executive function, theory of mind, and attribution bias. VBM and ALFF analyses were used to measure brain structure and function. The associations between global cognitive functions and brain regions in patients with EOS at the level of brain GMV and local neural activity were explored through correlation analyses.

Abbreviations: AIHQ, Ambiguous Intentions Hostility Questionnaire; ALFF, amplitude of low-frequency fluctuation; AVLT, auditory verbal learning test; BOLD, blood-oxygen-level-dependent; DARTEL, diffeomorphic anatomical registration through the exponentiated lie algebra; DPABI, Data Processing & Analysis for Brain Imaging; EOS, early onset schizophrenia; FA, flip angle; FD, frame-wise displacement; FOV, field of view; FWE, family wise error; GMV, gray matter volume; MFG, middle frontal gyrus; MNI, Montreal Neurological Institute; MRI, magnetic resonance imaging; MTG, middle temporal gyrus; *Pr*, partial correlation coefficient; ROI, region of interest; rTPJ, right temporoparietal junction; SD, standard deviation; TE, echo time; TIV, total intracranial volume; TP, temporal pole; TR, repetition time; VBM, voxel-based morphometry; VFT, verbal fluency test.

MATERIALS AND METHODS

Participants

This study consisted of 43 Chinese Han, right-handed patients with EOS within a restricted age range of 13–18 years. All patients were recruited consecutively from the Department of Child and Adolescent Mental Disorder, Affiliated Psychological Hospital of Anhui Medical University, Hefei. According to the International Classification of Diseases criteria, two well-trained clinical psychiatrists confirmed patients' diagnosis of EOS. The study's exclusion criteria were as follows: (1) the presence of other psychiatric disorders such as intellectual disability, bipolar disorder, substance-induced mood disorder, anxiety disorder, substance abuse or dependence; (2) a history of significant neurological or physical diseases; and (3) pregnancy or any contraindications for MRI. After a training to ensure consistent methodology of rating, two investigators completed the questionnaire assessment of patients. This study was approved by the Ethics Committee of the Affiliated Psychological Hospital of Anhui Medical University. After a complete description of the study was provided, all participants' legal guardians gave written informed consent. The demographic data of the participants are listed in **Table 1** and behavioral outcomes of the cognitive tests are listed in **Supplementary Table 1**.

Cognition Assessment

Neurocognition Assessment

The auditory verbal learning test (AVLT) was performed to evaluate verbal memory function, which included four indices such as immediate recall, short-term delayed recall, long-term delayed recall, and long-term delayed recognition (34). The test contains two different learning materials, each with 15 common Chinese vocabulary items. Participants would score one point for each correct recall of a word. In the immediate recall test, participants listened to the first set of words five times and recalled the words they heard within 2 min after each listening. Investigators recorded the score each time and calculated the average score as "immediate recall." Then, participants listened to the second set of words and immediately recalled it within 2 min after listening. After that, participants were asked to recall the first set of words, and investigators recorded the scores as "short-term delayed recall." Thirty minutes after the fifth listening session, participants needed to recall the first set of words again, and the scores were noted as the "long-term delayed recall." Finally, participants were asked to listen to a 50-word vocabulary consisting of the first set of words, the second set of words and other interference words, and recognized the words in the first set. The score recognized successfully was used as an index of "long-term delayed recognition."

The verbal fluency test (VFT) was used to assess verbal expression (35). Each participant had to list as many names as possible of household appliances, animals, and fruits within 1 min, respectively. Participants would score one point for each name. The investigators recorded the total scores as an index of verbal expression performance.

Attention was evaluated using the digit span tasks (36). The tasks consisted of two indices such as digit span forward and digit span backward. Span is defined as the maximum number of digits repeated by the participant. All participants completed a digit span forward task followed by a digit-span backward task. The former begins with a series of two digits orally presented to each participant, continuing to a maximum of 13 digits. Participants were asked to repeat the digits verbally. There were two trials per digit series. All participants began with the first digit series (i.e., two digits). If repeated correctly, the participant continued to the next one; otherwise, the second trial was performed with the same digit series. The task was discontinued when the participant failed in the second trial. The digit span backward task followed the same procedure, except that participants verbally repeated the digits in reverse order.

The Stroop color word test reflects executive function (37). There were three indices including Stroop-dot, Stroop-word and Stroop-color word in the test. The test materials consisted of three types of cards: A (dot), B (word), and C (color word). Card A had red, green, yellow, and blue dots arranged in a certain order in a 4×4 manner, and card B had four Chinese words (namely "Yin," "Zou," "Wen," "Sheng") with four colors of red, green, yellow, and blue arranged in the same order. Card C had four Chinese words (namely "red," "green," "yellow," "blue") with four colors of red, green, yellow, and blue arranged in the order of card A. The participants were asked to quickly read the color of the dots or Chinese words on the cards. The time taken to read each card was used as an index of executive function performance.

Social Cognition Assessment

The Theory of Mind Picture-Sequencing Task was performed to assess the ability of mentalization (38) through six stories. Each story consisted of four pictures, accompanied by 2∼6 questions. Participants composed a story with four pictures in a certain logical order and then answered questions from the investigators. Participants would get two points, respectively for the first and last pictures sequenced correctly of each story and get one point, respectively for the two pictures in the middle of each story. At the same time, one point would be awarded for each correct answer. These questions assessed the participants' ability to understand the mental state of the characters in the story, including primary beliefs, primary false beliefs, secondary

TABLE 1 | Demographic characteristics.

Characteristics	Mean ± SD	Range
Sex (female/male)	15/28	–
Age (years)	16.63 ± 1.36	13–18
Education (years)	10.37 ± 1.51	7–12
FD (mm)	0.13 ± 0.07	0.04–0.35
TIV (cm^3)	1401.54 ± 108.84	1186.71–1629.88
Chlorpromazine equivalent doses	389.21 ± 99.93	115.74–528.17
Course of disease (months)	18.77 ± 14.92	2–51
The age of onset of schizophrenia (years)	15.07 ± 4.56	12–18

SD, standard deviation; FD, frame-wise displacement; TIV, total intracranial volume.

beliefs, secondary false beliefs, tertiary false beliefs, sense of reality, understanding reciprocity, understanding deception, and detecting deception. Adding the total score, there were ten indices extracted from the test. The maximum score was 59. The scores were used as indices of mentalizing ability.

The Ambiguous Intentions Hostility Questionnaire (AIHQ) was used to evaluate attribution bias (39). The Chinese version of AIHQ is composed of three types of hypothetical scenarios describing the characters' behaviors: intentional (five vignettes), ambiguous (five vignettes), or accidental (five vignettes). After reading each vignette, participants were asked to imagine the scenario happening to them (e.g., "You walk past a bunch of teenagers at a mall and you hear them start to laugh"), and to write down why the other person (or persons) treated you this way. Two independent investigators subsequently rated this written response for the purpose of computing a "hostility index." Then, the participants rated, on Likert scales, whether the other person (or persons) performed the action on purpose (1 "definitely no" to 6 "definitely yes"), how angry it would make them feel (1 "not at all angry" to 5 "very angry"), and how much they would blame the other person (or persons) (1 "not at all" to 5 "very much"). Investigators calculated the average score of these three items as the "blame index." Finally, the participants were asked to write down how they would respond to the situation, which was later rated by two independent investigators to compute an "aggression index." For the hostility and aggression indices, two investigators independently evaluated each participant's reaction on 5-point Likert scales based on examples of high and low scores. The scales for the hostility and aggression indices were from 1 ("not at all hostile") to 5 ("very hostile"), and 1 ("not at all aggressive") to 5 ("very aggressive"), respectively. The hostility bias, blame bias, and aggression bias scores for each scenario type were averaged after being added up, respectively. Furthermore, the total scores for each bias in the three types of scenarios were added up as the total scores of hostility bias, total scores of blame bias, and total scores of aggression bias. On the whole, there were 12 indices extracted from the test. Higher scores indicated a more negative attribution bias.

MRI Data Acquisition

MRI scans were obtained using a 3.0-Tesla MR system (Discovery MR750w, General Electric, Milwaukee, WI, USA) with a 24-channel head coil. Earplugs were used to reduce scanner noise, and tight but comfortable foam padding was used to minimize head motion. Before the scanning, all participants were instructed to keep their eyes closed, think of nothing in particular, move as little as possible, and relax but not fall asleep during the scans. High-resolution 3D T1-weighted structural images were acquired by employing a brain volume (BRAVO) sequence with the following parameters: repetition time (TR) = 8.5 ms; echo time (TE) = 3.2 ms; inversion time = 450 ms; flip angle (FA) = 12°; field of view (FOV) = 256 mm × 256 mm; matrix size = 256 × 256; slice thickness = 1 mm, no gap; voxel size = 1 mm × 1 mm × 1 mm; 188 sagittal slices. Resting-state BOLD fMRI data were acquired using a gradient-echo single-shot echo planar imaging (GRE-SS-EPI) sequence with the following parameters: TR = 2,000 ms; TE = 30 ms; FA= 90°; FOV = 220 mm × 220 mm; matrix size = 64 × 64; slice thickness = 3 mm, slice gap = 1 mm; 35 interleaved axial slices; voxel size = 3 mm × 3 mm × 3 mm; 185 volumes. After the scanning, all images were visually inspected to ensure that only images without visible artifacts, lesions, and regional deformations were included in subsequent analyses.

Gray Matter Volume Analysis

The 3D T1-weighted structural images were processed using the VBM8 toolbox (http://dbm.neuro.uni-jena.de/vbm.html) implemented in the Statistical Parametric Mapping software (SPM8, http://www.fil.ion. ucl.ac.uk/spm). First, all the structural images were segmented into gray matter, white matter, and cerebrospinal fluid density maps using the standard segmentation model. After an initial affine registration of the gray matter density map into the Montreal Neurological Institute (MNI) space, the gray matter density images were non-linearly warped using the diffeomorphic anatomical registration through the exponentiated lie algebra (DARTEL) technique (40). They were then resampled to a voxel size of 1.5 mm × 1.5 mm × 1.5 mm. The GMV map was obtained by multiplying the gray matter density map by the non-linear determinants derived from the spatial normalization step. Finally, the resultant GMV images were smoothed with a Gaussian kernel of 8 mm × 8 mm × 8 mm full-width at half maximum.

ALFF Analysis

Resting-state BOLD data were preprocessed using SPM12 (http://www.fil.ion.ucl.ac.uk/spm) and Data Processing & Analysis for Brain Imaging (DPABI, http://rfmri.org/ dpabi) (41). The first ten volumes for each participant were discarded to allow the signal to reach equilibrium and the participants to adapt to the scanning noise. The remaining volumes were corrected for the acquisition time delay between slices. Then, realignment was performed to correct the motion between the time points. Head motion parameters were computed by estimating the translation in each direction and the angular rotation on each axis for each volume. All participants' BOLD data were within the defined motion thresholds (i.e., translational or rotational motion parameters <2 mm or 2°, respectively). The frame-wise displacement (FD), which indexes the volume-to-volume changes in the head position, was also calculated. Several nuisance covariates (the linear drift, estimated motion parameters based on the Friston-24 model, spike volumes with FD > 0.5, white matter signal, and cerebrospinal fluid signal) were regressed out from the data. In the normalization step, individual structural images were first co-registered with the mean functional image; thereafter, the transformed structural images were segmented and normalized to the MNI space using the diffeomorphic anatomical registration through the exponentiated lie algebra (DARTEL) technique (40). Finally, each functional volume was spatially normalized to the MNI space using the deformation parameters estimated during the above step and resampled into a 3 mm cubic voxel. After spatial normalization, all data sets were smoothed with a 6 mm full-width at half maximum Gaussian kernel.

ALFF analysis was conducted using DPABI software (http://rfmri.org/ dpabi). After preprocessing, each voxel's BOLD time course was filtered (bandpass, 0.01–0.1 Hz) to remove the effects of very-low-frequency drift and high frequency noise, e.g., respiratory and heart rhythms. The fast Fourier transform with default parameters from DPABI was used to transform the filtered BOLD time course of each voxel into frequency domain and the power spectrum was then obtained. Because the power of a given frequency is proportional to the square of the amplitude of this frequency component of the original BOLD time course in the time domain, the square root was calculated at each frequency of the power spectrum at each voxel. The averaged squared root was obtained across 0.01–0.1 Hz, which was defined as the ALFF value. Finally, the ALFF value of each voxel was divided by the global mean ALFF value for standardization.

Statistical Analysis

The statistical descriptive analyses of demographic and behavioral data were conducted using the SPSS software (version 23.0; SPSS, Chicago, IL, USA). This study examined the relationship between cognitive function indices and brain imaging parameters in a voxel-wise manner within the whole gray matter in EOS patients. The general linear model in Statistical Parametric Mapping software (SPM12, http://www.fil.ion.ucl.ac.uk/spm) with a multiple regression design was used to identify any voxels in the GMV and ALFF maps that showed a significant association with the behavioral outcomes while controlling for age, sex, and years of education. Total intracranial volume (TIV) and FD were additional covariates for the GMV and ALFF analyses, respectively. The resulting maps were thresholded at an uncorrected voxelwise level of $p < 0.001$, and then considered significant at $p < 0.05$ cluster-level family wise error (FWE)-corrected for multiple comparisons. For each subject, the GMV and ALFF values of each cluster with a significant correlation with behavioral outcomes were extracted by the RESTplus software (http://www.restfmri.net), and then used for region of interest (ROI)-based analyses that refers to the partial correlation analyses performed in SPSS while controlling the above covariates (**Supplementary Tables 2, 3**). To ensure the robustness of the findings, this study repeated the ROI-based partial correlation analyses after removing the outliers of outcomes (GMA and ALFF values, and behavioral outcomes) greater than mean + 3 × standard deviation (SD) or smaller than mean – 3 × SD. No corrections for multiple testing were conducted, as the objective for this study was to generate some hypotheses for further testing and confirmation in a larger sample.

Sensitivity Analysis

First, a previous study revealed the effect of antipsychotic drugs on brain structure and function (42). To test the possible effect of antipsychotic drugs on our results, chlorpromazine equivalent doses for antipsychotics were included as an additional nuisance covariate with repetition in the ROI-based partial correlation analyses (43). Second, the age of onset of schizophrenia might affect GMV and ALFF, so the ROI-based partial correlation analyses were repeated while adding this variable as an additional nuisance covariate.

RESULTS

Correlations Between Neurocognition and GMV

In the voxel-wise whole gray matter analysis, the significant correlations between neurocognition and GMV are shown in **Figure 1** (cluster-level $P < 0.05$, FWE corrected). After adjustment for age, sex, years of education, TIV, and outliers, significant positive correlations were found between the AVLT-immediate recall and GMV in the left temporal pole (TP) (cluster size: 1,602 voxels, peak MNI coordinate x/y/z: −39/4.5/-30, peak T: 4.872, partial correlation coefficient [pr]: 0.626, $P < 0.001$); positive correlations between the VFT and GMV in the left TP: middle temporal gyrus (cluster size: 762 voxels, peak MNI coordinate x/y/z: −46.5/12/-30, peak T: 5.319, pr: 0.635, $P < 0.001$); and positive correlations between the Stroop-word and GMV in the right middle frontal gyrus (MFG) (cluster size: 1,289 voxels, peak MNI coordinate x/y/z: 40.5/22.5/42, peak T: 4.951, pr: 0.472, $P = 0.003$). No significant correlations were observed between neurocognition and ALFF.

Correlations Between Social Cognition and ALFF

In the ALFF analysis, the significant correlations between social cognition and ALFF are shown in **Figure 2** (cluster-level $P < 0.05$, FWE corrected). After accounting for age, sex, years of education, FD, and outliers, the Theory of Mind-sense of reality showed significant negative correlations with ALFF in the left precentral gyrus (cluster size: 67 voxels, peak MNI coordinate x/y/z: −21/-24/66, peak T: −5.973, pr: −0.433, $P = 0.007$). The accidental hostility bias exhibited significant positive correlations with ALFF in the right middle temporal gyrus (MTG) (cluster size: 51 voxels, peak MNI coordinate x/y/z: 54/-36/-9, peak T: 6.187, pr: 0.380, $P = 0.022$). There were significant positive correlations between the accidental aggression bias and ALFF in the left precentral gyrus (cluster size: 51 voxels, peak MNI coordinate x/y/z: −30/-24/45, peak T: 5.854, pr: 0.377, $P = 0.021$). No significant correlations were observed between social cognition and GMV.

Sensitivity Analysis

First, after considering the influence of antipsychotics, the correlations between cognitive function indices and brain imaging parameters had slight changes in p values, but the main brain regions in the results had survived (**Supplementary Tables 4, 5**). Second, the correlations between cognitive function indices and brain imaging parameters remained unchanged after additionally adjusting for the age of onset of schizophrenia (**Supplementary Tables 6, 7**). These suggest that antipsychotics and the age of onset of schizophrenia did not influence the main results of this study.

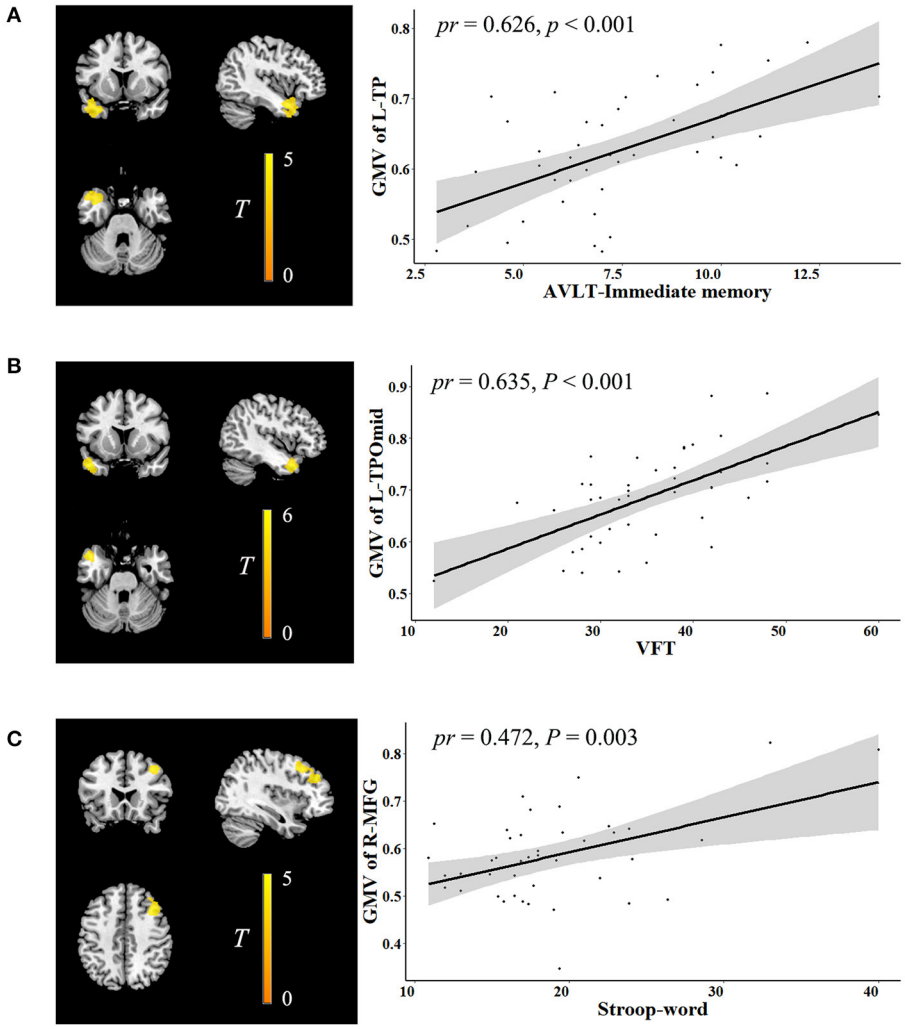

FIGURE 1 | Correlation between neurocognition and GMV. The left figure in **(A–C)** is voxel-based and the right is ROI-based. **(A)** Correlation between GMV in the left TP and AVLT-immediate recall. **(B)** Correlation between GMV in the left TPOmid and VFT. **(C)** Correlation between GMV in the right MFG and stroop-word. GMV, gray matter volume; ROI, region of interest; TP, temporal pole; AVLT, auditory verbal learning test; TPOmid, temporal pole: middle temporal gyrus; VFT, verbal fluency test; MFG, middle frontal gyrus; *pr*, partial correlation coefficient; L, left; R, right.

DISCUSSION

Using structural and resting-state functional MRI, we explored the relationships between neurocognitive function, social cognitive function, and brain imaging parameters in patients with EOS. There were two main findings in this study. The first was the relationship between neurocognitive function and brain structure. Higher language functions of verbal memory and expression were associated with increased GMV in the TP. Meanwhile, higher executive function was associated with increased GMV in the MFG. The second was the relationship between social cognitive function and brain function. This was characterized by lower theory of mind ability associated with increased ALFF in the precentral gyrus and more negative attribution bias with increased ALFF in the precentral gyrus, and MTG.

Previous studies have used VBM and ALFF methods to investigate changes in GMV and local neural activity in patients with schizophrenia (44–48). The TP, MFG, and MTG are the common brain areas consistently reported in previous studies and the current study. For instance, compared with healthy participants, some studies found that patients with schizophrenia demonstrate decreased GMV in the MFG and paralimbic system (including the orbitofrontal cortex, insular cortex, and TP) (44, 45). Li et al. found differences in the variability of dynamic ALFF between EOS patients and healthy controls in the bilateral precuneus, right superior marginal gyrus, right postcentral gyrus, and right MTG (48). However, the investigators focused solely on distinguishing this disease and paid no attention to changes in the global cognitive function of patients. We speculate that not only do EOS patients have altered GMV or local nerve activity in the common regions, but these alterations may also

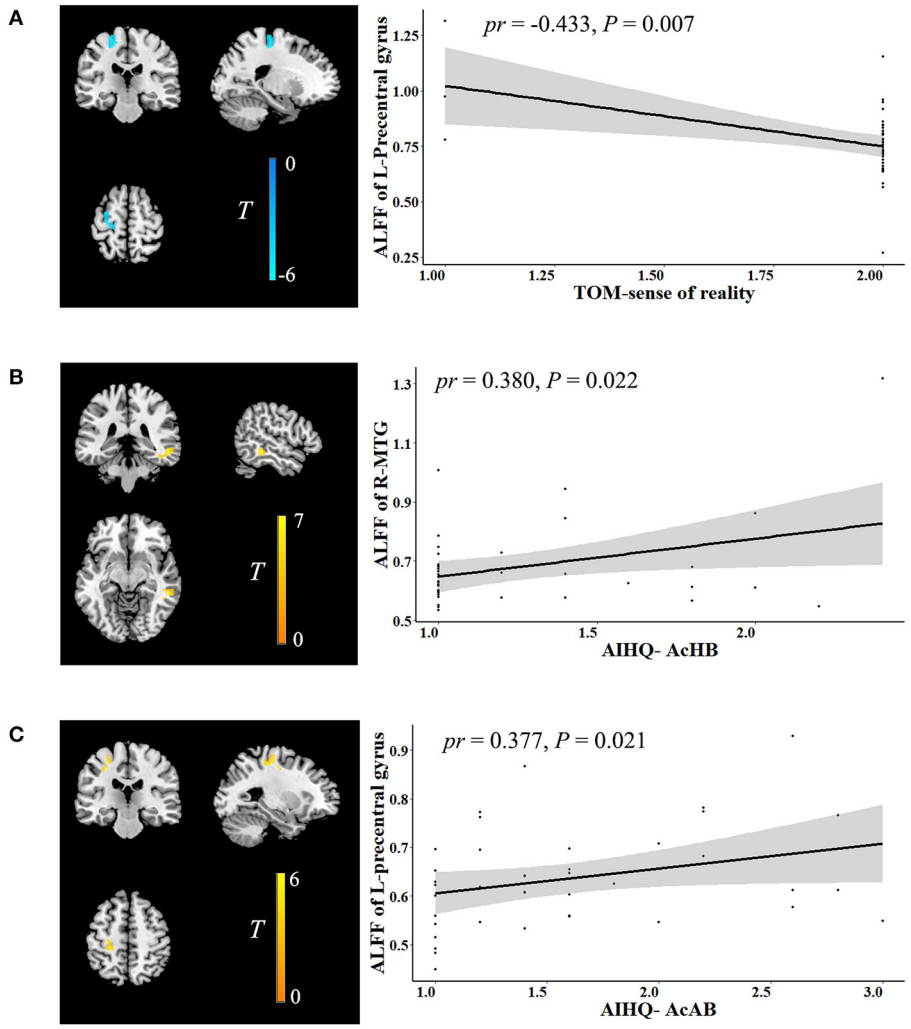

FIGURE 2 | Correlation between social cognition and ALFF. The left figure in **(A–C)** is voxel-based and the right is ROI-based. **(A)** Correlation between ALFF in the left precentral gyrus and TOM-sense of reality. **(B)** Correlation between ALFF in the right MTG and AIHQ-AcHB. **(C)** Correlation between ALFF in the left precentral gyrus and AIHQ-AcAB. ALFF, amplitude of low-frequency fluctuation; ROI, region of interest; TOM, theory of mind; AIHQ, ambiguous intentions hostility questionnaire; AcHB, accidental hostility bias; MTG, middle temporal gyrus; AcAB, accidental aggression bias; *pr*, partial correlation coefficient; L, left; R, right.

affect neurocognitive and social cognitive functions. There are some inconsistent findings between the current and previous studies. The differences across studies may be linked to patient characteristics (subtype of schizophrenia, age of onset, and course of disease), brain imaging methods (GMV, ALFF, and dynamic ALFF), and sample sizes.

The TP is the most rostral part of the temporal lobe, and its complex structure has been associated with a variety of advanced cognitive functions, including autobiographic memory (49–51), semantic memory (52, 53), generation of false memories (54), face processing (55) and processing of emotional understanding (56, 57). The "semantic hub" theory is one important theory about TP function, which considers the TP as a domain-general hub integrating semantic information from different modalities into a coherent representation (58, 59). Pehrs et al. showed that the TP plays a role in the integration of various semantic information and top-down modulation in the ventral visual stream (57). In patients with Alzheimer's disease, impaired semantic performance was associated with decreased GMV in the TP (60). Similarly, impaired semantic memory was also found in patients with epileptogenic lesions at the left TP (61). Consistent with these prior findings, a correlation between the TP and language function in EOS patients was found in this study. This suggests that damage to the TP may be a shared underlying neural mechanism leading to language dysfunction in a variety of neuropsychiatric diseases. The MFG is considered to be a component of the central executive network and involves processing of working memory information and the judgment and decision of goal-oriented behaviors (62–64). There is neuropsychological evidence that executive functions of schizophrenia, such as working memory and planning, are impaired (65), as well as neuroimaging evidence that specific deficits in an executive function known as goal maintenance in patients with schizophrenia are associated with reduced MFG

activity (66). Collectively, these prior findings, coupled with the results of this study, suggest that MFG dysfunction may serve as the basis of executive function deficits in patients with schizophrenia, including EOS.

One interesting aspect of the results of this study was the negative correlation between social cognitive performance and local neural activity in the precentral gyrus and MTG in patients with EOS. The precentral gyrus is considered to be the core area of the mirror-neuron system and plays a fundamental role in both action understanding and imitation (67), associated with the realization of a variety of social cognitive functions (68, 69). Previous studies found that the aberrant connectivity of the mirror neuron system network may be linked to social dysfunction in patients with schizophrenia, and this aberrant connectivity might even exist in the early stages of psychosis (70, 71). Together with our data, it is reasonable to assume that functional deficits of the precentral gyrus may be a neural characteristic of the impaired social cognition in EOS patients. The MTG plays a vital role in social cognition, semantic processing, auditory processing, action observation and language (72). Increasing number of studies have reported that the MTG is also an important component of the Theory of Mind network. For example, Schurz et al. found significant activation in the MTG during the tasks of social animations, mind in the eyes, and rational actions (73). Another study reported that, compared with false beliefs, social animations showed the strongest activation in the MTG (74). In patients with schizophrenia, a diffusion-weighted MRI study reported an increased trace in the right MTG and a correlation between trace and decreased social cognition (75). Taken together, our results support the idea that MTG dysfunction serves as the substrate underlying impaired social cognition in the EOS.

There are some limitations that should be noted in this study. First, healthy controls were not included in this study. Although our results are similar to those of previous controlled studies with healthy controls, future investigations are warranted to further strengthen our findings more rigorously and accurately by enrolling a sample of subjects with EOS and healthy adolescents. Second, causal relationships cannot be inferred from this cross-sectional design. Longitudinal studies with interventions targeting the improvement of cognitive function in EOS are required to establish the direction of causality. Third, the patients were receiving antipsychotic medication that may have influenced the interpretation of results. Although the main results remained after adjusting for antipsychotic dose equivalents, the medication effect could not be completely eliminated (43). Future studies with medication-naïve first-episode patients with EOS are needed to validate the preliminary findings of this study. Fourth, other indices (e.g., processing speed and emotional processing) would need to be analyzed to further clarify the cognitive function-brain relationship in the EOS. Finally, the results of this study were not corrected for multiple comparisons, because the results might not survive correction, likely due to the small sample size. However, our analyses were important for future hypothesis generation. Future studies are required to further expand the sample size and conduct the correction for multiple comparisons to make the results more reliable.

In conclusion, the present study is the first to explore the association between global cognitive function and the brain in patients with EOS. The observed relationships of neurocognition with GMV and social cognition with ALFF may help to expand the existing knowledge about the cognitive function-brain relationship in EOS. To some extent, this disassociation between anatomy and function also supports that neurocognition is the basic cognitive function that affects the ability of daily living, and social cognition, which is a more advanced cognitive function, can better predict social outcome (29). More broadly, these findings may have clinical significance for studying the neurological mechanism of cognitive impairment in patients with EOS and provide potential neural targets for their treatment and intervention.

DATA AVAILABILITY STATEMENT

The original contributions presented in the study are included in the article/**Supplementary Material**, further inquiries can be directed to the corresponding author/s.

ETHICS STATEMENT

The studies involving human participants were reviewed and approved by the Ethics Committee of the Affiliated Psychological Hospital of Anhui Medical University. Written informed consent to participate in this study was provided by the participants' legal guardian/next of kin.

AUTHOR CONTRIBUTIONS

PG and SH: methodology, data curation, software, and writing original draft. XJ, HoZ, DM, and XC: data collection, visualization, and investigation. JZ: conceptualization, methodology, software, and formal analysis. HuZ: conceptualization, supervision, and writing—review and editing. All authors contributed to the article and approved the submitted version.

FUNDING

This work was supported by the grants of Anhui Provincial Department of Science and Technology (No. 1804h08020251) and National Key Research and Development Program (No. 2018YFC1314300).

ACKNOWLEDGMENTS

The authors give special thanks to the patients and their families.

SUPPLEMENTARY MATERIAL

The Supplementary Material for this article can be found online at: https://www.frontiersin.org/articles/10.3389/fpsyt.2022.798105/full#supplementary-material

REFERENCES

1. Asarnow JR, Tompson MC, McGrath EP. Annotation: childhood-onset schizophrenia: clinical and treatment issues. *J Child Psychol Psychiatry*. (2004) 45:180–94. doi: 10.1111/j.1469-7610.2004.00213.x
2. Amminger GP, Henry LP, Harrigan SM, Harris MG, Alvarez-Jimenez M, Herrman H, et al. Outcome in early-onset schizophrenia revisited: findings from the Early Psychosis Prevention and Intervention Centre long-term follow-up study. *Schizophr Res.* (2011) 131:112–9. doi: 10.1016/j.schres.2011.06.009
3. Werry JS. Child and adolescent (early onset) schizophrenia: a review in light of DSM-III-R. *J Autism Dev Disord*. (1992) 22:601–24. doi: 10.1007/BF01046330
4. Joa I, Johannessen JO, Langeveld J, Friis S, Melle I, Opjordsmoen S, et al. Baseline profiles of adolescent vs. adult-onset first-episode psychosis in an early detection program. *Acta Psychiatr Scand.* (2009) 119:494–500. doi: 10.1111/j.1600-0447.2008.01338.x
5. Hollis C. Adult outcomes of child- and adolescent-onset schizophrenia: diagnostic stability and predictive validity. *Am J Psychiatry*. (2000) 157:1652–9. doi: 10.1176/appi.ajp.157.10.1652
6. Reichenberg A, Harvey PD. Neuropsychological impairments in schizophrenia: integration of performance-based and brain imaging findings. *Psychol Bull.* (2007) 133:833–58. doi: 10.1037/0033-2909.133.5.833
7. Harvey PD, Howanitz E, Parrella M, White L, Davidson M, Mohs RC, et al. Symptoms, cognitive functioning, and adaptive skills in geriatric patients with lifelong schizophrenia: a comparison across treatment sites. *Am J Psychiatry*. (1998) 155:1080–6. doi: 10.1176/ajp.155.8.1080
8. Keefe RS, Bilder RM, Davis SM, Harvey PD, Palmer BW, Gold JM, et al. Neurocognitive effects of antipsychotic medications in patients with chronic schizophrenia in the CATIE Trial. *Arch Gen Psychiatry*. (2007) 64:633–47. doi: 10.1001/archpsyc.64.6.633
9. Swartz MS, Perkins DO, Stroup TS, Davis SM, Capuano G, Rosenheck RA, et al. Effects of antipsychotic medications on psychosocial functioning in patients with chronic schizophrenia: findings from the NIMH CATIE study. *Am J Psychiatry*. (2007) 164:428–36. doi: 10.1176/ajp.2007.164.3.428
10. Iasevoli F, Razzino E, Altavilla B, Avagliano C, Barone A, Ciccarelli M, et al. Relationships between early age at onset of psychotic symptoms and treatment resistant schizophrenia. *Early Interv Psychiatry*. (2021). doi: 10.1111/eip.13174. [Epub ahead of print].
11. Oie MG, Sundet K, Haug E, Zeiner P, Klungsoyr O, Rund BR. Cognitive performance in early-onset schizophrenia and attention-deficit/hyperactivity disorder: a 25-year follow-up study. *Front Psychol.* (2020) 11:606365. doi: 10.3389/fpsyg.2020.606365
12. Javitt DC. Glutamate as a therapeutic target in psychiatric disorders. *Mol Psychiatry*. (2004) 9:984–97, 79. doi: 10.1038/sj.mp.4001551
13. Tsai GE, Yang P, Chang YC, Chong MY. D-alanine added to antipsychotics for the treatment of schizophrenia. *Biol Psychiatry*. (2006) 59:230–4. doi: 10.1016/j.biopsych.2005.06.032
14. Fachim HA, Loureiro CM, Corsi-Zuelli F, Shuhama R, Louzada-Junior P, Menezes PR, et al. GRIN2B promoter methylation deficits in early-onset schizophrenia and its association with cognitive function. *Epigenomics*. (2019) 11:401–10. doi: 10.2217/epi-2018-0127
15. Ferrarelli F, Tononi G. Reduced sleep spindle activity point to a TRN-MD thalamus-PFC circuit dysfunction in schizophrenia. *Schizophr Res.* (2017) 180:36–43. doi: 10.1016/j.schres.2016.05.023
16. Bartho P, Slezia A, Matyas F, Faradzs-Zade L, Ulbert I, Harris KD, et al. Ongoing network state controls the length of sleep spindles via inhibitory activity. *Neuron*. (2014) 82:1367–79. doi: 10.1016/j.neuron.2014.04.046
17. Epstein KA, Cullen KR, Mueller BA, Robinson P, Lee S, Kumra S. White matter abnormalities and cognitive impairment in early-onset schizophrenia-spectrum disorders. *J Am Acad Child Adoles Psychiatry*. (2014) 53:362–72 e1–2. doi: 10.1016/j.jaac.2013.12.007
18. Lui S, Zhou XJ, Sweeney JA, Gong Q. Psychoradiology: the frontier of neuroimaging in psychiatry. *Radiology*. (2016) 281:357–72. doi: 10.1148/radiol.2016152149
19. Lerch JP, van der Kouwe AJ, Raznahan A, Paus T, Johansen-Berg H, Miller KL, et al. Studying neuroanatomy using MRI. *Nat Neurosci.* (2017) 20:314–26. doi: 10.1038/nn.4501
20. Ashburner J, Friston KJ. Voxel-based morphometry–the methods. *Neuroimage*. (2000) 11:805–21. doi: 10.1006/nimg.2000.0582
21. Zang YF, He Y, Zhu CZ, Cao QJ, Sui MQ, Liang M, et al. Altered baseline brain activity in children with ADHD revealed by resting-state functional MRI. *Brain Dev*. (2007) 29:83–91. doi: 10.1016/j.braindev.2006.07.002
22. Tordesillas-Gutierrez D, Koutsouleris N, Roiz-Santianez R, Meisenzahl E, Ayesa-Arriola R, Marco de. Lucas E, et al. Grey matter volume differences in non-affective psychosis and the effects of age of onset on grey matter volumes: a voxelwise study. *Schizophrenia research*. (2015) 164:74–82. doi: 10.1016/j.schres.2015.01.032
23. Tang J, Liao Y, Zhou B, Tan C, Liu W, Wang D, et al. Decrease in temporal gyrus gray matter volume in first-episode, early onset schizophrenia: an MRI study. *PLoS ONE*. (2012) 7:e40247. doi: 10.1371/journal.pone.0040247
24. Zheng J, Zhang Y, Guo X, Duan X, Zhang J, Zhao J, et al. Disrupted amplitude of low-frequency fluctuations in antipsychotic-naive adolescents with early-onset schizophrenia. *Psychiatry Res Neuroimaging*. (2016) 249:20–6. doi: 10.1016/j.pscychresns.2015.11.006
25. Gao ZT Li YL, Guo SQ, Xia YH. [Brain gray matter volume alterations and cognitive function in first-episode childhood-and adolescence-onset schizophrenia]. *Zhonghua Yi Xue Za Zhi*. (2019) 99:3581–6. doi: 10.3760/cma.j.issn.0376-2491.2019.45.010
26. Kadriu B, Gu W, Korenis P, Levine JM. Do cognitive and neuropsychological functioning deficits coincide with hippocampal alteration during first-psychotic episode? *CNS Spectr*. (2019) 24:472–8. doi: 10.1017/S1092852918001293
27. Shi LJ, Zhou HY, Wang Y, Shen YM, Fang YM, He YQ, et al. Altered empathy-related resting-state functional connectivity in adolescents with early-onset schizophrenia and autism spectrum disorders. *Asian J Psychiatr*. (2020) 53:102167. doi: 10.1016/j.ajp.2020.102167
28. Harvey PD, Isner EC. Cognition, social cognition, and functional capacity in early-onset schizophrenia. *Child Adolesc Psychiatr Clin N Am*. (2020) 29:171–82. doi: 10.1016/j.chc.2019.08.008
29. Silberstein J, Harvey PD. Cognition, social cognition, and Self-assessment in schizophrenia: prediction of different elements of everyday functional outcomes. *CNS Spectr*. (2019) 24:88–93. doi: 10.1017/S1092852918001414
30. Bell M, Tsang HW, Greig TC, Bryson GJ. Neurocognition, social cognition, perceived social discomfort, and vocational outcomes in schizophrenia. *Schizophr Bull*. (2009) 35:738–47. doi: 10.1093/schbul/sbm169
31. Wexler BE, Bell MD. Cognitive remediation and vocational rehabilitation for schizophrenia. *Schizophr Bull*. (2005) 31:931–41. doi: 10.1093/schbul/sbi038
32. Green MF, Penn DL, Bentall R, Carpenter WT, Gaebel W, Gur RC, et al. Social cognition in schizophrenia: an NIMH workshop on definitions, assessment, and research opportunities. *Schizophr Bull*. (2008) 34:1211–20. doi: 10.1093/schbul/sbm145
33. Sergi MJ, Rassovsky Y, Widmark C, Reist C, Erhart S, Braff DL, et al. Social cognition in schizophrenia: relationships with neurocognition and negative symptoms. *Schizophr Res*. (2007) 90:316–24. doi: 10.1016/j.schres.2006.09.028
34. Van der Elst W, van Boxtel MP, van Breukelen GJ, Jolles J. Rey's verbal learning test: normative data for 1855 healthy participants aged 24-81 years and the influence of age, sex, education, and mode of presentation. *J Int Neuropsychol Soc*. (2005) 11:290–302. doi: 10.1017/S1355617705050344
35. Vasquez BP, Zakzanis KK. The neuropsychological profile of vascular cognitive impairment not demented: a meta-analysis. *J Neuropsychol*. (2015) 9:109–36. doi: 10.1111/jnp.12039
36. Groth-Marnat G, Baker S. Digit Span as a measure of everyday attention: a study of ecological validity. *Percept Mot Skills*. (2003) 97:1209–18. doi: 10.2466/pms.2003.97.3f.1209
37. Houx PJ, Jolles J, Vreeling FW. Stroop interference: aging effects assessed with the Stroop Color-Word Test. *Exp Aging Res*. (1993) 19:209–24. doi: 10.1080/03610739308253934

38. Van Rheenen TE, Rossell SL. Picture sequencing task performance indicates theory of mind deficit in bipolar disorder. *J Affect Disord.* (2013) 151:1132–4. doi: 10.1016/j.jad.2013.07.009
39. Combs DR, Penn DL, Wicher M, Waldheter E. The Ambiguous Intentions Hostility Questionnaire (AIHQ): a new measure for evaluating hostile social-cognitive biases in paranoia. *Cogn Neuropsychiatry.* (2007) 12:128–43. doi: 10.1080/13546800600787854
40. Ashburner J, A. fast diffeomorphic image registration algorithm. *Neuroimage.* (2007) 38:95–113. doi: 10.1016/j.neuroimage.2007.07.007
41. Yan CG, Wang XD, Zuo XN, Zang YF, DPABI. Data processing & analysis for (resting-state) brain imaging. *Neuroinformatics.* (2016) 14:339–51. doi: 10.1007/s12021-016-9299-4
42. Lesh TA, Tanase C, Geib BR, Niendam TA, Yoon JH, Minzenberg MJ, et al. A multimodal analysis of antipsychotic effects on brain structure and function in first-episode schizophrenia. *JAMA Psychiatry.* (2015) 72:226–34. doi: 10.1001/jamapsychiatry.2014.2178
43. Andreasen NC, Pressler M, Nopoulos P, Miller D, Ho BC. Antipsychotic dose equivalents and dose-years: a standardized method for comparing exposure to different drugs. *Biol Psychiatry.* (2010) 67:255–62. doi: 10.1016/j.biopsych.2009.08.040
44. Liao J, Yan H, Liu Q, Yan J, Zhang L, Jiang S, et al. Reduced paralimbic system gray matter volume in schizophrenia: correlations with clinical variables, symptomatology and cognitive function. *J Psychiatr Res.* (2015) 65:80–6. doi: 10.1016/j.jpsychires.2015.04.008
45. Jiang Y, Duan M, Chen X, Zhang X, Gong J, Dong D, et al. Aberrant prefrontal-thalamic-cerebellar circuit in schizophrenia and depression: evidence from a possible causal connectivity. *Int J Neural Syst.* (2019) 29:1850032. doi: 10.1142/S0129065718500326
46. Zhang YY, Liao JM, Li QQ, Zhang X, Liu LJ, Yan J, et al. Altered resting-state brain activity in schizophrenia and obsessive-compulsive disorder compared with non-psychiatric controls: commonalities and distinctions across disorders. *Front Psychiatry.* (2021) 12:681701. doi: 10.3389/fpsyt.2021.681701
47. Li Z, Lei W, Deng W, Zheng Z, Li M, Ma X, et al. Aberrant spontaneous neural activity and correlation with evoked-brain potentials in first-episode, treatment-naive patients with deficit and non-deficit schizophrenia. *Psychiatry Res Neuroimaging.* (2017) 261:9–19. doi: 10.1016/j.pscychresns.2017.01.001
48. Li Q, Cao X, Liu S, Li Z, Wang Y, Cheng L, et al. Dynamic alterations of amplitude of low-frequency fluctuations in patients with drug-naive first-episode early onset schizophrenia. *Front Neurosci.* (2020) 14:901. doi: 10.3389/fnins.2020.00901
49. Kapur N, Ellison D, Smith MP, McLellan DL, Burrows EH. Focal retrograde amnesia following bilateral temporal lobe pathology. A neuropsychological and magnetic resonance study. *Brain.* (1992) 115(Pt. 1):73–85. doi: 10.1093/brain/115.1.73
50. Maguire EA, Mummery CJ. Differential modulation of a common memory retrieval network revealed by positron emission tomography. *Hippocampus.* (1999) 9:54–61.
51. Tomadesso C, Perrotin A, Mutlu J, Mezenge F, Landeau B, Egret S, et al. Brain structural, functional, and cognitive correlates of recent versus remote autobiographical memories in amnestic Mild Cognitive Impairment. *Neuroimage Clin.* (2015) 8:473–82. doi: 10.1016/j.nicl.2015.05.010
52. Marinkovic K, Dhond RP, Dale AM, Glessner M, Carr V, Halgren E. Spatiotemporal dynamics of modality-specific and supramodal word processing. *Neuron.* (2003) 38:487–97. doi: 10.1016/S0896-6273(03)00197-1
53. Mesulam MM, Rogalski EJ, Wieneke C, Hurley RS, Geula C, Bigio EH, et al. Primary progressive aphasia and the evolving neurology of the language network. *Nat Rev Neurol.* (2014) 10:554–69. doi: 10.1038/nrneurol.2014.159
54. Chadwick MJ, Anjum RS, Kumaran D, Schacter DL, Spiers HJ, Hassabis D. Semantic representations in the temporal pole predict false memories. *Proc Natl Acad Sci USA.* (2016) 113:10180–5. doi: 10.1073/pnas.1610686113
55. Jimura K, Konishi S, Miyashita Y. Temporal pole activity during perception of sad faces, but not happy faces, correlates with neuroticism trait. *Neurosci Lett.* (2009) 453:45–8. doi: 10.1016/j.neulet.2009.02.012
56. Frith U, Frith CD. Development and neurophysiology of mentalizing. *Philosophical transactions of the Royal Society of London Series B, Biological sciences.* (2003) 358:459–73. doi: 10.1098/rstb.2002.1218
57. Pehrs C, Zaki J, Schlochtermeier LH, Jacobs AM, Kuchinke L, Koelsch S. The temporal pole top-down modulates the ventral visual stream during social cognition. *Cerebral Cortex.* (2017) 27:777–92. doi: 10.1093/cercor/bhv226
58. McClelland JL, Rogers TT. The parallel distributed processing approach to semantic cognition. *Nat Rev Neurosci.* (2003) 4:310–22. doi: 10.1038/nrn1076
59. Patterson K, Nestor PJ, Rogers TT. Where do you know what you know? The representation of semantic knowledge in the human brain. *Nat Rev Neurosci.* (2007) 8:976–87. doi: 10.1038/nrn2277
60. Joubert S, Gour N, Guedj E, Didic M, Gueriot C, Koric L, et al. Early-onset and late-onset Alzheimer's disease are associated with distinct patterns of memory impairment. *Cortex.* (2016) 74:217–32. doi: 10.1016/j.cortex.2015.10.014
61. Campo P, Poch C, Toledano R, Igoa JM, Belinchon M, Garcia-Morales I, et al. Visual object naming in patients with small lesions centered at the left temporopolar region. *Brain Struct Funct.* (2016) 221:473–85. doi: 10.1007/s00429-014-0919-1
62. Petrides M. Lateral prefrontal cortex: architectonic and functional organization. *Philos Trans R Soc Lond Ser B Biol Sci.* (2005) 360:781–95. doi: 10.1098/rstb.2005.1631
63. Muller NG, Knight RT. The functional neuroanatomy of working memory: contributions of human brain lesion studies. *Neuroscience.* (2006) 139:51–8. doi: 10.1016/j.neuroscience.2005.09.018
64. Koechlin E, Summerfield C. An information theoretical approach to prefrontal executive function. *Trends Cogn Sci.* (2007) 11:229–35. doi: 10.1016/j.tics.2007.04.005
65. Bortolato B, Miskowiak KW, Kohler CA, Vieta E, Carvalho AF. Cognitive dysfunction in bipolar disorder and schizophrenia: a systematic review of meta-analyses. *Neuropsychiatr Dis Treat.* (2015) 11:3111–25. doi: 10.2147/NDT.S76700
66. Poppe AB, Barch DM, Carter CS, Gold JM, Ragland JD, Silverstein SM, et al. Reduced frontoparietal activity in schizophrenia is linked to a specific deficit in goal maintenance: a multisite functional imaging study. *Schizophr Bull.* (2016) 42:1149–57. doi: 10.1093/schbul/sbw036
67. Rizzolatti G, Craighero L. The mirror-neuron system. *Annu Rev Neurosci.* (2004) 27:169–92. doi: 10.1146/annurev.neuro.27.070203.144230
68. Jani M, Kasparek T. Emotion recognition and theory of mind in schizophrenia: a meta-analysis of neuroimaging studies. *World J Biol Psychiatry.* (2018) 19:S86–96. doi: 10.1080/15622975.2017.1324176
69. Cook R, Bird G, Catmur C, Press C, Heyes C. Mirror neurons: from origin to function. *Behav Brain Sci.* (2014) 37:177–92. doi: 10.1017/S0140525X13000903
70. Sun F, Zhao Z, Lan M, Xu Y, Huang M, Xu D. Abnormal dynamic functional network connectivity of the mirror neuron system network and the mentalizing network in patients with adolescent-onset, first-episode, drug-naive schizophrenia. *Neurosci Res.* (2021) 162:63–70. doi: 10.1016/j.neures.2020.01.003
71. Choe E, Lee TY, Kim M, Hur JW, Yoon YB, Cho KK, et al. Aberrant within- and between-network connectivity of the mirror neuron system network and the mentalizing network in first episode psychosis. *Schizophr Res.* (2018) 199:243–9. doi: 10.1016/j.schres.2018.03.024
72. Xu J, Lyu H, Li T, Xu Z, Fu X, Jia F, et al. Delineating functional segregations of the human middle temporal gyrus with resting-state functional connectivity and coactivation patterns. *Hum Brain Mapp.* (2019) 40:5159–71. doi: 10.1002/hbm.24763
73. Schurz M, Radua J, Aichhorn M, Richlan F, Perner J. Fractionating theory of mind: a meta-analysis of functional brain imaging studies. *Neurosci Biobehav Rev.* (2014) 42:9–34. doi: 10.1016/j.neubiorev.2014.01.009
74. Schurz M, Tholen MG, Perner J, Mars RB, Sallet J. Specifying the brain anatomy underlying temporo-parietal junction activations for theory of mind: a review using probabilistic atlases from different imaging modalities. *Hum Brain Mapp.* (2017) 38:4788–805. doi: 10.1002/hbm.23675
75. Lee JS, Kim CY, Joo YH, Newell D, Bouix S, Shenton ME, et al. Increased diffusivity in gray matter in recent onset schizophrenia is associated with clinical symptoms and social cognition. *Schizophr Res.* (2016) 176:144–50. doi: 10.1016/j.schres.2016.08.011

Conflict of Interest: The authors declare that the research was conducted in the absence of any commercial or financial relationships that could be construed as a potential conflict of interest.

The Handling Editor YT declared a shared affiliation, though no other collaboration, with one of the authors PG, SH, XJ, HoZ, DM, XC, JZ, and HuZ at the time of the review.

Publisher's Note: All claims expressed in this article are solely those of the authors and do not necessarily represent those of their affiliated organizations, or those of the publisher, the editors and the reviewers. Any product that may be evaluated in this article, or claim that may be made by its manufacturer, is not guaranteed or endorsed by the publisher.

frontiers in Human Neuroscience

METHODS
published: 16 February 2022
doi: 10.3389/fnhum.2021.743846

Evidence Mapping Based on Systematic Reviews of Repetitive Transcranial Magnetic Stimulation on the Motor Cortex for Neuropathic Pain

Yaning Zang[1†], Yongni Zhang[2†], Xigui Lai[1], Yujie Yang[3], Jiabao Guo[4], Shanshan Gu[5] and Yi Zhu[6]*

[1] Department of Kinesiology, Shanghai University of Sport, Shanghai, China, [2] School of Health Sciences, Duquesne University, Pittsburgh, PA, United States, [3] Centre for Regenerative Medicine and Health, Hong Kong Institute of Science & Innovation, Chinese Academy of Sciences Limited, Hong Kong, Hong Kong SAR, China, [4] Department of Rehabilitation Medicine, The Second School of Clinical Medicine, Xuzhou Medical University, Xuzhou, China, [5] Department of Physical Therapy, University of Toronto, Toronto, ON, Canada, [6] Department of Musculoskeletal Pain Rehabilitation, The Fifth Affiliated Hospital of Zhengzhou University, Zhengzhou, China

OPEN ACCESS

Edited by:
Kai Wang,
Anhui Medical University, China

Reviewed by:
Joaquim Pereira Brazil-Neto,
Unieuro, Brazil
Gong-Jun Ji,
Anhui Medical University, China

***Correspondence:**
Yi Zhu
zhuyi1010@163.com

[†] These authors have contributed equally to this work

Specialty section:
This article was submitted to Brain Imaging and Stimulation, a section of the journal Frontiers in Human Neuroscience

Received: *02 August 2021*
Accepted: *15 November 2021*
Published: *16 February 2022*

Citation:
Zang Y, Zhang Y, Lai X, Yang Y, Guo J, Gu S and Zhu Y (2022) Evidence Mapping Based on Systematic Reviews of Repetitive Transcranial Magnetic Stimulation on the Motor Cortex for Neuropathic Pain. Front. Hum. Neurosci. 15:743846. doi: 10.3389/fnhum.2021.743846

Background and Objective: There is vast published literature proposing repetitive transcranial magnetic stimulation (rTMS) technology on the motor cortex (M1) for the treatment of neuropathic pain (NP). Systematic reviews (SRs) focus on a specific problem and do not provide a comprehensive overview of a research area. This study aimed to summarize and analyze the evidence of rTMS on the M1 for NP treatment through a new synthesis method called evidence mapping.

Methods: Searches were conducted in PubMed, EMBASE, Epistemonikos, and The Cochrane Library to identify the studies that summarized the effectiveness of rTMS for NP. The study type was restricted to SRs with or without meta-analysis. All literature published before January 23, 2021, was included. Two reviewers independently screened the literature, assessed the methodological quality, and extracted the data. The methodological quality of the included SRs was assessed by using the A Measurement Tool to Assess Systematic Reviews (AMSTAR-2). Data were extracted following a defined population, intervention, comparison, and outcome (PICO) framework from primary studies that included SRs. The same PICO was categorized into PICOs according to interventions [frequency, number of sessions (short: 1–5 sessions, medium: 5–10 sessions, and long: >10 sessions)] and compared. The evidence map was presented in tables and a bubble plot.

Results: A total of 38 SRs met the eligibility criteria. After duplicate primary studies were removed, these reviews included 70 primary studies that met the scope of evidence mapping. According to the AMSTAR-2 assessment, the quality of the included SRs was critically low. Of these studies, 34 SRs scored "critically low" in terms of methodological quality, 2 SR scored "low," 1 SR scored "moderate," and 1 SR scored "high."

Conclusion: Evidence mapping is a useful methodology to provide a comprehensive and reliable overview of studies on rTMS for NP. Evidence mapping also shows that further investigations are necessary to highlight the optimal stimulation protocols and standardize all parameters to fill the evidence gaps of rTMS. Given that the methodological quality of most included SRs was "critically low," further investigations are advised to improve the methodological quality and the reporting process of SRs.

Keywords: neuropathic pain, non-pharmacological, repetitive transcranial magnetic stimulation, evidence mapping, evidence synthesis, motor cortex

INTRODUCTION

Neuropathic pain (NP) is an ongoing and challenging condition due to its high morbidity rate of 7–10% in the general population; it usually results from lesions in the somatosensory nervous system, including the peripheral or central nervous system (Colloca et al., 2017). NP negatively impacts patients' quality of life by reducing functional mobility, activities of daily living, and participation in social roles, which may lead to psychological problems (Kalia and O'Connor, 2005; Gromisch et al., 2020). The initial treatment applied to NP is generally pharmacotherapy, such as use of antidepressants, anticonvulsants, and opioids (Finnerup et al., 2015). However, even with complex treatment regimens, the results of pharmacological approaches remain unsatisfactory, and some may lead to adverse events, such as toxicity, gastrointestinal events, or increased risk of addiction or drug abuse (Papanas and Ziegler, 2016; Urits et al., 2019). Therefore, non-pharmacological interventions, which are considered safe and effective, have been used to treat NP. Repetitive transcranial magnetic stimulation (rTMS) technology is widely accepted at present as a non-pharmacological intervention for treating NP.

The rTMS technique uses a transient high-intensity magnetic field acting on the cerebral cortex to generate induced currents. It alters the action potential of cortical nerve cells, depolarizes neurons in the targeted brain region, and ultimately leads to neuroplastic changes (Paulus et al., 2013). Stimulation target, frequency, and number of sessions are considered critical variables for analgesic efficacy. In terms of stimulation target, the primary motor cortex (M1) is the most commonly used target of stimulation for clinical treatment and has been the most extensively studied. In the 2020 guidelines for rTMS (Lefaucheur et al., 2020), the M1 was recommended as Level A evidence (definitive efficacy) for the treatment of NP. However, clinical promotion is still limited to some extent due to the heterogeneity of treatment protocols, such as frequency and sessions, and effectiveness among various studies. The European Society of Neurology encourages studies to collect and summarize evidence on the factors affecting these techniques (Cruccu et al., 2016). SRs are a common method for synthesizing research evidence. Nonetheless, SRs tend to address more specific research and practice questions and cannot provide a comprehensive overview of rTMS for NP. For example, the following research gaps are unknown: (1) SRs focus on a specific stimulation type or specific pain type (such as pain after spinal cord injury, post-stroke, and diabetic neuropathy), while research on other pain types needs to be developed. (2) The frequency, duration, and other parameters of interventions collected by the SRs varied, and the large amount of evidence with a lack of summarization and classification may lead to clinicians' confusion. (3) Differences in the quality between individual trials and SRs contributed to the heterogeneity of the evidence. The same primary study may be included in different SRs, which may yield various conclusions due to varying inclusion criteria.

A novel approach to evidence synthesis research called evidence mapping (Grant and Booth, 2009; Haddaway et al., 2016; Miake-Lye et al., 2016) has been developed. Evidence mapping is designed to provide an overview of a research area by including published SRs. Evidence mapping uses published SRs as units of analysis. In the population, intervention, control, and outcome (PICO) framework, evidence mapping extracts and categorizes these data from primary studies, which are included in the SRs. On the basis of the classification criteria, the obtained PICO is integrated into different PICOs, and the contribution of the number of primary studies related to that classification is also calculated to summarize the current interventions (Petersen et al., 2015). The characteristic of the evidence mapping method is to overcome the limitations of primary studies by using the selection of studies, effect size analysis, and bias evaluation of SRs. Considering that the quality of SRs affects the credibility of the evidence, the same primary studies may be included in SRs of different quality. Various conclusions may be drawn due to different inclusion criteria, such as random and double-blind bias. Therefore, evidence mapping uses AMSTAR-2 to evaluate the quality of SRs and the credibility of the results of SRs (Ballesteros et al., 2017; Madera Anaya et al., 2019). Evidence mapping can be translated into two visual products, namely, tables (general information tables and study-specific characteristic tables) and bubble plots (multidimensional composite presentation of classification criteria, quantity, and quality of evidence), which also provide a descriptive narrative summary of the results (Bragge et al., 2011; Haddaway et al., 2016).

Evidence mapping aims to summarize, identify, and analyze the current available evidence in SRs regarding rTMS on M1 for NP. Collecting and integrating data from primary studies on the basis of SRs provide breadth of evidence. Assessing the quality of SRs provides strength of evidence. This information is provided in a user-friendly manner that helps identify research gaps and assist evidence users in the decision-making process.

MATERIALS AND METHODS

Study Design

Evidence was mapped on the basis of the methodology proposed by Global Evidence Mapping (Bragge et al., 2011). The study process was divided into four phases (**Figure 1**: Core tasks performed to map evidence).

Boundaries and Context of Evidence Mapping

Studies and guidelines related to NP were referred, and an expert with research background in NP was consulted to frame the evidence map. With the help of the expert, the specific terminology of the search strategy was confirmed and the possible evidence users (pain, neurology, psychiatry, anesthesiology, and rehabilitation) involved were discussed. On the basis of the above information, the eligibility criteria have been established for inclusion in the study. Studies containing rTMS for NP were considered eligible. Studies on patients with NP were included, whereas experimental subjects that were animals or healthy people were excluded. The intervention should be rTMS, and the comparison could be rTMS, sham rTMS, other treatments of relieving pain, or no treatment. The outcome should be pain measured with various clinically validated tools [e.g., Visual Analog Scale (VAS), Numerical Rating Scale (NRS), Short-Form McGill Pain Questionnaire, and Brief Pain Inventory]. Studies that did not address intervention outcomes, such as those that aimed to explore NP-related pathophysiology and focus on cost-effectiveness, were excluded. Studies that reported other outcomes (e.g., fatigue, motor function, spasticity, sensory function, and cognition) but pain were also excluded. Only SRs (with or without meta-analysis) were included as they provided reliable evidence.

Evidence Search and Selection

We conducted searches of systematic literature on PubMed, EMBASE, Epistemonikos, and The Cochrane Library Published before January 23, 2021. Medical subject headings (mesh terms), free-text terms, and synonymous terms available for NP and transcranial magnetic stimulation, such as "neuralgia," "neurodynia," "atypical neuralgia," "nerve pain," and "stump neuralgia," were combined. Literature published in non-English languages was excluded. References of the relevant studies that met the inclusion criteria were added to potential additional reviews. The details of the search strategies are reported in **Supplementary Material 1**. EndNote (version X9) was applied to manage the search results. Duplicate SRs were removed, and two reviewers (YZa and XL) independently screened the titles and abstracts to exclude irrelevant studies. Full-text studies were obtained and reviewed to make a terminal decision. Any disagreements in the decision-making process were resolved through negotiation or by discussion with a third reviewer (YoZ).

Data Analysis

A data extraction table was designed to record the main characteristics and compare the methodological differences of the included SRs. Two authors (YZa and XL) assessed the methodological quality and extracted data independently. Any difference of opinions was discussed with the third author (YoZ). The original authors were contacted for missing information when necessary. Data were grouped into three categories:

(a) The Assessment Methodological Quality for Systematic Reviews (AMSTAR-2) was used to assess the methodological quality of SRs (Shea et al., 2017). AMSTAR-2 is a practical tool used to assess the quality of SRs that include randomized or non-randomized studies of healthcare interventions or both. It has 16 items, with an overall rating based on weaknesses in critical domains (items: 2, 4, 7, 9, 11, 13, and 15). In brief, the evaluation results of the SRs are generally divided into the following four categories: "High," no critical weakness and no more than one non-critical weakness; "Moderate," no critical weakness and more than one non-critical weakness; "Low," one critical flaw with or without non-critical weaknesses; and "Critically low," more than one critical flaw with or without non-critical weaknesses.

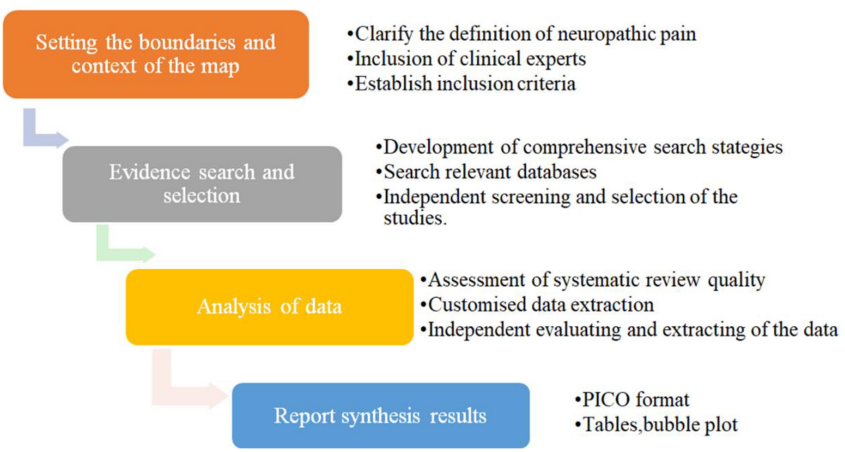

FIGURE 1 | Core tasks performed to map evidence.

(b) The following characteristics of SRs were extracted: authors, years of publication, types of SR (with or without meta-analysis), objectives, dates of search, sample sizes, designs, and numbers of included studies.

(c) The PICO framework was used to extract data from primary studies included in the SRs. The four key components are populations, intervention, comparison, and outcomes. Details including population characteristics (e.g., NP related to spinal cord injury, post-stroke symptoms, and complex regional pain syndrome), interventions (e.g., target area, frequency, and intensity of transcranial magnetic stimulation), comparative measures (e.g., placebo and sham stimulation), and outcomes were extracted. The obtained data of PICO from primary studies in SRs were classified into different groups based on similar characteristics (population; interventions: frequency, session, and intensity; control group; and outcome scale).

For descriptive purposes, the effect of rTMS on NP reported by the SR authors was grouped into the following five categories on the basis of the previously reported criteria: "Potentially better," the conclusions reported rTMS as more beneficial than the control group; "Mixed results," the same primary study had different findings among different studies (e.g., some studies found no difference in rTMS compared with the control group in the same population, whereas others found potential benefits of transcranial magnetic stimulation over the control group); "Unclear," insufficient evidence to draw definitive conclusions about the effectiveness of rTMS on pain; "No difference," the conclusions provided evidence of no difference between intervention and control; and "Potentially worse," the conclusions reported TMS as less beneficial than the control group. The same primary study may be included in multiple SRs. If the primary study has multiple consistent results, it would be added to the appropriate group, and multiple conflicting findings were included in the "Mixed Results" group (Miake-Lye et al., 2019).

Reporting Synthesized Findings

Each clinical question addressed in each included review was adapted into a PICO format that specified the types of participants, interventions (or comparison), and outcomes. Evidence mapping allows the reader to visualize any gaps in the literature base, with results presented in the form of tables and graphs.

(a) The basic characteristics, quality assessment of the included SRs, and characteristics of all integrated PICOs were described in tables.
(b) A heat map was used to present the quality of the included SRs.
(c) Graphical display was provided through bubble plots. The bubble plot displayed information in four dimensions: (1) bubble size (number of articles), the size of each bubble is proportional to the number of individual trials included in the SRs; (2) bubble color (research characteristics), bubbles labeled with different colors indicate different PICOs; (3) X-axis (effect of TMS on NP), the classification of authors' conclusions represented on the X-axis ("potentially better," "mixed results," "unclear," "no difference," and "worse"); and (4) Y-axis (AMSTAR-2 evaluation results), four different colors were used to indicate study quality, with red indicating critically low, orange indicating low, yellow indicating moderate, and green indicating high quality.

RESULTS

Selected Studies

This retrieval yielded 125 records. Another 11 articles were added from the references that met the inclusion criteria. After duplicates were removed, 97 articles remained for screening of the titles and abstracts. Subsequently, 44 articles were excluded after the screening. In the remaining 53 articles, 13 were excluded after full-text reviews. Finally, 38 articles met the eligibility criteria (**Figure 2**). The list of excluded studies along with exclusion rationales can be found in **Supplementary Material 2**.

Methodological Quality of Systematic Reviews

According to the AMSTAR-2 criteria, 34 SRs scored "critically low," 2 SR scored "low," 1 SR scored "moderate," and 1 SR scored "high" in terms of methodological quality (**Figure 3**). The most frequent drawbacks were as follows: no mention of the protocol in the systematic overview, no description of the rationale for the study designs included in the review, no report of excluded studies or reasons for exclusion, and no statement of funding for the included studies. The detailed assessment process is provided in **Supplementary Material 3**.

Characteristics of the Included Systematic Reviews

Table 1 shows the characteristics of the included SRs. All SRs were published between 2009 and 2020. Among the 38 included SRs, 17 SRs conducted a meta-analysis. The number of included studies ranged from 3 to 131, and they were conducted between 2001 and 2020. Each SR included patients ranging from 97 to 15,776. Six SRs did not report or incompletely reported the designs of the included individual studies. All studies reported study designs, and a total of 678 randomized controlled trials (RCTs) accounted for 86% of the included studies in all SRs. Of all SRs, 18 SRs included only RCTs, 15 SRs included patients with NP with different underlying causes, and 25 were exclusively conducted on NP with specific etiologies or due to a single disease. Six SRs included pain after spinal cord injury (SCI), another 5 SRs included central post-stroke pain (P), 3 SRs included phantom limb pain (PLP), 2 SRs included migraine, 2 SRs included complex regional pain syndrome (CRPS), 2 SRs included headache, 1 SR included diabetic peripheral neuropathy (DPN), 1 SR included multiple sclerosis (MS), and 1 SR included orofacial pain (OFP). As for the intervention, 13 SRs only assessed rTMS, 12 SRs assessed other non-invasive stimulations, 3 SRs assessed neuromodulation techniques, 4 SRs assessed non-pharmacological interventions, 5 SRs assessed pharmacological and non-pharmacological management of NP, and 1 SR assessed non-invasive brain stimulation combined with exercise.

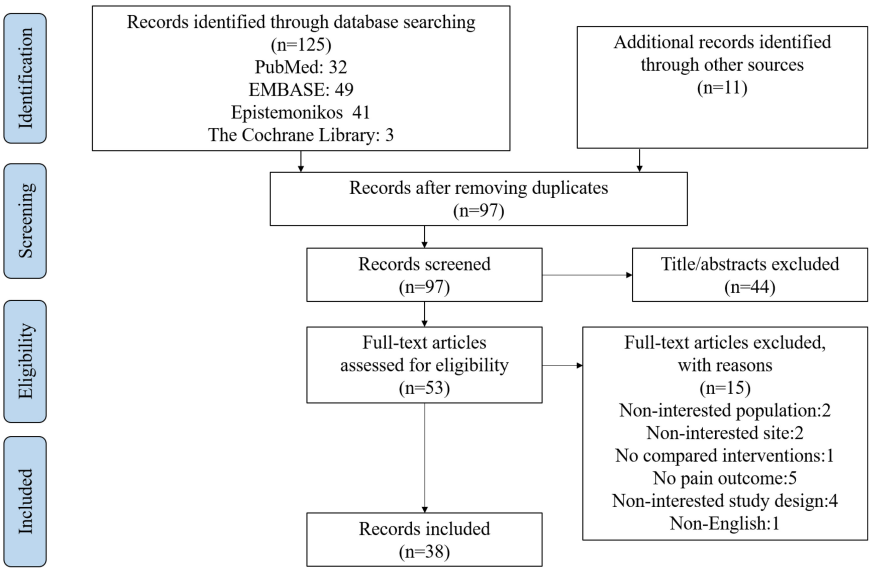

FIGURE 2 | PRISMA flow diagram detailing the selection process.

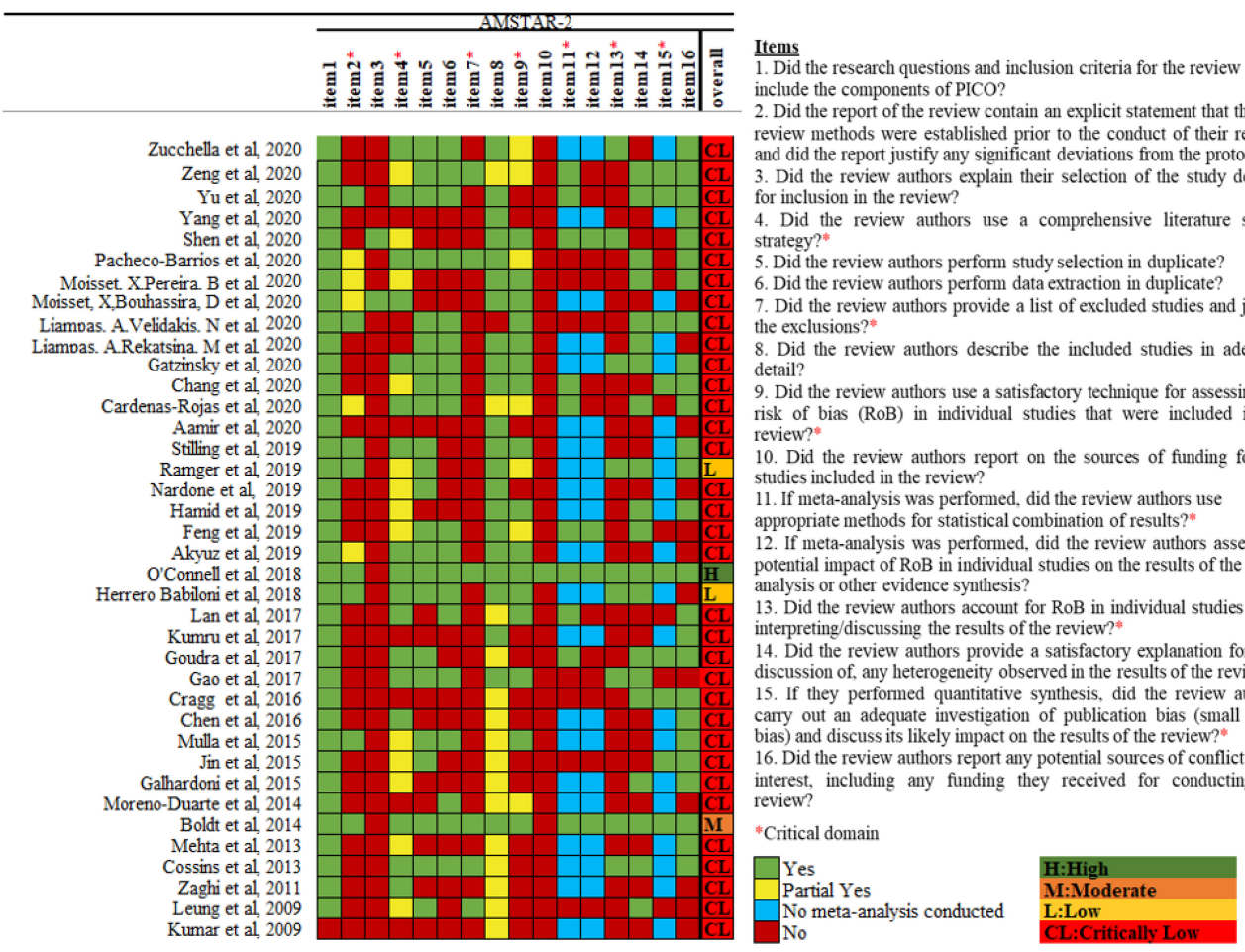

FIGURE 3 | Methodological quality of the included systematic reviews.

TABLE 1 | Characteristics of included systematic reviews.

Author and year	Study design	Search date	Objective	Number of studies included	Design and number of included studies	Participants (n)
Zucchella et al., 2020	SR	February 2020	To evaluate the effect of non-invasive brain and spinal cord stimulation in the treatment of pain in multiple sclerosis	9	RCT: 1 NCS: 6 FP: 1 CR: 1	175
Zeng et al., 2020	SRM	August 2019	To evaluate the effect of NINM in relieving pain intensity and improving nerve conduction velocity in patients with diabetic peripheral neuropathy	20	RCT: 18 QE: 2	1167
Yu et al., 2020	SRM	January 2019	To investigate the effect of non-invasive brain stimulation on NP in patients with SCI	11	RCT: 11	274
Yang and Chang, 2020	SR	June 2019	To explore the effect of rTMS on the control of various types of pain conditions	106	RCT: 69 OLT: 16 CR: 21	3264
Shen et al., 2020	SRM	November 2019	To evaluate the effect of non-invasive brain stimulation (rTMS and tDCS) on NP after SCI	10	RCT: 10	214
Pacheco-Barrios et al., 2020	SRM	February 2019	To assess the efficacy of neuromodulation techniques for the treatment of PLP in adults	14	RCT: 9 QE: 5	261
Moisset et al., 2020a	SRM	July 2020	To investigate the efficacy of neurostimulation techniques in migraine	38	RCT: 38	2899
Moisset et al., 2020b	SR	August 2019	To propose all the alternative treatment options for NP	131	RCT: 131	15776
Liampas et al., 2020a	SRM	November 2019	To describe the prevalence and characteristics of CPSP and investigate the relevant management methods	69	NR	NA
Liampas et al., 2020b	SR	April 2020	To assess the effect of non-pharmacological interventions in the management of peripheral NP	18	RCT: 13 OLT: 5	1613
Gatzinsky et al., 2020	SR	June 2019	To review primary research regarding the efficacy and safety of rTMS on M1	32	RCT: 24 CS: 8	682 (RCT)
Chang et al., 2020	SRM	February 2020	To assess the effectiveness of rTMS in the treatment of CRPS-related pain	3	RCT: 1 Prospective observational studies: 2	41
Cardenas-Rojas et al., 2020	SRM	November 2019	To assess the efficacy and safety of NIBS combined with exercise in the treatment of chronic pain	8	RCT: 8	219
Aamir et al., 2020	SR	June 2019	To evaluate the effect of rTMS in the management of peripheral NP	12	RCT: 5 CS: 2 CR: 5	188
Stilling et al., 2019	SR	September 2018	To review the use of TMS and tDCS for specific headache disorders	34	Randomized trials: 20 NRC/Prospective cohort/OLT: 14	1787
Ramger et al., 2019	SR	2018	To evaluate the efficacy of rTMS and tDCS in the treatment of CPSP	6	RCT: 1 Prospective cohort: 1 CS: 2 Cross-over: 2	109
Nardone et al., 2019	SR	April 2018	To evaluate the efficacy of TMS in treating patients with painful and non-painful phantom phenomena	18	NR	NA
Hamid et al., 2019	SR	2018	To evaluate the effect of rTMS on chronic refractory pain, especially in adults with central NP	12	RCT: 12	350
Feng et al., 2019	SRM	September 2018.	To evaluate the efficacy of rTMS and tDCS in RCTs in the treatment of migraine	9	RCT: 9	276
Akyuz and Giray, 2019	SR	August 2017	To assess the effectiveness and safety of rTMS and tDCS in the treatment of PLP	4	RCT: 4	97
O'Connell et al., 2018	SRM	October 2017	To assess the efficacy of non-invasive cortical stimulation techniques chronic pain	94	RCT: 94	2983
Herrero Babiloni et al., 2018	SR	NR	To evaluate the analgesic effect of TMS and tDCS in the treatment of different etiologies of chronic OFP	14	RCT: 14	228

(Continued)

TABLE 1 | (Continued)

Author and year	Study design	Search date	Objective	Number of studies included	Design and number of included studies	Participants (n)
Lan et al., 2017	SRM	April 2017	To evaluate the efficacy of TMS in the treatment of migraine	5	RCT: 5	313
Kumru et al., 2017	SR	August 2015	To assess the role of rTMS or peripheral magnetic stimulation for the treatment of NP	39	NR	892
Goudra et al., 2017	SRM	NR	To evaluate the effect of rTMS in the management of chronic pain	9	RCT: 6 Prospective observational: 3	183
Gao et al., 2017	SRM	March 2016	To assess the analgesic effect of rTMS in patients with SCI-related NP	6	RCT: 6	127
Cragg et al., 2016	SRM	May 2015	To explore the predictors of placebo responses in central NP clinical trials	39	RCT: 39	1153
Chen et al., 2016	SR	September 2015	To evaluate the antalgic effects of NIPMs on CPSP	16	NA	184
Mulla et al., 2015	SR	December 2013	To provide an overview of the evidence-based management of CPSP	8	RCT: 8	459
Jin et al., 2015	SRM	December 2014	To evaluate the optimal parameters of rTMS for NP	25	RCT: 20 Self-controlled: 5	589
Galhardoni et al., 2015	SR	2014	To review the literature on the analgesic effects of rTMS in chronic pain	33	RCT: 33	842
Moreno-Duarte et al., 2014	SR	2012	To evaluate the effectiveness and safety of neural stimulation techniques for the treatment of SCI pain	10	RCT: 8 OLT: 2	307
Boldt et al., 2014	SRM	March 2011	To review the available research evidence to explore the effectiveness of non-pharmacological interventions in patients with SCI	16	RCT: 16	616
Mehta et al., 2013	SR	April 2011	To review the literature on non-pharmacological treatment of post-SCI pain	17	RCT: 9 Prospective controlled trial: 2 CS: 1 Pre-post: 5	433
Cossins et al., 2013	SR	February 2012	To explore therapeutic methods for effective management of CRPS	29	RCT: 29	NR
Zaghi et al., 2011	SR	January 2010	To review the analgesic efficacy of TMS and tDCS and to discuss potential mechanisms of action	18	NR	413
Leung et al., 2009	SRM	August 2007	To evaluate the overall analgesic effect of rTMS in M1 for NP and evaluate the effect of treatment parameters. such as pulse, frequency, and number of sessions on the treatment effect	5	RCT: 5	149
Kumar et al., 2009	SR	September 2008	To review pathophysiology and treatment of CPSP	NA	NA	NA

SR, systematic review; SRM, systematic review with meta-analysis; NINM, non-invasive neuromodulation; NP, neuropathic pain; SCI, spinal cord injury; rTMS, repetitive transcranial magnetic stimulation; CPSP, central poststroke pain; tDCS, transcranial direct current stimulation; PLP, phantom limb pain; M1, motor cortex; CRPS, complex regional pain syndrome; NIBS, non-invasive brain stimulation; TMS, transcranial magnetic stimulation; OFP, orofacial pain; NIPMs, non-invasive physical modalities; RCT, randomized controlled trial; NCS, non-controlled trial; FP, feasibility pilot; CR, case report; QE, quasi-experiment; OLT, open-label trial; NR, not reported. NRT, non-randomized trial; CS, case series; NA, not available.

Characteristics of Population, Intervention, Comparison, and Outcomes From Systematic Reviews

After merging the duplicate primary studies included in the 38 SRs, 70 primary studies were integrated into 19 PICO groups based on the PICO characteristics. Studies that did not provide the mandatory parameter information were not included in the PICOs. Among the included SRs, populations with NP were from various diseases and etiologies, and the treatment protocols adopted various parameters, including frequency, sessions, and pulses. Sham stimulation or placebo was the most common intervention in the control group of rTMS on the M1. The primary outcome of the included studies was self-reported subjective nociception. VAS and NRS were the most commonly validated pain assessment scales. The details of the characteristics are enumerated in **Supplementary Material 4**.

As a result of unavoidable heterogeneity of the rTMS protocol among studies, classifying and categorizing all parameters can be difficult. Thus, the classification of PICO focused on interventions and comparison, as well as the population involved and outcome assessments, as presented in **Table 2**. We use **Figure 4** to explain the connection between the bubble polt and **Table 2**. In terms of interventions, we classified them to frequency

and session of rTMS, as they have been shown to influence the analgesic effects and are identified as clinically significant factors (Ahmed et al., 2012; O'Connell et al., 2018; Gatzinsky et al., 2020; Pacheco-Barrios et al., 2020). High and low frequency of rTMS can induce transient excitatory and inhibitory effects, respectively (Klein et al., 2015). Sessions of rTMS are considered an important factor in maintaining the effects. The characteristics of the interventions were categorized based on frequency (low or high frequency) and number of sessions (short: 1–5 sessions, medium: 5–10 sessions, and long: >10 sessions).

The key characteristics of PICOs are listed in **Supplementary Material 5**. A total of 19 PICOs were categorized based on stimulation target, frequency, and session (short, medium, and long). On the basis of the stimulation target, 17 PICOs used high-frequency rTMS (>1 Hz), and 2 used low-frequency rTMS (<1 Hz). In terms of the number of sessions, 1–5 sessions were considered short sessions, 6–10 were medium sessions, and more than 10 were regarded as long sessions. Twelve PICOs had short sessions, three had medium sessions, and four had long sessions. In addition, 12 PICOs used the same sessions of sham stimulation or placebo as a control to study the effectiveness of rTMS in patients with NP. Two PICOs studied the effects of different sessions of rTMS, while other PICOs involved different stimulation areas: M1 unilateral stimulation versus bilateral stimulation, rTMS compared with botulinum toxin injection, rTMS compared with transcranial direct current stimulation (tDCS), or rTMS combined with theta-burst stimulation. The PICOs were concentrated in the following characteristics: 20 Hz, short-term sessions versus sham stimulation (11 PICOs), and 10 Hz, short-term sessions versus sham stimulation (18 PICOs).

Specific Findings From Systematic Reviews in Evidence Mapping

The evidence map of rTMS for NP is presented in **Figure 5**. The bubble diagram is a visual display of data represented in **Supplementary Material 5**. We integrated similar intervention characteristics from primary studies into PICOs. In the bubble chart, different colors indicate varying PICOs. Each bubble was plotted in accordance with the conclusion of the effect of rTMS on NP (X-axis) and the quality of the related SRs (Y-axis), while the size of bubbles represented the number of primary studies included in PICOs. The evidence tables (**Supplementary Material 5**) provided details of the included SRs (**Supplementary Material 4**). Some primary studies may be included in multiple SRs. If SRs synthesized different conclusions for the same primary study, the same PICOs would appear in different classifications on the X-axis. If the same primary study was included by SRs of different quality, the same PICOs would appear in different classifications on the Y-axis. Evidence mapping showed that 5–20 Hz, high-frequency rTMS of M1 with short (1–5), medium (6–10), or long (>10) sessions usually lead to "potentially better" treatment effects compared with sham stimulation, although some had transient effects. By contrast, the synthesis results for the lower frequencies (1 and 0.5 Hz) showed either no difference or mixed effects. Thirteen PICOs included 52 primary studies rated as "potentially better," and four of these PICOs involved 13 primary studies that were also included in a high-quality meta-analysis. In accordance with the AMSTAR-2 quality assessment, the interventions in these four PICOs were considered beneficial in most cases. Nine PICOs included 18 primary studies with different findings in different SRs and were rated as "mixed," implying that the interventions in these eight PICOs had limited confidence in the effect estimates, and the true effect may be different from the study reports (Miake-Lye et al., 2019). One PICO conclusion was rated as "unclear" because its effect was not reported in the SR (Yang and Chang, 2020) with a critically low quality. Eight PICOs included 17 primary studies that concluded that rTMS showed no difference compared with controls. Of these, six studies showed a potentially better effect of rTMS in short-term follow-up but no difference during long-term follow up (**Supplementary Material 4** and **Supplementary Material 5**). After studies that were ineffective during follow-up were excluded, 8 of 11 primary studies were also included by a high-quality meta-analysis. This finding indicated less effectiveness of these intervention protocols or inapplicability to a particular NP, and the treatment effects could be uncertain. Two PICOs included two primary studies that showed a "potentially worse" conclusion.

DISCUSSION

Principal Findings of Evidence Mapping

This evidence map included 40 SRs, and the majority of the primary studies included were RCTs, which is the best study design to assess the effectiveness of interventions (Sylvester et al., 2017). Evidence mapping provided a broad overview of the available evidence of rTMS on NP, showing the focus and counting contributions of available studies by categorizing and generalizing them to help interpret the published SRs. (1) Research gaps: The included SRs covered most types of NP, including SCI, CPSP, CRPS, PLP, DNP, and headache; however, this left an evidence gap of the rTMS for some specific types of NP, such as postherpetic pain, radiculopathy pain, trigeminal neuralgia, post-traumatic brain injury pain, and cancer-related NP. In addition, the control groups were mostly given sham stimulation. Open questions about the effectiveness of rTMS associated with other therapies (such as pharmacotherapy, neurorehabilitation, and psychotherapy) are recommended. Future SRs are needed to analyze immediate, short-term, and long-term effects, which may help clarify the sessions of rTMS. Stimulation parameters, namely, frequency and intensity variable time, are also the direction for further research. (2) Summarization and classification of evidence: Evidence mapping showed that 5–20 Hz, high-frequency rTMS of M1 with short (1–5), medium (6–10), or long (>10) sessions usually lead to a "potentially better" conclusion compared with sham stimulation, suggesting that these interventions are beneficial in most cases. By contrast, the synthesis results for the low frequencies (1 and 0.5 Hz) showed no difference or were mixed, meaning these intervention protocols may be less effective or inappropriate for some specific NPs. (3) The impact of the quality

TABLE 2 | PICOs included in systematic reviews.

PICOS number	PICOs in bubble chart	Intervention	Parameters		Comparison	Population	Outcomes	Included SRs	Primary studies included in SRs				Conclusion
			Frequency (Hz)	Session schedule					RCT	Observation	Number of primary studies	Number of SRs involving the Quality (high/moderate/low/critically low) of primary studies	
1	50 Hz, short sessions versus sham rTMS	rTMS	50 Hz	1 session	Sham rTMS	Chronic OFP	VAS	Herrero Babiloni et al., 2018	Kohútová et al., 2017		1	0/0/0/1	Potentially better
		rTMS	50 Hz	1 session	Sham rTMS	Chronic OFP	VAS	Herrero Babiloni et al., 2018	Kohútová et al., 2017		1	0/0/0/1	No difference (long term)
2	20 Hz, long sessions versus sham rTMS	rTMS	20 Hz	11 sessions	Sham rTMS	Mixed NP	VAS	Yang and Chang, 2020		Pommier et al., 2016	1	0/0/0/1	Potentially better
3	20 Hz, medium sessions versus sham rTMS	rTMS	20 Hz	10 sessions	Sham rTMS	Pelvic pain (urinary bladder pain syndrome)/cancer and malignant NP	VAS	Gatzinsky et al., 2020; Moisset et al., 2020b; Yang and Chang, 2020	Khedr et al., 2015; Cervigni et al., 2018		2	0/0/0/2	Potentially better
		rTMS	20 Hz	10 sessions	Sham rTMS	Cancer and malignant NP	VAS	Jin et al., 2015; Gatzinsky et al., 2020; Moisset et al., 2020b; Yang and Chang, 2020	Jin et al., 2015; Khedr et al., 2015		2	0/0/0/2	No difference (1 month later)
4	20 Hz, short sessions versus sham rTMSr	TMS	20 Hz	5 sessions	Sham rTMS	LBP, non-specified OFP, TN after dental or neural surgery, atypical facial pain, CPSP, TN, PLP, Alzheimer, TGNP, and IBS	VAS	Kumar et al., 2009; Leung et al., 2009; Zaghi et al., 2011; Galhardoni et al., 2015; Jin et al., 2015; Chen et al., 2016; Goudra et al., 2017; Kumru et al., 2017; Herrero Babiloni et al., 2018; O'Connell et al., 2018*; Akyuz and Giray, 2019; Hamid et al., 2019; Nardone et al., 2019; Aamir et al., 2020; Gatzinsky et al., 2020; Liampas et al., 2020a; Moisset et al., 2020b; Pacheco-Barrios et al., 2020[I]; Yang and Chang, 2020	Khedr et al., 2005*; Ahmed et al., 2011*, 2012; Fricova et al., 2013; Melchior et al., 2014; Ambriz-Tututi et al., 2016		11	4/0/0/11	Potentially better
		rTMS	20 Hz	4 sessions	Sham rTMS	CPSP, SCI	NRS	Yang and Chang, 2020		Quesada et al., 2018			Potentially better
		rTMS	20 Hz	2 sessions	Sham rTMS	Mixed NP	VAS	Galhardoni et al., 2015; Kumru et al., 2017; O'Connell et al., 2018*; Gatzinsky et al., 2020; Yang and Chang, 2020	Andre-Obadia et al., 2008*				Potentially better (posteroanterior orientation of the coil)
		rTMS	20 Hz	2 sessions	Sham rTMS	Mixed NP and TN	NRS	Herrero Babiloni et al., 2018; Hamid et al., 2019; Yang and Chang, 2020	Andre-Obadia et al., 2018				Potentially better (with M1 hand)
		rTMS	20 Hz	1 session	Sham rTMS	Chronic neuropathic pain (mixed), CPSP, SCI, BPL, and TGNP	NRS	Jin et al., 2015; Kumru et al., 2017; O'Connell et al., 2018*; Hamid et al., 2019; Gatzinsky et al., 2020	Andre-Obadia et al., 2011*, 2014				Potentially better
		rTMS	20 Hz	5 sessions	Sham rTMS	DPN	VAS	Galhardoni et al., 2015; Jin et al., 2015; Kumru et al., 2017; O'Connell et al., 2018*; Aamir et al., 2020; Liampas et al., 2020b; Moisset et al., 2020b; Yang and Chang, 2020; Zeng et al., 2020	Onesti et al., 2013*		2	1/0/0/2	Mixed
		rTMS	20 Hz	1 session	Sham rTMS	LBP	Pain intensity	Zaghi et al., 2011; Galhardoni et al., 2015	Johnson et al., 2006				Mixed

(Continued)

TABLE 2 | (Continued)

PICOS number	PICOs in bubble chart	Intervention	Parameters		Comparison	Population	Outcomes	Included SRs	Primary studies included in SRs				Conclusion
			Frequency (Hz)	Session schedule					RCT	Observation	Number of primary studies	Number of SRs involving the Quality (high/moderate/low/critically low) of primary studies	
		rTMS	20 Hz	5 sessions	Sham rTMS	Rectal sensitivity in IBS		Goudra et al., 2017	Melchior et al., 2013		5	3/0/0/5	No difference
		rTMS	20 Hz	3 sessions	Sham rTMS	Mixed NP	VAS	Zaghi et al., 2011; Galhardoni et al., 2015; Jin et al., 2015; O'Connell et al., 2018*; Gatzinsky et al., 2020; Yang and Chang, 2020	Andre-Obadia et al., 2006*				No difference
		rTMS	20 Hz	2 sessions	Sham rTMS	Mixed NP	VAS	Galhardoni et al., 2015; Jin et al., 2015; Kumru et al., 2017; O'Connell et al., 2018*	Andre-Obadia et al., 2008*				No difference (lateromedial orientation of the coil)
		rTMS	20 Hz	2 sessions	Sham rTMS	Mixed NP	NRS	Herrero Babiloni et al., 2018	Andre-Obadia et al., 2018				No difference (with M1 face)
		rTMS	20 Hz	1 session	Sham rTMS	Mixed NP	VAS	Leung et al., 2009; Zaghi et al., 2011; Jin et al., 2015; Galhardoni et al., 2015; O'Connell et al., 2018*; Yang and Chang, 2020	Rollnik et al., 2002*				No difference
5	10 Hz, long sessions versus sham rTMS	rTMS	10 Hz	15 sessions	Sham rTMS	PHN	VAS	Moisset et al., 2020b	Pei et al., 2019		2	0/0/0/2	Potentially better
		rTMS	10 Hz	12 sessions	Sham rTMS	Migraine		Lan et al., 2017	Shehata et al., 2016				Potentially better
		rTMS	10 Hz	12 sessions	Sham rTMS	Migraine	VAS	Stilling et al., 2019; Yang and Chang, 2020	Shehata et al., 2016		1	0/0/0/1	Mixed
6	10 Hz, medium sessions versus sham rTMS	rTMS	10 Hz	10 sessions	Sham rTMS	SCI, chronic central pain after mild traumatic brain injury, thalamic pain, hemiplegic shoulder pain, PHN, PLP, and CPSP	NRS, VAS	Cragg et al., 2016; Gao et al., 2017; O'Connell et al., 2018*; Akyuz and Giray, 2019; Nardone et al., 2019; Aamir et al., 2020; Gatzinsky et al., 2020; Moisset et al., 2020b; Shen et al., 2020; Yang and Chang, 2020	Yilmaz et al., 2014*; Ma et al., 2015; Malavera et al., 2016; Choi et al., 2018; Choi and Chang, 2018	Lin et al., 2018	7	1/0/0/7	Potentially better
		rTMS	10 Hz	9 sessions	Sham rTMS	Mixed NP	VAS	Yang and Chang, 2020	Lawson et al., 2018				Potentially better
		rTMS	10 Hz	10 sessions	Sham rTMS	CRPS	VAS	Cossins et al., 2013; Galhardoni et al., 2015; Jin et al., 2015; O'Connell et al., 2018*; Cardenas-Rojas et al., 2020; Chang et al., 2020; Gatzinsky et al., 2020; Yang and Chang, 2020	Picarelli et al., 2010*		1	1/0/0/1	Mixed
		rTMS	10 Hz	10 sessions	Sham rTMS	SCI	VAS	Gao et al., 2017; Gatzinsky et al., 2020; Shen et al., 2020; Yang and Chang, 2020	Yilmaz et al., 2014		3	1/0/0/2	No difference (<6 weeks)
		rTMS	10 Hz	10 sessions	Sham rTMS	PLP	VAS	O'Connell et al., 2018*; Aamir et al., 2020; Gatzinsky et al., 2020; Moisset et al., 2020b; Pacheco-Barrios et al., 2020; Yang and Chang, 2020	Malavera et al., 2013**, 2016				No difference (30 days)
		rTMS	10 Hz	10 sessions	Sham rTMS	Migraine	Total HA days; overall HA index	Stilling et al., 2019	Teo et al., 2014		1	0/0/0/1	Potentially worse

(Continued)

TABLE 2 | (Continued)

PICOS number	PICOs in bubble chart	Intervention	Parameters		Comparison	Population	Outcomes	Included SRs	Primary studies included in SRs				Conclusion
			Frequency (Hz)	Session schedule					RCT	Observation	Number of primary studies	Number of SRs involving the Quality (high/moderate/low/critically low) of primary studies	
7	10 Hz, short sessions versus sham rTMS	rTMS	10 Hz	5 sessions	Sham rTMS	Mixed refractory neuropathic pain, radiculopathy, CPSP, mixed NP, pelvic pain, and facial NP	VAS, NRS	Kumru et al., 2017; O'Connell et al., 2018*; Gatzinsky et al., 2020; Yang and Chang, 2020	Lang et al., 2014; Nurmikko et al., 2016*	Pinot-Monange et al., 2019	18	5/0/0/18	Potentially better
		rTMS	10 Hz	3 sessions	Sham rTMS	Mixed NP, MBTI-HA, chronic migraine, CPSP, SCI, NTL, BPL,PLP, PNI, TGNP, and migraine	VAS, NRS	Zaghi et al., 2011; Galhardoni et al., 2015; Jin et al., 2015; Kumru et al., 2017; Gao et al., 2017; O'Connell et al., 2018*; Feng et al., 2019; Stilling et al., 2019; Gatzinsky et al., 2020; Yang and Chang, 2020	Lefaucheur et al., 2006*, 2008*; Saitoh et al., 2007*; Misra et al., 2013, 2017; Kalita et al., 2016; Leung et al., 2016	Lefaucheur et al., 2006, 2012; Misra et al., 2013; Kalita et al., 2017			Potentially better
		rTMS	10 Hz	1 session	Sham rTMS	Migraine, CPSP, SCI, PNP, mixed NP, CPSP, SCI, trigeminal nerve lesion (failure of TN surgery), BPL, and TGNI	VAS	Kumar et al., 2009; Leung et al., 2009; Zaghi et al., 2011; Galhardoni et al., 2015; Chen et al., 2016; Gao et al., 2017; Kumru et al., 2017; Herrero Babiloni et al., 2018; O'Connell et al., 2018*; Gatzinsky et al., 2020; Moisset et al., 2020a; Yang and Chang, 2020	Lefaucheur et al., 2004*, 2011; Misra et al., 2013, 2017				Potentially better
		rTMS	10 Hz	5 sessions	Sham rTMS	SCI	NRS	Zaghi et al., 2011; Mehta et al., 2013; Boldt et al., 2014[#]; Moreno-Duarte et al., 2014; Galhardoni et al., 2015; Jin et al., 2015; Cragg et al., 2016; Gao et al., 2017; Goudra et al., 2017; Kumru et al., 2017; O'Connell et al., 2018*; Gatzinsky et al., 2020; Moisset et al., 2020b; Shen et al., 2020; Yang and Chang, 2020; Yu et al., 2020	Kang et al., 2009*[#]		8	6/1/0/8	Mixed
		rTMS	10 Hz	3 sessions	Sham rTMS	Mixed NP, CPSP, and BPL	VAS	Jin et al., 2015; Gao et al., 2017; Kumru et al., 2017; O'Connell et al., 2018*; Yang and Chang, 2020	Lefaucheur et al., 2001b*	Lefaucheur, 2003			Mixed
		rTMS	10 Hz	2 sessions	Sham rTMS	Mixed NP, radiculopathy, TN after surgery, and atypical facial pain after dental surgery	VAS	Herrero Babiloni et al., 2018; Yang and Chang, 2020	Ayache et al., 2016				Mixed
		rTMS	10 Hz	1 session	Sham rTMS	SCI, CRPS, mixed NP, CPSP, and SCI	VAS, NRS	Cossins et al., 2013; Galhardoni et al., 2015; Jin et al., 2015; Chen et al., 2016[!]; Cragg et al., 2016; Gao et al., 2017; Kumru et al., 2017; Herrero Babiloni et al., 2018; O'Connell et al., 2018*; Chang et al., 2020; Gatzinsky et al., 2020; Shen et al., 2020; Yang and Chang, 2020	Lefaucheur et al., 2001a*; Pleger et al., 2004*; Lefaucheur et al., 2006*; Jetté et al., 2013*				Mixed

(Continued)

TABLE 2 | (Continued)

PICOS number	PICOs in bubble chart	Intervention	Parameters		Comparison	Population	Outcomes	Included SRs	Primary studies included in SRs				Conclusion
			Frequency (Hz)	Session schedule					RCT	Observation	Number of primary studies	Number of SRs involving the Quality (high/moderate/low/critically low) of primary studies	
8	5 Hz, long sessions versus sham rTMS	rTMS	5 Hz	15 sessions	Sham rTMS	PHN	VAS	Moisset et al., 2020b	Pei et al., 2019		2	0/0/1/2	Potentially better
		rTMS	5 Hz	12 sessions	Sham rTMS	CPSP	VAS	Kumru et al., 2017; Ramger et al., 2019[&]; Yang and Chang, 2020		Kobayashi et al., 2015[&]			Potentially better (up to 8 weeks)
9	5 Hz, medium sessions versus sham rTMS	rTMS	5 Hz	10 sessions	Sham rTMS	SCI, mixed NP, CPSP, BPL, PLP, TGNP, and PNI	VAS	Zaghi et al., 2011; Mehta et al., 2013; Boldt et al., 2014[#]; Moreno-Duarte et al., 2014; Galhardoni et al., 2015; Jin et al., 2015; Mulla et al., 2015; Chen et al., 2016; Cragg et al., 2016; Gao et al., 2017; Kumru et al., 2017; Herrero Babiloni et al., 2018; O'Connell et al., 2018[*]; Gatzinsky et al., 2020; Moisset et al., 2020b; Shen et al., 2020; Yang and Chang, 2020; Yu et al., 2020	Defrin et al., 2007[*#]; Hosomi et al., 2013[*]		2	2/1/0/2	Mixed
10	5 Hz, short sessions versus sham rTMS	rTMS	5 Hz	5 sessions	Sham rTMS	Mixed NP	VAS	Hamid et al., 2019; Liampas et al., 2020a; Yang and Chang, 2020	Shimizu et al., 2017		4	3/0/1/4	Potentially better
		rTMS	5 Hz	3 sessions	Sham rTMS	CPSP,SCI, PL, BPL, and PNI	VAS	Jin et al., 2015; Gao et al., 2017; Kumru et al., 2017; O'Connell et al., 2018[*]; Yang and Chang, 2020	Saitoh et al., 2007[*]				Potentially better
		rTMS	5 Hz	1 session	Sham rTMS	CPSP	VAS or NRS	Galhardoni et al., 2015; Jin et al., 2015; Kumru et al., 2017; Hamid et al., 2019; Ramger et al., 2019[&]; Yang and Chang, 2020	Hosomi et al., 2013[*]; Matsumura et al., 2013[*&]				Potentially better
		rTMS	5 Hz	1 session	Sham rTMS	PLP	VAS or NRS	Galhardoni et al., 2015; O'Connell et al., 2018[*]; Pacheco-Barrios et al., 2020	Irlbacher et al., 2006[*]			1/0/0/1	No difference
11	1 Hz, short sessions versus sham rTMS	rTMS	1 Hz	3 sessions	Sham rTMS	Mixed NP,CPSP, SCI, PNP, PLP, BPL, and TGNP	VAS, NRS	Leung et al., 2009; Zaghi et al., 2011; Galhardoni et al., 2015; Gao et al., 2017; Kumru et al., 2017; O'Connell et al., 2018[*]; Yang and Chang, 2020	Andre-Obadia et al., 2006[*]; Saitoh et al., 2007[*]; Lefaucheur et al., 2008[*]		4	4/0/0/4	No difference
		rTMS	1 Hz	1 session	Sham rTMS	PLP	VAS orNRS	Galhardoni et al., 2015; O'Connell et al., 2018[*]; Pacheco-Barrios et al., 2020	Irlbacher et al., 2006[*]				No difference

(Continued)

TABLE 2 | (Continued)

PICOS number	PICOs in bubble chart	Intervention	Parameters		Comparison	Population	Outcomes	Included SRs	Primary studies included in SRs				Conclusion
			Frequency (Hz)	Session schedule					RCT	Observation	Number of primary studies	Number of SRs involving the Quality (high/moderate/low/critically low) of primary studies	
12	0.5 Hz, short sessions versus sham rTMS	rTMS	0.5 Hz	3 sessions	Sham rTMS	Mixed NP, CPSP, and BPL	VAS	Zaghi et al., 2011; Galhardoni et al., 2015; Jin et al., 2015; Kumru et al., 2017; Yang and Chang, 2020	Lefaucheur et al., 2001b		1	0/0/0/1	Mixed
13	rTMS on M1 versusrTMS on S1, SMA, PMC, and sham	rTMS on M1 area	5 Hz	2 sessions	rTMS on S1,SMA,PMC area	CPSP, SCI, TGNI, PNI, and RA	VAS	Kumru et al., 2017	Saitoh et al., 2006		1	0/0/0/1	Potentially better
		rTMS on M1 area	5 Hz	4 sessions	rTMS on S2,SMA,PMC area	Mixed NP, CPSP, SCI, TGNP, and PNP	VAS	Leung et al., 2009; Galhardoni et al., 2015; Jin et al., 2015; Chen et al., 2016; Kumru et al., 2017; O'Connell et al., 2018*; Gatzinsky et al., 2020; Yang and Chang, 2020	Hirayama et al., 2006*		1	1/0/0/1	Mixed
14	bilateral M1 versus unilateral M1	rTMS:bilateral M1	10 Hz	1 session	rTMS, unilateral M1	TN		Yang and Chang, 2020	Henssen et al., 2019		1	0/0/0/1	Potentially better
15	Single rTMS versus 5 rTMS sessions	rTMS	10 Hz	1 session	rTMS, 5 sessions	CRPS	VAS, NRS	Chang et al., 2020; Yang and Chang, 2020		Gaertner et al., 2018	1	0/0/0/1	Mixed
16	3 true rTMS versus 1 true + 2 sham rTMS	rTMS	10 Hz	3 sessions true	1 true sessions and 2 sham sessions	Migraine	VAS	Stilling et al., 2019		Misra et al., 2017	1	0/0/0/1	Potentially better
		rTMS	10 Hz	3 sessions true	1 true sessions and 2 sham sessions	Migraine	VAS	Stilling et al., 2019; Moisset et al., 2020a	Kalita et al., 2016		1	0/0/0/1	No difference
17	rTMS versus BTX-A Injection	rTMS	10 Hz	12 sessions	BTX-A injection	Migraine		Yang and Chang, 2020	Shehata et al., 2016		1	0/0/0/1	Unclear
		rTMS	10 Hz	12 sessions	BTX-A 31 to 39 sites	Migraine	VAS	Stilling et al., 2019; Moisset et al., 2020a	Shehata et al., 2016		1	0/0/0/1	No difference
		rTMS	10 Hz	12 sessions	BTX-A 31 to 39 sites	Migraine	VAS	Stilling et al., 2019; Moisset et al., 2020a	Shehata et al., 2016		1	0/0/0/1	Potentially worse (at week 12)
18	rTMS + tDCS versussham rTMS and tDCS	rTMS and tDCS	10 Hz	3 sessions	Sham rTMS and2-mA tDCS	Radiculopathy	NRS	O'Connell et al., 2018; Aamir et al., 2020; Gatzinsky et al., 2020; Yang and Chang, 2020*	Attal et al., 2016*		1	1/0/0/1	Mixed
19	rTMS + TBS versus rTMS	rTMS+ TBS	10 Hz	1 session	rTMS	TGNP, CPSP, and SCI	VAS	Galhardoni et al., 2015; Kumru et al., 2017	Lefaucheur et al., 2012		1	0/0/0/1	Potentially better

PICO, population, intervention, control group, outcome; RCT, Randomized controlled trial; rTMS, Repetitive transcranial magnetic stimulation; M1, Motor cortex; S1, Primary somatosensory cortex; SMA, Supplementary motor cortex; PMC, Premotor cortex; BTX-A, Botulinum toxin type A; tDCS, Transcranial direct current stimulation; TBS, Theta-burst stimulation; OFP, Orofacial pain; NP, Neuropathic pain; LBP, Low back pain; TN, Trigeminal neuralgia; CPSP, Central post-stroke pain; PLP, Phantom limb pain; MBTI-HA, Mild traumatic brain injury related headache; NTL, Nerve trunk lesion; TGNP, Trigeminal neuropathic pain; IBS, Irritable bowel syndrome; SCI, Spinal cord injury; BPL, Brachial plexus lesion; DPN, Diabetic peripheral neuropathy; PHN, Postherpetic neuralgia; PNI, peripheral nerve injury; PNP, peripheral neuropathic pain; TGNI, trigeminal nerve injury; RA, root avulsion; VAS, Visual analog scale; NRS, Numerical rating scale.

Notes: *short, 1–5 sessions, medium, 5–10 sessions, long, >10 sessions.*

*In the [Included SRs], high-quality SRs are marked as *, moderate quality SRs are marked as #, low-quality SRs are marked as &, and the rest are critically-low-quality SRs.*

*In the [Primary studies included in SRs], *, included by high and critically-low-quality SRs; **, Only included by high-quality SRs; #, Included by moderate and critically-low-quality SRs; &, Included by low and critically-low-quality SRs.*

In the [Number of SRs involving the quality (high/moderate/low/critically low) of primary studies], Taking the 9th PICOs (5 Hz, medium sessions vs. sham rTMS), as an example, a total of 2 primary studies were involved. The meaning of 2/1/0/2 is shown in ***Figure 4****.*

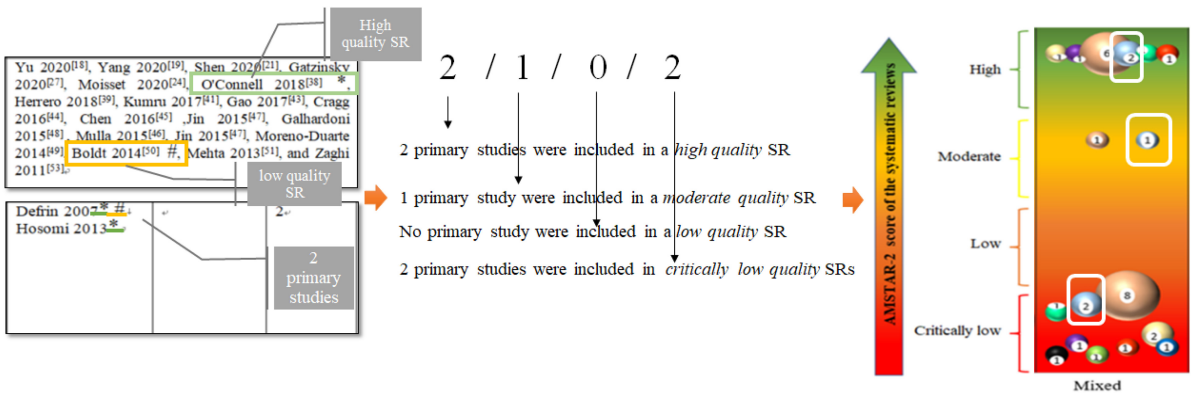

FIGURE 4 | Interpretation of evidence mapping.

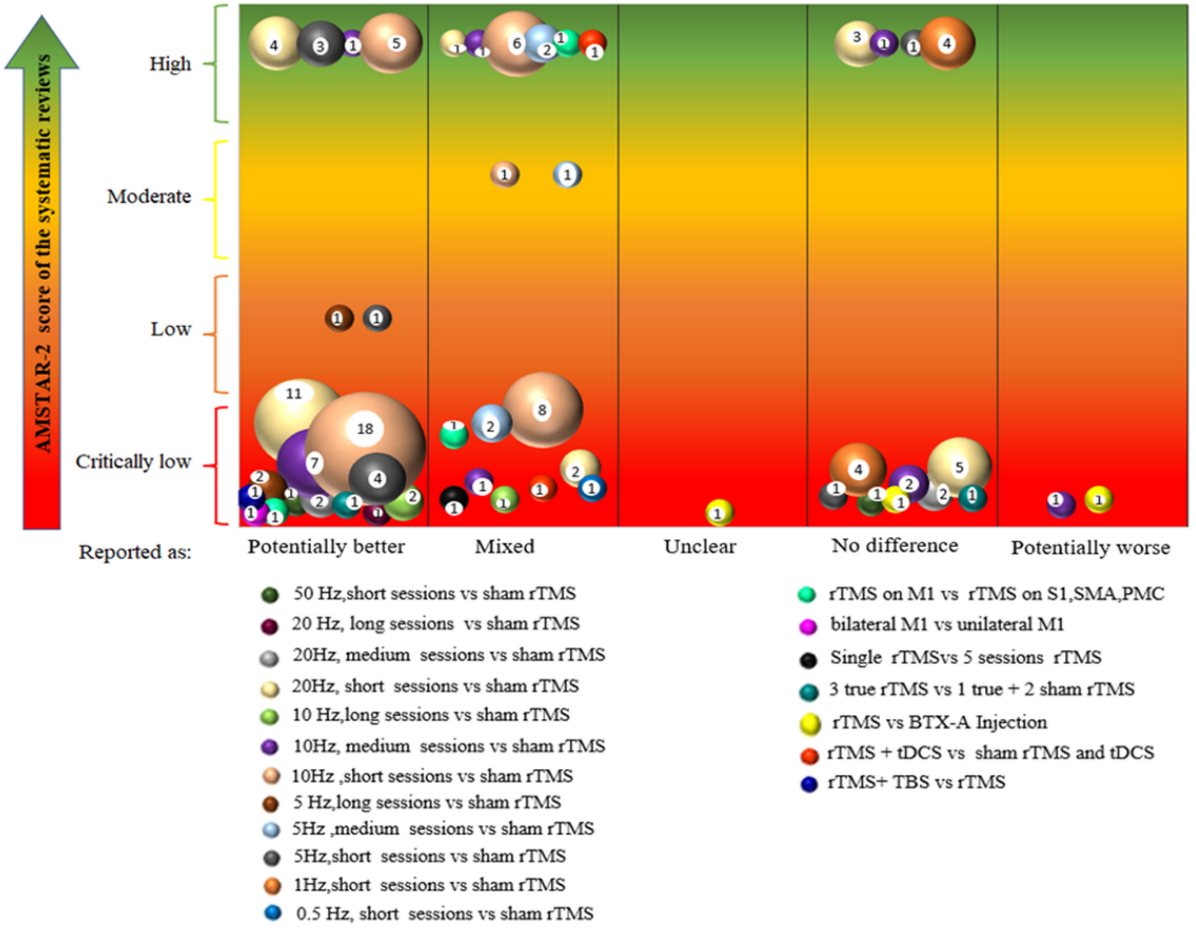

FIGURE 5 | Evidence mapping of the rTMS on neuropathic pain (NP). short, 1–5 sessions, medium, 5–10 sessions, long, >10 sessions. rTMS, repetitive transcranial magnetic stimulation; tDCS, transcranial direct current stimulation; TBS, theta-burst stimulation; M1,motor cortex, S1, primary somatosensory cortex; SMA, supplementary motor cortex; PMC, premotor cortex; BTX-A, botulinum toxin type A.

of the SRs on the strength of evidence: Some PICOs from high-quality SRs drew a potentially better conclusion, suggesting that these interventions were beneficial in most cases. Similarly, some PICOs from high-quality SRs did not show any difference in the conclusion, indicating that these interventions may be less effective or inappropriate for some specific NPs. This evidence map is not intended to replace any clinical protocol or guidelines, nor is it intended to provide a standardized protocol. Therefore,

the clinical diagnosis of each patient, the existing alternatives, cost-effectiveness, available resources, and other factors must be carefully considered before offering any recommendation (Nussbaumer-Streit et al., 2018).

Comparison of Results of Systematic Reviews

By comparing the results of the SRs, the same PICOs obtained from SRs were presented with different conclusions in the evidence map. The possible reasons were as follows: (1) some studies that reported different sessions had varied effects of rTMS. For example, a good outcome could be found in the short term, but not in the long term, that led to a mixed conclusion. Future SRs should focus on follow-up and explore the long-term effectiveness of the intervention. (2) Some SRs conducted meta-analysis but some did not. Qualitative studies may arrive at conclusions different from those in quantitative studies. For example, a primary study by Onesti et al. (2013) and meta-analysis of Zeng et al. (2020) had a "no difference" conclusion, while the review of Yang and Chang (2020), which only mentioned pain relief, showed a "potentially better" conclusion. The final conclusion in the evidence map of Onesti et al.'s study was "mixed." (3) Populations with different diseases that cause NP could cause heterogeneity. Previous studies have indicated that patients with orofacial pain have a better analgesic response than those with CPSP, SCI, or BPL (Lefaucheur et al., 2004). For example, a primary study on patients with CRPS (Picarelli et al., 2010) by Chang et al. (2020) and another one involving chronic pain by O'Connell et al. (2018) did not reach the same conclusion. This gap could also be a caveat to provide more reliable and reproducible data. Future studies must consider including more homogeneous groups of participants or stratifying patients in accordance with clinical characteristics and underlying pathogenesis.

If different SRs with varied conclusions included some primary studies that were overlapping and some unique studies, future investigations could synthesize studies that were included in these reviews and find new outcomes including all potential evidence. From the "mixed" results, future investigations could focus on comparing different stimulation protocols (doses, sessions, variable time, and intervals among sessions) of rTMS on NP.

Overall Completeness and Validity of Evidence Mapping

We evaluated the quality of SRs and the credibility of the results of SRs with a new version of AMSTAR. Compared with the previous version, AMSTAR-2 was adapted to include SRs on the basis of RCTs or non-randomized intervention studies or both and provide more refined and rigorous evaluation item criteria. Assessment in this field suggested room for improving SRs' quality. Future SRs should place more emphasis on the following domains to improve the quality of studies and the validity of the results: reporting an explicit statement about the description of the methodology prior to conducting the review; any significant deviations from the protocol should be justified; explaining the selection of the study designs for inclusion in the review; providing a list of excluded studies and justifying the exclusions; indicating the sources of funding or support for the individual studies included in the SRs; and interpreting or discussing the effect of the risk of bias in individual studies on the total effect.

Strengths and Limitations of This Evidence Mapping

This evidence map may be the first on rTMS for NP. Evidence mapping is a relatively new tool for the synthesis of available evidence, so we explain the methodology and results in more detail compared with published evidence maps and provide all the data of our study process to facilitate the reader's understanding and use. To avoid selection and data extraction bias, we constructed a rich search string for retrieving from four different databases. In addition, the reference lists of the selected studies were manually scanned for the detection of additional relevant studies, minimizing the risk of missing relevant studies. Study selection and data extraction were made via a double confirmation. Two authors conducted the process of selecting and extracting separately from one another, and any disagreements were then discussed with a third researcher until a final agreement was reached. Furthermore, results were mapped using various graphs, such as bubble plots, heat maps, and tables, which helped improve traceability between the extracted data and the conclusion.

Certain limitations in this evidence map should be considered. First, the map only chose studies published in English, which limited the scope of evidence mapping. Second, given that only SRs were included as a source of evidence, some studies, such as newly published or studies included in these SRs, could have been missed. Third, the methodologies of some SRs had limitations. Furthermore, several different types of studies in SRs comparing therapeutic interventions for NP were included. Although most trials were RCTs, some case reports and observational, open-label, and cohort studies were also available. Finally, evidence mapping synthesized the SRs as a unit rather than individual studies, which could lead to some primary studies being repeated.

CONCLUSION

Neuropathic pain is a complex and refractory group of diseases. Evidence mapping showed that rTMS, as a compliant and safety neuromodulation treatment, is promising for the treatment of NP. Evidence mapping could encourage clinicians and professionals involved in related areas, such as pain, neurology, psychiatry, and anesthesiology, to pay more attention to non-pharmacological treatments on patients with NPs, especially those with drug resistance. Evidence mapping is a useful and reliable method to identify the currently available evidence on therapeutic interventions and pinpoint gaps to suggest future research. In the future, when designing treatment protocols, rehabilitation practitioners are recommended to consider the duration and sessions of rTMS. More research efforts are needed

to highlight the optimal stimulation protocols and standardize all parameters to fill evidence gaps, and more homogeneous groups of participants should be considered. Meanwhile, as the methodological quality of most included SRs scored "critically low," further efforts are needed to improve the methodological quality and reporting process of SRs.

DATA AVAILABILITY STATEMENT

The original contributions presented in the study are included in the article/**Supplementary Material**, further inquiries can be directed to the corresponding author.

AUTHOR CONTRIBUTIONS

YZa, YoZ, and YiZ were designed the study. YZa and XL were collected the screening studies, extraction data and charted under the guidance of YoZ. YZa and YoZ analyzed the data and drafted the manuscript. YiZ reviewed the results. SG, YY, JG, and YiZ revised the manuscript for important intellectual content. All authors approved the final version of the manuscript.

FUNDING

This work was supported by National Natural Science Foundation of China Project (No. 81860875).

SUPPLEMENTARY MATERIAL

The Supplementary Material for this article can be found online at: https://www.frontiersin.org/articles/10.3389/fnhum.2021.743846/full#supplementary-material

REFERENCES

Aamir, A., Girach, A., Sarrigiannis, P. G., Hadjivassiliou, M., Paladini, A., Varrassi, G., et al. (2020). Repetitive magnetic stimulation for the management of peripheral neuropathic pain: a systematic review. *Adv. Ther.* 37, 998–1012. doi: 10.1007/s12325-020-01231-2

Ahmed, M. A., Darwish, E. S., Khedr, E. M., El Serogy, Y. M., and Ali, A. M. (2012). Effects of low versus high frequencies of repetitive transcranial magnetic stimulation on cognitive function and cortical excitability in Alzheimer's dementia. *J. Neurol.* 259, 83–92. doi: 10.1007/s00415-011-6128-4

Ahmed, M. A., Mohamed, S. A., and Sayed, D. (2011). Long-term antalgic effects of repetitive transcranial magnetic stimulation of motor cortex and serum beta-endorphin in patients with phantom pain. *Neurol. Res.* 33, 953–958. doi: 10.1179/1743132811Y.0000000045

Akyuz, G., and Giray, E. (2019). Noninvasive neuromodulation techniques for the management of phantom limb pain: a systematic review of randomized controlled trials. *Int. J. Rehabil. Res.* 42, 1–10. doi: 10.1097/mrr.0000000000000317

Ambriz-Tututi, M., Alvarado-Reynoso, B., and Drucker-Colin, R. (2016). Analgesic effect of repetitive transcranial magnetic stimulation (rTMS) in patients with chronic low back pain. *Bioelectromagnetics* 37, 527–535. doi: 10.1002/bem.22001

Andre-Obadia, N., Magnin, M., and Garcia-Larrea, L. (2011). On the importance of placebo timing in rTMS studies for pain relief. *Pain* 152, 1233–1237. doi: 10.1016/j.pain.2010.12.027

Andre-Obadia, N., Magnin, M., Simon, E., and Garcia-Larrea, L. (2018). Somatotopic effects of rTMS in neuropathic pain? A comparison between stimulation over hand and face motor areas. *Eur. J. Pain* 22, 707–715. doi: 10.1002/ejp.1156

Andre-Obadia, N., Mertens, P., Gueguen, A., Peyron, R., and Garcia-Larrea, L. (2008). Pain relief by rTMS: differential effect of current flow but no specific action on pain subtypes. *Neurology* 71, 833–840. doi: 10.1212/01.wnl.0000325481.61471.f0

Andre-Obadia, N., Mertens, P., Lelekov-Boissard, T., Afif, A., Magnin, M., Garcia-Larrea, L., et al. (2014). Is Life better after motor cortex stimulation for pain control?Results at long-term and their prediction by preoperative rTMS. *Pain Phys.* 17, 53–62. doi: 10.36076/ppj.2014/17/53

Andre-Obadia, N., Peyron, R., Mertens, P., Mauguière, F., Laurent, B., and Garcia-Larrea, L. (2006). Transcranial magnetic stimulation for pain control. Double-blind study of different frequencies against placebo, and correlation with motor cortex stimulation efficacy. *Clin. Neurophysiol.* 117, 1536–1544. doi: 10.1016/j.clinph.2006.03.025

Attal, N., Ayache, S. S., De Andrade, D. C., Mhalla, A., Baudic, S., and Jazat, F. (2016). Repetitive transcranial magnetic stimulation and transcranial direct-current stimulation in neuropathic pain due to radiculopathy: a randomized sham-controlled comparative study. *Pain* 157, 1224–1231. doi: 10.1097/j.pain.0000000000000510

Ayache, S. S., Ahdab, R., Chalah, M. A., Farhat, W. H., Mylius, V., Goujon, C., et al. (2016). Analgesic effects of navigated motor cortex rTMS in patients with chronic neuropathic pain. *Eur. J. Pain* 20, 1413–1422. doi: 10.1002/ejp.864

Ballesteros, M., Montero, N., López-Pousa, A., Urrútia, G., Solà, I., Rada, G., et al. (2017). Evidence mapping based on systematic reviews of therapeutic interventions for gastrointestinal stromal tumors (GIST). *BMC Med. Res. Methodol.* 17:135. doi: 10.1186/s12874-017-0402-9

Boldt, I., Eriks-Hoogland, I., Brinkhof, M. W. G., de Bie, R., Joggi, D., and von Elm, E. (2014). Non-pharmacological interventions for chronic pain in people with spinal cord injury. *Cochrane Database of Syst. Rev.* 28:CD009177. doi: 10.1002/14651858.CD009177.pub2

Bragge, P., Clavisi, O., Turner, T., Tavender, E., Collie, A., and Gruen, R. L. (2011). The Global Evidence Mapping Initiative: scoping research in broad topic areas. *BMC Med. Res. Methodol.* 11:92. doi: 10.1186/1471-2288-11-92

Cardenas-Rojas, A., Pacheco-Barrios, K., Giannoni-Luza, S., Rivera-Torrejon, O., and Fregni, F. (2020). Noninvasive brain stimulation combined with exercise in chronic pain: a systematic review and meta-analysis. *Exp. Rev. Neurother.* 20, 401–412. doi: 10.1080/14737175.2020.1738927

Cervigni, M., Onesti, E., Ceccanti, M., Gori, M. C., Tartaglia, G., Campagna, G., et al. (2018). Repetitive transcranial magnetic stimulation for chronic neuropathic pain in patients with bladder pain syndrome/interstitial cystitis. *Neurourol. Urodyn.* 37, 2678–2687. doi: 10.1002/nau.23718

Chang, M. C., Kwak, S. G., and Park, D. (2020). The effect of rTMS in the management of pain associated with CRPS. *Transl. Neurosci.* 11, 363–370. doi: 10.1515/tnsci-2020-0120

Chen, C. C., Chuang, Y. F., Huang, A. C., Chen, C. K., and Chang, Y. J. (2016). The antalgic effects of non-invasive physical modalities on central post-stroke pain: a systematic review. *J. Phys. Ther. Sci.* 28, 1368–1373. doi: 10.1589/jpts.28.1368

Choi, G. S., and Chang, M. C. (2018). Effects of high-frequency repetitive transcranial magnetic stimulation on reducing hemiplegic shoulder pain in patients with chronic stoke: a randomized controlled trial. *Int. J. Neurosci.* 128, 110–116. doi: 10.1080/00207454.2017.1367682

Choi, G. S., Kwak, S. G., Lee, H. D., and Chang, M. C. (2018). Effect of high-frequency repetitive transcranial magnetic stimulation on chronic central pain after mild traumatic brain injury: a pilot study. *J. Rehabil. Med.* 50, 246–252. doi: 10.2340/16501977-2321

Colloca, L., Ludman, T., Bouhassira, D., Baron, R., Dickenson, A. H., Yarnitsky, D., et al. (2017). Neuropathic pain. *Nat. Rev. Dis. Primers.* 3:17002. doi: 10.1038/nrdp.2017.2

Cossins, L., Okell, R. W., Cameron, H., Simpson, B., Poole, H. M., and Goebel, A. (2013). Treatment of complex regional pain syndrome in adults: a systematic

review of randomized controlled trials published from June 2000 to February 2012. *Eur. J. Pain* 17, 158–173. doi: 10.1002/j.1532-2149.2012.00217.x

Cragg, J. J., Warner, F. M., Finnerup, N. B., Jensen, M. P., Mercier, C., Richards, J. S., et al. (2016). Meta-analysis of placebo responses in central neuropathic pain: impact of subject, study, and pain characteristics. *Pain* 157, 530–540. doi: 10.1097/j.pain.0000000000000431

Cruccu, G., Garcia-Larrea, L., Hansson, P., Keindl, M., Lefaucheur, J. P., Paulus, W., et al. (2016). EAN guidelines on central neurostimulation therapy in chronic pain conditions. *Eur. J. Neurol.* 23, 1489–1499. doi: 10.1111/ene.13103

Defrin, R., Grunhaus, L., Zamir, D., and Zeilig, G. (2007). The effect of a series of repetitive transcranial magnetic stimulations of the motor cortex on central pain after spinal cord injury. *Arch. Phys. Med. Rehabil.* 88, 1574–1580. doi: 10.1016/j.apmr.2007.07.025

Feng, Y., Zhang, B., Zhang, J., and Yin, Y. (2019). Effects of non-invasive brain stimulation on headache intensity and frequency of headache attacks in patients with migraine: a systematic review and meta-analysis. *Headache* 59, 1436–1447. doi: 10.1111/head.13645

Finnerup, N. B., Attal, N., Haroutounian, S., McNicol, E., Baron, R., Dworkin, R. H., et al. (2015). Pharmacotherapy for neuropathic pain in adults: a systematic review and meta-analysis. *Lancet Neurol.* 14, 162–173. doi: 10.1016/s1474-4422(14)70251-0

Fricova, J., Klirova, M., Masopust, V., Novak, T., Verebova, K., and Rokyta, R. (2013). Repetitive transcranial magnetic stimulation in the treatment of chronic orofacial pain. *Physiol. Res.* 62, S125–S134.

Gaertner, M., Kong, J. T., Scherrer, K. H., Foote, A., Mackey, S., and Johnson, K. A. (2018). Advancing transcranial magnetic stimulation methods for complex regional pain syndrome: an open-label study of paired theta burst and high-frequency stimulation. *Neuromodulation* 21, 409–416. doi: 10.1111/ner.12760

Galhardoni, R., Correia, G. S., Araujo, H., Yeng, L. T., Fernandes, D. T., Kaziyama, H. H., et al. (2015). Repetitive transcranial magnetic stimulation in chronic pain: a review of the literature. *Arch. Phys. Med. Rehabil.* 96, S156–S172. doi: 10.1016/j.apmr.2014.11.010

Gao, F., Chu, H., Li, J., Yang, M., Du, L., Li, J., et al. (2017). Repetitive transcranial magnetic stimulation for pain after spinal cord injury: a systematic review and meta-analysis. *J. Neurosurg. Sci.* 61, 514–522. doi: 10.23736/s0390-5616.16.03809-1

Gatzinsky, K., Bergh, C., Liljegren, A., Silander, H., Samuelsson, J., Svanberg, T., et al. (2020). Repetitive transcranial magnetic stimulation of the primary motor cortex in management of chronic neuropathic pain: a systematic review. *Scand. J. Pain* 21, 8–21. doi: 10.1515/sjpain-2020-0054

Goudra, B., Shah, D., Balu, G., Gouda, G., Balu, A., Borle, A., et al. (2017). Repetitive transcranial magnetic stimulation in chronic pain: a meta-analysis. *Anesth. Essays Res.* 11, 751–757. doi: 10.4103/aer.AER_10_17

Grant, M. J., and Booth, A. (2009). A typology of reviews: an analysis of 14 review types and associated methodologies. *Health Info Libr. J.* 26, 91–108. doi: 10.1111/j.1471-1842.2009.00848.x

Gromisch, E. S., Kerns, R. D., and Beauvais, J. (2020). Pain-related illness intrusiveness is associated with lower activity engagement among persons with multiple sclerosis. *Mult. Scler. Relat. Disord.* 38, 101882. doi: 10.1016/j.msard.2019.101882

Haddaway, N. R., Bernes, C., Jonsson, B. G., and Hedlund, K. (2016). The benefits of systematic mapping to evidence-based environmental management. *Ambio* 45, 613–620. doi: 10.1007/s13280-016-0773-x

Hamid, P., Malik, B. H., and Hussain, M. L. (2019). Noninvasive transcranial magnetic stimulation (TMS) in chronic refractory pain: a systematic review. *Cureus* 11:e6019. doi: 10.7759/cureus.6019

Henssen, D. J. H. A., Hoefsloot, W., Groenen, P. S. M., Van Cappellen van Walsum, A. M., Kurt, E., and Kozicz, T. (2019). Bilateral vs. unilateral repetitive transcranial magnetic stimulation to treat neuropathic orofacial pain: a pilot study. *Brain Stimul.* 12, 803–805. doi: 10.1016/j.brs.2019.02.001

Herrero Babiloni, A., Guay, S., Nixdorf, D. R., de Beaumont, L., and Lavigne, G. (2018). Non-invasive brain stimulation in chronic orofacial pain: a systematic review. *J. Pain Res.* 11, 1445–1457. doi: 10.2147/jpr.S168705

Hirayama, A., Saitoh, Y., Kishima, H., Shimokawa, T., Oshino, S., Hirata, M., et al. (2006). Reduction of intractable deafferentation pain by navigation-guided repetitive transcranial magnetic stimulation of the primary motor cortex. *Pain* 122, 22–27. doi: 10.1016/j.pain.2005.12.001

Hosomi, K., Shimokawa, T., Ikoma, K., Nakamura, Y., Sugiyama, K., Ugawa, Y., et al. (2013). Daily repetitive transcranial magnetic stimulation of primary motor cortex for neuropathic pain: a randomized, multicenter, double-blind, crossover, sham-controlled trial. *Pain* 154, 1065–1072. doi: 10.1016/j.pain.2013.03.016

Irlbacher, K., Kuhnert, J., Ro richt, S., Meyer, B. U., and Brandt, S. A. (2006). Central and peripheral deafferent pain: therapy with repetitive transcranial magnetic stimulation. *Nervenarzt* 77, 1196–1203. doi: 10.1007/s00115-006-2148-1

Jetté, F., Cote, I., Meziane, H. B., and Mercier, C. (2013). Effect of single-session repetitive transcranial magnetic stimulation applied over the hand versus leg motor area on pain after spinal cord injury. *Neurorehabil. Neural. Repair* 27, 636–643. doi: 10.1177/1545968313484810

Jin, Y., Xing, G., Li, G., Wang, A., Feng, S., Tang, Q., et al. (2015). High frequency repetitive transcranial magnetic stimulation therapy for chronic neuropathic pain: a meta-analysis. *Pain Phys.* 18, E1029–E1046.

Johnson, S., Summers, J., and Pridmore, S. (2006). Changes to somatosensory detection and pain thresholds following high frequency repetitive TMS of the motor cortex in individuals suffering from chronic pain. *Pain* 123, 187–192. doi: 10.1016/j.pain.2006.02.030

Kalia, L. V., and O'Connor, P. W. (2005). Severity of chronic pain and its relationship to quality of life in multiple sclerosis. *Mult. Scler.* 11, 322–327. doi: 10.1191/1352458505ms1168oa

Kalita, J., Bhoi, S. K., and Misra, U. K. (2017). Effect of high rate rTMS on somatosensory evoked potential in migraine. *Cephalalgia* 37, 1222–1230. doi: 10.1177/0333102416675619

Kalita, J., Laskar, S., Bhoi, S. K., and Misra, U. K. (2016). Efficacy of single versus three sessions of high rate repetitive transcranial magnetic stimulation in chronic migraine and tension-type headache. *J. Neurol.* 263, 2238–2246. doi: 10.1007/s00415-016-8257-2

Kang, B. S., Shin, H. I., and Bang, M. S. (2009). Effect of repetitive transcranial magnetic stimulation over the hand motor cortical area on central pain after spinal cord injury. *Arch. Phys. Med. Rehabil.* 90, 1766–1771. doi: 10.1016/j.apmr.2009.04.008

Khedr, E. M., Kotb, H. I., Mostafa, M. G., Mohamad, M. F., Amr, S. A., Ahmed, M. A., et al. (2015). Repetitive transcranial magnetic stimulation in neuropathic pain secondary to malignancy: a randomized clinical trial. *Eur. J. Pain* 19, 519–527. doi: 10.1002/ejp.576

Khedr, E. M., Kotb, H., Kamel, N. F., Ahmed, M. A., Sadek, R., and Rothwell, J. C. (2005). Long-lasting analgic effects of daily sessions of repetitive transcranial magnetic stimulation in central and peripheral neuropathic pain. *J. Neurol. Neurosurg. Psychiatry* 76, 833–838. doi: 10.1136/jnnp.2004.055806

Klein, M. M., Treister, R., Raij, T., Pascual-Leone, A., Park, L., Nurmikko, T., et al. (2015). Transcranial magnetic stimulation of the brain: guidelines for pain treatment research. *Pain* 156, 1601–1614. doi: 10.1097/j.pain.0000000000000210

Kobayashi, M., Fujimaki, T., Mihara, B., and Ohira, T. (2015). Repetitive transcranial magnetic stimulation once a week induces sustainable long-term relief of central poststroke pain. *Neuromodulation* 18, 249–254. doi: 10.1111/ner.12301

Kohútová, B., Fricová, J., Klírová, M., Novák, T., and Rokyta, R. (2017). Theta burst stimulation in the treatment of chronic orofacial pain: a randomized controlled trial. *Physiol. Res.* 66, 1041–1047. doi: 10.33549/physiolres.933474

Kumar, B., Kalita, J., Kumar, G., and Misra, U. K. (2009). Central poststroke pain: a review of pathophysiology and treatment. *Anesthesia Anal.* 108, 1645–1657. doi: 10.1213/ane.0b013e31819d644c

Kumru, H., Albu, S., Vidal, J., and Tormos, J. M. (2017). Effectiveness of repetitive trancranial or peripheral magnetic stimulation in neuropathic pain. *Disabil. Rehabil.* 39, 856–866. doi: 10.3109/09638288.2016.1170213

Lan, L., Zhang, X., Li, X., Rong, X., and Peng, Y. (2017). The efficacy of transcranial magnetic stimulation on migraine: a meta-analysis of randomized controlled trails. *J. Headache Pain* 18, 86. doi: 10.1186/s10194-017-0792-4

Lang, M., Treister, R., Klein, M. M., and Oaklander, A. L. (2014). Repetitive transcranial magnetic stimulation (rTMS) of the primary motor cortex for treating facial neuropathic pain-preliminary results of arandomized, sham-controlled, cross-over study. *Mol. Pain* 10:6. doi: 10.1111/j.1526-4637.2009.00657.x

Lawson, M. A., Frank, S., Zafar, N., Waschke, A., Kalff, R., and Reichart, R. (2018). Time course of the response to navigated repetitive transcranial magnetic

stimulation at 10 Hz in chronic neuropathic pain. *Neurol. Res.* 40, 564–572. doi: 10.1080/01616412.2018.1453636

Lefaucheur, J. P. (2003). Evaluation électrophysiologique des boucles réflexes spinales potentiellement impliquées dans la spasticité [Electrophysiological assessment of reflex pathways involved in spasticity]. *Neurochirurgie* 49, 205–214.

Lefaucheur, J. P., Aleman, A., Baeken, C., Benninger, D. H., Brunelin, J., Di Lazzaro, V., et al. (2020). Evidence-based guidelines on the therapeutic use of repetitive transcranial magnetic stimulation (rTMS): an update (2014-2018). *Clin. Neurophysiol.* 131, 474–528. doi: 10.1016/j.clinph.2019.11.002

Lefaucheur, J. P., Ayache, S. S., Sorel, M., Farhat, W. H., Zouari, H. G., and Ciampi de Andrade, D. (2012). Analgesic effects of repetitive transcranial magnetic stimulation of the motor cortex in neuropathic pain: influence of theta burst stimulation priming. *Eur. J. Pain* 16, 1403–1413. doi: 10.1002/j.1532-2149.2012.00150.x

Lefaucheur, J. P., Drouot, X., Keravel, Y., and Nguyen, J. P. (2001a). Pain relief induced by repetitive transcranial magnetic stimulation of precentral cortex. *Neuroreport* 12, 2963–2965. doi: 10.1097/00001756-200109170-00041

Lefaucheur, J. P., Drouot, X., and Nguyen, J. P. (2001b). Interventional neurophysiology for pain control: duration of pain relief following repetitive transcranial magnetic stimulation of the motor cortex. *Neurophysiol. Clin.* 31, 247–252. doi: 10.1016/s0987-7053(01)00260-x

Lefaucheur, J. P., Drouot, X., Menard-Lefaucheur, I., Keravel, Y., and Nguyen, J. P. (2008). Motor cortex rTMS in chronic neuropathic pain: pain relief is associated with thermal sensory perception improvement. *J. Neurol. Neurosurg. Psychiatry* 79, 1044–1049. doi: 10.1136/jnnp.2007.135327

Lefaucheur, J. P., Drouot, X., Menard-Lefaucheur, I., Zerah, F., Bendib, B., Cesaro, P., et al. (2004). Neurogenic pain relief by repetitive transcranial magnetic cortical stimulation depends on the origin and the site of pain. *J. Neurol. Neurosurg. Psychiatry* 75, 612–616. doi: 10.1136/jnnp.2003.022236

Lefaucheur, J. P., Hatem, S., Nineb, A., Ménard-Lefaucheur, I., Wendling, S., Keravel, Y., et al. (2006). Somatotopic organization of the analgesic effects of motor cortex rTMS in neuropathic pain. *Neurology* 67, 1998–2004. doi: 10.1212/01.wnl.0000247138.85330.88

Lefaucheur, J. P., Menard-Lefaucheur, I., Goujon, C., Keravel, Y., and Nguyen, J. P. (2011). Predictive value of rTMS in the identification of responders to epidural motor cortex stimulation therapy for pain. *J. Pain* 12, 1102–1111. doi: 10.1016/j.jpain.2011.05.004

Leung, A., Donohue, M., Xu, R., Lee, R., Lefaucheur, J. P., Khedr, E. M., et al. (2009). rTMS for suppressing neuropathic pain: a meta-analysis. *J. Pain* 10, 1205–1216. doi: 10.1016/j.jpain.2009.03.010

Leung, A., Shukla, S., Fallah, A., Song, D., Lin, L., Golshan, S., et al. (2016). Repetitive transcranial magnetic stimulation in managing mild traumatic brain injury-related headaches. *Neuromodulation* 19, 133–141. doi: 10.1111/ner.12364

Liampas, A., Rekatsina, M., Vadalouca, A., Paladini, A., Varrassi, G., and Zis, P. (2020b). Non-pharmacological management of painful peripheral neuropathies: a systematic review. *Adv. Ther.* 37, 4096–4106. doi: 10.1007/s12325-020-01462-3

Liampas, A., Velidakis, N., Georgiou, T., Vadalouca, A., Varrassi, G., Hadjigeorgiou, G. M., et al. (2020a). Prevalence and management challenges in central post-stroke neuropathic pain: a systematic review and meta-analysis. *Adv. Ther.* 37, 3278–3291. doi: 10.1007/s12325-020-01388-w

Lin, H., Li, W., Ni, J., and Wang, Y. (2018). Clinical study of repetitive transcranial magnetic stimulation of the motor cortex for thalamic pain. *Medicine* 97:e11235. doi: 10.1097/md.0000000000011235

Ma, S. M., Ni, J. X., Li, X. Y., Yang, L. Q., Guo, Y. N., and Tang, Y. Z. (2015). High-frequency repetitive transcranial magnetic stimulation reduces pain in postherpetic neuralgia. *Pain Med.* 16, 2162–2170. doi: 10.1111/pme.12832

Madera Anaya, M., Franco, J. V. A., Ballesteros, M., Solà, I., Urrútia Cuchí, G., and Bonfill Cosp, X. (2019). Evidence mapping and quality assessment of systematic reviews on therapeutic interventions for oral cancer. *Cancer Manag. Res.* 11, 117–130. doi: 10.2147/cmar.S186700

Malavera, A., Silva, F. A., Fregni, F., Carrillo, S., and Garcia, R. G. (2016). Repetitive transcranial magnetic stimulation for phantom limb pain in land mine victims: a double-blinded, randomized, sham-controlled trial. *J. Pain.* 17, 911–918. doi: 10.1016/j.jpain.2016.05.003

Malavera, M., Silva, F., Garcia, R., Quiros, J., Dallos, M., and Pinzon, A. (2013). Effects of transcranial magnetic stimulation in the treatment of phantom limb pain in landmine victims: a randomized clinical trial. *J. Neurol. Sci.* 333:e534. doi: 10.1016/j.jns.2013.07.1880

Matsumura, Y., Hirayama, T., and Yamamoto, T. (2013). Comparison between pharmacologic evaluation and repetitive transcranial magnetic stimulation-induced analgesia in poststroke pain patients. *Neuromodulation* 16, 349–354. doi: 10.1111/ner.12019

Mehta, S., Orenczuk, K., McIntyre, A., Willems, G., Wolfe, D. L., Hsieh, J. T., et al. (2013). Neuropathic pain post spinal cord injury part 1: systematic review of physical and behavioral treatment. *Top. Spinal. Cord. Inj. Rehabil.* 19, 61–77. doi: 10.1310/sci1901-61

Melchior, C., Gourcerol, G., Chastan, N., Verin, E., Menard, J. F., Ducrotte, P., et al. (2014). Effect of transcranial magnetic stimulation on rectal sensitivity in irritable bowel syndrome: a randomized, placebo-controlled pilot study. *Colorectal. Dis.* 16, O104–O111. doi: 10.1111/codi.12450

Melchior, M., Chastang, J. F., Head, J., Goldberg, M., Zins, M., Nabi, H., et al. (2013). Socioeconomic position predicts long-term depression trajectory: a 13-year follow-up of the GAZEL cohort study. *Mol. Psychiatry* 18, 112–121. doi: 10.1038/mp.2011.116

Miake-Lye, I. M., Hempel, S., Shanman, R., and Shekelle, P. G. (2016). What is an evidence map? A systematic review of published evidence maps and their definitions, methods, and products. *Syst Rev.* 5, 28. doi: 10.1186/s13643-016-0204-x

Miake-Lye, I. M., Mak, S., Lee, J., Luger, T., Taylor, S. L., Shanman, R., et al. (2019). Massage for pain: an evidence map. *J. Alter. Comple. Med.* 25, 475–502. doi: 10.1089/acm.2018.0282

Misra, U. K., Kalita, J., Tripathi, G. M., and Bhoi, S. K. (2013). Is beta endorphin related to migraine headache and its relief? *Cephalalgia* 33, 316–322. doi: 10.1177/0333102412473372

Misra, U. K., Kalita, J., Tripathi, G., and Bhoi, S. K. (2017). Role of beta endorphin in pain relief following high rate repetitive transcranial magnetic stimulation in migraine. *Brain Stimul.* 10, 618–623. doi: 10.1016/j.brs.2017.02.006

Moisset, X., Bouhassira, D., Avez Couturier, J., Alchaar, H., Conradi, S., Delmotte, M. H., et al. (2020b). Pharmacological and non-pharmacological treatments for neuropathic pain: systematic review and French recommendations. *Rev. Neurol.* 176, 325–352. doi: 10.1016/j.neurol.2020.01.361

Moisset, X., Pereira, B., de Andrade, D., Fontaine, D., Lantéri-Minet, M., and Mawet, J. (2020a). Neuromodulation techniques for acute and preventive migraine treatment: a systematic review and meta-analysis of randomized controlled trials. *J. Headache Pain* 21:142. doi: 10.1186/s10194-020-01204-4

Moreno-Duarte, I., Morse, L. R., Alam, M., Bikson, M., Zafonte, R., and Fregni, F. (2014). Targeted therapies using electrical and magnetic neural stimulation for the treatment of chronic pain in spinal cord injury. *NeuroImage* 85, 1003–1013. doi: 10.1016/j.neuroimage.2013.05.097

Mulla, S. M., Wang, L., Khokhar, R., Izhar, Z., Agarwal, A., Couban, R., et al. (2015). Management of central poststroke pain: systematic review of randomized controlled trials. *Stroke* 46, 2853–2860. doi: 10.1161/strokeaha.115.010259

Nardone, R., Versace, V., Sebastianelli, L., Brigo, F., Christova, M., Scarano, G. I., et al. (2019). Transcranial magnetic stimulation in subjects with phantom pain and non- painful phantom sensations: a systematic review. *Brain Res. Bull.* 148, 1–9. doi: 10.1016/j.brainresbull.2019.03.001

Nurmikko, T., MacIver, K., Bresnahan, R., Hird, E., Nelson, A., and Sacco, P. (2016). Motor cortex reorganization and repetitive transcranial magnetic stimulation for pain-a methodological study. *Neuromodulation* 19, 669–678. doi: 10.1111/ner.12444

Nussbaumer-Streit, B., Grillich, L., Glechner, A., Affengruber, L., Gartlehner, G., Morche, J., et al. (2018). [GRADE: evidence to Decision (EtD) frameworks - a systematic and transparent approach to making well informed healthcare choices. 1: Introduction]. *Z. Evid. Fortbild. Qual. Gesundhwes.* 134, 57–66. doi: 10.1016/j.zefq.2018.05.004

O'Connell, N. E., Marston, L., Spencer, S., Desouza, L. H., and Wand, B. M. (2018). Non-invasive brain stimulation techniques for chronic pain. *Cochrane Database Syst. Rev.* 4:CD008208. doi: 10.1002/14651858.CD008208.pub5

Onesti, E., Gabriele, M., Cambieri, C., Ceccanti, M., Raccah, R., Di Stefano, G., et al. (2013). H-coil repetitive transcranial magnetic stimulation for pain relief

in patients with diabetic neuropathy. *Eur. J. Pain* 17, 1347–1356. doi: 10.1002/j.1532-2149.2013.00320.x

Pacheco-Barrios, K., Meng, X., and Fregni, F. (2020). Neuromodulation techniques in phantom limb pain: a systematic review and meta-analysis. *Pain Med.* 21, 2310–2322. doi: 10.1093/pm/pnaa039

Papanas, N., and Ziegler, D. (2016). Emerging drugs for diabetic peripheral neuropathy and neuropathic pain. *Exp. Opin. Emerg. Drugs* 21, 393–407. doi: 10.1080/14728214.2016.1257605

Paulus, W., Peterchev, A. V., and Ridding, M. (2013). Transcranial electric and magnetic stimulation: technique and paradigms. *Handb. Clin. Neurol.* 116, 329–342. doi: 10.1016/b978-0-444-53497-2.00027-9

Pei, Q., Wu, B., Tang, Y., Yang, X., Song, L., Wang, N., et al. (2019). Repetitive transcranial magnetic stimulation at different frequencies for postherpetic neuralgia: a double-blind, sham-controlled,randomized trial. *Pain Phys.* 22, E303–E313.

Petersen, K., Vakkalanka, S., and Kuzniarz, L. (2015). Guidelines for conducting systematic mapping studies in software engineering: an update. *Inform. Softw. Technol.* 64, 1–18. doi: 10.1016/j.infsof.2015.03.007

Picarelli, H., Teixeira, M. J., de Andrade, D. C., Myczkowski, M. L., Luvisotto, T. B., Yeng, L. T., et al. (2010). Repetitive transcranial magnetic stimulation is efficacious as an add-on to pharmacological therapy in complex regional pain syndrome (CRPS) type I. *J. Pain.* 11, 1203–1210. doi: 10.1016/j.jpain.2010.02.006

Pinot-Monange A, Moisset X, Chauvet P, Gremeau AS, Comptour A, Canis M, et al. (2019). Repetitive transcranial magnetic stimulation therapy. (rTMS) for endometriosis patients with refractory pelvic chronic pain: a pilot study. *J. Clin. Med.* 8:508. doi: 10.3390/jcm8040508

Pleger, B., Janssen, F., Schwenkreis, P., Volker, B., Maier, C., and Tegenthoff, M. (2004). Repetitive transcranial magnetic stimulation of the motor cortex attenuates pain perception in complex regional pain syndrome type I. *Neurosci. Lett.* 356, 87–90. doi: 10.1016/j.neulet.2003.11.037

Pommier, B., Creac'h, C., Beauvieux, V., Nuti, C., Vassal, F., and Peyron, R. (2016). Robot-guided neuronavigated rTMS as an alternative therapy for central. (neuropathic) pain: clinical experience and long-term follow-up. *Eur. J. Pain* 20, 907–916. doi: 10.1002/ejp.815

Quesada, C., Pommier, B., Fauchon, C., Bradley, C., Créac'h, C., Vassal, F., et al. (2018). Robot-guided neuronavigated repetitive transcranial magnetic stimulation. (rTMS) in Central neuropathic pain. *Arch. Phys. Med. Rehabil.* 99, 2203–2215. doi: 10.1016/j.apmr.2018.04.013

Ramger, B. C., Bader, K. A., Davies, S. P., Stewart, D. A., Ledbetter, L. S., Simon, C. B., et al. (2019). Effects of non-invasive brain stimulation on clinical pain intensity and experimental pain sensitivity among individuals with central post-stroke pain: a systematic review. *J. Pain Res.* 12, 3319–3329. doi: 10.2147/JPR.S216081

Rollnik, J. D., Wustefeld, S., Dauper, J., Karst, M., Fink, M., Kossev, A., et al. (2002). Repetitive transcranial magnetic stimulation for the treatment of chronic pain – a pilot study. *Eur. Neurol.* 48, 6–10.

Saitoh, Y., Hirayama, A., Kishima, H., Oshino, S., Hirata, M., Kato, A., et al. (2006). Stimulation of primary motor cortex for intractable deafferentation pain. *Acta Neurochir. Suppl.* 99, 57–59. doi: 10.1007/978-3-211-35205-2_11

Saitoh, Y., Hirayama, A., Kishima, H., Shimokawa, T., Oshino, S., Hirata, M., et al. (2007). Reduction of intractable deafferentation pain due to spinal cord or peripheral lesion by high-frequency repetitive transcranial magnetic stimulation of the primary motor cortex. *J. Neurosurg.* 107, 555–559. doi: 10.3171/jns-07/09/0555

Shea, B. J., Reeves, B. C., Wells, G., Thuku, M., Hamel, C., Moran, J., et al. (2017). AMSTAR 2: a critical appraisal tool for systematic reviews that include randomised or non-randomised studies of healthcare interventions, or both. *BMJ* 358, j4008. doi: 10.1136/bmj.j4008

Shehata, H. S., Esmail, E. H., Abdelalim, A., El-Jaafary, S., Elmazny, A., Sabbah, A., et al. (2016). Repetitive transcranial magnetic stimulation versus botulinum toxin injection in chronic migraine prophylaxis: a pilot randomized trial. *J. Pain Res.* 9, 771–777. doi: 10.2147/JPR.S116671

Shen, Z., Li, Z., Ke, J., He, C., Liu, Z., Zhang, D., et al. (2020). Effect of non-invasive brain stimulation on neuropathic pain following spinal cord injury: a systematic review and meta-analysis. *Medicine* 99:e21507. doi: 10.1097/md.0000000000021507

Shimizu, T., Hosomi, K., Maruo, T., Goto, Y., Yokoe, M., Kageyama, Y., et al. (2017). Efficacy of deep rTMS for neuropathic pain in the lower limb: a randomized, double-blind crossover trial of an H-coil and figure-8 coil. *J. Neurosurg.* 127, 1172–1180. doi: 10.3171/2016.9.JNS16815

Stilling, J. M., Monchi, O., Amoozegar, F., and Debert, C. T. (2019). Transcranial magnetic and direct current stimulation (TMS/tDCS) for the treatment of headache: a systematic review. *Headache* 59, 339–357. doi: 10.1111/head.13479

Sylvester, R. J., Canfield, S. E., Lam, T. B., Marconi, L., MacLennan, S., Yuan, Y., et al. (2017). Conflict of evidence: resolving discrepancies when findings from randomized controlled trials and meta-analyses disagree. *Eur. Urol.* 71, 811–819. doi: 10.1016/j.eururo.2016.11.023

Teo, W. P., Kannan, A., Loh, P. K., Chew, E., Sharma, V. K., and Chan, Y. C. (2014). Tolerance of motor cortex rTMS in chronic migraine. *J. Clin. Diagn. Res.* 8, MM01–MM02.

Urits, I., Adamian, L., Fiocchi, J., Hoyt, D., Ernst, C., Kaye, A. D., et al. (2019). Advances in the understanding and management of chronic pain in multiple sclerosis: a comprehensive review. *Curr. Pain Headache Rep.* 23:59. doi: 10.1007/s11916-019-0800-2

Yang, S., and Chang, M. C. (2020). Effect of repetitive transcranial magnetic stimulation on pain management: a systematic narrative review. *Front. Neurol.* 11:114. doi: 10.3389/fneur.2020.00114

Yilmaz, B., Kesikburun, S., Yasar, E., and Tan, A. K. (2014). The effect of repetitive transcranial magnetic stimulation on refractory neuropathic pain in spinal cord injury. *J. Spinal. Cord. Med.* 37, 397–400.

Yu, B., Qiu, H., Li, J., Zhong, C., and Li, J. (2020). Noninvasive brain stimulation does not improve neuropathic pain in individuals with spinal cord injury: evidence from a meta-analysis of 11 randomized controlled trials. *Am. J. Phys. Med. Rehabil.* 99, 811–820. doi: 10.1097/phm.0000000000001421

Zaghi, S., Thiele, B., Pimentel, D., Pimentel, T., and Fregni, F. (2011). Assessment and treatment of pain with non-invasive cortical stimulation. *Restorat. Neurol. Neurosci.* 29, 439–451. doi: 10.3233/RNN-2011-0615

Zeng, H., Pacheco-Barrios, K., Cao, Y., Li, Y., Zhang, J., Yang, C., et al. (2020). Non-invasive neuromodulation effects on painful diabetic peripheral neuropathy: a systematic review and meta-analysis. *Sci Rep.* 10:19184. doi: 10.1038/s41598-020-75922-9

Zucchella, C., Mantovani, E., De Icco, R., Tassorelli, C., Sandrini, G., and Tamburin, S. (2020). Non-invasive brain and spinal stimulation for pain and related symptoms in multiple sclerosis: a systematic review. *Front. Neurosci.* 14:547069. doi: 10.3389/fnins.2020.547069

Conflict of Interest: The authors declare that the research was conducted in the absence of any commercial or financial relationships that could be construed as a potential conflict of interest.

frontiers in Human Neuroscience

ORIGINAL RESEARCH
published: 04 March 2022
doi: 10.3389/fnhum.2022.848347

A Preliminary Study of the Efficacy of Transcranial Direct Current Stimulation in Trigeminal Neuralgia

*Babak Babakhani[1†], Narges Hoseini Tabatabaei[2†], Kost Elisevich[3], Narges Sadeghbeigi[4], Mojtaba Barzegar[4,5], Neda Mohammadi Mobarakeh[6,7], Fatemeh Eyvazi[7,8], Zahra Khazaeipour[1], Arman Taheri[2] and Mohammad-Reza Nazem-Zadeh[6,7]**

[1] Brain and Spinal Cord Injury Research Centre, Neuroscience Institute, Tehran University of Medical Sciences, Tehran, Iran, [2] Medical School, Tehran University of Medical Sciences, Tehran, Iran, [3] Department of Clinical Neurosciences, Spectrum Health, College of Human Medicine, Michigan State University, Grand Rapids, MI, United States, [4] National Brain Mapping Laboratory, Tehran, Iran, [5] Intelligent Quantitative Biomedical Imaging L.L.C, Tehran, Iran, [6] Medical Physics and Biomedical Engineering Department, Tehran University of Medical Sciences, Tehran, Iran, [7] Research Center for Molecular and Cellular Imaging, Advanced Medical Technologies and Equipment Institute, Tehran University of Medical Sciences, Tehran, Iran, [8] Cognitive Psychology Department, Shahid Beheshti University, Tehran, Iran

OPEN ACCESS

Edited by:
Jiaojian Wang, University of Electronic Science and Technology of China, China

Reviewed by:
Marcello Romano, Azienda Ospedaliera Ospedali Riuniti Villa Sofia Cervello, Italy
Cornelius Bachmann, Independent Researcher, Osnabrück , Germany

***Correspondence:**
Mohammad-Reza Nazem-Zadeh
mnazemzadeh@tums.ac.ir

† These authors have contributed equally to this work and share first authorship

Specialty section:
This article was submitted to Brain Imaging and Stimulation, a section of the journal Frontiers in Human Neuroscience

Received: *04 January 2022*
Accepted: *07 February 2022*
Published: *04 March 2022*

Citation:
Babakhani B, Tabatabaei NH, Elisevich K, Sadeghbeigi N, Barzegar M, Mobarakeh NM, Eyvazi F, Khazaeipour Z, Taheri A and Nazem-Zadeh M-R (2022) A Preliminary Study of the Efficacy of Transcranial Direct Current Stimulation in Trigeminal Neuralgia. Front. Hum. Neurosci. 16:848347. doi: 10.3389/fnhum.2022.848347

The purpose of this study is to assess the efficacy of transcranial direct current stimulation (tDCS) in patients with treatment-refractory trigeminal neuralgia (TN) and examine the utility of neuroimaging methods in identifying markers of such efficacy. Six patients with classical TN refractory to maximal medical treatment, underwent tDCS (three cases inhibitory/cathodic and three cases excitatory/anodic stimulation). All patients underwent pre- and posttreatment functional magnetic resonance imaging (fMRI) during block-design tasks (i.e., Pain, Pain + tDCS, tDCS) as well as single-shell diffusion MRI (dMRI) acquisition. The precise locations of tDCS electrodes were identified by neuronavigation. Five therapeutic tDCS sessions were carried out for each patient with either anodic or cathodic applications. The Numeric Rating Scale of pain (NRS) and the Headache Disability Index (HDI) were used to score the subjective efficacy of treatment. Altered activity of regional sites was identified by fMRI and associated changes in the spinothalamocortical sensory tract (STCT) were measured by the dMRI indices of fractional anisotropy (FA) and mean diffusivity (MD). Fiber counts of the bilateral trigeminal root entry zone (REZ) were performed as an added measure of fiber loss or recovery. All patients experienced a significant reduction in pain scores with a substantial decline in HDI (P value < 0.01). Following a course of anodic tDCS, the ipsilateral caudate, globus pallidus, somatosensory cortex, and the contralateral globus pallidus showed a significantly attenuated activation whereas cathodic tDCS treatment resulted in attenuation of the thalamus and globus pallidus bilaterally, and the somatosensory cortex and anterior cingulate gyrus contralaterally. dMRI analysis identified a substantial increase (>50%) in the number of contralateral sensory fibers in the STCT with either anodic or cathodic tDCS treatment in four of the six patients. A significant reduction in FA (>40%) was observed in the ipsilateral REZ in the posttreatment phase in five of the six patients. Preliminary evidence suggests that navigated tDCS presents

a promising method for alleviating the pain of TN. Different patterns of activation manifested by anodic and cathodic stimulation require further elaboration to understand their implication. Activation and attenuation of responses at various sites may provide further avenues for condition treatment.

Keywords: treatment efficacy, fMRI, neural bases, tDCS—transcranial direct current stimulation, brain stimulation, dMRI (diffusion magnetic resonance imaging), pain, trigeminal neuralgia

INTRODUCTION

Trigeminal neuralgia (TN) is a chronic neuralgic facial pain disorder that involves the territory of one or more branches of the trigeminal nerve and affects seniors and women more than men in a ratio of 3:1 with a prevalence of 0.03–0.3% (Cheshire, 2007; Olesen et al., 2013; Sivakanthan et al., 2014; CheshireJr., 2015; De Toledo et al., 2016). Added to the pain of the condition, patients with TN have an increased risk of anxiety and depression with significant life consequences (Morra et al., 2016). A variety of pathologies underlie the occurrence of TN with genetic, biologic and environmental factors implicated in its evolution affecting changes within both the central nervous system and nerve root itself (Pollack et al., 1988; Duff et al., 1999; Fleetwood et al., 2001; Devor et al., 2002; Gupta et al., 2002; Smyth et al., 2003; Hall et al., 2006; Hemminki et al., 2007; El et al., 2008; Ebner et al., 2010; Zakrzewska and Linskey, 2014).

Medical treatment is considered as firstline therapy for TN with preferences given to antiepileptic drugs and baclofen. Side effects of treatment with such drugs are typically dose-related (Zakrzewska, 2001) and age-related complications, intolerance of medical therapy, progression of pain severity, and the relapsing nature of TN limit efficacy. Evidence has identified neuromodulation as a potentially effective treatment of such conditions (Hansen et al., 2011; Hagenacker et al., 2014).

The processing of pain stimuli involves a complex arrangement of sites within the cerebral hemispheres that are accessible to neuromodulation. Reciprocal connections exist both between motor (MC) and premotor (PM) cortices and between the PM and ventrolateral nucleus (VLN) of the thalamus (Bosch-Bouju et al., 2013). Both the PM and globus pallidus interna (GPi) project to the anterior VLN while both the MC and cerebellum project to the posterior VLN. The ventromedial nucleus (VMN) of the thalamus similarly receives input from the PM as well as the substantia nigra pars reticulata (SNpr). Striatal GABAergic spiny neurons exert an inhibitory effect upon nigrothalamic and pallidothalamic neurons (Ueki et al., 1977; Uno et al., 1978; Chevalier and Deniau, 1982; Yamamoto et al., 1983) resulting in a disinhibition of the VMN and its projection onto the MC. The ventroposterior nucleus pars medialis (VPM) of the thalamus similarly has reciprocal connections with the somatosensory cortex (SSC) (Sherman and Guillery, 2011). It receives sensory information from the principal trigeminal nucleus. The posteromedial nucleus (POm) receives sensory information from the spinal trigeminal nucleus and from the SSC (Veinante et al., 2000; Sherman and Guillery, 2011; Groh et al., 2014). The POm additionally regulates SSC processing between it and secondary sensory cortical areas (Liao and Yen, 2008; Yam et al., 2018).

The basal ganglia-thalamus-cerebral cortex circuit consists of fibers projecting from the supplementary motor area (SMA), PM, MC, and SSC to the putamen which projects to both external and internal segments of the globus pallidus The circuit is completed with efferents from the GPi to the VLN and back to the SMA (Jürgens, 1984; Alexander et al., 1986). Two distinct pathways, direct and indirect, from the basal ganglia regulate the thalamic response with opposing effect. Activation of the striatum inhibits GPi neurons causing the direct pathway to release thalamic neurons from inhibition, and to excite the MC. The indirect pathway involves striatal inhibition of the external globus pallidus (GPe) which then disinhibits neurons of the subthalamic nucleus to bring about excitation of the GPi. The latter results in an inhibition of the thalamus and subsequent inhibition of the MC.

Medical treatment is considered as firstline therapy for TN with preferences given to antiepileptic drugs (AEDs) and baclofen. Side effects of treatment with such drugs are typically dose-related and underestimated by clinicians (Zakrzewska, 2001). Age-related complications, intolerance of medical therapy, progression of pain severity and the relapsing nature of TN limit efficacy. Nonmedical treatment has primarily involved minimally invasive surgical procedures while neuromodulatory methods have more recently become acknowledged as effective interventions (Hansen et al., 2011; Hagenacker et al., 2014). Stimulation of the MC (Attal et al., 2016) and caudate nucleus (Ervin et al., 1966; Lineberry and Vierck, 1975) have both been shown to mitigate pain. Noxious stimulation activates the SSC bilaterally but does so more ipsilaterally (Becerra et al., 2008).

A recent review analyzed the therapeutic effect of repeated transcranial magnetic stimulation (rTMS) and transcranial direct current stimulation (tDCS) on different types of chronic headache (Stilling et al., 2019). Cases of mild-moderate grade headache have responded with a reduced frequency of events using anodic tDCS applied to either the left MC or the dorsolateral prefrontal cortex (DLPFC) with the cathode overlying the contralateral fp2 site of the 10-20 EEG system. Orofacial pain disorders likewise have responded to similar stimulation of the MC, DLPFC, and the secondary sensory cortex (Ferreira et al., 2019).

Different applications of navigated tDCS in six patients with treatment-refractory TN, specifically the locations of anode and cathode, were evaluated to determine response to treatment. Magnetic resonance imaging was undertaken to identify coincident structural and functional changes underlying the effect of the stimulation. Activation and attenuation of

responses at various sites and with a larger TN cohort may provide further avenues for treatment of the condition.

MATERIALS AND METHODS

Study Design

This research study was approved by Institutional Review Board (IRB) of the Tehran University of Medical Sciences. Six otherwise healthy patients with unilateral primary TN (five left, one right; Table S1) refractory to maximal medical therapy (including Carbamazepine, Pregabalin, and Clonidine) were enrolled in the study following informed consent. None suffered from depression or other psychological disorder. All had failed to achieve treatment goals with recommended standard medical treatment (International Headache Society). Inclusion eligibility was drawn from the criteria established by the Headache Classification Committee for TN [International Headache Society (HIS)] (Ettlin, 2013); specifically, recurrent paroxysmal unilateral facial pain in the distribution(s) of one or more divisions of the 5th cranial nerve, without radiation beyond. Attacks of neuralgiform pain can be precipitated by innocuous stimuli within the affected territory of trigeminal division. Morphological changes of Trigeminal nerve are evident in MRI study. Exclusion criteria included: (1) Presence of any severe systemic comorbidity, (2) History of arrhythmia or seizure, and (3) Any contraindication for magnetic resonance imaging (MRI). Both SSC and MC were determined using standard neuronavigation technique. Three patients underwent inhibitory cathodic tDCS over the SSC and three had anodic excitatory tDCS over the MC, both contralateral to the side of the TN.

Functional MRI-based navigation was used to identify sites within the SSC and MC corresponding to the region of facial pain. The precise locations of tDCS electrodes were determined using a transcranial magnetic stimulation (TMS)-based navigator (LOCALITE GmbH, Bonn, Germany, Personal Communication). A high spatial resolution T1-MPRAGE MRI with voxel size 1 mm^3, 3D brain segmentation and registration tools confirmed the stimulation target sites for subsequent imaging and therapeutic sessions. A conductive paste (Ten20) was manually applied as a conductor between the electrodes and skin, with the resultant impedance checked for the subject's safety. MR-compatible tDCS equipment (NeuroConn DC-stimulator) was used to apply 2 mA direct current concurrently with fMRI paradigm. A pair of MR-compatible rectangular rubber electrodes with dimensions of 35 cm^2 (7 × 5) were used with rubber band fixation to keep the electrodes in place during imaging. The pretreatment session with fMRI consisted of the standard three stages in the block-design imaging analysis approach: (1) "tDCS" stimulation task targeting optimal regions in the block design; (2) Pain stimulation task with pain triggered in the block design; (3) "Pain + tDCS" stimulation task with pain triggered instantaneously with tDCS in the block design between rest phases. During activation blocks in the "Pain" task, the patients were instructed to bite their ipsilateral interior cheek next to the second upper molar tooth in order to reproduce their neuralgiform pain in the territory of trigeminal nerve. The same scenario was applied for the "Pain + tDCS" task, while an electrical stimulus was directed to the motor (anodic/excitatory stimulation) or sensory (cathodic/inhibitory stimulation) cortex. For the "tDCS" task, only the electrical current was applied during activation blocks with the patients instructed to do nothing during the task. A diffusion MRI (dMRI) study was also performed in the pretreatment phase. The patients then underwent five sessions of tDCS treatment with either cathodic stimulation delivered onto the contralateral SSC or anodic stimulation upon the contralateral MC. Again, a direct current of 2mA was applied by the same tDCS for a 20-min duration with 30s fade in/out. A saturated sponge with normal saline (0.9%) was used as a conductor between the electrode and skin with impedance checking for the subject's safety. A one-day interval was provided between sessions and the posttreatment study was performed two days after the last treatment session. Both fMRI and DTI were performed with the same tasks and imaging parameters as in the initial study. The Numeric Rating Scale (NRS) and the Headache Disability Index (HDI) were used to score the subjective efficacy of treatment. NRS and HDI were registered before and one week after completion of the study (Jacobson et al., 1994).

Imaging Protocols, Preprocessing, and Analysis

All subjects underwent high-resolution structural MRI and fMRI block-design stimulation tasks, along with a single-shell dMRI acquisition using a 64-channel phased array head coil and a 3-Tesla scanner (Siemens Prisma, Erlangen, Germany) using the software version "Syngo MR E11." A structural MRI was acquired using a standardized protocol as follows: transverse T1-weighted images using the MPRAGE protocol with imaging parameters, TR = 1840 ms, TI = 900 ms, TE = 2.43ms, flip angle = 8°, matrix = 224 × 224, in-plane resolution = 1.0 × 1.0 mm^2, slice thickness = 1.0 mm, pixel bandwidth = 250 Hz/pixel. The volumes of the task-related fMRI (120 measurements) covering the whole brain were acquired in the transverse plane using an echo planar imaging (EPI) sequence (TR = 3,000 ms, TE = 30 ms, flip angle = 90, matrix = 640 × 640, slice thickness = 2.4 mm). In the "Pain" stimulation task, sic blocks of activation were applied, each followed by a rest period. The duration of each fMRI task block was 6 min. Single shell dMRI (b-value of 1,000 s/mm^2 involved 64 diffusion gradient directions acquired using EPI with the same unit in an anteroposterior phase direction with the following imaging parameters: TR = 9,600 ms, TE = 92 ms, flip angle = 90, matrix = 110 110, in-plane resolution = 2.0 × 2.0 mm^2, slice thickness = 2.0 mm, pixel bandwidth = 1,420 Hz/pixel. Two sets of null volumes using the above-mentioned imaging parameters and without applying diffusion synthesizing gradients (b-value of 0 s/mm^2 were acquired using two opposite phase-encoding directions (AP and PA) to perform distortion correction.

Preprocessing steps included motion correction and eddy current correction, followed by a two-step registration protocol. First, each dMRI or fMRI volume was registered to its own T1 space. A transformation of dMRI or fMRI was then undertaken

to register the individual subject's T1 space to standard MNI space. After preprocessing, FEAT in FSL tools (Linux) was used to extract the activation areas for each of the three tasks. The ExploreDTI (v4.8.6) package in MATLAB 2015b was used to perform tensor fitting for all subjects and establish index maps for FA and MD.

To determine the effectiveness of tDCS upon network activation, particular sites such as the caudate, SSC, globus pallidus GP, putamen, thalamus, and cingulate gyrus, believed to be influenced by TN, were extracted using FEAT in FSL. Both MD and FA were determined at the trigeminal root entry zone (REZ). The number of sensory fibers, speculated to be involved in the pain propagation of TN, were extracted using ExploreDTI and manual ROI insertion. Finally, the method of constraint spherical deconvolution (CSD) was implemented for analysis of high angular resolution of dMRI data and fiber tracking (Leemans et al., 2009; Jeurissen et al., 2010, 2011; Kristo et al., 2013).

Statistical Assessment: Effect of Pain, tDCS Stimulation and Treatment

We assessed the effect of unilateral pain application upon ipsilateral vs. contralateral brain structures with the "Pain" stimulation task alone. This was followed by assessing the sites of activation generated by application of the "Pain + tDCS" task expected to bring about a dynamic suppression of pain induced. The effect of tDCS treatment upon site activation was examined in pre- and posttreatment sessions.

RESULTS

Assessment of Treatment Efficacy

Repeated measurement analysis showed no differences between groups with cathodic and anodic stimulations for HDI (F test = 0.237, $P = 0.6$) and NPRS (F test = 0.14, $P = 0.7$). Conversely, significant differences for HDI (F test = 190.125, $P < 0.001$) and NRS (F test = 224.733, $P < 0.001$) (**Figure 1** and **Supplementary Table 2**) were found between pre- and postintervention.

Assessment of Unilateral Pain Upon Activation of Brain Structures

A significantly greater activation was found with anodic tDCS, after Bonferroni adjustment, of the caudate and SSC within the ipsilateral pain zone compared to that of the contralateral side as determined in the pretreatment session. No significant difference was identified, otherwise, in any other brain structure in the posttreatment session.

Assessment of Pain Suppression Effects of tDCS Upon Brain Structures

Concurrent application of tDCS stimulation during the "Pain task" ("tDCS + Pain") in the pretreatment session significantly reduced activation in both ipsilateral and contralateral caudate and ipsilateral SSC in cases of anodic tDCS treatment. The same occurred in both ipsilateral and contralateral thalamus in cases treated by cathodic tDCS treatment. There was no significant difference between "Pain" and "Pain + tDCS" stimulation tasks for these structures during the posttreatment session (**Supplementary Figure 1** and **Supplementary Table 2**). The findings of fMRI correlated with the effectiveness of tDCS of both MC and SSC using anodic and cathodic stimulation, respectively.

Transcranial DCS Application

A significant increase in activation was found within the caudate and putamen bilaterally with anodic stimulation. A similar significant increase in activation was identified in the contralateral caudate, GP, lateral SSC, and in the putamen bilaterally with cathodic stimulation (**Supplementary Figure 1** and **Supplementary Table 2**).

Assessment of Therapeutic Effects of tDCS

Following a course of five tDCS treatments, regardless of stimulation methodology, we observed a significant decrease in activation of the ipsilateral caudate, SSC, GP, and thalamus, and in the contralateral GP during the posttreatment session compared to that of pretreatment. With anodic stimulation, the observed significant decrease from pre- to posttreatment occurred only in the ipsilateral caudate and SSC. On the other hand, cathodic stimulation brought about increased activation in the ipsilateral thalamus. The decrease within the ipsilateral and contralateral GP occurred with both anodic and cathodic applications. These observations prompted investigation of anodic and cathodic cases separately. For cases of anodic stimulation, a significant decrease in activation occurred in the ipsilateral caudate, SSC and GP, and the contralateral GP. With cathodic stimulation, a significant decrease in activation was observed in the contralateral SSC, GP, thalamus, and anterior cingulate gyrus (ACG), and the ipsilateral GP and thalamus in the posttreatment compared to the pretreatment situation (**Supplementary Figure 1** and **Supplementary Table 4**).

The dMRI analysis showed a substantial increase (>50%) in the number of contralateral sensory fibers in the spinothalamocortical sensory tract (STCT) following the complete course of tDCS stimulation in three of the six patients (**Supplementary Figures 2A,B**). A significant reduction in fractional anisotropy (FA) (>40%) was observed in the ipsilateral trigeminal REZ, after Bonferroni adjustment, in the posttreatment phase compared to pretreatment in five of the six patients (**Supplementary Figure 3**). Three patients showed a substantial increase (>32%) while a single case was found to have a relatively minor decrease (13%) in FA within the contralateral REZ in the posttreatment phase (**Supplementary Figure 3**). A reduction in mean diffusivity (MD) (>12%) within the contralateral REZ in the posttreatment phase was a consistent finding across all patients (**Supplementary Figure 4**).

DISCUSSION

The concurrent application of anodic tDCS and a relevant pain stimulus significantly attenuates activation in both the ipsilateral

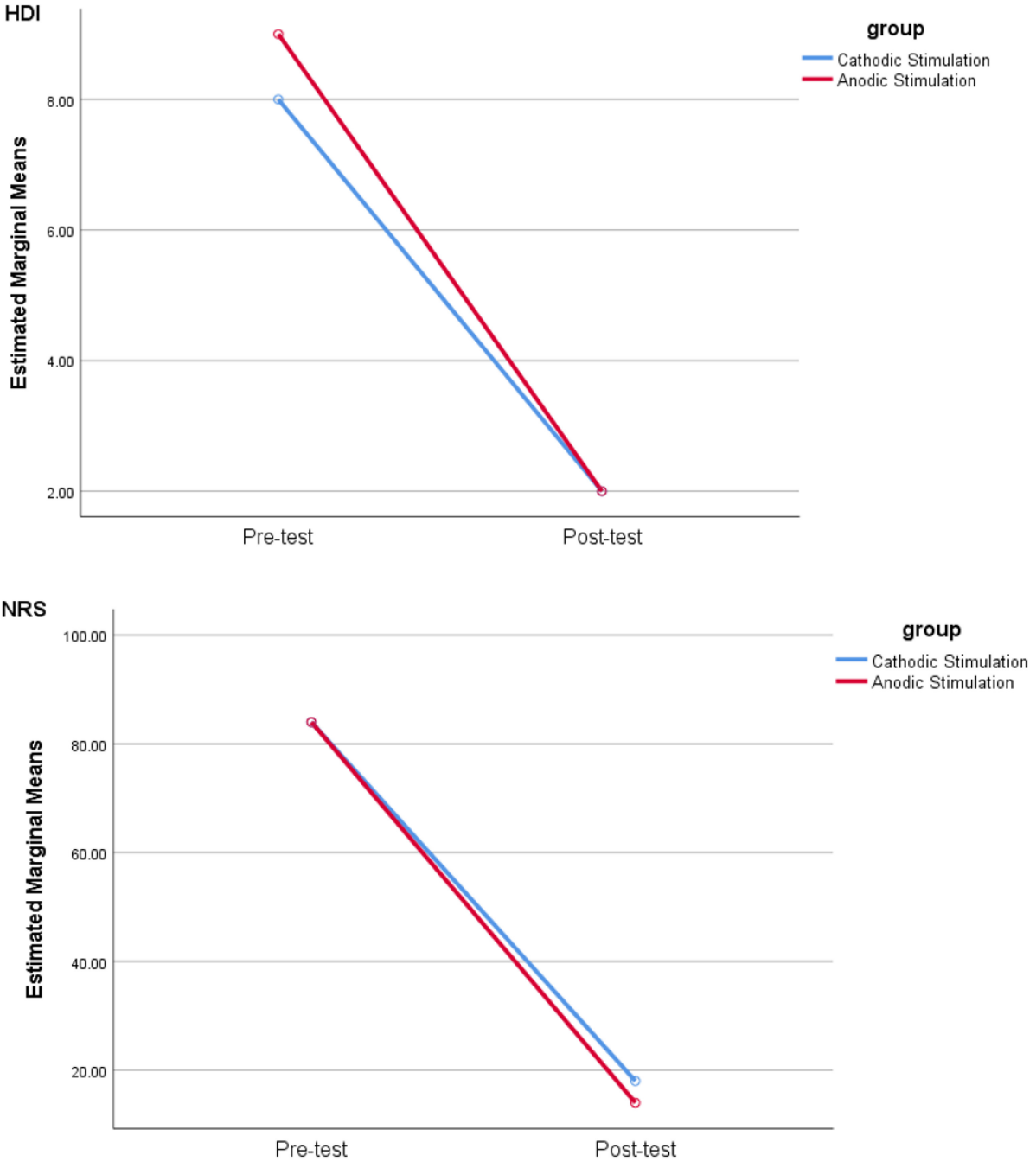

FIGURE 1 | Comparison of HDI and NRS scores in pre- and postsessions by cathodic and anodic stimulation. Note that NRS is used to quantify the severity of pain stipulating "0" as no pain and "10" as the greatest imaginable pain, while HDI provides a score for the level of disability suffered with TN.

and contralateral caudate and the ipsilateral SSC. Likewise, following a course of anodic tDCS, the ipsilateral caudate, GP and SSC and the contralateral GP showed a significantly attenuated activation as assessed by the "Pain" stimulation task. Stimulation rendered within the TN pain zone revealed an area of activation within the ipsilateral caudate and SSC that was significantly greater when compared to the contralateral side. This difference disappeared following a course of anodic tDCS treatment. Concurrent application of cathodic tDCS and pain stimulation significantly reduced activation in both ipsilateral and contralateral thalamus. After a course of cathodic tDCS treatment, a significant decrease with the "Pain" stimulation task was identified in the thalamus and GP bilaterally, and the SSC and ACG contralaterally.

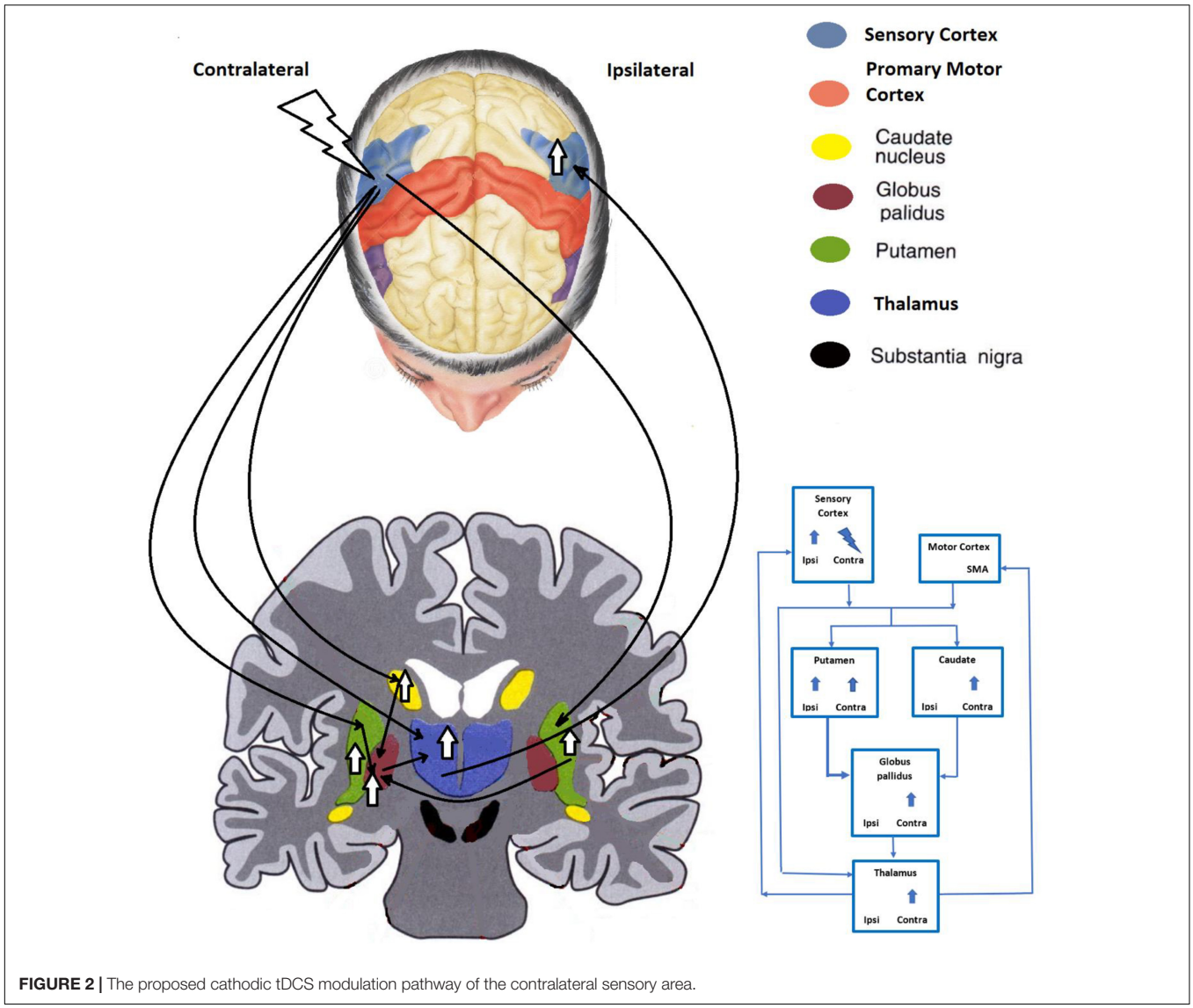

FIGURE 2 | The proposed cathodic tDCS modulation pathway of the contralateral sensory area.

Findings in the current study are consistent with prior formulations of a pain neuromatrix (Moissetl et al., 2011). The remarkable feature here, however, was the significant success achieved with both cathodic and anodic tDCS in relieving pain. The functional outcomes achieved with activation of different sets of anatomical elements by each of the two neuromodulatory applications implicate different mechanisms in achieving the same effect.

FMRI Findings: Cathodic tDCS Stimulation

Cathodic tDCS of the SSC alters activity within the ipsilateral SSC, the contralateral caudate, GP and thalamus and the putamen bilaterally (**Figure 2**). A proposed pathway makes use of the GP-thalamus-cerebral cortex circuit previously described (Alexander et al., 1986). Unilateral cutaneous stimulation activates the SSC bilaterally[35], although the effect is more contralateral. Application of tDCS tends to equalize the activation. After a course of treatment, the pain score during pain induction is reduced significantly, along with a reduced activation of the GP and thalamus bilaterally, and the contralateral SSC and ACG (Rainville et al., 1997; Yesudas and Lee, 2015).

The cathodic tDCS course of treatment resulted in greater contralateral thalamic activation compared to pretreatment acquisition. With pain induction, the thalamus bilaterally was shown to manifest less activation. Such relative hypoactivity would be interpreted subjectively as a reduced sense of pain. The final outcome could be attributable to a conveyance of lesser input to the sensorimotor cortex. Transcranial DCS alone increased bilateral putamenal activation in both phases, more significantly on the ipsilateral side. The subjective perception of pain has been shown to be influenced by putamenal activation with a functional connection identified between it and the sensorimotor area (Starr et al., 2011). An animal model has also shown activation of striatal dopamine receptors to be effective in suppressing

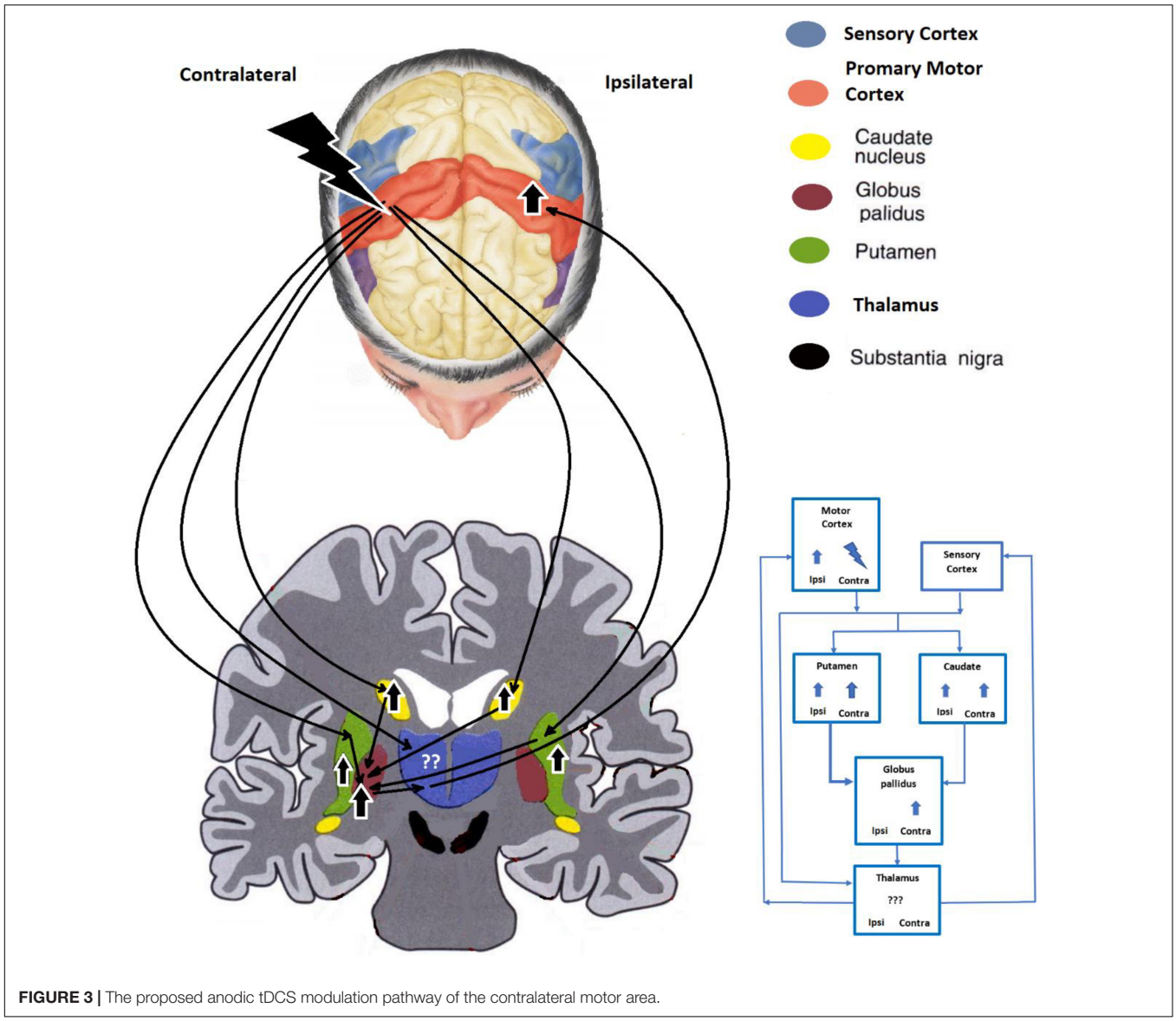

FIGURE 3 | The proposed anodic tDCS modulation pathway of the contralateral motor area.

induced pain (Lin et al., 1981; Magnusson and Fisher, 2000). In this regard, patients with Parkinson's disease have been presumed to have greater susceptibility toward pain because of the progressive loss of nigrostriatal dopaminergic neurons (Defazio et al., 2008; Cheon et al., 2009). Altogether, these studies support the important role of striatal dopamine in processing pain. Hence, cathodic tDCS of the contralateral SSC may exert its mitigation of pain through the activation of the putamen.

fMRI Findings: Anodic tDCS Stimulation

In cases undergoing anodic tDCS stimulation of the contralateral MC, activation of the caudate and putamen bilaterally and the contralateral GP ostensibly brought about a pain suppressive effect. The net pain-relieving effect was reflected in the ipsilateral SSC and caudate and GP bilaterally in the posttreatment phase (**Figure 3**).

Prior to application of the treatment protocol, anodic stimulation of the MC with simultaneous pain induction showed both caudate nuclei to be activated much less than by pain induction alone. Following treatment, pain delivery resulted in less activation of the caudate ipsilaterally than during the pretreatment phase along with a corresponding subjective relief of pain. Suppression of the caudate and the resultant suppression of the thalamus again would bring about the same pain mitigation as with cathodic tDCS stimulation.

In a previous study, painful electrical stimulation accompanied by a suppression task in the early phase of stimulation (i.e., initial 13 s) resulted in bilateral caudate activation while in the late phase (i.e., after 39 s) caudate activation was reduced significantly (Wunderlich et al., 2011). The authors interpreted the activation in the early phase as a feature of the pain-suppression task or an effort required to suppress the pain. Another study using painful thermal

stimulation accompanied by a suppression task resulted in bilateral caudate activation in the early phase of pain suppression while activation of the prefrontal cortex was identified in the late phase. Here, the caudate was implicated in the initiation of pain suppression and the prefrontal cortex in its maintenance (Freund et al., 2009).

Caudate activation by tDCS is consistent with these findings. The subsequent reduced activation of the caudate after anodic tDCS treatment coincides with the sustained subjective relief of pain in our cases. Caudate suppression and its putative disinhibition of the thalamus (Chevalier and Deniau, 1990) would ultimately bring about a reduction of SSC activity. Putamenal activation is known to have a similar effect (Lin et al., 1981; Magnusson and Fisher, 2000; Starr et al., 2011). Likewise, activation of the GP in the same manner would influence thalamocortical activity resulting in the same outcome.

dMRI Findings

Reduced FA within the ipsilateral and reduced MD within the contralateral trigeminal root entry zone following a course of tDCS in the majority of patients suggests an induced neuroplasticity coinciding with pain relief. This partly supports but also contrasts with findings of a previous study that investigated structural changes in TN after decompression surgery which showed reduction in FA and an increase in MD at the affected trigeminal REZ (Zhang et al., 2018) and may point to differences in effect brought about by cerebrocortical neuromodulation (Jürgens, 1984). The quantity of fibers within the STCT was also substantially increased indicating a more widespread effect. In another study, episodic central pain was evaluated in a patient with multiple sclerosis and demonstrated an abnormal unilateral temporary FA increase in the thalamus contralateral to the affected body side and normal values pre- and postepisodic pain (Attal et al., 2016). This finding implies the increase of directional uniformity of the water diffusion in the thalamus, perhaps due to the participation and integration of more fiber tracts during the pain which is comparable with our findings in the ipsilateral trigeminal nerve pre- and post-tDCS intervention. The increased sensory fiber number in the STCT does raise support for the notion that cerebrocortical reinnervation may play a significant role in mitigating the symptoms of TN.

Limitations

Limitations of this study include the absence of a control group and determination of a placebo effect related to the application of tDCS. Although the imaging features accompanying the positive findings in the study remain compelling, the sample size is insufficient to declare efficacy and further study of the effect with a larger patient population is required. A fatigue aspect in the study may have affected a number of patients and contributed to a desire for completion of the study prematurely resulting in a bias toward a favorable effect. In addition to a larger sample size of randomized patients treated with cathodal and anodal tDCS (e.g., $N = 12$), a separate cohort undergoing sham treatment is advisable to evaluate any placebo effects.

Patients in the current study were not subject to any recent changes in medical therapy and served as their own control. Nevertheless, future study must also exclude any mitigation of the therapeutic effect by psychological comorbidity or the effect of any medical treatment.

DATA AVAILABILITY STATEMENT

The raw data supporting the conclusions of this article will be made available by the authors, without undue reservation.

ETHICS STATEMENT

The studies involving human participants were reviewed and approved by Tehran University of Medical Sciences, Ethical Board. The patients/participants provided their written informed consent to participate in this study.

AUTHOR CONTRIBUTIONS

BB contributed in proposing the research idea, providing the research funding, and writing the manuscript's Introduction. NT contributed in designing and carrying out the research, supervising the data processing, neuroscience modeling, and writing the manuscript's Discussion. KE contributed in data interpretation and revising and finalizing the manuscript. NS contributed in carrying out the fMRI task and tDCS treatments on the patients in therapeutic sessions. MB contributed in carrying out the MRI data acquisition. FE and NM contributed in functional MRI data analysis. ZK and AT contributed in proposing the research idea and patient recruitment. M-RN-Z contributed in conducting the research, supervising the data acquisition and processing, and writing the manuscript's Summary, Methods, and Results. All authors contributed to the article and approved the submitted version.

FUNDING

This work was partially granted and funded by the Brain and Spinal Cord Injury Research Centre, Neuroscience Institute, Tehran University of Medical Sciences (Project No. 97-02-85-39457).

ACKNOWLEDGMENTS

We acknowledge the contribution of the National Brain Mapping Lab (NBML) toward MRI data acquisition and brain stimulation during imaging and treatment sessions.

SUPPLEMENTARY MATERIAL

The Supplementary Material for this article can be found online at: https://www.frontiersin.org/articles/10.3389/fnhum.2022.848347/full#supplementary-material

REFERENCES

Alexander, G. E., DeLong, M. R., and Strick, P. L. (1986). Parallel organization of functionally segregated circuits linking basal ganglia and cortex. *Annu. Rev. Neurosci.* 9, 357–381.

Attal, N., Ayache, S. S., De Andrade, D. C., Mhalla, A., Baudic, S., Jazat, F., et al. (2016). Repetitive transcranial magnetic stimulation and transcranial direct-current stimulation in neuropathic pain due to radiculopathy: a randomized sham-controlled comparative study. *Pain* 157, 1224–1231. doi: 10.1097/j.pain.0000000000000510

Becerra, L., Harris, W., Joseph, D., Huppert, T., Boas, D. A., and Borsook, D. (2008). Diffuse optical tomography of pain and tactile stimulation: activation in cortical sensory and emotional systems. *Neuroimage* 41, 252–259. doi: 10.1016/j.neuroimage.2008.01.047

Bosch-Bouju, C., Hyland, B. I., and Parr-Brownlie, L. C. (2013). Motor thalamus integration of cortical, cerebellar and basal ganglia information: implications for normal and parkinsonian conditions. *Front. Comput. Neurosci.* 7:163. doi: 10.3389/fncom.2013.00163

Cheon, S.-M., Park, M. J., Kim, W.-J., and Kim, J. W. (2009). Non-motor off symptoms in Parkinson's disease. *J. Korean Med. Sci.* 24, 311–314.

Cheshire, W. P. (2007). Trigeminal neuralgia: for one nerve a multitude of treatments. *Expert Rev. Neurother.* 7, 1565–1579. doi: 10.1586/14737175.7.11.1565

Cheshire, W. P. Jr. (2015). Cranial neuralgias. *Continuum.* 21, 1072–1085.

Chevalier, G., and Deniau, J. (1982). Inhibitory nigral influence on cerebellar evoked responses in the rat ventromedial thalamic nucleus. *Exp. Brain Res.* 48, 369–376. doi: 10.1007/BF00238613

Chevalier, G., and Deniau, J. (1990). Disinhibition as a basic process in the expression of striatal functions. *Trends Neurosci.* 13, 277–280.

De Toledo, I. P., Réus, J. C., Fernandes, M., Porporatti, A. L., Peres, M. A., Takaschima, A., et al. (2016). Prevalence of trigeminal neuralgia: a systematic review. *J. Am. Dent. Assoc.* 147, 570–576.e2.

Defazio, G., Berardelli, A., Fabbrini, G., Martino, D., Fincati, E., Fiaschi, A., et al. (2008). Pain as a nonmotor symptom of Parkinson disease: evidence from a case-control study. *Arch. Neurol.* 65, 1191–1194. doi: 10.1001/archneurol.2008.2

Devor, M., Amir, R., and Rappaport, Z. H. (2002). Pathophysiology of trigeminal neuralgia: the ignition hypothesis. *Clin. J. Pain* 18, 4–13. doi: 10.1097/00002508-200201000-00002

Duff, J., Spinner, R., Lindor, N. M., Dodick, D. W., and Atkinson, J. L. (1999). Familial trigeminal neuralgia and contralateral hemifacial spasm. *Neurology* 53, 216–218. doi: 10.1212/wnl.53.1.216

Ebner, F. H., Tatagiba, M., and Roser, F. (2010). Familial trigeminal neuralgia—Microsurgical experience and psychological observations. *Acta neurochir.* 152:381. doi: 10.1007/s00701-009-0413-3

El, H. O., Moutaouakil, F., Fadel, H., and Slassi, I. (2008). Familial trigeminal neuralgia. *Revue Neurol.* 164, 384–387.

Ervin, F., Brown, C., and Mark, V. (1966). Striatal influence on facial pain. *Stereotactic Funct. Neurosurg.* 27, 75–90. doi: 10.1159/000103936

Ettlin, D. A. (2013). The international classification of headache disorders, (beta version). *Cephalalgia* 33, 629–808.

Ferreira, N. R., Junqueira, Y. N., Corrêa, N. B., Fonseca, E. O., Brito, N. B., Menezes, T. A., et al. (2019). The efficacy of transcranial direct current stimulation and transcranial magnetic stimulation for chronic orofacial pain: a systematic review. *PloS one* 14:e0221110. doi: 10.1371/journal.pone.0221110

Fleetwood, I. G., Innes, A. M., Hansen, S. R., and Steinberg, G. K. (2001). Familial trigeminal neuralgia: case report and review of the literature. *J. Neurosurg.* 95, 513–517.

Freund, W., Klug, R., Weber, F., Stuber, G., Schmitz, B., and Wunderlich, A. (2009). Perception and suppression of thermally induced pain: a fMRI study. *Somatosens. Motor Res.* 26, 1–10. doi: 10.1080/08990220902738243

Groh, A., Bokor, H., Mease, R. A., Plattner, V. M., Hangya, B., Stroh, A., et al. (2014). Convergence of cortical and sensory driver inputs on single thalamocortical cells. *Cereb. Cortex* 24, 3167–3179. doi: 10.1093/cercor/bht173

Gupta, V., Singh, A., Kumar, S., and Sinha, S. (2002). Familial trigeminal neuralgia. *Neurol. India* 50:87.

Hagenacker, T., Bude, V., Naegel, S., Holle, D., Katsarava, Z., Diener, H.-C., et al. (2014). Patient-conducted anodal transcranial direct current stimulation of the motor cortex alleviates pain in trigeminal neuralgia. *J. Headache Pain* 15:78. doi: 10.1186/1129-2377-15-78

Hall, G. C., Carroll, D., Parry, D., and McQuay, H. J. (2006). Epidemiology and treatment of neuropathic pain: the UK primary care perspective. *Pain* 122, 156–162. doi: 10.1016/j.pain.2006.01.030

Hansen, N., Obermann, M., Poitz, F., Holle, D., Diener, H.-C., Antal, A., et al. (2011). Modulation of human trigeminal and extracranial nociceptive processing by transcranial direct current stimulation of the motor cortex. *Cephalalgia* 31, 661–670. doi: 10.1177/0333102410390394

Hemminki, K., Li, X., and Sundquist, K. (2007). Familial risks for nerve, nerve root and plexus disorders in siblings based on hospitalisations in Sweden. *J. Epidemiol. Commun. Health* 61, 80–84. doi: 10.1136/jech.2006.046615

Jacobson, G. P., Ramadan, N. M., Aggarwal, S. K., and Newman, C. W. (1994). The Henry Ford hospital headache disability inventory (HDI). *Neurology* 44, 837–842.

Jeurissen, B., Leemans, A., Jones, D. K., Tournier, J. D., and Sijbers, J. (2011). Probabilistic fiber tracking using the residual bootstrap with constrained spherical deconvolution. *Hum. Brain Mapp.* 32, 461–479. doi: 10.1002/hbm.21032

Jeurissen, B., Leemans, A., Tournier, J., Jones, D., and Sijbers, J. (eds) (2010). "Estimating the number of fiber orientations in diffusion MRI voxels: a constrained spherical deconvolution study," in *Proceedings of the International Society of Magnetic Resonance Medicine*, Stockholm.

Jürgens, U. (1984). The efferent and afferent connections of the supplementary motor area. *Brain Res.* 300, 63–81. doi: 10.1016/0006-8993(84)91341-6

Kristo, G., Leemans, A., Raemaekers, M., Rutten, G. J., de Gelder, B., and Ramsey, N. F. (2013). Reliability of two clinically relevant fiber pathways reconstructed with constrained spherical deconvolution. *Magn. Reson. Med.* 70, 1544–1556. doi: 10.1002/mrm.24602

Leemans, A., Jeurissen, B., Sijbers, J., and Jones, D. (eds) (2009). "ExploreDTI: a graphical toolbox for processing, analyzing, and visualizing diffusion MR data," in *Proceedings of the 17th Annual Meeting of International Society of Magnetic Resonance Medicine*, Hawaii.

Liao, C. C., and Yen, C. T. (2008). Functional connectivity of the secondary somatosensory cortex of the rat. *Anat. Rec.* 291, 960–973. doi: 10.1002/ar.20696

Lin, M., Wu, J., Chandra, A., and Tsay, B. (1981). Activation of striatal dopamine receptors induces pain inhibition in rats. *J. Neural Transm.* 51, 213–222. doi: 10.1007/BF01248953

Lineberry, C., and Vierck, C. (1975). Attenuation of pain reactivity by caudate nucleus stimulation in monkeys. *Brain Res.* 98, 119–134. doi: 10.1016/0006-8993(75)90513-2

Magnusson, J. E., and Fisher, K. (2000). The involvement of dopamine in nociception: the role of D1 and D2 receptors in the dorsolateral striatum. *Brain Res.* 855, 260–266. doi: 10.1016/s0006-8993(99)02396-3

Moissetl, X., Villainl, N., Ducreuxl, D., Serriel, A., Cuninl, G., Valadel, D., et al. (2011). Functional brain imaging of trigeminal neuralgia. *Eur. J. Pain* 15, 124–131.

Morra, M. E., Elgebaly, A., Elmaraezy, A., Khalil, A. M., Altibi, A. M., Vu, T. L.-H., et al. (2016). Therapeutic efficacy and safety of botulinum toxin A therapy in trigeminal neuralgia: a systematic review and meta-analysis of randomized controlled trials. *J. Headache Pain.* 17:63. doi: 10.1186/s10194-016-0651-8

Olesen, J., Bes, A., Kunkel, R., Lance, J. W., Nappi, G., Pfaffenrath, V., et al. (2013). The international classification of headache disorders, (beta version). *Cephalalgia* 33, 629–808.

Pollack, I. F., Jannetta, P. J., and Bissonette, D. J. (1988). Bilateral trigeminal neuralgia: a 14-year experience with microvascular decompression. *J. Neurosurg.* 68, 559–565. doi: 10.3171/jns.1988.68.4.0559

Rainville, P., Duncan, G. H., Price, D. D., Carrier, B., and Bushnell, M. C. (1997). Pain affect encoded in human anterior cingulate but not somatosensory cortex. *Science* 277, 968–971. doi: 10.1126/science.277.5328.968

Sherman, S. M., and Guillery, R. (2011). Distinct functions for direct and transthalamic corticocortical connections. *J. Neurophysiol.* 106, 1068–1077. doi: 10.1152/jn.00429.2011

Sivakanthan, S., Van Gompel, J. J., Alikhani, P., Van Loveren, H., Chen, R., and Agazzi, S. (2014). Surgical management of trigeminal neuralgia: use and cost-effectiveness from an analysis of the medicare claims database. *Neurosurgery* 75, 220–226.

Smyth, P., Greenough, G., and Stommel, E. (2003). Familial trigeminal neuralgia: case reports and review of the literature. *Headache* 43, 910–915. doi: 10.1046/j.1526-4610.2003.03172.x

Starr, C. J., Sawaki, L., Wittenberg, G. F., Burdette, J. H., Oshiro, Y., Quevedo, A. S., et al. (2011). The contribution of the putamen to sensory aspects of pain: insights from structural connectivity and brain lesions. *Brain* 134, 1987–2004. doi: 10.1093/brain/awr117

Stilling, J. M., Monchi, O., Amoozegar, F., and Debert, C. T. (2019). Transcranial magnetic and direct current stimulation (TMS/tDCS) for the treatment of headache: a systematic review. *Headache* 59, 339–357. doi: 10.1111/head.13479

Ueki, A., Uno, M., Anderson, M., and Yoshida, M. (1977). Monosynaptic inhibition of thalamic neurons produced by stimulation of the substantia nigra. *Experientia* 33, 1480–1482. doi: 10.1007/BF01918820

Uno, M., Ozawa, N., and Yoshida, M. (1978). The mode of pallido-thalamic transmission investigated with intracellular recording from cat thalamus. *Exp. Brain Res.* 33, 493–507. doi: 10.1007/BF00235570

Veinante, P., Jacquin, M. F., and Deschênes, M. (2000). Thalamic projections from the whisker−sensitive regions of the spinal trigeminal complex in the rat. *J. Comp. Neurol.* 420, 233–243. doi: 10.1002/(sici)1096-9861(20000501)420:2<233::aid-cne6>3.0.co;2-t

Wunderlich, A. P., Klug, R., Stuber, G., Landwehrmeyer, B., Weber, F., and Freund, W. (2011). Caudate nucleus and insular activation during a pain suppression paradigm comparing thermal and electrical stimulation. *Open Neuroimag. J.* 5:1–8. doi: 10.2174/1874440001105010001

Yam, M. F., Loh, Y. C., Tan, C. S., Khadijah Adam, S., Abdul Manan, N., and Basir, R. (2018). General pathways of pain sensation and the major neurotransmitters involved in pain regulation. *Int. J. Mol. Sci.* 19:2164. doi: 10.3390/ijms19082164

Yamamoto, T., Hassler, R., Huber, C., Wagner, A., and Sasaki, K. (1983). Electrophysiologic studies on the pallido-and cerebellothalamic projections in squirrel monkeys (Saimiri sciureus). *Exp. Brain Res.* 51, 77–87. doi: 10.1007/BF00236805

Yesudas, E. H., and Lee, T. (2015). The role of cingulate cortex in vicarious pain. *BioMed. Res. Int.* 2015:719615. doi: 10.1155/2015/719615

Zakrzewska, J. (2001). Consumer views on management of trigeminal neuralgia. *Headache* 41, 369–376. doi: 10.1046/j.1526-4610.2001.111006369.x

Zakrzewska, J. M., and Linskey, M. E. (2014). Trigeminal neuralgia. *BMJ.* 348: g474.

Zhang, Y., Mao, Z., Cui, Z., Ling, Z., Pan, L., Liu, X., et al. (2018). Diffusion tensor imaging of axonal and myelin changes in classical trigeminal neuralgia. *World Neurosurg.* 112, e597–e607. doi: 10.1016/j.wneu.2018.01.095

Conflict of Interest: MB was employed by Intelligent Quantitative Biomedical Imaging L.L.C.

The remaining authors declare that the research was conducted in the absence of any commercial or financial relationships that could be construed as a potential conflict of interest.

Publisher's Note: All claims expressed in this article are solely those of the authors and do not necessarily represent those of their affiliated organizations, or those of the publisher, the editors and the reviewers. Any product that may be evaluated in this article, or claim that may be made by its manufacturer, is not guaranteed or endorsed by the publisher.

frontiers in Human Neuroscience

HYPOTHESIS AND THEORY
published: 31 March 2022
doi: 10.3389/fnhum.2022.837972

Possible Mechanisms Underlying Neurological Post-COVID Symptoms and Neurofeedback as a Potential Therapy

Mária Orendáčová[1] and Eugen Kvašňák[2]*

[1] Department of Medical Biophysics and Medical Informatics, Third Faculty of Medicine, Charles University in Prague, Prague, Czechia, [2] Department of Medical Biophysics and Medical Informatics, Third Faculty of Medicine, Charles University in Prague, Prague, Czechia

Theoretical considerations related to neurological post-COVID complications have become a serious issue in the COVID pandemic. We propose 3 theoretical hypotheses related to neurological post-COVID complications. First, pathophysiological processes responsible for long-term neurological complications caused by COVID-19 might have 2 phases: (1) Phase of acute Sars-CoV-2 infection linked with the pathogenesis responsible for the onset of COVID-19-related neurological complications and (2) the phase of post-acute Sars-CoV-2 infection linked with the pathogenesis responsible for long-lasting persistence of post-COVID neurological problems and/or exacerbation of another neurological pathologies. Second, post-COVID symptoms can be described and investigated from the perspective of dynamical system theory exploiting its fundamental concepts such as system parameters, attractors and criticality. Thirdly, neurofeedback may represent a promising therapy for neurological post-COVID complications. Based on the current knowledge related to neurofeedback and what is already known about neurological complications linked to acute COVID-19 and post-acute COVID-19 conditions, we propose that neurofeedback modalities, such as functional magnetic resonance-based neurofeedback, quantitative EEG-based neurofeedback, Othmer's method of rewarding individual optimal EEG frequency and heart rate variability-based biofeedback, represent a potential therapy for improvement of post-COVID symptoms.

Keywords: post-COVID symptoms, neurological complications, mechanisms, therapy, dynamical system theory, neurofeedback

OPEN ACCESS

Edited by:
Hongming Li,
University of Pennsylvania,
United States

Reviewed by:
Francesco Motolese,
Campus Bio-Medico University, Italy
Thorsten Rudroff,
The University of Iowa, United States

****Correspondence:***
Mária Orendáčová
maria.orendacova@lf3.cuni.cz

Specialty section:
This article was submitted to Brain Imaging and Stimulation, a section of the journal Frontiers in Human Neuroscience

Received: *17 December 2021*
Accepted: *26 January 2022*
Published: *31 March 2022*

Citation:
Orendáčová M and Kvašňák E (2022) Possible Mechanisms Underlying Neurological Post-COVID Symptoms and Neurofeedback as a Potential Therapy. Front. Hum. Neurosci. 16:837972. doi: 10.3389/fnhum.2022.837972

INTRODUCTION

Neurological post-COVID complications include long-term presence of the symptoms such as headache, insomnia, depression, anxiety, dizziness, seizures and mood swings (Asadi-Pooya and Simani, 2020; Caronna et al., 2021; Fernández-De-las-Peñas et al., 2021c; Townsend et al., 2021). They may originate from neural or extra-neural COVID-19-related pathology (Libby and Lüscher, 2020). The prevalence of post-COVID complications ranges from 8 to 47.5% (Fernández-De-las-Peñas et al., 2021d; Kayaaslan et al., 2021; Pilotto et al., 2021) thereby making it likely to be a

public health threat and a formidable challenge for a health care system. Neurological complications associated with COVID-19 may exacerbate either during the acute Sars-CoV-2 infection or during its post-acute phase (Collantes et al., 2021; Delorme et al., 2021; Fernández-De-las-Peñas et al., 2021a,e). In this hypothetical article, we propose that there are several pathological processes responsible for exacerbation and persistence of neurological disturbances in acute and post-acute phase of Sars-CoV-2 infection. We postulate that these mechanisms can take place during acute COVID-19, during post-acute COVID-19 or during the both phases. In the second part of this work, we will try to discuss post-COVID complications from the perspective of dynamical system theory using its underlying concepts such as attractors, system parameters and criticality of system behavior. In the final part of this paper, we will discuss the potential beneficial effects of biofeedback therapy on post-COVID neurological complications.

GENERAL CHARACTERISTICS OF COVID-19-RELATED NEUROLOGICAL SYMPTOMS

COVID-19-related complications include long-term disturbances occurring in nervous, cardio-respiratory, immune, endocrine and gastro-intestinal body systems (Ellul et al., 2020; Dennis et al., 2021; Selvaraj et al., 2021). Some post-COVID symptoms seem to be attributed to the isolated dysfunction of a single body system whereas other symptoms may stem from COVID-19-related dysfunction of multiple body systems. For example, symptoms such as anosmia and ageusia are likely to be caused by isolated dysfunction of nervous system. On the other hand, COVID-19-related fatigue, which is defined as reduction of physical and mental performance due to COVID-19, can be caused by dysfunction of both neural and extra-neural systems (Rudroff et al., 2020; Bilgin et al., 2021; Morgul et al., 2021; Workman et al., 2021). Long-term post-COVID complications occur in COVID-19 survivors regardless their age (Morand et al., 2021) and sex (Blitshteyn and Whitelaw, 2021; Delorme et al., 2021; Fernández-De-las-Peñas et al., 2021b). Female sex was consistently found to be associated with the higher risk of increased probability of exacerbation of long-lasting post-COVID disturbances (Mahmud et al., 2021; Stavem et al., 2021; Thye et al., 2022). The longer recovery period for some post-COVID disturbances such as anosmia and ageusia was observed in women (Meini et al., 2020). Interestingly, some post-COVID complications seem to occur more frequently in men and vice versa, some symptoms are more frequent in women (Meini et al., 2020; Huang et al., 2021; Xiong et al., 2021). For instance, fatigue and myalgia are more common in women (Huang et al., 2021; Stavem et al., 2021; Xiong et al., 2021). On the contrary, anosmia and ageusia were documented to occur more frequently in men (Meini et al., 2020). To the best of our knowledge, it is currently unknown what underlying causes are responsible for these sex differences. Prolonged time for clinical improvement of COVID-19 symptoms and long duration of acute Sars-CoV-2 infection measured by duration of positive RT-PCR test were found to represent risk factors for increased probability of occurrence of long-term post-COVID-19 complications (Mahmud et al., 2021). In addition, some acute COVID-19 symptoms, such as dyspnea (Stavem et al., 2021), chest pain (Walsh-Messinger et al., 2021), fatigue (Mahmud et al., 2021), fever (Mahmud et al., 2021; Walsh-Messinger et al., 2021), headaches (Walsh-Messinger et al., 2021) and olfactory impairment (Walsh-Messinger et al., 2021), were associated with the higher probability of exacerbation of post-COVID complications. In relation to the link between severity of initial acute COVID-19 symptoms and the higher risk of occurrence of post-COVID problems, some studies found the correlation between these two entities (Stavem et al., 2021) whereas other studies did not (Townsend et al., 2020).

In this theoretical work, we will focus on neurological manifestations of COVID-19. Neurological disturbances linked with acute and post-acute period of COVID-19 include disturbances such as dizziness, headaches, epileptic seizures, paresthesia, fatigue, anxiety, depression, sleep disturbances, cognitive dysfunctions and others (Fernández-De-las-Peñas et al., 2021c; Sun et al., 2021). Neurological COVID-19-related disturbances may originate from dysfunctions related to central nervous system (CNS), peripheral nervous system (PNS), autonomous nervous system (ANS), but they may also stem from dysfunctions of extraneural sorgans (Ayat et al., 2021). Since post-COVID-19- symptoms may overlap with the acute COVID-19 symptoms (Mahmud et al., 2021), we postulate that there can be some common mechanism responsible for exacerbation and occurrence of acute and post-acute COVID-19-related disturbances. In the following chapter, we will discuss potential similarities and differences between the pathological processes which may be possibly responsible for neurological complications occurring in acute and post-acute period of COVID-19.

MECHANISMS RESPONSIBLE FOR THE EXACERBATION AND MAINTENANCE OF COVID-19-RELATED NEUROLOGICAL COMPLICATIONS

Acute COVID-19 infection may be accompanied with the neurological complications such as headaches, dizziness, seizures, sleep disturbances, anxiety, depression, alterations of taste and smell etc. (Mao et al., 2020; Najjar et al., 2020; Paterson et al., 2020; Collantes et al., 2021). However, these neurological conditions sometimes persist for a long-term period after acute infection, or alternatively, they may exacerbate and develop with some latency for a longer period following acute infection (Delorme et al., 2021; Fernández-De-las-Peñas et al., 2021a). If there is no other objective explanation for the etiology of neurological complications following COVID-19 and at the same time if they occur/persist for more than 3 months after acute COVID-19 infection, then there are attributed to be direct or indirect result of COVID-19 infection and are termed as post-COVID complications (Fernández-De-las-Peñas et al., 2021e).

There are probably several pathological processes responsible for COVID-19-related neurological problems: direct and indirect damage to CNS associated with Sars-CoV-2, long-term recovery of damaged neural tissue, dysfunction of extraneural tissues, psychological factors and mutual co-occurrence and interference between the multiple COVID-19-related symptoms. We believe that these pathogenetic processes may take place in two phases, namely, during the phase of acute Sars-CoV-2 infection and during its post-acute phase. In this chapter, we will discuss possible differences and similarities between these two phases of the aforementioned pathogenetic processes.

COVID-Related Damage to Neural Tissue

The evidence of the link between COVID-19 and neuronal injury comes from studies which detected elevated serum levels of neurofilament light chain protein, which is the marker of neuronal injury, in mild-to-moderate and moderate-to-severe cases of COVID-19 (Ameres et al., 2020; Kanberg et al., 2020). In relation to COVID-19, damage to neural tissue, responsible for the exacerbation of various neurological disturbances, can manifest as a result of direct and indirect interaction of Sars-CoV-2 with the CNS of the host (Ellul et al., 2020; Mayi et al., 2021; Meinhardt et al., 2021).

Direct Damage to Brain Caused by Sars-Cov-2

In acute COVID-19, as a direct viral entry to CNS, pathways through angiotensin 2 (ACE2) and neuropilin-1 in olfactory epithelium has been strongly considered (Ellul et al., 2020; Lukiw et al., 2020; Meinhardt et al., 2021). This can be supported by findings of the study done by Bryche et al. (2020), in which damaged olfactory epithelium has been associated with Sars-Cov-2 infection (Bryche et al., 2020). Also, hematogenic route has been proposed (Kumar et al., 2020; Bodnar et al., 2021). Several autopsy studies done on the victims of COVID-19 patients found evidences of neurotropism of Sars-CoV-2 as the viral RNA has been detected in a various brain regions such olfactory system, brainstem, cerebellum (Meinhardt et al., 2021) and frontal lobes (Gagliardi et al., 2021). Apart from neurons, Sars-CoV-2 presence was detected in astrocytes as well (Crunfli et al., 2021). It may be important to mention that it is possible that dynamics and replication of Sars-CoV-2 may differ with regard to the particular brain cells. In Crunfli et al. (2021) study, both neurons and astrocytes have been infected but the vast majority of infected cells were represented by astrocytes. Viability of the astrocytes was showed to be reduced (Crunfli et al., 2021). Based on these findings and different roles of neurons and glias, it might be interesting to study whether and how clinical representations of COVID-19-related symptoms differ between those patients with prevalent Sars-CoV-2 infection in neurons and in those in whom Sars-CoV-2 predominantly infected astrocytes. The exact mechanisms of interaction between Sars-CoV-2 and neural host cells and their pathological consequences remain elusive so far. There are some implications that Sars-CoV-2 is capable of alterations of gene expressions since it was found that Sars-CoV-2 presence in frontal lobes is associated with down-regulation of genes connected to hypoxia and up-regulations of hemoglobin genes (Gagliardi et al., 2021).

Not much is known about the long-term presence of Sars-CoV-2 in brain in post-acute period of COVID-19. Positive Sars-CoV-2 presence was documented in cytological samples of olfactory mucosa in the participants with and without anosmia approximately 6 months after the initial Sars-CoV-2 infection (de Melo et al., 2021). Viral load was found to be significantly higher in post-COVID-19 participants with long-lasting or relapsing anosmia than in those with no anosmia (de Melo et al., 2021) which suggests positive association between long-lasting viral presence in brain and neurologic symptoms. Damage to the olfactory neuro-epithel was indirectly proven *via* positive detection of increased caspase-3 signal indicating cell death caused by apoptosis (de Melo et al., 2021). Taking into consideration fact that nasopharyngeal RT-PCR was negative in the participants, it is possible that acute and post-acute phases of Sars-CoV-2 infection, accompanied by the presence of Sars-CoV-2 in the brain, differ with regard to the dynamics of distribution of the virus in the various parts of the organism since acute and sub-acute period of Sars-Cov-2 infection is frequently linked with positive nasopharyngeal positive RT-PCR test (Wang et al., 2020; Zhou et al., 2021).

Damage to Brain Tissue Caused Indirectly by Sars-CoV-2

Neurological symptoms connected to the acute period of Sars-CoV-2 infection can manifest even without the presence of Sars-CoV-2 in the brain tissue (Ellul et al., 2020). One of the possible explanations for this phenomenon may consist in damage to brain tissue caused by indirect effects of Sars-CoV-2 infection. Indirect effect of Sars-CoV-2 infection may include maladaptive-immune response to the infection (Hussman, 2021),thromboembolism (Wichmann et al., 2020), endothelial dysfunction (Libby and Lüscher, 2020), hypoxia and neurotoxic metabolities released from extraneural organs affected by COVID-19 (Wu et al., 2020. All these factors can cause damage to blood-brain barrier, infiltrate to CNS and cause further damage to brain tissues (Chaparro-Huerta et al., 2005; Takagishi et al., 2010; Slevin et al., 2020; Bobermin and Quincozes-Santos, 2021). In acute COVID-19, neural damage is likely to be caused primarily due to direct or indirect interaction of Sars-Cov-2 with the host organism. This may lead to various neurological consequences. Documented post-mortem brain lesions of COVID-19 non-survivors (Coolen et al., 2020) and neural atrophy associated with the presence of neurological complications were documented in acute COVID-19 (Chiu et al., 2021). This may support the hypothesis of occurrence of neurological problems due to damage to brain tissue caused by Sars-CoV-2 infection.

Apart from neurological complications and brain lesions linked with acute COVID-19, neurological complications accompanied by atrophy of a various brain regions were already documented in post-acute period of COVID-19 (Carroll et al., 2020; Douaud et al., 2021). We believe that one of the possible mechanisms responsible for this phenomenon may include secondary damage to neural tissue. Secondary damage to neural tissues can potentially come into play as a consequence of mechanisms responsible for long-term post-COVID

complications. There are probably multiple possible ways of how such secondary damage to neural tissue may arise. For instance, breathing problems such as dyspnea, pulmonary and cardiological pathologies, which occur in post-COVID condition (Goërtz et al., 2020; Zarei et al., 2021) may lead to insufficient distribution of oxygen and/or blood to brain causing hypoxia-related damage to neural tissue. Another possible mechanism may consist in excitotoxic effects of some pro-inflammatory cytokines (Takagishi et al., 2010; Slevin et al., 2020) which may initiate apoptosis in some neural tissues (Chaparro-Huerta et al., 2005). Some post-COVID-19 neurological complications were found to be associated with elevated levels of excitotoxic pro-inflammatory cytokines (Lorkiewicz and Waszkiewicz, 2021; Sun et al., 2021). It is therefore possible that elevated concentrations of these pro-inflammatory cytokines may cause secondary damage to neural tissue which can lead to increasing severity and long-term persistence of the particular existing neurological problems and/or to exacerbations of new neurological pathologies.

We believe that neuroimaging studies done before, during and after acute period of COVID-19 might help to distinguish between primary damage to brain tissue associated to acute COVID-19 and secondary brain damage associated with post-COVID period. Although, both processes can probably overlap in some points, predominance of brain injury in acute COVID-19 might point toward pathogenesis linked with primary damage associated with Sars-CoV-2 infection. On the other hand, the predominance of occurrence of brain injury in Sars-CoV-2 negative COVID-19 survivors in post-acute period might indicate predominance of secondary brain damage linked with post-infectious condition.

Long-Term Recovery of Damaged Neural Tissue

Long-term recovery of direct or indirect damage of neural tissue, associated with Sars-CoV-2 infection was suggested to be one of the possible causes responsible for the persistence of long-term COVID-19 neurological complications (Yong, 2021). The large time window during which the slow recovery of damaged neural tissues takes place, may give rise to a wide spectrum of a various possible pathophysiological processes which may occur and contribute to long-term and complex post-COVID-19 neurological complications. Furthermore, compensatory brain plasticity which may occur in the period of recovery of neural tissues, may sometimes turn into maladaptive plastic processes (Takeuchi and Izumi, 2012). For instance, hypertrophy of the affected brain area (Shaikh et al., 2010) and compensatory neurogenesis (Lu et al., 2020) were proposed to the possible causes responsible for the volume increase of the selected brain regions in post-COVID state (Lu et al., 2020). Due to possible emergence of maladaptive plasticity in the processes of brain recovery and its long-lasting period, compensatory plasticity might represent a risk factor for long-lasting persistence of post-COVID-19 symptoms and/or for exacerbation of secondary neurological complications.

In the connection to the possible link between COVID-19 and occurrence of long-term recovery of damaged neural tissues and compensatory maladaptive plasticity, we postulate that neurological problems originating from the processes linked with long-term neural recovery are more likely to manifest in sub-acute and/or post-acute phase of Sars-CoV-2 infection than in the early phases of the acute infection.

Immune-Mediated Adaptation of Central Nervous System

Neurological complications linked with acute COVID-19 may not be always accompanied by damage to a neural tissue (Solomon et al., 2020). One of the possible explaining mechanisms may consist in adaptation of CNS to ongoing inflammatory processes. In order to differentiate between immune-mediated adaptation of CNS to inflammatory processes and damage to neural tissues caused by excitotoxic influence of maladaptive immune response to Sars-CoV-2, which was mentioned in the previous chapter, we feel that definitions of both are necessary to be mentioned in this section. Damage to neural tissues, caused by excitotoxic influence of maladaptive immune response to Sars-CoV-2, is defined as a pathological process leading to the death of neurons. On the other hand, immune-mediated adaptation of CNS to inflammatory processes is defined as quantitative or qualitative change of activation patterns of neurons caused by their interaction with pro-inflammatory cytokines. Even though these two processes are probably not mutually exclusive, in the following section we would focus solely on our perspective of possible immune-mediated adaptation of CNS to acute and post-acute COVID-19.

During inflammatory condition, such as viral or bacterial infection, there comes to a rapid increase of pro-inflammatory markers such as interleukin 4 (il-4), interleukin 6 (il-6), tumor necrosis factor (TNF) and C reactive protein (CRP) (Slaats et al., 2016). Elevated levels of these cytokines are frequently present in acute COVID-19 (Effenberger et al., 2021). The role of these cytokines seems to consist not only in a successful mobilization of immune system to combat the pathogen, but it also seems to consist in a modulation of CNS functioning with regard to ongoing infectious processes (Felger, 2017). Pro-inflammatory cytokines were found to be capable of affecting regions such as amygdala, insula, cingulate gyrus, prefrontal cortex (PFC) (Felger, 2017). They can propagate into CNS by the following ways: through leak regions in blood brain barrier (BBB), by inducing of activation of cytokine uptake mechanisms in BBB and by activation of afferents of vagal nerve which are capable to relay cytokine signals to relevant brain structures (Felger, 2017). Increased levels of inflammatory markers were found to alter a variety of brain regions, for instance, in chronic fatigue syndrome, elevated concentrations of pro-inflammatory cytokines are associated with reduced activity in reward-related neuronal circuitries (Capuron et al., 2012). On the other hand, elevated levels of il-6 and TNF were coupled with increased activity in amygdala associated with the feelings of a social disconnection and socially threatening images (Inagaki et al., 2012). From the evolutionary point of view, immune-mediated

inhibition of reward systems and increased activation of brain structures responsible for a greater awareness of a potential threats, were proposed to serve as adaptive behavioral adjustment of CNS activity to ongoing infection (Felger, 2017). Its main purpose is thought to consist in decreasing motivation of exploratory behavior and mobility that would prevent from a successful recovery from ongoing infections (Felger, 2017).

In relation to post-acute COVID-19 period, this kind of immune-mediated adaptations of CNS might probably occur as well, for instance, due to the presence of a long-term persistence of SARS-CoV-2 in brain or its presence in some other tissues. Immune-mediated adaptation of CNS to long-term elevations of pro-inflammatory cytokines may possibly also come into play as a result of dysautonomia which can occur in COVID-19 survivors (Barizien et al., 2021; Blitshteyn and Whitelaw, 2021; Goodman et al., 2021). Elevated levels of some pro-inflammatory markers may lead to decreased activity of reward neural circuitry and increased activity in the parts of amygdala responsible for fear-related responses (Felger, 2017). Such alterations in CNS functioning might likely lead to conditions such as permanent anxiety, mood disturbances, insomnia and depression, which are quite a frequent post-COVID problems (Fernández-De-las-Peñas et al., 2021c; Lorkiewicz and Waszkiewicz, 2021; Townsend et al., 2021). This hypothesis might be at least partially supported by the fact that brain structures, which are responsive to cytokine signaling such as insula, amygdala and gyrus cingulate (Felger, 2017) were repeatedly found to exhibit various abnormalities in post-COVID-19 condition (Lu et al., 2020; Guedj et al., 2021a; Morand et al., 2021; Sollini et al., 2021). Also, elevated levels of pro-inflammatory cytokines were found to accompany neuropsychological disturbances such as depression and anxiety (Young et al., 2014; Tang et al., 2018) thereby speaking in favor of the existence of the potential link between post-COVID neurological and psychiatric disturbances and immune-mediated adaption of CNS to COVID-related inflammatory processes. This may be at least partly supported by positive correlation between the level of pro-inflammatory cytokines and severity of post-COVID depression (Lorkiewicz and Waszkiewicz, 2021). Occurrence of lymphadenopathia (Walsh-Messinger et al., 2021) and long-term persistence/repeated occurrence of elevated temperature and fever in post-acute period in COVID survivors (Goërtz et al., 2020), together with positive associations between severity of post-COVID neurological symptoms and elevated levels of pro-inflammatory markers (Lorkiewicz and Waszkiewicz, 2021; Sun et al., 2021) may speak in favor of the role of immune deregulation which may be coupled with immune-mediated adaptation of CNS to inflammatory processes linked with post-acute COVID-19.

However, future research investigating the relation between immune profiles, clinical representations and neuroimaging data is necessary to distinguish between the effects of immune-mediated adaptation to CNS and damage to neural tissue caused by excitotoxic effects of maladaptive immune responses to Sars-CoV-2. Furthermore, it is possible that pathogenesis of COVID-19-related neurological complications caused by immune-mediated processes can differ with regard to sex and age due to age and sex-dependent different patterns of immune responses to acute Sars-CoV-2 infection. In women, there was found a more robust response of T-cells to Sars-CoV-2 infection and worse disease outcome was associated with the higher levels of innate immune cytokines (Takahashi et al., 2020). On the other hand, men were found to display the greater activation of innate immunity and worse disease outcome was associated with poor response of T cells (Takahashi et al., 2020). Poor T-cells were also negatively correlated with the age of the patients (Takahashi et al., 2020). Furthermore, new Sars-CoV-2 variant (mutant S24L), which induces more active responses of immune system to acute Sars-CoV-2 infection in females than in males, has been discovered (Wang et al., 2021). Therefore, it is possible that COVID-19-related neurological complications caused by immune-mediated adaption of CNS and/or immune-mediated damage to neural tissues in acute and/or post-acute phase of COVID-19 may be qualitatively and quantitatively different in females than in males.

COVID-19 Related Malfunctions of Extra-Neural Organs

Apart from COVID-19-related pathological processes taking place in CNS, COVID-19-related alteration of proper functioning of extra-neural tissues and organs might play an important role in exacerbation of neurological disturbances. For instance, endocrine glands producing hormones such as cortisol and sex hormones are heavily integrated in regulation of CNS functioning *via* hypothalamic-pituitary axis (HPA) (Pittman, 2011). Cortisol depletion caused by intense and/or long-term inflammatory processes might serve as an example for extra-neural etiologies of COVID-19-related neurological disturbances. Possibly due to the fear of death and/or neuro-endocrine-immune regulatory processes in acute COVID-19, high concentrations of cortisol levels were documented (Tan et al., 2020). Possibly because of cortisol depletion in acute COVID-19, in post-acute COVID-19 condition, hypocortisolism linked with neurological disturbances, such as inability to concentrate and fatigue, were already reported (Ayat et al., 2021). Possible extraneural etiology of long-term post-COVID neurological symptoms may be at least partially supported by documented long-lasting dysfunctions of one or more organs in COVID-19 survivors (Dennis et al., 2021; Selvaraj et al., 2021). Another example of hypothetical causal link between the injury to extra-neural tissues caused by COVID-19 and neurological problems, might be associated with the cases of COVID-19-related pathophysiological processes in neuromuscular junction. Damage to muscle, which seems to be vulnerable target to Sars-CoV-2 infection (Rudroff et al., 2021) due to sensitivity to some pro-inflammatory markers (Tay et al., 2020) and the presence of ACE2 receptors (Ferrandi et al., 2020), may lead to decreased motor performance resulting in peripheral fatigue (Hunter, 2018; Rudroff et al., 2020). Neural and muscular parts of neuromuscular junction have reciprocal trophic effects on each other (Guth, 1968; Funakoshi et al., 1995). Consequently, muscle dysfunction may cause secondary dysfunction of adjacent neural structures due to the trophic influences of muscle on motor unit (Funakoshi et al., 1995). The lack of muscular trophic factors for motor unit might trigger tertiary dysfunctions of

higher-order adjacent brain systems leading to the exacerbation of central fatigue and/or other neurologic complications.

Psychological Factors

Psychological factors may represent one of the important mechanisms responsible for the exacerbation and/or maintenance of a various neurological COVID-19-related symptoms in acute and post-acute period of COVID-19. In acute COVID-19, depression, fears and social isolation can worsen clinical condition and lead or contribute to exacerbation of a various neurologic and psychiatric conditions, such as anxiety and post-traumatic stress disorder (PTSD) (Fu et al., 2021; Samkaria et al., 2021) and fatigue (Morgul et al., 2021). Psychological stress related to acute COVID-19 is likely to be caused by the fear of death, fear of infecting family and other people and by social isolation due to quarantine.

In relation to post-acute COVID-19 period, psychological factors are also very likely to play an important role in exacerbation of new post-COVID-19 symptoms and/or maintenance or worsening of the actual ones. This notion can be at least partly supported by documented effects of psychological factors such as stress, fears and anxiety on exacerbation of fatigue in recovering COVID-19 survivors (Rudroff et al., 2020). Psychological stress related to post-acute COVID-19 is likely to be present due to multiple causes such as fear of the unknown health consequences of that disease, fear of re-infection and fear of decreased general functioning in daily life due to the reconvalescent period.

Contribution of psychological factors to neurological consequences of COVID-19 can be at least partly supported by the promising outcomes of psychotherapy (Hu et al., 2020; Yang et al., 2020) and positive thinking therapy (Alhempi et al., 2021) which were both demonstrated to be capable of reduction of some physical and psycho-social problems caused by COVID-19. Evidence speaking in favor of the existence of the link between psychological factors and COVID-19-related long-lasting disturbances comes from the study done by Thye et al. (2022). In that study, positive association between pre-existing worsened psychological status and increased risk of exacerbation of long-term post-COVID disturbances was documented (Thye et al., 2022).

Mutual Co-occurrence and Interference Between Multiple Post-COVID-19 Neurological Symptoms

COVID-19-related neurological complications may occur as a single isolated symptom or the co-occurrence of multiple symptoms (Pilotto et al., 2021). Simultaneous co-occurrence of multiple neurological problems might possibly implicate the following two scenarios: (1) multiple neurological complications might have occurred approximately at the same time as a consequence of the COVID-19-related direct or indirect damage to the brain structure/s which is/are naturally responsible for multiple functions. For instance, amygdala, which is responsible for the functions such as emotional regulation (Kim et al., 2011), autonomic regulation (Reisert et al., 2021) and is also involved in olfactory functions (Kevetter and Winans, 1981; Zald and Pardo, 1997; Buchanan et al., 2003), was repeatedly found to exhibit abnormalities in post-COVID-19 condition (Douaud et al., 2021; Guedj et al., 2021a; Morand et al., 2021; Sollini et al., 2021). (2) Secondly, some complications may develop earlier and they may secondarily trigger other ones. That may be one of the possible explanations of why some disturbances linked with COVID-19 occur at the early phases of this infection whereas other problems develop after a longer elapsed time (Delorme et al., 2021; Fernández-De-las-Peñas et al., 2021a). Therefore, co-occurrence and co-interaction of multiple co-morbidities may lead to exacerbation of new co-morbidities and/or long-lasting maintenance of them. For instance, dizziness, migraines and anxiety found in post- COVID patients were found to precede the later development of seizures (Park et al., 2021). In another study, the severity of headaches in acute COVID-19 infection was positively associated with the severity level of post-COVID-19 fatigue and headaches (Fernández-De-las-Peñas et al., 2021b). There are some studies finding a positive correlation between some post-COVID-19 neurological problems, such as between fatigue and anxiety (Townsend et al., 2021), fatigue and anhedonia (El Sayed et al., 2021). These findings may implicate some kind of interdependency between these post-COVID-19 complications. This hypothesis may be at least partially supported by the fact that some neurological complications are likely to co-occur, for instance, depression, fatigue and pain are frequently present in people suffering from chronic fatigue syndrome (Komaroff and Lipkin, 2021) and from multiple sclerosis (Workman et al., 2020). The severity of these symptoms may be cross-correlated with each other (Bould et al., 2013). Such co-occurrence of some particular neurological complications in a various pathological conditions may speak in favor of their casual interrelatedness irrespective of their etiology. For instance, the positive correlation between the level of fatigue and the level of anxiety found in post-COVID-19 condition (Townsend et al., 2021) may indicate that the level of fatigue is casually dependent on the level of anxiety and vice versa. In other words, anxiety may generate fatigue due to permanent anxiety-related hyperarousal and conversely, a permanent fatigue may represent a source of anxiety as fatigued individuals may feel anxious of finding the way of overcoming their burden of fatigue.

Based on these findings, it can be postulated that mutual co-occurrence and interference between multiple COVID-19 related symptoms can be responsible for the exacerbation and/or maintenance of another disturbances during both, acute and post-acute period of COVID-19.

It can be seen that our proposed factors possibly responsible for exacerbation and long-term persistence of COVID-19-related neurological conditions are likely to overlap with each other and they can probably co-exist together. Also, it is necessary to bear in mind that there are probably no strict boundaries between damages to CNS caused by Sars-CoV-2, long-term recovery of damaged neural tissues, immune-mediated adaption of CNS to inflammatory state, COVID-19-related damage to extraneural tissues, psychological factors and co-interaction and mutual interference between multiple post-COVID symptoms. For that

TABLE 1 | Summarization of possible manifestations of pathophysiological mechanisms responsible for occurrence of COVID-19-related neurological problems in relation to acute and post-acute phase of Sars-CoV-2 infection.

Possible pathophysiological mechanisms responsible for occurrence of COVID-19-related neurological problems	Possible manifestation of the particular pathophysiological mechanism in ACUTE Sars-CoV-2 infection	Possible manifestation of the particular pathophysiological mechanism in POST-ACUTE Sars-CoV-2 infection
1. Direct damage of Sars-CoV-2 to neural tissue	Yes	Yes
2. Indirect damage of Sars-CoV-2 to neural tissue	Yes	Yes
3. Long-term recovery of damaged neural tissues	It probably does not manifest in the early phases of the acute infection. Rather, it is likely to start to manifest in its later phases (sub-acute phase)	Yes
4. COVID-19-related dysfunction of extraneural tissue	Yes	Yes
5. Psychological factors	Yes	Yes
6. Mutual co-occurrence and interference between multiple post-COVID-19 neurological symptoms	Yes	Yes

reason, our proposed classification of these factors is likely to be a simplification and approximation of the reality.

To summarize this chapter, the following **Table 1** is supposed to summarize all 6 aforementioned proposed pathophysiological mechanisms responsible for COVID-19-related neurological problems in relation to acute and post-acute phase of Sars-CoV-2 infection.

POST-COVID-19 NEUROLOGICAL COMPLICATIONS FROM THE PERSPECTIVE OF DYNAMIC SYSTEM THEORY

Investigation of the link between behavior of biological organisms and dynamic system theory has recently become a widely investigated topic of interest (Ros et al., 2014; Zimmern, 2020; Burrows et al., 2021; Nemzer et al., 2021). Its outcomes bring many valuable papers integrating concepts from neuroscience, physics and information theory (Stam, 2005). Based on the current knowledge related to post-COVID-19 neurological complications and system's behavior, we speculate that post-COVID-19 complications may be understood and viewed as a consequence of deregulation and/or disruption of system parameters and emergence of maladaptive attractors turning brain into operating out of its critical regime.

First of all, it is necessary to define the basic terms from dynamic system theory such as system parameters, attractors and criticality.

System Parameters

System parameters refer to the term of system attributes whose values determine system's behavior (Stam, 2005). For instance, physical quantities such as temperature, volume and pressure are examples of system parameter. The modulation of the system parameters values cause changes in system's behavior (Hesse and Gross, 2014). Analogically, biological systems possess an enormous number of hormones, enzymes, neurotransmitters and cytokines which all can be viewed as system parameters as alterations in their concentrations and/or activity will cause significant changes in the behavior of the organism. For example, gamma-aminobutyric acid (GABA) represents the major inhibitory neurotransmitter in CNS. It participates in a variety of functions such as regulation of sleep (Watanabe et al., 2002), seizure prevention (Möhler, 2006) and others (Möhler, 2006; Hepsomali et al., 2020). Pathological enhancement of GABAergic activity can cause abnormal somnolence (Trotti et al., 2015) whereas over-reduction of GABA levels and/or its receptors can cause exacerbation of epileptic seizures (Schiene et al., 1996). In relation to post-COVID-19 problems, post-COVID-19 central fatigue was proposed to stem from COVID-19-related alterations of the levels of neurotransmitters such as serotonine and dopamine (Rudroff et al., 2020). Although, to the best of our knowledge, the relationship between the levels of neurotransmitters and post-COVID-19 disturbances has not been investigated yet, it is possible that neurotransmitters and their levels might represent important system parameters involved in determination of various post-COVID-19 symptoms and their dynamics. Based on the findings from the studies dedicated to the investigation of post-COVID-19 complications, we postulate that post-COVID-19 complications may portray manifestations of pathological alterations of system parameters, emergence of new pathological attractors which are responsible for disruption of homeostasis and consequent disability to operate in/near the critical point of the system. In relation to acute COVID-19 and post-COVID-19 condition, levels of inflammatory cytokines and leukocytes seem to represent important system parameters influencing the system's behavior. Increased pro-inflammatory cytokines and altered levels of leukocytes plus levels of lymphopenia were associated with increased risk of exacerbation of COVID-related neurological complications (Sun et al., 2021) and with higher severity of them (Sun et al., 2021; Visvabharathy et al., 2021). Immunotherapy has been found to be effective in normalizing immune profile and improvement of post-COVID neurological pathological conditions (Carroll et al., 2020; Sangare et al., 2020). It is currently unknown how many cytokines, enzymes, neurotransmitters and hormones are directly or indirectly affected by COVID-19 and how such alterations in the levels of these system parameters and their activity would manifest in acute and post-acute phase of COVID-19.

Attractors

When the change of system parameters is very rapid and/or intense, new attractors may emerge (Stam, 2005). Attractor of the system represents the most probable state which the system has the greatest tendency to evolve to Stam (2005). According to thermodynamics laws, each system has a tendency to evolve into the state requiring the minimal energy cost (Haddad, 2013). Within the reign of living organisms, the ideal state, which biosystems try to evolve to, should meet these two following conditions: (1) there should be the minimal energy cost and (2) it should be the most efficient for a proper functioning of the whole system (Johnson, 1992).

New pathological attractors, emerging from COVID-19-related structural and functional abnormalities documented in a various brain regions, might be responsible for making brain to turn into conditions of post-COVID-19 complications such as seizures, dizziness, headaches etc.

From neurological point of view, in relation to excitatory or inhibitory manifestation of the symptoms, there are two types of neurological symptoms- so-called positive and negative symptoms (Berman et al., 1997; Brown and Pluck, 2000; Strauss and Cohen, 2017). Positive symptoms are manifested as the states of over-increased and/or disorganized brain functions, for example, pain, anxiety and delirium may belong to this category (Berman et al., 1997). On the other hand, negative symptoms manifest as the occurrence of conditions characterized by decreased level/loss of the brain functions, such as loss of memory (Strauss and Cohen, 2017). In the connection to post-COVID-19 neurological complications, both types of symptoms can be found within the realm of post-COVID-19 symptoms. Positive symptoms might include conditions such as headaches, seizures, pain, anxiety and delirium. Negative symptoms might involve conditions such as memory loss, hypo/anosmia and hypo/ageusia. Occurrence of positive and negative symptoms or the co-occurrence of both might theoretically correspond to neurological profiles of misbalance between activation levels within the particular brain areas affected by COVID-19. In other words, some areas may get hyperactivated whereas other ones hypoactivated and the mutual misbalance of their activity levels may generate various pathological conditions.

Criticality

Critical behavior of the system refers to the state of the system in which there is a balance between order and entropy (Hellyer et al., 2014). In this state, the system is the most capable of switching between a multiple different states managing to benefit from each of these states but at the same time the stability of the system is maintained (Stam, 2005; Pastukhov et al., 2013). In relation to critical behavior of CNS, homeostatic plasticity has been proven to play a very important role in critical behavior (Ma et al., 2019) as it tunes CNS functioning to the state of balance between excitatory and inhibitory influences (Turrigiano and Nelson, 2000). When there comes to disruption of homeostatic regulation of biosystem, the system is likely to turn into either supercritical or subcritical regimes (Stam, 2005; Ma et al., 2019). Supercritical regime refers to the condition in which there is almost no order and entropy becomes dominant (Stam, 2005; Freyer et al., 2011). The system loses its stability, its behavior becomes chaotic and disorganized (Stam, 2005; Freyer et al., 2011) and there comes to hyper-responsiveness due to increased but chaotic information transfer (Poel et al., 2021). On the other hand, subcritical regime refers to the state in which there comes to maximal level of order and minimal level of entropy. In this regime, the system becomes rigid and unresponsive to stimuli due to hyper-organization which prevents from flexibility (Stam, 2005; Freyer et al., 2011). Post-COVID-19 coma was found to be characterized by dominant large-scale prevalence of alpha activity in EEG with minimal or no-reactivity to amplitude modulation (Koutroumanidis et al., 2021) which might be hallmarks of the manifestation of subcritical regime. On the other hand, possible occurrence of supercritical regime or the possible risk factor for being likely to turn into operating in supercritical regime, might be hypothesized to occur in COVID-19 survivors with PTSD in which altered organization of dynamic functional connectivity has been found (Fu et al., 2021). Reduction of node strengths and their degrees and efficacy, which was found in neural networks of these COVID survivors (Fu et al., 2021), may be linked with increased level of entropy or with higher risk of increased entropy levels causing consequent increase of information noise in neuronal communication.

However, so far, our proposed perspective of viewing post-COVID-19 complications from the perspective of dynamical system theory suffers from the lack of studies investigating the link between post-COVID-19 complications and critical behavior of the systems. We believe that future studies, using mathematical analytical approaches for studying links between neuroimaging data and clinical manifestations of post-COVID complications, may shed more light on this issue. Nevertheless, based on the current clinical and neuroimaging studies, we propose that post-COVID-19 complications are linked with maladaptive alterations of system parameters and emergence of new pathological attractors responsible for turning the brain to operate far from its critical (optimal) state.

For that reason, we propose that therapy targeting post-COVID-19 complication should be capable of elimination of pathological attractor, renormalization of system parameters and tuning of system to operate in its critical regime.

BIOFEEDBACK THERAPY AS A POTENTIAL TREATMENT FOR POST-COVID CONDITION

So far, post-COVID-19 complications have been treated pharmacologically (Blitshteyn and Whitelaw, 2021; Pattnaik et al., 2021), immunologically (Carroll et al., 2020; Sangare et al., 2020), by oxygen therapy (Kamal et al., 2021) and by rehabilitation exercises (Spielmanns et al., 2021). In relation to non-invasive brain modulation techniques, potential benefits of transcranial magnetic and transcranial direct current stimulation have been proposed for the treatment of COVID-19-related complications (Baptista et al., 2020). Transcranial direct current

stimulation has been already documented to be effective for reduction of subjective fatigue in COVID-19 survivors (Workman et al., 2021).

Biofeedback (BFB) represents non-invasive therapy based on self-regulation of one's internal state based on delivering information of biosignal changes to the participant (Gruzelier, 2014; Enriquez-Geppert et al., 2017). Once the amplitude of biosignal (e.g., EEG activity) reaches the level, which is at least as high as the level set by BFB therapist; the participant receives auditory and/or visual feedback. Due to repeated receiving of these feedbacks, the brain is able to associate these feedbacks with the underlying mental and psycho-physiological states linked with rewarded activity. Consequently, due to associative learning, it is becoming easier and easier for the participant to reach the states associated with increased levels of rewarded targeted activity (Gruzelier, 2014; Enriquez-Geppert et al., 2017). Biosignal modalities may include heartbeats patterns, electroencephalogram (EEG) changes, blood oxygen-dependent changes and others (Gruzelier, 2014; Collura, 2017; Watanabe et al., 2017; Lehrer et al., 2020). Biofeedback modalities, which are targeted to modify brain biosignals, such as EEG or blood oxygen-dependent changes in brain, are termed neurofeedback (NFB). Rewarded levels of targeted biosignals are set in accordance with the scientific and clinical knowledge related to the particular functions of the biosignals and the particular values of these biosignals documented in healthy and pathological conditions (Gruzelier, 2014; Collura, 2017; Enriquez-Geppert et al., 2017). BFB has been found to be capable of improving various neurological problems such as headaches (Walker, 2011), insomnia (Hammer et al., 2011), depression (Paquette et al., 2009; Tsuchiyagaito et al., 2021), fatigue (Hammond, 2001), epileptic seizures (Walker and Kozlowski, 2005) which overlap with the symptoms frequently found in post-COVID-19 conditions as well (Carroll et al., 2020; Dono et al., 2021; Guedj et al., 2021b; Kincaid et al., 2021; Lorkiewicz and Waszkiewicz, 2021; Park et al., 2021). Furthermore, NFB was found to be effective for treatment of chronic fatigue syndrome (CFS) (Hammond, 2001) and multiple sclerosis (MS) (Ayache et al., 2021) which both share similar symptoms to post-COVID-19 complications, such as pain, fatigue and depression (Workman et al., 2020; Komaroff and Lipkin, 2021; Wostyn, 2021). In addition, as well as in case of post-COVID-19 syndrome, both CFS and MS may stem from infectious agents (Steiner et al., 2001; Ghasemi et al., 2017; Komaroff and Lipkin, 2021). For that reason, we believe that BFB may represent a promising therapy for post-COVID-19 complications. Our proposal might be supported by the fact that NFB has been found to initiate micro-structural changes of white and gray matter associated with the improvement of functions of the trained brain areas (Ghaziri et al., 2013). In addition, NFB-induced behavioral improvements of brain functions were repeatedly documented to have a long-term persistence (Kerson et al., 2009; Alexeeva et al., 2012; Van Boxtel et al., 2012; Mottaz et al., 2015). Neurofeedback (NFB) was also shown to be capable of tuning EEG oscillations to operate near the state of criticality (Zhigalov et al., 2016; Ros et al., 2017) which may be possibly the hallmark of NFB capability to help to restore system behavior to operate in its optimal (critical) state which may be possibly of particular significance for post-COVID-19 complications. Furthermore, NFB therapy was also associated with increased levels of brain derived neurotrophic factor (Markiewicz and Dobrowolska, 2020), which is involved in regulating homeostatic plasticity (Turrigiano and Nelson, 2000), and which plays an essential role for successful maintenance of critical regime of brain dynamics (Ma et al., 2019).

In the following sections, we will discuss a potential role of biofeedback as a possible therapy for the treatment of post-COVID-19 complications. The proposed biofeedback modalities involve: (1) fMRI-based neurofeedback, (2) QEEG-based neurofeedback, (3) Othmer's method of rewarding individual optimal EEG frequency and (4) HRV biofeedback.

fMRI-Based Neurofeedback

fMRI neurofeedback (fMRI-NFB) is based on increasing or decreasing amplitude of fMRI signal which is averaged across the regions of interest (ROIs) in a brain (Watanabe et al., 2017). fMRI-NFB signal consists in the extraction of online blood level oxygen dependent (BOLD) signal (Haller et al., 2013; Watanabe et al., 2017). There are two major approaches of fMRI-NFB: The training of a particular targeted area, and the training of a neural network which may consist of two or more brain regions (Haller et al., 2013; Watanabe et al., 2017). The former type of fMRI-based NFB consists in increasing or decreasing the activity in the particular ROI, whereas the latter one relates to the modulation of activity within 2 or more brain areas (Watanabe et al., 2017). FMRI-based NFB was found to be capable of improving various neuro-pathological conditions (Bauer et al., 2020; Tsuchiyagaito et al., 2021). FMRI-based NFB has been found to be capable of altering connectivity strength in a targeted neural network (Haller et al., 2013; Koush et al., 2013). This kind of NFB modality can promote recovery from a neurological disorders accompanied with abnormalities in brain connectivity (Haller et al., 2013). The following **Figure 1** illustrates the underlying principles of fMRI-based NFB.

In post-COVID-19 condition, various abnormalities have been found in a various brain regions including damage to gray and white matter, abnormal hypometabolism and hypermetabolism of a various brain areas and impairment in brain connectivity (Carroll et al., 2020; Sangare et al., 2020; Dono et al., 2021; Douaud et al., 2021; Fu et al., 2021; Guedj et al., 2021a; Morand et al., 2021; Younger, 2021).

Since fMRI-based NFB can modulate brain network abnormalities and down-regulate abnormalities even in subcortical areas (Haller et al., 2013; Tsuchiyagaito et al., 2021) which are frequently found to exhibit functional and structural abnormalities in post-COVID condition (Guedj et al., 2021a; Sollini et al., 2021; Younger, 2021), we propose that fMRI-NFB may be beneficial for the treatment of post-COVID-19 conditions accompanied by aberrant patterns of brain activity. FMRI-based NFB for up-regulation of activity of target brain area/areas might be beneficial for hypometabolic condition in which activity in affected areas is reduced. On the other hand, down-regulation of brain activity might be beneficial for conditions of hypermetabolism and hyperconnectivity which can

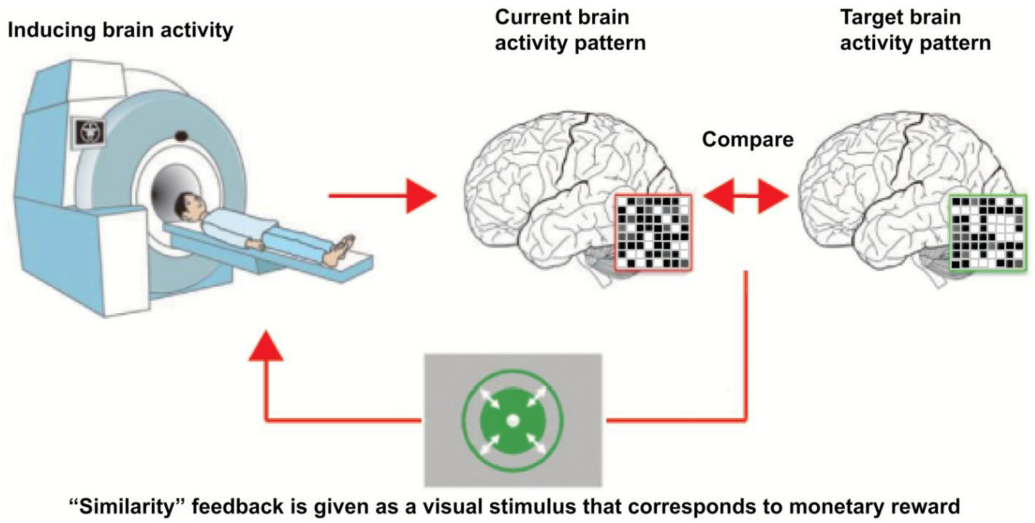

FIGURE 1 | Underlying principles of fMRI-based neurofeedback. This figure describes the underlying principles of fMRI-based neurofeedback. Magnetic activity of the participant head is monitored. Neurofeedback system constantly compares the current brain activity pattern with target brain activity pattern. As soon as the current brain activity pattern is sufficiently close to the target brain activity pattern, neurofeedback system generates rewarding feedback for the participant [taken from Yamada et al. (2017), taken with the permission of the author].

also occur in post-acute COVID period (Fu et al., 2021; Kincaid et al., 2021). In case of focal brain damage, patients might be likely to benefit from fMRI-NFB targeted to train activity in single ROI. On the contrary, connectivity-based NFB-fMRI might be useful for abnormal hypo/hyperconnectivity within multiple brain regions.

The following mentioned hypometabolic and hypermetabolic brain areas correlated with a various post-COVID-19 disturbances may serve as potential therapeutic target areas to fMRI-based NFB. Higher severity of hyposmia was positively associated with hypometabolism in bilateral gyrus rectus, medial frontal gyri and right middle temporal cortex (Morbelli et al., 2022). Positive correlation was documented between fronto-parietal hypometabolism and impairment of memory and executive functions measured by Montreal Cognitive Assessment performance (Hosp et al., 2021) which is consistent with the functional involvement of fronto-parietal network in executive functions (Sauseng et al., 2005). The findings documented in Hosp et al. (2021) study are at least partly consistent with another study which documented positive link between impairment in cognitive performance and reduction of metabolic activity in fronto-parietal network and temporal areas in COVID-19 survivors (Blazhenets et al., 2021). Hypometabolism in the right temporal lobe was also found to be positively correlated with pain, insomnia and longer duration of initial infectious symptoms (Guedj et al., 2021b). Positive linkage was also observed between hypometabolism of frontal areas and the presence of pain and high blood pressure (Guedj et al., 2021b), possibly indicating disturbances of central autonomous nervous system. In addition, cerebellar hypometabolism was positively correlated with increased number of various post-COVID-19 complaints (Guedj et al., 2021b). Apart from documented positive correlations between increased number and severity of post-COVID-19 disturbances, there are also existing reports of existing link between brain hypermetabolism and severity of post-COVID-19 problems. Namely, positive link between the levels of metabolism in orbitofrontal and parietal cortices and greater severity and longer duration of COVID-19-related dysosmia was observed (Niesen et al., 2021). However, apart from documented positive correlations between severity of post-COVID-19 symptoms and the level of decreased or increased metabolism in a various brain regions, there are also existing reports of more complex relationships between brain metabolism and severity of post-COVID-19 disturbances. The study done by Du et al. (2022) discovered positive correlation between amplitude of low frequency fluctuations in the left caudate nucleus and severity of sleep problems measured by Athens Insomnia Scale (Du et al., 2022). For that reason, advanced mathematical analysis of biosignals may be helpful to come up with successful NFB therapy for COVID-19 survivors in which positive association between neurological problems and complex brain metabolic patterns is present.

Nevertheless, fMRI-NFB was found to be capable of alteration of activity in other non-trained regions (Shibata et al., 2019) and therefore complex NFB outcomes might be expected. Our proposal of possible benefits from fMRI-based NFB on post-COVID neurological symptoms may be at least partly supported by the findings from other studies discovering that fMRI-based NFB is capable of improving various neurological disturbances that overlap with post-COVID-19 symptoms (Patel et al., 2020; Barizien et al., 2021; El Sayed et al., 2021; Fernández-De-las-Peñas et al., 2021c; Lorkiewicz and Waszkiewicz, 2021; Townsend et al., 2021; Tsuchiyagaito et al., 2021). Furthermore, fMRI-based NFB was demonstrated to improve neuro-immune regulatory pathway by up-regulation of activity in left amygdala (Tsuchiyagaito

et al., 2021). Such fMRI-NFB-based improvement in neuro-immune regulation might be beneficial for post-COVID-19 patients suffering from long-term inflammation and deregulation of immune system.

Limitation of our proposal of suitability of fMRI-based NFB for treatment of a post-COVID-19 neurological complication may consist in several aspects. First, we do not know whether post-COVID-19 neurological problems would successfully respond to that kind of treatment. Second, it is not known yet whether and which neurological post-COVID-19 symptoms are causally associated to the brain abnormalities found in neuroimaging studies done on COVID survivors. The last but not least, occurrence of post-COVID-19 neurological complications may not accompanied by abnormalities in brain structures (Fischer et al., 2020; Lim et al., 2020; Paterson et al., 2020). For that reason, COVID-19 survivors suffering from neurological complications having no structural brain abnormalities might be more likely to benefit from other types of NFB modalities.

Quantitative Electroencephalogram-Based Neurofeedback as a Potential Training for Electroencephalogram Abnormalities in Post-COVID-19 Condition

Quantitative EEG (QEEG) is based on enhancing or inhibiting certain EEG activity which is selected as a target NFB reward activity in accordance with pre-NFB EEG assessment (Collura, 2017). QEEG-based NFB protocols share a special narrative EEG databases containing statistically huge collection of EEG values of healthy people and EEG values of neuro-pathological condition as well as links between EEG patterns and various clinical conditions (Collura, 2017). Abnormal EEG activity may therefore represent a potential pathological attractor responsible for turning brain behavior into maladaptive regimes of operating far from optimal set-point. QEEG-based NFB is used for normalizing the pathological EEG activity by NFB-induced reduction of abnormally high coherence/amplitude and for up-regulation of abnormally low EEG amplitude/coherence values (Walker, 2010; Collura, 2017). Numerous QEEG NFB studies showed that QEEG-based NFB down-regulation of abnormal EEG patterns is connected with various behavioral improvements such as cessation or reduction of epileptic seizures (Walker and Kozlowski, 2005), improvement in cognitive abilities (Kerson et al., 2009) and others (Hammond, 2001; Paquette et al., 2009). NFB-induced reduction of aberrant EEG activity can be associated with the level of behavioral improvement (Hammer et al., 2011). These findings may speak in favor of ability of QEEG-based NFB to restore homeostatic set-point by teaching brain to operate in regimes which are far away from pathological regimes generated from pathological attractors linked with aberrant EEG activity. There have been documented a numerous aberrant pathological patterns found in a various neuropathological conditions (Díaz et al., 1998; Hammer et al., 2011; Walker, 2011) including post-COVID-19 condition as well (Kincaid et al., 2021). To the best of our knowledge, no study has been done to investigate the potential link between the severity of post-COVID-19 neurological complications and EEG profile yet. However, in acute COVID-19 condition, in which pathological EEG activity can occur (Flamand et al., 2020; Pellinen et al., 2020; Kubota et al., 2021), positive correlation between the level of EEG slowing and severity of clinical symptoms of the patients has been already documented (Pasini et al., 2020). These findings indicate that the investigation of EEG profiles and their links with clinical symptoms in post-COVID conditions may bring fruitful and valuable findings which may serve as a therapeutic target. We propose that QEEG-based NFB may serve as a beneficial non-invasive therapy for post-COVID neurological complications which are accompanied with abnormal EEG profiles. This proposal is based on the findings of multiple QEEG-NFB studies which managed to improve similar pathological conditions as those that frequently occurs in post-COVID period such as epileptic seizures (Wyler et al., 1976; Walker and Kozlowski, 2005; Walker, 2011) depressions (Paquette et al., 2009), fatigue (Hammond, 2001) and insomnia (Hammer et al., 2011) by NFB-induced reduction of pathological EEG associated with these conditions. Furthermore, level of behavioral improvement was repeatedly found to correlate with the level of NFB-induced reduction of target aberrant EEG activity (Paquette et al., 2009; Hammer et al., 2011). These positive associations might be in line with positive associations found between the severity of some particular neurological symptoms and the level of aberrant EEG activity (Díaz et al., 1998; Askew, 2001). So far, it is unknown whether post-COVID-19 neurological complications are associated with some specific EEG patterns. So far, various abnormal EEG patterns were repeatedly found in COVID-19 survivors suffering from *de novo* seizure conditions (Carroll et al., 2020; Dono et al., 2021; Kincaid et al., 2021). However, to the best our knowledge, no study has investigated the link between the severity of pathological EEG and severity of seizures yet. Furthermore, to the best of our knowledge, it is unknown by now if there is a specific EEG pattern found in other post-COVID-19 neurological complications, such as migraines, dizziness, anxiety, depression etc. and whether there exists a causal link between these post-COVID-19 problems and particular EEG profile. Apart from the lack of this knowledge, post-COVID-19 neurological complications do not have to be always accompanied with abnormalities in EEG profile (Lim et al., 2020). For that reason, other NFB modalities might be more suitable for such cases.

Othmer's Method of Training of Individual Optimal Electroencephalogram Frequency

Othmer's method of rewarding optimal training EEG frequency is based on individual adjustment of NFB-rewarded EEG frequency band width (Othmer and Othmer, 2017; Othmer, 2020). Optimal rewarded EEG frequency (ORF) is associated with mental state during which one feels calm, alert and relaxed and it is connected with the state of so-called optimal arousal (Othmer and Othmer, 2017; Othmer, 2020). On the other hand, too high NFB-rewarded frequency is linked with irritating symptoms such as headaches,

anxiety, onset insomnia, and nightmares which are the signs of high arousal (Othmer and Othmer, 2017; Othmer, 2020). This may be in accordance with positive linkages between excessive high beta activity and neurological disturbances such as anxiety (Walker, 2010; Díaz et al., 2019), headaches (Walker, 2011) and insomnia (Perlis et al., 2001; Hammer et al., 2011). On the contrary, hypoarousal (low arousal) occurs when the training NFB frequency is too low and it results in symptoms such as somnolence, fatigue, apathy and sadness (Othmer and Othmer, 2017; Othmer, 2020). This notion might be in line with the prevalence of low frequency activity in conditions such as fatigue (Klimesch, 1999; Lafrance and Dumont, 2000) and somnolence (Hammer et al., 2011). ORF and the corresponding optimal arousal can be analogous to Yerkes-Dodson model of inverted U-like relationship between the arousal level and level of learning and Hebb's model of U-like relation between level of arousal and level of cognitive performance (Teigen, 1994). In both of these models, low arousal is linked with the states of coma or sleep coupled with low level of behavioral performance whereas high arousal levels are associated with the states of anxiety and panic and are also linked with lower levels of behavioral performance. On the other hand, moderate levels of arousal are associated with the highest levels of behavioral cognitive performance (Teigen, 1994). Hebb's and Yerkes-Dodson's models of relationship between behavioral performance and levels of arousal may be also reminiscent of system's behavior according to dynamical system theory. In this analogy, critical system's behavior would be linked with rewarding of individual ORF, whereas subcritical regime might be the result of rewarding too low EEG frequency and supercritical regime might occur as a result of NFB training of too high EEG frequency.

Post-COVID-19 complications involve symptoms such as headaches, anxiety and insomnia (Fernández-De-las-Peñas et al., 2021c,d; Townsend et al., 2021) which are typical for presence of state of high arousal (Hammer et al., 2011; Walker, 2011; Othmer and Othmer, 2017; Díaz et al., 2019; Othmer, 2020) as well as symptoms reminiscent of low arousal such as somnolence and fatigue (Othmer and Othmer, 2017; Othmer, 2020). Therefore, we propose that NFB training of ORF may lead to normalization of arousal level leading to improvement of the aforementioned post-COVID-19 symptoms. As post-COVID-19 complications may not be necessarily accompanied with any structural and/or electrophysiological brain abnormalities (Fischer et al., 2020; Lim et al., 2020; Park et al., 2021), the advantage of this Othmer's method of ORF would consist in its methodology that does not rely on neuroimaging data of the patient. Instead, individualized NFB protocol is entirely based on the symptomatology of the patient (Othmer and Othmer, 2017; Othmer, 2020). Othmer's method of ORF has been successfully applied on a variety of neurophysiological problems (Putman, 2004; Sime, 2004; Legarda et al., 2011; Carlson and Ross, 2021) which greatly overlap with post-COVID-19 neurological complications (Caronna et al., 2021; Fernández-De-las-Peñas et al., 2021b; Pilotto et al., 2021).

In relation to possible limitations, we do not know whether post-COVID-19 symptoms would successfully respond to this kind of treatment compared to analogical symptoms of different etiologies which have been already found to be successfully treated by Othmer's method of ORF. Another important notion that should be taken into consideration is the possibility that some symptoms portraying the characteristics of low arousal might be in fact caused by high arousal and vice versa, symptoms reminiscent of high arousal may be in fact the consequence of low arousal. For instance, fatigue can be the result of high arousal-like states such as insomnia (Hammer et al., 2011) and/or anxiety (Díaz et al., 2019) and in this case lowering training EEG frequency instead of its increase can be the successful strategy. In post-COVID-19 condition, significant positive correlation has been found between the level of fatigue and anxiety (Townsend et al., 2021) which may indicate mutual interrelatedness of these symptoms and their potential causal inter-relation and this kind of inter-relation may be that case in one needs to be very careful in proper classification of symptoms resulting from high or low arousal condition. All in all, we believe that Othmer's method may represent a promising therapy for post-COVID-19 neurological complications.

Heart Rate Variability-Based Biofeedback

Heart rate variability-based biofeedback (HRV-based BFB) is based on feeding back heart rate data to the participant during breathing, such that the participant tries to maximize his/her respiratory sinus arrhythmia (RSA). When breathing, RSA is the heart activity corresponding to the changes of heart rate which is influenced by breathing such that heart rate increases during inspiration and decreases during expiration and gas-exchange efficacy in lungs becomes maximized when breathing and heart oscillations become coherent (Gevirtz, 2013; Lehrer et al., 2020). During HRV-based BFB training, RSA oscillations become more simple and sinusoidal which is often achieved within a several of minutes, even though the participant is completely naive to HRV-based BFB treatment (Gevirtz, 2013; Lehrer and Gevirtz, 2014). RSA is controlled by parasymphatetic autonomous nervous system (PANS) (Lehrer and Gevirtz, 2014; Lehrer et al., 2020). These postulates are also supported by studies which managed to find greater baroreflex after (Lehrer et al., 2003; Hassett et al., 2007) and/or during HRV-based BFB (Lehrer et al., 2003) and higher HRV after BFB-HRV (Hassett et al., 2007; Lin et al., 2019) and during BFB-based HRV (Caldwell and Steffen, 2018) since both high HRV and baroreflex are markers of PANS (Cowley and Guyton, 1975; Swenne, 2013; Tracy et al., 2016; Beltrán et al., 2020). Additionally, HRV-based BFB was reported to decrease blood pressure and heart rate (May et al., 2019) which may also speak in favor of its capability to modulate ANS toward the greater influence of PANS. Activation of baroreflex and activation of vagal afferents *via* subdiaphragmatic breathing accompanying HRV-based BFB are proposed mechanisms of HRV-based BFB-mediated effects on central autonomous nervous system (CANS) (Lehrer and Gevirtz, 2014; Lehrer et al., 2020) *via* activation of nucleus tractus solitarii which regulates baroreflex (Takagishi et al., 2010; Lin et al., 2013) and is also responsible for transferring signals to higher-ordered CANS (Reisert et al., 2021). Based

on these notions, we hypothesize that post-COVID-19 haulers, especially those suffering from dysautonomia, might benefit from HRV-based BFB treatment. First of all, this proposal is based on the significant overlap between post-COVID-19 symptoms and symptoms of other etiologies that were successfully treated by HRV-BFB (Karavidas et al., 2007; Reiner, 2008; van der Zwan et al., 2015; Windthorst et al., 2017; Lin et al., 2019). Secondly, since HRV-BFB was found to be capable of enhancing markers of PANS, such as increased HRV (Hassett et al., 2007; Caldwell and Steffen, 2018) and increased baroreflex (Lehrer et al., 2003; Hassett et al., 2007), post-COVID-19 patients with under-activated/inhibited PANS and/or over-activated sympathetic autonomous nervous system (SANS) might represent a suitable candidates for HRV-BFB treatment. This proposal might be at least partially supported by reported alterations in HRV pattern found between fatigued post-COVID-19 and non-fatigued post-COVID-19 participants (Barizien et al., 2021). Thirdly, successful acquisition of the proper breathing pattern leading to success in HRV-BFB training can help to restore better breathing habits leading to more effective gas exchange in lungs resulting in greater oxygenation facilitating regeneration and/or reparation of damaged tissue in post-COVID-19 condition. Therapy involving HRV-BFB training might be especially of a great significance to those people who display maladaptive breathing patterns and/or other breathing complications that often occur in post-COVID-19 condition (Becker, 2021). Last but not least, ANS is strongly connected with the proper functioning of immune system (Andersson, 2005; Hilderman et al., 2019). SANS is involved in driving pro-inflammatory changes whereas PANS mediates suppression of pro-inflammatory markers (Andersson, 2005; Hilderman et al., 2019). HRV-BFB was found to enhance resilience to inflammatory marker, particularly, to lipopolysaccharide (Lehrer et al., 2010). HRV-based BFB was documented to decline lipopolysaccharide-related attenuation effects on HRV showing neuro-immune-regulatory potential of HRV-based BFB which may be indicative of its potential therapeutic benefits for post-COVID-19 participants suffering from long-term deregulation of immune system (Lehrer et al., 2010).

Another supporting evidence of potential therapeutic effect of HRV-based BFB for post-COVID-19 haulers comes from neuroimaging studies demonstrating increases in blood flow in amygdala, hippocampus, gyrus cingulate plus greater connectivity between sub-cortical limbic areas and prefrontal cortex during HRV-based BFB (Mather and Thayer, 2018; Vaschillo et al., 2019). The aforementioned limbic areas hugely overlap with the areas which were repeatedly found hypo-metabolic in post-COVID-19 period (Guedj et al., 2021a; Morand et al., 2021; Sollini et al., 2021) and were associated with some post-COVID-19 neurological complications (Douaud et al., 2021; Sollini et al., 2021) and at the same time they belong to CANS (Reisert et al., 2021). For that reason, we suggest that HRV-based BFB might help to normalize activity in CANS and restore its underlying functions in post-COVID-19 condition.

However, it is necessary to mention that no link has been found/investigated between the levels of alteration in ANS markers and severity of post-COVID-19 complications yet. Also, the particular type of dysautonomia is likely to play a crucial role. For instance, dysautonomia exhibiting reduced SANS and/or over/activated PANS might not be as suitable candidate as dysautonomia with predominant SANS for HRV-BFB therapy in which PANS is stimulated. Despite these limitations, we believe that HRV-BFB is worth-investigating as a potential and promising therapy for post-COVID-19 complications.

TABLE 2 | Suitability of biofeedback modalities for post-COVID-19 neurological symptoms with regard to the presence of electrophysiological and functional brain abnormalities.

Biofeedback modality	Necessity of the presence of structural or functional brain abnormalities documented by neuro-imaging methods
1. fMRI-based neurofeedback	Yes
2. QEEG-based neurofeedback	Yes
3. Othmer's neurofeedback method	No
4. HRV-based biofeedback	No

To summarize our considerations of suitability of aforementioned biofeedback modalities for post-COVID-19 neurological symptoms with regard to the presence of electrophysiological and/or functional brain abnormalities, **Table 2** is proposed.

CONCLUSION

In our view, there are several mechanisms, responsible for the onset and persistence of COVID-19-related neurological disturbances, which may take place in two phases, in the phase of acute and in the phase of post-acute Sars-CoV-2 infection. We also proposed the point of view by approaching post-COVID-19 complications from the perspective of dynamical system theory. Last but not least, we propose that neurofeedback may represent a potential therapy for post-COVID-19 neurological complications. We have discussed potential limiting factors specific to BFB treatment. Apart from them, we feel it is necessary to mention some general limitation of our considerations. Firstly, there is limited knowledge about overall duration of post-COVID-19 complications and their dynamics. Secondly, it is not clear whether and how the post-COVID-19 complications caused by new variants of SARS-CoV-2 differ in their severity, types and responsiveness to the treatment. Also, the type of particular post-COVID-19 complication might also influence its responsiveness to the treatment. For instance, post-COVID-19 complications caused by direct viral invasion might respond differently to the therapy than post-COVID-19 complications caused indirectly by SARS-CoV-2 effects on CNS. Regarding neurofeedback as proposed possible therapy for neurological post-COVID-19 problems, the exact etiology of these neurological problems may play a crucial role in the level of effectiveness of neurofeedback. It might be of a considerable relevance whether particular neurological problems originate from COVID-19-related damage to brain or whether the particular neurological

consequence is the result of extra-neural etiology. Last but not least, it is necessary to say that interdisciplinary approach and combination of other therapies than neurofeedback, for instance rehabilitation, breathing exercise and psychotherapy, should be included for increasing the efficacy of the treatment of post-COVID-19 complications.

All in all, in spite of these limitations, we believe our considerations are worth-studying and we hope they will help to broaden the research horizons in the related neuroscience research.

AUTHOR CONTRIBUTIONS

MO wrote the preliminary and final manuscript. EK helped with administration issues. Both authors contributed to the article and approved the submitted version.

FUNDING

This article has been funded by the programme Cooperatio, Neuroscience Charles University in Prague.

REFERENCES

Alexeeva, M. V., Balios, N. V., Muravlyova, K. B., Sapina, E. V., and Bazanova, O. M. (2012). Training for voluntarily increasing individual upper α power as a method for cognitive enhancement. *Hum. Physiol.* 38, 40–48. doi: 10.1134/S0362119711060028

Alhempi, R. R., Salamah, I., and Lastriani, E. (2021). Effect of positive thinking on Covid-19 patient healing. *Ann. Romanian Soc. Cell Biol.* 25, 5546–5554.

Ameres, M., Brandstetter, S., Toncheva, A. A., Kabesch, M., Leppert, D., Kuhle, J., et al. (2020). Association of neuronal injury blood marker neurofilament light chain with mild-to-moderate COVID-19. *J. Neurol.* 267, 3476–3478. doi: 10.1007/s00415-020-10050-y

Andersson, J. (2005). The inflammatory reflex - Introduction. *J. Intern. Med.* 257, 122–125. doi: 10.1111/j.1365-2796.2004.01440.x

Asadi-Pooya, A. A., and Simani, L. (2020). Central nervous system manifestations of COVID-19: a systematic review. *J. Neurol. Sci.* 413:116832. doi: 10.1016/j.jns.2020.116832

Askew, J. H. (2001). *The Diagnosis of Depression Using Psychometric Instruments and Quantitative Measures of Electroencephalographic Activity*. ProQuest Dissertations. Knoxville, TN: The University of Tennessee.

Ayache, S. S., Bardel, B., Lefaucheur, J. P., and Chalah, M. A. (2021). Neurofeedback therapy for the management of multiple sclerosis symptoms: current knowledge and future perspectives. *NeuroSignals* 20, 745–754. doi: 10.31083/j.jin2003079

Ayat, P., Burza, A., and Habeeb, C. (2021). Hypocortisolism in a patient with Covid-19: a case report and discussion on management. *Chest* 160:A715. doi: 10.1016/j.chest.2021.07.678

Baptista, A. F., Baltar, A., Okano, A. H., Moreira, A., Campos, A. C. P., Fernandes, A. M., et al. (2020). Applications of non-invasive neuromodulation for the management of disorders related to COVID-19. *Front. Neurol.* 11:573718. doi: 10.3389/fneur.2020.573718

Barizien, N., Le Guen, M., Russel, S., Touche, P., Huang, F., and Vallée, A. (2021). Clinical characterization of dysautonomia in long COVID-19 patients. *Sci. Rep.* 11:14042. doi: 10.1038/s41598-021-93546-5

Bauer, C. C. C., Okano, K., Gosh, S. S., Lee, Y. J., Melero, H., Angeles, C., et al. (2020). Real-time fMRI neurofeedback reduces auditory hallucinations and modulates resting state connectivity of involved brain regions: part 2: default mode network -preliminary evidence. *Psychiatry Res.* 284:112770. doi: 10.1016/j.psychres.2020.112770

Becker, R. C. (2021). Autonomic dysfunction in SARS-COV-2 infection acute and long-term implications COVID-19 editor's page series. *J. Thromb. Thrombolysis* 52, 692–707. doi: 10.1007/s11239-021-02549-6

Beltrán, A. R., Arce-Álvarez, A., Ramirez-Campillo, R., Vásquez-Muñoz, M., von Igel, M., Ramírez, M. A., et al. (2020). Baroreflex modulation during acute high-altitude exposure in rats. *Front. Physiol.* 11:1049. doi: 10.3389/fphys.2020.01049

Berman, I., Viegner, B., Merson, A., Allan, E., Pappas, D., and Green, A. I. (1997). Differential relationships between positive and negative symptoms and neuropsychological deficits in schizophrenia. *Schizophr. Res.* 25, 1–10. doi: 10.1016/S0920-9964(96)00098-9

Bilgin, A., Kesik, G., and Ozdemir, L. (2021). 'The body seems to have no life': the experiences and perceptions of fatigue among patients after COVID-19. *J. Clin. Nurs.* 1–11. doi: 10.1111/jocn.16153

Blazhenets, G., Schroeter, N., Bormann, T., Thurow, J., Wagner, D., Frings, L., et al. (2021). Slow but evident recovery from neocortical dysfunction and cognitive impairment in a series of chronic COVID-19 patients. *J. Nucl. Med.* 62, 910–915. doi: 10.2967/jnumed.121.262128

Blitshteyn, S., and Whitelaw, S. (2021). Postural orthostatic tachycardia syndrome (POTS) and other autonomic disorders after COVID-19 infection: a case series of 20 patients. *Immunol. Res.* 69, 205–211. doi: 10.1007/s12026-021-09185-5

Bobermin, L. D., and Quincozes-Santos, A. (2021). COVID-19 and hyperammonemia: potential interplay between liver and brain dysfunctions. *Brain Behav. Immun. - Heallth* 14:100257. doi: 10.1016/j.bbih.2021.100257

Bodnar, B., Patel, K., Ho, W., Luo, J. J., and Hu, W. (2021). Cellular mechanisms underlying neurological/neuropsychiatric manifestations of COVID-19. *J. Med. Virol.* 93, 1983–1998. doi: 10.1002/jmv.26720

Bould, H., Collin, S. M., Lewis, G., Rimes, K., and Crawley, E. (2013). Depression in paediatric chronic fatigue syndrome. *Arch. Dis. Child.* 98, 425–428. doi: 10.1136/archdischild-2012-303396

Brown, R. G., and Pluck, G. (2000). Negative symptoms: the "pathology" of motivation and goal-directed behaviour. *Trends Neurosci.* 23, 412–417. doi: 10.1016/S0166-2236(00)01626-X

Bryche, B., St Albin, A., Murri, S., Lacôte, S., Pulido, C., Ar Gouilh, M., et al. (2020). Massive transient damage of the olfactory epithelium associated with infection of sustentacular cells by SARS-CoV-2 in golden Syrian hamsters. *Brain. Behav. Immun.* 89, 579–586. doi: 10.1016/j.bbi.2020.06.032

Buchanan, T. W., Tranel, D., and Adolphs, R. (2003). A specific role for the human amygdala in olfactory memory. *Learn. Mem.* 10, 319–325. doi: 10.1101/lm.62303

Burrows, D. R., Diana, G., Pimpel, B., Moeller, F., Richardson, M. P., Bassett, D. S., et al. (2021). Single-cell networks reorganise to facilitate whole-brain supercritical dynamics during epileptic seizures. *bioRxiv [preprint]* 2021.10.14.464473. doi: 10.1101/2021.10.14.464473

Caldwell, Y. T., and Steffen, P. R. (2018). Adding HRV biofeedback to psychotherapy increases heart rate variability and improves the treatment of major depressive disorder. *Int. J. Psychophysiol.* 131, 96–101. doi: 10.1016/j.ijpsycho.2018.01.001

Capuron, L., Pagnoni, G., Drake, D. F., Woolwine, B. J., Spivey, J. R., Crowe, R. J., et al. (2012). Dopaminergic mechanisms of reduced basal ganglia responses to hedonic reward during interferon alfa administration. *Arch. Gen. Psychiatry* 69, 1044–1053. doi: 10.1001/archgenpsychiatry.2011.2094

Carlson, J., and Ross, G. W. (2021). Neurofeedback impact on chronic headache, sleep, and attention disorders experienced by veterans with mild traumatic brain injury: a pilot study. *Biofeedback* 49, 2–9. doi: 10.5298/1081-5937-49.01.01

Caronna, E., Alpuente, A., Torres-Ferrus, M., and Pozo-Rosich, P. (2021). Toward a better understanding of persistent headache after mild COVID-19: three migraine-like yet distinct scenarios. *Headache* 61, 1277–1280. doi: 10.1111/head.14197

Carroll, E., Neumann, H., Aguero-Rosenfeld, M. E., Lighter, J., Czeisler, B. M., Melmed, K., et al. (2020). Post–COVID-19 inflammatory syndrome manifesting as refractory status epilepticus. *Epilepsia* 61, e135–e139. doi: 10.1111/epi.16683

Chaparro-Huerta, V., Rivera-Cervantes, M. C., Flores-Soto, M. E., Gómez-Pinedo, U., and Beas-Zárate, C. (2005). Proinflammatory cytokines and apoptosis

following glutamate-induced excitotoxicity mediated by p38 MAPK in the hippocampus of neonatal rats. *J. Neuroimmunol.* 165, 53–62. doi: 10.1016/j.jneuroim.2005.04.025

Chiu, A., Fischbein, N., Wintermark, M., Zaharchuk, G., Yun, P. T., and Zeineh, M. (2021). COVID-19-induced anosmia associated with olfactory bulb atrophy. *Neuroradiology* 63, 147–148. doi: 10.1007/s00234-020-02554-1

Collantes, M. E. V., Espiritu, A. I., Sy, M. C. C., Anlacan, V. M. M., and Jamora, R. D. G. (2021). Neurological manifestations in COVID-19 infection: a systematic review and meta-analysis. *Can. J. Neurol. Sci.* 48, 66–76. doi: 10.1017/cjn.2020.146

Collura, T. F. (2017). Quantitative EEG and Live Z -Score neurofeedback—current clinical and scientific context. *Biofeedback* 45, 25–29. doi: 10.5298/1081-5937-45.1.07

Coolen, T., Lolli, V., Sadeghi, N., Rovai, A., Trotta, N., Taccone, F. S., et al. (2020). Early postmortem brain MRI findings in COVID-19 non-survivors. *Neurology* 95, e2016–e2027. doi: 10.1212/WNL.0000000000010116

Cowley, A. W., and Guyton, A. C. (1975). Baroreceptor reflex effects on transient and steady state hemodynamics of salt loading hypertension in dogs. *Circ. Res.* 36, 536–546. doi: 10.1161/01.RES.36.4.536

Crunfli, F., Carregari, V. C., Veras, F. P., Vendramini, P. H., Valença, G. F., Saraiva, A., et al. (2021). SARS-CoV-2 infects brain astrocytes of COVID-19 patients and impairs neuronal viability. *medRxiv [preprint]* doi: 10.1101/2020.10.09.20207464

de Melo, G. D., Lazarini, F., Levallois, S., Hautefort, C., Michel, V., Larrous, F., et al. (2021). COVID-19-related anosmia is associated with viral persistence and inflammation in human olfactory epithelium and brain infection in hamsters. *Sci. Transl. Med.* 13:eabf8396. doi: 10.1126/scitranslmed.abf8396

Delorme, C., Houot, M., Rosso, C., Carvalho, S., Nedelec, T., Maatoug, R., et al. (2021). The wide spectrum of Covid-19 neuropsychiatric complications within a multidisciplinary center. *Brain Commun.* 3:fcab135. doi: 10.1093/braincomms/fcab135

Dennis, A., Wamil, M., Alberts, J., Oben, J., Cuthbertson, D. J., Wootton, D., et al. (2021). Multiorgan impairment in low-risk individuals with post-COVID-19 syndrome: a prospective, community-based study. *BMJ Open* 11, 2–7. doi: 10.1136/bmjopen-2020-048391

Díaz, G. F., Virués, T., San Martín, M., Ruiz, M., Galán, L., Paz, L., et al. (1998). Generalized background qEEG abnormalities in localized symptomatic epilepsy. *Electroencephalogr. Clin. Neurophysiol.* 106, 501–507. doi: 10.1016/S0013-4694(98)00026-1

Díaz, H. M., Cid, F. M., Otárola, J., Rojas, R., Alarcón, O., and Cañete, L. (2019). EEG Beta band frequency domain evaluation for assessing stress and anxiety in resting, eyes closed, basal conditions. *Procedia Comput. Sci.* 162, 974–981. doi: 10.1016/j.procs.2019.12.075

Dono, F., Carrarini, C., Russo, M., De Angelis, M. V., Anzellotti, F., Onofrj, M., et al. (2021). New-onset refractory status epilepticus (NORSE) in post SARS-CoV-2 autoimmune encephalitis: a case report. *Neurol. Sci.* 42, 35–38. doi: 10.1007/s10072-020-04846-z

Douaud, G., Lee, S., Alfaro-Almagro, F., Arthofer, C., Wang, C., Lange, F., et al. (2021). Brain imaging before and after COVID-19 in UK Biobank. *medRxiv [preprint]* doi: 10.1101/2021.06.11.21258690

Du, Y.-Y., Zhao, W., Zhou, X. L., Zeng, M., Yang, D. H., Xie, X. Z., et al. (2022). Survivors of COVID-19 exhibit altered amplitudes of low frequency fluctuation in the brain: a resting-state functional magnetic resonance imaging study at 1-year follow-up. *Neural Regen. Res.* 17, 1576–1581. doi: 10.4103/1673-5374.327361

Effenberger, M., Grander, C., Grabherr, F., Griesmacher, A., Ploner, T., Hartig, F., et al. (2021). Systemic inflammation as fuel for acute liver injury in COVID-19. *Dig. Liver Dis.* 53, 158–165. doi: 10.1016/j.dld.2020.08.004

El Sayed, S., Shokry, D., and Gomaa, S. M. (2021). Post-COVID-19 fatigue and anhedonia: a cross-sectional study and their correlation to post-recovery period. *Neuropsychopharmacol. Rep.* 41, 50–55. doi: 10.1002/npr2.12154

Ellul, M. A., Benjamin, L., Singh, B., Lant, S., Michael, B. D., Easton, A., et al. (2020). Neurological associations of COVID-19. *Lancet Neurol.* 19, 767–783. doi: 10.1016/S1474-4422(20)30221-0

Enriquez-Geppert, S., Huster, R. J., and Herrmann, C. S. (2017). EEG-neurofeedback as a tool to modulate cognition and behavior: a review tutorial. *Front. Hum. Neurosci.* 11:51. doi: 10.3389/fnhum.2017.00051

Felger, J. C. (2017). Imaging the role of inflammation in mood and anxiety-related disorders. *Curr. Neuropharmacol.* 15, 533–558. doi: 10.2174/1570159x15666171123201142

Fernández-De-las-Peñas, C., Gómez-Mayordomo, V., de-la-Llave-Rincón, A. I., Palacios-Ceña, M., Rodríguez-Jiménez, J., Florencio, L. L., et al. (2021c). Anxiety, depression and poor sleep quality as long-term post-COVID sequelae in previously hospitalized patients: a multicenter study. *J. Infect.* 83, 496–522. doi: 10.1016/j.jinf.2021.06.022

Fernández-De-las-Peñas, C., Navarro-Santana, M., Gómez-Mayordomo, V., Cuadrado, M. L., García-Azorín, D., Arendt-Nielsen, L., et al. (2021d). Headache as an acute and post-COVID-19 symptom in COVID-19 survivors: a meta-analysis of the current literature. *Eur. J. Neurol.* 28, 3820–3825. doi: 10.1111/ene.15040

Fernández-De-las-Peñas, C., Florencio, L. L., Gómez-Mayordomo, V., Cuadrado, M. L., Palacios-Ceña, D., and Raveendran, A. V. (2021a). Proposed integrative model for post-COVID symptoms. *Diabetes Metab. Syndr. Clin. Res. Rev.* 15, 15–17. doi: 10.1016/j.dsx.2021.05.032

Fernández-De-las-peñas, C., Palacios-Ceña, D., Gómez-Mayordomo, V., Cuadrado, M. L., and Florencio, L. L. (2021e). Defining post-covid symptoms (Post-acute covid, long covid, persistent post-covid): an integrative classification. *Int. J. Environ. Res. Public Health* 18:2621. doi: 10.3390/ijerph18052621

Fernández-de-las-Peñas, C., Gómez-Mayordomo, V., Cuadrado, M. L., Palacios-Ceña, D., Florencio, L. L., Guerrero, A. L., et al. (2021b). The presence of headache at onset in SARS-CoV-2 infection is associated with long-term post-COVID headache and fatigue: a case-control study. *Cephalalgia* 41, 1332–1341. doi: 10.1177/03331024211020404

Ferrandi, P. J., Alway, S. E., and Mohamed, J. S. (2020). The interaction between SARS-CoV-2 and ACE2 may have consequences for skeletal muscle viral susceptibility and myopathies. *J. Appl. Physiol.* 129, 864–867. doi: 10.1152/applphysiol.00321.2020

Fischer, D., Threlkeld, Z. D., Bodien, Y. G., Kirsch, J. E., Huang, S. Y., Schaefer, P. W., et al. (2020). Intact brain network function in an unresponsive patient with COVID-19. *Ann. Neurol.* 88, 851–854. doi: 10.1002/ana.25838

Flamand, M., Perron, A., Buron, Y., and Szurhaj, W. (2020). Pay more attention to EEG in COVID-19 pandemic. *Clin. Neurophysiol.* 131, 2062–2064. doi: 10.1016/j.clinph.2020.05.011

Freyer, F., Roberts, J. A., Becker, R., Robinson, P. A., Ritter, P., and Breakspear, M. (2011). Biophysical mechanisms of multistability in resting-state cortical rhythms. *J. Neurosci.* 31, 6353–6361. doi: 10.1523/JNEUROSCI.6693-10.2011

Fu, Z., Tu, Y., Calhoun, V. D., Zhang, Y., Zhao, Q., Chen, J., et al. (2021). Dynamic functional network connectivity associated with post-traumatic stress symptoms in COVID-19 survivors. *Neurobiol. Stress* 15:100377. doi: 10.1016/j.ynstr.2021.100377

Funakoshi, H., Belluardo, N., Arenas, E., Yamamoto, Y., Casabona, A., Persson, H., et al. (1995). Muscle-derived neurotrophin-4 as an activity-dependent trophic signal for adult motor neurons. *Science* 268, 1495–1499. doi: 10.1126/science.7770776

Gagliardi, S., Poloni, E. T., Pandini, C., Garofalo, M., Dragoni, F., Medici, V., et al. (2021). Detection of SARS-CoV-2 genome and whole transcriptome sequencing in frontal cortex of COVID-19 patients. *Brain. Behav. Immun.* 97, 13–21. doi: 10.1016/j.bbi.2021.05.012

Gevirtz, R. (2013). The promise of heart rate variability biofeedback: evidence-based applications. *Biofeedback* 41, 110–120. doi: 10.5298/1081-5937-41.3.01

Ghasemi, N., Razavi, S., and Nikzad, E. (2017). Multiple sclerosis: pathogenesis, symptoms, diagnoses and cell-based therapy. *Cell J.* 19, 1–10. doi: 10.22074/cellj.2016.4867

Ghaziri, J., Tucholka, A., Larue, V., Blanchette-Sylvestre, M., Reyburn, G., Gilbert, G., et al. (2013). Neurofeedback training induces changes in white and gray matter. *Clin. EEG Neurosci.* 44, 265–272. doi: 10.1177/1550059413476031

Goërtz, Y. M. J., Van Herck, M., Delbressine, J. M., Vaes, A. W., Meys, R., Machado, F. V. C., et al. (2020). Persistent symptoms 3 months after a SARS-CoV-2 infection: the post-COVID-19 syndrome? *ERJ Open Res.* 6, 00542–02020. doi: 10.1183/23120541.00542-2020

Goodman, B. P., Khoury, J. A., Blair, J. E., and Grill, M. F. (2021). COVID-19 Dysautonomia. *Front. Neurol.* 12:624968. doi: 10.3389/fneur.2021.624968

Gruzelier, J. H. (2014). Neuroscience and biobehavioral reviews EEG-neurofeedback for optimising performance . III?: a review of methodological and theoretical considerations. *Neurosci. Biobehav. Rev.* 44, 159–182. doi: 10.1016/j.neubiorev.2014.03.015

Guedj, E., Million, M., Dudouet, P., Tissot-Dupont, H., Bregeon, F., Cammilleri, S., et al. (2021a). 18F-FDG brain PET hypometabolism in post-SARS-CoV-2 infection: substrate for persistent/delayed disorders? *Eur. J. Nucl. Med. Mol. Imaging* 48, 592–595. doi: 10.1007/s00259-020-04973-x

Guedj, E., Campion, J. Y., Dudouet, P., Kaphan, E., Bregeon, F., Tissot-Dupont, H., et al. (2021b). 18F-FDG brain PET hypometabolism in patients with long COVID. *Eur. J. Nucl. Med. Mol. Imaging* 48, 2823–2833. doi: 10.1007/s00259-021-05215-4

Guth, L. (1968). "Trophic" influences of nerve on muscle. *Physiol. Rev.* 48, 645–687. doi: 10.1152/physrev.1968.48.4.645

Haddad, W. M. (2013). A unification between dynamical system theory and thermodynamics involving an energy, mass, and entropy state space formalism. *Entropy* 15, 1821–1846. doi: 10.3390/e15051821

Haller, S., Kopel, R., Jhooti, P., Haas, T., Scharnowski, F., Lovblad, K. O., et al. (2013). Dynamic reconfiguration of human brain functional networks through neurofeedback. *Neuroimage* 81, 243–252. doi: 10.1016/j.neuroimage.2013.05.019

Hammer, B. U., Colbert, A. P., Brown, K. A., and Ilioi, E. C. (2011). Neurofeedback for insomnia: a pilot study of Z-score SMR and individualized protocols. *Appl. Psychophysiol. Biofeedback* 36, 251–264. doi: 10.1007/s10484-011-9165-y

Hammond, D. C. (2001). Treatment of chronic fatigue with neurofeedback and self-hypnosis. *NeuroRehabilitation* 16, 295–300. doi: 10.3233/nre-2001-16415

Hassett, A. L., Radvanski, D. C., Vaschillo, E. G., Vaschillo, B., Sigal, L. H., Karavidas, M. K., et al. (2007). A pilot study of the efficacy of heart rate variability (HRV) biofeedback in patients with fibromyalgia. *Appl. Psychophysiol. Biofeedback* 32, 1–10. doi: 10.1007/s10484-006-9028-0

Hellyer, P. J., Shanahan, M., Scott, G., Wise, R. J. S., Sharp, D. J., and Leech, R. (2014). The control of global brain dynamics: opposing actions of frontoparietal control and default mode networks on attention. *J. Neurosci.* 34, 451–461. doi: 10.1523/JNEUROSCI.1853-13.2014

Hepsomali, P., Groeger, J. A., Nishihira, J., and Scholey, A. (2020). Effects of Oral Gamma-Aminobutyric Acid (GABA) administration on stress and sleep in humans: a systematic review. *Front. Neurosci.* 14:923. doi: 10.3389/fnins.2020.00923

Hesse, J., and Gross, T. (2014). Self-organized criticality as a fundamental property of neural systems. *Front. Syst. Neurosci.* 8:166. doi: 10.3389/fnsys.2014.00166

Hilderman, M., Qureshi, A. R., Abtahi, F., Witt, N., Jägren, C., Olbers, J., et al. (2019). The cholinergic anti-inflammatory pathway in resistant hypertension treated with renal denervation. *Mol. Med.* 25:39. doi: 10.1186/s10020-019-0097-y

Hosp, J. A., Dressing, A., Blazhenets, G., Bormann, T., Rau, A., Schwabenland, M., et al. (2021). Cognitive impairment and altered cerebral glucose metabolism in the subacute stage of COVID-19. *Brain* 144, 1263–1276. doi: 10.1093/brain/awab009

Hu, C. C., Huang, J. W., Wei, N., Hu, S. H., Hu, J. B., Li, S. G., et al. (2020). Interpersonal psychotherapy-based psychological intervention for patient suffering from COVID-19: a case report. *World J. Clin. Cases* 8, 6064–6070. doi: 10.12998/wjcc.v8.i23.6064

Huang, C., Huang, L., Wang, Y., Li, X., Ren, L., Gu, X., et al. (2021). 6-month consequences of COVID-19 in patients discharged from hospital: a cohort study. *Lancet* 397, 220–232. doi: 10.1016/S0140-6736(20)32656-8

Hunter, S. K. (2018). Performance fatigability: mechanisms and task specificity. *Cold Spring Harb. Perspect. Med.* 8, 1–22. doi: 10.1101/cshperspect.a029728

Hussman, J. P. (2021). Severe clinical worsening in COVID-19 and potential mechanisms of immune-enhanced disease. *Front. Med.* 8:949. doi: 10.3389/fmed.2021.637642

Inagaki, T. K., Muscatell, K. A., Irwin, M. R., Cole, S. W., and Eisenberger, N. I. (2012). Inflammation selectively enhances amygdala activity to socially threatening images. *Neuroimage* 59, 3222–3226. doi: 10.1016/j.neuroimage.2011.10.090

Johnson, L. (1992). An ecological approach to biosystem thermodynamics. *Biol. Philos.* 7, 35–60. doi: 10.1007/BF00130163

Kamal, M., Abo Omirah, M., Hussein, A., and Saeed, H. (2021). Assessment and characterisation of post-COVID-19 manifestations. *Int. J. Clin. Pract.* 75:e13746. doi: 10.1111/ijcp.13746

Kanberg, N., Ashton, N. J., Andersson, L. M., Yilmaz, A., Lindh, M., Nilsson, S., et al. (2020). Neurochemical evidence of astrocytic and neuronal injury commonly found in COVID-19. *Neurology* 95, e1754–e1759. doi: 10.1212/WNL.0000000000010111

Karavidas, M. K., Lehrer, P. M., Vaschillo, E., Vaschillo, B., Marin, H., Buyske, S., et al. (2007). Preliminary results of an open label study of heart rate variability biofeedback for the treatment of major depression. *Appl. Psychophysiol. Biofeedback* 32, 19–30. doi: 10.1007/s10484-006-9029-z

Kayaaslan, B., Eser, F., Kalem, A. K., Kaya, G., Kaplan, B., Kacar, D., et al. (2021). Post-COVID syndrome: a single-center questionnaire study on 1007 participants recovered from COVID-19. *J. Med. Virol.* 93, 6566–6574. doi: 10.1002/jmv.27198

Kerson, C., Sherman, R. A., and Kozlowski, G. P. (2009). Alpha suppression and symmetry training for generalized anxiety symptoms. *J. Neurother.* 13, 146–155. doi: 10.1080/10874200903107405

Kevetter, G. A., and Winans, S. S. (1981). Connections of the corticomedial amygdala in the golden hamster. II. Efferents of the "olfactory amygdala.". *J. Comp. Neurol.* 197, 99–111. doi: 10.1002/cne.901970108

Kim, M. J., Loucks, R. A., Palmer, A. L., Brown, A. C., Solomon, K. M., Marchante, A. N., et al. (2011). The structural and functional connectivity of the amygdala: from normal emotion to pathological anxiety. *Behav. Brain Res.* 223, 403–410. doi: 10.1016/j.bbr.2011.04.025

Kincaid, K. J., Kung, J. C., Senetar, A. J., Mendoza, D., Bonnin, D. A., Purtlebaugh, W. L., et al. (2021). Post-COVID seizure: a new feature of "long-COVID.". *eNeurologicalSci* 23:100340. doi: 10.1016/j.ensci.2021.100340

Klimesch, W. (1999). EEG alpha and theta oscillations reflect cognitive and memory performance: a review and analysis. *Brain Res. Rev.* 29, 169–195. doi: 10.1016/S0165-0173(98)00056-3

Komaroff, A. L., and Lipkin, W. I. (2021). Insights from myalgic encephalomyelitis/chronic fatigue syndrome may help unravel the pathogenesis of postacute COVID-19 syndrome. *Trends Mol. Med.* 27, 895–906. doi: 10.1016/j.molmed.2021.06.002

Koush, Y., Rosa, M. J., Robineau, F., Heinen, K., Rieger, S. W., Weiskopf, N., et al. (2013). Connectivity-based neurofeedback: dynamic causal modeling for real-time fMRI. *Neuroimage* 81, 422–430. doi: 10.1016/j.neuroimage.2013.05.010

Koutroumanidis, M., Gratwicke, J., Sharma, S., Whelan, A., Tan, S. V., and Glover, G. (2021). Alpha coma EEG pattern in patients with severe COVID-19 related encephalopathy. *Clin. Neurophysiol.* 132, 218–225. doi: 10.1016/j.clinph.2020.09.008

Kubota, T., Gajera, P. K., and Kuroda, N. (2021). Meta-analysis of EEG findings in patients with COVID-19. *Epilepsy Behav.* 115:107682. doi: 10.1016/j.yebeh.2020.107682

Kumar, A., Pareek, V., Prasoon, P., Faiq, M. A., Kumar, P., Kumari, C., et al. (2020). Possible routes of SARS-CoV-2 invasion in brain: in context of neurological symptoms in COVID-19 patients. *J. Neurosci. Res.* 98, 2376–2383. doi: 10.1002/jnr.24717

Lafrance, C., and Dumont, M. (2000). Diurnal variations in the waking EEG: comparisons with sleep latencies and subjective alertness. *J. Sleep Res.* 9, 243–248. doi: 10.1046/j.1365-2869.2000.00204.x

Legarda, S. B., McMahon, D., Othmer, S., and Othmer, S. (2011). Clinical neurofeedback: case studies, proposed mechanism, and implications for pediatric neurology practice. *J. Child Neurol.* 26, 1045–1051. doi: 10.1177/0883073811405052

Lehrer, P., Karavidas, M. K., Lu, S. E., Coyle, S. M., Oikawa, L. O., MacOr, M., et al. (2010). Voluntarily produced increases in heart rate variability modulate autonomic effects of endotoxin induced systemic inflammation: an exploratory study. *Appl. Psychophysiol. Biofeedback* 35, 303–315. doi: 10.1007/s10484-010-9139-5

Lehrer, P., Kaur, K., Sharma, A., Shah, K., Huseby, R., Bhavsar, J., et al. (2020). Heart rate variability biofeedback improves emotional and physical health and performance: a systematic review and meta analysis. *Appl. Psychophysiol. Biofeedback* 45, 109–129. doi: 10.1007/s10484-020-09466-z

Lehrer, P. M., and Gevirtz, R. (2014). Heart rate variability biofeedback: how and why does it work? *Front. Psychol.* 5:756. doi: 10.3389/fpsyg.2014.00756

Lehrer, P. M., Vaschillo, E., Vaschillo, B., Lu, S. E., Eckberg, D. L., Edelberg, R., et al. (2003). Heart rate variability biofeedback increases baroreflex gain and peak expiratory flow. *Psychosom. Med.* 65, 796–805. doi: 10.1097/01.PSY.0000089200.81962.19

Libby, P., and Lüscher, T. (2020). COVID-19 is, in the end, an endothelial disease. *Eur. Heart J.* 41, 3038–3044. doi: 10.1093/eurheartj/ehaa623

Lim, S. T., Janaway, B., Costello, H., Trip, A., and Price, G. (2020). Persistent psychotic symptoms following COVID-19 infection. *BJPsych Open* 6:e105. doi: 10.1192/bjo.2020.76

Lin, I. M., Fan, S. Y., Yen, C. F., Yeh, Y. C., Tang, T. C., Huang, M. F., et al. (2019). Erratum: and improved symptoms of depression and insomnia among patients with major depression disorder. *Clin. Psychopharmacol. Neurosci.* 17:458.

Lin, L. H., Moore, S. A., Jones, S. Y., McGlashon, J., and Talman, W. T. (2013). Astrocytes in the rat nucleus tractus solitarii are critical for cardiovascular reflex control. *J. Neurosci.* 33, 18608–18617. doi: 10.1523/JNEUROSCI.3257-13.2013

Lorkiewicz, P., and Waszkiewicz, N. (2021). Biomarkers of post-COVID depression. *J. Clin. Med.* 10:4142. doi: 10.3390/jcm10184142

Lu, Y., Li, X., Geng, D., Mei, N., Wu, P. Y., Huang, C. C., et al. (2020). Cerebral micro-structural changes in COVID-19 patients – an MRI-based 3-month follow-up study: a brief title: cerebral changes in COVID-19. *EClinicalMedicine* 25:100484. doi: 10.1016/j.eclinm.2020.100484

Lukiw, W. J., Pogue, A., and Hill, J. M. (2020). SARS-CoV-2 infectivity and neurological targets in the brain. *Cell. Mol. Neurobiol.* 42, 217–224. doi: 10.1007/s10571-020-00947-7

Ma, Z., Turrigiano, G. G., Wessel, R., and Hengen, K. B. (2019). Cortical circuit dynamics are homeostatically tuned to criticality in vivo. *Neuron* 104, 655.e4–664.e4. doi: 10.1016/j.neuron.2019.08.031

Mahmud, R., Rahman, M. M., Rassel, M. A., Monayem, F. B., Sayeed, S. K. J. B., Islam, M. S., et al. (2021). Post-COVID-19 syndrome among symptomatic COVID-19 patients: a prospective cohort study in a tertiary care center of Bangladesh. *PLoS One* 16:e249644. doi: 10.1371/journal.pone.0249644

Mao, L., Jin, H., Wang, M., Hu, Y., Chen, S., He, Q., et al. (2020). Neurological manifestations of hospitalized patients with coronavirus disease 2019 in Wuhan, China. *JAMA Neurol.* 77, 683–690. doi: 10.1001/jamaneurol.2020.1127

Markiewicz, R., and Dobrowolska, B. (2020). Cognitive and social rehabilitation in schizophrenia—from neurophysiology to neuromodulation. Pilot study. *Int. J. Environ. Res. Public Health* 17, 7–10. doi: 10.3390/ijerph17114034

Mather, M., and Thayer, J. F. (2018). How heart rate variability affects emotion regulation brain networks. *Curr. Opin. Behav. Sci.* 19, 98–104. doi: 10.1016/j.cobeha.2017.12.017

May, R. W., Seibert, G. S., Sanchez-Gonzalez, M. A., and Fincham, F. D. (2019). Self-regulatory biofeedback training: an intervention to reduce school burnout and improve cardiac functioning in college students. *Stress* 22, 1–8. doi: 10.1080/10253890.2018.1501021

Mayi, B. S., Leibowitz, J. A., Woods, A. T., Ammon, K. A., Liu, A. E., and Raja, A. (2021). The role of Neuropilin-1 in COVID-19. *PLoS Pathog.* 17:e1009153. doi: 10.1371/journal.ppat.1009153

Meinhardt, J., Radke, J., Dittmayer, C., Franz, J., Thomas, C., Mothes, R., et al. (2021). Olfactory transmucosal SARS-CoV-2 invasion as a port of central nervous system entry in individuals with COVID-19. *Nat. Neurosci.* 24, 168–175. doi: 10.1038/s41593-020-00758-5

Meini, S., Suardi, L. R., Busoni, M., Roberts, A. T., and Fortini, A. (2020). Olfactory and gustatory dysfunctions in 100 patients hospitalized for COVID-19: sex differences and recovery time in real-life. *Eur. Arch. Oto-Rhino-Laryngology* 277, 3519–3523. doi: 10.1007/s00405-020-06102-8

Möhler, H. (2006). GABAA receptors in central nervous system disease: anxiety, epilepsy, and insomnia. *J. Recept. Signal Transduct.* 26, 731–740. doi: 10.1080/10799890600920035

Morand, A., Campion, J. Y., Lepine, A., Bosdure, E., Luciani, L., Cammilleri, S., et al. (2021). Similar patterns of [18F]-FDG brain PET hypometabolism in paediatric and adult patients with long COVID: a paediatric case series. *Eur. J. Nucl. Med. Mol. Imaging [Online ahead of print]* 1–8. doi: 10.1007/s00259-021-05528-4

Morbelli, S., Chiola, S., Donegani, M. I., Arnaldi, D., Pardini, M., Mancini, R., et al. (2022). Metabolic correlates of olfactory dysfunction in COVID-19 and Parkinson's disease (PD) do not overlap. *Eur. J. Nucl. Med. Mol. Imaging [Online ahead of print]* doi: 10.1007/s00259-021-05666-9

Morgul, E., Bener, A., Atak, M., Akyel, S., Aktaş, S., Bhugra, D., et al. (2021). COVID-19 pandemic and psychological fatigue in Turkey. *Int. J. Soc. Psychiatry* 67, 128–135. doi: 10.1177/0020764020941889

Mottaz, A., Solcà, M., Magnin, C., Corbet, T., Schnider, A., and Guggisberg, A. G. (2015). Clinical Neurophysiology Neurofeedback training of alpha-band coherence enhances motor performance. *Clin. Neurophysiol.* 126, 1754–1760. doi: 10.1016/j.clinph.2014.11.023

Najjar, S., Najjar, A., Chong, D. J., Pramanik, B. K., Kirsch, C., Kuzniecky, R. I., et al. (2020). Central nervous system complications associated with SARS-CoV-2 infection: integrative concepts of pathophysiology and case reports. *J. Neuroinflammation* 17:231. doi: 10.1186/s12974-020-01896-0

Nemzer, L. R., Cravens, G. D., Worth, R. M., Motta, F., Placzek, A., Castro, V., et al. (2021). Critical and Ictal Phases in Simulated EEG Signals on a Small-World Network. *Front. Comput. Neurosci.* 14:583350. doi: 10.3389/fncom.2020.583350

Niesen, M., Trotta, N., Noel, A., Coolen, T., Fayad, G., Leurkin-Sterk, G., et al. (2021). Structural and metabolic brain abnormalities in COVID-19 patients with sudden loss of smell. *Eur. J. Nucl. Med. Mol. Imaging* 48, 1890–1901. doi: 10.1007/s00259-020-05154-6

Othmer, S., and Othmer, S. F. (2017). *Toward a Frequency-Based Theory of Neurofeedback*. Woodland Hills, CA: The EEG Institute, doi: 10.1016/B978-0-12-803726-3.00008-0

Othmer, S. F. (2020). "History of the Othmer method: an evolving clinical model and process," in *Neurofeedback*, eds J. R. Evans, M. B. Dellinger, and H. L. Russell (Cambridge, MA: Academic Press), 327–334.

Paquette, V., Beauregard, M., and Beaulieu-Prévost, D. (2009). Effect of a psychoneurotherapy on brain electromagnetic tomography in individuals with major depressive disorder. *Psychiatry Res. - Neuroimag.* 174, 231–239. doi: 10.1016/j.pscychresns.2009.06.002

Park, S., Majoka, H., Sheikh, A., and Ali, I. (2021). A presumed case of new-onset focal seizures as a delayed complication of COVID-19 infection. *Epilepsy Behav. Rep.* 16:100447. doi: 10.1016/j.ebr.2021.100447

Pasini, E., Bisulli, F., Volpi, L., Minardi, I., Tappatà, M., Muccioli, L., et al. (2020). EEG findings in COVID-19 related encephalopathy. *Clin. Neurophysiol.* 131, 2265–2267. doi: 10.1016/j.clinph.2020.07.003

Pastukhov, A., García-Rodríguez, P. E., Haenicke, J., Guillamon, A., Deco, G., and Braun, J. (2013). Multi-stable perception balances stability and sensitivity. *Front. Comput. Neurosci.* 7:17. doi: 10.3389/fncom.2013.00017

Patel, K., Sutherland, H., Henshaw, J., Taylor, J. R., Brown, C. A., Casson, A. J., et al. (2020). Effects of neurofeedback in the management of chronic pain: a systematic review and meta-analysis of clinical trials. *Eur. J. Pain (United Kingdom)* 24, 1440–1457. doi: 10.1002/ejp.1612

Paterson, R. W., Brown, R. L., Benjamin, L., Nortley, R., Wiethoff, S., Bharucha, T., et al. (2020). The emerging spectrum of COVID-19 neurology: clinical, radiological and laboratory findings. *Brain* 143, 3104–3120. doi: 10.1093/brain/awaa240

Pattnaik, J. I., Deepthi, R. A., Dua, S., Padhan, P., and Ravan, J. R. (2021). Role of tofisopam in post COVID neuro-psychiatric sequelae: a case series. *Indian J. Psychol. Med.* 43, 174–176. doi: 10.1177/0253717621994285

Pellinen, J., Carroll, E., Friedman, D., Boffa, M., Dugan, P., Friedman, D. E., et al. (2020). Continuous EEG findings in patients with COVID-19 infection admitted to a New York academic hospital system. *Epilepsia* 61, 2097–2105. doi: 10.1111/epi.16667

Perlis, M. L., Merica, H., Smith, M. T., and Giles, D. E. (2001). Beta EEG activity and insomnia. *Sleep Med. Rev.* 5, 365–376. doi: 10.1053/smrv.2001.0151

Pilotto, A., Cristillo, V., Cotti Piccinelli, S., Zoppi, N., Bonzi, G., Sattin, D., et al. (2021). Long-term neurological manifestations of COVID-19: prevalence and predictive factors. *Neurol. Sci.* 42, 4903–4907. doi: 10.1007/s10072-021-05586-4

Pittman, Q. J. (2011). A neuro-endocrine-immune symphony. *J. Neuroendocrinol.* 23, 1296–1297. doi: 10.1111/j.1365-2826.2011.02176.x

Poel, W., Daniels, B. C., Sosna, M. M. G., Twomey, C. R., Leblanc, S. P., Couzin, I. D., et al. (2021). Subcritical escape waves in schooling fish. *arXiv* [Preprint]. arXiv:2108.05537

Putman (2004). *Supported Projects Presented at the 12th Annual ISNR Conference*, Vol. 9. Abu Dhabi: International Society for Neuroregulation & Research, 99–101.

Reiner, R. (2008). Integrating a portable biofeedback device into clinical practice for patients with anxiety disorders: results of a pilot study. *Appl. Psychophysiol. Biofeedback* 33, 55–61. doi: 10.1007/s10484-007-9046-6

Reisert, M., Weiller, C., and Hosp, J. A. (2021). Displaying the autonomic processing network in humans – a global tractography approach. *Neuroimage* 231:117852. doi: 10.1016/j.neuroimage.2021.117852

Ros, T., Baars, B. J., Lanius, R. A., and Vuilleumier, P. (2014). Tuning pathological brain oscillations with neurofeedback: a systems neuroscience framework. *Front. Hum. Neurosci.* 8:1008. doi: 10.3389/fnhum.2014.01008

Ros, T., Frewen, P., Théberge, J., Michela, A., Kluetsch, R., Mueller, A., et al. (2017). Neurofeedback tunes scale-free dynamics in spontaneous brain activity. *Cereb. Cortex* 27, 4911–4922. doi: 10.1093/cercor/bhw285

Rudroff, T., Kamholz, J., Fietsam, A. C., Deters, J. R., and Bryant, A. D. (2020). Post-covid-19 fatigue: potential contributing factors. *Brain Sci.* 10:1012. doi: 10.3390/brainsci10121012

Rudroff, T., Workman, C. D., and Ponto, L. L. B. (2021). 18 F-FDG-PET imaging for post-COVID-19 brain and skeletal muscle alterations. *Viruses* 13:2283. doi: 10.3390/v13112283

Samkaria, A., Punjabi, K., Sharma, S., Joon, S., Sandal, K., Dasgupta, T., et al. (2021). Brain stress mapping in COVID-19 survivors using MR spectroscopy: new avenue of mental health status monitoring. *J. Alzheimer's Dis.* 83, 523–530. doi: 10.3233/JAD-210287

Sangare, A., Dong, A., Valente, M., Pyatigorskaya, N., Cao, A., Altmayer, V., et al. (2020). Neuroprognostication of consciousness recovery in a patient with covid-19 related encephalitis: preliminary findings from a multimodal approach. *Brain Sci.* 10:845. doi: 10.3390/brainsci10110845

Sauseng, P., Klimesch, W., Schabus, M., and Doppelmayr, M. (2005). Fronto-parietal EEG coherence in theta and upper alpha reflect central executive functions of working memory. *Int. J. Psychophysiol.* 57, 97–103. doi: 10.1016/j.ijpsycho.2005.03.018

Schiene, K., Bruehl, C., Zilles, K., Qü, M., Hagemann, G., Kraemer, M., et al. (1996). Neuronal hyperexcitability and reduction of GABA(A)-receptor expression in the surround of cerebral photothrombosis. *J. Cereb. Blood Flow Metab.* 16, 906–914. doi: 10.1097/00004647-199609000-00014

Selvaraj, K., Ravichandran, S., Krishnan, S., Radhakrishnan, R. K., Manickam, N., and Kandasamy, M. (2021). Testicular atrophy and hypothalamic pathology in COVID-19: possibility of the incidence of male infertility and HPG axis abnormalities. *Reprod. Sci.* 28, 2735–2742. doi: 10.1007/s43032-020-00441-x

Shaikh, A. G., Hong, S., Liao, K., Tian, J., Solomon, D., Zee, D. S., et al. (2010). Oculopalatal tremor explained by a model of inferior olivary hypertrophy and cerebellar plasticity. *Brain* 133, 923–940. doi: 10.1093/brain/awp323

Shibata, K., Lisi, G., Cortese, A., Watanabe, T., Sasaki, Y., and Kawato, M. (2019). Toward a comprehensive understanding of the neural mechanisms of decoded neurofeedback. *Neuroimage* 188, 539–556. doi: 10.1016/j.neuroimage.2018.12.022

Sime, A. (2004). Case study of trigeminal neuralgia using neurofeedback and peripheral biofeedback. *J. Neurother.* 8, 59–71. doi: 10.1300/J184v08n01_05

Slaats, J., ten Oever, J., van de Veerdonk, F. L., and Netea, M. G. (2016). IL-1β/IL-6/CRP and IL-18/ferritin: distinct inflammatory programs in infections. *PLoS Pathog.* 12:e1005973. doi: 10.1371/journal.ppat.1005973

Slevin, M., Elisa Garcia-Lara, E., Capitanescu, B., Sanfeliu, C., Zeinolabediny, Y., Albaradie, R., et al. (2020). Monomeric c-reactive protein aggravates secondary degeneration after intracerebral haemorrhagic stroke and may function as a sensor for systemic inflammation. *J. Clin. Med.* 9:3053. doi: 10.3390/jcm9093053

Sollini, M., Morbelli, S., Ciccarelli, M., Cecconi, M., Aghemo, A., Morelli, P., et al. (2021). Long COVID hallmarks on [18F]FDG-PET/CT: a case-control study. *Eur. J. Nucl. Med. Mol. Imaging* 48, 3187–3197. doi: 10.1007/s00259-021-05294-3

Solomon, I. H., Normandin, E., Bhattacharyya, S., Mukerji, S. S., Keller, K., Ali, A. S., et al. (2020). Neuropathological features of Covid-19. *N. Engl. J. Med.* 383, 989–992. doi: 10.1056/NEJMc2019373

Spielmanns, M., Pekacka-Egli, A. M., Schoendorf, S., Windisch, W., and Hermann, M. (2021). Effects of a comprehensive pulmonary rehabilitation in severe post-covid-19 patients. *Int. J. Environ. Res. Public Health* 18:2695. doi: 10.3390/ijerph18052695

Stam, C. J. (2005). Nonlinear dynamical analysis of EEG and MEG: review of an emerging field. *Clin. Neurophysiol.* 116, 2266–2301. doi: 10.1016/j.clinph.2005.06.011

Stavem, K., Ghanima, W., Olsen, M. K., Gilboe, H. M., and Einvik, G. (2021). Prevalence and determinants of fatigue after covid-19 in non-hospitalized subjects: a population-based study. *Int. J. Environ. Res. Public Health* 18:2030. doi: 10.3390/ijerph18042030

Steiner, I., Nisipianu, P., and Wirguin, I. (2001). Infection and the etiology and pathogenesis of multiple sclerosis. *Curr. Neurol. Neurosci. Rep.* 1, 271–276. doi: 10.1007/s11910-001-0030-x

Strauss, G. P., and Cohen, A. S. (2017). A transdiagnostic review of negative symptom phenomenology and etiology. *Schizophr. Bull.* 43, 712–729. doi: 10.1093/schbul/sbx066

Sun, B., Tang, N., Peluso, M. J., Iyer, N. S., Torres, L., Donatelli, J. L., et al. (2021). Characterization and biomarker analyses of post-covid-19 complications and neurological manifestations. *Cells* 10:386. doi: 10.3390/cells10020386

Swenne, C. A. (2013). Baroreflex sensitivity: mechanisms and measurement. *Netherlands Hear. J.* 21, 58–60. doi: 10.1007/s12471-012-0346-y

Takagishi, M., Waki, H., Bhuiyan, M. E. R., Gouraud, S. S., Kohsaka, A., Cui, H., et al. (2010). IL-6 microinjected in the nucleus tractus solitarii attenuates cardiac baroreceptor reflex function in rats. *Am. J. Physiol. - Regul. Integr. Comp. Physiol.* 298, 183–190. doi: 10.1152/ajpregu.00176.2009

Takahashi, T., Ellingson, M. K., Wong, P., Israelow, B., Lucas, C., Klein, J., et al. (2020). Sex differences in immune responses that underlie COVID-19 disease outcomes. *Nature* 588, 315–320. doi: 10.1038/s41586-020-2700-3

Takeuchi, N., and Izumi, S. I. (2012). Maladaptive plasticity for motor recovery after stroke: mechanisms and approaches. *Neural Plast.* 2012:359728. doi: 10.1155/2012/359728

Tan, T., Khoo, B., Mills, E. G., Phylactou, M., Patel, B., Eng, P. C., et al. (2020). Association between high serum total cortisol concentrations and mortality from COVID-19. *Lancet Diabetes Endocrinol.* 8, 659–660. doi: 10.1016/S2213-8587(20)30216-3

Tang, Z., Ye, G., Chen, X., Pan, M., Fu, J., Fu, T., et al. (2018). Peripheral proinflammatory cytokines in Chinese patients with generalised anxiety disorder. *J. Affect. Disord.* 225, 593–598. doi: 10.1016/j.jad.2017.08.082

Tay, M. Z., Poh, C. M., Rénia, L., MacAry, P. A., and Ng, L. F. P. (2020). The trinity of COVID-19: immunity, inflammation and intervention. *Nat. Rev. Immunol.* 20, 363–374. doi: 10.1038/s41577-020-0311-8

Teigen, K. H. (1994). Yerkes-Dodson: a law for all seasons. *Theory Psychol.* 4, 525–547. doi: 10.1177/0959354394044004

Thye, A. Y.-K., Law, J. W. F., Tan, L. T. H., Pusparajah, P., Ser, H. L., Thurairajasingam, S., et al. (2022). Psychological symptoms in COVID-19 Patients (2022): insights into pathophysiology and risk factors of long COVID-19. *Biology* 11:61. doi: 10.3390/biology11010061

Townsend, L., Dyer, A. H., Jones, K., Dunne, J., Mooney, A., Gaffney, F., et al. (2020). Persistent fatigue following SARS-CoV-2 infection is common and independent of severity of initial infection. *PLoS One* 15:e0240784. doi: 10.1371/journal.pone.0240784

Townsend, L., Moloney, D., Finucane, C., McCarthy, K., Bergin, C., Bannan, C., et al. (2021). Fatigue following COVID-19 infection is not associated with autonomic dysfunction. *PLoS One* 16:e0247280. doi: 10.1371/journal.pone.0247280

Tracy, L. M., Ioannou, L., Baker, K. S., Gibson, S. J., Georgiou-Karistianis, N., and Giummarra, M. J. (2016). Meta-analytic evidence for decreased heart rate variability in chronic pain implicating parasympathetic nervous system dysregulation. *Pain* 157, 7–29. doi: 10.1097/j.pain.0000000000000360

Trotti, L. M., Saini, P., Bliwise, D. L., Freeman, A. A., Jenkins, A., and Rye, D. B. (2015). Clarithromycin in γ-aminobutyric acid-Related hypersomnolence: a randomized, crossover trial. *Ann. Neurol.* 78, 454–465. doi: 10.1002/ana.24459

Tsuchiyagaito, A., Smith, J. L., El-Sabbagh, N., Zotev, V., Misaki, M., Al Zoubi, O., et al. (2021). Real-time fMRI neurofeedback amygdala training may influence kynurenine pathway metabolism in major depressive disorder. *NeuroImage Clin.* 29:102559. doi: 10.1016/j.nicl.2021.102559

Turrigiano, G. G., and Nelson, S. B. (2000). Hebb and homeostasis in neuronal plasticity. *Curr. Opin. Neurobiol.* 10, 358–364. doi: 10.1016/S0959-4388(00)00091-X

Van Boxtel, G. J. M., Denissen, A. J. M., Jäger, M., Vernon, D., Dekker, M. K. J., Mihajlović, V., et al. (2012). A novel self-guided approach to alpha activity training. *Int. J. Psychophysiol.* 83, 282–294. doi: 10.1016/j.ijpsycho.2011.11.004

van der Zwan, J. E., de Vente, W., Huizink, A. C., Bögels, S. M., and de Bruin, E. I. (2015). Physical activity, mindfulness meditation, or heart rate variability biofeedback for stress reduction: a randomized controlled trial. *Appl. Psychophysiol. Biofeedback* 40, 257–268. doi: 10.1007/s10484-015-9293-x

Vaschillo, E., Vaschillo, B., Buckman, J., and Bates, M. (2019). New approach for brain stimulation. *Brain Stimul.* 12:393. doi: 10.1016/j.brs.2018.12.263

Visvabharathy, L., Hanson, B., Orban, Z., Lim, P. H., Palacio, N. M., Jain, R., et al. (2021). Neuro-COVID long-haulers exhibit broad dysfunction in T cell memory generation and responses to vaccination. *medRxiv [Preprint]*. doi: 10.1101/2021.08.08.21261763

Walker, J. E. (2010). Recent advances in quantitative EEG as an aid to diagnosis and as a guide to neurofeedback training for cortical hypofunctions, hyperfunctions, disconnections, and hyperconnections: improving efficacy in complicated neurological and psychological disorder. *Appl. Psychophysiol. Biofeedback* 35, 25–27. doi: 10.1007/s10484-009-9107-0

Walker, J. E. (2011). QEEG-guided neurofeedback for recurrent migraine headaches. *Clin. EEG Neurosci.* 42, 59–61. doi: 10.1177/155005941104200112

Walker, J. E., and Kozlowski, G. P. (2005). Neurofeedback treatment of epilepsy. *Child Adolesc. Psychiatr. Clin. N. Am.* 14, 163–176. doi: 10.1016/j.chc.2004.07.009

Walsh-Messinger, J., Manis, H., Vrabec, A., Sizemore, Bs, J., Bishof, K., Debidda, M., et al. (2021). The kids are not alright: a preliminary report of Post-COVID syndrome in university students. *J. Am. Coll. Health [Online ahead of print]* 1–7. doi: 10.1080/07448481.2021.1927053

Wang, R., Chen, J., Gao, K., Hozumi, Y., Yin, C., and Wei, G. W. (2021). Analysis of SARS-CoV-2 mutations in the United States suggests presence of four substrains and novel variants. *Commun. Biol.* 4:228. doi: 10.1038/s42003-021-01754-6

Wang, X., Tan, L., Wang, X., Liu, W., Lu, Y., Cheng, L., et al. (2020). Comparison of nasopharyngeal and oropharyngeal swabs for SARS-CoV-2 detection in 353 patients received tests with both specimens simultaneously. *Int. J. Infect. Dis.* 94, 107–109. doi: 10.1016/j.ijid.2020.04.023

Watanabe, M., Maemura, K., Kanbara, K., Tamayama, T., and Hayasaki, H. (2002). GABA and GABA receptors in the central nervous system and other organs. *Int. Rev. Cytol.* 213, 1–47. doi: 10.1016/S0074-7696(02)13011-7

Watanabe, T., Sasaki, Y., Shibata, K., and Kawato, M. (2017). Advances in fMRI Real-Time Neurofeedback. *Trends Cogn. Sci.* 21, 997–1010. doi: 10.1016/j.tics.2017.09.010

Wenting, A., Gruters, A., van Os, Y., Verstraeten, S., Valentijn, S., Ponds, R., et al. (2020). COVID-19 neurological manifestations and underlying mechanisms: a scoping review. *Front. Psychiatry* 11:860. doi: 10.3389/fpsyt.2020.00860

Wichmann, D., Sperhake, J. P., Lütgehetmann, M., Steurer, S., Edler, C., Heinemann, A., et al. (2020). Autopsy findings and venous thromboembolism in patients with COVID-19: a prospective cohort study. *Ann. Intern. Med.* 173, 268–277. doi: 10.7326/M20-2003

Windthorst, P., Mazurak, N., Kuske, M., Hipp, A., Giel, K. E., Enck, P., et al. (2017). Heart rate variability biofeedback therapy and graded exercise training in management of chronic fatigue syndrome: an exploratory pilot study. *J. Psychosom. Res.* 93, 6–13. doi: 10.1016/j.jpsychores.2016.11.014

Workman, C., Boles-Ponto, L., Kamholz, J., Bryant, A., and Rudroff, T. (2021). Transcranial direct current stimulation and Post-COVID-19-Fatigue. *Brain Stimul.* 14, 1672–1673. doi: 10.1016/j.brs.2021.10.268

Workman, C. D., Kamholz, J., and Rudroff, T. (2020). Transcranial direct current stimulation (tDCS) for the treatment of a Multiple Sclerosis symptom cluster. *Brain Stimul.* 13, 263–264. doi: 10.1016/j.brs.2019.09.012

Wostyn, P. (2021). COVID-19 and chronic fatigue syndrome: is the worst yet to come? *Med. Hypotheses* 146:110469. doi: 10.1016/j.mehy.2020.110469

Wu, T., Zuo, Z., Kang, S., Jiang, L., Luo, X., Xia, Z., et al. (2020). Multi-organ dysfunction in patients with COVID-19: a systematic review and meta-analysis. *Aging Dis.* 11, 874–894. doi: 10.14336/AD.2020.0520

Wyler, A. R., Lockard, J. S., Ward, A. A., and Finch, C. A. (1976). Conditioned EEG desynchronization and seizure occurrence in patients. *Electroencephalogr. Clin. Neurophysiol.* 41, 501–512. doi: 10.1016/0013-4694(76)90062-6

Xiong, Q., Xu, M., Li, J., Liu, Y., Zhang, J., Xu, Y., et al. (2021). Clinical sequelae of COVID-19 survivors in Wuhan, China: a single-centre longitudinal study. *Clin. Microbiol. Infect.* 27, 89–95. doi: 10.1016/j.cmi.2020.09.023

Yamada, T., Hashimoto, R. I., Yahata, N., Ichikawa, N., Yoshihara, Y., Okamot, Y., et al. (2017). Resting-state functional connectivity-based biomarkers and functional MRI-based neurofeedback for psychiatric disorders: a challenge for developing theranostic biomarkers. *Int. J. Neuropsychopharmacol.* 20, 769–781. doi: 10.1093/ijnp/pyx059

Yang, X., Yang, X., Kumar, P., Cao, B., Ma, X., and Li, T. (2020). Social support and clinical improvement in COVID-19 positive patients in China. *Nurs. Outlook* 68, 830–837. doi: 10.1016/j.outlook.2020.08.008

Yong, S. J. (2021). Persistent brainstem dysfunction in long-COVID: a hypothesis. *ACS Chem. Neurosci.* 12, 573–580. doi: 10.1021/acschemneuro.0c00793

Young, J. J., Bruno, D., and Pomara, N. (2014). A review of the relationship between proinflammatory cytokines and major depressive disorder. *J. Affect. Disord.* 169, 15–20. doi: 10.1016/j.jad.2014.07.032

Younger, D. S. (2021). Post-acute sequelae of SARS-Cov-2 infection associating peripheral, autonomic and central nervous system disturbances: case report and review of the literature. *World J. Neurosci.* 11, 17–21. doi: 10.4236/wjns.2021.111003

Zald, D. H., and Pardo, J. V. (1997). Emotion, olfaction, and the human amygdala: amygdala activation during aversive olfactory stimulation. *Proc. Natl. Acad. Sci. U.S.A.* 94, 4119–4124. doi: 10.1073/pnas.94.8.4119

Zarei, M., Bose, D., Nouri-Vaskeh, M., Tajiknia, V., Zand, R., and Ghasemi, M. (2021). Long-term side effects and lingering symptoms post COVID-19 recovery. *Rev. Med. Virol.* e2289. doi: 10.1002/rmv.2289

Zhigalov, A., Kaplan, A., and Palva, J. M. (2016). Modulation of critical brain dynamics using closed-loop neurofeedback stimulation. *Clin. Neurophysiol.* 127, 2882–2889. doi: 10.1016/j.clinph.2016.04.028

Zhou, M., Cai, J., Sun, W., Wu, J., Wang, Y., Gamber, M., et al. (2021). Do post-COVID-19 symptoms exist? A longitudinal study of COVID-19 sequelae in Wenzhou, China. *Ann. Med. Psychol. (Paris).* 179, 818–821. doi: 10.1016/j.amp.2021.03.003

Zimmern, V. (2020). Why brain criticality is clinically relevant: a scoping review. *Front. Neural Circuits* 14:54. doi: 10.3389/fncir.2020.00054

Conflict of Interest: The authors declare that the research was conducted in the absence of any commercial or financial relationships that could be construed as a potential conflict of interest.

Publisher's Note: All claims expressed in this article are solely those of the authors and do not necessarily represent those of their affiliated organizations, or those of the publisher, the editors and the reviewers. Any product that may be evaluated in this article, or claim that may be made by its manufacturer, is not guaranteed or endorsed by the publisher.

frontiers | Frontiers in Psychiatry

ORIGINAL RESEARCH
published: 04 July 2022
doi: 10.3389/fpsyt.2022.822677

The Neural Correlates of the Abnormal Implicit Self-Esteem in Major Depressive Disorder: An Event-Related Potential Study

Chen-guang Jiang[1†], Heng Lu[1†], Jia-zhao Zhang[2], Xue-zheng Gao[1], Jun Wang[1] and Zhen-he Zhou[1*]*

[1] Department of Psychiatry, The Affiliated Wuxi Mental Health Center of Nanjing Medical University, Wuxi, China, [2] 3 Grade 2019 Class 6, Basic Medicine College of Jinzhou Medical University, Jinzhou, China

OPEN ACCESS

Edited by:
Jiaojian Wang,
University of Electronic Science and Technology of China, China

Reviewed by:
Alexander Nikolaevich Savostyanov,
State Scientific Research Institute of Physiology and Basic Medicine, Russia
Drozdstoy Stoyanov Stoyanov,
Plovdiv Medical University, Bulgaria

***Correspondence:**
Jun Wang
woodfish2@126.com
Zhen-he Zhou
zhouzh@njmu.edu.cn

[†]These authors share first authorship

Specialty section:
This article was submitted to Neuroimaging and Stimulation, a section of the journal Frontiers in Psychiatry

Received: 26 November 2021
Accepted: 08 June 2022
Published: 04 July 2022

Citation:
Jiang C-g, Lu H, Zhang J-z, Gao X-z, Wang J and Zhou Z-h (2022) The Neural Correlates of the Abnormal Implicit Self-Esteem in Major Depressive Disorder: An Event-Related Potential Study. Front. Psychiatry 13:822677. doi: 10.3389/fpsyt.2022.822677

Implicit self-esteem (ISE) has been considered a critical factor in the development and maintenance of major depressive disorder (MDD). Further investigating the event-related potential (ERP) characteristics underlying abnormal ISE in MDD would be helpful for understanding the neural mechanism of MDD. For this purpose, 32 MDD patients and 31 age- and sex-matched healthy controls (HCs) were enrolled in this study. The Rosenberg Self-Esteem Scale (RSES) was used to evaluate explicit self-esteem (ESE), and a self-esteem go/no-go association task (GNAT) was used to assess ISE. Electroencephalograms were synchronously recorded when performing the self-esteem GNAT. Behavioral data and ERP characteristics under different conditions were analyzed and compared within and across groups. The results showed that compared to HCs, MDD patients had significantly lower RSES scores and *self*-D scores of GNAT, which reflected lower levels of ESE and ISE, respectively. No significant correlation was found between RESE and *self*-D scores, and only RESE scores were significantly negatively correlated with the Hamilton Depression Rating Scale (HAMD) score. The averaged centroparietal go-P3 amplitude under the *self-positive* condition was significantly smaller in MDD than in HCs. Moreover, HCs had a significantly larger average centroparietal go-P3 amplitude in *self-positive* than in *self-negative* conditions, while this pattern was opposite in the MDD group. The neural activity patterns for *other* conditions were similar between MDD and HCs. Our results suggested that patients with MDD have a decreased level of both ESE and ISE, and ISE might be more independent of clinical symptoms. Decreased neural processing that implicitly associate *self* with *positive* conditions (and relatively increased implicit association between *self* and *negative* conditions) might be important neural correlates for abnormal ISE in MDD.

Keywords: major depressive disorder, implicit self-esteem, event-related potentials, go/no-go association task, neural mechanism

INTRODUCTION

Major depressive disorder (MDD) is one of the most common and disabling mental disorders worldwide. The link between MDD and negative clinical outcomes such as suicidality is strong, and people at high risk for suicidal behavior usually approached suicide through many ways (1). Proper self-esteem, that is, an appropriate and positive subjective evaluation of one's own worth, is of great importance in maintaining a person's mental health and wellbeing. Nevertheless, people with MDD often have low self-esteem, which is typically characterized by self-exclusion, self-denial, and self-contempt (2).

Self-esteem can be divided into two different psychological constructs, namely, explicit self-esteem (ESE) and implicit self-esteem (ISE). The former can be assessed using simple measurement strategies like self-reported questionnaires [e.g., Rosenberg Self-Esteem Scale (RSES)] (2). ISE, however, is thought to be outside of conscious control and cannot be realized through introspection. Greenwald and Banaji first proposed the definition of ISE, which grew out of the dual signal system (3). Distinct from ESE, ISE refers to a person's disposition to evaluate themselves positively or negatively in a spontaneous, automatic, or unconscious manner. Accordingly, ISE is expected to unveil aspects of *self* that are not captured by ESE.

Both ESE and ISE have a relationship with MDD. It has been repeatedly reported that people with MDD often have lower ESE than the general population, while studies regarding ISE in MDD have yielded inconsistent results (4–9). It is worth noting that some evidence indicated that ISE may be more important than ESE as a target for interventions to prevent the recurrence of MDD. For instance, a previous study reported that ISE, but not ESE, could predict future depressive symptomatology (10). Another study also found that ISE is an important variable of vulnerability for MDD relapse (11). Recently, a 3-year follow-up study with a large sample size further confirmed that ISE could predict recurrence of depression even when statistically controlling for confounding factors at baseline, while the prediction value of ESE is relatively smaller (4). Interpretation of abnormal ISE was varied in previous studies. Some stated that lower ISE in MDD would be the marker of how deeply negative self-views are internalized (7), but some hold that increased positive implicit associations with others would have also played an important role in MDD (12). Taken together, further studies on characteristics of ISE in patients with MDD are warranted. In the present study, we aimed to verify the characteristics of ISE in clinically diagnosed MDD patients. Given that ISE is thought to be outside of conscious control and cannot be realized through introspection, it may represent more stable and deep-seated part of self-esteem than ESE. Hence, we expected that ISE would be less correlated with depressive symptom severity than ESE.

On the other hand, the neural mechanism behind abnormal ISE in MDD is far from being clarified. Event-related potential (ERP) is a powerful technique in neuroscience that can simultaneously provide information on neural electrical activity during behavioral tasks. Due to its high temporal resolution up to milliseconds, ERP may have advantages even over functional magnetic resonance imaging (fMRI) for studying ISE because ISE is detected using experimental paradigms requiring rapid response, such as the Implicit Association Test (IAT). In fact, the ERP technique has been adopted by many researchers to study the neural correlates of ISE. For instance, by combining the ERP and IAT, a study (13) reported that participants demonstrated a more positive ERP deflection between 350 and 450 ms after the onset of *self*-stimuli in congruent conditions (*self-positive*) than in incongruent conditions (*self-negative*). Another study combined ERP with the go/no-go association task (GNAT), a variant of IAT, and found that positive ISE was manifested on neural activity around 270 ms after the presentation of self-relevant stimuli (14). Notably, these studies were carried out in the general population, rather than MDD patients. Meanwhile, studies have found differences between healthy controls (HCs) and subclinical depressive individuals. As a recent study reported (15), relative to people without depressive symptoms, the neural activity pattern during the self-esteem IAT was reversed in dysphoric participants. This left an open question of whether clinically diagnosed patients with MDD have similar neural activity patterns.

It is considered that self-referential processing has a close relationship with self-esteem (16), and several studies have explored the implicit self-referential processing in patients with MDD. For instance, Dainer-Best et al. found that sustained attention involvement was related to the increased negative self-referential processing in patients with MDD (17). Recently, Benau et al. found that depressive participants were more likely to endorse negative self-referent sentences, and this could be reflected as larger late positive potential (LPP) to negative stimuli (18). It should be noted that the self-referent encoding task (SRET) or adapted SRET used in these studies is distinct from the IAT or the GNAT. SRET is an affective decision task in which participants make binary-choice decisions on whether positive and negative words or sentences are self-descriptive (19). In other words, SRET, at least in part, requires participants to consciously, rather than implicitly, judge whether the stimulus is relevant to them. Therefore, it remains unclear whether the findings obtained using the SRET paradigm well reflect the ISE characteristics of people with MDD.

In the present study, we aim to reveal the potential neural correlates of abnormal ISE in clinically diagnosed MDD patients by combining a self-esteem GNAT paradigm and the ERP technique. According to Beck's cognitive theory (19), uncontrollable automatic biases toward negative information play an important role in the development and maintenance of depression. Therefore, MDD patients are likely to have more spontaneous attention toward a negative stimulus and stronger *self-negativity* association. In addition, anhedonia, an inability to experience pleasure, is common among MDD patients (20). From this perspective, positive stimuli may capture less attention than negative stimuli and thus induce less neural activity in this population. Based on the aforementioned theory and findings, we hypothesized that when performing the GNAT, MDD patients would have much smaller amplitudes of ERP

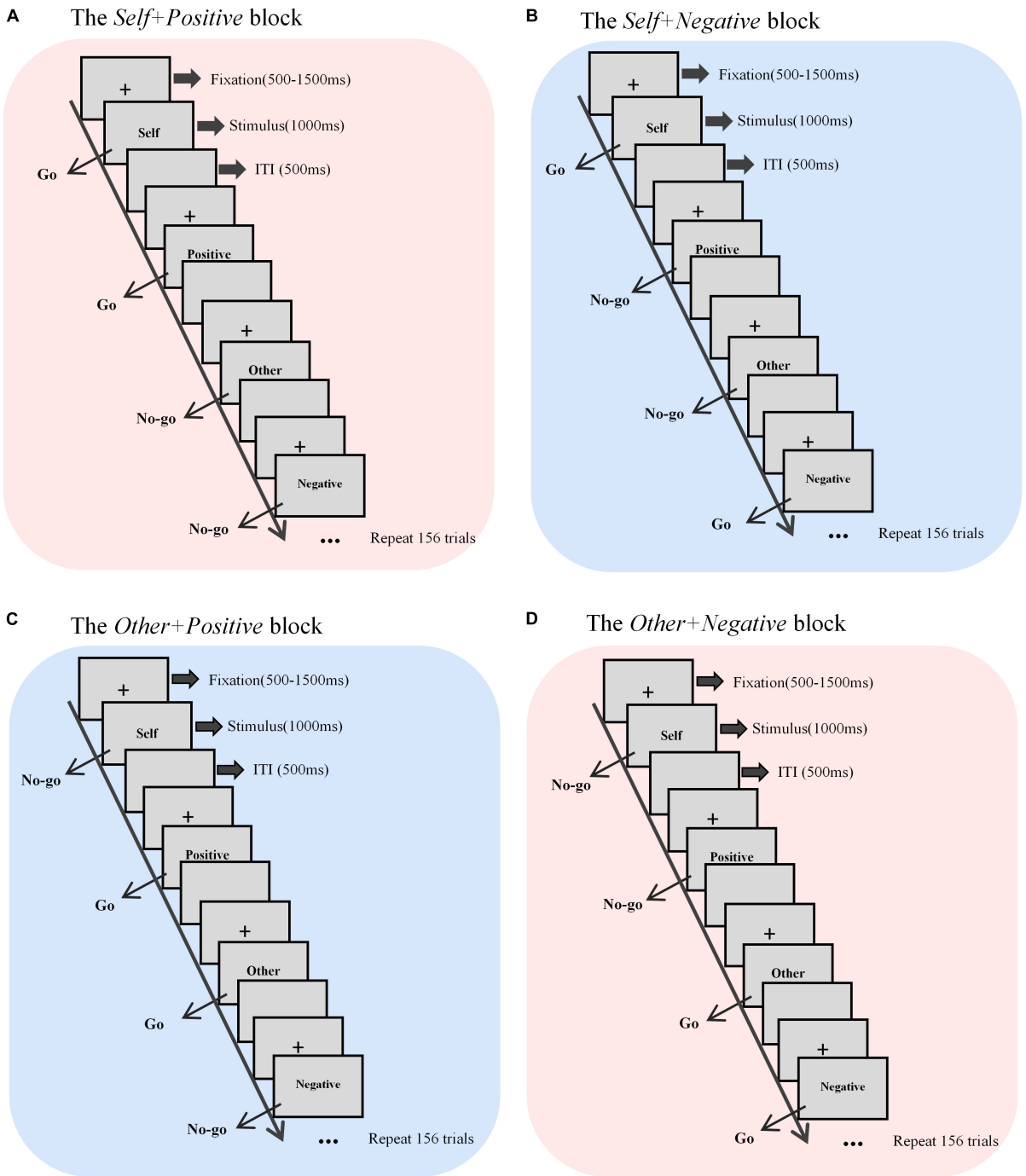

FIGURE 1 | Sketch map of the self-esteem GNAT process. There were four blocks with different target stimuli, that is, **(A)** *self + positive*, **(B)** *self + negative*, **(C)** *other + positive*, and **(D)** *other + negative*. Each block contained 160 trials. ITI, inter-trial interval.

components that reflect attention and emotional processing (like P3/LPP) than their counterparts; moreover, MDD patients *per se* would have lower ERP amplitudes to *self* items under *positive* conditions than under *negative* conditions, which represents a neural process bias to implicit association between *self* and *negativity*.

MATERIALS AND METHODS

Time and Setting

The present study was carried out from 1 July 2018 to 31 March 2021, in the Affiliated Wuxi Mental Health Center of Nanjing Medical University, Wuxi city, the People Republic of China.

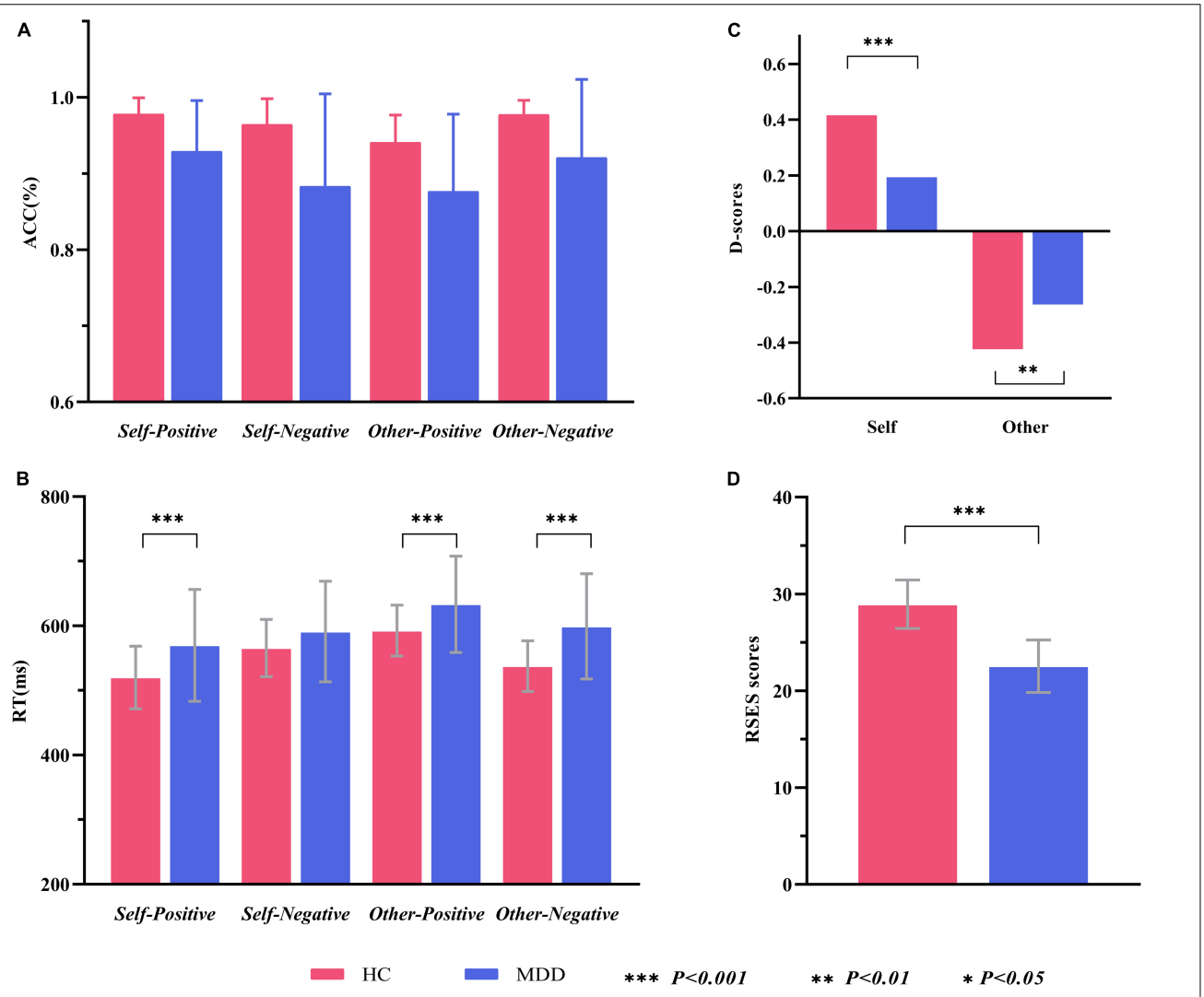

FIGURE 2 | Within- and between-group comparisons of behavioral data in the self-esteem GNAT. **(A)** Grand average hit rate of go-task in different conditions and groups. **(B)** Grand average reaction time of go-task in different conditions and groups. **(C)** *Self-D* scores and *Other-D* socres in two groups. **(D)** Average RSES scores of two groups. ACC, accuracy (hit rate of go-task); RT, reaction time; RSES, Rosenberg Self-Esteem Scale.

This study was approved by the Ethics Committee of the Wuxi Mental Health Center and conducted in accordance with the Declaration of Helsinki.

Participants

All MDD patients were recruited from inpatients of the Wuxi Mental Health Center. The inclusion criteria were (a) individuals meeting the criteria of MDD according to the Diagnostic and Statistical Manual of Mental Disorders, Fourth Edition (DSM-IV) (21), (b) Chinese Han aged 18–65 years, and (c) volunteer to participate in this study. The exclusion criteria were individuals (a) meeting the criteria of any other mental disorder according to DSM-IV, (b) received electroconvulsive therapy in the last 24 weeks, (c) having neurological illness or other severe physical illness as determined by clinical evaluations and medical records, (d) having nicotine/other substance misuse or dependence, and (e) having taken any medication known to affect cognition within the past 2 weeks. All HCs were recruited from the local residential communities through advertisement. The inclusion criteria of HCs were (a) individuals meeting no criteria of any kind of mental disorder according to DSM-IV, and (b) and (c) criteria same as the MDD group. The exclusion criteria of HCs were the same as (c) to (e) criteria as the MDD group.

Both MDD patients and HCs provided written informed consent to participate in this study. For MDD patients whose capacity to consent was compromised, we obtained consent from their next of kin or guardians. Each participant was compensated 300.00 Chinese yuan (CNY).

Clinical Assessments

The Hamilton Depression Rating Scale (HAMD, 24-item version) (22) was employed to evaluate the severity of

depressive symptoms of MDD patients by an experienced senior psychiatrist. Higher HAMD scores indicate more severe depression. The RSES (2), a widely used ESE evaluation tool, was employed for all participants. This self-rating scale has 10 items regarding the overall feelings of self-worth and self-acceptance. The RSES score ranges from 4 to 40, with higher scores suggesting a higher level of ESE.

Self-Esteem Go/No-Go Association Task

We employed a self-esteem GNAT paradigm to study the characteristics of ISE. Relative to the IAT, the GNAT may have some unique advantages. For instance, the GNAT relies on fewer blocks, which can reduce cognitive confounds like task switching, which frequently occurs in the IAT (23). Moreover, the GNAT requires the participants to press only one button (only one category and one evaluative attribute) over two buttons, which can not only detect the approach function but also the inhibition ability. In addition, the GNAT is more flexible in measuring automatic cognition (24). Despite studies comparing the IAT and GNAT have confirmed that they can effectively measure the automatic self-evaluation and are both valid measurement tools for ISE (23), a recent study has shown that the GNAT may detect some implicit bias that are not easily detected by the IAT (24).

Referring to a recent study in this field (13), we programmed a self-esteem GNAT paradigm by E-Prime 3.0 software (Psychology Software Tools Incorporated, Pittsburgh, United States) (25) to assess the level of ISE. Stimuli included 90 Chinese words: 40 *positive* words, 40 *negative* words, 5 words served as the self category [I ("我" in Chinese), mine ("我的" in Chinese), self ("自己" in Chinese), own ("自己的" in Chinese), and self ("本人" in Chinese)], and 5 words served as the *other* category [for male participants: he ("他" in Chinese), his ("他的" in Chinese), others ("别人" in Chinese), other's ("别人的" in Chinese), and others ("外人" in Chinese); for female patients: she ("她" in Chinese), hers ("她的" in Chinese), others ("别人" in Chinese), other's ("别人的" in Chinese), and others ("外人" in Chinese)]. Overall, 80 attribute (positive and negative) words were selected from the Chinese Affective Words System (16), matched in the number of Chinese characters, strokes, arousal, and familiarity. Through the combination of stimulus categories, the self-esteem GNAT consisted of four conditions (i.e., *self* + *positive*, *self* + *negative*, *other* + *positive*, and *other* + *negative*). The participants were asked to respond as quickly and accurately as possible to target stimuli (i.e., go task) by pressing the spacebar on the keyboard, or do nothing to the non-target stimuli (i.e., no-go task). Taking the *self* + *positive* condition as an example, the participants should press the spacebar when words of either *self* category or *positive* category are displayed on the screen but do nothing when words of either *other* category or *negative* category are displayed.

The self-esteem GNAT paradigm has a total of four blocks corresponding to the aforementioned four different conditions (**Figure 1**). At the beginning of each trial, there was a fixation ("+") presented in the center of the screen, with a randomized duration between 500 and 1500 millisecond (ms). Then the word stimulus was displayed in the center of the screen, and the participants were required to respond to the go-task and do nothing to the no-Go task, as described before. Regardless of whether there was a response, the presentation time of each stimulus was fixed at 1000 ms, and the next trial began right after a 500-ms inter-trial interval (ITI). Each block had 160 trials, with each category (*self*, *other*, *positive*, and *negative*) of words displaying 40 times in a random order. Before each test block, the participants completed a practice block (10 trials) to ensure that they understood the rules. The participants were asked to complete all four blocks in a counterbalanced order between groups, with a 5-min break between each two blocks.

Behavioral indicators of interest mainly included the hit rate of the go-task under each condition and its corresponding response time (RT), which were calculated from the automatically recorded E-Data in E-Prime software. To exclude arbitrary answers, we also calculated the false alarm rate under the no-go task. If the participants arbitrarily presses the spacebar over and over to obtain a high hit rate in the go-task (e.g., *self-positive*), they would also get a high false alarm rate in the relative no-go task (e.g., *other negative*). To reflect participants' ISE levels, D-scores for self-esteem were calculated using the method introduced in previous studies (25, 26). Briefly, we first calculated the difference of mean RTs between the *self-negative* condition and the *self-positive* condition and then divided the difference by the standard deviation (SD) for all RTs in these two conditions. Higher *self*-D-scores indicate stronger implicit bias toward *self-positive* association; that is to say, the higher the *self*-D-scores, the higher the level of ISE. Similarly, the D-score of "other esteem" was also calculated.

EEG Recording and Analysis

To explore neural activity associated with ISE, EEG data were synchronously and continuously recorded during the self-esteem GNAT from a customized 64 Ag/AgCl channel EasyCap using a BrainAmp Standard recorder (Brain Products GmbH, Germany) at a 500-hertz (Hz) sampling rate. The FPz electrode was used as the recording reference and the left clavicle electrode as ground. The horizontal electrooculogram (HEOG) recording electrodes were placed 1 cm away from the outer corner of both eyes, and the vertical electrooculogram (VEOG) recording electrode was placed at the lower orbit of the left eye. Electrode impedances were kept below 5 kOhm (kΩ) during the recording.

Brain Vision Analyzer (version 2.0, Brain Products GmbH, Germany) was used for offline data analysis, according to established methods (26). In short, the EEG data were re-referenced to the averaged to the averaged left and right mastoids and band-pass-filtered between 0.1 and 30 Hz using a zero-phase shift Butterworth filter. A bad electrode was interpolated, and the independent component analysis (ICA) was applied to remove artifacts such as eye movement, myoelectricity, and electrocardiogram signals. For ERP analysis, continuous EEG data were segmented by a stimulus marker from −200 to 800 ms and then baseline-corrected using a −200 to 0−ms pre-stimulus. A given segment was rejected if the voltage gradient exceeded 50 microvolts (μV)/ms, the absolute amplitude was more than 75 μV, or the signal was flat (less than 0.5 μV for more than 100 ms). Finally, after a thorough manually check of artifacts, the individual ERPs for different

categories of words in go tasks with correct responses were averaged separately.

Although the neural processes associated with ISE may involve more than a single ERP component, results from most of the previous research studies (13, 14, 27–29) in this field have suggested that the most critical one may be a late positive component (LPC) that begins approximately 300 ms after and continues to the end of the stimulation. Accordingly, we also focused on this component in the present study. In previous studies, researchers named this component P3 (or P300) or LPP. Task-relevant P3 is parietally maximal and often called P3b, whose amplitude is often considered to be related to task difficulty and effort devoted to the task and can be used as a measure of attention and other resource allocation. Many studies have drawn a conclusion that P3 amplitude is reduced in people with MDD (30, 31). LPP is a positive deflection that usually has the same onset time and scalp distribution as the P3 waveform (i.e., onset around 300 ms post-stimulation and the parietal maximum). LPP may become more centrally distributed over time, and its initial part may actually consist of an enlarged P3, reflecting an effect of the intrinsic task relevance of emotion-related stimuli (32). There is evidence that P3 and LPP are not identical (33); however, as a recent review concluded, they might reflect a common response to stimulus significance (34).

In the present study, by visual inspection of the grand averaged waveforms, we obtained such a positive potential that started about 300 ms and with a peak amplitude below 600 ms after the target stimuli. Evidence on whether P3 and LPP are the same ERP component remains controversial, whereas they may reflect output from a general system that tracks the time-course of stimulus importance (34). To this end, we named this P3/LPP waveform go-P3 in this study because our main interest was the neural correlates when participants made a correct response in go-tasks. Go-P3 was measured within a time window between 300 and 600 ms following the stimulus onset. ERP indicators of interest were mainly the peak amplitude of go-P3 that correctly responded under different conditions. Since the task-relevant P3 is parietally maximal and LPP may be more centrally distributed (32), we focused on centroparietal electrodes (Cz, CPz, and Pz) to better control the potential statistical error risk caused by multiple comparisons, referring to a recent study that employed P300 and LPP to investigate mechanisms of cognitive control training in MDD patients (35).

Statistical Analyses

IBM SPSS Statistics version 22 (IBM Corp., Armonk, NY, United States) was used for data analysis. Comparisons of mean age, education, duration of illness, RSES scores, HAMD scores, and D-scores were conducted between the MDD group and the HC group with independent sample *t*-tests. D-scores of both groups were also independently compared to zero using the one-sample *t*-test. Comparisons of handedness and sex were conducted with the Pearson Chi-square test. A 2-group (MDD vs. HC) × 2-target (self vs. other) × 2-valence (positive vs. negative) mixed-model analysis of variance (ANOVA) was employed to compare the behavioral and ERP data, with group as a between-subject variable and target and valence as within-subject variables. The Greenhouse–Geisser method was employed to correct the degrees of freedom when the sphericity assumption was violated. Effect sizes were also estimated using partial eta-squared (η_p^2). *Post hoc* analyses were conducted when a significant interaction was found, and Bonferroni correction was used to control possible type I error caused by multiple comparisons.

RESULTS

Demographic and Clinical Characteristics

In line with the inclusion and exclusion criteria, a total of 33 MDD patients and 32 HCs participated and finished this study. Data from one MDD patient and one HC were excluded because of technical reasons. Remaining data of 32 MDD patients (12 males and 20 females) and 31 HCs (15 males and 16 females) were analyzed. This sample size was sufficient to detect a medium-size effect with 80% power in mixed-model ANOVA. As shown in **Table 1**, there were no significant between-group differences in mean age, education level, handedness, and male-to-female ratio. The MDD group had a significantly lower RSES score than HCs (t = 9.733, $p < 0.001$), suggesting a decreased level of ESE in MDD (**Figure 2D**).

Behavioral Data of Self-Esteem Go/No-Go Association Task

Accuracy and Response Times

The grand average hit rate of go-task and the false alarm rate of no-go tasks for both groups is shown in **Table 2** and **Figure 2A**. For the hit rate of go-tasks, mixed-model ANOVA indicated no significant interaction effect for group × target × valence ($F_{1,61}$ = 2.041, p = 0.158, η_p^2 = 0.032), while a significant interaction between the target and valence ($F_{1,61}$ = 24.722, $p < 0.001$, η_p^2 = 0.288) was found. *Post hoc* analyses revealed that the participants had higher accuracy in the *self-positive* condition than in the *self-negative* condition (p = 0.007) but higher in the *other negative* condition than in the *other positive* condition ($p < 0.001$). The main effect of group was significant ($F_{1,61}$ = 18.445, $p < 0.001$, η_p^2 = 0.232), with higher accuracy for HCs than for MDD patients. For the false alarm rate of no-go tasks, a significant main effect for group ($F_{1,61}$ = 11.418, p = 0.001, η_p^2 = 0.158) was found, which showed that the HCs had a much lower false alarm rate than the MDD group. Overall, both groups had high hit rates in all go-tasks and low false alarm rates in the corresponding no-go tasks, indicating that no participants pressed the spacebar continuously (or never) during the tasks.

The average RTs for go tasks of two groups in different conditions are shown in **Table 2** and **Figure 2B**. Mixed-model ANOVA indicated a significant interaction effect for group × target × valence ($F_{1,61}$ = 10.545, p = 0.002, η_p^2 = 0.147). *Post hoc* tests revealed significant higher RTs for the MDD group than for the HC group in the *self-positive* condition ($F_{1,61}$ = 7.859, p = 0.007, η_p^2 = 0.114), *other positive* condition ($F_{1,61}$ = 7.265, p = 0.009, η_p^2 = 0.106), and *other negative* condition

($F_{1,61}$ = 14.351, $p < 0.001$, η_p^2 = 0.190), but not in the *self-negative* condition ($F_{1,61}$ = 2.528, p = 0.117, η_p^2 = 0.040). The participants responded faster in the *self-positive* condition than in the *self-negative* condition (both $p < 0.01$), while slower in the *other positive* condition than in the *other negative* condition (both $p < 0.01$).

D-Scores

Figure 2C shows that comparisons between all D-scores and zero were significant (for MDD, *self* condition: t = 2.675, p = 0.012; *other* condition, t = 4.860, $p < 0.001$; for HCs, *self* condition, t = 9.805, $p < 0.001$; *other* condition, t = 8.837, $p < 0.001$). Interestingly, D-scores of the *self* condition (*self*-D-scores) were positive, while those of the *other* condition (*other* D-scores) were negative. Compared to the HCs, the MDD group had significantly lower *self*-D-scores (t = 3.516, p = 0.001), suggesting a remarkable decrease in ISE in MDD patients. The absolute *other* D-scores were larger in HCs than in MDD (t = 2.184, p = 0.033), indicating the implicit association between *other* and *negative* conditions in the MDD group is reduced. Because the direction of *self*-D-scores was opposite to that of *other* D-scores, we did not compare them from the perspective of target (self vs. other).

Event-Related Potential Data of Self-Esteem Go/No-Go Association Task

The averaged peak go-P3 amplitude in centroparietal sites (Cz, CPz, and Pz) was analyzed by mixed-model ANOVA. The grand averaged amplitude of go-P3 that correctly responded to both groups under different conditions are shown in **Figure 3**. To better illustrate its overall distribution and within- and between-group differences, we also provided the topographical map and violin plots in **Figure 4**.

The interaction effect for group × target × valence was significant ($F_{1,61}$ = 12.954, p = 0.001, η_p^2 = 0.175). There was no significant interaction effect for group × target ($F_{1,61}$ = 0.175, p = 0.677, η_p^2 = 0.003), valence × group ($F_{1,61}$ = 0.259, p = 0.612, η_p^2 = 0.004), and target × valence ($F_{1,61}$ = 1.858, p = 0.178, η_p^2 = 0.030). The main effects of group ($F_{1,61}$ = 3.582, p = 0.063, η_p^2 = 0.055), target ($F_{1,61}$ = 1.569, p = 0.215, η_p^2 = 0.025), and valence ($F_{1,61}$ = 0.034, p = 0.854, η_p^2 = 0.001) were also not significant. *Post hoc* tests revealed that on the group level (MDD vs. HCs), the average amplitude in the *self-positive* condition was significantly smaller in MDD than in HCs ($F_{1,61}$ = 13.401, p = 0.001, η_p^2 = 0.180), while no such group difference was detected in the *self-negative* condition ($F_{1,61}$ = 0.698, p = 0.407, η_p^2 = 0.011). Moreover, in the HC group, go-P3 amplitude in the *self-positive* condition was larger than that in the *self-negative* condition ($F_{1,61}$ = 7.655, p = 0.007, η_p^2 = 0.111); remarkably, a reversed pattern was found in MDD groups where amplitude was smaller in the *self-positive* condition than in the *self-negative* condition, although this difference did not reach the significant threshold ($F_{1,61}$ = 2.655, p = 0.108, η_p^2 = 0.042). No significant difference was observed in both *other positive* and *other negative* conditions between groups (p = 0.671 and 0.076, respectively). On the target level (*self* vs. *other*), HCs demonstrated a larger go-P3 amplitude in the *other negative* condition than in the *self-negative* condition ($F_{1,61}$ = 5.466, p = 0.023, η_p^2 = 0.082), but no significant difference was found between the *self-positive* condition and the *other positive* condition ($F_{1,61}$ = 2.228, p = 0.141, η_p^2 = 0.035). For the MDD group, no significant difference was observed in aforementioned comparisons (both $p > 0.05$).

We also had a look at the go-P3 latencies; however, mixed-model ANOVA did not find significant interaction effect for group × target × valence. Furthermore, no significant second-order interaction effect or main effect was observed (all $p > 0.05$).

Correlations Among Indicators in Major Depressive Disorder

The Pearson correlation analysis was employed to detect correlations among HAMD scores, RSES scores, D-scores, and go-P3 amplitudes (pooled by electrode sites) in the MDD group. Since there was no significant group difference in the go-P3 latencies, this indicator was not included here. As shown in **Figure 5**, HAMD scores were significantly negatively correlated with RSES scores (r = −0.47, p = 0.006), but not with either *self*-*r*-D-scores (r = −0.22, $p > 0.05$), *other* D-scores (r = 0.24, $p > 0.05$), or any of the go-P3 indicators (r = −0.095–0.2, all $p > 0.05$). In addition, RSES scores were also neither significantly correlated with *self*- and *other* D-scores (r = 0.16 and −0.29, respectively, both $p > 0.05$) nor with any of the go-P3 indicators (r = −0.15–0.22, all $p > 0.05$). *Other* D-scores were negatively correlated with the go-P3 amplitude under self-positive (r = −0.4, p = 0.002) and other positive conditions (r = −0.36, p = 0.004).

TABLE 1 | Demographic characteristics and clinical information of two groups.

Variable	MDD (n = 32)	HC (n = 31)	Statistics	p-Value
Age range (years)	21–54	23–0	–	
Mean age (SD)	38.03 (9.12)	36.42 (6.80)	t = 0.784	0.431
Sex (M/F)	12/20	15/16	χ^2 = 0.762	0.383
Handedness (R/M/L)	13/10/10	12/10/9	χ^2 = 0.190	0.879
Year of education (SD)	11.69 (3.36)	12.74 (3.08)	t = 1.299	0.199
RSES (SD)	22.53 (2.71)	28.94 (2.50)	t = 90.733	<0.001
HAMD (SD)	29.47 (6.67)	–	–	
Duration of illness (year, SD)	3.66 (2.48)	–	–	

MDD, major depressive disorder; HC, healthy control; SD, standard deviation; R, right; M, mixed; L, left; RSES, Rosenberg Self-Esteem Scale; HAMD, Hamilton Depression Scale.

TABLE 2 | Behavior data of two groups in the self-esteem GNAT.

Variable	Self + positive		Self + negative		Other + positive		Other + negative	
	HC	MDD	HC	MDD	HC	MDD	HC	MDD
Hit rate of go-task (SD)	0.98 (0.02)	0.93 (0.07)	0.96 (0.03)	0.88 (0.12)	0.94 (0.04)	0.88 (0.10)	0.98 (0.02)	0.92 (0.10)
False alarm rate of no-go task (SD)	0.04 (0.04)	0.08 (0.06)	0.03 (0.03)	0.05 (0.04)	0.07 (0.07)	0.13 (0.11)	0.02 (0.03)	0.04 (0.03)
RTs for hit (SD)	520.15 (48.50)	569.90 (86.50)	565.70 (44.42)	591.23 (77.96)	592.69 (39.51)	633.43 (74.62)	537.78 (39.10)	599.11 (81.50)

HC, healthy control; MDD, major depressive disorder; RT, response time; SD, standard deviation.

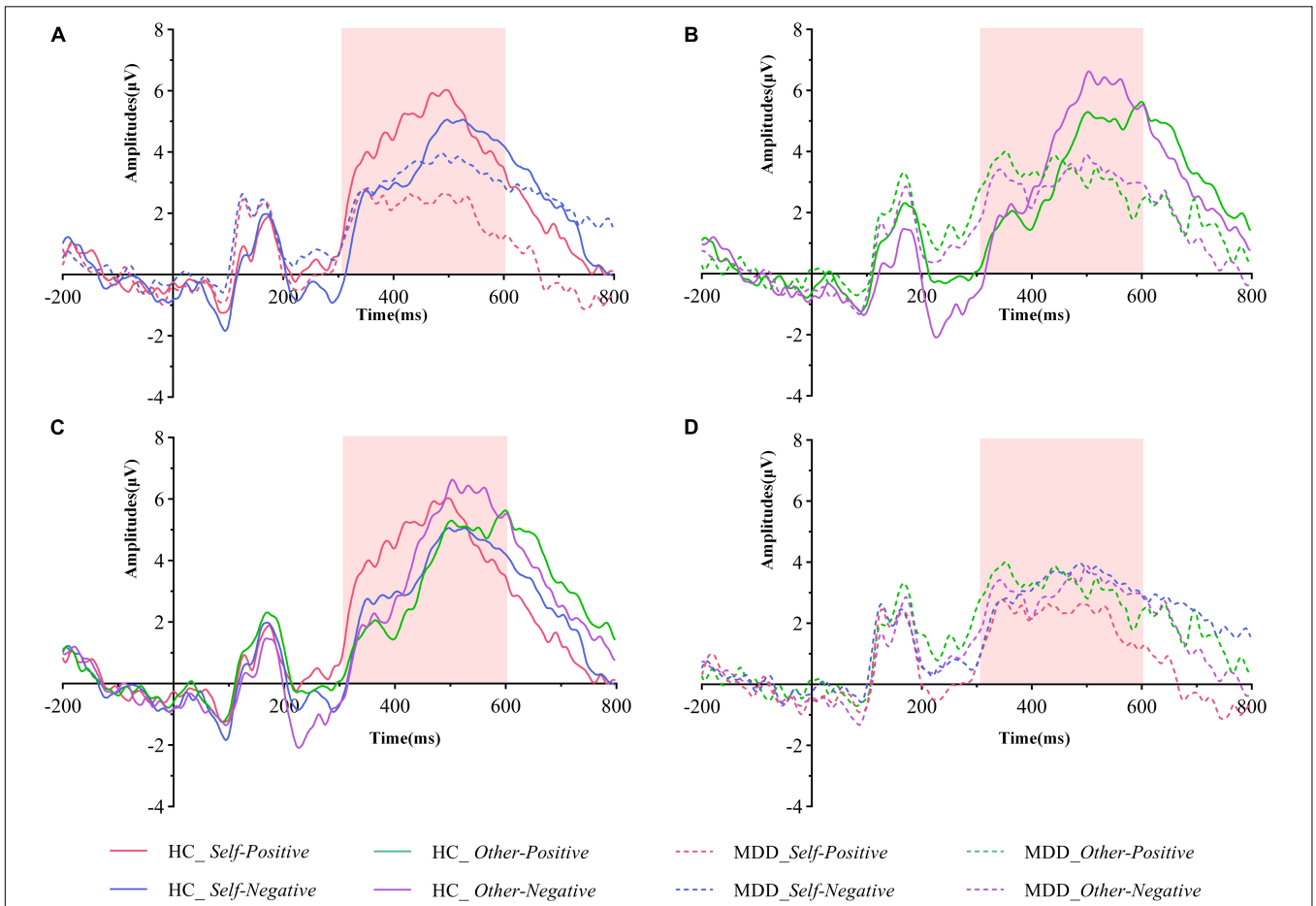

FIGURE 3 | Grand averaged ERPs of both groups under different conditions of the pooling electrodes site (averaged Cz, CPz, and Pz sites). **(A)** Grand averaged ERPs in the HC group (solid lines) and the MDD group (dashed lines) during the self-positive (red lines) and the self-negative (blue lines) conditions. **(B)** Grand averaged ERPs in the HC group (solid lines) and the MDD group (dashed lines) during the other positive (green lines) and the self-negative (purple lines) conditions. **(C)** Grand averaged ERPs in the HC group during the self-positive (red lines), the self-negative (blue lines), the other positive (green lines), and the self-negative (purple lines) conditions. **(D)** Grand averaged ERPs in the MDD group during the self-positive (red lines), the self-negative (blue lines), the other positive (green lines), and the self-negative (purple lines) conditions. The go-P3 time windows are marked with light pink shadow. MDD, major depressive disorder; HC, healthy control.

In addition, there are broadly positive correlations among go-P3 amplitudes under different conditions (r = 0.37–0.64, all $p < 0.05$).

DISCUSSION

In the present study, in targeted clinically diagnosed patients with MDD, we found that both the ESE and ISE levels were reduced in this population. ISE indicators were not correlated with HAMD scores as ESE did, indicating that ISE may be more independent of clinical symptoms. Furthermore, we found that MDD patients, in comparison to HCs, had significantly smaller centroparietal go-P3 amplitude in the *self-positive* condition, but not in *self-negative* or both *other* conditions, suggesting that decreased neural processing that implicitly associate *self* with the *positive* condition might be important neural correlates of abnormal ISE in MDD.

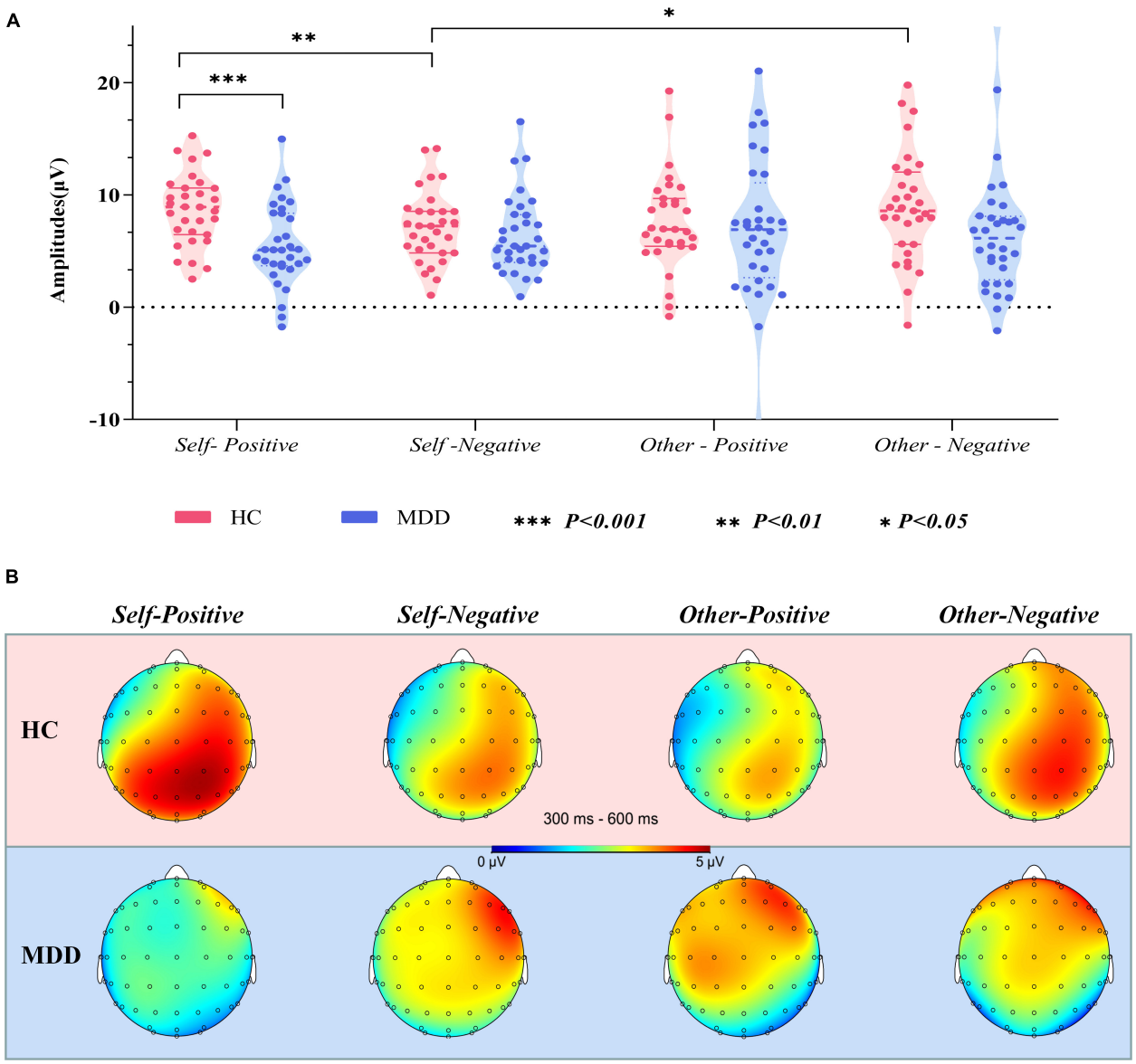

FIGURE 4 | (A) Violin plots of pooled (Cz, CPz, and Pz) averaged go-P3 amplitudes in different groups and conditions. **(B)** Topographical distribution of grand averaged go-P3 within a time window of 300–600 ms post-stimuli under different conditions. MDD, major depressive disorder; HC, healthy control; SD, standard deviation.

It has been repeatedly reported that self-esteem is abnormal in depressive patients. Reduced ESE in MDD patients has been well established in previous studies; however, whether there exists lower ISE in this population remains unclear yet. Our results verified that the ESE level of MDD patients was reduced, as reflected by significant lower RSES scores in this group. As for ISE, we found a much lower level of *self*-D-scores in the MDD group. According to the calculation method mentioned previously, lower *self*-D-scores indicate higher implicit bias toward *self-negative* association, which represents a reduced level of ISE. This finding is consistent with those of previous studies. Discrepancies with some studies that failed to find a similar result might be due to differences in subject characteristics. For example, Risch et al. found that there was no significant difference in ISE between remitted depressive patients and HCs, but the times of depressive episodes would significantly aggravate the reduction of ISE (6). Smeijers et al. reported that remitted depressed patients demonstrated lower ESE, but not ISE, than never depressed controls (36). Different from these studies, the MDD patients in our study were all in their depressive episodes and had an average HAMD score closed to 30 points, corresponding to moderate level of severity. According to the dual process model, cognitive vulnerability to depression is observed when negatively biased associative

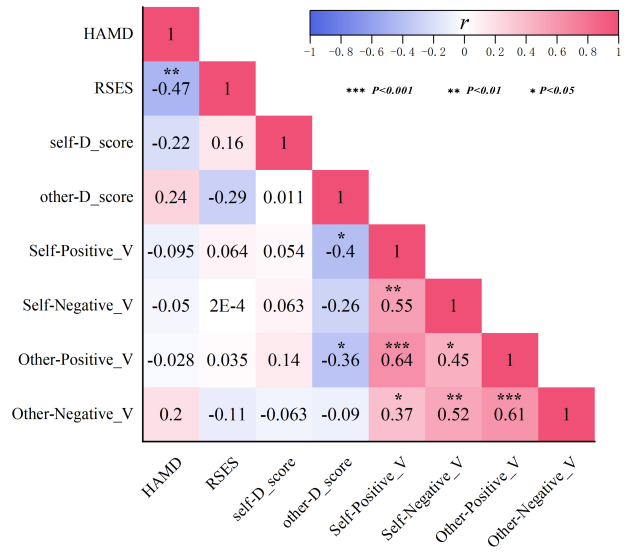

FIGURE 5 | Correlations among indicators of HAMD scores, RSES scores, D-scores, and go-P3 amplitudes in the MDD group. HAMD, Hamilton Depression Rating Scale; RSES, Rosenberg Self-Esteem Scale.

(implicit, automatic, non-conscious, and intuitive) processing is uncorrected by reflective (explicit, controlled, conscious, and rational) processing (37, 38). In this way, it is understandable that lower ESE and lower ISE coexist in patients with major depressive episodes. Contrary to lower *self*-D-scores, we detected higher (less negative) *other* D-scores in MDD patients, indicating that when they view themselves negatively, they tend to have an increased bias to view others positively in relative terms. This result was in line with a previous large-sample size study and suggested that not only reduced ISE but also relatively increased implicit other esteem would play a role in depression (12).

We also found that MDD patients' HAMD scores were significantly negatively correlated with their RSES scores, indicating that the more severe the depressive symptoms, the lower the ESE. This result was not surprising, since the RSES can be regarded as a comprehensive evaluation of some certain depressive symptoms, like "sense of inferiority," which is common in MDD patients and is also assessed in the HAMD. Meanwhile, no significant correlation between the HAMD scores and *self*-D-scores was found, suggesting that ISE in MDD might be more independent of clinical symptoms. In this respect, abnormal ISE has more potential to be an endophenotype of MDD. As supporting evidence, a recent twin study (39) has proved the heritability of ISE, although the current mainstream view is that ISE is mainly determined by environmental factors. Our result further supported the assumption that ISE reflects different psychological constructs of self-esteem from ESE. In fact, previous studies have already shown that ISE and ESE having different neural bases. Using fMRI, Izuma et al. (40) found that although both ISE and ESE were related to neural signals in regions involved in self-processing, there were obvious differences; moreover, neural signals in reward-related brain regions were strongly related to ISE, but not to ESE. Together with previous evidence that ISE would have a better prediction value for relapse or recurrence of depression (10, 11), our data from psychological assessment and behavioral test, as well as their interconnections, provided new evidence that ISE may represent different aspects of self-esteem and have more potential to be an endophenotype of MDD. Further studies are also worth paying attention to the relations of ISE and other psychological characteristics relating to self-acceptance and negative clinical outcomes, such as affective temperaments (41).

We further investigated the neural correlates of abnormal ISE through the ERP technique, which can provide more direct information about brain activity during the GNAT than behavioral data. We found that the overall go-P3 amplitude of MDD was relatively smaller than that of HCs among different conditions (although in some cases, the between-group difference did not reach a significant threshold). In fact, it has been suggested that reduced P3 amplitude would play a central role in clinical depression, and reduced P3 amplitude in current depressive patients has been reported by numerous studies using different ERP paradigms that require quick response (42). Previous studies have revealed that many factors could influence the amplitude of the P3 component, mainly including the probability of target stimuli, the difficulty of task, the uncertainty of stimuli, and the amount of available resource allocation (43). In our GNAT paradigm, the frequency and probability among each task and condition are equal and counterbalanced. In addition, there were high correct response rates and low false alarm rate under different conditions in both groups. Therefore, it is unlikely that the overall reduction of P3 amplitude in the MDD group was caused by features of the GNAT paradigm itself. The reduction of P3 amplitude at the overall level has been largely interpreted as insufficient allocation of brain resources in this population (34, 42, 44), which is commensurate with the clinical phenomenon that people with depression often complain of slow thinking and reaction.

The most striking finding in the present study was that in the MDD group, the go-P3 amplitude under the *self-positive* condition was smaller than that under the *self-negative* condition, the pattern of which was just the opposite to that of HCs (**Figure 3A**). By contrast, the two groups had similar patterns under the *other* conditions (**Figure 3B**), that is, beyond a general decrease in neural reactivity, MDD patients were particularly less responsive to *self* items under the positive condition. Since P3 has been suggested as an index of ISE (13), the aforementioned findings would be important neural correlates of abnormal ISE in MDD. Our results coincided with those of previous studies. A recent study (15) using self-esteem IAT found that the self-positive condition induced smaller LPC amplitudes than the self-negative condition in dysphoric individuals, whereas the pattern was reversed in the control group.

Another study also found that small LPC amplitudes existed in response to positive than to negative self-referent items in patients with current depression. Studies (16, 18) using the SRET paradigm also found that MDD patients had larger LPP to negative self-referent stimuli than to positive or neutral ones. Although these studies differ from the present study in terms of subjects' clinical characteristics or experimental paradigm, their findings can be seen as supporting evidence for our results. In the present study, a larger go-P3 amplitude was observed in the *self-positive* condition relative to the *self-negative* condition for the HCs. As interpreted by previous studies, enhanced amplitude of P3/LPP was regarded as indicative of more voluntary attention and increased stimulus evaluation (28, 45). However, for the MDD group, go-P3 amplitude was smallest under the *self-positive* condition, suggesting that MDD patients were unable to engage similar voluntary attention and stimulus assessments under the *self-positive* condition. In other words, there was an implicit self-negativity bias in this population. Together with the lower *self*-D-scores in the MDD group (also indicates an implicit bias toward *self-negative* association), our finding provides support for Beck's cognitive theory of depression (46). Previous studies have reported that ISE was robustly associated with reward-related brain regions (40). Moreover, patients with MDD tended to exhibit blunted amplitude of feedback-related negativity (FRN) in response to positive outcomes like monetary reward, rather than increased changes in response to negative outcomes (47). Our results have similarity to these findings, that is, changes in go-P3 amplitude are more obviously reflected as a decrease under *positive* conditions, rather than an increase under *negative* conditions. Thereby, fundamental processes of abnormal ISE in MDD patients may be mainly due to decreased attention and resource allocation toward positive stimuli.

Some limitations should be addressed in this study. First, we only focused on the go-P3 in this study, which might have missed some other valuable ERP components, such as no-Go N2, which is thought to be related to response inhibition. Moreover, the effect of medication on self-esteem in MDD participants may not be fully excluded, even if we have ruled out those who had recently taken any drugs known to affect the cognitive function. Similarly, the age range of the participants was broad, which might also have some potential influence on the results, although no significant group differences existed. In addition, due to the nature of the cross-sectional study and limited sample size, our results were unable to clarify the relationship between abnormal ISE and the process of MDD; therefore, well-designed longitudinal studies are warranted to address this question. Finally, neural processes underlying self-esteem are related to not only local cortical areas but also functional networks (48). Since ERPs have disadvantages in spatial resolution, other neuroimaging techniques with better balanced temporal and spatial resolution, such as functional near-infrared spectroscopy (fNIRS) or magnetoencephalography, are warranted to further exploring the neural mechanism of abnormal ISE in MDD.

CONCLUSION

Taken together, by using a self-esteem GNAT paradigm and the ERP technique, our study verified that MDD patients had significantly lower ESE and ISE and found that the latter was more independent of clinical symptoms. Moreover, as indexed by the centroparietal go-P3 amplitude, we found that MDD patients exhibited decreased neural processing, which implicitly associates the *self* with the *positive* condition and relatively increased implicit association between the *self* and the *negative* condition. Our results provide new evidence for characteristics and underlying neural mechanisms of abnormal self-esteem in clinically diagnosed MDD patients, which also have some implications for optimizing treatment strategies, especially psychological intervention for this population.

DATA AVAILABILITY STATEMENT

The original contributions presented in the study are included in the article/supplementary material, further inquiries can be directed to the corresponding authors.

ETHICS STATEMENT

The studies involving human participants were reviewed and approved by the Ethics Committee on Human Studies, The Affiliated Wuxi Mental Health Center of Nanjing Medical University. The patients/participants provided their written informed consent to participate in this study. Written informed consent was obtained from the individual(s) for the publication of any potentially identifiable images or data included in this article.

AUTHOR CONTRIBUTIONS

Z-HZ conceived the study and designed the study together with C-GJ and JW. C-GJ, HL, J-ZZ, and X-ZG recruited the subjects and collected the EEG and clinical data. C-GJ, Z-HZ, and JW performed the data analysis and drafted and revised the manuscript. All authors reviewed and commented on the final manuscript.

FUNDING

This study was supported by the Wuxi Taihu Talent Project (No. WXTTP2020008) and the Science and Technology Development Program of Wuxi City (No. N20192034).

ACKNOWLEDGMENTS

We thank all the subjects for participating in this study.

REFERENCES

1. Solano P, Ustulin M, Pizzorno E, Vichi M, Pompili M, Serafini G, et al. A Google-based approach for monitoring suicide risk. *Psychiatry Res.* (2016) 246:581–6. doi: 10.1016/j.psychres.2016.10.030
2. Rosenberg M. *Society and the Adolescent Self-Image*. Princeton, NJ: Princeton University Press (1965). doi: 10.1515/9781400876136
3. Greenwald AG, Banaji MR, Rudman LA, Farnham SD, Nosek BA, Mellott DS. A unified theory of implicit attitudes, stereotypes, self-esteem, and self-concept. *Psychol Rev.* (2002) 109:3–25. doi: 10.1037/0033-295x.109.1.3
4. van Tuijl LA, Bennik EC, Penninx B, Spinhoven P, de Jong PJ. Predictive value of implicit and explicit self-esteem for the recurrence of depression and anxiety disorders: a 3-year follow-up study. *J Abnorm Psychol.* (2020) 129:788–98. doi: 10.1037/abn0000634
5. Cvencek D, Greenwald AG, McLaughlin KA, Meltzoff AN. Early implicit-explicit discrepancies in self-esteem as correlates of childhood depressive symptoms. *J Exp Child Psychol.* (2020) 200:104962. doi: 10.1016/j.jecp.2020.104962
6. Risch AK, Buba A, Birk U, Morina N, Steffens MC, Stangier U. Implicit self-esteem in recurrently depressed patients. *J Behav Ther Exp Psychiatry.* (2010) 41:199–206. doi: 10.1016/j.jbtep.2010.01.003
7. van Randenborgh A, Pawelzik M, Quirin M, Kuhl J. Bad roots to grow: deficient implicit self-evaluations in chronic depression with an early onset. *J Clin Psychol.* (2016) 72:580–90. doi: 10.1002/jclp.22275
8. Franck E, De Raedt R, Dereu M, Van den Abbeele D. Implicit and explicit self-esteem in currently depressed individuals with and without suicidal ideation. *J Behav Ther Exp Psychiatry.* (2007) 38:75–85. doi: 10.1016/j.jbtep.2006.05.003
9. Roberts JE, Porter A, Vergara-Lopez C. Implicit and explicit self-esteem in previously and never depressed individuals: baseline differences and reactivity to rumination. *Cogn Ther Res.* (2015) 40:164–72. doi: 10.1007/s10608-015-9732-2
10. Franck E, Raedt RD, Houwer JD. Implicit but not explicit self-esteem predicts future depressive symptomatology. *Behav Res Ther.* (2007) 45:2448–55. doi: 10.1016/j.brat.2007.01.008
11. Elgersma HJ, Glashouwer KA, Bockting CL, Penninx BW, de Jong PJ. Hidden scars in depression? Implicit and explicit self-associations following recurrent depressive episodes. *J Abnorm Psychol.* (2013) 122:951–60. doi: 10.1037/a0034933
12. Hobbs C, Sui J, Kessler D, Munafò MR, Button KS. Self-processing in relation to emotion and reward processing in depression. *Psychol Med.* (2021). [Eupb ahead of print]. doi: 10.1017/s0033291721003597
13. Yang J, Zhang Q. P300 as an index of implicit self-esteem. *Neurol Res.* (2009). [Epub ahead of print]. doi: 10.1179/174313209x431138
14. Wu L, Cai H, Gu R, Luo YL, Zhang J, Yang J, et al. Neural manifestations of implicit self-esteem: an ERP study. *PLoS One.* (2014) 9:e101837. doi: 10.1371/journal.pone.0101837
15. Lou Y, Lei Y, Astikainen P, Peng W, Otieno S, Leppänen PHT. Brain responses of dysphoric and control participants during a self-esteem implicit association test. *Psychophysiology.* (2021) 58:e13768. doi: 10.1111/psyp.13768
16. Yang J, Qi M, Guan L. Self-esteem modulates the latency of P2 component in implicit self-relevant processing. *Biol Psychol.* (2014) 97:22–6. doi: 10.1016/j.biopsycho.2014.01.004
17. Dainer-Best J, Trujillo LT, Schnyer DM, Beevers CG. Sustained engagement of attention is associated with increased negative self-referent processing in major depressive disorder. *Biol Psychol.* (2017) 129:231–41. doi: 10.1016/j.biopsycho.2017.09.005
18. Benau EM, Hill KE, Atchley RA, O'Hare AJ, Gibson LJ, Hajcak G, et al. Increased neural sensitivity to self-relevant stimuli in major depressive disorder. *Psychophysiology.* (2019) 56:e13345. doi: 10.1111/psyp.13345
19. Derry PA, Kuiper NA. Schematic processing and self-reference in clinical depression. *J Abnorm Psychol.* (1981) 90:286–97. doi: 10.1037//0021-843x.90.4.286
20. Stein DJ. Depression, anhedonia, and psychomotor symptoms: the role of dopaminergic neurocircuitry. *CNS Spectr.* (2008) 13:561–5. doi: 10.1017/s1092852900016837
21. American Psychiatric Association [APA]. *Diagnostic and Statistical Manual of Mental Disorders*. 4th ed. Washington, DC: American Psychiatric Association. (1994)
22. Hamilton M. A rating scale for depression. *J Neurol Neurosurg Psychiatry.* (1960) 23:56–62. doi: 10.1136/jnnp.23.1.56
23. Cai H, Wu L. The self-esteem implicit association test is valid: evidence from brain activity. *Psych J.* (2021) 10:465–77. doi: 10.1002/pchj.422
24. Nosek BA, Banaji MR. The go/no-go association task. *Soc Cogn.* (2001) 19:161–76.
25. Greenwald AG, Nosek BA, Banaji MR. Understanding and using the implicit association test: I. An improved scoring algorithm. *J Pers Soc Psychol.* (2003) 85:197–216. doi: 10.1037/0022-3514.85.2.197
26. Monaghan CK, Brickman S, Huynh P, Öngür D, Hall MH. A longitudinal study of event related potentials and correlations with psychosocial functioning and clinical features in first episode psychosis patients. *Int J Psychophysiol.* (2019) 145:48–56. doi: 10.1016/j.ijpsycho.2019.05.007
27. Yang J, Guan L, Dedovic K, Qi M, Zhang Q. The neural correlates of implicit self-relevant processing in low self-esteem: an ERP study. *Brain Res.* (2012) 1471:75–80. doi: 10.1016/j.brainres.2012.06.033
28. Wu L, Gu R, Cai H, Zhang J. Electrophysiological evidence for executive control and efficient categorization involved in implicit self-evaluation. *Soc Neurosci.* (2016) 11:153–63. doi: 10.1080/17470919.2015.1044673
29. Gray HM, Ambady N, Lowenthal WT, Deldin P. P300 as an index of attention to self-relevant stimuli. *J Exp Soc Psychol.* (2004) 40:216–24. doi: 10.1016/S0022-1031(03)00092-1
30. Klawohn J, Joyner K, Santopetro N, Brush CJ, Hajcak G. Depression reduces neural correlates of reward salience with increasing effort over the course of the progressive ratio task. *J Affect Disord.* (2022) 307:294–300. doi: 10.1016/j.jad.2022.03.051
31. Zhang J, Li X, Du J, Tan X, Zhang J, Zhang Y, et al. Impairments of implicit emotional neurocognitive processing in college students with subthreshold depression: an ERP study. *J Clin Neurophysiol.* (2021) 38:192–7. doi: 10.1097/wnp.0000000000000680
32. Luck SJ. *An Introduction to the Event-Related Potential Technique*. 2nd ed. Cambrige: The MIT Press (2014).
33. Nowparast Rostami H, Ouyang G, Bayer M, Schacht A, Zhou C, Sommer W. Dissociating the influence of affective word content and cognitive processing demands on the late positive potential. *Brain Topogr.* (2016) 29:82–93. doi: 10.1007/s10548-015-0438-2
34. Hajcak G, Foti D. Significance?.... Significance! Empirical, methodological, and theoretical connections between the late positive potential and P300 as neural responses to stimulus significance: an integrative review. *Psychophysiology.* (2020) 57:e13570. doi: 10.1111/psyp.13570
35. Sommer A, Fallgatter AJ, Plewnia C. Investigating mechanisms of cognitive control training: neural signatures of PASAT performance in depressed patients. *J Neural Transm.* (2021) 129:649–59. doi: 10.1007/s00702-021-02444-7
36. Smeijers D, Vrijsen JN, van Oostrom I, Isaac L, Speckens A, Becker ES, et al. Implicit and explicit self-esteem in remitted depressed patients. *J Behav Ther Exp Psychiatry.* (2017) 54:301–6. doi: 10.1016/j.jbtep.2016.10.006
37. Suslow T, Bodenschatz CM, Kersting A, Quirin M, Günther V. Implicit affectivity in clinically depressed patients during acute illness and recovery. *BMC Psychiatry.* (2019) 19:376. doi: 10.1186/s12888-019-2365-3
38. Beevers CG. Cognitive vulnerability to depression: a dual process model. *Clin Psychol Rev.* (2005) 25:975–1002. doi: 10.1016/j.cpr.2005.03.003
39. Cai H, Luo YLL. The heritability of implicit self-esteem: a twin study. *Pers Individ Differ.* (2017) 119:249–51. doi: 10.1016/j.paid.2017.07.028
40. Izuma K, Kennedy K, Fitzjohn A, Sedikides C, Shibata K. Neural activity in the reward-related brain regions predicts implicit self-esteem: a novel validity test of psychological measures using neuroimaging. *J Pers Soc Psychol.* (2018) 114:343–57. doi: 10.1037/pspa0000114
41. Baldessarini RJ, Innamorati M, Erbuto D, Serafini G, Fiorillo A, Amore M, et al. Differential associations of affective temperaments and diagnosis of major affective disorders with suicidal behavior. *J Affect Disord.* (2017) 210:19–21. doi: 10.1016/j.jad.2016.12.003
42. Klawohn J, Santopetro NJ, Meyer A, Hajcak G. Reduced P300 in depression: evidence from a flanker task and impact on ERN, CRN, and Pe. *Psychophysiology.* (2020) 57:e13520. doi: 10.1111/psyp.13520
43. Polich J. Updating P300: an integrative theory of P3a and P3b. *Clin Neurophysiol.* (2007) 118:2128–48. doi: 10.1016/j.clinph.2007.04.019

44. Shahaf G. Neuropsychiatric Disorders as Erratic Attention Regulation - Lessons from Electrophysiology. *Psychiatr Q.* (2019) 90:793–801.
45. Fleischhauer M, Strobel A, Diers K, Enge S. Electrophysiological evidence for early perceptual facilitation and efficient categorization of self-related stimuli during an Implicit Association Test measuring neuroticism. *Psychophysiology.* (2014) 51:142–51. doi: 10.1111/psyp.12162
46. Beck AT. Beyond belief: A theory of modes, personality, and psychopathology. In: Salkovskis PM editor. *Frontiers of Cognitive Therapy*. New York, NY: The Guilford Press (1996). p. 1–25.
47. Whitton AE, Kakani P, Foti D, Van't Veer A, Haile A, Crowley DJ, et al. Blunted neural responses to reward in remitted major depression: a high-density event-related potential study. *Biol Psychiatry Cogn Neurosci Neuroimaging.* (2016) 1:87–95. doi: 10.1016/j.bpsc.2015.09.007
48. Knyazev GG, Savostyanov AN, Bocharov AV, Rudych PD. How self-appraisal is mediated by the brain. *Front Hum Neurosci.* (2021) 15:700046. doi: 10.3389/fnhum.2021.700046

Conflict of Interest: The authors declare that the research was conducted in the absence of any commercial or financial relationships that could be construed as a potential conflict of interest.

Frontiers in Psychiatry

Explores and communicates innovation in the field of psychiatry to improve patient outcomes

The third most-cited journal in its field, using translational approaches to improve therapeutic options for mental illness, communicate progress to clinicians and researchers, and consequently to improve patient treatment outcomes.

Discover the latest Research Topics

See more →

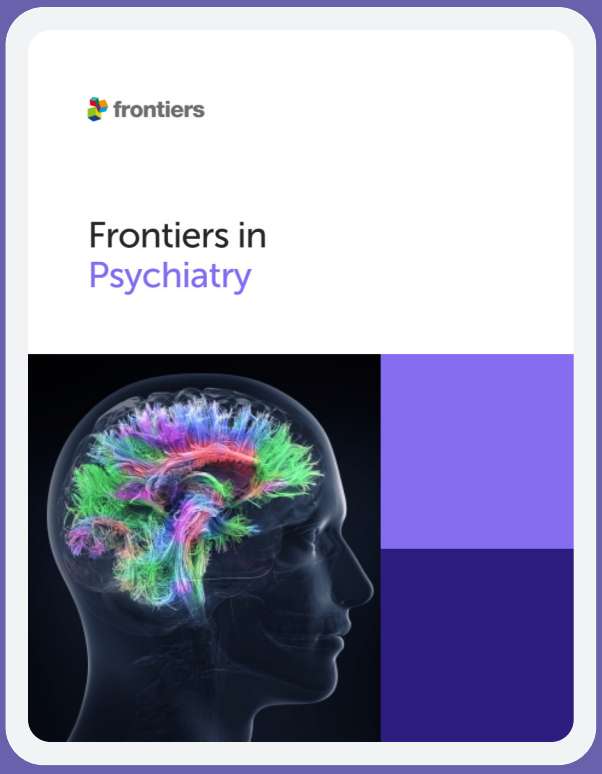

Frontiers

Avenue du Tribunal-Fédéral 34
1005 Lausanne, Switzerland
frontiersin.org

Contact us

+41 (0)21 510 17 00
frontiersin.org/about/contact